

Monitoring Recovery Trends in Key Spring Chinook Habitat: Annual Report 2011

publication date: March 31, 2011

Authors: Dale A. McCullough, Casey Justice, Seth White, Rishi Sharma, Denise Kelsey, David Graves, Nicole Tursich, Laurinda Hill, Tarin Lewis, Robert Lessard, and Henry Franzoni



Technical Report

11-05

Columbia River Inter-Tribal Fish Commission

700 NE Multnomah St, Ste 1200, Portland OR 97232 • (503)238-0667 • www.critfc.org

Funding for this work came from the Columbia Basin Fish Accords (2008-2018), a ten-year tribal/federal partnership between the Bonneville Power Administration, Bureau of Reclamation, Columbia River Inter-Tribal Fish Commission, The Confederated Tribes of the Umatilla Indian Reservation, The Confederated Tribes of the Warm Springs Reservation of Oregon, US Army Corps of Engineers, and The Confederated Tribes and Bands of the Yakama Nation.

Annual Report (2011)

Monitoring Recovery Trends in Key Spring Chinook Habitat

Columbia River Inter-Tribal Fish Commission

Authors: Dale A. McCullough, Casey Justice, Seth White, Rishi Sharma, Denise Kelsey, David Graves, Nicole Tursich, Laurinda Hill, Tarin Lewis, Robert Lessard, and Henry Franzoni

Project Number: 2009-004-00

Proposer: CRITFC

Short Description: Monitoring recovery trends in key spring Chinook habitat

Province(s): Blue Mountain

Subbasin(s): Grande Ronde

Contact Name: Dale A. McCullough

Contact email: mccd@critfc.org



Table of Contents

Contents

A : 165. Produce Environmental Compliance Documentation - Provide proof of all EC and permits to BPA.....	5
A. Stream work permit-NOAA.....	5
B. Stream work.....	5
B : 191. Watershed Coordination - Coordinate with regional agencies, tribes, and landowners.....	6
A. Coordinate with regional agencies, tribes, and landowners.....	6
B. Tribal coordination.....	7
C. Deliverable: Coordination on Research, Monitoring and Evaluation.....	7
C : 157. Collect/Generate/Validate Field and Lab Data - Collect water temperature, sediment, streamflow and habitat condition data.....	8
A. Environmental compliance requirements complete.....	8
B. Calibrate and install water temperature monitoring devices.....	8
C. Streamflow data.....	8
D. Snorkel sample to estimate fish densities by reach.....	10
E. Collect macroinvertebrate samples.....	12
F. Process macroinvertebrate samples.....	13
G. Map habitat units using CHaMP protocol.....	14
H. Water temperature field data collection.....	16
I. Conduct sediment infiltration study with gravel-filled buckets in spawning.....	16
J. Data entry.....	17
See Appendix A. Database Development and Implementation for Temperature and flow database (raFT).....	17
K. Data summaries.....	18
L. Deliverable: L. 2011 data collection on key fish habitat parameters.....	18
D : 156. Develop RM&E Methods and Designs - Review and refine monitoring protocols and statistical designs.....	18
A. Field manual for fine sediment, water temperature, streamflow monitoring, climate.....	18
See Appendix B. Draft Revisions to the Solar Input and Riparian Canopy Protocol that Incorporates use of the Solmetric SunEye.....	19
See Appendix C. Protocol for Snorkel Surveys of Fish Densities.....	19

See Appendix D. Summary of fine sediment conditions in Catherine Creek and Upper Grande Ronde River during summer 2011	19
See Appendix E. Study Design for Evaluation of Fine Sediment Infiltration and Chinook Embryo Survival in the Upper Grande Ronde River and Catherine Creek	19
See Appendix F. Compilation of Diagrams and Literature Illustrating the Options for Implementing Radiation Shielding of Air Temperature Sensors	20
B. Training in use of field equipment	20
C. Sampling Design	21
D. Develop draft life cycle model	21
E. Training in monitoring methods and statistics	22
F. Training in habitat restoration methods and principles	23
G. Deliverable: G. Monitoring plan and model for temperature, sediment and flow measures on the Grande Ronde	23
See Appendix G. Upper Grande Ronde River Basin Stream Temperature Modeling	23
See Appendix E	23
See Appendix H. Work Plan for Hydrological Analysis	23
E : 160. Create/Manage/Maintain Database - Develop and manage fish habitat condition database	23
A. Continue database development and implementation	23
B. Deliverable: B. Habitat Variables Database	24
F : 162. Analyze/Interpret Data - Summarize and integrate findings	24
A. GIS Analysis	24
See Appendix I. Aerial images of terrain for all CHaMP sites; Summary of Stream Statistics	24
See Appendix J. Report on the acquisition, mapping, and quality control of ODFW Aquatic Habitat Inventory data	26
B. Analysis of temperature, sediment, streamflow, riparian canopy	26
See Appendix K. Summary of Stream Temperature in the Upper Grande Ronde River and Catherine Creek During Summer 2011	26
See Appendix L. Joint Probabilities for Air Temperature and Streamflows	26
See Appendix M. Streamflow Statistics Summaries	26
See Appendix N. Correlations among USGS stream gauges in the Grande Ronde River and Catherine Creek and selected statistics for these long term gauges	26
See Appendix F.	26
See Appendix O. Upper Grande Ronde River Basin Stream Temperature Modeling: Scenarios	27
See Appendix P. Summary of Solar Input in the Upper Grande River and Catherine Creek during Summer 2011	27

C.	Hydrological analysis.....	27
	This proposal is available in Appendix Q (Kelly 2012, Characterizing Low-Flow Regime in Upper Grande Ronde River Basin, Oregon).	27
D.	Final development and testing of water temperature model.....	27
E.	Deliverable: E. GIS Analysis on existing data layers	28
G :	161. Disseminate Raw/Summary Data and Results - Present findings and procedures in professional meetings	28
A.	Presentation in AFS, JNABS, JASA or other symposia	28
B.	Post data to the internet.....	29
C.	Present findings and procedures in routine professional meetings	29
	See Appendix R. Measuring Shade and Solar Radiation Using the Solmetric SunEye.....	29
H :	183. Produce Journal Article - Produce draft journal publications on fish/habitat relationships.....	30
A.	Produce draft journal article on fish-habitat relationships	30
B.	Deliverable: B. Draft paper on monitoring or modeling in the Grande Ronde basin.	31
	See Appendix S. The landscape context of fish-habitat relationships: implications for restoring wood recruitment processes in U.S. Pacific Northwest rivers	31
I :	119. Manage and Administer Projects – Project Administration	31
A.	Accrual - Submit September 2011 estimate to BPA.....	31
B.	Submit Draft 2012 SOW/budget to COTR.....	31
C.	Funding Package - Conduct internal review (e.g., Supervisor or Interagency)	31
D.	Submit Final 2012 SOW/budget/property	32
E.	Submit 2011 Cost Share Data to BPA	32
F.	Obtain bids for potential subcontracts prior to 2012.....	32
J :	132. Produce (Annual) Progress Report - Annual Report - April 1, 2011 to March 31, 2012.....	32
A.	Review progress report format requirements.....	32
B.	Submit progress report for internal contractor review	32
C.	Submit progress report for external review.....	32
D.	Deliverable: D. Attach Annual Report in Pisces for April 2010 to March 2011	33

A : 165. Produce Environmental Compliance Documentation - Provide proof of all EC and permits to BPA

A. Stream work permit-NOAA

4/1/2011 5/15/2011

On June 8, 2010 we received a letter from William W. Stelle, Regional Administrator of NOAA in response to our May 24, 2010 permit request with the subject: Endangered Species Act Section 7 Informal Consultation and Magnuson-Stevens Fishery Conservation and Management Act Essential Fish Habitat Consultation for the Columbia River Inter-Tribal Fish Commission's (CRITFC's) proposal to conduct stream and riparian monitoring in the upper Grande Ronde River, Minam River, and Catherine Creek, Oregon. NOAA concurred that the proposed actions in our Accords habitat monitoring project are "not likely to adversely affect (NLAA) critical habitat or species listed as threatened or endangered under the Endangered Species Act (ESA)." This permit will be operative through this Accords project unless the scope of our activities changes. At some point, we wish to include studies of survival to emergence of Chinook eggs from Lookingglass Hatchery (Grande Ronde captive broodstock) placed in gravel-filled buckets in the Upper Grande Ronde. Even this would be done using the stock currently used in supplementation, this activity will require special permitting to ensure that taking 4000 eggs would not affect the stock viability.

Instream work in the Grande Ronde and Catherine Creek under the permit involves placing thermistors in the stream; maintaining our 2 depth gauge recorders in place and taking streamflows periodically to establish stage height/flow relationships; taking macroinvertebrate samples at times when the listed fish are not present; snorkeling to obtain juvenile fish density estimates; conduct summertime habitat measurements using CHaMP methodology after steelhead emergence and before Chinook spawning; embedding gravel-filled buckets into streambed substrate to measure fine sediment infiltration; conducting habitat surveys according to NOAA's CHaMP protocol; measuring streamflow at all 25 monitoring reaches.

B. Stream work

4/1/2011 5/15/2011

On June 2, 2010 the USFWS sent Jennifer Stolz a memo concerning the permit for our instream work in the Grande Ronde, Catherine Creek, and the Minam River. The memo subject was: proposed CRITFC Accord Monitoring Project, Grande Ronde Subbasin, Union and Wallowa Counties, Oregon-Informal Consultation (FWS reference 13420-2010-I-0112). This memo provided the USFWS's concurrence on this project in accordance with the ESA of 1973 that this project would not adversely affect threatened bull trout. This permit will be operative through this Accords project unless the scope of our activities changes.

Work under the permit will involve placing thermistors in the stream; maintaining streamflow depth gauge recorders in the stream (this was approved by BPA in year 2009); taking streambed substrate samples in spawning zones during the time period when listed fish are not spawning (prior to Sept. 1); taking macroinvertebrate samples at times when the listed fish are not spawning; snorkeling to estimate juvenile fish densities, collecting habitat condition data according to CHaMPs protocol.

B : 191. Watershed Coordination - Coordinate with regional agencies, tribes, and landowners

A. Coordinate with regional agencies, tribes, and landowners

4/1/2011 3/31/2012

- We coordinated our activities with Oregon Department of Fisheries and Wildlife, the Confederated Tribes of the Umatilla Indian Reservation (CTUIR), and local landowners. Coordination with ODFW was primarily through Rich Carmichael, Ted Sedell, and Chris Horn. Coordination with CTUIR involved coordination primarily with Les Naylor, Allan Childs, Steve Boe, and Gene Shippentower. Coordination with local landowners was conducted through the Grande Ronde Model Watershed by contact with Jeff Ovesen, Mason Bailie, and Coby Menton. Coordination with the USFS was conducted with Paul Boehne, Joe Platts, and their hydrologist (Kayla Morinaga). Coordination with EPA was conducted by cooperative work with Phil Larsen. Coordination with the CHaMP team involved cooperative work, conference calls, and meetings with Chris Jordan (NOAA, Program Manager), Michael Ward (Terraqua, Inc., CHaMP program coordinator), Boyd Bouwes (Quantitative Consultants Inc., Monitoring Coordinator, protocol development lead), Andrew Hill (protocol development, EcoLogical Research), Nick Bouwes (protocol development, Utah State University), Carol Volk (sampling design, protocol development), Steve Rentmeester (Sitkatech, data management, data logger), Kelly Whitehead (post-field processing of GIS data in ForeSight and ArcGIS), Meagan Polino (EcoLogical, equipment selection and purchase), and David Byrnes (BPA, Program COTR).
- We coordinated with PNAMP concerning macroinvertebrate sample collection methodologies.
- We attended two expert panel workshops sponsored by BPA in La Grande seeking to apply their methodology for accounting for restoration activities in addressing limiting factors.
- We contacted Dr. Paul Anderson, OSU Department of Forestry, to evaluate best options for measurement of solar radiation using a hemispherical image from a fish eye lens camera. Dr. Anderson advised that we use the HemiView software (<http://www.dynamax.com/hemiview.htm>) for analysis of view to sky (i.e., % open sky). He provided us with a protocol his lab uses (J. Sewell, 2004, Hemispherical Photographs, Image Capture Ver. 1.0), which we incorporated into our protocol that we developed for CHaMP.
- Participation with NW Biological Assessment Workgroup (26-28 Oct 2011, Skamania, WA) in order to integrate Tribal monitoring of benthic macroinvertebrates and fish distribution into regional assessments.

- Participation with PNAMP Habitat Data Sharing Macroinvertebrate Planning Group. This group promotes using standard field and laboratory protocols related to benthic macroinvertebrate collection, and facilitates data sharing across the region.
- CHaMP: Two presentations at November post-season workshop on preliminary analyses of 2011 CHaMP data. Participation on CHaMP-ISEMP conference calls coordinating statistical analyses of fish habitat conditions. Significant involvement on revisions to protocol.
- Literature review, development, and training of CRITFC and ODFW field crews on macroinvertebrate sampling according to PNAMP standards and snorkel estimates of fish density modified from published protocols to meet specific project needs (see attached White et al. 2011).
- Initiation of cooperative agreement with USGS on stream flow project, including development of objectives, revisions to work plan, and administration of budget (see attached Kelly 2012).
- Presentation of CRITFC habitat project at Grande Ronde Model Watershed landowner meeting, Cove, OR.
- Presentation to Nez Perce Watershed Department re: CRITFC habitat monitoring program, November 2012.
- Presentation at Expert Panel workshop, La Grande, February 2012.

B. Tribal coordination

4/1/2011 3/31/2012

Coordinate with CRITFC member tribes that are developing or implementing sound RM&E plans. We have scheduled a presentation of our CHaMP and Accords work to the CRITFC Commission in April 2012. We hope to communicate the importance of this work as a means of understanding trends in spring Chinook habitat conditions and related survival of the population. Our monitoring project in the Upper Grande Ronde, Catherine Creek, and the Minam River entails work under CHaMP and the Accords for the Umatilla, Warm Springs and Yakama, and coordination with the Nez Perce due to their ceded area interest in the Minam and Wenaha drainages. This project will serve as a reference model for other similar projects conducted by these four tribes in other areas. We will learn from these projects collectively, and share information about monitoring methods and study designs for different sets of objectives.

C. Deliverable: Coordination on Research, Monitoring and Evaluation

3/31/2012

We shared LiDAR data with the CTUIR so that they could effectively plan their restoration activities on Rock Creek, which enters the Grande Ronde near Five Points Creek mouth. CTUIR biologist noticed from snorkeling that spring Chinook juveniles use Rock Creek heavily. Conducting riparian restoration projects on Rock Creek will improve rearing survival during summer, given that water temperatures are adverse in Rock Creek.

The CTUIR and USFS shared their water temperature with CRITFC and CRITFC shared our data with CTUIR. The USFS intends to share their streamflow data with CRITFC, but this has not occurred in FY 2011 to date.

CRITFC received streambed substrate (McNeil) samples from ODFW that it processed for use by both CRITFC and ODFW. CRITFC has access to ODFW habitat and water quality data through involvement in CHaMP.

We kept partners informed of our monitoring activities

C : 157. Collect/Generate/Validate Field and Lab Data - Collect water temperature, sediment, streamflow and habitat condition data

A. Environmental compliance requirements complete

4/1/2011 5/16/2011

Documentation of environmental compliance was submitted to BPA environmental compliance staff. BPA ensured the concurrence of NOAA and USFWS in their permitting of our project and also completed a HIP document of their own covering our work, which was filed in Pisces.

B. Calibrate and install water temperature monitoring devices

6/1/2011 7/1/2011

We calibrated thermistors against a NIST standard thermometer and assembled water temperature thermistor units with housings and attachment fittings for placing them in sampling locations. Thermistors (HoboTemp by Onset) were installed in approximately 25 stream locations in the mainstem or tributaries representing habitat monitoring locations and positions in the stream network and in selected additional locations used in our long-term winter temperature monitoring throughout the mainstem. The extensive network of year-around monitoring stations will be used for water temperature model validation. Site selection was conducted in consultation with the water temperature modeling contractor (Watershed Sciences, Inc.) and as part of the CHaMP study design. Sites will provide extensive spatial coverage in the stream system to permit high accuracy water temperature modeling longitudinally in the stream system.

C. Streamflow data

6/1/2011 3/31/2012

We measured streamflow at approximately 25 locations in the upper Grande Ronde and Catherine Creek where we conducted CHaMP habitat monitoring. These data, along with continuous streamflow measurements from our two gaging stations, USGS and USFS gaging stations, and other miscellaneous measurements, will be used to further calibrate and then validate a temperature-flow model that will be run based on measurements of air temperature, riparian condition, and cloud cover and other meteorological conditions. We collected data on the 2 gauge sites continuously throughout 2011 to adequately represent streamflows at various stage heights. A data summary will be included in the annual progress report.

In summer through fall of 2011, we redeployed water and air pressure sensors at two stream gauges that we operate in South Fork Catherine Creek and Sheep Creek. Sheep Creek was first visited 29 June to deploy sensors and take discharge measurements (total of 6 discharge measurements throughout season) but because of high flows, South Fork Catherine Creek was first visited later when flows began to subside, on 13 July (4 total discharge measurements throughout season). Figures (1 and 2) below show 2011 stage-discharge relationships for both gauges. Because of an air sensor failure in Sheep Creek, site-specific corrections for barometric pressure could not be made, but we are currently exploring the use of local weather data as a correction factor. Remaining analyses includes merging stage-discharge relationships from 2010 data and extrapolating flow estimates to unmeasured time periods based on the rating curves.

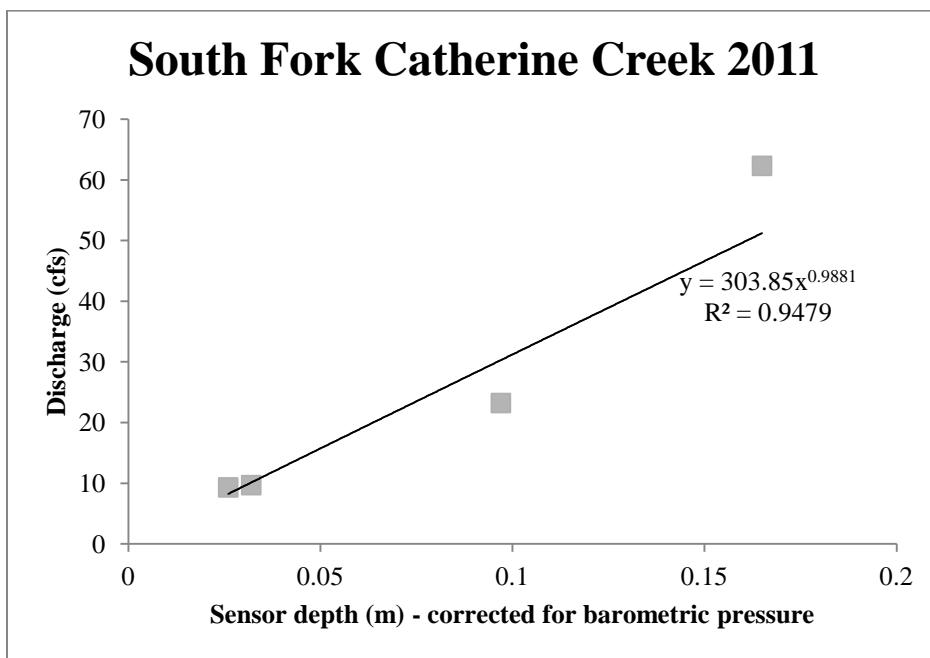


Figure 1. Stage height (water depth at depth logger cross section)-discharge relationship for the CRITFC gauging station at South Fork Catherine Creek for 2011.

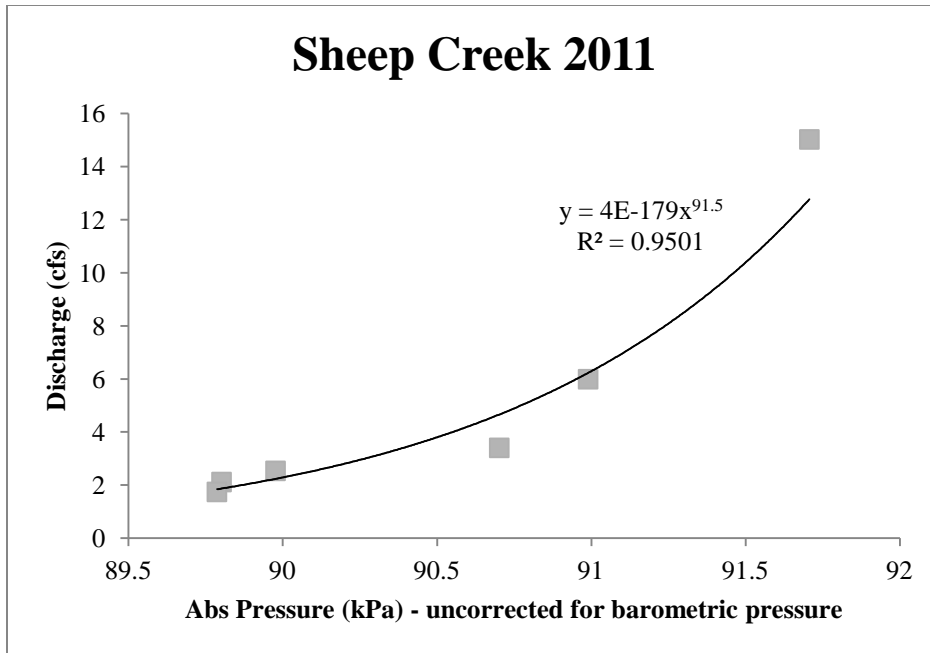


Figure 2. Stage height (water depth at depth logger cross section)-discharge relationship for the CRITFC gauging station at Sheep Creek (Upper Grande Ronde) for 2011.

D. Snorkel sample to estimate fish densities by reach

6/1/2011 10/1/2011

In summer of 2011, CRITFC and ODFW conducted snorkel surveys at 52 CHaMP locations according to the procedures of White et al. (2011). We conducted snorkel sampling in all CHaMP stream reaches to estimate fish species presence and densities in relation to key environmental factors of channel units. We counted numbers of salmonids (Chinook, steelhead, bull trout) by length classes and by channel unit. We noted the presence of other fish species observed.

A map of juvenile Chinook presence/absence reveals that Chinook presence extended beyond the expected distribution based on information provided by ODFW (Figure 3). Average pool areas, Chinook abundance, and Chinook density are reported for each tributary (Table 1).

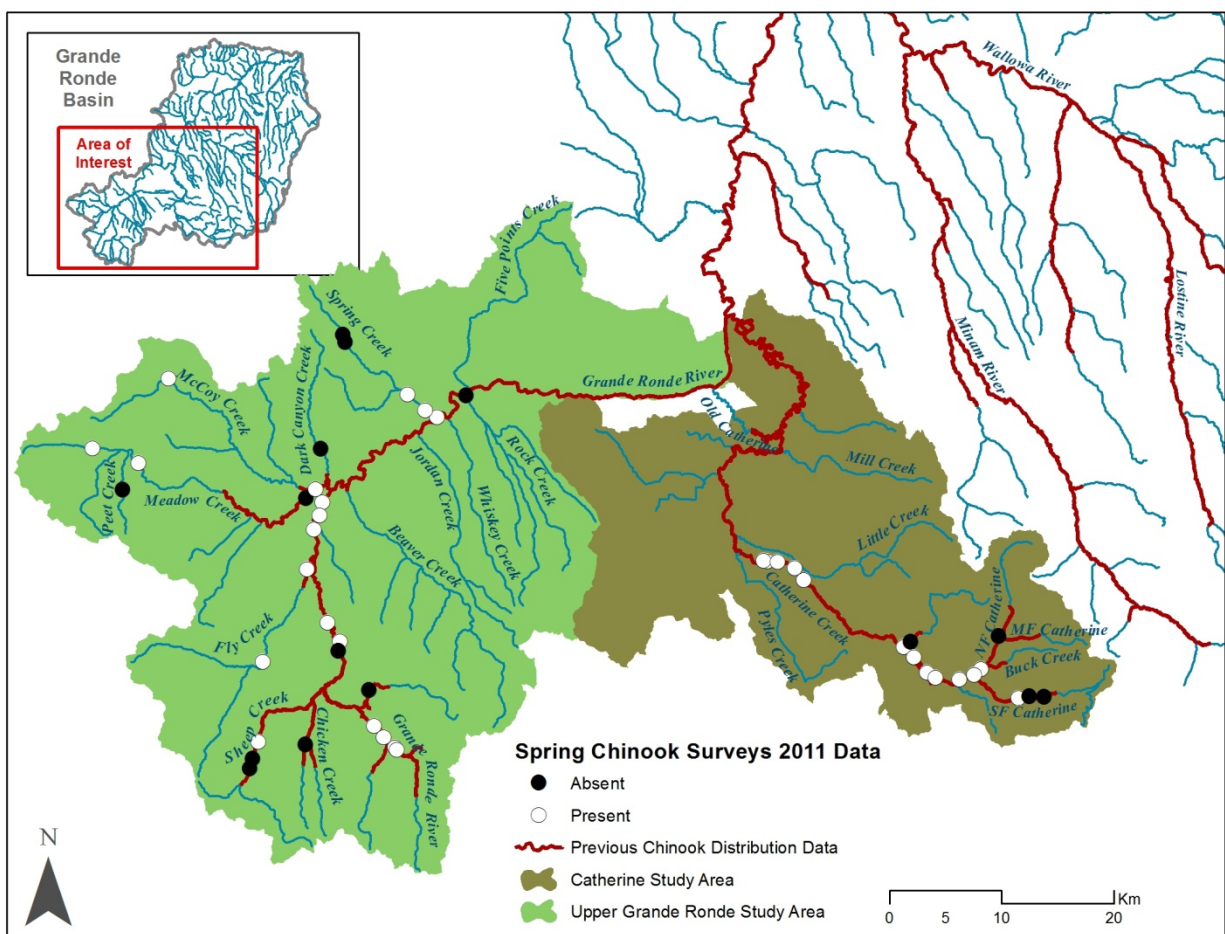


Figure 3. Presence/absence of spring Chinook salmon in the upper Grande Ronde and Catherine Creek basins in 2011.

Table 2. Average pool areas, Chinook abundance, and Chinook density reported for each tributary.

Stream	Average pool area (m ²)	Average juvenile Chinook abundance	Average juvenile Chinook density (fish/m ²)
Burnt Corral Creek	27.50	0.00	0.00
Catherine Creek	293.97	337.56	0.92
Clark Creek	0.00	0.00	0.00
Dark Canyon	0.00	0.00	0.00
Fly Creek	334.75	30.00	0.08
Gordon Creek	43.00	0.00	0.00
Grande Ronde River	410.21	178.36	0.40
Limber Jim Creek	275.89	0.00	0.00
Little Catherine Creek	146.60	0.00	0.00
Little Indian Creek	145.31	0.00	0.00
Little Phillips Creek	30.00	0.00	0.00
Meadow Creek	436.13	20.25	0.03

North Fork			
Catherine Creek	37.67	3.00	0.13
Peet Creek	0.00	0.00	0.00
Rock Creek	0.00	0.00	0.00
Sheep Creek	202.83	25.67	0.07
South Fork			
Catherine Creek	61.67	0.33	0.00
Spring Creek	54.15	2.00	0.04
Summer Creek	0.00	0.00	0.00
West Chicken Creek	0.00	0.00	0.00
Willow Creek	0.00	0.00	0.00

E. Collect macroinvertebrate samples

6/15/2011 10/15/2011

We used a quantitative sampling device (Hess sampler) to take benthic macroinvertebrate samples from riffles in spawning zones in all CHaMP study reaches. This will be an indicator of habitat quality of each stream site, water quality at the site, and overall watershed condition upstream. It also indicates the availability of a food base for rearing juveniles in relation to overall habitat quality and water temperature in particular. We composited 8 benthic samples (each 1 ft²) collected using a Hess sampler (500 um mesh) randomly in riffle habitat in a manner that represents the typical substrate composition. We took composite samples from each of the 25 stream CHaMP monitoring reaches.

We also collected two side-by-side daytime drift samples from a shallow, flowing section in the thalweg of each site according to CHaMP protocols. This produced a total of 2 drift samples for each of the 25 monitoring sites. The benthic and drift samples collected during the hot summer period reflect food availability when fish bioenergetic demands are greatest.

While benthic samples are still being processed by a contractor (ABR), drift samples have been processed in the laboratory including estimates of taxonomic composition; contribution of biomass by aquatic, aquatic-terrestrial, and terrestrial; and total biomass. Average biomass of drifting invertebrates was summarized by tributary in the upper Grande Ronde River basin, with notably high values in Gordon, Little Indian, and Peet, and Spring Creeks (Figure 4).

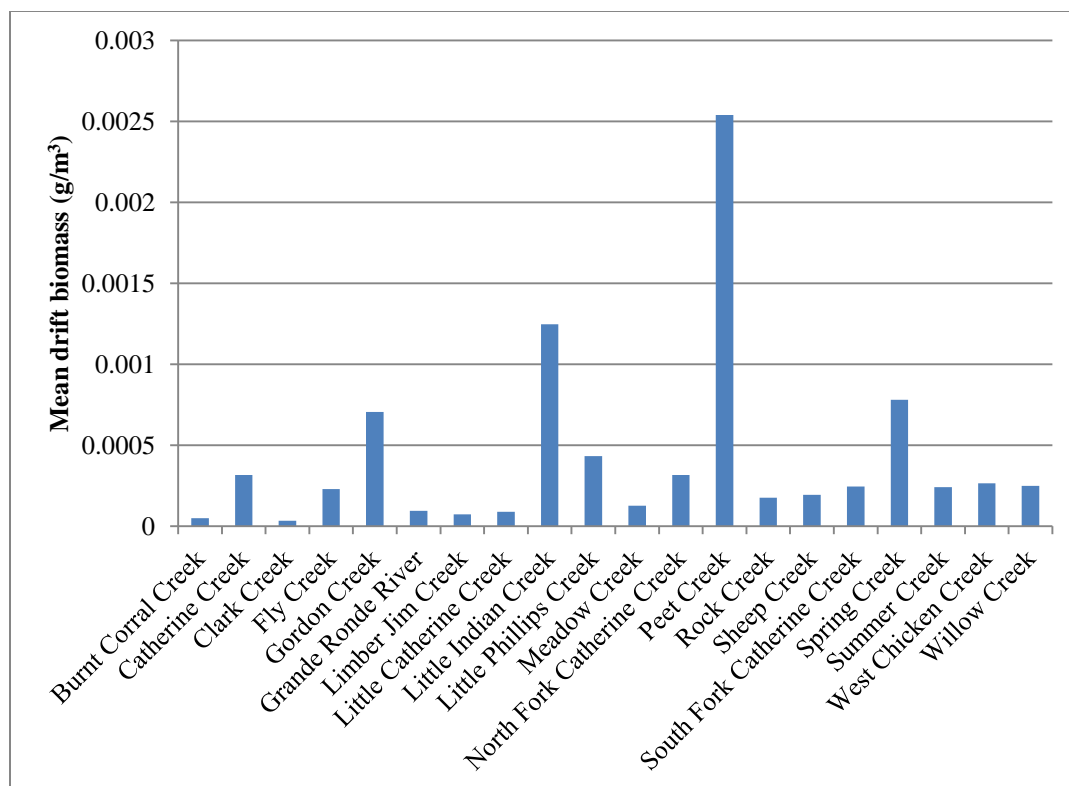


Figure 4. Average biomass of drifting invertebrates per volume of water in upper Grande Ronde River tributaries, 2011.

F. Process macroinvertebrate samples

4/1/2011 3/31/2012

In the 2011 contract year, laboratory processing of drift and benthic macroinvertebrates was completed on samples collected in 2010. A total of 21 samples were collected including four 24-hour drift samples in the Minam River and 17 benthic samples in the upper Grande Ronde, Catherine Creek, and Minam basins. Table 3 Summarizes the average benthic macroinvertebrate density, number of temperature sensitive indicator taxa, and number of fine sediment sensitive indicator taxa by tributary. Macroinvertebrate benthic and drift samples from 2010 were processed by ABR, Inc. Our 2011 benthic samples being processed by ABR, Inc. will be completed by April 2011.

Our 2011 drift samples were processed by Rhithron, Inc. using a protocol developed by CHaMP. Both labs counted individuals by taxa and measured lengths. Benthic data will be loaded to a CRITFC database for future access and analysis. Drift sample data will be located on the CHaMP server. For benthic samples, ABR conducted a basic statistical description using a wide variety of standard multimetric statistical indices. In addition, for QA/QC we employed ABA (Aquatic Biology Associates) to validate the taxonomic identification done by ABR by reviewing the voucher collection.

Table 3. Average benthic macroinvertebrate density, number of temperature sensitive indicator taxa, and number of fine sediment sensitive indicator taxa by tributary.

Stream name	Average of Invertebrate density (indiv/m ²)	Average of # Temperature Sensitive Indicator Taxa	Average of # Fine Sediment Sensitive Indicator Taxa
Catherine Creek	5347.52	4.50	6.00
Fly Creek	6294.86	3.00	3.00
Grande Ronde River	13421.70	2.60	3.20
Little Minam River	3215.70	7.50	7.00
Meadow Creek	4479.30	10.00	8.00
Minam River	3721.41	7.50	7.00
NF Catherine Creek	2719.58	10.00	10.00
SF Catherine Creek	8100.00	9.00	6.00
West Chicken Creek	10793.25	1.00	4.00

G. Map habitat units using CHaMP protocol

6/15/2011 10/1/2011

Habitat units (riffles, pools, glides) were mapped using the CHaMP protocol. This involved ocular recognition of channel units, flagging their boundaries, and then using a Total Station to survey their perimeters and internal topography. This will show potential spawning areas, deep pools that could be holding pools for adults and juveniles, smaller pools that could be rearing habitat, etc. This information is needed to follow trends in available spawning and rearing area. This is a habitat quantity issue. Habitat quality will be assessed with the measures of water temperature, substrate composition, etc. Habitat quality and quantity enter our production model to estimate carrying capacity. We used a McNeil sampler to collect subsurface fine sediment samples. CHaMP elected not to collect subsurface samples, but instead recommended use of ocular estimates of surface substrate composition, measurement of pool tail fine sediments using a grid intersection technique, and Wolman pebble counts. We believe the McNeil sampler provides a reliable and accurate assessment of egg incubation conditions that relates to survival to emergence. It may be that estimates of surface fine sediment by the ocular method, pool tail fines tallying, or pebble counts will be correlated with depth fines, but this will require continued subsurface monitoring.

Following the CHaMP protocol, a total of 311 habitat units were mapped in the upper Grande Ronde basin. Figure 5 demonstrates the concept of mapping habitat units using GIS, with darker blue areas indicating deeper pools and lighter areas indicating shallow habitat units such as riffles. The majority of mapped habitat in all CHaMP reaches from the upper Grande Ronde River was riffles, followed by rapids, runs, and pools (Figure 6).

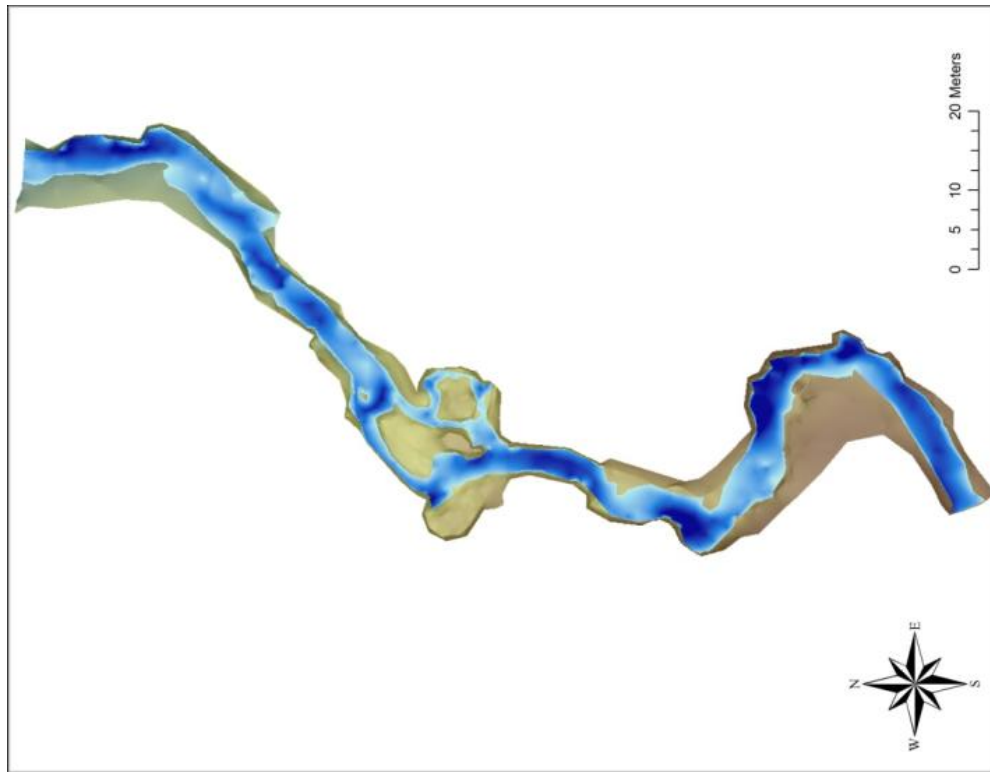


Figure 5. Example of processed DEM of CHaMP reach, with darker blue areas indicating deeper pools and lighter areas indicating shallow habitat units such as riffles.

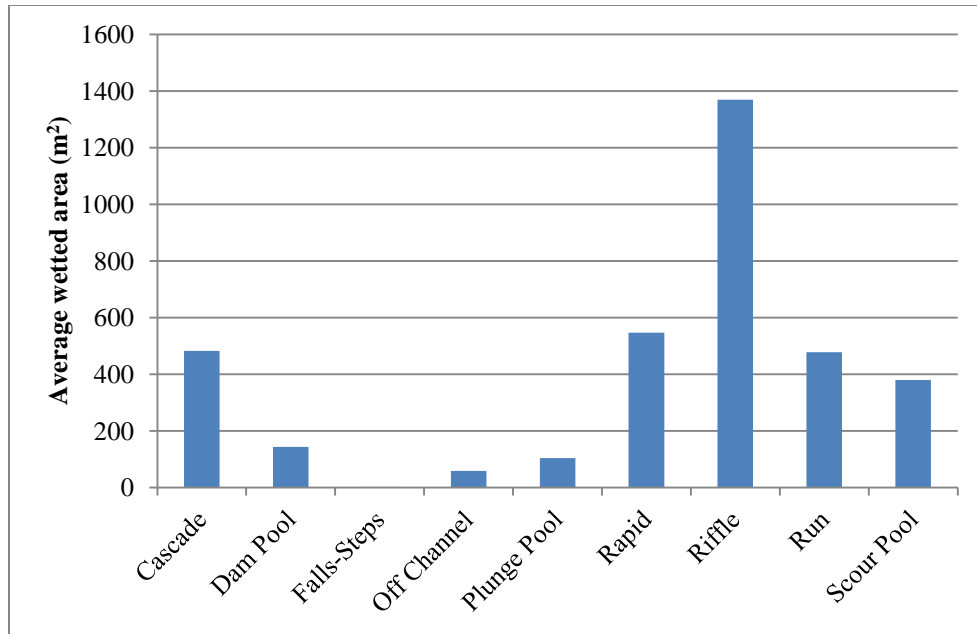


Figure 6. Average wetted area by tier II channel unit type for all CHaMP reaches in the upper Grande Ronde River basin.

H. Water temperature field data collection

8/1/2011 10/15/2011

We collected water temperature data using Hobo water temperature loggers at approximately 25 CHaMP monitoring locations in the Grand Ronde River and Catherine Creek plus other long-term sites on the mainstems of these rivers that act as our complete monitoring network. Data were transferred electronically to a data shuttle and then to a computer for transport back to the office for upload to the CHaMP cloud and analysis.

I. Conduct sediment infiltration study with gravel-filled buckets in spawning

9/1/2011 3/31/2012

We have intended for 2010 and 2011 to conduct an infiltration study. However, for reasons to be described below, we not able to implement this study in 2011. This study would involve placing plastic buckets into spawning beds to study fine sediment infiltration into simulated spawning gravel mixtures. These gravel mixtures would be created using sieved gravel fractions from previous sediment studies. We anticipated that rates of infiltration will be related to levels of fine sediments stored upstream in mainstem and tributary stream channels and the original (cleaned) gravel mixtures. We will randomly select potential spawning substrate that does not contain a redd by September 1 in which to embed buckets filled

with known gravel mixtures. We plan to use 3 different mixtures; 2 buckets per mixture type pulled from the streambed on December 1, January 15, March 1, and June 1 to allow plotting of infiltration rate. 3 mixtures, 2 replicates per mixture, and 4 dates for removal of buckets comprise 24 buckets per stream. Monitoring in the GR and CC will require 48 buckets total. In the future we hope to introduce fertilized eggs from supplementation stock to measure survival to emergence in relation to percentage of fines.

In 2011 we were not able to conduct this study. Streamflows were high until mid-July, causing us to begin field surveys with CHaMP methodology so late that we needed the entire summer to complete all sites that were part of our study design. This work has a high importance to the future success of our production model to represent reality. Consequently, we wish to keep this project in our annual tool kit to implement whenever we get the opportunity.

J. Data entry

9/1/2011 3/31/2012

For all habitat monitoring variables collected in the field using CHaMP protocols, data were entered to an electronic data logger and then downloaded each night to the computer and then to the CHaMP cloud. Other data such as photos were uploaded and photo IDs were indexed to specific sites, transects, and dates. Solar radiation data collected using the Solmetric SunEye were downloaded to folders specific to each site code. Snorkel survey data were recorded on paper data entry forms devised by CRITFC in preparation for transfer to a Sequel database. McNeil substrate data were entered after completion of processing of each sample by site. Data were comprised by dry weights for each particle size fraction computed after dry sieving and weighing on an analytical balance. Macroinvertebrate data were compiled by ABR on Excel spreadsheets and sent to CRITFC for maintenance on our database. GIS data were added to the CRITFC geodatabase structure for our study basins. All map products developed in the process of spatial analysis are available in the CRITFC network.

We applied QA/QC procedures to ensure data accuracy.

We applied a data entry form developed by CRITFC data management staff for digital entry of data from snorkel surveys. This data entry form was also available online for remote data entry by ODFW crews.

Significant effort was applied in further development of the CRITFC database for water temperature, flow, and snorkel survey data entry.

See [Appendix A](#). Database Development and Implementation for Temperature and flow database (raFT)

K. Data summaries

2/1/2012 3/31/2012

From data entered into Excel spreadsheets or GIS geodatabases, staff created data summaries and displays that portray trends. Water temperatures, streamflows, GPS site locations, substrate particle size characterization, macroinvertebrate communities, salmonid presence and densities are among the data collected. Analysis of trends will be needed to estimate statistically appropriate sample sizes. A data summary for water temperature and streamflows will be included in the annual progress report. The annual report will include raw data and graphics portraying these data.

Data coverage will become more spatially comprehensive as we continue to add more sites in our split panel design. The annual report will include increasing amounts of data interpretation, such as relating sediment conditions or infiltration to monitored levels of fines, watershed conditions, road densities in the watershed or riparian area, etc. Also, stream gradient and/or stream power calculations will be used to explain the distribution of bed substrate fine sediments. LiDAR, FLIR, and stream water temperature measurements were put together by Watershed Sciences to develop a working water temperature model. We will begin to explore the use of the model to predict future water temperatures as riparian restoration is targeted to specific stream reaches. The use of our growing database on habitat conditions, basin characteristics, and fish and macroinvertebrate distribution and abundance will be an increasing element in our annual reports. However, for 2011 the demands of the CHaMP program on CRITFC staff were very high. CRITFC staff spent weeks in doing QA/QC on data on the cloud, in reviewing and critiquing the CHaMP protocol, in helping modify and improve protocol elements, contributing to the “Lessons Learned” document, and in revising Total Station topographic site survey data and DEMs so that the RBT tool could handle the data available from surveys. The Total Station revisions would not have been necessary if the RBT tool were adequately developed to handle the variety of survey results captured.

L. Deliverable: L. 2011 data collection on key fish habitat parameters.

All data on key fish habitat parameters were uploaded to either the CHaMP cloud or, for Accord project only data, to the CRITFC database server.

3/31/2012

D : 156. Develop RM&E Methods and Designs - Review and refine monitoring protocols and statistical designs

A. Field manual for fine sediment, water temperature, streamflow monitoring, climate

4/1/2011 6/1/2011

CRITFC staff contributed significantly to further improvements in the CHaMP protocol in coordination with various other CHaMP staff. This involved critical review of the entire monitoring protocol and writing of draft revisions, followed by coordinated review and revision with other CHaMP protocol developers.

CRITFC staff had the responsibility to develop a module based on measurement of solar radiation using the Solmetric SunEye. In addition, staff researched the ability to use the SunEye's fish-eye lens to capture riparian canopy images for analysis of percentage view to sky (essentially a measure of the percentage of the hemispherical image that is clear sky as opposed to tree canopy or other obstructions to the sky).

See [Appendix B](#). Draft Revisions to the Solar Input and Riparian Canopy Protocol that Incorporates use of the Solmetric SunEye

We developed a protocol for snorkel surveys and uploaded this to www.monitoringmethods.org.

See [Appendix C](#). Protocol for Snorkel Surveys of Fish Densities

Staff conducted a statistical analysis of all 2011 McNeil core sediment collections made in pool tailout habitats and spawning patches within all CRITFC and ODFW CHaMP sites. Samples were collected according to already published CRITFC monitoring methodology.

See [Appendix D](#). Summary of fine sediment conditions in Catherine Creek and Upper Grande Ronde River during summer 2011

We are contemplating making adjustments to the McNeil fine sediment analysis by removing the armor layer prior to taking a core sample. Surface armor layers are typically coarser than subsurface materials. The presence of some of the large particles that are not eliminated from analysis by use of our size threshold could skew the percentage by weight measure used to report percentage fines. However, our procedure of applying large particle thresholds would probably tend to eliminate or reduce the impact of presence of a coarse surface layer that is not representative of materials at egg pocket depth.

Staff reviewed literature on the effect of fine sediment on survival to emergence (STE) in development of a draft protocol for measuring STE in the field in key spawning areas in the Upper Grande Ronde.

See [Appendix E](#). Study Design for Evaluation of Fine Sediment Infiltration and Chinook Embryo Survival in the Upper Grande Ronde River and Catherine Creek

CRITFC staff put together a compilation of information on radiation shields that would be used to improve the collection of air temperature data. The 2011 protocol called for the use of a very lightweight reflective insulation material to construct small, natural air-flow boxes that shield light from air temperature loggers. These boxes are nailed to trees as much as 30 m upslope from the riparian zone.

Major concerns with this design (shown at http://www.fs.fed.us/rm/boise/AWAE/projects/stream_temp/blogs/06ThoughtsOn%20monitoringAirTemperaturesInComplexForestedTerrain.pdf) are that:

- 1) they are fairly weak and could be affected by high winds and heavy snows

2) they get many holes drilled into lids that can provide an entry point for water to get inside. This could mean that loggers would be sitting in water that then acts as an evaporative cooling mechanism.

3) in winter the collection of water inside and lack of a reliable means of draining moisture, could result in icing and spurious temperature readings.

4) the variable spacing in the multiple plates in this modified Gill design allows variable amounts of light to enter the interior of the shield. Reflected light entering the shields gets converted to longwave radiation and heats up the interior.

The good points about the 2011 housings seem to be that they are made of highly reflective material that has a very low thermal conductivity and they are inexpensive. A brief comparison that Zack Holden did of the shield used by CHaMP in 2011 showed good performance of this design. This may be representative of certain conditions that he tested. However, the large variations that have been reported in the literature among varying designs is cause for some concern about how good our data are for air temperature. Under harsh field conditions, it seems that these shields won't hold up well. Maybe if these shields themselves could be mounted on something that would partially shield and support them, they might work better.

The alternative could be to build our own Gill type shields using inverted white plastic bowls and steel threaded rod. But this may be too laborious. A company called Ambient Weather seems to offer one for about \$35. It would be good to buy one and take it apart to see how it is built and compare it with a Hobo design, which in at least one study I reviewed used this as a standard for evaluating other designs.

Another option could be to put out fewer numbers of air temperature loggers, but to place them in the most protected locations in annual sites where we could get the best idea of the change in air temperature that occurs with altitude change. This could aid in figuring out an average regional lapse rate that could be applied to data from a good, long-term air temperature station.

After discussion with the CHaMP partners, the option that they chose was to select a Gill type natural air flow shield for all site locations. Presumably the vendor will be Onset.

See [Appendix F](#). Compilation of Diagrams and Literature Illustrating the Options for Implementing Radiation Shielding of Air Temperature Sensors

B. Training in use of field equipment

4/1/2011 7/15/2011

With the CHaMP 10-day training session held in Brewster, Washington in June 2011, we provided training to all professional and technical staff in use of: the Total Station, GPS equipment; water and air temperature data logger devices; water chemistry probes; channel unit recognition; collection of drifting macroinvertebrates; post-processing of Total Station survey data; Wolman pebble count process; pool tail fines; ocular substrate composition; riparian canopy evaluation; solar radiation; alkalinity. This training is required to collect accurate and standardized surveys of stream channel morphology, water temperature,

water chemistry, habitat, and streamflow data. In addition, we provided training in the field prior to collecting Accord related monitoring data. This training included use of the engineering level and rod; stream hydrograph equipment; McNeil sediment sample collection; benthic macroinvertebrate collection using the Hess sample.

C. Sampling Design

4/1/2011 3/31/2012

Continue work on sampling designs needed to obtain precise, unbiased estimators. Modeling staff will become familiarized in application of GRTS and its application in obtaining variance estimators. All sampling protocols are designed to be effective in capturing patterns and have inherent tradeoffs.

CRITFC staff worked in cooperation with Phil Larsen (EPA) and Carol Volk (NOAA) in refinement of the 2011 CRITFC sample frame and GRTS draw. The sample frame was adjusted to create a division of effort between CRITFC and ODFW. This also involved CRITFC concentrating its sample effort into currently used Chinook habitat rather than distributing effort downstream on the mainstem and upstream into tributaries to capture historically used habitats. Our 2010 legacy sample locations were integrated into the GRTS program so that we could continue to use these sites as annual sites.

Finalized protocol for snorkel surveys of fish abundance by species and size class (see attached White et al. 2011); published here: <http://monitoringmethods.org/Protocol/Details/499>

D. Develop draft life cycle model

4/1/2011 3/31/2012

In coordination with the monitoring framework program, continue development of draft life cycle model. This model will incorporate components of the habitat model (e.g., water temperature physical model, streamflow model relating watershed characteristics to streamflow statistics, streamflow/water temperature model), habitat characteristic/survival models (water temperature biological model, fine sediment biological model), and integrate these into a Chinook life cycle model. A life-cycle model will be constructed to characterize the environmental influences on salmon survival and, by virtue of being a full life-cycle model, will predict the potential production of the population given the past, present and predicted future conditions. Life-cycle modeling will involve four phases: Construction of a conceptual model, Historical reconstruction of system conditions, Historical reconstruction of population dynamics, and Forecast population dynamics under various scenarios of environmental conditions in the future. Using population and environmental reconstructions, the impact of the environment on stage to stage survival will be inferred. These estimated coefficients will be used as the basis for relating future conditions to commensurate increases or decreases in survival.

Developed model to examine the effect of spatial and temporal variability in habitat conditions on the estimation of population dynamics parameters. This was performed for the purpose of establishing the optimal subpopulation structure (lumping vs splitting) to assume in the spring run Chinook population model. A model was constructed to examine the interaction between process and observation errors in

subpopulation models and the effect on estimating the magnitude of environmental influences on survival as observed in aggregated data. The model assumed that individual spawning populations react to local conditions and that those effects are not seen in the data until all subpopulations are observed as an aggregate during smolt outmigration, i.e., we know about fine-scale stream conditions, but only coarse scale juvenile abundance. The model simulated stream specific conditions with a random effects model that incorporated temporal autocorrelation, thus simultaneously simulating spatial and temporal variation and temporal trends analogous to climate change. The analysis compared the predicted vs observed smolts when using subpopulations vs a single aggregated population. Environmental conditions were simulated for 20 years and Beverton Holt productivity and capacity parameters were simulated to change in relation to changes in 3 key environmental conditions. The variables are theoretical for the purpose of the analysis. Values were normalized such that no one effect would be dominant. For the aggregated case, the environmental condition was treated as the average of all fine scale simulated conditions and those conditions were used to drive the population. All populations act as one. For the split-combined case, populations act independently, but are recombined and treated as one for analysis. In the fully split case, each population is compared independently. The results showed that if the prediction errors are relatively low ($CV=0.3$), we can detect with good precision what the population response will be when we sample 6 populations in detail. However, when the prediction error reaches $CV=0.6$, the fully aggregated model does as well as either the split-combined analysis or the fully split population model. This preliminary result suggests that unless the environmental effects explain 70% or greater of the variation in survival, the remaining prediction error would make it impossible to accurately predict fine scale population response to environmental change without fine scale monitoring of stream specific abundances. However, with process error below 30%, a reasonable accuracy in predicted response to fine scale changes in environmental conditions appears feasible.

Another model (HoneaEval) was developed for the purpose of evaluating the published work of Honea et al (2009), where a Shiraz model was parameterized for Wenatchee Chinook. The Honea analysis showed that the percent fine sediment was the strongest predictor of survival and concluded that 160% improvements in smolt production could result from reductions in fine sediments. The HoneaEval model was developed to evaluate the effect of process error on the prediction of smolt abundances that arise from changes in fine sediment. The model will be used to gauge the expected population response when different functional forms for survival at each stage are combined with different process error terms. It will serve as a validation tool to compare other empirical work with the CRITFC population model.

E. Training in monitoring methods and statistics

4/1/2011 3/31/2012

Attended workshop “Using unmarked- An R package for fitting hierarchical models of species abundance and occurrence,” USGS, January 25-26, 2012.

Visual Basic 2008 Level 1. Online course through Education to Go. Course dates Jan 18 - Feb 24, 2012.

F. Training in habitat restoration methods and principles

4/1/2011 3/31/2012

Three science staff attended River Restoration Northwest symposium (Jan. 31-Feb. 2) at Skamania Lodge. This workshop is oriented toward methods and principles of salmon habitat restoration.

G. Deliverable: G. Monitoring plan and model for temperature, sediment and flow measures on the Grande Ronde

3/31/2012

Watershed Sciences, Inc. completed its draft of its Heat Source water temperature model, which incorporates past LiDAR, FLIR, and distributed water temperature measurements.

See [Appendix G](#). Upper Grande Ronde River Basin Stream Temperature Modeling

A protocol for monitoring fine sediment infiltration and related survival to emergence of spring Chinook embryos under field conditions.

See [Appendix E](#).

A long-term plan for evaluating streamflow statistics was devised.

See [Appendix H](#). Work Plan for Hydrological Analysis

E : 160. Create/Manage/Maintain Database - Develop and manage fish habitat condition database

A. Continue database development and implementation

4/1/2011 3/31/2012

Most monitoring data is being housed on the CHaMP cloud server. This database is supported by Steve Rentmeester. A number of standard data analysis reports will be produced using this database and a set of mathematical procedures agreed to by participants that will provide a basic set of information common to all basins.

The CRITFC database will not need to house the bulk of CHaMP data but will support those elements not part of CHaMP. The database will link to the GIS system using GPS lat/long points for spatial representation of habitat condition. Key data entered will be water temperature, streamflow, stage height at gages, substrate particle size distribution from McNeil core samples, fish snorkel counts, macroinvertebrate taxonomic distribution and diversity, and fine sediment infiltration rates. In future

years, additional habitat information will be added to this database, such as pool frequency and location, streambank stability, and intragravel dissolved oxygen.

B. Deliverable: B. Habitat Variables Database

3/31/2012

The 2011 habitat variables database has been uploaded to either the CHaMP cloud server or the CRITFC habitat database, or is stored on the CRITFC network.

F : 162. Analyze/Interpret Data - Summarize and integrate findings

A. GIS Analysis

4/1/2011 3/31/2012

A draft article linking landscape and reach characteristics to site-level fish habitat and fish distribution describes GIS analysis conducted on 2011 CHaMP data and snorkel surveys (White et al., in preparation). See also section H:183.A. of this report.

We ordered a computer program that will allow assessment of a wide variety of watershed indices that will be used in a variety of applications, such as relating streamflow statistics to basin characteristics. This program is available from: <http://www.nvisionsolutions.com/products/BasinTools.php>. Among the indices available from GIS analysis with this program are drainage density, basin length, circularity, relief, hypsometric integral, channel slope, basin azimuth, etc.

We used the USGS StreamStats program to extract watershed characteristics for all stream sample sites. The latitude/longitude of sites were downloaded from <http://www.champmonitoring.org>. From that point, sites were located using Google Earth. Using the map measuring tool, sites were located on USGS maps with a corresponding measurement tool. Site characteristics and basin areas upstream of sites were extracted from StreamStats website after placing points on the stream layer at scales of <1:15K.

See **Appendix I**. Aerial images of terrain for all CHaMP sites; Summary of Stream Statistics

Once we have the BasinTools program, we will assign GIS staff to attribute all current and future CHaMP monitoring sites with watershed and channel characteristics that will comprise a database by which biological response can be related. Among the basin and channel characteristics (inherent and current) that will be developed using ArcMap (ESRI) are: mean annual precipitation by grid cell and cumulative precipitation at watershed scale; basin area; hypsometric integral; relief ratio; valley width by stream reach; channel longitudinal gradient; road density; road density for riparian zones for the entire stream network upstream of the site; road density in riparian zones for stream segments upstream by a fixed distance considered to have an effective influence on sites; land use; livestock density by tributary; lithology underlying stream reaches; hillslope lithology; soil type frequency; streamside soil types. We

also need to develop indices to historic land use impacts. Beechie has suggested to us the utility of General Land Office survey data as a guide to historic vegetation coverage.

A plan was outlined for expanding GIS analysis of current land use in the effective environment to study sites. The effective environment can be conceived of as the adjacent riparian zone to a site, the riparian zone within a fixed distance upstream, the entire riparian system upstream, the entire watershed upstream, or that portion of the watershed between the upper end of a study site and a mainstem point within a fixed distance upstream. If we want to get more refined, we can make assumptions about the effect of sediment delivery from sediment sources being related to their proximity. Sources that are adjacent or immediately upstream by a certain distance would be more effective than other sources further upslope or upstream in defining the amount of fine sediment. The distribution of cattle AUMs spatially would also be important information by which to model sediment delivery.

A brief summary of plans to digitize the roads not currently shown on existing GIS roads layers is the following:

- 1) gather any map data on roads from all available sources--USFS, ODOT, and others
- 2) overlay the compiled roads information with Google satellite imagery. Digitize the additional roads that are visible.
- 3) Roads should be differentiated somehow by quality if possible. Paved roads, gravel, dirt, trails, log landings.
- 4) If there is any information available on the age of unpaved roads, this would be helpful in sediment delivery models.
- 5) Once the road layers are all available, we need to assess how many miles and km/km² exist in the various tributary watersheds and the UGR as a whole, or to various key locations, such as at our sampling locations. Road quality would also factor into the calculation of potential sediment. Road quality on terrain of various characteristics (e.g., slope gradient) also plays a role in surface erosion modeling. We need road density (km/km²) by riparian zone and for the entire watershed.

CRITFC staff devoted considerable effort to a compilation of all ODFW Aquatic Habitat Inventory data into a database. In the Grande Ronde River basin and elsewhere in the state, Oregon Department of Fish & Wildlife (ODFW) has conducted spatially continuous, habitat-unit scale fish habitat surveys every decade since the 1990s. The Aquatic Habitat Inventory (AHI) surveys (Moore et al. 2008) employ rapid assessment techniques to collect coarse resolution information over large areas using modified rapid fish-habitat assessment procedures (Hankin and Reeves 1988). While more recent fish-habitat surveys such as the Columbia habitat monitoring protocol (CHaMP) (Bouwes et al. 2010) compromise extensive spatial coverage for precise measurements collected at a few, probabilistic random locations, we felt that AHI data were useful for describing coarse resolution habitat change through space and among decades. This report briefly describes our work in acquiring, mapping, summarizing metrics, and performing initial quality control procedures on AHI data. The final version of AHI data will be used by CRITFC for analysis of fish-habitat relationships, and the resulting database will be shared with ODFW, which will have the option of replacing the current dataset, which is available to the public, with the corrected dataset.

See [Appendix J](#). Report on the acquisition, mapping, and quality control of ODFW Aquatic Habitat Inventory data

B. Analysis of temperature, sediment, streamflow, riparian canopy

4/1/2011 2/1/2012

Field data will be linked to GPS coordinates in a database that will be captured by a GIS project map for the study areas. Temperature analysis will include basic statistics (hourly, daily, monthly values for min., mean, max.; and 7DADMax).

See [Appendix K](#). Summary of Stream Temperature in the Upper Grande Ronde River and Catherine Creek During Summer 2011

Correlations of water temperature with air temperature statistics will be computed.

See [Appendix L](#). Joint Probabilities for Air Temperature and Streamflows

Streamflow data will be computed for days sampled at all 25 monitored stream sites plus additional mainstem sites needed to track downstream water temperature trends. Longitudinal trends will be evaluated for pattern and anomalies. These data have been uploaded to the CHaMP cloud, but delays in QA/QC by the entire program have inhibited the database managers from implementing all calculation procedures on available data.

Streamflow statistics were calculated using the USGS StreamStats program.

See [Appendix M](#). Streamflow Statistics Summaries

Known irrigation diversions will be accounted for.

Correlations with existing USGS gages will be made.

See [Appendix N](#). Correlations among USGS stream gauges in the Grande Ronde River and Catherine Creek and selected statistics for these long term gauges.

The stream water temperature model (Heat Source) was developed by Watershed Sciences, Inc. based on LiDAR, FLIR, and water temperature and streamflow data and calibrated to replicate empirical measurements.

See [Appendix F](#).

Watershed Sciences, Inc. also produced several riparian restoration scenarios showing the system-wide thermal consequences in the modeled spring Chinook habitat. These results reveal the current thermal patterns against alternative combinations of streamflow and air temperature, and also contrast this with

potential natural riparian condition (PNV). The PNV conditions were the same as previously assumed by ODEQ in its earlier use of Heat Source in the Grande Ronde. The current model makes use of much more precise measures of current riparian condition from LiDAR and more robust water temperature and flow monitoring data. In the near future CRITFC is planning to use the LiDAR data and other available information to develop more ecologically accurate estimates of PNV to revise these scenarios.

See [Appendix O](#). Upper Grande Ronde River Basin Stream Temperature Modeling: Scenarios

CRITFC staff analyzed the solar radiation inputs to all CHaMP sites for 2011 using the Solmetric SunEye 210 handheld device. Data were entered into a computer database from the device. CSV files from this database provided the ability to compute mean daily or monthly solar radiation to each transect for each site accounting for riparian canopy shading.

See [Appendix P](#). Summary of Solar Input in the Upper Grande River and Catherine Creek during Summer 2011

C. Hydrological analysis

10/1/2011 3/31/2012

We will take the stream cross-sectional streamflow measurements made at each sampling site and place these streamflows in a regional context by comparison to long-term regional streamflow statistics from a combination of USGS gages, USFS gages, and the two gages that we installed (Sheep Creek on the upper Grande Ronde and South Fork Catherine Creek). After the computation of streamflows by site are available as described in Section B above, this process can take place.

In 2011 we initiated a cooperative agreement with USGS Water Science Center, which will begin April 1, 2012. The project has the goal of describing and modeling low flow statistics in tributaries of the Grande Ronde River, but the framework will be applicable to the broader region. We are drawing from extensive experience of USGS in helping us with this subject, the results of which will be directly relevant to one of the main goals of the Habitat Accords project: building a life cycle model for spring Chinook salmon in the upper Grande Ronde basin to evaluate restoration potential. The project is designed to estimate low flow statistics in ungaged streams and determine the influence of groundwater in buffering low flow events, which has important implications for salmon, especially with projected low flows from climate change.

This proposal is available in [Appendix Q](#) (Kelly 2012, Characterizing Low-Flow Regime in Upper Grande Ronde River Basin, Oregon).

D. Final development and testing of water temperature model

4/1/2011 11/30/2011

The Heat Source water temperature model, which incorporates the previously collected LiDAR and FLIR data, water temperature and streamflow data, and potential riparian vegetation estimates was calibrated for a 3-week period in August.

See [Appendix F](#).

In 2012 we plan to have Watershed Sciences extend the calibration of this model to include July-September. This will make the model more robust and usable as a predictor of water temperatures under a variety of summertime flows and air temperature conditions.

Watershed Sciences, Inc. is expected to provide CRITFC with 3 scenarios of riparian restoration to allow water temperature prediction consequences as its conclusion to the 2011 contract. Watershed Science has provided brief training to CRITFC staff in the use of the model. We anticipate needing additional training as we become more engaged in use of the model and WS indicated their willingness to help us become proficient.

E. Deliverable: E. GIS Analysis on existing data layers

3/31/2012

G : 161. Disseminate Raw/Summary Data and Results - Present findings and procedures in professional meetings

A. Presentation in AFS, JNABS, JASA or other symposia

4/1/2011 3/31/2012

Attend professional meetings to communicate Accord research to peers and/or make formal presentation based on monitoring work or planning.

R Lessard presented findings from the lumping vs splitting analysis “Multi-Stock Life Cycle Modeling” at the American Fisheries Society 2011 annual meeting in Seattle, WA.

White, S.M. 2011 (June). Concepts, meanings, and metaphors of biodiversity. Invited panelist, Biodiversity Perspectives Workshop, National River Rally, Charleston, South Carolina.

White, S.M., C. Justice, D. McCullough, and P. Roger. 2011 (April). Storytelling and structural equations modeling for linked watershed processes: common ground for indigenous perspectives and western science. Oral presentation, Annual Meeting of the Association of American Geographers, Seattle, Washington.

White, S.M., C. Justice, and D. McCullough. 2012 (March). Simplifying complex relationships between salmon and their habitat in the Pacific Northwest. Oral presentation, Oregon Chapter of the American Fisheries Society, Eugene, Oregon.

White, S.M. 2012 (March). A riverscape perspective of salmon habitat assessments on Tribal ceded lands. Invited speaker, U.S. Geological Survey (Water Science Center) Seminar Series, Portland, Oregon.

B. Post data to the internet

8/1/2011 3/31/2012

All monitoring data that was developed strictly for the CRITFC Accord work is housed on the CRITFC network and the Tribal Data Network. These data have associated metadata.

All data collected according to CHaMP protocols have been posted on CHaMPs cloud server site.

C. Present findings and procedures in routine professional meetings

8/1/2011 3/31/2012

Science staff presented a comparison of the Solmetric SunEye vs. Solar Pathfinder devices for measuring solar radiation reaching the stream sites at transects. This presentation and a related one presented on a CHaMP conference call showing the deficiencies in the Solar Pathfinder led to adoption of the SunEye 201 as the preferred monitoring tool.

The conference call presentation pointed out several key issues:

- (1) The Solar Pathfinder images were often too affected by solar flare on the hemispherical surface to be interpretable.
- (2) There was a significant discrepancy between the Pathfinder and the SunEye under conditions of high canopy cover (or low solar radiation at the stream level). At low surface radiation levels, the Pathfinder values were typically about 30% of those for the SunEye. This may mean that heavy canopy was generally interpreted to be dense and continuous, but the SunEye has the ability to account for radiation passing through large gaps in the canopy.
- (3) The SunEye instantly creates output data files, but images can be easily edited to correct color assignment to indicate obstructions or open sky.
- (4) CRITFC suggested a protocol that could be adopted to use the SunEye to capture hemispherical images that could then be analyzed using HemiView software.

See [Appendix R](#). Measuring Shade and Solar Radiation Using the Solmetric SunEye

Staff contributed to the following CHaMP document that was a culmination of a BPA and CHaMP partners meeting held in December, 2011:

Ward, M.B., S.M. Walker, P. Nelle, and C.E. Jordan, (editors). 2011. CHaMP: 2011 Pilot Year Draft Lessons Learned Project Synthesis Report. Prepared for the Bonneville Power Administration by CHaMP. Published by Bonneville Power Administration, Portland, OR. 94 pages

Deliverable: D. Presentation in AFS/JASA/FSBI

3/31/2012.

H : 183. Produce Journal Article - Produce draft journal publications on fish/habitat relationships

A. Produce draft journal article on fish-habitat relationships

4/1/2011 3/31/2012

White, S.M., C. Justice, and D. McCullough, (In prep). The landscape context of fish-habitat relationships: implications for restoring wood recruitment processes in U.S. Pacific Northwest rivers. Intended for Ecological Restoration.

Abstract:

The Columbia River Inter-Tribal Fish Commission (CRITFC) is conducting a monitoring program in Northeast Oregon basins designed to evaluate whether aggregate habitat restoration actions can positively affect threatened spring Chinook salmon populations. According to literature, common impediments to salmon survival are high water temperatures, fine sediment in spawning gravel, loss of riparian vegetation, channelization, lack of large woody debris in the channel, loss of large pools for adult fish to hold in prior to spawning, and summertime depletion of streamflows. However, the effects on salmon of these and other factors are often inter-correlated and the influence of each is dependent upon the entire suite of relationships, which can be difficult or impossible to tease out using classic univariate statistics. This presentation describes a “riverscape approach,” including the use of landscape classification, multivariate analyses, and structural equations modeling as tools for simplifying complex relationships. A multivariate ordination was conducted of reach-scale habitat data collected by the Columbia Habitat Monitoring Program (CHaMP) in 2011 across nine watersheds in the Pacific Northwest to discover an appropriate landscape-level classification, which in turn helped reveal patterns of anthropogenic impacts on site-level fish habitat. In the upper Grande Ronde River basin, estimates of juvenile Chinook salmon density (via snorkeling) were linked to landscape classification and site-level habitat conditions. Across the entire basin, large woody debris volume and frequency of pool area positively affected fish density, but their effects were swamped by mean annual streamflow. However, these relationships varied across landscape classes, with high elevation mountain reaches behaving differently than lower elevation floodplain and constrained reaches. These results demonstrate an approach to habitat modeling that CRITFC is currently employing, with the eventual outcome of informing a habitat-based life cycle model for spring Chinook salmon.

White, S.M., G.R. Giannico, and H.W. Li. (In Prep.) Application of a multi-species habitat selection theory to salmonid movement and foraging behavior in natural streams. Intended for J. Animal Ecol.

McCullough., D.A. 2011. The impact on coldwater-fish populations of interpretative differences in the application of the United States Clean Water Act 1972 by individual State legislatures. *Freshwater Reviews* 4:43-79.

B. Deliverable: B. Draft paper on monitoring or modeling in the Grande Ronde basin.

Based on work done to provide a preliminary assessment of habitat conditions and fish/habitat relationships from CHaMP data, a draft paper has been in development since November 2011. This paper was first presented in the December 2011 CHaMP workshop held between BPA and CHaMP partners. This material was refined for presentation to the Oregon AFS. The following Appendix material presents a draft of a paper on this subject.

See [Appendix S](#). The landscape context of fish-habitat relationships: implications for restoring wood recruitment processes in U.S. Pacific Northwest rivers

3/31/2012.

I : 119. Manage and Administer Projects – Project Administration

A. Accrual - Submit September 2011 estimate to BPA

8/16/2011 9/9/2011

BPA was provided with an estimate of contract work that will occur prior to September 30 but was not to be billed until October 1 or later.

B. Submit Draft 2012 SOW/budget to COTR

12/1/2011 2/3/2012

A draft SOW and a draft line item budget in excel were uploaded to PISCES and our COTR was notified. All COTR suggestions for amending the SOW/budget were addressed in developing the final package. Because we received the 2012 Watershed Sciences, Inc. proposal after the draft was approved, we asked that this be included in the final budget, which was approved by the CO.

C. Funding Package - Conduct internal review (e.g., Supervisor or Interagency)

1/2/2012 1/27/2012

The 2012 SOW and Budget were reviewed internally at CRITFC for compliance with CRITFC budget procedures. An evaluation was also completed of this Accord project's full 10-year budget projection,

given that annual spending occurs in cycles where some years have a high level of activity followed by a lower level of activity.

D. Submit Final 2012 SOW/budget/property

1/2/2012 2/24/2012

Work with COTR to finalize 2012 contract package - responding to comments and suggestions. Providing final line item budgets and property if applicable. Allows BPA contracting officer 1 month to issue a new contract and CRITFC 1 month for internal review and return of package to BPA with signatures.

E. Submit 2011 Cost Share Data to BPA

10/3/2011 12/30/2011

Prepare and submit cost share data to BPA via PISCES.

F. Obtain bids for potential subcontracts prior to 2012

1/2/2012 2/7/2012 We anticipate a continuing need for services of subcontractors to provide work such as hydrological analysis of data collected by CRITFC staff; macroinvertebrate species processing and identification of samples collected by CRITFC staff; . Competitive bids would be required for these subcontracts, but the detailed budgets will be needed prior to Year 4 budget in order to include it in the SOW.

J : 132. Produce (Annual) Progress Report - Annual Report - April 1, 2011 to March 31, 2012

A. Review progress report format requirements

1/2/2012 3/31/2012

CRITFC staff reviewed the BPA-required format described at <http://www.efw.bpa.gov/IntegratedFWP/technicalreports.aspx> in producing a non-technical annual report.

B. Submit progress report for internal contractor review

2/15/2012 to 2/28/2012

This annual report did not have full internal technical review except in part and did not have a policy review.

C. Submit progress report for external review

3/1/2012 3/15/2012

Although external review is desirable, this provision was not used due to the time constraints produced in participating in the CHaMP process, whereby CRITFC staff devoted large blocks of time in QA/QC work, revising Total Station survey data so that it would be compatible, if possible, with a River Bathymetry Toolkit model that was not sufficiently developed, and in reviewing, editing, and re-writing protocol elements, and devising new protocol elements. Significant time was also spent in lengthy conference calls with protocol developers.

D. Deliverable: D. Attach Annual Report in Pisces for April 2010 to March 2011

3/31/2012

Appendix A.

Database Development and Implementation for

Temperature and flow database (raFT)

Database Development and Implementation for Temperature and flow database (raFT)

Start-Date: 4/1/2011-End-Date: 3/31/2012

I. Introduction

The continual development of an extensive database to house data collected for the habitat monitoring project is detailed in this section. The raw flow and temperature database (raFT) was established in 2009 using a relational database model with a two-dimensional structure of rows and columns to store data within Microsoft SQL Server 2008 R2. This provides a central repository for all data, eliminates the need for database version control, and provides an easily shareable data source. The SQL Server is loaded on a virtual server running Microsoft Server 2008 operating system. SQL Maintenance plans routinely backed up to an external portable Sony hard drive, Drobo SATA device and an additional virtual server housed at the Hood River office on a routine basis. Data stored in this system includes: temperature, flow, sediment and will eventually if warranted chemistry data.

In 2011, an extensive study of gauge locations for flow data was conducted as well as a study of all available water quality site monitoring locations. Additionally, web applications that enable the user to view, import, and report data using a secure protocol have been deployed to share data efficiently. These developments to enter and report data were incorporated to assist the habitat group with maintaining secure, organized and reliable data products. Several of the data products include tables that can be accessed through Microsoft Access Database, several web sites for loading, viewing, and reporting data, and a secured database. Future goals include site maps that enable the user to click on gauge locations to download the most recent data reports.

II. Data Collection, Entry and Validation of Field Collected Data for Water Temperature, StreamFlow, Sediment and Water Quality Habitat

Temperature

Temperature data is entered, validated and summarized for 266 CRITFC, US Forest Service (USFS), Confederated Tribes of the Umatilla Indian Reservation (CTUIR), and Oregon Department of Fish and Wildlife (ODFW).temperature monitoring locations annually (Appendix 1). Some of the locations included over 20 years of collected data. The flow and temperature data locations are housed in a single table (Temperature_Flow_Locations, Appendix 1). Table 1 describes the data stored in this table and Figure 1 a, b and c displays the spatial locations of the temperature, flow, and water chemistry data monitoring stations. Nineteen USFS Temperature stations do not have coordinate information and are not included in Figure 1 (email correspondence with Kayla Morinaga, Fish Technician for USFS in 2011).

In 2011/2012 updates included: data updates for 2011, data entry web applications, access to the tables from everyone using ODBC connection to Microsoft Access 2010 and summarized data tables for all temperature data collected. The Data entry application provides an easier method to load data from the different organizations (CRITFC, ODFW, CTUIR, and USFS). The application converts data to Celsius if necessary and loops through the data to ensure duplicates are ignored and all data is imported to the database with the correct site name. Values for temperature are stored in the database to the tenth decimal place due to the accuracy of most temperature probes (± 0.2 °Celsius). Figure 2a provides a screen shot of the data entry application for temperature data. The green values indicate those that are entered to the database. Red records would indicate duplicates or bad values, which assists in detecting errors in values. Appendix 1 displays the temperature locations, coordinating agency, and the date each location had been updated. Several sites from USFS that have annual data are not included in the database (Indian Creek, Little Indian Creek, and Clarks Creek Sites).

CTUIR performed validation of the probe data collected and methods are included in Appendix 2. However, in 2011 several sites contained duplicate values. The duplicates resulted from testing of new temperature probes (email correspondence Les Naylor, CTUIR, 2011). Results from the new temperature probe were the only ones imported in to raFT (correspondence Casey Justice, CRITFC, 2011). The database provides additional validation for temperature and flow data using indexing for eliminating duplicates, indexing and ordering for missing data, and flagging outliers following guidelines set forth in recent publications directing the management of fisheries data (Dunham et al. 2005). If data is found to be suspect, then the data are flagged in the validation column. Additionally, data typing for each of the columns as shown in Table 1 ensures that certain values are acceptable in the columns.

Flow

In 2011 CRITFC conducted an extensive survey of water flow station location sites in the Grande Ronde Basin. Several more station locations have been included in raFT for a total of 53 flow station locations of the total 85 that are located in the Grande Ronde Basin ([http://www.hydro.washington.edu/SurfaceWaterGroup/Data/ARCINFO.html#usgs_gages_correspondences with Richard Marvin and Ken Stahr, OWRD, 2011](http://www.hydro.washington.edu/SurfaceWaterGroup/Data/ARCINFO.html#usgs_gages_correspondences%20with%20Richard%20Marvin%20and%20Ken%20Stahr,%20OWRD,%202011)). Figure 1b shows the 85 locations of the flow monitoring stations and indicates which of the 85 are included in raFT. The reasons for not including the stations in raFT include:

- No data reported
- Only peak flows reported
- Only staff gauge data reported

Of the 53 sites, 17 are active (not decommissioned). This database houses flow data in two related tables, a locations (Temperature_flow_locations) and mean daily flow data (Flow_Data_Master). Refer to Table 1 for the column headers, data types and data descriptions.

The 15 minute interval logging data is collected by stations that record the height of surface water. This data is then transformed using a stage discharge curve or rating table. This discharge curve or rating table was created by measuring flow at cross sections with known areas (OWRD 2011). This data is

maintained and transformed to the mean daily flow in cubic feet per second (MDF) by the Oregon Water Resources Department (OWRD 2011). The MDF is uploaded to raFT using the automated application. This application has been created to automate the process of gathering MDF data from active OWRD station locations. Data is downloaded automatically from the following address: http://apps.wrd.state.or.us/apps/sw/hydro_near_real_time/hydro_download.aspx?station_nbr and updated weekly using Automate 8 Professional Version 8.0.1.01 (Figure 3). Appendix 1 shows the site names and dates for database updates of data within raFT.

At this time, preliminary data is loaded into the database then updated after it has been qualified as published by OWRD. A field key of Site and date information was created to enforce additional referential integrity. OWRD validation has been adopted by CRITFC, which suggests that data qualified as “preliminary” should not be used. Data should at least meet the “provisional” status (http://apps.wrd.state.or.us/apps/sw/hydro_near_real_time/faq.aspx). This data has been shared with numerous individuals using ODBC connection to Microsoft Access 2010.

Sediment/Water Chemistry Data

Data collected in 2010 that includes site locations for sediment samples and sediment sample data is also stored in raFT. Several stored procedures transform these data to reportable formats. It is not decided if this database will continue to house 2011 sediment data.

The Department of Environmental Quality (DEQ) maintains a LASAR database that stores and reports water quality data monitoring locations for the Grande Ronde Basin. CRITFC found a GIS layer that extensively displays the spatial variability of this water quality data. Figure 1c displays these water quality monitoring locations. CRITFC will create an application to loop through data and summarize potential contaminants that are stored in the Lasar database. These data will then be stored in raFT as warranted. The database structure will include a similar relational database structure adopted by EQUIS and validation of the data will be verified by CRITFC.

Table 1. Descriptions of the tables within the raFT database including: column headers, data types and data descriptions.

Column Headers	Data Type	Description
Temperature Flow Locations Table		
fid	int	is a unique number used in the GIS analysis so links to this table are seamless. This data is an auto-generated sequential id.
longname	Varchar	is a variable character which includes a unique column of data that is Organization. is the name of the site given by the contributing organization from which this data originates. Is the unique probe number. Probes were generally used at the same locations each year but some were moved and/or replaced.
site	Varchar	
start_date	date	is the date the probe was first deployed or date data is available (mm/dd/yyyy).
end_date	date	is the date the probe was last removed (mm/dd/yyyy).
update_date	date/time	is the date/time of the most recent data upload (mm/dd/yyyy 24:00:00.00).
easting_utm	Varchar	is the location information for the probe.
northing_utm	Varchar	is the location information for the probe.

utm_zone	integer	is the UTM zone at the location (11).
huc6	Varchar	is the sub-basin id of the probe, which is a 12-digit integer.
season	Varchar	is the monitoring season (summer, winter, or both).
parameter	Varchar	is the type of information that this probe is collecting such as temperature, flow, or sediment
stream	Varchar	is the stream from where this probe is located
project_area	Varchar	is the reference area from which all probes within a certain area are located within such as: Catherine Creek, Grande Ronde, Imnaha, or Minam.
monitoring_status	Varchar	is the status of the probe is it decommissioned or on-going.
other	Varchar	is the comment field for additional information.
coordinator	Varchar	is the organization responsible for gathering the probes information.

Temperature Data Master

site	Varchar	is the name of the site given by the contributing organization from which this data originates. Links to locations table.
modified_date	date/time	is the date/time the data was collected (mm/dd/yyyy 24:00:00.00).
air_temperature_c	float	is the value of the recorded hourly air temperature in degrees celcius.
temperature_c	float	is the value of the recorded hourly stream temperature in degrees celcius.
nist_audit_c	Varchar	is the result of the audit from USFS using criteria from NIST checks on the probes recording the air temperatures.
air_nist_audit_c	Varchar	is the result of the audit from USFS using criteria from NIST checks on the probes recording the stream temperatures.
rhumidity_min	float	is the value of the recorded hourly minimum percent relative humidity.
rhumidity_max	float	is the value of the recorded hourly maximum percent relative humidity.
rhumidity_per	float	is the value of the recorded hourly percent relative humidity.
validation	Varchar	is the result from the qa/qc checks performed by CRITFC using following recommended procedures of USDA Dunham et al. 2005
comments	Varchar	is the comment field for additional information.

Temperature Summary Table

site_name	Varchar	is a variable character which includes a unique column of data that is Organization. is the name of the site given by the contributing organization from which this data originates. Is the unique probe number. Probes were generally used at the same locations each year but some were moved and/or replaced.
site	Varchar	
start_date	date	is the date the probe was deployed or date data is available (mm/dd/yyyy).
end_date	date	is the date the probe was removed (mm/dd/yyyy).
update_date	date/time	is the date/time the probe was updated (mm/dd/yyyy 24:00:00.00).
easting_utm	Varchar	is the location information for the probe.
northing_utm	Varchar	is the location information for the probe.
utm_zone	integer	is the UTM zone at the location (11).
huc6	Varchar	is the sub-basin id of the probe, which is a 12-digit integer.
season	Varchar	is the monitoring season (summer, winter, or both).
coordinator	Varchar	is the organization responsible for gathering the probes information.
average	float	is the daily average of temperature recorded on hourly basis in degrees celcius
7day_average	float	is the 7day average of temperature recorded on hourly basis in degrees celcius
max_temp	float	is the daily maximum recorded temperature on hourly basis in degrees celcius

7day_max	float	is the 7 day maximum recorded temperature on hourly basis in degrees celcius
validation	varchar	is the results of the QA/QC on the temperature data. "a" -
Flow Master Table		
station_nbr	Varchar	is the name of the site given by the contributing organization from which this data originates. Links to locations table.
record_date	date/time	is the date/time the data was collected (mm/dd/yyyy 24:00:00.00).
mean_daily_flow_cfs	float	is the value of the recorded mean daily flow in cubic feet per second.
published_status	Varchar	is the value of the result based on qa/qc checks. http://apps.wrd.state.or.us/apps/sw/hydro_near_real_time/faq.aspx
estimated	Varchar	is the value of the result based on estimation.
revised	Varchar	is the value of the result that is to replace any other previously reported value.
download_date	date/time	is the date/time the data was uploaded to database(mm/dd/yyyy 24:00:00.00).
Flow Summary Table		
site_name	Varchar	is a variable character which includes a unique column of data that is Organization_OrganizationCode.
site	Varchar	is the name of the site given by the contributing organization from which this data originates. Is the unique probe number. Probes were generally used at the same locations each year but some were moved and/or replaced.
start_date	date	is the date the probe was deployed or date data is available (mm/dd/yyyy).
end_date	date	is the date the probe was removed (mm/dd/yyyy).
update_date	date/time	is the date/time the probe was updated (mm/dd/yyyy 24:00:00.00).
easting_utm	Varchar	is the location information for the probe.
northing_utm	Varchar	is the location information for the probe.
utm_zone	integer	is the UTM zone at the location (11).
huc6	Varchar	is the sub-basin id of the probe,which is a 12-digit integer.
season	Varchar	is the monitoring season (summer, winter,or both).
record_date	date/time	is the date/time the data was collected (mm/dd/yyyy 24:00:00.00).
mean_daily_flow_cfs	float	is the value of the recorded mean daily flow in cubic feet per second.
Flow Summary Table cont.		
published_status	Varchar	is the value of the result based on qa/qc checks. http://apps.wrd.state.or.us/apps/sw/hydro_near_real_time/faq.aspx
estimated	Varchar	is the value of the result based on estimation.
revised	Varchar	is the value of the result that is to replace any other previously reported value.
download_date	date/time	is the date/time the data was uploaded to database(mm/dd/yyyy 24:00:00.00).

Grande Ronde Basin - Water Temperature Sites

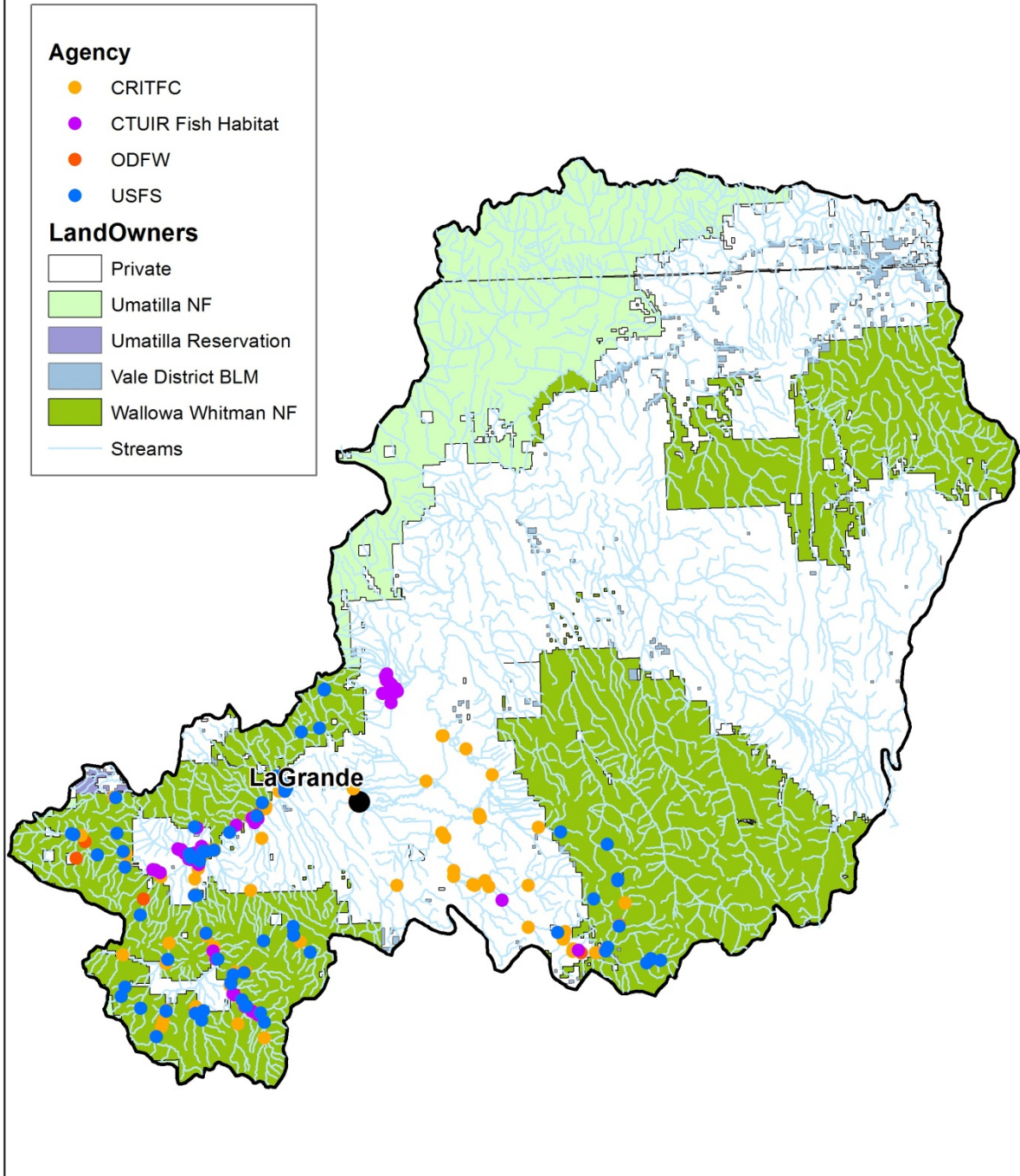


Figure 1a. Map of Grande Ronde Basin showing locations of temperature monitoring stations for each coordinating agency (CRITFC, CTUIR, ODFW, and USFS) and land use designation.

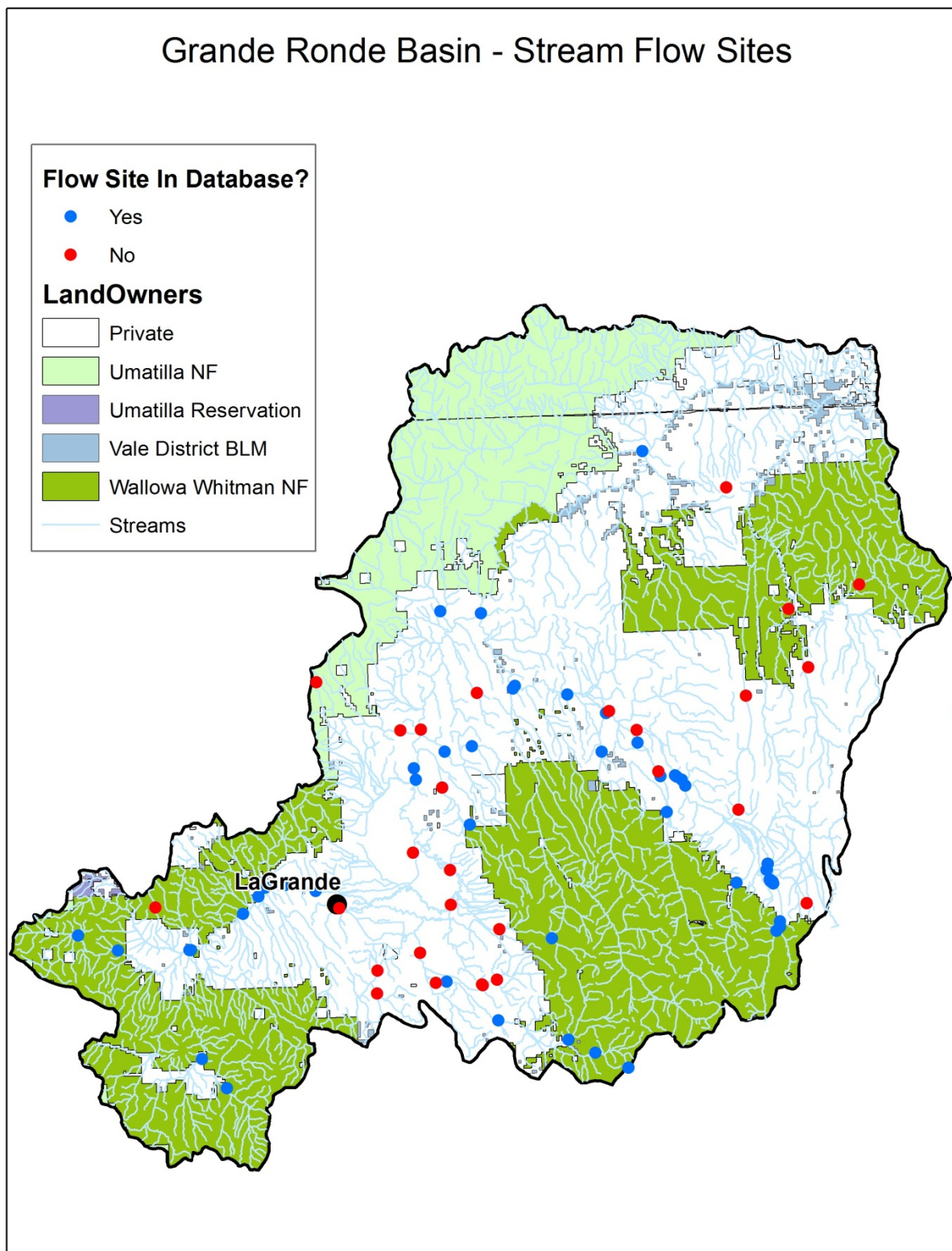


Figure 1a. Map of Grande Ronde Basin showing locations of flow monitoring stations that are included in raFT (yes, no) and land use designation (managed by: USGS, OWRD, and other unknown).

Grande Ronde Basin - Water Quality Sites

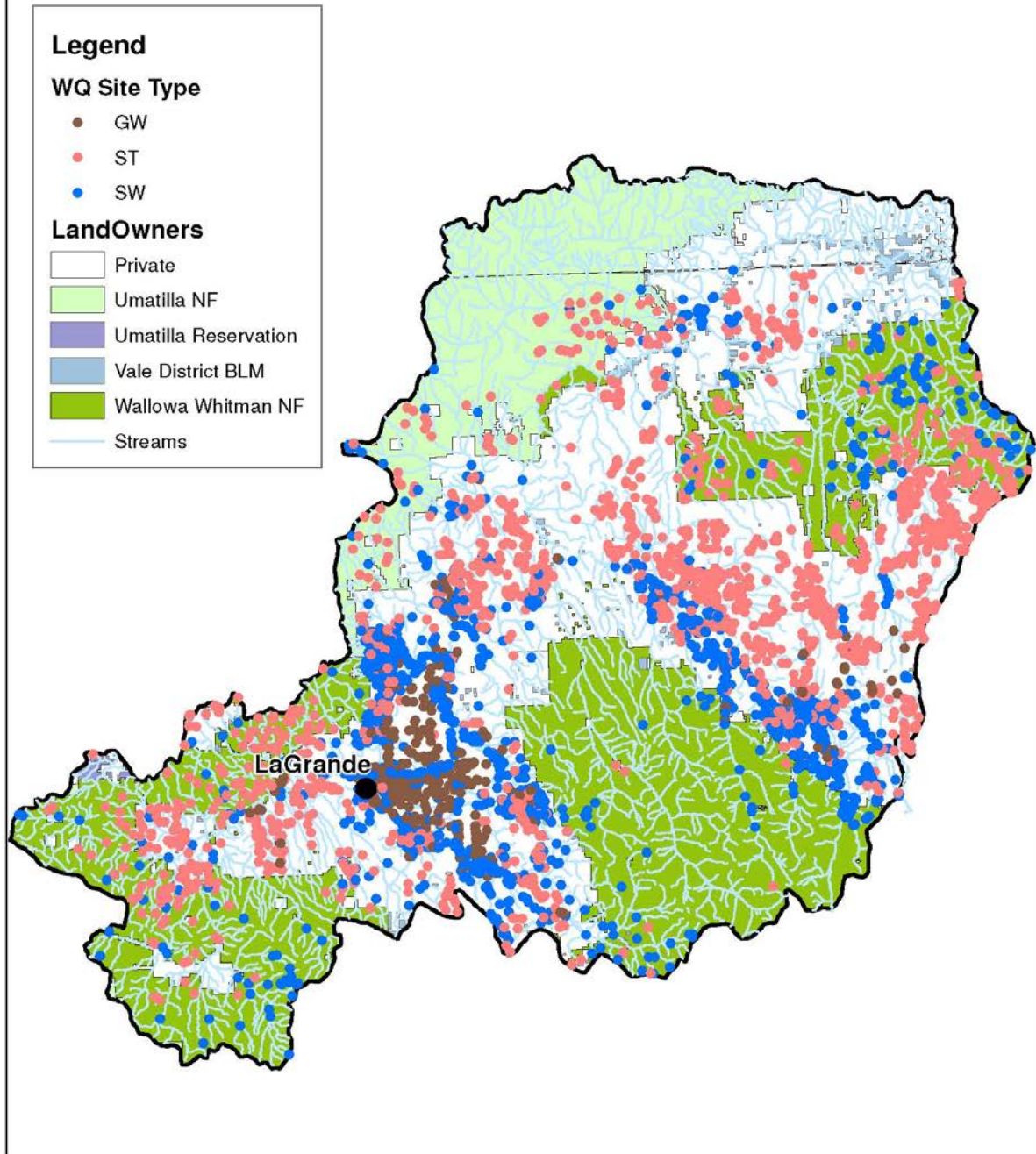


Figure 1a. Map of Grande Ronde Basin showing locations of water quality monitoring stations included in Lasar (DEQ) by monitoring medium (groundwater (GW), surface water (SW) and staff gauges (ST)) and land use designation.

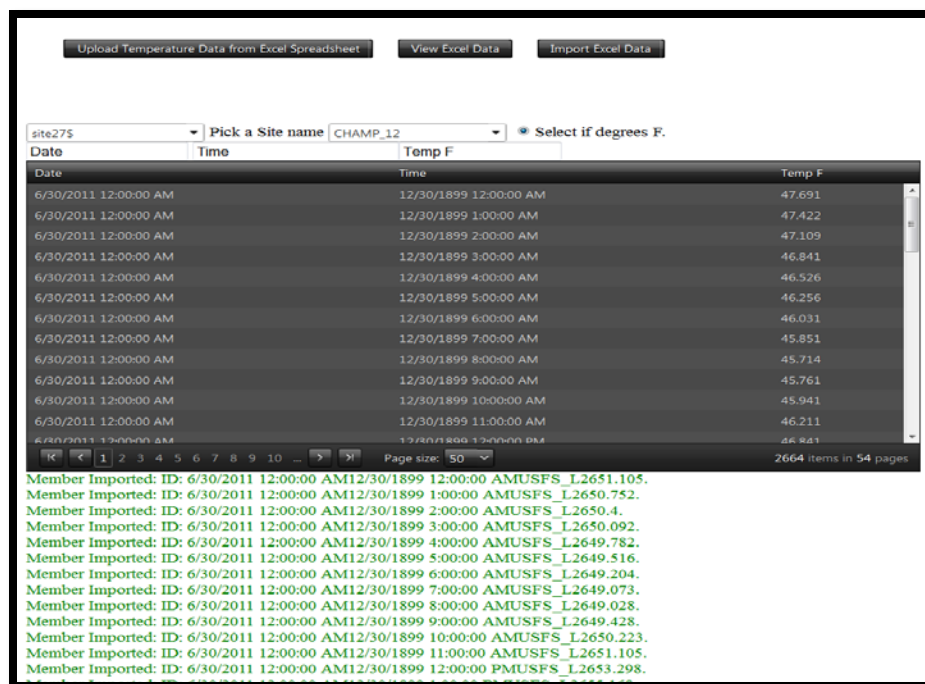


Figure 2. Screen shot showing the data import application for temperature data CRITFC receives from various agencies, in this case, USFS. The green records indicate which rows have been entered into the raFT. A red record would indicate a record data that was not loaded.

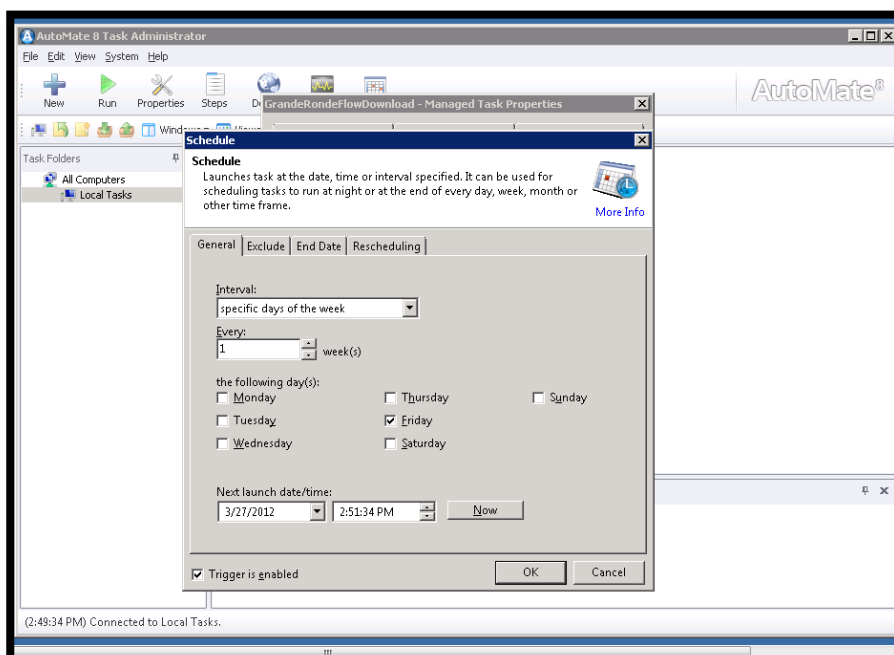


Figure 3. Screen shot showing the Automate 8 routine that automatically downloads data from http://apps.wrd.state.or.us/apps/sw/hydro_near_real_time/hydro_download.aspx and loads to SQL server for active flow gauges in Grande Ronde Basin (Appendix 1).

Database Development and Implementation for Shared Snorkel Survey and Human Disturbance Database and Web Application

Start-Date: 4/1/2011-End-Date: 3/31/2012

I. Introduction

The Development of a database (SSHD) for housing snorkel survey data and human disturbance data was finalized in 2011. The database was created using a relational database model with a two-dimensional structure of rows and columns to store data within Microsoft SQL Server 2008 R2, which provides a central repository for all data, eliminates the need for database version control, and provides an easily shareable data source. This system is loaded on a virtual server with Microsoft Server 2008 operating system. SQL Maintenance plans provide back routines.

A secured website was developed to facilitate the sharing of data and data processing of the snorkel survey and human disturbance data collected by ODFW and CRITFC. The website was created using Microsoft Visual Studio 2008, Telerik Version Q3 2010 tools and Microsoft virtual server running Microsoft Web Server 2008, which is secured using Secure Sockets Layering (SSL). Additional security is provided by the use of usernames and passwords to access the web application. Dynamic web reports are created on demand using SQL Server 2008 R2 reporting tools and SQL Server Stored procedures.

I. Data Collection, Entry and Validation of Field Collected Data for Snorkel Survey and Human Disturbance Survey Data

Snorkel Survey and Human Disturbance data collected during the 2011 field season by ODFW and CRITFC in the Grande Ronde Basin has been included in the SSHD. The validation is maintained using primary keys, foreign keys, strong data typing, valid value lists and sorting for determining missing data. The web application also includes some data validation to help the user minimize data entry errors. For instance, red lettering will show when an invalid entry is included in the web application and the user will not be able to leave the entry until it is corrected. Figure 4 a/b show the web applications for the entry of data for snorkel surveys and human disturbance surveys, respectively. The web reports generated are not shown in this section. The reports are created from Stored Procedures running on the SQL server that generate numerous data tables with data values that have been computed from the raw survey data. SQL Server reports application was used to generate these automated reports since they allow these reported to be exported in a variety of application formats.

Three tables make up the SSHD that includes:Hb_Field_FieldData, Hb_Field_SnorkelSurvey, Hb_Field_Human_Disturbance, and numerous valid values tables. Table 2 provides the column headers, data types, and data descriptions of the three main related data tables housed in the SSHD.

Table 2. Descriptions of the tables within the SSHD database including: column headers, data types and data descriptions.

Column Headers	Data Type	Description
Hb_Field_FieldData		
fid	int	is an auto-generated sequential id.
reach_id_prefix	Varchar	is a variable character that starts the reach id.
Reach_id_suffix	Varchar	is the name ending id for the reach snorkeled.
snk_date	date	is the date the survey was started (mm/dd/yyyy).
Water_temp	date	is the temperature of the water at start of survey (degrees Celsius).
Water_visibility	date/time	is the scale of water visibility through the column (0-3).
Snk_time_start	Varchar	is the time of day the snorkel survey started 24 hr format (hh.mm.ss).
Snk_time_end	Varchar	is the time of day the snorkel survey ended 24 hr format (hh.mm.ss).
Snk_crew	integer	is the UTM zone at the location (11).
Snk_notetaker	Varchar	is the sub-basin id of the probe, which is a 12-digit integer.
Snk_comments	Varchar	is the field person's comments for the snorkel data survey
Entered_dat	date/time	is the date the snorkel field data was entered to SSHD
Stream_nm	Varchar	is the stream from where this probe is located
Agency	Varchar	Is the name of the organization coordinating the survey
Snk_weather	Varchar	is the status of weather at the start of the snorkel survey.
other	Varchar	is the comment field for additional information.
Hb_Field_Snorkel_Survey		
Snrk_id	Int	is an auto-generated sequential id.
Field_id	Varchar	Is the foreign key for the primary key in the field data table.
Chnl_typ	Varchar	Is the
Unit_no	int	is the value of the recorded hourly stream temperature in degrees celcius.
Chnl_unit_length	Varchar	is the result of the audit from USFS using criteria from NIST checks on the probes recording the air temperatures.
Chnl_unit_width	Varchar	is the result of the audit from USFS using criteria from NIST checks on the probes recording the stream temperatures.
Diver1_lane_width	Varchar	is the value of the recorded hourly minimum percent relative humidity.
Diver2_lane_width	Varachar	is the value of the recorded hourly maximum percent relative humidity.
70_130	Int	is the number of Chinook species caught between 70_130 mm.
130_200	Int	is the number of Chinook species caught between 130-200 mm
200_250	int	is the number of Chinook species caught between 200-250.
250	Int	is the number of steelhead species caught between 250mm
50_80	Int	is the number of Chinook species caught between 50_80 mm
100	Int	is the number of Chinook species caught ~100 mm
Other	Int	is the number of Chinook species caught outside of other ranges listed above
Adult	Int	is the number of Chinook species adult
Unidentified	Varchar	is yes/no for unidentified fish
Dominant	Varchar	Is the dominant species

Common	Varchar	Is the common species
Rare	Varchar	Is the rare species
Notes	Varchar	Is the notes for each lane width surveyed
Upl_dat	Date/time	Is the date the data were loaded in database
Human Disturbance Table		
Field_id	Varchar	Is the foreign key for the primary key in the field data table
hdi_date	Date/time	Is the date the human disturbance survey was conducted (mm/dd/yyyy).
hdi_crew	Varchar	is names of individuals who performed the survey.
hdi_comments	Varchar	is the date the probe was removed (mm/dd/yyyy).
hdi_ag_cafo	int	is the score for cattle & poultry
hdi_ag_chan	int	is the score for channelization
hdi_ag_chem	int	is the score for chemical treatment/liming
hdi_ag_cnst	int	is the score for construction/storm water
hdi_ag_crop	int	is the score for cropland
hdi_ag_dam	int	is the score for dams
hdi_ag_ind	int	is the score for industrial plants/commercial
hdi_ag_irr	int	is the score for irrigation equipment
hdi_ag_lwn	int	is the score for maintained lawns/run-off
hdi_ag_orch	int	is the score for orchards, tree farms
hdi_ag_pav	int	is the score for pavement/cleared lot
hdi_ag_pwr	int	is the score for power plants/oil/gas wells
hdi_ag_rsd	int	is the score for residences/buildings
hdi_ag_ripr	int	is the score for riprap/wall/dike
hdi_ag_swg	int	is the score for sewage/pipes/outfalls/drains
hdi_ag_flct	int	is the score for water level fluctuations
hdi_ag_oth	int	is the score for other disturbances in the agriculture-urban category
hdi_ag_max	int	is the score for maximum score in the above agriculture-urban category
hdi_rng_catt	int	is the score for cattle, livestock use
hdi_rng_past	int	is the score for pasture/range/hayfield
hdi_rng_oth	int	is the score for other disturbances in the rangeland category
hdi_rng_max	int	is the score for maximum score in the above rangeland category
hdi_rd_brdg	int	is the score for bridges/culverts/rr crossings
hdi_rd_rr	int	is the score for railroads
hdi_rd_rd	int	is the score for roads paved/gravel/dirt
hdi_rd_oth	int	is the score for other disturbances in the roads category
hdi_rd_max	int	is the score for maximum score in the above roads category
hdi_slv_lgact	int	is the score for logging ops
hdi_slv_lgrec	int	is the score for logging ops
hdi_slv_lghis	int	is the score for logging ops
hdi_slv_oth	int	is the score for other disturbances in the silviculture category

hdi_slv_max	int	is the score for maximum score in the above silviculture category
hdi_msc_angl	int	is the score for angling pressure
hdi_msc_drdg	int	is the score for dredging
hdi_msc_dmp	int	is the score for dumping/garbage/trash/litter
hdi_agriculture_ max scores	int	is the max score the agriculture section
hdi_rangeland_ max scores	int	is the max score the rangeland section
hdi_silviculture_ max scores	int	is the max score the silviculture section
hdi_road_max scores	int	is the max score the road section
hdi_agriculture_ max scores	int	is the max score the agriculture section

Grande Ronde Basin - Fish Habitat Data Access

Snorkel Survey
DEQ Human Disturbance

Use Drop down box to select reach of interest. If it doesn't exist enter the field data by selecting the "New Reach" link, prior to entering channel unit data. Please use lower case when entering channel unit data.

[Click here to view report](#)

Field Data

CBW05583-013882

Stream

Peet Creek

Start(HH:MM):

End(HH:MM):

Reach:

CBW05583-013882

H20temp:

Visibility:

Date:

Notetaker:

Snorkler(s):

Weather:

Comments:

Agency:

[New Reach](#)
[Delete Reach](#)
[Edit Reach](#)

Delete Row

Add New Row
Save
Last Row

Steelhead length (mm)
Chin length (mm)

Type	unit no.	length (m)	width (m)	Lane1 (m)	Lane2 (m)	70_130	130_200	200_250	250	50_80	100	other	adult	YOY	dominant	common	rare	notes
No records to display.																		

Figure 4a. Screen shot showing the web application for entering field data from snorkel survey sites during the 2011 field season. This web application was used by ODFW and CRITFC staff.

Grande Ronde Basin - Fish Habitat Data Access

Special Survey
ODFW Human Disturbance

[Click here for report.](#)

Field Data

Select a field id from the combobox or use the page selector at bottom of page to select a field id prior to selecting edit.

Stream:

Date:

Comments:

Reach:

Crew:

Agency:

Activity Checklist

[Edit](#)

Agriculture-Urban

Cattle/Poultry

Channelization

Chemical Treatment

Construction/stormwater

Cropland

Dams

Industrial plants

Irrigation

Maintained lawn/runoff

Orchards

Pavement

Powerplants/oil-gas wells

Residences/buildings

Riprap/wall/dike

Sewage

Water Fluctuations

Other

Silviculture

Logging Active

Logging Recent(<5yrs)

Logging Historic

Silv Other

Miscellaneous

Angling Press.

Dredging

Dumping/Garbage

Exotic Plants

Fish Stocking

Hiking Trails

Mines Quarries

Parks/Orgrds

Primitive parks/orgrds

Surface films odors

Misc Other

Rangeland

Cattle/Livestock

Pasture/Range

Range other

Roads

Bridges/culverts/RRX

Railroads

Roads (paved/gravel)

Roads Other

Reference Site

Reference Site Cand.

Best Judgement

Natural Disturbance

Fire

Floods

Mass Wasting

Nat. Other

Rank Score Calculation by Category

Agriculture & urban

Rangeland

Roads

Silviculture

Miscellaneous

Total Score

Website Created By:

Version 1.2.2 | Compiled 01/10/2012

Figure 4b. Screen shot showing the web application for entering field data from human disturbance surveys during the 2011 field season. This web application was used by ODFW and CRITFC staff.

Appendix 1. Summary of the temporal data for the temperature and flow Monitoring Locations available in the database.

Site Name	Site ID	Start Date	End Date	Update Date	Missing Years	Northing UTM	Easting UTM	Coor-dinator	Stream
Temperature									
NF_CC_above_MF_CC	CHAMP_12	23-Sep-10	27-Sep-11	9-Dec-11	NULL	5000096	451504	CRITFC	North Fork Catherine Creek
CBW05583-155818	CHAMP_14	24-Aug-11	NULL	NULL	NULL	4999556	443707	CRITFC	Little Catherine Creek
Jim_Cr_mouth	CHAMP_19	2-Jun-10	NULL	NULL	NULL	5003344	452560	CRITFC	Jim Creek
DSGN4-000009	CHAMP_2	15-Jul-11	22-Sep-11	9-Dec-11	NULL	4989992	397788	CRITFC	Grande Ronde River
CBW05583-456106	CHAMP_28	12-Aug-11	21-Sep-11	9-Dec-11	NULL	4996871	445092	CRITFC	Catherine Creek
CBW05583-382778	CHAMP_29	25-Jul-11	5-Oct-11	9-Dec-11	NULL	5006892	382829	ODFW	Burnt Corral Creek
CBW05583-013882	CHAMP_30	4-Aug-11	4-Oct-11	9-Dec-11	NULL	5013214	373300	ODFW	Peet Creek
DSGN4-000213	CHAMP_31	14-Jul-11	5-Oct-11	9-Dec-11	NULL	5013167	390632	ODFW	Meadow Creek
DSGN4-000094	CHAMP_32	28-Jun-11	5-Oct-11	9-Dec-11	NULL	4997845	385829	ODFW	Fly Creek
CBW05583-108010	CHAMP_33	15-Jul-11	22-Sep-11	9-Dec-11	NULL	4995300	395296	CRITFC	Limber Jim Creek
DSGN4-000093	CHAMP_34	29-Jun-11	4-Oct-11	9-Dec-11	NULL	5015553	374714	ODFW	Meadow Creek
DSGN4-000161	CHAMP_35	3-Aug-11	3-Oct-11	9-Dec-11	NULL	4994727	455566	ODFW	SF Catherine Creek
CBW05583-138554	CHAMP_36	30-Jun-11	22-Sep-11	9-Dec-11	NULL	4990674	385429	CRITFC	Sheep Creek
DSGN4-000245	CHAMP_37	11-Jul-11	23-Sep-11	9-Dec-11	NULL	5013613	392853	CRITFC	Grande Ronde River
DSGN4-000277	CHAMP_38	14-Jul-11	22-Sep-11	9-Dec-11	NULL	4998754	392550	CRITFC	Grande Ronde River
CBW05583-280042	CHAMP_39	29-Jul-11	22-Sep-11	9-Dec-11	NULL	4990084	397713	CRITFC	Grande Ronde River
CBW05583-368042	CHAMP_40	20-Sep-11	NULL	NULL	NULL	4996300	448020	CRITFC	Catherine Creek
CBW05583-252730	CHAMP_41	18-Jul-11	5-Oct-11	9-Dec-11	NULL	5012421	389685	ODFW	Meadow Creek
DSGN4-000202	CHAMP_42	12-Jul-11	22-Sep-11	9-Dec-11	NULL	5010920	390905	CRITFC	Grande Ronde River
CBW05583-206314	CHAMP_43	15-Jul-11	22-Sep-11	9-Dec-11	NULL	4992143	395754	CRITFC	Grande Ronde River
CBW05583-235322	CHAMP_44	13-Jul-11	22-Sep-11	9-Dec-11	NULL	5001173	391697	CRITFC	Grande Ronde River
DSGN4-000001	CHAMP_45	11-Aug-11	3-Oct-11	9-Dec-11	NULL	4996779	449528	ODFW	NF Catherine Creek
CBW05583-228666	CHAMP_46	30-Jun-11	22-Sep-11	9-Dec-11	NULL	4988282	384614	CRITFC	Sheep Creek
DSGN4-000006	CHAMP_48	21-Jun-11	5-Oct-11	9-Dec-11	NULL	4990392	389619	ODFW	West Chicken Creek
CBW05583-527786	CHAMP_49	8-Aug-11	3-Oct-11	9-Dec-11	NULL	4996427	445937	ODFW	Catherine Creek
DSGN4-000168	CHAMP_50	1-Aug-11	3-Oct-11	9-Dec-11	NULL	5000228	451613	ODFW	NF Catherine Creek
CBW05583-148970	CHAMP_51	4-Aug-11	22-Sep-11	9-Dec-11	NULL	4991057	396606	CRITFC	Grande Ronde River
CBW05583-457530	CHAMP_52	16-Jul-11	22-Sep-11	9-Dec-11	NULL	5009478	390356	CRITFC	Grande Ronde River
CBW05583-321338	CHAMP_53	13-Jul-11	22-Sep-11	9-Dec-11	NULL	4999615	392694	CRITFC	Grande Ronde River
CBW05583-490810	CHAMP_54	14-Jul-11	22-Sep-11	9-Dec-11	NULL	4989128	384890	CRITFC	Sheep Creek
CBW05583-269114	CHAMP_55	5-Aug-11	23-Sep-11	9-Dec-11	NULL	5011937	391164	CRITFC	Grande Ronde River
DSGN4-000205	CHAMP_56	26-Jul-11	5-Oct-11	9-Dec-11	NULL	5018485	399954	ODFW	Grande Ronde River
CBW05583-430250	CHAMP_6	21-Sep-11	NULL	NULL	NULL	5006930	430620	CRITFC	Catherine Creek
CBW05583-217258	CHAMP_9	12-Aug-11	20-Sep-11	9-Dec-11	NULL	5006809	430896	CRITFC	Catherine Creek
Bear_Cr_below_Little_Bear_Cr	CRITFC_1	27-Jul-09	21-Sep-10	6-May-11	NULL	5011812	380432	CRITFC	Bear Creek

Site Name	Site ID	Start Date	End Date	Update Date	Missing Years	Northing UTM	Easting UTM	Coordinator	Stream
CC_above_Little_Cr	CRITFC_10	30-Jun-10	17-Aug-10	6-May-11	NULL	5008245	427929	CRITFC	Catherine Creek
CC_above_Milk_Cr	CRITFC_11	10-Jul-10	20-Sep-10	6-May-11	NULL	4998502	443440	CRITFC	Catherine Creek
CC_above_Mill_Cr	CRITFC_12	30-Jun-10	20-Sep-10	6-May-11	NULL	5016584	432041	CRITFC	Catherine Creek
CC_Booth_Rd_bridge	CRITFC_13	10-Jul-10	20-Sep-10	6-May-11	NULL	5022739	434105	CRITFC	Catherine Creek
CC_E_Union	CRITFC_14	29-Jul-09	20-Sep-10	6-May-11	NULL	5006556	432938	CRITFC	Catherine Creek
CC_Geckler_Rd_bridge	CRITFC_15	30-Jun-10	20-Sep-10	6-May-11	NULL	5017103	431960	CRITFC	Catherine Creek
CC_Hwy_203	CRITFC_16	29-Jul-09	27-Sep-11	9-Dec-11	NULL	5000410	438423	CRITFC	Catherine Creek
CC_Market_Ln_bridge	CRITFC_17	30-Jun-10	7-Jul-10	6-May-11	NULL	5026634	430467	CRITFC	Catherine Creek
CC_mouth	CRITFC_18	30-Jun-10	11-Jul-10	6-May-11	NULL	5028675	427232	CRITFC	Catherine Creek
Chicken_Cr_below_W_Chicken_Cr	CRITFC_19	29-Jun-10	23-Sep-10	6-May-11	NULL	4990991	389699	CRITFC	Chicken Creek
Bear_Cr_mouth	CRITFC_2	10-Jul-10	20-Sep-10	6-May-11	NULL	5017922	399000	CRITFC	Bear Creek
Clear_Cr_mouth	CRITFC_20	26-Jul-09	22-Sep-11	9-Dec-11	NULL	4990798	396784	CRITFC	Clear Creek
Clear_Cr_upper	CRITFC_21	26-Jul-09	29-Sep-10	6-May-11	NULL	4988225	395704	CRITFC	Clear Creek
Five_Points_Cr_above_Little_JD_Cr	CRITFC_22	28-Jul-09	21-Sep-10	6-May-11	NULL	5030106	406691	CRITFC	Five Points Creek
Five_Points_Cr_above_Pelican_Cr	CRITFC_23	25-Jul-09	20-Sep-10	6-May-11	NULL	5023787	402922	CRITFC	Five Points Creek
Five_Points_Cr_mouth	CRITFC_24	28-Jul-09	23-Sep-11	9-Dec-11	NULL	5022231	404207	CRITFC	Five Points Creek
Five_Points_Cr_upper	CRITFC_25	23-Jun-10	21-Sep-10	6-May-11	NULL	5030563	409404	CRITFC	Five Points Creek
Fly_Cr_below_Little_Fly_Cr	CRITFC_26	27-Jul-09	23-Sep-10	6-May-11	NULL	4997459	385647	CRITFC	Fly Creek
Fly_Cr_below_Squaw_Cr	CRITFC_27	27-Jul-09	6-Oct-09	16-Feb-11	NULL	4998954	379438	CRITFC	Fly Creek
Fly_Cr_canyon	CRITFC_28	30-Jun-10	23-Sep-10	6-May-11	NULL	5000369	386242	CRITFC	Fly Creek
Fly_Cr_mouth	CRITFC_29	24-Jun-10	22-Sep-11	9-Dec-11	NULL	5007242	390356	CRITFC	Fly Creek
Bear_Cr_Upper	CRITFC_3	11-Jul-10	29-Sep-10	6-May-11	NULL	5014993	400307	CRITFC	Bear Creek
GR_2nd_St_Bridge	CRITFC_30	28-Jul-09	21-Sep-10	6-May-11	NULL	5021553	413891	CRITFC	Grande Ronde River
GR_above_Bear_Cr	CRITFC_31	10-Jul-10	20-Sep-10	6-May-11	NULL	5017964	398984	CRITFC	Grande Ronde River
GR_above_Beaver_Cr	CRITFC_32	1-Jul-10	21-Sep-10	6-May-11	NULL	5013641	393358	CRITFC	Grande Ronde River
GR_above_CC_mouth	CRITFC_33	30-Jun-10	4-Jul-10	6-May-11	NULL	5028695	427121	CRITFC	Grande Ronde River
GR_above_Clear_Cr	CRITFC_34	26-Jul-09	20-Sep-10	6-May-11	NULL	4990808	396891	CRITFC	Grande Ronde River
GR_above_Five_Points_Cr	CRITFC_35	28-Jul-09	14-Jul-11	9-Dec-11	NULL	5022161	404219	CRITFC	Grande Ronde River
GR_above_Fly_Cr	CRITFC_36	26-Jul-09	20-Sep-10	6-May-11	NULL	5007051	390402	CRITFC	Grande Ronde River
GR_above_Jordan_Cr	CRITFC_37	10-Jul-10	20-Sep-10	6-May-11	NULL	5018280	399658	CRITFC	Grande Ronde River
GR_above_Meadow_Cr	CRITFC_38	26-Jul-09	20-Sep-10	6-May-11	NULL	5013003	391800	CRITFC	Grande Ronde River
GR_above_Spring_Cr	CRITFC_39	1-Jul-10	20-Sep-10	6-May-11	NULL	5019221	401063	CRITFC	Grande Ronde River
Beaver_Cr_below_Dry_Beaver_Cr	CRITFC_4	1-Jul-10	26-Sep-10	6-May-11	NULL	5007510	398402	CRITFC	Beaver Creek
GR_acclimation_site	CRITFC_40	26-Jul-09	24-Aug-09	16-Feb-11	NULL	4992610	395171	CRITFC	Grande Ronde River
GR_below_Tanner_Gulch	CRITFC_41	29-Jun-10	27-Sep-10	6-May-11	NULL	4985997	399477	CRITFC	Grande Ronde River
GR_below_Vey	CRITFC_42	27-Jul-09	22-Sep-11	9-Dec-11	NULL	4998018	393019	CRITFC	Grande Ronde River

Site Name	Site ID	Start Date	End Date	Update Date	Missing Years	Northing UTM	Easting UTM	Coordinator	Stream
GR_Hilgard_Park	CRITFC_43	1-Jul-10	20-Sep-10	6-May-11	NULL	5021682	403115	CRITFC	Grande Ronde River
GR_mine_tailings	CRITFC_44	8-Oct-09	27-Jun-10	27-Apr-11	NULL	4989460	398740	CRITFC	Grande Ronde River
GR_Peach_Rd_bridge	CRITFC_45	30-Jun-10	20-Sep-10	6-May-11	NULL	5022243	424528	CRITFC	Grande Ronde River
GR_Reach_U155154	CRITFC_46	11-Jul-10	27-Sep-10	6-May-11	NULL	4989992	397788	CRITFC	Grande Ronde River
GR_Time_and_Half_Bridge	CRITFC_47	26-Jul-09	20-Sep-10	6-May-11	NULL	5001541	391497	CRITFC	Grande Ronde River
Jordan_Cr_mouth	CRITFC_48	10-Jul-10	19-Aug-10	6-May-11	NULL	5018226	399725	CRITFC	Jordan Creek
Ladd_Cr_mouth	CRITFC_49	14-Jul-10	20-Sep-10	6-May-11	NULL	5014624	426459	CRITFC	Ladd Creek
Beaver_Cr_below_reservoir	CRITFC_5	1-Jul-10	28-Sep-10	6-May-11	NULL	4999737	405224	CRITFC	Beaver Creek
Ladd_Cr_upper	CRITFC_50	1-Jul-10	28-Sep-10	6-May-11	NULL	5007327	419609	CRITFC	Ladd Creek
Limber_Jim_Cr_below_NF	CRITFC_51	26-Jul-09	27-Sep-10	6-May-11	NULL	4995796	395658	CRITFC	Limber Jim Creek
Limber_Jim_Cr_mouth	CRITFC_52	26-Jul-09	27-Sep-10	6-May-11	NULL	4993859	394822	CRITFC	Limber Jim Creek
Limber_Jim_Cr_upper	CRITFC_53	26-Jul-09	27-Sep-10	6-May-11	NULL	4995705	397179	CRITFC	Limber Jim Creek
Little_CC_mouth	CRITFC_56	29-Jul-09	20-Sep-10	6-May-11	NULL	4998817	443477	CRITFC	Little Catherine Creek
Little_Cr_High_Valley_Rd	CRITFC_57	29-Jul-09	22-Sep-10	6-May-11	NULL	5006477	438641	CRITFC	Little Creek
Little_Cr_mouth	CRITFC_58	30-Jun-10	20-Sep-10	6-May-11	NULL	5009109	427945	CRITFC	Little Creek
Little_Cr_N_Union	CRITFC_59	29-Jul-09	20-Sep-10	6-May-11	NULL	5007439	432455	CRITFC	Little Creek
Beaver_Cr_mouth	CRITFC_6	1-Jul-10	29-Sep-10	6-May-11	NULL	5013482	393402	CRITFC	Beaver Creek
McCoy_Cr_below_Ensign_Cr	CRITFC_60	24-Jun-10	21-Sep-10	6-May-11	NULL	5021821	379120	CRITFC	McCoy Creek
McCoy_Cr_mouth	CRITFC_61	24-Jun-10	21-Sep-10	6-May-11	NULL	5013242	390396	CRITFC	McCoy Creek
Meadow_Cr_above_Bear_Cr	CRITFC_62	27-Jul-09	21-Sep-10	6-May-11	NULL	5013595	380605	CRITFC	Meadow Creek
Meadow_Cr_above_Dark_Canyon_Cr	CRITFC_63	1-Jul-10	20-Sep-10	6-May-11	NULL	5014075	391559	CRITFC	Meadow Creek
Meadow_Cr_above_McCoy_Cr	CRITFC_64	24-Jun-10	21-Sep-10	6-May-11	NULL	5013171	390424	CRITFC	Meadow Creek
Meadow_Cr_above_Waucup_Cr	CRITFC_65	24-Jun-10	21-Sep-10	6-May-11	NULL	5016747	373014	CRITFC	Meadow Creek
Meadow_Cr_below_FS22_Bridge	CRITFC_66	27-Jul-09	7-Oct-09	16-Feb-11	NULL	5016513	374169	CRITFC	Meadow Creek
Meadow_Cr_mouth	CRITFC_67	26-Jul-09	23-Sep-11	9-Dec-11	NULL	5013246	391914	CRITFC	Meadow Creek
MF_CC_mouth	CRITFC_68	29-Jul-09	27-Sep-11	9-Dec-11	NULL	5003345	452560	CRITFC	Middle Fork Catherine Creek
Milk_Cr_below_unnamed_trib	CRITFC_69	25-Jun-10	20-Sep-10	6-May-11	NULL	4996989	444763	CRITFC	Milk Creek
Burnt_Corral_Cr_mouth	CRITFC_7	27-Jul-09	21-Sep-10	6-May-11	NULL	5010023	385480	CRITFC	Burnt Corral Creek
Milk_Cr_mouth	CRITFC_70	25-Jun-10	20-Sep-10	6-May-11	NULL	4998470	443382	CRITFC	Milk Creek
Milk_Cr_upper	CRITFC_71	25-Jun-10	20-Sep-10	6-May-11	NULL	4996639	444678	CRITFC	Milk Creek
Mill_Cr_mouth	CRITFC_72	30-Jun-10	20-Sep-10	6-May-11	NULL	5016610	432166	CRITFC	Mill Creek
Mill_Cr_upper	CRITFC_73	30-Jun-10	20-Sep-10	6-May-11	NULL	5014864	440465	CRITFC	Mill Creek
NF_CC_above_Jim_Cr	CRITFC_74	25-Jun-10	28-Sep-10	6-May-11	NULL	5003345	452560	CRITFC	North Fork Catherine Creek

Site Name	Site ID	Start Date	End Date	Update Date	Missing Years	Northing UTM	Easting UTM	Coordinator	Stream
NF_CC_above_MF_CC	CRITFC_75	29-Jul-09	6-Oct-09	16-Feb-11	NULL	5000181	451579	CRITFC	North Fork Catherine Creek
NF_CC_mouth	CRITFC_76	29-Jul-09	27-Sep-11	9-Dec-11	NULL	4996591	449231	CRITFC	North Fork Catherine Creek
NF_CC_upper	CRITFC_77	25-Jun-10	28-Sep-10	6-May-11	NULL	5006701	451715	CRITFC	North Fork Catherine Creek
Pelican_Cr_mouth	CRITFC_78	25-Jul-09	3-Aug-09	16-Feb-11	NULL	5023929	402828	CRITFC	Pelican Creek
Rock_Cr_mouth	CRITFC_79	24-Jun-10	20-Sep-10	6-May-11	NULL	5021613	403995	CRITFC	Rock Creek
CC_above_Ladd_Cr	CRITFC_8	14-Jul-10	20-Sep-10	6-May-11	NULL	5013954	426890	CRITFC	Catherine Creek
SF_CC_mouth	CRITFC_80	29-Jul-09	27-Sep-11	9-Dec-11	NULL	4996531	449253	CRITFC	South Fork Catherine Creek
Sheep_Cr_below_5160_Rd	CRITFC_81	27-Jul-09	22-Sep-11	9-Dec-11	NULL	4990521	385376	CRITFC	Sheep Creek
Sheep_Cr_below_E_Sheep_Cr	CRITFC_82	27-Jul-09	23-Sep-10	6-May-11	NULL	4986932	383815	CRITFC	Sheep Creek
Spring_Cr_mouth	CRITFC_84	1-Jul-10	26-Aug-10	6-May-11	NULL	5019565	401163	CRITFC	Spring Creek
Spring_Cr_upper	CRITFC_85	11-Jul-10	25-Jul-10	6-May-11	NULL	5007439	432455	CRITFC	Spring Creek
Waucup_Cr_mouth	CRITFC_86	24-Jun-10	21-Sep-10	6-May-11	NULL	5016670	373011	CRITFC	Waucup Creek
CC_above_Little_CC	CRITFC_9	10-Jul-10	20-Sep-10	6-May-11	NULL	4998749	443313	CRITFC	Catherine Creek
Battle Creek Lower	CTUIR_BATTLE1	30-Mar-10	31-Oct-11	18-Jan-12		5011010	384715	CTUIR	Battle Creek
Bear Creek Upper	CTUIR_BEAR1	8-Jun-03	13-Oct-05	9-Jun-10		5017287	399393	CTUIR	Bear Creek
Bear Creek Lower	CTUIR_BEAR2	28-Apr-04	13-Oct-05	9-Jun-10		5017963	399270	CTUIR	Bear Creek
CC Acclimation	CTUIR_CCAclimation	5-Mar-04	30-Oct-10	10-May-11	NULL	4996770	445479	CTUIR	Catherine Creek
CC Weir	CTUIR_CCWeir	25-Apr-02	30-Oct-10	10-May-11	NULL	5004495	434756	CTUIR	Catherine Creek
Clear Creek lower	CTUIR_CLC1	22-Jul-09	23-Oct-11	18-Jan-12	NULL	4990709	396831	CTUIR	Clear Creek
CoonCr1	CTUIR_COONCR1	NULL	NULL	NULL		5037107	419390	CTUIR	Coon Creek
Dark Canyon lower	CTUIR_DC1	4-Aug-09	31-Oct-11	18-Jan-12	NULL	5014172	391585	CTUIR	Dark Canyon Creek
Dark Canyon upper	CTUIR_DC2	4-Aug-09	31-Oct-11	18-Jan-12	NULL	5016873	391028	CTUIR	Dark Canyon Creek
Dry Cr McKenzie upper property	CTUIR_DRYCR1	14-Jun-11	26-Oct-11	18-Jan-12		5038035	419460	CTUIR	Dry Creek
End Creek Davidson	CTUIR_END1	28-Jun-03	30-Oct-11	18-Jan-12	NULL	5035239	418707	CTUIR	End Creek
End Creek Lower	CTUIR_END2	28-Jun-03	30-Oct-11	18-Jan-12	NULL	5035119	420142	CTUIR	End Creek
End Creek Davidson	CTUIR_ENDAIR	14-Jun-11	30-Oct-11	18-Jan-12	NULL	5035239	418707	CTUIR	End Creek
Fir Creek Lower	CTUIR_FIR1	14-Jun-11	26-Oct-11	18-Jan-12		5037640	419280	CTUIR	Fir Creek
Bird Track Springs	CTUIR_GR1	7-Jun-03	10-Oct-07	9-Jun-10	NULL	5017003	396714	CTUIR	Grande Ronde River
Mouth Moss Creek	CTUIR_GR2	7-Jun-03	13-Oct-05	9-Jun-10	NULL	5017980	399035	CTUIR	Grande Ronde River
Mouth Jordan Creek	CTUIR_GR3	7-Jun-03	10-Oct-07	9-Jun-10	NULL	5018253	399704	CTUIR	Grande Ronde River
Grande Ronde River lower Vey	CTUIR_GR4	22-Jul-09	23-Oct-11	18-Jan-12	NULL	4997765	392973	CTUIR	Grande Ronde River
Grande Ronde Acclimation Facility	CTUIR_GR5	22-Jul-09	23-Oct-11	18-Jan-12	NULL	4992447	395396	CTUIR	Grande Ronde River

Site Name	Site ID	Start Date	End Date	Update Date	Missing Years	Northing UTM	Easting UTM	Coordinator	Stream
Grande Ronde River Mid	CTUIR_GR6	22-Jul-09	23-Oct-11	18-Jan-12	NULL	4989952	397816	CTUIR	Grande Ronde River
East Fork Grande Ronde River	CTUIR_GR7	22-Jul-09	23-Oct-11	18-Jan-12	NULL	4989473	398779	CTUIR	East Fork Grande Ronde River
Grand Ronde River upper	CTUIR_GR8	22-Jul-09	23-Oct-11	18-Jan-12	NULL	4989391	398767	CTUIR	Grande Ronde River
GR Acclimation	CTUIR_GRAcclimation	19-Apr-04	15-Apr-10	10-May-11	NULL	4992610	395171	CTUIR	Grande Ronde River
GR Weir River Campground	CTUIR_GRWeircmgrd	26-Apr-01	1-Jul-06	10-May-11	NULL	4998923	392560	CTUIR	Grande Ronde River
GR Weir Starkey	CTUIR_GRWeirstarkey	27-Jan-05	1-Nov-10	10-May-11	NULL	5011544	390993	CTUIR	Grande Ronde River
Jordan Creek Lower	CTUIR_JORDAN1	7-Jun-03	10-Oct-07	9-Jun-10	NULL	5017804	399888	CTUIR	Jordan Creek
Jordan Creek Upper	CTUIR_JORDAN2	30-Jul-02	10-Oct-07	9-Jun-10	NULL	5018193	399731	CTUIR	Jordan Creek
McCoythermo upper	CTUIR_MCCOY1	26-Jul-02	31-Oct-11	18-Jan-12	NULL	5013925	388128	CTUIR	McCoy Creek
McCoythermo2	CTUIR_MCCOY2	26-Jul-02	5-Nov-08	8-Jun-10	NULL	5013825	388344	CTUIR	McCoy Creek
McCoythermo3	CTUIR_MCCOY3	26-Jul-02	14-Oct-06	8-Jun-10	NULL	5013806	388602	CTUIR	McCoy Creek
McCoythermo5 above bridge	CTUIR_MCCOY5	26-Jul-02	23-Nov-09	9-Jun-10	2010, 2011	5013306	389041	CTUIR	McCoy Creek
McCoythermo6 below bridge	CTUIR_MCCOY6	26-Jul-02	31-Oct-11	18-Jan-12	NULL	5013298	389037	CTUIR	McCoy Creek
McCoythermo7 lower	CTUIR_MCCOY7	7-Jun-03	31-Oct-11	18-Jan-12	NULL	5013241	390466	CTUIR	McCoy Creek
McCoythermo8	CTUIR_MCCOY8	26-Jul-02	5-Nov-08	9-Jun-10	NULL	5013258	390480	CTUIR	McCoy Creek
Meadow Creek 1	CTUIR_MEADOW1	26-Jul-02	31-Oct-11	18-Jan-12	NULL	5012393	389614	CTUIR	Meadow Creek
Meadowstarlogger1	CTUIR_MEADOW1ST	NULL	NULL	NULL	NULL	5012393	389614	CTUIR t	Meadow Creek
Meadow Creek 2	CTUIR_MEADOW2	26-Jul-02	31-Oct-11	18-Jan-12	NULL	5013175	390427	CTUIR	Meadow Creek
Meadowstarlogger2	CTUIR_MEADOW2ST	NULL	NULL	NULL	NULL	5013175	390427	CTUIR	Meadow Creek
Meadowwetlandchannel1	CTUIR_MEADOW3	11-May-09	21-Jun-11	18-Jan-12	NULL	5012358	389876	CTUIR	Meadow Creek
Meadowwetlandchannel2	CTUIR_MEADOW4	11-May-09	21-Jul-10	6-May-11	NULL	5013156	390742	CTUIR	Meadow Creek
Meadow Creek	CTUIR_MEADOW5	17-Jul-09	31-Oct-11	18-Jan-12	NULL	5011105	384373	CTUIR	Meadow Creek
Habberstad1 Upper	CTUIR_MEADOW5H	11-May-09	23-Nov-09	9-Jun-10	NULL	5011092	384337	CTUIR	Meadow Creek
Meadow Creek	CTUIR_MEADOW6	17-Jul-09	31-Oct-11	18-Jan-12	NULL	5010609	385359	CTUIR	Meadow Creek
Habberstad2 Lower	CTUIR_MEADOW6	17-Jul-09	31-Oct-11	18-Jan-12	NULL	5010609	385359	CTUIR	Meadow Creek
Meadow Creek	CTUIR_MEADOW	22-May-	17-Nov-09	9-Jun-10	NULL	5010609	385359	CTUIR	Meadow Creek

Site Name	Site ID	Start Date	End Date	Update Date	Missing Years	Northing UTM	Easting UTM	Coordinator	Stream
Habberstad2 Lower H	6H	09							
Rock Cr lower	CTUIR_Rock1	1-Jul-11	29-Nov-11	18-Jan-12	NULL	5021358	403954	CTUIR	Rock Creek
Rock Cr below Graves Cr	CTUIR_Rock2	30-Jun-11	29-Nov-11	18-Jan-12	NULL	5019210	405635	CTUIR	Rock Creek
South Fork Willow Upper	CTUIR_SFW1	14-Jun-11	30-Oct-11	18-Jan-12		5033817	419907	CTUIR	South Fork Willow Creek
South Fork Willow Lower	CTUIR_SFW2	NULL	NULL	NULL		5035086	420229	CTUIR	South Fork Willow Creek
Spring Trib 2	CTUIR_SPRTRIB2	NULL	NULL	NULL		5036530	419902	CTUIR	Willow Creek
Spring Trib 3	CTUIR_SPRTRIB3	NULL	NULL	NULL		5036855	419638	CTUIR	Willow Creek
Willow Creek 1	CTUIR_WILL1	14-Jun-11	26-Oct-11	18-Jan-12		5035434	420889	CTUIR	Willow Creek
Willow Creek 2	CTUIR_WILL2	14-Jun-11	26-Oct-11	18-Jan-12		5035773	420738	CTUIR	Willow Creek
Willow Creek 3	CTUIR_WILL3	14-Jun-11	26-Oct-11	18-Jan-12		5036453	420053	CTUIR	Willow Creek
Willow Creek 4	CTUIR_WILL4	14-Jun-11	26-Oct-11	18-Jan-12		5036866	419692	CTUIR	Willow Creek
Willow Creek 5	CTUIR_WILL5	14-Jun-11	26-Oct-11	18-Jan-12		5037651	419320	CTUIR	Willow Creek
Pelican Creek	USFS_L1	30-Jul-91	23-Sep-93	28-Dec-09	1994	5023928	402804	USFS	Pelican Creek
Dark Canyon Creek	USFS_L10	2-Aug-91	14-Sep-96	3-Feb-10	1995	5017067	390620	USFS	Dark Canyon Creek
Five Points below Mt. Emily Creek	USFS_L100	28-Jul-00	18-Oct-00	3-Feb-10	NULL	5036107	410290	USFS	Five Points Creek
Sheep.85F.102	USFS_L102	30-May-02	18-Oct-11	26-Mar-12	NULL	4990563	385394	USFS	Sheep Creek
Collins Creek at mouth	USFS_L105	19-Jun-08	3-Oct-11	26-Mar-12	NULL	4994818	457375	USFS	Collins Creek
Prong Creek at mouth	USFS_L106	19-Jun-08	11-Oct-10	2-May-11	NULL	4994501	455308	USFS	Prong Creek
Big Creek at Bridge	USFS_L107	3-Jul-08	27-Sep-11	26-Mar-12	NULL	4983531	453920	USFS	Big Creek
McCoy Creek	USFS_L11	2-Aug-91	29-Jul-92	15-Dec-09	NULL	5013128	389744	USFS	McCoy Creek
Meadow Creek near McIntyre Rd.	USFS_L12	2-Aug-91	8-Apr-93	28-Dec-09	NULL	5012617	389906	USFS	Meadow Creek
Burnt Corral Creek	USFS_L13	2-Aug-91	10-Sep-07	4-Feb-10	1993-2001	5000081	399964	USFS	Burnt Corral Creek
Bear Creek	USFS_L14	2-Aug-91	12-Oct-11	23-Mar-12	1992-1995,1997-1999	5011656	380343	USFS	Bear Creek
Meadow Cr. Gauging station (upper)	USFS_L15	30-Jul-91	12-Oct-11	26-Mar-12	1993-2001, 2003, portion of 2011	5013943	380185	USFS	Meadow Creek
Meadow Cr. above smolt trap	USFS_L16	30-Jul-91	27-Jul-94	4-Jan-10	1993	5013595	376427	USFS	Meadow Creek
Beaver Pond at Starkey store	USFS_L17	2-Aug-91	8-Apr-93	28-Dec-09	NULL	5012090	391148	USFS	Beaver Pond
Fly.85B.18	USFS_L18	30-Jul-91	18-Oct-11	26-Mar-12	1995-1997,2006	5007082	390232	USFS	Fly Creek
Upper Grande	USFS_L19	29-Jul-91	18-Oct-11	26-Mar-12	2000	5007086	390500	USFS	Grande Ronde River

Site Name	Site ID	Start Date	End Date	Update Date	Missing Years	Northing UTM	Easting UTM	Coordinator	Stream
Ronde.85E.19									
Five Points above Pelican Creek	USFS_L2	30-Jul-91	10-Jul-92	15-Dec-09	NULL	5023770	402920	USFS	Five Points Creek
Grande Ronde Below Vey Meadow	USFS_L20	31-Jul-91	29-Sep-10	6-May-11	1999-2000, 2011	4997764	393193	USFS	Grande Ronde River
Limber Jim above South Fork	USFS_L21	2-Aug-91	26-Sep-93	28-Dec-09	NULL	4995357	395336	USFS	Limber Jim Creek
South Fork Limber Jim	USFS_L22	31-Jul-91	31-Aug-92	16-Dec-09	NULL	4994262	394955	USFS	South Fork Limber Creek
Limber Jim. 85J.23 below south fork confluence	USFS_L23	31-Jul-91	18-Oct-11	26-Mar-12	199,619,99 2,003	4994107	394966	USFS	Limber Jim Creek
Clear.85I.24	USFS_L24	31-Jul-91	18-Oct-11	26-Mar-12	199,619,99 2,003	4990799	396899	USFS	Clear Creek
Upper Grande Ronde.85I.25 above clear Cr.	USFS_L25	31-Jul-91	18-Oct-11	26-Mar-12	1993,1994, 1996,1997, 1999-2001	4990722	397086	USFS	Grande Ronde River
West Chicken.85G.26	USFS_L26	27-Jul-91	18-Oct-11	26-Mar-12	19,941,998	4990037	389602	USFS	West Chicken Creek
Chicken. 85G.27	USFS_L27	28-Jul-91	18-Oct-11	28-Mar-12	1996, 2000-2001	4988966	390475	USFS	Chicken Creek
Sheep Creek	USFS_L28	28-Jul-91	30-Sep-91	14-Dec-09	1992	4990496	385348	USFS	Sheep Creek
Little Fly Creek	USFS_L29	28-Jul-91	18-Oct-11	28-Mar-12	1996- 1997,2007	4991109	381703	USFS	Little Fly Creek
Grande Ronde above Five Points	USFS_L3	1-Aug-91	3-Sep-92	15-Dec-09	NULL	5022177	404289	USFS	Grande Ronde River
Fly.85B.30 Fly Cr. Below vey	USFS_L30	2-Aug-91	12-Oct-11	28-Mar-12	1994,1996- 1999,2006	4997981	385975	USFS	Fly Creek
Catherine Creek above State Park	USFS_L31	21-Aug-91	15-Sep-96	3-Feb-10	1995	4999492	442625	USFS	Catherine Creek
South Fork Catherine Creek	USFS_L33a	15-Aug-91	22-Oct-00	8-Feb-10	199,419,95 1,998	NULL	NULL	USFS	South Fork Catherine Creek
North Fork Catherine Creek	USFS_L33b	15-Aug-91	22-Oct-00	27-Apr-11	1995	NULL	NULL	USFS	North Fork Catherine Creek
Birdtrack Springs, Second pool	USFS_L34	21-Aug-91	7-Aug-93	31-Dec-09	NULL	NULL	NULL	USFS	Bird Track Springs
S.F. Catherine below Bottle Creek	USFS_L35	15-Aug-91	19-Aug-94	5-Jan-10	1992-1993	NULL	NULL	USFS	South Fork Catherine Creek
Five Points below Tie Creek	USFS_L36	5-Jun-92	12-Sep-96	3-Feb-10	1993-1995	5030539	409386	USFS	Five Points Creek
MF Catherine.12M.37	USFS_L37	15-Aug-91	27-Sep-11	28-Mar-12	1995,1997- 2000,2008	5000065	451564	USFS	Middle Fork Catherine Creek
North Fork Catherine Creek	USFS_L38	15-Aug-91	25-Sep-94	5-Jan-10	NULL	NULL	NULL	USFS	North Fork Catherine Creek
Five Points below Mt. Emily Creek	USFS_L39	20-Aug-91	4-Jun-92	22-Dec-09	NULL	5036067	410267	USFS	Five Points Creek

Site Name	Site ID	Start Date	End Date	Update Date	Missing Years	Northing UTM	Easting UTM	Coordinator	Stream
Rock Creek	USFS_L4	1-Aug-91	3-Sep-92	15-Dec-09	1993-1995	5021634	403929	USFS	Rock Creek
Mt Emily Creek	USFS_L40a	20-Aug-91	28-Jul-97	8-Feb-10	1993-1995	NULL	NULL	USFS	Mount Emily Creek
Middle Fork Five Points	USFS_L40b	20-Aug-91	28-Jul-97	8-Feb-10	1993-1995	NULL	NULL	USFS	Middle Fork Five Points Creek
Big Creek	USFS_L41	15-Aug-91	30-Aug-92	22-Dec-09	1993-2002	4984098	455003	USFS	Big Creek
Little Catherine Tributary #1	USFS_L42	26-May-94	4-Oct-94	5-Jan-10	NULL	NULL	NULL	USFS	Little Catherine Creek
Little Catherine Creek at 2036	USFS_L43	15-Aug-91	4-Oct-94	5-Jan-10	1992-1993	5004111	448016	USFS	Little Catherine Creek
Lick Creek	USFS_L44	4-Jun-92	21-Sep-93	31-Dec-09	NULL	NULL	NULL	USFS	Lick Creek
S.F. Catherine below 600rd bridge	USFS_L45	4-Jun-92	24-Sep-94	5-Jan-10	1993	4994931	455826	USFS	South Fork Catherine Creek
Burnt Corral Creek @ 2444040 Rd.	USFS_L46	9-Jul-92	4-Oct-94	5-Jan-10	NULL	5004600	382205	USFS	Burnt Corral Creek
Lookout Creek at 5160	USFS_L47	9-Jul-92	18-Oct-11	28-Mar-12	199,619,98 2,002	4994279	379571	USFS	Lookout Creek
Lookout Creek Tributary #1	USFS_L49	9-Jul-92	28-Aug-94	5-Jan-10	NULL	4992965	378934	USFS	Lookout Creek
Spring Creek	USFS_L5	1-Aug-91	1-Oct-02	3-Feb-10	1996-2001	5020136	400637	USFS	Spring Creek
East Fork Grande Ronde	USFS_L50	15-Jul-93	13-Nov-00	11-Oct-10	1998	4989694	399053	USFS	East Fork Grande Ronde River
Waucup Creek @ 21 road	USFS_L51	14-Jul-93	12-Oct-11	28-Mar-12	1992,1994- 1998,1999	5016679	373076	USFS	Waucup Creek
Upper Grande Ronde above Blowout	USFS_L53	9-Jul-92	29-Oct-95	3-Feb-10	1994	4988284	399585	USFS	Grande Ronde River
Beaver.16D.54 above reservoir	USFS_L54	24-Jun-94	27-Sep-11	28-Mar-12	199,520,00 2,005	4998160	406640	USFS	Beaver Creek
WF Beaver.16C.55 above 270 rd.	USFS_L55	10-Jul-92	27-Sep-11	28-Mar-12	1,996,199, 820,002,00 0	5000690	404328	USFS	Beaver Creek
Hoodoo.16B.56	USFS_L56	10-Jul-92	10-Oct-07	9-Feb-10	1993,1996- 1997,1999- 2000	4995030	409975	USFS	Hoodoo Creek
Middle Fork Limber Jim	USFS_L59	12-Jul-92	4-Nov-97	3-Feb-10	1995	4995598	396928	USFS	Middle Fork Limber Jim Creek
Jordan Creek	USFS_L6	1-Aug-91	3-Sep-92	15-Dec-09	NULL	5018221	399754	USFS	Jordan Creek
Meadow Creek @ Waucup Creek	USFS_L60	14-Jul-93	21-Sep-93	4-Jan-10	NULL	5016627	379385	USFS	Meadow Creek
Sheep Creek @ Road 5182500	USFS_L61	14-Jul-93	8-Oct-01	3-Feb-10	1994-1999	4986882	383800	USFS	Sheep Creek
East Sheep Cr. @ Rd.	USFS_L62	4-May-94	8-Oct-01	3-Feb-10	1996,1998-	4986882	383800	USFS	East Sheep Creek

Site Name	Site ID	Start Date	End Date	Update Date	Missing Years	Northing UTM	Easting UTM	Coordinator	Stream
5182500 Mill Creek	USFS_L63	10-Jul-93	17-Oct-00	9-Feb-10	1999 1995- 1996,1999	5014020	443684	USFS	Mill Creek
Catherine Creek	USFS_L64k	2-Jun-93	19-Jul-93	4-Jan-10	NULL	NULL	NULL	USFS	Catherine Creek
SF Catherine.12K.65a	USFS_L65a	23-Aug-95	3-Oct-11	26-Mar-12	2007	4994989	455953	USFS	South Fork Catherine Creek
Pole.12K.65b	USFS_L65b	23-Aug-95	3-Oct-11	26-Mar-12	20,002,007	4995107	455972	USFS	Pole Creek
Beaver below 4305 road	USFS_L66	12-Jun-93	9-Aug-98	3-Feb-10	19,941,996	5001967	404350	USFS	Beaver Creek
Grande Ronde at Red Bridge	USFS_L7	1-Aug-91	10-Jul-92	15-Dec-09	NULL	5016026	395688	USFS	Grande Ronde River
Upper Grande Ronde.85E.74	USFS_L74	9-Jun-95	12-Oct-11	26-Mar-12	19,961,998	5001530	391606	USFS	Grande Ronde River
NF Catherine.12N.75 NF Catherine Meadows	USFS_L75	22-Jun-93	23-Sep-07	9-Feb-10	1994- 1999,2001	5011931	450320	USFS	North Fork Catherine Creek
North Fork Catherine Meadows	USFS_L76	4-Aug-93	5-Oct-93	4-Jan-10	NULL	NULL	NULL	USFS	North Fork Catherine Creek
Jordan Creek	USFS_L77	29-Jul-95	27-Aug-95	3-Feb-10	NULL	NULL	NULL	USFS	Jordan Creek
North Fork Catherine below NF/SF	USFS_L78	26-Jul-96	3-Sep-96	3-Feb-10	NULL	NULL	NULL	USFS	North Fork Catherine Creek
Milk Creek	USFS_L79	23-Jul-96	12-Sep-96	3-Feb-10	NULL	NULL	NULL	USFS	Milk Creek
Beaver Creek	USFS_L8	1-Aug-91	3-Sep-92	15-Dec-09	1993	5013556	393323	USFS	Beaver Creek
Whiskey Creek	USFS_L80	23-Jul-96	12-Sep-96	3-Feb-10	NULL	NULL	NULL	USFS	Whiskey Creek
McCoy.86D.81	USFS_L81	24-Jul-96	12-Oct-11	28-Mar-12	1997-2000	5021742	379400	USFS	McCoy Creek
Rock Creek	USFS_L82	23-Jul-96	12-Sep-96	3-Feb-10	NULL	NULL	NULL	USFS	Rock Creek
Upper Grande Ronde.85I.86 Woodley Cr Gage	USFS_L86	16-Feb-94	26-Oct-11	28-Mar-12	1995-2000	4991723	396424	USFS	Grande Ronde River
NF Catherine.12L.87 Gage	USFS_L87	1-Jan-01	25-Oct-11	28-Mar-12	2001- 2004,2006	4997055	449757	USFS	North Fork Catherine Creek
Five Points Gauging Station	USFS_L88	24-Apr-94	26-Oct-11	28-Mar-12	1995-2000	5022726	403801	USFS	Five Points Creek
Meadow.86A.89 Lower Meadow gage	USFS_L89	1-Jan-94	25-Oct-11	26-Mar-12	1995- 2002,2003, 2005,2008	5013453	391717	USFS	Meadow Creek
Grande Ronde below Meadow Cr.	USFS_L9	2-Aug-91	5-Sep-92	15-Dec-09	NULL	5013386	392310	USFS	Grande Ronde River
SF Catherine.12K.90 @ mouth	USFS_L90	9-Jul-02	27-Sep-10	6-May-11	2006, 2011	4996512	449427	USFS	South Fork Catherine Creek
Beaver Creek @ Spillway	USFS_L91	14-Jul-00	29-Sep-03	3-Feb-10	2001	4992727	411733	USFS	Beaver Creek
NF Catherine.12N.92 mdw below Amelia Cr	USFS_L92	29-Jul-00	28-Sep-11	26-Mar-12	NULL	5006839	451672	USFS	North Fork Catherine Creek
Chicken/Dry Cr @ 5178 Rd	USFS_L93	4-May-01	29-Aug-04	29-Apr-11	NULL	4990324	390775	USFS	Dry Creek

Site Name	Site ID	Start Date	End Date	Update Date	Missing Years	Northing UTM	Easting UTM	Coordinator	Stream
NF Cath Cr Mdw below project	USFS_L94	28-Jul-00	11-Oct-00	3-Feb-10	NULL	5006627	451629	USFS	North Fork Catherine Creek
Meadow Cr above 21 Rd	USFS_L95	18-May-01	12-Oct-11	28-Mar-12	2009	5016795	372780	USFS	Meadow Creek
Five Points @ Camp One	USFS_L96	30-May-01	25-Oct-11	28-Mar-12	2003	5030102	406685	USFS	Five Points Creek
Five Points above Mt. Emily Cr	USFS_L98	28-Jul-00	19-Sep-07	9-Feb-10	20,012,004	5036163	410323	USFS	Five Points Creek
Mt. Emily Cr @ Mouth	USFS_L99	28-Jul-00	19-Sep-07	9-Feb-10	20,012,004	5036141	410336	USFS	Mount Emily Creek
GRR @ spool cart	USFS_LUtahL	18-Jun-01	5-Oct-01	3-Feb-10	NULL	NULL	NULL	USFS	Grande Ronde River
GRR @ 5125 Bridge	USFS_LUtahM	18-Jun-01	5-Oct-01	3-Feb-10	NULL	NULL	NULL	USFS	Grande Ronde River
GRR above Woodley Campground	USFS_LUtahU	17-Jun-01	5-Oct-01	3-Feb-10	NULL	NULL	NULL	USFS	Grande Ronde River
NF_CC_above_MF_CC	CHAMP_12	23-Sep-10	27-Sep-11	9-Dec-11	NULL	5000096	451504	CRITFC	North Fork Catherine Creek
CBW05583-155818	CHAMP_14	24-Aug-11	NULL	NULL	NULL	4999556	443707	CRITFC	Little Catherine Creek
Jim_Cr_mouth	CHAMP_19	2-Jun-10	NULL	NULL	NULL	5003344	452560	CRITFC	Jim Creek
DSGN4-000009	CHAMP_2	15-Jul-11	22-Sep-11	9-Dec-11	NULL	4989992	397788	CRITFC	Grande Ronde River
CBW05583-456106	CHAMP_28	12-Aug-11	21-Sep-11	9-Dec-11	NULL	4996871	445092	CRITFC	Catherine Creek
CBW05583-382778	CHAMP_29	25-Jul-11	5-Oct-11	9-Dec-11	NULL	5006892	382829	ODFW	Burnt Corral Creek
CBW05583-013882	CHAMP_30	4-Aug-11	4-Oct-11	9-Dec-11	NULL	5013214	373300	ODFW	Peet Creek
DSGN4-000213	CHAMP_31	14-Jul-11	5-Oct-11	9-Dec-11	NULL	5013167	390632	ODFW	Meadow Creek
DSGN4-000094	CHAMP_32	28-Jun-11	5-Oct-11	9-Dec-11	NULL	4997845	385829	ODFW	Fly Creek
CBW05583-108010	CHAMP_33	15-Jul-11	22-Sep-11	9-Dec-11	NULL	4995300	395296	CRITFC	Limber Jim Creek
Flow									
Bear Cr. at Wallowa	13330700	9-May-95	30-Sep-03			457936	5047574	OWRD	Bear Creek
Bear Cr. nr Wallowa	13330500	1-Apr-15		22-Feb-11		456954	5041638	OWRD	Bear Creek
Flow_Bear_Cr_at_Wallowa	13330700	9-May-95	30-Sep-03			457936	5047574	OWRD	Bear Creek
Flow_Bear-Cr_nr_Wallowa	13330500	1-Apr-15		22-Feb-11		456954	5041638	OWRD	Bear Creek
Flow_CatherineCreek_near Union	13320000	1-Aug-11		22-Feb-11		439170	5000514	OWRD	Catherine Creek
Flow_Five_Points_CR	13318920	1-Oct-92		22-Feb-11		403802	5022671	OWRD	Five Points Creek
Flow_GR_at_Hilgard	13318800	1-Oct-66	30-Nov-81			402526	5021396	OWRD	Grande Ronde
Flow_GR_near_Imbler	13323495	28-Jan-97	18-Sep-03			427854	5038543	OWRD	Grande Ronde
Flow_GR_near_Perry	13318960	1-Oct-96		22-Feb-11		407442	5022746	OWRD	Grande Ronde
		15-May-36	31-Oct-37			392630	4996477	OWRD	Grande Ronde
Flow_GR_near_Starkey	13317900								
Flow_Imnaha_at_Imnaha	13292000	1-Oct-28		22-Feb-11		5045409	512973	OWRD	Imnaha River
Flow_IndianCr_near_Imbler	13323600	1-Mar-38	30-Sep-50			435929	5031155	OWRD	Indian Creek
Flow_LittleMinamR_near_Cove	13331400	16-Jun-38	30-Sep-43			447920	5012912	OWRD	Minam River

Site Name	Site ID	Start Date	End Date	Update Date	Missing Years	Northing UTM	Easting UTM	Coordinator	Stream
Flow_Lostine_at_Baker_rd_nr_Lostine	13330300	1-Jun-95		22-Feb-11		462633	5042790	OWRD	Lostine River
Flow_Lostine_at_Caudle_Ln_at_Lostine	13330050	1-Aug-95		22-Feb-11		465965	5037441	OWRD	Lostine River
Flow_LostineR_near_Lostine	13330000	1-Sep-12		22-Feb-11		466651	5031849	OWRD	Lostine River
Flow_MeadowCR_above_BearCr	13318060	1-Jul-77		22-Feb-11		380731	5013575	OWRD	Meadow Creek
Flow_MeadowCR_below_DarkCanyon	13318210	1-Oct-92		22-Feb-11		391681	5013502	OWRD	Meadow Creek
Flow_MeadowCR_below_SmithCR	13318050	1-Jul-77	31-Oct-79			374187	5016542	OWRD	Meadow Creek
Flow_MeadowCR_near_Starkkey	13318200	1-Oct-31	30-Sep-35			391391	5013476	OWRD	Meadow Creek
Flow_MinamR_near_Minam	13331500	1-Jun-12		22-Feb-11		443434	5052051	OWRD	Minam River
Flow_NFKCatherineCR_near_MedicalSprings	13319900	1-Oct-92		22-Feb-11		450261	4997463	OWRD	Catherine Creek
Flow_S_Catherine_Ditch	13319700	31-May-66	30-Sep-84			458987	4992247	OWRD	Catherine Creek
Flow_S_Catherine_MedicalSprings	13319800	1-May-26	20-Sep-27			453912	4994843	OWRD	Catherine Creek
Flow_WallowaR_below_watertcan	13331450	16-Aug-95		22-Feb-11		452042	5050717	OWRD	Wallowa River
Flow_WallowaR_Enterprise	13329765	1-Jun-12		22-Feb-11		469714	5035802	OWRD	Wallowa River
Lostine R. at Baker Rd. nr Lostine	13330300	1-Jun-95		22-Feb-11		462633	5042790	OWRD	Lostine River
Lostine R. at Caudle Ln at Lostine	13330050	1-Aug-95	22-Feb-11	22-Feb-11		465965	5037441	OWRD	Lostine River
Wallowa R. Ab. XC canal nr. Enterprise	13329770	28-Apr-95	24-Jun-09			468526	5037312	OWRD	Wallowa River

Appendix 2-Les Naylor

Notes on how CTUIR temperature data were organized and collated

These data are from the Confederated Tribes of the Umatilla Indian Reservation Grande Ronde Fish Habitat program.

Data covered by this document span the years 2002 to 2009.

1. Data in the raw ASCII files has not been edited or altered. Any edits were carried out and saved in either a Microsoft Excel or Access format.
2. The date for the probes activation and termination were not the same as deployment and/or retrieval, therefore, data outside the deployment/retrieval dates was not used (but is retained in the raw ASCII files).
3. Data for the day of deployment and day of retrieval were removed from the dataset. This was done to provide data where probes at the upstream and downstream sites were recording water temperature at the same time/date.
4. When field notes indicated errors with the probe the data for that time period was removed. These errors could be due to a dead battery or the probes being out of the water.
5. Some probes recorded erratically due to failing batteries and/or being out of the water. These probes/years are detailed as follows:
 - a. BEAR1 (2003) weeks 30 through 33 the probe was out of the water so data deleted for that time period.
 - b. BEAR1 (2006) probe not working correctly so data deleted.
 - c. BEAR2 (2003) no data.
 - d. BEAR2 (2006) probe not working correctly.
 - e. END1H (2006) no data.
 - f. END1H (2008) probe not working correctly weeks 29 through 38 so data deleted for that time period.
 - g. END2H (2006) weeks 36 through 39 probe not working.
 - h. GR1 (2003) weeks 28 through 30 the probe was out of the water so data for that period was deleted.
 - i. GR1 (2006) probe not working correctly so data deleted.
 - j. GR2 (2006) probe not working correctly so data deleted.
 - k. GR3 (2007) for weeks 31 through 40 probe was out of water so data for that period was deleted.
 - l. JORDAN1 (2002) no data.

- m. JORDAN1 (2006) probe not working correctly data deleted.
 - n. JORDAN1 (2007) probe out of the water weeks 40 through 41 so data deleted.
 - o. JORDAN2 (2004) no data.
 - p. JORDAN1 and 2 (2005) probes were out of the water during week 23 so data for that week was deleted.
 - q. JORDAN2 the channel dries up approximately June through September; however these data are retained so that the timing of this dry period can be plotted each year.
 - r. LONGLEYAIR (2007) no data.
 - s. MCCOY1H (2007) data ends week 39.
 - t. MCCOY2H (2005) record period ends week 41.
 - u. MCCOY3H (2007) data lost when stream bank collapsed.
 - v. MCCOY5H (2005) data collection ends week 41.
 - w. MCCOY5H (2007) week 22 the probe was out of the water so data deleted for that week. Data collection ends week 39.
 - x. MCCOY6H (2007) probe was in the dry for weeks 22 and 23, then weeks 30 through 33 so these data were deleted.
 - y. MCCOYAIR (2005) no data.
 - z. MEADOW1H (2003) no data.
 - aa. MEADOW1H (2007) probe not working correctly, data deleted.
 - i. MEADOW1H and 2H (2008) no data as Starlogger deployed instead of Hobo's.
6. Probe locations were plotted in ARCGIS with the projection being in UTM NAD 83 zone 11N.
7. Problems with the date format in Microsoft Excel made it necessary to import the data table into Microsoft Access with all dates formatted as text, and then export the table back to Excel. The spreadsheet for McCoy Meadows is approximately 154,000 rows and is a compilation of several years of data. This size may contribute to potential problems in Excel, therefore, it may be necessary to split these data into smaller chunks and re-combine them after calculating the 7-day maximum temperatures.
8. Table headers were:
- a. **Date_id and Time_id.** Are the date and hour of recording (split into two columns when imported into Excel).
 - b. **Temp_C.** Is the recorded temperature in degrees Celsius.
 - c. **Probe_id.** Is the unique probe number. Probes were generally used at the same locations each year but some were moved and/or replaced. A combination of the "Probe_id", "Location" and "Year" will give a unique reference.
 - d. **Location.** Is a unique identifier for each monitoring site and is used to link the temperature data table to an X/Y coordinate table in Microsoft Access.
 - e. **WeekNum.** Is the week of the year (numbered from 1 to 52) and is used when calculating the 7-day maximum temperatures.
 - f. **Comments.** Is a column for general comments about a probe, particular date or weather conditions etc.

Citations

Dunham, J., C. Gwynne, B. Reiman, and D. Martin. 2005. Measuring stream temperature with digital data loggers: A user's guide. USDA Forest Service, Report RMRS-GTR-150WWW, Fort Collins, CO.

OWRD 2011. Oregon Water Resources Department. Accessed site on: March 21, 2011. Using:
http://apps.wrd.state.or.us/apps/sw/hydro_near_real_time and
http://apps.wrd.state.or.us/apps/sw/hydro_near_real_time/hydro_download.aspx

Appendix B.

Draft Revisions to the Solar Input and Riparian Canopy Protocol that Incorporates use of the Solmetric SunEye



COLUMBIA RIVER INTER-TRIBAL FISH COMMISSION

729 NE Oregon, Suite 200, Portland, Oregon 97232

Telephone 503 238 0667

Fax 503 235 4228

Draft Revisions to the Solar Input and Riparian Canopy Protocol that Incorporates use of the Solmetric SunEye

A component of

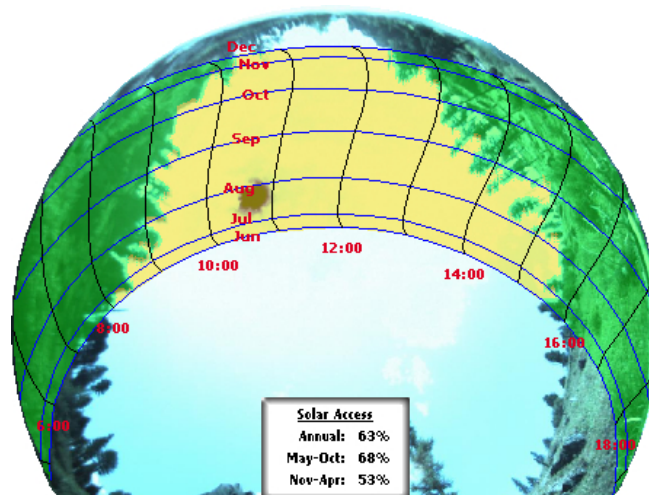
Monitoring Recovery Trends in Key Spring Chinook Habitat Variables and Validation of
Population Viability Indicators

March 2012

Casey Justice

Dale McCullough

Seth White



Data by Solmetric SunEye™ -- www.solmetric.com

9.3 Solar Input

Equipment: Solmetric SunEye

The Solmetric SunEye device is used to measure potential solar radiation at the center of the bankfull channel at all odd-numbered transects from 1 to 21 for a total of 11 transects. To ensure accuracy in estimation of solar radiation, it is critical to capture good quality images. Adequate atmospheric conditions are necessary to achieve usable images. These conditions include low sun angle (dawn or dusk is ideal) or uniform overcast sky and absence of sun “flares” or “spots”. Because ideal conditions may not exist during a survey, solar input measurements should be completed at the beginning or end of a survey to ensure the best possible atmospheric conditions. It is also important to hold the SunEye as level and steady as possible to ensure that images are clear and representative of the vegetation directly overhead. The SunEye automatically adjusts for its tilt and heading orientation for every image, but the best results are achieved if the SunEye is steady within +/- 5° of level and within 30° of South.

- i. All solar input measurements will be collected in the center of the bankfull channel.
- ii. Turn on the SunEye by pushing the yellow power button on the upper left side of the device.
- iii. Begin a new session for the site by tapping the “New session...” button on the left side of the screen. Name the session using the DCE id (e.g., CBW06683-457806-20110801), then tap “Next”.
- iv. Select the location for the session using the “SunEye GPS” option. Do not check the box that says “Get new GPS location for each skyline”. After the coordinates have been obtained, tap “Done” in the upper right corner.
- v. A total of 11 images (skylines) will be captured for each site. Tap the yellow circle in the lower left corner of the screen, then tap “Skyline”. Next tap “New”. Alternatively, push the blue button with the star icon to start a new skyline. Leave the default settings as is (i.e., Type = Fixed, Azim = 180°, Tilt = 0°) and tap “OK”.
- vi. The SunEye has different camera settings which allow it to more accurately differentiate between open sky, and vegetation or other structures. The three setting options are “Clouds and Blue Sky”, “Normal”, and “Shaded”. For our purposes, the shaded option is generally preferred because it provides the best delineation between vegetation and open sky. To select the camera setting, tap the ► icon in the upper left corner, then tap the drop down button next to “Sky” and select “Shaded”. Tap “Close”.
- vii. Holding the SunEye 30 cm above the wetted or dry surface, align the SunEye compass so the heading is centered on true South and ensure that the level indicator is centered. Push the round green button on the keypad or tap “Snap” to capture the skyline. Hold the SunEye steady until the skyline is successfully captured.
- viii. After the skyline is captured, a new skyline view automatically appears on the screen. Tap “Cancel” to close this new skyline. After tapping “Cancel”, an image of the skyline will appear. Review the image to ensure that it is not blurry and that your head is not blocking the sun path. If the image looks good, “Tap here to add a note” at the top of the screen. Record the transect number (T1, T3, ..., T21) and (mid channel “mc”). If the skyline image is of low quality, it can be deleted by tapping the yellow circle in the lower left corner of the screen, then tapping “Skyline”, then “Browse”. Scroll down to the skyline you want to delete, highlight the skyline, then tap “Delete”.

- ix. Proceed to the next transect, and push the blue button with the star symbol to start a new skyline, or tap the yellow circle in the lower left corner of the screen and then tap “Skyline”, then “New”.
- x. After skyline images have been captured for all 11 transects, simply press the power button to shut down the device. All data is automatically saved until it is transferred off of the device.

9.4 Riparian Structure

References: Modified protocol from Kaufmann et al. (1999) and Peck et al. (2001)

Riparian assessments are collected on both stream banks at transects 1, 6, 11, 16, and 21 using a combination of visual estimation of riparian structure and quantitative estimation of total areal cover from hemispherical images captured using the Solmetric SunEye. This rapid assessment protocol is designed to provide a quantitative index of the effective areal cover, size and type of riparian vegetation at each site.

To ensure accuracy in estimation of canopy cover from hemispherical images of riparian vegetation, it is critical to capture good quality images. Adequate atmospheric conditions are necessary to achieve usable images. These conditions include low sun angle (dawn or dusk is ideal) or uniform overcast sky and absence of sun “flares” or “spots”. It is also important to hold the SunEye as level and steady as possible to ensure that images are clear and representative of the vegetation directly overhead. The SunEye automatically adjusts for its tilt and heading orientation for every image, but the best results are achieved if the SunEye is steady within $\pm 5^\circ$ of level and within 30° of South.

- i. **Lay out plots:** Visually estimate a 10 by 10 m square plot on both the right and left banks centered on each transect. The plot boundaries should extend 5 m upstream and downstream from the transect and a distance of 10 m back into the riparian vegetation from the bankfull stage. Within this 10 m by 10 m square, visually divide the riparian vegetation into three vertical layers: canopy layer (>5 m), understory layer (0.5 to 5 m), and a ground cover layer (<0.5 m).
- ii. **Canopy Layer (>5 m):**
 - a. *By vegetation type:* Estimate the percentage areal cover in the canopy layer alone that is contributed by each of the following vegetation types: 1) woody broadleaf evergreen, 2) woody coniferous, or 3) woody deciduous. Record percentages as 0, 1, 5, or multiples of 5 from 10 – 100%. Areal cover is defined as the amount of shadow cast by a particular layer alone when the sun is directly overhead. The sum of these percentages represents the total areal vegetation cover in the canopy layer, and generally will not sum to 100%.
 - b. *By size:* Estimate the percentage areal cover in the canopy layer alone that is contributed by each of the following size categories: 1) large trees (>0.3 m diameter at breast height (DBH)), and 2) small trees (<0.3 m DBH).
- iii. **Understory Layer (0.5 to 5 m):**
 - a. *By vegetation type:* Estimate the percentage areal cover in the understory layer alone that is contributed by each of the following vegetation types: 1) woody broadleaf evergreen, 2) woody coniferous, 3) woody deciduous, or 4) non-woody forbs and grasses.

- b. *By size*: Estimate the percentage areal cover in the understory layer alone that is contributed by each of the following size categories: 1) large trees (>0.3 m diameter at breast height (DBH)), 2) small trees (<0.3 m DBH), woody shrubs and saplings.
- iv. **Ground Cover Layer (<0.5 m)**: Estimate the percentage of the ground covered by the following categories: 1) trees, woody shrubs and tree seedlings, 2) non-woody forbs and grasses, 3) bare dirt, 4) duff or woody debris, or 5) rock. Cover percentages should sum to 100%.
- v. **Quantitative Total Areal Cover**: Hold the SunEye in the center of the plot, or within 1 m of the plot center, at an elevation of 0.5 m. Ensure that the SunEye is at least 1 m from large obstructions (tree, stump, rock outcroppings, etc.). To the extent possible, ensure that no obstructions (branches, leaves, fronds, etc.) are within 0.5 m of the 180 degree hemisphere above the SunEye device. Also, it will be necessary to extend the SunEye away from your body, and crouch below the horizontal plane of the SunEye lens to ensure that the surveyor's head is not captured in the image. Use the same methods as described in the Solar Input section to capture an image of the canopy overhead. Record the transect number (T1, T3, ..., T21) and location (left bank "lb", right bank "rb", or mid channel "mc") in the notes for each SunEye image. Recording the transect number and location is critical for linking the SunEye data with the other riparian vegetation data and for separating the images used for estimating solar input from those used for characterizing riparian structure.

Appendix C.

Protocol for Snorkel Surveys of Fish Densities



COLUMBIA RIVER INTER-TRIBAL FISH COMMISSION

729 NE Oregon, Suite 200, Portland, Oregon 97232

Telephone 503 238 0667

Fax 503 235 4228

Protocol for Snorkel Surveys of Fish Densities

A component of

Monitoring Recovery Trends in Key Spring Chinook Habitat Variables
and Validation of Population Viability Indicators

May 2011

Seth White

Casey Justice

Dale McCullough



TABLE OF CONTENTS

TABLE OF CONTENTS.....	2
Table of Figures	3
Introduction.....	4
Methods for Snorkel Surveys.....	4
Required Conditions for Snorkeling	4
Detailed Procedures.....	5
References.....	8
Appendix A: Some Common Fishes of the upper Grande Ronde River	9
Appendix B: Equipment List	13
Appendix C: Datasheet	14

Table of Figures

Figure 1. In small streams, one snorkeler counts fish in a single pass, zigzagging through an entire channel unit while moving upstream. The dashed line represents the approximate path of the snorkeler who counts fish left and right (from Thurow 1994).	7
Figure 2. In wider streams, two snorkelers count fish in a channel unit while moving upstream. In a stream smaller than the combined lane width of both snorkelers, observers count fish on their respective side of the stream. In stream wider than the combined lane width of both snorkelers, each observer records all the fish in their respective lanes and records lane width (from Thurow 1994).	7
Figure 3. Juvenile steelhead/rainbow trout. Note the oval parr marks, prevalent spotting, and white tips on the pelvic and anal fins (from Thurow 1994).	9
Figure 4. Juvenile Chinook salmon. Note the broad, vertical parr marks, large eye, unspotted dorsal fin, forked tail, and dorsal spotting. The adipose fin has been clipped from this hatchery-reared fish (From Thurow 1994).	9
Figure 5. Adult bull trout. Note the large mouth, pale yellow spots, white fin margins, and unpigmented dorsal fin (from Thurow 1994).	10
Figure 6. Adult mountain whitefish. Note slender body, small terminal mouth, silver color, large scales reflecting light, and forked tail (from Thurow 1994).	10
Figure 7. Adult northern pikeminnow. Note the large mouth, forked tail, lack of spots, and absence of an adipose fin (from Thurow 1994).	10
Figure 8. Juvenile redbreasted shiner. Note the lack of parr marks, lack of spots and parr marks, absence of adipose fin, and a distinct, laterally-compressed shape (from Thurow 1994).	11
Figure 9. Sucker sp. Note the large head, small eye, oval cross section, and ventral mouth (from Thurow 1994).	11
Figure 10. Longnose dace. Note the elongated body shape and nose (courtesy of Ohio Department of Natural Resources).	11
Figure 11. Speckled dace. Note the elongated, fusiform body shape and shorter nose as compared with longnose dace (photo by Dave Giordano, University of California).	12

Introduction

This report describes a protocol for monitoring fish densities and fish assemblage structure using snorkel surveys. The Columbia River Inter-Tribal Fish Commission (CRITFC), Oregon Department of Fish & Wildlife (ODFW), and Confederated Tribes of the Umatilla Indian Reservation (CTUIR) have recognized the need to use a common snorkel survey so that information collected by individual entities can help managers determine whether aggregate habitat restoration actions will yield a net improvement in basin-wide habitat quality for ESA-listed fish species (NOAA 2007). To this end, we developed a snorkeling protocol drawing heavily from the protocols of Thurow (1994) and O’Neal (2007), intended for use among all agencies responsible for data collection in the upper Grande Ronde, Catherine Creek, Minam River, and potentially other nearby basins.

Methods for Snorkel Surveys

During baseflow conditions after fish habitat surveys have been completed, fish abundance and size, along with a semi-quantitative description of fish assemblage structure, will be enumerated at each reach. It is important to note that although this snorkel survey occurs over the length of an entire reach, the data is collected at the channel unit scale. *If snorkeling occurs in reaches where habitat surveys were conducted, the field crew should ensure that all channel units can be referenced to the corresponding channel units in the habitat survey.*

A single snorkeler or a team of two snorkelers (depending on channel unit size and visibility, see below) will identify and count fish species and size classes in all slow water habitats (e.g., pools and runs) and 25% of all fast water, turbulent habitats (e.g., riffles, rapids, and cascades) . Fish counts will be standardized by area sampled and reported by habitat unit type and total reach densities.

Before surveys commence each field season, snorkelers will spend a morning and/or afternoon training in habitat types where different species are likely to occur, and will calibrate estimates of fish length by using plastic cut outs of fish in 50 mm size classes. Periodic calibrations of fish size will ensure precise estimates. Field identification of fish species should be practiced and validated by occasional capture of fish using a hand net or electrofisher and checked against the keys of Bond (1973), Dauble (2009), Martinson *et al.* [no date], or other relevant sources. Additional, plates of a few of the commonly-encountered fish species are listed in Appendix A.

Required Conditions for Snorkeling

- ✓ During low stream flows and when flow conditions are similar to those recorded during the habitat survey.
- ✓ When visibility is equal to or greater than 1.5 m (as measured by minimum distance that a plastic fish cut-out with parr marks can be discerned).
- ✓ Between late morning and early afternoon (i.e., 1000-1600 hrs) when the sun is directly overhead, or during cloudy or overcast conditions if reaches have significant cover.
- ✓ When both stream banks can be observed by a single observer, one snorkeler will be sufficient. When the stream is larger, two snorkelers are required.

Detailed Procedures

- 1) Locate the downstream-most channel unit to be surveyed in the reach and record the site ID indicated on the flag or marker. If the flag or marker cannot be found record the UTM with accuracy ≤ 10 m using a GPS. Complete the top portion of the snorkel survey data sheet; including stream name, date, weather conditions, water temperature using a hand-held thermometer, underwater visibility ranking, note taker and snorkeler names, and start time.
- 2) Determine snorkeler lane widths and decide upon the number of snorkelers that will conduct the survey. Lane widths are defined as the width of stream that an observer can effectively survey, and are determined by doubling the distance which a snorkeler can clearly identify a 100 mm plastic cut-out of a fish with parr marks. Estimates of lane widths may differ among individual channel units in a reach—these estimates should be adjusted when physical obstructions such as shallow water, boulders, or turbulence impede visibility. Where the wetted stream width is greater than the combined lane widths of snorkelers, each observer counts fish only in their lane and fish density estimates are scaled to the area observed.
- 3) Snorkeler(s) enter the stream a short distance below the downstream end of the channel unit to be surveyed, slowly and quietly assuming the face-down snorkeling position. After scanning the channel unit for fish from a stationary position, begin surveying in an upstream direction. A single snorkeler moves in a zig-zag pattern upstream (Figure 1). Or if two people are required, snorkelers move slowly upstream adjacent to one another and at the same speed in the midline of the stream, each snorkeler enumerating only the fish observed between himself and the adjacent stream bank as the snorkelers pass fish. Depending on the type of habitat, the two snorkelers may instead agree upon a centerline in the stream and count fish only on their respective half of the stream (Figure 2). Enumerate steelhead/rainbow trout and juvenile Chinook salmon by species and size classes noted on the data sheet *only after the snorkeler passes upstream of fish* (to reduce double counting). Note presence/absence but do not identify or enumerate young-of-the-year salmonids except Chinook salmon, which can be accurately counted and identified (Thurow 1994). Also record the number of adult Chinook salmon observed. All microhabitats are surveyed (e.g., behind log jams, in pocket waters behind boulders, stream margins). Even during daylight hours, handheld lights are useful for searching for fish in complex habitats such as substrate crevices, undercut banks, and logjams.
- 4) In certain low-visibility conditions such as large, deep pools or turbulent channel units, some fish may remain undetected in the upstream pass. In those cases, an additional downstream pass by a single snorkeler may be required. At the top of the channel unit, a snorkeler will turn around and drift facing downstream, *noting only additional fish species or size classes not previously counted*.
- 5) At the end of each channel unit survey, each snorkeler calls out fish counts by species and size class to a note taker, who remains downstream of snorkelers so as not to disturb fish before they are surveyed. Snorkelers may also “download” fish data to the note taker at any point during the channel unit survey if fish are numerous or fish assemblages are

complex with several size classes. If a note taker is not available, the snorkeler may record data onto plastic tablets attached to the snorkeler's arm.

- 6) Record the relative abundance of all fish species present in the channel unit, including salmonids and non-salmonids, as per Torgersen *et al.* (2006): each species is recorded as dominant (> 50%), common (10-50%), or rare (< 10%) in relation to the total number of fish observed in a channel unit. See Appendix A for identification of a few commonly-encountered fish species.
- 7) The note taker records the length and average width of each channel unit surveyed. Width measurements are made at 25%, 50%, and 75% of the channel length, and the average of these three measurements is recorded on the datasheet. If a fastwater channel unit is surveyed, the length of the actual distance surveyed replaces the channel unit length. After the first channel unit is surveyed, continue to reference individual site IDs from flags, habitat datasheet, or acquire UTM's for each channel unit. *Ensure that each channel unit can be referenced to the corresponding habitat survey data.* The previously-drawn reach map can also be used for reference.
- 8) At the end of the survey, record the time and any additional comments.



Figure 1. In small streams, one snorkeler counts fish in a single pass, zigzagging through an entire channel unit while moving upstream. The dashed line represents the approximate path of the snorkeler who counts fish left and right (from Thurow 1994).

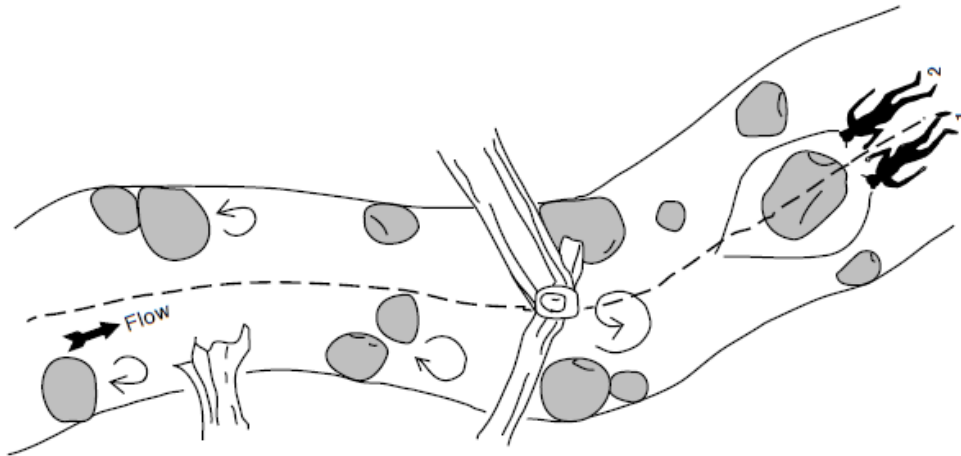


Figure 2. In wider streams, two snorkelers count fish in a channel unit while moving upstream. In a stream smaller than the combined lane width of both snorkelers, observers count fish on their respective side of the stream. In stream wider than the combined lane width of both snorkelers, each observer records all the fish in their respective lanes and records lane width (from Thurow 1994).

References

- Bond, C.E. 1973. *Keys to Oregon freshwater fishes*. Corvallis, OR: Agricultural Experiment Station, Oregon State University.
- Dauble, D.D. 2009. *Fishes of the Columbia Basin: A Guide to Their Natural History and Identification*. Sandpoint, ID: Kokee Books.
- Martinson, R., G. Kovalchuk, D. Ballinger, and L. Cowger. *Columbia River basin juvenile fish field guide, including common injuries, diseases, tags, and invertebrates - 4th edition*. Bonneville Power Administration & Pacific States Marine Fisheries Commission, [no date].
- NOAA. 2007. Tributary Habitat Proposed Action Summary. May 21, 2007. NOAA, Portland, Oregon. 295 p.
- O'Neal, J. 2007. Snorkel surveys. In *Salmonid Field Protocols Handbook*, ed. D.H. Johnson, B.M. Shrier, J. O'Neal, J.A. Knutzen, X. Augerot, T.A. O'Neil, and T.N. Pearsons, 325-339. Bethesda, Maryland: American Fisheries Society.
- Thurow, R.F. 1994. *Underwater Methods for Study of Salmonids in the Intermountain West*. General Technical Report. Ogden, UT: US Department of Agriculture, Forest Service, Intermountain Research Station.
- Torgersen, C.E., C.V. Baxter, H.W. Li, and B.A. McIntosh. 2006. Landscape influences on longitudinal patterns of river fishes: spatially continuous analysis of fish-habitat relationships. *American Fisheries Society Symposium* 48: 473-492.

Appendix A: Some Common Fishes of the upper Grande Ronde River



Figure 3. Juvenile steelhead/rainbow trout. Note the oval parr marks, prevalent spotting, and white tips on the pelvic and anal fins (from Thurow 1994).



Figure 4. Juvenile Chinook salmon. Note the broad, vertical parr marks, large eye, unspotted dorsal fin, forked tail, and dorsal spotting. The adipose fin has been clipped from this hatchery-reared fish (From Thurow 1994).



Figure 5. Adult bull trout. Note the large mouth, pale yellow spots, white fin margins, and unpigmented dorsal fin (from Thurow 1994).



Figure 6. Adult mountain whitefish. Note slender body, small terminal mouth, silver color, large scales reflecting light, and forked tail (from Thurow 1994).



Figure 7. Adult northern pikeminnow. Note the large mouth, forked tail, lack of spots, and absence of an adipose fin (from Thurow 1994).



Figure 8. Juvenile redbreasted sunfish. Note the lack of parr marks, lack of spots and parr marks, absence of adipose fin, and a distinct, laterally-compressed shape (from Thurow 1994).



Figure 9. Sucker sp. Note the large head, small eye, oval cross section, and ventral mouth (from Thurow 1994).



Figure 10. Longnose dace. Note the elongated body shape and nose (courtesy of Ohio Department of Natural Resources).



Figure 11. Speckled dace. Note the elongated, fusiform body shape and shorter nose as compared with longnose dace (photo by Dave Giordano, University of California).

Appendix B: Equipment List

Equipment	Quantity	Check	Notes
Snorkel Surveys			
Fish identification guides (Bond 1973; Dauble 2009; Martinson <i>et al.</i> [no date])	1	<input type="checkbox"/>	
Plastic fish cutouts (with parr marks) of various multiples of 50 mm in length	7	<input type="checkbox"/>	
Drysuit	2	<input type="checkbox"/>	
Wet suit hood	2	<input type="checkbox"/>	
Neoprene gloves	2	<input type="checkbox"/>	
Neoprene socks	2	<input type="checkbox"/>	
Mask w/ extra strap	2	<input type="checkbox"/>	
Snorkel	2	<input type="checkbox"/>	
Handheld dive light	2	<input type="checkbox"/>	
Handheld thermometer	1	<input type="checkbox"/>	
Meter tape or graduated wading staff (for measuring visibility distance)	1	<input type="checkbox"/>	
GPS, datasheets, clipboard, pencils, wading boots (see "General Field Equipment")		<input type="checkbox"/>	
Completed habitat data sheets		<input type="checkbox"/>	
Rangefinder (for measuring channel unit length & width)	1	<input type="checkbox"/>	
Blank snorkel survey datasheets and pencils		<input type="checkbox"/>	
Personal Field Equipment		<input type="checkbox"/>	
Wading boots	1	<input type="checkbox"/>	
Wading socks	1	<input type="checkbox"/>	
Waders	1	<input type="checkbox"/>	
Rain gear	1	<input type="checkbox"/>	
Hat	1	<input type="checkbox"/>	
Sunscreen	1	<input type="checkbox"/>	
Sun glasses (polarized preferable)	1	<input type="checkbox"/>	
Bug repellent	1	<input type="checkbox"/>	
Pocket knife or multi-tool	1	<input type="checkbox"/>	
Water bottle (1 qt)	1	<input type="checkbox"/>	
Backpack	1	<input type="checkbox"/>	
Cell phone	1	<input type="checkbox"/>	
Cell phone charger	1	<input type="checkbox"/>	
Toilet paper	2	<input type="checkbox"/>	
Food for lunch and lunch bag		<input type="checkbox"/>	
First aid kit	1	<input type="checkbox"/>	

Appendix C: Datasheet

Stream:_____Start time:_____End time:_____Notetaker:_____

Reach ID:_____Water temp (°C):_____Snorkeler(s):_____

Date:_____Visibility* (0-3):_____Weather/other comments:_____

Channel Unit Surveyed				Lane widths		ST length (mm)				chin length (mm)				Unident. salmonid YOY?	Juvenile-Adult Fish Species Present*** (inc. salmonids)		
Type**	ID	Length (m)	Width (m)	Lane 1 (m)	Lane 2 (m)	70-130	130-200	200-250	250+	50-80	100+	Other	Adult		Dominant (> 50%)	Common (10-50%)	Rare (< 10%)
														Y / N			
														Y / N			
														Y / N			
														Y / N			
														Y / N			
														Y / N			
														Y / N			
														Y / N			
														Y / N			
														Y / N			
														Y / N			
														Y / N			
														Y / N			
														Y / N			
														Y / N			
														Y / N			
														Y / N			
														Y / N			

Notes:

* Visibility: 0 = not snorkelable due to high turbidity or cover, 1 = high amount of cover and/or poor water clarity, 2 = moderate cover and/or moderate water clarity, 3 = little hiding cover and good water clarity. ** Channel unit types are fastwater non-turbulent (FNT), riffle (RI), cascade (CA), rapid (RA), falls and steps (FA), scour pool (SP), plunge pool (PP), dam pool (DP), and beaver pool (BP). *** Fish codes are steelhead/rainbow trout (ST), Chinook salmon (chin), redbelt shiner (RS), northern pikeminnow (NP), mountain whitefish (MW), bridgelip sucker (BS), mountain sucker (MS), largescale sucker (LS), longnose dace (LD), speckled dace (SD), carp (CR), lamprey (LY), chiselmouth (CM), Cottidae (scuplins) (CT), Ichthiluridae (catfishes) (IC), and Centrarchids (sunfishes) (CN).

Appendix D.

Summary of fine sediment conditions in Catherine Creek and Upper Grande Ronde River during summer 2011



COLUMBIA RIVER INTER-TRIBAL FISH COMMISSION

729 NE Oregon, Suite 200, Portland, Oregon 97232

Telephone 503 238 0667

Fax 503 235 4228

Summary of fine sediment conditions in Catherine Creek and Upper Grande Ronde River during summer 2011

A component of

Monitoring Recovery Trends in Key Spring Chinook Habitat Variables and Validation of
Population Viability Indicators

March 2012

Casey Justice

Dale McCullough

Seth White



Summary

We measured fine sediment levels in the streambed at 23 sites in Catherine Creek and the Upper Grande Ronde River basins during the summer of 2011 as a component of a broad-scale habitat monitoring project designed to evaluate status and trends in habitat conditions for spring Chinook salmon. The proportion of subsurface fine sediment < 6.35 mm ranged from 0.07 to 0.44 (mean = 0.30) across all sites. According to literature-derived formulas that describe the relationship between fine sediment and Chinook egg-to-fry survival (Tappel and Bjornn 1983), estimated survival across all sites ranged from 30 to 96% (mean = 78%). No significant relationships were observed between subsurface fines and landscape characteristics such as gradient, forest cover, road density, or geomorphic reach type. Visual estimates of surface fines in pools were positively correlated with depth fines, suggesting that visual estimation methods may serve as a useful surrogate for more intensive subsurface sediment sampling methods. Overall, these data provide a useful preliminary assessment of fine sediment conditions in the Grande Ronde and Catherine Creek basins and their potential implications for Chinook egg-to-fry survival.

Introduction

High levels of fine sediment in salmon bearing streams can have serious detrimental effects on fish survival through reductions in inter-gravel dissolved oxygen during egg incubation or entombment of emergent fry (Tappel and Bjornn 1983; Everest *et al.* 1986; Chapman 1988; Reiser 1999), or through infilling of interstitial spaces between streambed particles which provide refuge from predation and high flows. We measured the quantity of fine sediment in the streambed at 23 sites in Catherine Creek and the Upper Grande Ronde River basins in order to characterize the suitability of streambed gravels for spawning fish and associated embryo survival and to examine relationships between habitat conditions and landscape characteristics. This information will be used to parameterize a life cycle model for Spring Chinook salmon which simulates long term fish response to changes in habitat conditions.

We also compared measurements of subsurface fine sediment with several different estimates of surface fines to determine the extent to which rapid surface sediment sampling methods may be used as a surrogate for more intensive subsurface sediment sampling. Although subsurface sediment sampling is more laborious and expensive compared with relatively rapid surface sediment methods such as pebble counts or ocular estimation, subsurface sediment data likely provides a more accurate and directly applicable estimate of the fine sediment levels potentially impacting egg survival. However, most large-scale habitat monitoring programs such as the Columbia Habitat Monitoring Program (CHaMP) (Bouwes *et al.* 2011), PACFISH/INFISH Biological Opinion effectiveness monitoring program (PIBO) (Heitke *et al.* 2010), and Environmental Monitoring and Assessment Program (EMAP) (Kaufmann *et al.* 1999) only measure fine sediment on the surface of the streambed and do not attempt to quantify the substrate size composition at depth. If these data are ultimately intended to make inferences about the influence of habitat conditions on fish productivity, it is important to know the extent to which surface sediment metrics are correlated with subsurface metrics.

The objectives of this study were to 1) examine the relationship between subsurface fine sediment and landscape characteristics (e.g., gradient, forest cover, road density, etc.), 2) estimate egg-to-fry survival rates for Chinook salmon using literature-derived relationships between fine sediment and embryo survival, and 3) evaluate the extent to which surface and subsurface measures of fine sediment were correlated.

Methods

We measured fine sediment levels in the streambed surface and subsurface at 23 randomly distributed sites during summer of 2011 including 8 sites in the Catherine Creek basin and 15 sites in the Upper Grande Ronde River basin (Table 2; Figure 1). Sample sites were randomly selected using the Generalized Random Tessellation Stratified (GRTS) survey design in coordination with the Columbia Habitat Monitoring Program (CHaMP). At each site, we quantified the proportion of sediment particles in the streambed surface and subsurface that was smaller than 2 mm and 6.3 mm in accordance with commonly cited studies examining the effects of fine sediment on egg-to-fry survival of salmonid fishes (Tappel and Bjornn 1983, Chapman and McLeod 1987).

Subsurface sediment

We used a modified McNeil sampler to collect between 5 and 9 replicate core samples within qualifying pool tail and spawning patch habitats at each site. Sample locations were limited to areas of the wetted channel that were classified as suitable spawning habitat based on literature-derived criteria for depth, velocity, area, and dominant substrate size (Justice et al. 2011). We selected a target sample size of 9 per site based on a power analysis of sediment data collected during a pilot study in 2009. However, the number of samples collected at each site fell below our target sample size of 9 in a small number of cases because of limited availability of suitable spawning habitat or errors in labeling and processing of samples. Core dimensions on the sampler were 20 cm diameter by 20 cm height, producing bulk samples ranging in mass from 8 to 13 kg (mean = 11 kg).

Bulk samples were transported to the lab where they were dried in an oven at approximately 120°C. After returning samples to room temperature, particles were sorted into discrete size classes using an automatic sieve shaker for a period of 12 minutes. Sieve sizes included 0.125, 0.355, 0.85, 2, 3.35, 4, 6.3, 8, 11.2, 16, 31.5, and 63 mm. The mass of particles in each size class was weighed to the nearest 0.1 grams. Prior to calculating the fraction of fine sediment in each sample, we truncated the data by removing all sediment particles > 63mm from the sample to ensure that estimates of percent fines were not disproportionately affected by the presence of a few anomalously large cobbles as recommended by Church et al. (1987).

We examined the potential implications of observed levels of subsurface fine sediment on Chinook egg-to-fry survival using predictive formulas developed from laboratory studies. Perhaps the most thorough evaluation of the effects of fine sediment on salmonid survival to emergence was done by Tappel and Bjornn (1983), who evaluated the survival impacts of different combinations of fine sediment including particles ranging from 0.85 to 9.5 mm. We used a relationship developed by Irving and Bjornn (1984) based on data from Tappel and Bjornn (1983) to estimate survival to emergence s_e as a function of the proportion of sediment particles finer than 6.35 mm p_f :

$$s_e = 1 - 0.0001 p_f^2 + 0.0009 p_f$$

We evaluated the relationship between the proportion of fine sediment < 2 and < 6.35 mm and landscape characteristics including gradient, road density, forest cover and two different channel morphology classifications to determine if the variation in fine sediment was explained by differences in land use or natural geomorphic channel characteristics. The two classification systems include a modification of the Montgomery and Buffington (1997) channel reach classification system for mountain streams applied to the entire Columbia River basin (Beechie and Imaki 2008) and a simplified version of the same classification system developed by White et al. (in prep).

The Beechie classification system used landscape characteristics such as bankfull width, gradient, and valley width index to divide the stream network into 9 different reach types with relatively homogeneous morphologies and channel processes. The White classification system essentially pooled all classification types from the Beechie classification into two channel types: floodplain and constrained reaches (i.e., bankfull width ≥ 8 m) and mountain reaches (bankfull width < 8 m). Each of our 23 study sites were superimposed over the classified reaches from Beechie et al. (2010) in GIS and the channel class and gradient for the nearest reach was assigned to each study site. Land use variables (i.e., road density and forest cover) were derived from the work of Whittier et al. (2010) (unpublished report). Road density was calculated as the total length of roads divided by the total area in each HUC6 watershed. Forest cover was estimated as the proportion of the total area in each HUC6 watershed that is covered by forest. The land use information for each HUC6 watershed was assigned to all study sites falling within that HUC6 unit.

We built a candidate set of 15 *a priori* logistic regression models using the proportion of fine sediment < 6.35 mm as the dependent variable and different combinations of the 5 landscape characteristics as independent variables (Table 1). We limited the analysis to fines < 6.35 mm because this response variable was highly correlated with fines < 2 mm, and therefore relationships between fines and landscape characteristics would likely be very similar. Rather than examining every possible combination of variables, we limited the analysis to a small set of models representing our hypotheses about the relationship between fine sediment and landscape characteristics as informed by the scientific literature and professional experience. We used Akaike's Information Criterion (AIC) to select the best fitting model from the candidate set (Burnham and Anderson 2002). Models with the lowest AIC_c values were selected as the best fitting models. Models with ΔAIC_c values less than or equal to 2.0 were considered strong competing models.

Prior to running any of the models, we used logistic regression to test whether there was a significant difference in mean fine sediment levels between the Upper Grande Ronde River and

Catherine Creek basins. After confirming that there was no statistical difference between the two basins ($P > 0.05$), we pooled the samples from both basins to increase statistical power.

Logistic regression was used for analysis because the dependent variable (i.e., proportion fine sediment) was binomially distributed and therefore constrained between 0 and 1. All continuous independent variables were normalized prior to analysis to ensure that they were all in the same scale of measurement and that any one variable was not attributed undue weight in the analysis.

Table 1. Candidate set of logistic regression models used to analyze the relationship between the proportion of fine sediment < 2 and < 6.35 mm and landscape characteristics.

Model Number	Independent variables
1	<i>1 (null model)</i>
2	<i>classw¹</i>
3	<i>classb²</i>
4	<i>gradient</i>
5	<i>classw + forest</i>
6	<i>classw + roads</i>
7	<i>gradient + roads</i>
8	<i>gradient + forest</i>
9	<i>classw + roads + forest</i>
10	<i>gradient + forest + roads</i>
11	<i>classw + forest + classw*forest</i>
12	<i>classw + roads + classw*roads</i>
13	<i>gradient + forest + gradient*forest</i>
14	<i>gradient + roads + gradient*roads</i>
15	<i>gradient + roads + forest + gradient*roads + gradient*forest</i>

¹ White classification ² Beechie classification

Surface sediment

We estimated the proportion of fine sediment (< 2 and < 6 mm) on the streambed surface at each site using 4 different methods including McNeil core samples in pool tails and spawning patches, pebble counts in riffles, grid counts of fine sediment at pool tails, and ocular estimates of substrate size by channel unit. In addition, we visually estimated the proportion of cobbles in riffles that were embedded by fine sediment. A detailed description of these methods is described in Bouwes et al. (2011).

We computed standard Pearson correlation coefficients to evaluate pairwise relationships among a set of 9 different fine sediment metrics including: 1) McNeil fines < 2 mm (*mnfines2*), 2) McNeil fines < 6.35 mm (*mnfines6*), 3) pool tail fines < 2 mm (*ptfines2*), 4) pool tail fines < 6 mm (*ptfines6*), 5) pebble count fines < 2 mm in riffles (*pcfines2*), 6) pebble count fines < 6 mm in riffles (*pcfines6*), 7) ocular fines < 2 mm in all habitat types (*ocfinesall*), 8) ocular fines < 2 mm in scour pools (*ocfinessp*), and 9) cobble embeddedness in riffles (*embed*). Relationships with correlation coefficients > 0.50 were subsequently analyzed using linear regression to compute R² and P-Values.

Table 2. Description of sediment sampling sites in the upper Grande Ronde River and Catherine Creek during summer, 2011.

Site ID	Basin	Stream	Replicates	UTM E	UTM N	Crew
CBW05583-090282	Catherine Creek	Catherine Creek	9	443053	4999153	ODFW
CBW05583-430250	Catherine Creek	Catherine Creek	9	430541	5006856	CRITFC
CBW05583-446634	Catherine Creek	Catherine Creek	8	433286	5006178	ODFW
CBW05583-456106	Catherine Creek	Catherine Creek	9	445093	4996877	CRITFC
CBW05583-527786	Catherine Creek	Catherine Creek	9	445880	4996414	ODFW
DSGN4-000010	Catherine Creek	Catherine Creek	9	443969	4998225	CRITFC
DSGN4-000001	Catherine Creek	North Fork Catherine Creek	5	449305	4996660	ODFW
CBW05583-316330	Catherine Creek	South Fork Catherine Creek	9	453284	4994577	ODFW
DSGN4-000094	Grande Ronde River	Fly Creek	9	385811	4997843	ODFW
CBW05583-148970	Grande Ronde River	Grande Ronde River	7	396628	4991086	CRITFC
CBW05583-235322	Grande Ronde River	Grande Ronde River	9	391609	5001324	CRITFC
CBW05583-269114	Grande Ronde River	Grande Ronde River	8	391118	5012095	CRITFC
CBW05583-280042	Grande Ronde River	Grande Ronde River	9	397642	4990189	CRITFC
CBW05583-457530	Grande Ronde River	Grande Ronde River	9	390371	5009661	CRITFC
DSGN4-000009	Grande Ronde River	Grande Ronde River	9	397787	4989995	CRITFC
DSGN4-000202	Grande Ronde River	Grande Ronde River	9	390902	5010926	CRITFC
DSGN4-000205	Grande Ronde River	Grande Ronde River	6	400009	5018736	ODFW
CBW05583-108010	Grande Ronde River	Limber Jim Creek	9	395317	4995296	CRITFC
DSGN4-000093	Grande Ronde River	Meadow Creek	9	374732	5015568	ODFW
DSGN4-000213	Grande Ronde River	Meadow Creek	9	390546	5013237	ODFW
CBW05583-138554	Grande Ronde River	Sheep Creek	7	385425	4990678	CRITFC
CBW05583-490810	Grande Ronde River	Sheep Creek	9	384880	4989154	CRITFC
DSGN4-000006	Grande Ronde River	West Chicken Creek	9	389626	4990427	ODFW

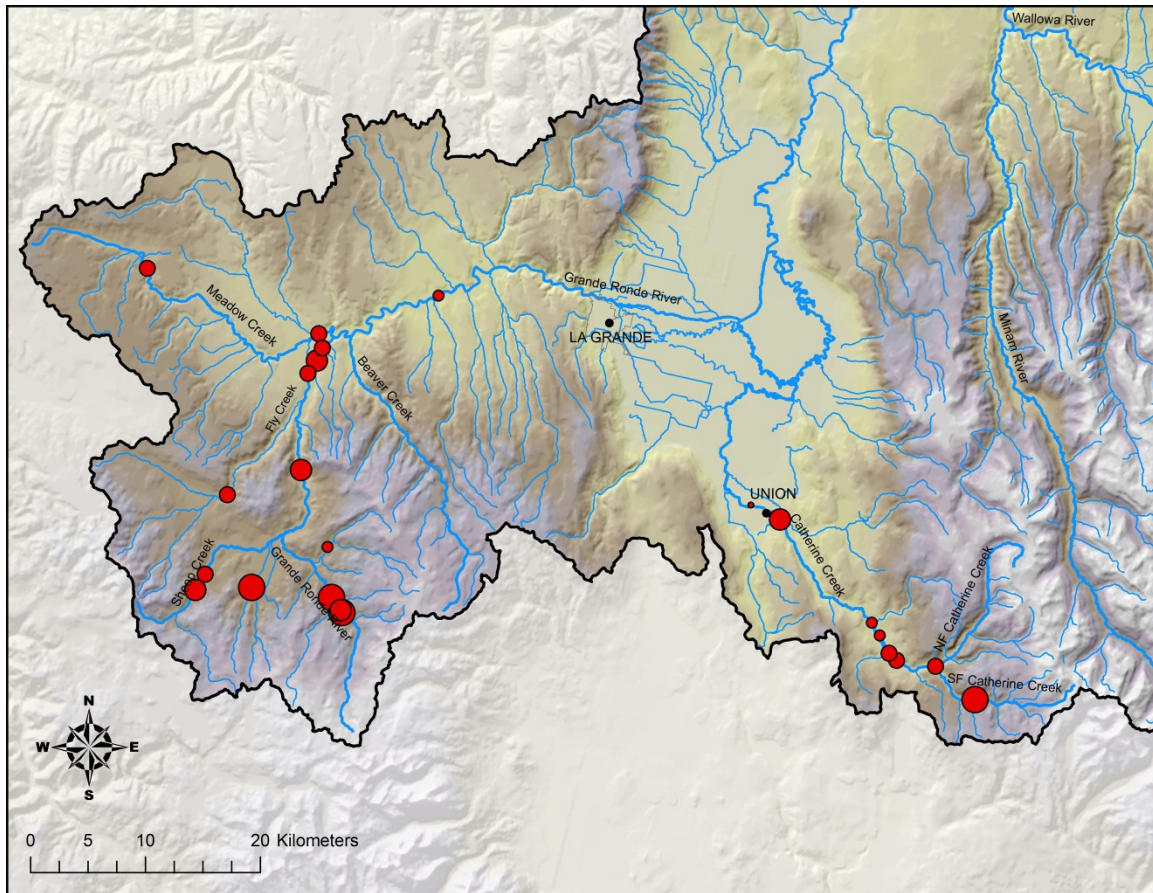


Figure 1. Subsurface sediment sampling sites in the Upper Grande Ronde River and Catherine Creek basins during summer, 2011. The size of each red circle is proportional to the amount of fines < 6.35 mm measured at each site.

Results and Discussion

The average proportion of subsurface fine sediment < 2 mm across all sites ranged from 0.06 to 0.23 (mean = 0.14) (Table 3, Figure 2). The proportion of fine sediment < 6.35 mm ranged from 0.07 to 0.44 (mean = 0.30). Fine sediment levels were not statistically different between the Upper Grande Ronde River and Catherine Creek basins ($P > 0.05$).

Within-site variation in fine sediment was generally low to moderate with the exception of two sites with very high within-site variation. The coefficient of variation (CV) within sites ranged from 12 to 118% (mean = 40%) for fine sediment < 2 mm and from 9 to 148% (mean = 35%) for fine sediment < 6.35 mm. Variability in average fine sediment levels across sites was moderate with a CV of 33% for fines < 2 mm and 28% for fines < 6.35 mm.

Egg-to-fry survival estimates ranged from 30 to 96% (mean = 78%). This mean survival rate is considerably higher than the average egg-to-fry survival rate of 38% reported by Quinn (2005), which represents a compilation of data from 215 published and unpublished estimates of survival for naturally-rearing Chinook populations. Although these survival rates may be useful as a preliminary assessment of the relative importance of fine sediment conditions on overall Chinook salmon productivity in the Grande Ronde and Catherine Creek basins, they should be interpreted with caution. Because these estimates were based on a laboratory-derived relationship between fine sediment and survival, it is not clear how well this relationship reflects expected survival rates under natural stream conditions where environmental factors such as discharge, temperature, and fine sediment infiltration rates are considerably more variable. A study that explicitly measures egg-to-fry survival would be required to verify the relationship between fines sediment and embryo survival.

The best fitting model from the candidate set of models used to evaluate the relationship between fine sediment and landscape characteristics was the null model (Model 1), indicating that none of the landscape variables we examined explained a significant proportion of the variation in fine sediment < 6.35 mm (Table 4). Models 2 and 4 were considered strong competing models on the basis of their low $\Delta AICc$ values. However, proportion of variation explained by these two models was very low ($R^2 < 0.13$) and the effect of both gradient and the white classification were not statistically significant ($P > 0.05$).

The fact that none of the landscape characteristics explained a significant amount of variation in fine sediment levels may be due in part to the way that the independent variables were calculated. For example, forest cover and road density were measure for each HUC6 watershed, and any sediment sampling site that fell within that HUC6 was assigned the corresponding value for forest cover or road density without regard for the proportion of the watershed area upstream of that point. In addition, age of roads or proximity to the stream were not considered in this analysis, but these factors likely play a role in the relationship between land use and fine sediment in streams. We intend to complete a more thorough analysis of landscape

characteristics in the future which takes into account issues such as upstream drainage area, age and type of roads, and proximity of land use impacts.

Table 3. Proportion of fine sediment in subsurface bulk samples (truncated data^a) measured at 23 sites in Catherine Creek and the Upper Grande Ronde River basins during summer 2011.

	Basin		
	Catherine Creek	Grande Ronde River	Total
<i>Fines < 2 mm</i>			
Min	0.06	0.09	0.06
Max	0.19	0.23	0.23
Mean	0.13	0.15	0.14
Standard Deviation	0.04	0.05	0.05
Coefficient of Variation	0.33	0.32	0.33
Replicates	8	15	23
Standard Error	0.01	0.01	0.01
95% CI Lower Bound	0.09	0.12	0.12
95% CI Upper Bound	0.16	0.18	0.16
<i>Fines < 6.35 mm</i>			
Min	0.07	0.21	0.07
Max	0.40	0.44	0.44
Mean	0.26	0.32	0.30
Standard Deviation	0.10	0.07	0.08
Coefficient of Variation	0.37	0.21	0.28
Replicates	8	15	23
Standard Error	0.03	0.02	0.02
95% CI Lower Bound	0.18	0.28	0.26
95% CI Upper Bound	0.34	0.36	0.33

^aData were truncated at 64 mm (i.e., all particles > 63 mm were excluded from the sample) to minimize the influence of very large cobbles.

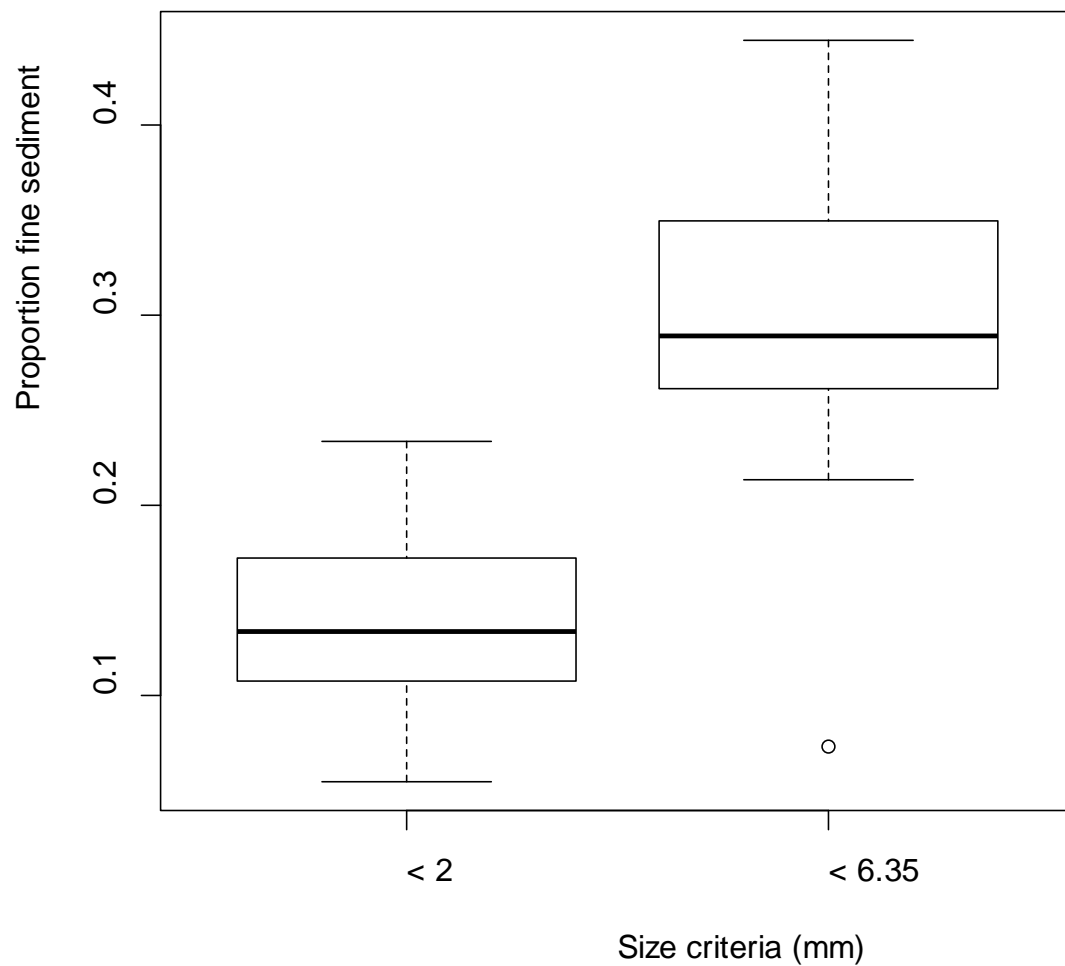


Figure 2. Proportion of sediment < 2 and 6.35 mm from subsurface core samples collected at 23 sites in the Upper Grande Ronde River and Catherine Creek basins. Dark horizontal bars represent median values, bottom and top of boxes represent 25th and 75th percentiles, and whiskers represent roughly 2 standard deviations from the mean.

Table 4. Comparison of model fit from 15 candidate models used to evaluate the relationship between fine sediment < 6.35. Models are sorted by AICc, with the best fitting model (i.e., smallest AICc value) shown at the top.

Model	AICc	Δ AICc	R ²
1	66.1	0.0	NA
4	67.5	1.4	0.13
2	67.6	1.5	0.10
8	70.1	4.1	0.21
5	70.3	4.3	0.19
7	70.3	4.3	0.13
6	70.4	4.3	0.11
14	73.0	6.9	0.23
13	73.2	7.1	0.27
10	73.3	7.2	0.22
9	73.4	7.4	0.20
11	73.5	7.4	0.19
12	73.5	7.5	0.11
3	76.7	10.6	0.16
15	80.2	14.2	0.33

The proportion of fine sediment at depth was significantly correlated with some of the more rapid surface sediment metrics we evaluated (Table 5). Most notably, the proportion of subsurface fines < 6.35 mm was positively correlated with pool tail fines < 6 mm (Figure 3; $R^2 = 0.51$, $p < 0.001$). Interestingly, the proportion of fines at depth was consistently higher than the surface estimates of pool tail fines. For example, the proportion of subsurface fines < 6.35 mm averaged 0.30 compared with 0.13 for pool tail fines < 6 (difference = 0.17, % difference = 60 %). Similarly, the proportion of subsurface fines < 2 mm was positively correlated with pool tail fines < 2 mm, although the relationship was not as strong (Figure 4; $R^2 = 0.39$, $p = 0.002$). Subsurface fines < 2 mm were also higher than pool tail fines < 2 mm on average, with a mean difference (depth fines – pool tail fines) of 0.06 (% difference = 0.43).

Ocular estimates of fine sediment < 2 mm in scour pools were also positively correlated with subsurface fines < 2 mm (Figure 5). Unlike pool tail fines, ocular fines were not consistently higher or lower than depth fines. None of the other surface sediment metrics including pebble

count fines < 2 mm in riffles, pebble count fines < 6 mm in riffles, ocular fines < 2 mm in all habitat types, and cobble embeddedness in riffles were significantly correlated with depth fines. This result is not surprising considering that these metrics were estimated in different channel unit types where hydraulic conditions and sediment transport and depositional processes are different.

Although visual estimates of surface fines in pools explained a relatively low proportion of the variation in depth fines, these statistically significant relationships could prove very useful in linking surface sediment data with subsurface sediment conditions and making more meaningful assessments about potential implications for fish survival.

Table 5. Pearson correlation coefficients for comparisons among 9 different fine sediment metrics calculated from sediment samples collected in the Upper Grande Ronde River and Catherine Creek basins during summer 2011.

	<i>mnfines2</i>	<i>mnfines6</i>	<i>ptfines2</i>	<i>ptfines6</i>	<i>embed</i>	<i>pcfines2</i>	<i>pcfines6</i>	<i>ocfinesall</i>	<i>ocfinessp</i>
<i>mnfines2</i>	1								
<i>mnfines6</i>	0.92	1							
<i>ptfines2</i>	0.62	0.59	1						
<i>ptfines6</i>	0.71	0.72	0.91	1					
<i>embed</i>	0.16	0.28	0.41	0.47	1				
<i>pcfines2</i>	0.20	0.17	0.36	0.34	-0.25	1			
<i>pcfines6</i>	0.23	0.23	0.35	0.35	-0.24	0.96	1		
<i>ocfinesall</i>	0.43	0.33	0.49	0.58	0.14	0.24	0.28	1	
<i>ocfinessp</i>	0.50	0.42	0.62	0.68	0.26	0.21	0.23	0.96	1

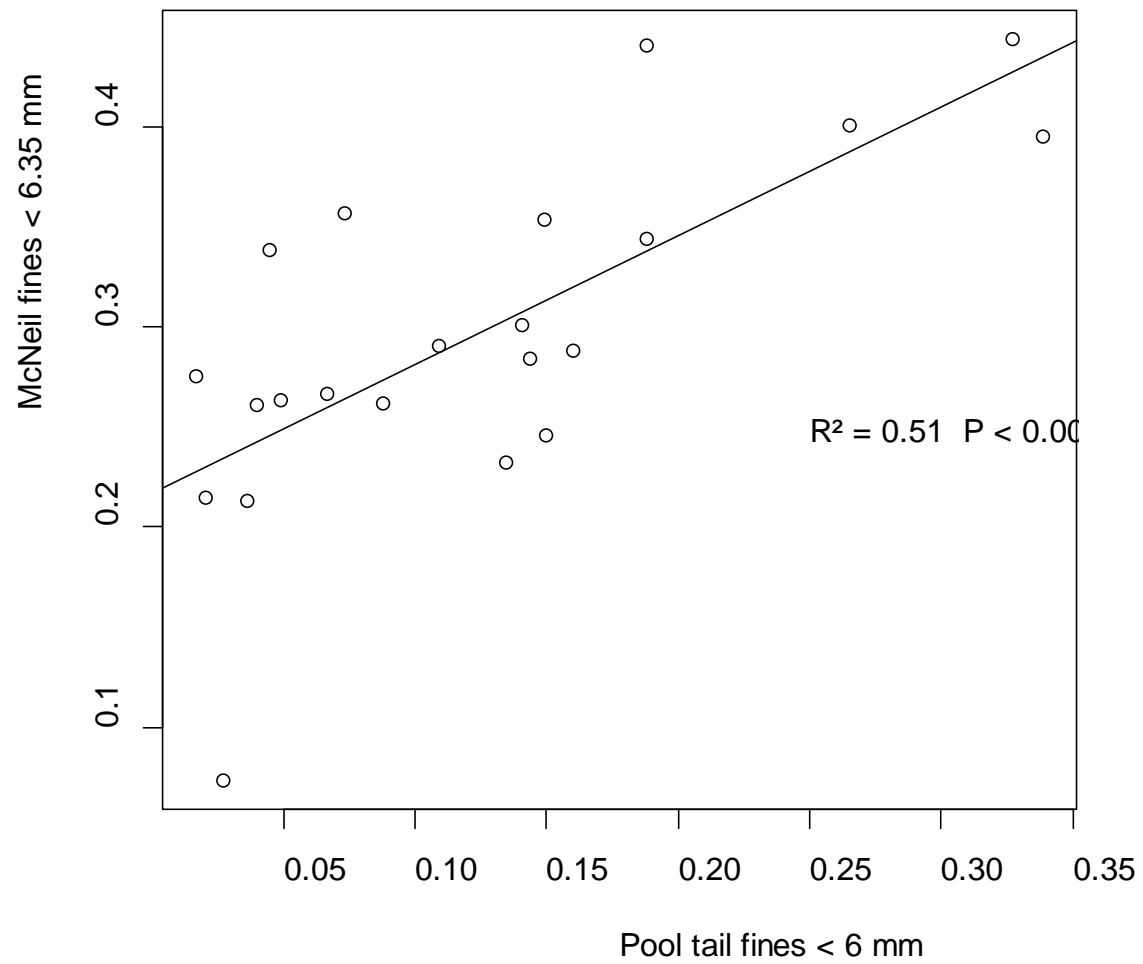


Figure 3. Relationship between pool tail fines < 6 mm and McNeil fines < 6.35 mm estimated from 23 sites in the Upper Grande Ronde River and Catherine Creek basins.

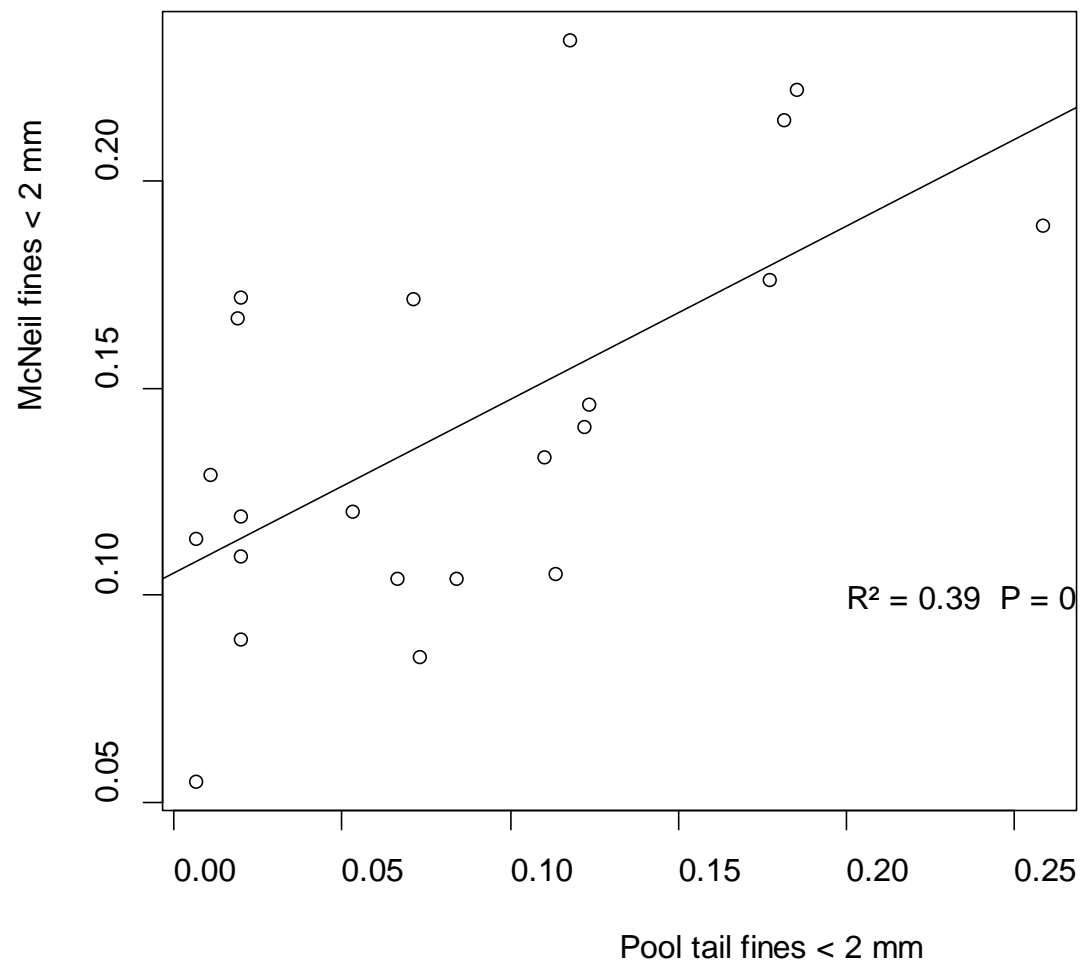


Figure 4. Relationship between pool tail fines < 2 mm and McNeil fines < 2 mm estimated from 23 sites in the Upper Grande Ronde River and Catherine Creek basins.

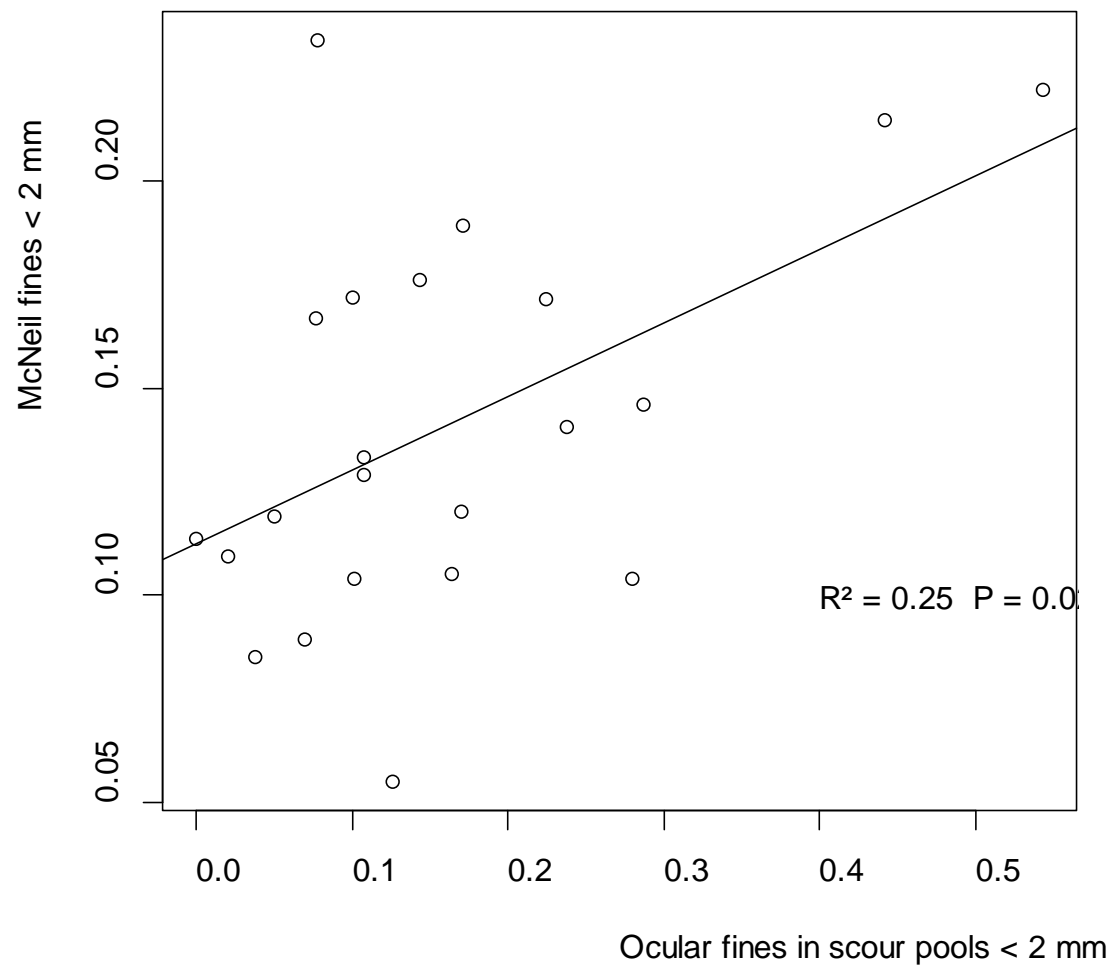


Figure 5. Relationship between ocular fines < 2mm in scour pools and McNeil fines < 6.35 mm estimated from 23 sites in the Upper Grande Ronde River and Catherine Creek basins.

References

- Beechie, T., and H. Imaki. 2008. Predicting Natural Channel Typology for River Restoration in the Columbia River Basin. American Geophysical Union, Fall Meeting.
- Bouwes, N., J. Moberg, N. Weber, B. Bouwes, C. Beasley, S. Bennett, A.C. Hill, et al. 2011. Scientific Protocol for Salmonid Habitat Surveys Within the Columbia Habitat Monitoring Program. Prepared by the Integrated Status and Effectiveness Monitoring Program. Wauconda, WA: Terraqua, Inc.
- Burnham, K.P. and D.R. Anderson. 2002. Model selection and multimodel inference. A practical information-theoretic approach. Springer-Verlag New York, Inc. New York. 488 pages.
- Chapman, D.W., and K.P. McLeod. 1987. Development of criteria for fine sediment in the Northern Rockies ecoregion. Final Report. Boise, Idaho: Battelle Columbus Laboratories. 279 p.
- Chapman, D.W. 1988. Critical Review of Variables Used to Define Effects of Fines in Redds of Large Salmonids. Transactions of the American Fisheries Society 117 (1988): 1–21.
- Church, M., D.G. McLean, and J.F. Wolcott. 1987. River Bed Gravels: Sampling and Analysis. In Sediment Transport in Gravel-Bed Rivers, 43–88. C.R. Thorne, J.D. Bathurst and R.D. Hey (eds.). Chichester: John Wiley and Sons.
- Everest, F.H., R.L. Beschta, J.C. Scrivener, K.V. Koski, J.R. Sedell, and C.J. Cederholm. 1986. Fine Sediment and Salmonid Production: a Paradox. In Streamside Management: Forestry and Fishery Interactions, 98–142. Proceedings of a Symposium Held at University of Washington Contribution No. 57. College of Forest Resources, University of Washington, Seattle.

- Heitke, J.D., E.K. Archer, and B.B. Roper. 2010. Effectiveness Monitoring for Streams and Riparian Areas: Sampling Protocol for Stream Channel Attributes. Logan, UT: PACFISH/INFISH Biological Opinion Effectiveness Monitoring Program (PIBO-EMP).
- Irving, J.S., and T.C. Bjornn. 1984. Effects of substrate size composition on survival of kokanee salmon and cutthroat and rainbow trout. Technical Report. Idaho Cooperative Fishery Research Unit, University of Idaho, Moscow, ID. 21 p.
- Justice, C.J., S. White, D. McCullough. 2011. Field protocol for the spawning gravel composition survey. A component of Monitoring Recovery Trends in Key Spring Chinook Habitat Variables and Validation of Population Viability Indicators. Columbia River Inter-Tribal Fish Commission. 14 pages.
- Kaufmann, P.R., P. Levine, E.G. Robison, C. Seeliger, and D.V. Peck. 1999. Quantifying Physical Habitat in Wadeable Streams. Washington, DC: U.S. Environmental Protection Agency.
- Montgomery, D.R., and J.M. Buffington. 1997. Channel-reach Morphology in Mountain Drainage Basins. GSA Bulletin 109, no. 5: 596–611.
- Quinn, T.P. 2005. The behavior and ecology of Pacific salmon and trout. University of Washington Press. Seattle. 363 pages.
- Reiser, D.W. 1999. Sediment in Gravel Bed Rivers: Ecological and Biological Consideration. In Gravel-bed Rivers in the Environment, 199–225. Edited by P.C. Klingeman, R.L. Beschta, P.D. Komar, and J.B. Bradely. Highlands Ranch, Colorado: Water Resources Publications.
- Tappel, P.D., and T.C. Bjornn. 1983. A new method of relating size of spawning gravel to salmonid embryo survival. North American Journal of Fisheries Management 3: 123-135.

White, S.M., Justice, C., and McCullough, D. (In prep) The landscape context of fish-habitat relationships: implications for restoring wood recruitment processes in U.S. Pacific Northwest rivers. Intended for Ecological Restoration.

Whittier, T.R., A.T. Herlihy, C. Jordan, C. Volk, and J. Sifneos. 2010. Unpublished Report. A Landscape Classification to Support Intensively Monitored Watersheds in the Pacific Northwest. Corvallis, OR: Department of Fisheries and Wildlife, Oregon State University.

Appendix E.

Study Design for Evaluation of Fine Sediment Infiltration and Chinook Embryo Survival in the Upper Grande Ronde River and Catherine Creek

Study Design for Evaluation of Fine Sediment Infiltration and Chinook Embryo Survival in the Upper Grande Ronde River and Catherine Creek

Authors: Casey Justice, Dale McCullough, and Seth White

Columbia River Inter-Tribal Fish Commission

Portland, Oregon

May 10, 2011

Introduction

High levels of fine sediment in salmonid spawning gravels can have serious detrimental effects on embryo survival through reductions in inter-gravel dissolved oxygen or entombment of emergent fry (Tappel and Bjornn 1983; Everest *et al.* 1986; Chapman 1988; Reiser 1999). Natural resource scientists often measure the quantity of fine sediment in streambed substrate in order to characterize the suitability of the gravel for spawning fish and associated embryo survival or to examine relationships between habitat conditions and land use. However, most habitat monitoring programs measure fine sediment in potential spawning areas during summer base flow (Heitke *et al.* 2010; Kaufmann *et al.* 1999; USDA 2006), and fail to account for gravel cleaning that occurs during spawning (Everest *et al.* 1986; Kondolf *et al.* 1993), or infiltration of fine sediment during the incubation period (Levasseur *et al.* 2006a). The negative effect of fine sediment on embryo survival may be more related to the amount of fine sediment that accumulates in the gravel during the incubation period, and to a much lesser extent on the gravel composition immediately before or after spawning (Acornley and Sear 1999; Julien and Bergeron 2006). We plan to evaluate fine sediment infiltration rates and embryo survival in the Upper Grande Ronde River and Catherine Creek basins where fine sediment levels have been identified as key limiting factors for threatened spring Chinook salmon populations (Nowak 2004). These data will provide a better understanding of fine sediment dynamics in these basins as well as improve our ability to accurately model the impacts of fine sediment on salmonid embryo survival.

Sediment infiltration traps have been frequently used to measure infiltration rates of fine sediment into spawning gravels (Frostick *et al.* 1984; Lisle 1989; Lisle and Eads 1991; Wesche *et al.* 1989; Lachance and Dube 2004; Zimmerman and Lapointe 2005) and to evaluate impacts of fine sediment on embryo survival in the field (Sowden and Power 1985; Weaver and Fraley 1993; Pauwels and Haines 1994; Malcolm *et al.* 2003; Julien and Bergeron 2006; Levasseur *et al.* 2006a; Fudge *et al.* 2008). Infiltration traps generally consist of some type of container filled with gravel of known size distribution that is buried in the stream bed, flush with the bed surface (Lisle and Eads 1991). The containers are removed approximately at the time of fry

emergence, or periodically during the incubation period and the gravel mixture is subsequently sieved and weighed to determine the percentage of fine sediment.

Most studies examining fine sediment dynamics have relied on sediment traps or incubation baskets that allow for an unknown quantity of fine sediment to wash out of the trap during removal from the stream. Loss of very fine sediment particles upon retrieval of the traps may introduce unwanted error in estimates of fine sediment quantity and evaluations of fine sediment and embryo survival relationships. Recent studies have increasingly shown that, although they comprise a relatively small proportion of the total gravel composition, very fine sediment fractions (< 0.125 mm) are more detrimental to embryo survival than coarser particle fractions (Julien and Bergeron 2006; Levasseur *et al.* 2006a). Infiltration bags (Levasseur *et al.* 2006b) and porous-walled containers with holes that close prior to extraction (Lachance and Dube 2004) provide useful alternatives for concurrent measurements of fine sediment infiltration and embryo survival by permitting unhindered lateral infiltration of fines with minimal loss of fines during retrieval.

Fine sediment infiltration rates are usually measured using traps filled with well-sorted mixtures of experimental gravel that aren't reflective of the full size distribution of gravels in natural salmonid redds. In addition, gravel mixtures in sediment traps are often replaced periodically during the incubation period with freshly cleaned gravel (Lisle 1989; Zimmermann and Lapointe 2005), which doesn't mimic the natural process of fine sediment accumulation. The infiltration rate of fine sediment is strongly influenced by the size and shape of the bed material (Frostick *et al.* 1984; Carling 1984; Lisle 1989), and the degree of saturation of fine sediment in the gravel (Zimmermann and Lapointe 2005; Wooster *et al.* 2008). Consequently, studies seeking to describe natural fine sediment dynamics in spawning gravels should use gravel mixtures that closely resemble the natural size distribution of gravel found in salmonid redds.

Estimates of fine sediment in streams are commonly used in simulation models to predict effects of fine sediment on fish production (Lisle and Lewis 1992; Mobrand and Lestelle 1997; McHugh *et al.* 2004; Scheuerell *et al.* 2006). One important application of these types of models is to evaluate potential population responses to stream restoration actions (Honea *et al.* 2009), which may include activities that reduce fine sediment delivery to stream channels such as planting trees in riparian zones or decommissioning roads. However, most of these models rely on laboratory-derived relationships between fine sediment and embryo survival for predictions of fish response, and do not attempt to correct for the reduction in fine sediment that occurs during the redd building process (Everest *et al.* 1987; Kondolf *et al.* 1993), or subsequent increases in fine sediment resulting from infiltration during the incubation period (Levasseur *et al.* 2006a). This study would provide the information necessary to adjust estimates of fine sediment derived from standard substrate samples collected during summer base flow conditions to account for gravel cleaning and fine sediment infiltration, thereby improving the utility of sediment data in population modeling.

We designed a field experiment to quantify the rate of fine sediment infiltration into Chinook salmon spawning gravels and associated effects on embryo survival in the Upper Grande Ronde River and Catherine Creek, NE Oregon. More specifically, the objectives of this study are to (i) estimate average infiltration rates of fine sediment and dissolved oxygen in infiltration traps deployed in two currently used spawning areas, (ii) estimate average survival rates from egg-to-hatching and egg-to-emergence, (iii) examine relationships between survival of Chinook salmon embryos and measures of fine sediment and dissolved oxygen, and (iv) compare observed survival rates with model-predicted survival based on laboratory-derived functional relationships.

Study Area

This study will be conducted in two 4th order streams in the Grande Ronde River basin including the Upper Grande Ronde River and Catherine Creek (Figure 1). The study area in the Upper Grande Ronde River is limited to the segment between the Vey Meadows boundary above Limber Jim Creek (rkm 313) and East Fork Grande Ronde River (rkm 319). This portion of the Grande Ronde River drains approximately 118 km² of forested terrain in the Blue Mountains, with an average summer (July – September) discharge of 16 cfs and average annual peak discharge of 243 cfs. The active channel in this segment averages approximately 8.6 m wide with an average gradient of 1.6%. The study area within Catherine Creek includes the river segment between Milk Creek (rkm 44.5) and the confluence of North Fork and South Fork Catherine Creek (rkm 52) and drains approximately 173 km² of steep, forested terrain in the southwest corner of the Wallowa Mountains, with an average summer discharge of 49 cfs and average peak discharge of 741 cfs. This river segment has an average gradient of 1.5% and average active channel width of 11.2 m.

Spring Chinook populations in both of these streams are listed as threatened under the Endangered Species Act, and are heavily supplemented with hatchery stocks. Habitat conditions in these streams are severely degraded as a result of intensive anthropogenic disturbances including timber harvest, cattle grazing, levee and road construction, and stream diversions for irrigation. Specifically, high stream temperatures, excessive levels of fine sediment, and decreased streamflow have been identified as key limiting factors for recovery of Chinook populations in these basins (Nowak 2004).

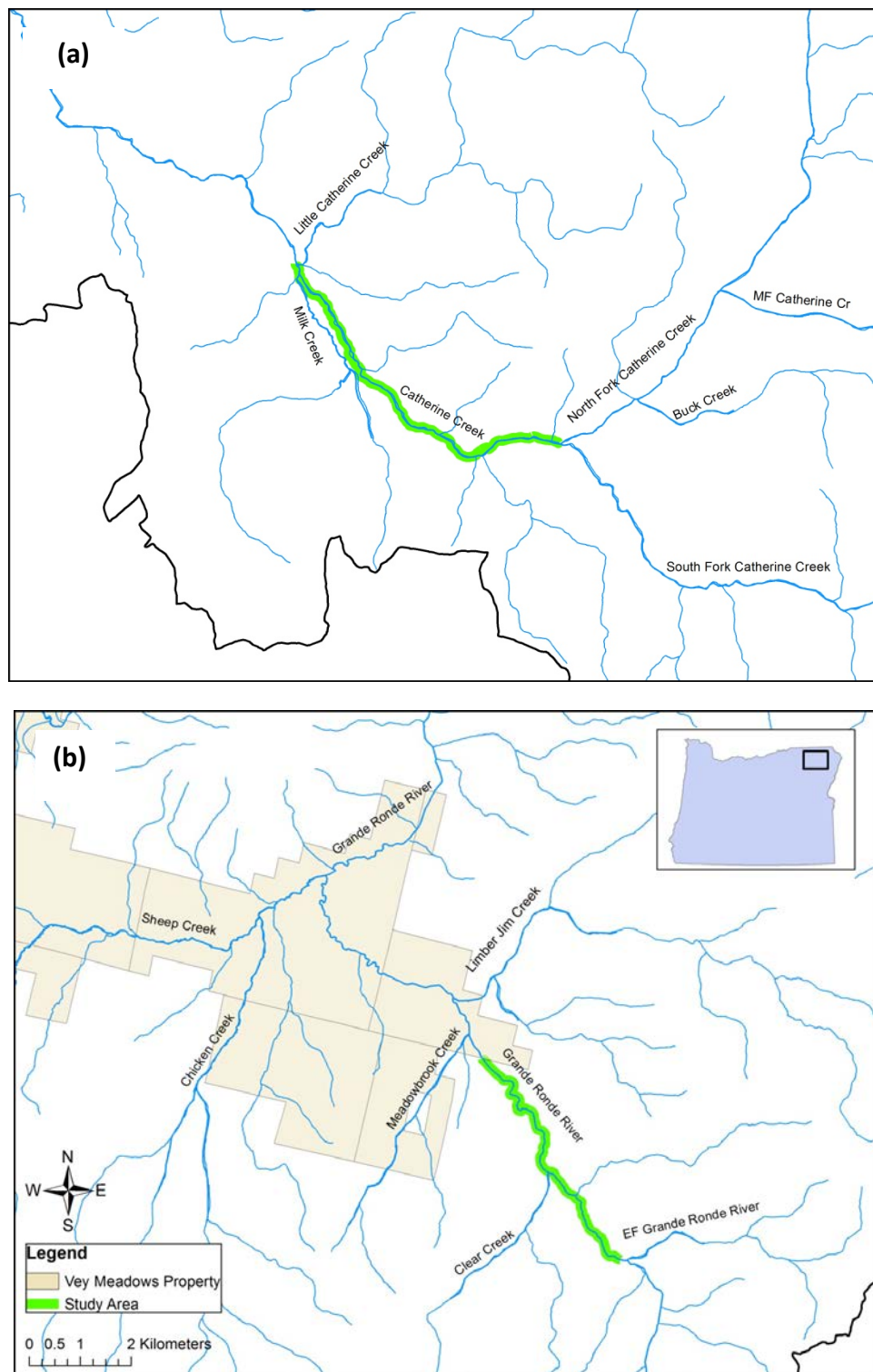


Figure 1. Study areas in (a) Catherine Creek (b) the Upper Grande Ronde River.

Methods

Field measurements of fine sediment infiltration and embryo survival will be conducted during the Fall-to-Spring egg incubation period (late September – late June) in 2011 and 2012 (Table 1). The experimental design will consist of 10 randomly selected sites in each of the two streams, with three replicate samples collected at each site. Potential study sites will be selected by walking each study reach at the end of spawning (mid-September) and recording GPS coordinates at all pool tail habitats that do not contain newly constructed redds. Because flagging and GPS data will be available from previous spawning surveys, we will be able to ensure that we do not disturb any recently-constructed redds in the study area. Only pool tail habitats meeting the following criteria will be included as a potential study site: 1) dominant substrate size is between 11 and 90 mm; 2) water is flowing; and 3) water depth is between 0.15 and 1.0 m. Potential study sites meeting these criteria will then be assigned a unique ID number, and a random sample of size $n = 10$ will be drawn from the sample population for each stream.

Fine sediment infiltration rates and Chinook embryo survival will be measured at each site using sediment traps similar to those described in Lachance and Dube (2004) (Figure 3). Each trap will consist of two 6-liter cylindrical buckets (dimensions 22 cm length by 21 cm diameter) fitted inside one another. The buckets are perforated with 6.35 mm diameter holes to allow for lateral infiltration of fines into the buckets. Alignment of the holes on the two buckets is marked with metal pins. Upon removal from the stream, the inner bucket can be rotated to close the holes and prevent loss of fine sediment. The inner bucket is lined with 3 mm Nitex netting and capped with a screened lid of 3mm mesh to prevent escape of alevins and fry during the incubation period.

A brightly colored latex extraction tube with 5 mm internal diameter and screened with mesh at the sampler end will be used to draw water from the bottom of each trap for measurement of intra-gravel dissolved oxygen (Malcolm *et al.* 2003). Water will be slowly pumped through the tube using a small hand pump and funneled into a flow cell where dissolved oxygen will be measured using a YSI Professional Plus multi-parameter probe. Dissolved oxygen samples will be collected at roughly monthly intervals for a total of 9 samples over the course of the incubation period. The brightly colored extraction tube will be fitted with a foam float at the extraction end to aid in relocation of each trap.

A total of three substrate samples will be collected at each site after spawning is completed in late September or early October. At each site, the location of the riffle crest line will be visually estimated, and each of the three samples will be randomly assigned to a location along the horizontal length of the riffle crest including 25, 50, and 75%. All three samples will be cleaned of fine sediment (see description below), and two of the samples will be transferred to infiltration traps and buried in the stream. The third sample will be returned immediately to the lab for the purpose of estimating the fraction of fines remaining in the traps immediately after cleaning. The fine sediment removed from the gravel during cleaning will also be retained for each sample to provide an estimate of the quantity of fine sediment present in the gravel

immediately before and after cleaning. The location of the sediment traps will be marked by driving a rebar stake with a brightly colored cap into the stream bank across from the sediment traps. Nylon flagging will also be attached to a nearby tree to mark the site.

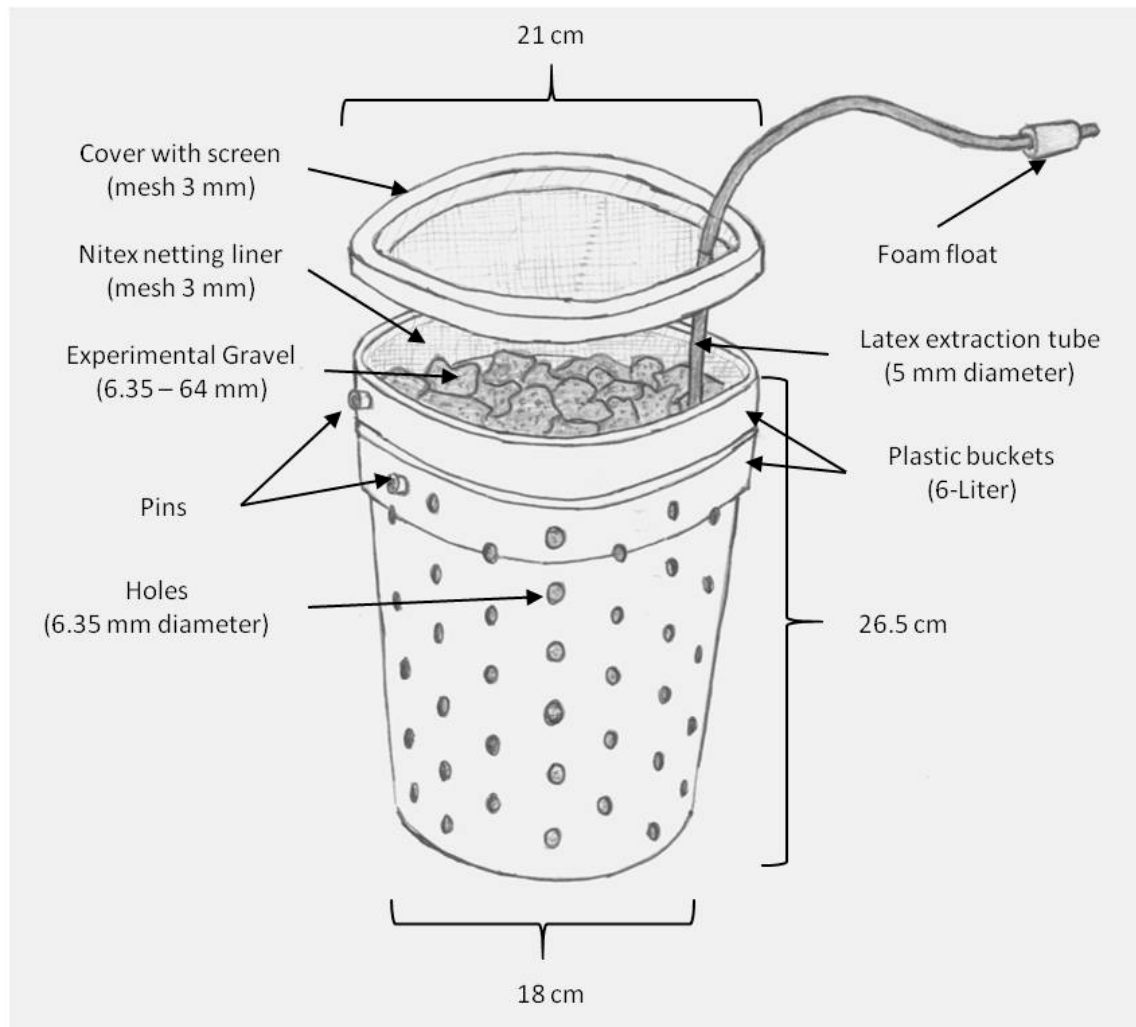


Figure 2. Fine sediment infiltration trap modified from Lachance and Dube (2004).

At each sample point, we will use a standard round point shovel to dig a hole of dimensions 25 cm deep by 25 cm wide. Extracted gravel will be placed in a gravel cleaning apparatus (hereby referred to as “gravel cleaner”) designed to separate and retain most of the particles smaller than 6.35 mm from the rest of the gravel mixture. The gravel cleaner consists of a 5 gallon bucket with 6.35 mm holes drilled in the bottom and a fine mesh net (mesh size 0.1 μm) attached to the bottom. The purpose of the net is to retain all fine sediment washed out of each gravel sample. The perforated bucket and net are placed inside another 5 gallon bucket

with 6.35 mm holes in the bottom. Stream water will be poured into the gravel cleaner while rocking it back and forth for a period of no less than 10 minutes to facilitate removal of the fine sediment fraction. Fines collected in the net will then be transferred to a 6 liter bucket, and a wash bottle will be used to remove any remaining fine sediment from the inside of the net. In addition, any coarse particles larger than 64 mm diameter will be measured with a gravelometer and removed from the gravel mixture. Coarse particles > 64 mm will be combined with the fine sediment fraction and returned to the lab for analysis. The remaining gravel mixture will be dumped into a fine mesh bag or bucket and stored along the stream bank in preparation for addition of the Chinook salmon eggs.

Chinook salmon eggs will be obtained from the Lookingglass Hatchery near Elgin, Oregon in coordination with the Confederated Tribes of the Umatilla Indian Reservation (CTUIR) and Oregon Department of Fish and Wildlife (ODFW). Chinook stocks used for this study will be specific to the stream of origin. Approximately 2000 eggs from each stock will be fertilized and water hardened and then placed in cool, sterile glass containers for transport. Eggs will be transported in a cooler to the study sites and installed in the stream within 16 hours post fertilization to reduce handling related mortality.

Eggs will be incubated inside Whitlock-Vibert (W-V) boxes (Whitlock 1977) installed in the bottom of each infiltration trap. After filling each W-V box half full with the pre-cleaned gravel mixture, a total of 100 eggs will be carefully transferred into each box and distributed evenly across the gravel surface. In order to reduce damage to the eggs, the transfer of eggs will occur inside a 5-gallon bucket filled with water. The eggs will then be covered carefully with more gravel until the box is full. The W-V boxes will then be placed inside the bottom of the infiltration traps with the lids left open, covered with the remaining gravel mixture, and buried flush with the stream bed. Any extra gravel mixture that doesn't fit inside the sediment trap will be returned to the lab for analysis.

In order to evaluate the influence of transport and handling on egg fertilization rates, 3 replicate samples of 100 green eggs each will be incubated at the hatchery as control samples for a period of 12 hours post fertilization. After this period, the eggs will be fixed in Stockard's solution and returned to the lab for analysis. Fertilization success will be calculated as the proportion of eggs reaching the 2nd cleavage stage (Ballard 1973; Stoeckel and Neves 1992). Similarly, 3 replicate samples of 100 eggs each will be transported to the stream and subjected to the same handling process as the eggs intended for long-term deployment. These eggs will be recovered after a period of approximately 12 hours post fertilization, fixed in Stockard's solution, and examined in the lab to determine fertilization success. The ratio of fertilization rates between transported and control samples will provide an estimate of the handling effect on egg fertilization.

Decomposition of eggs and fry during incubation can produce bias in survival estimates. For example, if a proportion of the fry that successfully emerge from the gravel decompose before the sample is collected, the estimate of survival-to-emergence will be biased low. To account for this possibility, we will deploy four additional W-V boxes containing eggs or fry in each

stream during the incubation period to measure decomposition rates. Two of the boxes will contain 100 green eggs each and the other two boxes will contain 20 Chinook fry. Fry used for this study will consist of fish that had recently died in the hatchery. These fish will be stored in a freezer prior to deployment in the stream. Eggs will be killed prior to deployment by placing them in a freezer. The W-V boxes will be partially filled with cleaned gravel and placed inside steel cages buried just under the surface of the streambed. Steel cages will be secured to rebar stakes driven into the streambed. The cages are intended to aid in repeated collection and redeployment of the W-V boxes and to reduce the chance of loss during high flows.

The W-V boxes used to measure egg decomposition rates will be deployed at the same time as the infiltration traps and the W-V boxes containing fry will be deployed during retrieval of the first set of infiltration traps (i.e., at the end of hatching). The boxes will be retrieved on monthly intervals coincident with measurements of dissolved oxygen. Upon retrieval, the boxes will be emptied onto a tray and the number of intact or partially decomposed eggs or fry will be tallied. After enumeration, all contents will be transferred back into the boxes and the boxes will be redeployed in the stream.

Sediment traps will be removed from the streams at two different times corresponding approximately with the end of hatching and emergence (Figures 4 and 5; Table 1). We used a temperature-dependent model developed by Beacham and Murray (1990) to predict the timing of hatching and emergence using average stream temperature data from 2004 to 2010. Because hatching and emergence dates are considerably different between the two streams due to differences in thermal regime, sediment traps will be removed from each stream on different dates. In addition to thermal regime, predicted timing of hatching and emergence depends largely on the date that eggs are fertilized and installed in the stream, and will therefore vary depending on when eggs are available from the hatchery. Assuming the eggs will be deployed in the stream between September 12 and 30, approximate dates for retrieval of traps following hatching range from January 30 to April 7 for Catherine Creek and from April 16 to May 25 for the Upper Grande Ronde River. Dates of trap removal corresponding with post-emergence range from May 8 to June 6 for Catherine Creek and from June 15 to June 30 for the Upper Grande Ronde River. Real-time temperature data collected at each stream will be used to revise estimates of hatch and emergence timing, and adjust trap retrieval dates accordingly. In addition, dates of trap retrieval will likely vary somewhat from this schedule according to logistical considerations and streamflows.

After removal from the stream, all infiltration traps will be immediately returned to the lab and carefully sorted to remove any eggs, alevins, or fry. The top 5 cm of gravel in each trap will be removed and examined separately for the presence of emergent alevins or fry. The Whitlock-Vibert boxes will be carefully excavated from the infiltration trap and the gravel sorted to remove any eggs or alevins. The gravel from the W-V boxes will be kept separate from the surrounding gravel in the infiltration trap in order to estimate the fine sediment fraction at egg depth. All eggs, alevins, and fry will be fixed in Stockard solution and stored in labeled glass vials prior to analysis. The number of eggs, alevins, and fry in each of the following categories will be enumerated: pre-eyed eggs (PEE), eyed eggs (EE), alevins in top 5 cm of trap (AT), alevins in

bottom 17 cm of trap (AB), fry in top 5 cm of trap (FT), fry in bottom 17 cm of trap (FB). Fry will be distinguished from alevins based on the absence of a yolk sac. Survival rates will be calculated for each of three life stages as follows:

$$\text{Survival-to-eyed stage (STE)} = (EE + AT + AB + FT + FB)/100$$

$$\text{Survival-to-hatching (STH)} = (AT + AB + FT + FB)/100$$

$$\text{Survival-to-emergence (STE)} = (AT + FT)/100$$

Substrate size composition will be measured in the lab for all substrate samples including initial gravel samples, W-V boxes, infiltration traps, and fine sediment samples removed during gravel cleaning. Substrate samples will be oven dried, sieved, and weighed to obtain percent composition by weight. Fine sediment particles < 6.35 mm will be sieved into the following size classes: fine gravel (4 – 6.35 mm); very fine gravel (2 – 4 mm); very coarse sand (1 – 2 mm); coarse sand (0.85 – 1 mm); medium coarse sand (0.35 – 0.85 mm); fine sand (0.125 – 0.35 mm); very fine sand (0.063 – 0.125 mm); and silt and clay (< 0.063 mm). These data will provide estimates of fine sediment composition at four different periods including 1) immediately prior to cleaning, 2) immediately after cleaning, 3) after hatching, and 4) after emergence.

The relationship between embryo survival rates and measures of fine sediment and dissolved oxygen will be examined using logistic regression analysis. In addition, observed survival rates will be compared with model-predicted survival rates generated from fine sediment fractions measured prior to gravel cleaning and laboratory-derived relationships between percent fines and embryo survival (Tappel and Bjornn 1983). Finally, methods will be developed to correct for potential bias in model-predicted estimates of embryo survival to account for gravel cleaning during spawning and subsequent infiltration of fine sediment into spawning gravels.

Table 1. Schedule of study activities.

Activity	Date	
	Catherine Creek	Upper Grande Ronde River
Infiltration traps with eggs deployed (100 eggs per trap, 2 traps per site, 10 sites per stream, 2 streams, 4000 eggs total)	Sep 12 - Sep 30	Sep 12 - Sep 30
Initial gravel samples collected (1 bucket per site, 20 buckets total)		
Eggs in W-V boxes deployed for decomposition analysis (100 eggs per box, 2 boxes per stream, 400 eggs total)		
Transport and handling effects on fertilization success (100 eggs per sample, 3 samples retained at hatchery, 3 samples transported, 600 eggs total)		
Infiltration traps retrieved at hatching (1 trap per site, 20 traps total)	Jan 30 - Apr 7	Apr 16 - May 25
Fry in W-V boxes deployed for decomposition analysis (20 fry per box, 2 boxes per stream, 80 fry total)		
Infiltration traps retrieved at emergence (1 trap per site, 20 traps total)	May 8 - Jun 6	Jun 15 - Jun 30
Dissolved oxygen measured (9 measurements per stream)	Monthly (Sep 12 - Jun 6)	Monthly (Sep 12 - Jun 30)
Eggs in W-V boxes enumerated for decomposition analysis (9 measurements per stream)		
Fry in W-V boxes enumerated for decomposition analysis (4 measurements per stream)	Monthly (Jan 30 - Jun 6)	Monthly (Apr 16 - Jun 30)

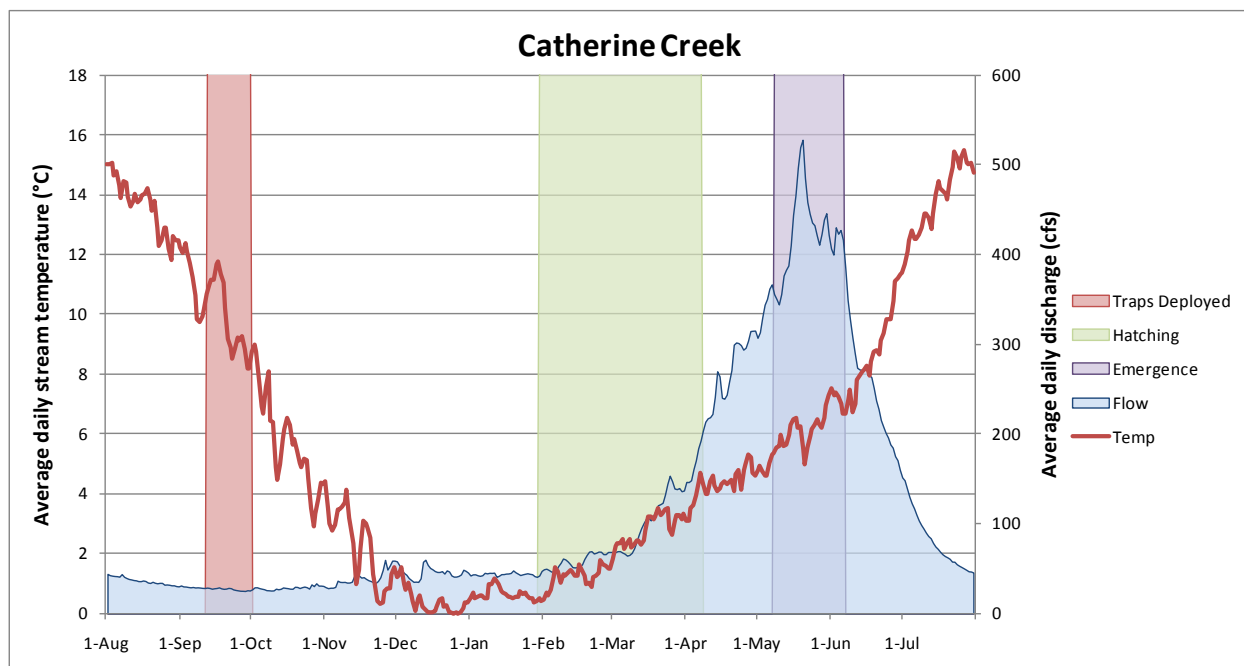


Figure 3. Stream temperature, discharge, and predicted hatch and emergence timing for Chinook salmon incubated in traps in Catherine Creek between Milk Creek and the confluence of North Fork and South Fork Catherine Creek.

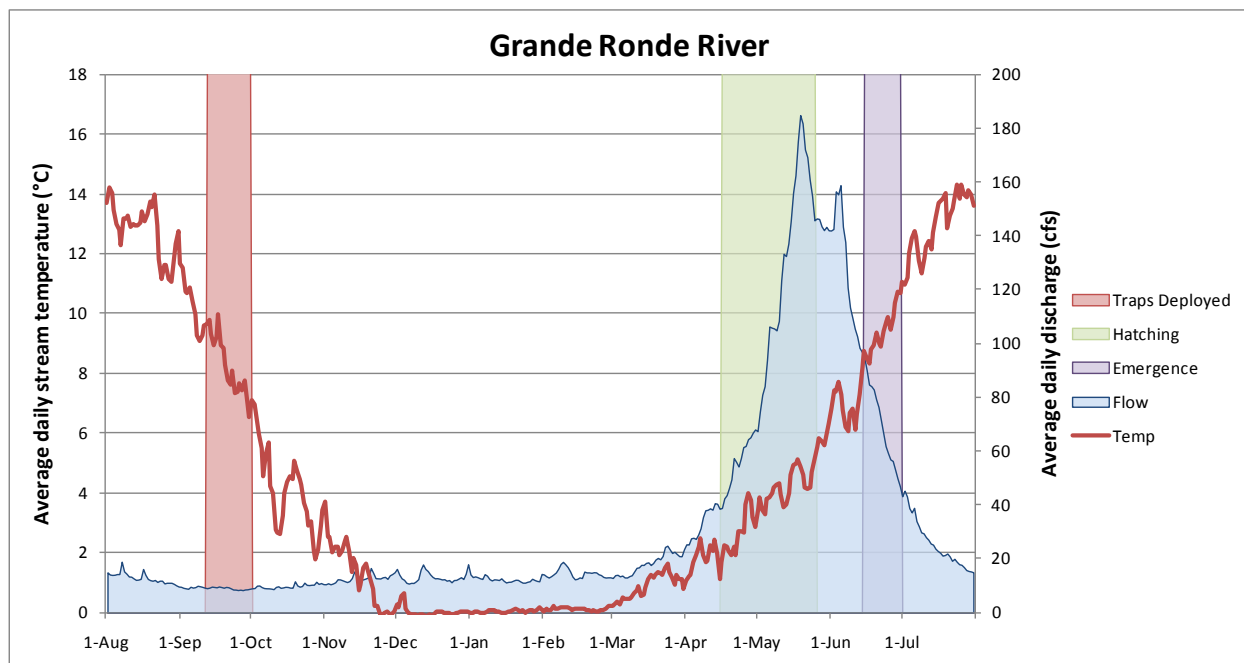


Figure 4. Stream temperature, discharge, and predicted hatch and emergence timing for Chinook salmon incubated in traps in the Upper Grande Ronde River between Limber Jim Creek and East Fork Grande Ronde River.

References

- Acornely, R.M., and D.A. Sear. 1999. Sediment transport and siltation of brown trout (*Salmo trutta* L.) spawning gravels in chalk streams. *Hydrological Processes* 13: 447-458.
- Ballard, W.W. 1973. "Normal embryonic stages for salmonid fishes, based on *Salmo gairdneri* Richardson and *Salvelinus fontinalis* (Mitchill)." *Journal of Experimental Zoology* 184: 7-26.
- Beacham, T.D., and C.B. Murray. Temperature, egg size, and development of embryos and alevins of five species of Pacific salmon: a comparative analysis. *Transactions of the American Fisheries Society* 119 (6): 927-945.
- Carling, P.A. 1984. Deposition of fine and coarse sand in an open-work gravel bed. *Canadian Journal of Fisheries and Aquatic Sciences* 41: 263-270.
- Chapman, D.W. 1988. Critical review of variables used to define effects of fines in redds of large salmonids. *Transactions of the American Fisheries Society* 117: 1-21.
- Everest, F.H., R.L. Beschta, J.C. Scrivener, K.V. Koski, J.R. Sedell, and C.J. Cederholm. 1986. Fine sediment and salmonid production: a paradox. In *Streamside management: forestry and fishery interactions*, 98-142. Proceedings of a symposium held at University of Washington Contribution No. 57. College of Forest Resources, University of Washington, Seattle, February 12.
- Frostick, L.E., P.M. Lucas, and I. Reid. 1984. The infiltration of fine matrices into coarse-grained alluvial sediments and its implications for stratigraphical interpretation. *Journal of the Geological Society of London* 141: 955-965.
- Fudge, Thomas, Kerry Wautier, Robert Evans, and Vince Palace. 2008. Effect of different levels of fine-sediment loading on the escapement success of rainbow trout fry from artificial redds. *North American Journal of Fisheries Management* 28 (3): 758-765. doi:10.1577/M07-084.1.
- Heitke, J.D., E.K. Archer, and B.B. Roper. 2010. Effectiveness monitoring for streams and riparian areas: sampling protocol for stream channel attributes. Logan, UT: PACFISH/INFISH Biological Opinion Effectiveness Monitoring Program (PIBO-EMP).
- Honea, J.M., J.C. Jorgensen, M.M. McClure, T.D. Cooney, K. Engie, D.M. Holzer, and R. Hilborn. 2009. Evaluating habitat effects on population status: influence of habitat restoration on spring-run Chinook salmon. *Freshwater Biology* 54: 1576-1592.
- Julien, H.P., and N.E. Bergeron. 2006. Effect of fine sediment infiltration during the incubation period on Atlantic salmon (*Salmo salar*) embryo survival. *Hydrobiologia* 563: 61-71.

- Kaufmann, P.R., P. Levine, E.G. Robison, C. Seeliger, and D.V. Peck. 1999. Quantifying physical habitat in wadeable streams. Washington, DC: U.S. Environmental Protection Agency.
- Kondolf, G.M., M.J. Sale, and M.G. Wolman. 1993. Modification of fluvial gravel size by spawning salmonids. *Water Resources Research* 29 (7): 2265-2274.
- Lachance, S., and M. Dube. 2004. A new tool for measuring sediment accumulation with minimal loss of fines. *North American Journal of Fisheries Management* 24: 303-310.
- Levasseur, M., N.E. Bergeron, M.F. Lapointe, and F. Berube. 2006a. Effects of silt and very fine sand dynamics in Atlantic salmon (*Salmo salar*) redds on embryo hatching success. *Canadian Journal of Fisheries and Aquatic Sciences* 63: 1450-1459.
- Levasseur, M., F. Berube, and N.E. Bergeron. 2006b. A field method for the concurrent measurement of fine sediment content and embryo survival in artificial salmonid redds. *Earth Surface Processes and Landforms* 31: 526-530.
- Lisle, T.E. 1989. Sediment transport and resulting deposition in spawning gravels, North Coastal California. *Water Resources Research* 25 (6): 1303-1319.
- Lisle, T., and R.E. Eads. 1991. Methods to measure sedimentation of spawning gravels. Research Note. Berkeley, CA: Pacific Southwest Research Station, Forest Service, U.S. Department of Agriculture.
- Lisle, T.E., and J. Lewis. 1992. Effects of sediment transport on survival of salmonid embryos in a natural stream: a simulation approach. *Canadian Journal of Fisheries and Aquatic Sciences* 49: 2337-2344.
- Malcolm, Iain A., Alan F. Youngson, and Chris Soulsby. 2003. Survival of salmonid eggs in a degraded gravel-bed stream: effects of groundwater-surface water interactions. *River Research and Applications* 19 (4): 303-316. doi:10.1002/rra.706.
- McHugh, P., P. Budy, and H. Schaller. 2004. A model-based assessment of the potential response of Snake River Spring-Summer Chinook salmon to habitat improvements. *Transactions of the American Fisheries Society* 133: 622-638.
- Mobrand, L., and L. Lestelle, L.C. 1997. Application of the Ecosystem Diagnosis and Treatment method to the Grande Ronde Model Watershed Project. Prepared for U.S. Department of Energy, Bonneville Power Administration. Vashon Island, WA: Mobrand Biometrics.
- Nowak, M.C. 2004. Grande Ronde Subbasin Plan. Prepared for Northwest Power and Conservation Council.
- Pauwels, S.J., and T.A. Haines. 1994. Survival, hatching, and emergence success of Atlantic salmon eggs planted in three Maine streams. *North American Journal of Fisheries Management* 14: 125-130.

- Reiser, D.W. 1999. Sediment in gravel bed rivers: ecological and biological consideration. In Gravel-bed rivers in the environment, 199-225. Edited by P.C. Klingeman, R.L. Beschta, P.D. Komar, and J.B. Bradely. Highlands Ranch, Colorado: Water Resources Publications.
- Scheuerell, M.D., R. Hilborn, M.H. Ruckelshaus, K.K. Bartz, K.M. Lagueur, A.D. Haas, and K. Rawson. 2006. The Shiraz model: a tool for incorporating anthropogenic effects and fish–habitat relationships in conservation planning. *Canadian Journal of Fisheries and Aquatic Sciences* 63: 1596-1607.
- Sowden, T.K., and G. Power. 1985. Prediction of rainbow trout embryo survival in relation to groundwater seepage and particle size of spawning substrates. *Transactions of the American Fisheries Society* 114: 804-812.
- Stoeckel, J. N. and Neves, R. J. (1992) Comparison of methods for viewing the germinal vesicle in fish oocytes. *Progressive Fish-Culturist* 54 , pp. 115-118.
- Tappel, P.D., and T.C. Bjornn. 1983. A new method of relating size of spawning gravel to salmonid embryo survival. *North American Journal of Fisheries Management* 3: 123-135.
- USDA. 2006. Stream inventory handbook Level I and II: U.S. Department of Agriculture, Forest Service, Pacific Northwest Region, Region 6.
- Weaver, T.M., and J.J. Fraley. 1993. A method to measure emergence success of Westslope cutthroat trout fry from varying substrate compositions in a natural stream. *North American Journal of Fisheries Management* 13: 817-822.
- Wesche, T.A., D.W. Reiser, V.R. Hasfurther, W.A. Hubert, and Q.D. Skinner. 1989. New technique for measuring fine sediment in streams. *North American Journal of Fisheries Management* 9: 234-238.
- Whitlock, D. 1977. The Whitlock-Vibert box handbook. El Segundo, California: Federation of Fly Fishermen.
- Wooster, John K., Scott R. Dusterhoff, Yantao Cui, Leonard S. Sklar, William E. Dietrich, and Mary Malko. 2008. Sediment supply and relative size distribution effects on fine sediment infiltration into immobile gravels. *Water Resources Research* 44 (3). doi:10.1029/2006WR005815. <http://www.agu.org/pubs/crossref/2008/2006WR005815.shtml>.
- Zimmermann, A.E., and M. Lapointe. 2005. Sediment infiltration traps: their use to monitor salmonid spawning habitat in headwater tributaries of the Cascapedia River, Quebec. *Hydrological Processes* 19: 4161-4177.

Appendix F.

Compilation of Diagrams and Literature Illustrating the Options for Implementing Radiation Shielding of Air Temperature Sensors

Compilation of Diagrams and Literature Illustrating the Options for Implementing Radiation Shielding of Air Temperature Sensors

A component of

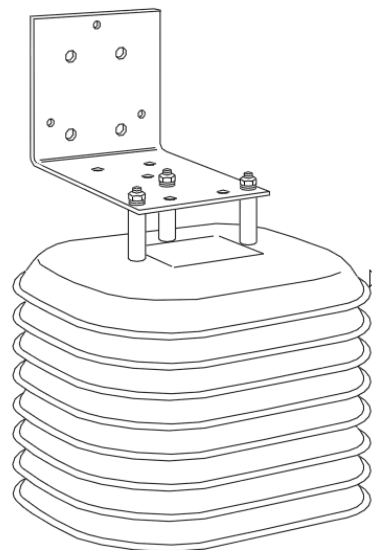
Monitoring Recovery Trends in Key Spring Chinook Habitat Variables and Validation of Population
Viability Indicators

March 2012

Dale McCullough

Casey Justice

Seth White



Davis radiation shield (7714). This is the model used by Onset.

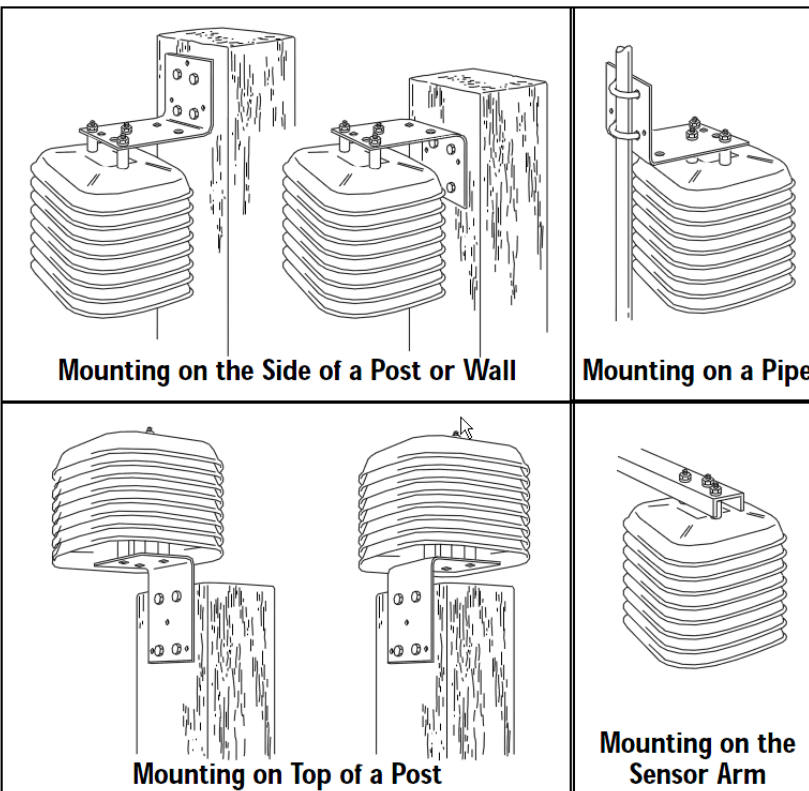
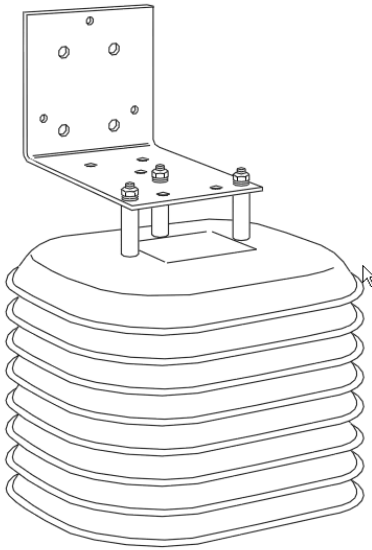
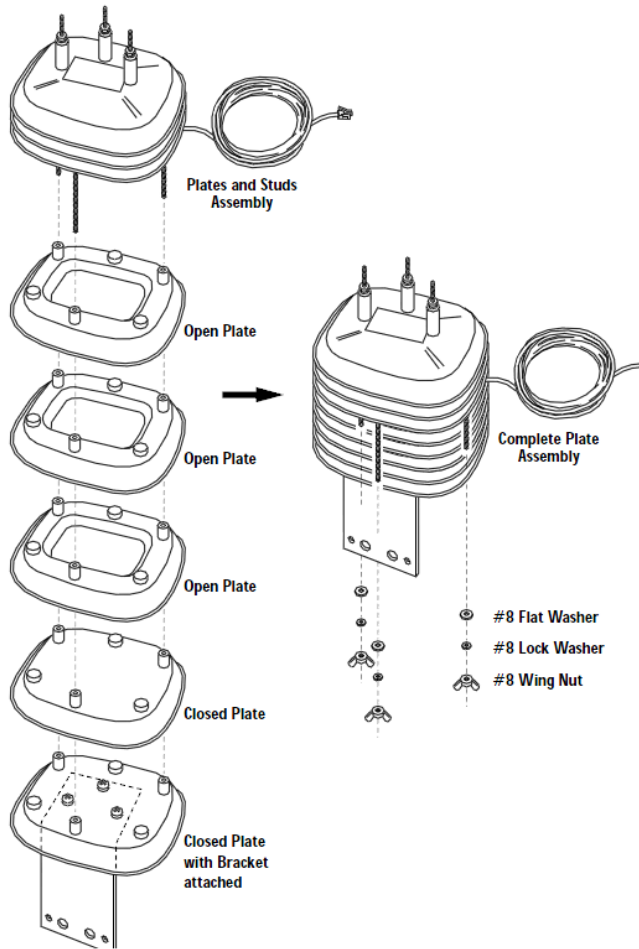


Diagram from the Davis shield manual (similar to what is in the Onset manual) showing how mounting is accomplished.



This diagram illustrates that the bottom plate is closed. The benefit of this would be that radiation reflected from the ground upward into the shield is eliminated. This problem can be severe in winter with snow on the ground where exposed to full sunlight. Also, the most desirable ground cover for temperature sensors is over grass. Surfaces with widely varying albedos can create differences in the way sensors respond. This diagram also illustrates the opening in the center of the series of the device where the temperature sensor would be placed.

XXXXXXXXXXXXXXXXXXXX

RS-1 Radiation shield from Onset

Solar Radiation Shield - RS1



Qty.	1-9	10-99	100+	1
\$US	\$79	\$73	\$67	Add

XXXXXXXXXXXXXXXXXXXXXXXXXXXX

Reina Nakamura and L. Mahrt. 2005. Air Temperature Measurement Errors in Naturally Ventilated Radiation Shields. JOURNAL OF ATMOSPHERIC AND OCEANIC TECHNOLOGY 22:1046-1058.

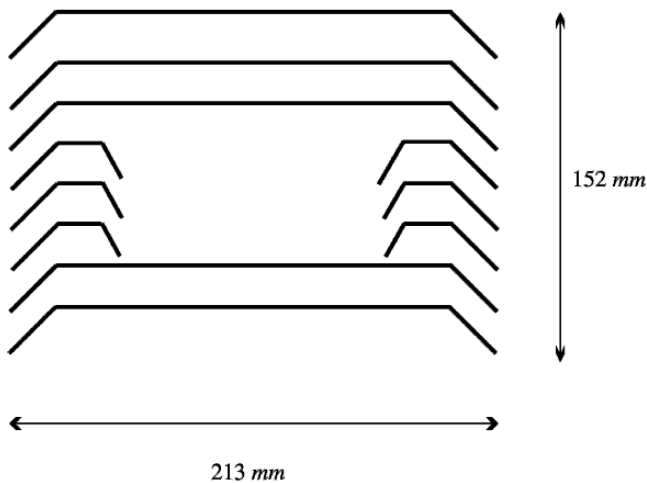


FIG. 3. Cross section of Davis Instruments multiplate shield model 7714 (Onset Computer Radiation Shield RS1). Dimension of the shield is 213 mm (length) \times 188 mm (depth) \times 152 mm (height). Individual plates are 3 mm thick. All of the plates are separated by 15 mm, except for the top two, which are separated by 20 mm. The vertical overlap between a plate and the one underneath is 4 mm.

Ambient Weather SRS100LX Temperature and Humidity Solar Radiation Shield. According to Ambient Weather, this model is for larger sensors than the SRS100. Can be purchased from Amazon.com for Price: **\$44.99**



Also, check Ambient Weather SRS100 Temperature and Humidity Solar Radiation Shield;

Sku: SRS100 **\$35.99**

Phone: 480 - 346 - 3380

<http://www.ambientweather.com/amwesrpatera.html>

[Note: my questions about this shield have to do with:]

- 1) Will our temperature loggers fit inside these housings?
- 2) What is the internal structure of these housings like? Are they comparable to the Onset housings in design? Are they painted black to reduce reflection of sunlight into the housing? Do they allow collection of condensation inside the housing that could affect accurate readings?

XXXXXXXXXXXXXXXXXXXXXXXXXXXX

Matthias Mauder, R. L. Desjardins, Zhiling Gao, And Ronald Van Haarlem. 2008. Errors of Naturally Ventilated Air Temperature Measurements in a Spatial Observation Network. American Meteorological Society. Notes and Correspondence. P. 2145-2151.

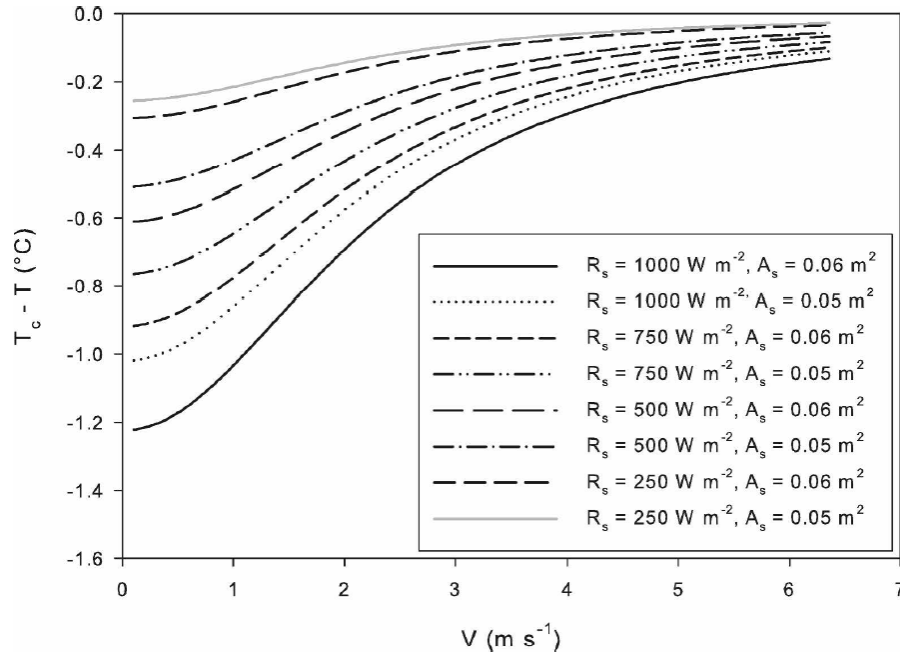


FIG. 2. Difference between corrected and measured HOBO temperature ($T_c - T$) as a function of wind speed V for various combinations of R_s and A_s values.

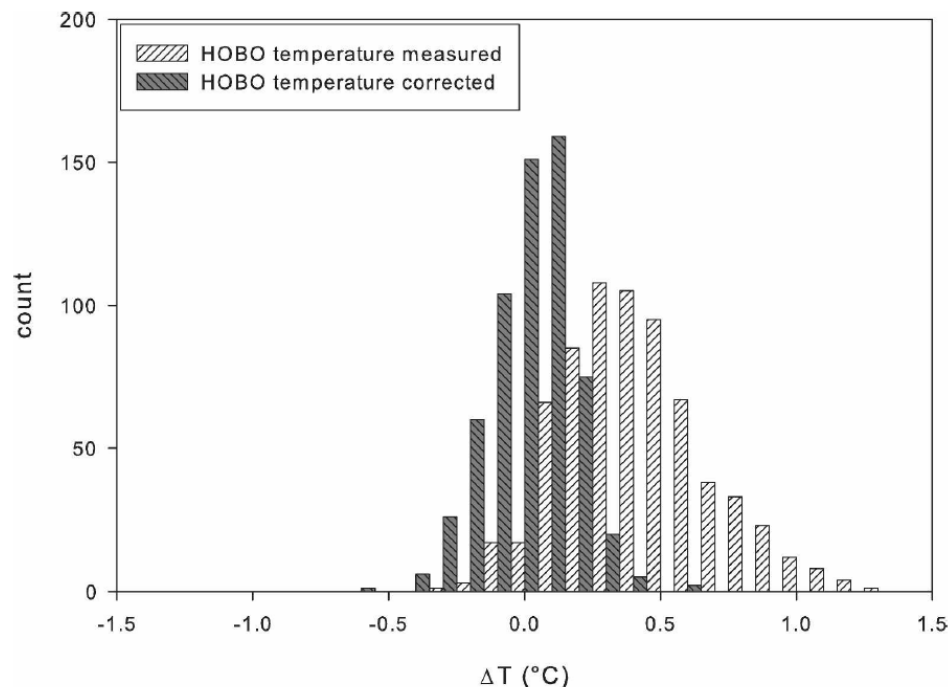


FIG. 4. Histograms of the difference between the HOBOTemperature and the aspirated temperature before and after applying the radiation correction.

Mauder was able to show from a spatially distributed set of Hobo temperature sensors using a HOBOT M-RSA radiation shield the ability to adjust readings for direct radiation intensity and wind speed. The Hobo readings were compared against a high-precision temperature sensor of type 063 (MetOne Instruments, Inc., Grants Pass, Oregon) in an aspirated radiation shield of type 076B, also produced by MetOne. This system served as reference for determining the correction coefficients h_0 , C , and m , since its fan-aspirated shield reduces the radiative error to 0.03°C according to the manufacturer (MetOne Instruments 1997).

The 25 Hobo readings were corrected for wind speed, using local wind speed data. The root mean-square difference between the HOBOTemperature measurements and the fan-aspirated reference measurements was reduced from 0.49° to 0.15°C . The remaining error is only slightly larger than the precision of the HOBOT sensor-shield combinations themselves.

[Note: this comparison is between a Hobo sensor with a commercial Gill shield and a high precision instrument with an aspirated shield (generally considered the most reliable type of shield).]

xxxxxxxxxxxxxxxxxxxxxxxxxxxx

Lundquist, J., and B. Huggett (2008). Evergreen trees as inexpensive radiation shields for temperature sensors, *Water Resour. Res.*, 44, XXXXXX, doi:10.1029/2008WR006979.



Figure 1. An iButton in a funnel radiation shield in a tree.

[1] Evergreen trees provide temperature sensors with shielding from solar radiation and an elevated location above snowfall. Sensors were deployed with simple funnel radiation shields in the Sierra Nevada, California, and Rocky Mountains, Colorado. Compared with unaspirated, Gill-shielded thermistors, inexpensive self-recording temperature sensors hung in dense stands of trees have less than 0.8°C (0.4°C) mean difference in daily maximum (mean) temperature. In contrast, sensors in sparse and isolated trees had a bias of $2\text{--}5^{\circ}\text{C}$ ($0.3\text{--}1.3^{\circ}\text{C}$) in daily maximum (mean) temperature. Sensors on poles were biased $5\text{--}13^{\circ}\text{C}$ ($0.5\text{--}3.0^{\circ}\text{C}$) for daily maximum (mean) temperatures. In locations with deep winter snowpacks, sensors can be raised high into a tree using a pulley system.

(*Abies lasiocarpa*). All sensors were deployed with an upside-down funnel shield developed by Jason Hubbart (personal communication, 2005), which shielded them from solar radiation from above but not reflected solar radiation from below (Figure 1). The funnel shield is less important than the tree in providing shielding from solar radiation (see section 3) but protects the sensors from rain and snow and helps researchers find the sensors again.

[Note: while the deployment in a dense stand of trees has the advantage of protecting the sensor from direct solar radiation, it might be vulnerable to upward radiation from a snowpack and the ground. For this reason, I would think the use of a Gill type shield that protects from upward radiation would be warranted.]

5. Conclusions

[11] Evergreen trees provide shielding from solar radiation for temperature sensors, with average biases less than 0.4°C for T_{mean} and 0.8°C for T_{max} , as compared to naturally ventilated Gill-shielded thermistors. Thus, trees provide a cost-effective way to distribute inexpensive, self-recording temperature sensors. Sensors placed on poles above treeline are likely to be exposed to large amounts of solar radiation, with average warm biases of 2°C for T_{mean} and 8°C for T_{max} . The difference in temperature between a sensor placed in a tree and one placed on a pole is correlated with changes in solar radiation and thus provides proxy information about cloud cover.

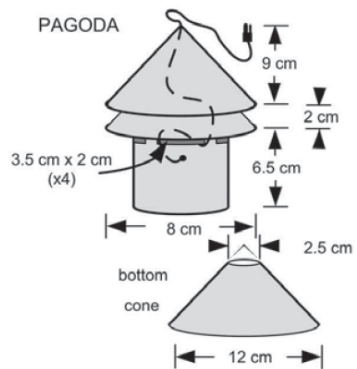
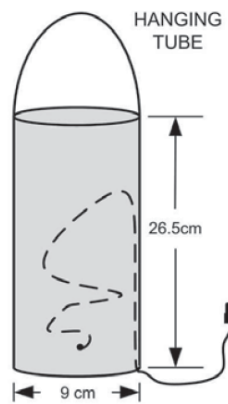
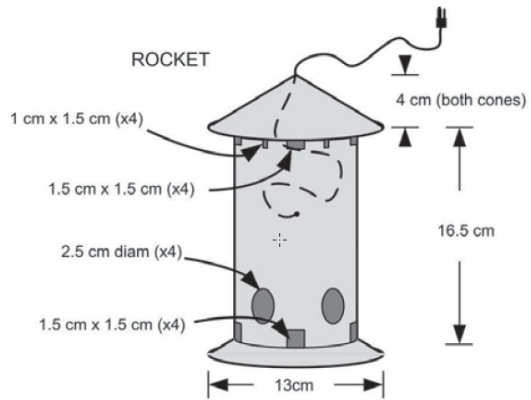
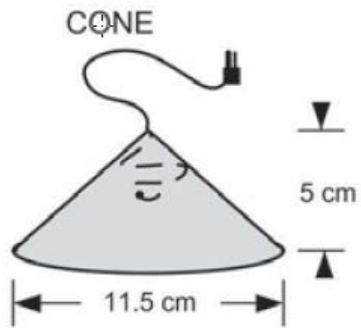
[12] **Acknowledgments.** Thanks are due to John Selker, Bob Westfall, and three anonymous reviewers for providing editorial guidance. Thanks are due to Mark Losleben, Caitlin Rochford, and Dave Clow for temperature deployment help in the Rocky Mountains. Thanks are due to Lucia Harrop and Jenn Kelly for help with funnel shield construction. Thanks are due to Janneke Hille Ris Lambers for help developing the pulley system for temperature sensor deployments. This work was supported by a University of Colorado, Boulder and NOAA Western Water Assessment–sponsored CIRES Innovative Research Grant, and by the National Science Foundation under grant CBET-0729838.

[Note: this publication was reviewed by John Selker, a professor at OSU in Corvallis who is well known for innovations in temperature sensor technology, so it has received top-notch peer review. So, I would conclude from this that the suggestion that suspending an air temperature sensor in a dense stand of conifers is a reasonable way to shield a sensor, even though it goes against the conventional recommendations, such as below:]

Julie M. Tarara and Gwen-Alyn Hoheisel. 2007. Low-cost Shielding to Minimize Radiation Errors of Temperature Sensors in the Field. *HORTSCIENCE* 42(6):1372–1379. 2007.

Additional index words. Gill shield, solar, global irradiance, reflectance, albedo, aspiration, thermocouple, relative humidity

Abstract. The importance of shielding temperature sensors from solar radiation is understood, but there is a lack of prescriptive advice for plant scientists to build inexpensive and effective shields for replicated field experiments. Using the general physical principles that govern radiation shielding, a number of low-cost, passively ventilated radiation shields built in-house was assessed for the measurement of air temperature against the same type of sensor in a meteorological “standard” Gill radiation shield. The base shield material had high albedo (≈ 0.9) and low emissivity (0.03). Aspirated shields were included for simultaneous measurements of temperature and relative humidity. Differences in air temperature (ΔT) between low-cost shields and the standard Gill were greatest for shields with open bottoms (up to $+7.4^\circ\text{C}$) and for those with poorly perforated sidewalls. Open-bottomed shields were prone to heating from reflected radiation. Tube-shaped shields appeared to require more than 30% sidewall perforation for convection by ambient wind (up to $4\text{ m}\cdot\text{s}^{-1}$) to offset the midday radiation load of the shield. The smallest daytime ΔT were between aspirated shields and the standard Gill, averaging less than $\pm 0.5^\circ\text{C}$. Among passively ventilated shields, the smallest daytime ΔT consistently were produced by a shield that emulated the stacked plate design of the standard Gill for a total of U.S. \$4.00 in materials and 45 min construction time. Eighty-nine percent of all daytime ΔT for the “homemade Gill” shield was 1.5°C or less. The combination of low ambient wind speed (less than $1\text{ m}\cdot\text{s}^{-1}$) and high global irradiance (greater than $600\text{ W}\cdot\text{m}^{-2}$) produced the largest ΔT for all passively ventilated shields, the magnitude of which varied with shield design; stacked plate configurations were more effective shields than were tube-based configurations. Night-time ΔT were inconsequential for all shields. Cost-effective radiation shielding can be achieved by selecting shield materials and a configuration that minimize daytime radiation loading on the shield while maximizing the potential for convective transfer of that radiation load away from the shield and the sensor it houses.



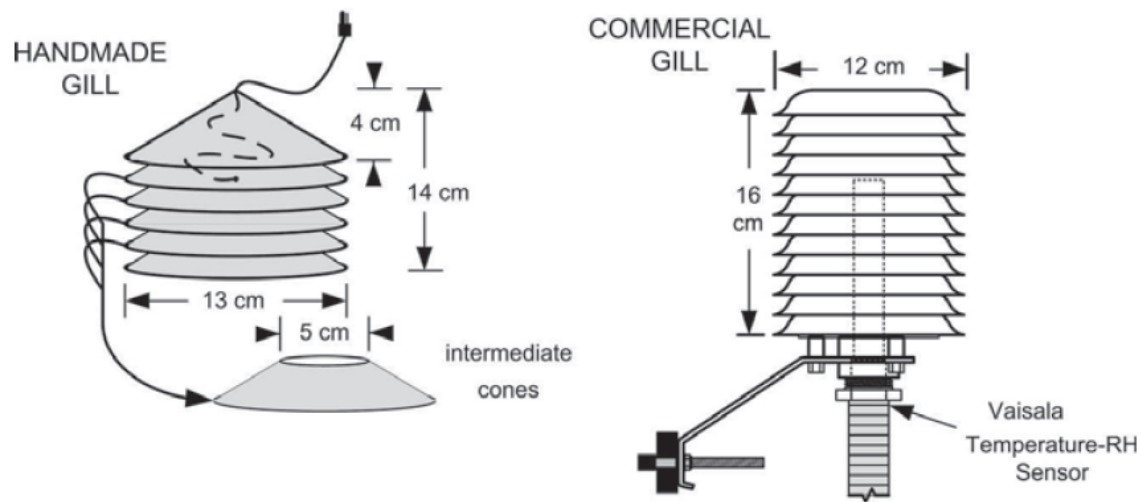


Fig. 1. Schematic diagrams of plate-shaped, passively ventilated radiation shields. The commercial Gill shield housed both a thermocouple and a temperature–relative humidity sensor. All in-house built shields housed a thermocouple, the location of which is denoted by the dashed line (lead wire) and black dot (junction).

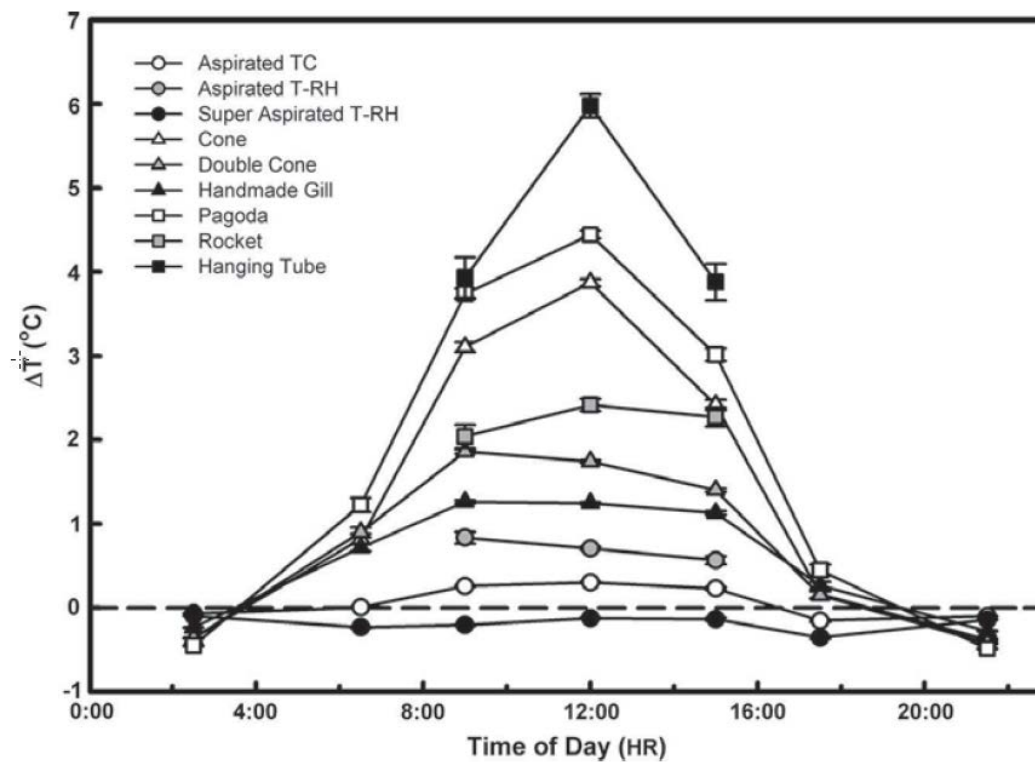


Fig. 5. Mean difference in measured air temperature (ΔT) between sensors in an experimental radiation shield and the same type of sensor in a standard commercial Gill shield for each of seven periods into which the day was divided. Symbols are plotted at the midpoint of the period (HR). Error bars represent ± 1 SE.

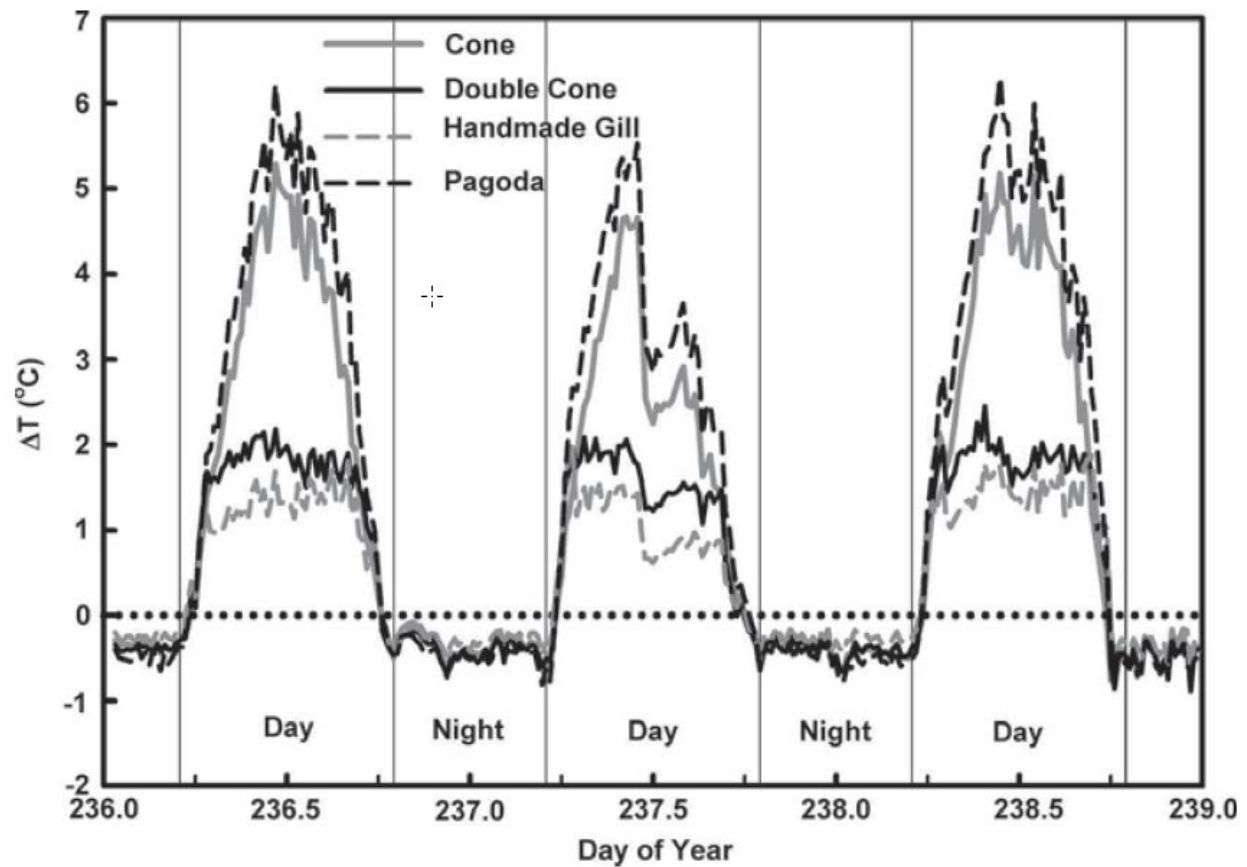


Fig. 6. Difference in measured air temperature (ΔT) between sensors in a passively ventilated experimental radiation shield and the same type of sensor in a standard commercial Gill shield over three exemplary days with clear skies and maximum global irradiance of 800 to 830 $\text{W}\cdot\text{m}^{-2}$. Vertical lines demarcate day (periods 2 to 6) and night (periods 1, 7).

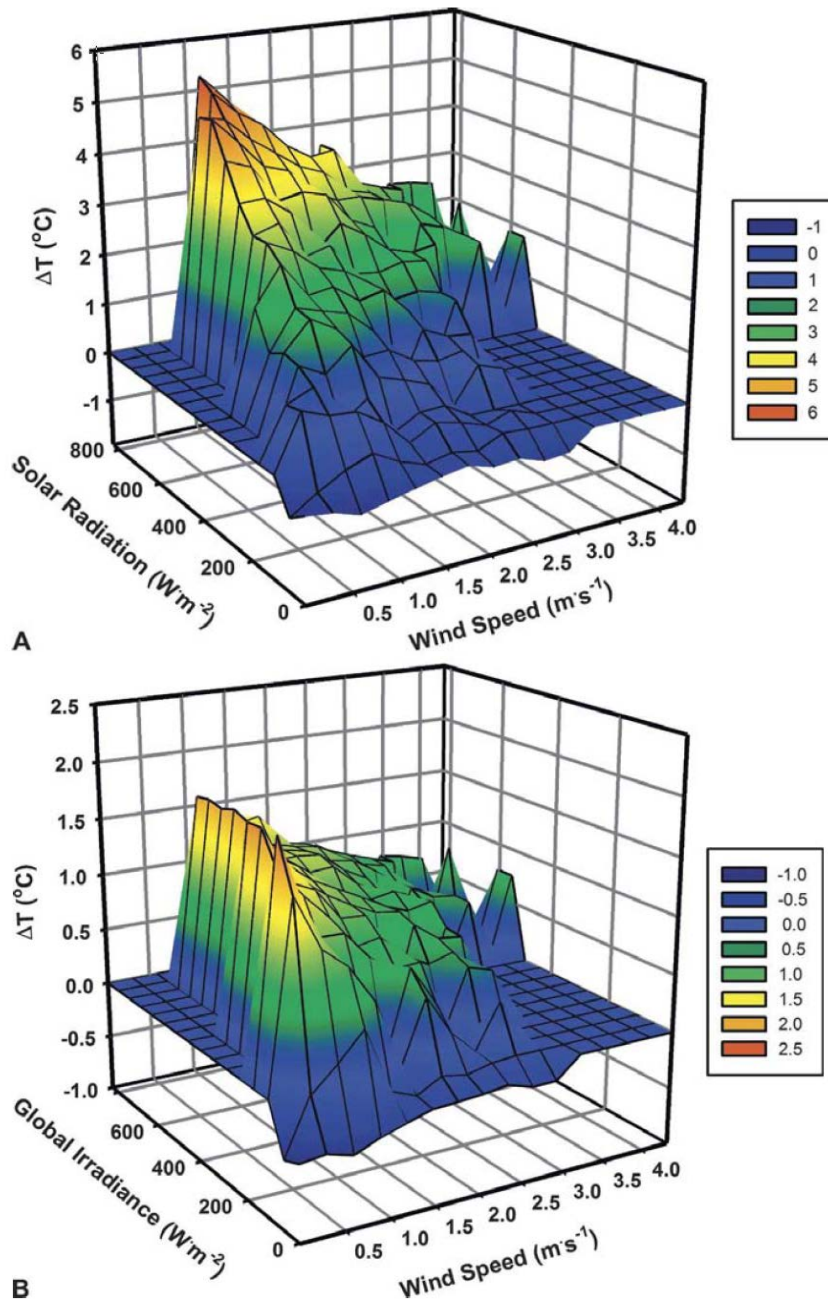


Fig. 7. Response surface of the difference in measured air temperature (ΔT) between sensors in an experimental radiation shield and the same type of sensor in a standard commercial Gill shield against the two main driving forces of ΔT , solar radiation [global irradiance (R_g)] and wind speed. (A) Cone shield, the simplest plate configuration, with an open bottom. (B) Handmade Gill shield, a low-cost mockup of a standard commercial Gill shield.

This paper by Tarara and Hoheisel shows a few key things. As the solar radiation increases and the wind speeds decrease, the deviation in temperature readings between the low cost cone shield and the commercial Gill shield becomes large. For reference, 1 m/sec = 2.24 mph. 3 m/sec = 6.7 mph.

Also, most of their handmade shields had temperature deviations from the Commercial Gill shield of up to 6 $^{\circ}\text{C}$.

The open-bottomed cone, like many of the non-Gill designs, performed poorly. Lundquist used an open-bottomed cone, but hers was suspended in a dense conifer stand, so most of the radiation shielding was provided by the tree. The shield served to keep the weather off the sensor. However, it seems that the performance of this sensor would be better in all seasons if it had a shielded bottom like the Gill designs.

XXXXXXXXXXXXXXXXXXXX

Evyatar Erell, Vitor Leal, Eduardo Maldonado. ON THE MEASUREMENT OF AIR TEMPERATURE IN THE PRESENCE OF STRONG SOLAR RADIATION

“The effects of radiant exchange on thermometer readings of air temperature were recognized over 150 years ago, and eventually led to the design of the Stevenson screen in 1864. This white wooden cupboard has since become the standard instrument screen, whereby indirect ventilation is provided through the bottom, double roof and louvered sides, and thermometers placed within it give a close approximation to the true air temperature, undisturbed by the effects of direct solar or terrestrial radiation. However, the Stevenson screen is unsuitable for many applications: It is too bulky to be portable; it is too large for measurements in confined spaces; it is too obtrusive to be installed in locations accessible to the public; it may be considered too expensive when a large number of screens is required for simultaneous measurements in different locations; and it does not give full protection from radiant exchange (WMO, 1971). Many other thermometer screens have been shown to introduce measurement error, too (Sparks, 1972; Andersson and Mathisson, 1992; Van der Meulen, 1998), so where electric power is available, aspirated sensors may be preferable: they can provide extremely accurate temperature readings. However, while aspirated sensors may be more accurate than non-aspirated ones, they are expensive, and their dependence on electric power is a limitation.

A variety of instrument screens are currently available. However, while temperature sensors are generally calibrated carefully and their accuracy is specified in most research papers, there is no standard procedure for assessing the effect of instrument screens on radiant exchange, and hence on the accuracy of the resulting readings. Furthermore, although changes in instrumentation (including screen) at a meteorological station are usually accompanied by a homogeneization procedure, comparison of data from non-adjacent stations using different types of screens is troublesome and prone to error.”

3. EXPERIMENTAL EVALUATION

Copper-constantan thermocouples with a wire diameter of about 0.5mm and junction diameter of about 1.2mm were used to measure air temperature in a location exposed to the sun and under an adjacent shed open on all sides, exposed to diffuse radiation only. In a period with light wind ($\bar{u}=3\text{m/s}$), global radiation of about 570W/m^2 and diffuse radiation of only 70W/m^2 , the exposed sensor showed a temperature that was about 2.2K warmer, but was about 0.3K cooler at night.

The performance of a variety of instrument screens was then evaluated by comparison of concurrent temperature readings from sensors in these screens and in a standard Stevenson screen. Two commercial screens were included in the sample: This selection is of course by no means exhaustive - it was merely intended to illustrate the differences in temperature readings even in screens produced by the same manufacturer. The thermistors used in this case, though small, were substantially larger than the TC used previously: they are disc-shaped, with a diameter of 3mm and thickness of about 1.5mm. The sensors have a dark maroon color, with an estimated solar absorptivity of 0.7.

- - - - -

Passively ventilated instrument shields are apparently incapable of providing protection from radiant exchange that is sufficient to ensure highly accurate temperature measurement in all conditions. In the absence of calibration procedures for instrument screens – and sufficiently detailed meteorological information on-site to assess the likely measurement error – the best approach to achieving accurate temperature measurement in the presence of high levels of radiation would appear to be the use of very small sensors. As the analysis in the first part of this article shows, the surface convective heat exchange coefficient depends on the size of the sensor. If the sensor diameter is less than about 0.2mm, the error from full exposure to bright sunshine is estimated to be less than 0.3K, even at very low ambient wind speed. Such small sensors may be suitable for use in restricted spaces where a radiation shield is too bulky, or where the presence of the shield would alter conditions, especially air flow, to an extent that is unacceptable.

[This conclusion has been suggested in other studies also. The size of the sensor has a lot to do with the effectiveness of any screen. Because we are using sensors that are internal to an Onset datalogger, I doubt that we benefit from having a sensor of very small dimension, which I think means a bare, small wire sensor that is connected by wire to a data logger.]

Designs for jury-rigged thermometer screens

The makeshift screens tested may be classified into three general categories (below), according to the means of providing the sensor with ventilation. Additional variations included the type of exterior finish (glossy white or aluminum foil), and modifications to the basic form to improve protection from direct radiation:

- *Vertical pipes* (cases 1-9): 50mm or 75mm PVC (or cardboard) pipes, with T-section at top. Some variants had a second external 110mm pipe, creating a double-barreled screen. Exterior finish - aluminum foil or glossy white paint. This type of screen was expected to allow efficient convective air flow, but less exposure to horizontal flow (wind).
- *Horizontal pipes* (cases 10-12): 75mm PVC pipes 50cm long; External finish – aluminum foil or glossy white paint. One variant had lightweight cardboard louvers added to both ends. This type of screen was expected to allow efficient exposure to wind, but relatively poorer exposure to vertical flows.
- *Multi-plate gill-type* (cases 13-14): Inverted plastic bowls with the center cut out to create a cavity for the sensor (except in the top and bottom bowls), attached by means of threaded metal rods, with thin plastic pipes serving as spacers to maintain a 30mm gap for ventilation. Exterior finish: glossy white. Interior: matt black. This type of screen, which is also used in most commercial designs, allows multi-directional horizontal air flow, but restricts vertical flow to a certain extent.

Table 1 summarizes the performance of the various instrument screen in comparison with the Stevenson screen:

#	Description of shield	Difference in temp. vs. Stevenson screen [°C]			
		mean	max	min	stdev
1	Vertical pipe: 50mm, T top, white	0.44	2.85	-1.78	1.77
2	Vertical pipe: 50mm, T top, alum foil	0.78	6.76	-1.92	2.15
3	Vertical pipe: 75mm, T top, white	0.80	5.19	-1.69	1.83
4	Vertical pipe: 50mm, T top, insulation + alum foil	0.44	3.77	-1.79	1.52
5	Vertical pipe: 50mm, white, T top & bottom	0.52	3.71	-1.15	1.17
6	Double vertical pipe: internal 50mm, external 110mm, alum foil	0.65	3.76	-1.25	1.32
7	Double vertical pipe: internal perforated 50mm, external 110mm, alum foil	0.45	2.98	-1.63	1.11
8	Double vertical pipe: internal 50mm, external 110mm, alum foil, bottom cone	0.37	2.78	-1.51	1.06
9	Inverted styrofoam cup + alum foil	2.59	10.56	-1.25	3.54
10	Horizontal pipe: 75mm diameter, 500mm long, white	0.33	4.47	-2.06	1.63
11	Horizontal pipe: 75mm diameter, 500mm long, alum foil	0.22	2.25	-1.40	0.77
12	Horizontal pipe: 75mm diameter, 500mm long, alum foil, louvers at both ends	0.87	4.78	-1.10	1.61
13	Gill type: 150mm dia. Inverted bowls, 30mm spacing	0.00	1.76	-1.40	0.65
14	Gill type: 122mm dia. Inverted bowls, 30mm spacing	0.08	2.04	-1.28	0.79
15	Commercial gill - "Type A": 170mm anodized aluminum	0.40	2.81	-1.30	1.08
16	Commercial gill - "Type B": 120mm white plastic	0.36	2.38	-1.03	0.87

- Exposure to horizontal airflow may be more efficient than exposure to vertical flow: The best designs were those that comprised horizontal pipes or gill-plates, rather than vertical pipes.
- The use of shiny aluminum foil at the external surface resulted in lower daytime temperatures than white paint, as illustrated by comparing the two horizontal pipes (#10 and #11), which were otherwise identical. Concurrently, the lower infra red emissivity of the aluminum foil also resulted in higher night-time temperatures, as radiant loss from this shield was less efficient than in the white-painted version.
- Temperature readings in two makeshift gill-type shields were very close to those of commercial screens of similar construction. However, a simple PVC pipe 50cm long and 75mm in diameter, covered with aluminum foil and suspended horizontally, gave similar readings – and is much easier to construct.

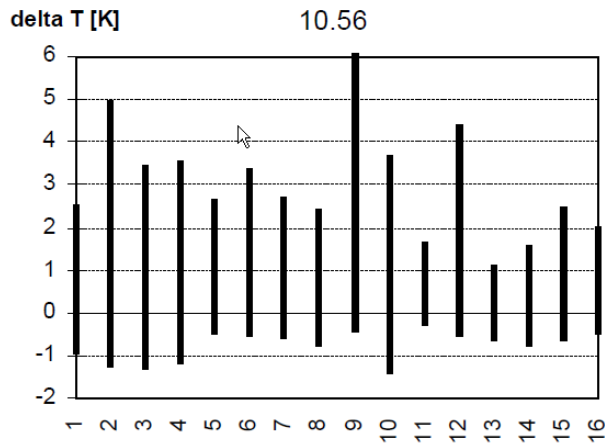


Figure 3: Accuracy of screens

[Note: shields such as No. 11, 13, and 14 above seem to perform well compared to the same sensors in a Stevenson shield. It is possible that we could create our own Gill type shields. Otherwise, something that may be equivalent could be purchased relatively cheaply from Ambient Weather.]

XXXXXXXXXXXXXXXXXXXX

Site Selection for Installation of an Air Temperature Sensor

WORLD METEOROLOGICAL ORGANIZATION. 2006. Guide to Meteorological Instruments and Methods of Observation Preliminary seventh edition. WMO-No. 8. Secretariat of the World Meteorological Organization – Geneva – Switzerland.

1.3.3.1 SITE SELECTION

Meteorological observing stations are designed to enable representative measurements (or observations) to be made according to the type of station involved. Thus, a station in the synoptic network should make observations to meet synoptic-scale requirements whereas an aviation meteorological observing station should make observations that describe the conditions specific to the local (aerodrome) site. Where stations are used for several purposes, e.g. aviation, synoptic and climatology, the most stringent requirement will dictate the precise location of an observing site and its associated sensors. A detailed study on siting and exposure is published by WMO (1993 *a*).

As an example, the following considerations apply to the selection of site and instrument exposure requirements for a typical synoptic or climatological station in a regional or national network:

- (a) Outdoor instruments should be installed on a level piece of ground, approximately 10 metres by seven metres (the enclosure), covered with short grass or a surface representative of the locality, and surrounded by open fencing or palings to exclude unauthorized persons. Within the enclosure, a bare patch of ground about two metres by two metres is reserved for observations of the state of the ground and of soil temperature at depths of equal or less than 20 centimetres (Chapter 2 in this Part); soil temperatures at depths larger greater than 20 cm can be measured outside this bare patch of ground); a good example of the layout of such a station is given in Figure 1.1 (taken from WMO, 1989);
- (b) There should be no steeply sloping ground in the vicinity and the site should not be in a hollow. If these conditions are not complied with, the observations may show peculiarities of entirely local significance;
- (c) The site should be well away from trees, buildings, walls or other obstructions. The distance of any such obstacle (including fencing) from the raingauge should not be less than twice the height of the object above the rim of the gauge, and preferably four times the height;

[note: The WMO is the standard reference for meteorological investigations. We have located sensors on sloping ground; under trees; in hollows. These installations may be unavoidable in our work and maybe for our purposes we want to know what kinds of air temperatures are actually occurring near our streams.]

Sources of Error

- (d) The effectiveness of the heat transfer between the thermometer element and the air in the thermometer shelter, which should ensure that the element is at thermal equilibrium with the air (related to system time constant or lag coefficient). In a well-designed aspirated shelter this error will be very small, but it may be large otherwise;
- (e) The effectiveness of the thermometer shelter, which should ensure that the air in the shelter is at the same temperature as the air immediately surrounding it. In a well-designed case this error is small, but the difference between an effective and an ineffective shelter may be 3°C or more in particular circumstances;
- (f) The exposure, which should ensure that the shelter is at a temperature which is representative of the region to be monitored. Nearby sources and sinks of heat (buildings, other unrepresentative surfaces below and around the shelter) and topography (hills, land-water boundaries) may introduce large errors. The station metadata should contain a good and regularly updated description of the exposure (see Annex 1.C) to inform data users about possible exposure errors.

XXXXXXXXXXXXXXXXXXXX

Zack Holden wrote a blog report for his work for the USFS in which he recommended his corrugated plastic housings that CHaMP had used in 2011.

Xxxxxxxxxxxxx

Shield providers:

Onset

<http://www.onsetcomp.com/products/mounting/rs3>

R.M. Young radiation shield

<http://www.youngusa.com/products/2/11.html>

This shield seems to provide cable hookups used by high performance systems that would not apply to our needs.

Davis shield

http://www.davisnet.com/weather/products/weather_product.asp?pnum=07714

Ambient Weather

<http://www.ambientweather.com/amwesrpatera.html>

My concern about this is whether it is constructed well and has all the technical features found in shields such as sold by Onset. Does it adequately reduce light penetration internally into the shield? Is the plastic made of materials that provide good reflective characteristics? Is it capable of accepting a temp logger such as we have been using? How does it open up to receive the logger?

Appendix G.

Upper Grande Ronde River Basin Stream Temperature Modeling

Upper Grande Ronde River Basin Stream Temperature Modeling



Prepared for:

Columbia River Inter-Tribal Fish Commission

729 NE Oregon Street, Suite 200
Portland, Oregon 97232

Prepared by:

Watershed Sciences, Inc.

529 SW Third Avenue, Suite 300
Portland, OR 97204



- DRAFT - August 3, 2011

TABLE OF CONTENTS

1. Overview and Scope	1
2. Data Summary	2
2.1 Remote Sensing Data	2
2.1.1 LiDAR.....	2
2.1.2 Thermal Infrared.....	6
2.2 Ground Level Data	9
2.2.1 Hourly Temperature Data	9
2.2.2 Seasonal Variation.....	10
2.2.3 Instantaneous Flow Data	11
2.2.4 Gaged Flow Data.....	12
2.2.5 Climate Data	13
3. GIS Data Sampling for Heat Source Input - TTools.....	15
3.1 Stream Mapping	17
3.2 Wetted Edge Mapping	18
3.3 Active Channel Mapping	19
3.4 Near Stream Land Cover Mapping.....	20
3.5 Automated GIS Sampling - TTools.....	21
3.5.1 TTools Step 1	21
3.5.2 TTools Step 2	22
3.5.3 TTools Step 3	22
3.5.4 TTools Step 4	23
3.5.5 TTools Step 5	24
3.5.6 TTools Step 6	25
4. Heat Source Overview	26
5. North Fork Catherine Creek.....	32
5.1 North Fork Catherine Creek TTools.....	33
5.2 North Fork Catherine Creek Heat Source Calibration	36
6. South Fork Catherine Creek.....	41
6.1 South Fork Catherine Creek TTools Results.....	42
6.2 South Fork Catherine Creek Heat Source Calibration	45
7. Milk Creek	50
7.1 Milk Creek TTools Results	51
7.2 Milk Creek Heat Source Calibration Results	54
8. Little Catherine Creek	58
8.1 Little Catherine Creek TTools Results.....	59
8.2 Little Catherine Creek Effective Shade Simulation	62

9. Little Creek	64
9.1 Little Creek TTools Results.....	65
9.1 Little Creek Heat Source Calibration Results	68
10. Ladd Creek	73
10.1 Ladd Creek TTools Results	74
10.2 Ladd Creek Effective Shade Simulation	77
11. Catherine Creek	80
11.1 Catherine Creek TTools Results.....	81
11.2 Catherine Creek Heat Source Calibration Results	84
12. Clear Creek	90
12.1 Clear Creek TTools Results	91
12.2 Clear Creek Heat Source Calibration Results	94
13. Limber Jim Creek	98
13.1 Limber Jim Creek TTools Results	99
13.2 Limber Jim Creek Heat Source Calibration Results.....	102
14. Chicken Creek	107
14.1 Chicken Creek TTools Results	108
14.2 Chicken Creek Heat Source Calibration Results.....	112
15. Sheep Creek	116
15.1 Sheep Creek TTools Results	117
15.2 Sheep Creek Heat Source Calibration Results	120
16. Fly Creek	125
16.1 Fly Creek TTools Results	126
16.2 Fly Creek Heat Source Calibration Results.....	129
17. McCoy Creek	134
17.1 McCoy Creek TTools Results	135
17.2 McCoy Creek Heat Source Calibration Results.....	138
18. Meadow Creek	140
18.1 Meadow Creek TTools Results.....	141
18.2 Meadow Creek Heat Source Calibration Results	144
19. Beaver Creek	151
19.1 Beaver Creek TTools Results	152
19.2 Beaver Creek Heat Source Calibration Results	155
20. Five Points Creek	160
20.1 Five Points Creek TTools Results	161
20.2 Five Points Creek Heat Source Calibration Results.....	164
21. Grande Ronde River	169
21.1 Grande Ronde River TTools Results	170
21.2 Grande Ronde River Heat Source Calibration Results.....	173

LIST OF FIGURES

Figure 1 - Streams of interest in the upper Grande Ronde River subbasin.....	1
Figure 2 - LiDAR data coverage.	2
Figure 3 - LiDAR point cloud cross section over Beaver Creek.	3
Figure 4 - LiDAR point cloud with RGB extraction (top) and bare earth digital terrain model (bottom). .	4
Figure 5 - LiDAR digital elevation model of the Grande Ronde River near Hilgard.	5
Figure 6 - TIR data extents.	6
Figure 7 - Example of a TIR longitudinal stream temperature profile.	6
Figure 8 - Example of TIR imagery.	7
Figure 9 - Example of TIR imagery overlaid on LiDAR bare earth DTM.	8
Figure 10 - Example of TIR imagery where there is an active diversion.....	8
Figure 11 - Hourly stream temperature monitoring locations.	9
Figure 12 - Example of hourly temperature data collected by CRITFC.	9
Figure 13 - Grande Ronde River stream temperature variability during the summer of 2010.....	10
Figure 14 - Catherine Creek stream temperature variability during the summer of 2010.	10
Figure 15 - Instantaneous flow measurement locations.	11
Figure 16 - Flow gage locations.	12
Figure 17- Climate station locations.	13
Figure 18 - Hourly cloud cover values recorded at La Grande airport.	13
Figure 19 - Hourly air temperature, relative humidity and wind speed data.....	14
Figure 20 - TTools sampling extents	15
Figure 21 - General workflow to prepare Heat Source model inputs.	16
Figure 22 - Raw stream polyline.	17
Figure 23 - Smoothed stream polyline.	17
Figure 24 - Stream polyline overlaid on LiDAR intensity image.	18
Figure 25 - Estimated wetted area based on LiDAR intensity image.	18
Figure 26 - Wetted channel edges (yellow) and active channel edges (red).	19
Figure 27 - Manually digitized near stream land cover polygons.	20
Figure 28 - 50-meter stream segments (yellow dots).	21
Figure 29 - Stream channel edges and the TTools point shapefile.	22
Figure 30 - Stream elevations sampled at each 50-meter node.	22
Figure 31 - Topographic features to the west (green triangles), south (red circles) and east (white squares).	23
Figure 32 - Near stream land cover radial sampling pattern.	24
Figure 33 - Example of 50-meter stream nodes and TIR data points.....	25
Figure 34 - Parameters included within the Heat Source methodology.	26
Figure 35 - Example of the TTools data input worksheet in Heat Source.	27
Figure 36 - Example of the continuous data input worksheet in Heat Source.....	28
Figure 37 - Example of the morphology data input worksheet in Heat Source.....	28
Figure 38 - Example of the longitudinal temperature output worksheet in Heat Source.	29
Figure 39 - Example of the hydraulics output worksheet in Heat Source.	30
Figure 40 - Example of heat flux output worksheet in Heat Source.....	31
Figure 41 - North Fork Catherine Creek elevation and gradient.	33
Figure 42 - North Fork Catherine Creek wetted width.....	33
Figure 43 - North Fork Catherine Creek stream aspect.....	34
Figure 44 - North Fork Catherine Creek topographic shade angles.....	34
Figure 45 - North Fork Catherine Creek land cover heights sampled from highest hit LiDAR.	35
Figure 46 - North Fork Catherine Creek TIR temperature profile.....	35
Figure 47 - North Fork Catherine Creek simulation extent.	36
Figure 48 - North Fork Catherine Creek simulated and measured hydraulics values.....	37
Figure 49 - North Fork Catherine Creek simulated and measured daily flow volumes at the gage near Medical Springs.	38
Figure 50 - North Fork Catherine Creek longitudinal stream temperature calibration.	39

Figure 51 - North Fork Catherine Creek simulated effective shade.	40
Figure 52 - South Fork Catherine Creek elevation and gradient.	42
Figure 53 - South Fork Catherine Creek wetted width.	42
Figure 54 - South Fork Catherine Creek stream aspect.	43
Figure 55 - South Fork Catherine Creek topographic shade angles.	43
Figure 56 - South Fork Catherine Creek land cover heights sampled from highest hit LiDAR.	44
Figure 57 - South Fork Catherine Creek TIR stream temperature profile.	44
Figure 58 - South Fork Catherine Creek simulation extent.	45
Figure 59 - South Fork Catherine Creek simulated and measured hydraulic values.	46
Figure 60 - South Fork Catherine Creek simulated daily stream flow at the mouth.	47
Figure 61 - South Fork Catherine Creek simulated and measured stream temperature.	48
Figure 62 - South Fork Catherine Creek simulated and measured hourly temperatures.	48
Figure 63 - South Fork Catherine Creek simulated effective shade.	49
Figure 64 - Milk Creek stream elevation and gradient.	51
Figure 65 - Milk Creek stream aspect.	51
Figure 66 - Milk Creek topographic shade angles.	52
Figure 67 - Milk Creek TIR stream temperature profile.	52
Figure 68 - Milk Creek land cover heights sampled from highest hit LiDAR.	53
Figure 69 - Milk Creek simulation extent.	54
Figure 70 - Milk Creek simulated and measured hydraulic values for 8/19/2010.	55
Figure 71 - Milk Creek simulated daily stream flow at the mouth.	56
Figure 72 - Milk Creek simulated and measured longitudinal temperatures.	56
Figure 73 - Milk Creek simulated and measured hourly temperatures.	57
Figure 74 - Milk Creek simulated effective shade values.	57
Figure 75 - Little Catherine Creek elevation and gradient.	59
Figure 76 - Little Catherine Creek stream aspect.	59
Figure 77 - Little Catherine Creek topographic shade angles.	60
Figure 78 - Little Catherine Creek TIR stream temperature profile.	60
Figure 79 - Little Catherine Creek digitized near stream land cover.	61
Figure 80 - Little Catherine Creek simulation extent.	62
Figure 81 - Little Catherine Creek simulated effective shade.	63
Figure 82 - Little Creek elevation and gradient.	65
Figure 83 - Little Creek stream aspect.	65
Figure 84 - Little Creek topographic shade angles.	66
Figure 85 - Little Creek land cover heights sampled from highest hit LiDAR.	66
Figure 86 - Little Creek TIR stream temperatures.	67
Figure 87 - Little Creek simulation extent.	68
Figure 88 - Little Creek simulated and measured hydraulic values.	69
Figure 89 - Little Creek simulated flow volume at the mouth of Little Creek.	70
Figure 90 - Little Creek simulated and measured longitudinal temperatures.	71
Figure 91 - Little Creek simulated and measured hourly temperatures.	71
Figure 92 - Little Creek simulated effective shade.	72
Figure 93 - Ladd Creek elevation and gradient.	74
Figure 94 - Ladd Creek stream aspect.	74
Figure 95 - Ladd Creek topographic shade angles.	75
Figure 96 - Ladd Creek TIR stream temperature profile.	75
Figure 97 - Ladd Creek digitized near stream land cover.	76
Figure 98 - Ladd Creek simulation extent.	77
Figure 99 - Ladd Creek simulated effective shade.	79
Figure 100 - Catherine Creek elevation and gradient.	81
Figure 101 - Catherine Creek wetted widths.	81
Figure 102 - Catherine Creek stream aspect.	82
Figure 103 - Catherine Creek topographic shade angles.	82
Figure 104 - Catherine Creek land cover heights sampled from highest hit LiDAR.	83
Figure 105 - Catherine Creek TIR stream temperature profile.	83

Figure 106 - Catherine Creek simulation extent.	84
Figure 107 - Catherine Creek simulated and measured hydraulic values.	85
Figure 108 - Catherine Creek simulated and measured daily flow volumes at select locations.	86
Figure 109 - Catherine Creek simulated and measured longitudinal temperatures.	87
Figure 110 - Catherine Creek simulated and measured hourly stream temperatures.	87
Figure 111 - Catherine Creek simulated effective shade values.	89
Figure 112 - Clear Creek elevation and gradient.	91
Figure 113 - Clear Creek stream aspect.	91
Figure 114 - Clear Creek topographic shade angles.	92
Figure 115 - Clear Creek land cover heights sampled from highest hit LiDAR.	92
Figure 116 - Clear Creek TIR stream temperature profile.	93
Figure 117 - Clear Creek simulation extent.	94
Figure 118 - Clear Creek simulated and measured hydraulics values for 8/19/2010.	95
Figure 119 - Clear Creek daily flow volumes at the mouth.	96
Figure 120 - Clear Creek simulated and measured longitudinal temperatures.	96
Figure 121 - Clear Creek simulated and measured hourly temperatures.	97
Figure 122 - Clear Creek simulated effective shade.	97
Figure 123 - Limber Jim Creek elevation and gradient.	99
Figure 124 - Limber Jim Creek stream aspect.	99
Figure 125 - Limber Jim Creek topographic shade angles.	100
Figure 126 - Limber Jim Creek land cover heights sampled from highest hit LiDAR.	100
Figure 127 - Limber Jim TIR stream temperature profile.	101
Figure 128 - Limber Jim Creek simulation extent.	102
Figure 129 - Limber Jim Creek simulated and measured hydraulic values.	103
Figure 130 - Limber Jim Creek simulated flows at the mouth.	104
Figure 131 - Limber Jim Creek simulated and measured longitudinal stream temperatures.	105
Figure 132 - Limber Jim Creek simulated and measured hourly stream temperatures.	105
Figure 133 - Limber Jim Creek simulated effective shade.	106
Figure 134 - Chicken Creek elevation and gradient.	108
Figure 135 - Chicken Creek stream aspect.	108
Figure 136 - Chicken Creek topographic shade angles.	109
Figure 137 - Chicken Creek TIR stream temperature profile.	109
Figure 138 - Chicken Creek digitized near stream land cover.	110
Figure 139 - Chicken Creek simulation extent.	112
Figure 140 - Chicken Creek simulated hydraulic values.	113
Figure 141 - Chicken Creek simulated flow volumes at the mouth.	114
Figure 142 - Chicken Creek simulated and measured longitudinal stream temperatures.	114
Figure 143 - Chicken Creek simulated effective shade.	115
Figure 144 - Sheep Creek elevation and gradient.	117
Figure 145 - Sheep Creek wetted widths.	117
Figure 146 - Sheep Creek stream aspect.	118
Figure 147 - Sheep Creek topographic shade angles.	118
Figure 148 - Sheep Creek land cover heights sampled from highest hit LiDAR.	119
Figure 149 - Sheep Creek TIR stream temperature profile.	119
Figure 150 - Sheep Creek simulation extent.	120
Figure 151 - Sheep Creek simulated and measured hydraulic values.	121
Figure 152 - Sheep Creek simulated flow volumes at the mouth.	122
Figure 153 - Sheep Creek simulated and measured longitudinal stream temperatures.	123
Figure 154 - Sheep Creek simulated and measured hourly stream temperatures.	123
Figure 155 - Sheep Creek simulated effective shade.	124
Figure 156 - Fly Creek elevation and gradient.	126
Figure 157 - Fly Creek wetted widths.	126
Figure 158 - Fly Creek stream aspect.	127
Figure 159 - Fly Creek topographic shade angles.	127
Figure 160 - Fly Creek land cover heights sampled from highest hit LiDAR.	128

Figure 161 - Fly Creek TIR stream temperature profile.	128
Figure 162 - Fly Creek simulation extent.	129
Figure 163 - Fly Creek simulated and measured hydraulic values.	130
Figure 164 - Fly Creek simulated flow volumes at the mouth.	131
Figure 165 - Fly Creek simulated and measured longitudinal stream temperatures.	132
Figure 166 - Fly Creek simulated and measured hourly stream temperatures.	132
Figure 167 - Fly Creek simulated effective shade.	133
Figure 168 - McCoy Creek elevation and gradient.	135
Figure 169 - McCoy Creek stream aspect.	135
Figure 170 - McCoy Creek topographic shade angles.	136
Figure 171 - McCoy Creek land cover heights sampled from highest hit LiDAR.	136
Figure 172 - McCoy Creek TIR stream temperature profile.	137
Figure 173 - McCoy Creek simulation extent.	138
Figure 174 - McCoy Creek simulated effective shade.	139
Figure 175 - McCoy Creek typical terrain and vegetation.	139
Figure 176 - Meadow Creek elevation and gradient.	141
Figure 177 - Meadow Creek wetted width.	141
Figure 178 - Meadow Creek stream aspect.	142
Figure 179 - Meadow Creek topographic shade angles.	142
Figure 180 - Meadow Creek land cover heights sampled from highest hit LiDAR.	143
Figure 181 - Meadow Creek TIR stream temperature profile.	143
Figure 182 - Meadow Creek simulation extent.	144
Figure 183 - Meadow Creek simulated and measured hydraulic values.	145
Figure 184 - Meadow Creek simulated flows at mouth.	146
Figure 185 - Meadow Creek simulated and measured longitudinal stream temperatures.	147
Figure 186 - Meadow Creek simulated and measured hourly stream temperatures.	147
Figure 187 - Meadow Creek simulated effective shade.	150
Figure 188 - Beaver Creek elevation and gradient.	152
Figure 189 - Beaver Creek wetted widths.	152
Figure 190 - Beaver Creek stream aspect.	153
Figure 191 - Beaver Creek topographic shade angles.	153
Figure 192 - Beaver Creek land cover heights sampled from highest hit LiDAR.	154
Figure 193 - Beaver Creek TIR stream temperature profile.	154
Figure 194 - Beaver Creek simulation extent.	155
Figure 195 - Beaver Creek simulated and measured hydraulic values.	156
Figure 196 - Beaver Creek simulated flows at the mouth.	157
Figure 197 - Beaver Creek simulated and measured longitudinal stream temperatures.	158
Figure 198 - Beaver Creek simulated and measured hourly stream temperatures.	158
Figure 199 - Beaver Creek simulated effective shade.	159
Figure 200 - Five Points Creek elevation and gradient.	161
Figure 201 - Five Points Creek wetted widths.	161
Figure 202 - Five Points Creek stream aspect.	162
Figure 203 - Five Points Creek topographic shade angles.	162
Figure 204 - Five Points Creek land cover heights sampled from highest hit LiDAR.	163
Figure 205 - Five Points Creek TIR stream temperature profile.	163
Figure 206 - Five Points Creek simulation extent.	164
Figure 207 - Five Points Creek simulated and measured hydraulic values.	165
Figure 208 - Five Points Creek simulated flow at mouth.	166
Figure 209 - Five Points Creek simulated and measured longitudinal stream temperatures.	167
Figure 210 - Five Points Creek simulated and measured hourly stream temperatures.	167
Figure 211 - Five Points Creek simulated effective shade.	168
Figure 212 - Grande Ronde River elevation and gradient.	170
Figure 213 - Grande Ronde River channel widths.	170
Figure 214 - Grande Ronde River stream aspect.	171
Figure 215 - Grande Ronde River topographic shade angles.	171

Figure 216 - Grande Ronde River TIR stream temperature profile.	172
Figure 217 - Grande Ronde River simulation extent.	173
Figure 218 - Grande Ronde River simulated and measured hydraulic values.	175
Figure 219 - Grande Ronde River simulated and measured flows at the gages.	176
Figure 220 - Grande Ronde River simulated and measured longitudinal stream temperatures.	177
Figure 221 - Grande Ronde River simulated and measured hourly stream temperatures.	177
Figure 222 - Grande Ronde River simulated effective shade.	183

LIST OF TABLES

Table 1 - LiDAR products and their applications for stream temperature modeling.	2
Table 2 - Stream flow gages within the study area.	12
Table 3 - Streams where TTools sampling was completed.	15
Table 4 - TTools steps and data sources.	21
Table 5 - North Fork Catherine Creek general Heat Source parameters.	36
Table 6 - North Fork Catherine Creek mass inflow locations and assumptions.	38
Table 7 - South Fork Catherine Creek general Heat Source parameters.	45
Table 8 - South Fork Catherine Creek mass inflow locations and assumptions.	47
Table 9 - Milk Creek general Heat Source parameters.	54
Table 10 - Little Catherine Creek general Heat Source parameters.	62
Table 11 - Little Catherine Creek land cover codes and descriptions.	63
Table 12 - Little Creek general Heat Source parameters.	68
Table 13 - Little Creek mass inflow features and assumptions.	70
Table 14 - Ladd Creek general Heat Source parameters.	77
Table 15 - Ladd Creek near stream land cover codes and descriptions.	78
Table 16 - Catherine Creek general Heat Source parameters.	84
Table 17 - Catherine Creek mass inflow and outflow features and assumptions.	86
Table 18 - Clear Creek general Heat Source parameters.	94
Table 19 - Limber Jim Creek general Heat Source parameters.	102
Table 20 - Limber Jim Creek mass inflow features and assumptions.	104
Table 21 - Chicken Creek near stream land cover codes and descriptions.	111
Table 22 - Chicken Creek general Heat Source parameters.	112
Table 23 - Sheep Creek general Heat Source parameters.	120
Table 24 - Chicken Creek mass inflow feature and assumption.	122
Table 25 - Fly Creek general Heat Source parameters.	129
Table 26 - Fly Creek mass inflows and assumptions.	131
Table 27 - McCoy Creek general Heat Source parameters.	138
Table 28 - Meadow Creek general Heat Source parameters.	144
Table 29 - Meadow Creek mass inflow features and assumptions.	146
Table 30 - Beaver Creek general Heat Source parameters.	155
Table 31 - Beaver Creek mass inflow features and assumptions.	157
Table 32 - Five Points Creek general Heat Source parameters.	164
Table 33 - Five Points Creek mass inflow features and assumptions.	166
Table 34 - Grande Ronde River general Heat Source parameters.	173
Table 35 - Grande Ronde River mass inflow and outflow features and assumptions.	176

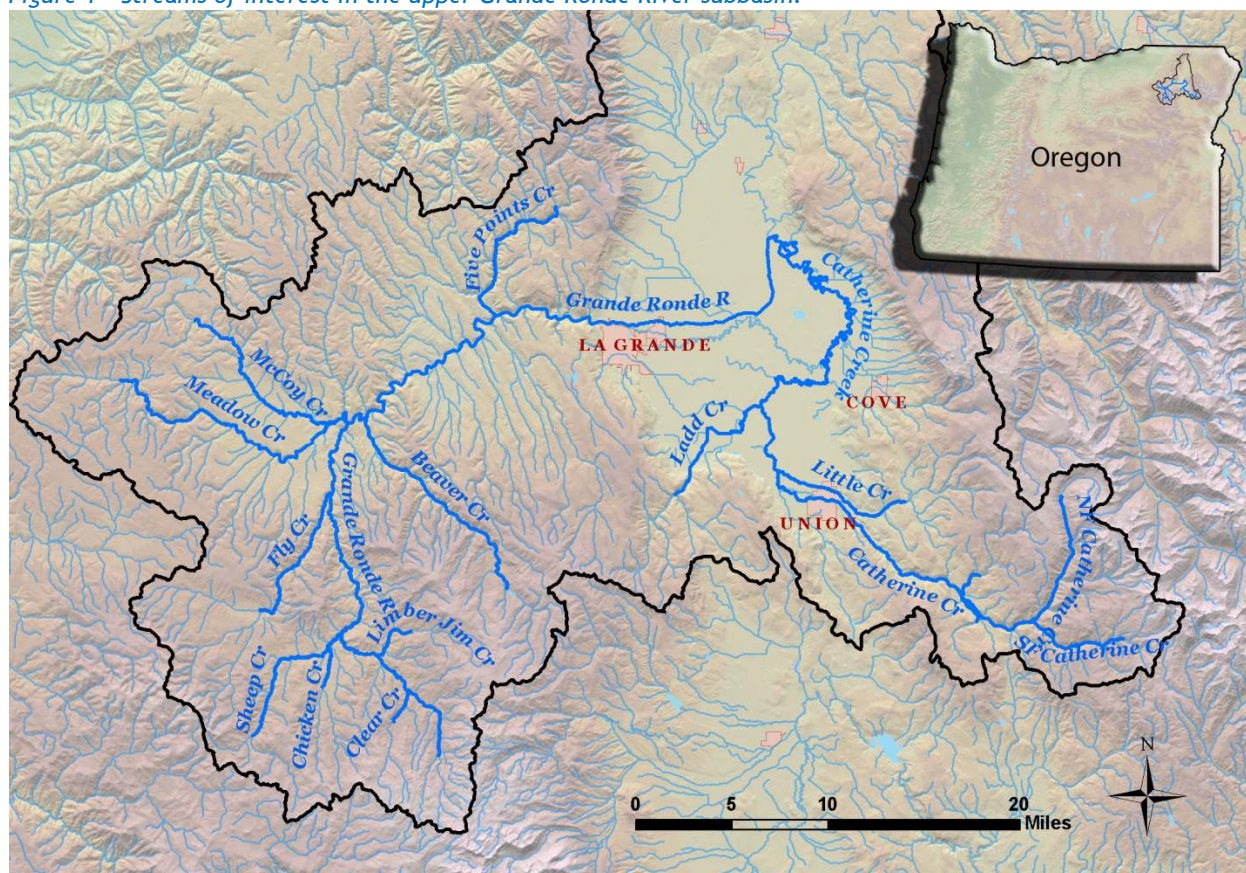
1. OVERVIEW AND SCOPE

The Columbia River Inter-Tribal Fish Commission (CRITFC) contracted with Watershed Sciences, Inc. (WSI) to collect LiDAR and thermal infrared data and simulate stream temperature in the upper Grande Ronde River subbasin in northeastern Oregon. This report summarizes the remote sensing and ground level data and describes the stream temperature modeling results.

The goal of the project was to collect high-resolution landscape and water quality data for use in the Heat Source stream temperature model. Stream temperature was simulated for the Grande Ronde River, Catherine Creek, and several of their tributaries for a 3-week period between August 6 and August 27, 2010. The simulation period is representative of low-flow and high stream temperature conditions, when salmonid habitat is at its most critical condition. Potential near stream vegetation conditions were then incorporated into the models in order to simulate stream temperatures after restoration.

Figure 1 shows the location of the study area within northeastern Oregon. Approximately 247 stream miles were simulated above the confluence of Catherine Creek and the Grande Ronde River. The streams of interest are either historic or current salmonid habitat.

Figure 1 - Streams of interest in the upper Grande Ronde River subbasin.



2. DATA SUMMARY

2.1 Remote Sensing Data

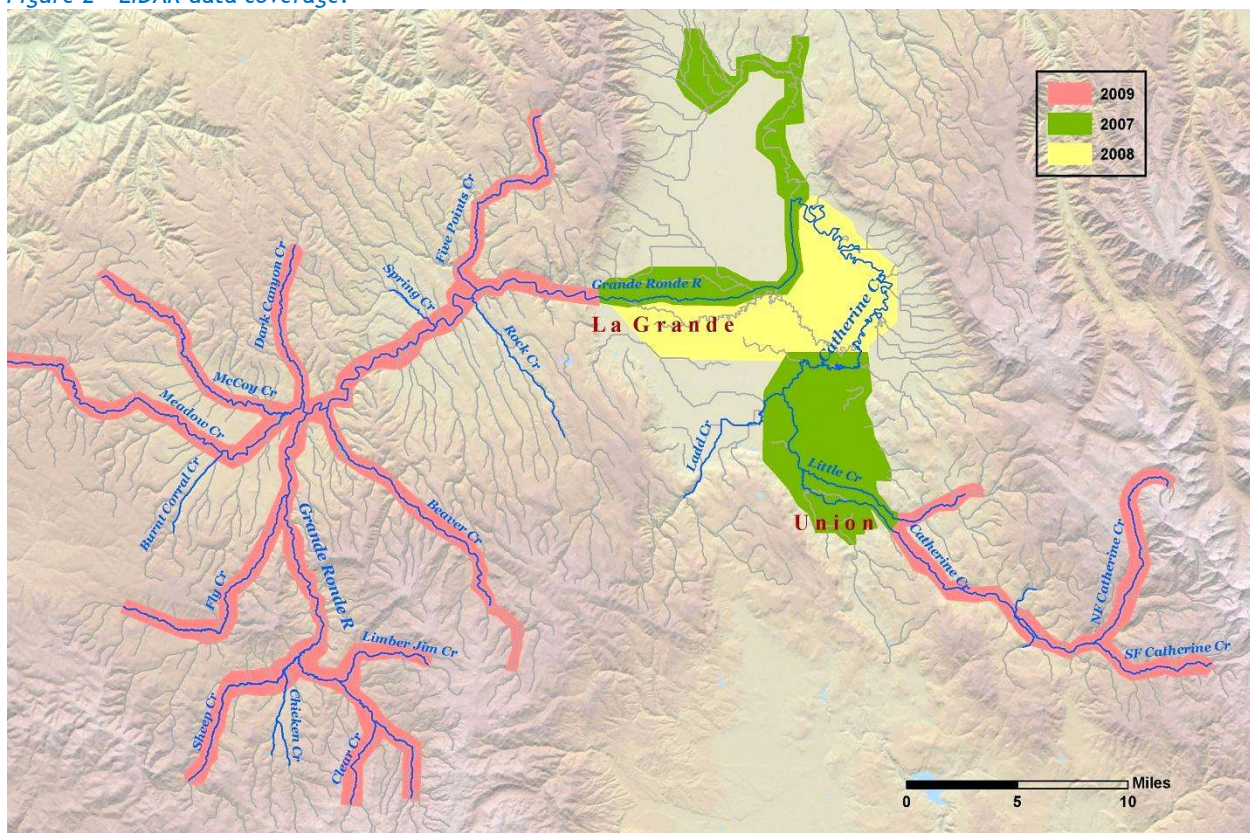
2.1.1 LiDAR

Light detection and ranging (LiDAR) data was collected by Watershed Sciences in September 2009 in order to supplement two existing LiDAR datasets that were collected in 2007 and 2008 (Figure 2). Together, the three LiDAR datasets provide high resolution land cover and bare earth elevation data for stream temperature model input. Table 1 summarizes the LiDAR products and their applicability to Heat Source modeling.

Table 1 - LiDAR products and their applications for stream temperature modeling.

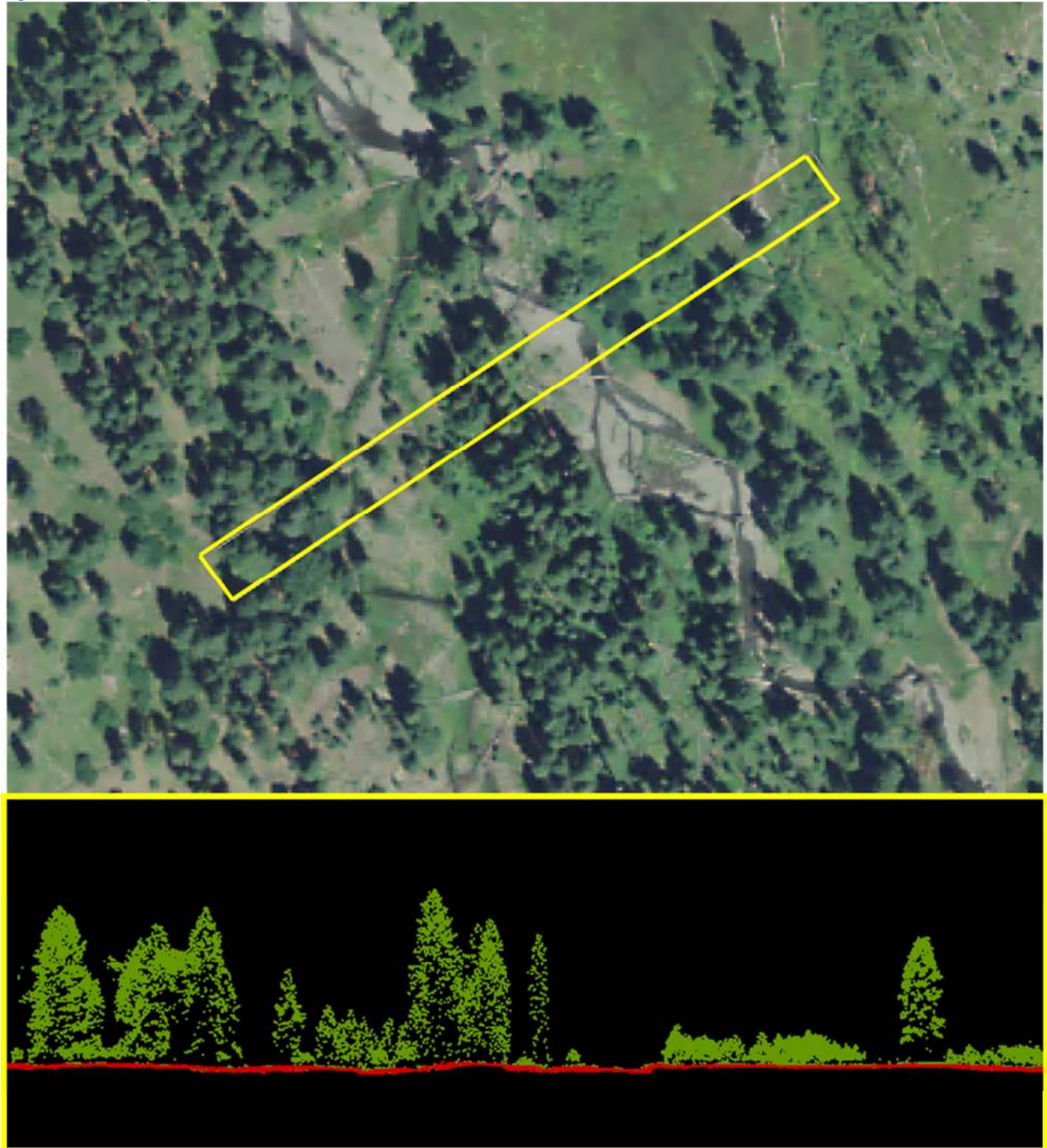
LiDAR Product	Applications
1-meter highest hit raster	Sampling near-stream land cover heights.
1-meter bare earth raster	Deriving high-resolution stream maps - including centerlines and banks. Sampling stream elevations and near-stream land surface elevations.
1-meter intensity images	Mapping stream centerlines and estimating wetted edges.

Figure 2 - LiDAR data coverage.



The LiDAR data consists of three-dimensional point clouds at approximately 8 points per square meter, with a relative accuracy of 5 centimeters. Each LiDAR data point is classified as either “ground” or “default”. “Default” includes all non-ground features such as vegetation, buildings, and other human made structures. Figure 3 shows a cross section of LiDAR data over Beaver Creek. Default points are green, while the ground points are colored red.

Figure 3 - LiDAR point cloud cross section over Beaver Creek.



LiDAR point data can be associated with RGB values from orthophotographs in order to produce more realistic or true-color oblique imagery. The default points can also be “turned off” to reveal a bare earth surface model which is useful for studying ground surface features that are normally obscured by vegetation. Figure 4 shows a LiDAR point cloud with RGB extraction and the corresponding bare earth model for a section of Beaver Creek. Complex channel geometry within the floodplain is easily visible in the bare earth LiDAR model.

Figure 4 - LiDAR point cloud with RGB extraction (top) and bare earth digital terrain model (bottom).

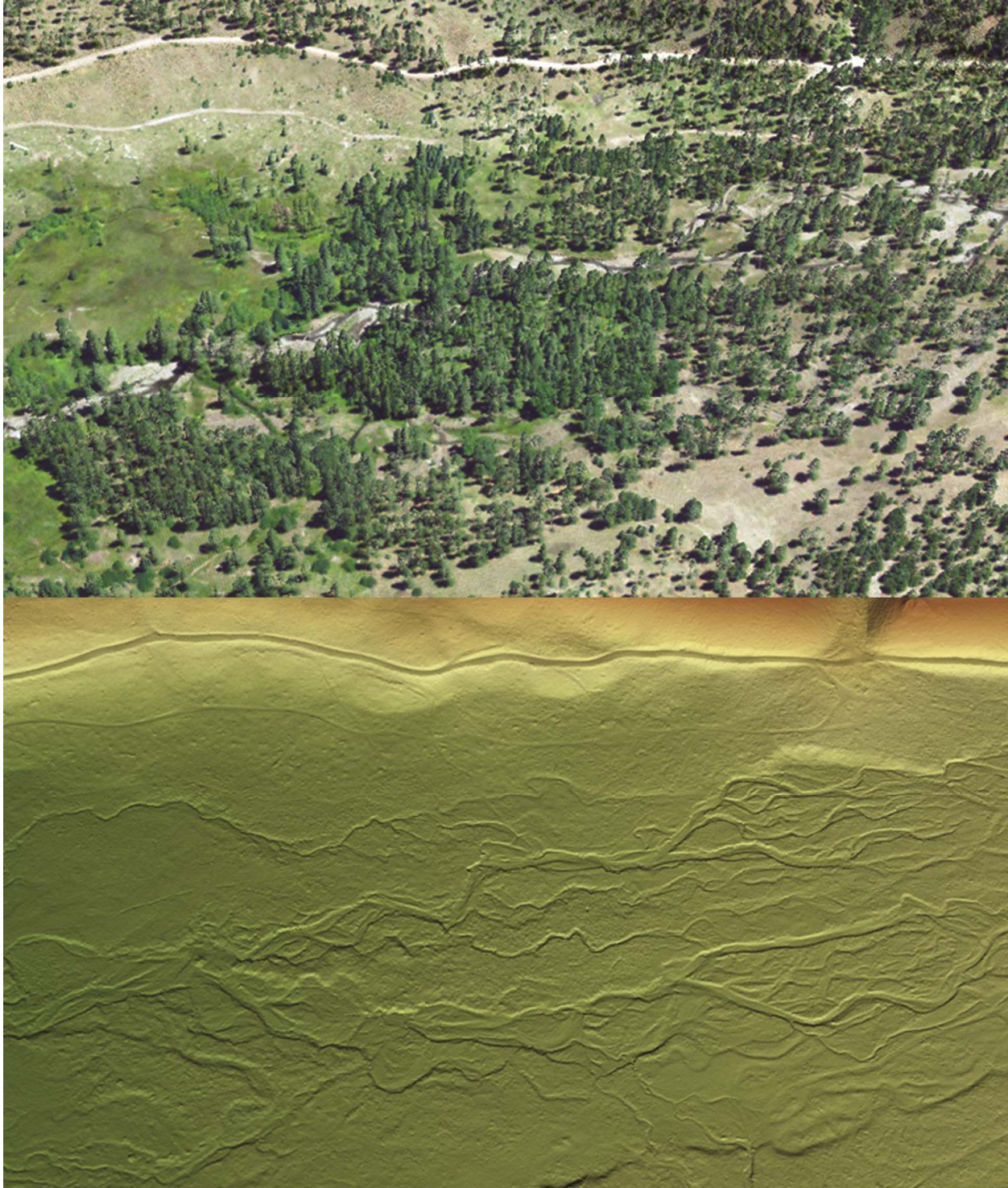


Figure 5 is another example of LiDAR digital elevation models (DEMs). The top image is the bare earth LiDAR model and the lower image is the highest hit LiDAR model. The DEM cell size is one meter. This type of raster data is commonly used within GIS applications such as ArcMap. For this project, the bare earth and highest hit rasters were used for stream mapping, tree height sampling, and other stream temperature model inputs.

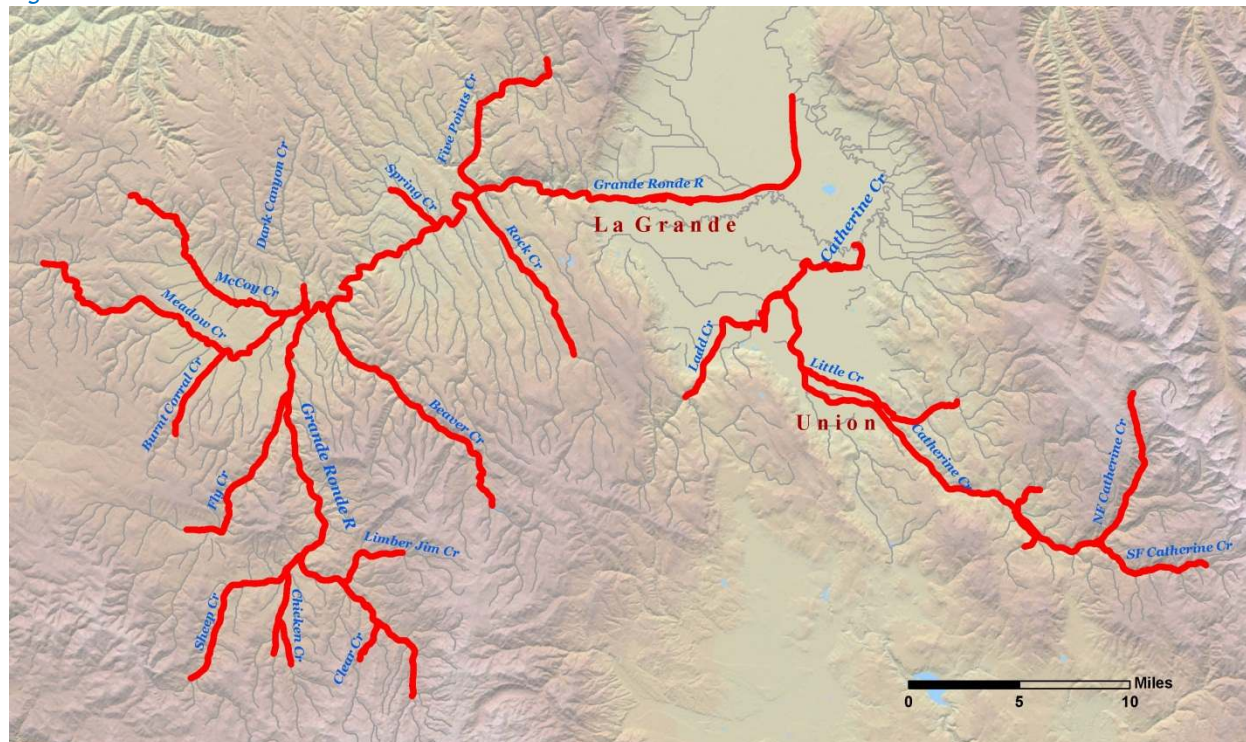
Figure 5 - LiDAR digital elevation model of the Grande Ronde River near Hilgard.



2.1.2 Thermal Infrared

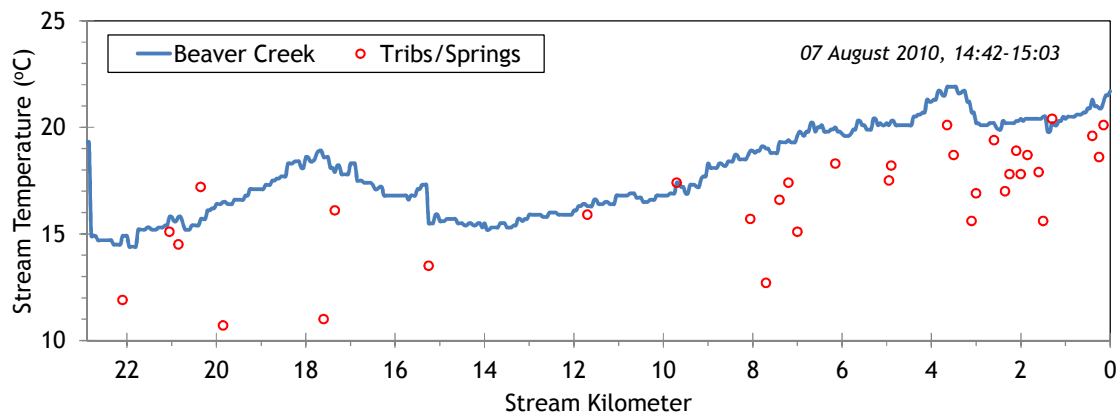
Watershed Sciences collected thermal infrared (TIR) stream temperature data for approximately 226 river miles during August 2010 (Figure 6). The TIR data was collected during the warmest part of the afternoon in order to capture near-daily maximum stream temperatures, when aquatic life is most at risk. Additionally, the August data collection was intended to target the low-flow and high seasonal temperature window when salmonid habitat is most impaired. Coinciding with the TIR data collection window, CRITFC crews were collecting ground-level flow measurements and hourly stream temperature data (see the following sections).

Figure 6 - TIR data extents.



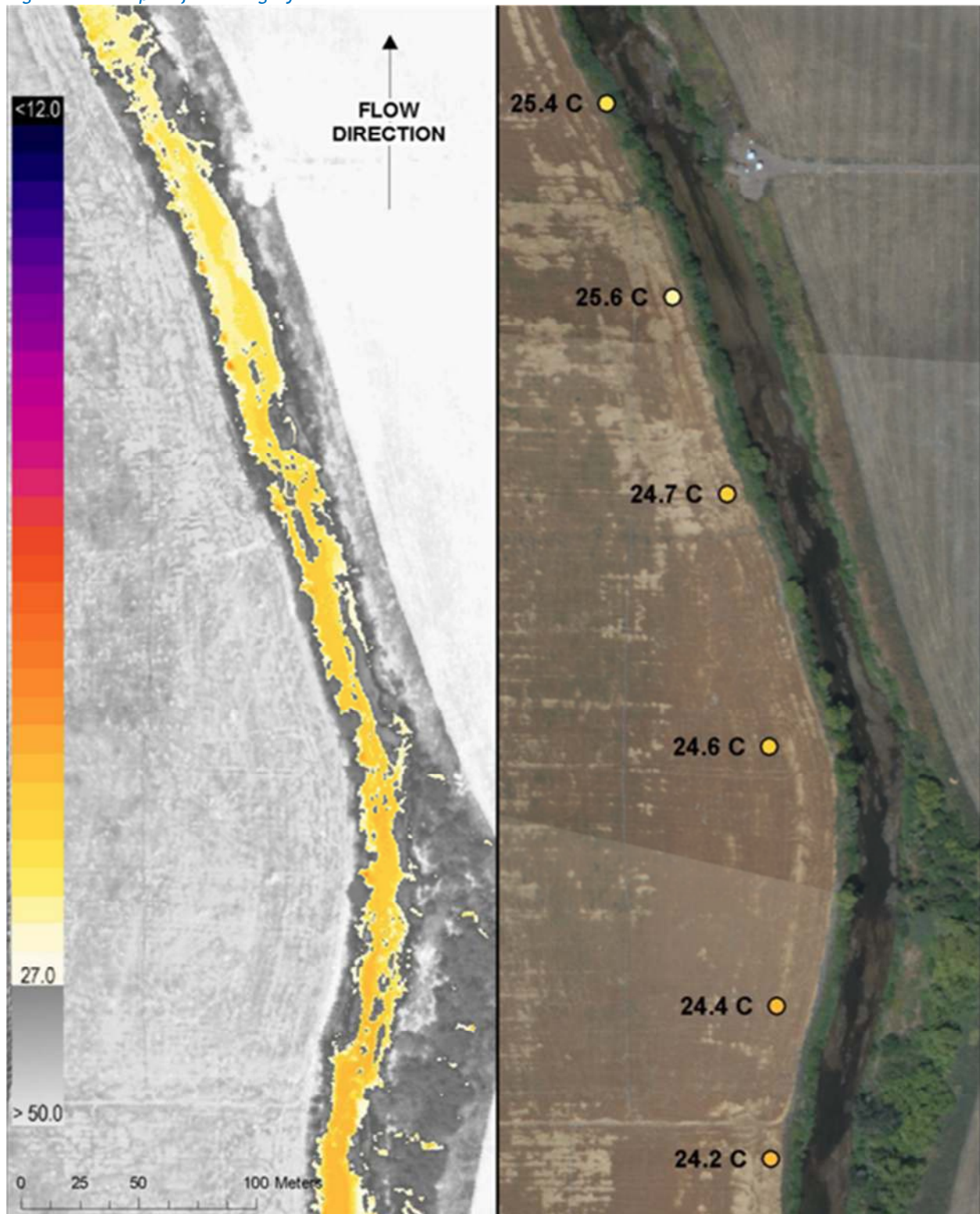
Following is an example of a TIR longitudinal temperature profile (Figure 7). In addition to the stream temperature profile, the temperatures of springs and tributaries are captured by the survey.

Figure 7 - Example of a TIR longitudinal stream temperature profile.



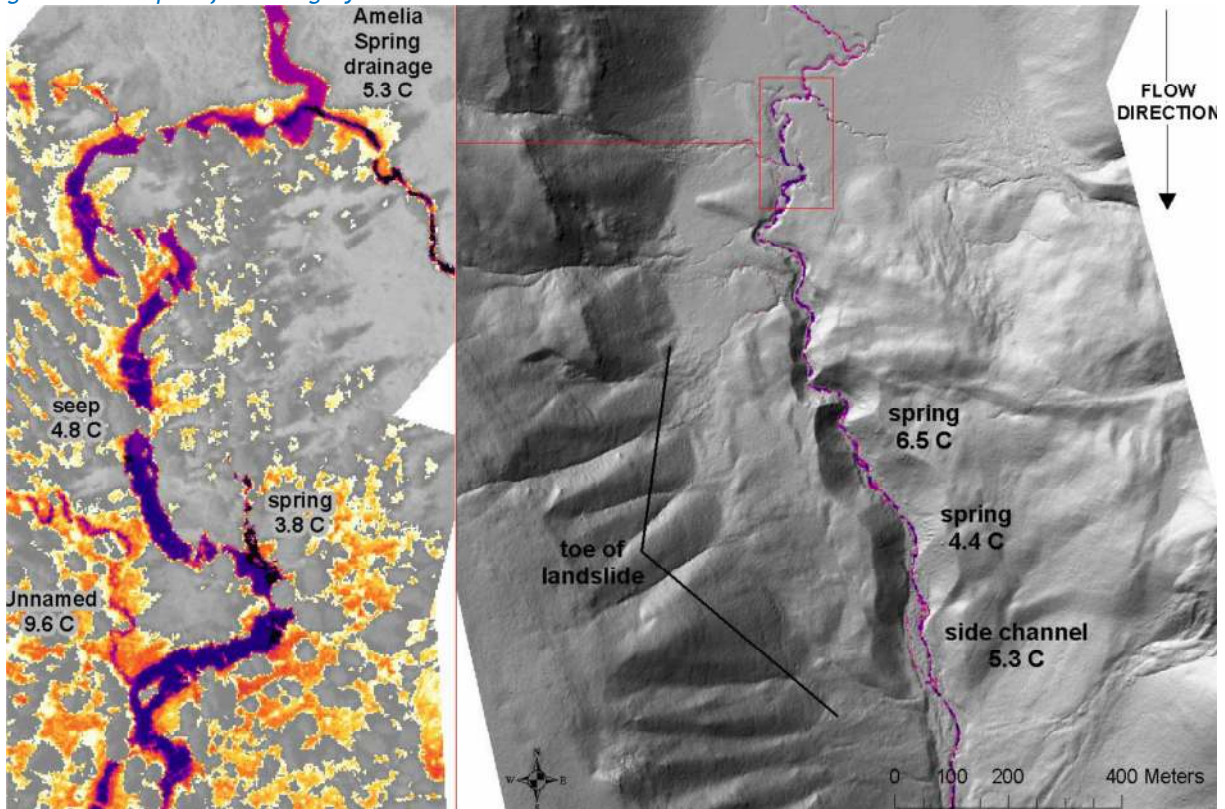
TIR surveys record only the surface temperatures and do not penetrate into the water column. Figure 8 shows an example of TIR imagery and the temperatures sampled from it. The points represent the position of the helicopter at the time the image was recorded.

Figure 8 - Example of TIR imagery.



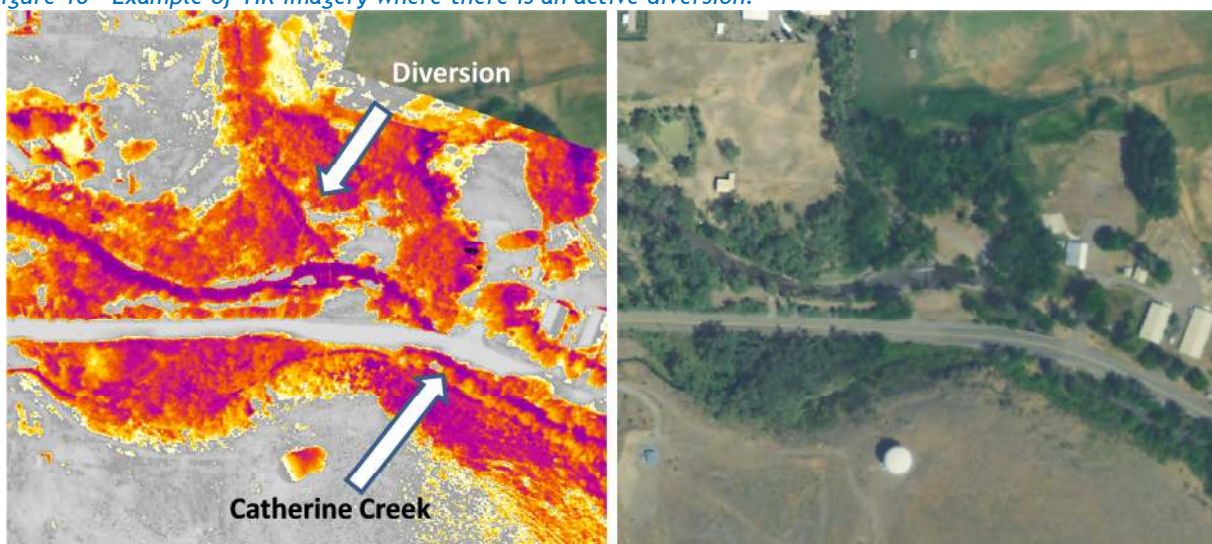
The TIR stream temperature imagery is useful for identifying features such as tributaries and springs. Temperatures can be sampled from those inflows and then mass balance calculations can be made to estimate their volumes. Significant inflows (ones that are large enough to accurately measure and are impacting stream temperature) are often included within the stream temperature models.

Figure 9 - Example of TIR imagery overlaid on LiDAR bare earth DTM.



The TIR imagery can also be used to identify diversion canals that were active at the time of the survey (Figure 10).

Figure 10 - Example of TIR imagery where there is an active diversion.

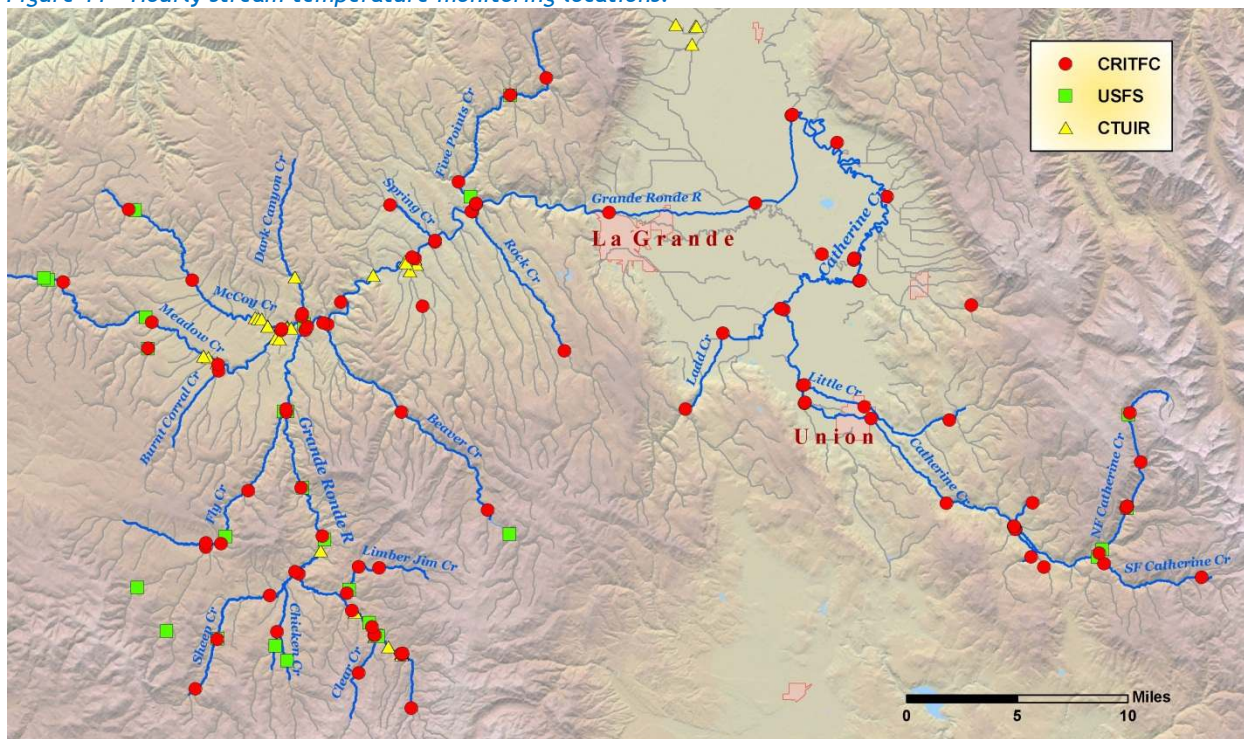


2.2 Ground Level Data

2.2.1 Hourly Temperature Data

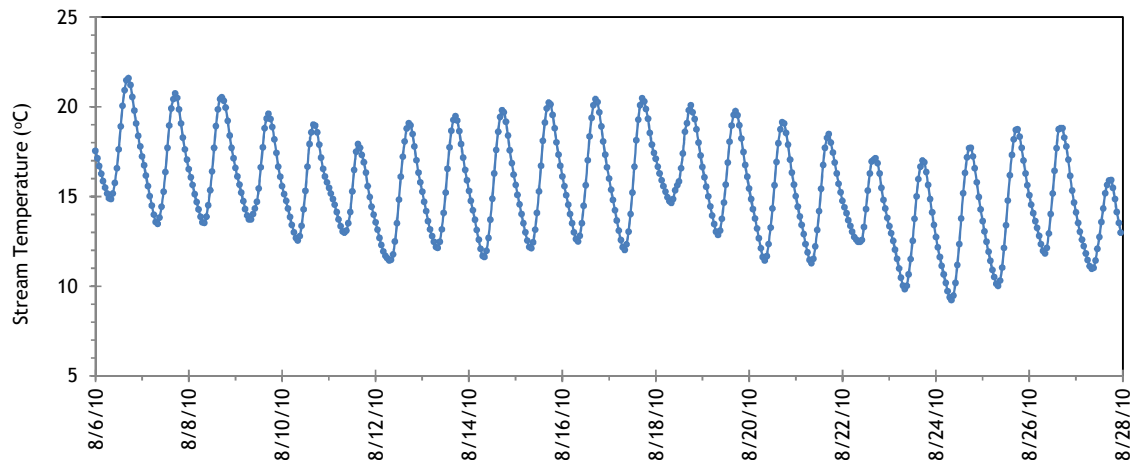
During the summer of 2010, CRITFC deployed thermistors throughout the study area in order to record hourly stream temperatures. The United States Forest Service (USFS) and Confederated Tribes of the Umatilla Indian Reservation (CTUIR) also provided hourly temperature data they had collected during that time. Figure 11 shows the hourly stream temperature monitoring locations.

Figure 11 - Hourly stream temperature monitoring locations.



Hourly stream temperature data was used to calibrate and verify the TIR data. It was also used for Heat Source input - to seed the uppermost boundary temperatures and for validating simulation results at various locations along the modeled streams. Figure 12 is an example of hourly temperature data.

Figure 12 - Example of hourly temperature data collected by CRITFC.



2.2.2 Seasonal Variation

A few stream temperature monitoring locations were selected in order to assess variability throughout the summertime period. The highest stream temperatures generally occurred in August. Figure 13 and Figure 14 display the stream temperature variability of sites along the Grande Ronde River and Catherine Creek.

Figure 13 - Grande Ronde River stream temperature variability during the summer of 2010.

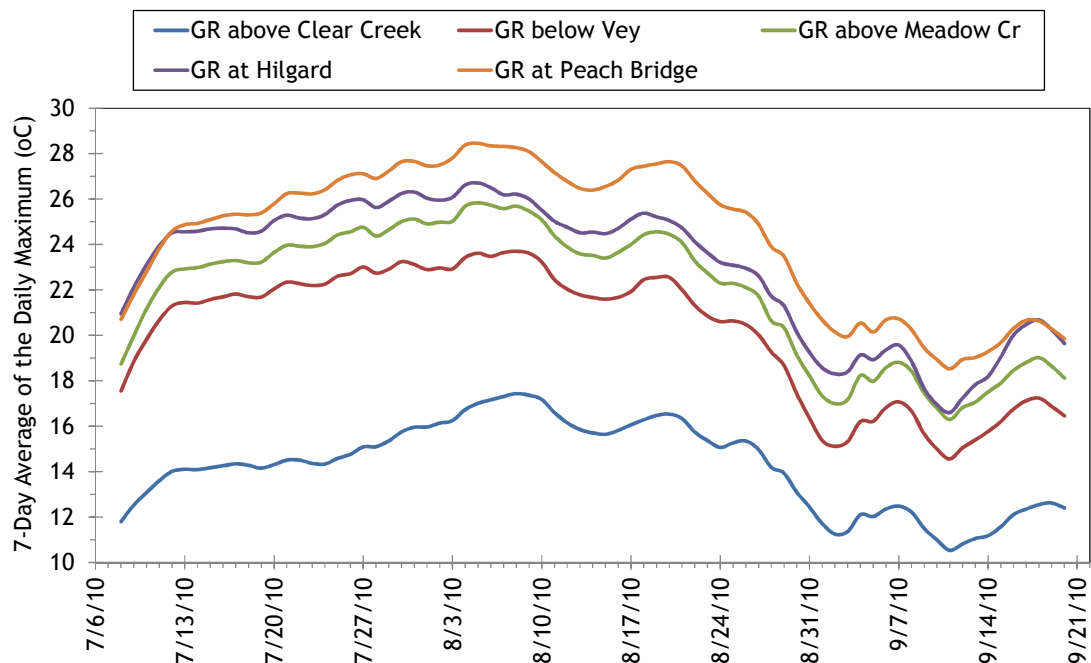
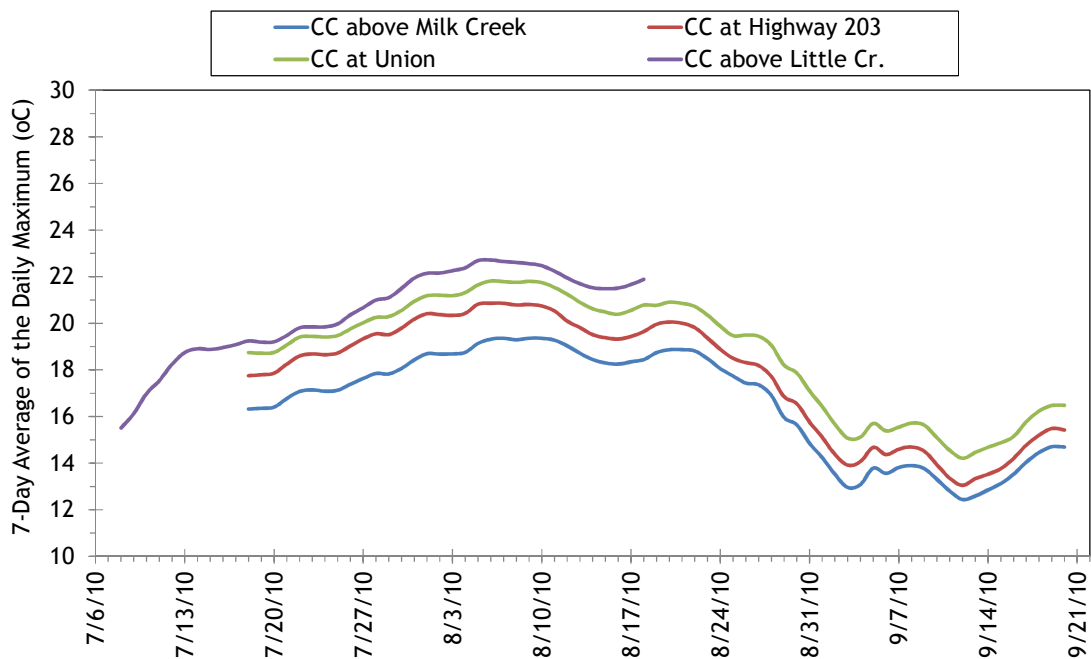


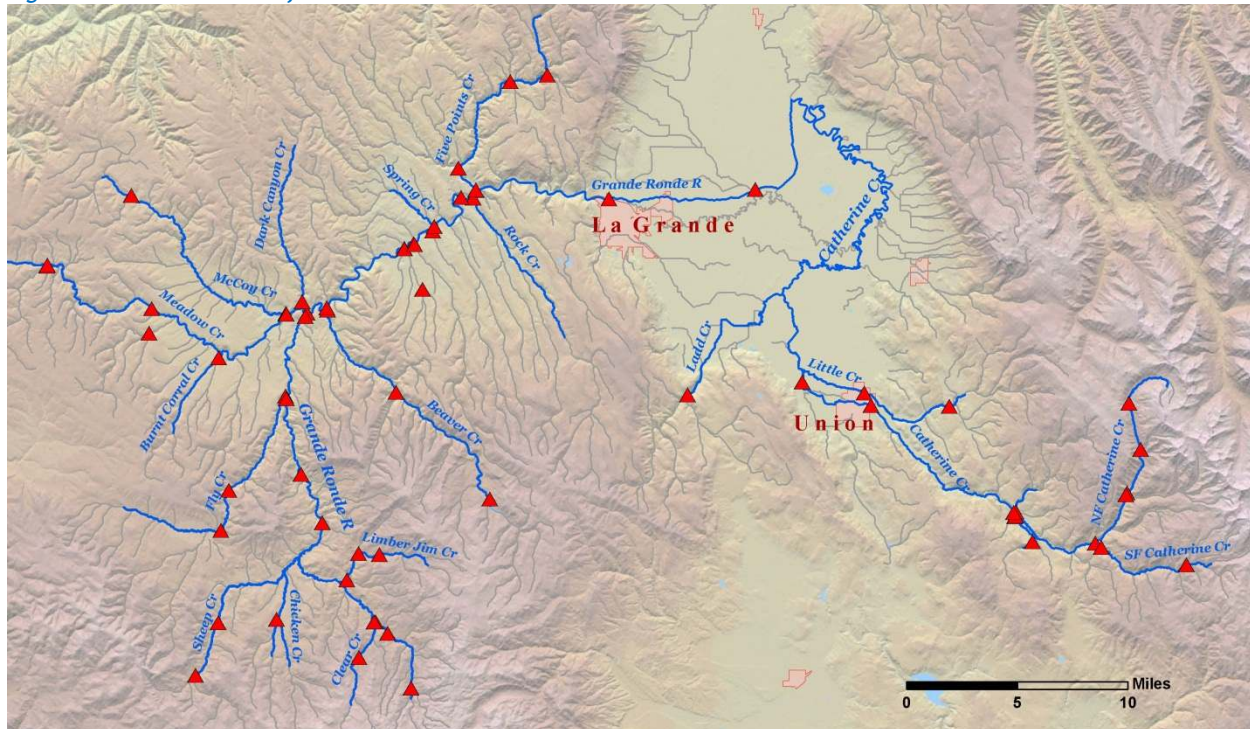
Figure 14 - Catherine Creek stream temperature variability during the summer of 2010.



2.2.3 Instantaneous Flow Data

CRITFC collected instantaneous ground-level flow data at various locations in August 2010 in order to coincide with the TIR flight window (Figure 15). Flow volume, velocity, depth and width were recorded at each location. The data was used to set up Heat Source hydraulics and to validate the simulation results.

Figure 15 - Instantaneous flow measurement locations.



The following data were recorded at each flow measurement site:

- Date and time
- Discharge volume
- Minimum, maximum and average velocity
- Minimum, maximum and average depth
- Wetted width
- Latitude and longitude

One measurement was taken at each site sometime during the simulation time period (August 6-27, 2010). The measurements were used to “seed” mass balance calculations of daily flow volume for streams where daily gage data was unavailable. The data were also used to validate the Heat Source simulated hydraulics.

2.2.4 Gaged Flow Data

Daily flow volumes were recorded at several USGS/OWRD gages within the study area (Figure 16). The daily average flows recorded at these locations were used to set up Heat Source hydraulics and validate the simulation results.

Figure 16 - Flow gage locations.

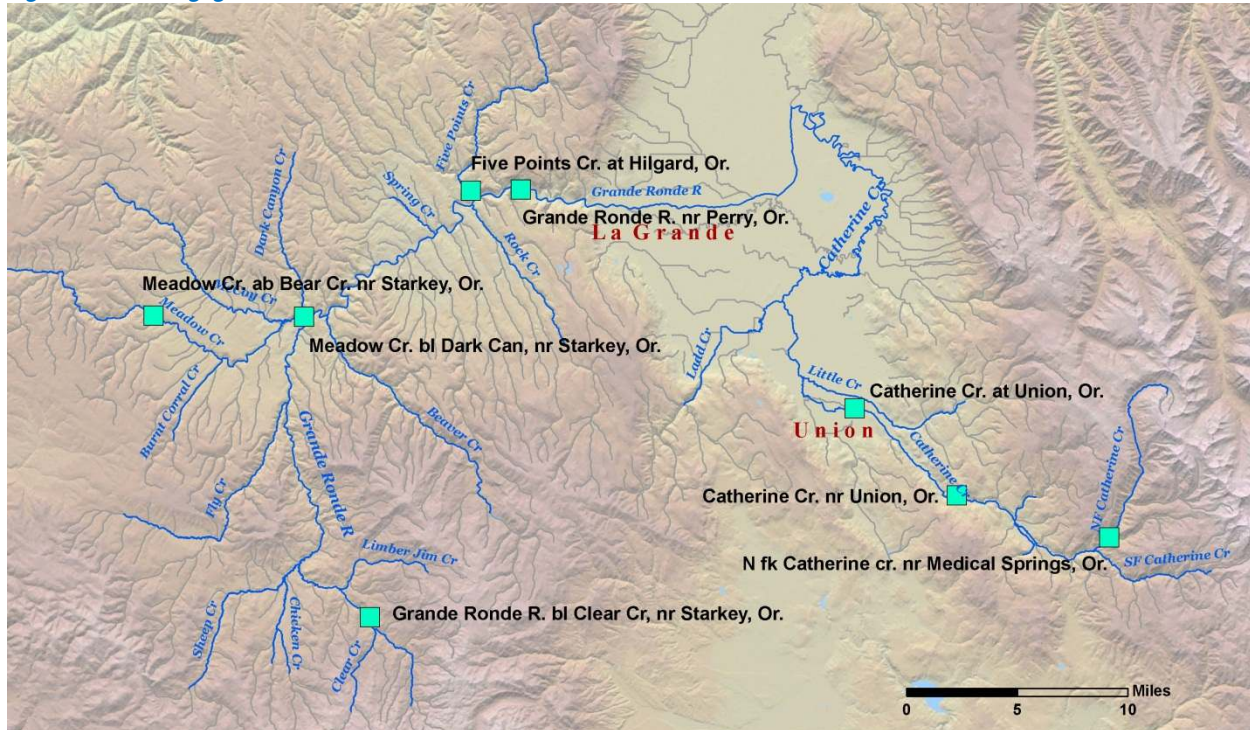


Table 2 lists the gages that were active during August 2010 within the study area. Data were downloaded from the Oregon Water Resources Department website. The original records were in 15-minute intervals and daily average values were calculated.

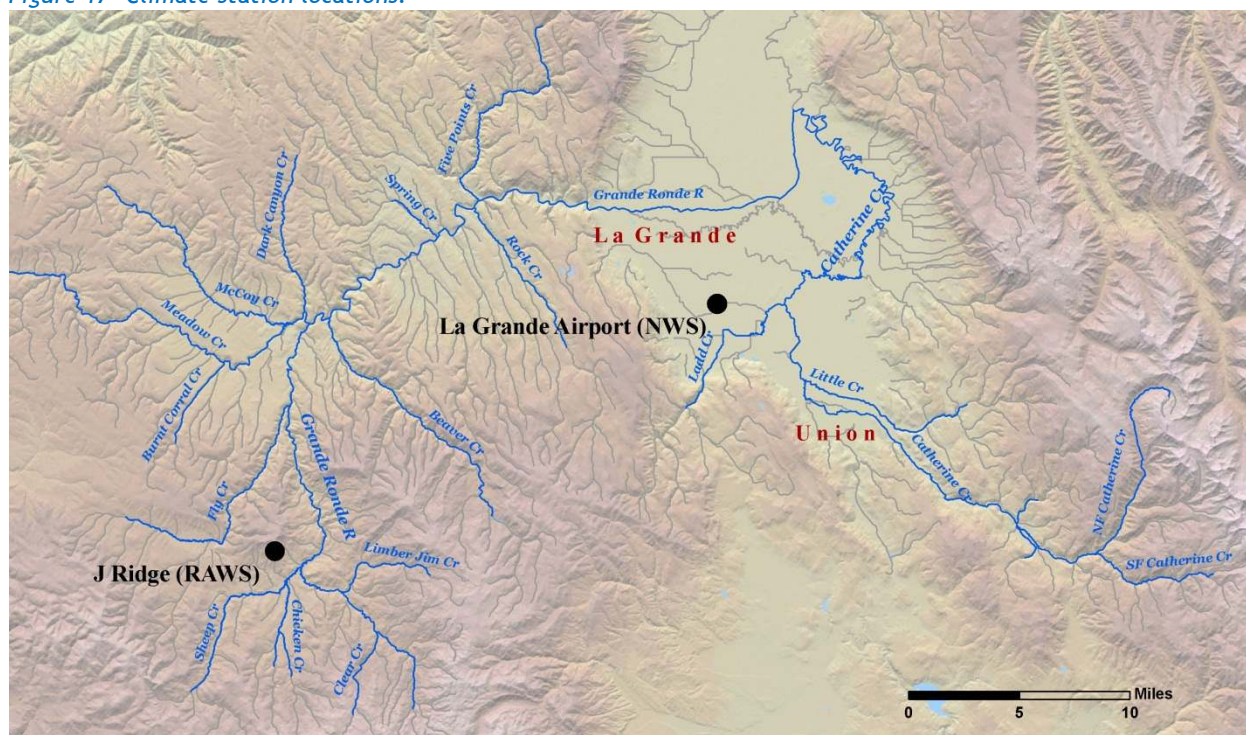
Table 2 - Stream flow gages within the study area.

ID #	Gage	Stream
13320300	Catherine Cr. at Union, OR	Catherine Creek
13320000	Catherine Cr. near Union, OR	Catherine Creek
13318920	Five Points Cr. at Hilgard, OR	Five Points Creek
13317850	Grande Ronde R. bl Clear Cr, nr Starkey, OR	Grande Ronde River
13318960	Grande Ronde R. nr Perry, OR	Grande Ronde River
13318060	Meadow Cr. above Bear Cr. nr Starkey, OR	Meadow Creek
13318210	Meadow Cr. below Dark Can, nr Starkey, OR	Meadow Creek
13319900	NF Catherine Cr. nr Medical Springs, OR	North Fork Catherine Creek

2.2.5 Climate Data

Hourly climate data was recorded by the National Weather Service at the La Grande airport. The U.S. Forest Service also recorded hourly temperature data at the J Ridge remote automated weather station (RAWS) site in the upper Grande Ronde basin. Figure 17 shows the climate station locations. For most Heat Source models, data from the La Grande airport was used. Some upper basin models used the USFS RAWS climate data. Further details and assumptions are provided in the following sections for each simulated stream.

Figure 17- Climate station locations.



For all simulations, the cloud cover data recorded at the La Grande airport was used (Figure 18). Cloud cover was reported as eighths of sky and the data were translated into percentages for Heat Source input.

Figure 18 - Hourly cloud cover values recorded at La Grande airport.

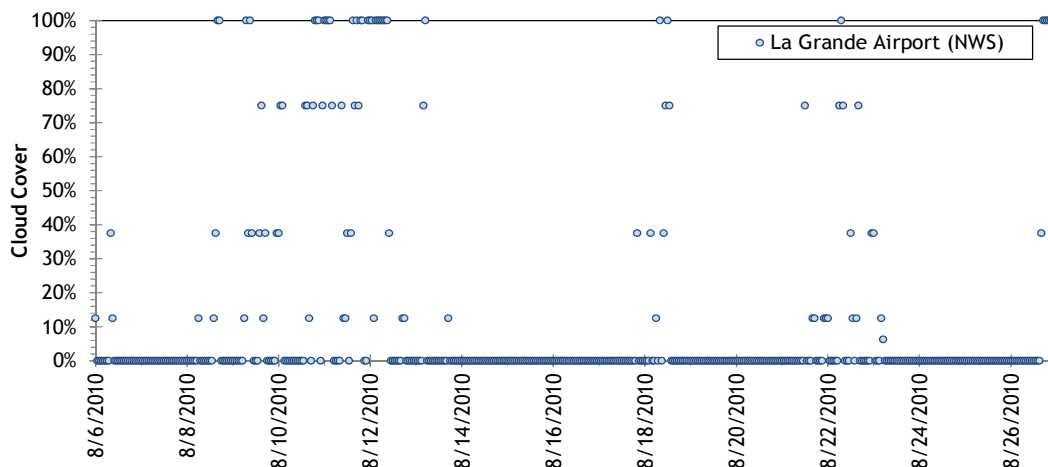
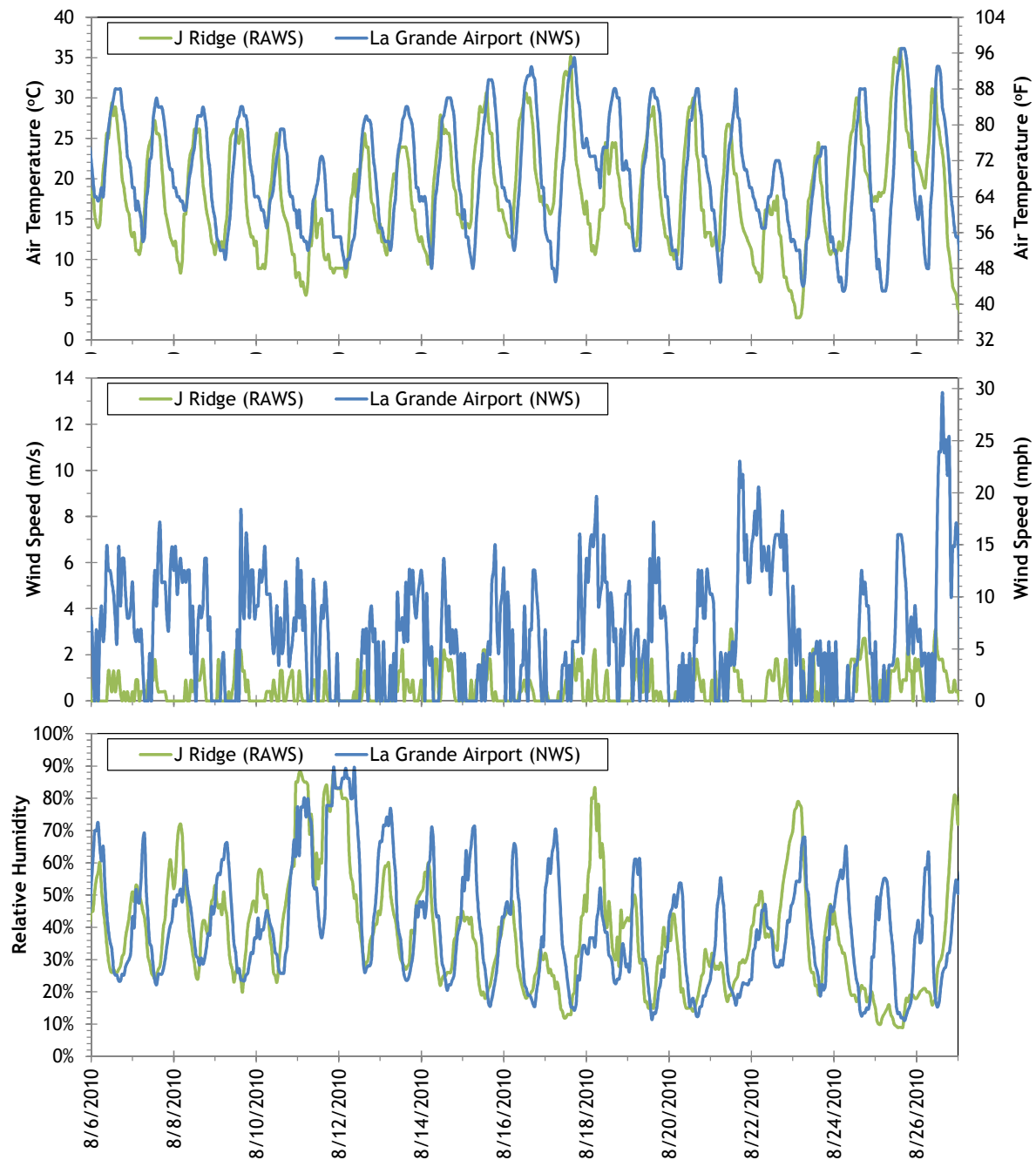


Figure 19 shows the recorded hourly air temperature, relative humidity and wind speed data recorded at the J Ridge (RAWS) and La Grande airport (NWS) weather stations between August 6 and August 27, 2010. Wind speeds at the airport were higher than at J Ridge because the airport is located in wide open valley bottom.

Figure 19 - Hourly air temperature, relative humidity and wind speed data.



3. GIS DATA SAMPLING FOR HEAT SOURCE INPUT - TTOOLS

Streams were mapped from the bare earth LiDAR data and TTools, a set of automated GIS sampling tools, was used to create an input database for Heat Source model. Figure 20 is a map of where stream channels were mapped and TTools was run. Table 3 summarizes the streams and lengths that were mapped and sampled with TTools.

Figure 20 - TTools sampling extents

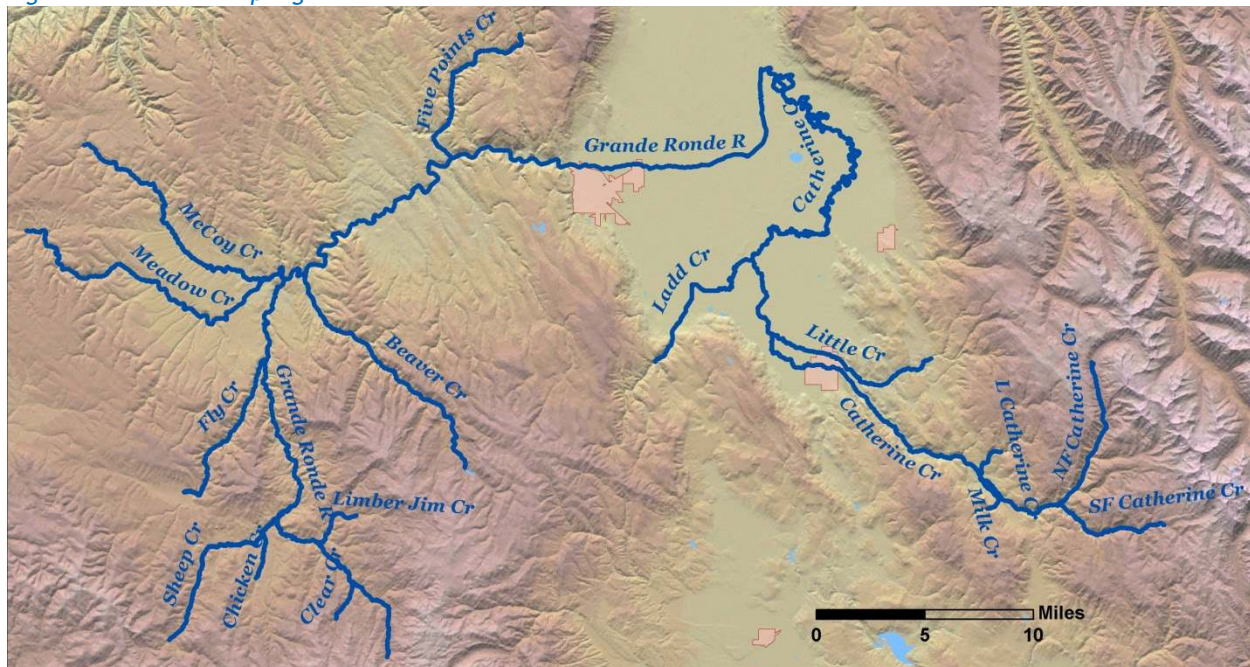


Table 3 - Streams where TTools sampling was completed.

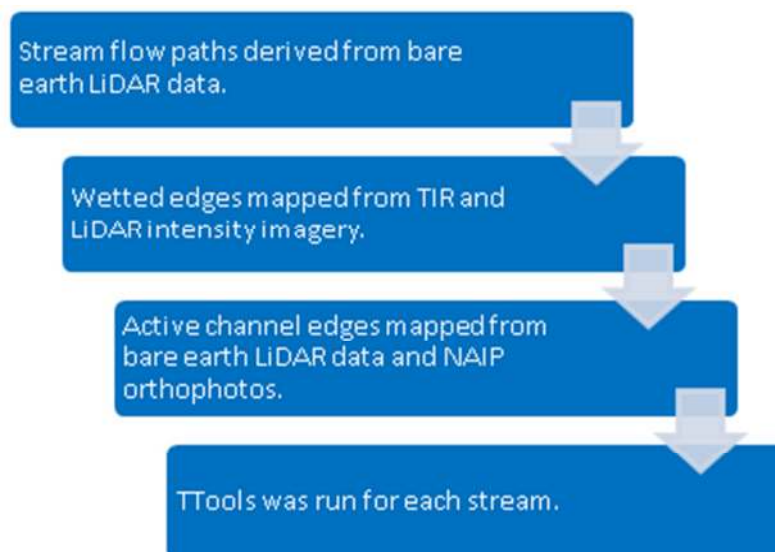
Watershed	Stream	Km	Miles
Catherine Creek	North Fork Catherine Creek	13.4	8.3
	South Fork Catherine Creek	10.4	6.5
	Milk Creek	3.4	2.1
	Little Catherine Creek	3.2	2.0
	Little Creek	16.5	10.3
	Ladd Creek	15.3	9.5
	Catherine Creek	88.7	55.1
	Clear Creek	3.5	2.2
	Limber Jim Creek	5.9	3.7
	Chicken Creek	6.5	4.0
	Sheep Creek	22.2	13.8
	Fly Creek	15.5	9.6
	Meadow Creek	31.5	19.6
	McCoy Creek	23.9	14.9
	Beaver Creek	22.9	14.2
	Five Points Creek	16.4	10.2
	Grande Ronde River	98.1	61.0
Upper Grande Ronde River	TOTAL:	397.3	246.9

Heat Source stream temperature modeling incorporates high-resolution LiDAR, TIR, and stream mapping. This section describes how stream channels were mapped from LiDAR data and how the various GIS data sources were sampled to create Heat Source input databases. Following is a brief overview of the methodology:

1. Stream flow paths were derived from 1-meter bare earth LiDAR rasters.
 - a. Smoothing algorithms were applied.
 - b. Results verified and manually corrected where needed.
2. Wetted edges were digitized.
3. Active channel edges were digitized.
4. TTools was used to segment the stream every 50 meters and sample the following:
 - a. Stream elevation, gradient, and aspect
 - b. Channel widths
 - c. Topographic shade angles
 - d. Near stream land cover heights
 - e. TIR stream temperatures

Figure 21 summarizes the general workflow used to create, assemble, and sample GIS data for Heat Source model input. Once the TTools shapefile database was created for each stream, Heat Source models were set up and the calibration process was ready to commence.

Figure 21 - General workflow to prepare Heat Source model inputs.



3.1 Stream Mapping

Existing stream layers were outdated and had fairly coarse resolutions (1:24,000 or coarser). Since Heat Source relies on high resolution LiDAR inputs, new stream layers were mapped from the bare earth LiDAR data. Following are the steps used to create the high-resolution stream layers:

1. One-meter rasters of the bare earth LiDAR were mosaicked for each stream to be modeled.
2. The bare earth rasters were filled and flow direction and accumulation rasters were derived.
3. The flow accumulation raster was then converted to polylines using a minimum drainage area.
4. The stream of interest was isolated and all extraneous segments were deleted.
5. Smoothing algorithms were applied to remove “kinks”.
6. Smoothed stream polylines were verified against LiDAR, TIR, and aerial photography and manually corrected where necessary.

Figure 22 - Raw stream polyline.

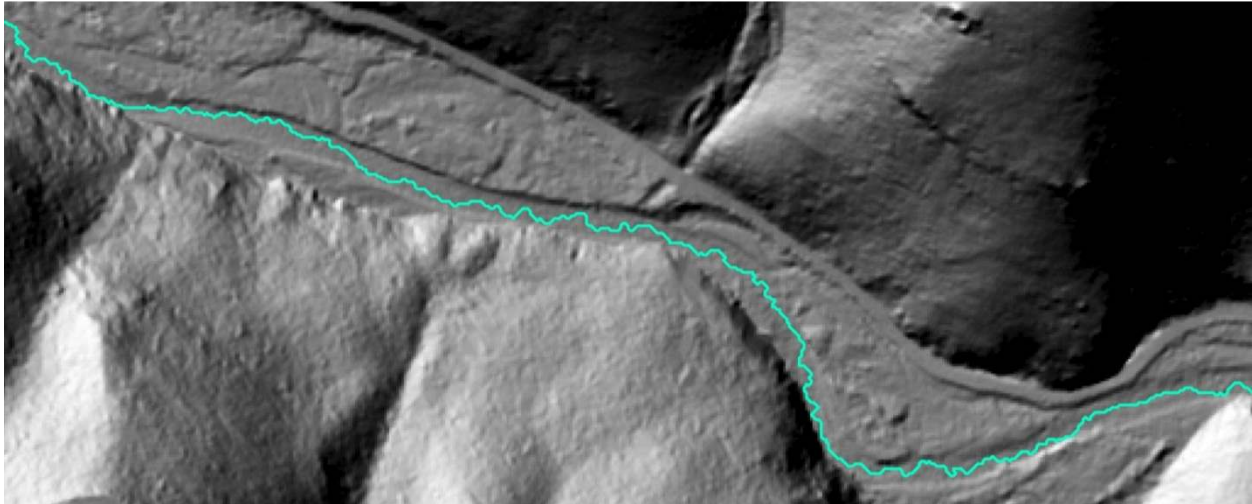
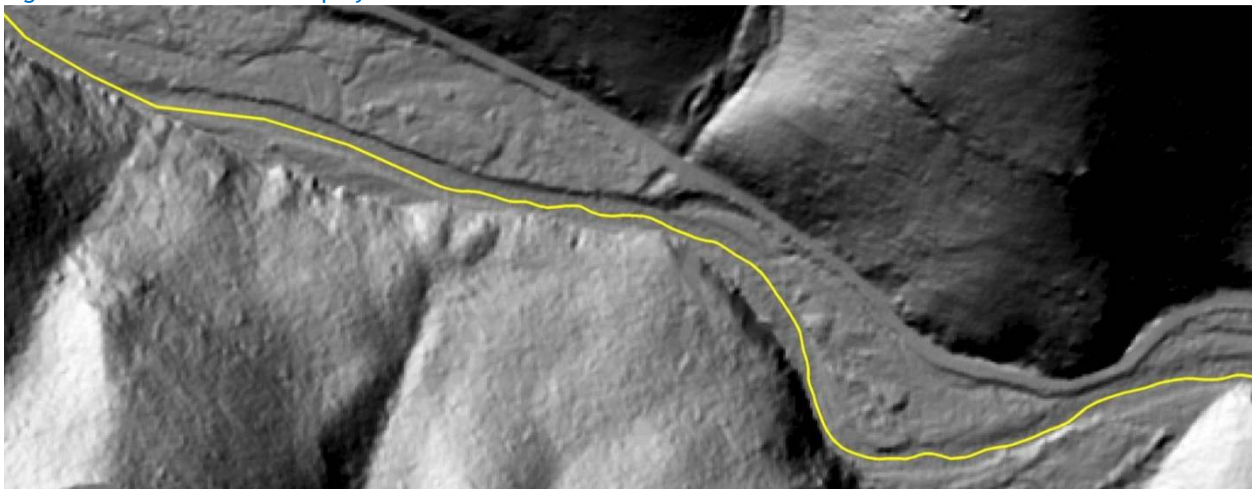


Figure 23 - Smoothed stream polyline.



3.2 Wetted Edge Mapping

Wetted widths are an important input parameter for the Heat Source model because accurate hydraulics is essential for a robust modeling effort. LiDAR intensity images and TIR imagery provided clear depictions of the stream surface in most cases. The right and left wetted edges were digitized from those sources. Then TTools was used to measure the wetted width at each 50-meter segment.

Figure 24 - Stream polyline overlaid on LiDAR intensity image.

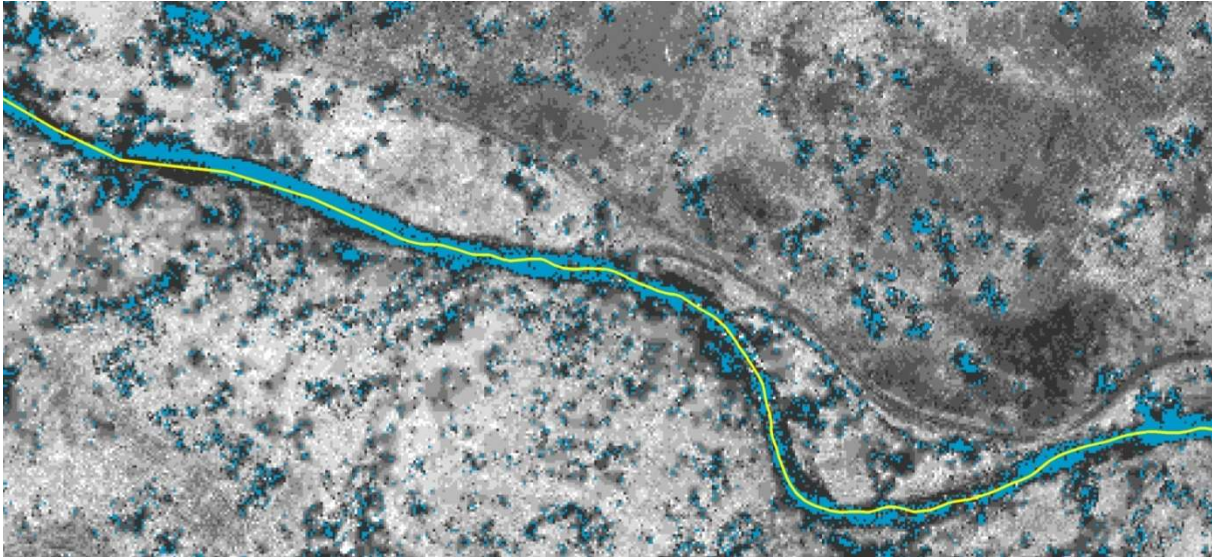
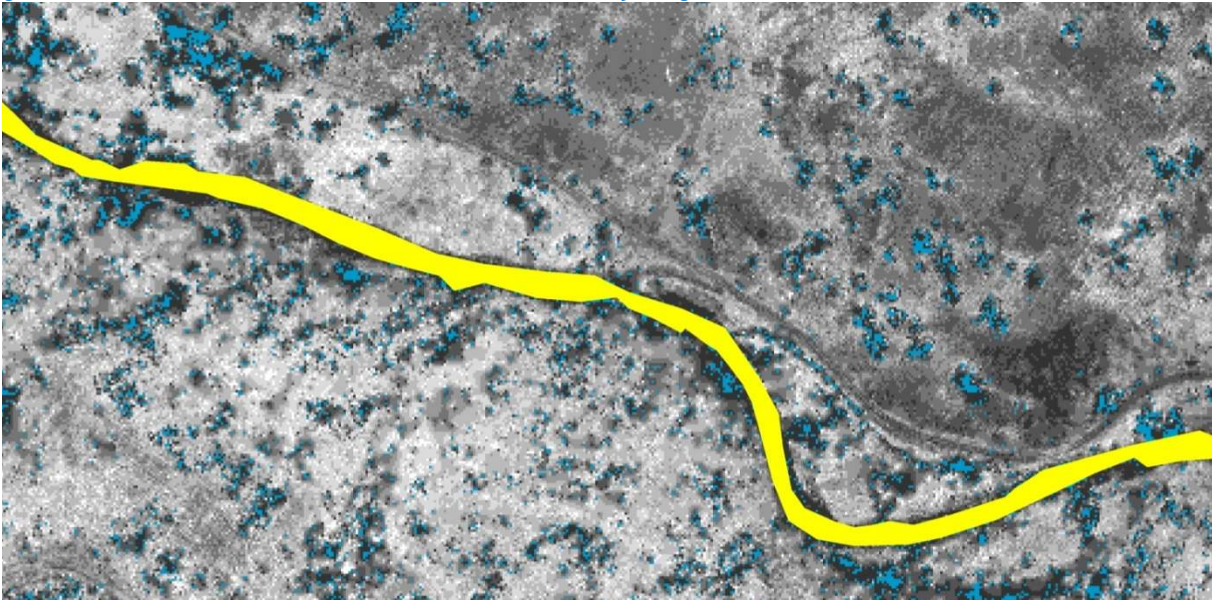


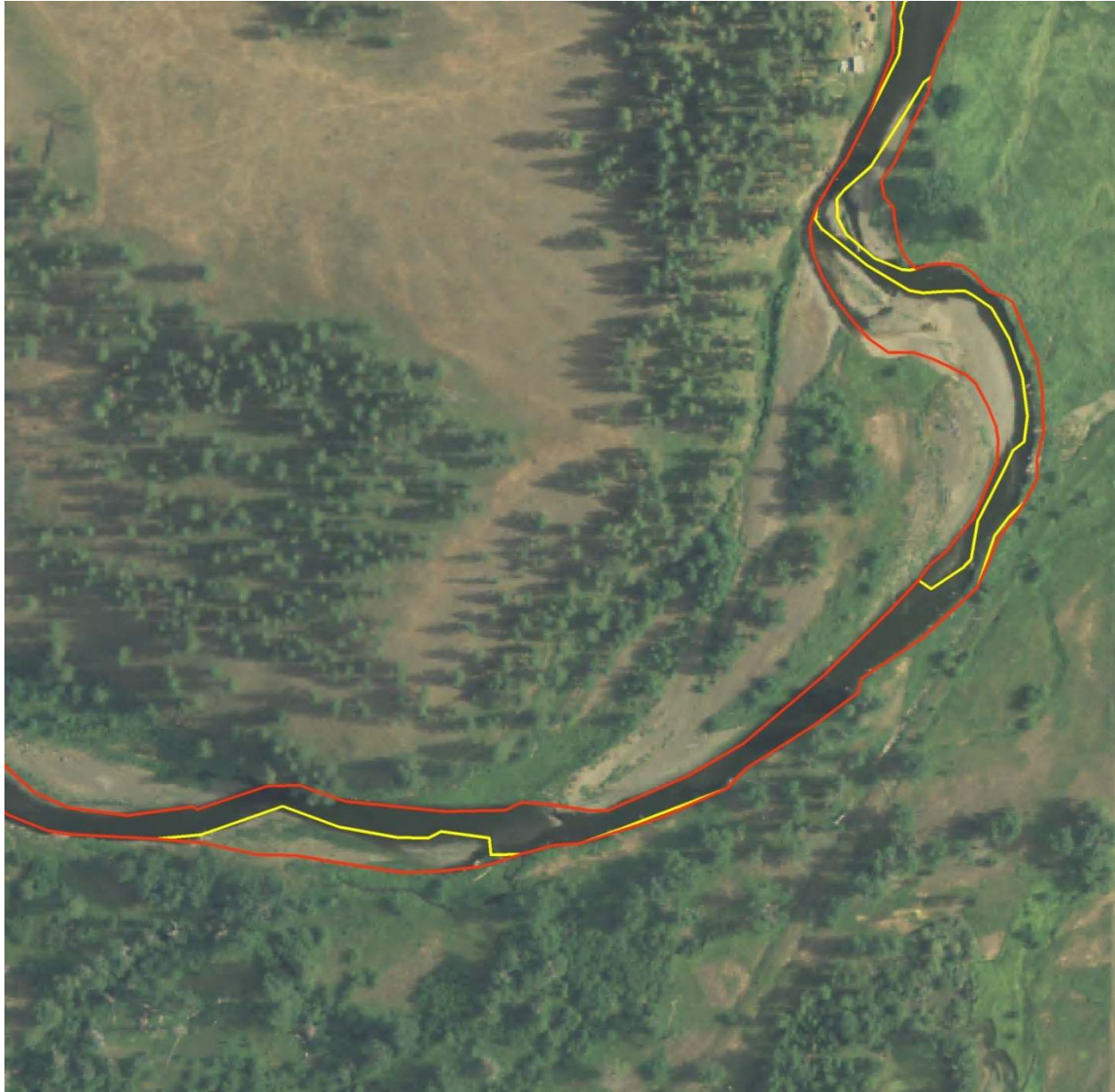
Figure 25 - Estimated wetted area based on LiDAR intensity image.



3.3 Active Channel Mapping

Active channel edges are an important consideration when applying potential vegetation for “what-if” model runs. In most cases, the active channel should remain free of vegetation during the potential vegetation scenarios. Active channel edges were digitized from the bare earth LiDAR data and aerial photography. TTools was used to sample the active channel widths at each 50-meter stream segment.

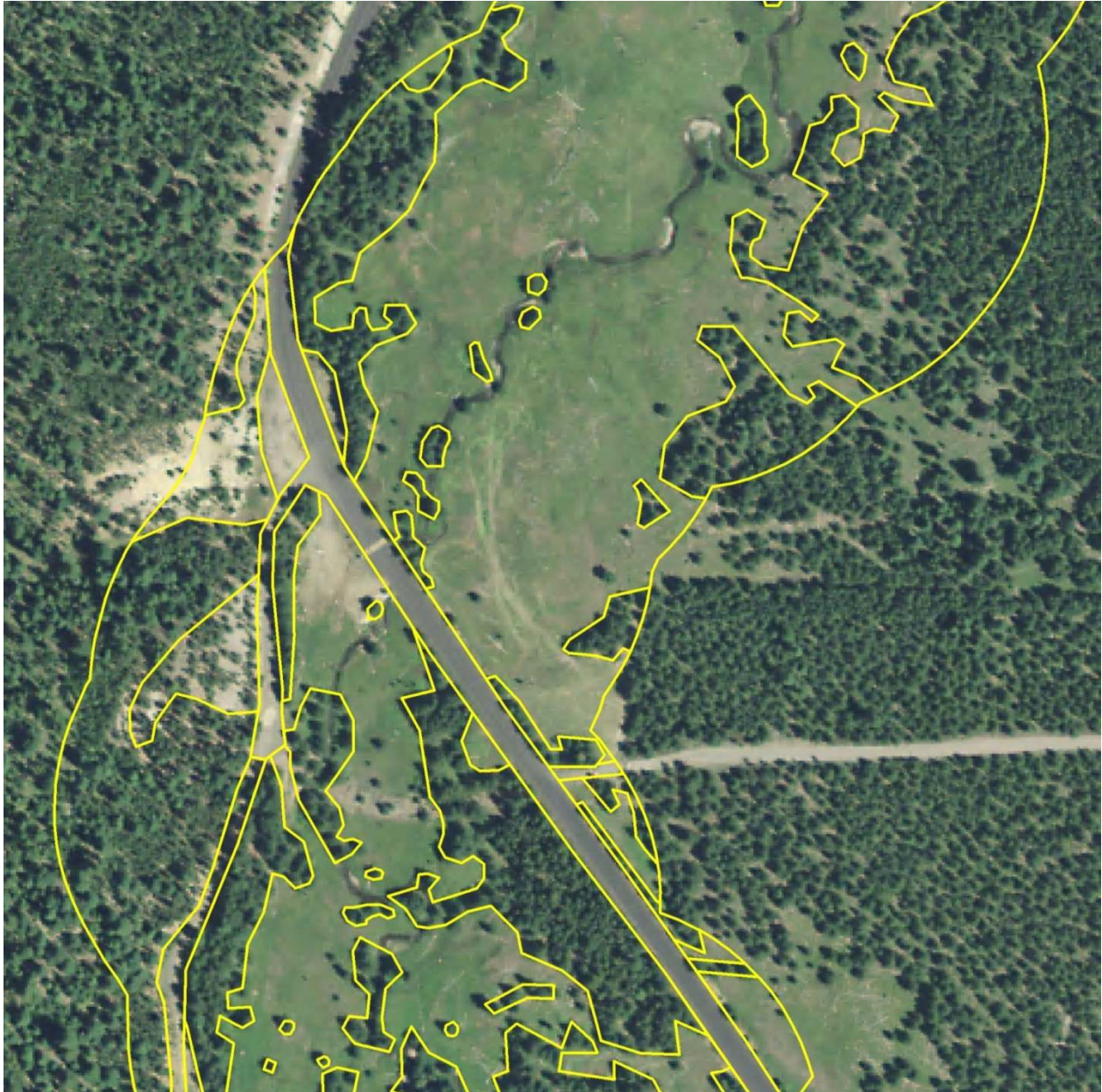
Figure 26 - Wetted channel edges (yellow) and active channel edges (red).



3.4 Near Stream Land Cover Mapping

Some streams had partial or no LiDAR data available. In those cases, the near stream land cover was manually digitized from aerial imagery (NAIP orthophotography). The stream was buffered 100 meters from each bank and that buffer was divided into polygons based on land cover type, height class, and density class. General height estimates were made based on nearby LiDAR data (see following sections for individual stream details).

Figure 27 - Manually digitized near stream land cover polygons.



3.5 Automated GIS Sampling - TTools

TTools is an ArcMap tool set that is designed to sample high-resolution GIS data and create an input database for Heat Source. Table 4 summarizes the TTools functions.

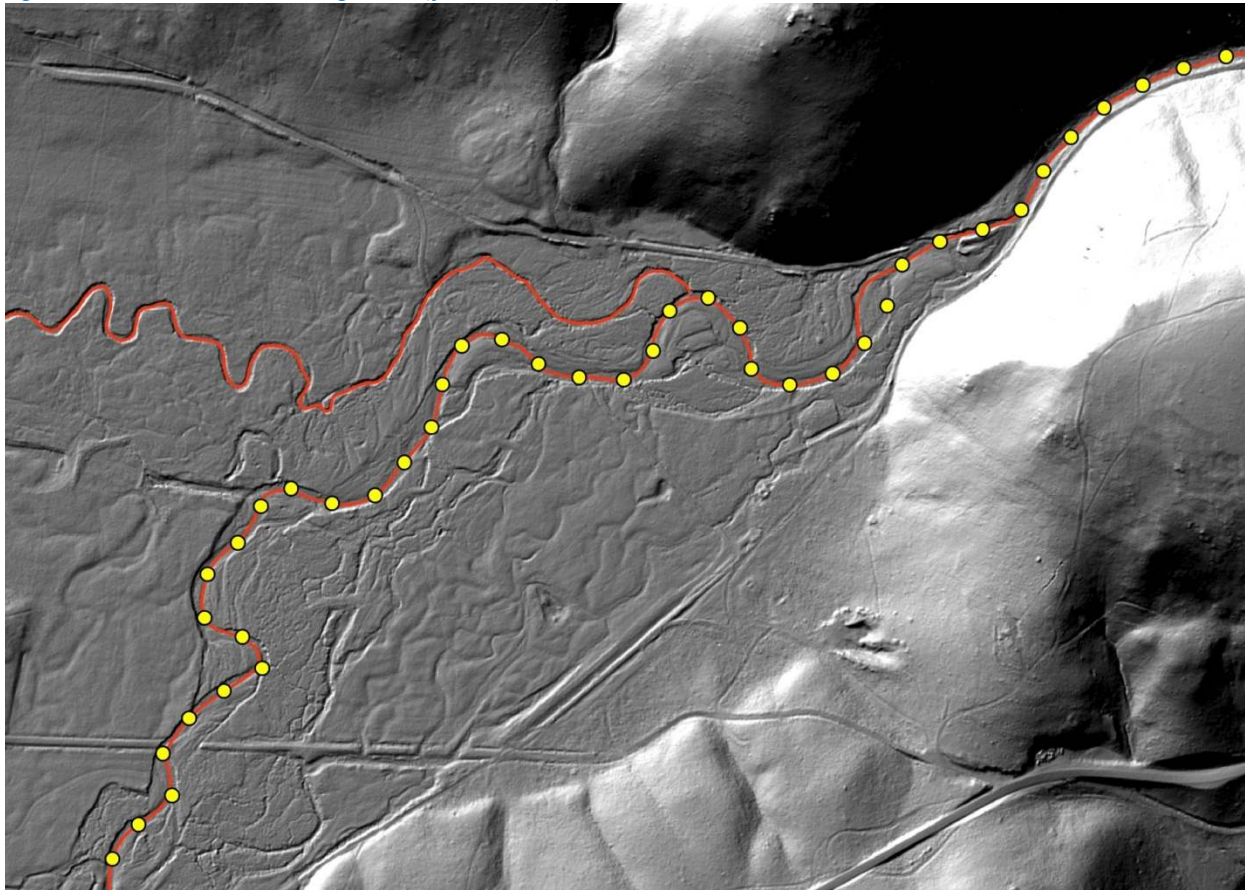
Table 4 - TTools steps and data sources.

Step	Description	Data Sources
1	Segments stream polyline every 50 meters and calculates aspect	Stream polyline
2	Measures channel width at each 50-meter node	Wetted and active channel edge polylines
3	Measures stream elevation and gradient	Bare earth LiDAR data
4	Measures topographic shade angles	10-meter DEM
5	Samples near stream land cover heights	Highest hit and bare earth LiDAR data / manually digitized polygons
6	Samples TIR temperature data	TIR point shapefile

3.5.1 TTools Step 1

In the first step of TTools, the stream polyline is segmented every 50 meters and a point shapefile is created that will house the data from all subsequent steps. Figure 28 shows an example of a stream polyline that has been segmented using TTools.

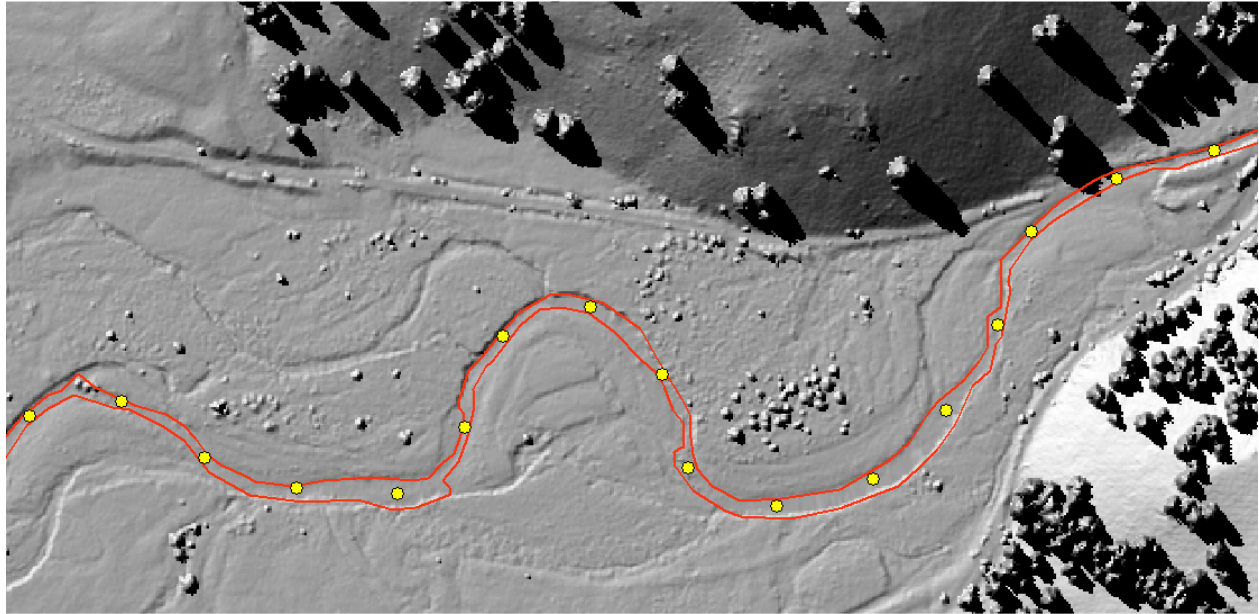
Figure 28 - 50-meter stream segments (yellow dots).



3.5.2 TTools Step 2

The second step of TTools is to sample the channel widths at each 50-meter node (Figure 29). The right and left banks or channel edges must have been mapped and represented as individual polyline shapefiles. Channel widths are measured perpendicular to the stream flow. The user may use this step to sample wetted edges, active bank edges, floodplain widths, or various other widths relative to the stream.

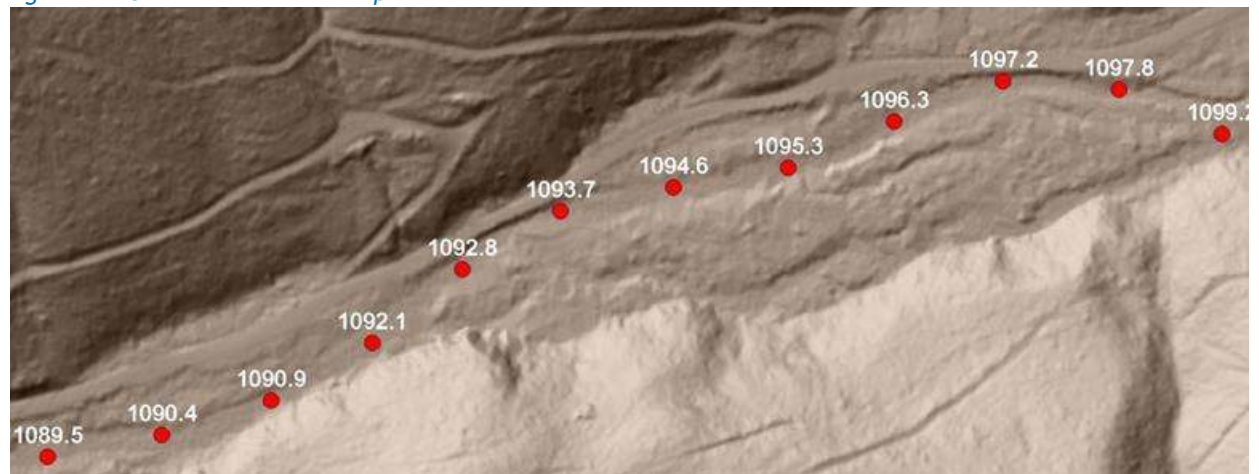
Figure 29 - Stream channel edges and the TTools point shapefile.



3.5.3 TTools Step 3

In the third step of TTools, stream elevation is sampled at each 50-meter node (Figure 30) and then the gradient is calculated as rise/run. Where LiDAR data is available, the elevations were sampled from the bare earth LiDAR data. Where LiDAR was not available, the 10-meter DEM was used.

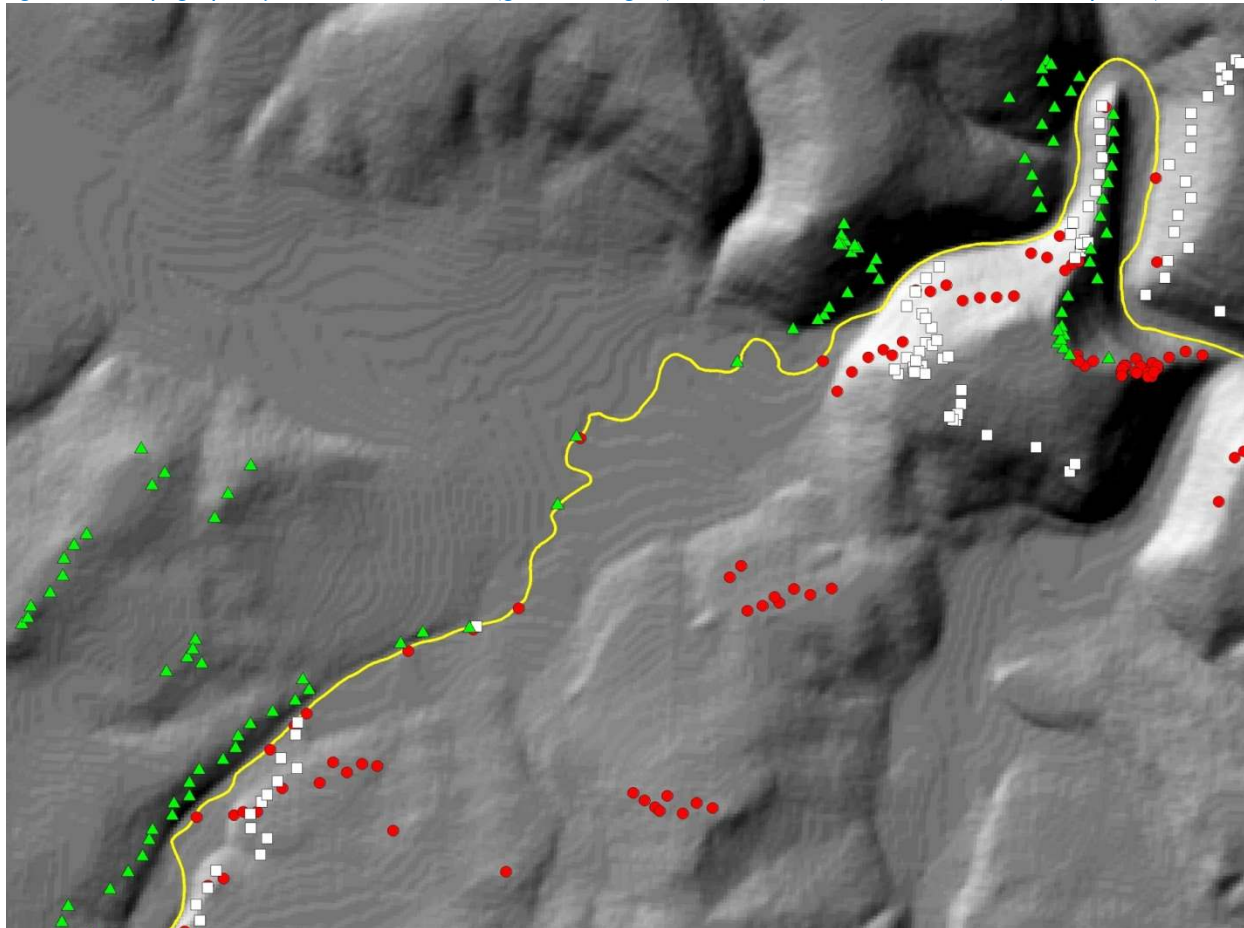
Figure 30 - Stream elevations sampled at each 50-meter node.



3.5.4 TTools Step 4

The maximum topographic angles to the east, south and west are sampled for each 50-meter node from the 10-meter DEM. The sampling routine looks up to 10 kilometers in each direction. Figure 31 shows the stream polyline (yellow) and the highest topographic shade producing features in each of the three directions. The TTools sampling routing is optimized to assess both near-field (<1 km) and far field (up to 10 km) topographic features. In many cases, the highest topographic shade feature is the bank where the stream has become down-cut or flows along cliffs.

Figure 31 - Topographic features to the west (green triangles), south (red circles) and east (white squares).



3.5.5 TTools Step 5

Near stream land cover heights are sampled at each 50-meter node using a dense radial sampling pattern. Where LiDAR is available, the bare earth elevation and the highest hit elevation are both sampled and the height is calculated as the difference between the two. Where near stream land cover was manually digitized, the unique land cover code is sampled and recorded in the database. The distance between samples was either 10 or 15 meters, depending upon stream size.

Figure 32 - Near stream land cover radial sampling pattern.



The radial sampling pattern produces extensive overlap between each 50-meter node which ensures dense sampling of the near stream area. While there is no direct canopy cover input in the Heat Source model, the extensive land cover sampling and complex solar flux algorithms indirectly account for the density of tree stands within each radial sampling area. For example, in the figure above, approximately 50% of the ground is visible within the sampling area and since the model calculates solar flux through each radial sampling location for every minute of the day, the overall canopy density is indirectly accounted for and varies for each 50-meter stream node.

Note that there is an input in Heat Source for “land cover density”. This term is not the same as “canopy density” as it is classically used in the forest industry. Land cover density in Heat Source refers to the relative density of the vegetation that is being sampled. It can also be thought of as the amount of sky that is blocked by the trunk, branches, and leaves of a tree. In most Heat Source simulations of eastern and central Oregon, the land cover density value is set to 75%, which is representative of conifers in the region. Ground level solar pathfinder measurements have been used to successfully validate the Heat Source effective shade predictions using the 75% land cover density value.

3.5.6 TTools Step 6

One of the TIR deliverables was a point shapefile containing sampled stream temperatures. Step 6 of TTools associates the nearest TIR sample point with each 50-meter stream node. Figure 33 shows section of Catherine Creek with the 50-meter nodes and the TIR data points. The TIR data points are typically more than 50-meters apart and are located according to the helicopter position at the time the TIR image frame was collected. TTools walks through each of the 50-meter stream nodes and locates the nearest TIR data point then incorporates that data into the TTools shapefile database.

Figure 33 - Example of 50-meter stream nodes and TIR data points.

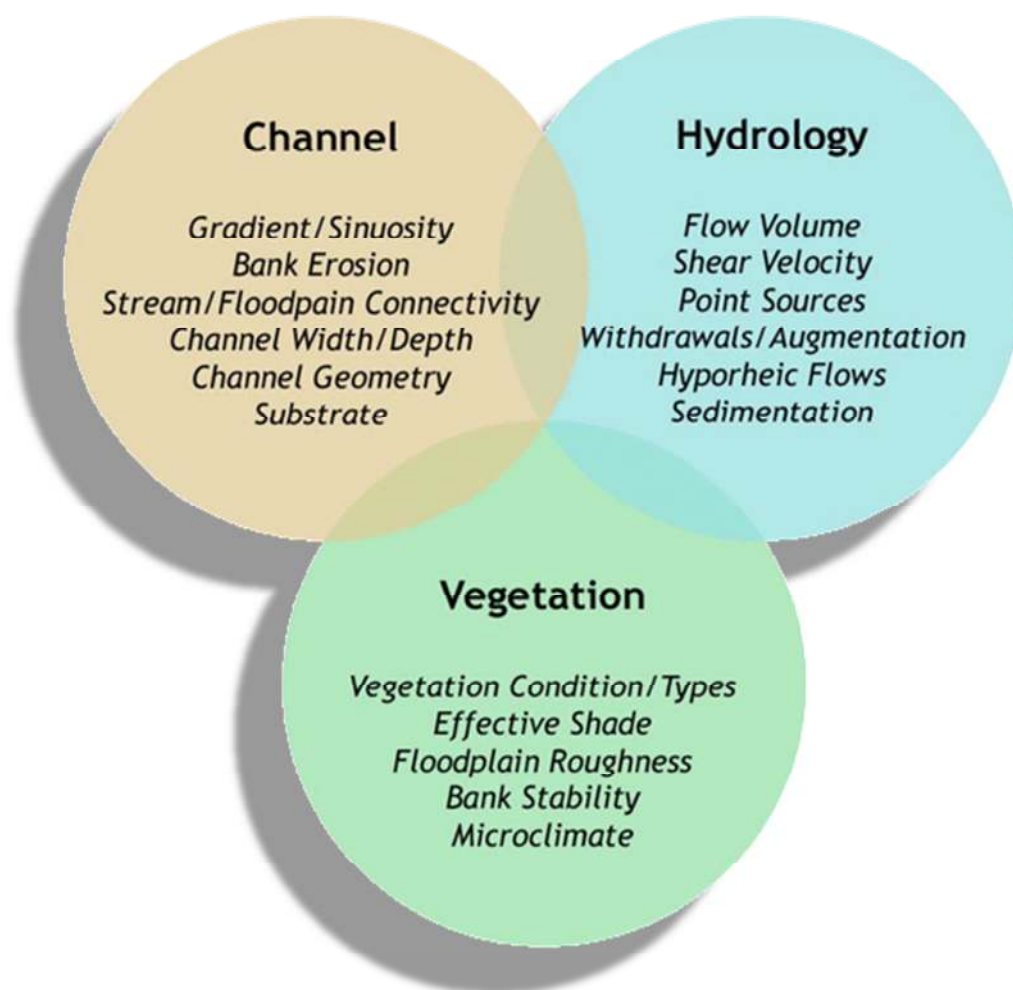


4. HEAT SOURCE OVERVIEW

Heat Source is a high-resolution stream temperature model that incorporates both remote sensing and ground level data. It has been used for stream temperature studies (including Total Maximum Daily Load development) throughout the Pacific Northwest since 1998. Some of the Heat Source characteristics are listed below:

- Input distance step = 50 meters.
- Output distance step = 100 meters.
- Time step = 1 minute.
- Hourly air temperature, relative humidity, wind speed and cloud cover inputs.
- Accommodates high-resolution LiDAR bare earth and highest hit data.
- Calibrated to TIR longitudinal profile and to hourly instream temperature measurements.
- Can be set up to simulate a connected stream network (i.e., outputs from tributaries can become inputs to receiving stream models).
- Strives to account for all factors that influence stream temperature (Figure 34).

Figure 34 - Parameters included within the Heat Source methodology.



Heat Source has a Microsoft Excel user interface and is driven by Visual Basic, Python, and C+ code. Inputs are inserted into various spreadsheet tabs within the model. Outputs are written to text files that can then be accessed within the Excel interface to be plotted or listed within the spreadsheets.

The shapefile database created from TTools sampling contains much of the information required to set up a Heat Source model. Most of the data can be copied from the shapefile database and pasted directly into Heat Source's Excel interface. Figure 35 shows one of the input worksheets where TTools data is stored.

Figure 35 - Example of the TTools data input worksheet in Heat Source.

Reach Label (optional)	Longitude (deg)	Latitude (deg)	Topographic Elev. (deg)			Emergent Veg	Veg 1	NE Veg 2	NE Veg 3	NE Veg 4	NE Veg 1	E
			West	South	East							
16.4	-118.16	45.43	30.6	9.0	28.1	0	3.2	0.1	2.5	0.5	2.2	2.2
16.35	-118.16	45.43	29.6	9.6	29.9	0	13.8	9.8	3.5	1.9	0.4	0.4
16.3	-118.16	45.43	28.2	10.0	31.6	0	0.9	2.6	1.7	25.7	0.6	0.6
16.25	-118.16	45.43	28.0	10.3	25.9	0	3.7	0.5	5.4	14.7	0.6	0.6
16.2	-118.16	45.43	28.3	10.8	13.4	0	15.6	9.2	0.3	0.3	19.1	19.1
16.15	-118.16	45.43	29.2	11.3	15.0	0	32.0	1.7	23.7	5.2	32.1	32.1
16.1	-118.16	45.43	34.1	18.1	15.2	0	1.4	4.8	8.0	8.2	37.6	37.6
16.05	-118.16	45.43	34.3	22.9	19.4	0	4.7	26.7	25.2	13.9	31.0	31.0
16	-118.16	45.43	31.2	14.0	24.5	0	1.3	0.2	2.6	0.4	8.6	8.6
15.95	-118.16	45.43	28.9	13.2	28.8	0	1.6	0.9	0.5	0.4	0.1	0.1
15.9	-118.16	45.43	27.8	13.7	32.3	0	1.0	0.3	0.6	0.6	0.6	0.6
15.85	-118.16	45.43	28.6	14.5	31.5	0	9.8	16.1	15.4	18.3	0.1	0.1
15.8	-118.16	45.43	31.2	15.4	29.6	0	0.1	0.0	5.9	0.4	0.1	0.1
15.75	-118.16	45.43	28.9	15.8	31.9	0	4.7	19.6	5.5	2.4	5.8	5.8
15.7	-118.16	45.42	30.2	17.0	30.2	0	1.1	23.3	13.6	11.8	13.3	13.3
15.65	-118.16	45.42	31.1	18.0	30.8	0	3.6	2.5	19.5	0.5	3.2	3.2
15.6	-118.16	45.42	36.6	18.1	19.0	0	0.1	0.1	0.0	0.1	0.4	0.4
15.55	-118.16	45.42	32.1	19.7	16.1	0	0.4	2.2	2.0	0.6	0.4	0.4

Heat Source uses hourly climate and stream temperature data as input. Figure 36 is an example of the continuous data input worksheet. Continuous data nodes are locations where hourly stream temperature was recorded.

Figure 36 - Example of the continuous data input worksheet in Heat Source.

Continuous Data Node 1				Boundary Condition		Continuous Data Node 1		Continuous Data Node 1		Continuous Data Node 1		Continuous Data Node 1	
Continuous Data Node Locational Information (optional)				Node	Notes (optional)	Stream km	Flow (cms)	Temperature (°C)	Cloudiness (0 - 1)	Wind Speed (m/s)	Humidity (0 - 1)	Air Temp (°C)	Stream Temp (°C)
Five Points above Little JD Creek				1		12.00	0.02971	11.2	0.1	0.9	0.5	19.9	16.2
Five Points above Pelican Creek				2		2.35	0.02971	11.1	0.0	0.5	0.6	17.7	16.0
Five Points at Mouth				3		0.10	0.02971	10.9	0.0	0.0	0.7	15.5	15.7
							0.02971	10.8	0.0	0.8	0.7	15.5	15.4
							0.02971	10.7	0.0	0.0	0.7	14.9	15.1
							0.02971	10.5	0.0	0.8	0.7	15.5	14.9
							0.02971	10.4	0.0	1.0	0.6	16.6	14.6
							0.02971	10.3	0.0	0.6	0.7	15.5	14.5
							0.02971	10.3	0.4	0.9	0.5	18.8	14.7
							0.02971	10.5	0.1	1.7	0.4	21.6	15.5
							0.02971	11.1	0.0	1.4	0.4	23.8	16.7
							0.02971	12.2	0.0	1.4	0.4	25.5	17.9
							0.02971	13.3	0.0	1.3	0.3	26.6	19.0
							0.02971	14.2	0.0	1.2	0.3	27.7	19.8
							0.02971	14.9	0.0	0.9	0.3	28.8	20.6
							0.02971	14.9	0.0	0.6	0.3	28.8	20.9
							0.02971	14.3	0.0	1.7	0.2	28.8	20.7
							0.02971	13.6	0.0	1.0	0.2	28.8	20.3
							0.02971	12.8	0.0	1.5	0.3	26.6	19.6
							0.02971	12.4	0.0	1.5	0.3	25.5	18.6

Typically, Heat Source uses a 50-meter input distance step. Figure 37 shows the morphology data input worksheet. Manning's n, sediment heat exchange, and hyporheic flow are some of the most commonly adjusted inputs during model calibration.

Figure 37 - Example of the morphology data input worksheet in Heat Source.

Microsoft Excel - Five Points, Calibration, xsm - Microsoft Excel non-commercial use

FileHomeInsertPage LayoutFormulasDataReviewViewDeveloperAdd-InsAcrobat

PasteClipboard

Font

Alignment

Number

Conditional Formatting

Format as Table

Cell Styles

Insert

Delete

Format

AutoSum

Fill

Clear

Sort & Find & Filter

Select

Editing

E10=A10*0.66

A

B

C

D

E

F

G

H

I

J

K

L

M

N

1

2

3

4

5

6

7

8

9

10

11

12

13

14

15

16

17

18

19

20

21

22

23

24

Five Points Creek

Bottom Width

z

1

Locational Information (optional)	Elevation	Gradient	Bottom Width (m)	Channel Angle z	Manning's n	Parameters for sediment heat exchange and hyporheic flow				Optional				
						Sediment Thermal Conductivity (W/m°C)	Sediment Thermal Diffusivity (cm²/sec)	Sediment / hyporheic zone thickness (m)	Percent Hyporheic Exchange	Porosity (0 - 1)	TIR Date/Time	TIR Temp. (°C)		
6	4.7367	16.4	1131.63	2.400%	3.13	0.000	0.700	1.6	0.0064	0.03	5.00%	0.4	8/7/10 13:58	15.40
7	4.09236	16.35	1130.40	2.460%	2.70	0.000	0.700	1.6	0.0064	0.03	5.00%	0.4	8/7/10 13:58	15.40
8	2.26737	16.3	1129.30	2.200%	1.50	0.000	0.700	1.6	0.0064	0.03	5.00%	0.4	8/7/10 13:58	15.40
9	2.29536	16.25	1128.30	2.000%	1.51	0.000	0.700	1.6	0.0064	0.03	5.00%	0.4	8/7/10 13:58	15.90
10	2.07227	16.2	1127.66	1.25%	1.37	0.000	0.700	1.6	0.0064	0.20	5.00%	0.4	8/7/10 13:58	15.90
11	3.15135	16.15	1126.39	2.540%	2.08	0.000	0.700	1.6	0.0064	0.20	5.00%	0.4	8/7/10 13:58	15.90
12	2.50744	16.1	1125.64	1.500%	1.65	0.000	0.700	1.6	0.0064	0.20	5.00%	0.4	8/7/10 13:58	15.90
13	4.4833	16.05	1124.19	2.900%	2.96	0.000	0.700	1.6	0.0064	0.20	5.00%	0.4	8/7/10 13:58	13.20
14	3.76598	16	1123.27	1.840%	2.49	0.000	0.700	1.6	0.0064	0.20	5.00%	0.4	8/7/10 13:58	13.20
15	4.17356	15.95	1122.52	1.500%	2.75	0.000	0.700	1.6	0.0064	0.20	5.00%	0.4	8/7/10 13:58	13.20
16	3.68258	15.9	1121.66	1.720%	2.43	0.000	0.700	1.6	0.0064	0.20	5.00%	0.4	8/7/10 13:58	15.90
17	4.06346	15.85	1121.09	1.140%	2.68	0.000	0.700	1.6	0.0064	0.20	5.00%	0.4	8/7/10 13:58	15.90
18	2.20694	15.8	1120.33	1.520%	1.46	0.000	0.700	1.6	0.0064	0.03	5.00%	0.4	8/7/10 13:58	15.90
19	4.53882	15.75	1118.65	3.360%	3.00	0.000	0.700	1.6	0.0064	0.03	5.00%	0.4	8/7/10 13:58	15.40
20	2.70296	15.7	1118.11	1.080%	1.78	0.000	0.700	1.6	0.0064	0.03	5.00%	0.4	8/7/10 13:58	15.40
21	4.8671	15.65	1117.02	2.180%	3.21	0.000	0.700	1.6	0.0064	0.03	5.00%	0.4	8/7/10 13:58	15.40
22	2.01133	15.6	1115.88	2.280%	1.33	0.000	0.700	1.6	0.0064	0.03	5.00%	0.4	8/7/10 13:58	17.50
23	3.05033	15.55	1114.87	2.020%	2.01	0.000	0.700	1.6	0.0064	0.03	5.00%	0.4	8/7/10 13:58	15.80
24	3.70035	15.5	1114.01	1.720%	2.44	0.000	0.700	1.6	0.0064	0.03	5.00%	0.4	8/7/10 13:58	16.50

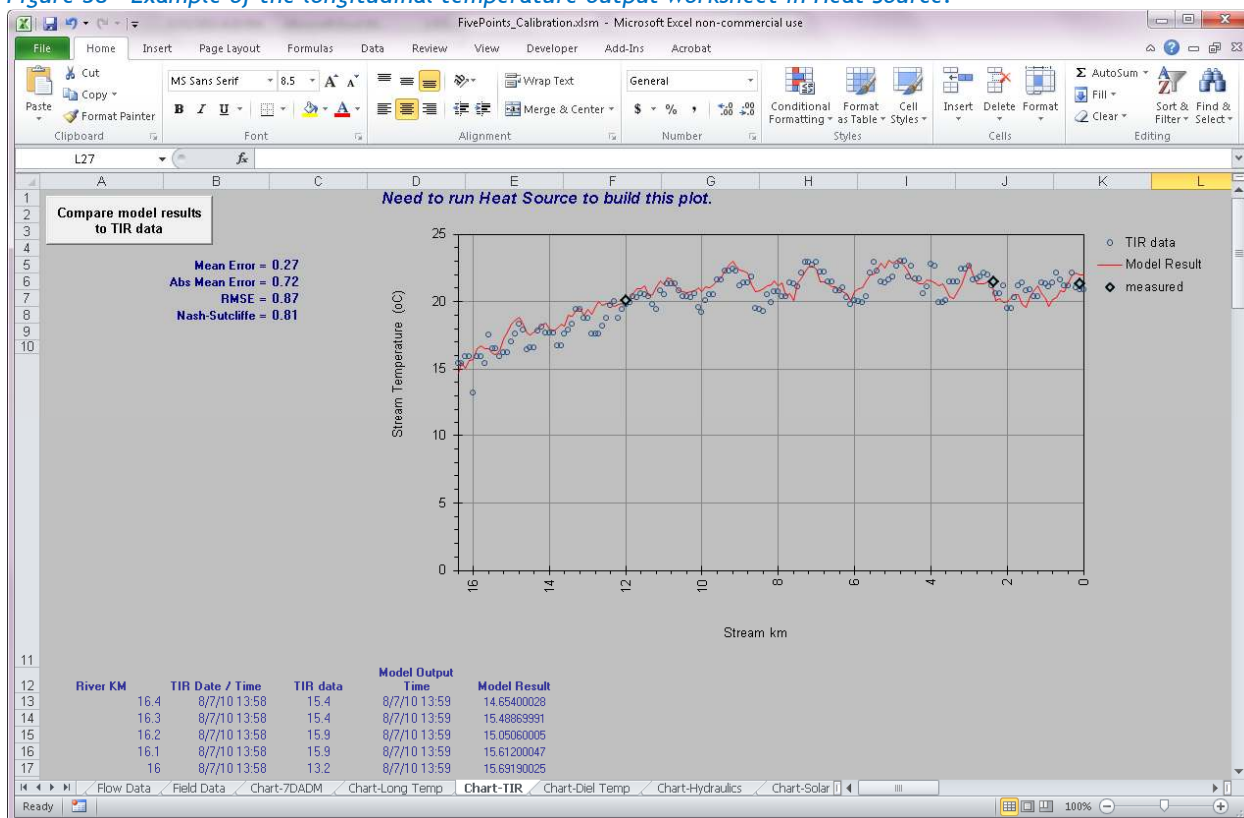
TTools DataLand Cover CodesMorphology DataContinuous DataFlow DataField DataChart-7ADAMChaJ

Ready

100%

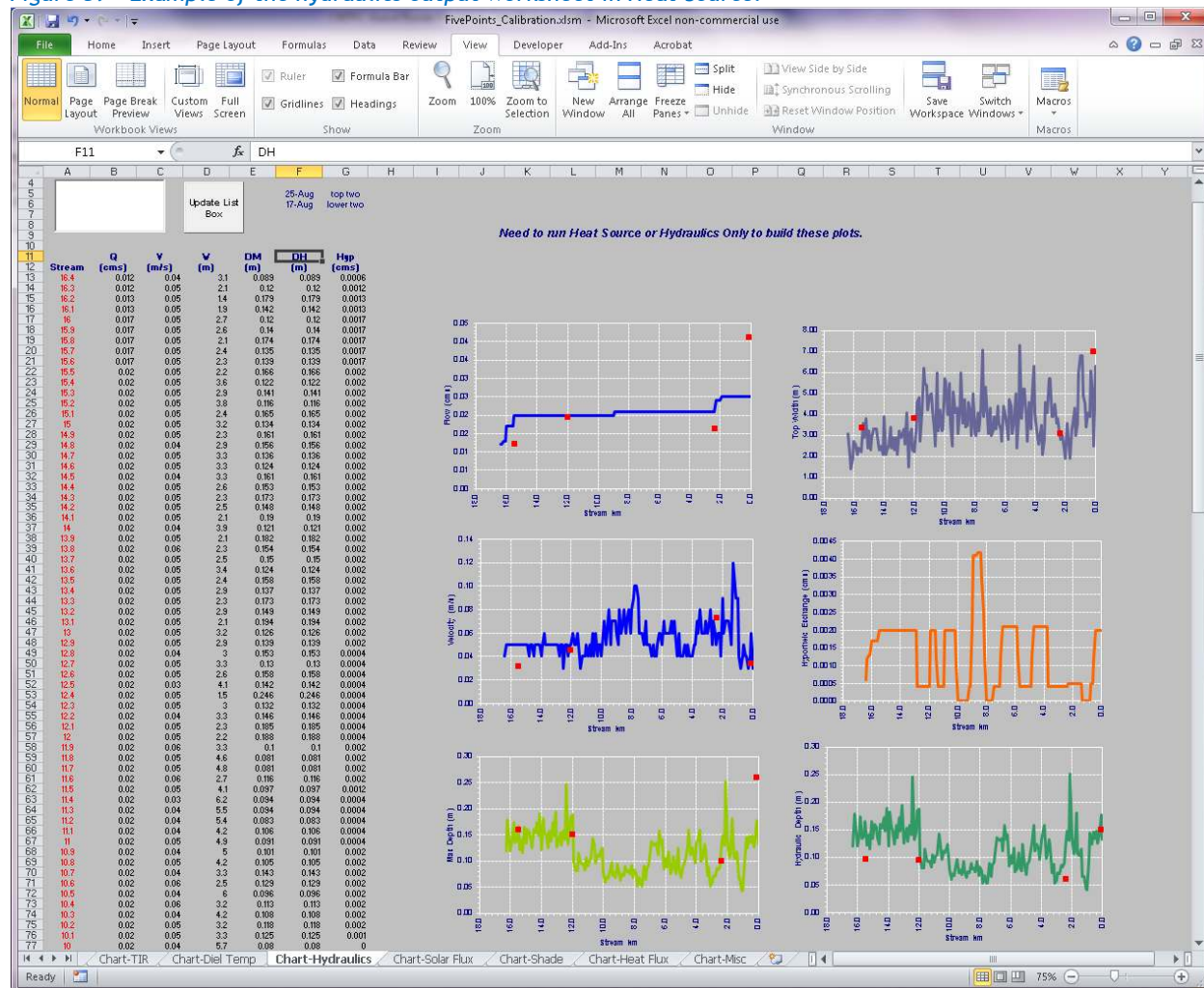
The Heat Source model contains several worksheets that use data from the output text files to display temporal and longitudinal data. Figure 38 shows the longitudinal temperature calibration worksheet. After the model is run, this chart is updated for the user to compare simulated and measured values. There are similar charts that compare the hourly simulated and measured data for each continuous monitoring location.

Figure 38 - Example of the longitudinal temperature output worksheet in Heat Source.



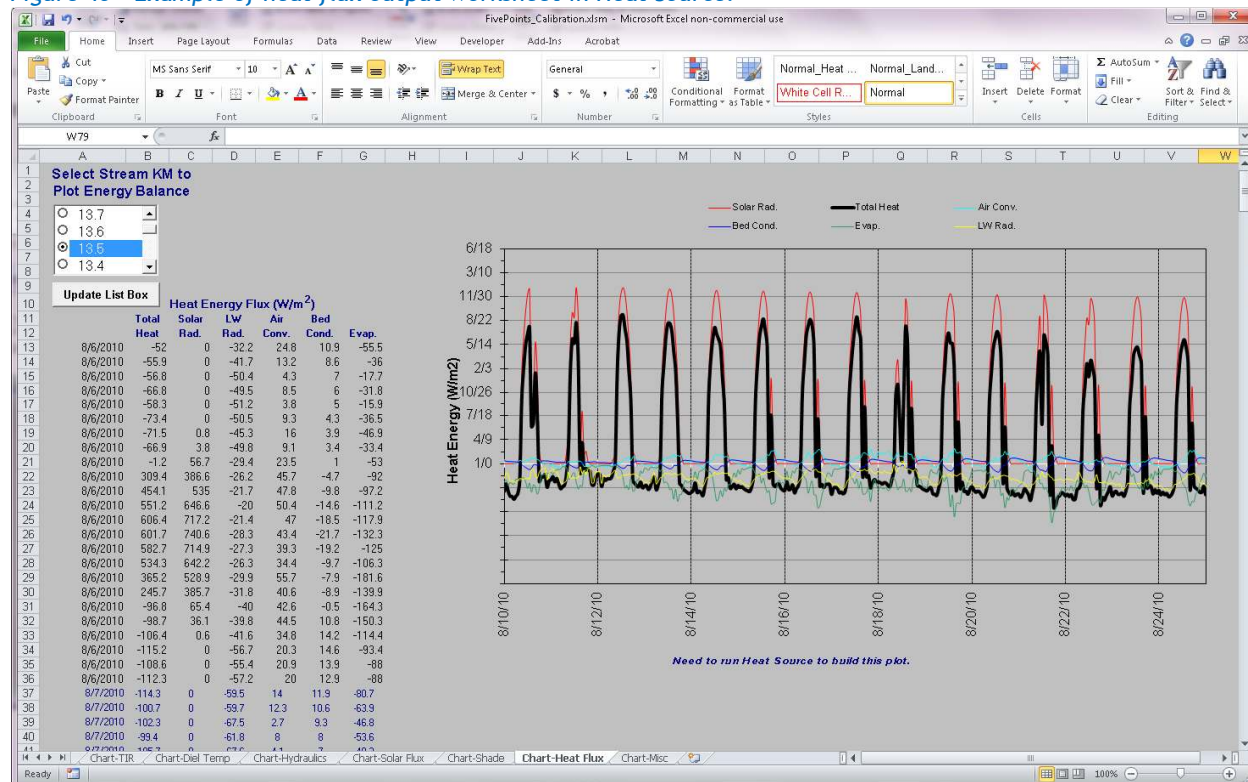
Model hydraulics is another important output worksheet in Heat Source (Figure 39). The simulation outputs can be plotted within this worksheet for model validation purposes. Any available ground level measurements can be included within these charts to compare simulated and measured values. The data can be plotted for each day of the simulation.

Figure 39 - Example of the hydraulics output worksheet in Heat Source.

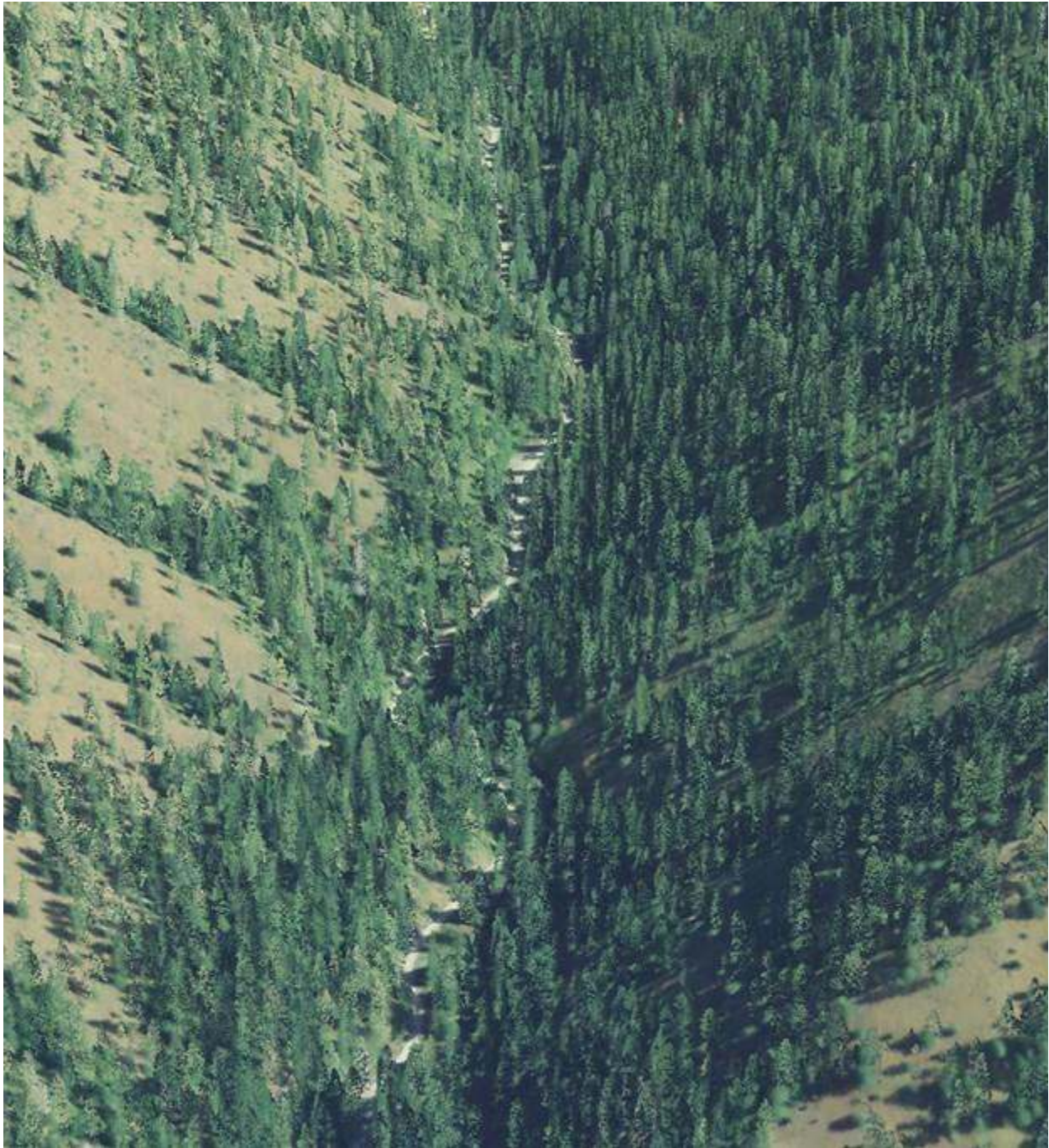


Heat Source also records the hourly heat flux values for each 100-meter output node. There is a worksheet where the user can view various simulated heat flux values (Figure 40). These outputs are useful during calibration to make sure that the simulation is within reasonable boundaries for solar flux, bed conduction, evaporation, air convection, longwave radiation, etc.

Figure 40 - Example of heat flux output worksheet in Heat Source.



5. NORTH FORK CATHERINE CREEK



RGB-colored LiDAR point cloud - North Fork Catherine Creek looking upstream just above mouth (road visible alongside stream).

5.1 North Fork Catherine Creek TTools

The North Fork Catherine Creek has a moderate gradient, typically between 2% and 8%. Figure 41 shows the TTools-sampled stream elevations and calculated gradients for each 50-meter node.

Figure 41 - North Fork Catherine Creek elevation and gradient.

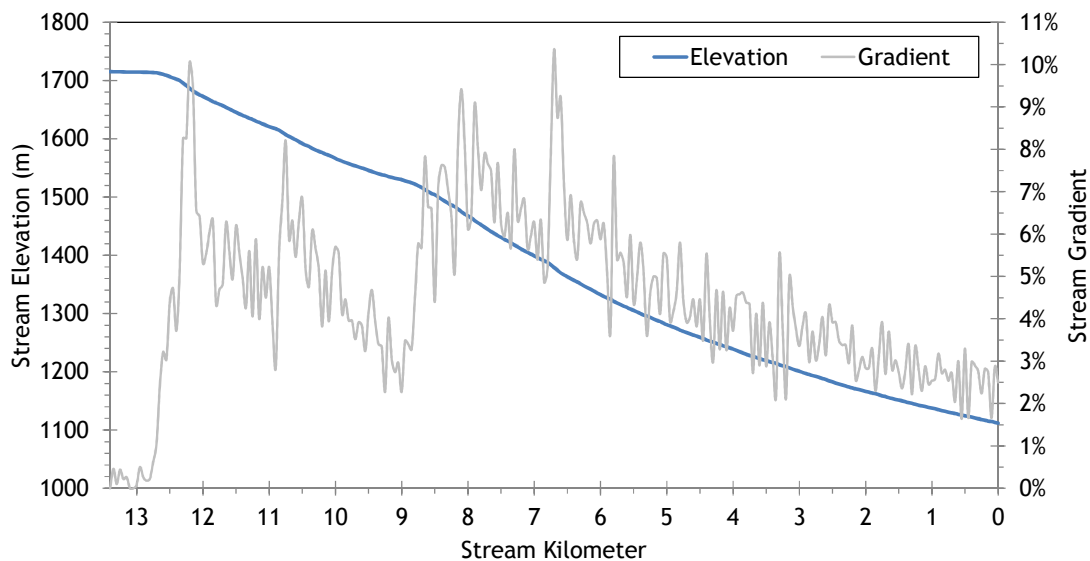
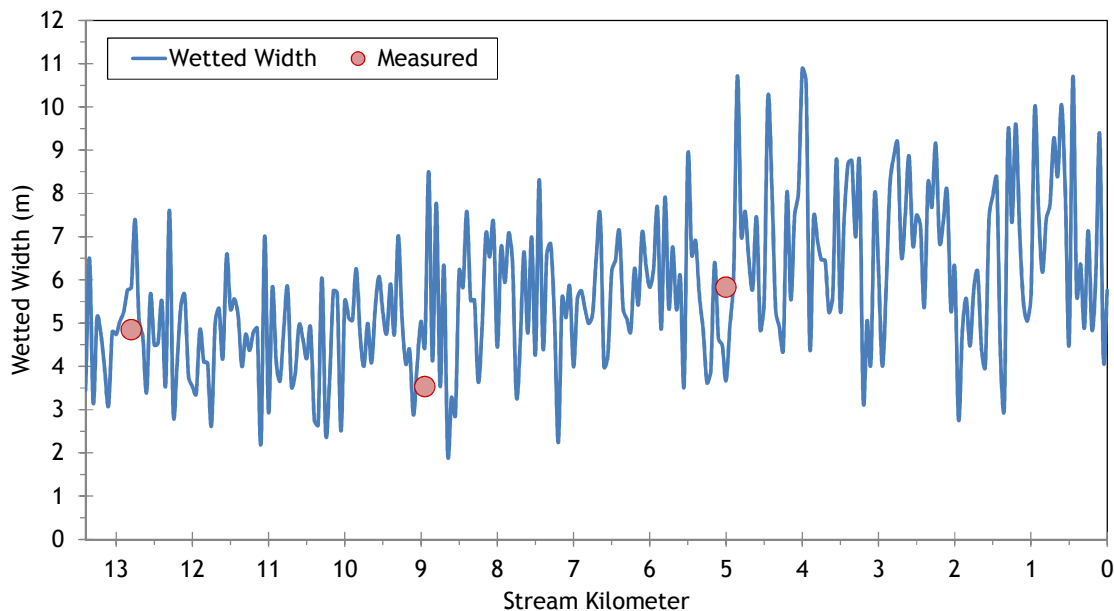


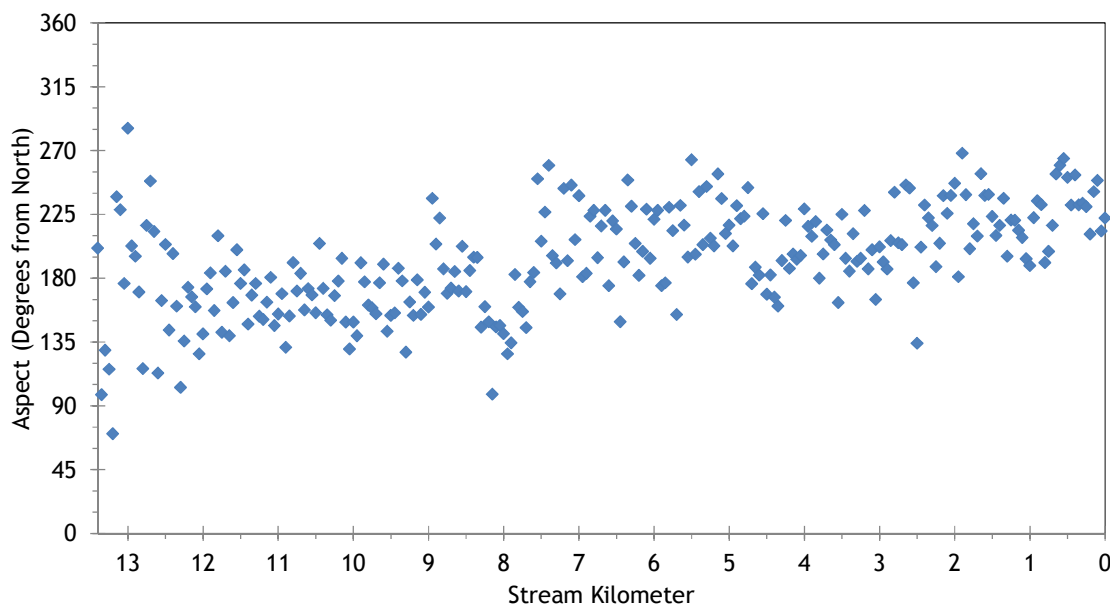
Figure 42 shows the TTools-sampled and measured wetted widths for the North Fork Catherine Creek which are used as estimates for the simulation time period. Generally, the stream was between 4 and 8 meters wide during August 2010.

Figure 42 - North Fork Catherine Creek wetted width.



The North Fork Catherine Creek generally flows from north to south. Figure 43 shows the TTools-sampled stream aspect for each 50-meter node. Aspect is an important Heat Source input parameter because it is used to calculate solar flux at the stream surface.

Figure 43 - North Fork Catherine Creek stream aspect.



The North Fork Catherine Creek flows through mountainous foothills and eastern and western topographic shade angles are typically over 20 degrees from the horizon (Figure 44). Since the stream flows down a predominately south-facing slope, the southern topographic shade angles are smaller.

Figure 44 - North Fork Catherine Creek topographic shade angles.

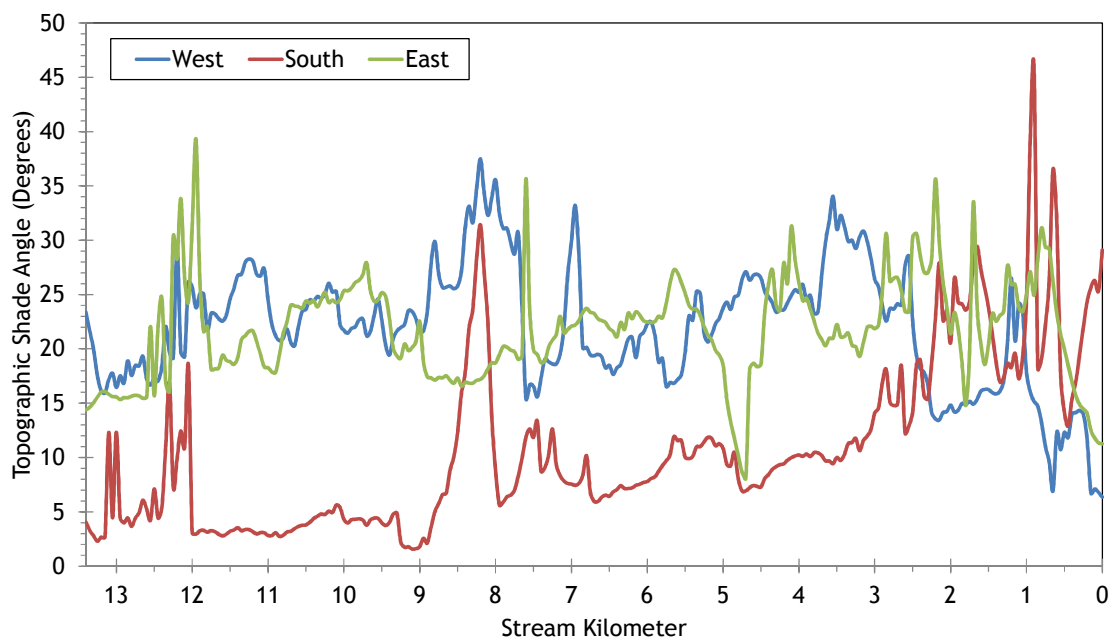
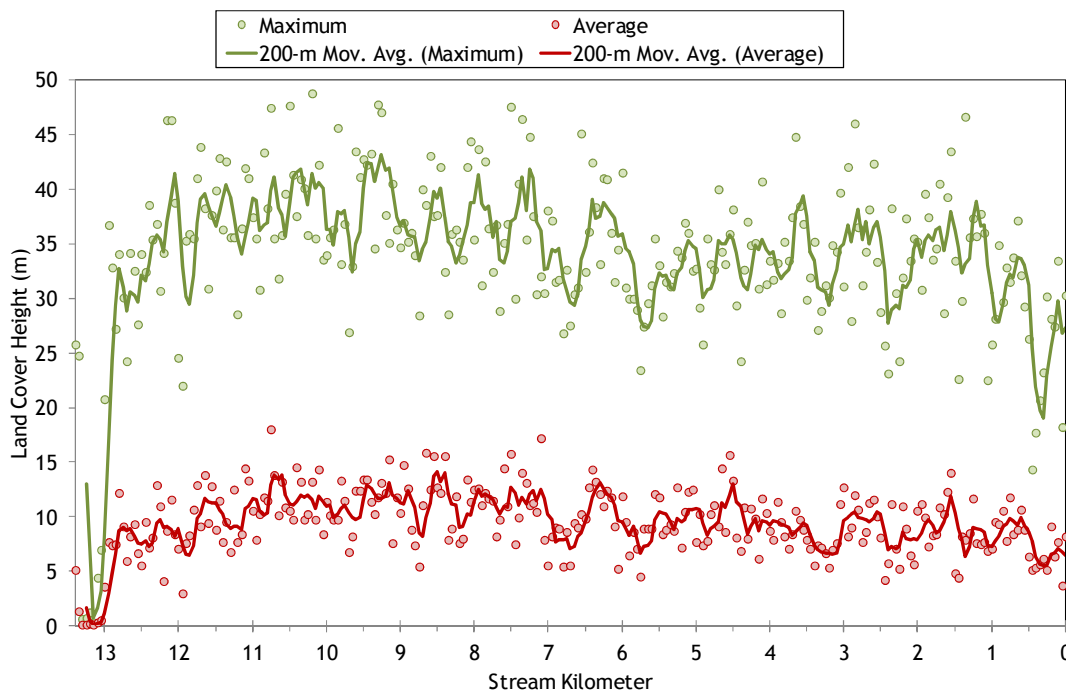


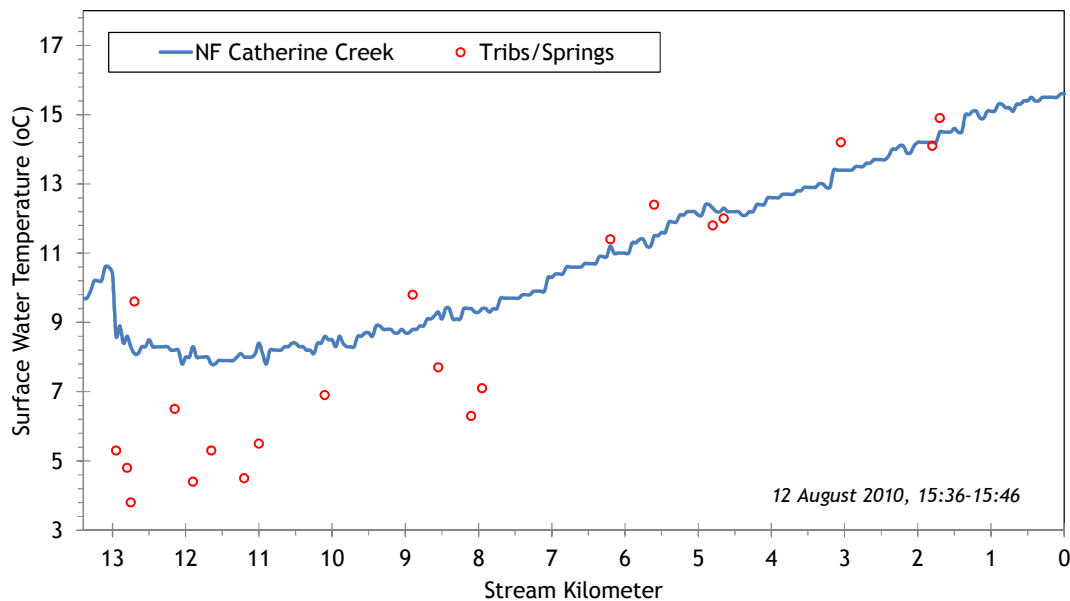
Figure 45 shows the land cover heights sampled along North Fork Catherine Creek. The maximum and average of the 28 radial samples were calculated for each 50-meter stream node. The stream is well-forested throughout most of its length. (Note: Heat Source uses each of the 28 radial samples for each 50-meter node. The maximum and average are shown here for simplification purposes.)

Figure 45 - North Fork Catherine Creek land cover heights sampled from highest hit LiDAR.



TTools was used to associate TIR temperatures with each 50-meter node (Figure 46). Heat Source is calibrated to the TIR longitudinal temperature profile. The North Fork Catherine Creek was cool, relative to other streams in the watershed at the time of the survey (12 August 2010, 15:36-15:46).

Figure 46 - North Fork Catherine Creek TIR temperature profile.



5.2 North Fork Catherine Creek Heat Source Calibration

The North Fork Catherine Creek was simulated from just above Amelia Spring to the mouth (13.4 stream kilometers). The largest tributaries are the Middle Fork Catherine Creek, Buck Creek, and Lick Creek. There were four sites where hourly stream temperature data collection was attempted; however there were data quality issues at some locations. Figure 47 shows the simulation extent and continuous temperature monitoring locations.

Figure 47 - North Fork Catherine Creek simulation extent.

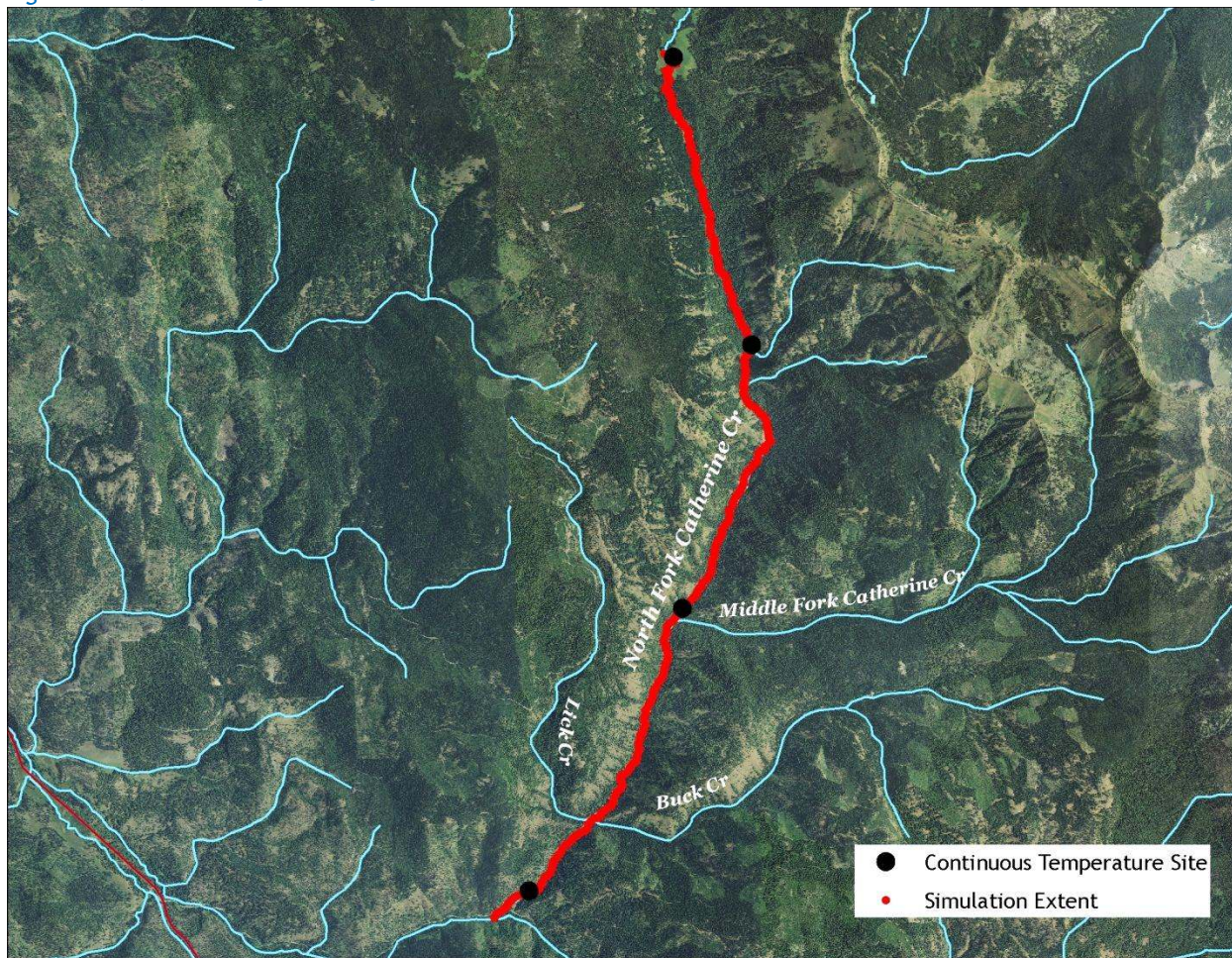


Table 5 - North Fork Catherine Creek general Heat Source parameters.

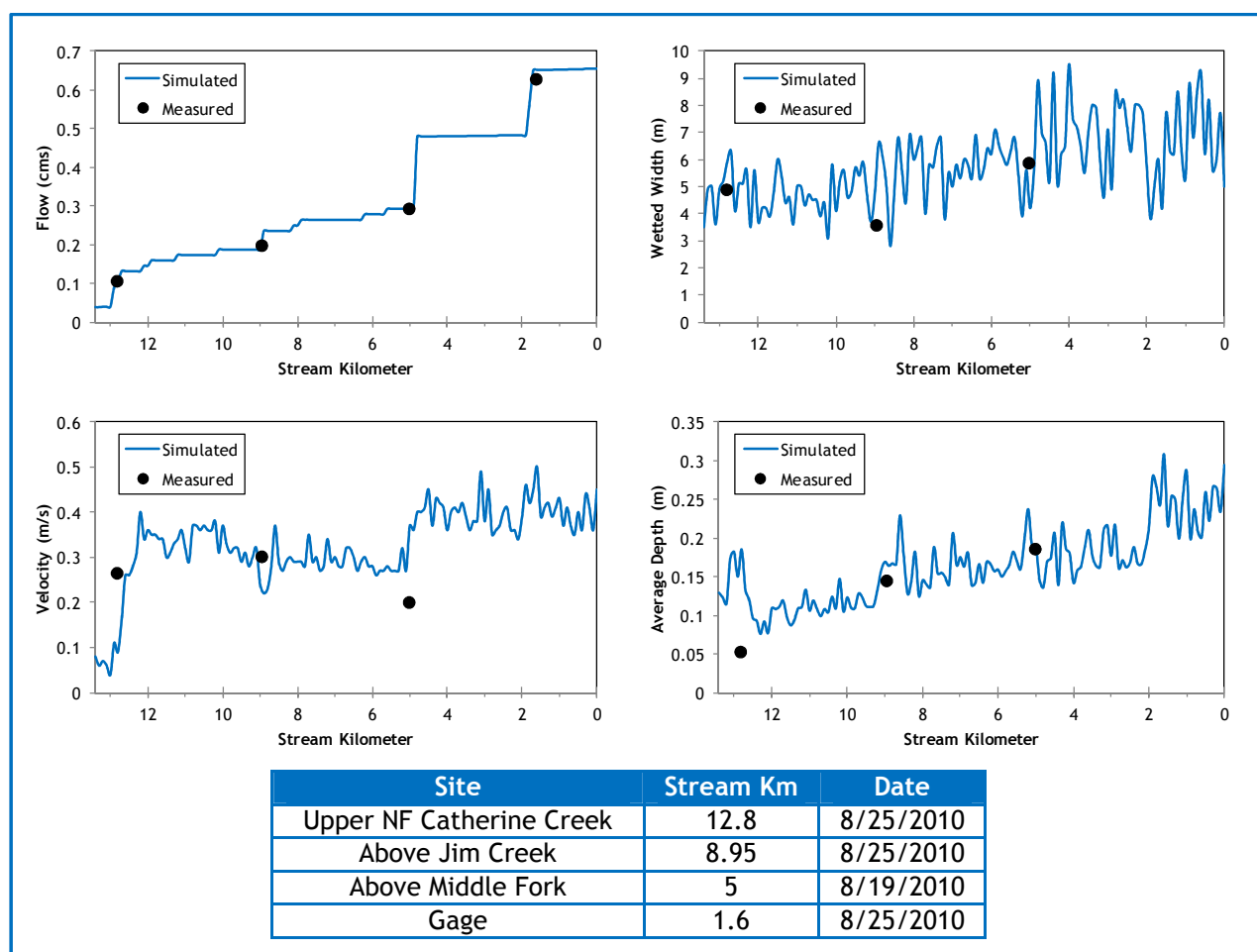
Stream:	North Fork Catherine Creek
Length:	13.4 kilometers
Time Period:	August 6-27, 2010
Input Distance Step:	50 meters
Output Distance Step:	100 meters
Time Step:	1 minute
Flush Initial Condition:	7 days
TIR Date and Time:	August 12, 2010 15:36-15:46
Land Cover Data Source:	LiDAR
Land Cover Sampling Distance Step:	15 meters

Following is a list of assumptions that were used during Heat Source calibration:

- Hourly climate data was obtained from the La Grande Airport (NWS). Air temperature was adjusted using the adiabatic lapse rate of 1°C per 100 meters elevation.
- Daily flow volumes vary based on extrapolation (back-calculation) from the gage data recorded on the North Fork Catherine Creek at Medical Springs (stream kilometer 1.6).
- There were no observed diversions or withdrawals on the stream.
- Small springs and seeps were assumed constant volumes and temperatures.
- Jim Creek, Buck Creek, Lick Creek, and Middle Fork Catherine Creek were included using daily variable flow volume and hourly temperatures (see Table 6).

Figure 48 shows the simulated and measured hydraulic values for the calibrated model. The simulated data was plotted for August 25, 2010 because that is the day most of the field measurements were collected. The simulated values vary daily based upon flow volume.

Figure 48 - North Fork Catherine Creek simulated and measured hydraulics values.



Daily flow values used in the model were based upon data recorded at the gage near Medical Springs. Figure 49 compares the simulated and measured flow volumes at the gage for the entire simulation time period. The simulated daily flow values are identical to the gage values because those gage data were used as the starting point for the stream flow mass balance calculations. Tributary and spring inflows were estimated and applied within the model in order to meet the recorded gage values.

Figure 49 - North Fork Catherine Creek simulated and measured daily flow volumes at the gage near Medical Springs.

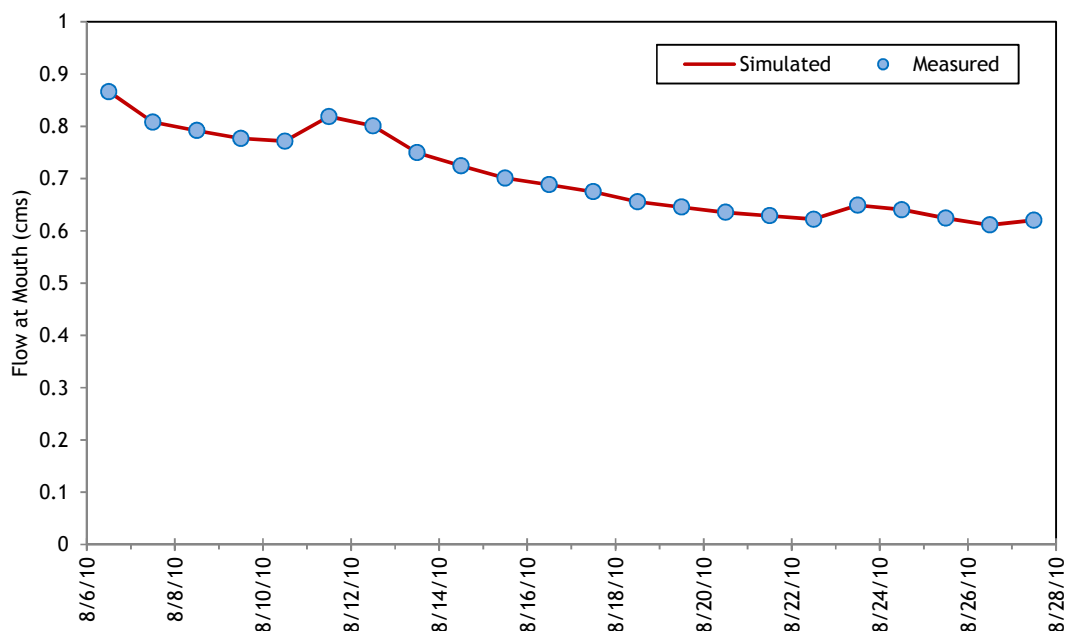


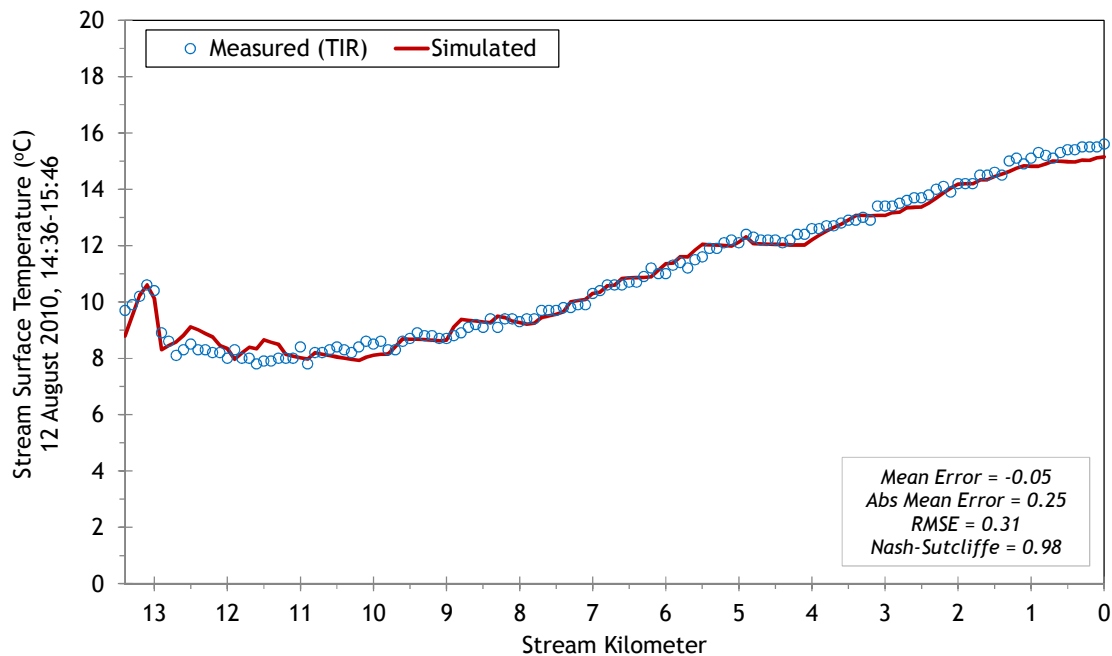
Table 6 summarizes the mass flow inputs that were included within the calibrated Heat Source model. They are features that were identified from the TIR imagery.

Table 6 - North Fork Catherine Creek mass inflow locations and assumptions.

Feature	Stream Km	Assumptions
Amelia Spring	12.95	0.05 cms at 5.3°C (constant)
Seep	12.8	0.014 cms at 4.8°C (constant)
Spring	12.75	0.014 cms at 3.8°C (constant)
Unnamed Trib	12.7	0.014 cms at 9.6°C (constant)
Spring	12.15	0.014 cms at 6.5°C (constant)
Spring	11.9	0.014 cms at 4.4°C (constant)
Spring	11.2	0.014 cms at 4.5°C (constant)
Seep	10.1	0.014 cms at 6.9°C (constant)
Jim Creek	8.9	Estimated daily flow (mass balance) and MF temperatures minus 2°C.
Spring	8.1	0.014 cms at 8.1°C (constant)
Spring	7.95	0.014 cms at 7.1°C (constant)
Unnamed Trib	6.2	0.014 cms at variable temperature
Unnamed Trib	5.6	0.014 cms at variable temperature
Middle Fork Catherine Cr	4.8	Estimated daily flow (mass balance) and measured hourly temperatures.
Buck Creek	1.8	Estimated daily flow (mass balance) and MF temperatures minus 2.3°C.
Lick Creek	1.7	Estimated daily flow (mass balance) and MF temperatures minus 3.1°C.

The North Fork Catherine Creek simulated and measured longitudinal temperatures are shown in Figure 50. Amelia Spring is responsible for the sudden temperature drop near stream kilometer 13. Then the stream gradually heats without any significant thermal fluctuations. The springs and seeps were small, while the tributaries were also relatively small and cool. The RMSE of the longitudinal temperature calibration is 0.31°C , which means the simulated instantaneous values match well to the measured TIR data.

Figure 50 - North Fork Catherine Creek longitudinal stream temperature calibration.

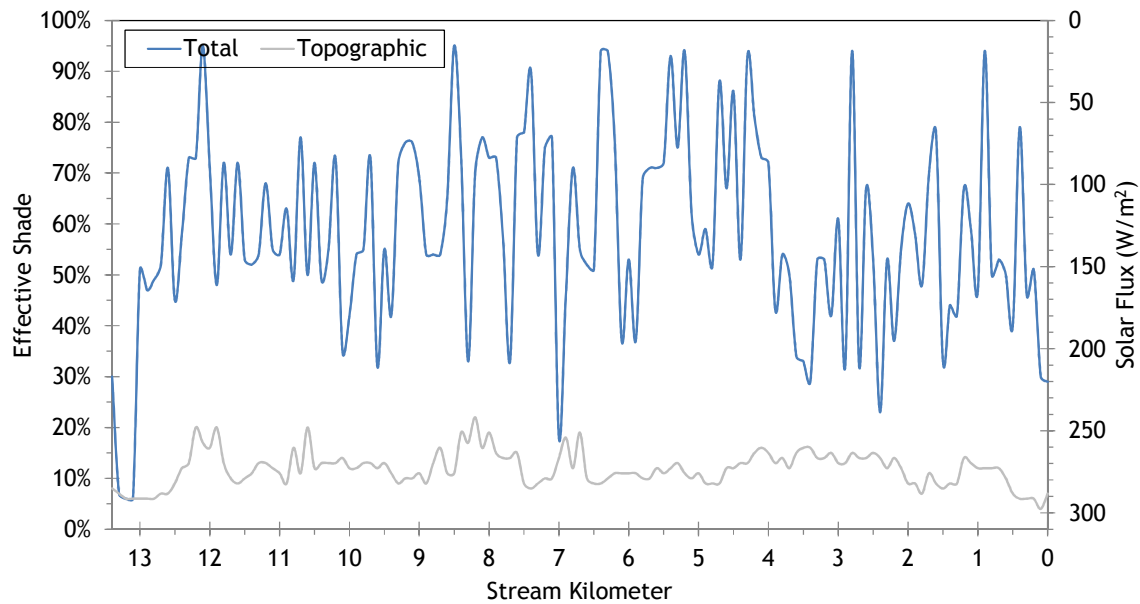


NOTE: There were no valid hourly stream temperature data available besides that which was used for the boundary condition. Data was not retrieved for the two middle sites. The data recorded at the mouth was out of the water and did not record valid stream temperatures. Therefore, there are no hourly temperature calibration results or statistics.

Effective shade is one of the Heat Source simulation outputs (Figure 51). The North Fork Catherine Creek is well-forested and the stream is shaded through much of the day, resulting in effective shade values over 50% for most areas.

Topographic shade was simulated by removing all land cover from within the model. Topographic shade was typically 10% or greater throughout the stream. The difference between the total effective shade and the topographic shade shown in Figure 51 is the amount that can be attributed to land cover.

Figure 51 - North Fork Catherine Creek simulated effective shade.



LiDAR point cloud with RGB extraction - North Fork Catherine Creek upper reach.

6. SOUTH FORK CATHERINE CREEK

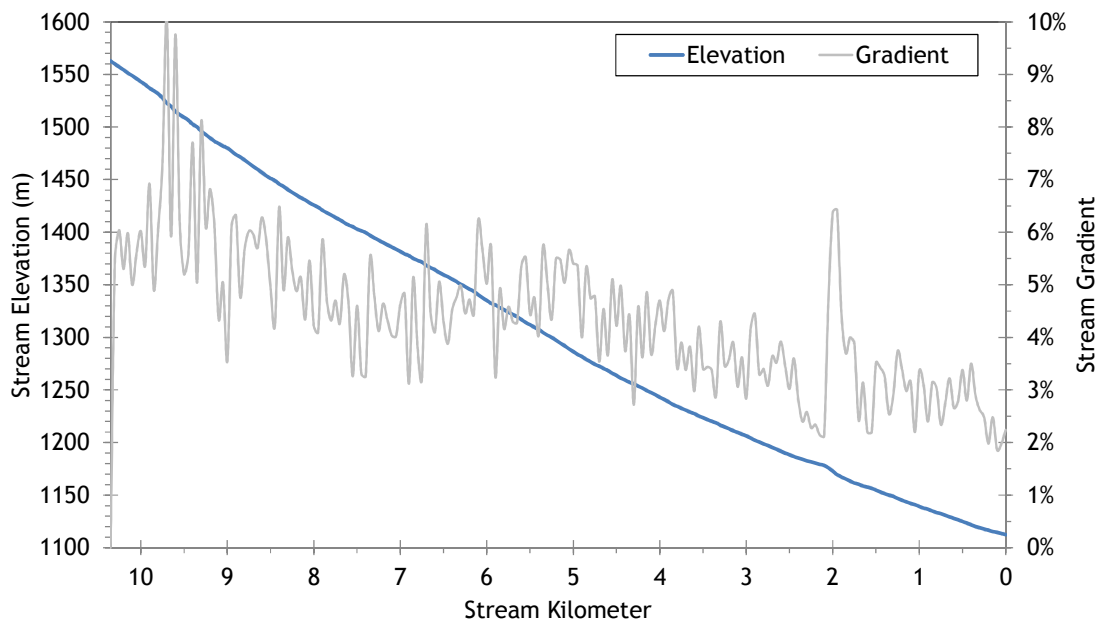


RGB-colored LiDAR point cloud - South Fork Catherine Creek looking upstream toward Corral Creek confluence.

6.1 South Fork Catherine Creek TTools Results

The South Fork Catherine Creek has a moderately steep gradient that ranges between 2% and 8% (Figure 52). It drops about 450 meters in elevation in the lower 10 stream kilometers.

Figure 52 - South Fork Catherine Creek elevation and gradient.



The South Fork Catherine Creek wetted widths were sampled at each 50-meter node (Figure 53). Ground level measurements are included in the chart for validation purposes. Generally, the stream is between 3 and 6 meters wide.

Figure 53 - South Fork Catherine Creek wetted width.

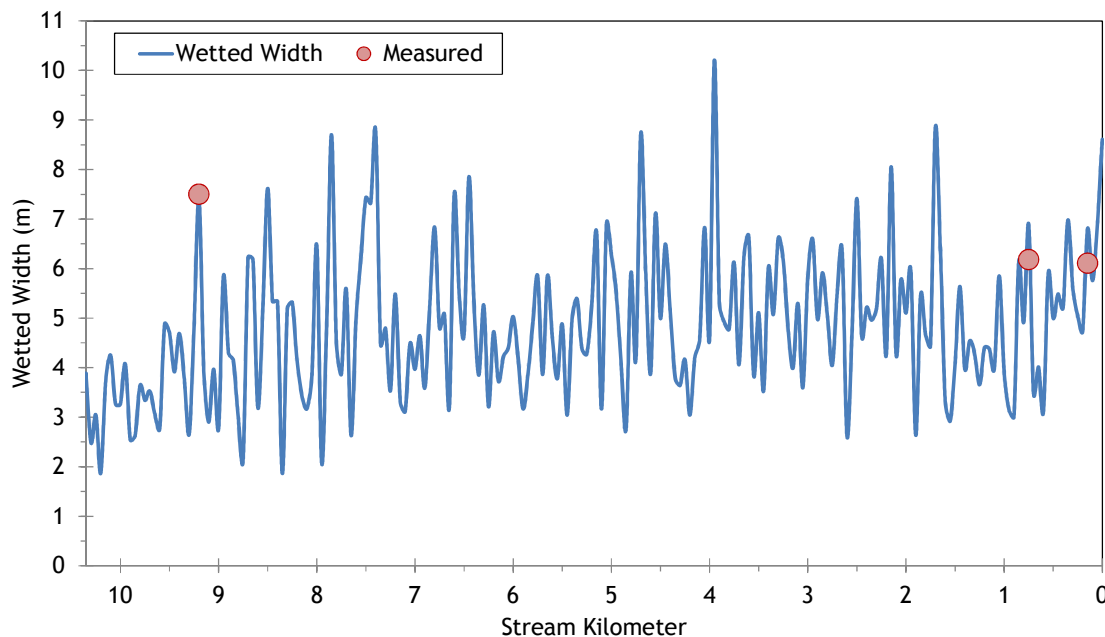
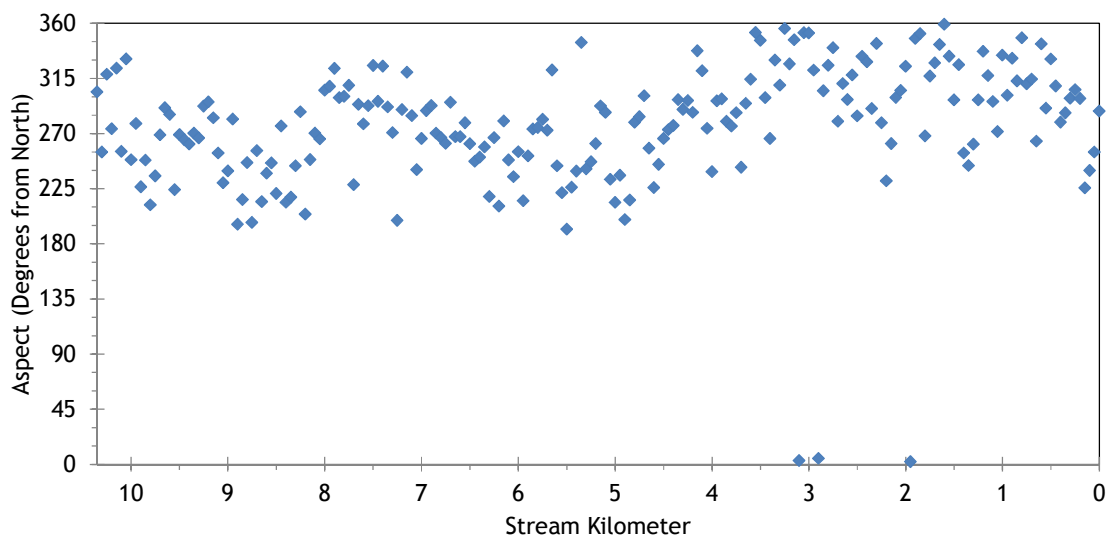


Figure 54 shows the stream aspect for each 50-meter reach of the South Fork Catherine Creek. The stream flows generally from east to west. Since it flows within a confined mountain valley, the stream meanders very little.

Figure 54 - South Fork Catherine Creek stream aspect.



Topographic shade angles of the South Fork Catherine Creek are shown in Figure 55. Since the stream flows east to west, the highest topographic shade angles are produced by hills or mountains to the south.

Figure 55 - South Fork Catherine Creek topographic shade angles.

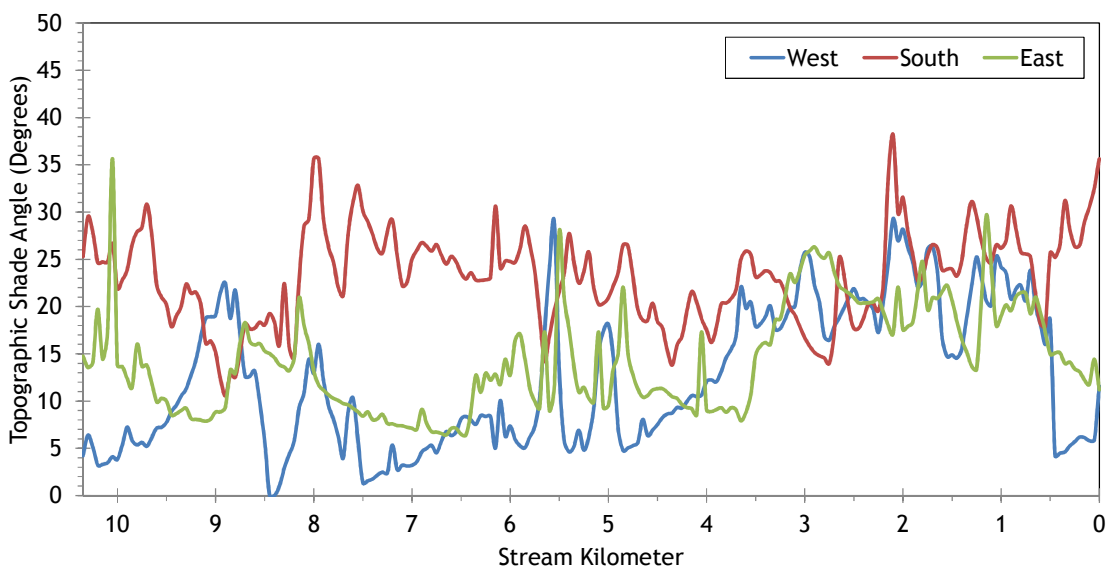
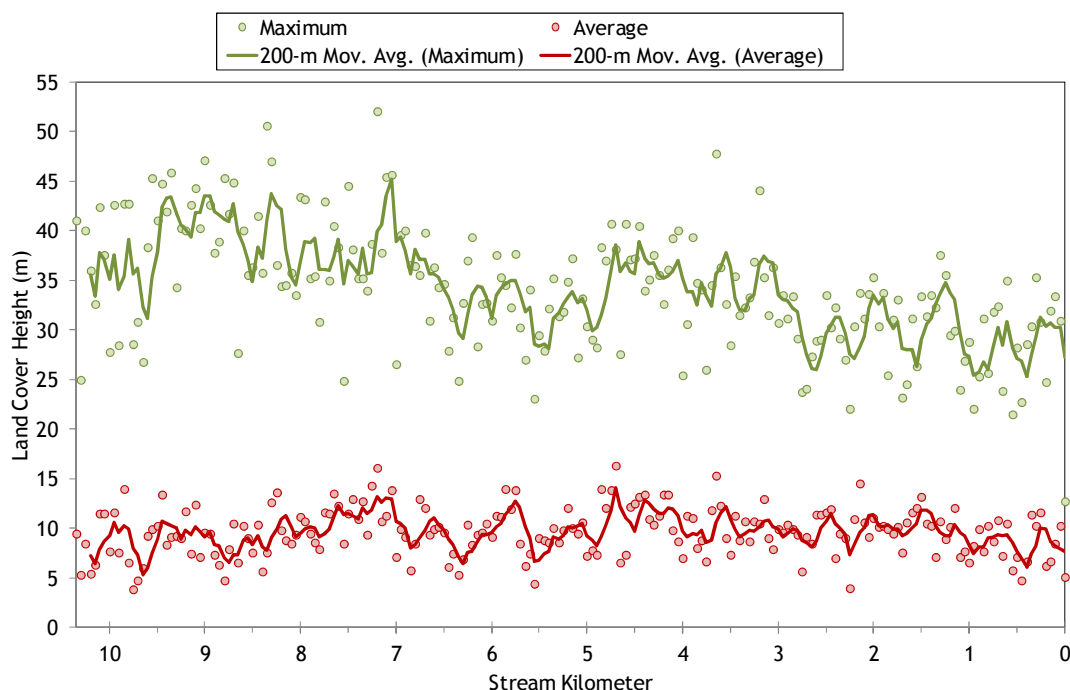


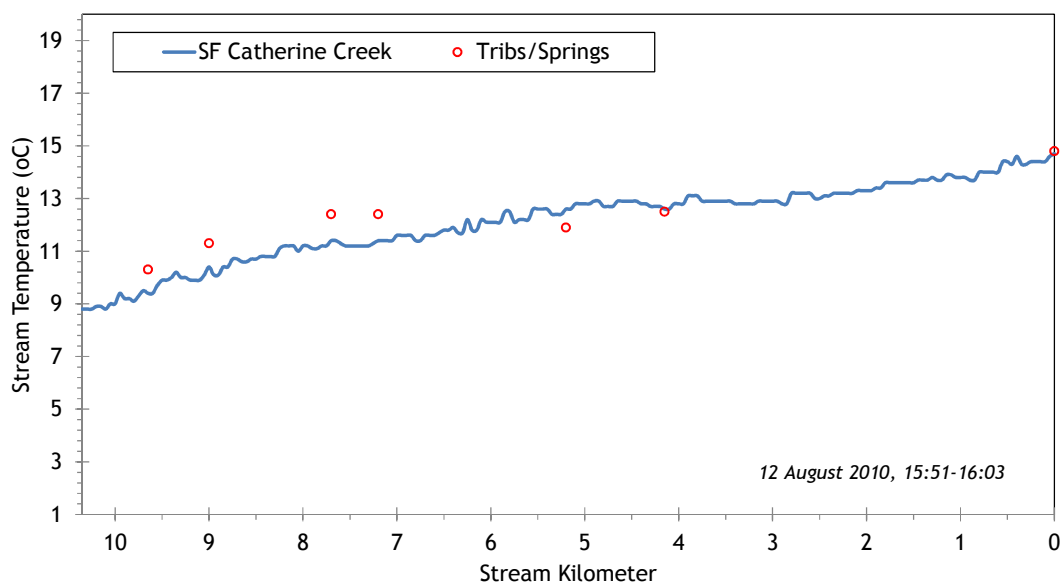
Figure 56 shows the land cover heights sampled along South Fork Catherine Creek. The maximum and average of the 28 radial samples were calculated for each 50-meter stream node. The stream is flanked by mature conifers and riparian trees through most of its length. (Note: Heat Source uses each of the 28 radial samples for each 50-meter node. The maximum and average are shown here for simplification purposes.)

Figure 56 - South Fork Catherine Creek land cover heights sampled from highest hit LiDAR.



The South Fork Catherine Creek flows through predominantly forested mountain foothills, is well-shaded and remains relatively cool compared to other streams in the watershed (Figure 57). The stream barely reached 15°C at the mouth at the time of the TIR survey.

Figure 57 - South Fork Catherine Creek TIR stream temperature profile.



6.2 South Fork Catherine Creek Heat Source Calibration

The lower 10.4 kilometers of South Fork Catherine Creek were simulated (Figure 58). The stream originates in the Eagle Cap Wilderness area and flows westward until joining with the North Fork to form the Catherine Creek mainstem. The South Fork Catherine Creek is primarily forested and flows within a v-shaped mountain valley. There are several small tributaries as well.

Figure 58 - South Fork Catherine Creek simulation extent.

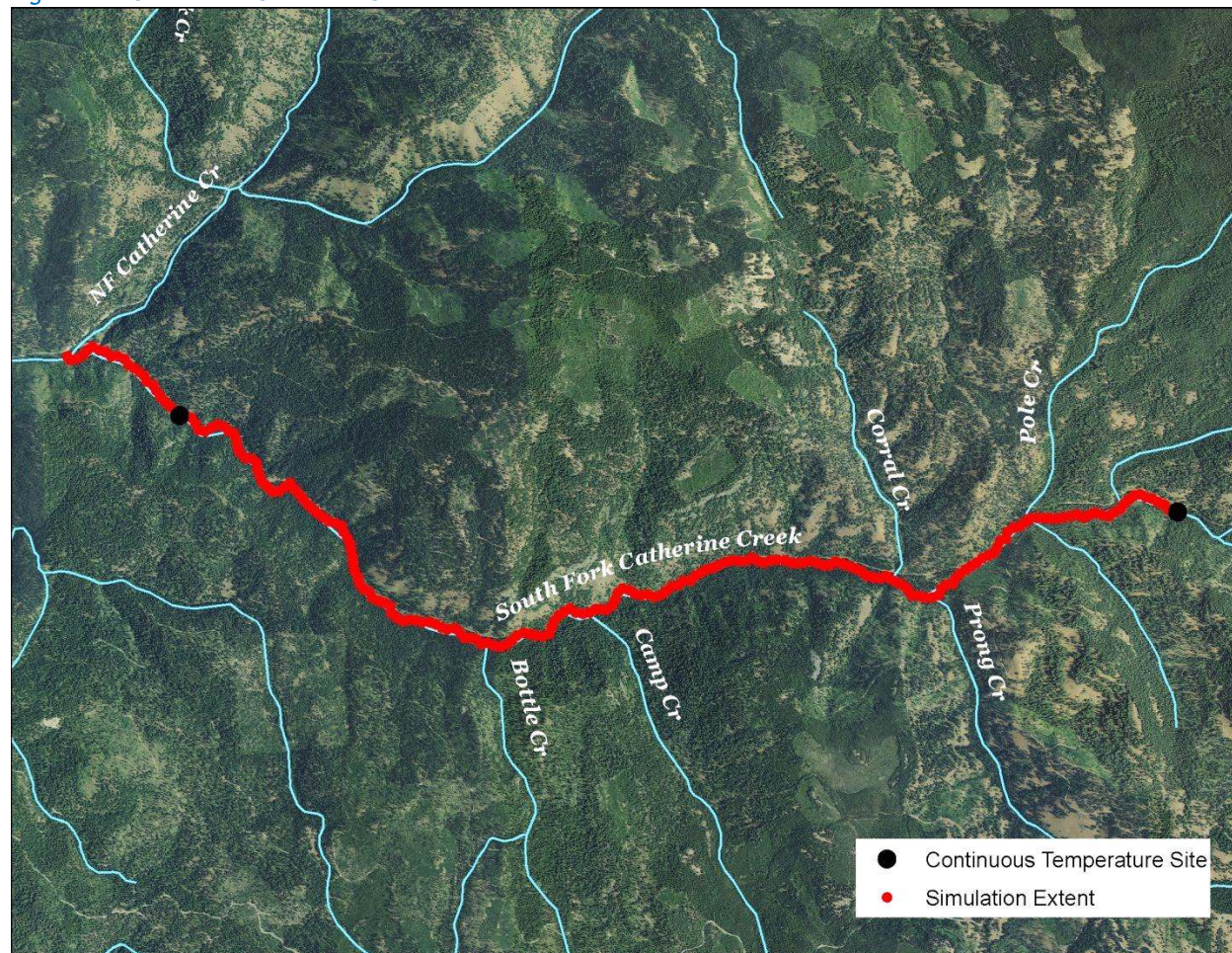


Table 7 - South Fork Catherine Creek general Heat Source parameters.

Stream:	South Fork Catherine Creek
Length:	10.4 kilometers
Time Period:	August 6-27, 2010
Input Distance Step:	50 meters
Output Distance Step:	100 meters
Time Step:	1 minute
Flush Initial Condition:	7 days
TIR Date and Time:	August 12, 2010 15:51-16:03
Land Cover Data Source:	LiDAR
Land Cover Sampling Distance Step:	15 meters

The following assumptions were used when calibrating the South Fork Catherine Creek Heat Source model:

- The upstream monitoring site had no hourly temperature data available, so 5.5°C were subtracted from the values recorded at the mouth and used as the upstream boundary condition. This assumption adds unquantifiable uncertainty to the model. However, since the stream is well-forested and the longitudinal profile has little variability, this assumption is considered a “best estimate” of actual boundary temperatures.
- Hourly climate data was obtained from the La Grande Airport (NWS). Air temperature was adjusted using the adiabatic lapse rate of 1°C per 100 meters elevation.
- Sand Pass, Pole, Prong, Camp and Butte Creek were all assumed to be contributing equal flow volumes.
- Wetted widths used in the final calibration are 130% of the raw TTools values, based on the ground level hydraulics data.
- Daily flow volumes vary based on extrapolation (back-calculation) from the gage data recorded in the North Fork Catherine Creek and Catherine Creek.

Figure 59 shows the hydraulic input parameters for the South Fork Catherine Creek for August 19, 2010. The ground level data was measured on August 19, 2010 at two locations.

Figure 59 - South Fork Catherine Creek simulated and measured hydraulic values.

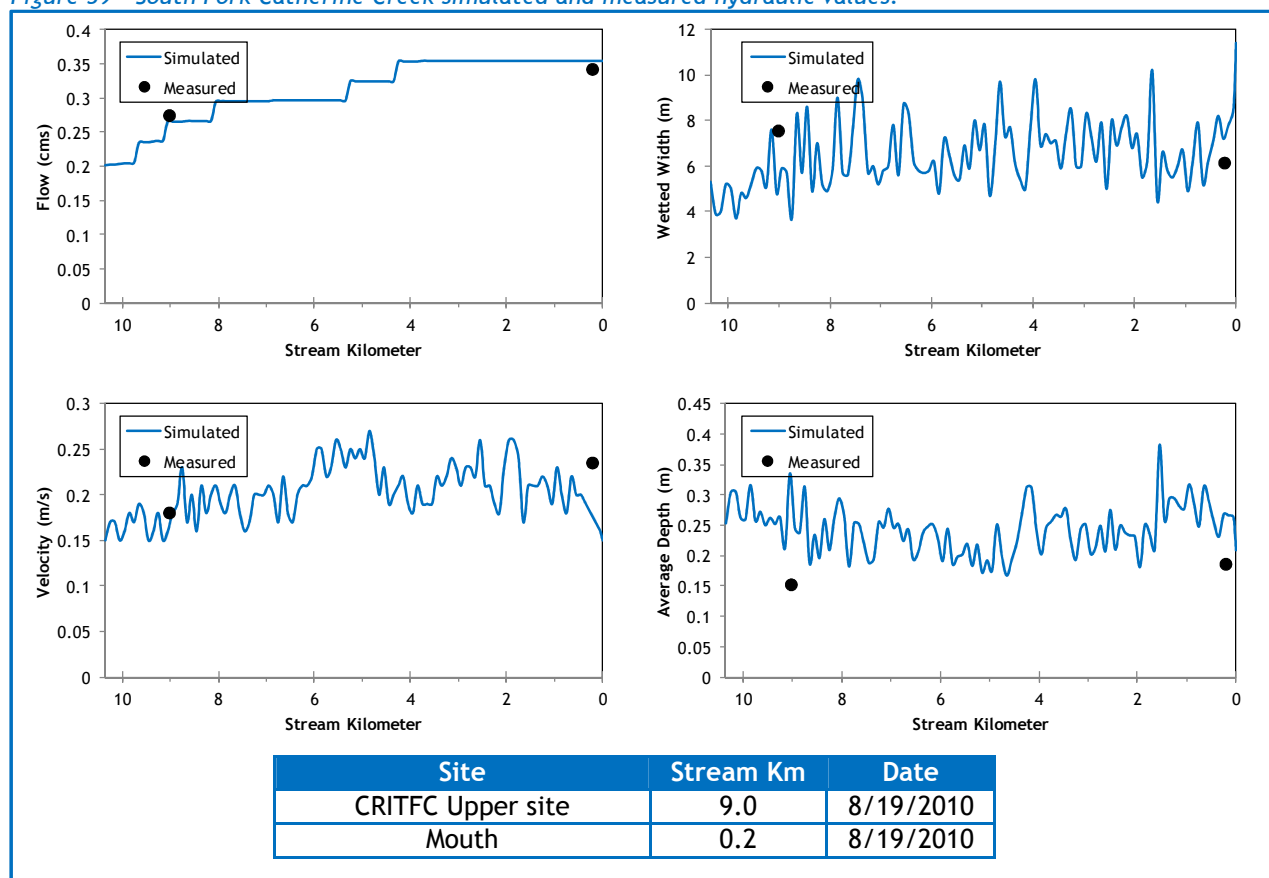
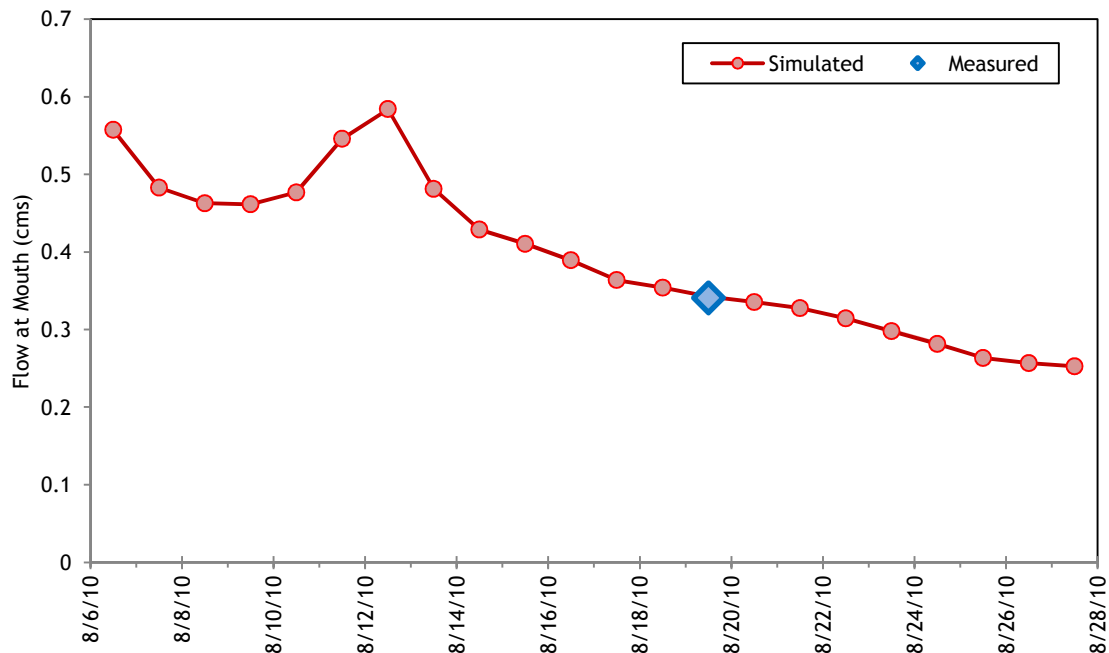


Figure 60 shows the simulated daily stream flow volume at the mouth of the South Fork Catherine Creek. Daily values for the simulation were extrapolated from gage data on the North Fork and Catherine Creek. The increased flows beginning on August 11th were caused by a small rain event.

Figure 60 - South Fork Catherine Creek simulated daily stream flow at the mouth.



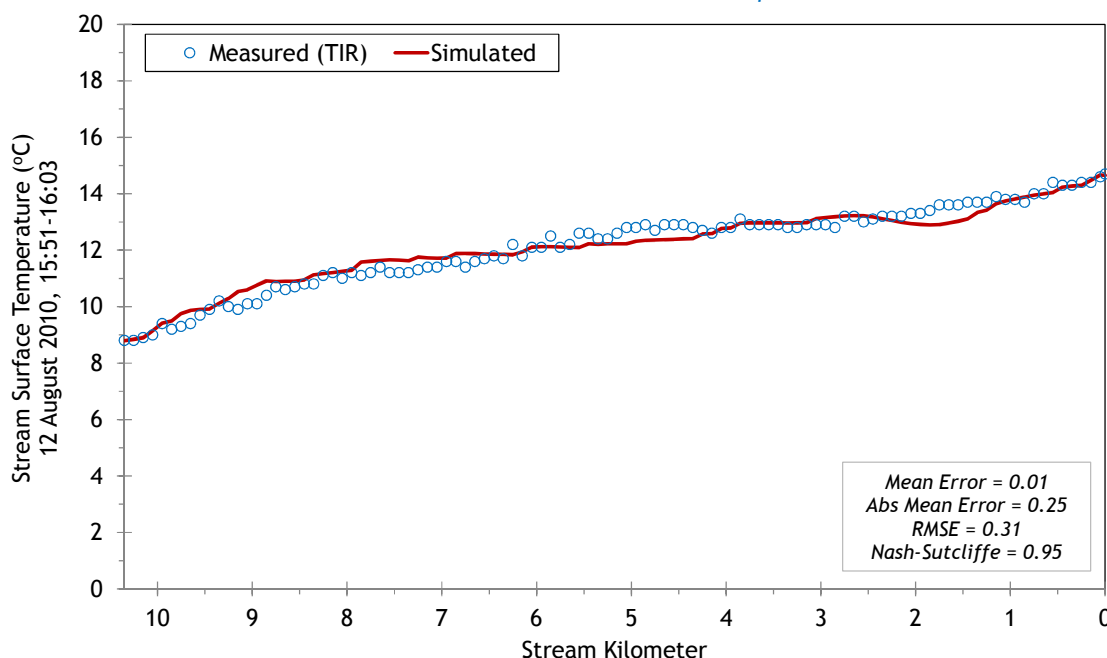
There were 5 tributaries observed in the TIR imagery. They were small enough that they did not have a measurable impact on the South Fork Catherine Creek temperatures; therefore mass balance flow estimates were not possible and simple conservative estimates were used. Hourly temperatures of the tributaries were assumed by adjusting hourly data recorded at the South Fork mouth based on temperature of the tributary observed in the TIR data.

Table 8 - South Fork Catherine Creek mass inflow locations and assumptions.

Feature	Stream Km	Assumptions
Sand Pass Creek	9.65	Daily flow estimated and hourly temperatures estimated by adjusting SF mouth data according to TIR imagery.
Pole Creek	9.05	Daily flow estimated and hourly temperatures estimated by adjusting SF mouth data according to TIR imagery.
Prong Creek	8.1	Daily flow estimated and hourly temperatures estimated by adjusting SF mouth data according to TIR imagery.
Camp Creek	5.25	Daily flow estimated and hourly temperatures estimated by adjusting SF mouth data according to TIR imagery.
Butte Creek	4.3	Daily flow estimated and hourly temperatures estimated by adjusting SF mouth data according to TIR imagery.

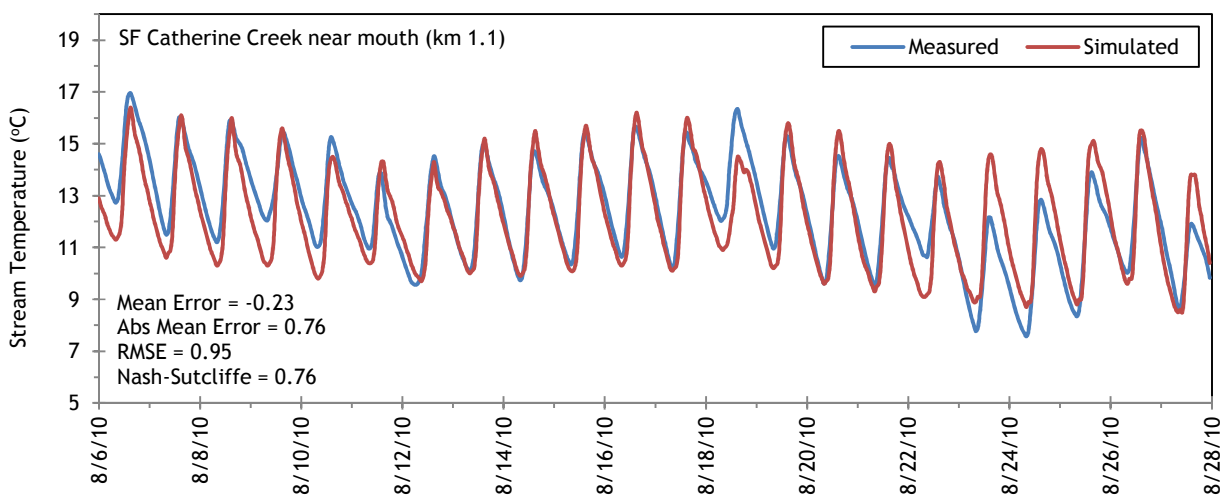
The South Fork Catherine Creek simulated and measured longitudinal temperatures are shown in Figure 61. The calibration statistics are also presented on the chart.

Figure 61 - South Fork Catherine Creek simulated and measured stream temperature.



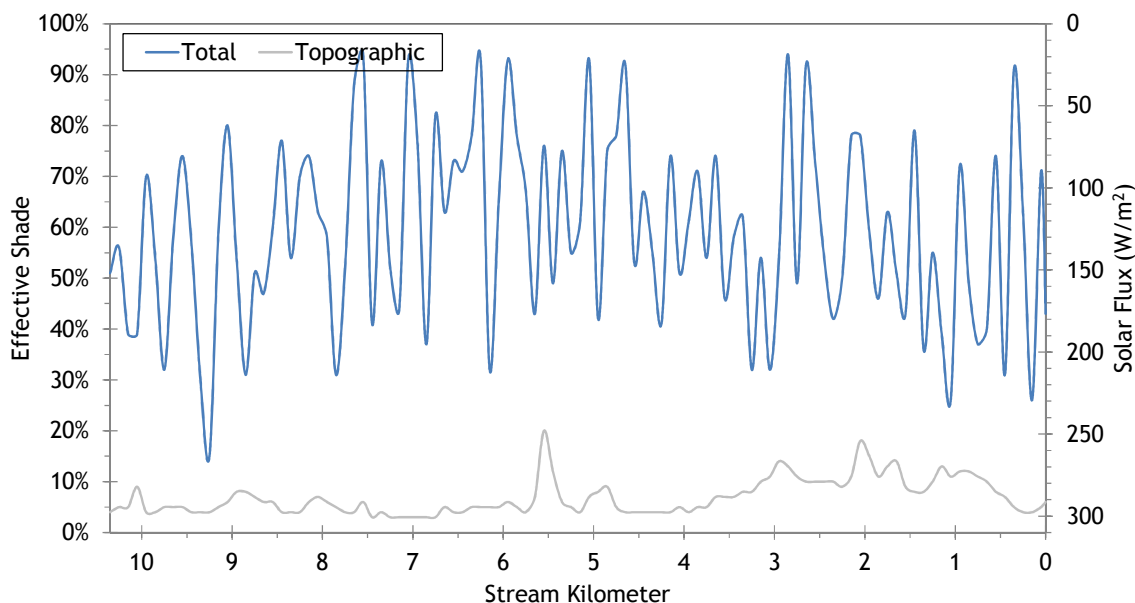
Besides the boundary condition (stream kilometer 10.4), there was one other hourly temperature monitoring site located near the mouth. Figure 62 shows the simulated and measured hourly stream temperatures near the mouth.

Figure 62 - South Fork Catherine Creek simulated and measured hourly temperatures.

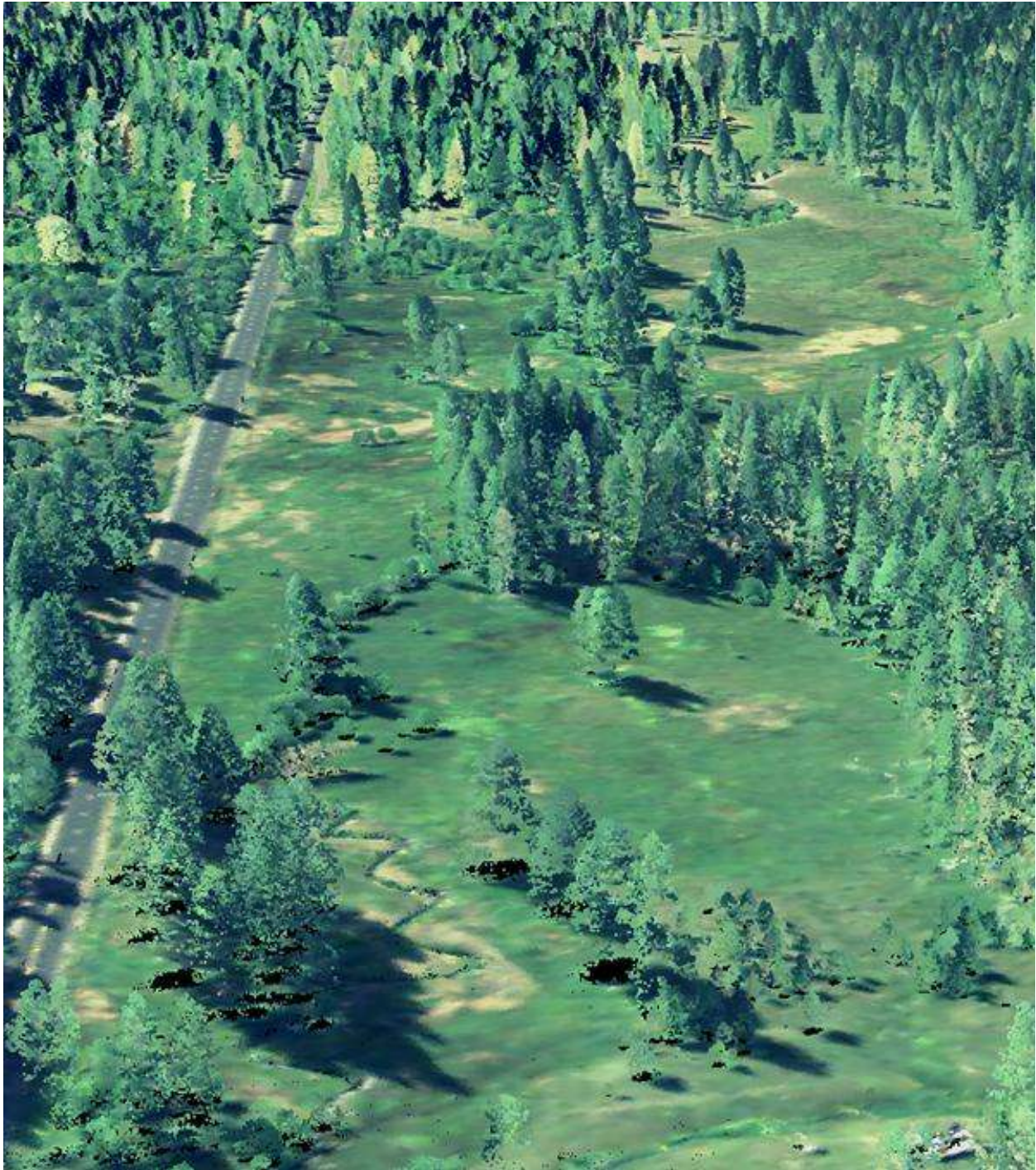


The simulated effective shade values for South Fork Catherine Creek are presented in Figure 63. The total effective shade is that which the stream experiences from both topography and vegetation. The topographic effective shade is the amount received by the stream in the absence of vegetation. The difference between the two is the amount of effective shade provided by the near stream land cover. Since the South Fork Catherine Creek is well forested, effective shade values are substantial for most of the stream.

Figure 63 - South Fork Catherine Creek simulated effective shade.



7. MILK CREEK

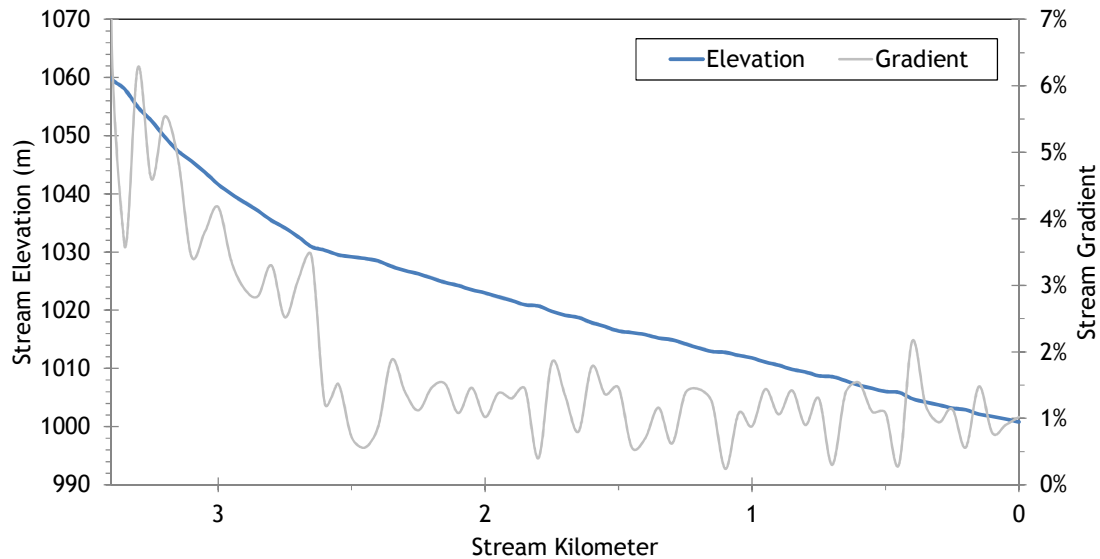


RGB-colored LiDAR point cloud - Looking upstream from mouth of Milk Creek (Medical Springs Highway on left).

7.1 Milk Creek TTools Results

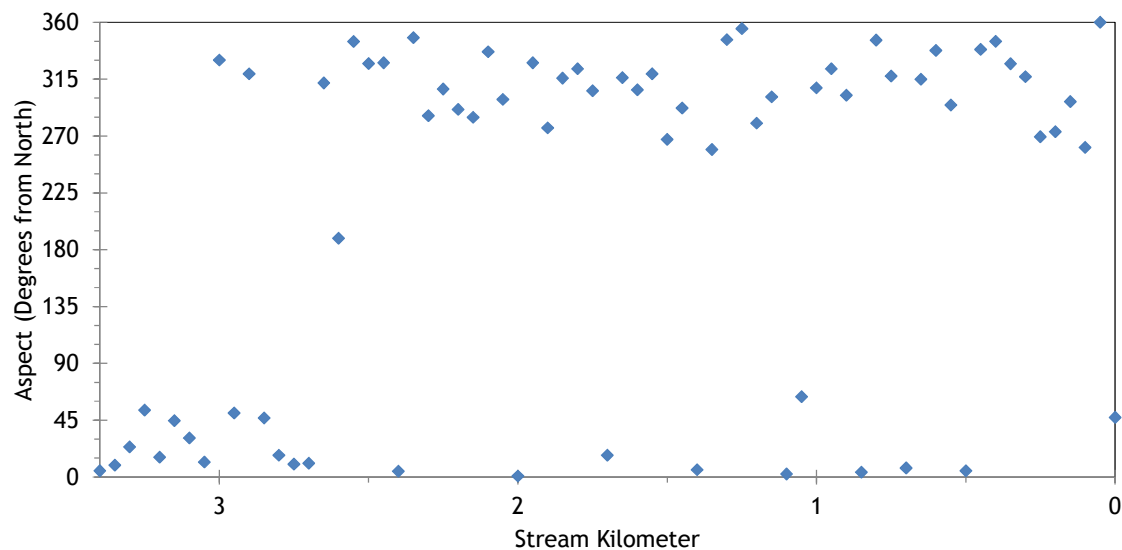
The lower 2.5 kilometers of Milk Creek flow through mostly open meadow and is low gradient. Figure 64 shows the elevation and gradient of the lower 3.4 kilometers where LiDAR data was available.

Figure 64 - Milk Creek stream elevation and gradient.



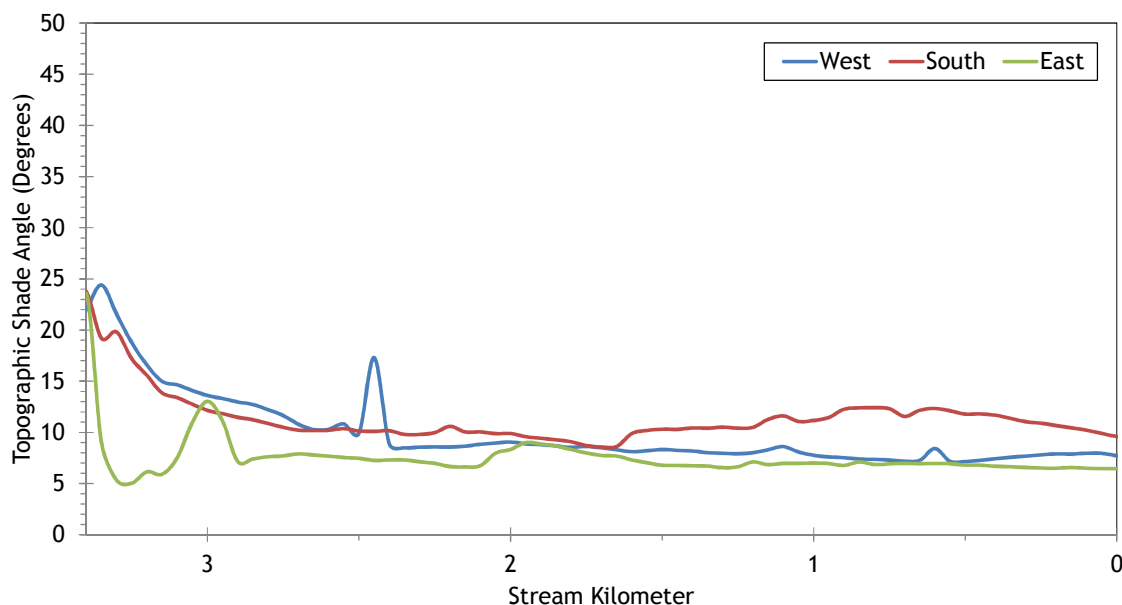
Milk creek generally flows in the northwesterly direction. Figure 65 displays the stream aspect for each 50 meter node of the lower 3.4 kilometers.

Figure 65 - Milk Creek stream aspect.



Topographic shade angles are around 10 degrees for Milk Creek (Figure 66). The highest topographic shade producing features are located to the south of the stream.

Figure 66 - Milk Creek topographic shade angles.



Milk Creek is a small stream so TIR stream temperature samples were sparser than for larger streams (Figure 67). Overall, Milk Creek was about 15-16°C during the TIR flight. This data is used for Heat Source calibration purposes.

Figure 67 - Milk Creek TIR stream temperature profile.

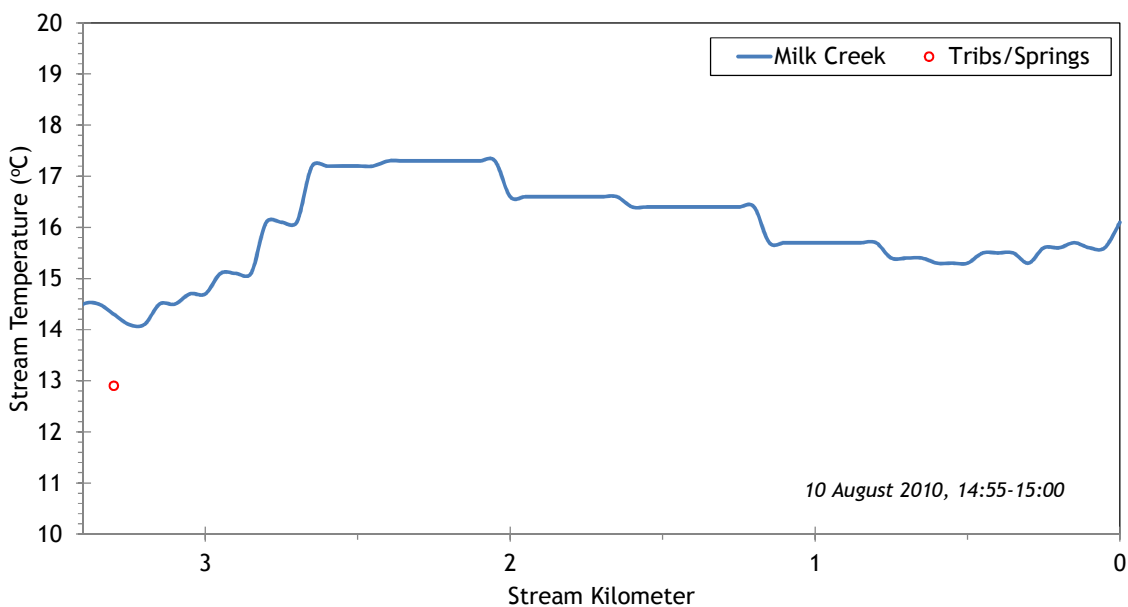
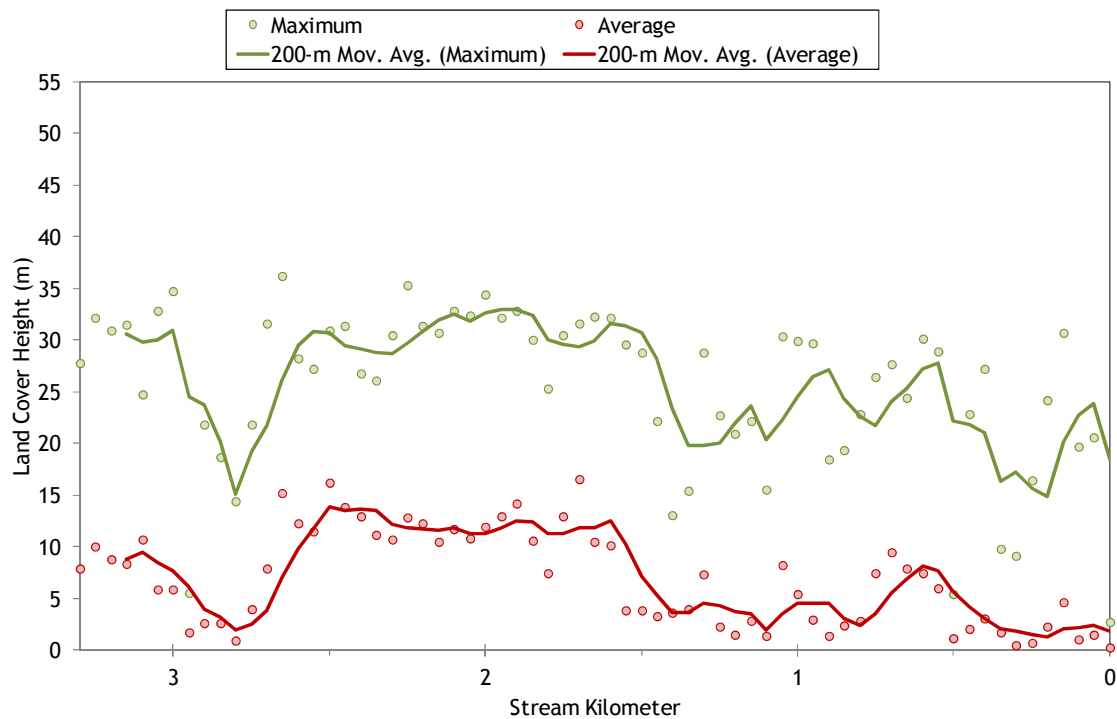


Figure 68 shows the land cover heights sampled along Milk Creek. The maximum and average of the 28 radial samples were calculated for each 50-meter stream node. Average heights are small in the lower 1.5 kilometers because there are fewer trees and many of the radial samples are of meadow grasses. (Note: Heat Source uses each of the 28 radial samples for each 50-meter node. The maximum and average are shown here for simplification purposes.)

Figure 68 - Milk Creek land cover heights sampled from highest hit LiDAR.



7.2 Milk Creek Heat Source Calibration Results

The lower 3.3 kilometers for Milk Creek were simulated (Figure 69). There were two ground level monitoring sites which determined the simulation extent.

Figure 69 - Milk Creek simulation extent.

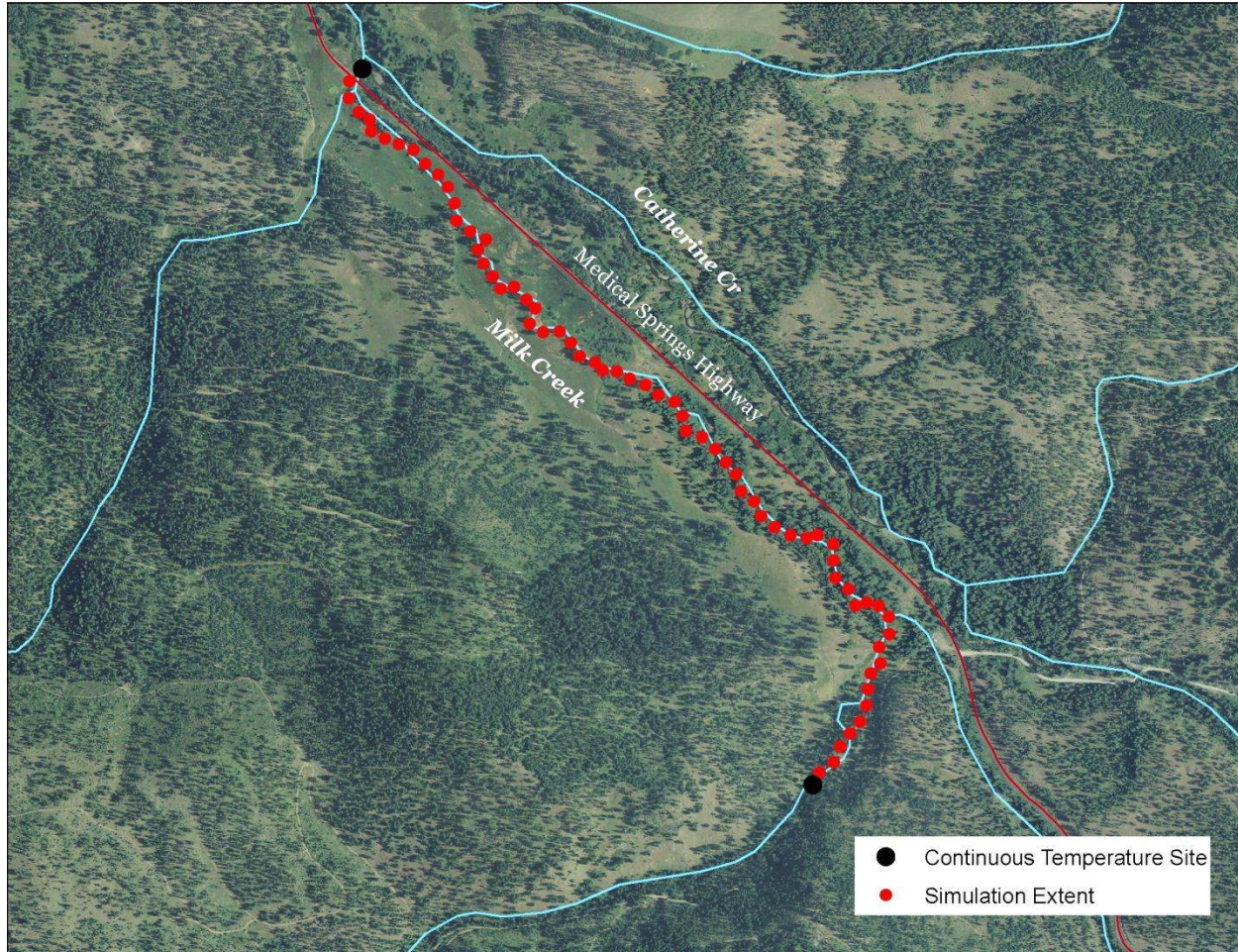


Table 9 - Milk Creek general Heat Source parameters.

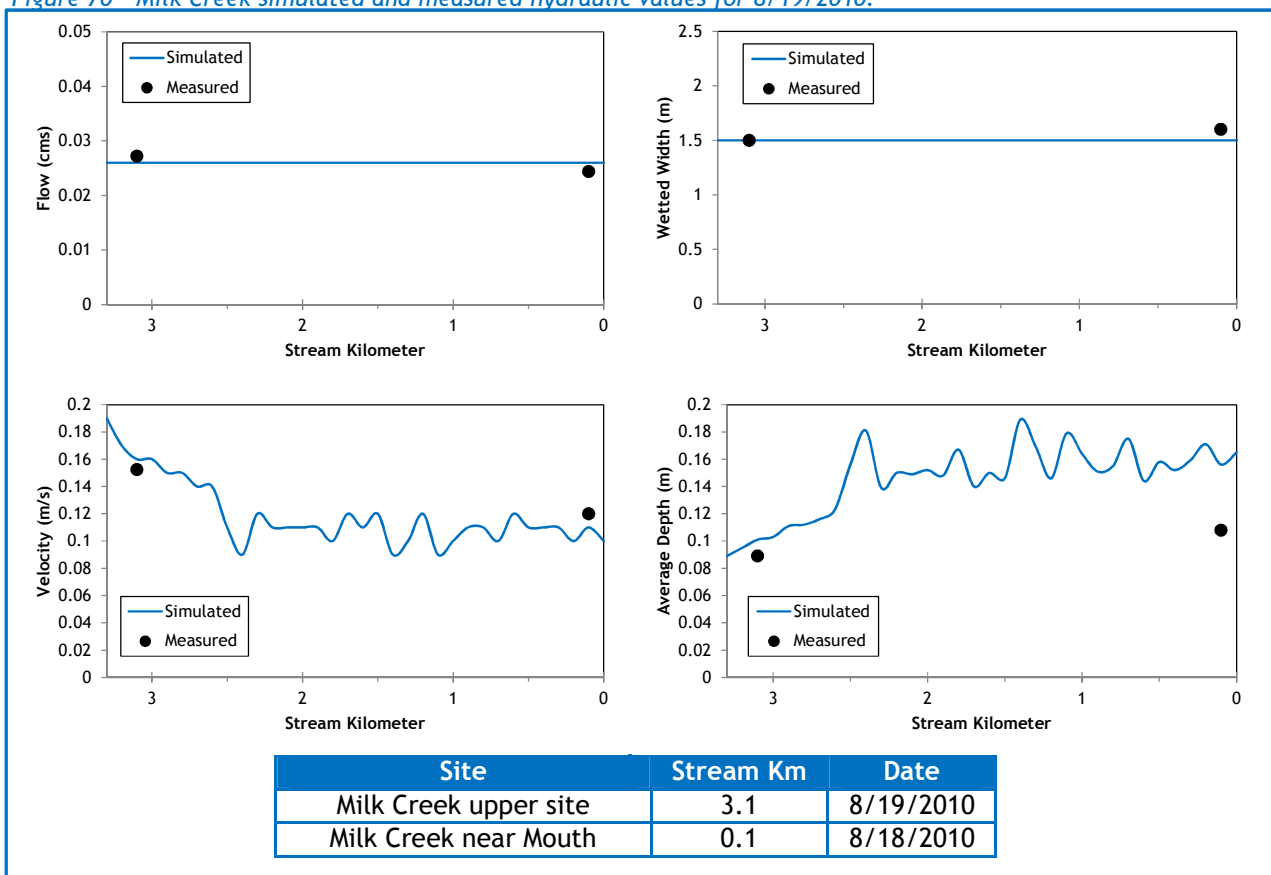
Stream:	Milk Creek
Length:	3.3 kilometers
Time Period:	August 6-27, 2010
Input Distance Step:	50 meters
Output Distance Step:	100 meters
Time Step:	1 minute
Flush Initial Condition:	7 days
TIR Date and Time:	August 10, 2010 14:55-15:00
Land Cover Data Source:	LiDAR
Land Cover Sampling Distance Step:	10 meters

The following assumptions were used when calibrating the Milk Creek Heat Source model:

- Hourly climate data was obtained from the La Grande Airport (NWS). Air temperature was adjusted using the adiabatic lapse rate of 1°C per 100 meters elevation.
- Wetted widths used in the final calibration were 1.5 meters for the entire length. The stream was too small to digitized wetted edges from the remote sensing imagery, so this value was estimated based on the two field measurements.
- Daily flow volumes vary based on extrapolation (back-calculation) from the gage data recorded in the North Fork Catherine Creek and Catherine Creek.
- Since the stream is so small, the land cover sampling distance step was reduced to 10 meters in order to capture the land cover nearest the stream.

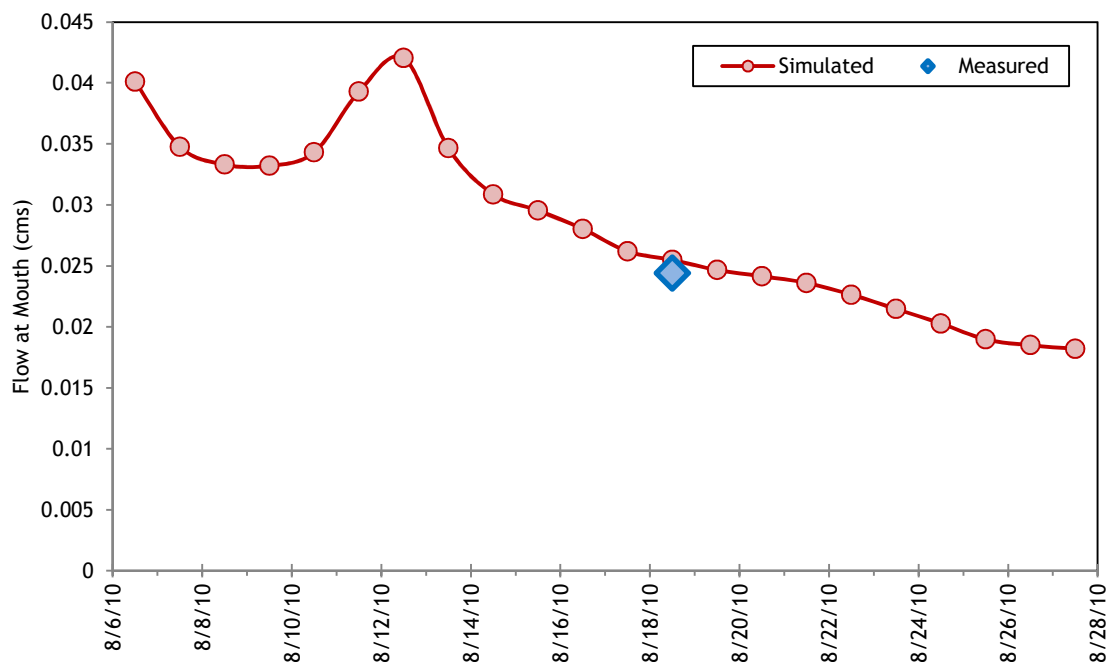
Figure 70 shows the simulated and measured hydraulic parameters for Milk Creek. The simulated data are for August 19, 2010. The field measurements were collected on August 18th and 19th.

Figure 70 - Milk Creek simulated and measured hydraulic values for 8/19/2010.



The simulated flow volumes at the mouth of Milk Creek are shown in Figure 71. The data were extrapolated/estimated from daily gage records in Catherine Creek. There was a small rain event in the basin that increased flows during the second week of August. Since there were no tributary or spring inputs to Milk Creek, these are the flow volumes that were simulated throughout the length of the stream.

Figure 71 - Milk Creek simulated daily stream flow at the mouth.



The simulated and measured longitudinal stream temperatures are shown in Figure 72. Due to the small size of Milk Creek, few TIR samples were obtained.

Figure 72 - Milk Creek simulated and measured longitudinal temperatures.

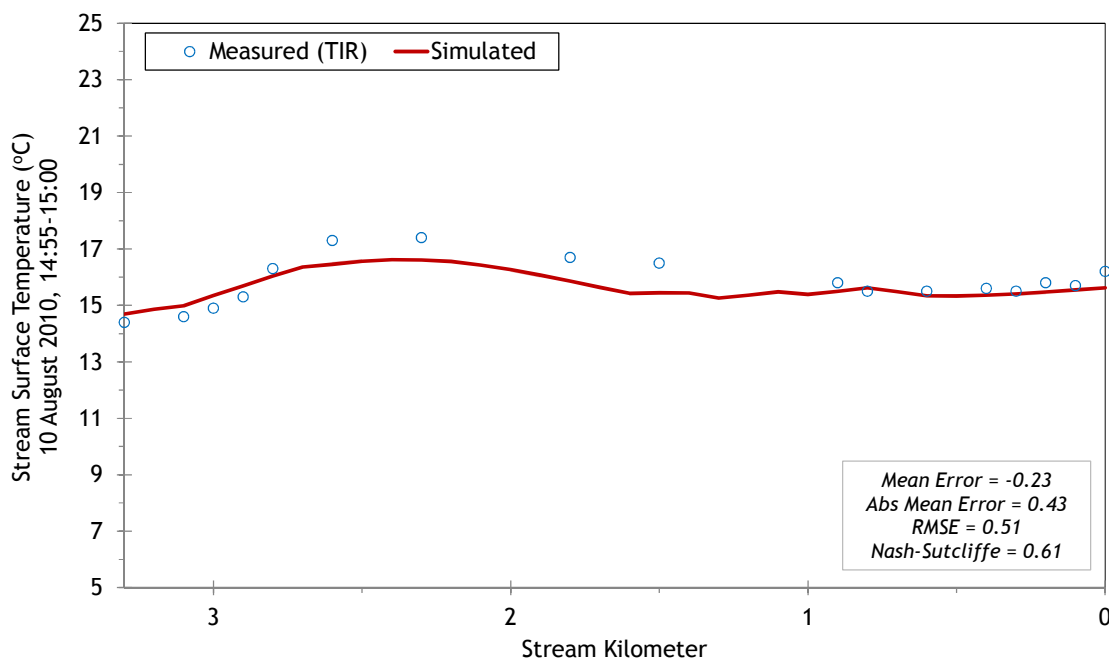
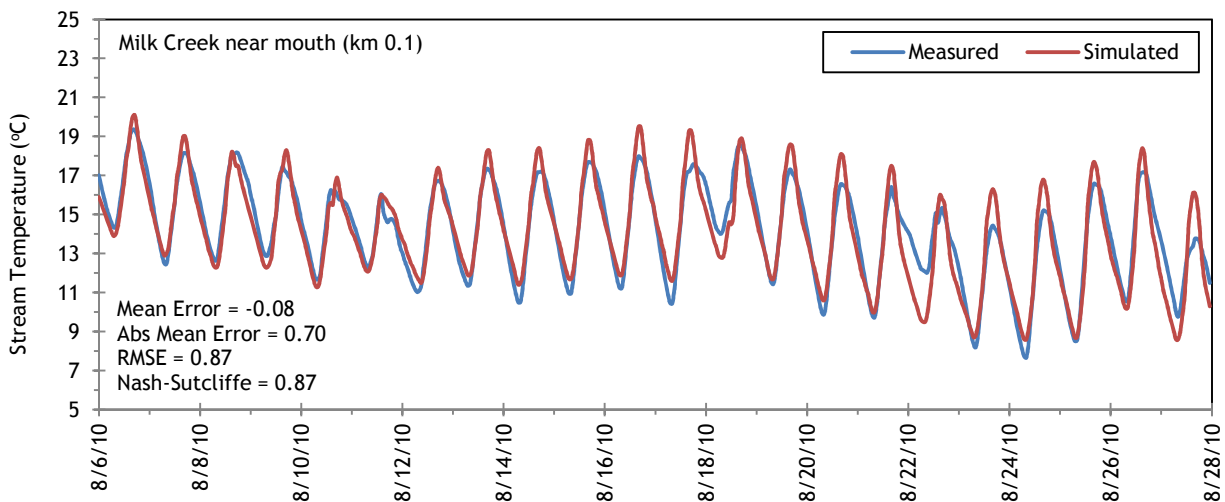


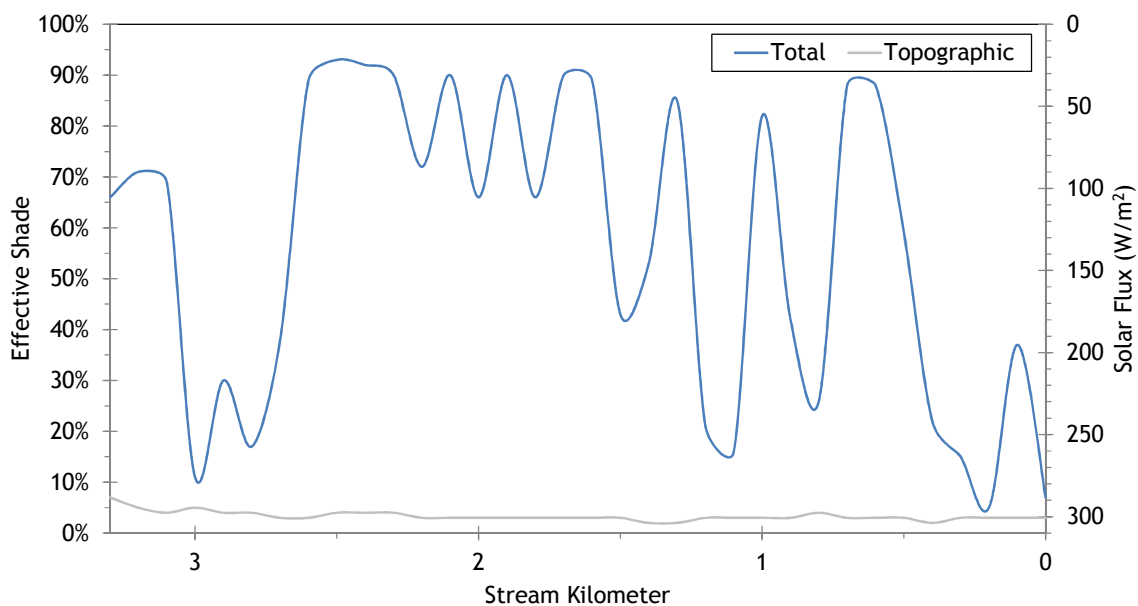
Figure 73 shows the simulated and measured hourly stream temperatures for Milk Creek.

Figure 73 - Milk Creek simulated and measured hourly temperatures.

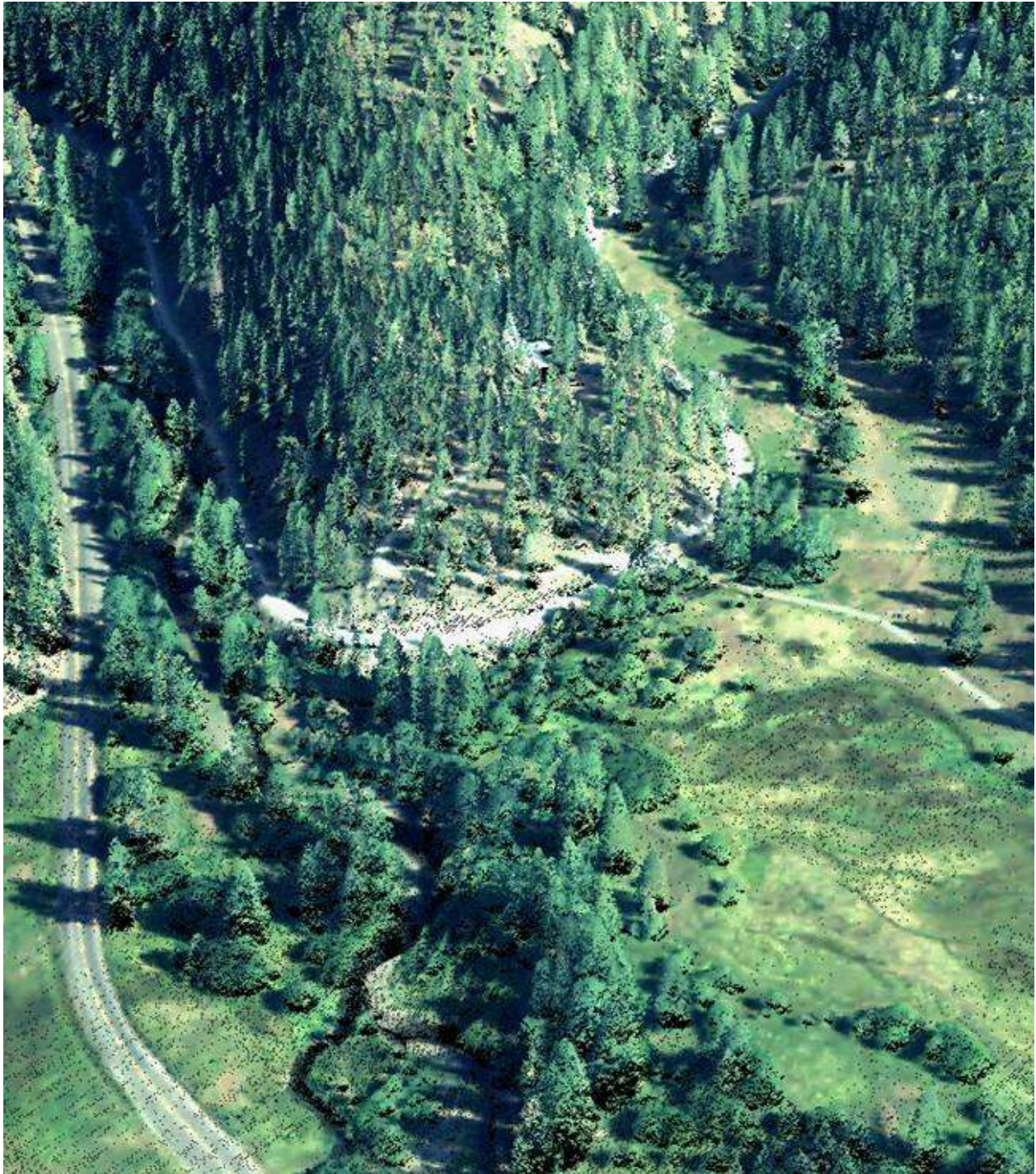


The simulated effective shade values of Milk Creek are presented in Figure 74. The total effective shade is variable because Milk Creek is flowing through a meadow with occasional stands of trees. There is fairly little topographic shade within the meadow.

Figure 74 - Milk Creek simulated effective shade values.



8. LITTLE CATHERINE CREEK

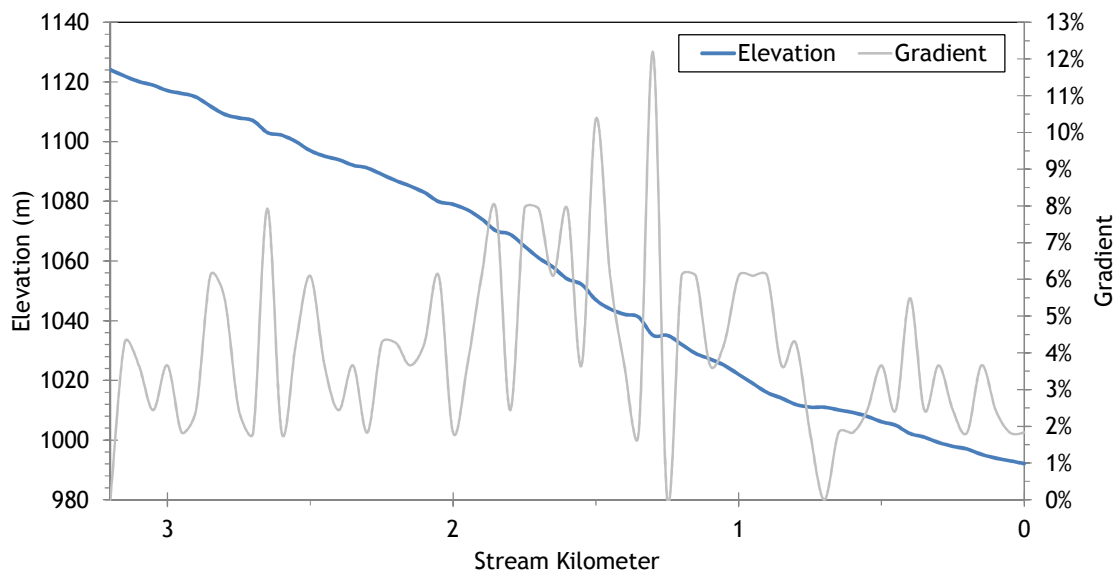


RGB-colored LiDAR point cloud - Little Catherine Creek (flowing top right to middle of image) confluence with Catherine Creek (flowing from bottom to top left of image).

8.1 Little Catherine Creek TTools Results

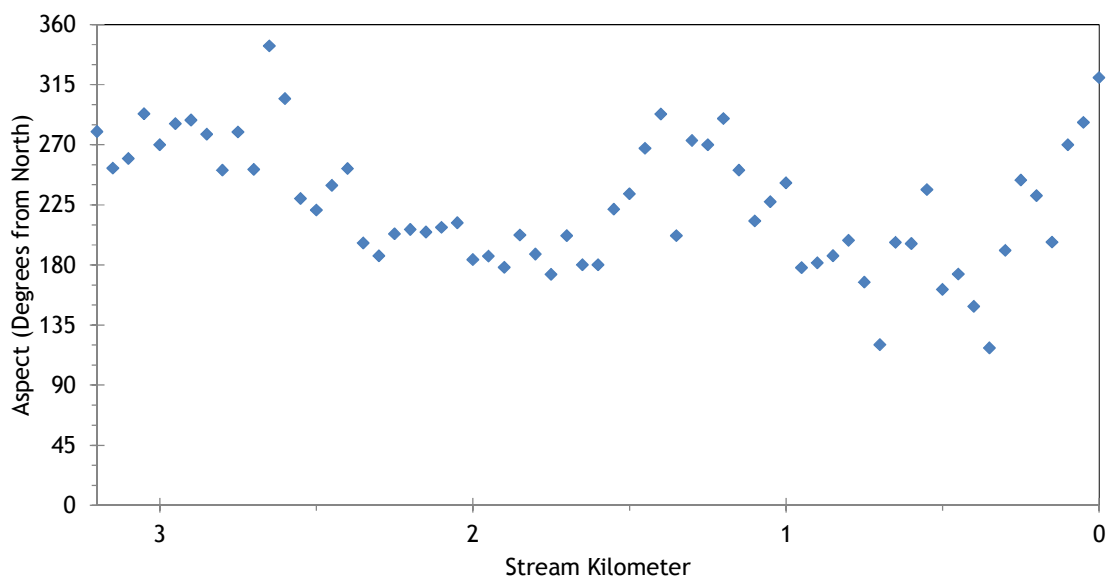
Little Catherine Creek did not have LiDAR coverage (except for a small reach near the mouth). Therefore, stream elevations and gradients were sampled from the 10-meter DEM. Figure 75 shows the elevations and gradients for Little Catherine Creek.

Figure 75 - Little Catherine Creek elevation and gradient.



Little Catherine Creek flows generally toward the southwest until it reaches Catherine Creek just upstream of the city of Union. Figure 76 shows the stream aspect for each 50-meter node of Little Catherine Creek.

Figure 76 - Little Catherine Creek stream aspect.



Topographic shade angles are relatively high on Little Catherine Creek, with some values over 30 degrees (Figure 77). This is due to the fact that the stream is flowing out of mountain foothills within a deep v-shaped valley.

Figure 77 - Little Catherine Creek topographic shade angles.

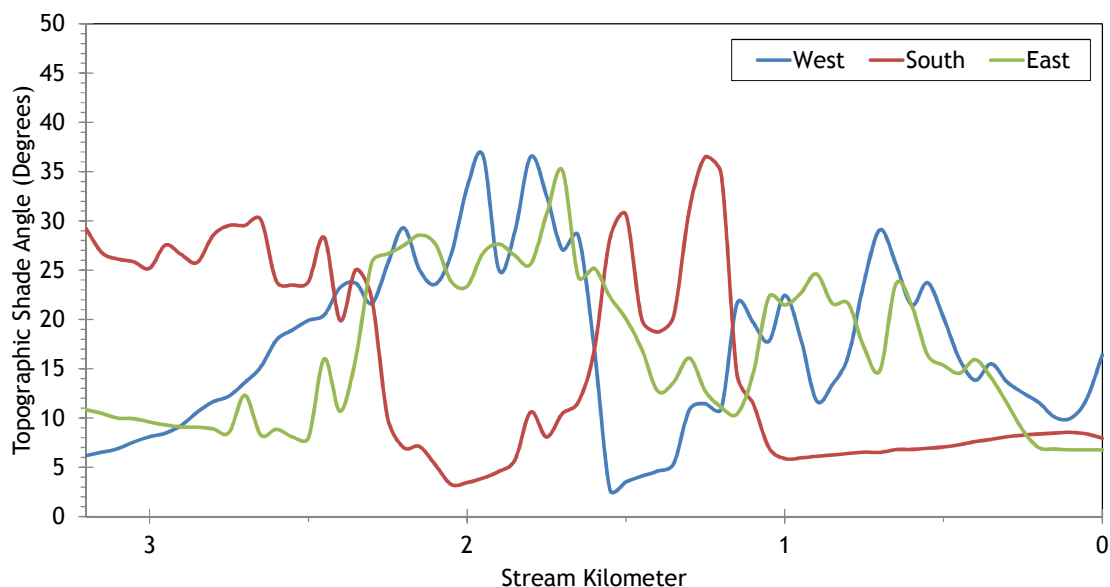
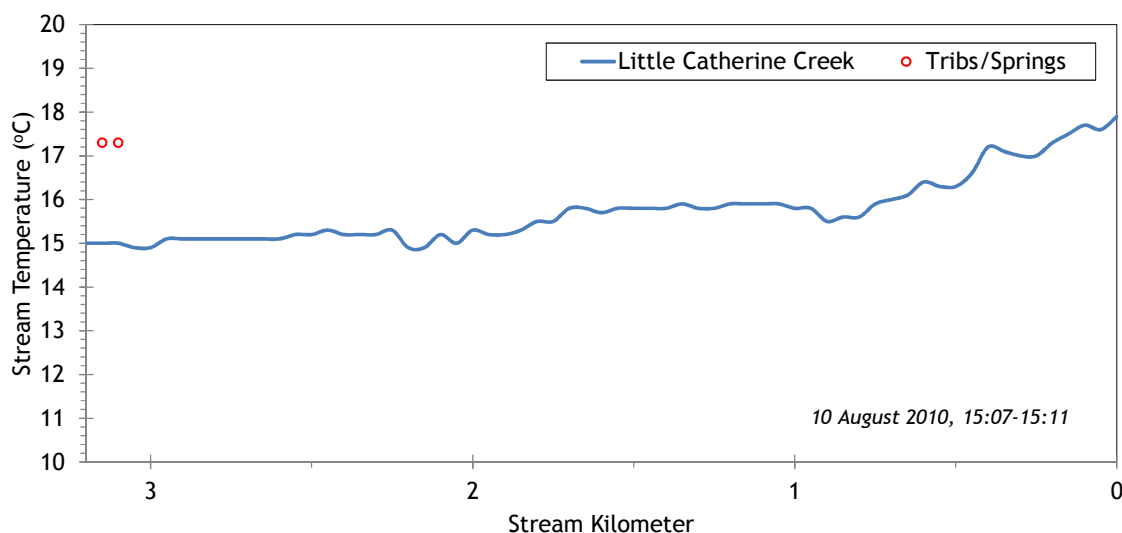


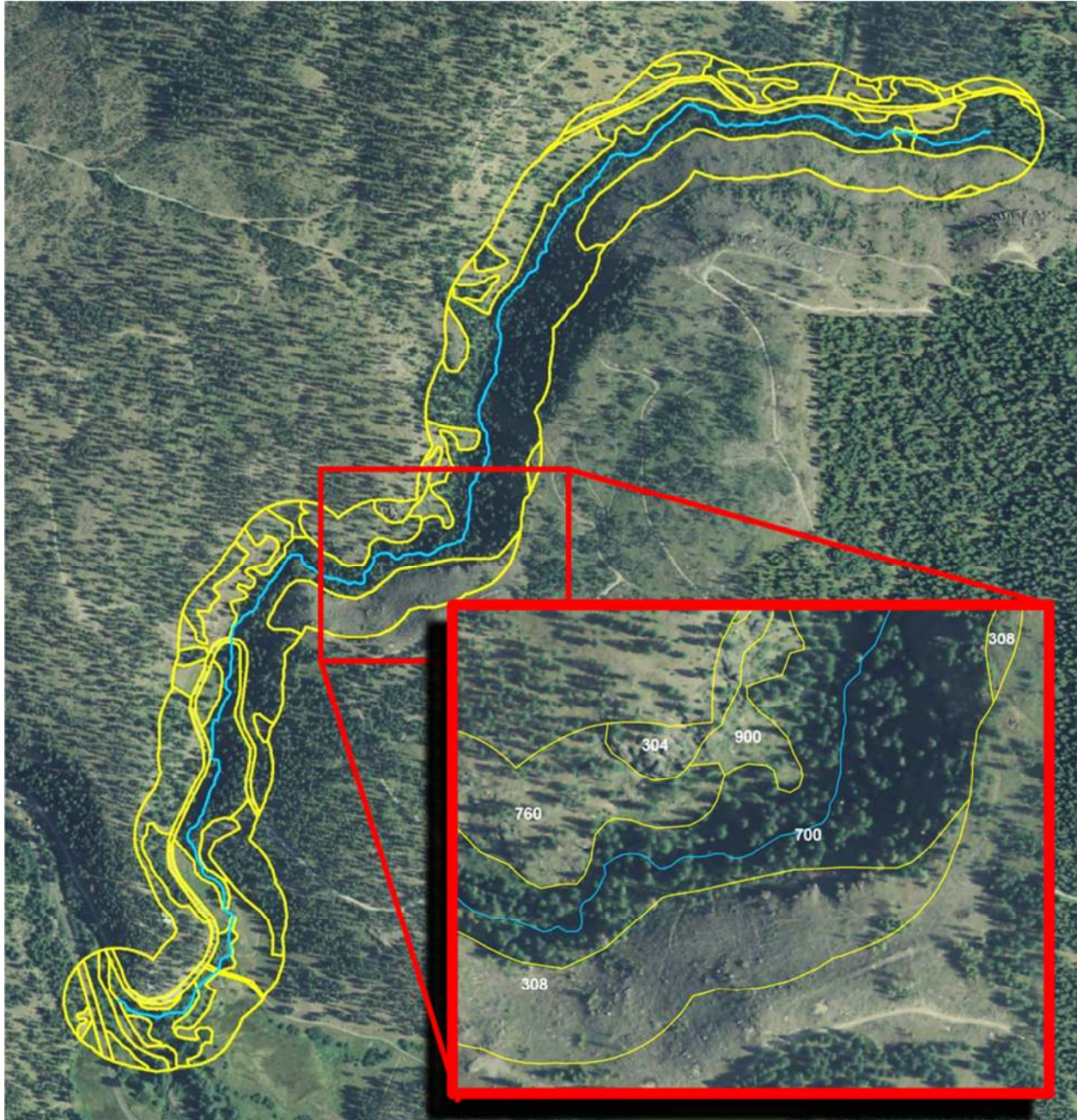
Figure 78 shows the TIR stream temperature profile of Little Catherine Creek. Stream temperature ranged from 15-18°C during the TIR flight.

Figure 78 - Little Catherine Creek TIR stream temperature profile.



Since there was no LiDAR available for Little Catherine Creek, the near stream land cover was digitized from the NAIP imagery within 100 meters of the stream. Figure 79 shows the near stream land cover polygons along Little Catherine Creek. Each polygon contains a code that signifies the land cover type, height class, and density class.

Figure 79 - Little Catherine Creek digitized near stream land cover.



8.2 Little Catherine Creek Effective Shade Simulation

Little Catherine Creek was simulated for effective shade only. There was insufficient ground-level flow and temperature for stream temperature modeling. Figure 80 shows the effective shade simulation extent.

Figure 80 - Little Catherine Creek simulation extent.

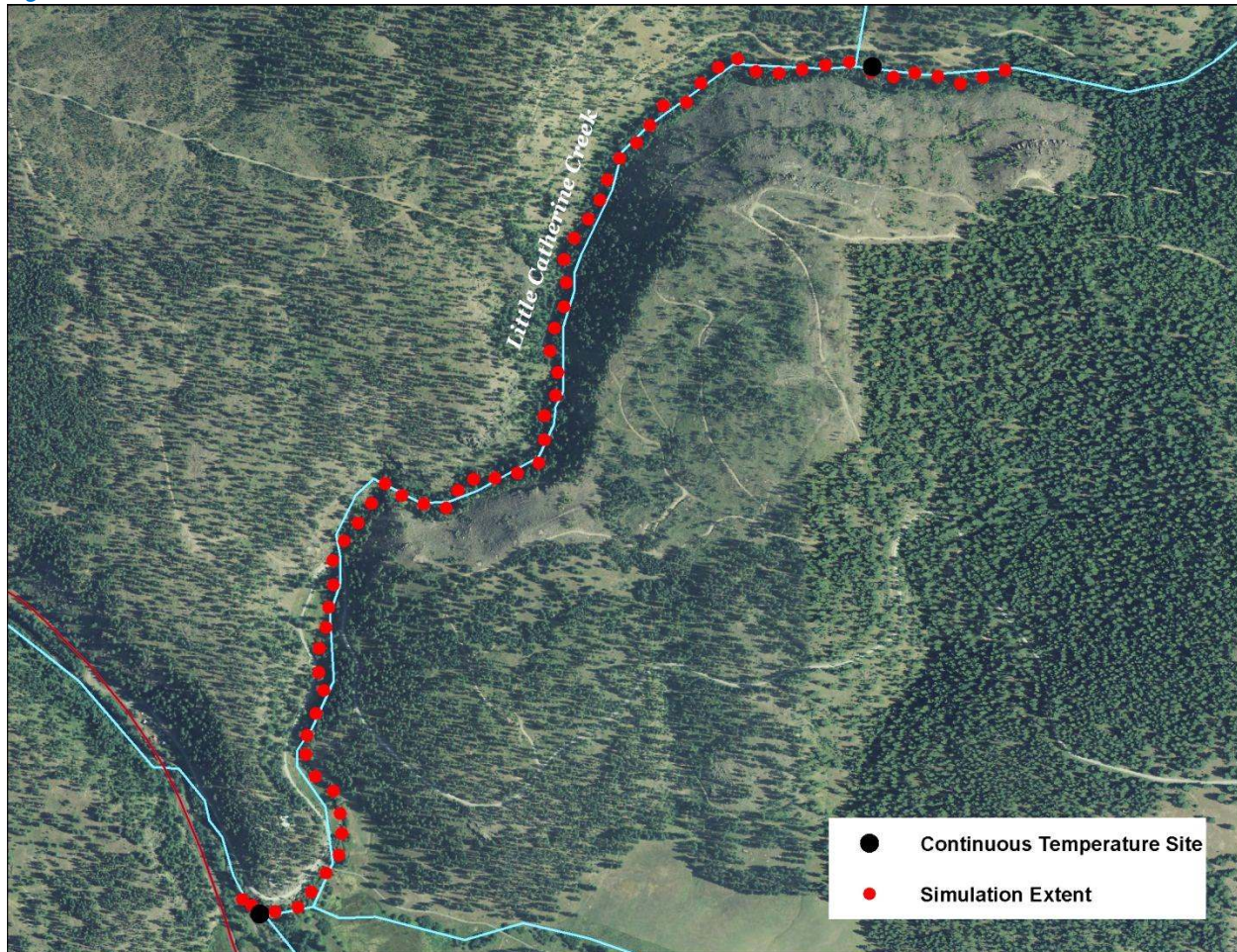


Table 10 - Little Catherine Creek general Heat Source parameters.

Stream:	Little Catherine Creek
Length:	3.2 kilometers
Time Period:	August 6-27, 2010
Input Distance Step:	50 meters
Output Distance Step:	100 meters
Time Step:	1 minute
Flush Initial Condition:	NA
TIR Date and Time:	NA
Land Cover Data Source:	LiDAR
Land Cover Sampling Distance Step:	10 meters

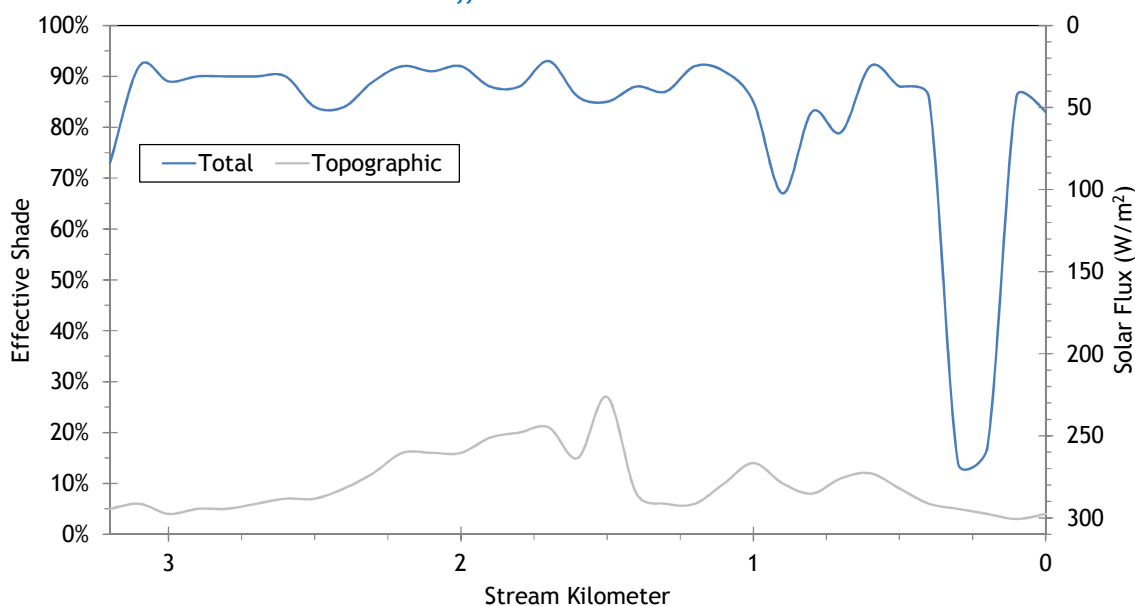
The near stream land cover codes used for Little Catherine Creek are shown in Table 11. The height values were derived from the tree heights sampled from the LiDAR data on the North Fork and South Fork Catherine Creek. The large conifer height value is the 75th percentile of all samples greater than 3 meters. The small conifer height is the 25th percentile of all samples greater than 3 meters. Density was estimated. Overhang was set at zero.

Table 11 - Little Catherine Creek land cover codes and descriptions.

Land Cover Name	Code	Height (m)	Density	Overhang (m)
Rock	304	0	0	0.0
Embankment	305	0	0	0.0
Clearcut	308	0	0	0.0
Road - paved	400	0	0	0.0
Road - unpaved	401	0	0	0
Large Conifer Forest	700	24.2	0.6	0
Small Conifer Forest	701	6.8	0.6	0
Large Conifer Forest	750	24.2	0.2	0
Small Conifer Forest	751	6.8	0.2	0
Conifer, small, sparse	760	3	0.1	0
shrubs	800	2	0.75	0
dry upland grass	900	0.5	0.9	0
floodplain grasses	901	0.5	0.9	0
active stream channel	3011	0	0	0

Figure 81 shows the simulated effective shade for Little Catherine Creek. The stream is well-forested throughout most of its length and thus well shaded by near stream land cover. Using manually digitized land cover for Heat Source inputs is less robust than using LiDAR and captures less of the natural variability. As a result, simulated effective shade also shows less variability and is more likely to be over-estimated. Ground level measurements could be used as validation if available.

Figure 81 - Little Catherine Creek simulated effective shade.



9. LITTLE CREEK

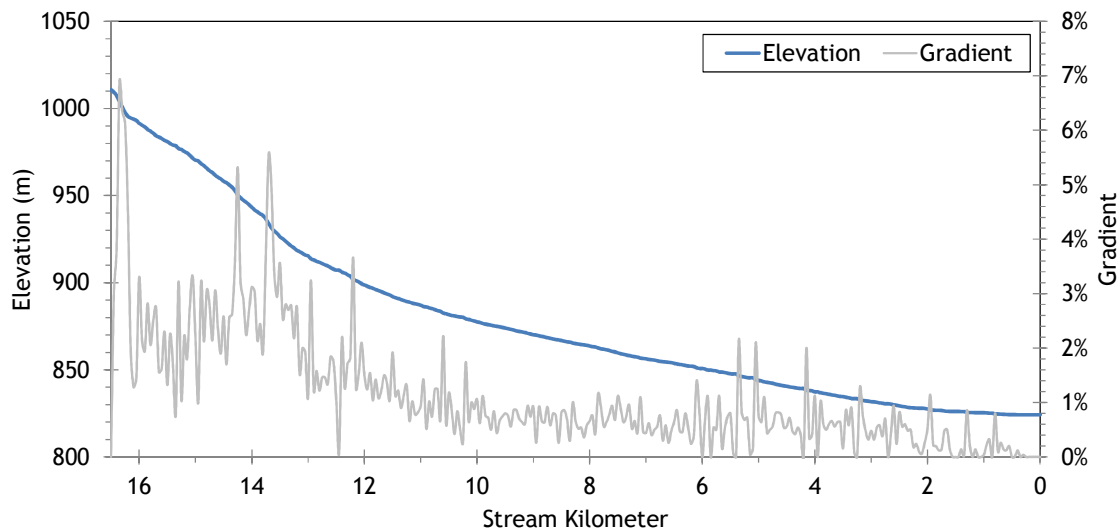


RGB-colored LiDAR point cloud - Little Creek looking downstream where it enters valley bottom.

9.1 Little Creek TTools Results

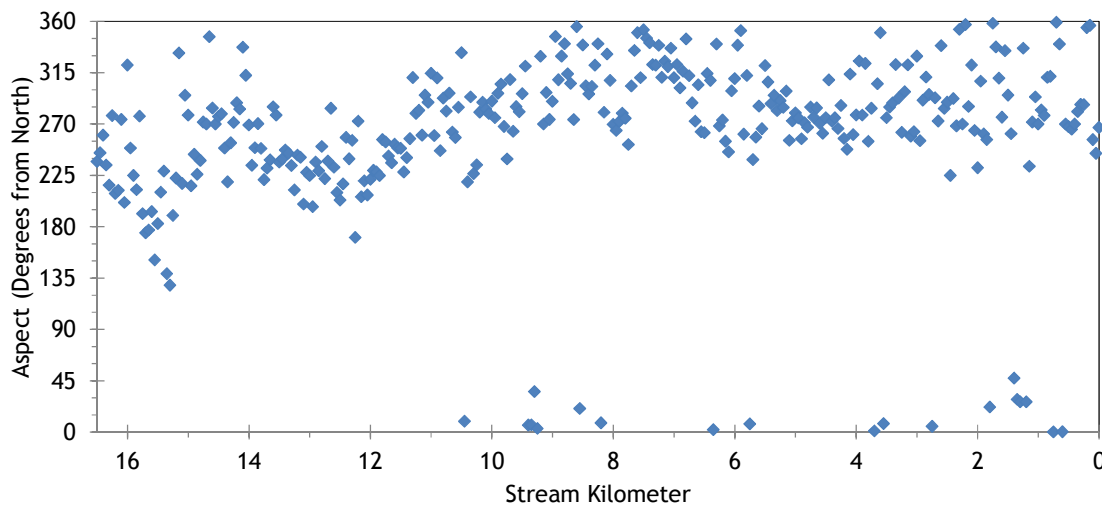
Figure 82 shows Little Creek elevations and gradients sampled from bare earth LiDAR data. The lower 10 stream kilometers are fairly low gradient because that reach flows through flat agricultural valley bottom.

Figure 82 - Little Creek elevation and gradient.



Little Creek flows mostly in the southwest-westerly direction before joining Catherine Creek below the city of Union. Figure 83 shows stream aspects for each 50-meter node.

Figure 83 - Little Creek stream aspect.



Topographic shade angles on Little Creek are highest above stream kilometer 10, where the terrain is hilly (Figure 84). The lower 10 stream kilometers have much lower topographic shade angles because the terrain is broad flat valley bottom.

Figure 84 - Little Creek topographic shade angles.

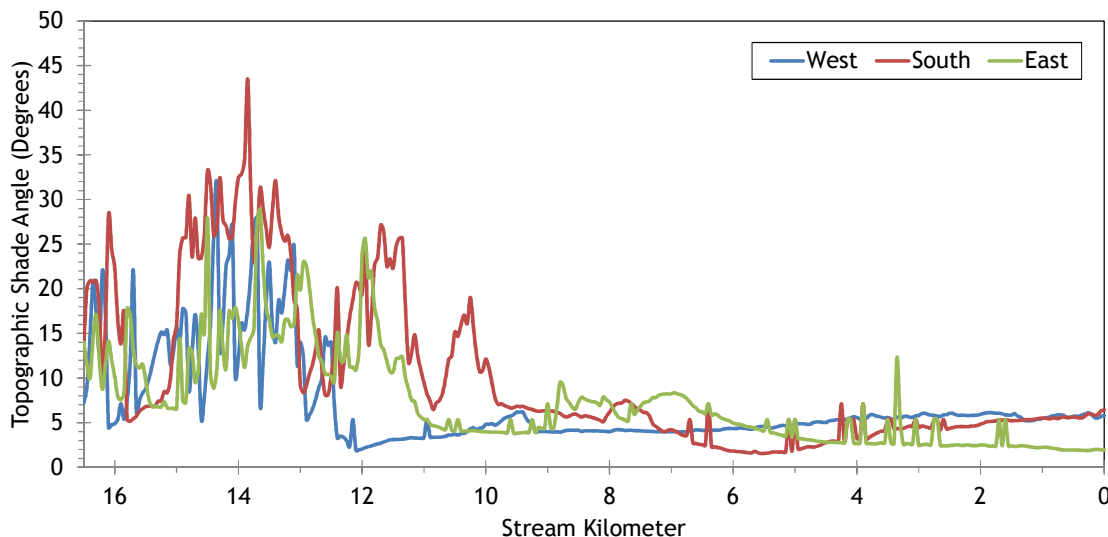
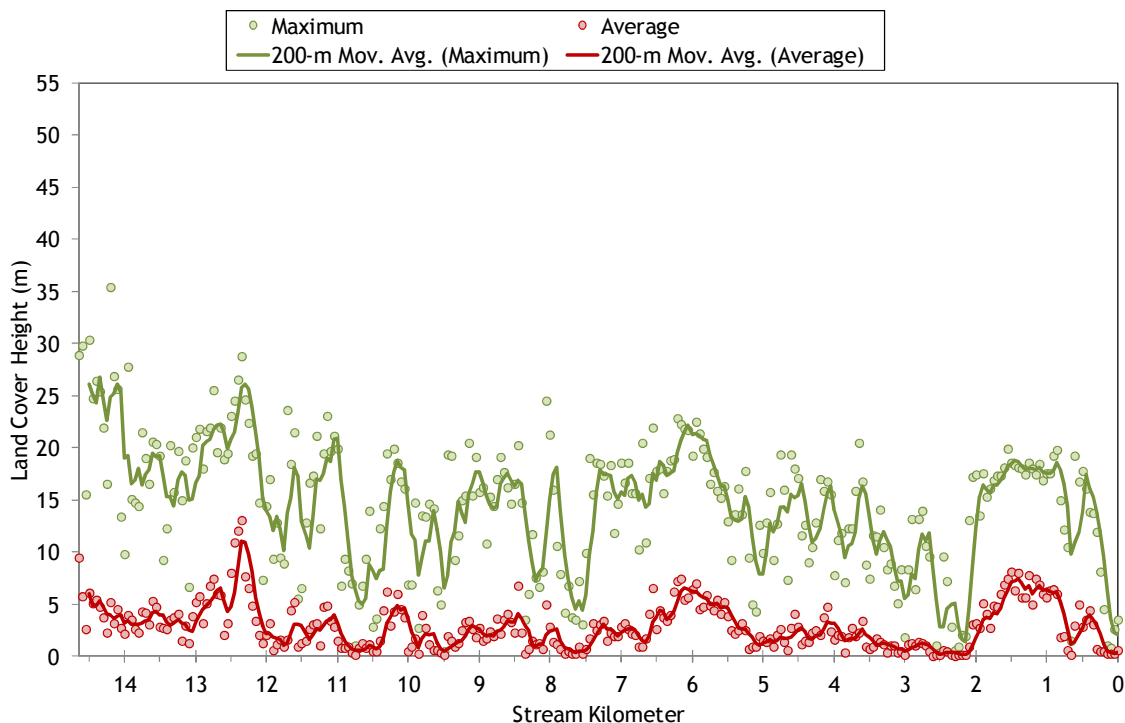


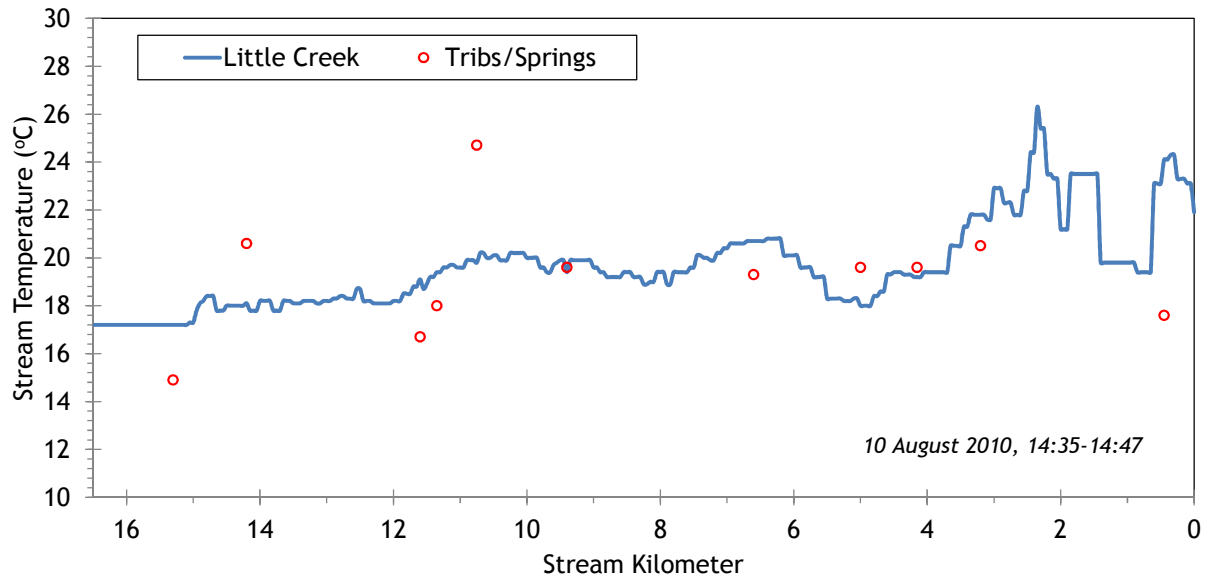
Figure 85 shows the land cover heights sampled along Little Creek. The maximum and average of the 28 radial samples were calculated for each 50-meter stream node. (Note: Heat Source uses each of the 28 radial samples for each 50-meter node. The maximum and average are shown here for simplification purposes.)

Figure 85 - Little Creek land cover heights sampled from highest hit LiDAR.



Little Creek TIR stream temperatures are presented in Figure 86. Overall, stream temperatures were 18-24°C during the TIR flight. There are areas of potential thermal stratification in the lower 3 kilometers where the stream velocities were very slow due to the low gradients. TIR only records the surface water temperature.

Figure 86 - Little Creek TIR stream temperatures.



9.1 Little Creek Heat Source Calibration Results

Little Creek was simulated from High Valley Road to the mouth (14.7 kilometers). Figure 87 shows the simulation extent and temperature monitoring sites.

Figure 87 - Little Creek simulation extent.



Table 12 - Little Creek general Heat Source parameters.

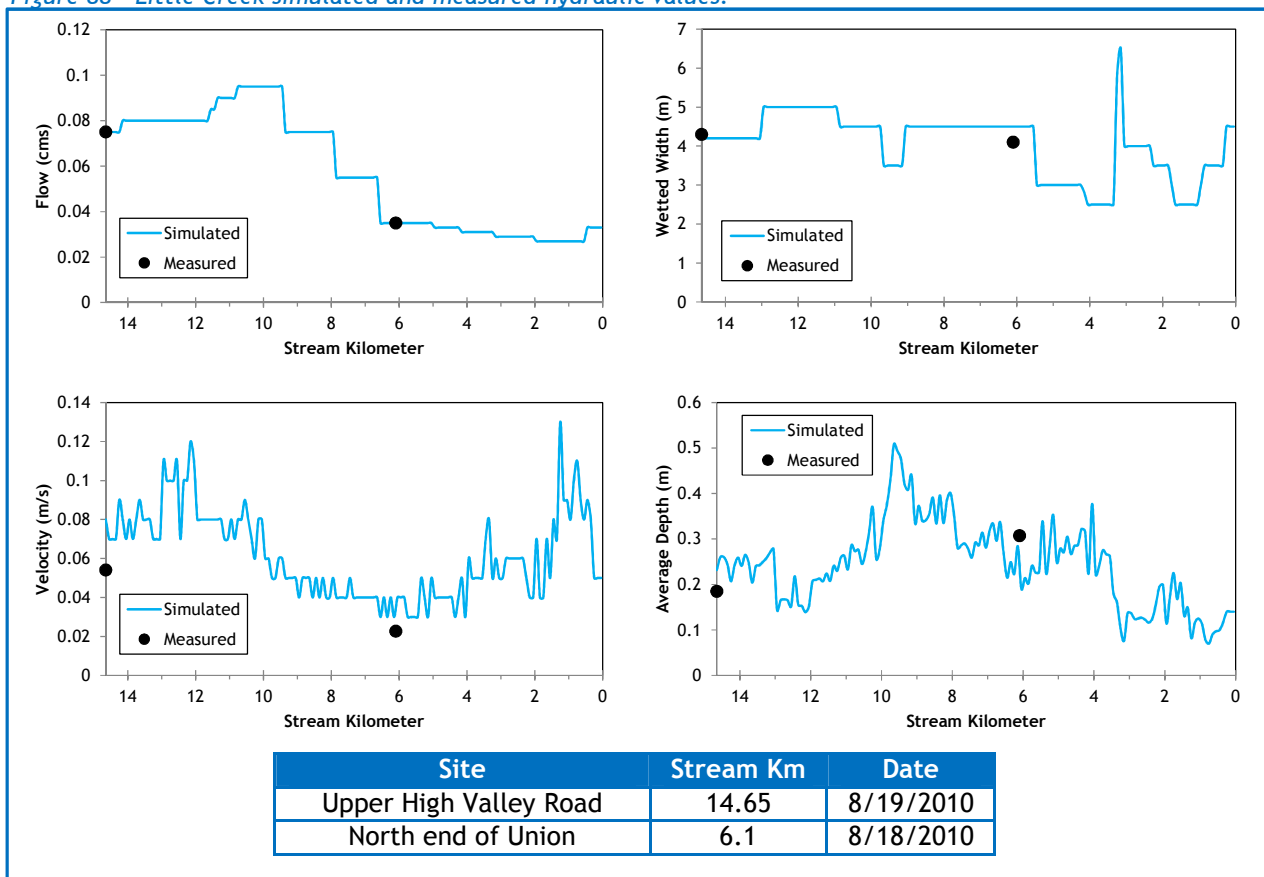
Stream:	Little Creek
Length:	14.65 kilometers
Time Period:	August 6-27, 2010
Input Distance Step:	50 meters
Output Distance Step:	100 meters
Time Step:	1 minute
Flush Initial Condition:	7 days
TIR Date and Time:	August 10, 2010 14:34-14:46
Land Cover Data Source:	LiDAR
Land Cover Sampling Distance Step:	15 meters

The following assumptions were used when calibrating the Little Creek Heat Source model:

- Hourly climate data was obtained from the La Grande Airport (NWS). Air temperature was adjusted using the adiabatic lapse rate of 1°C per 100 meters elevation.
- In many reaches, the stream was too small to digitize right and left banks. Therefore, wetted widths were estimated by taking several manual measurements from the TIR imagery.
- Since the flow of Little Creek was so small and highly regulated by irrigation withdrawals, a constant volume was used for the entire simulation time period (i.e., daily variability was not applied).
- There were 6 active diversion canals identified in the TIR imagery. The uppermost three were each assumed to withdraw 0.02 cms during the simulation time period while the lower three were assumed to withdraw 0.002 cms. No measured data was available for the canals.

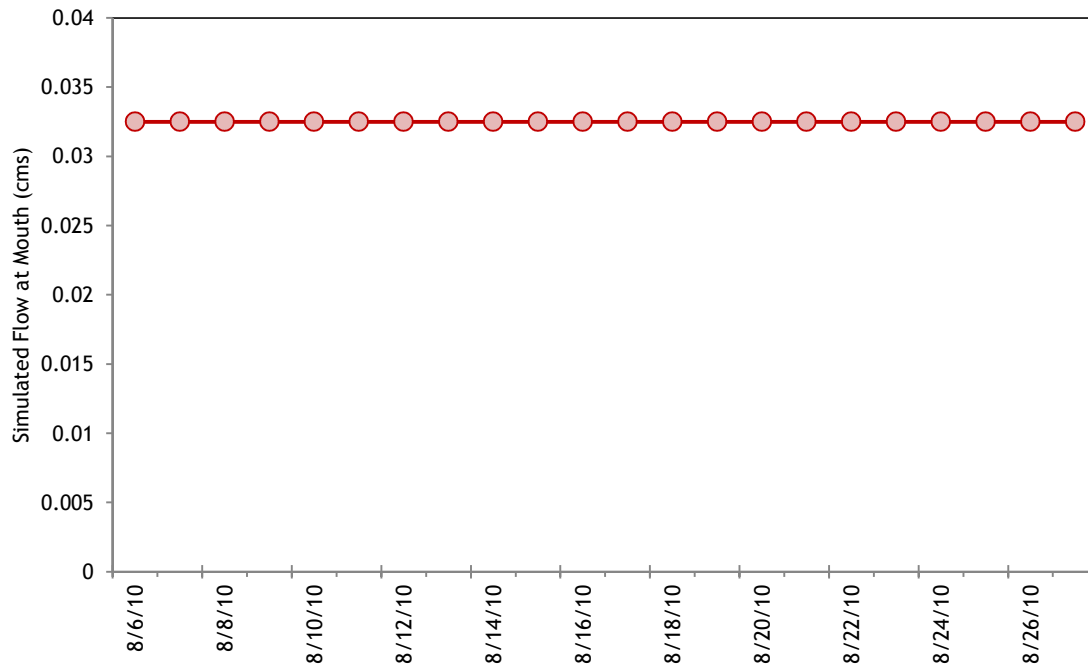
The simulated and measured hydraulic values for Little Creek are presented in Figure 88. The simulated values are for August 19, 2010. There were two ground level measurement sites, including the upstream boundary at High Valley Road, where data was collected on August 18th and 19th.

Figure 88 - Little Creek simulated and measured hydraulic values.



As mentioned previously, Little Creek simulated flows do not have daily variability. The same values were used for each day of the simulation (Figure 89). This assumption was used because of the low flow volumes and un-monitored irrigation withdrawals. (Estimating daily variability for such a stream adds unquantifiable uncertainty and also tends to make the Heat Source model unstable.) The closest field measurement was 0.035 cms on August 18, 2010 at stream kilometer 6.1.

Figure 89 - Little Creek simulated flow volume at the mouth of Little Creek.



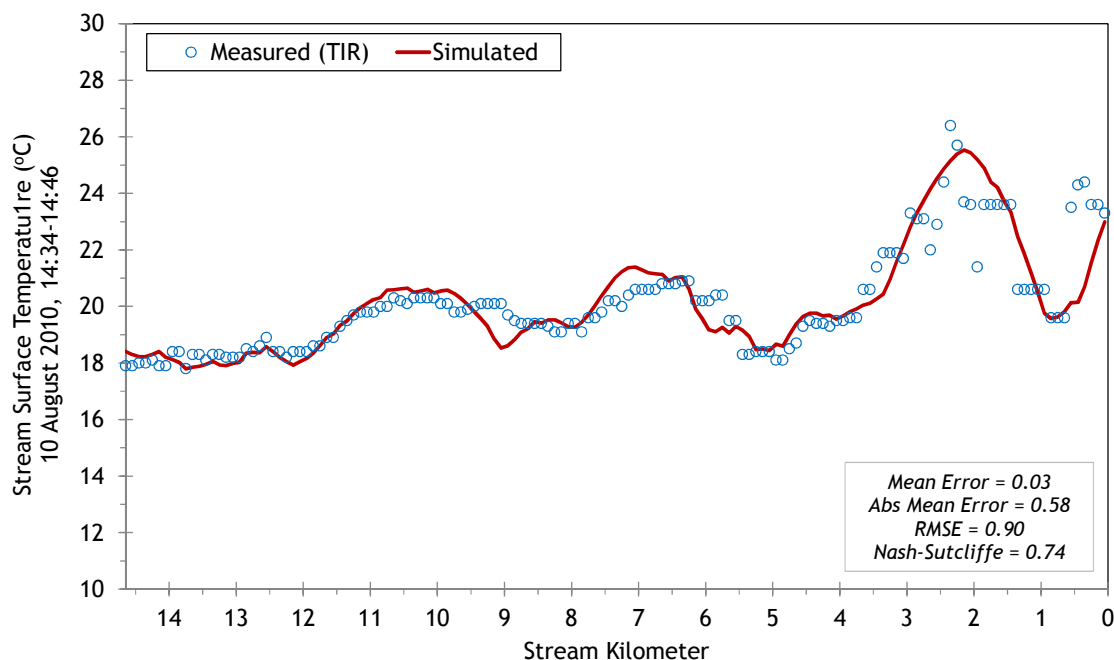
There was one unnamed tributary and several seeps identified within the TIR imagery. Those features were not large enough to compute a mass balance flow volume (i.e., did not produce a measurable thermal signature in Little Creek's longitudinal temperature profile), so volumes were estimated for each. Temperatures were measured from the TIR imagery. No daily variation was applied to these inputs because of their insignificant size relative to Little Creek.

Table 13 - Little Creek mass inflow features and assumptions.

Feature	Stream Km	Assumptions
Unnamed Trib	14.2	0.005 cms at 19.6°C (constant)
seep	11.6	0.005 cms at 16.4°C (constant)
seep	11.35	0.005 cms at 17.8°C (constant)
seep	10.75	0.005 cms at 24.4°C (constant)
seep	0.45	0.005 cms at 17.4°C (constant)

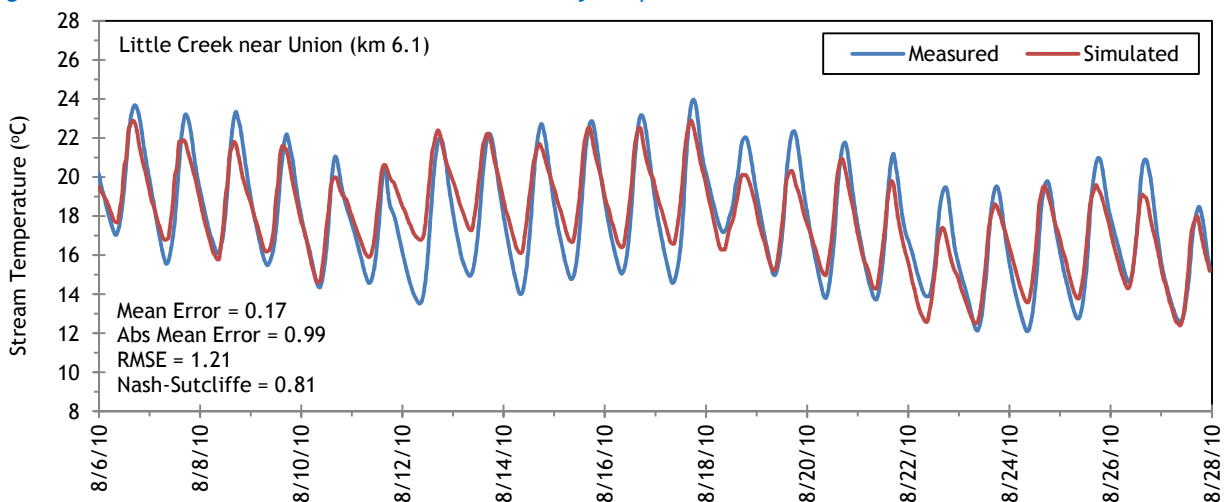
The simulated and measured longitudinal stream temperatures for Little Creek are shown in Figure 90. The lower 3 kilometers are uncertain because there is possible (but unverified) thermal stratification occurring.

Figure 90 - Little Creek simulated and measured longitudinal temperatures.



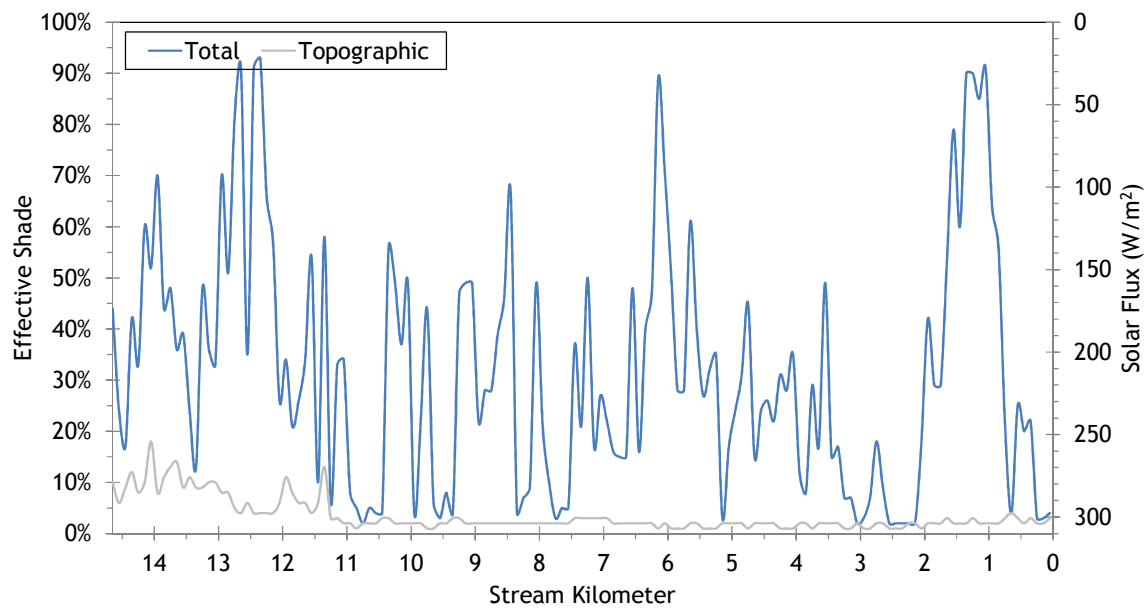
There was one site with valid hourly temperatures besides the upstream boundary condition. Figure 91 shows the simulated and measured hourly temperatures near the city of Union (stream kilometer 6.1).

Figure 91 - Little Creek simulated and measured hourly temperatures.



Simulated effective shade values for Little Creek are presented in Figure 92. The total effective shade is variable because much of the stream has intermittent riparian vegetation limited to a small strip along the banks.

Figure 92 - Little Creek simulated effective shade.



10. LADD CREEK



RGB-colored LiDAR point cloud - Looking downstream Ladd Creek at the mouth.

10.1 Ladd Creek TTools Results

Ladd Creek did not have LiDAR data available, except for a small section near the mouth. The elevations and gradients were sampled from the 10-meter DEM (Figure 93). The lower 9 stream kilometers are extremely low-gradient as they flow through agricultural lands and are often channelized.

Figure 93 - Ladd Creek elevation and gradient.

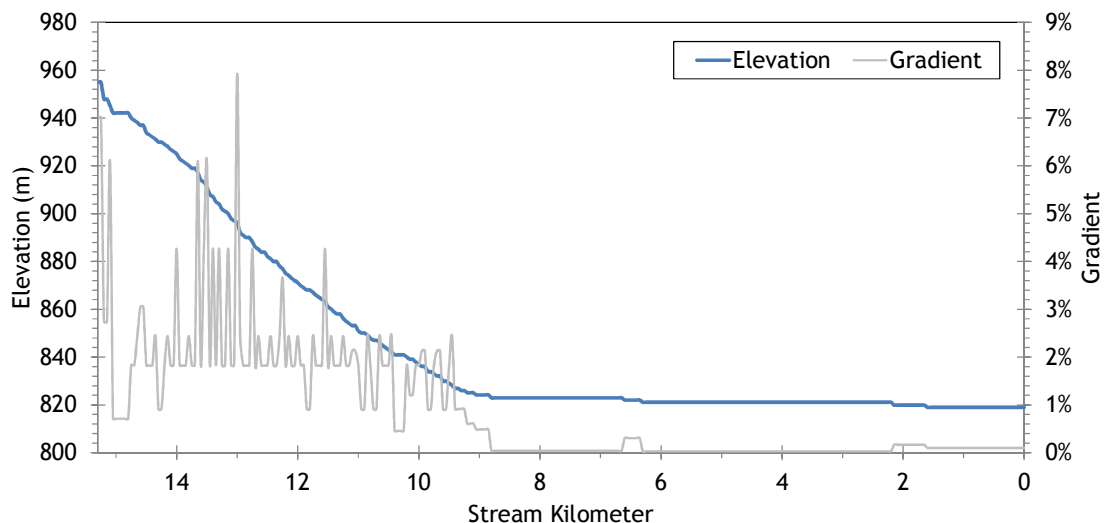
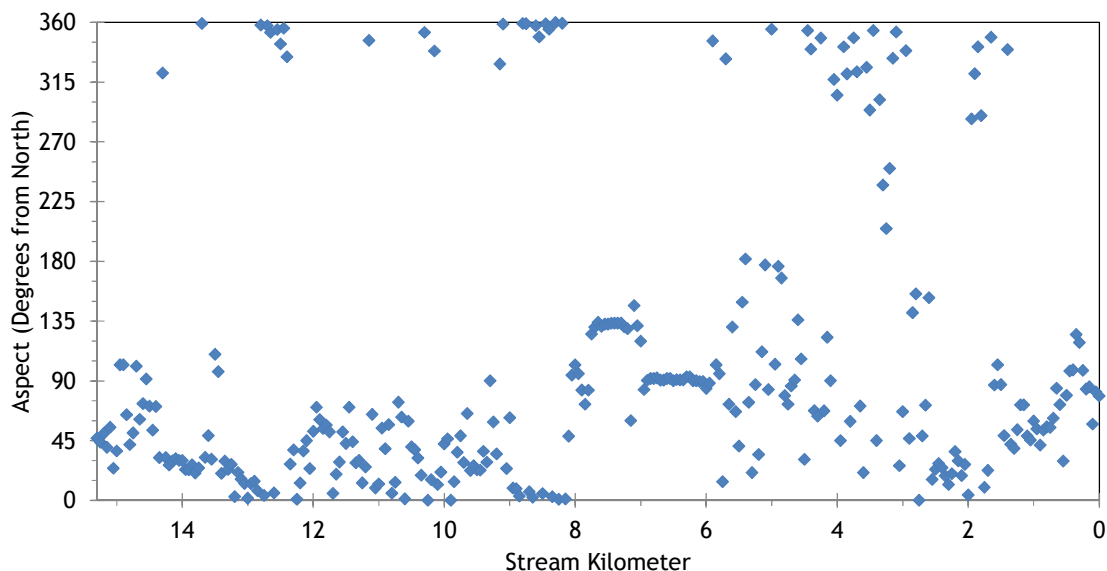


Figure 94 displays the stream aspect for each 50-meter segment of Ladd Creek. The stream flows mostly northeasterly and easterly until it merges with Catherine Creek.

Figure 94 - Ladd Creek stream aspect.



The lower 12 stream kilometers of Ladd Creek have little topographic shade because the stream is flowing through flat agricultural valley bottom (Figure 95). The upper 3 kilometers that were sampled are within more hilly terrain.

Figure 95 - Ladd Creek topographic shade angles.

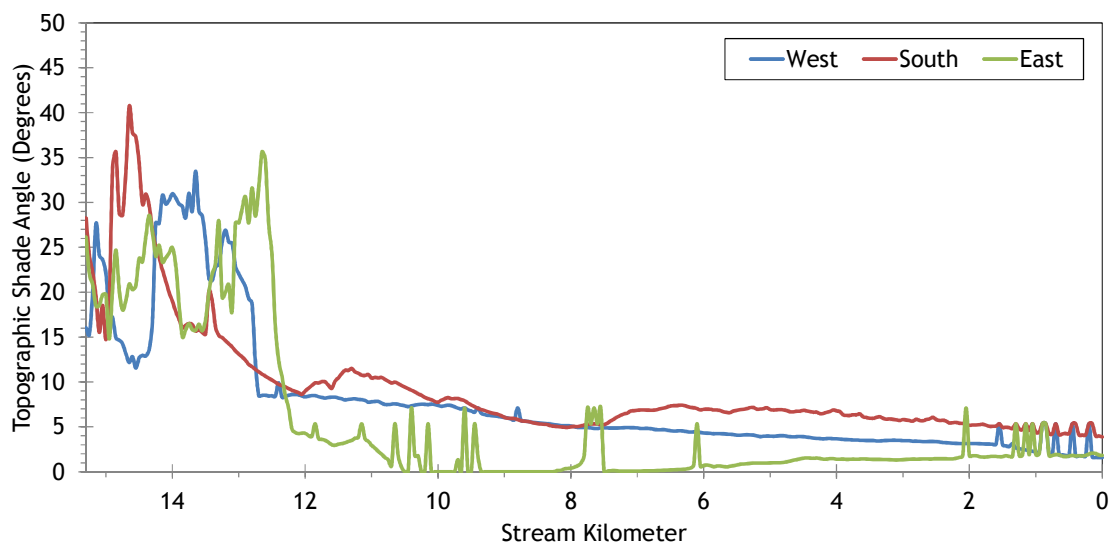
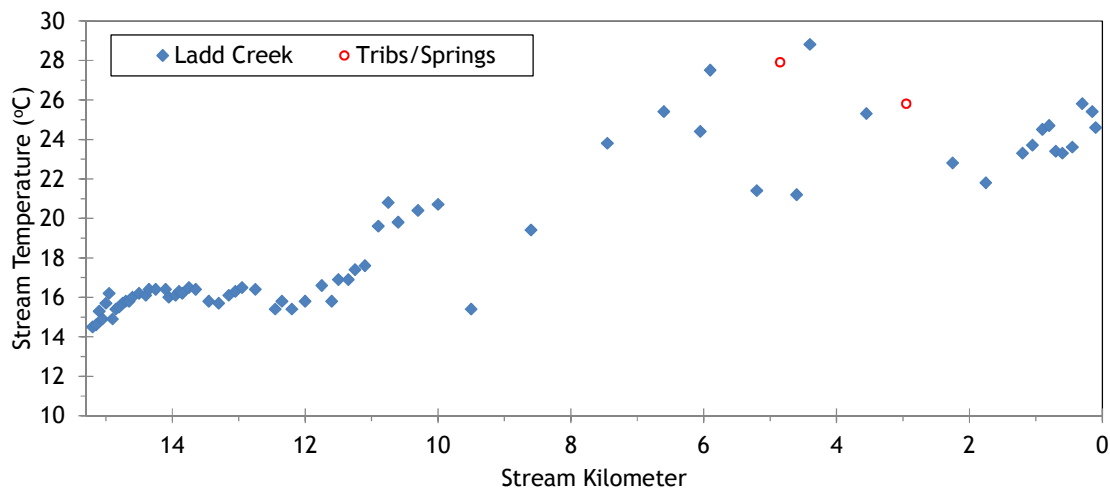


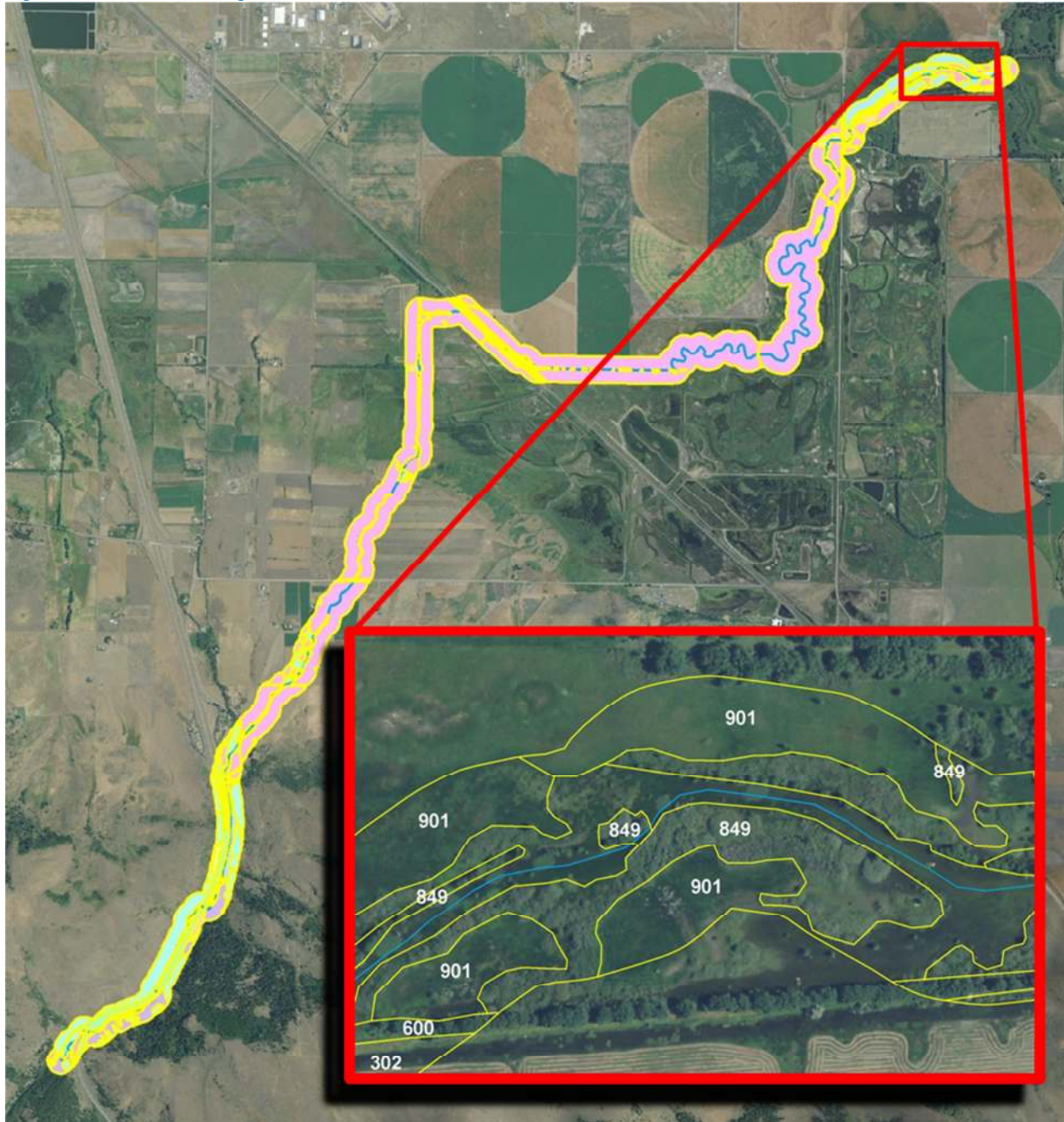
Figure 96 shows the TIR profile of Ladd Creek. The TIR temperature data is sparse throughout much of Ladd Creek and of limited value for multiple reasons. The stream flow was very low (~1 cfs) at the time of the survey. The stream is very small and difficult to sample in the TIR imagery. Much of the stream is channelized and flow volumes and paths are regulated for irrigation purposes. And many areas are very low gradient and likely to have been thermally stratified during the TIR flight.

Figure 96 - Ladd Creek TIR stream temperature profile.



LiDAR data was not available for Ladd Creek, so the near stream land cover was manually digitized from the NAIP orthophotos within 100 meters of the stream (Figure 97). Each polygon was coded to represent a specific land cover type, height class, and density class.

Figure 97 - Ladd Creek digitized near stream land cover.



10.2 Ladd Creek Effective Shade Simulation

Stream temperature was unable to be simulated for Ladd Creek because of its extreme low flow volume and a lack of sufficient ground level data. Effective shade was simulated for the extent shown in Figure 98.

Figure 98 - Ladd Creek simulation extent.

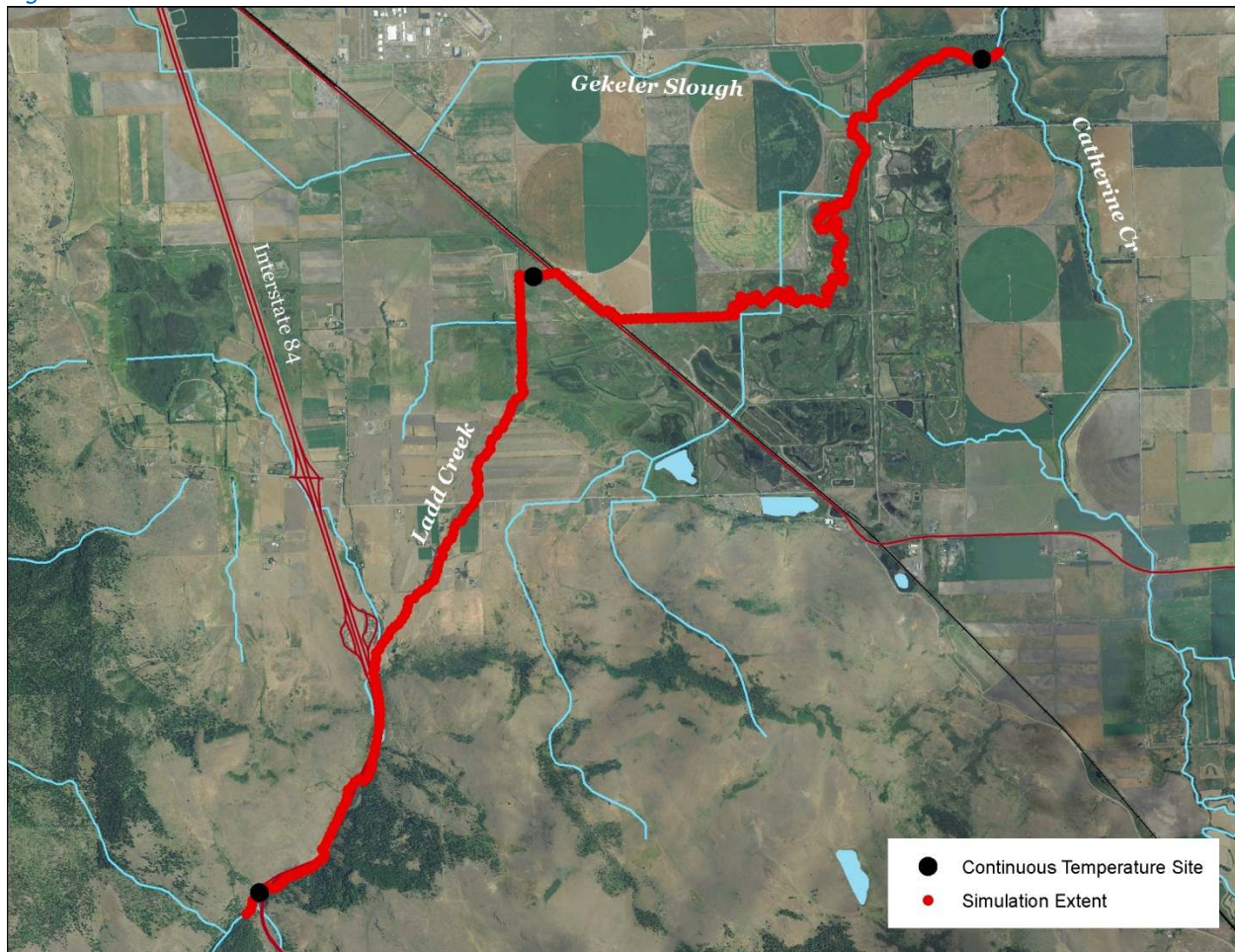


Table 14 - Ladd Creek general Heat Source parameters.

Stream:	Ladd Creek
Length:	15.3 kilometers
Time Period:	August 6-27, 2010
Input Distance Step:	50 meters
Output Distance Step:	100 meters
Time Step:	1 minute
Flush Initial Condition:	NA
TIR Date and Time:	NA
Land Cover Data Source:	LiDAR
Land Cover Sampling Distance Step:	15 meters

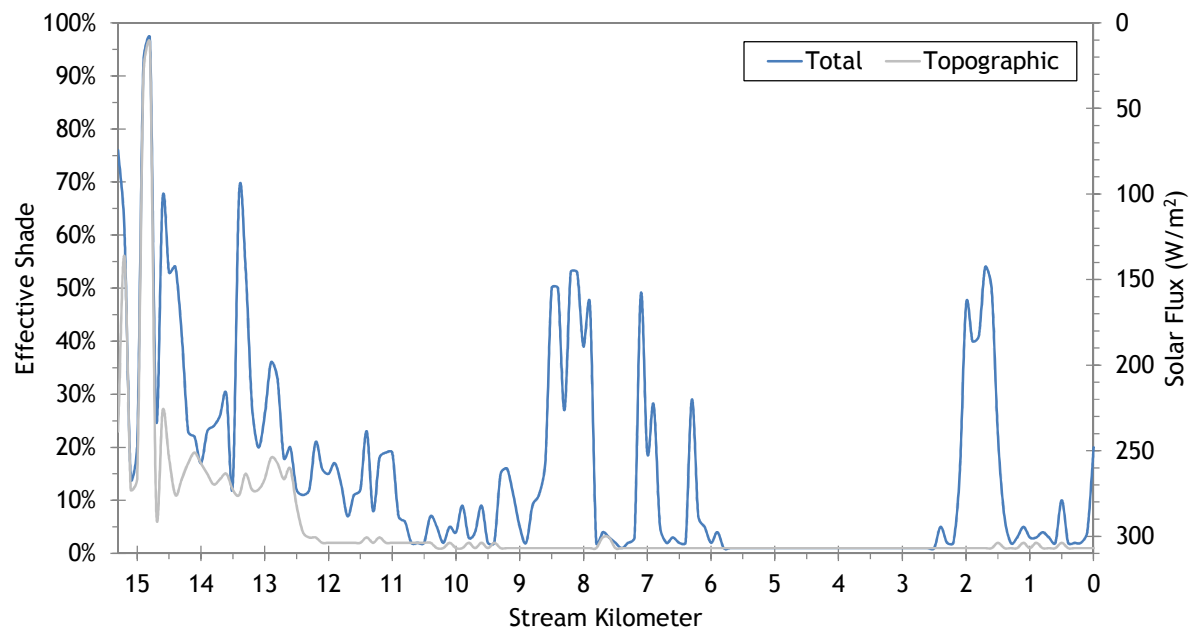
Table 15 shows the near stream land cover codes that were used in the manually digitized layer for Ladd Creek. Height values are based on the lower 66.5 kilometers of Catherine Creek, where LiDAR data was sampled. Values over 3 meters were evaluated for the 75th and 25th percentile. The large height class for Ladd Creek was 9.7 meters, which is equivalent to the 75th percentile of trees on lower Catherine Creek. The small height class used the 25th percentile of 4.4 meters. Values within the regions of Ladd Creek and lower Catherine Creek are smaller than in the upper watershed, primarily because the vegetation consists of smaller riparian shrubs and trees as opposed to large conifer stands.

Table 15 - Ladd Creek near stream land cover codes and descriptions.

Land Cover Name (optional)	Code	Height (m)	Density	Overhang (m)
water	301	0	0	0
pasture, field, cultivated, agriculture	302	0.5	0.9	0
rock	304	0	0	0
road (paved)	400	0	0	0
road (unpaved)	401	0	0	0
Road (unpaved)	403	0	0	0
mixed forest, large	500	9.7	0.75	0
mixed forest, small	501	4.4	0.75	0
deciduous, large	600	9.7	0.75	0
deciduous, small	601	4.4	0.75	0
conifer forest, large	700	9.7	0.75	0
conifer forest, small	701	4.4	0.75	0
conifer forest, large	750	4.4	0.25	0
conifer forest, small and sparse	760	4.4	0.1	0
riparian shrubs, large	849	4.5	0.75	0
shrubs	850	4.5	0.75	0
riparian shrubs, small	899	1	0.75	0
dry upland grasses	900	0.5	0.9	0
floodplain grasses	901	0.5	0.9	0
active channel	3011	0	0	0
building	3248	4	1	0

The simulated effective shade for Ladd Creek is shown in Figure 99. In the upper reaches, most of the effective shade is provided by topographic features. Below stream kilometer 12.5, the stream is flowing through the flat valley bottom and has relatively little streamside vegetation.

Figure 99 - Ladd Creek simulated effective shade.



11. CATHERINE CREEK

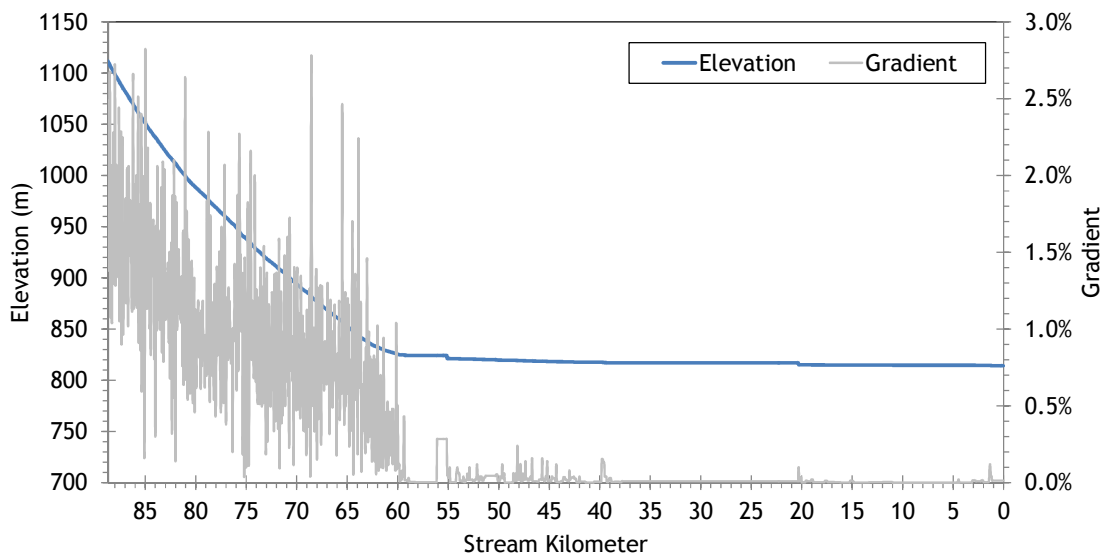


RGB-colored LiDAR point cloud - Catherine Creek in Union (looking upstream).

11.1 Catherine Creek TTools Results

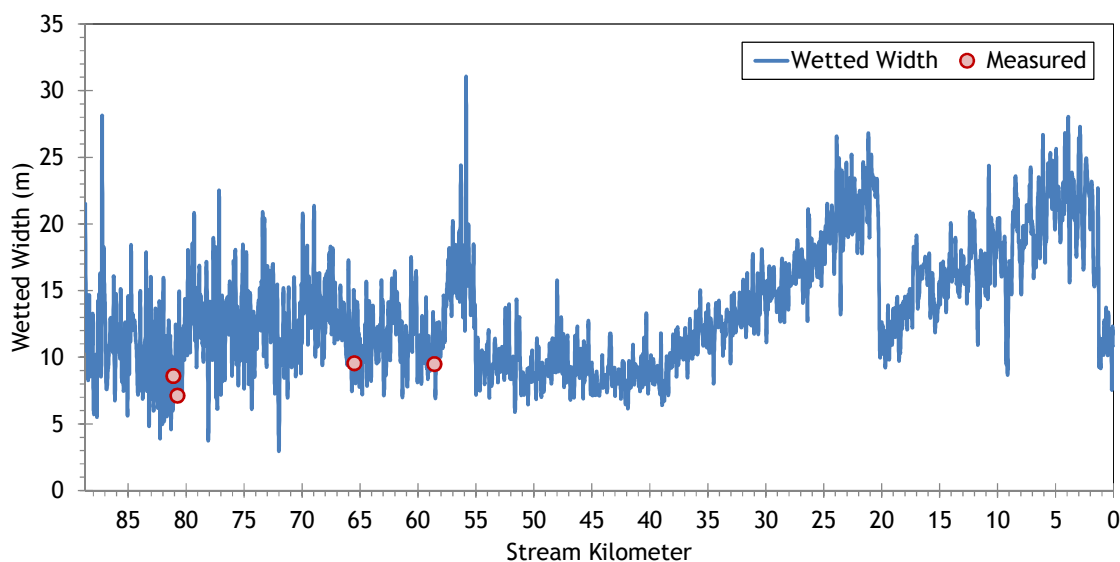
Catherine Creek elevations and gradients are shown in Figure 100. The upper reaches are flowing through mountain foothills, while the lower 60 stream kilometers run through flat agricultural valley bottom. In addition, the lower 60 stream kilometers have much higher sinuosity, thereby further decreasing the stream gradient.

Figure 100 - Catherine Creek elevation and gradient.



Wetted widths were digitized using the TIR, LiDAR intensity, and NAIP imagery. Figure 101 shows the sampled wetted widths along with the ground level measurements. These wetted widths were used as estimates for setting up the Heat Source model hydraulics.

Figure 101 - Catherine Creek wetted widths.



Overall, Catherine Creek flows northwesterly; however, there is huge variation in the lower 60 kilometers where the stream is very sinuous and has large meander bends (Figure 102).

Figure 102 - Catherine Creek stream aspect.

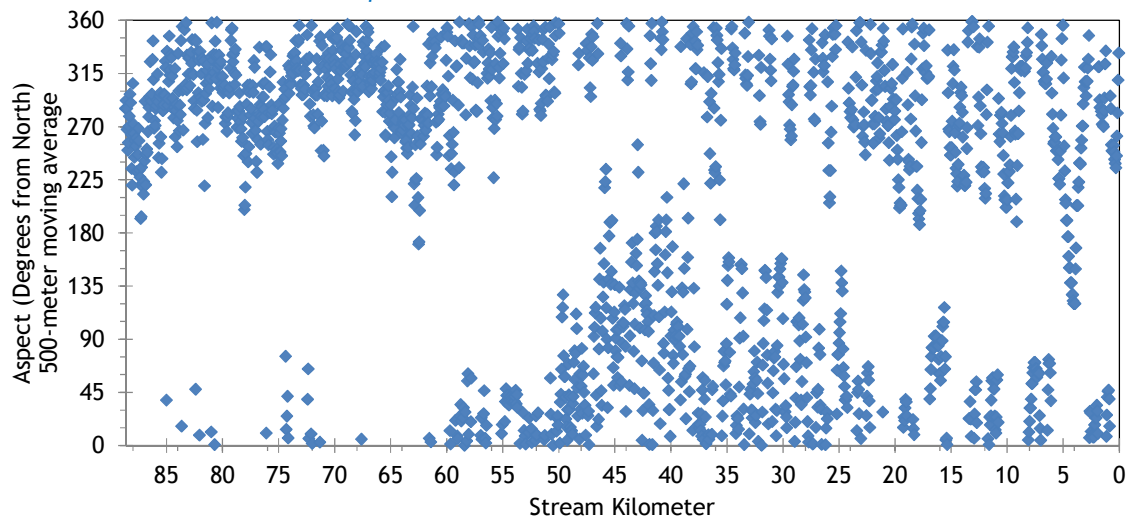


Figure 103 shows the topographic shade angles for Catherine Creek. The upper reaches have more topographic shade because the stream is flowing through a confined valley. The lower reaches have less topographic shade because they are within the Grande Ronde valley bottom.

Figure 103 - Catherine Creek topographic shade angles.

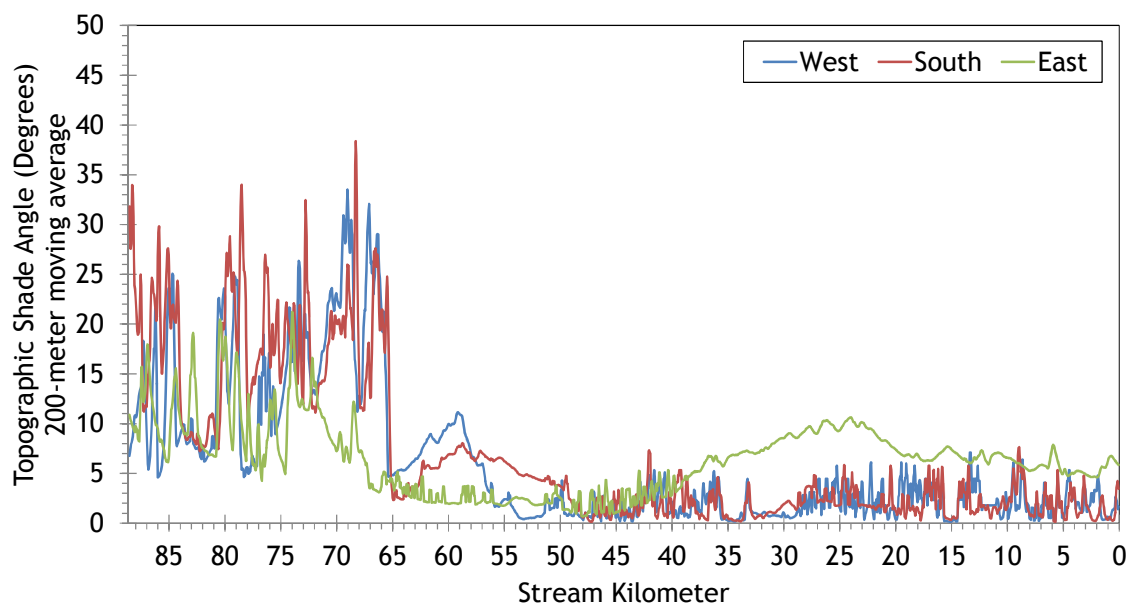
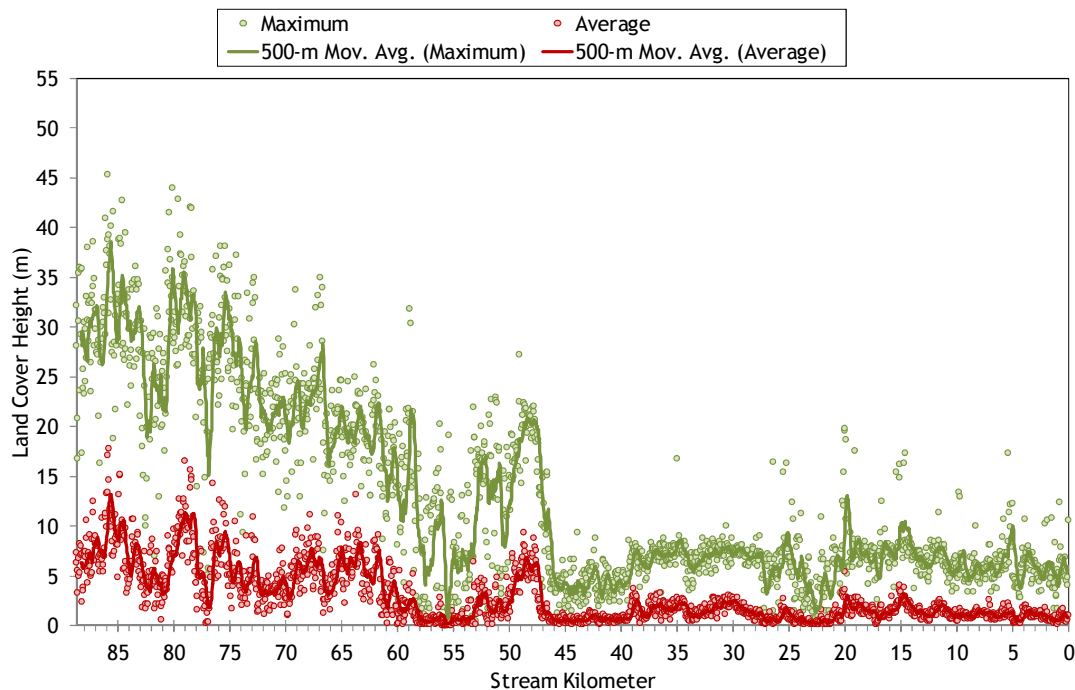


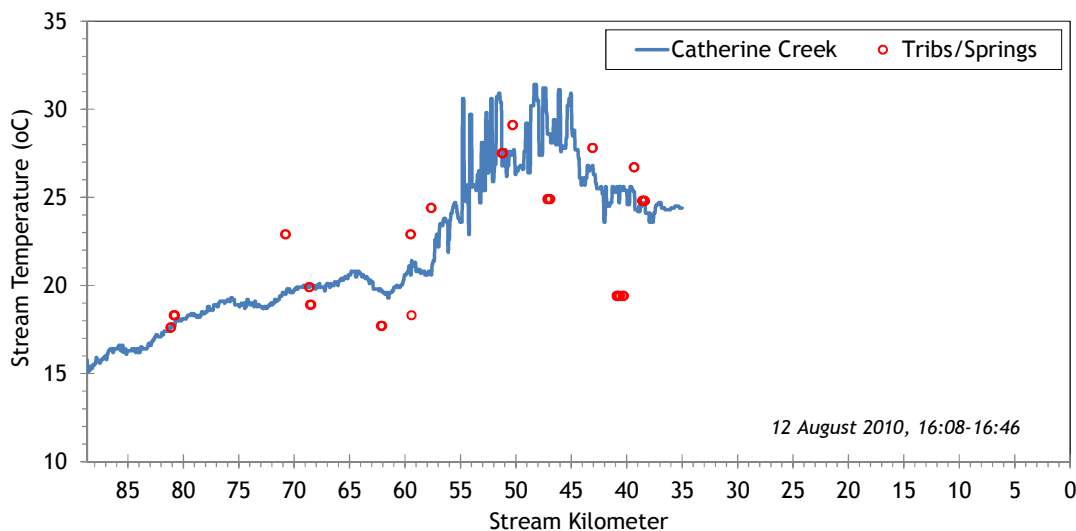
Figure 104 shows the land cover heights sampled along Catherine Creek. The maximum and average of the 28 radial samples were calculated for each 50-meter stream node. (Note: Heat Source uses each of the 28 radial samples for each 50-meter node. The maximum and average are shown here for simplification purposes.)

Figure 104 - Catherine Creek land cover heights sampled from highest hit LiDAR.



TIR data was available for approximately the upper 50 stream kilometers of Catherine Creek (Figure 105). Between the forks and the city of Union (stream kilometer 60), stream temperatures were more stable because there was more volume within the river. At Union, most of the water had been diverted for irrigation use, leaving relatively little volume in the stream. At this point, the stream temperatures rise rapidly and become variable. There are most likely areas of thermal stratification in the lower section as well.

Figure 105 - Catherine Creek TIR stream temperature profile.



11.2 Catherine Creek Heat Source Calibration Results

Catherine Creek was simulated for temperature from the forks to the city of Union. The entire stream was simulated for effective shade.

Below Union, the flow is heavily regulated by irrigation withdrawals which use most of the water. The reach between Union and the mouth was unable to be simulated for temperature. In addition, there are many stratified reaches below Union, which cannot be simulated using Heat Source because it is a 2-D model.

Figure 106 - Catherine Creek simulation extent.

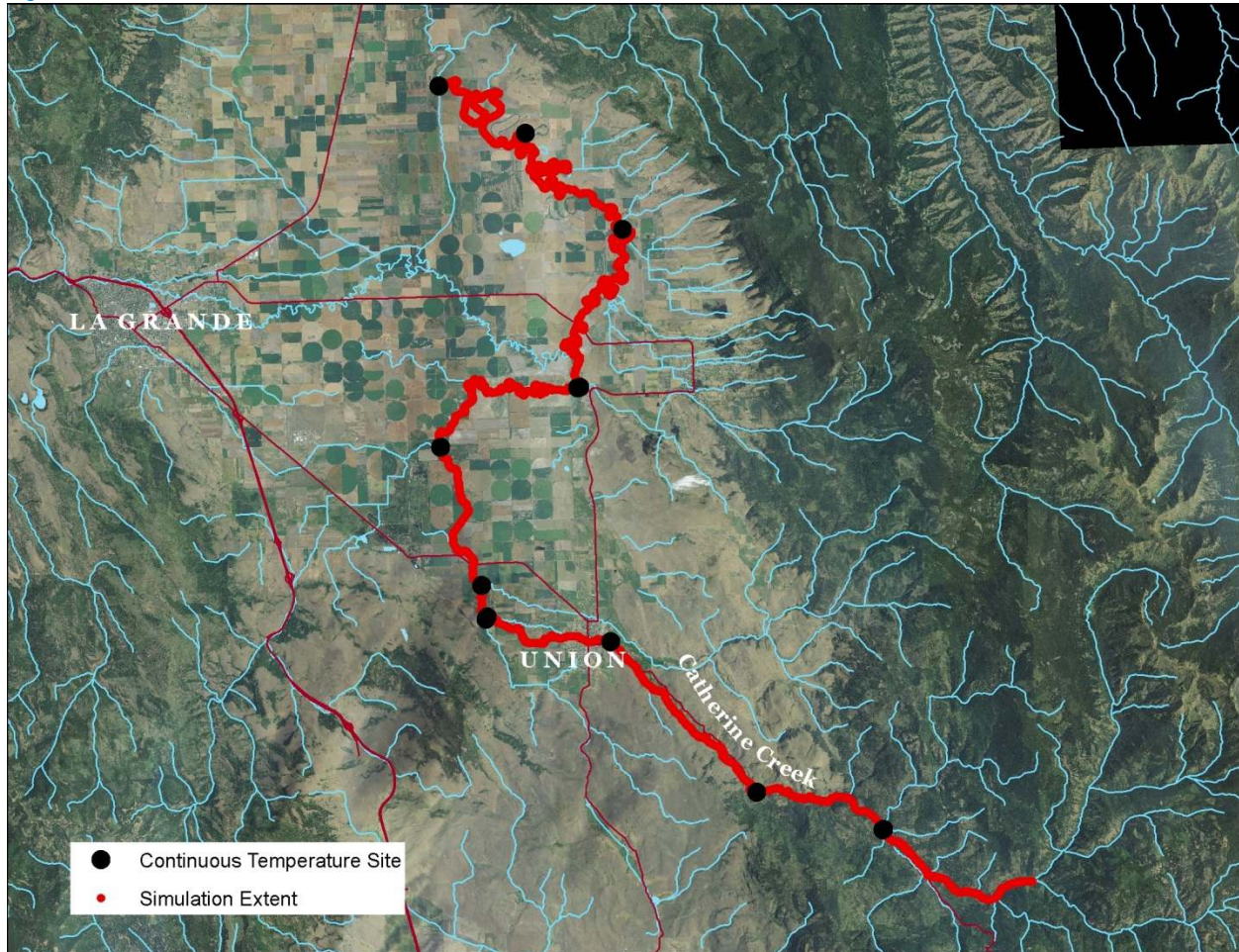


Table 16 - Catherine Creek general Heat Source parameters.

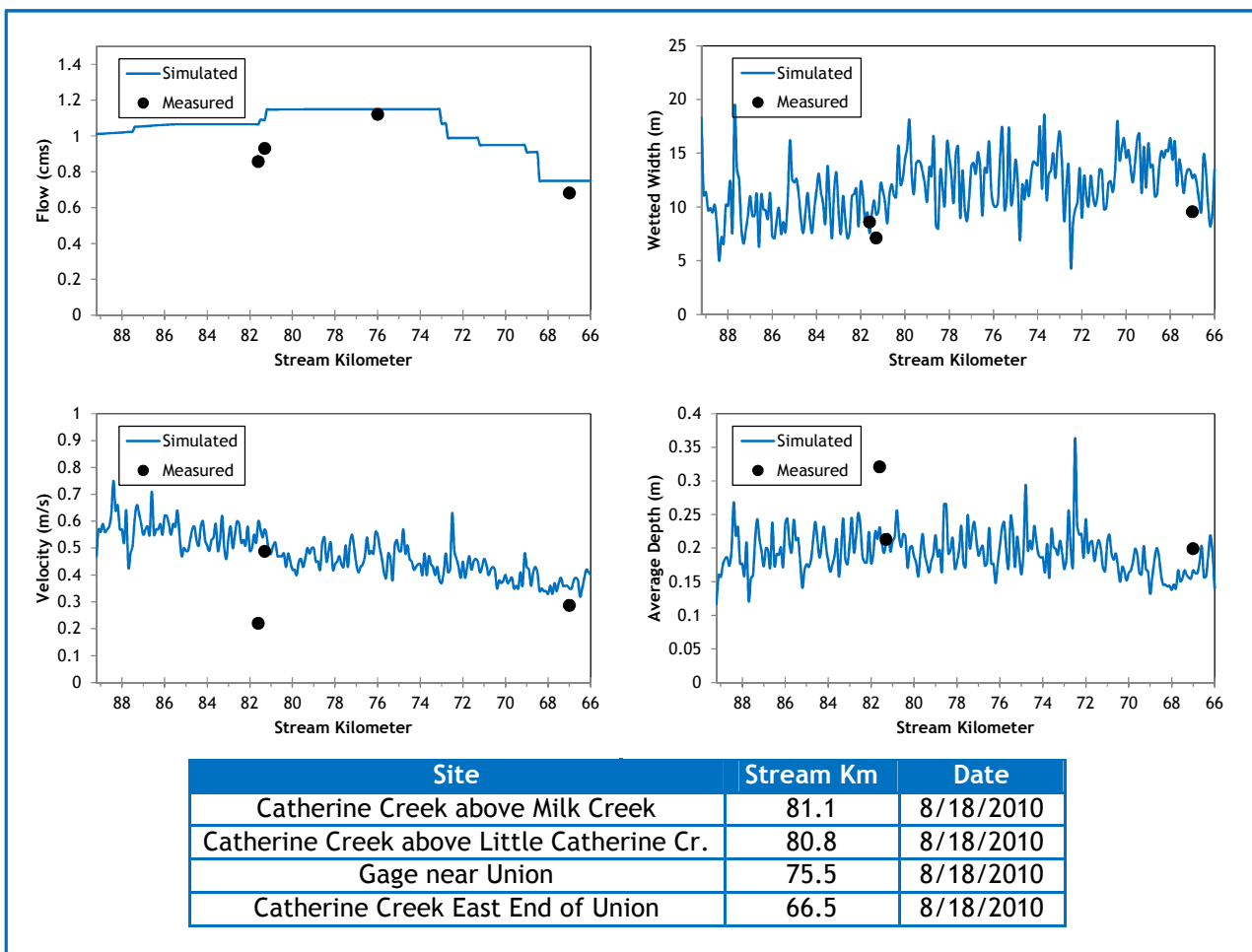
Stream:	Catherine Creek
Length:	88.7 kilometers
Time Period:	August 6-27, 2010
Input Distance Step:	50 meters
Output Distance Step:	100 meters
Time Step:	1 minute
Flush Initial Condition:	7 days
TIR Date and Time:	August 12, 2010 16:08-16:46
Land Cover Data Source:	LiDAR
Land Cover Sampling Distance Step:	15 meters

The following assumptions were used when calibrating the Catherine Creek Heat Source model:

- Hourly climate data was obtained from the La Grande Airport (NWS). Air temperature was adjusted using the adiabatic lapse rate of 1°C per 100 meters elevation.
- The upstream boundary condition is a mass balance of data from the mouths of the North and South Forks.
- There is a large diversion in the city of Union where most of the water was being diverted for irrigation use. Below this point there were additional diversions, very low flow, and thermal stratification which prohibited stream temperature modeling; however, effective shade was simulated the entire length from the forks to the confluence with the Grande Ronde River.

Figure 107 shows the simulated and measured hydraulic values for the calibrated Heat Source model for August 18, 2010. The upstream boundary flow volume is a mass balance of the North and South Forks. The Catherine Creek simulated flow volumes are based on the daily values recorded at the gage above Union (stream kilometer 75.5).

Figure 107 - Catherine Creek simulated and measured hydraulic values.



The simulated and daily gage flows for select locations are shown in Figure 108. The flow below the forks is a mass balance of the simulated flows at the mouths of the North and South Forks. The Catherine Creek simulated flows were then calibrated to target the values recorded at the gage near (upstream of) Union. There is a large diversion that was occurring between the lower end of the simulation and the gage in Union. Very little water was left in the stream and those volumes fluctuated each day. The very low flows below Union, thermal stratification, and unmonitored diversions prohibited Heat Source temperature simulation of lower Catherine Creek (effective shade was still simulated for the entire stream).

Figure 108 - Catherine Creek simulated and measured daily flow volumes at select locations.

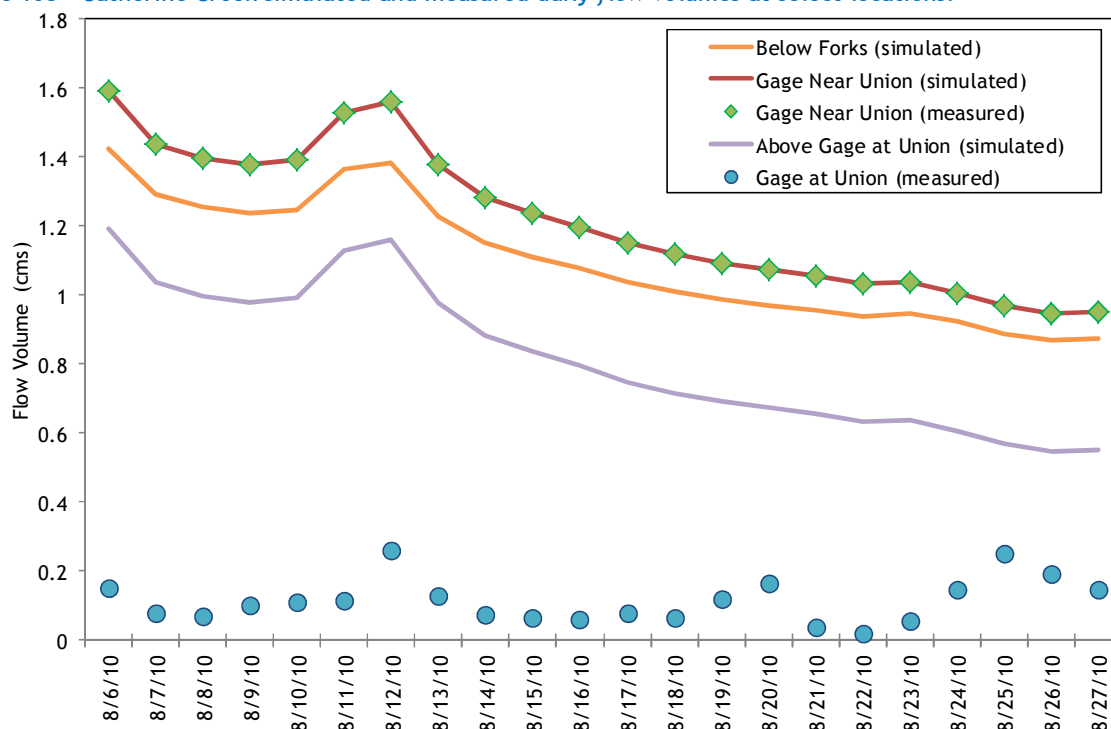


Table 17 summarizes the mass inflows and outflows included in the calibrated Heat Source model. Scout, Milk, and Little Catherine Creek flows were calculated based on the difference between the boundary condition and the gage above Union and vary daily.

Table 17 - Catherine Creek mass inflow and outflow features and assumptions.

Feature	Stream Km	Assumptions
Scout Creek	87.0	0.02-0.04 cms, used Little Catherine Creek at mouth hourly temperatures
Milk Creek	81.1	0.02-0.04 cms, measured hourly temperatures
Little Catherine Cr.	80.7	0.04-0.09 cms, measured hourly temperatures
Diversion (small)	72.5	-0.08 cms (constant)
Diversion (small)	72.2	-0.08 cms (constant)
Diversion	70.8	-0.04 cms (constant)
Hatchery / Ponds	68.5	-0.04 cms (constant)
Dam and Diversion	68.0	-0.16 cms (constant)

The simulated and measured longitudinal stream temperatures above Union are shown in Figure 109.

Figure 109 - Catherine Creek simulated and measured longitudinal temperatures.

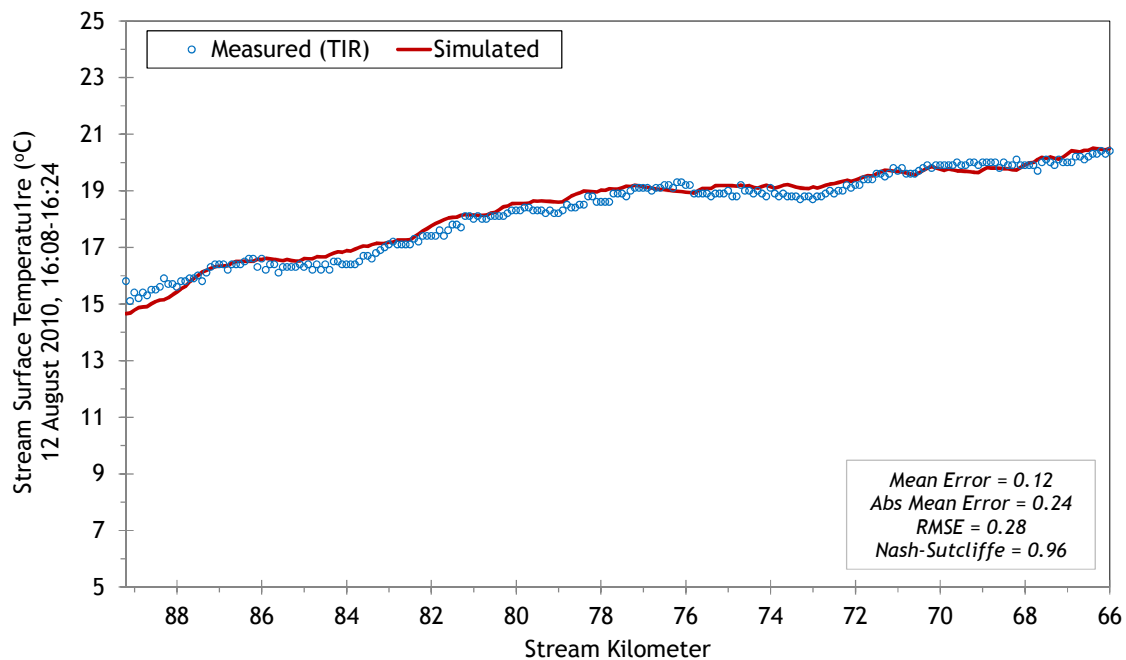
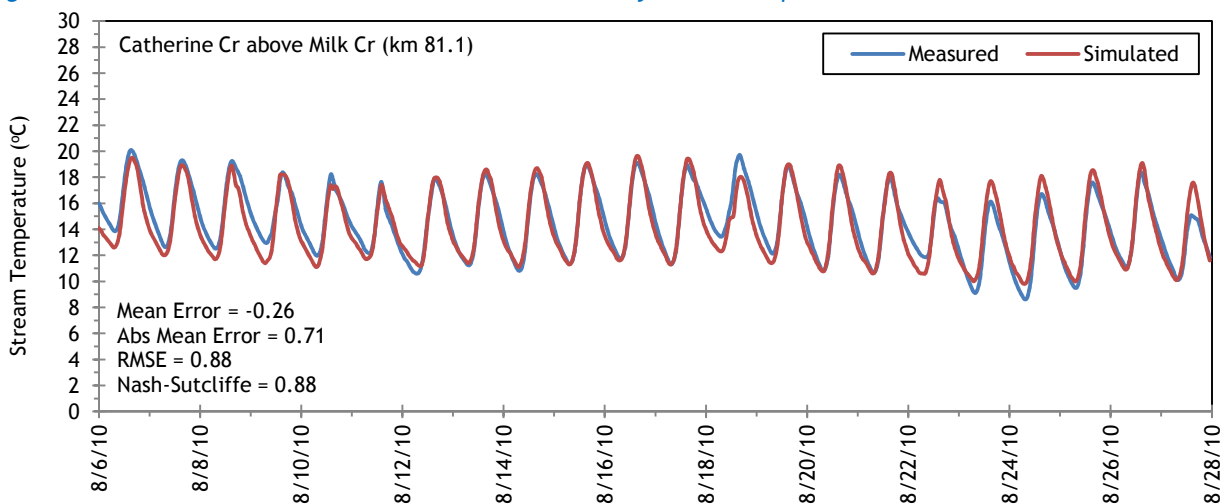
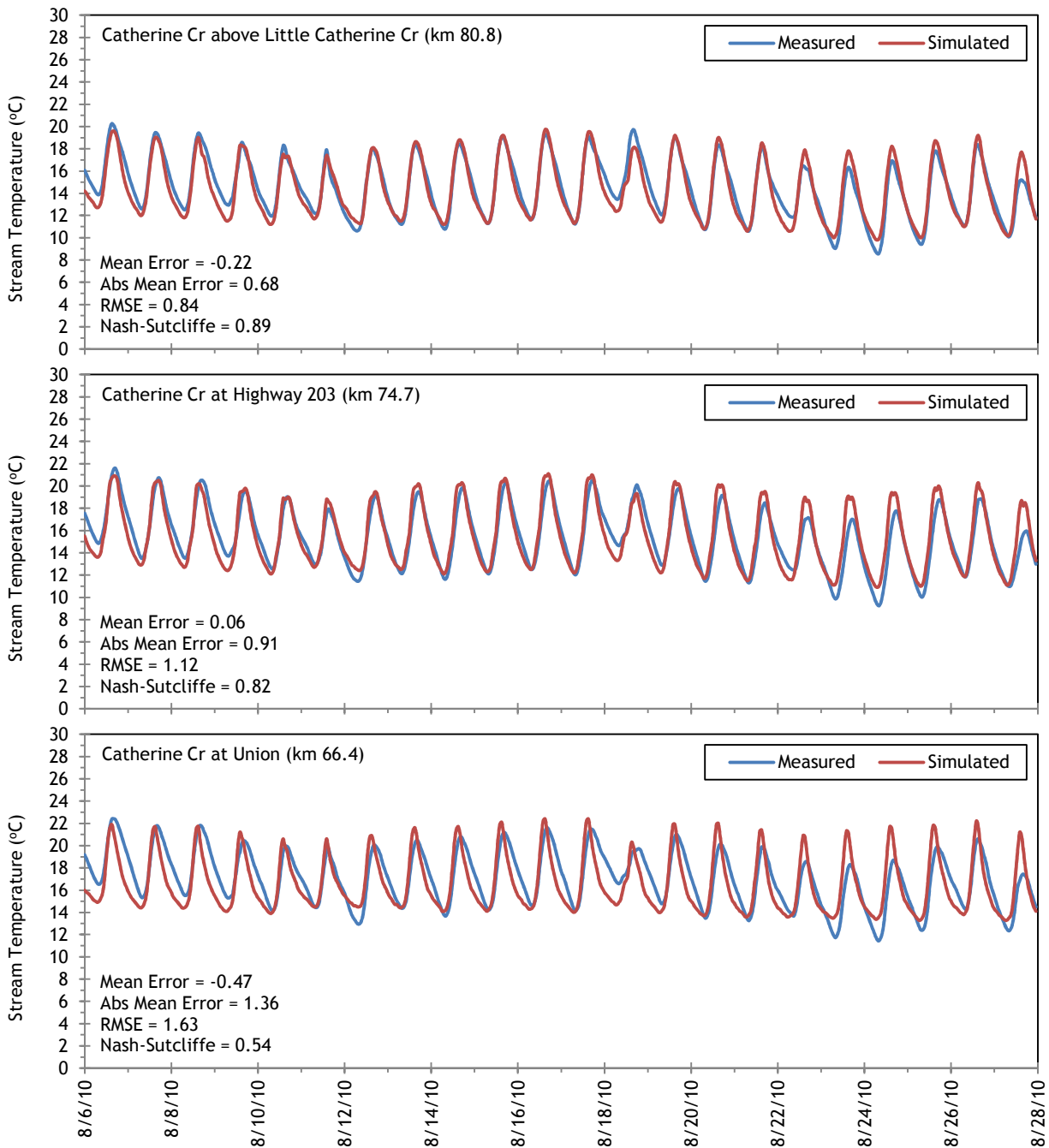


Figure 110 shows the simulated and measured hourly temperatures at 4 locations along the simulated reach between the forks and Union.

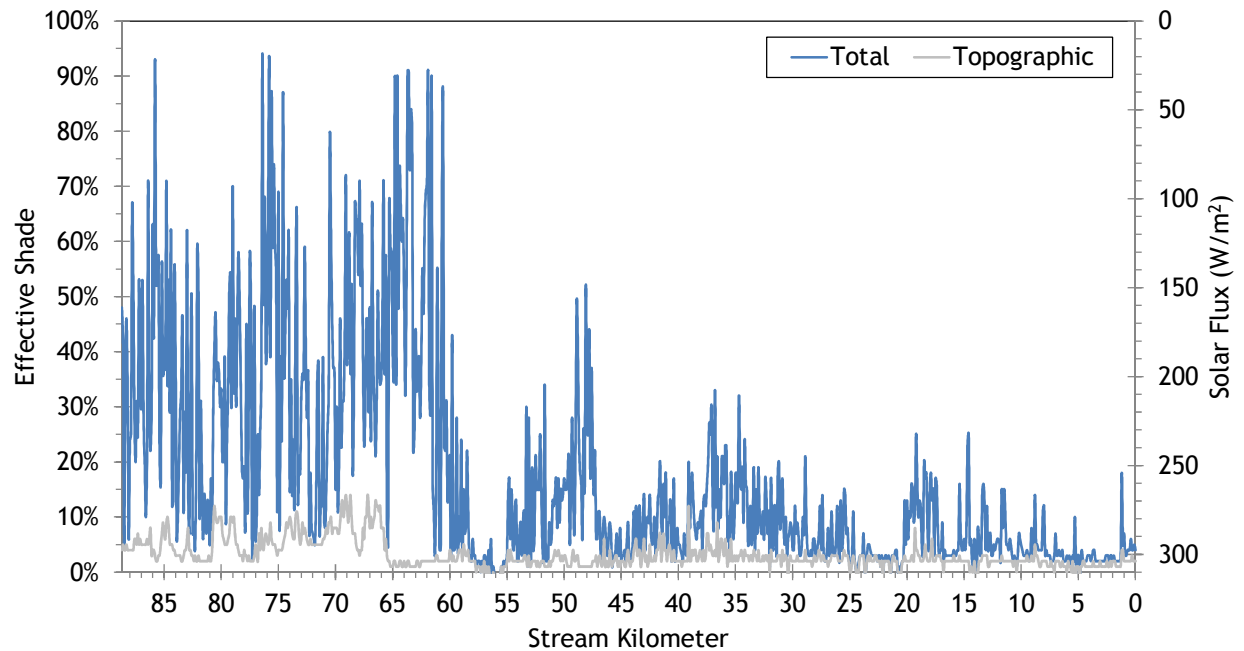
Figure 110 - Catherine Creek simulated and measured hourly stream temperatures.





The simulated effective shade values for Catherine Creek are presented in Figure 111. Above the city of Union (approximately kilometer 65) the stream is flowing through a more confined valley in the foothills and is well forested. Below Union, the land use is primarily agriculture and there is little stream side vegetation, so effective shade is lower.

Figure 111 - Catherine Creek simulated effective shade values.



RGB-colored LiDAR point cloud - Catherine Creek downstream of Warm Creek.

12. CLEAR CREEK

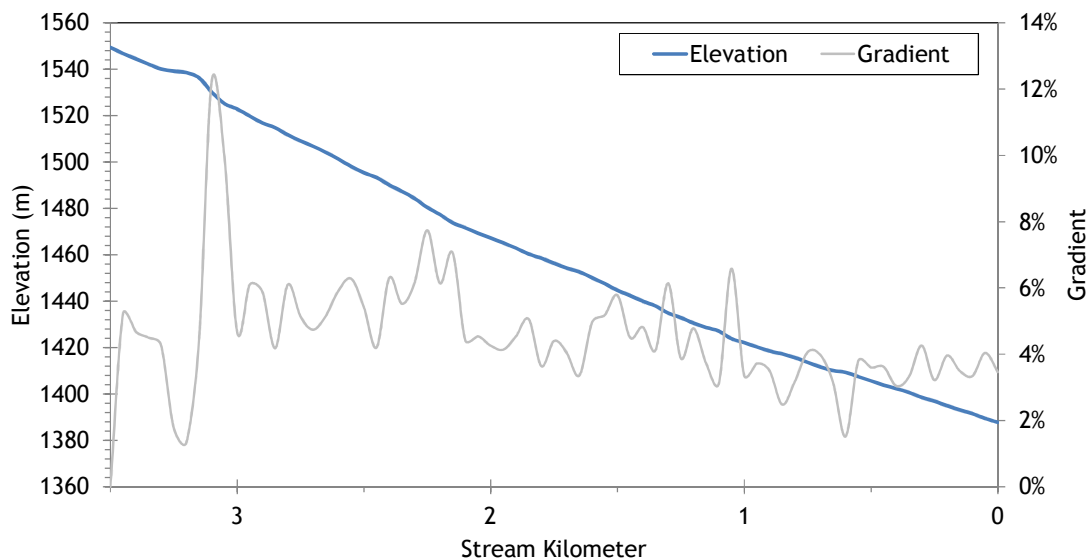


RGB-colored LiDAR point cloud - Clear Creek looking upstream from near mouth.

12.1 Clear Creek TTools Results

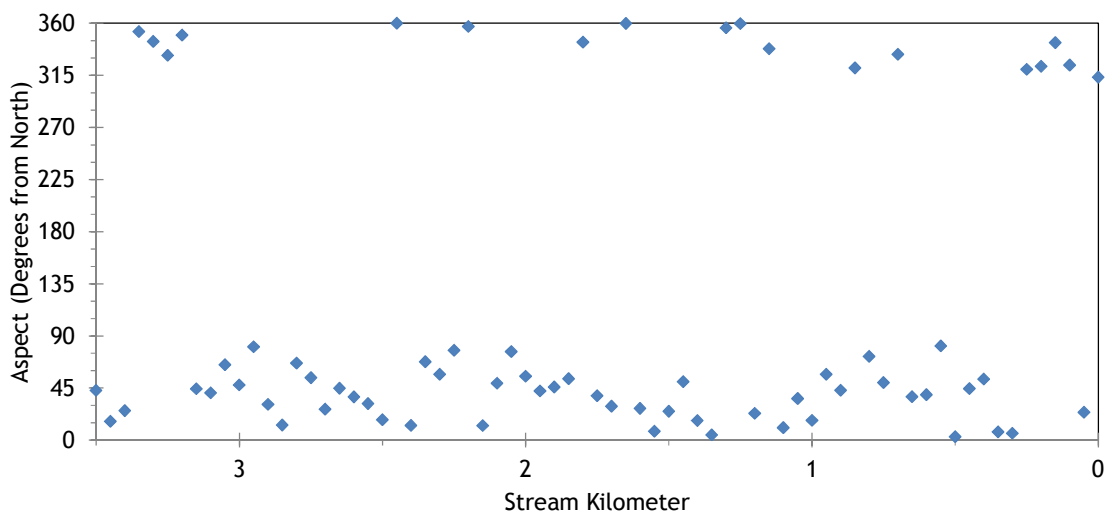
Clear Creek elevations and gradients were sampled from bare earth LiDAR data (Figure 112). The stream is located in the Blue Mountains area of the upper watershed and has a moderately steep gradient.

Figure 112 - Clear Creek elevation and gradient.



Clear Creek flows mostly toward the northeast until it reaches the Grande Ronde River (Figure 113).

Figure 113 - Clear Creek stream aspect.



Topographic shade angles for Clear Creek are shown in Figure 114. There is a significant amount of topographic shade provided by the surrounding mountains.

Figure 114 - Clear Creek topographic shade angles.

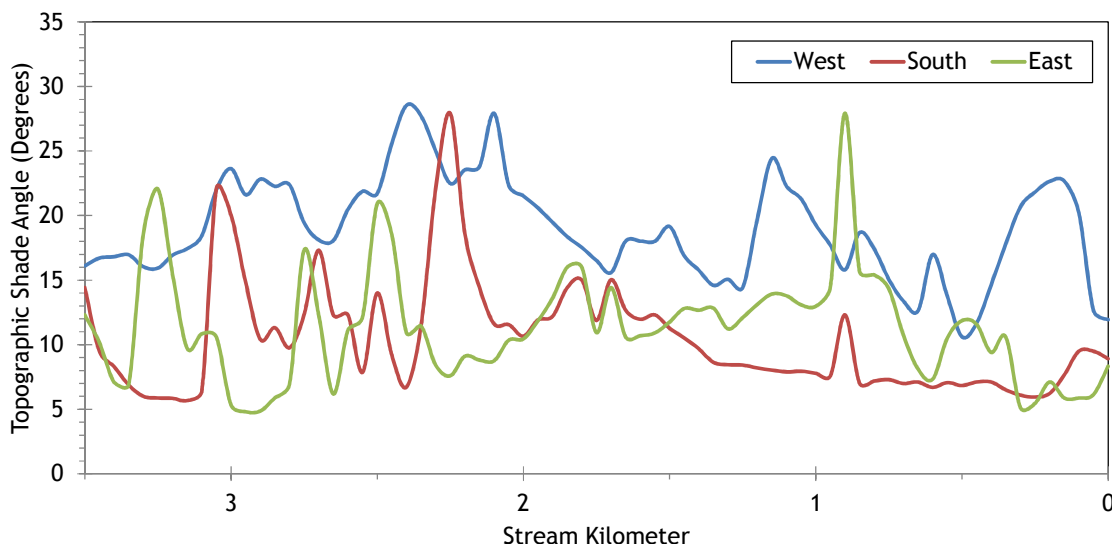
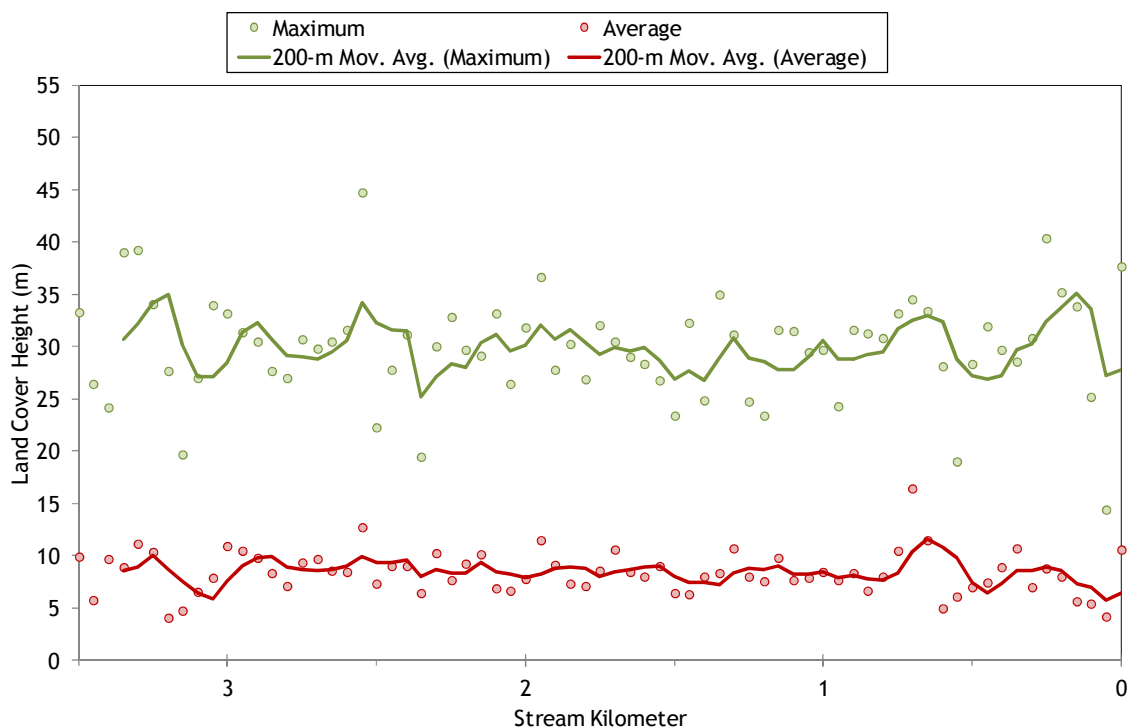


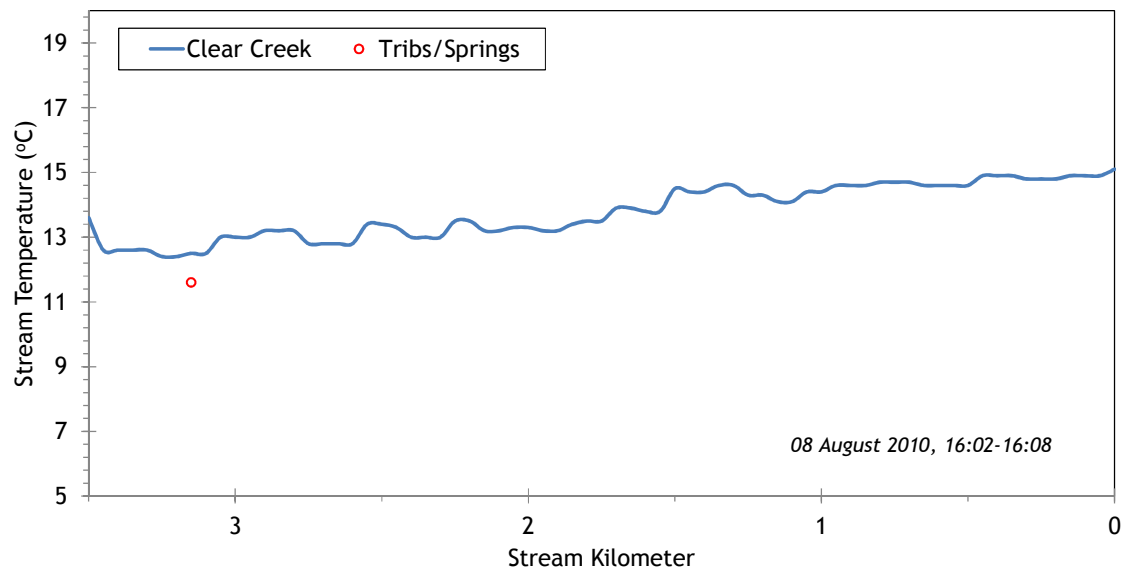
Figure 115 shows the land cover heights sampled along Clear Creek. The maximum and average of the 28 radial samples were calculated for each 50-meter stream node. (Note: Heat Source uses each of the 28 radial samples for each 50-meter node. The maximum and average are shown here for simplification purposes.)

Figure 115 - Clear Creek land cover heights sampled from highest hit LiDAR.



The TIR stream temperature profile for Clear Creek is shown in Figure 116. Clear Creek is well-forested and remains fairly cool throughout the day.

Figure 116 - Clear Creek TIR stream temperature profile.



12.2 Clear Creek Heat Source Calibration Results

Stream temperature was simulated for the lower 3.5 kilometers of Clear Creek (Figure 117).

Figure 117 - Clear Creek simulation extent.

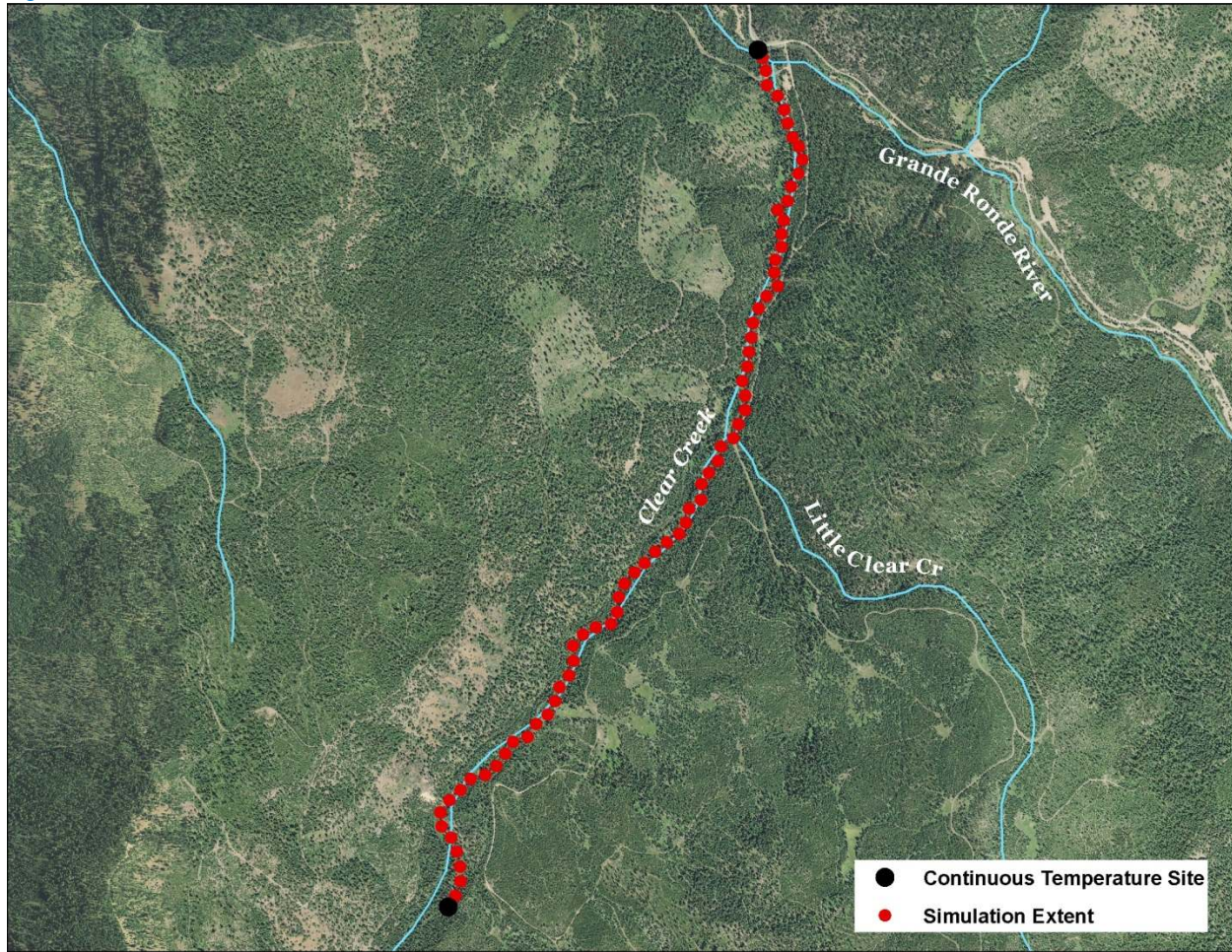


Table 18 - Clear Creek general Heat Source parameters.

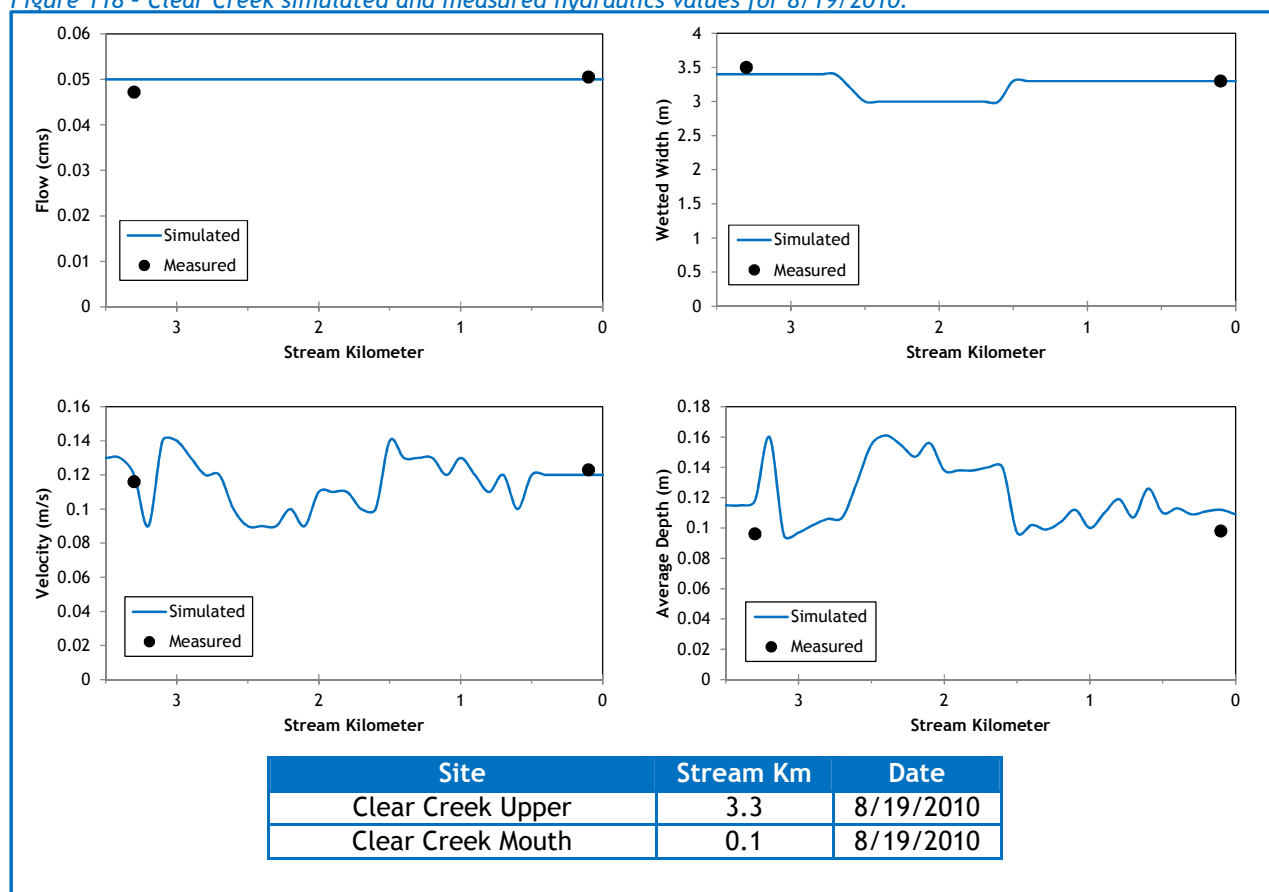
Stream:	Clear Creek
Length:	3.5 kilometers
Time Period:	August 6-27, 2010
Input Distance Step:	50 meters
Output Distance Step:	100 meters
Time Step:	1 minute
Flush Initial Condition:	7 days
TIR Date and Time:	August 8, 2010 16:01-16:07
Land Cover Data Source:	LiDAR
Land Cover Sampling Distance Step:	15 meters

The following assumptions were used when calibrating the Clear Creek Heat Source model:

- Hourly climate data was obtained from the J Ridge RAWs (USFS) site. Air temperature was adjusted using the adiabatic lapse rate of 1°C per 100 meters elevation.
- Wetted widths were too small to be digitized from the remote sensing data and were therefore estimated based on the field measurements.
- Daily flow variability was extrapolated from Grande Ronde River gage data.
- There were no significant springs or tributaries observed in the TIR imagery, and therefore none were included within the model.

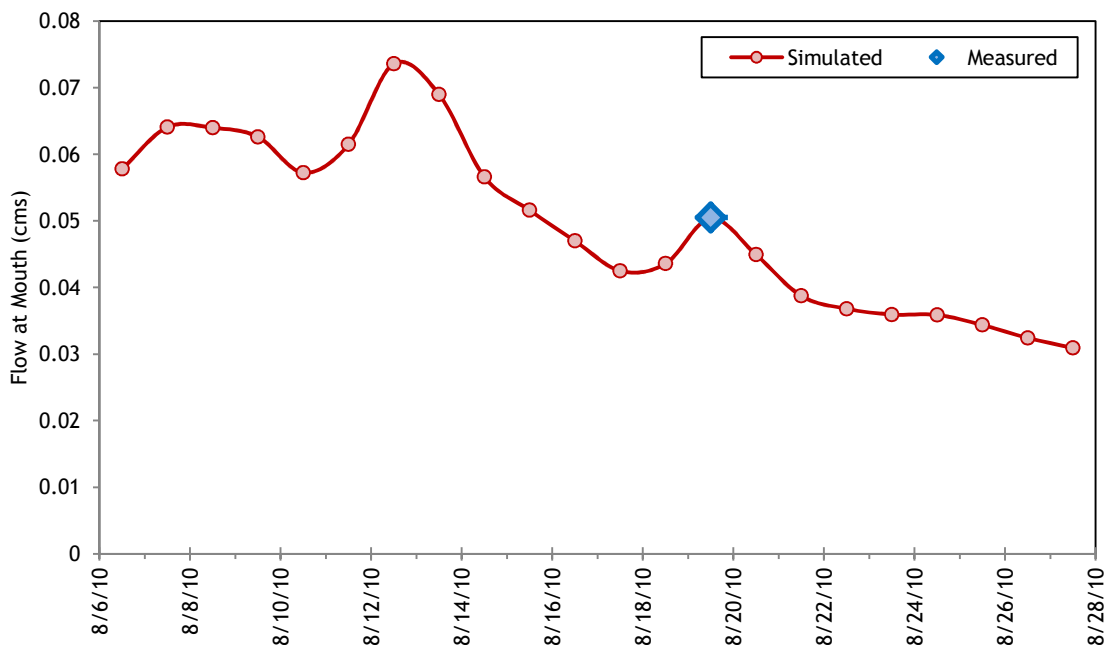
Figure 118 displays the simulated and measured hydraulic values for Clear Creek for August 19, 2010.

Figure 118 - Clear Creek simulated and measured hydraulics values for 8/19/2010.



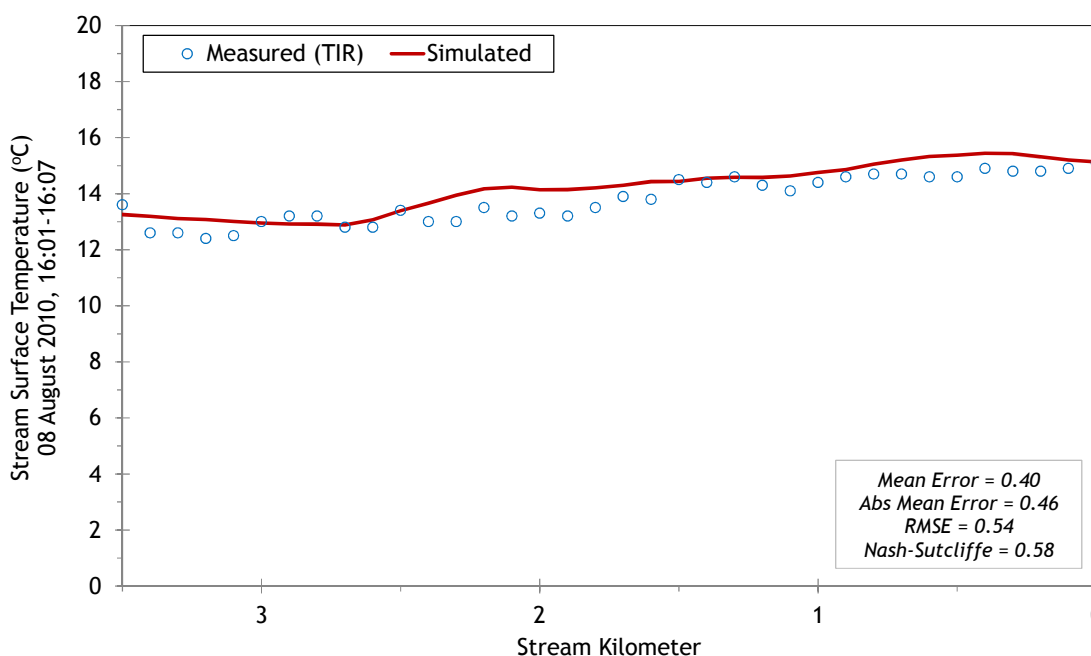
The simulated daily flow volumes at the mouth of Clear Creek are shown in Figure 119. The daily values were extrapolated from gage data recorded on the Grande Ronde River. There were two small rain events which are responsible for the slight flow increases around August 11th and 19th.

Figure 119 - Clear Creek daily flow volumes at the mouth.



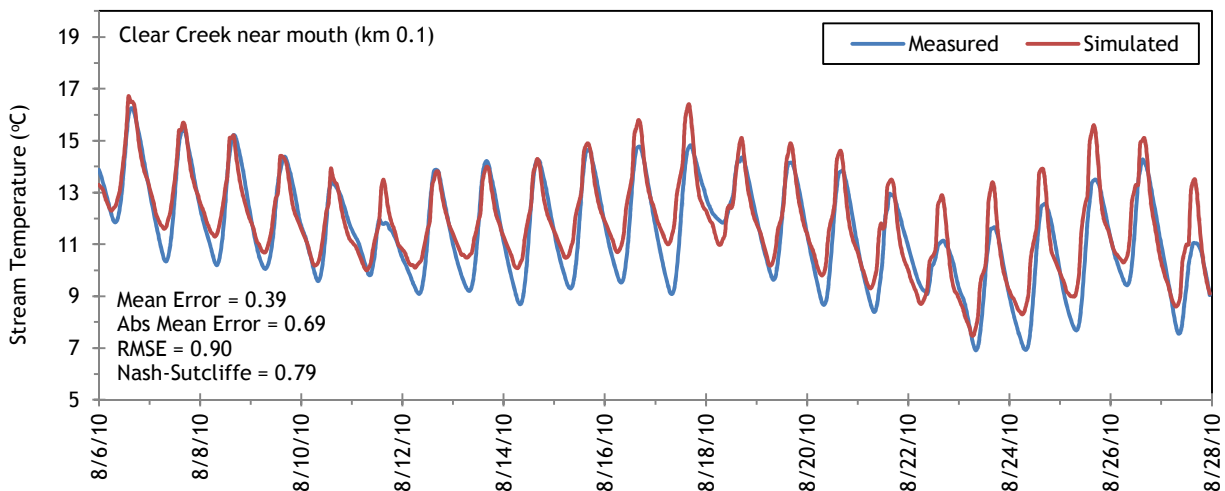
The simulated and measured longitudinal stream temperatures and calibration statistics are shown in Figure 120. There was little thermal variability in the lower 3.5 stream kilometers.

Figure 120 - Clear Creek simulated and measured longitudinal temperatures.



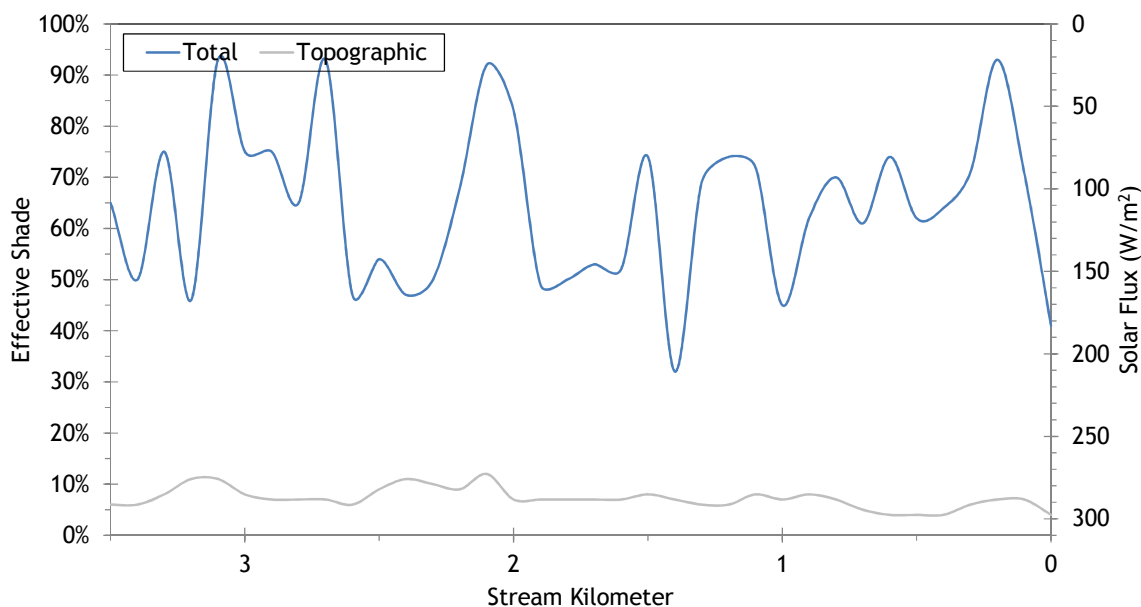
Clear Creek simulated and measured hourly temperatures are plotted in Figure 121.

Figure 121 - Clear Creek simulated and measured hourly temperatures.

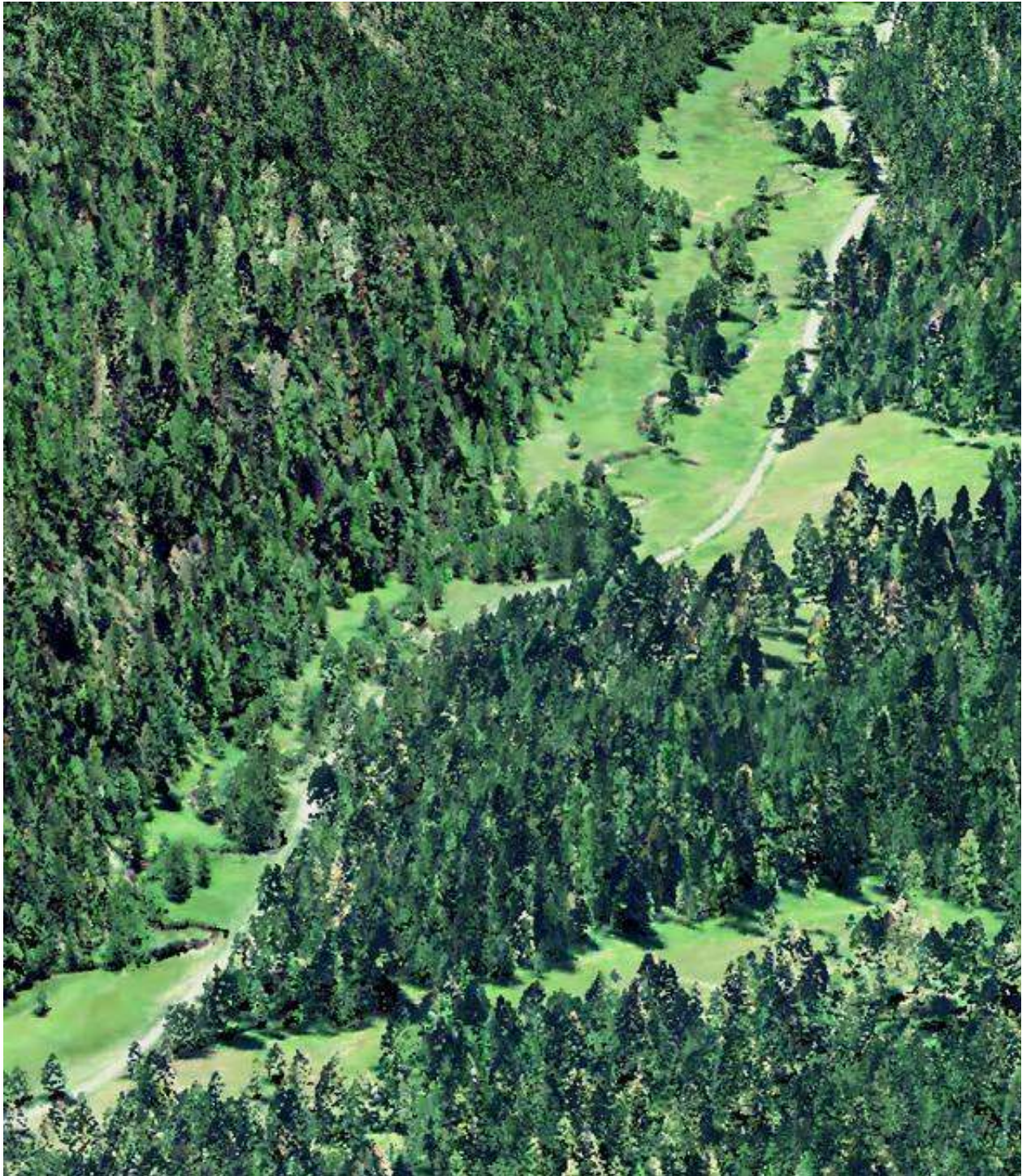


The simulated effective shade values for Clear Creek are shown in Figure 122. There is less than 10% topographic shade along the simulated reach. The majority of the total effective shade is produced by near stream vegetation.

Figure 122 - Clear Creek simulated effective shade.



13. LIMBER JIM CREEK

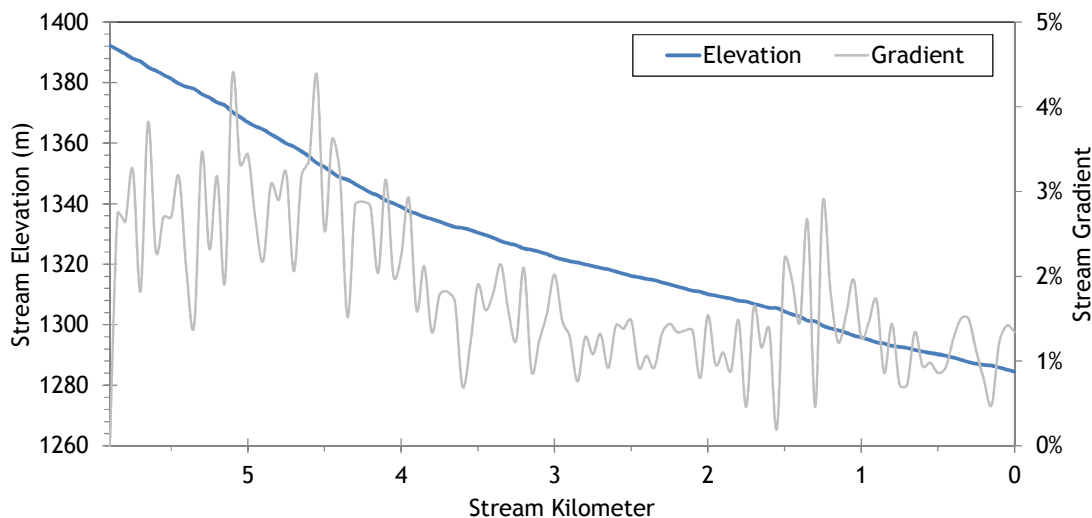


RGB-colored LiDAR point cloud - Limber Jim Creek look downstream just below the North Fork.

13.1 Limber Jim Creek TTools Results

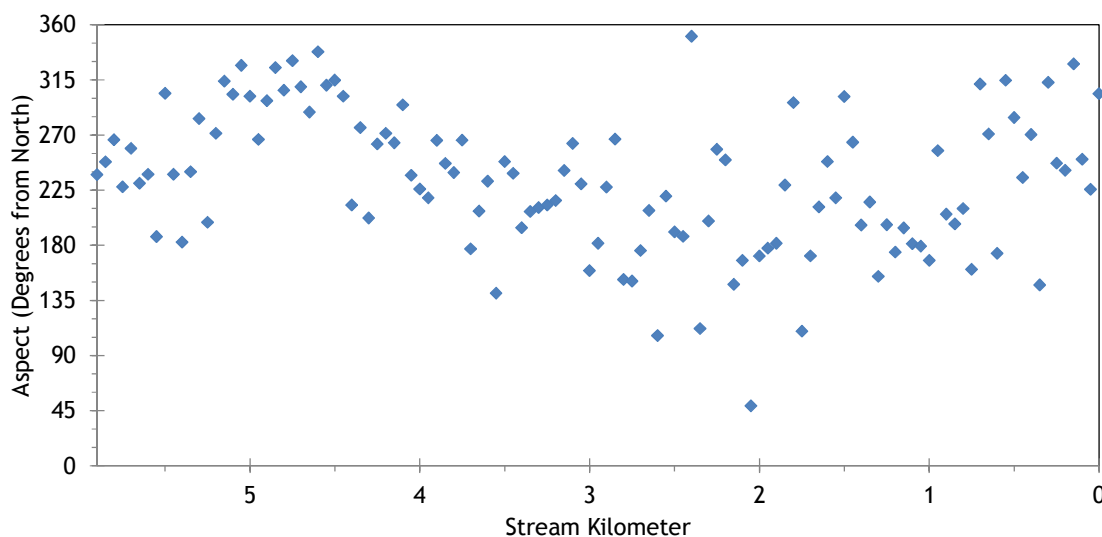
Limber Jim Creek elevations and gradients are shown in Figure 123. The values were sampled from the bare earth LiDAR data. The stream goes from a more constricted valley to a more flat valley bottom in the lower 3 kilometers, where it meanders more and has a lower gradient.

Figure 123 - Limber Jim Creek elevation and gradient.



Limber Jim Creek stream aspects are shown in Figure 124 for each 50-meter reach. Overall, the stream flows in the westerly direction before reaching the Grande Ronde River.

Figure 124 - Limber Jim Creek stream aspect.



Limber Jim Creek has a good amount of topographic shade features provided by the surrounding mountains (Figure 125). Values range between 5 and 25 degrees in general.

Figure 125 - Limber Jim Creek topographic shade angles.

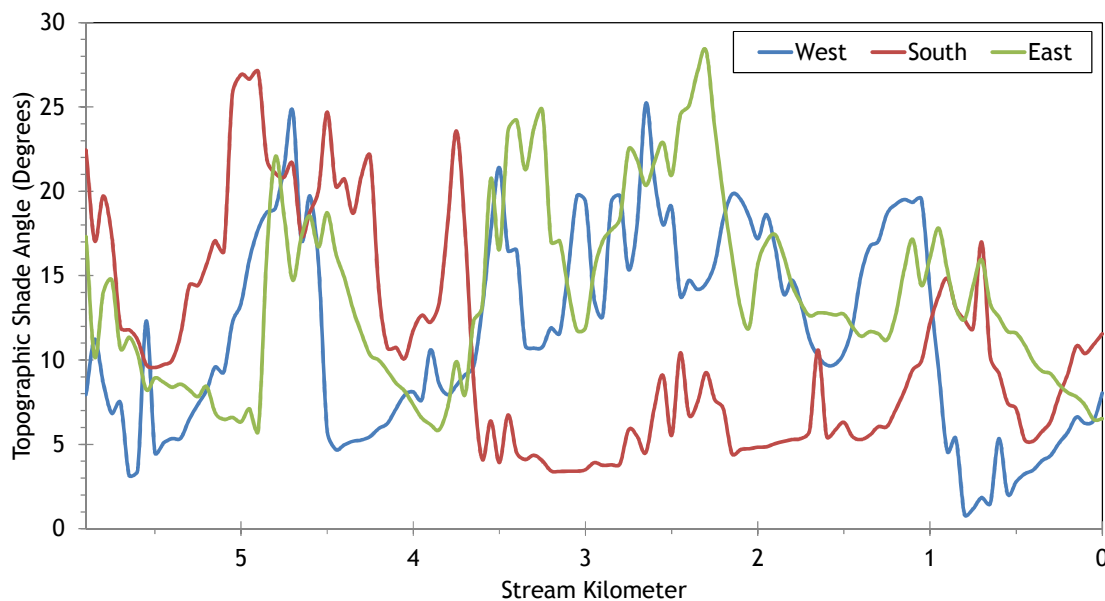
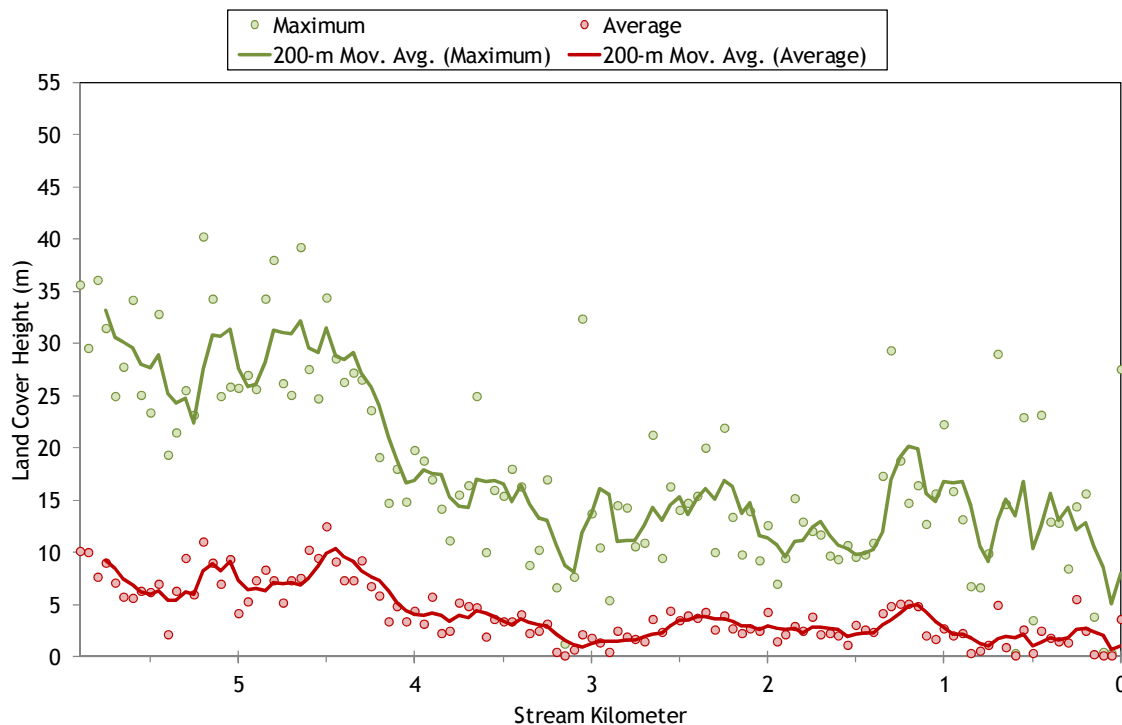


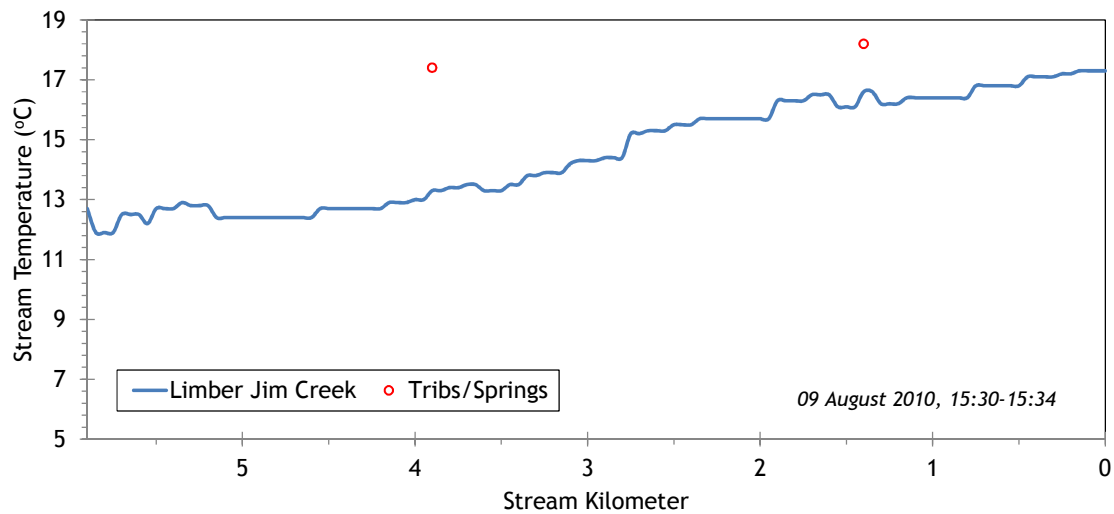
Figure 126 shows the land cover heights sampled along Limber Jim Creek. The maximum and average of the 28 radial samples were calculated for each 50-meter stream node. (Note: Heat Source uses each of the 28 radial samples for each 50-meter node. The maximum and average are shown here for simplification purposes.)

Figure 126 - Limber Jim Creek land cover heights sampled from highest hit LiDAR.



Limber Jim Creek is a fairly cool mountain stream relative to others in the basin (Figure 127). The TIR stream temperature profile shows a steady increase within the lower 6.5 kilometers.

Figure 127 - Limber Jim TIR stream temperature profile.



13.2 Limber Jim Creek Heat Source Calibration Results

The lower 5.9 stream kilometers of Limber Jim Creek were simulated for temperature. Figure 128 shows the simulation extent and hourly temperature data sites.

Figure 128 - Limber Jim Creek simulation extent.

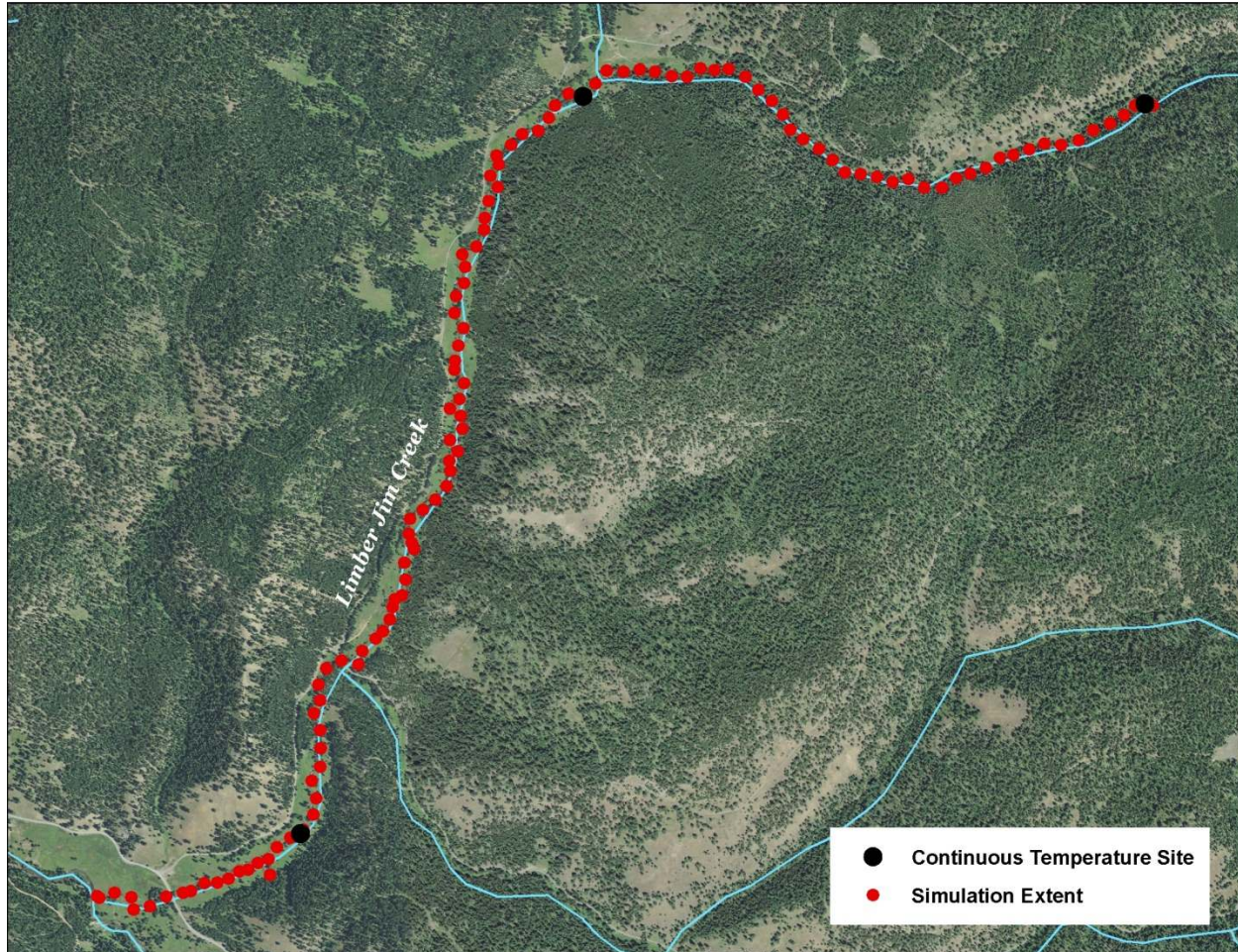


Table 19 - Limber Jim Creek general Heat Source parameters.

Stream:	Limber Jim Creek
Length:	5.9 kilometers
Time Period:	August 6-27, 2010
Input Distance Step:	50 meters
Output Distance Step:	100 meters
Time Step:	1 minute
Flush Initial Condition:	7 days
TIR Date and Time:	August 8, 2010 15:30-15:34
Land Cover Data Source:	LiDAR
Land Cover Sampling Distance Step:	10 meters

The following assumptions were used when calibrating the Limber Jim Creek Heat Source model:

- Hourly climate data was obtained from the J Ridge RAWS (USFS) site. Air temperature was adjusted using the adiabatic lapse rate of 1°C per 100 meters elevation.
- Wetted widths were digitized from the remote sensing imagery and then had to be reduced in some reaches in order to accommodate the stream hydraulics and measured data.
- Daily flow values were extrapolated from the Grande Ronde River gage data.

Figure 129 displays the simulated and measured hydraulic values for Limber Jim Creek for August 14, 2010. The ground-level data was collected at three locations, including the upstream boundary of the model extent.

Figure 129 - Limber Jim Creek simulated and measured hydraulic values.

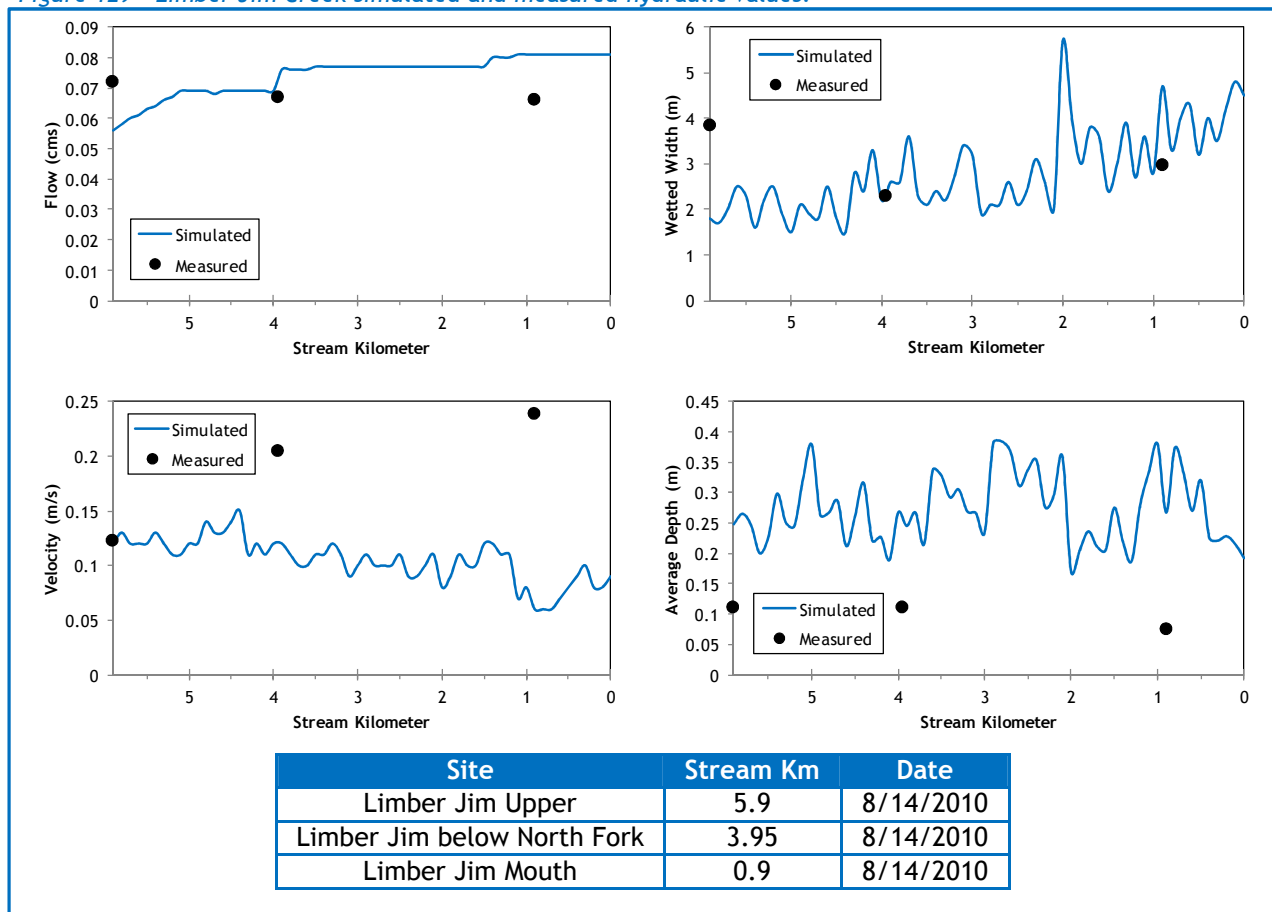
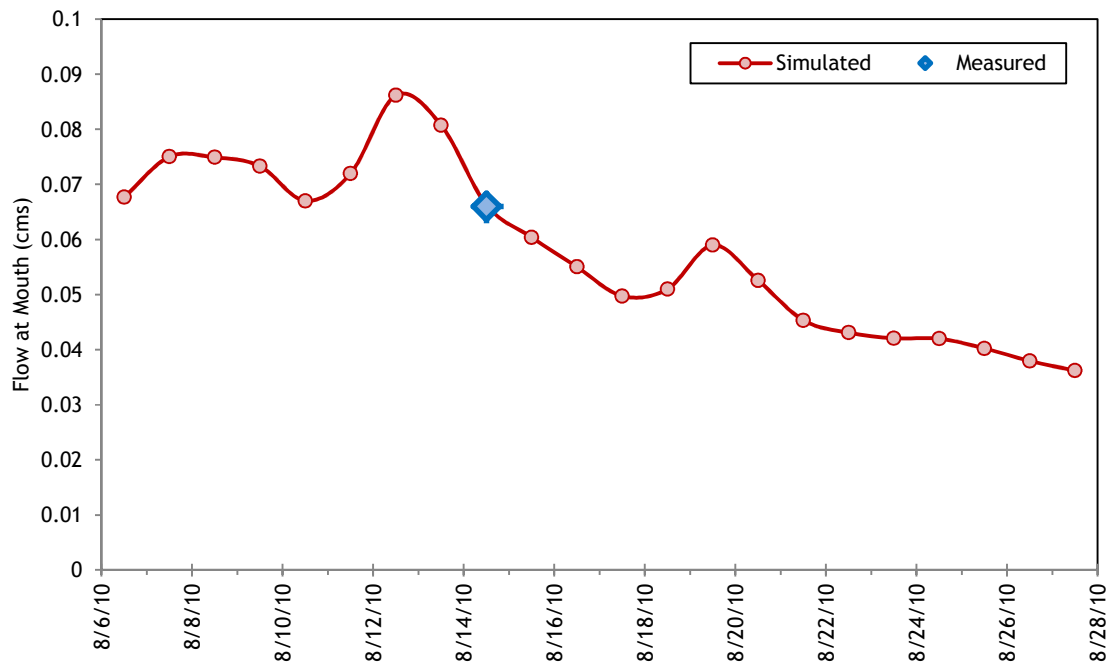


Figure 130 displays the simulated daily flow volumes at the mouth of Limber Jim Creek. The values were extrapolated from gage data on the Grande Ronde River, assuming that each stream in the watershed exhibited similar degrees of daily variability.

Figure 130 - Limber Jim Creek simulated flows at the mouth.



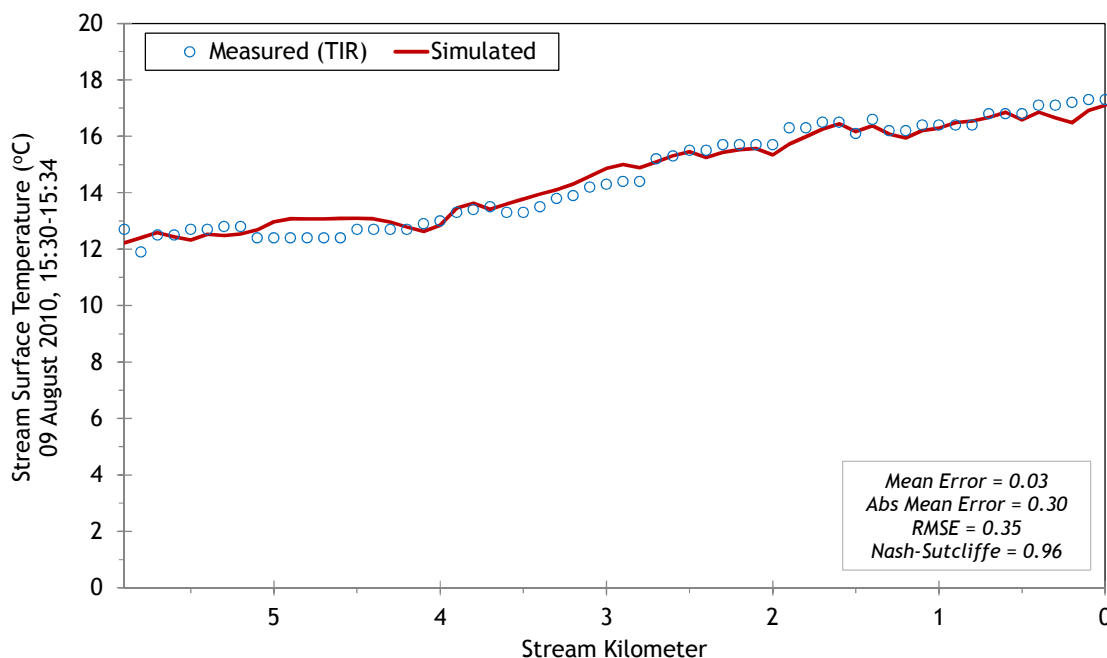
There were two tributaries observed in the TIR data (Table 20). Their daily flow volumes were estimated and daily variability was extrapolated from gage data on the Grande Ronde River. Overall, the tributaries were estimated to be much smaller than the mainstem Limber Jim Creek; therefore their flow estimates were small and temperatures were included as constants.

Table 20 - Limber Jim Creek mass inflow features and assumptions.

Feature	Stream Km	Assumptions
North Fork Limber Jim Cr.	3.9	0.004-0.009 cms at 17.4°C
South Fork Limber Jim Cr.	1.4	0.002-0.004 cms at 18.2°C

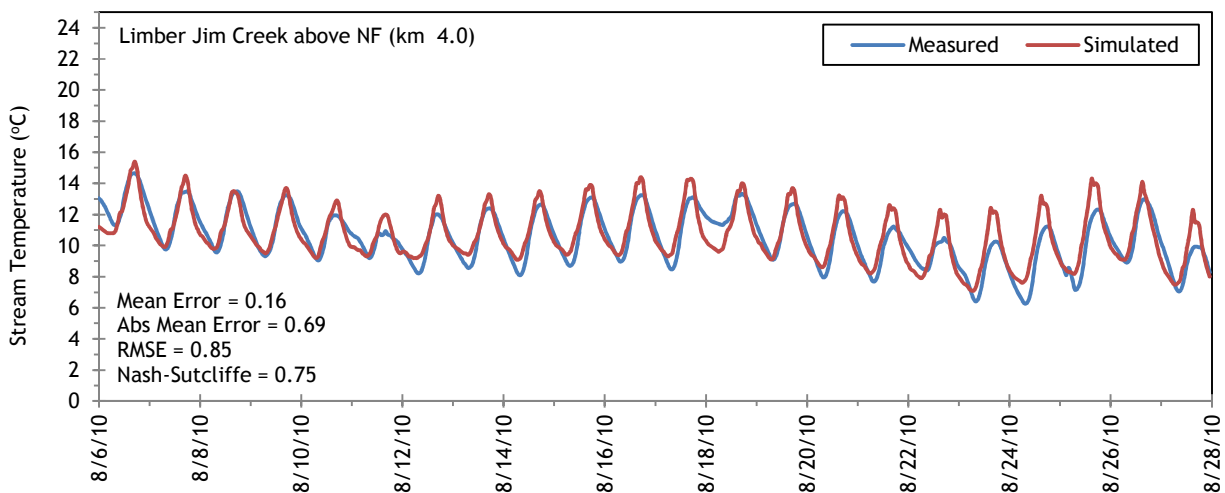
The simulated and measured longitudinal stream temperatures for Limber Jim Creek are shown in Figure 131. The stream gradually heated approximately 5°C in its lower six kilometers at the time that the TIR data was collected

Figure 131 - Limber Jim Creek simulated and measured longitudinal stream temperatures.



Simulated and measured hourly stream temperatures are presented in Figure 132. Calibration statistics are also shown in each plot.

Figure 132 - Limber Jim Creek simulated and measured hourly stream temperatures.



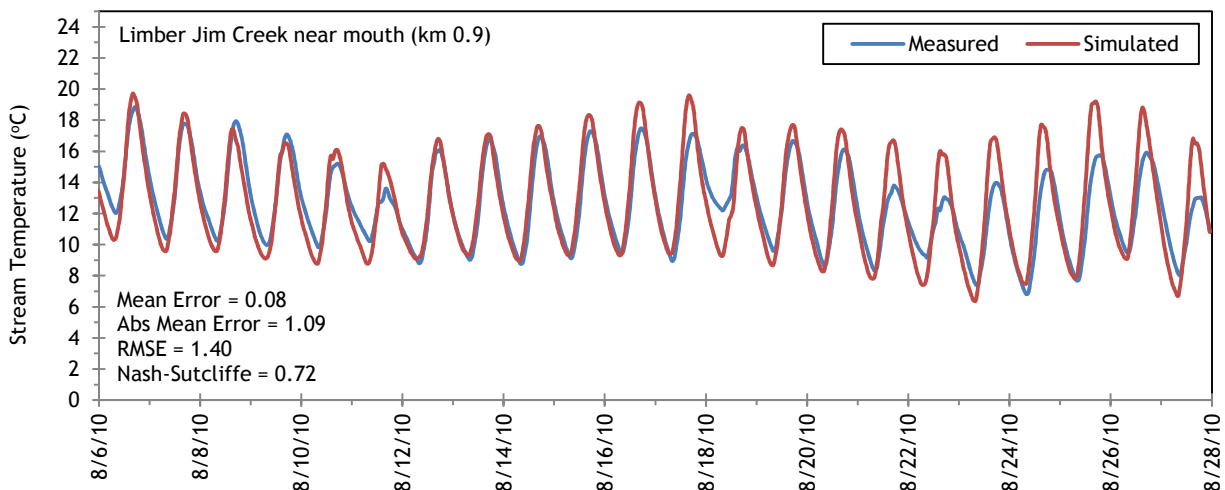
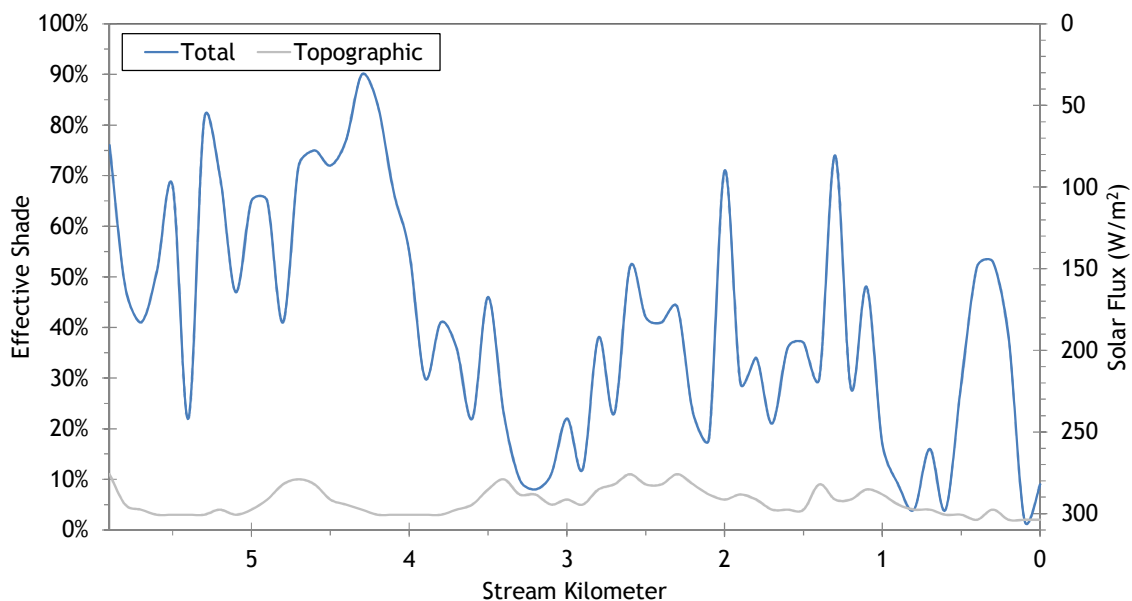


Figure 133 shows the simulated effective shade values for Limber Jim Creek. Between stream kilometer 4 and the mouth, there is less effective shade because the stream is flowing through a meadow-forest complex. Topographic shade is generally less than 10%.

Figure 133 - Limber Jim Creek simulated effective shade.



14. CHICKEN CREEK

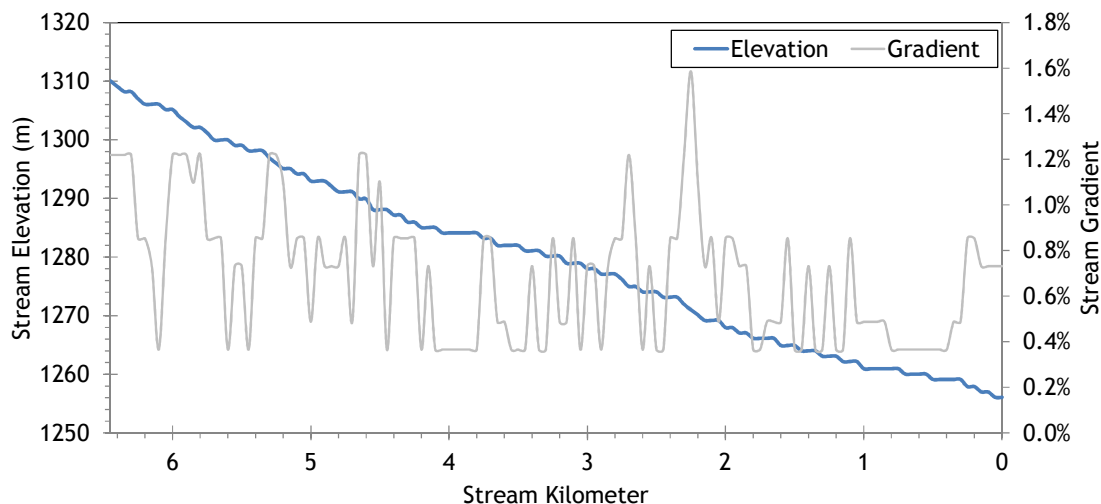


RGB-colored LiDAR point cloud - Chicken Creek (flowing from bottom of image) at confluence with Sheep Creek.

14.1 Chicken Creek TTools Results

Chicken Creek elevations and gradients are shown in Figure 134. The values were sampled from the 10-meter DEM because there LiDAR data was only available for a short reach near the mouth. Of the sampled reach, gradients were usually less than 1%.

Figure 134 - Chicken Creek elevation and gradient.



Stream aspects for every 50 meters of Chicken Creek are shown in Figure 135. Chicken Creek generally flows northward until it reaches Sheep Creek; however there is significant small scale variation due to the meandering nature of the stream within the valley bottom.

Figure 135 - Chicken Creek stream aspect.

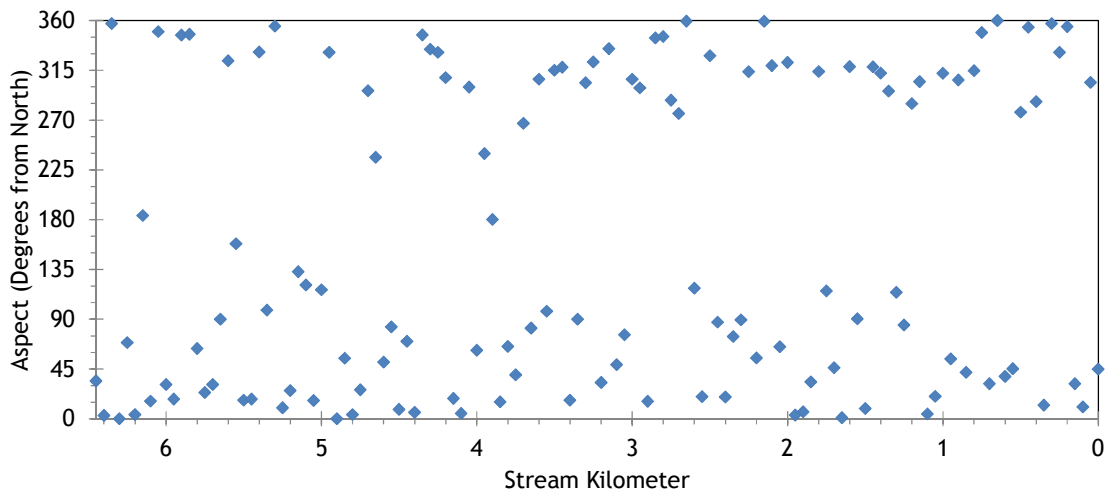
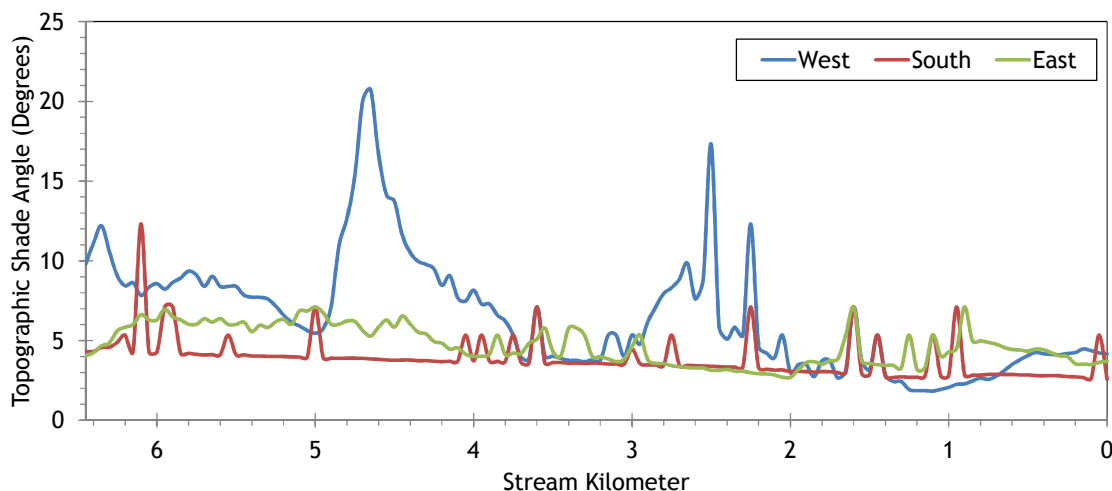


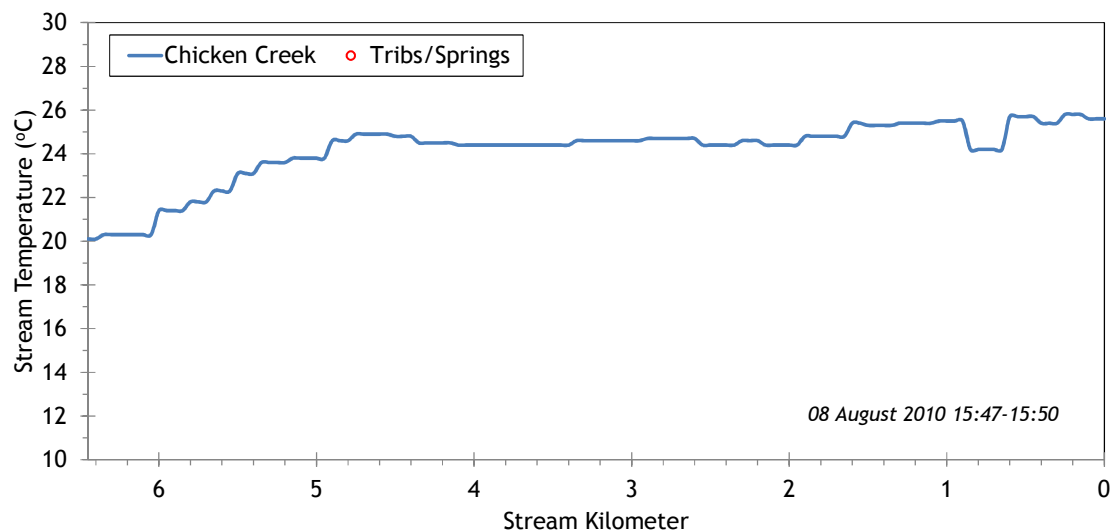
Figure 136 shows the topographic shade angles. Overall, topographic shade is minor because of the wide flat valley morphology through which this section of stream flows.

Figure 136 - Chicken Creek topographic shade angles.



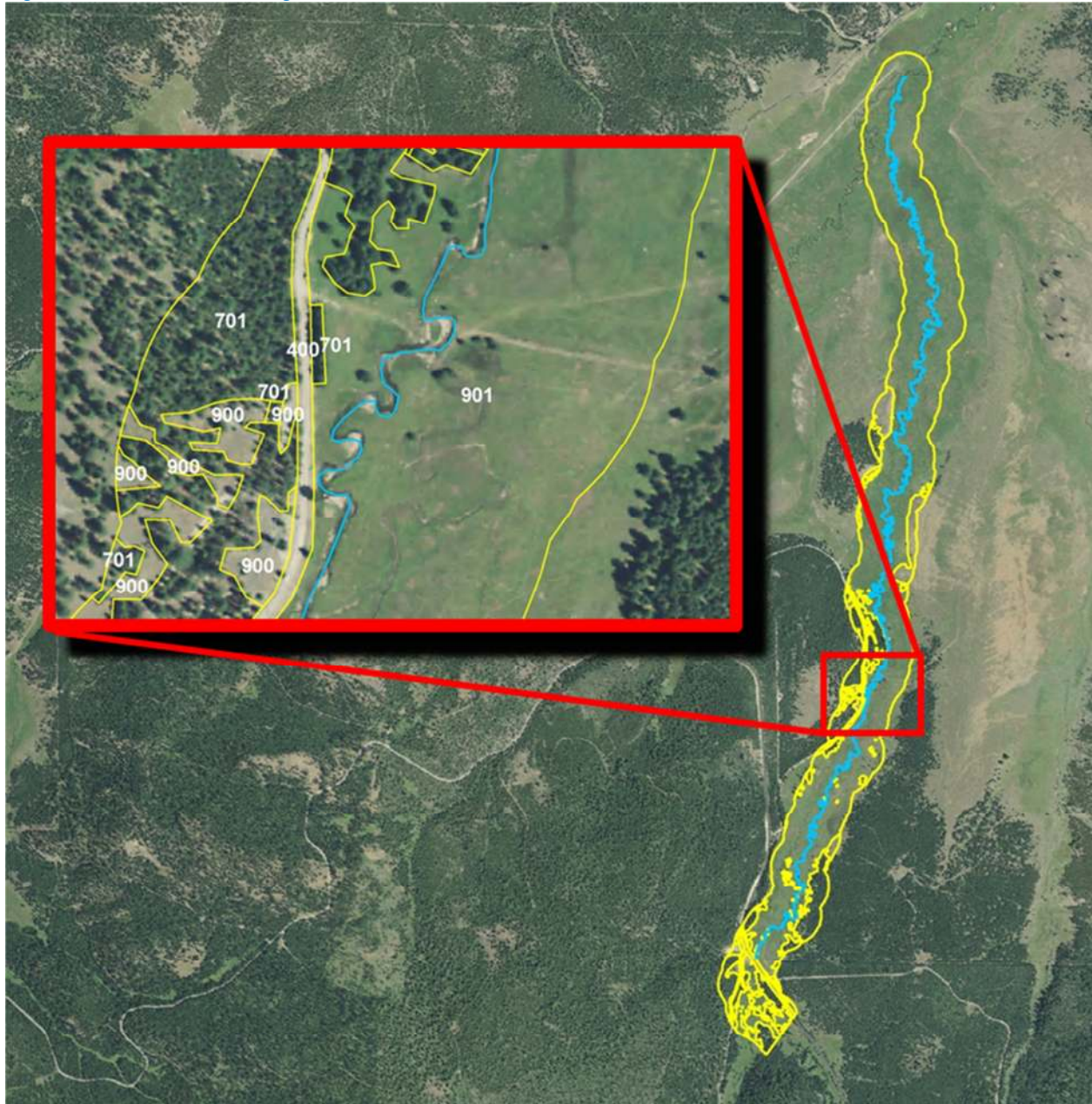
The Chicken Creek TIR stream temperature profile is shown in Figure 137. In this section of lower Chicken Creek, the temperatures were fairly warm and reached a maximum of about 25°C during the TIR flight.

Figure 137 - Chicken Creek TIR stream temperature profile.



LiDAR data was unavailable for Chicken Creek, so the near stream land cover was manually digitized within 100 meters of the stream using NAIP orthoimages (Figure 138). Most of the lower 6.5 kilometers of Chicken Creek flow through open grassy areas and has few trees.

Figure 138 - Chicken Creek digitized near stream land cover.



Chicken Creek land cover height estimates were derived from the LiDAR samples of Sheep Creek (Table 21). The 25th and 75th percentiles of values over 3 meters were calculated from the Sheep Creek TTools data. The 75th percentile was 14.1 meters, which was applied to tall tree classes for Chicken Creek. The 25th percentile was 6.3 meters, which was applied to the short tree classes for Chicken Creek.

Table 21 - Chicken Creek near stream land cover codes and descriptions.

Land Cover Name	Code	Height (m)	Density	Overhang (m)
Upland dry grasses	900	0.5	0.9	0.0
Lowland wet grasses	901	0.5	0.9	0.0
large conifer - dense	700	14.1	0.75	1.0
small conifer - dense	701	6.2	0.75	1.0
large conifer - sparse	750	14.1	0.25	1.0
small conifer - sparse	751	6.2	0.25	1.0
paved road	400	0	0	0
unpaved road	401	0	0	0
water	3011	0	0	0

14.2 Chicken Creek Heat Source Calibration Results

The lower 6.5 kilometers of Chicken Creek were simulated for temperature (Figure 139).

Figure 139 - Chicken Creek simulation extent.

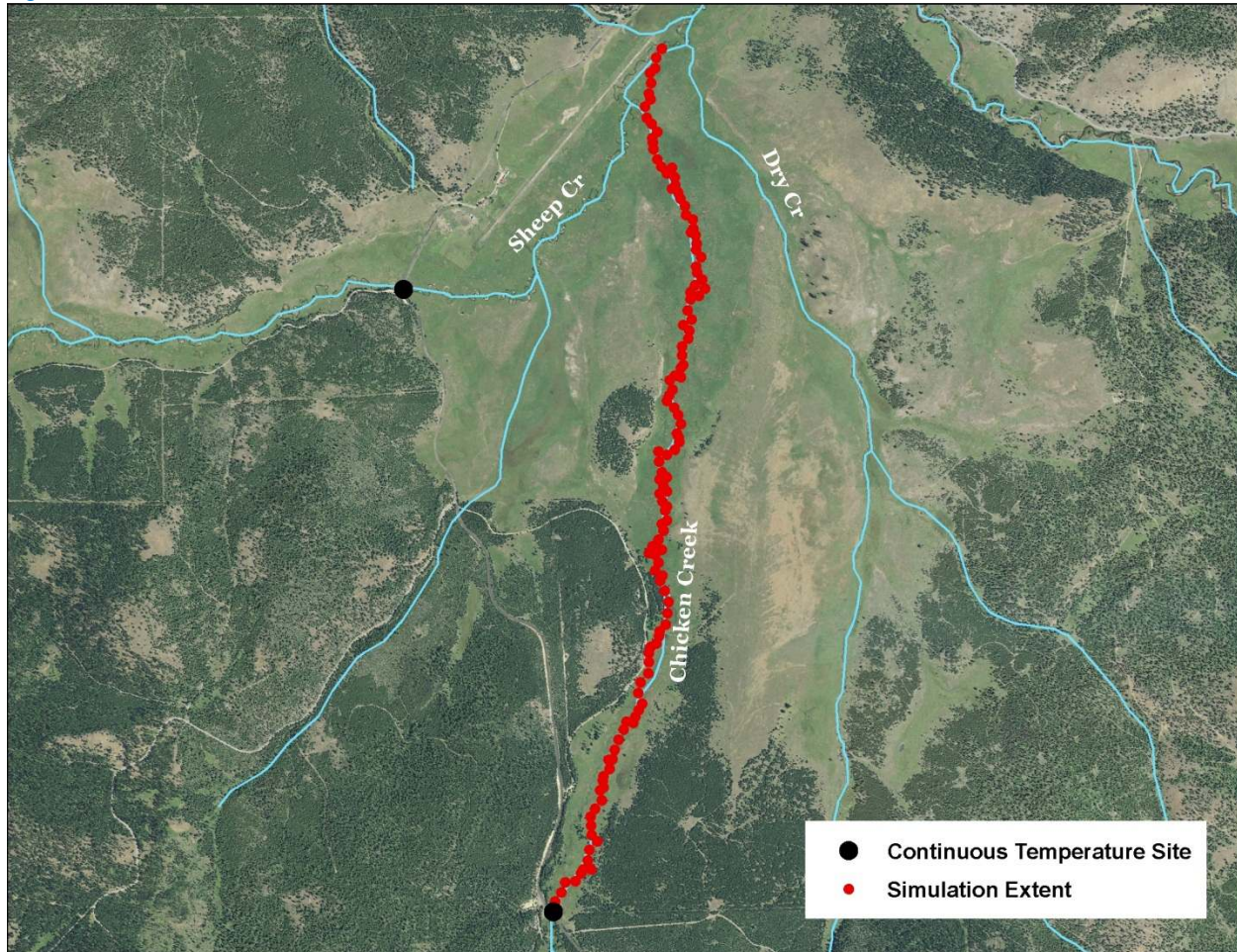


Table 22 - Chicken Creek general Heat Source parameters.

Stream:	Chicken Creek
Length:	6.5 kilometers
Time Period:	August 6-27, 2010
Input Distance Step:	50 meters
Output Distance Step:	100 meters
Time Step:	1 minute
Flush Initial Condition:	7 days
TIR Date and Time:	August 8, 2010 15:30-15:34
Land Cover Data Source:	Manually Digitized
Land Cover Sampling Distance Step:	15 meters

The following assumptions were used when calibrating the Chicken Creek Heat Source model:

- Hourly climate data was obtained from the J Ridge RAWS (USFS) site. Air temperature was adjusted using the adiabatic lapse rate of 1°C per 100 meters elevation.
- The stream was too small to digitize the banks from the remote sensing imagery. Several measurements were made from the NAIP images and the in-between values were interpolated for each 50-meter model node.
- Daily flow variability was extrapolated from Grande Ronde River gage data.
- The only available hourly temperature data was for the upstream boundary condition, therefore there is no hourly calibration validation. This model is calibrated strictly to the TIR data, which increases the uncertainty associated with it.
- Since there was no LiDAR available, the near stream land cover was digitized within a 100-meter buffer of the stream. Height estimates were applied based on values observed in the LiDAR data along other streams in the vicinity.

Figure 140 shows the simulated hydraulic parameters for Chicken Creek for August 19, 2010. There were no available ground level data for the lower 6.5 kilometers, except for the boundary condition.

Figure 140 - Chicken Creek simulated hydraulic values.

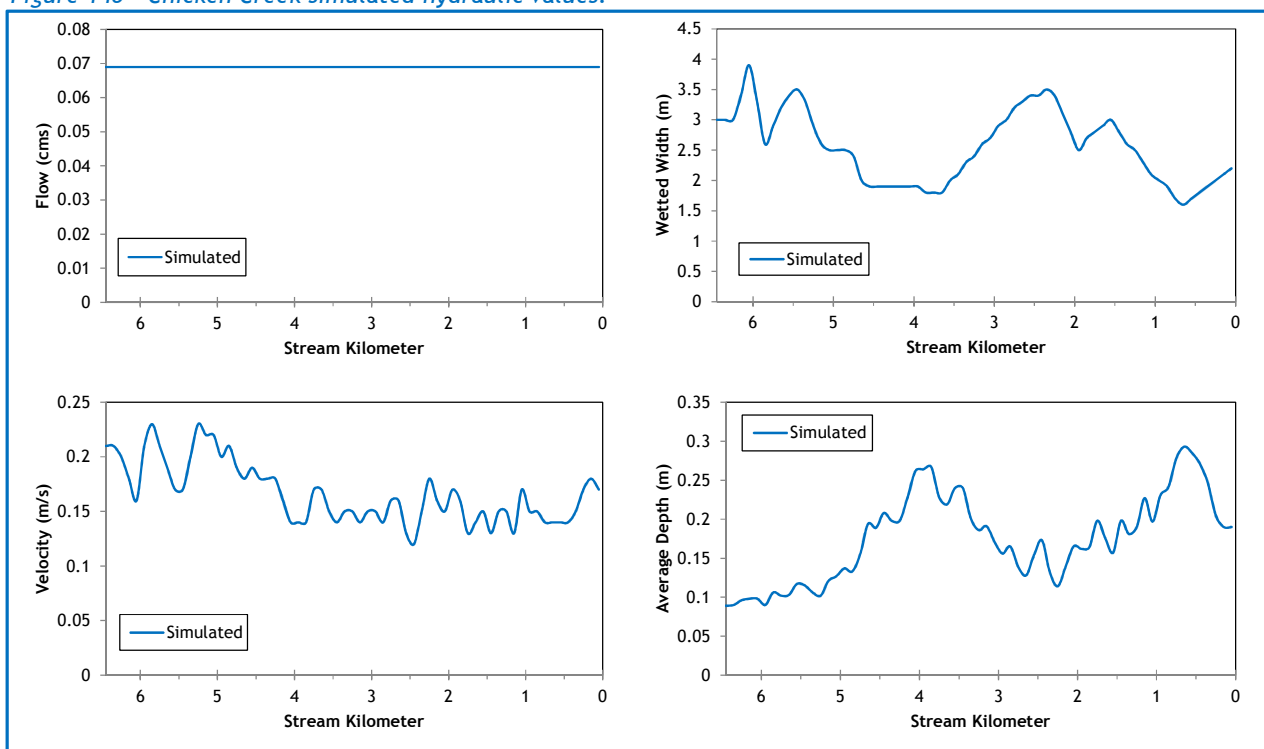
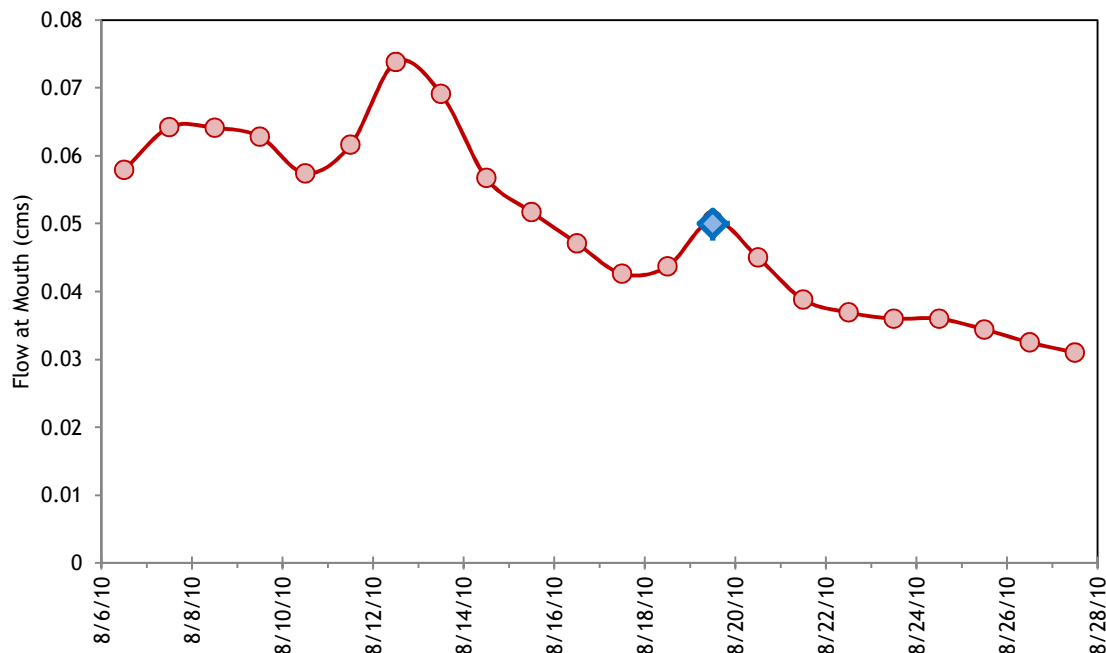


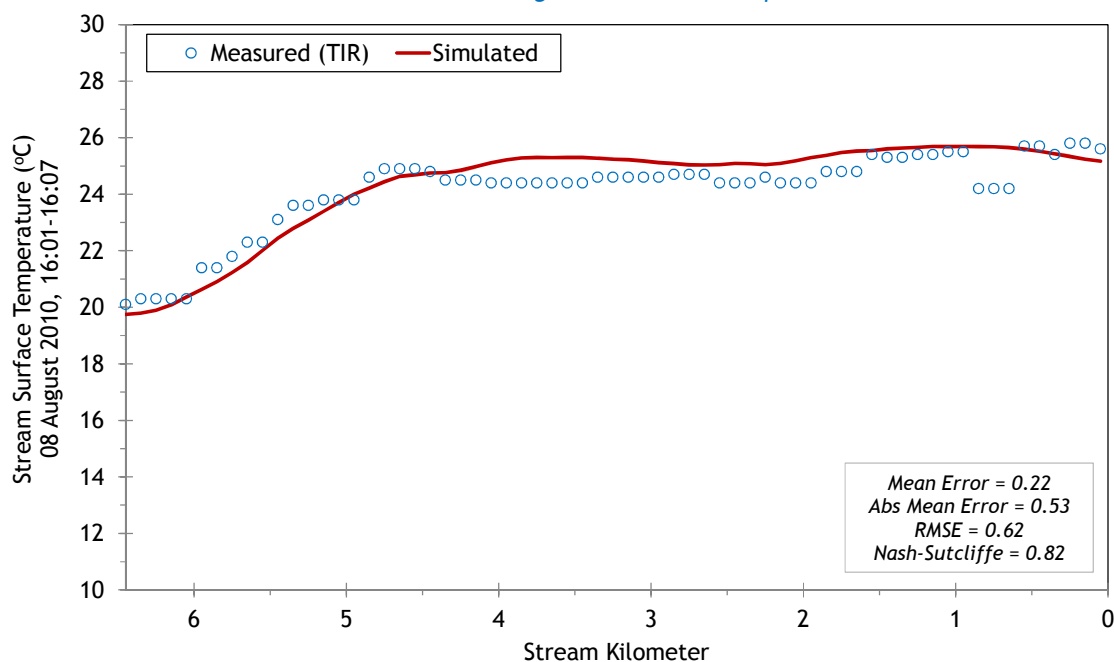
Figure 141 shows the simulated flows at the mouth of Chicken Creek. Since there were no tributaries or diversions, this is also the flow for the entire simulation length. The values were extrapolated through back-calculations from Sheep Creek. The measured flow on August 19, 2010 below the forks was 0.05 cms (1.8 cfs).

Figure 141 - Chicken Creek simulated flow volumes at the mouth.



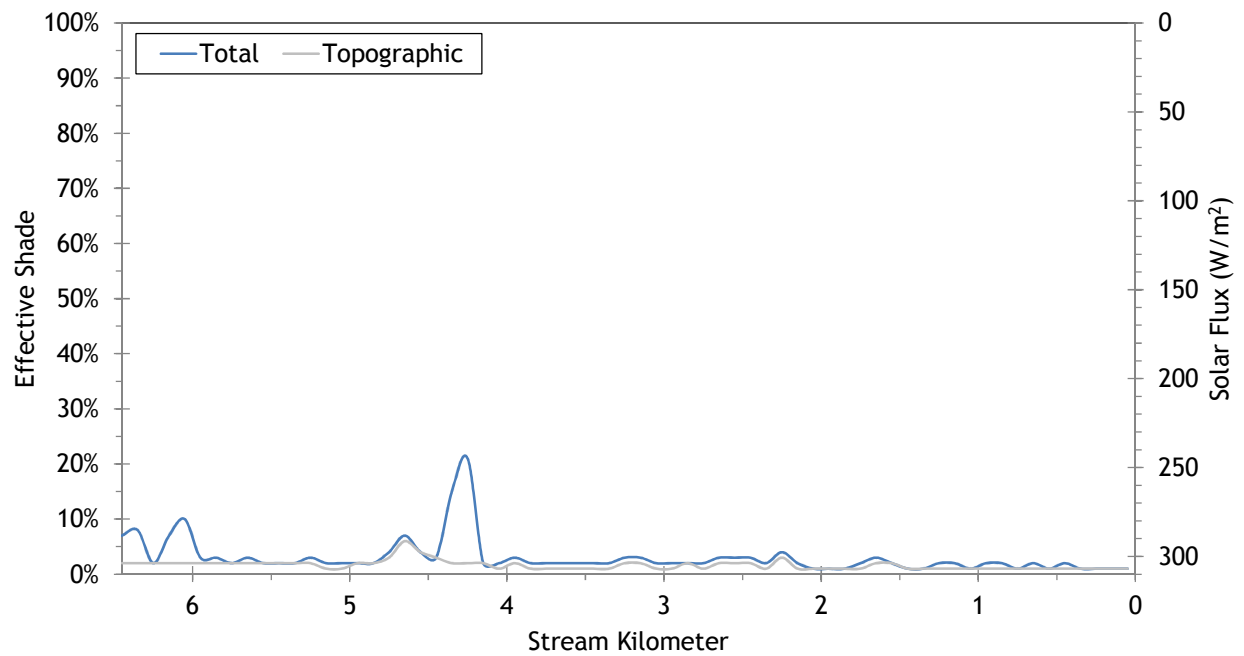
The simulated and measure longitudinal temperatures for Chicken Creek are presented in Figure 142. It appears that the stream heated more rapidly once it entered the open meadow, and then reached a maximum temperature of approximately 25°C until the mouth.

Figure 142 - Chicken Creek simulated and measured longitudinal stream temperatures.



The lower 6.5 kilometers of Chicken Creek flow through mostly open meadow and hence there is very little effective shade (Figure 143).

Figure 143 - Chicken Creek simulated effective shade.



15. SHEEP CREEK

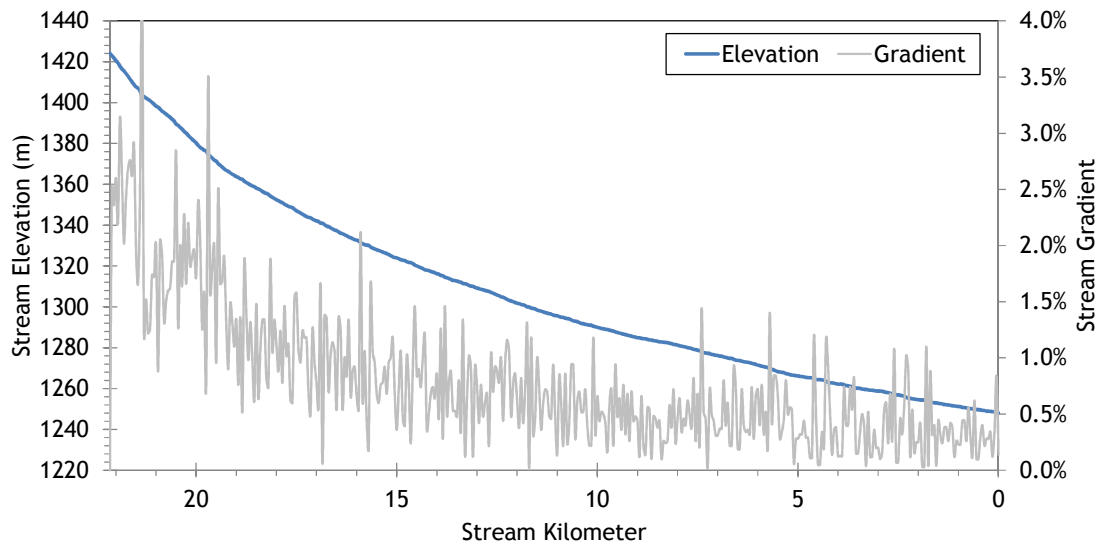


RGB-colored LiDAR point cloud - Sheep Creek downstream of East Sheep Creek (looking upstream).

15.1 Sheep Creek TTools Results

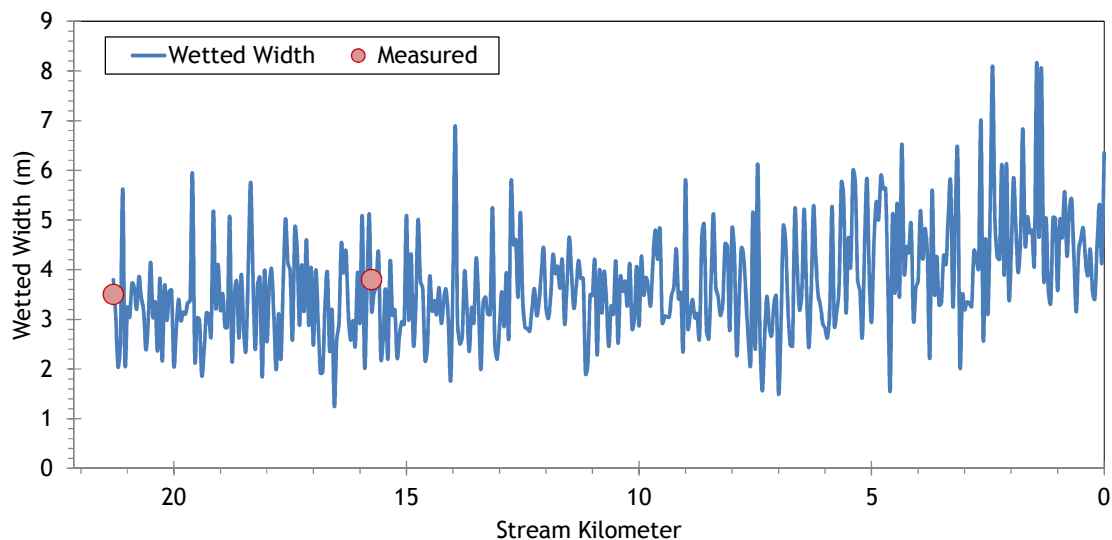
Sheep Creek elevations and gradients were sampled from the bare earth LiDAR data (Figure 144). The stream is steeper in the upper 7 kilometers, while the lower 15 kilometers meander more through a less confined valley.

Figure 144 - Sheep Creek elevation and gradient.



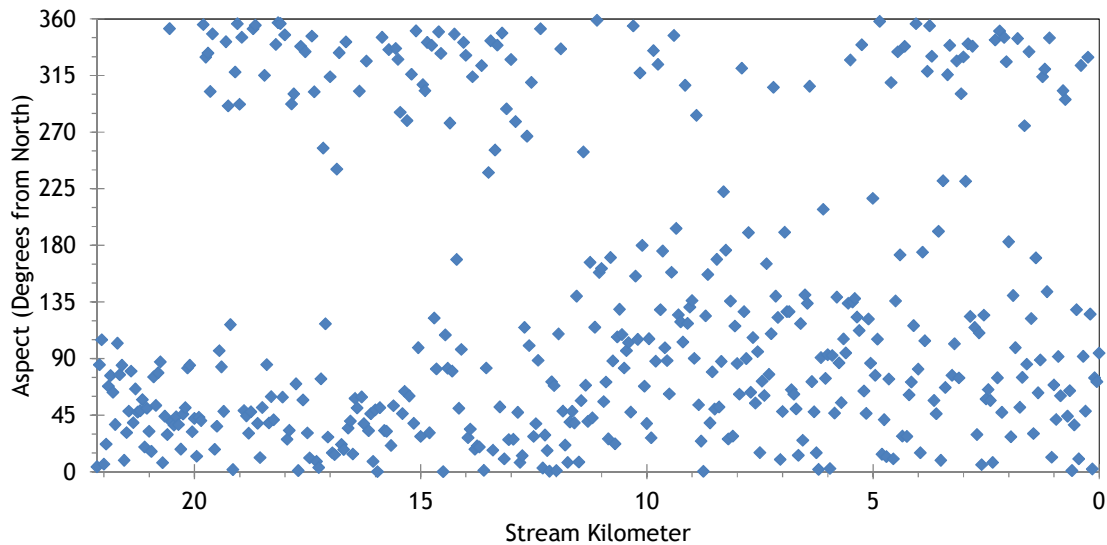
Sheep Creek wetted widths were digitized from the LiDAR intensity, TIR, and NAIP images. Figure 145 shows the sampled and measured values. Sheep Creek is a small stream, with wetted widths between about 3 and 5 meters on average during the simulation time period.

Figure 145 - Sheep Creek wetted widths.



The stream aspect for every 50 meters of Sheep Creek is presented in Figure 146. The stream is oriented northeasterly.

Figure 146 - Sheep Creek stream aspect.



Topographic shade angles for Sheep Creek are shown in Figure 147. There is a moderate amount of topographic shade produced by surrounding mountains.

Figure 147 - Sheep Creek topographic shade angles.

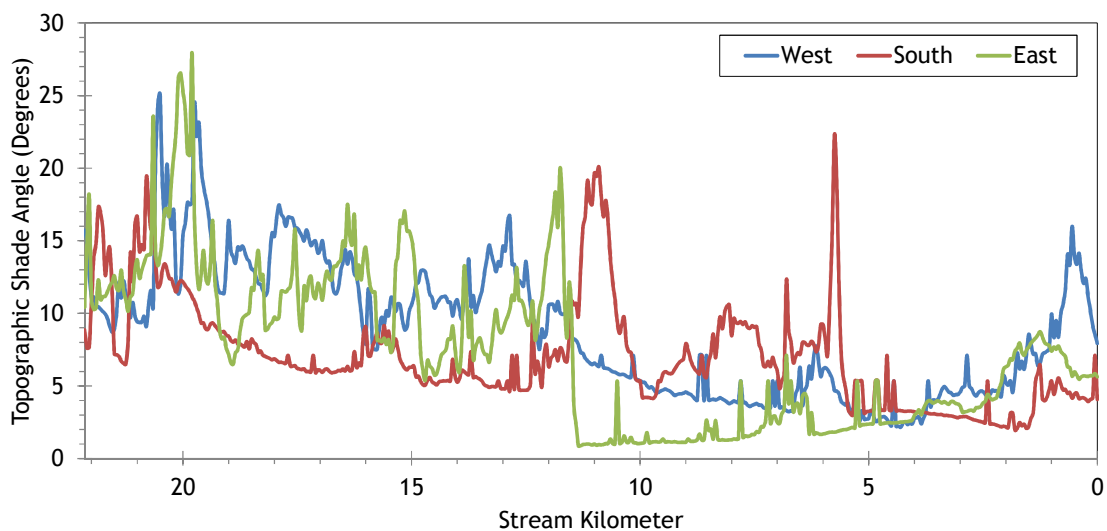
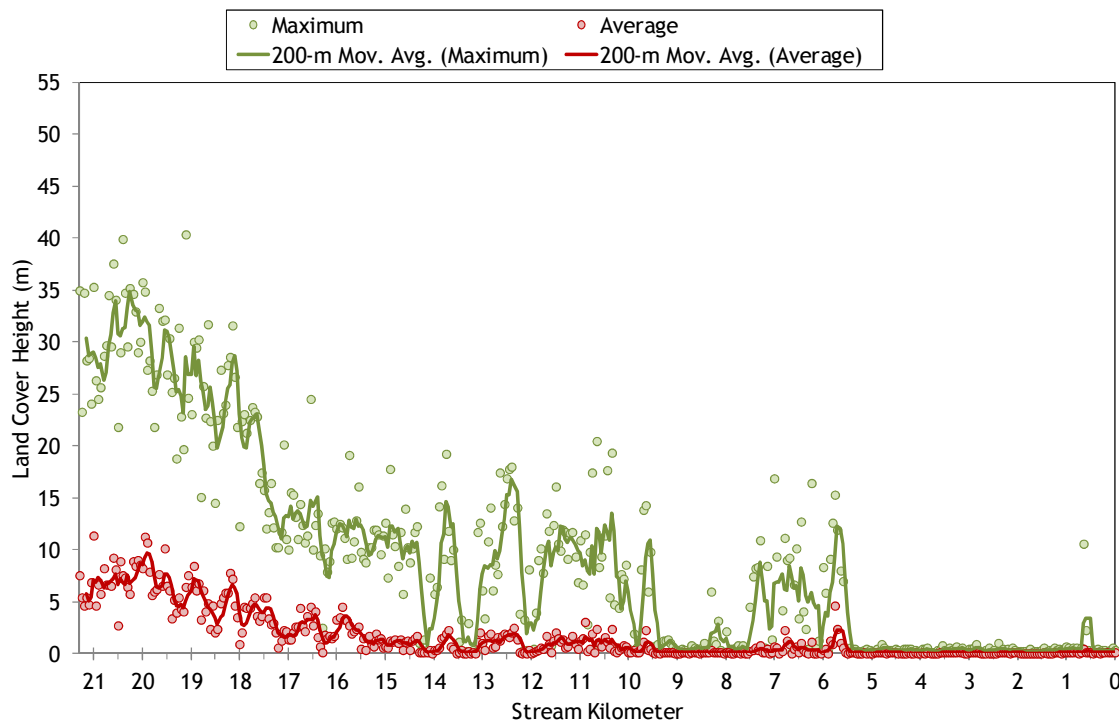


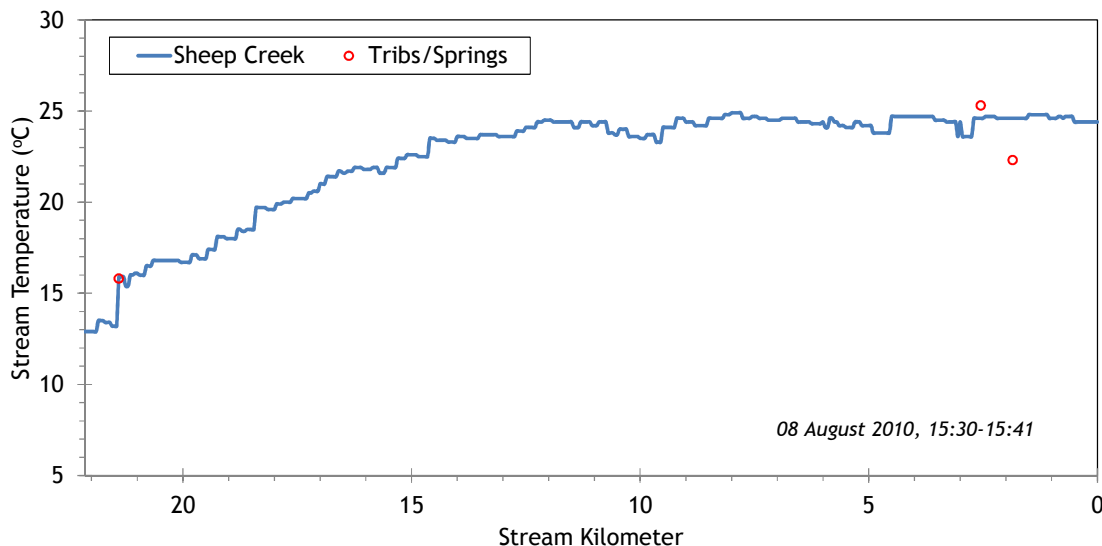
Figure 148 shows the land cover heights sampled along Sheep Creek. The maximum and average of the 28 radial samples were calculated for each 50-meter stream node. (Note: Heat Source uses each of the 28 radial samples for each 50-meter node. The maximum and average are shown here for simplification purposes.)

Figure 148 - Sheep Creek land cover heights sampled from highest hit LiDAR.



The TIR stream temperature profile of Sheep Creek is presented in Figure 149. The stream gained about 10°C between kilometers 20 and 14, and then remained around 25°C until the mouth during the TIR flight.

Figure 149 - Sheep Creek TIR stream temperature profile.



15.2 Sheep Creek Heat Source Calibration Results

Sheep Creek was simulated from East Sheep Creek to the mouth (Figure 150).

Figure 150 - Sheep Creek simulation extent.

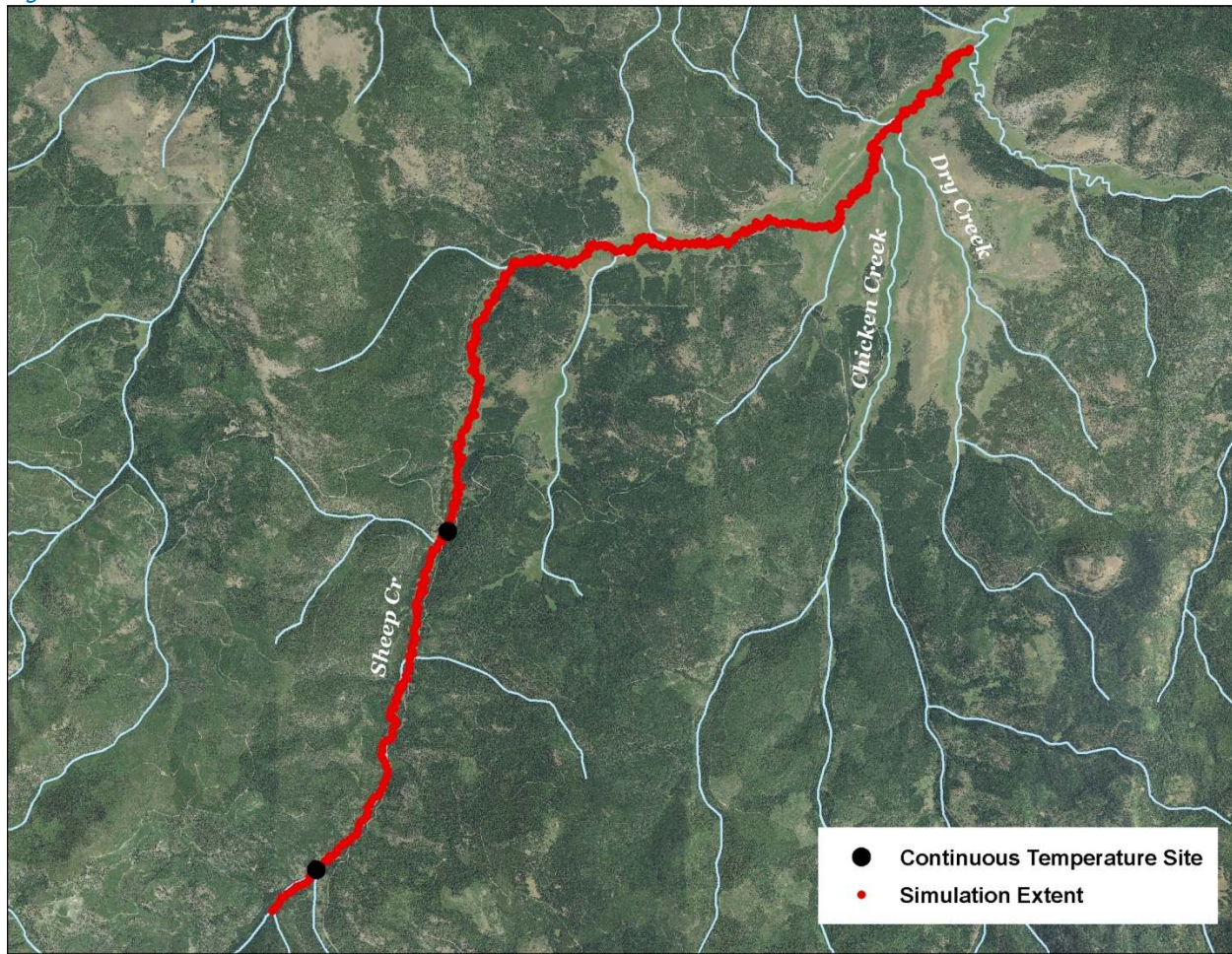


Table 23 - Sheep Creek general Heat Source parameters.

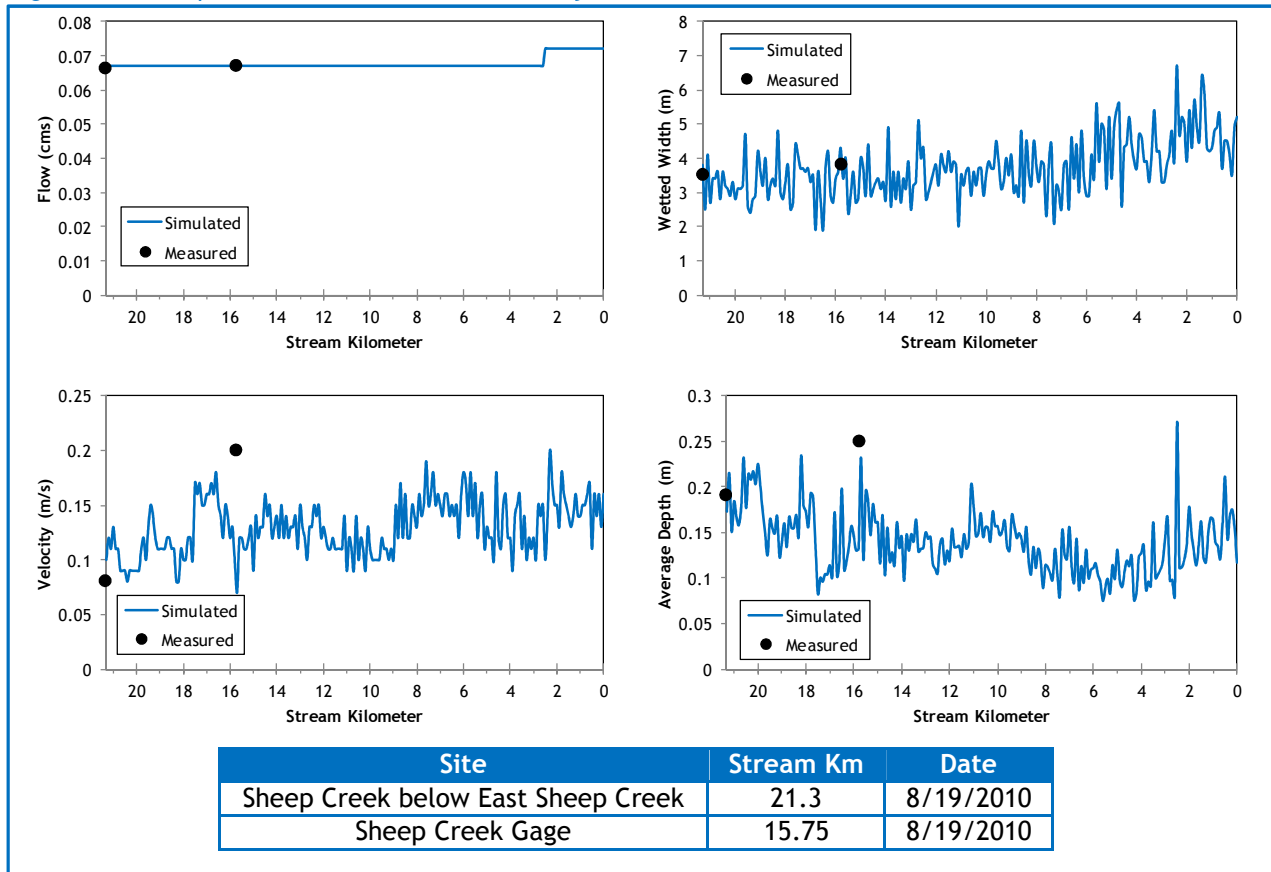
Stream:	Sheep Creek
Length:	21.3 kilometers
Time Period:	August 6-27, 2010
Input Distance Step:	50 meters
Output Distance Step:	100 meters
Time Step:	1 minute
Flush Initial Condition:	7 days
TIR Date and Time:	August 8, 2010 15:29-15:40
Land Cover Data Source:	LiDAR
Land Cover Sampling Distance Step:	15 meters

The following assumptions were used when calibrating the Sheep Creek Heat model:

- Hourly climate data was obtained from the J Ridge RAWS (USFS) site. Air temperature was adjusted using the adiabatic lapse rate of 1°C per 100 meters elevation.
- Daily flow variability was extrapolated from Grande Ronde River gage data.

Figure 151 shows the simulated and measured hydraulic values for the calibrated Sheep Creek model. There were only two available ground level data points, one of which was at the upstream boundary of the model. The data are plotted for August 19, 2010 when the ground level measurements were taken.

Figure 151 - Sheep Creek simulated and measured hydraulic values.



The simulated daily flow volumes for the mouth of Sheep Creek are shown in Figure 152. Daily values were extrapolated based on gage data from the Grande Ronde River. No field measurements were recorded at the mouth of Sheep Creek; however measurements were taken in the upper reaches.

Figure 152 - Sheep Creek simulated flow volumes at the mouth.

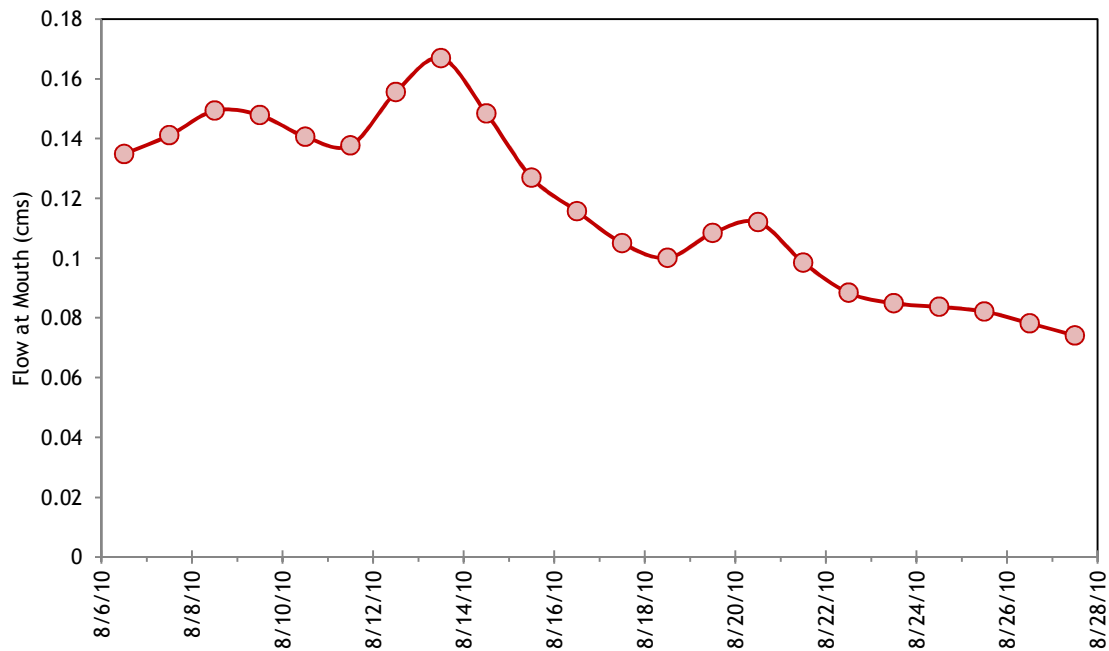


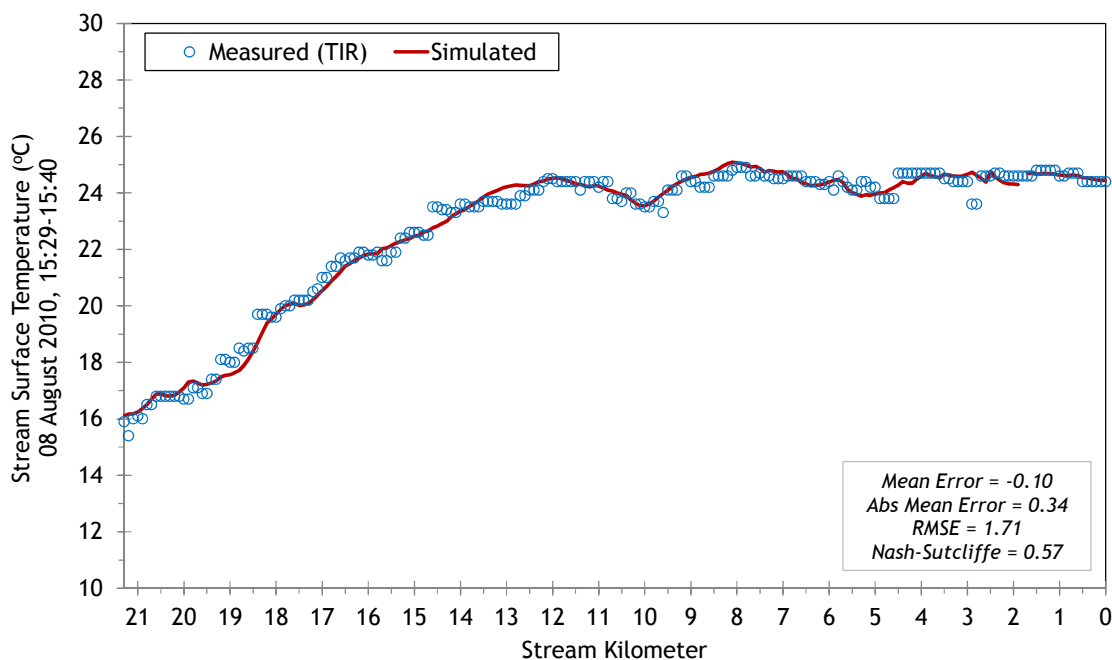
Table 24 summarizes the mass inflow input for the Sheep Creek model. There was only one significant tributary observed in the TIR data, which was Chicken Creek. There was no measured data available for Chicken Creek at the mouth, so the simulation outputs from the Chicken Creek model were used as inputs to the Sheep Creek model.

Table 24 - Chicken Creek mass inflow feature and assumption.

Feature	Stream Km	Assumptions
Chicken Creek	2.5	Used simulation outputs from Chicken Creek model as inputs to Sheep Creek model.

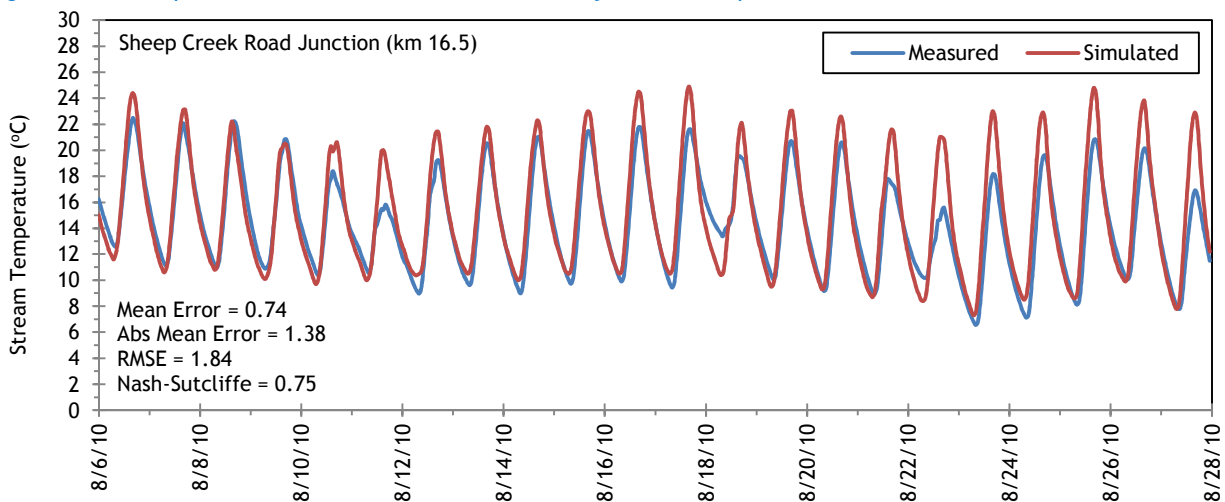
The simulated and measured longitudinal stream temperatures are shown in Figure 144. Validation statistics are also included within the plot.

Figure 153 - Sheep Creek simulated and measured longitudinal stream temperatures.



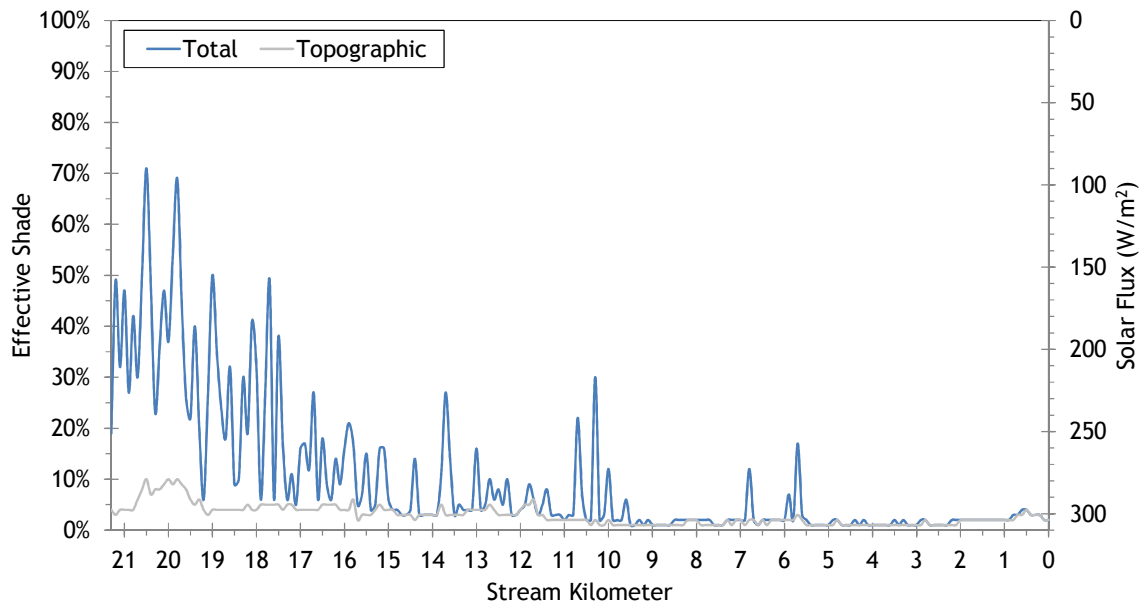
There was one site where measured hourly temperature data was available (stream kilometer 16.5). Figure 154 compares the measured and simulated hourly temperatures at that site. Validation statistics are also included in the figure.

Figure 154 - Sheep Creek simulated and measured hourly stream temperatures.

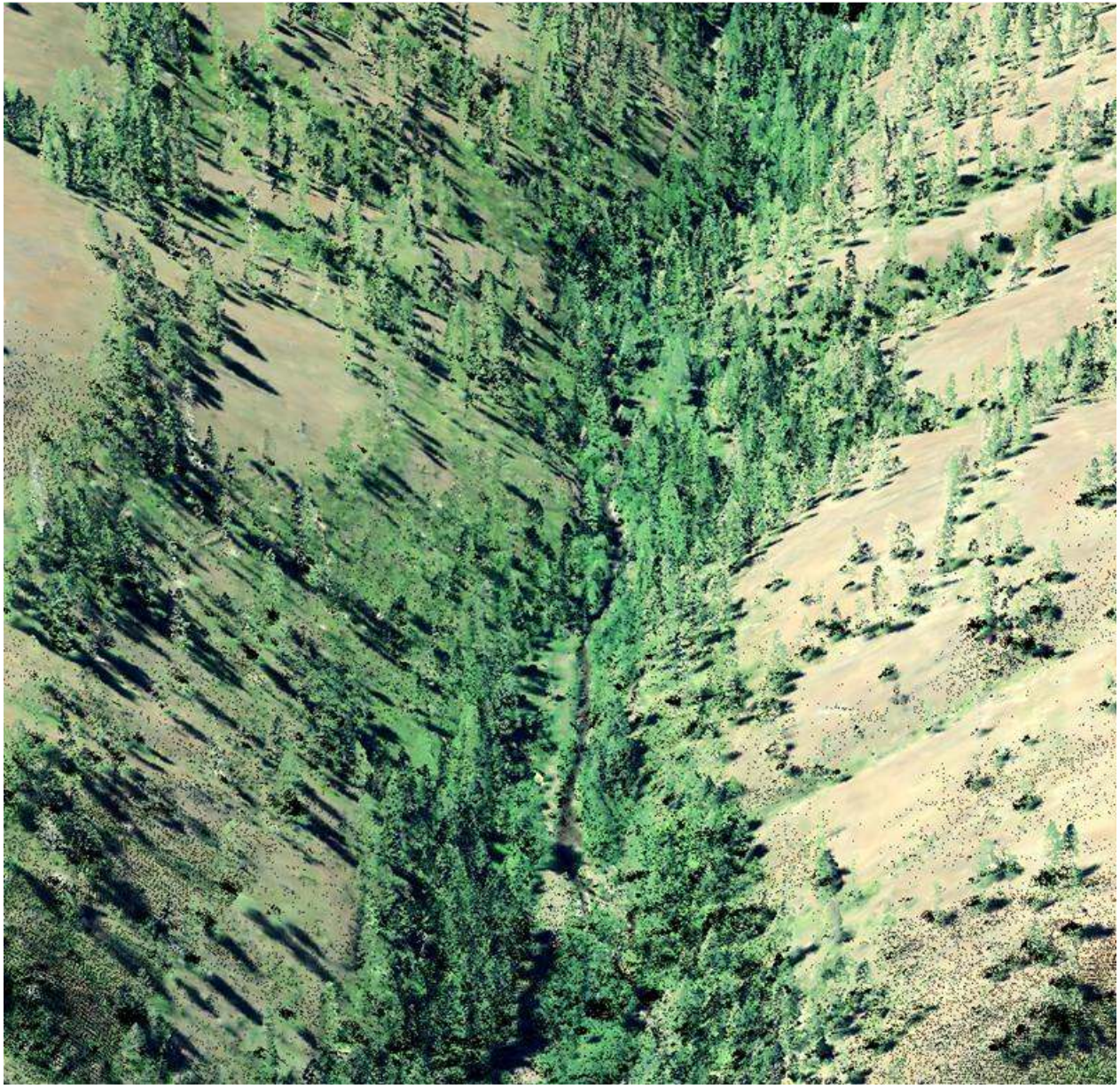


Simulated effective shade values are shown in Figure 155. Sheep Creek flows from more forested areas into wide open valley bottom meadows, so effective shade decreases in the lower reaches where there are very few trees.

Figure 155 - Sheep Creek simulated effective shade.



16. FLY CREEK

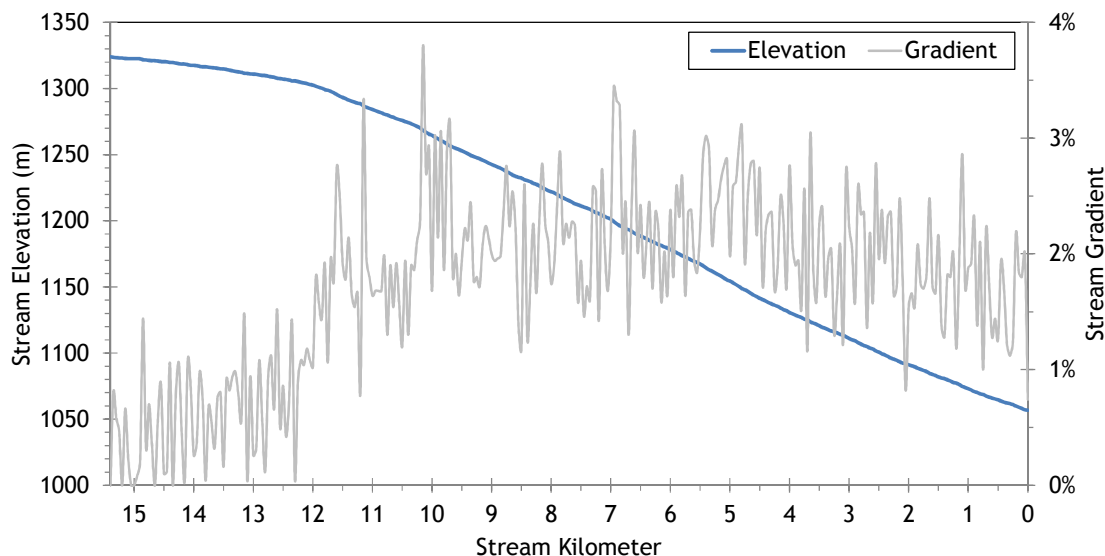


RGB-colored LiDAR point cloud - Fly Creek just above mouth (looking upstream).

16.1 Fly Creek TTools Results

Fly Creek elevations and gradients are shown in Figure 156. The upper 4 kilometers flow through a low-gradient meadow. Then the stream enters steeper and more confined valley terrain, so the gradients are higher in the lower 12 kilometers.

Figure 156 - Fly Creek elevation and gradient.



The wetted widths for Fly Creek were digitized from the LiDAR intensity, TIR, and NAIP imagery. Figure 157 shows the sampled and measured wetted widths. Overall, Fly Creek is a small stream with widths between about 3 and 5 meters.

Figure 157 - Fly Creek wetted widths.

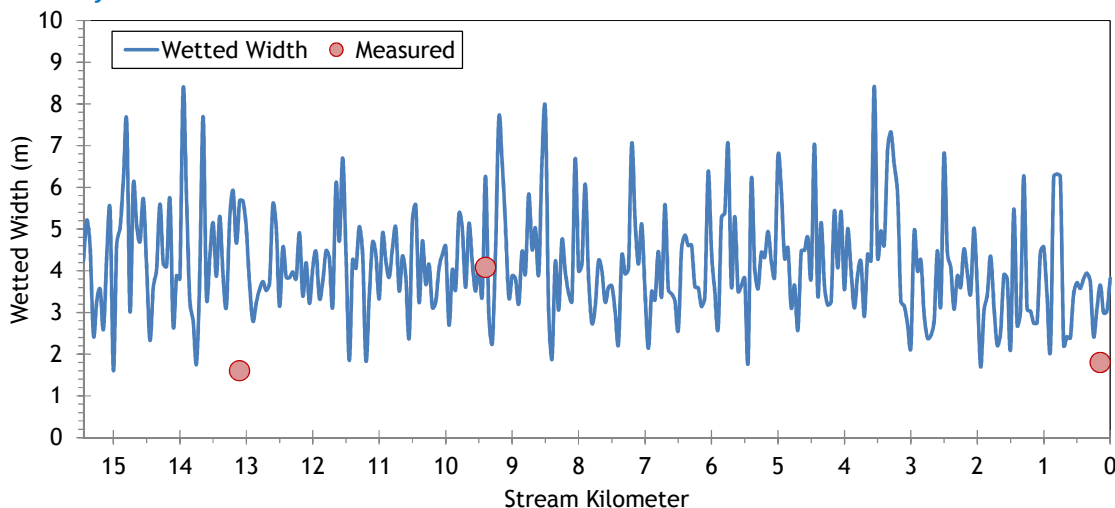
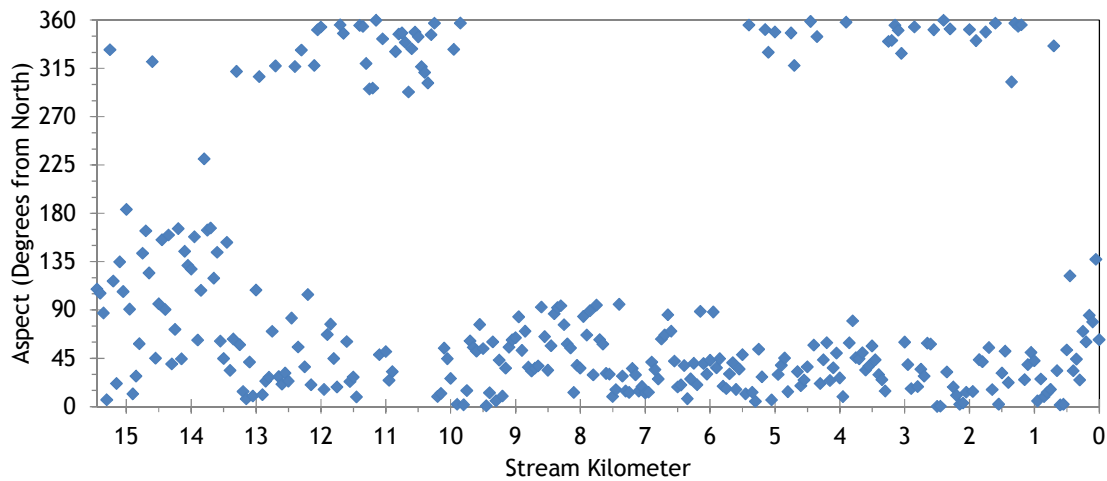


Figure 158 shows the stream aspect for every 50 meters of Fly Creek. The stream generally flows toward the northeast.

Figure 158 - Fly Creek stream aspect.



Fly Creek topographic shade angles are shown in Figure 159. The values for Fly Creek are relatively large, reaching up to 30 degrees in many locations.

Figure 159 - Fly Creek topographic shade angles.

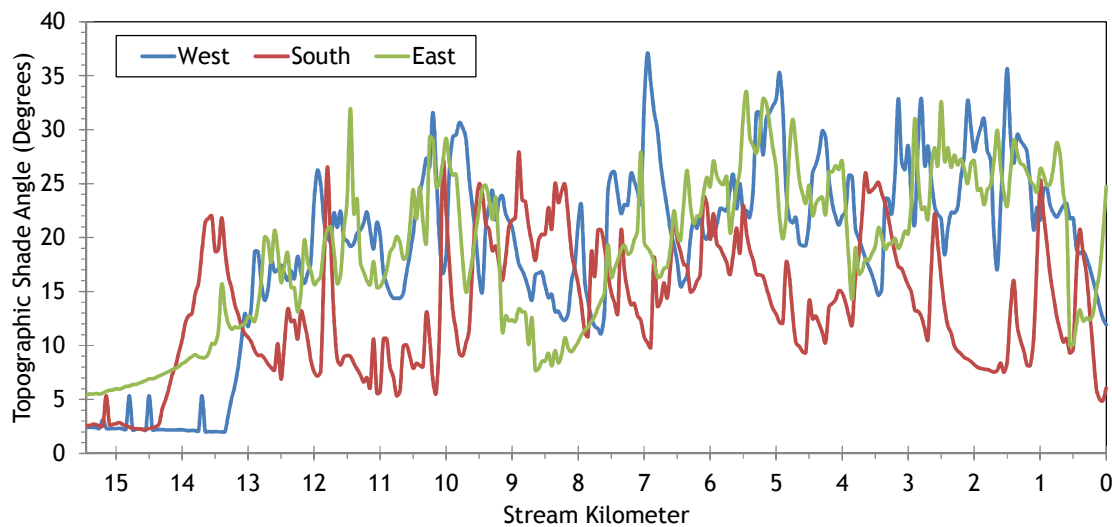
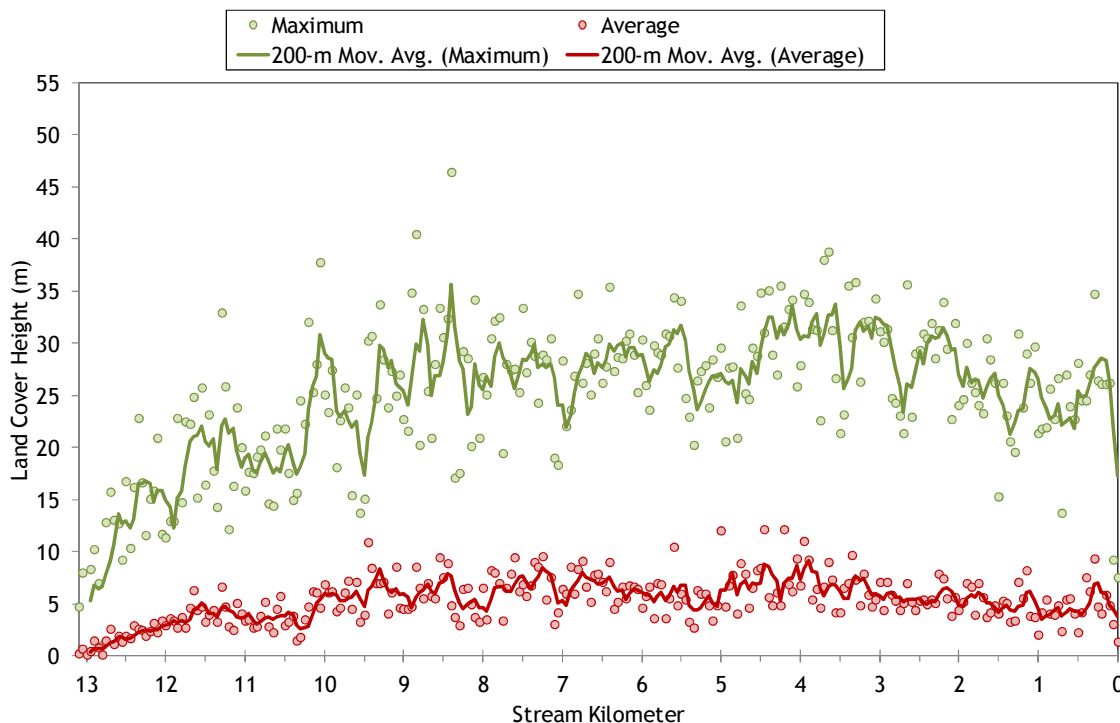


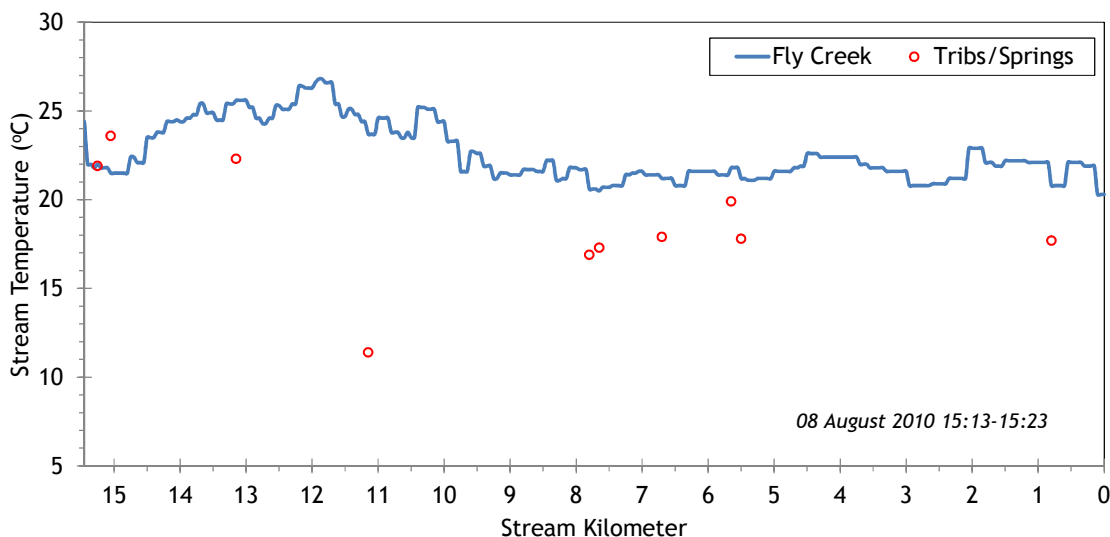
Figure 160 shows the land cover heights sampled along Fly Creek. The maximum and average of the 28 radial samples were calculated for each 50-meter stream node. (Note: Heat Source uses each of the 28 radial samples for each 50-meter node. The maximum and average are shown here for simplification purposes.)

Figure 160 - Fly Creek land cover heights sampled from highest hit LiDAR.



The TIR stream temperature profile of Fly Creek is shown in Figure 161. Interestingly, the stream temperature drops slightly in the downstream direction. The upper reaches are lower gradient open meadow, so the temperatures become quite warm. Then the stream enters a steeper and more confined valley, where some of that heat is lost from the stream.

Figure 161 - Fly Creek TIR stream temperature profile.



16.2 Fly Creek Heat Source Calibration Results

Fly Creek was simulated from below Little Fly Creek to the mouth (Figure 162). The total simulation length was 13.1 kilometers.

Figure 162 - Fly Creek simulation extent.

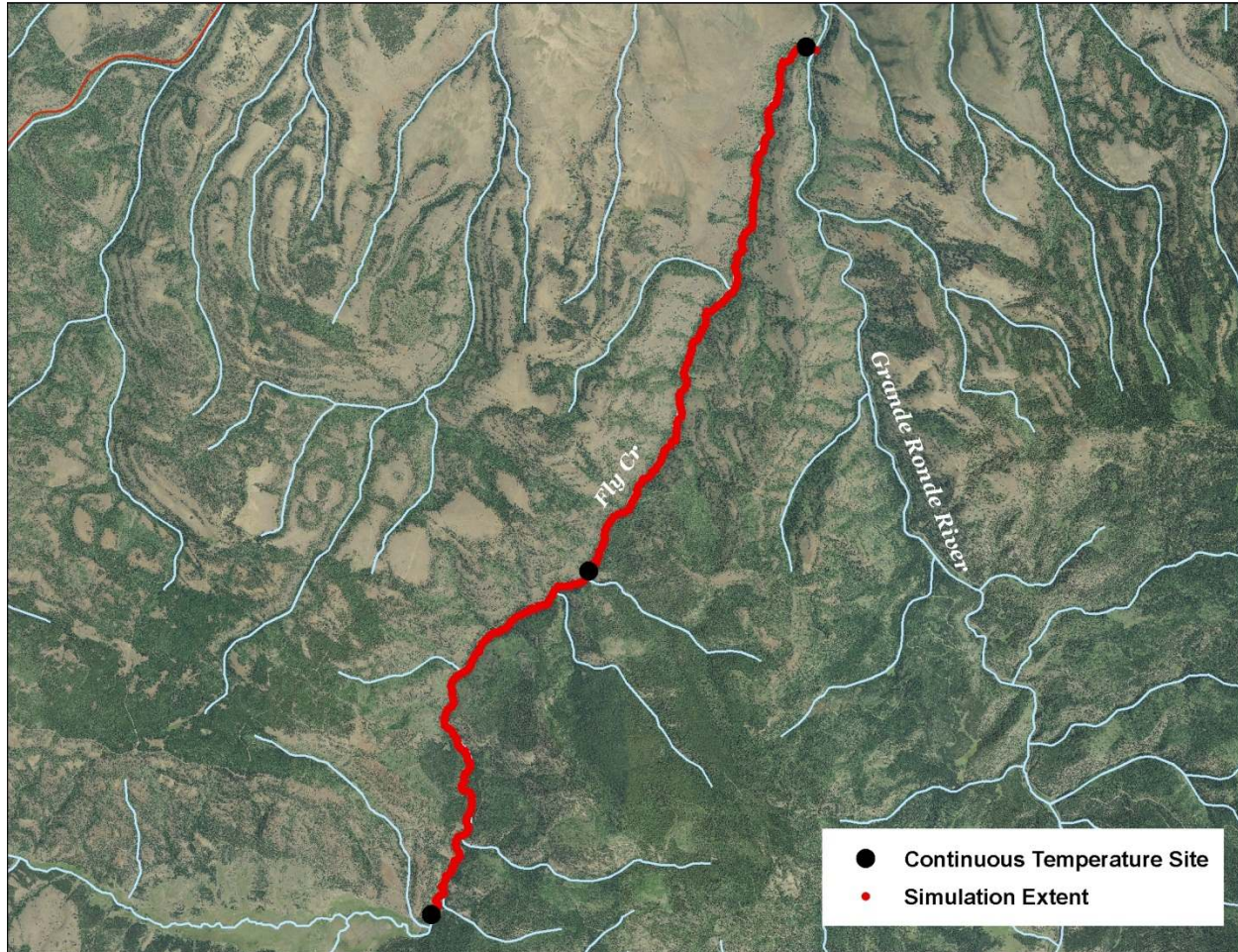


Table 25 - Fly Creek general Heat Source parameters.

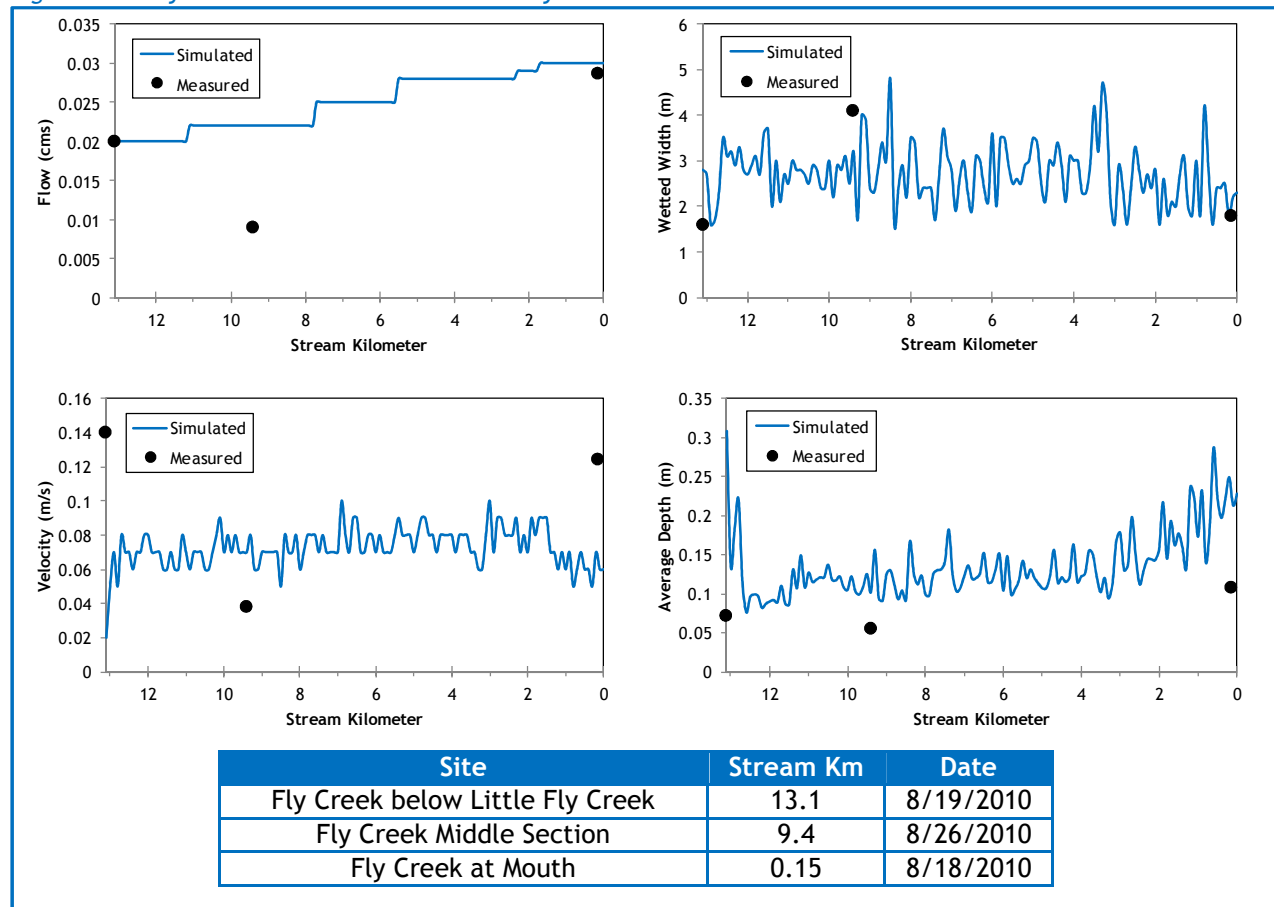
Stream:	Fly Creek
Length:	13.1 kilometers
Time Period:	August 6-27, 2010
Input Distance Step:	50 meters
Output Distance Step:	100 meters
Time Step:	1 minute
Flush Initial Condition:	7 days
TIR Date and Time:	August 8, 2010 15:12-15:21
Land Cover Data Source:	LiDAR
Land Cover Sampling Distance Step:	15 meters

The following assumptions were used when calibrating the Fly Creek Heat Source model:

- Hourly climate data was obtained from the J Ridge RAWS (USFS) site. Air temperature was adjusted using the adiabatic lapse rate of 1°C per 100 meters elevation.
- Daily flow variability was extrapolated from Grande Ronde River gage data.
- The wetted widths were reduced 33-50% from the raw TTools values in order to match the ground level measurements and calibrate the hydraulics.

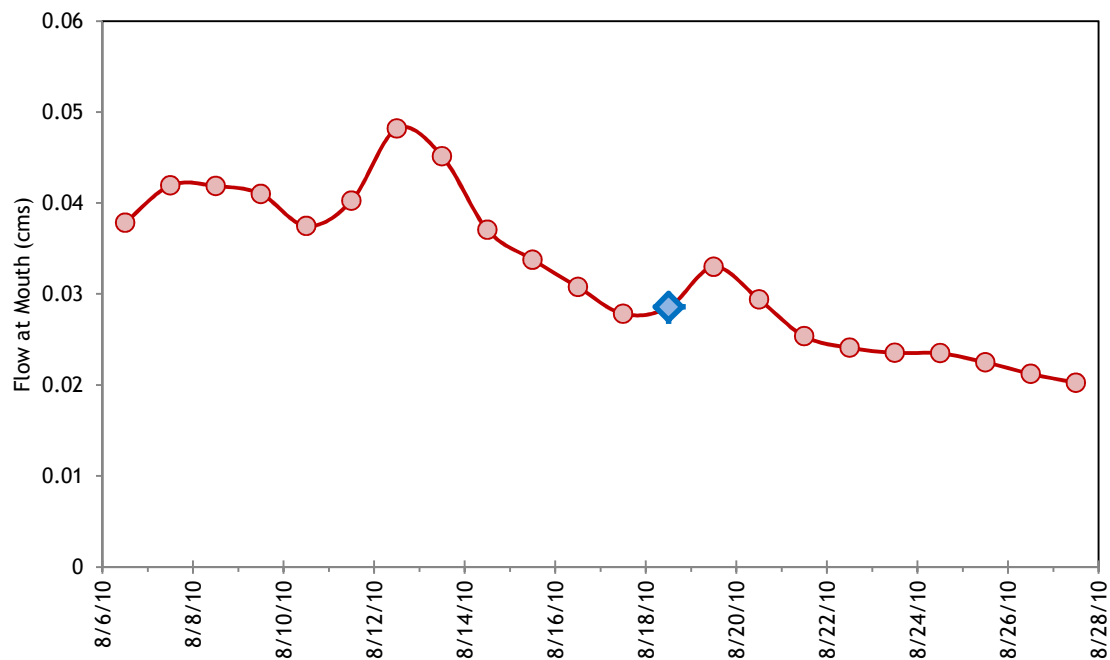
Fly Creek's simulated and measured hydraulic values are shown in Figure 163. The simulated values are from August 18th, while the measured values' dates vary. There were three ground level measurement sites. The measurements at kilometer 9.4 were taken on August 26 and do not match the simulated values for August 18 as well.

Figure 163 - Fly Creek simulated and measured hydraulic values.



The simulated daily flows at the mouth of Fly Creek are shown in Figure 164. The daily values were extrapolated from gage data on the Grande Ronde River.

Figure 164 - Fly Creek simulated flow volumes at the mouth.



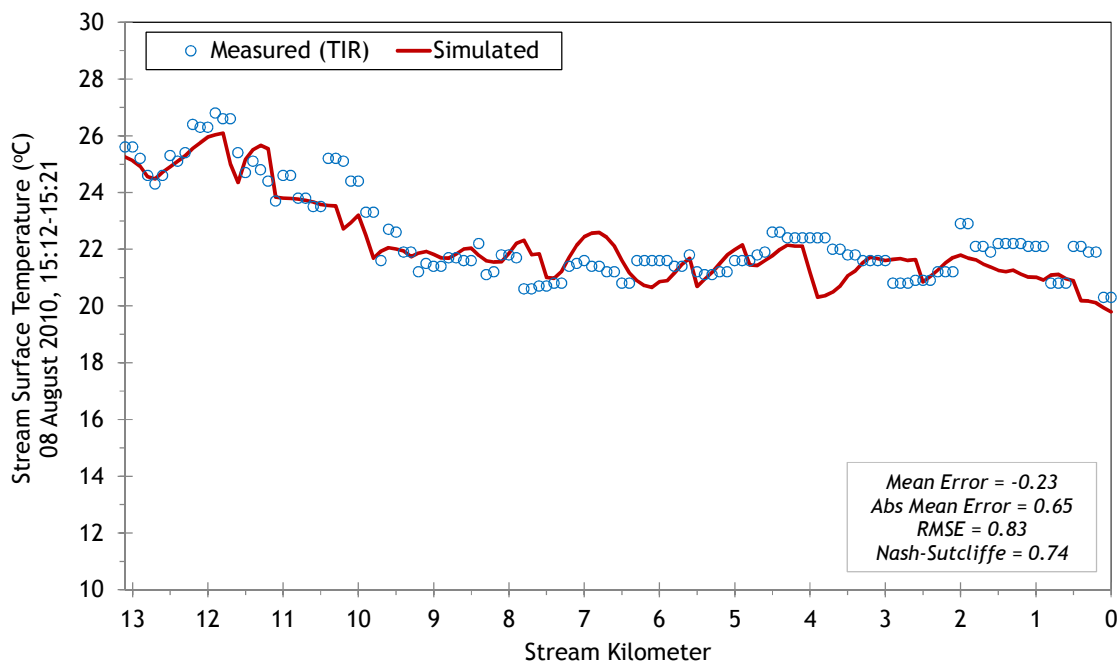
There were 2 springs and one tributary included within the Fly Creek model (Table 26). Their flow volumes were varied daily in order to mimic the variation assumed for the flows at the mouth of Fly Creek. Their temperatures were held at a constant value because of their insignificant volumes.

Table 26 - Fly Creek mass inflows and assumptions.

Feature	Stream Km	Assumptions
Spring	11.1	0.002-0.005 cms at constant 11.4°C
Spring	7.7	0.002-0.005 cms at constant 16.9°C
Unnamed Tributary	5.5	0.002-0.005 cms at constant 17.8°C

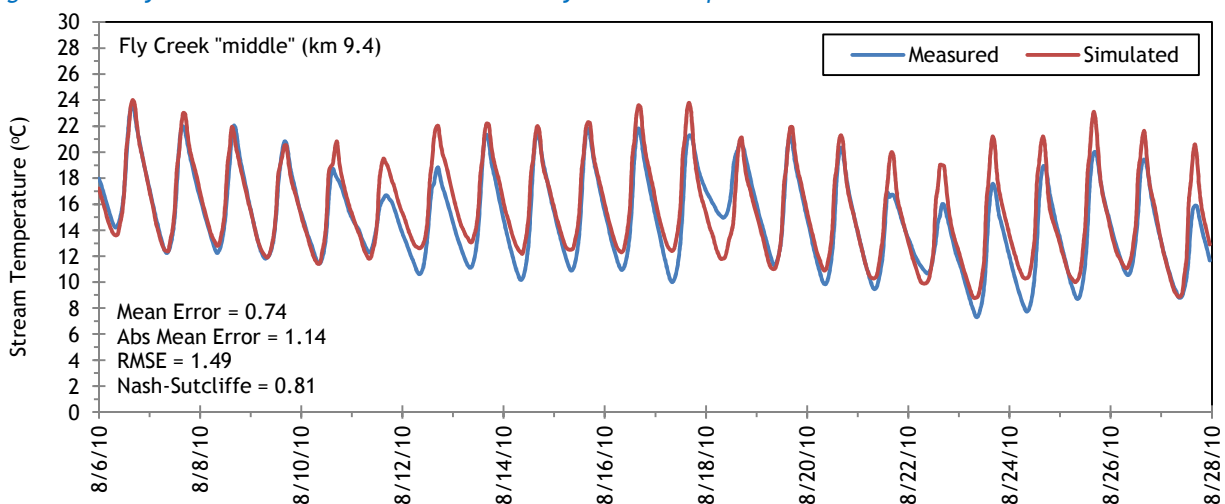
Figure 165 shows the simulated and measured longitudinal stream temperatures for Fly Creek. As previously mentioned, Fly Creek temperatures decline in the downstream direction because the stream is flowing from lower gradient meadows at the upper end into a more confined and steeper valley.

Figure 165 - Fly Creek simulated and measured longitudinal stream temperatures.



The simulated and measured hourly stream temperatures are presented in Figure 166.

Figure 166 - Fly Creek simulated and measured hourly stream temperatures.



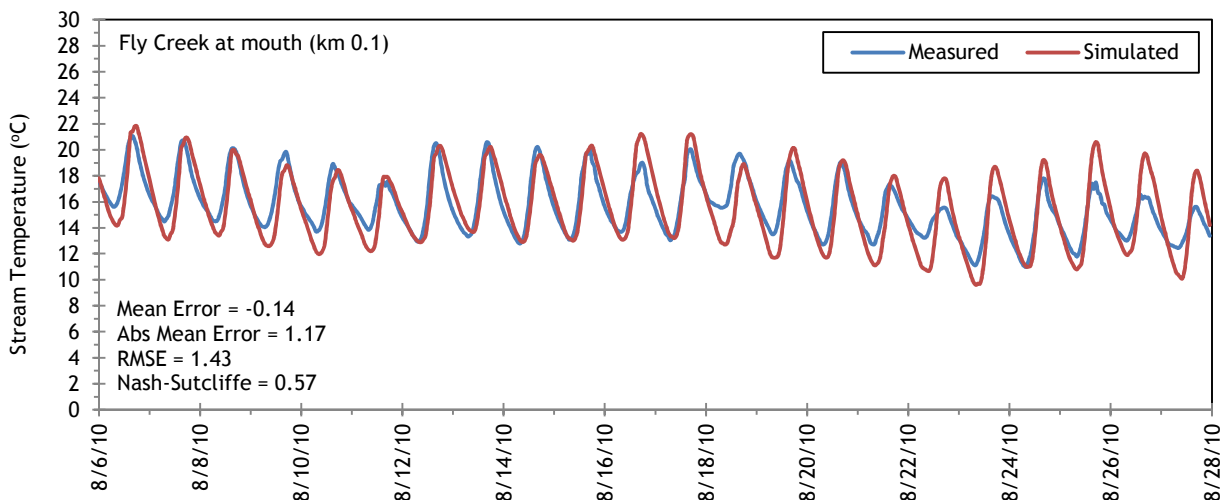
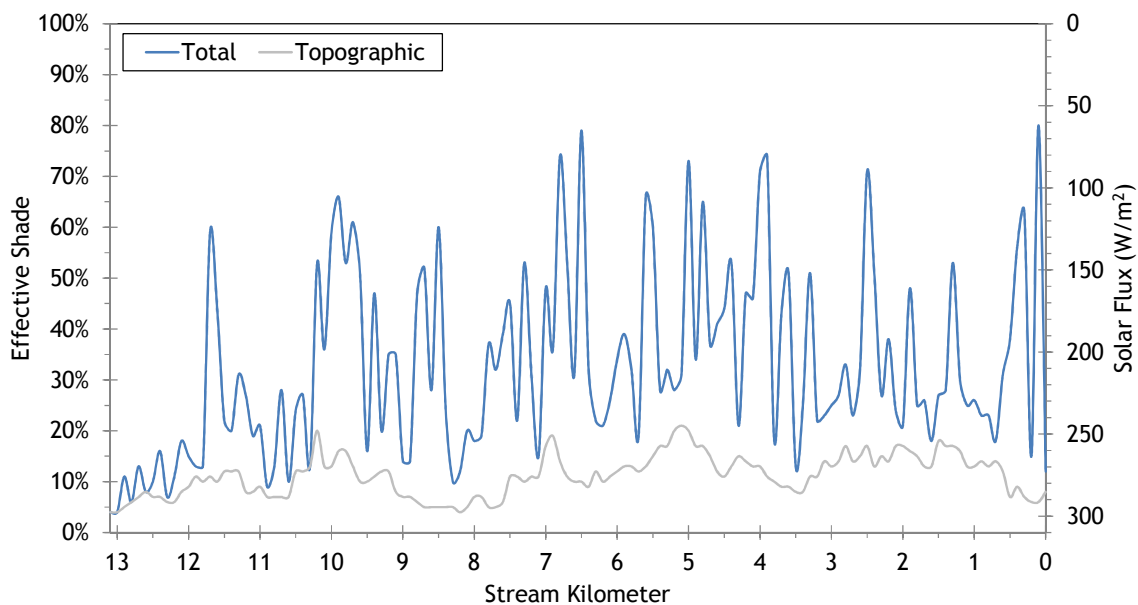


Figure 167 shows the simulated effective shade for Fly Creek. The upper few kilometers have less shade because the stream is flowing through a mixed meadow-forest complex. The lower 10 stream kilometers have more topographic shade and more total effective shade produced by the surrounding forest.

Figure 167 - Fly Creek simulated effective shade.



17. MCCOY CREEK

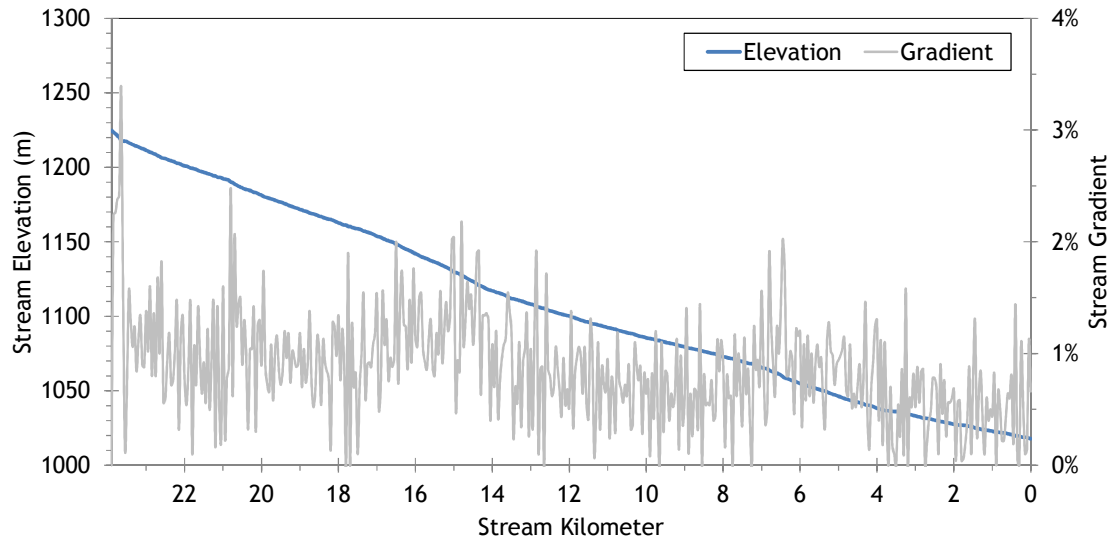


RGB-colored LiDAR point cloud - McCoy Creek just above mouth - the once channelized stream has been restored to its original channel.

17.1 McCoy Creek TTools Results

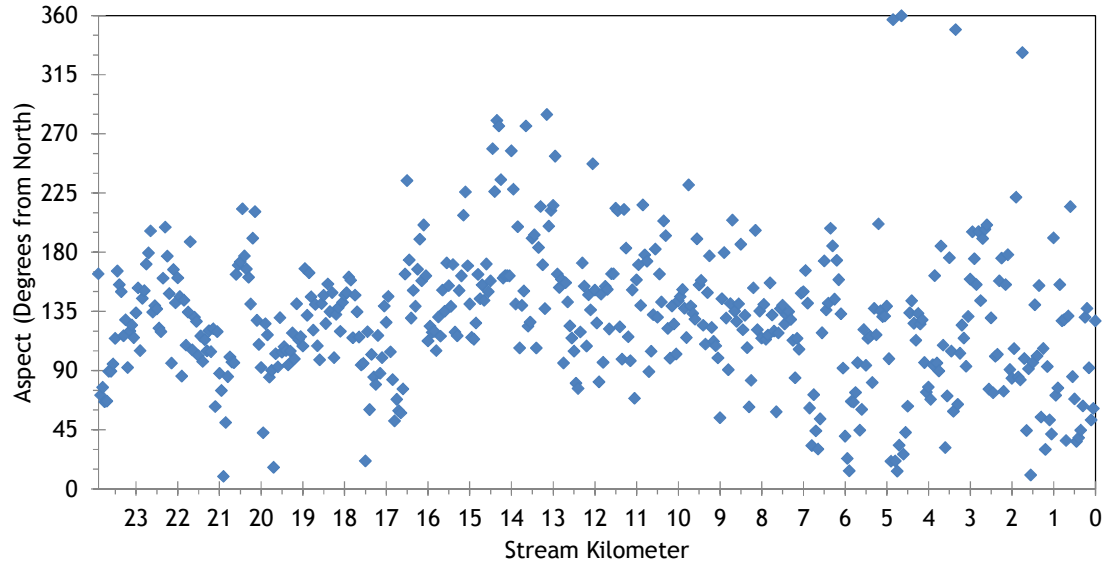
McCoy Creek elevations and gradients were sampled from the bare earth LiDAR data (Figure 168). The stream has a moderately low gradient due to the gradual elevation drop and meandering nature.

Figure 168 - McCoy Creek elevation and gradient.



McCoy Creek flows generally toward the southeast (Figure 169).

Figure 169 - McCoy Creek stream aspect.



Topographic shade is variable along McCoy Creek (Figure 170). As the stream enters more confined valleys, the topographic shade angles increase. In the lower 3.5 kilometers, the stream flows through a wide flat valley and has less topographic shade.

Figure 170 - McCoy Creek topographic shade angles.

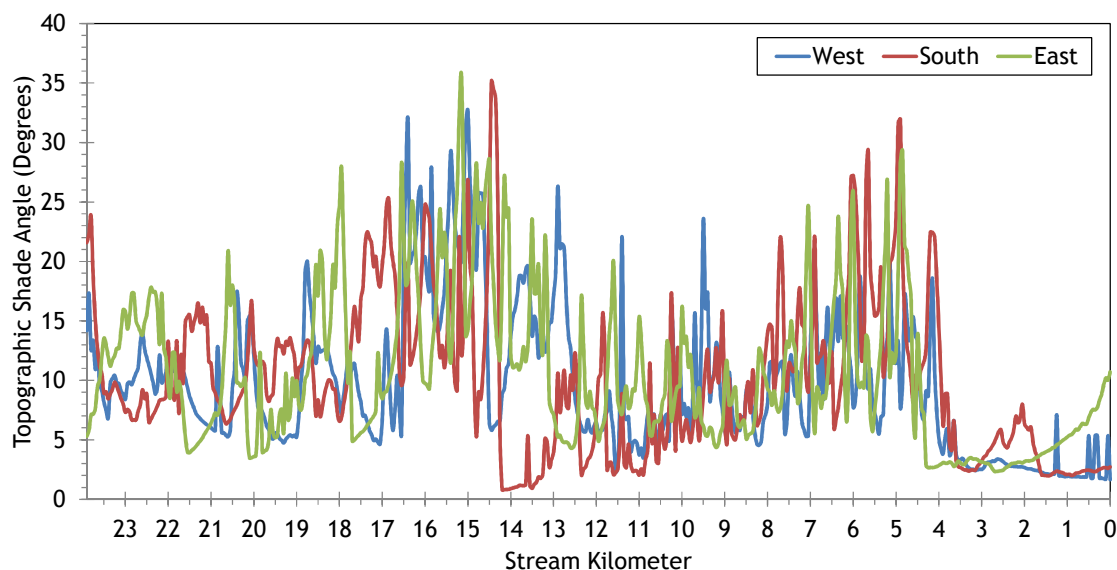


Figure 171 shows the land cover heights sampled along McCoy Creek. The maximum and average of the 28 radial samples were calculated for each 50-meter stream node. (Note: Heat Source uses each of the 28 radial samples for each 50-meter node. The maximum and average are shown here for simplification purposes.)

Figure 171 - McCoy Creek land cover heights sampled from highest hit LiDAR.

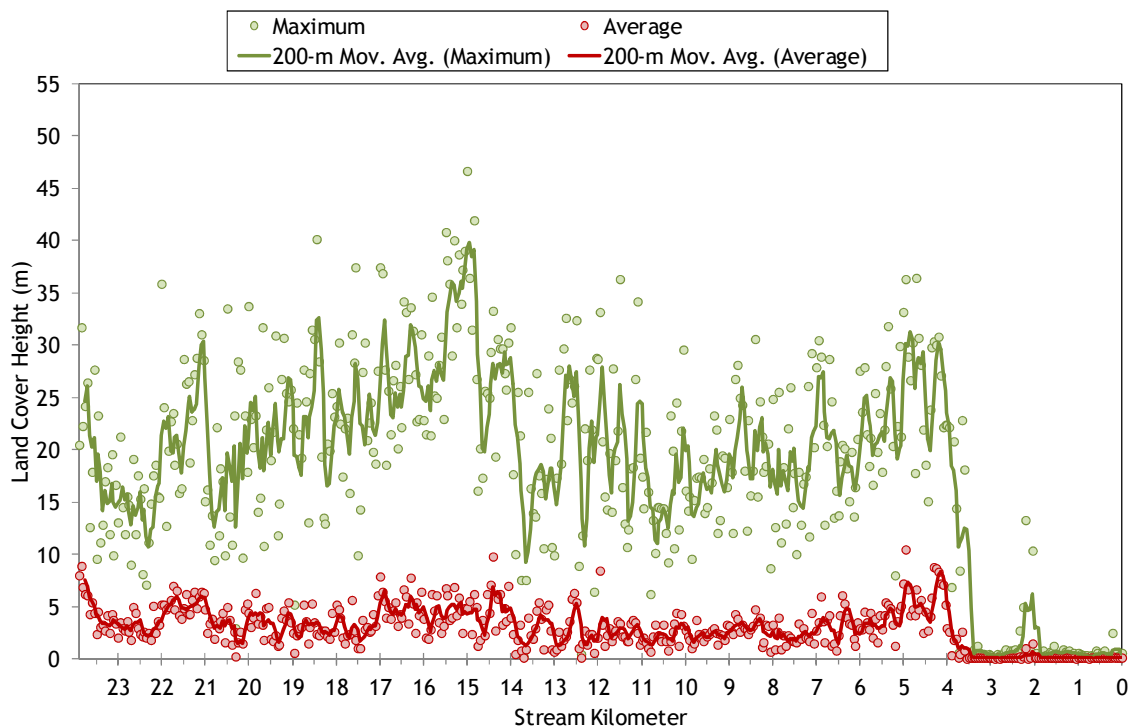
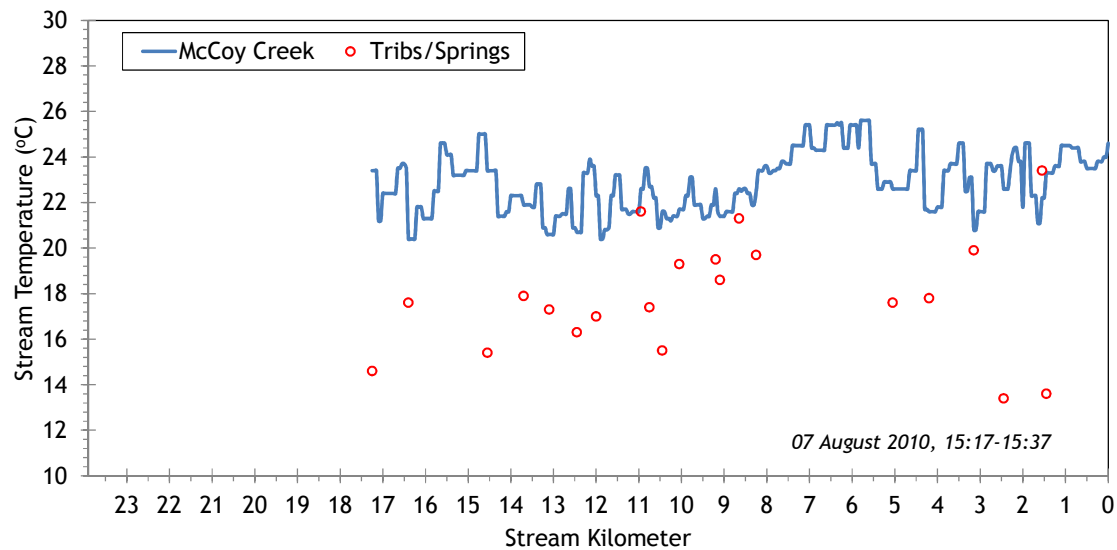


Figure 172 shows the TIR stream temperature profile of McCoy Creek. It is a fairly small stream with low summertime flows; therefore temperatures are fairly high and variable. The small flows (less than 1 cfs) are the main factor contributing to the highly variable stream temperatures.

Figure 172 - McCoy Creek TIR stream temperature profile.



17.2 McCoy Creek Heat Source Calibration Results

McCoy Creek effective shade was simulated for the lower 23.9 stream kilometers. The flow was too low in August 2010 to simulate temperature.

Figure 173 - McCoy Creek simulation extent.

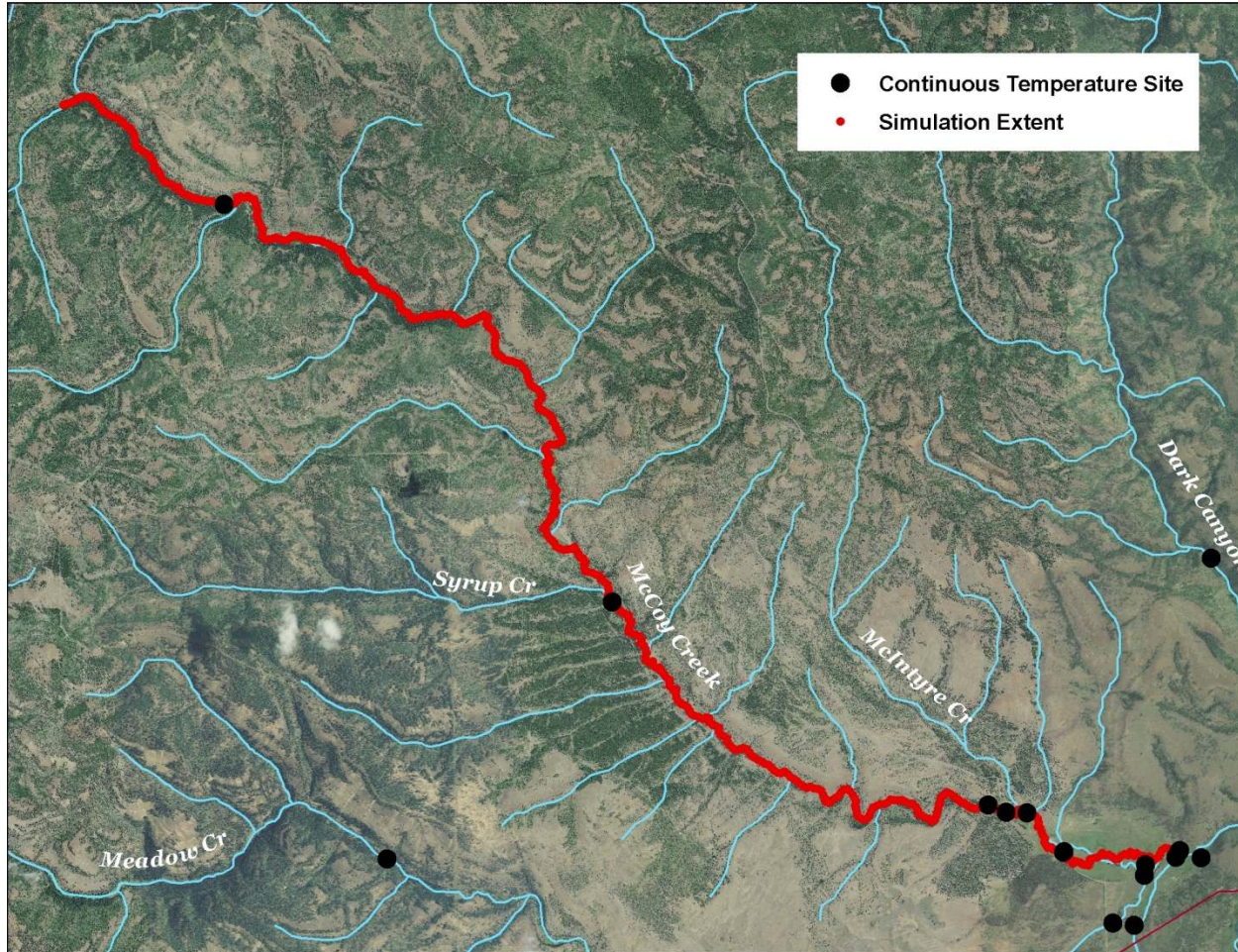


Table 27 - McCoy Creek general Heat Source parameters.

Stream:	McCoy Creek
Length:	23.9 kilometers
Time Period:	August 6-27, 2010
Input Distance Step:	50 meters
Output Distance Step:	100 meters
Time Step:	1 minute
Flush Initial Condition:	NA
TIR Date and Time:	NA
Land Cover Data Source:	LiDAR
Land Cover Sampling Distance Step:	15 meters

Figure 174 shows the simulated effective shade values for McCoy Creek. There is moderate effective shade along most of the stream, and much of the total effective shade is often created by topographic features. The lower 4 kilometers are where the stream flows in open meadow and through the restoration area.

Figure 174 - McCoy Creek simulated effective shade.

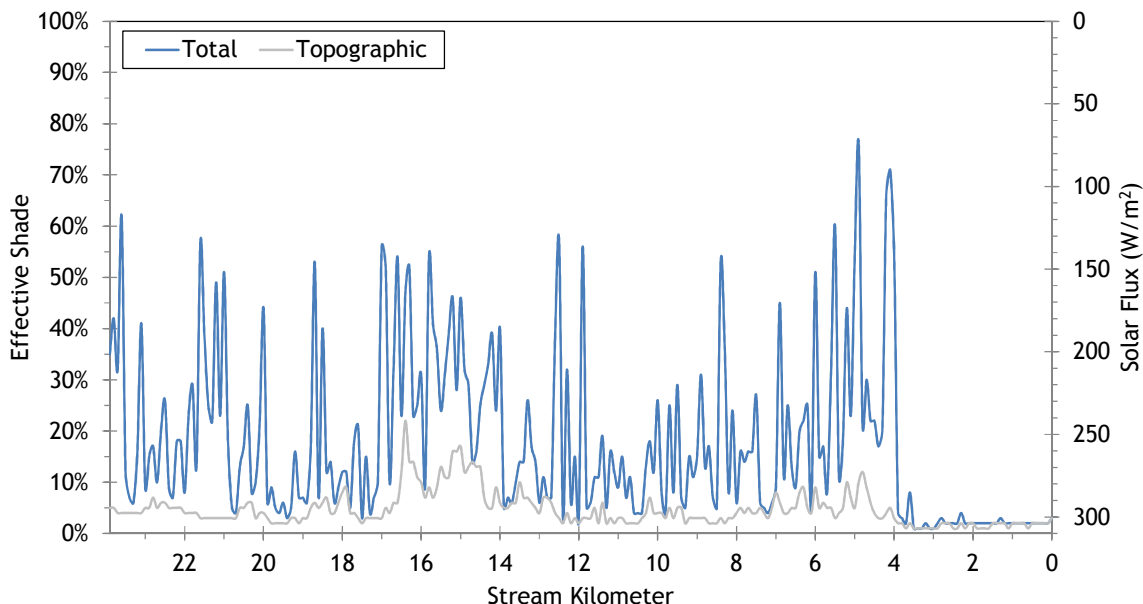
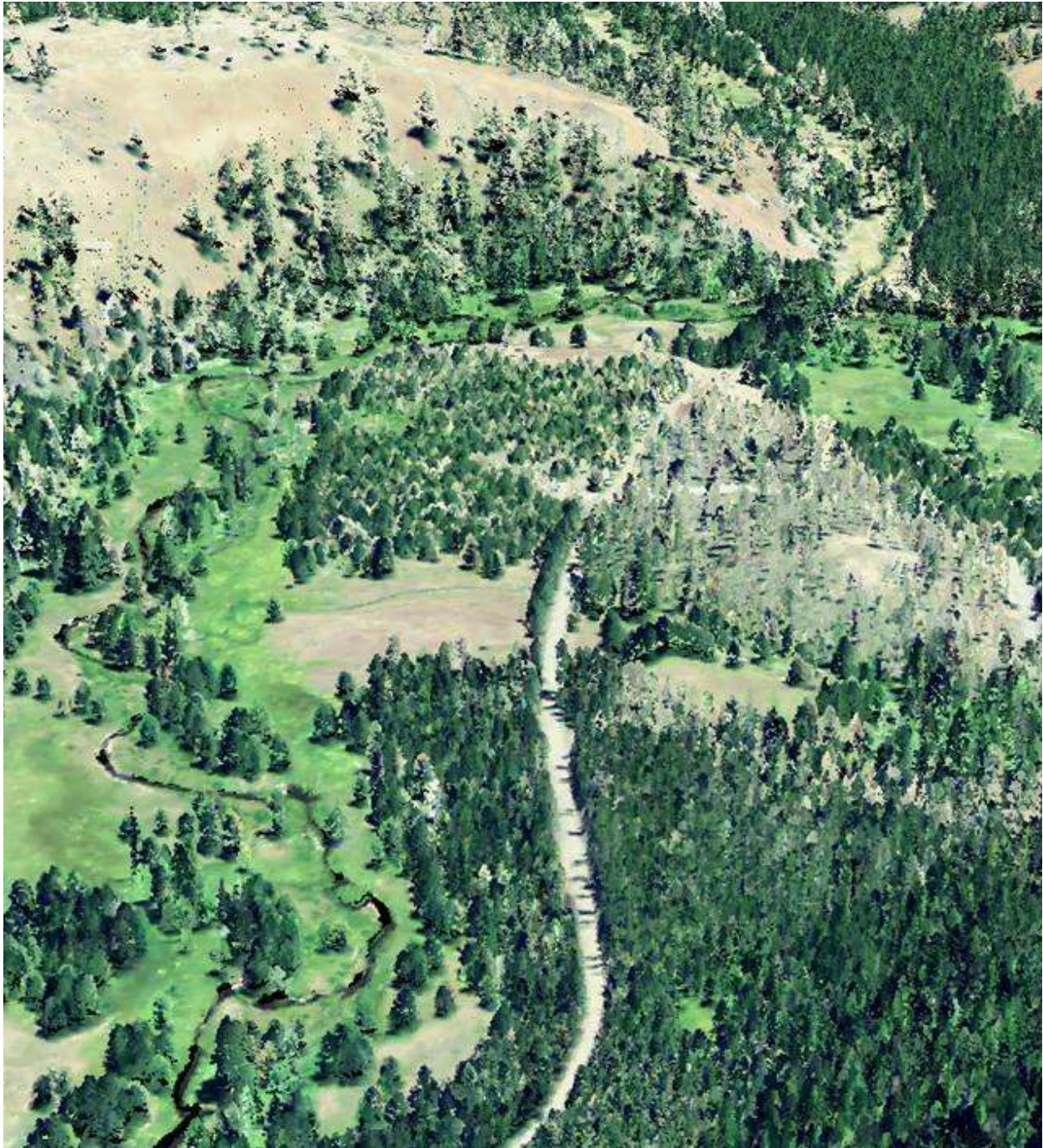


Figure 175 shows the typical terrain and vegetation along McCoy Creek. The stream often has a wide flat floodplain and intermittently is flanked by large trees. The image gives a better understanding of why effective shade is relatively low compared to other streams in the basin.

Figure 175 - McCoy Creek typical terrain and vegetation.



18. MEADOW CREEK

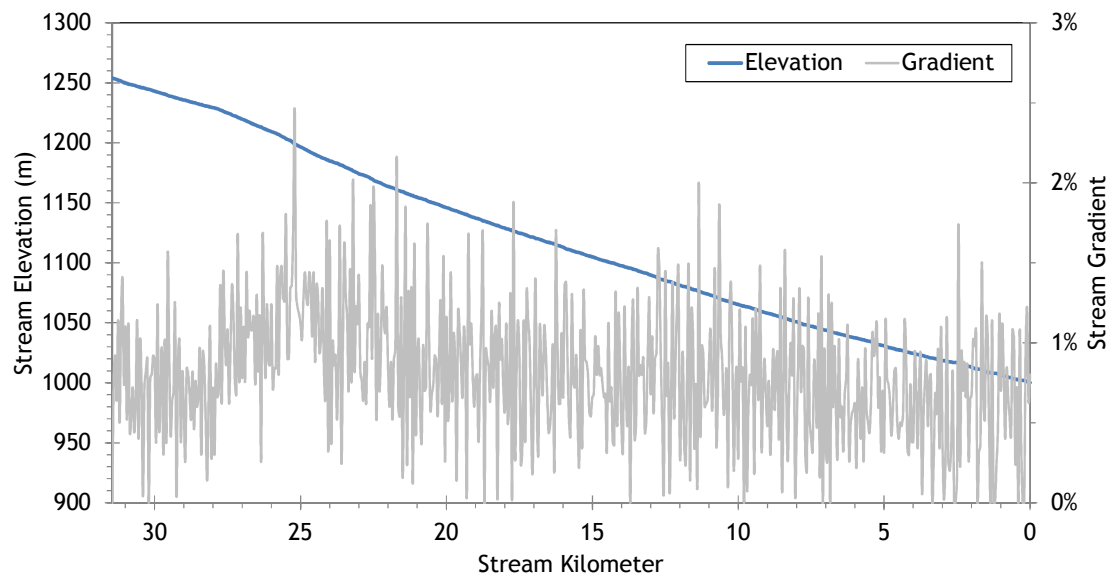


RGB-colored LiDAR point cloud - Meadow Creek looking downstream near Smith Creek.

18.1 Meadow Creek TTools Results

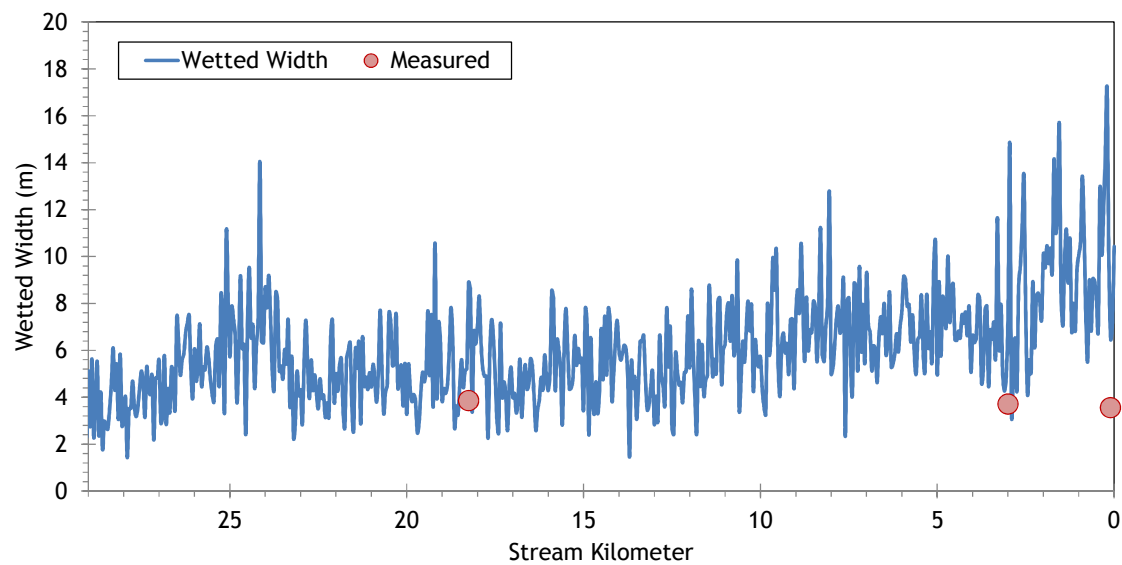
Meadow Creek elevations and gradients are shown in Figure 176. The stream has a fairly gradual descent, is moderately sinuous, and hence gradient is moderated throughout.

Figure 176 - Meadow Creek elevation and gradient.



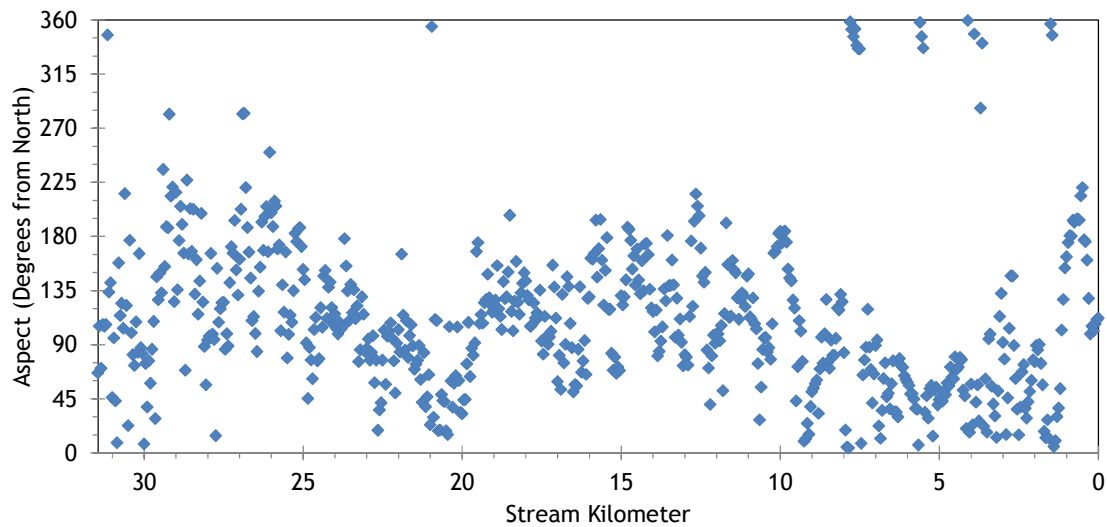
The wetted widths for Meadow Creek are shown in Figure 177. There is a slight increase in widths in the downstream direction, but overall the stream is relatively small.

Figure 177 - Meadow Creek wetted width.



Meadow Creek flows from west to east before joining the Grande Ronde River (Figure 178).

Figure 178 - Meadow Creek stream aspect.



The mountainous terrain surrounding Meadow Creek creates moderately high topographic shade angles (Figure 179). Values vary between about 5 and 30 degrees.

Figure 179 - Meadow Creek topographic shade angles.

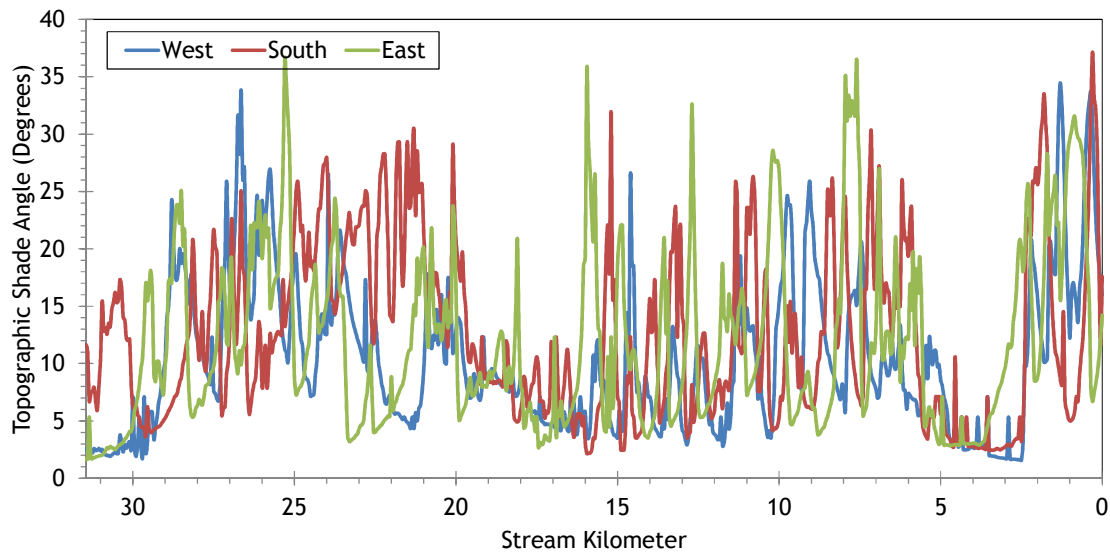
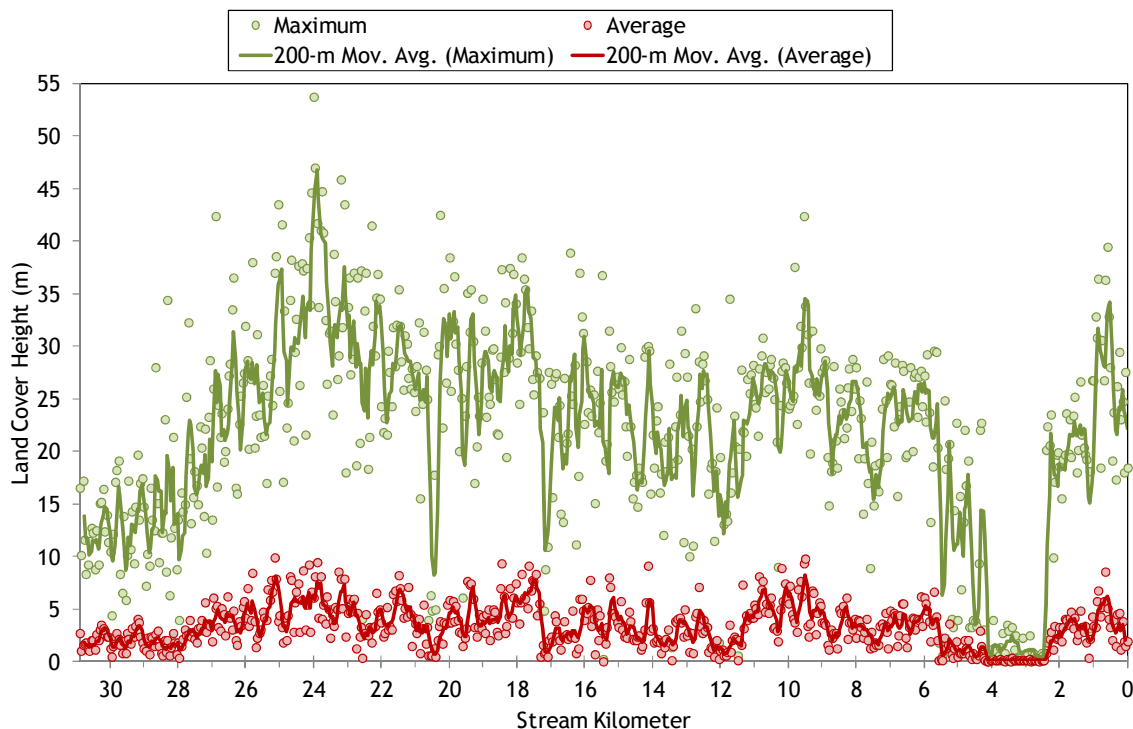


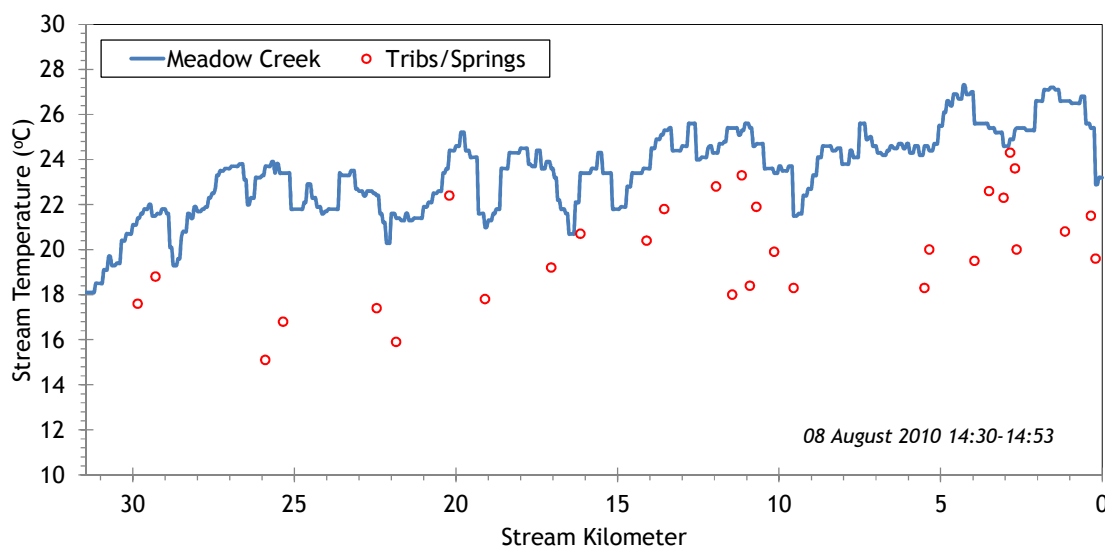
Figure 180 shows the land cover heights sampled along Meadow Creek. The maximum and average of the 28 radial samples were calculated for each 50-meter stream node. (Note: Heat Source uses each of the 28 radial samples for each 50-meter node. The maximum and average are shown here for simplification purposes.)

Figure 180 - Meadow Creek land cover heights sampled from highest hit LiDAR.



The moderate gradients and low stream flows make the longitudinal thermal profile quite variable (Figure 181). Maximum stream temperatures were about 27°C during the TIR flight.

Figure 181 - Meadow Creek TIR stream temperature profile.



18.2 Meadow Creek Heat Source Calibration Results

Meadow Creek was simulated from Waucup Creek to the mouth (Figure 182). The total simulation length was 30.9 stream kilometers.

Figure 182 - Meadow Creek simulation extent.

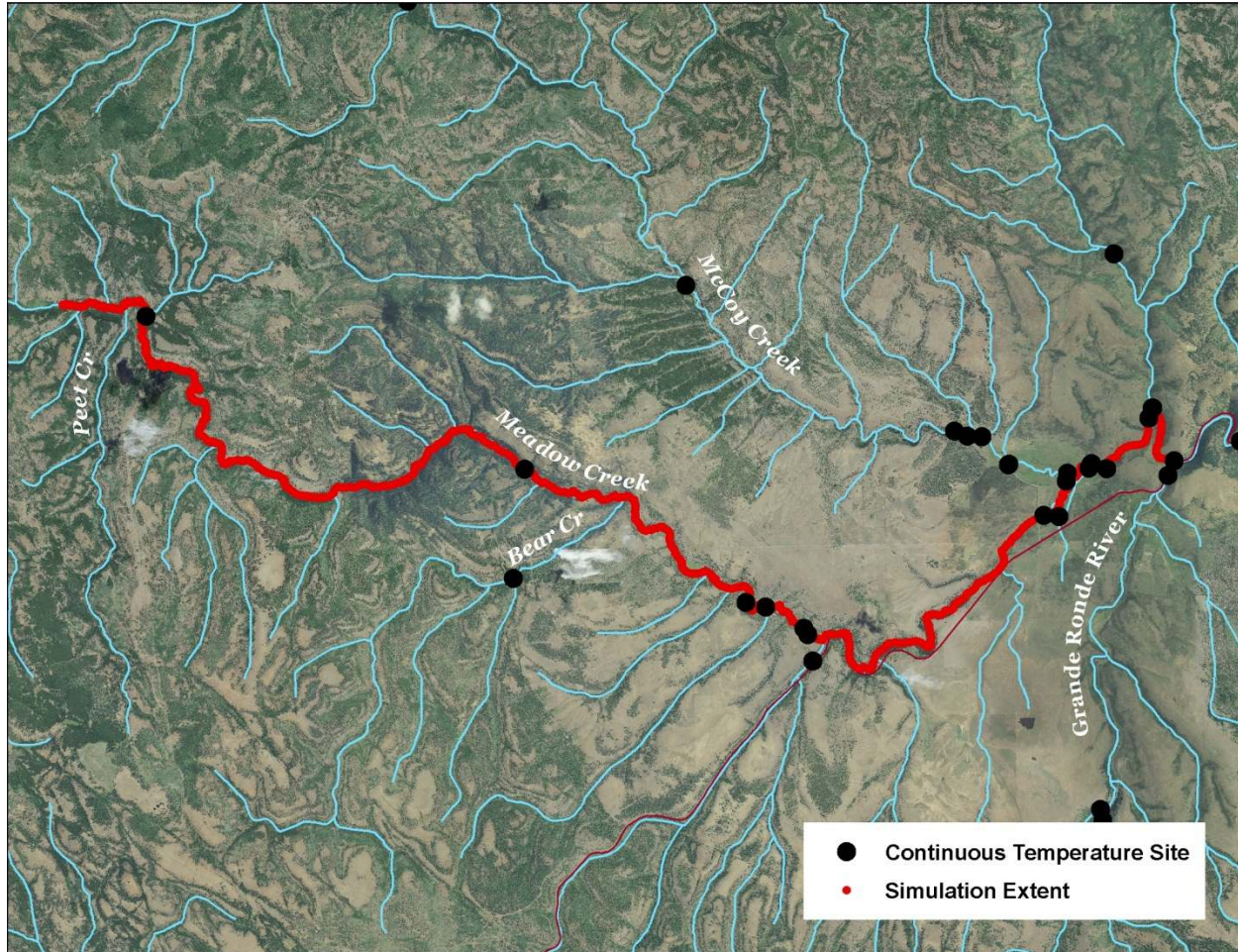


Table 28 - Meadow Creek general Heat Source parameters.

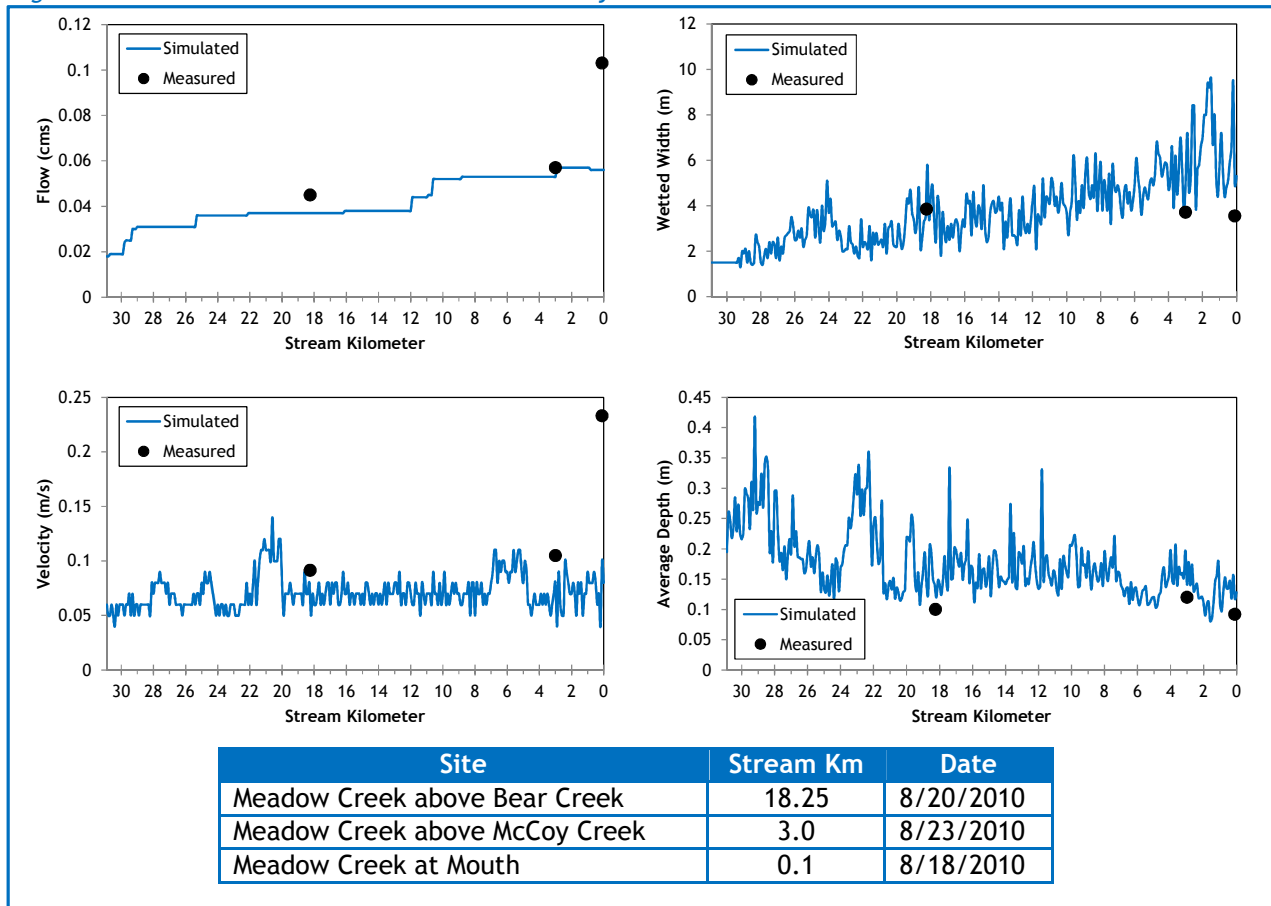
Stream:	Meadow Creek
Length:	30.9 kilometers
Time Period:	August 6-27, 2010
Input Distance Step:	50 meters
Output Distance Step:	100 meters
Time Step:	1 minute
Flush Initial Condition:	7 days
TIR Date and Time:	August 8, 2010 14:30-14:53
Land Cover Data Source:	LiDAR
Land Cover Sampling Distance Step:	15 meters

The following assumptions were used when calibrating the Meadow Creek Heat Source model:

- Hourly climate data was obtained from the La Grande Airport (NWS). Air temperature was adjusted using the adiabatic lapse rate of 1°C per 100 meters elevation.
- Daily flow variability was extrapolated from Grande Ronde River gage data.

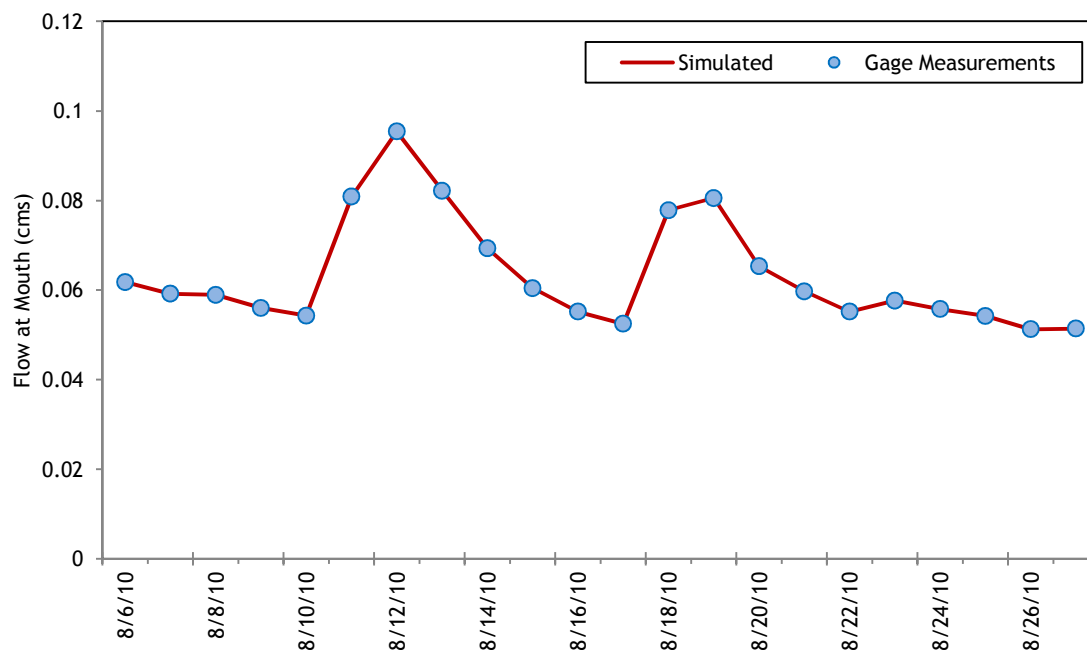
Figure 183 summarized the simulated and measured hydraulic values used in the calibrated Meadow Creek model. The simulated data was plotted for August 26th, while the ground level measurements were collected on three different days.

Figure 183 - Meadow Creek simulated and measured hydraulic values.



The simulated daily flow values at the mouth are presented in Figure 184. The daily values were extrapolated from gage data recorded on the Grande Ronde River.

Figure 184 - Meadow Creek simulated flows at mouth.



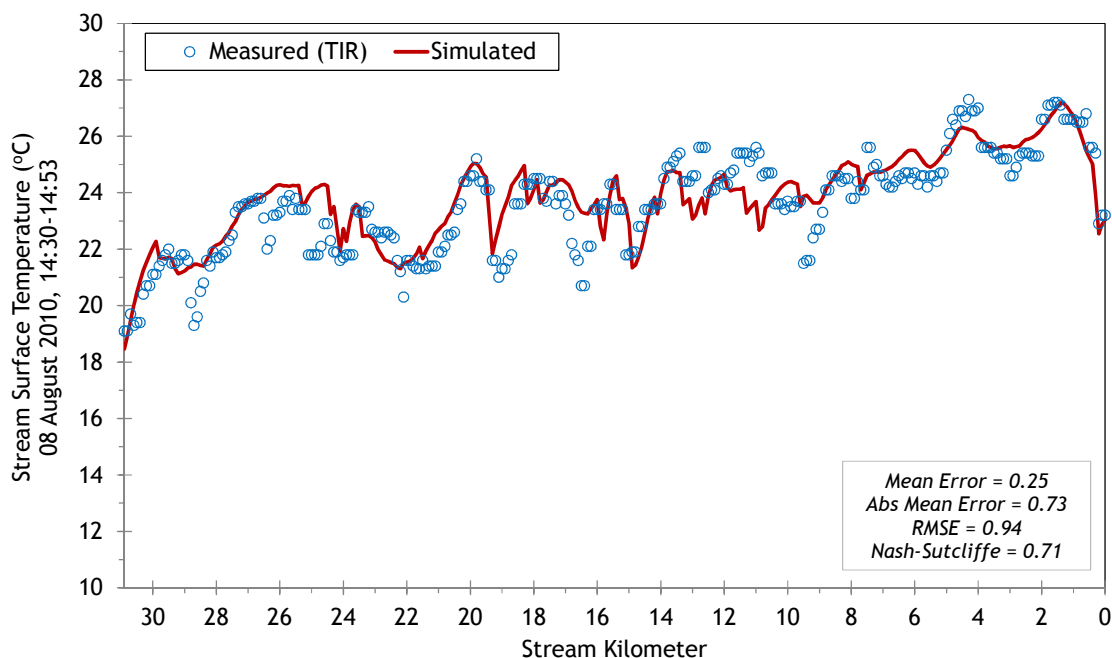
The tributaries included within the Meadow Creek Heat Source model are summarized in Table 29. Dark Canyon Creek had intermittent flow during August 2010 and was assumed dry during the simulation time period.

Table 29 - Meadow Creek mass inflow features and assumptions.

Feature	Stream Km	Assumptions
Peet Creek	29.8	0.006-0.01 cms, used Bear Cr temps
Smith Creek	29.3	0.006-0.01 cms, used Bear Cr temps
Cougar Canyon	25.3	0.006-0.01 cms, used Bear Cr temps
Bear Creek	16.15	0.0006-0.001 cms, measured hourly temps
Battle Creek	11.95	0.006-0.01 cms, used Bear Cr temps
Burnt Corral Creek	10.65	0.007-0.01 cms, measured hourly temps
McCoy Creek	2.9	0.004-0.007 cms, measured hourly temps

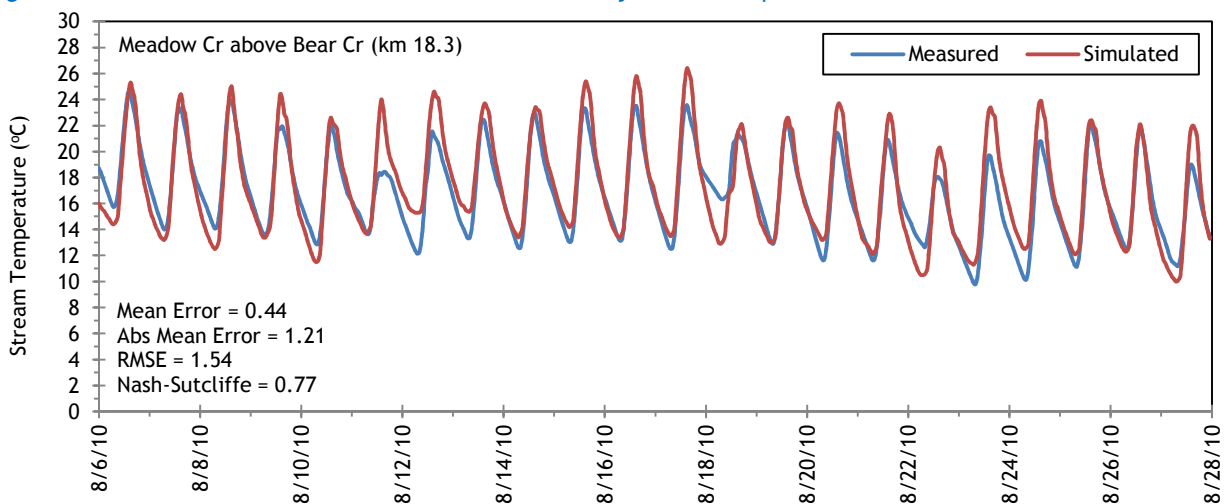
Meadow Creek simulated and measured longitudinal temperatures are shown in Figure 185. There is a great deal of variability over short distances because the stream flows were quite low during August 2010.

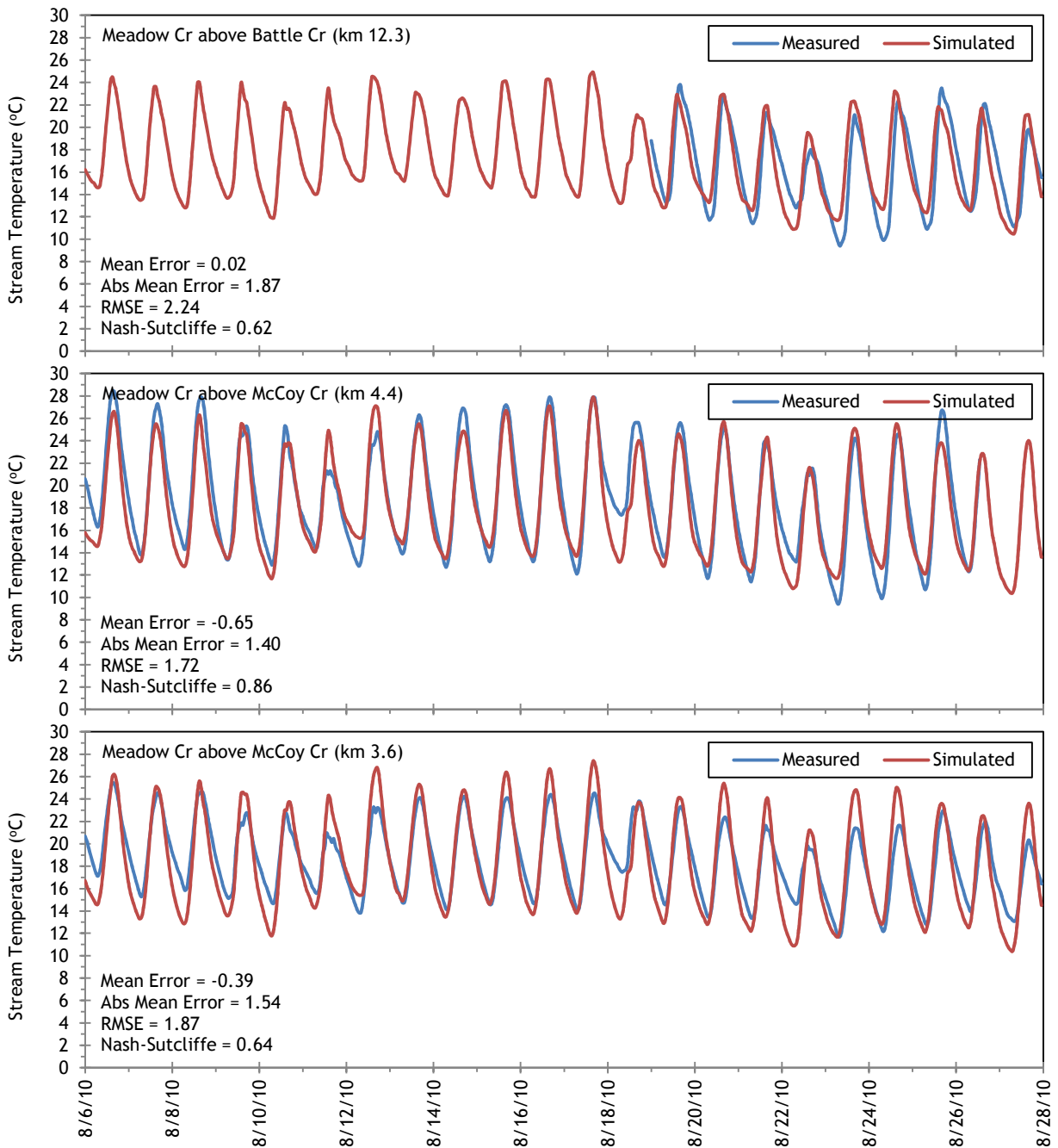
Figure 185 - Meadow Creek simulated and measured longitudinal stream temperatures.



Simulated and measured hourly stream temperatures are compared in Figure 186. Meadow Creek had very low flow which makes the stream temperatures more variable over shorter distances. Calibration of the Heat Source model was more challenging than for other streams and the resulting calibration statistics reflect that.

Figure 186 - Meadow Creek simulated and measured hourly stream temperatures.





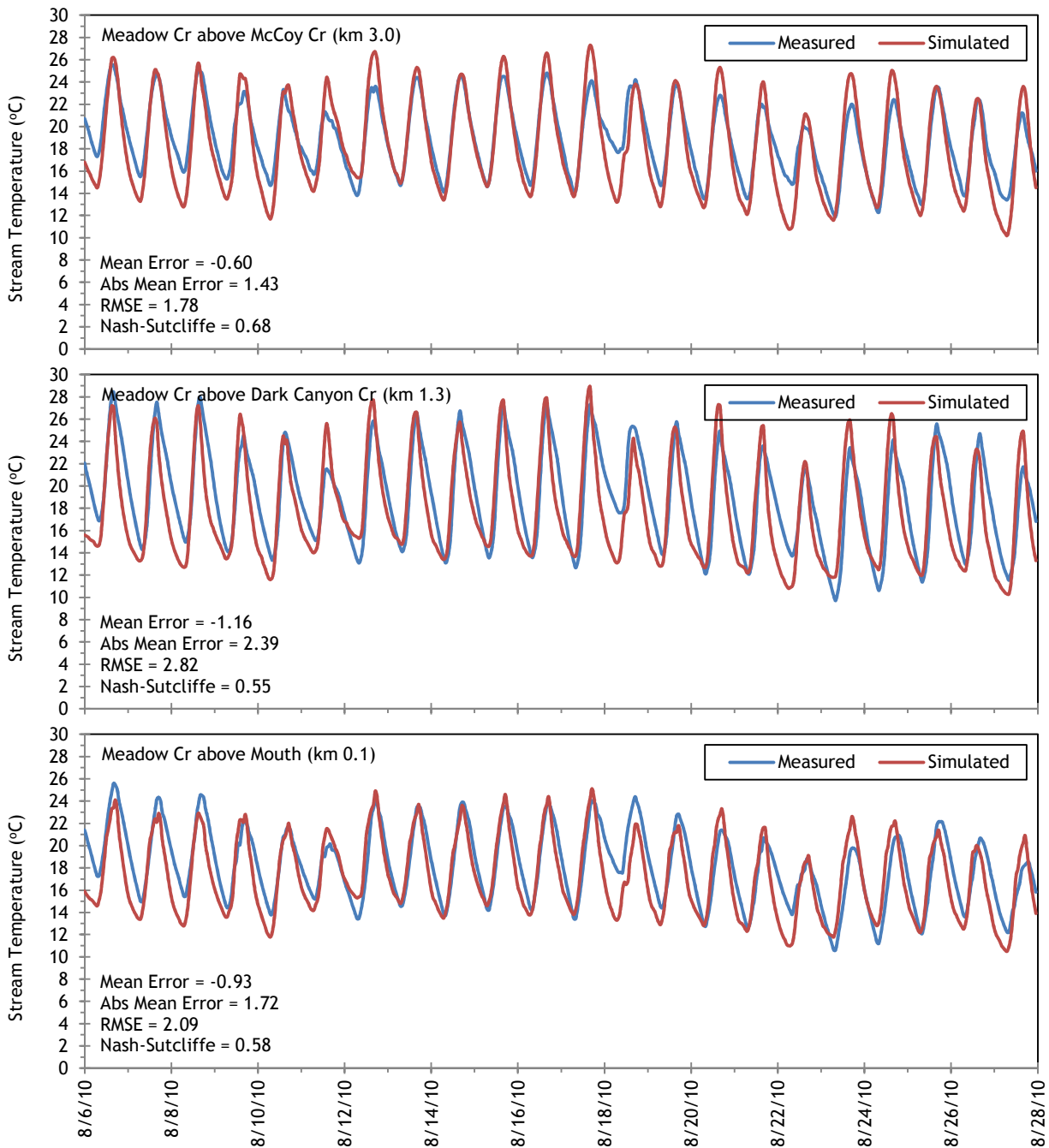
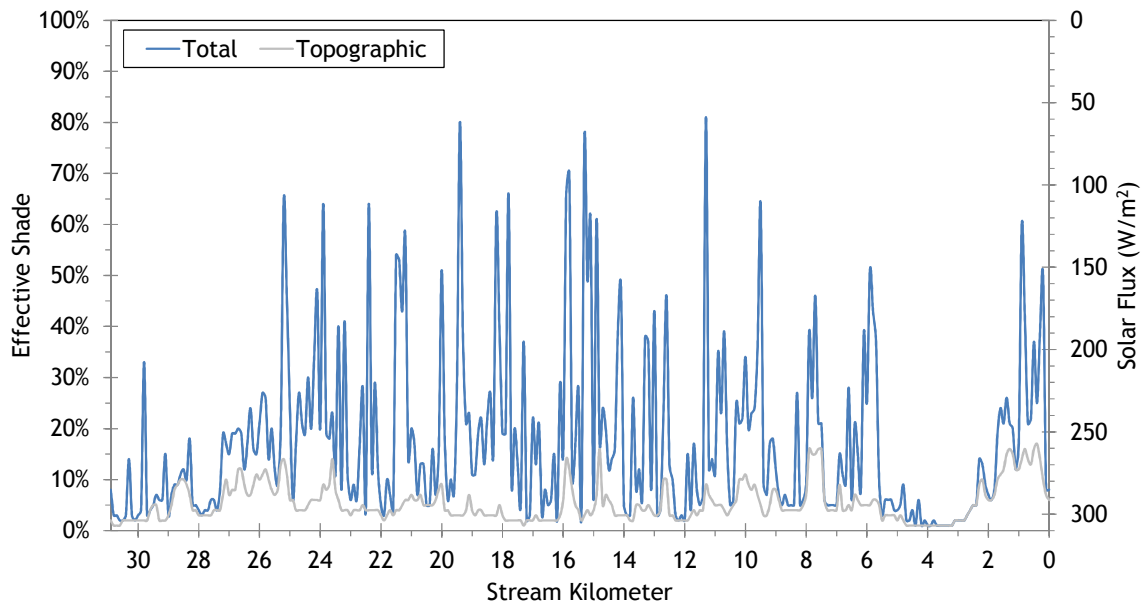
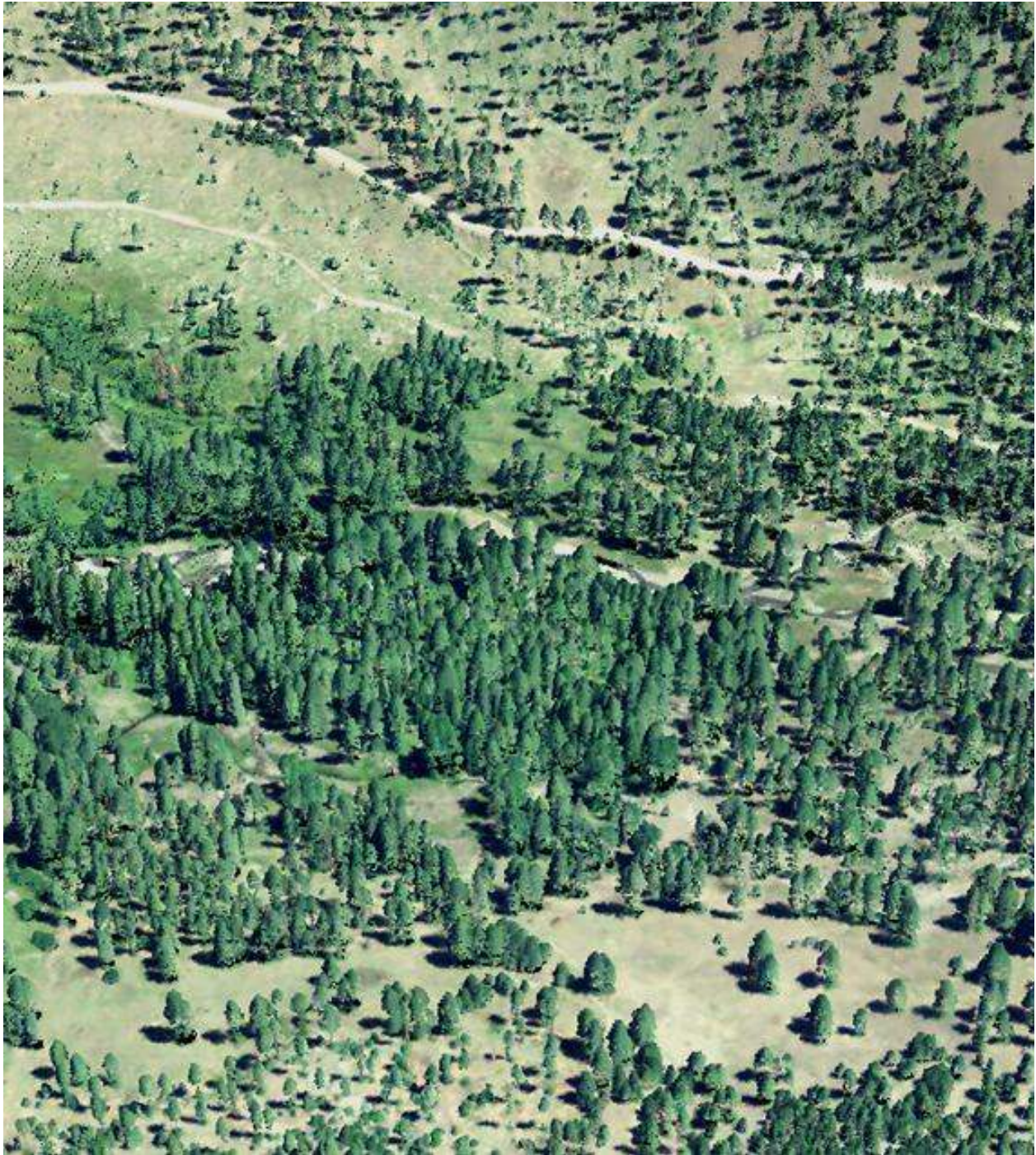


Figure 187 shows the simulated effective shade values for Meadow Creek. The total effective shade is somewhat moderate because the meanders through meadows that are a mix of grass and trees. There is upwards of 10% effective shade produced by topography throughout much of the stream length.

Figure 187 - Meadow Creek simulated effective shade.



19. BEAVER CREEK



RGB-colored LiDAR point cloud - Beaver Creek near Little Beaver Creek (stream flowing from right to left of image).

19.1 Beaver Creek TTools Results

Beaver Creek elevations and gradients were sampled from the bare earth LiDAR data (Figure 188). The reaches just below La Grande Reservoir (kilometer 22.9) are the steepest, and then gradients are generally between 1% and 4%.

Figure 188 - Beaver Creek elevation and gradient.

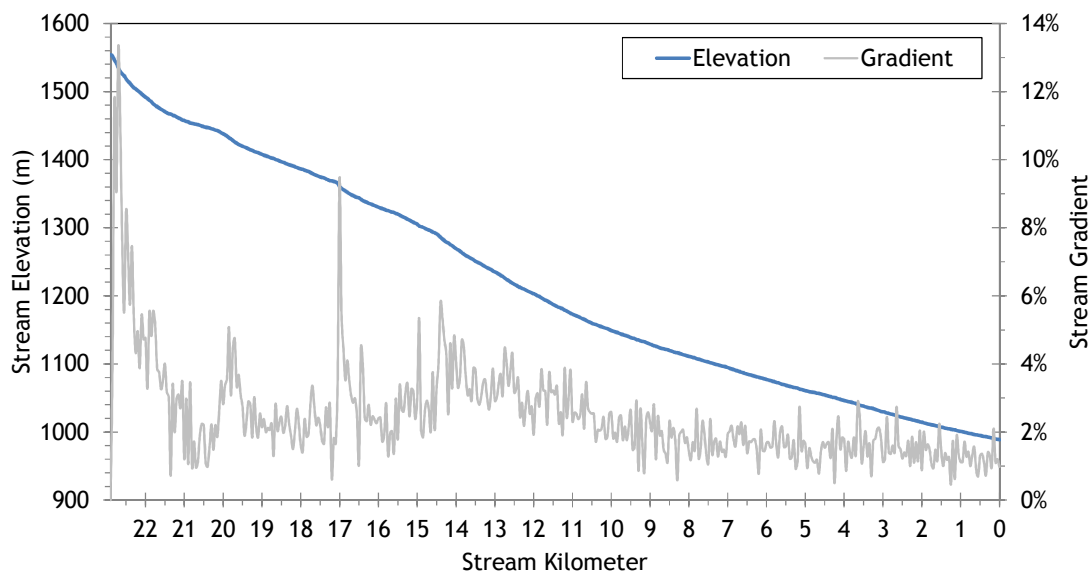
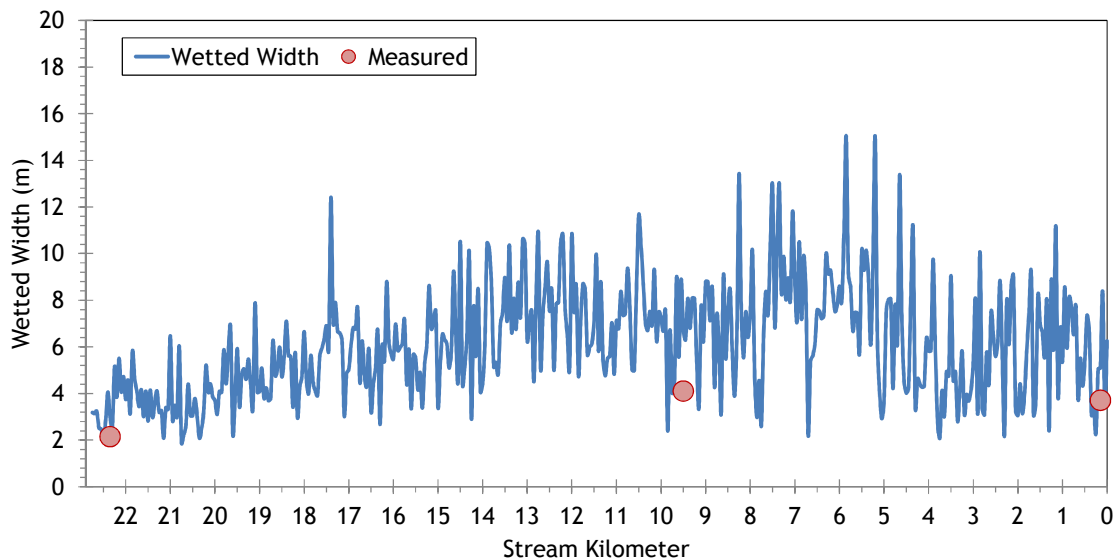


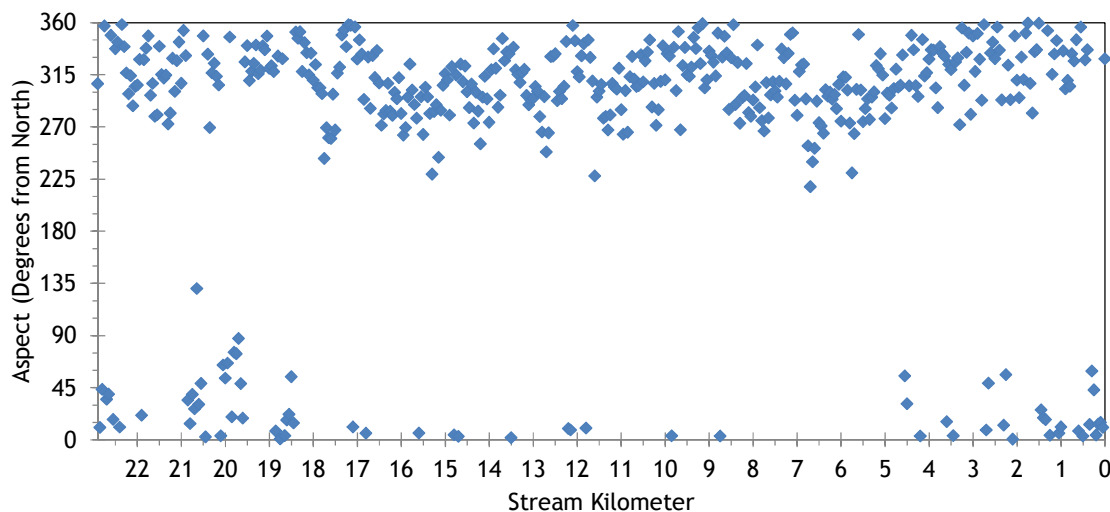
Figure 189 displays the measured and sampled wetted widths for Beaver Creek. The average width was about 6 meters during the simulation time period.

Figure 189 - Beaver Creek wetted widths.



Beaver Creek flows generally in the northwesterly direction (Figure 190).

Figure 190 - Beaver Creek stream aspect.



Topographic shade angles on Beaver Creek are somewhat higher than other streams in the watershed (Figure 191). Maximum values regularly exceed 30 degrees, while the minimums are generally above 10 degrees in most reaches.

Figure 191 - Beaver Creek topographic shade angles.

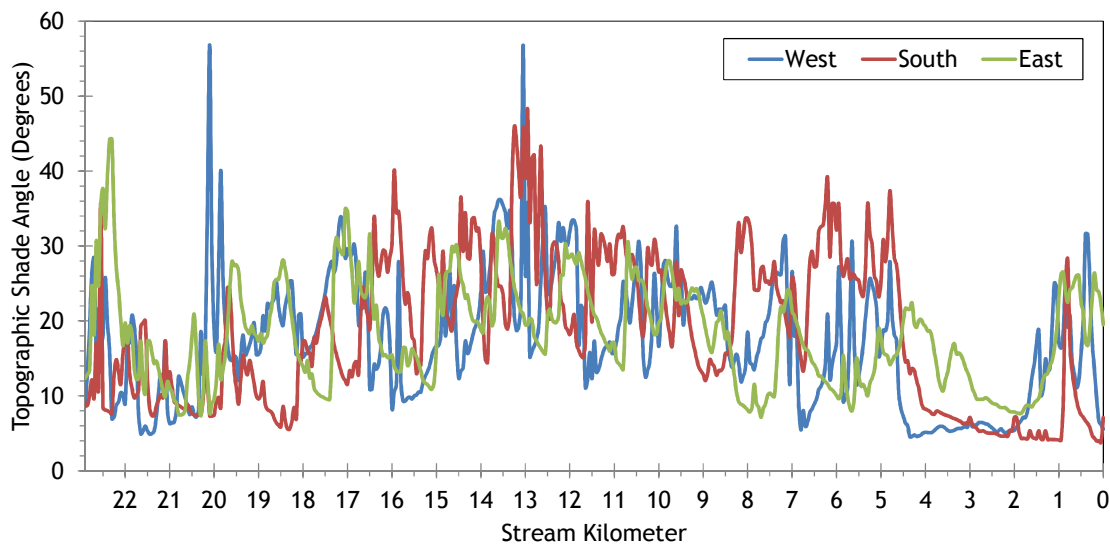


Figure 192 shows the land cover heights sampled along Beaver Creek. The maximum and average of the 28 radial samples were calculated for each 50-meter stream node. (Note: Heat Source uses each of the 28 radial samples for each 50-meter node. The maximum and average are shown here for simplification purposes.)

Figure 192 - Beaver Creek land cover heights sampled from highest hit LiDAR.

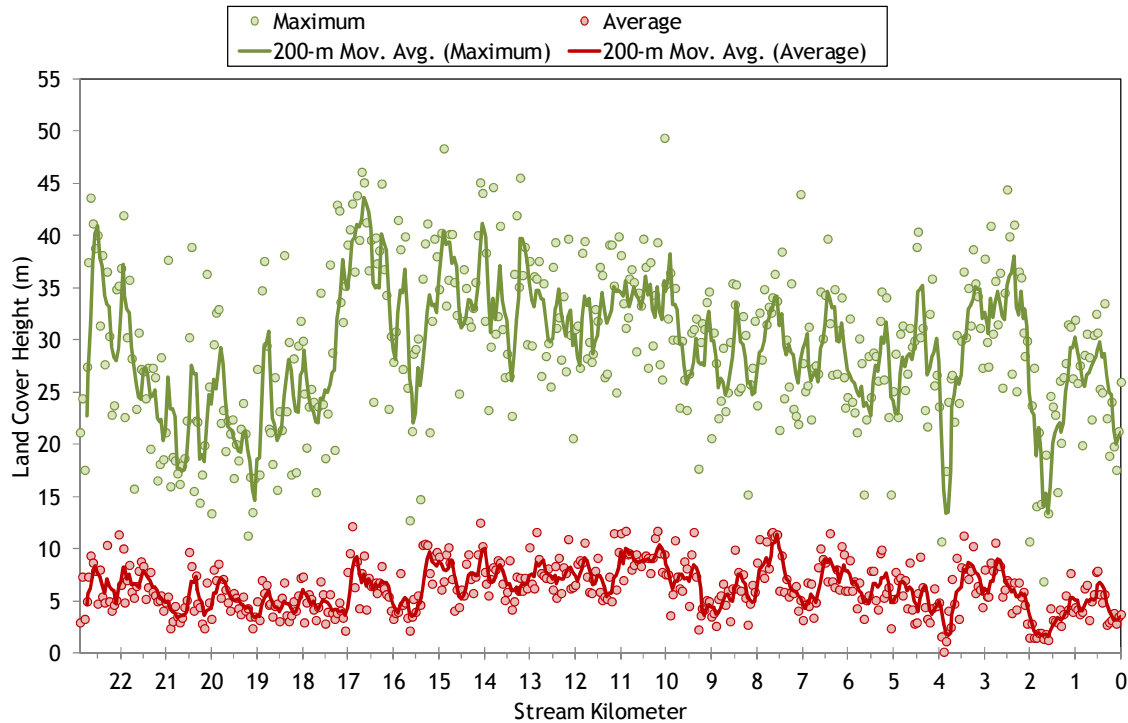
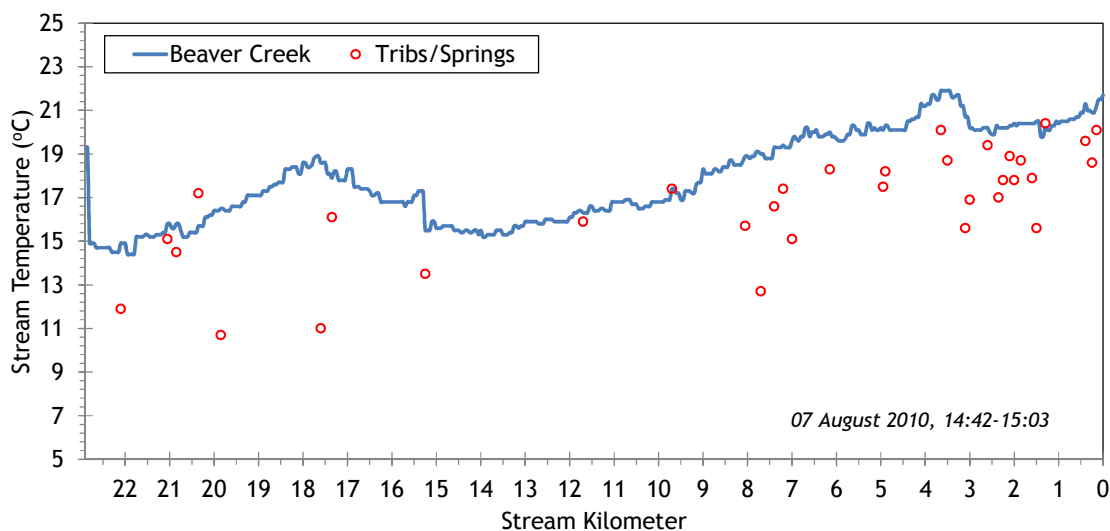


Figure 193 shows the TIR stream temperature profile of Beaver Creek. The stream was leaving the La Grande Reservoir at approximately 15°C at the time of the TIR flight.

Figure 193 - Beaver Creek TIR stream temperature profile.



19.2 Beaver Creek Heat Source Calibration Results

Beaver Creek was simulated from La Grande Reservoir to the mouth (Figure 194).

Figure 194 - Beaver Creek simulation extent.

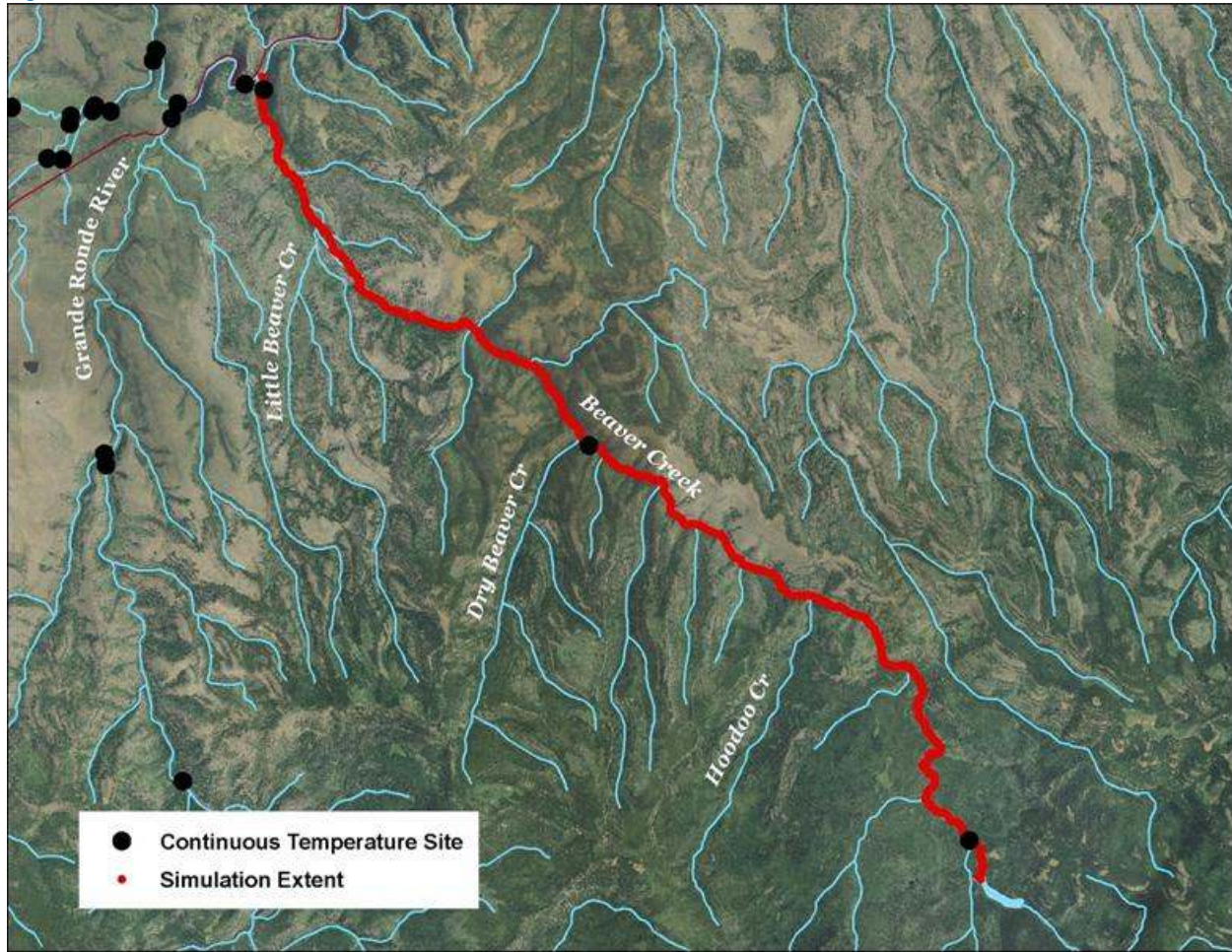


Table 30 - Beaver Creek general Heat Source parameters.

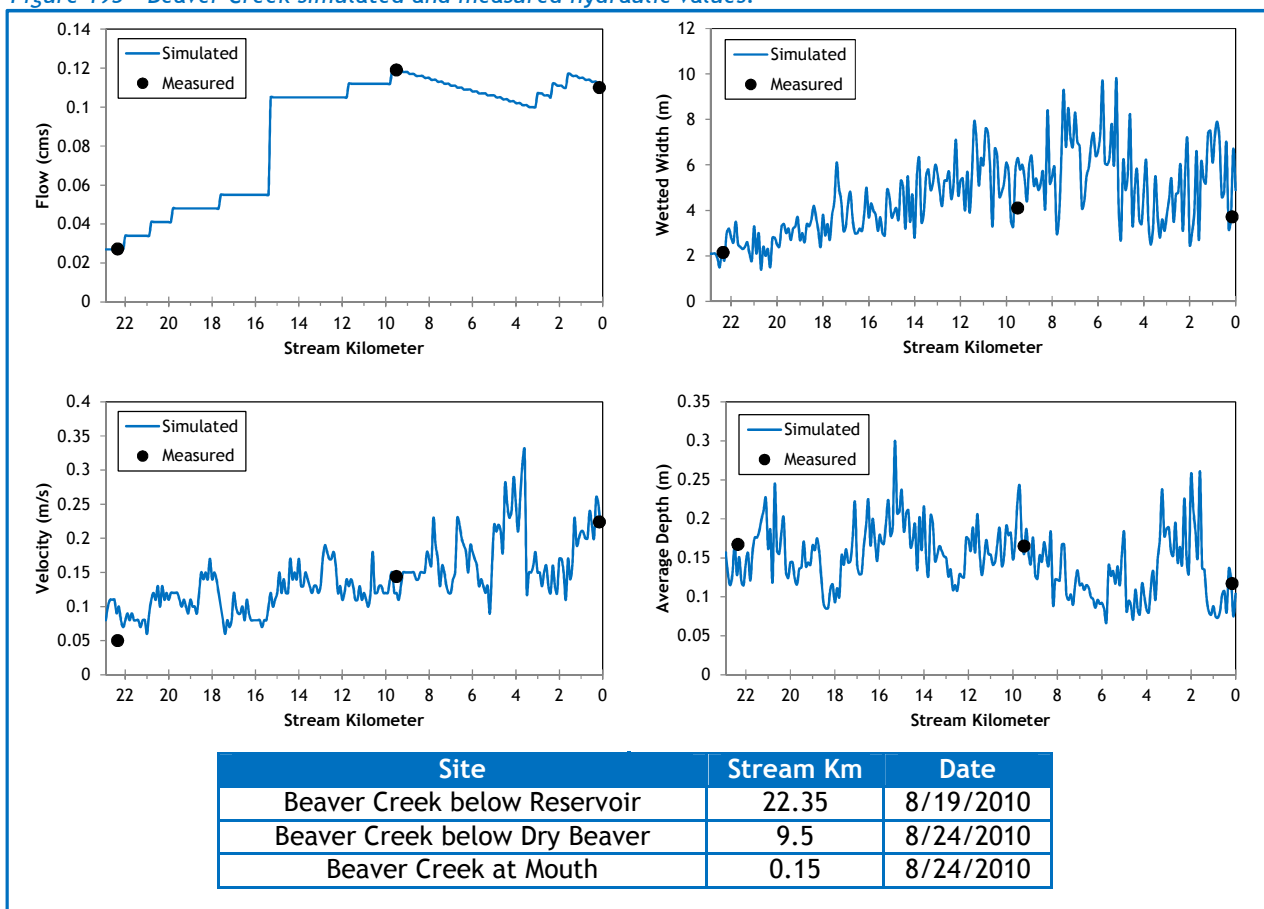
Stream:	Beaver Creek
Length:	22.9 kilometers
Time Period:	August 6-27, 2010
Input Distance Step:	50 meters
Output Distance Step:	100 meters
Time Step:	1 minute
Flush Initial Condition:	7 days
TIR Date and Time:	August 7, 2010 14:42-15:03
Land Cover Data Source:	LiDAR
Land Cover Sampling Distance Step:	15 meters

The following assumptions were used when calibrating the Beaver Creek Heat Source model:

- Hourly climate data is from the La Grande airport. Wind speeds were reduced 50% and air temperatures were adjusted using the adiabatic lapse rate.
- Wetted widths were roughly digitized from the TIR and LiDAR intensity images. The model reduced the value sampled by TTools by 20-34% in order to accommodate the other hydraulic values.

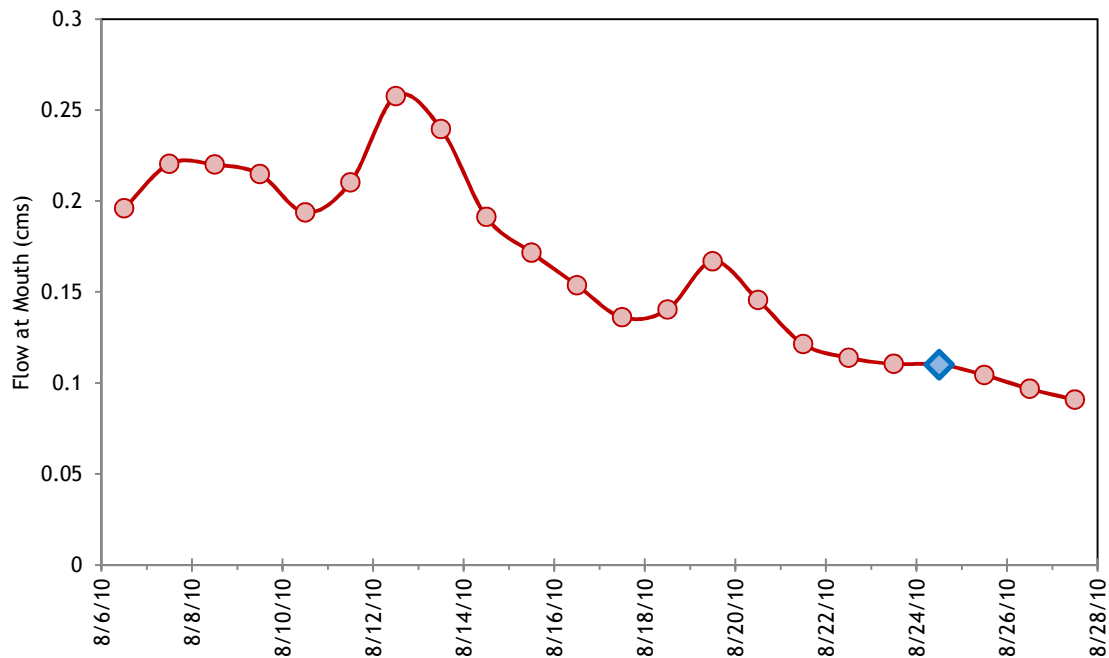
Figure 195 summarizes the simulated and measured hydraulic values from the calibrated model. The simulated values are from August 24th, while the measurements were taken on various days. There was an unverified losing reach between kilometer 9.5 and the mouth, based on measurements taken on August 24, 2010. The loss was accounted for in the simulation by gradually removing 1 cfs across the lower 9.5 kilometers.

Figure 195 - Beaver Creek simulated and measured hydraulic values.



The simulated daily flow volumes at the mouth of Beaver Creek are shown in Figure 196. The daily values were extrapolated from gage measurements on the Grande Ronde River.

Figure 196 - Beaver Creek simulated flows at the mouth.



The tributaries and springs included in the calibrated model are listed in Table 31. Hoodoo Creek was the largest tributary and was creating a significant thermal signature in the TIR imagery. The other tributaries were all assumed to be of equal (small) volume. Hourly temperature data was estimated by using the values recorded on Beaver Creek upstream of Dry Beaver Creek, minus the difference between the tributary (TIR temperature) and the Beaver Creek upstream of Dry Beaver Creek temperature.

Table 31 - Beaver Creek mass inflow features and assumptions.

Feature	Stream Km	Assumptions
Cove Creek	22.0	0.006-0.01 cms, hourly temps based on Beaver Cr. u/s Dry Beaver Cr. minus difference of TIR observation.
West Fork Beaver Cr.	20.85	0.006-0.01 cms, hourly temps based on Beaver Cr. u/s Dry Beaver Cr. minus difference of TIR observation.
Unnamed Tributary	19.8	0.006-0.01 cms, hourly temps based on Beaver Cr. u/s Dry Beaver Cr. minus difference of TIR observation.
Spring	17.6	0.006-0.01 cms, hourly temps based on Beaver Cr. u/s Dry Beaver Cr. minus difference of TIR observation.
Hoodoo Creek	15.3	0.04-0.1 cms, hourly temps based on Beaver Cr. u/s Dry Beaver Cr. minus difference of TIR observation.
Watermelon Creek	11.75	0.006-0.01 cms, hourly temps based on Beaver Cr. u/s Dry Beaver Cr. minus difference of TIR observation.
Dry Beaver Creek	9.75	0.006-0.01 cms, hourly temps based on Beaver Cr. u/s Dry Beaver Cr. minus difference of TIR observation.
Little Beaver Creek	3.0	0.006-0.01 cms, hourly temps based on Beaver Cr. u/s Dry Beaver Cr. minus difference of TIR observation.
Unnamed Tributary	2.35	0.006-0.01 cms, hourly temps based on Beaver Cr. u/s Dry Beaver Cr. minus difference of TIR observation.

The simulated and measured longitudinal stream temperatures are shown in Figure 197.

Figure 197 - Beaver Creek simulated and measured longitudinal stream temperatures.

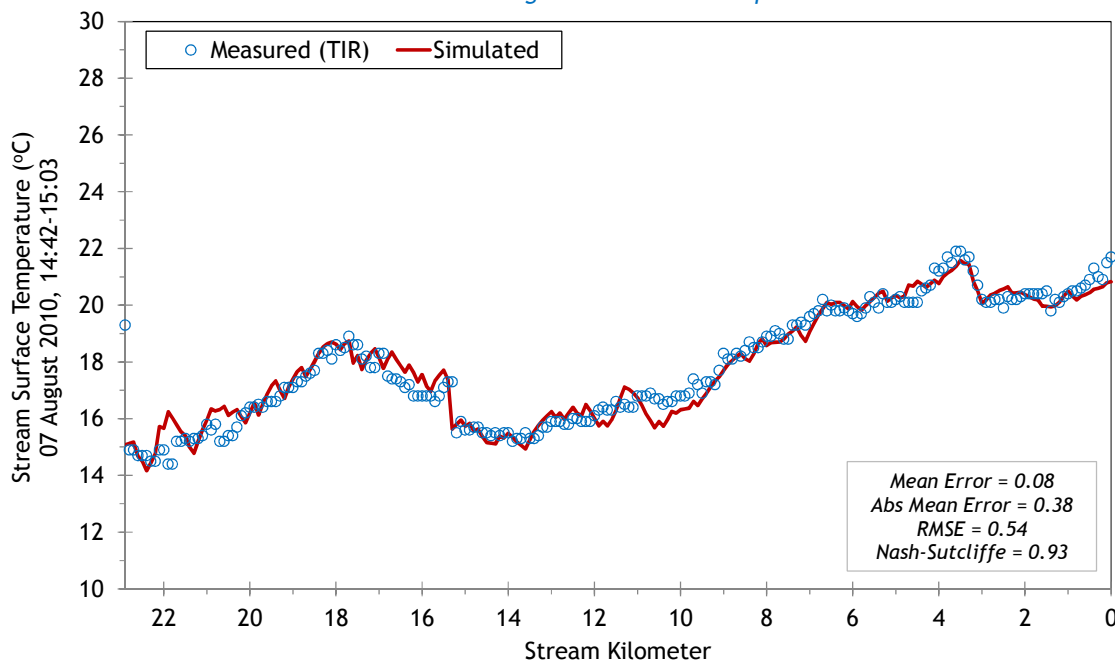
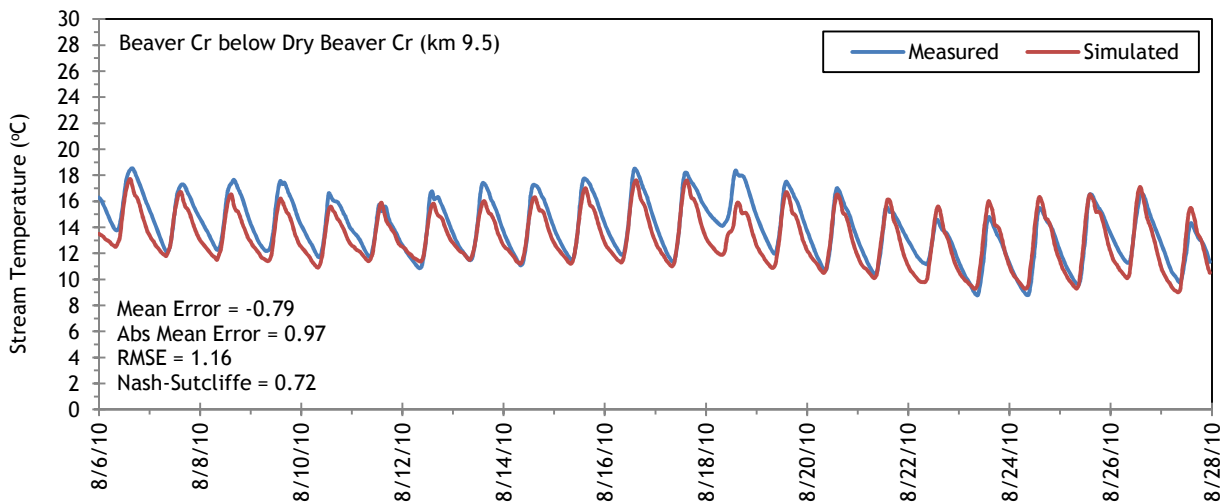
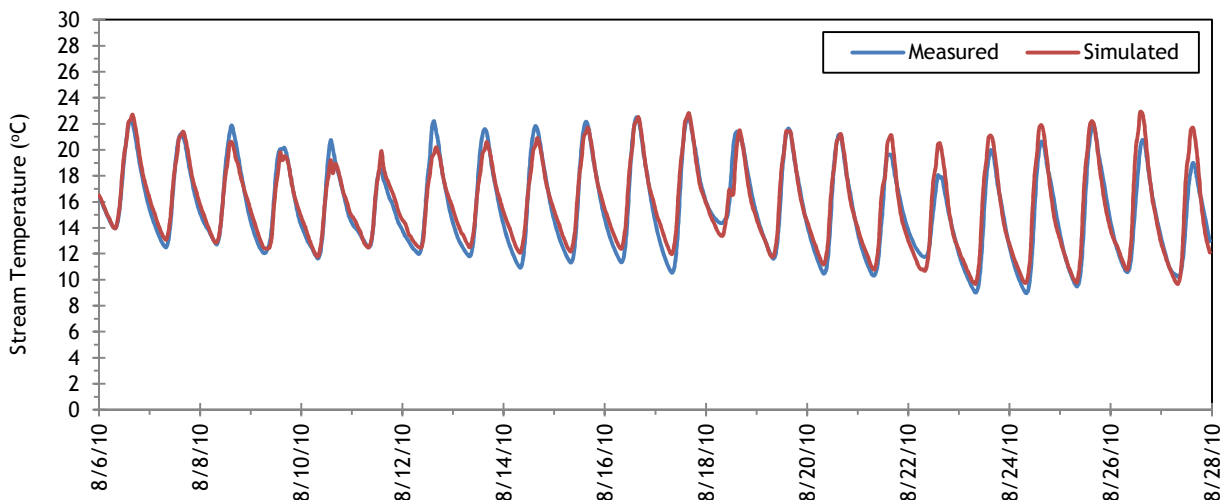


Figure 198 shows the simulated and measured hourly stream temperatures. Error statistics are also presented for each location.

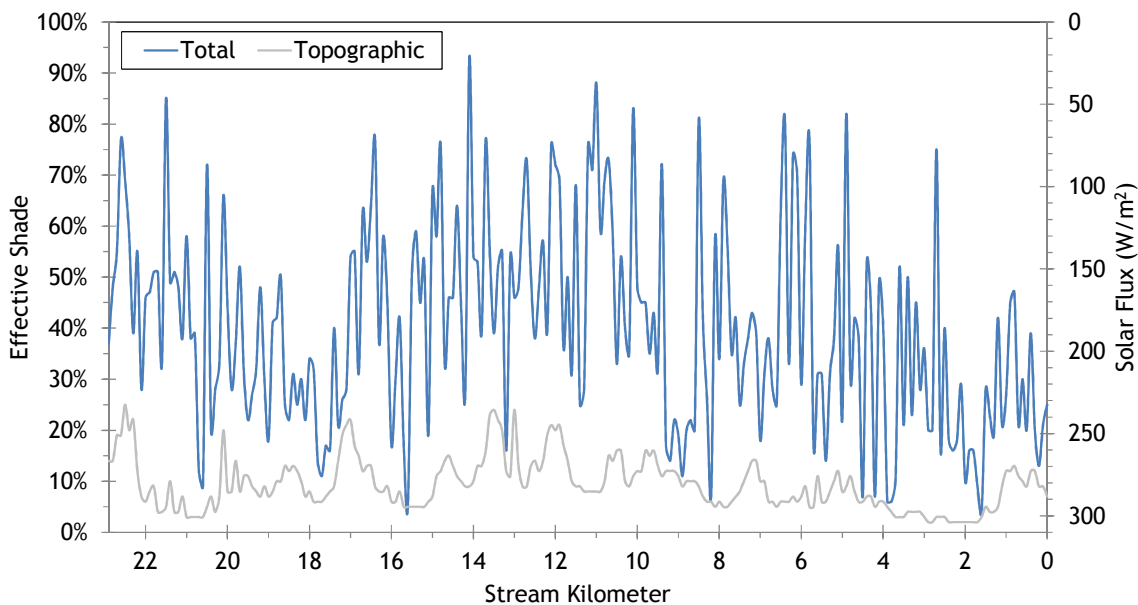
Figure 198 - Beaver Creek simulated and measured hourly stream temperatures.





The simulated effective shade values for Beaver Creek are presented in Figure 199. A fair amount of topographic shade occurs along Beaver Creek - upwards of 20% effective shade is created by topographic features in many locations. Beaver Creek is not very densely forested because of the wide grassy floodplain that occurs in so many reaches.

Figure 199 - Beaver Creek simulated effective shade.



20. FIVE POINTS CREEK

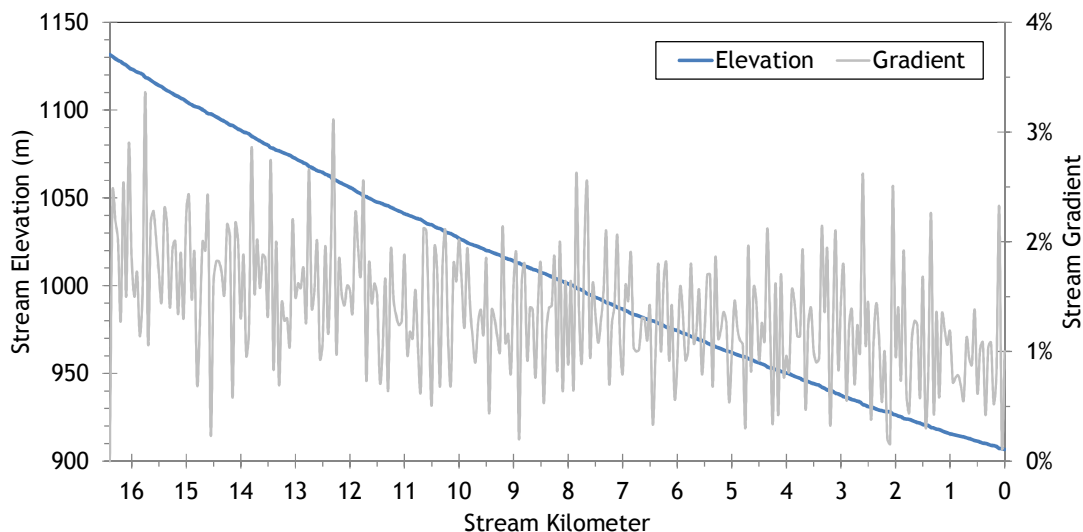


RGB-colored LiDAR point cloud - Five Points Creek below Little John Day Creek (looking downstream).

20.1 Five Points Creek TTools Results

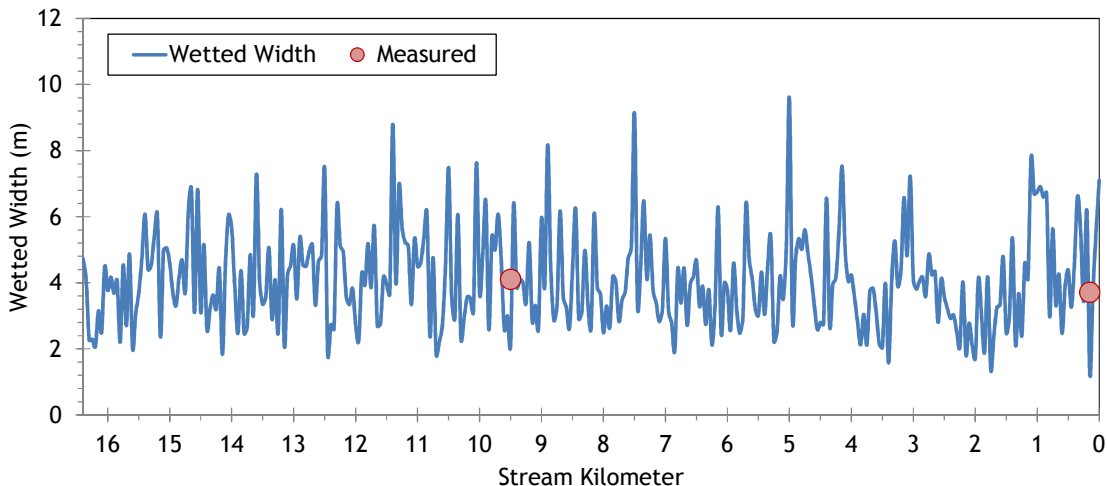
Figure 200 shows the sampled elevations and gradients for Five Points Creek. Gradients were generally between 1% and 2%. The stream flows through mostly confined valley in a mountainous terrain.

Figure 200 - Five Points Creek elevation and gradient.



Five Points Creek is also relatively small during the summertime. Figure 201 shows the measured and sampled wetted widths. The average width was about 4 meters for most of the stream.

Figure 201 - Five Points Creek wetted widths.



Five Points Creek flows from north to south, before joining the Grande Ronde River (Figure 202).

Figure 202 - Five Points Creek stream aspect.

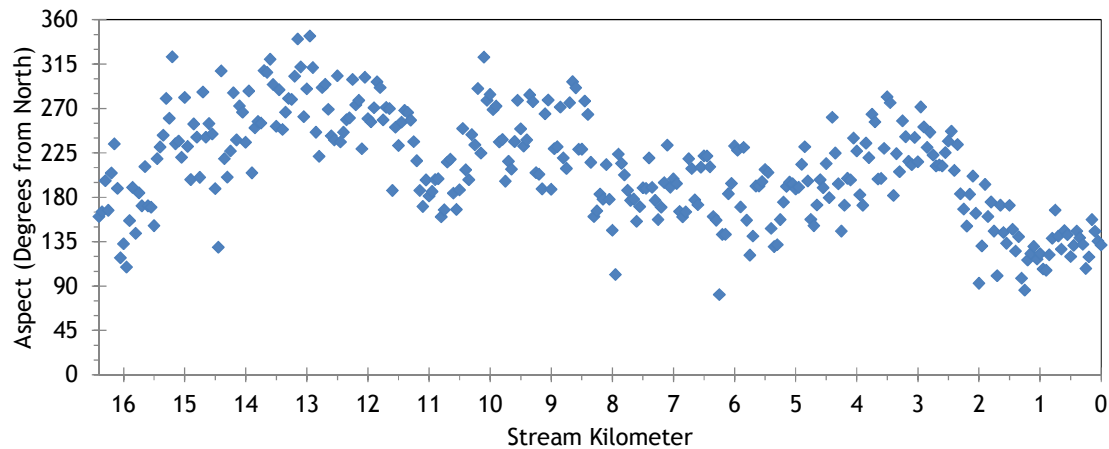


Figure 203 shows the topographic shade angles sampled for Five Points Creek. Overall, there is a significant amount of topographic shade on Five Points Creek.

Figure 203 - Five Points Creek topographic shade angles.

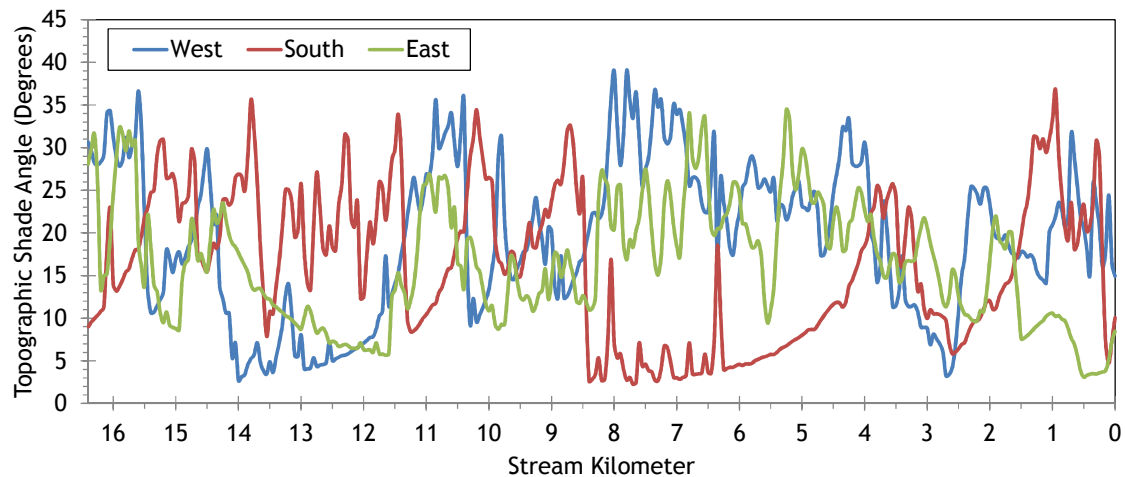
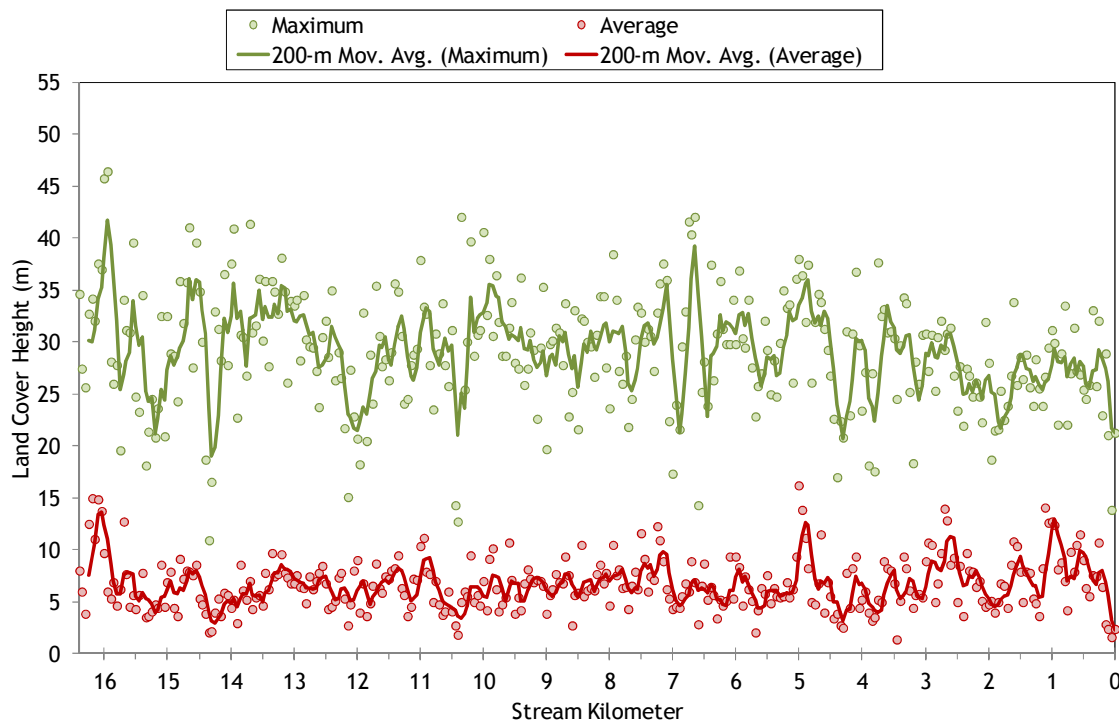


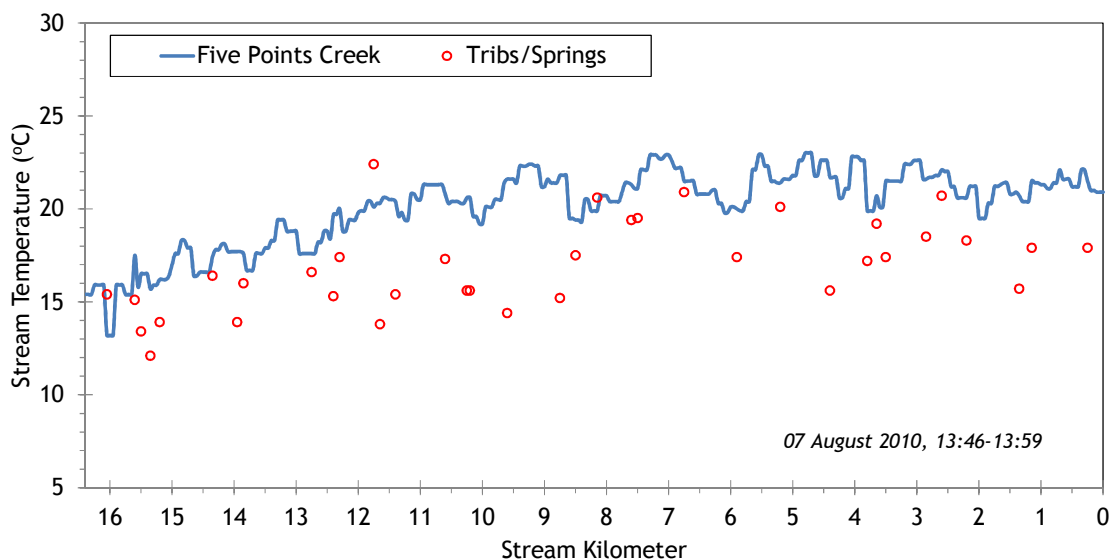
Figure 204 shows the land cover heights sampled along Five Points Creek. The maximum and average of the 28 radial samples were calculated for each 50-meter stream node. (Note: Heat Source uses each of the 28 radial samples for each 50-meter node. The maximum and average are shown here for simplification purposes.)

Figure 204 - Five Points Creek land cover heights sampled from highest hit LiDAR.



The TIR stream temperature profile of Five Points Creek is shown in Figure 205. The low flow volumes at the time of the flight are the primary reason for so much variability in the temperature profile. Smaller stream volumes are more sensitive to environmental factors that influence stream temperature.

Figure 205 - Five Points Creek TIR stream temperature profile.



20.2 Five Points Creek Heat Source Calibration Results

Five Points Creek flows from the north to the south and joins the Grande Ronde River. Figure 206 shows the simulation extent of the Heat Source model.

Figure 206 - Five Points Creek simulation extent.

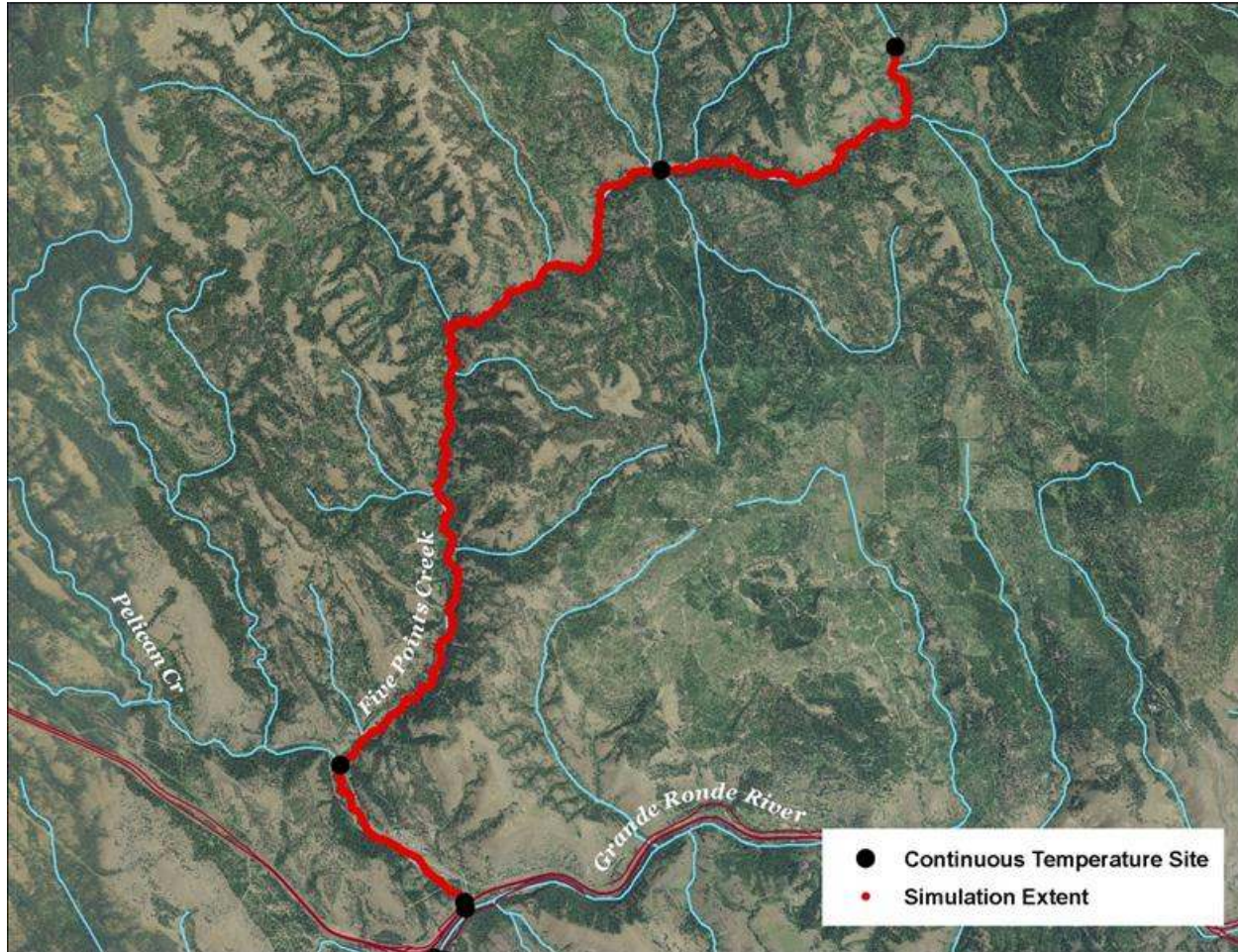


Table 32 - Five Points Creek general Heat Source parameters.

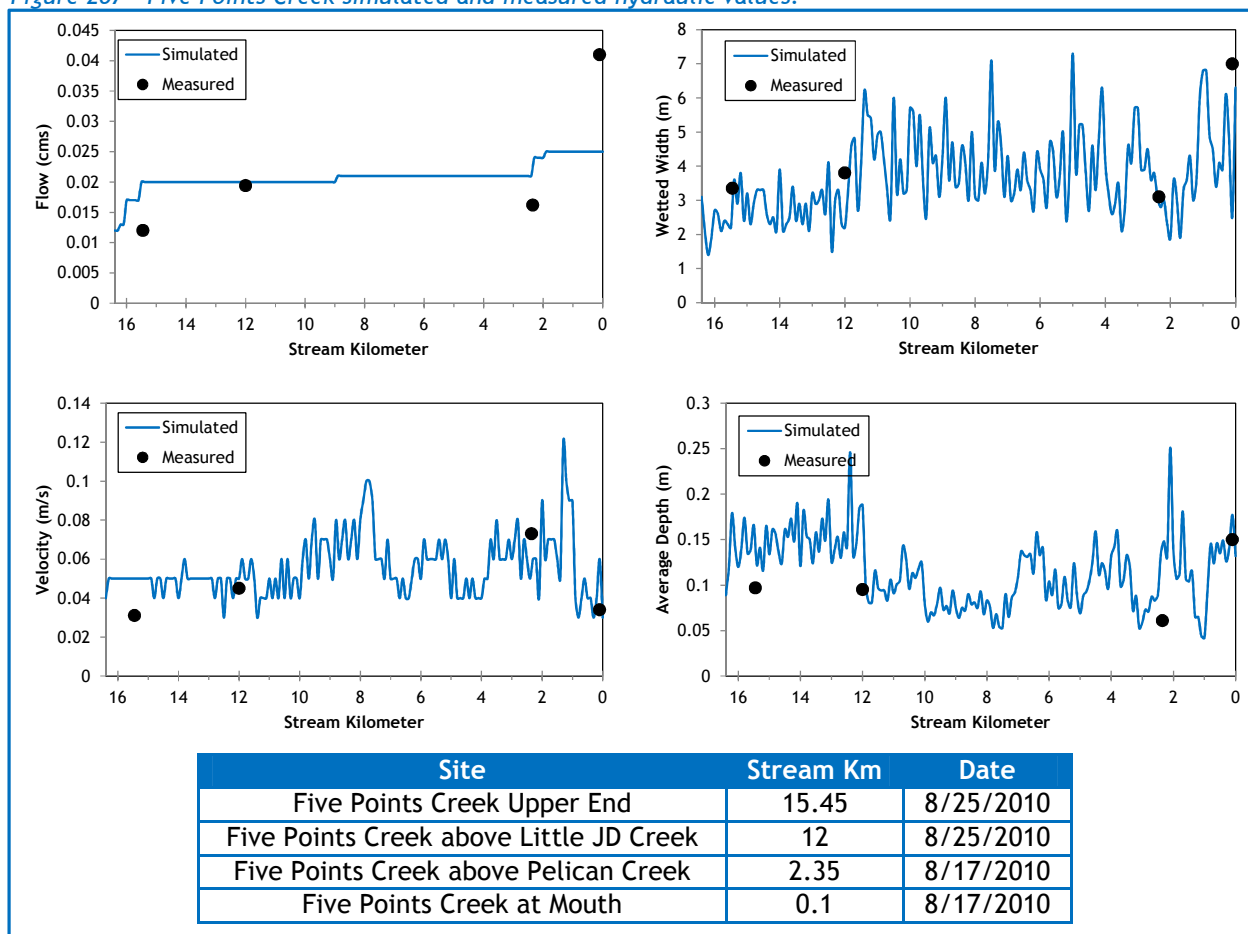
Stream:	Beaver Creek
Length:	22.9 kilometers
Time Period:	August 6-27, 2010
Input Distance Step:	50 meters
Output Distance Step:	100 meters
Time Step:	1 minute
Flush Initial Condition:	7 days
TIR Date and Time:	August 7, 2010 14:42-15:03
Land Cover Data Source:	LiDAR
Land Cover Sampling Distance Step:	15 meters

The following assumptions were used when calibrating the Five Points Creek Heat Source model:

- Hourly climate data was obtained from the La Grande airport (NWS). Wind speeds were reduced to better represent forested mountain terrain. Air temperatures were adjusted using the adiabatic lapse rate.
- Wetted widths were digitized from the TIR and LiDAR intensity images. The calibrated model used 66% of the TTools-sampled value in the upper 4.4 stream kilometers, while 100% of sampled wetted width was used in the lower 12 kilometers.

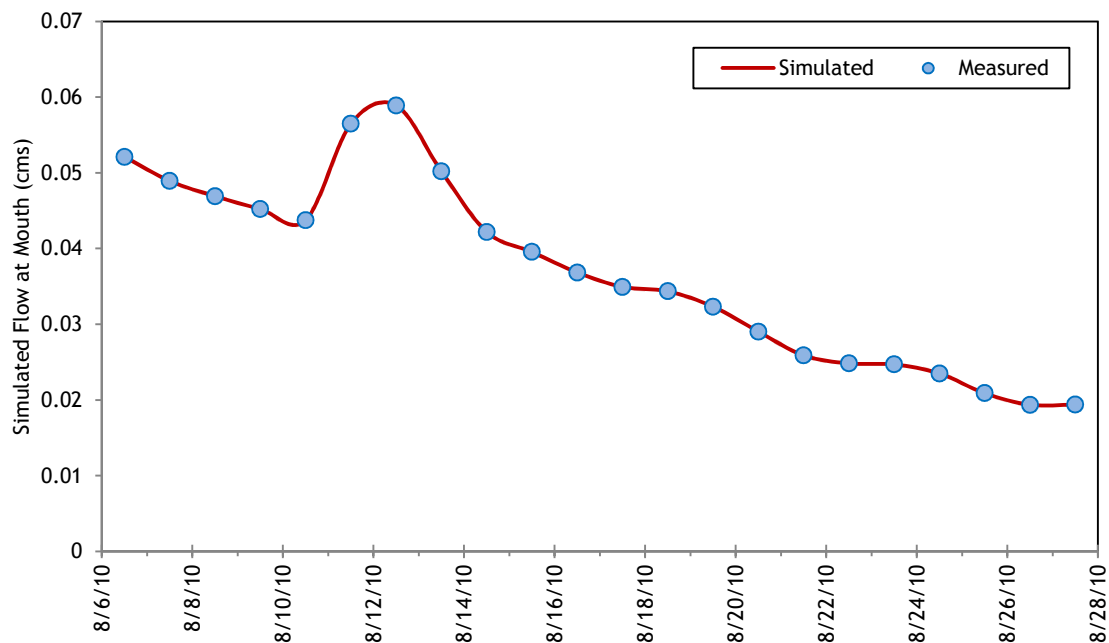
Figure 207 summarizes the simulated and measured hydraulic values for Five Points Creek. The simulated values are from August 25th, while the measured values were obtained on various dates.

Figure 207 - Five Points Creek simulated and measured hydraulic values.



The simulated daily flows at the mouth of Five Points Creek are presented in Figure 208. Daily variability was extrapolated from data measured at the Grande Ronde River gage near Perry.

Figure 208 - Five Points Creek simulated flow at mouth.



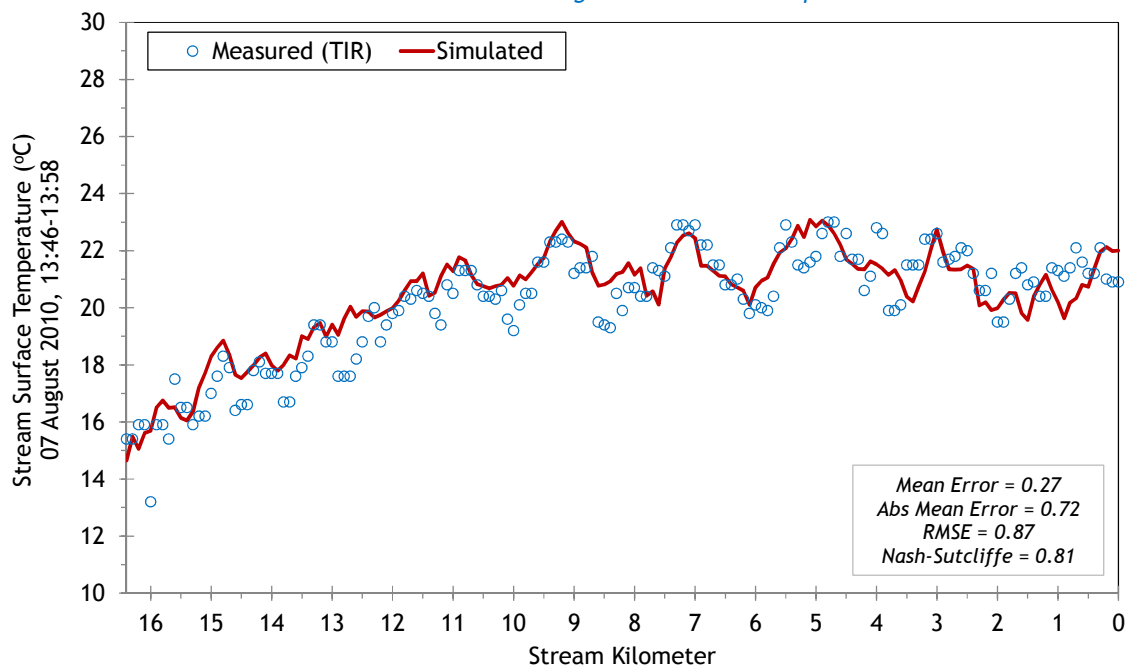
There were three active tributaries observed in the TIR imagery (Table 33). The flow volumes for each were estimated to be the same, while the TIR sampled temperatures were used for each.

Table 33 - Five Points Creek mass inflow features and assumptions.

Feature	Stream Km	Assumptions
Fiddlers Hell Creek	16.0	0.003-0.008 cms at constant 15.4°C
Tie Creek	15.5	0.003-0.008 cms at constant 13.4°C
Pelican Creek	2.3	0.003-0.008 cms at constant 18.3°C

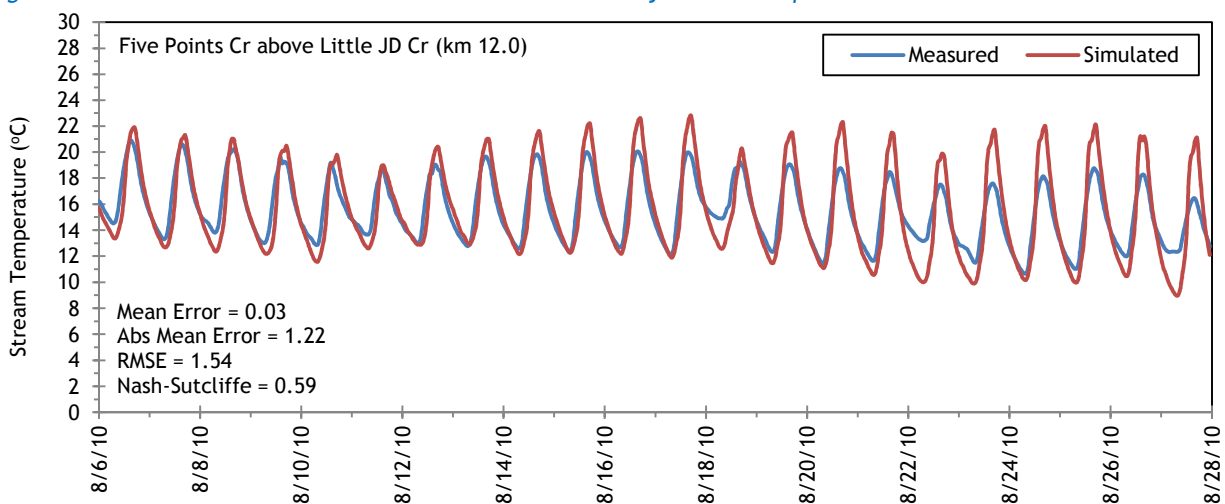
Figure 209 shows the simulated and measured longitudinal stream temperatures for Five Points Creek. There is a great deal of variability in the longitudinal temperatures mainly because of the low flow volume during the simulation time period.

Figure 209 - Five Points Creek simulated and measured longitudinal stream temperatures.



The simulated and measured hourly stream temperatures are presented in Figure 210. There were three locations where hourly stream temperatures were recorded.

Figure 210 - Five Points Creek simulated and measured hourly stream temperatures.



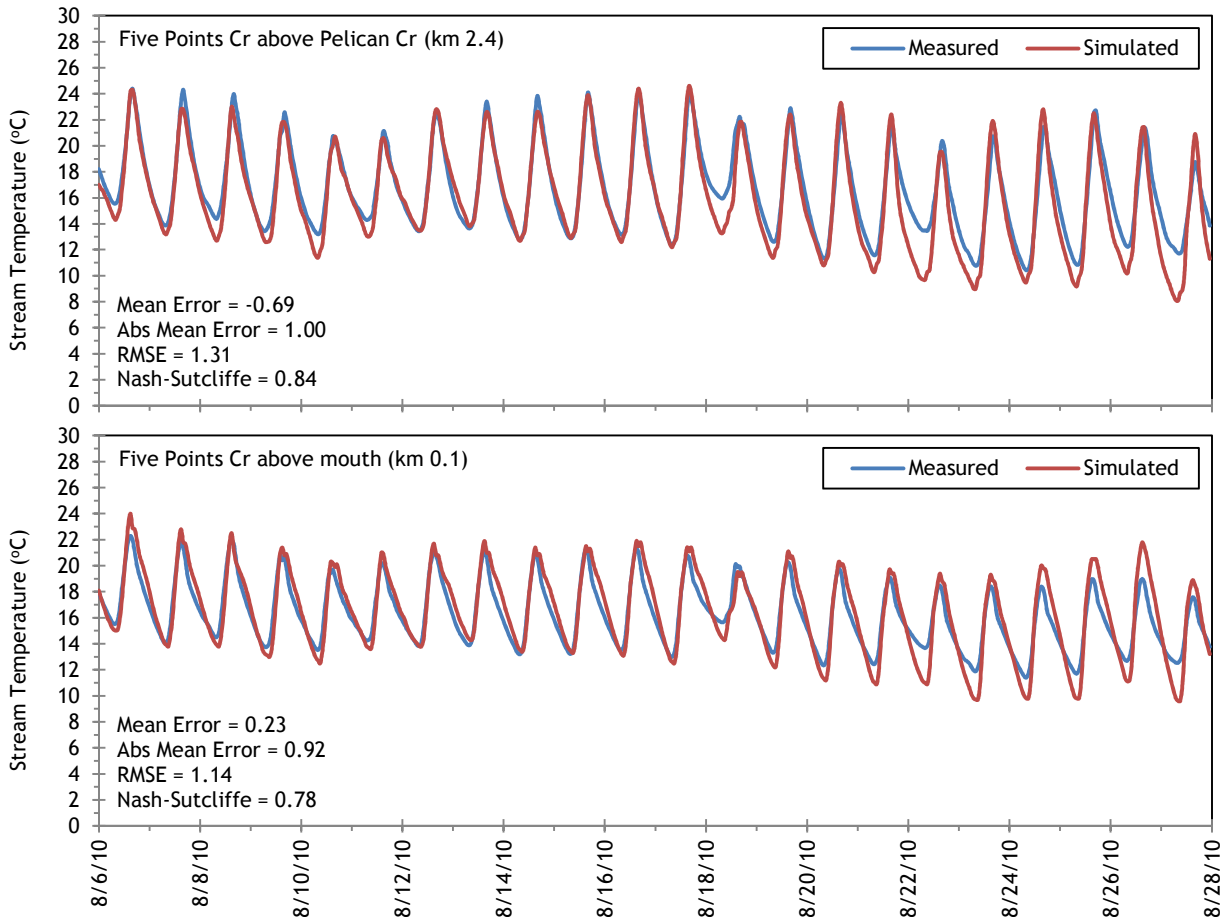
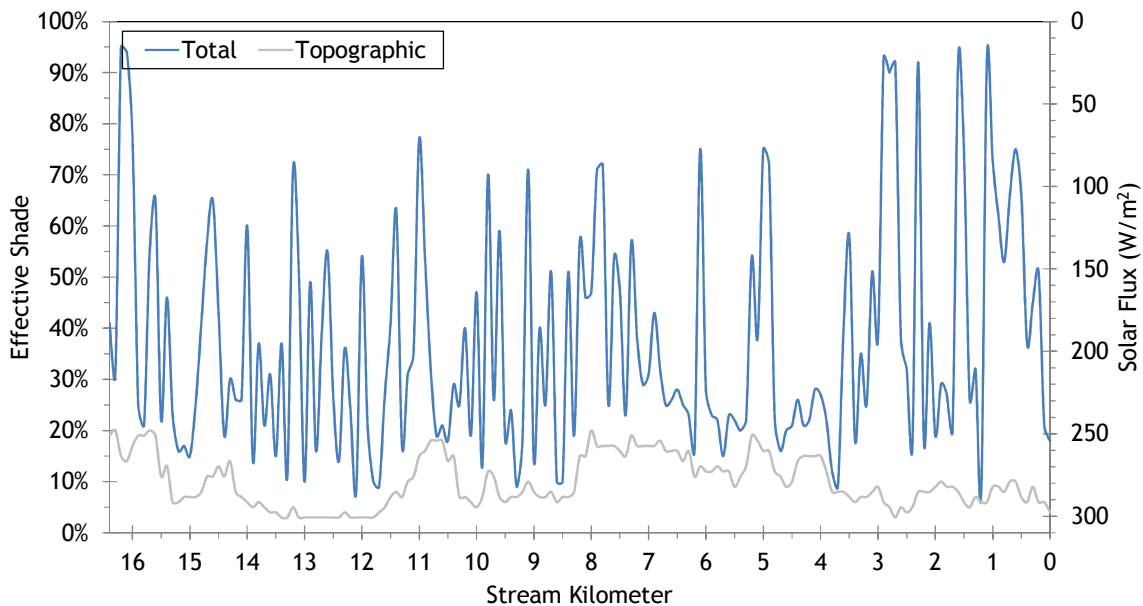
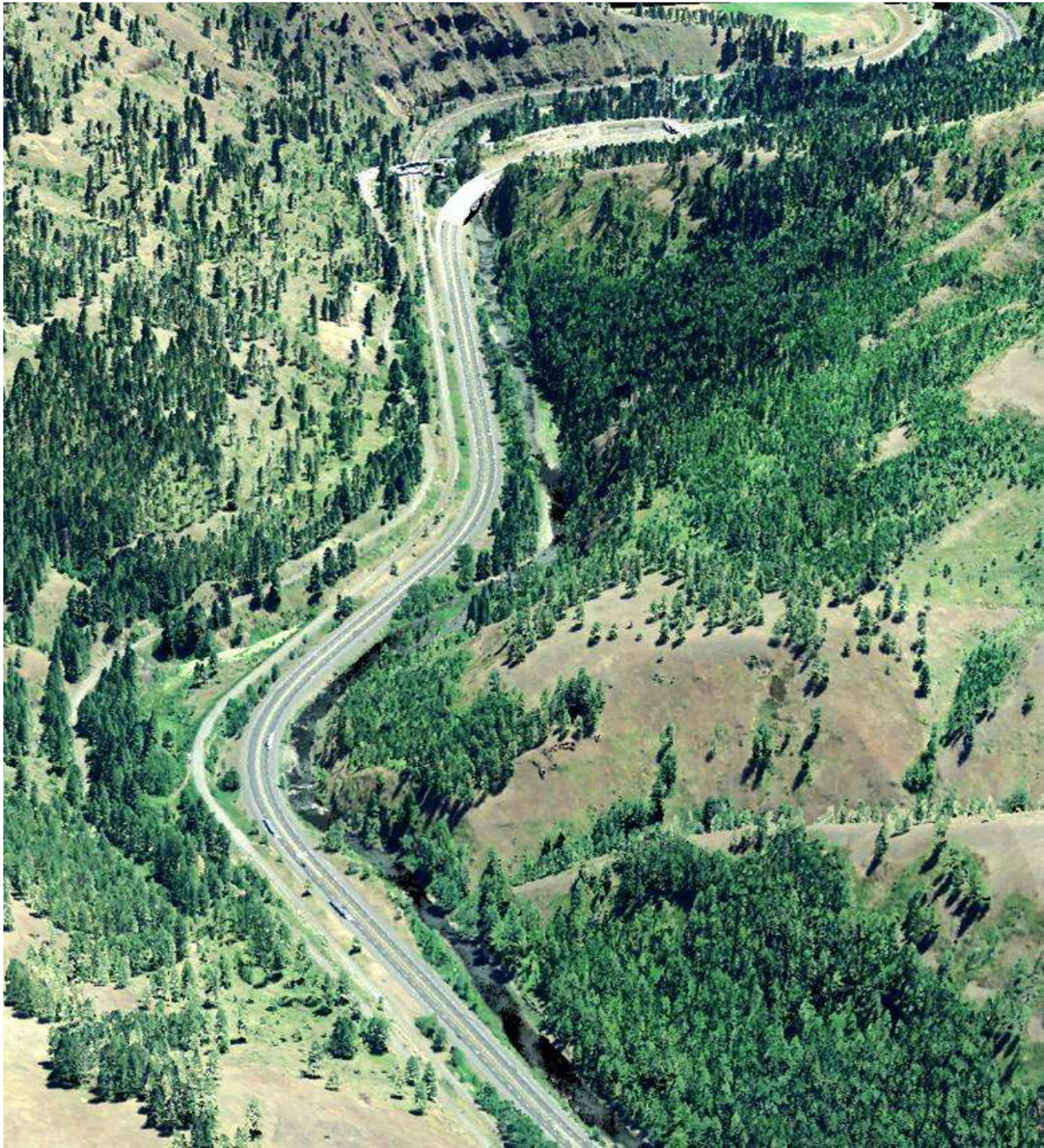


Figure 211 shows the simulated effective shade values for Five Points Creek. There is a fair amount of topographic shade created by the mountainous terrain.

Figure 211 - Five Points Creek simulated effective shade.



21. GRANDE RONDE RIVER



RGB-colored LiDAR point cloud - Grande Ronde River alongside Interstate 84, below Five Points Creek (looking downstream).

21.1 Grande Ronde River TTools Results

The Grande Ronde River elevations and gradients were sampled from the bare earth LiDAR data (Figure 212). The upper reaches have a much higher gradient than the lower sections.

Figure 212 - Grande Ronde River elevation and gradient.

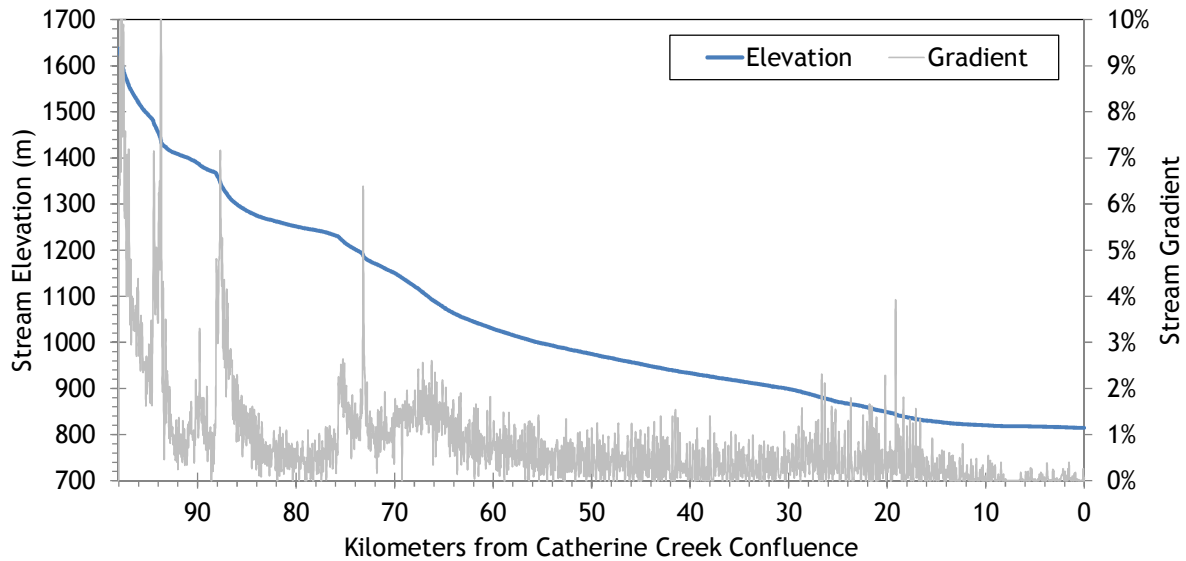


Figure 213 shows the sampled active and wetted channel widths along with the measured wetted widths. The Grande Ronde River generally gets wider as it flows downstream. Below stream kilometer 10, the channel is mostly diked and flows through a canal “State Ditch”.

Figure 213 - Grande Ronde River channel widths.

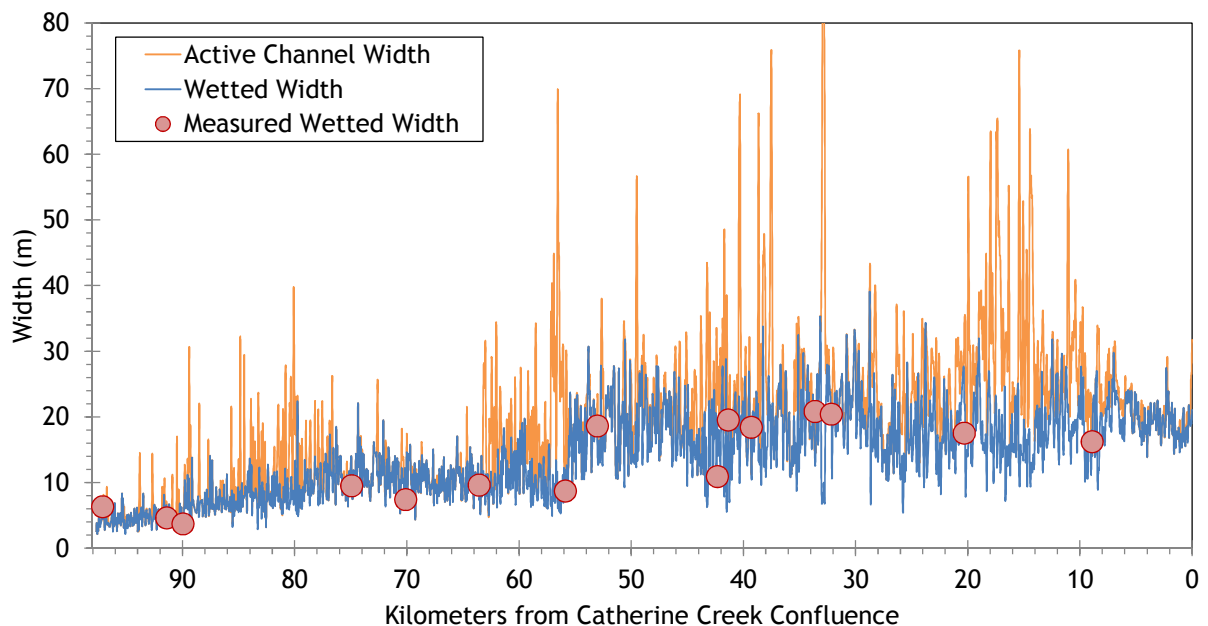
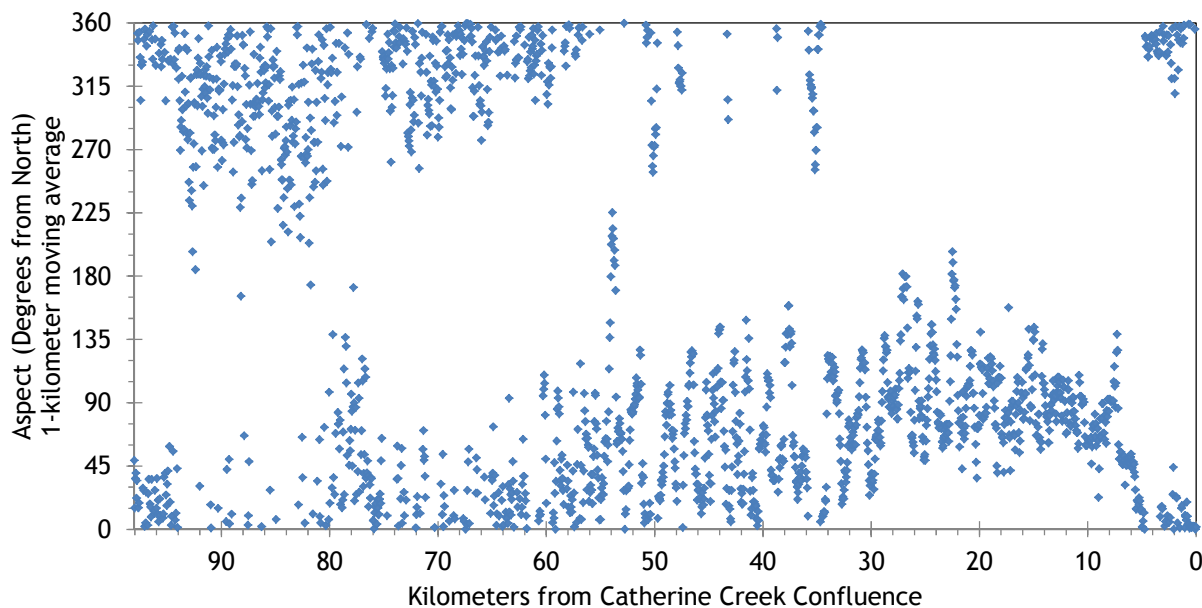


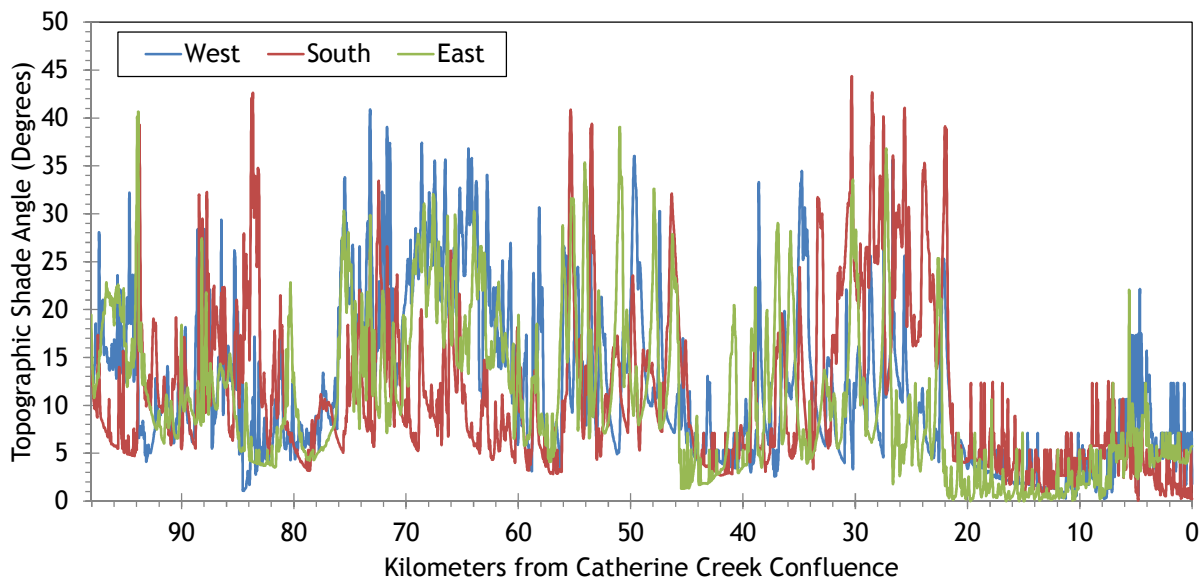
Figure 214 shows the stream aspect for each 50-meter segment of the Grande Ronde River. The river starts out flowing northerly, bends to the northeast between kilometers 60 and 30, then flows east through La Grande and the State Ditch.

Figure 214 - Grande Ronde River stream aspect.



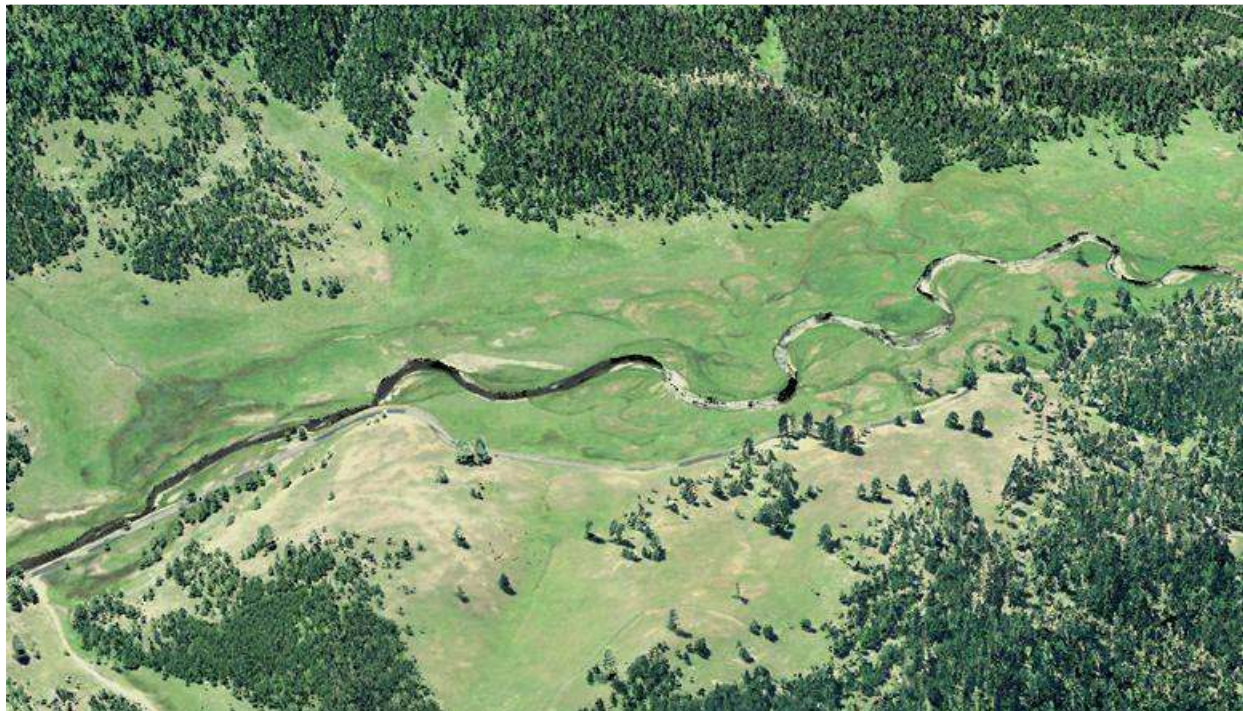
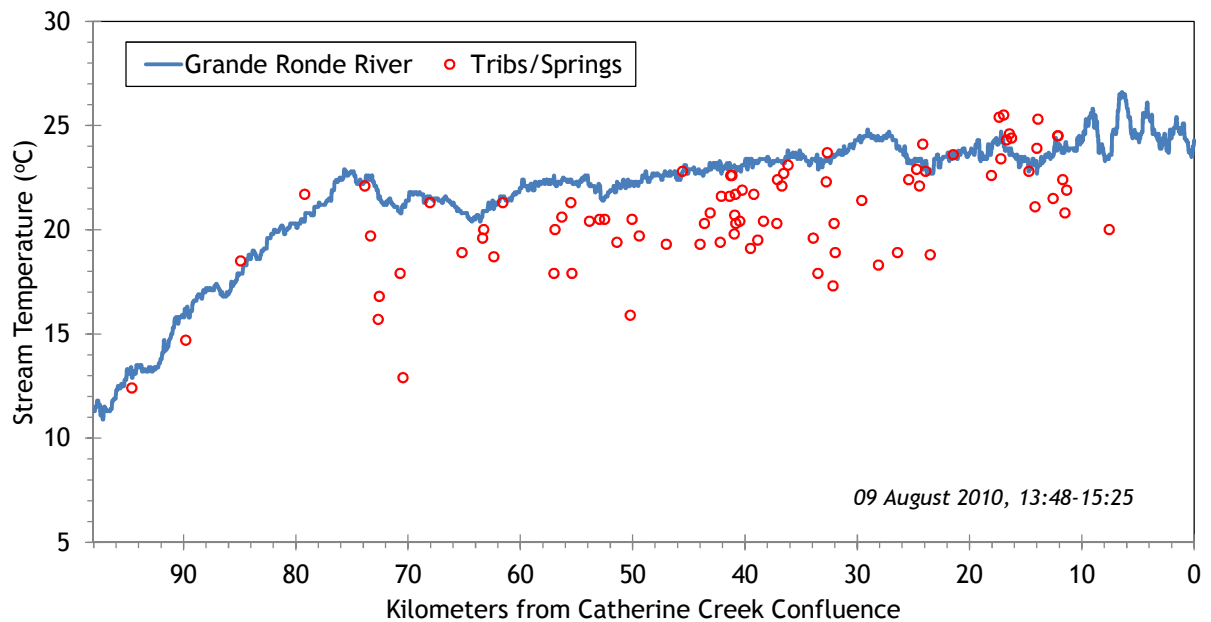
Topographic shade angles for the Grande Ronde River are shown in Figure 215. The upper river has a fair amount of topographic shade. The lower 20 kilometers are in the wide valley bottom and have much less topographic shade. In many of those lower 20 kilometers, the river banks are severely down-cut and it is the riverbanks that are producing the topographic shade.

Figure 215 - Grande Ronde River topographic shade angles.



The TIR stream temperature profile of the Grande Ronde River is shown in Figure 216. In the upper watershed, the stream is relatively cool, but heats steadily until approximately stream kilometer 75. Below that, stream temperatures hovered between 21 and 25°C during the TIR flight.

Figure 216 - Grande Ronde River TIR stream temperature profile.



RGB-colored LiDAR point cloud - Grande Ronde River at Vey Meadow (flowing from right to left of image).

21.2 Grande Ronde River Heat Source Calibration Results

The Grande Ronde River was simulated from just below Tanner Gulch to the Catherine Creek confluence (Figure 217).

Figure 217 - Grande Ronde River simulation extent.

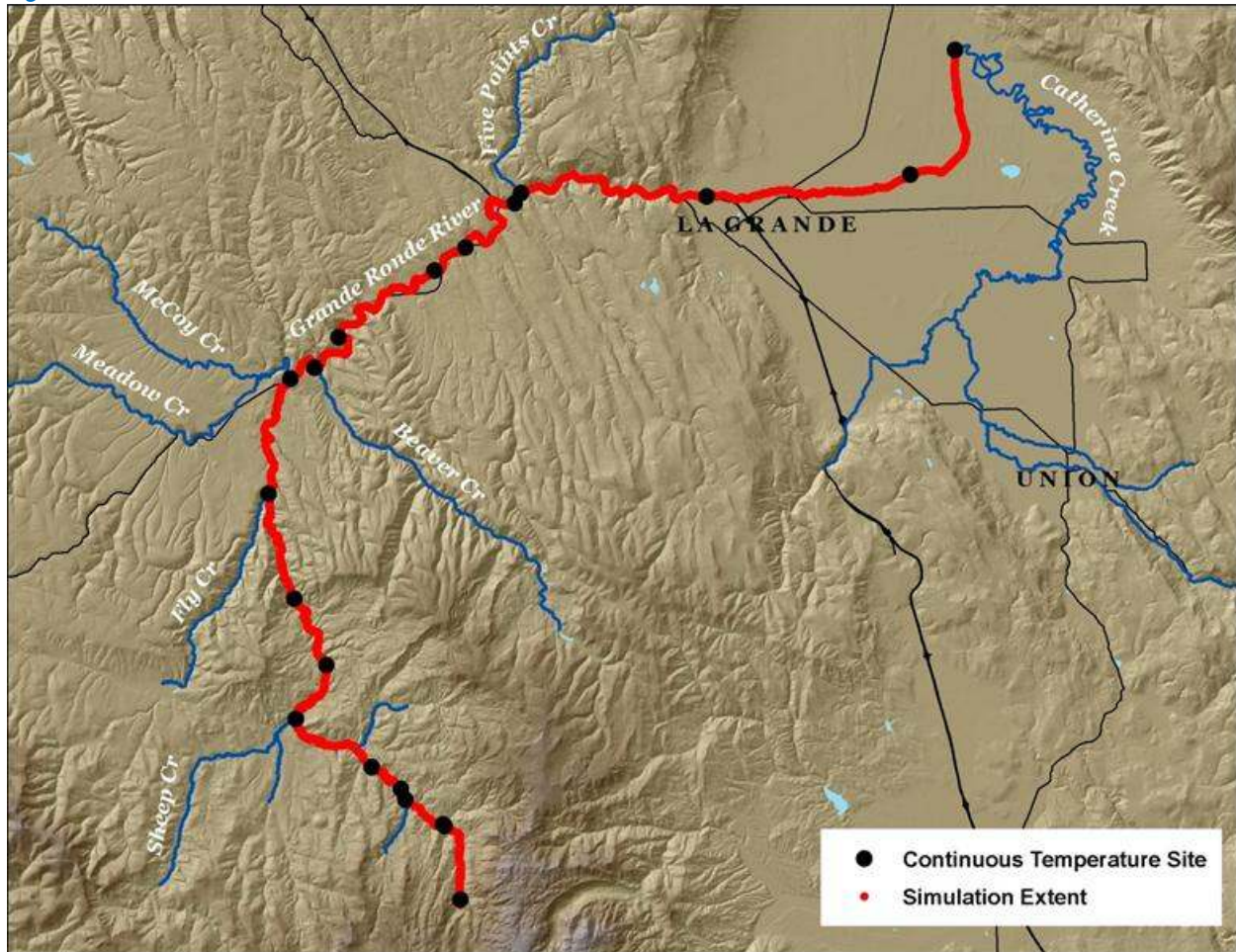


Table 34 - Grande Ronde River general Heat Source parameters.

Stream:	Grande Ronde River
Length:	97.2 kilometers
Time Period:	August 6-27, 2010
Input Distance Step:	50 meters
Output Distance Step:	100 meters
Time Step:	1 minute
Flush Initial Condition:	7 days
TIR Date and Time:	August 9, 2010 13:48-15:25
Land Cover Data Source:	LiDAR
Land Cover Sampling Distance Step:	15 meters

The following assumptions were used when calibrating the Grande Ronde River Heat Source model:

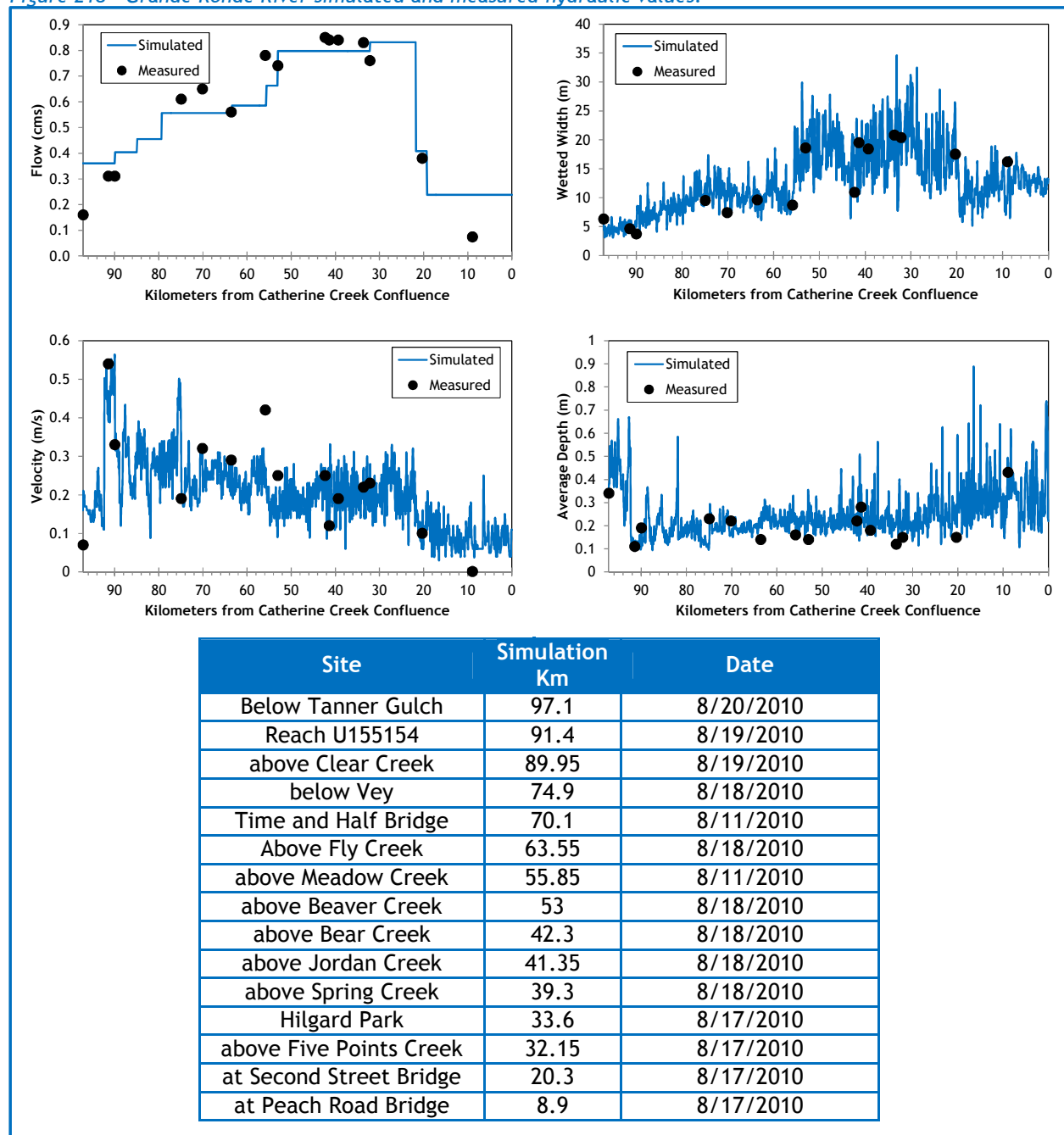
- Hourly climate data is from the La Grande airport. Wind speeds were reduced and air temperatures were adjusted for the adiabatic lapse rate of 1°C per 100 meters elevation.
- Wetted widths were digitized from the TIR and LiDAR intensity images.
- Most inflows observed in the TIR data were very small compared to the Grande Ronde River flow and did not produce measurable thermal influences. Therefore, only the larger inflows were included within the model, which includes but is not limited to the other simulated tributaries.
- There is significant withdrawal that occurs in La Grande. The withdrawals are not monitored and are likely to vary greatly during the simulation time period. Since the majority of water is consumed starting in the reaches through and below La Grande and the gradient is very low, the model exhibited instability below simulation kilometer 10. In addition, there is likely thermal stratification occurring in those low-gradient reaches below La Grande, which Heat Source is incapable of simulating. For these reasons, less water was removed at simulation the diversions than was probably actually occurring.
- **Model results below simulation kilometer 21.75 should be considered as rough estimates only and should not be used for regulatory or planning purposes.**



RGB-colored LiDAR point cloud - Grande Ronde River above Meadow Creek (looking downstream).

Figure 218 shows the simulated and measured hydraulics values for the Grande Ronde River. Note that the measured data was collected on several different days, while the simulated values are plotted only for August 18, 2010.

Figure 218 - Grande Ronde River simulated and measured hydraulic values.



The simulated and measured flows at each gage are shown in Figure 219. The flow volumes were set up within the model to target the measured daily average flows at each gage. There were small rain events around August 11th and 18th that resulted in elevated flow volumes.

Figure 219 - Grande Ronde River simulated and measured flows at the gages.

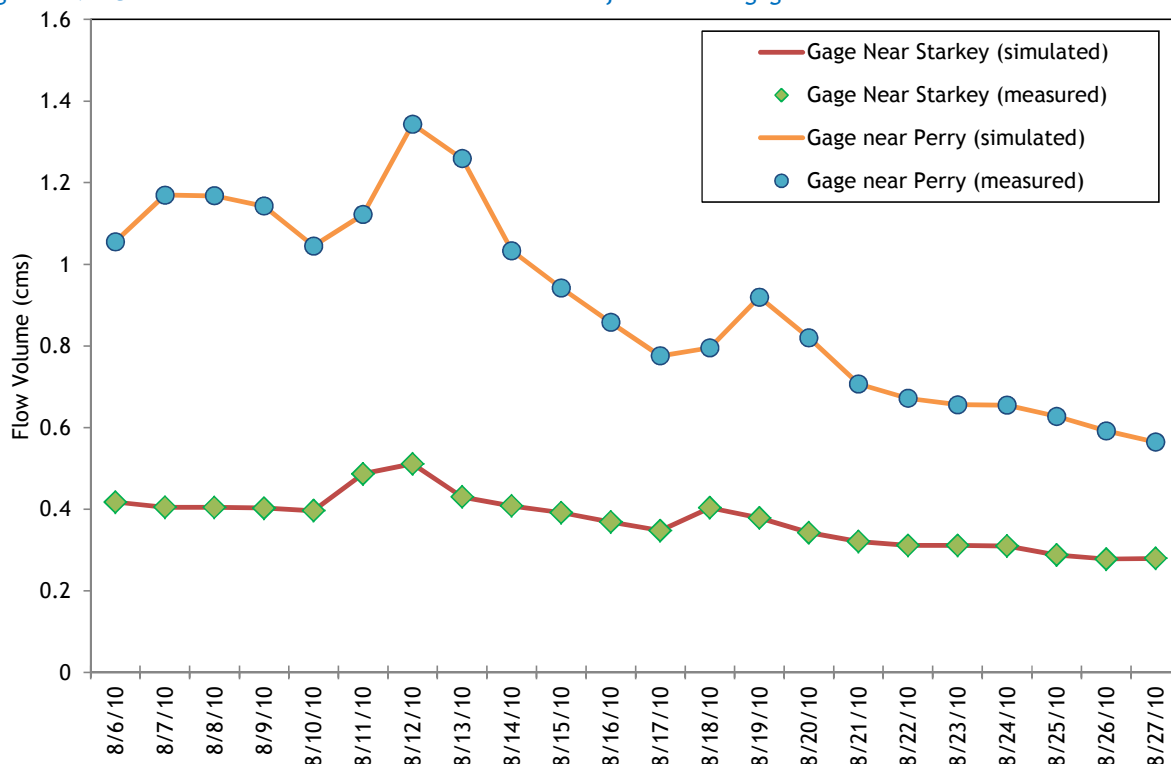


Table 1 summarizes the inflows and outflows included in the Grande Ronde River Heat Source model. All tributary flows had daily values estimated based on CRITFC measurements and patterns derived from Grande Ronde River gage data (see previous sections). Hourly stream temperatures were measured near the mouth of each tributary. The diversion rates were estimated as a constant percentage of the stream flow. The diversions were not monitored and values are uncertain; therefore, the simulation below

Table 35 - Grande Ronde River mass inflow and outflow features and assumptions.

Feature	Stream Km	Assumptions
Clear Creek	89.85	Simulated flow volume, measured hourly temperatures.
Limber Jim Creek	84.9	Simulated flow volume, measured hourly temperatures.
Sheep Creek	79.3	Simulated flow volume, measured hourly temperatures.
Fly Creek	63.35	Simulated flow volume, measured hourly temperatures.
Meadow Creek	55.55	Simulated flow volume, measured hourly temperatures.
Beaver Creek	52.95	Simulated flow volume, measured hourly temperatures.
Bear Creek	42.1	Simulated flow volume, measured hourly temperatures.
Spring Creek	38.95	Simulated flow volume, measured hourly temperatures.
Rock Creek	32.75	Simulated flow volume, measured hourly temperatures.
Five Points Creek	32.1	Simulated flow volume, measured hourly temperatures.
Dobbins Diversion	21.75	Estimated to be 51% of stream flow - based on 8/17/2010 CRITFC upstream and downstream flow measurements.
Diversion	19.2	Estimated to be 40% of stream flow (further reduction causes model instability)

The simulated and measured longitudinal stream temperatures are shown in Figure 220. There is an apparent “drop” in the simulated temperature near kilometer 38, but that is an artifact of the model changing times for its output data. Upstream of that location, the simulation output is for the 14:00 hour, and downstream the simulation output is for the 15:00 hour, causing an artificial temperature drop. The results below kilometer 21.75 should be considered for information purposes only because the diversions were not monitored and there is likely thermal stratification occurring.

Figure 220 - Grande Ronde River simulated and measured longitudinal stream temperatures.

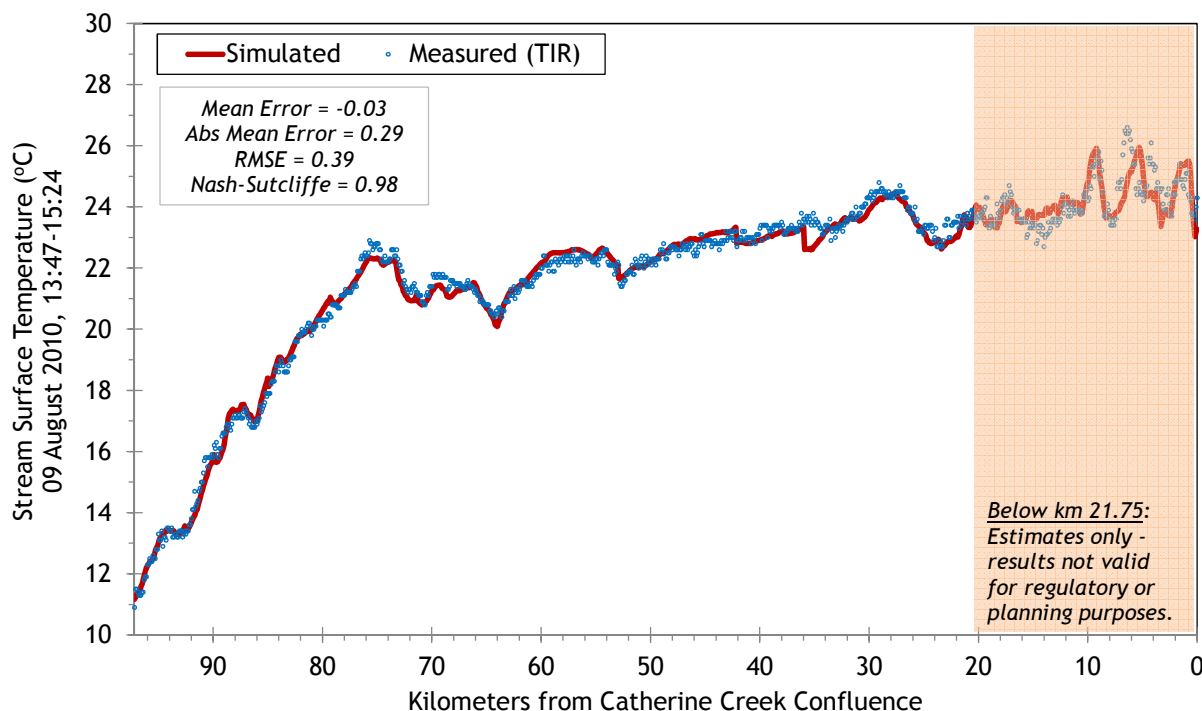
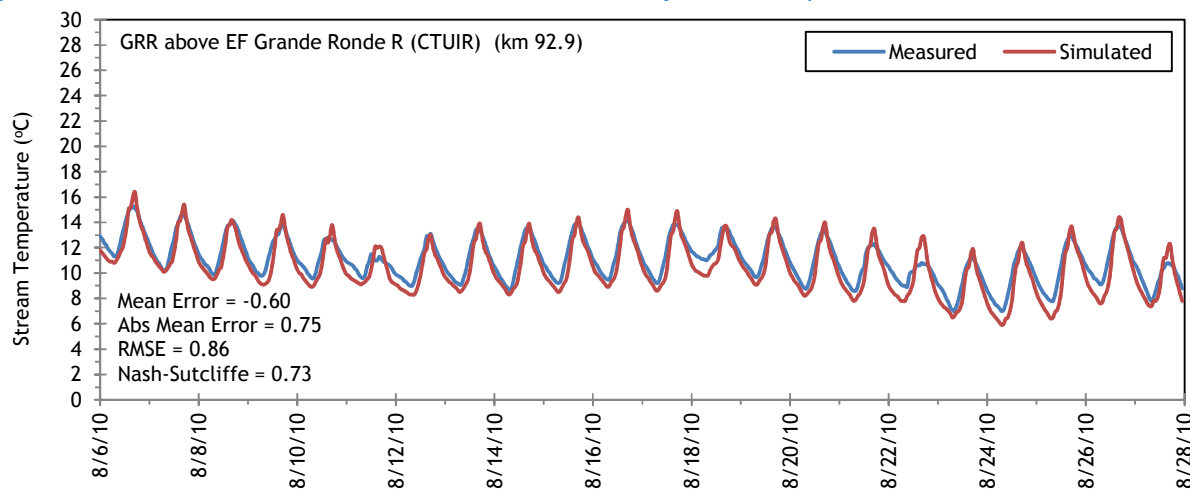
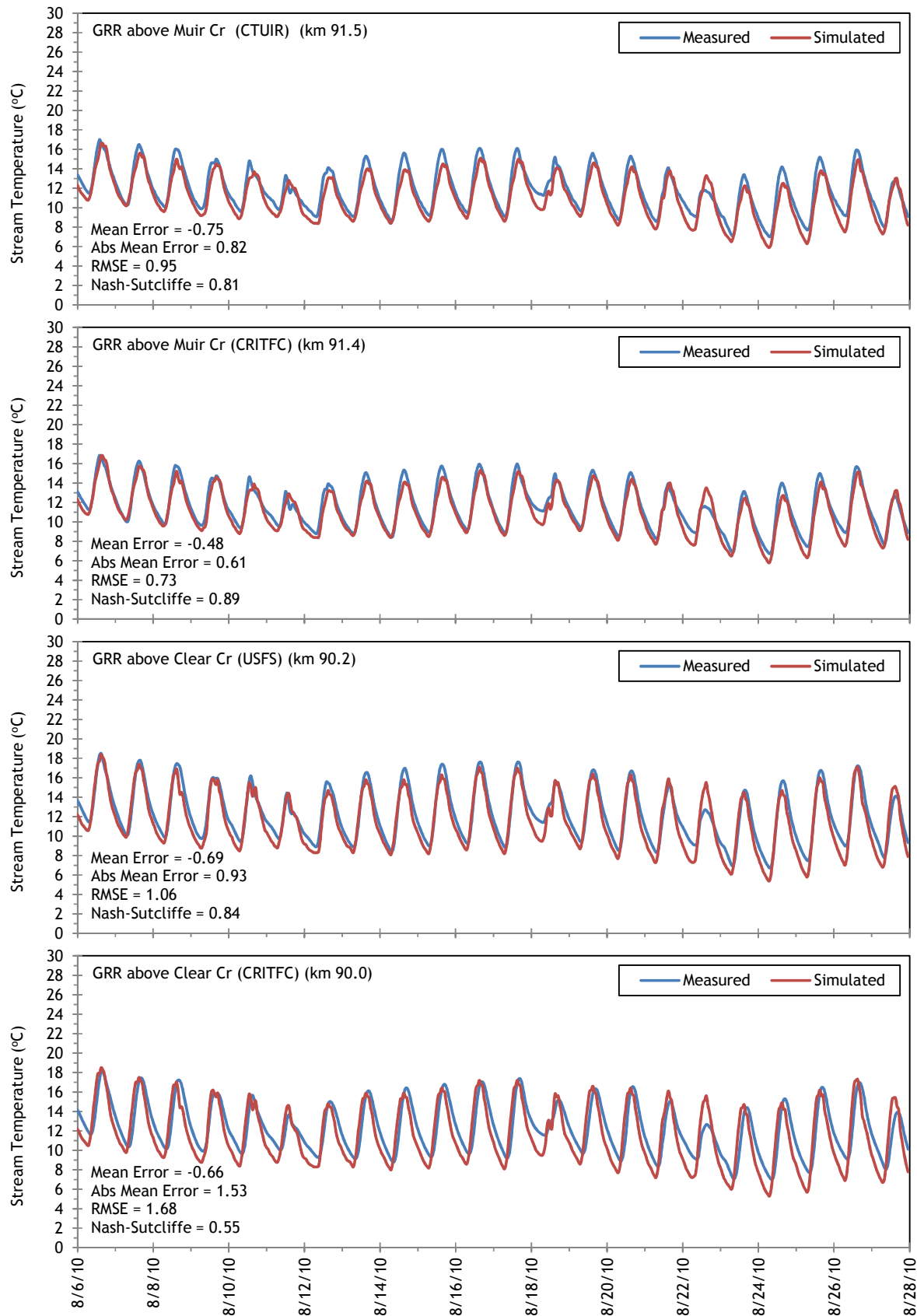
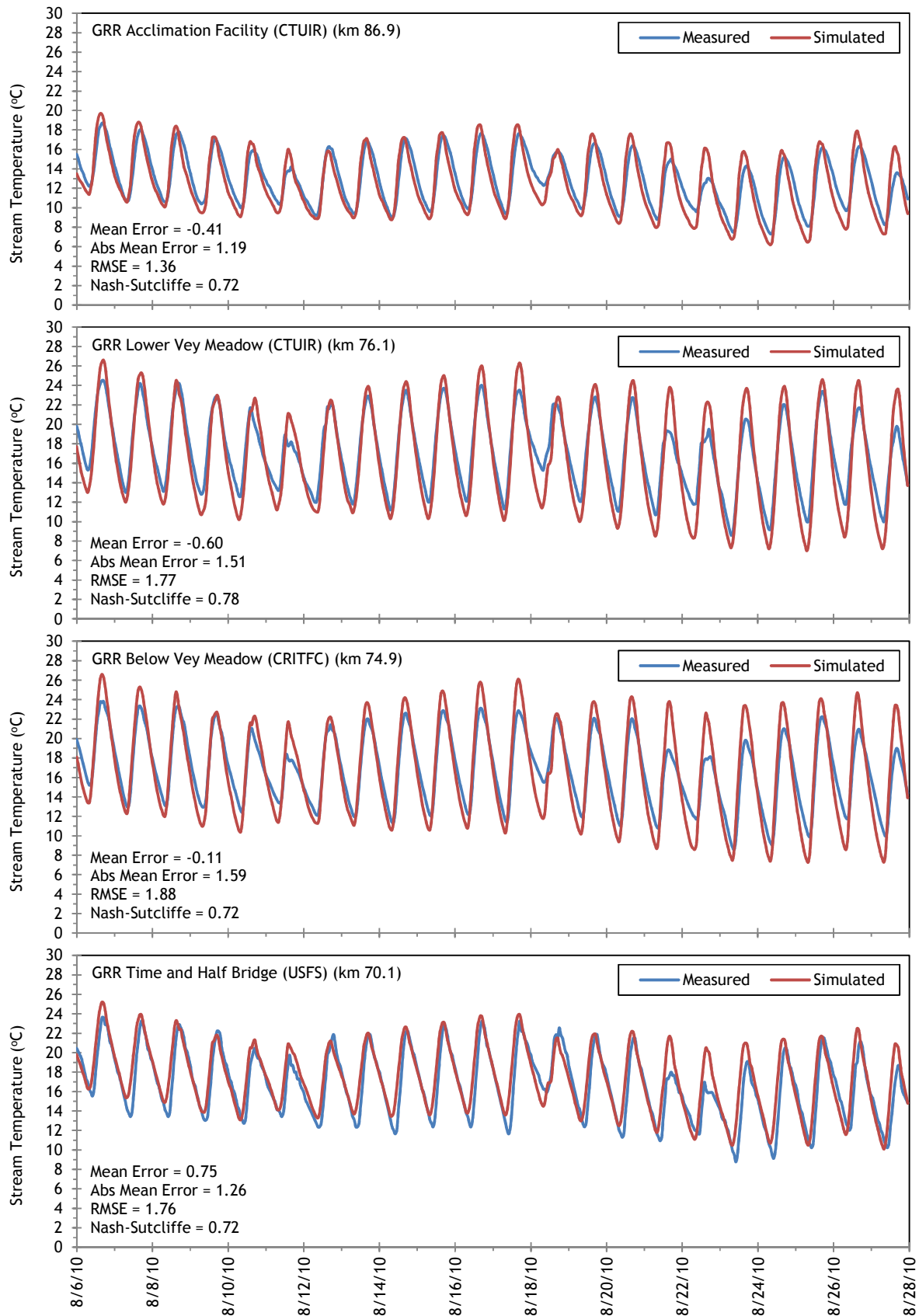


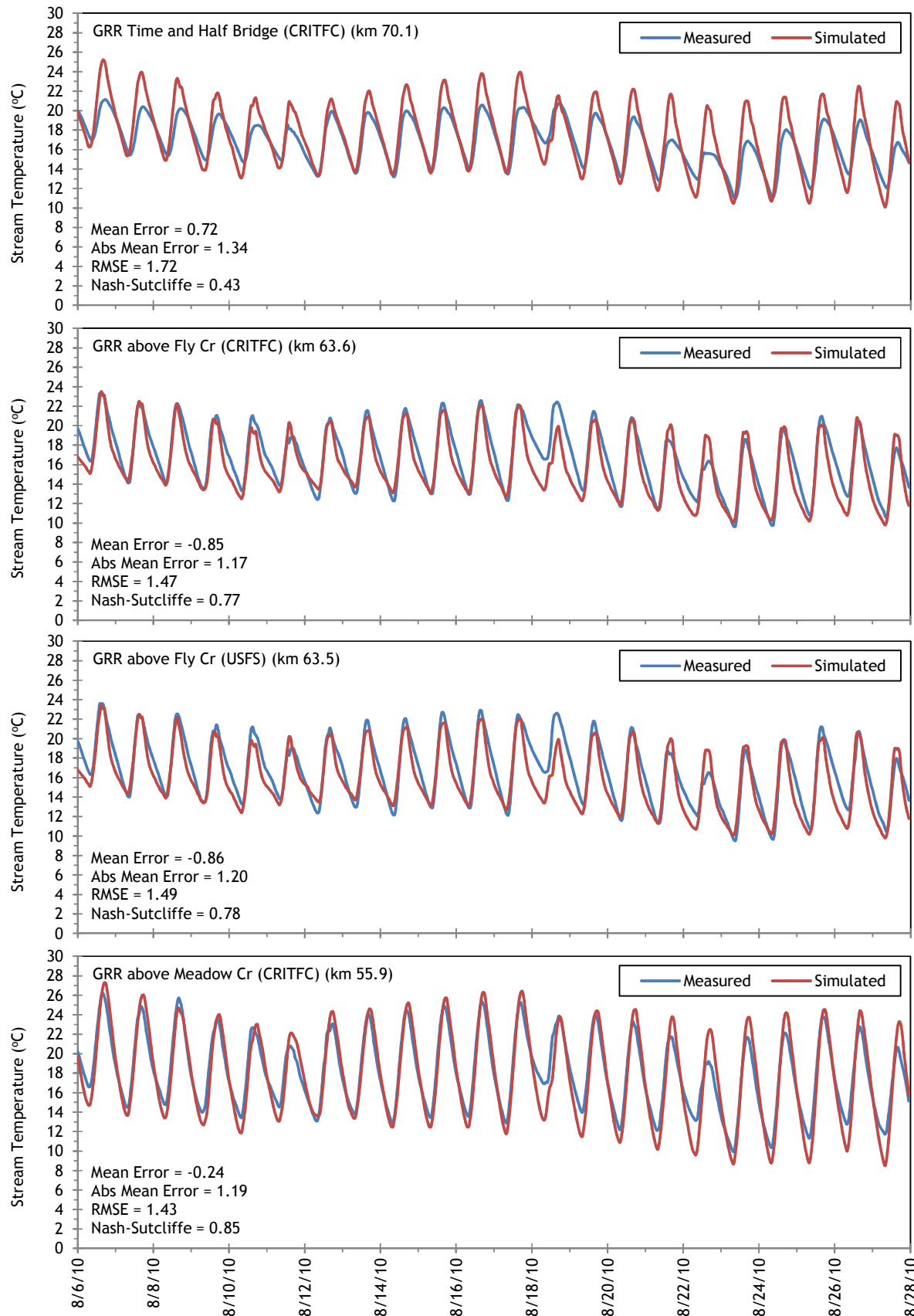
Figure 221 shows the simulated and measured hourly stream temperatures at locations along the Grande Ronde River where thermistors were deployed. Calibration statistics are included on each plot.

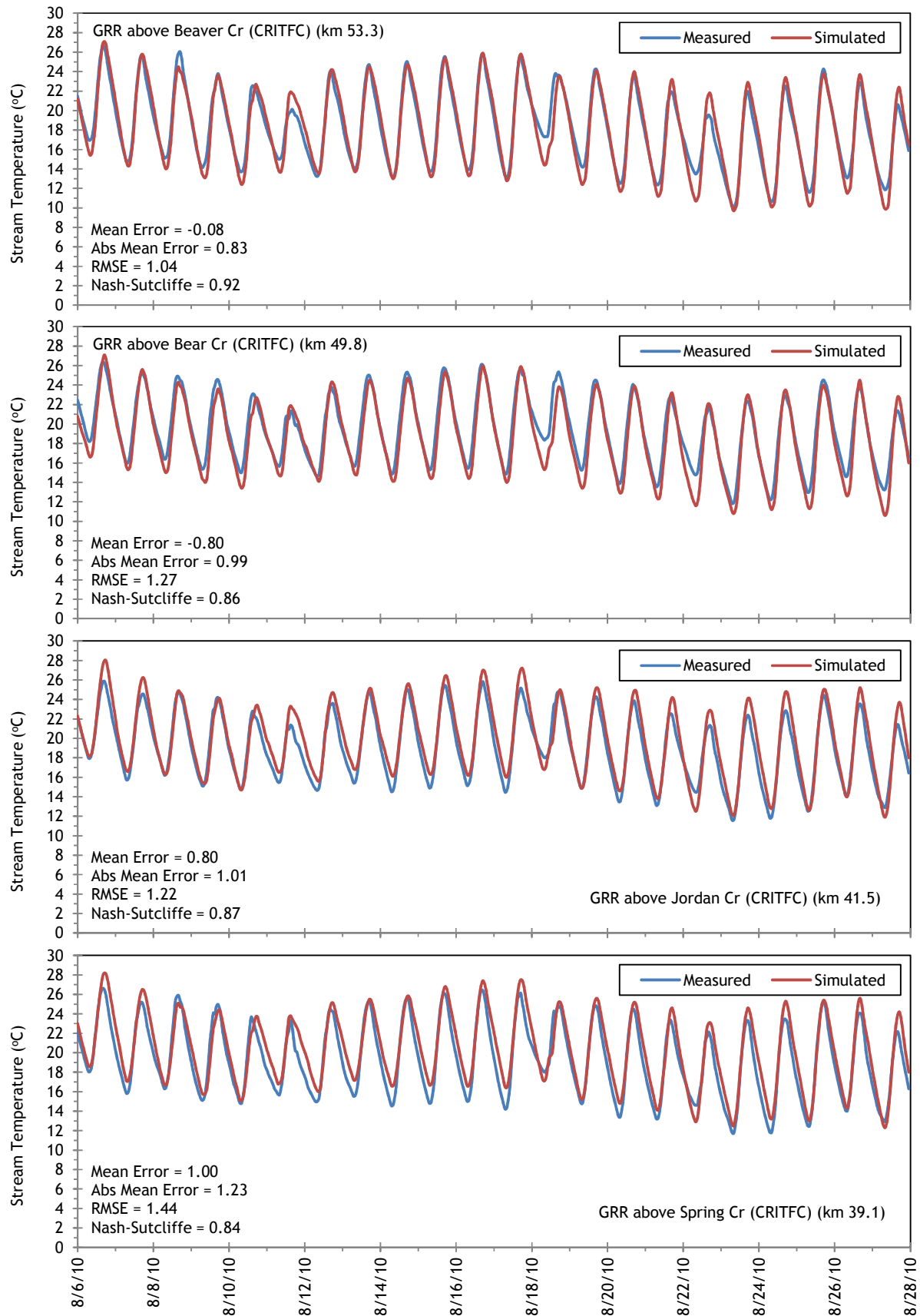
Figure 221 - Grande Ronde River simulated and measured hourly stream temperatures.

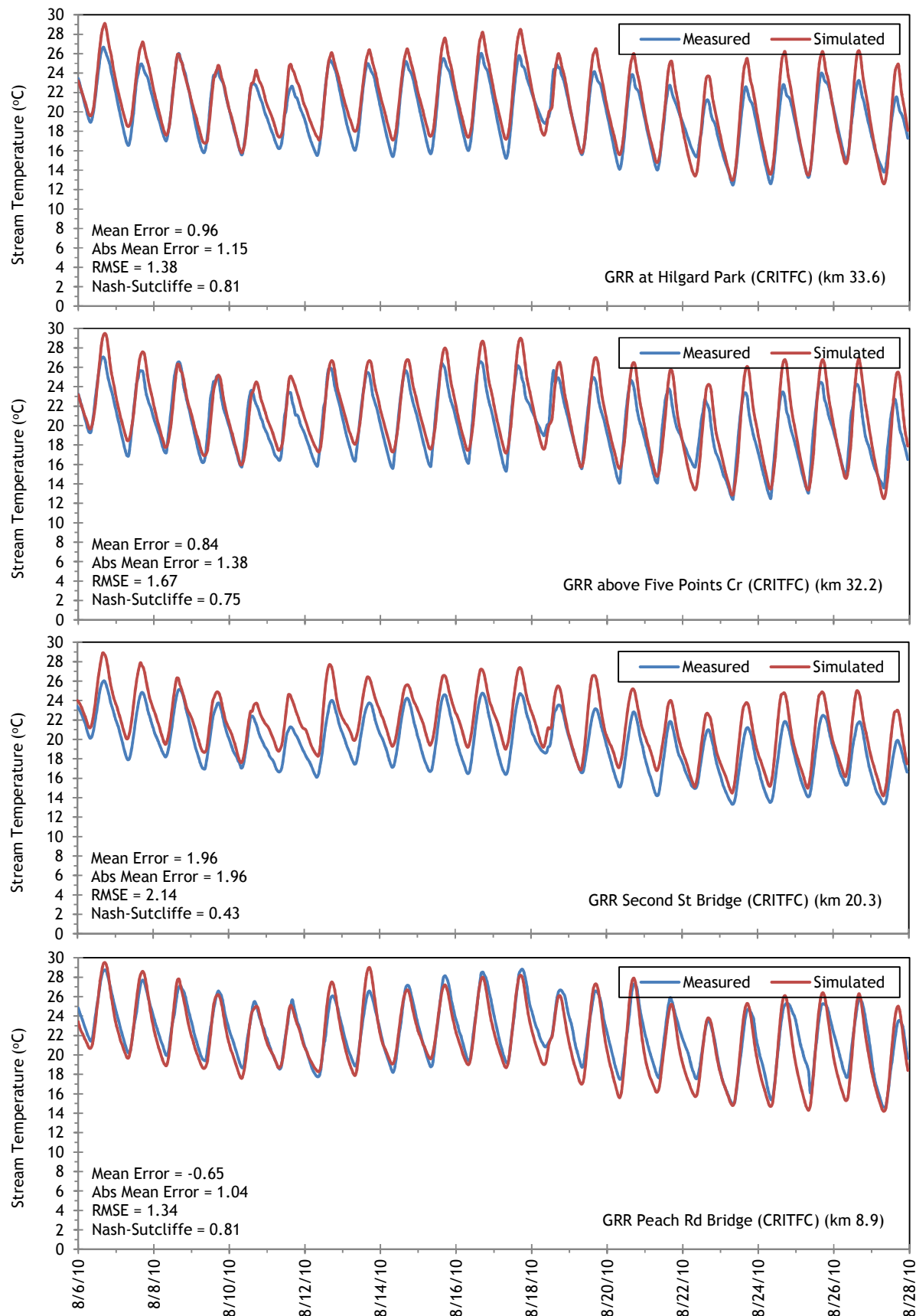






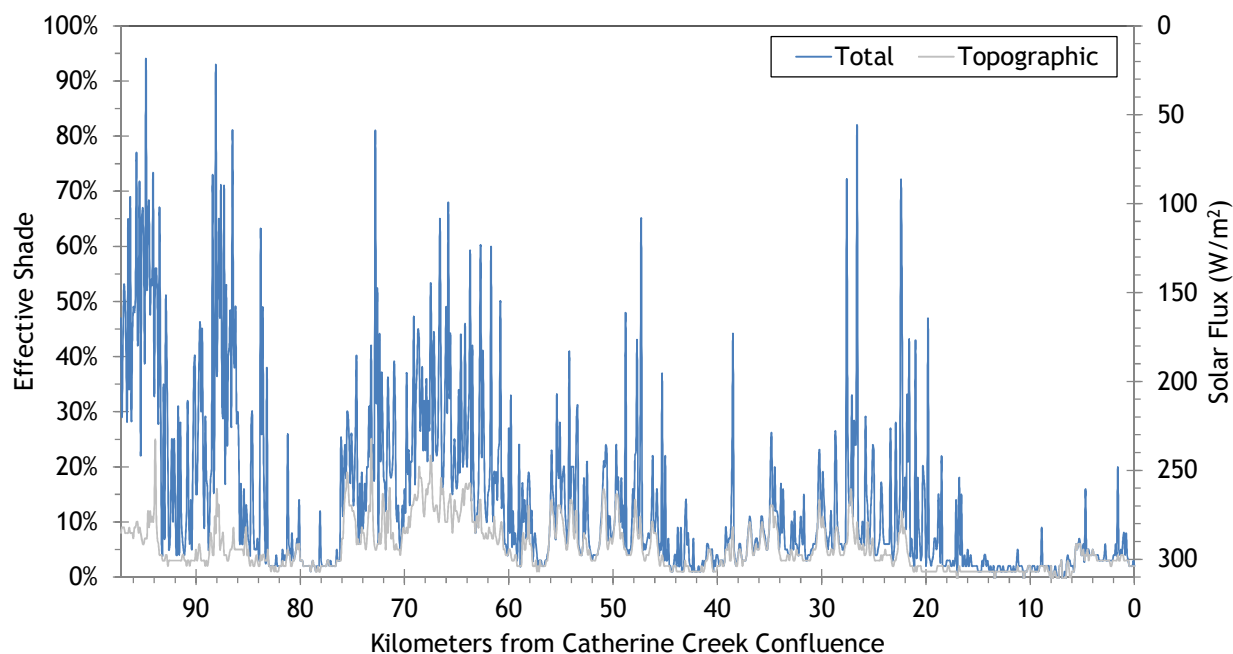






The simulated effective shade for the Grande Ronde River is presented in Figure 222. In many reaches, topography is producing the majority of effective shade. The Grande Ronde River is also wider than its tributaries and some reaches have less effective shade for that reason. Additionally, there is often a road or interstate highway alongside the river, which reduces the amount of near stream land cover. Below La Grande (approximately kilometer 22, there is less effective shade because the river is within the agricultural valley bottom where there are few large trees.

Figure 222 - Grande Ronde River simulated effective shade.





RGB-colored LiDAR point cloud - Grande Ronde River below the city of La Grande (looking upstream).

Appendix H.

Work Plan for Hydrological Analysis



COLUMBIA RIVER INTER-TRIBAL FISH COMMISSION

729 NE Oregon, Suite 200, Portland, Oregon 97232

Telephone 503 238 0667

Fax 503 235 4228

Work Plan for Hydrological Analysis

A component of

Monitoring Recovery Trends in Key Spring Chinook Habitat Variables and Validation of
Population Viability Indicators

March 2012

Dale McCullough



1. USGS data for Grande Ronde at La Grande can be found at this website:
http://waterdata.usgs.gov/nwis/inventory/?site_no=13319000&
2. Data for the Grande Ronde River at La Grande can also be found at the Climate Impacts Group website at <http://www.hydro.washington.edu/2860/products/sites/?site=4012>. What is the reason for the differences in the data. For example, the raw data from the Climate Impacts Group does not match the data from the USGS gauge. Also, the USGS data is missing for 1925 and 1926 but is present in the CIG data. It appears that the adjusted CIG data is better than the raw data, but we need to find out why there are differences. Learn about how the data were adjusted by reading the project report at: <http://www.hydro.washington.edu/2860/report/>.
3. Go to StreamStats website at: <http://water.usgs.gov/osw/streamstats/>. Click on “state applications.” Click on Oregon on the map. Click on “interactive map” button. Become familiar with how to acquire watershed characteristics for any point on the stream network. You need to be at a scale of 1:20K or higher resolution.
4. In StreamStats, click on “USGS station statistics.” Click on station 13319000, the Grande Ronde River at La Grande. Acquire the station statistics for the streamflows at that station. You can see whether you can derive the same streamflow statistics for this station by conducting the calculation manually. Also, you can use the regression equations from Risley to calculate streamflow statistics for this station.
5. Go to <http://pubs.usgs.gov/sir/2008/5126/> to acquire the publication Risley, J.C., A.Stonewall,, and T. Haluska. 2008. Estimating flow-duration and low-flow frequency statistics for unregulated streams in Oregon. U.S. Geological Survey Scientific Investigations Report 08-5126, 23 p. Download the report. Also, download the Tables 1-17 that are provided in a Microsoft® Excel workbook, which can be accessed at http://pubs.usgs.gov/sir/2008/5126/sir20085126_tables.xls. (4.25 MB). This Excel file contains the regional regression equations used to estimate streamflow statistics for any site for which watershed characteristics are available. These watershed characteristics should be acquired from StreamStats.
6. Get the GIS map of locations of all water temperature monitoring sites. Locate the same point on the StreamStats site. Click on the exact spot where each temperature logger was installed. Acquire the upstream watershed characteristics for each point. Build a table of watershed characteristics for all points that had water temperature loggers.
7. Use the Excel file from the Risley et al. (2008) report to compile formulas for each regression equation that predicts streamflows. These formulas are in Table 12 in the Excel spreadsheet. The streamflow statistics that it calculates are: P5, P10, P25, P50, P95, 7Q2, and 7Q10. For the USGS station 13319000, compare these statistics computed from the Risley et al. equations with those calculated directly from the USGS data.
8. Acquire the streamgage statistics for gauge 13319000 from StreamStats website:
<http://streamstatsags.cr.usgs.gov/gages/viewer14.htm?stabbr=GAGES>
9. Compute streamflow statistics directly for peak flows and 7-day low flows for gauge 13319000. To do this, use the OSU website at:
http://streamflow.engr.oregonstate.edu/analysis/floodfreq/meandaily_tutorial.htm. Download

the tutorial Excel spreadsheet to use as a model for how to calculate these. You will need the file USGS Bulletin #17B (Guidelines for determining flood flow frequency) to find the “k” coefficients to use in the computations. This publication can be found at: http://water.usgs.gov/osw/bulletin17b/bulletin_17B.html. Use the CIG data to make these calculations and also use the raw USGS data. Compare the results.

10. Also, refer to this text for how to conduct streamflow statistical analysis: Philip B. Bedient, Wayne Charles Huber, Baxter E. Vieux. 2007. Hydrology and floodplain analysis (4th edition). This text is cited in the Oregon Engineering Department website.
11. Use the following references to evaluate peak flow statistics:
 - a. Berenbrock, C. 2002. Estimating the magnitude of peak flows at selected recurrence intervals for streams in Idaho. U.S. Geological Survey Water-Resources Investigation Report Report 02-4170, 59 p.
 - b. Berenbrock, C. 2002. Estimating the Magnitude of Peak Flows at Selected Recurrence Intervals for Streams in Idaho. USGS Water Resources Investigations Report 02-4170.
 - c. Harris, D.D. and L.E. Hubbard. 1982. Magnitude and frequency of floods in eastern Oregon. USGS Water-Resources Investigations Report 82-4078. 45 p. :ill., maps ;28 cm.
 - d. Hortness, J.E. and C. Berenbrock. 2001. Estimating monthly and annual streamflow statistics at ungaged sites in Idaho. U.S. Geological Survey Water-Resources Investigation Report Report 01-4093, 36 p.
 - e. These publications have statistical calculations for gaged sites in NE Oregon, including station 13319000.
12. Calculate low flow statistics using the 7-day running mean of the daily mean streamflows. Refer to the following documents, although Riggs is the key document. Refer also to Bedient et al. (2007).
 - a. Riggs, H.C. 1972. Low flow investigations: U.S.G.S. Techniques of water-resources investigations. Book 4, Chapter B1. 18 pp.
 - b. Orsborn, J.F. 1975. Predicting ungaged low flows in diverse hydrologic provinces using river basin geomorphic characteristics. Internat.Assoc. Sci. Hydrol. 117:157-167.
 - c. Bingham, R.H. 1985. Low flows and flow duration of Tennessee streams through 1981. U.S. Geological Survey Water-Resources Investigations Report 84-4347.
 - d. Bingham, R.H.. 1986. Regionalization of low-flow characteristics of Tennessee streams. U.S. Geological Survey Water-Resources Investigations Report 85-4191.
 - e. Giese, G.L. and R.R. Mason. 1990. Low-flow frequency characteristics of streams in North Carolina. U.S. Geological Survey Open-File Report 90-399.
 - f. Hayes, D.C. 1991. Low-flow characteristics of streams in Virginia. U.S. Geological Survey Water-Supply Paper 2374.
 - g. Ludwig, A.H.. 1992. Flow duration and low-flow characteristics of selected Arkansas streams. U.S. Geological Survey Water-Resources Investigations Report 92-4026, 77 p.
 - h. Ruhl, K.J., and G.R. Martin. 1991. Low-flow characteristics of Kentucky streams. U.S. Geological Survey Water-Resources Investigations Report 91-4097, 51 p.

- i. Telis, P.A.. 1991. Low-flow and flow-duration characteristics of Mississippi streams. U.S. Geological Survey Water-Resources Investigations Report 90-4087, 214 p.
 - j. Flynn, R.H. 2003. Development of regression equations to estimate flow durations and low-flow-frequency statistics in New Hampshire Streams. Water-Resources Investigations Report 02-4298U. U.S. Geological Survey Water-Resources Investigations Report 02-4298 In Cooperation with the New Hampshire Department of Environmental Services.
 - k. Orsborn, J.F. 1975. A geomorphic method for estimating low flows. Am. Soc. Civil Eng. Annual Meeting, Denver, Colorado, Nov. 3-7. 38 p.
 - l. Tasker, G.D. 1987. A comparison of methods for estimating low flow characteristics of streams. Water Res. Bull 23:1077-1084.
 - m. Hortness, J.E. 2006. Estimating low-flow frequency statistics for unregulated streams in Idaho. U.S. Geological Survey Scientific Investigations Report 2006-5035. 31 p.
13. The air temperature data for La Grande and Union were acquired by purchase from NOAA starting at <http://www.ncdc.noaa.gov/oa/mpp/digitalfiles.html#DIG>. The hourly data are from A and the daily surface data are from B. We acquired daily data. For Union station, we have data from 1911 to 2010. Data from the La Grande station was available from 1965 to 2010.
- a. Compute annual total precipitation from this record for each station.
 - b. Do a correlation of daily precipitation between the two sites.
 - c. Compare the precipitation for these two stations at their respective altitudes with the mean annual precipitation by elevation within the watersheds of the Upper Grande Ronde and Catherine Creek. We need GIS assistance to compute mean annual precipitation using the new PRISM maps for each watershed above all sites where water temperatures were measured. The new high resolution PRISM data is available from http://www.climateSource.com/400_meter.html and has been ordered.
 - d. Plot air temperature and precipitation by altitude for various watersheds with the UGR and CC. Find a value for a regional lapse rate for air temperature.
 - e. Correlate maximum and mean daily air temperature on the day that our FLIR flight was flown with water temperatures for the same day. The air temperature would be the value for either the La Grande or Union station, corrected using information available from PRISM or a regional lapse rate to each specific stream site where water temperatures were measured. Air temperatures that would affect stream temperatures might need to be averaged by weighting by the air temperatures above the stream network that is within a 1-day flow distance upstream.
 - f. Compute recurrence intervals for the air temperature data from Union station. What is the frequency of air temperatures high enough to cause stress in the UGR or CC given current riparian conditions.
 - g. Based on the correlation of water temperature and air temperature for the dates that the 2010 and 1999 FLIR flights were flown, estimate water temperatures for the past 20 years for various stream sites.

- h. Acquire daily water temperature records for various stream sites (either the 2009 and 2010 CRITFC data or longer term USFS data). Compute a regression of daily maximum (or mean) water temperature on daily maximum (or mean) air temperature.
14. Use the publication Orsborn, J.F. 1990. Quantitative modeling of the relationships among basin, channel and habitat characteristics for classification and impact assessment. Timber/Fish/Wildlife Program. CMER Project 16D to compute the relationships between streamflow statistics at ungaged sites from watershed characteristics.
15. Use the NSS (National Streamflow Statistics) program to calculate streamflow statistics. The NSS program is found at: <http://water.usgs.gov/software/NSS/>. This program requires entry of approximately 3 parameters that can be obtained from the StreamStats website.
 - a. Ries III, K.G., J.B. Atkins, P.R. Hummel, M.H. Gray, R.A. Dusenbury, M.E. Jennings, W.H. Kirby, H.C. Riggs, V.B. Sauer, W.O. Thomas Jr. 2007. The National Streamflow Statistics Program: A Computer Program for Estimating Streamflow Statistics for Ungaged Sites. Techniques and Methods 4-A6. U.S. Geological Survey, Reston, VA.
 - b. Ries, K.G., III. 2006. The National Streamflow Statistics Program: A computer program for estimating streamflow statistics for ungaged sites. U.S. Geological Survey Techniques and Methods Report TM Book 4, Chapter A6, 45 p.
 - c. Turnipseed, D.P. and K.G. Ries, III. 2007. The National Streamflow Statistics Program: Estimating high and low streamflow statistics for ungaged sites. U.S. Geological Survey Fact Sheet 2007-3010, 4 p.
16. Using the daily air temperature and precipitation data downloaded from NOAA for the La Grande and Union weather stations, develop a watershed hydrology model using the PRMS model from USGS. This model will predict daily streamflows for any ungaged site. Use the model to predict streamflows at USGS gage site 13319000. Determine the degree of correlation. The PRMS model can be obtained from: http://wwwbrr.cr.usgs.gov/projects/SW_MoWS/software/software.shtml. This would be an alternative to using StreamStats. This model can be used to create long time series of simulated daily streamflows from flow statistics can be computed. The model can also be used to estimate the effect of land alteration or climate change scenarios.
17. Go to http://gis.wrd.state.or.us/apps/map/owrd_map/Default.aspx or http://gis.wrd.state.or.us/apps/map/owrd_map/Default.aspx or http://www.wrd.state.or.us/OWRD/SW/peak_flow.shtml. You can click the button "Perform a peak discharge estimate at this point." You can navigate to any point on the map and do this calculation. Do this for all points at tributary mouths and along the mainstem UGR and CC where
18. Go to <http://www1.wrd.state.or.us/files/wars/summary.out> to get my file: Grande Ronde-natural streamflow for selected watersheds.pdf. This is NATURAL STREAMFLOW FOR SELECTED WATERSHEDS.


Appendix I.

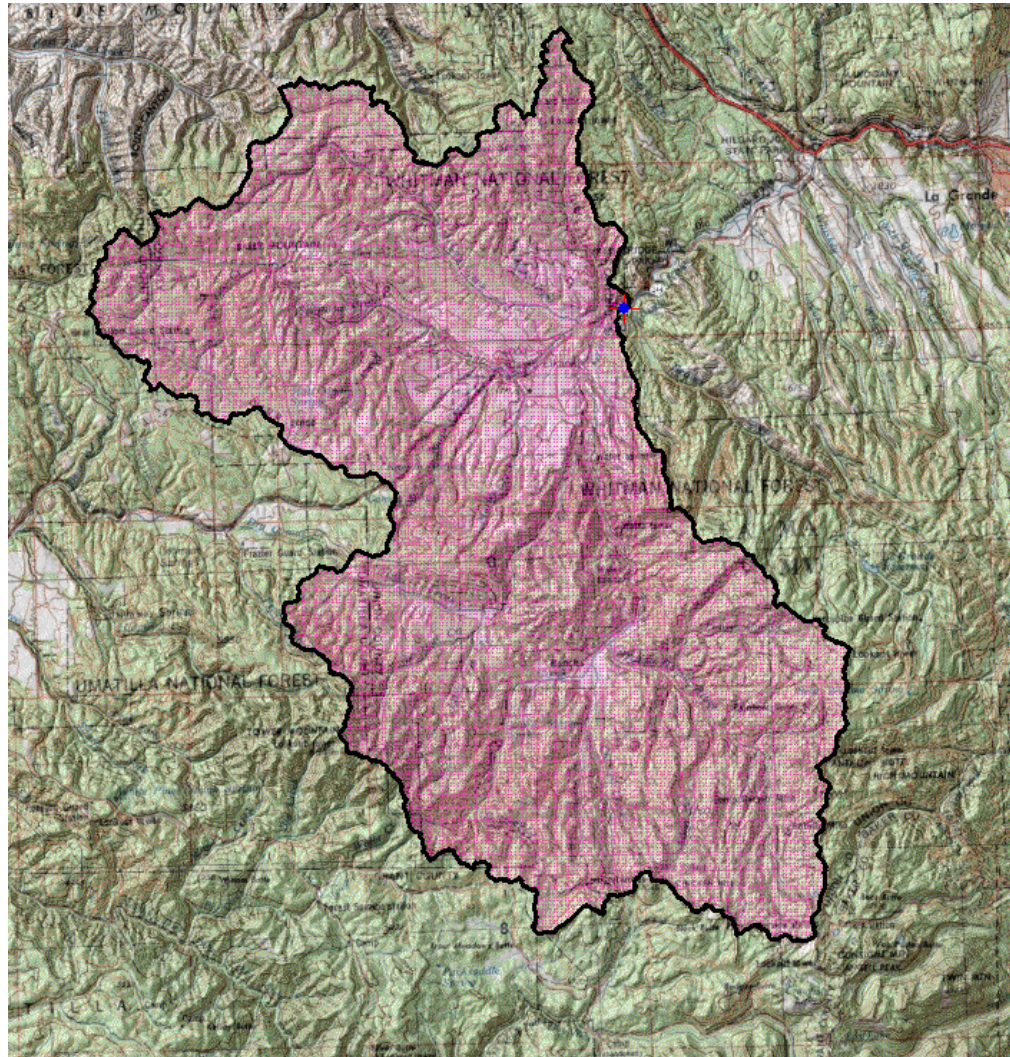
Aerial images of terrain for all CHaMP sites surveyed by CRITFC in 2011 (from www.champmonitoring.org), tables of immutable characteristics of these CHaMP survey sites (from www.champmonitoring.org), and outlines of the watersheds upstream of each CHaMP survey site in 2011 (from USGS StreamStats).



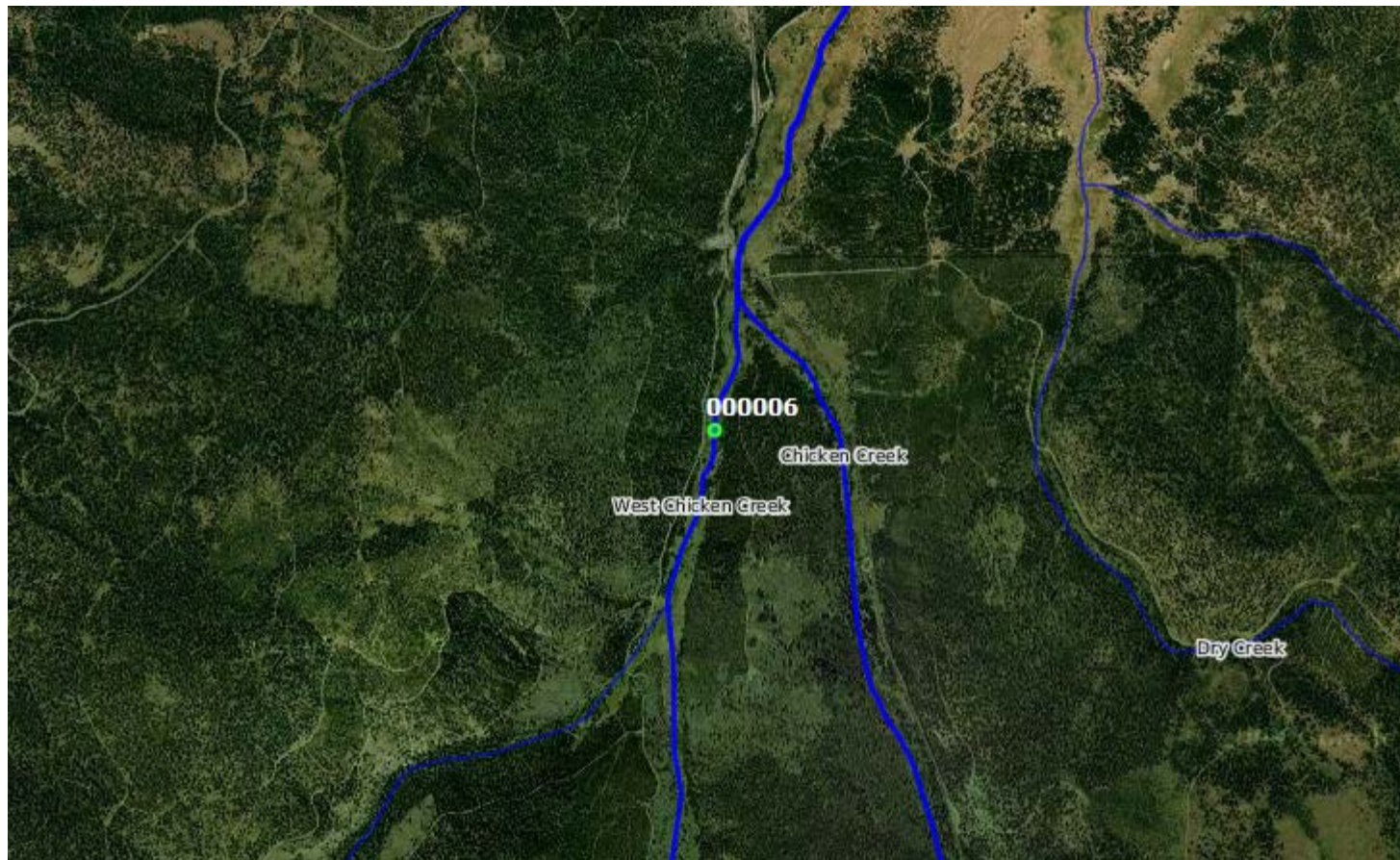
Immutable Characteristics

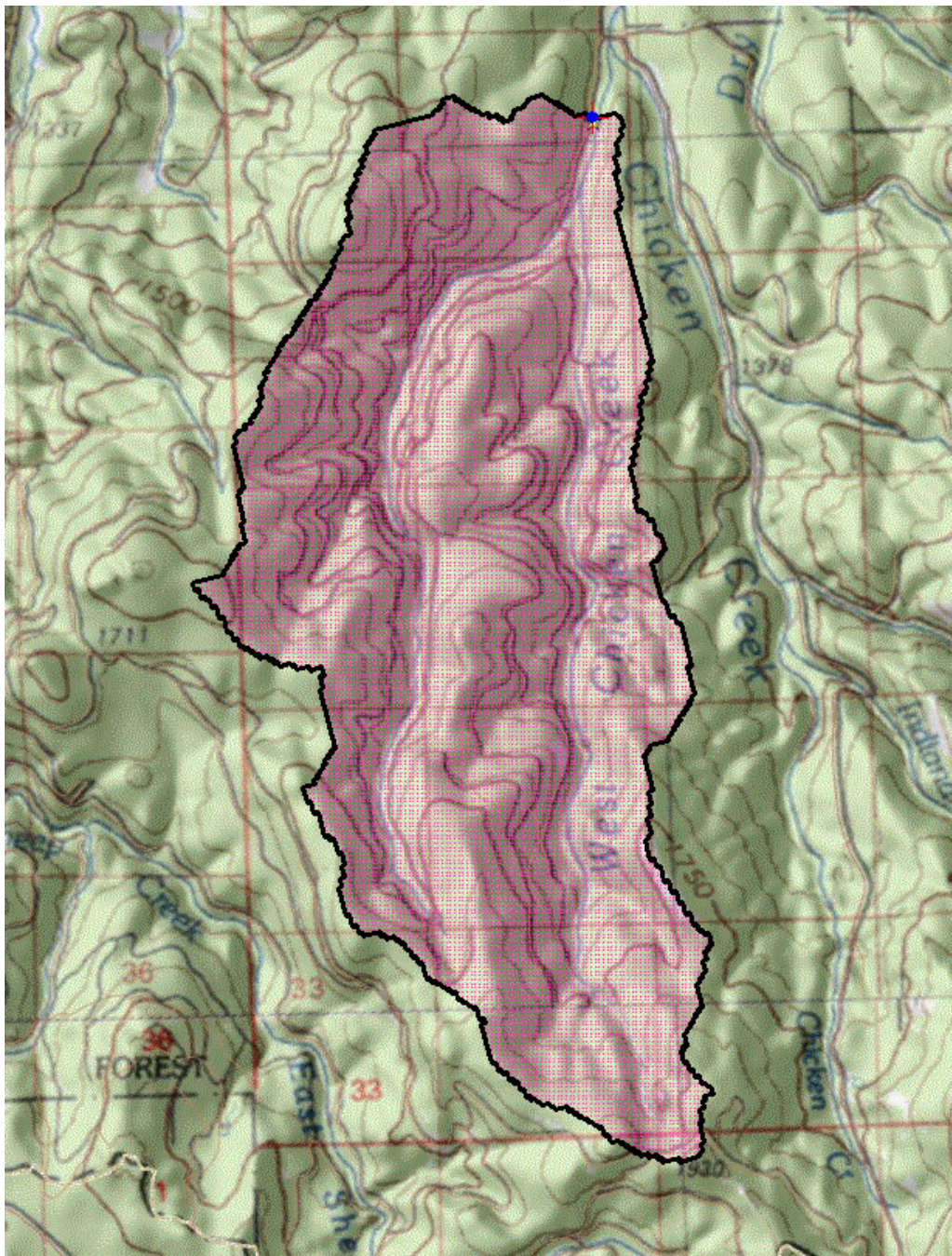
Here are some of the immutable characteristics of this site, many of these come from the Master Sample.

UTM	11N 392921 5013827
Township Range Section 	3S 36E 30
Category	Upper Grande Ronde Chinook
Panel	Annual
Owner Type	Private Lands
Ownership	Private Lands
State	OR
County	Union
HUC6	170601040307
Stream	Grande Ronde River
Strahler Order	5
Latitude	45.26978
Longitude	-118.36503

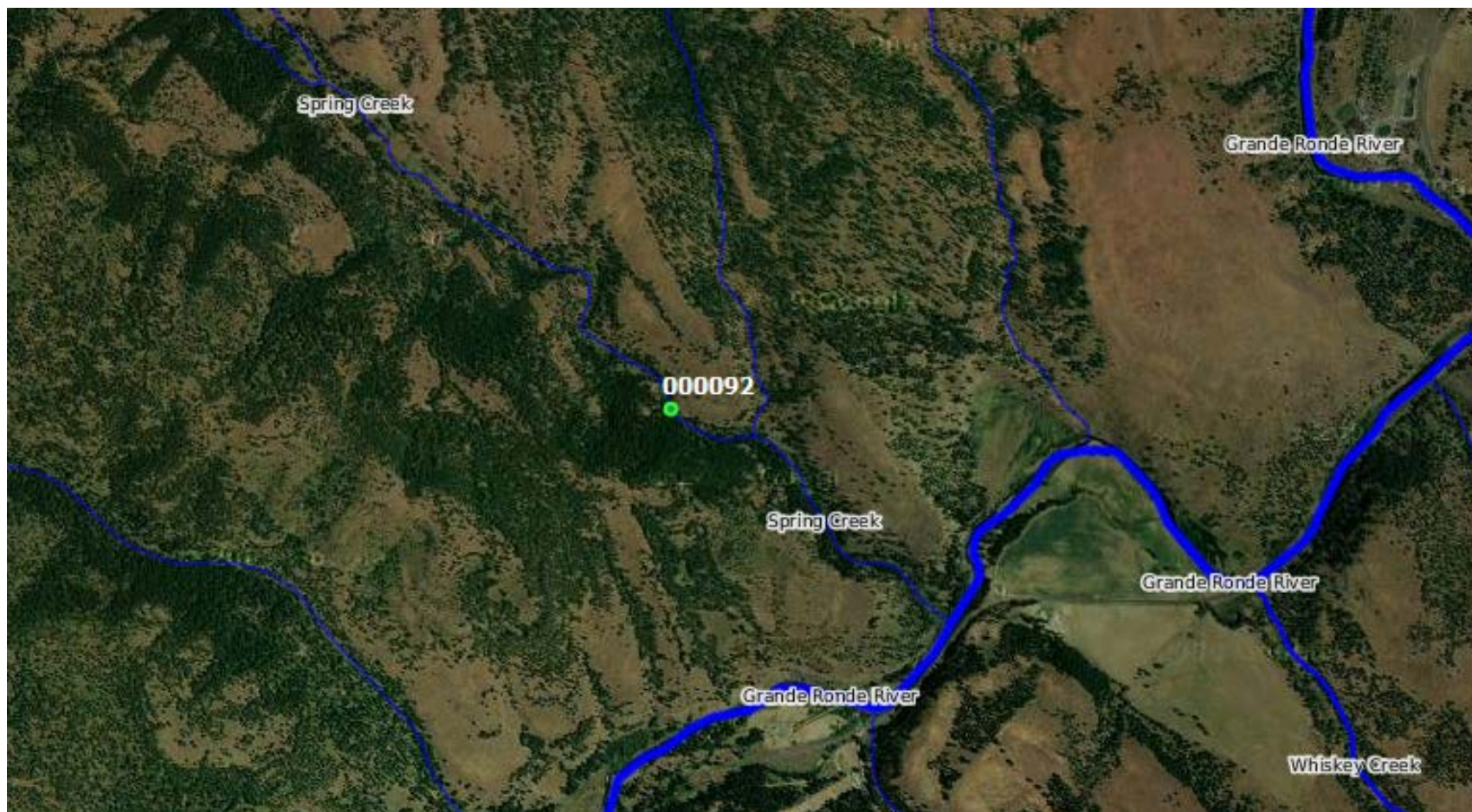


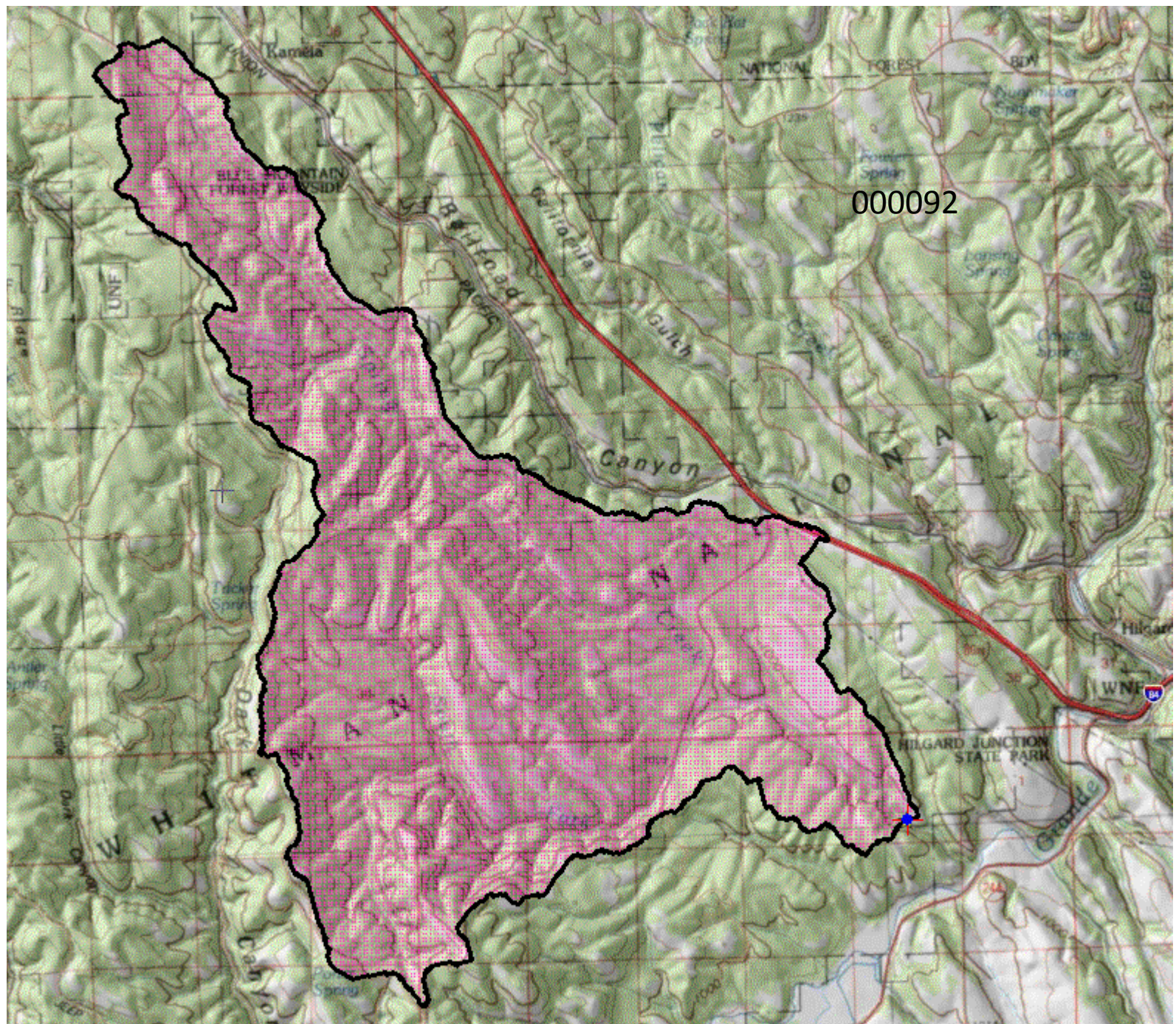
000245



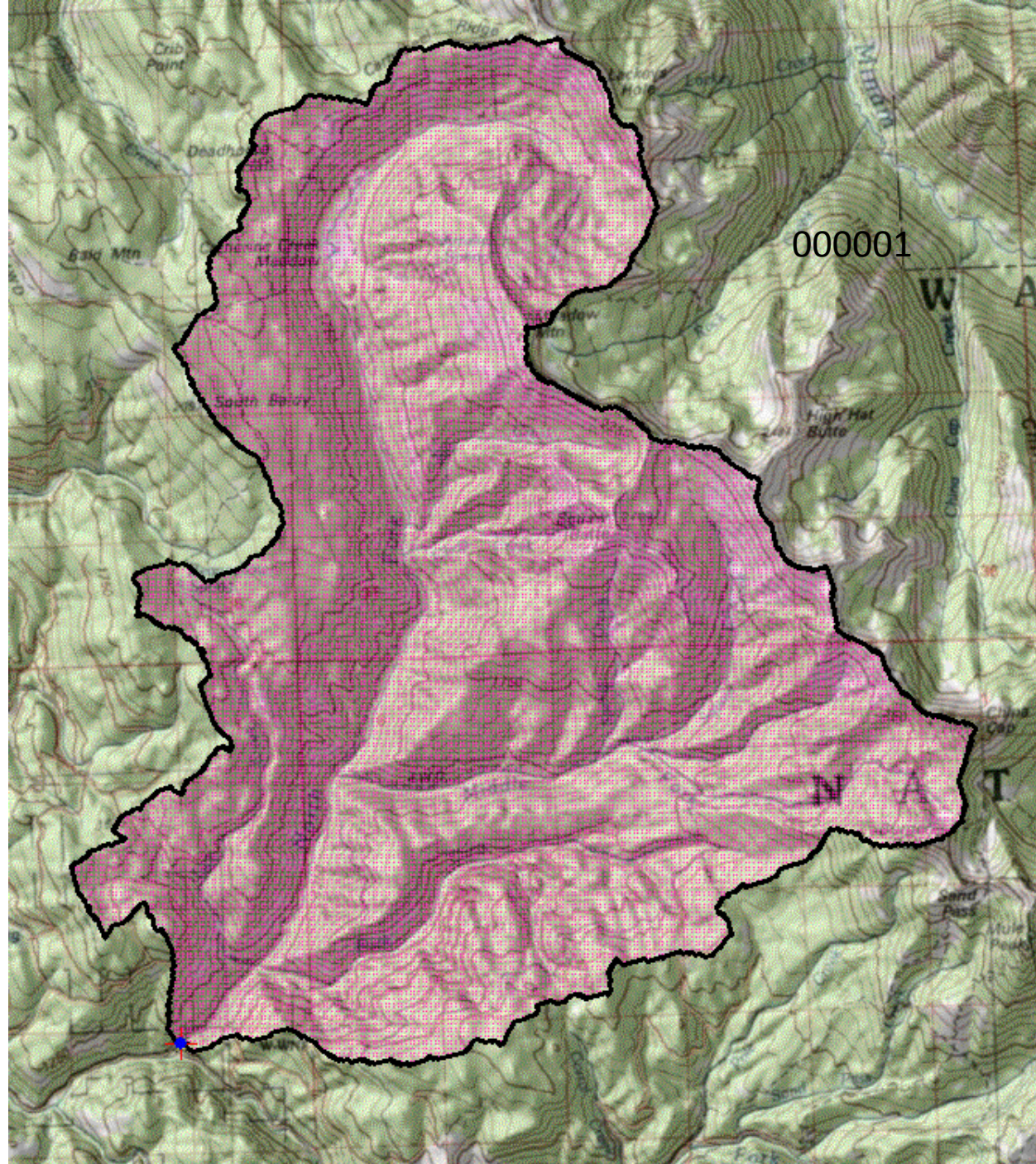


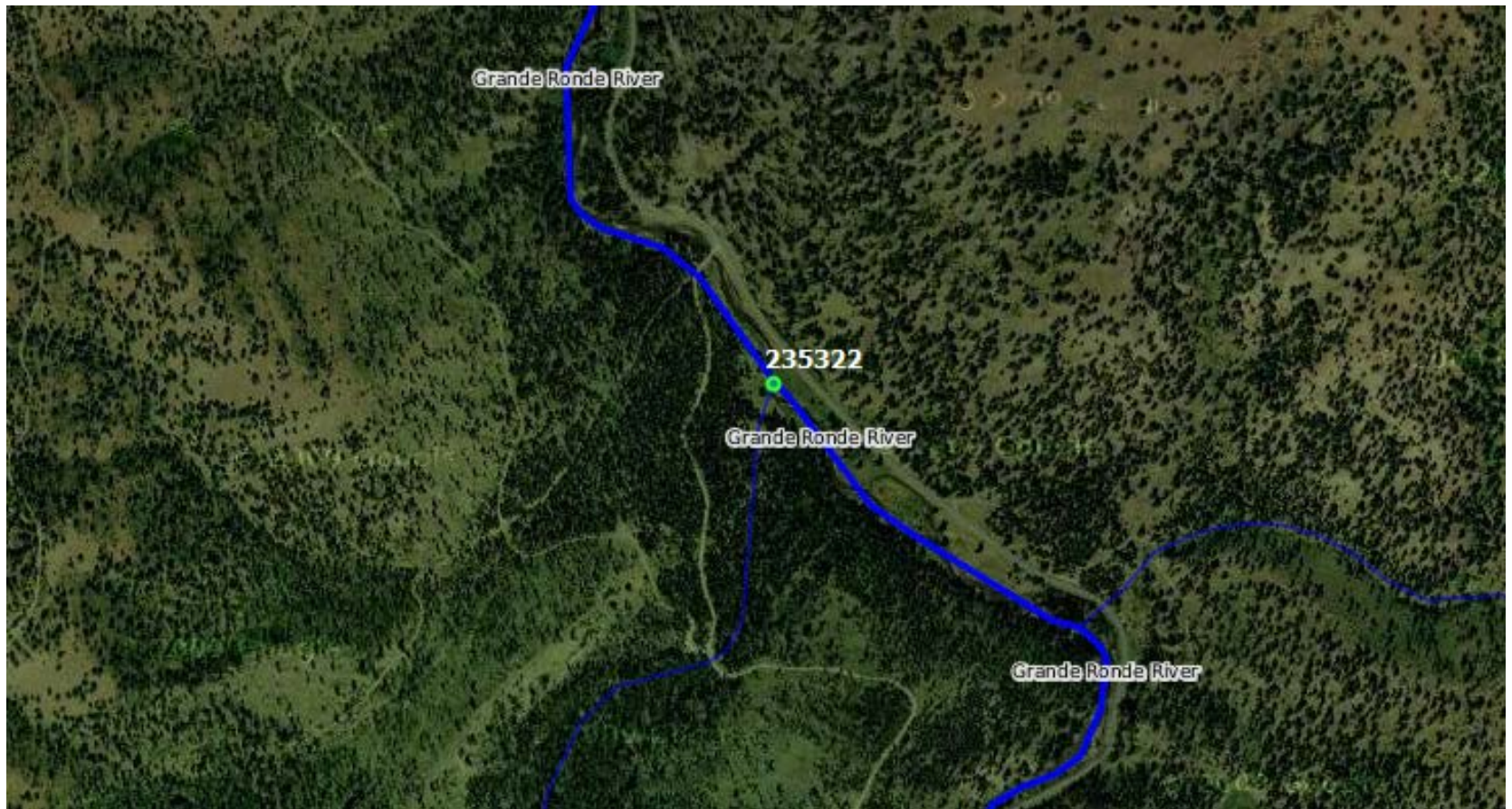
000006

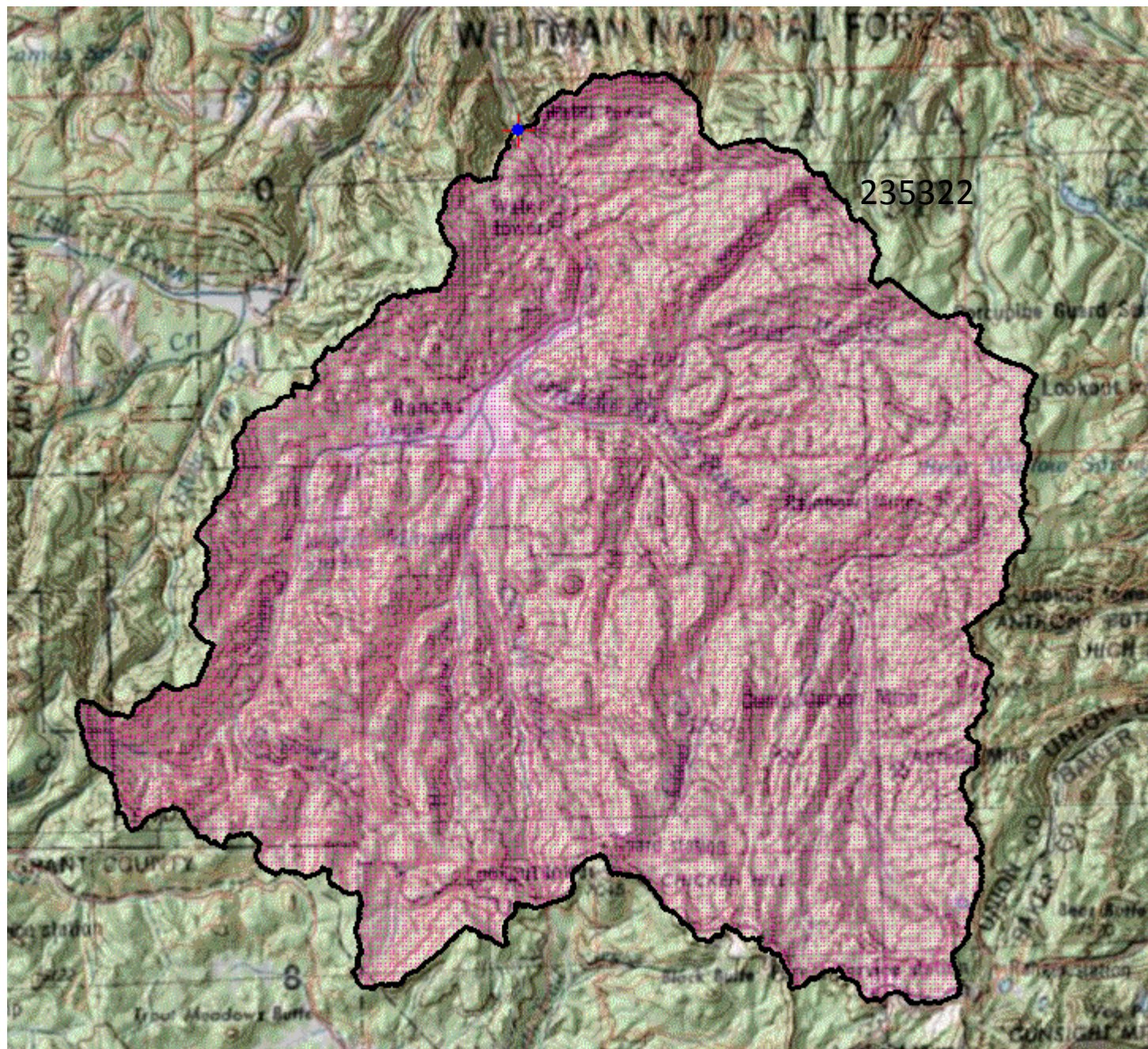


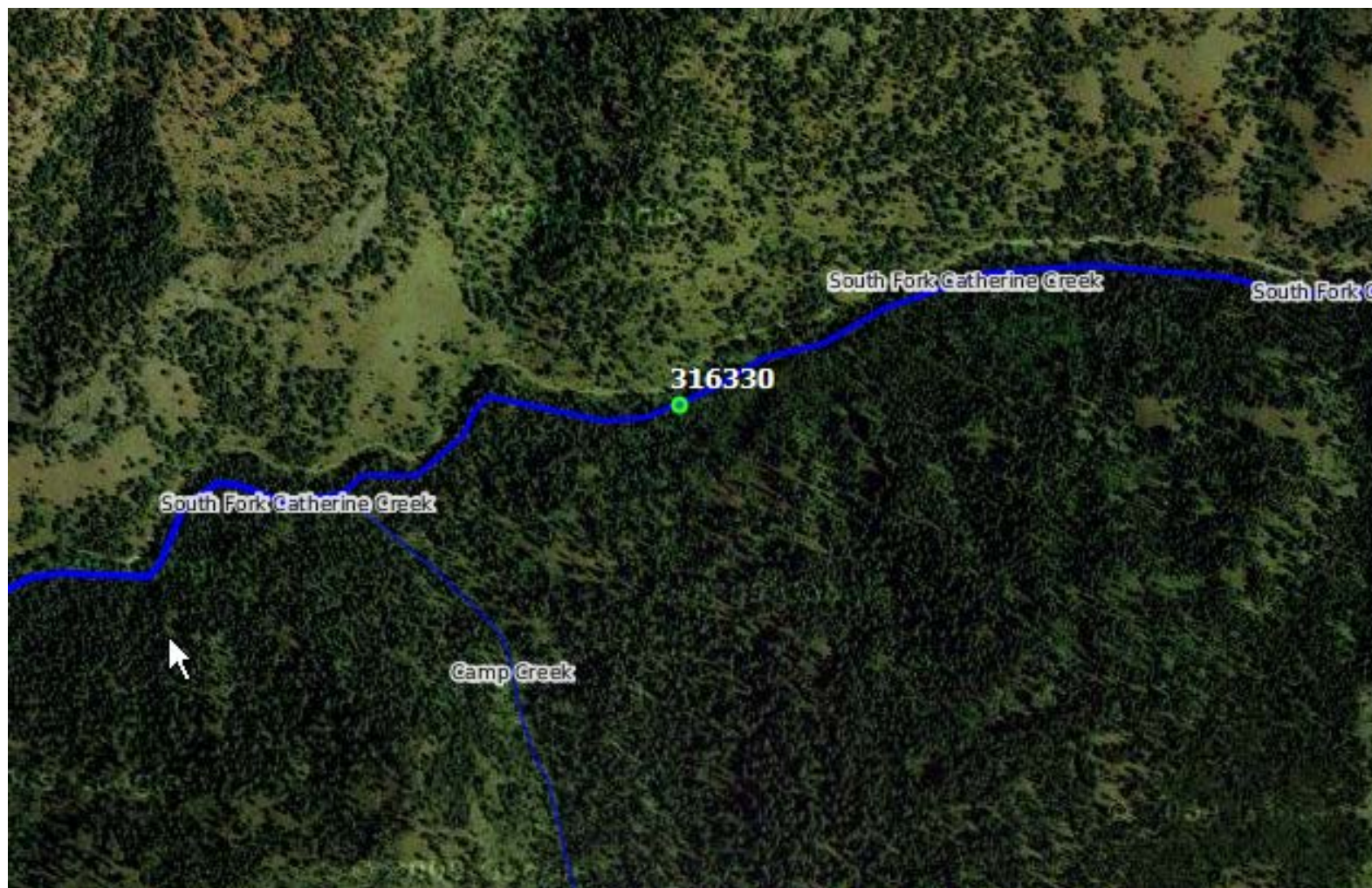


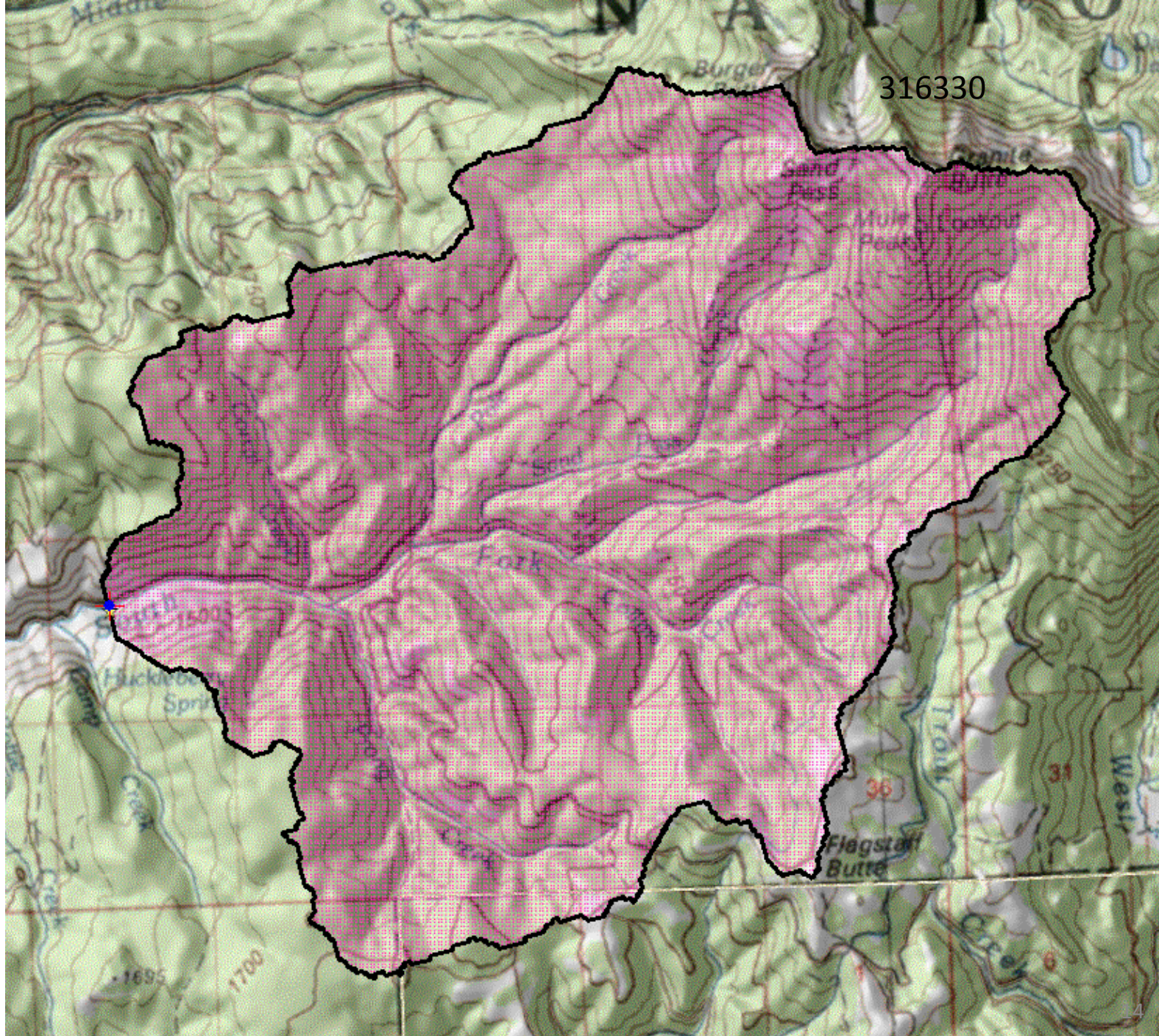




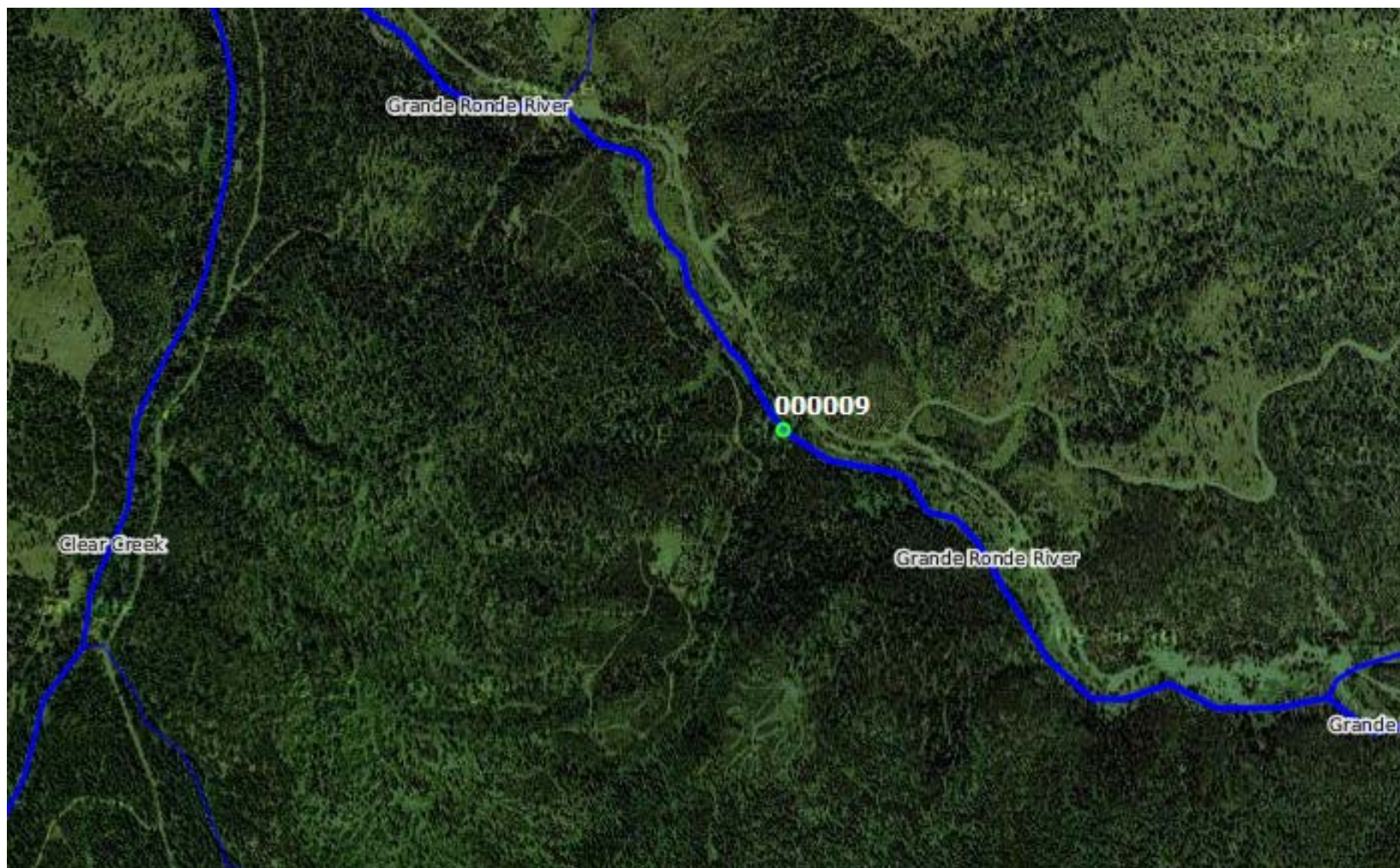


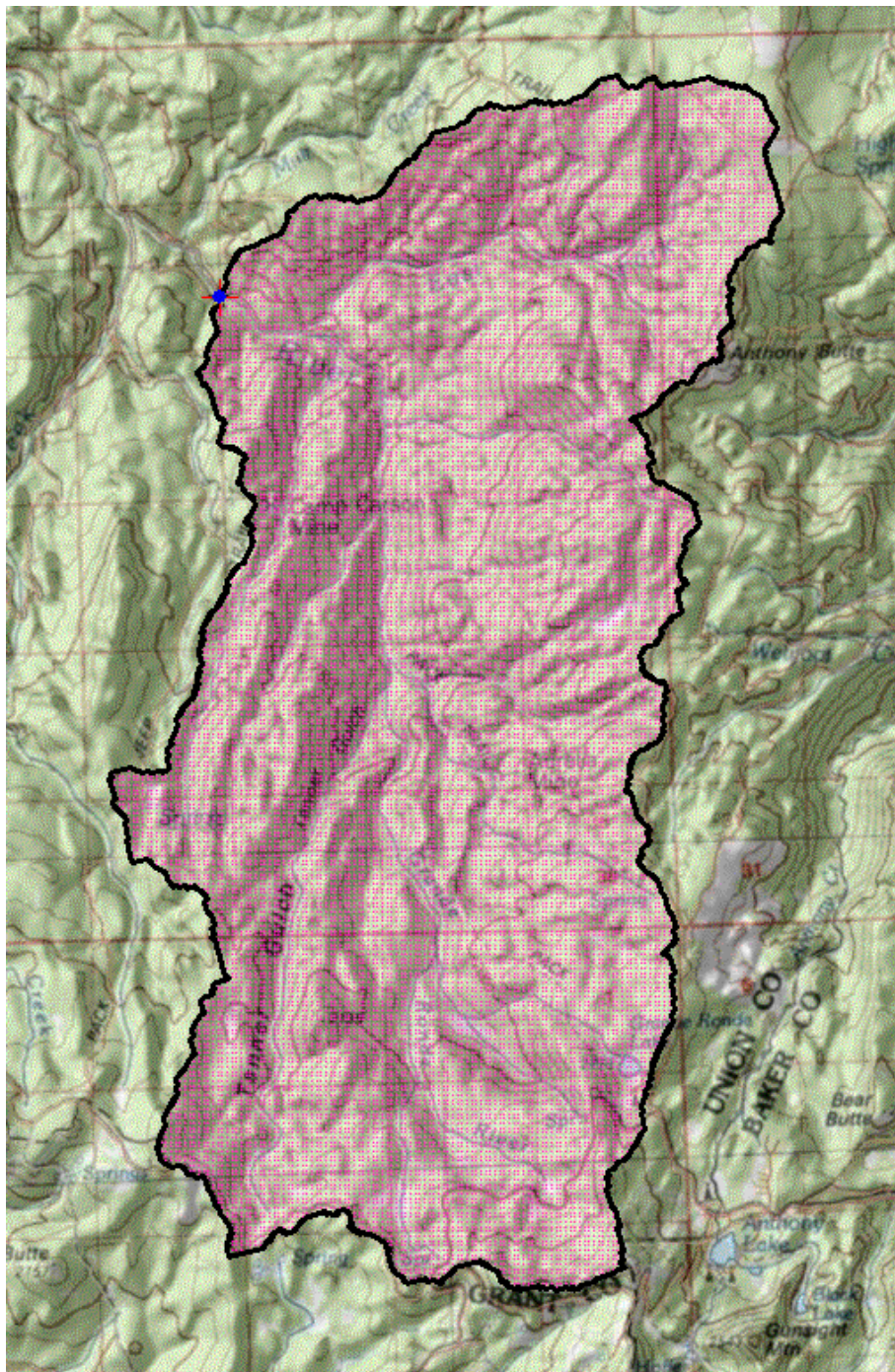






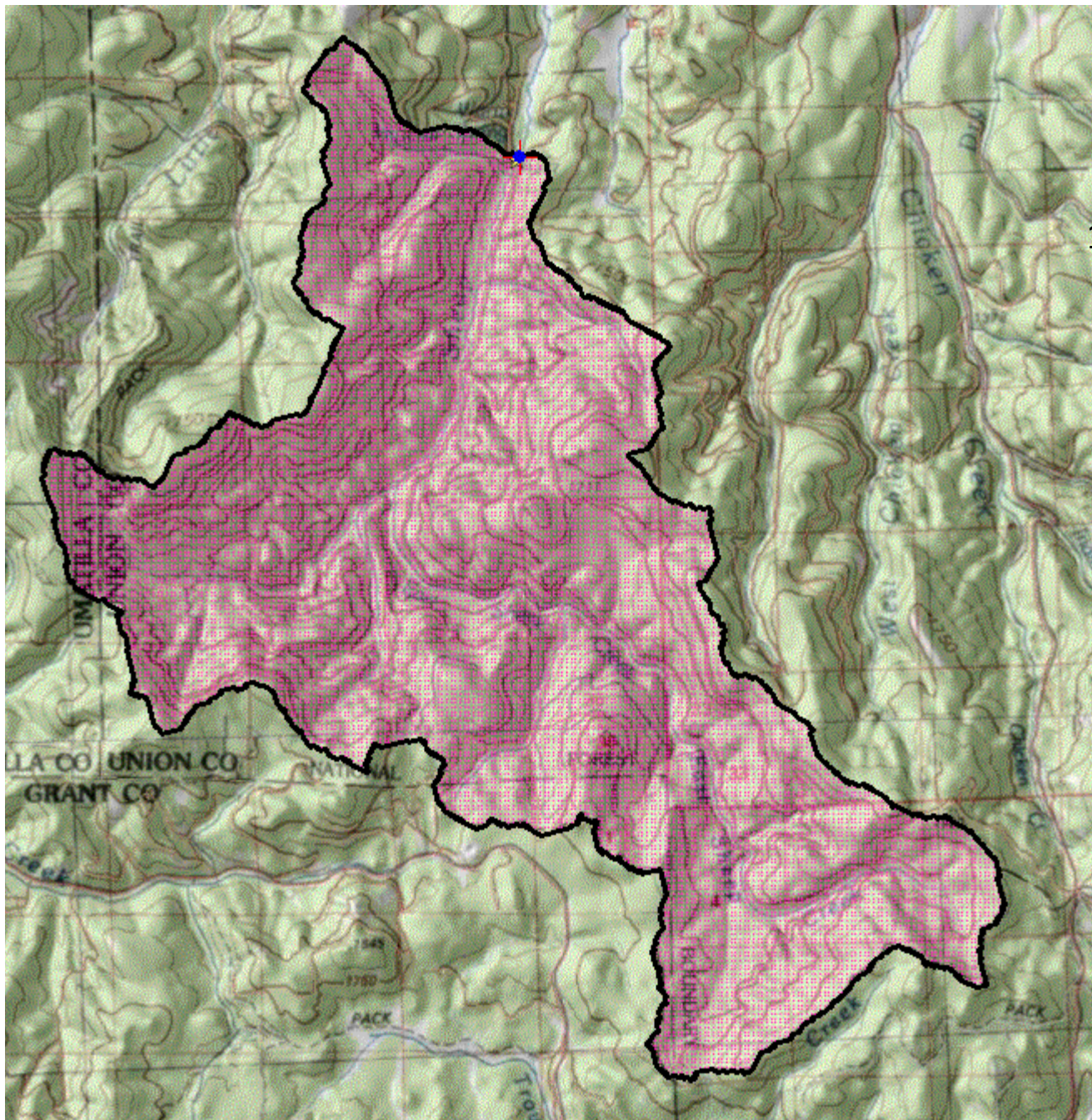
316330





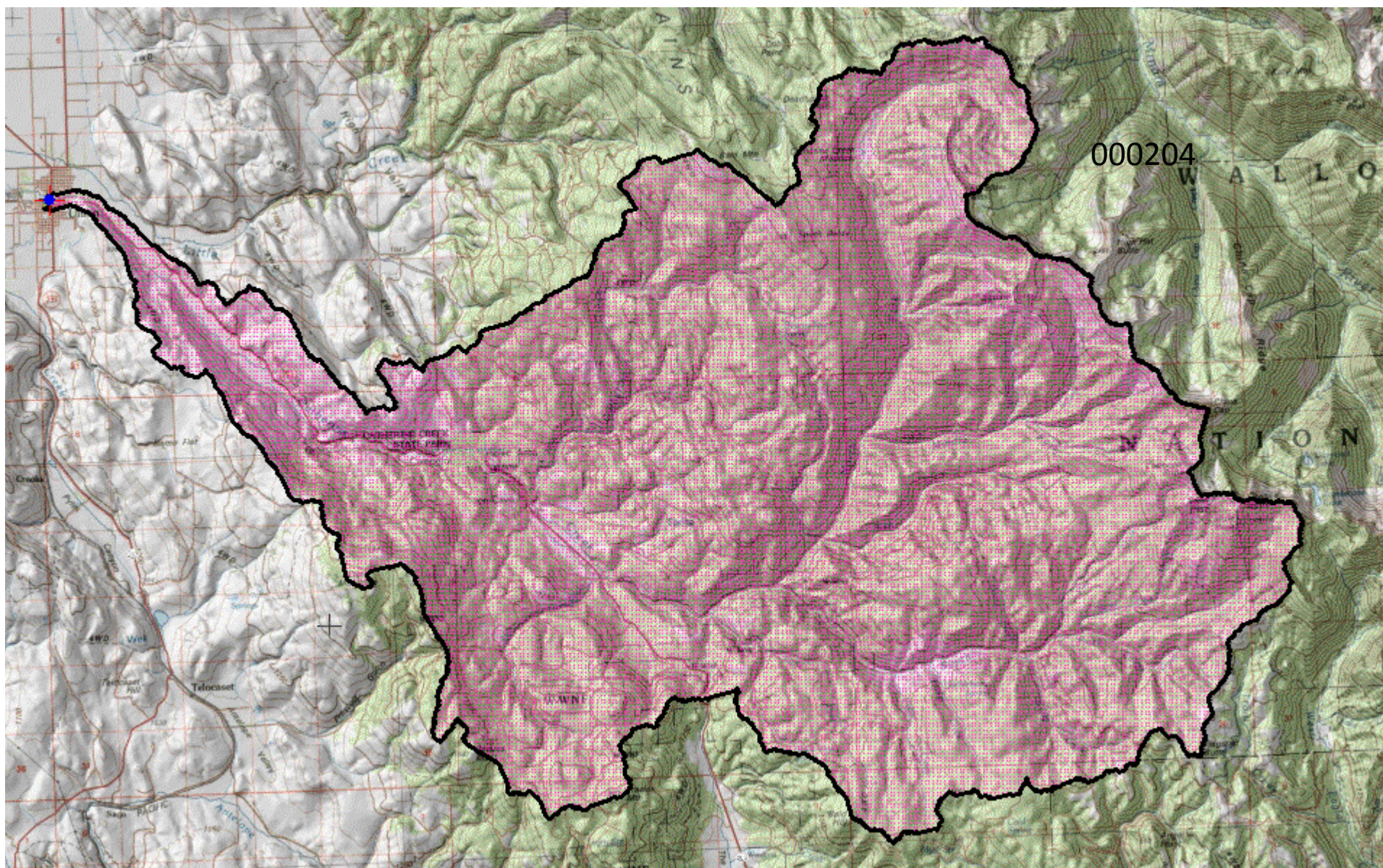
000009

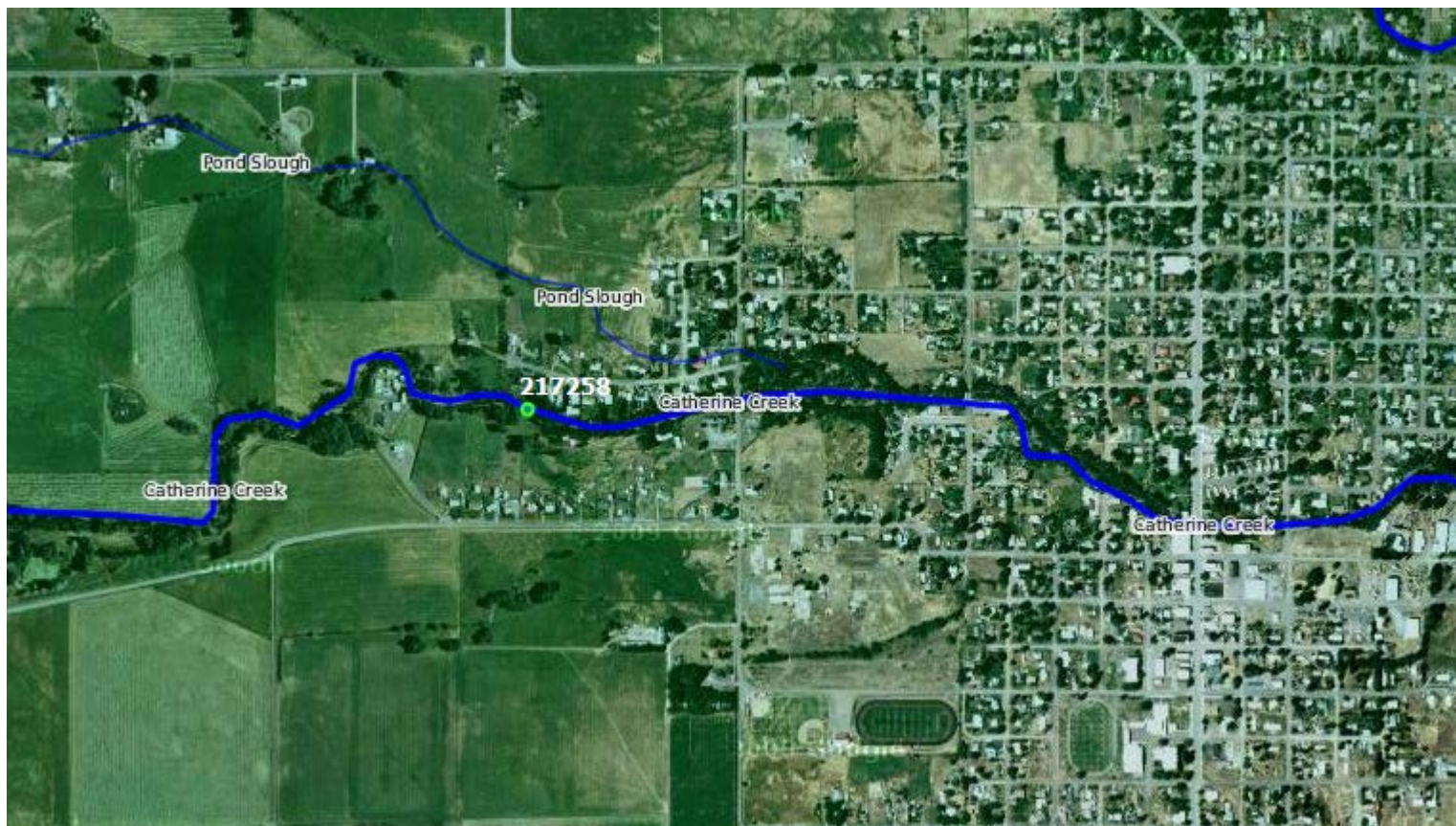




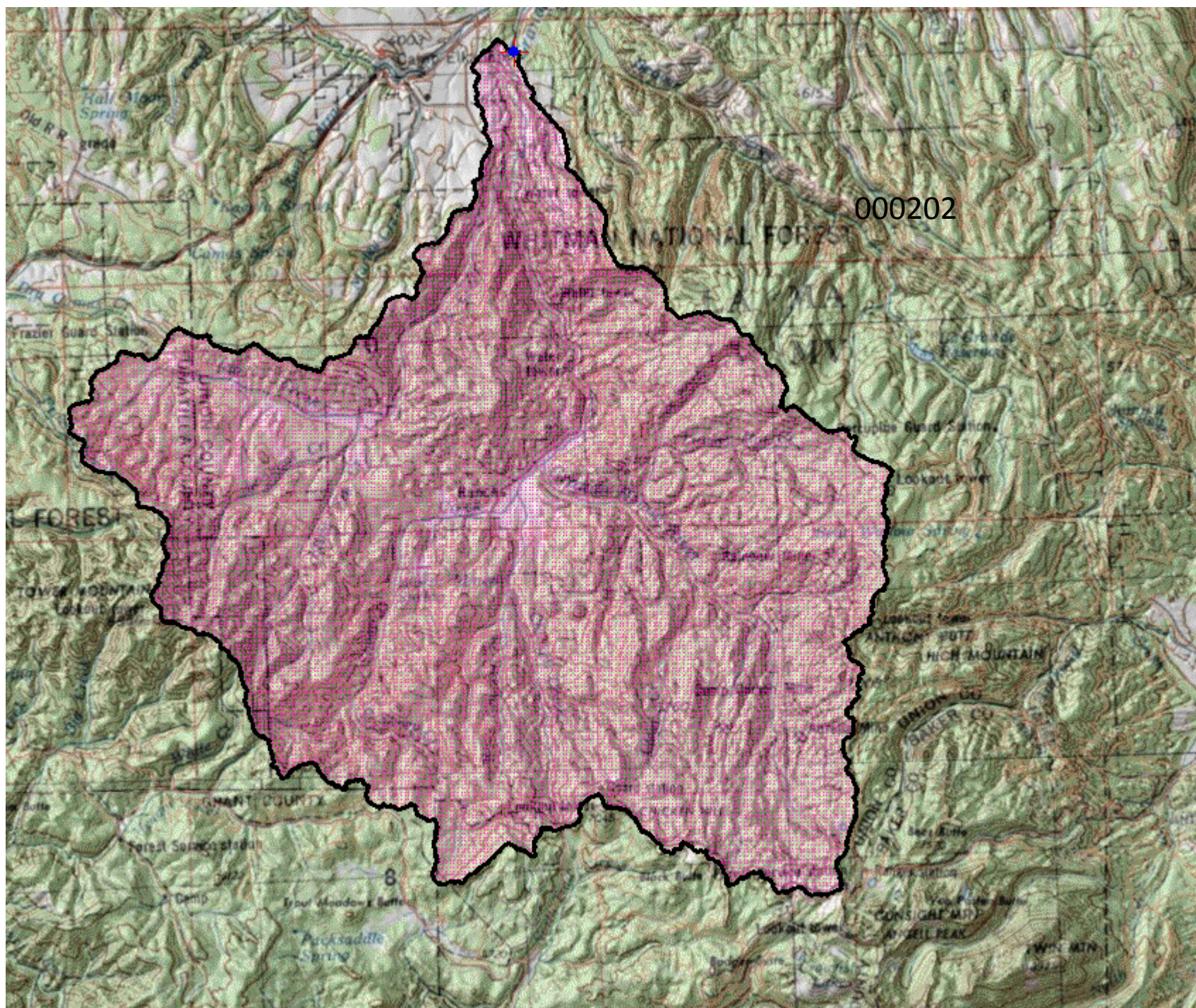
138554

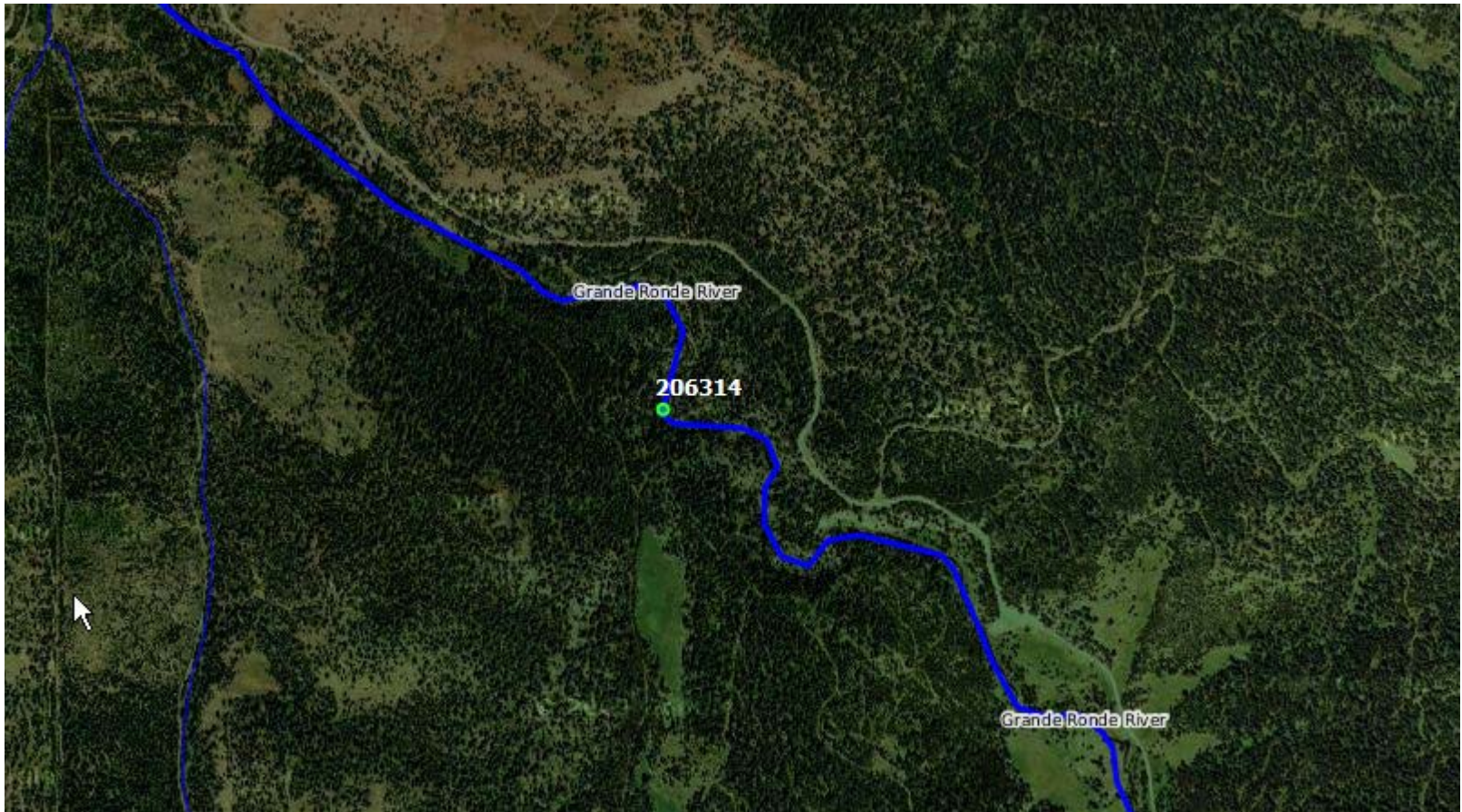


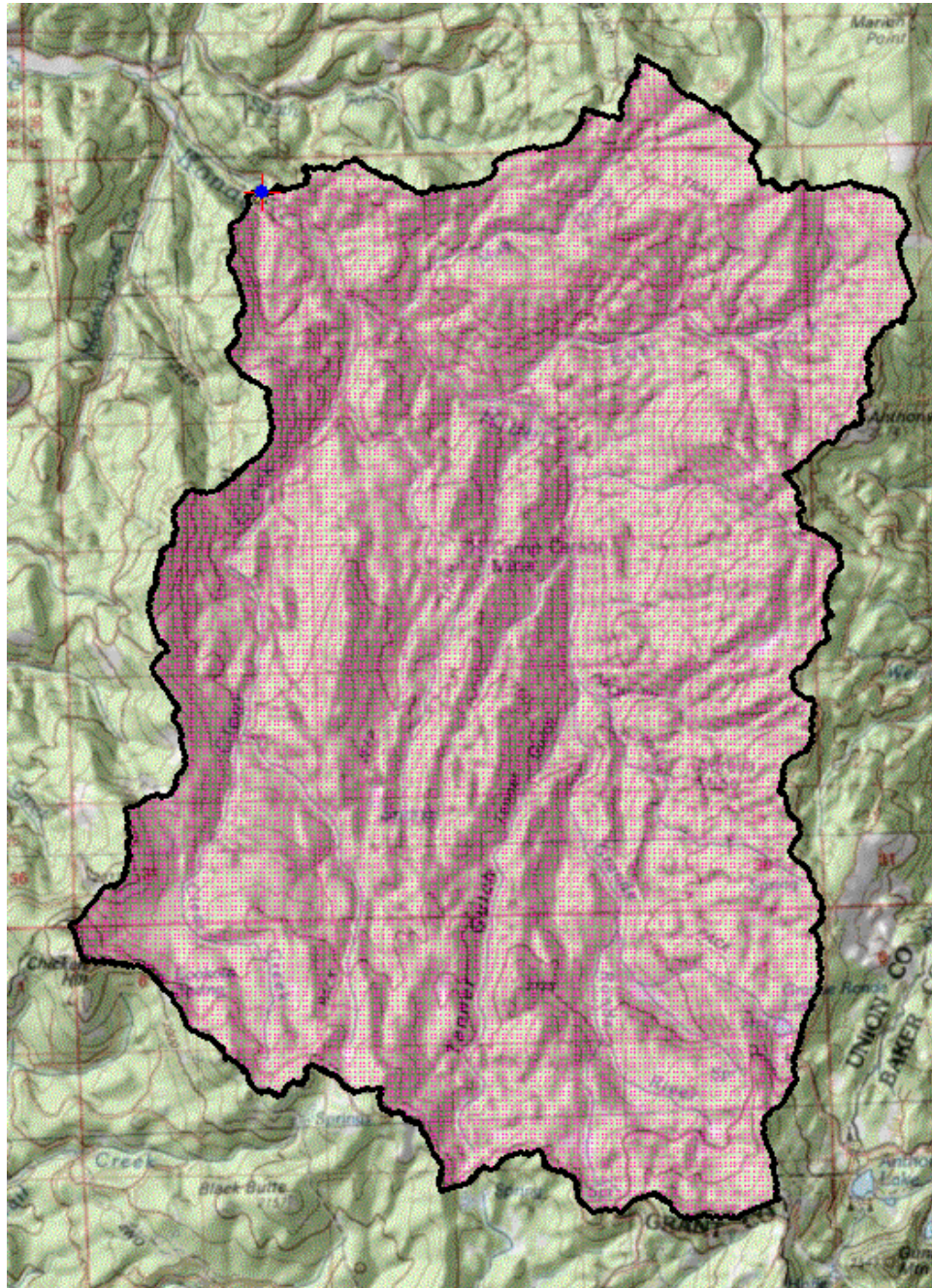






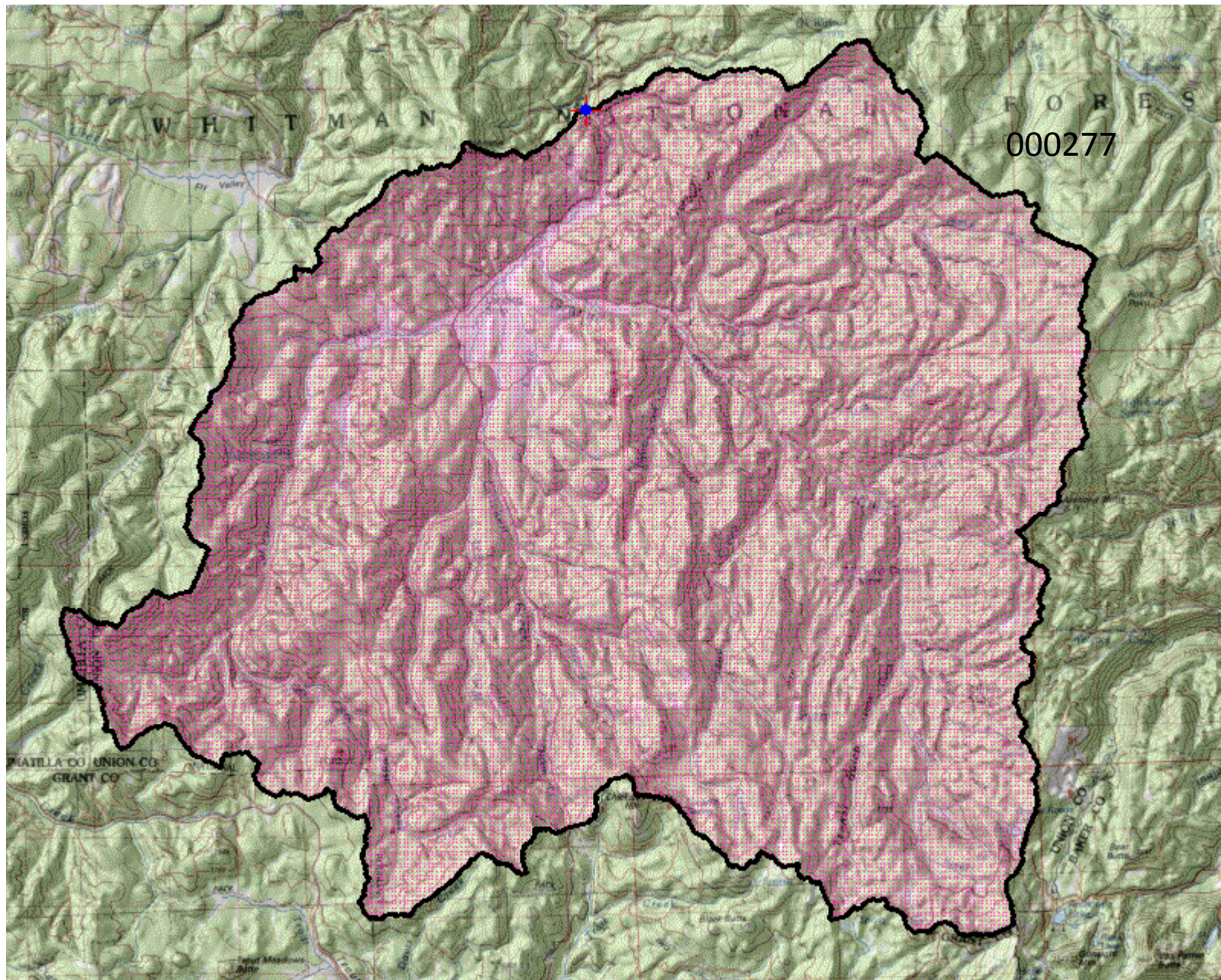




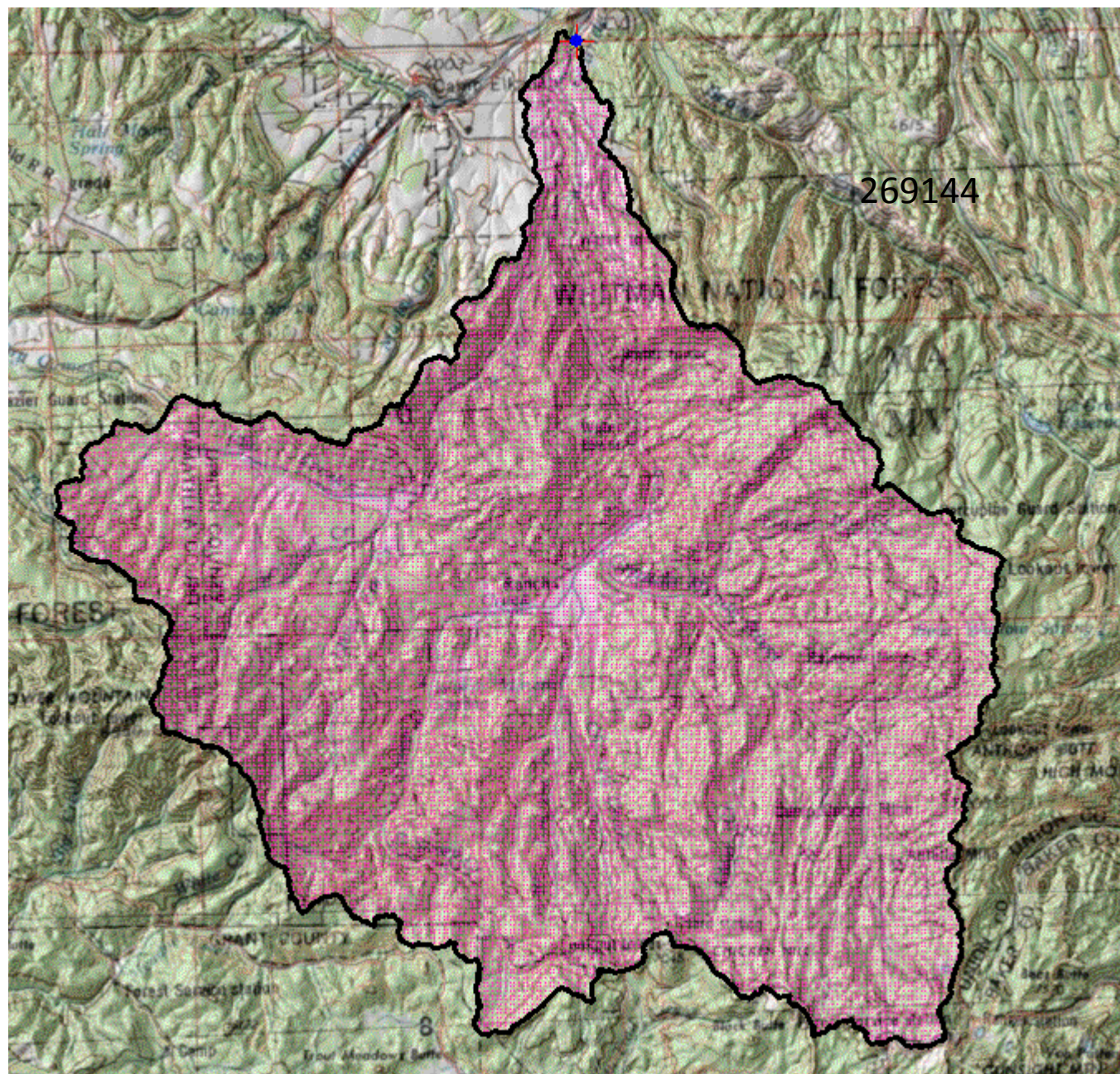


206314



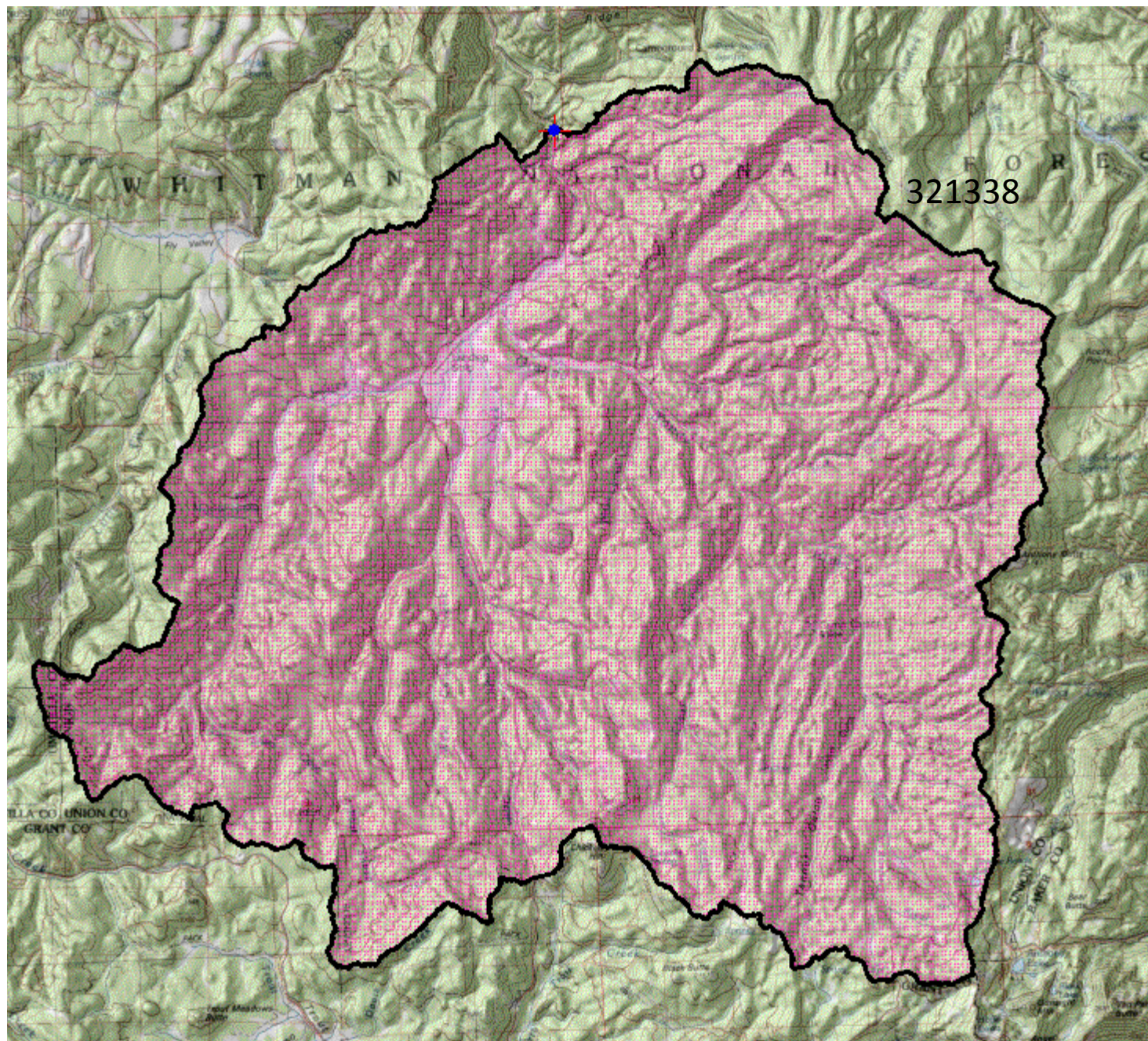




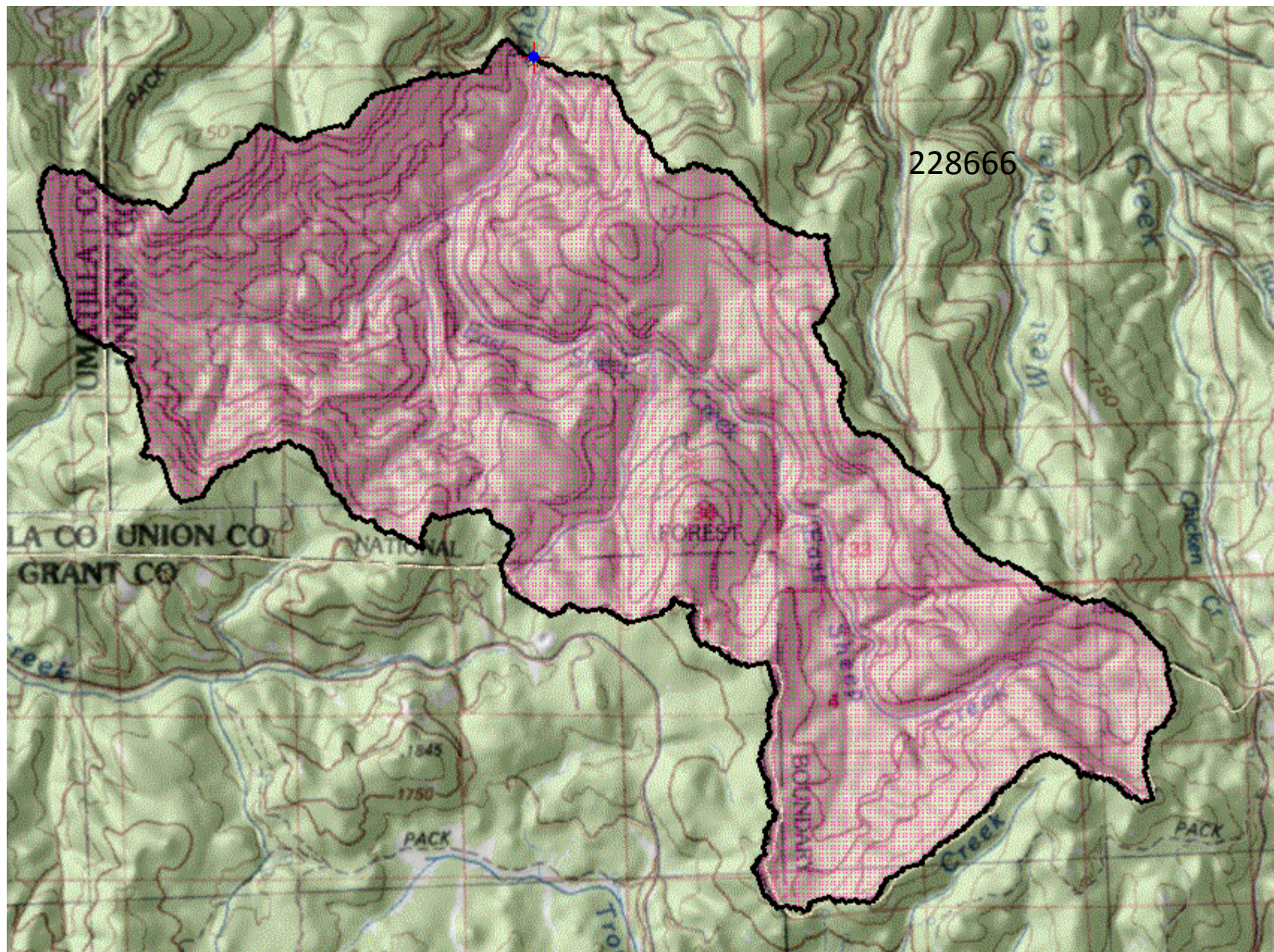


269144

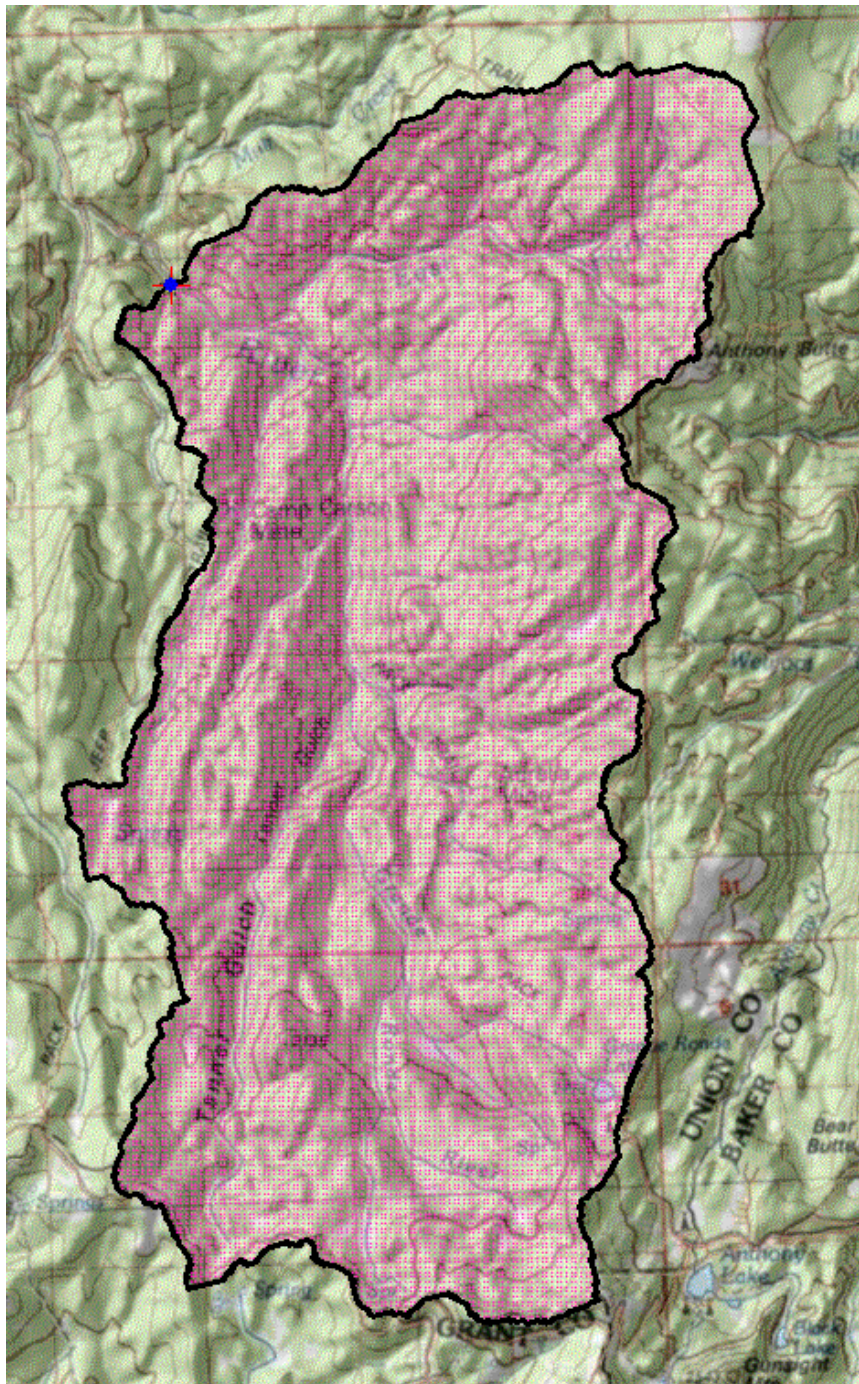






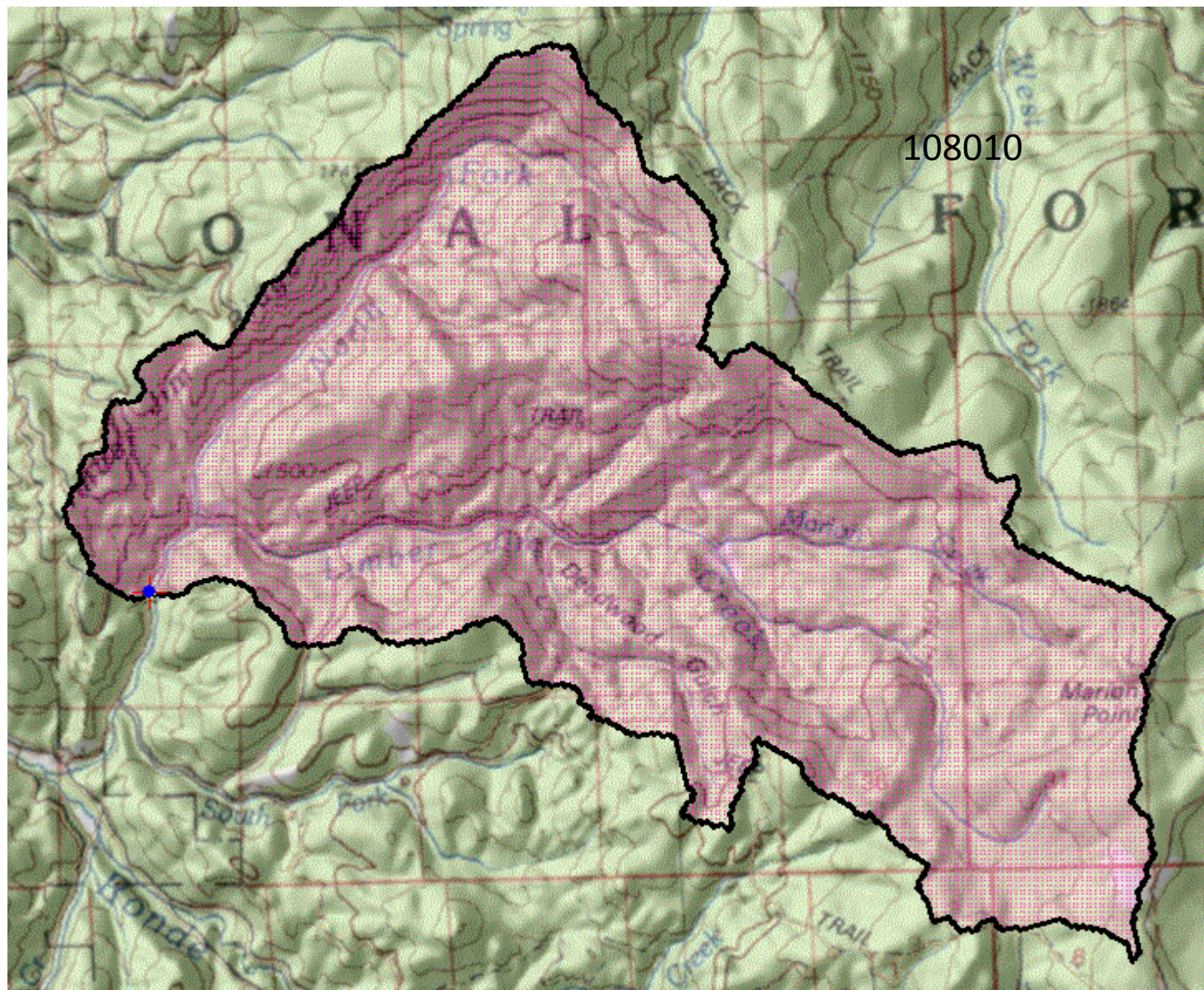




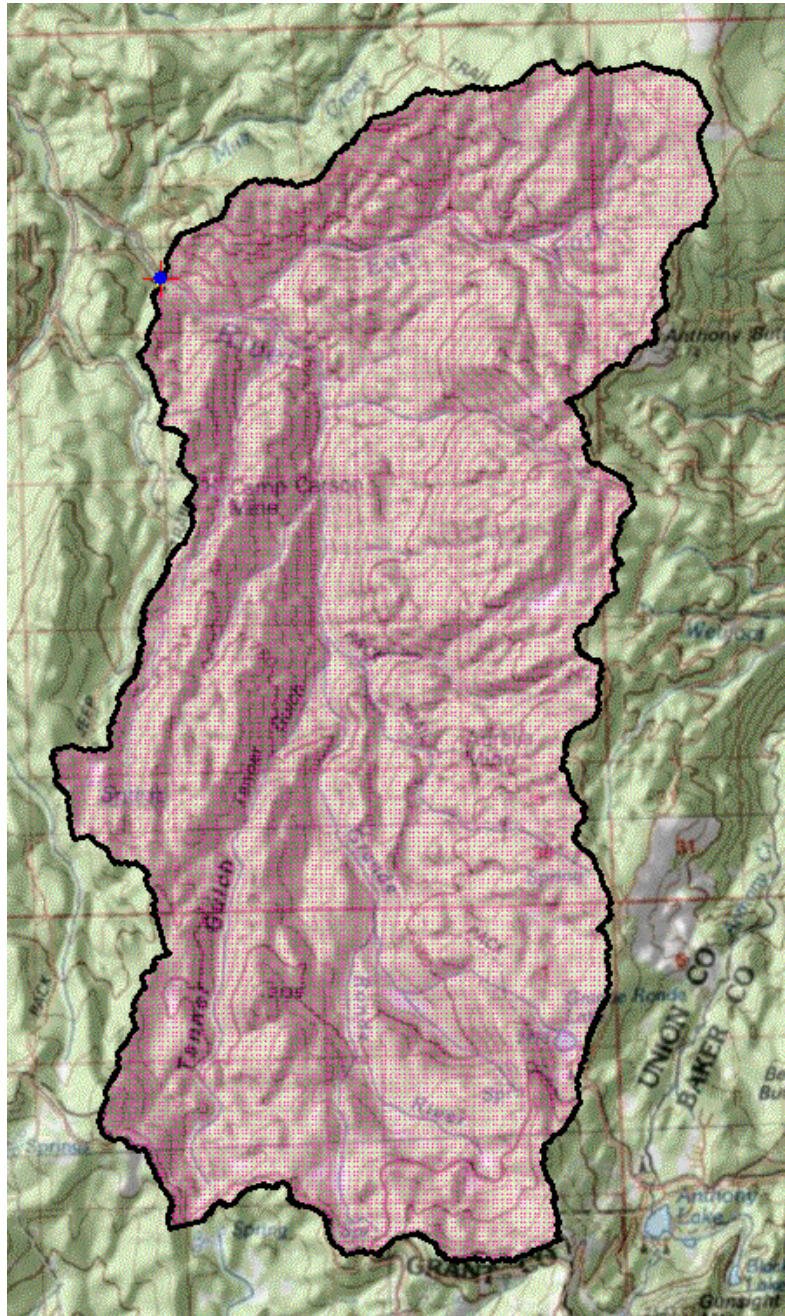


148977



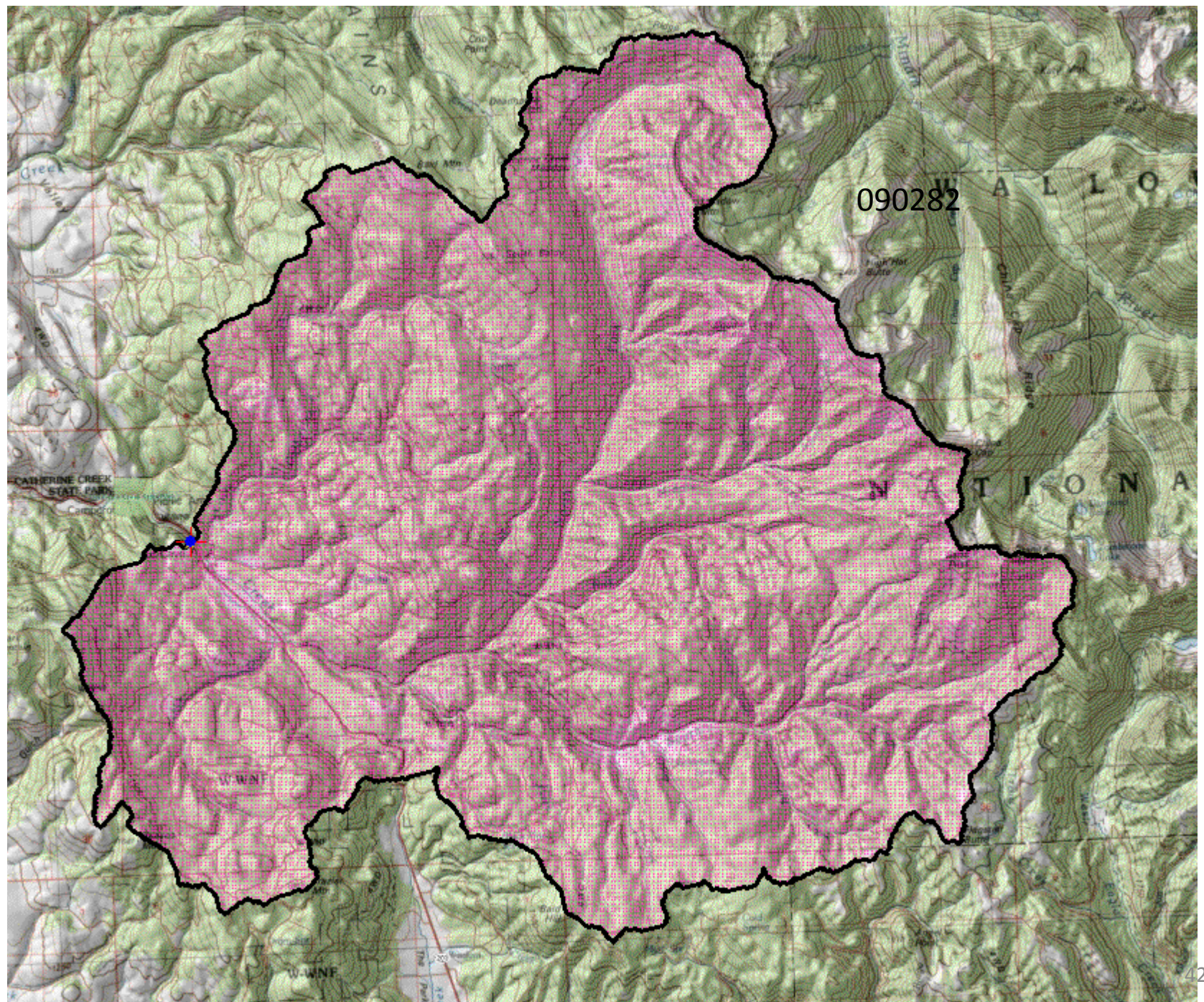


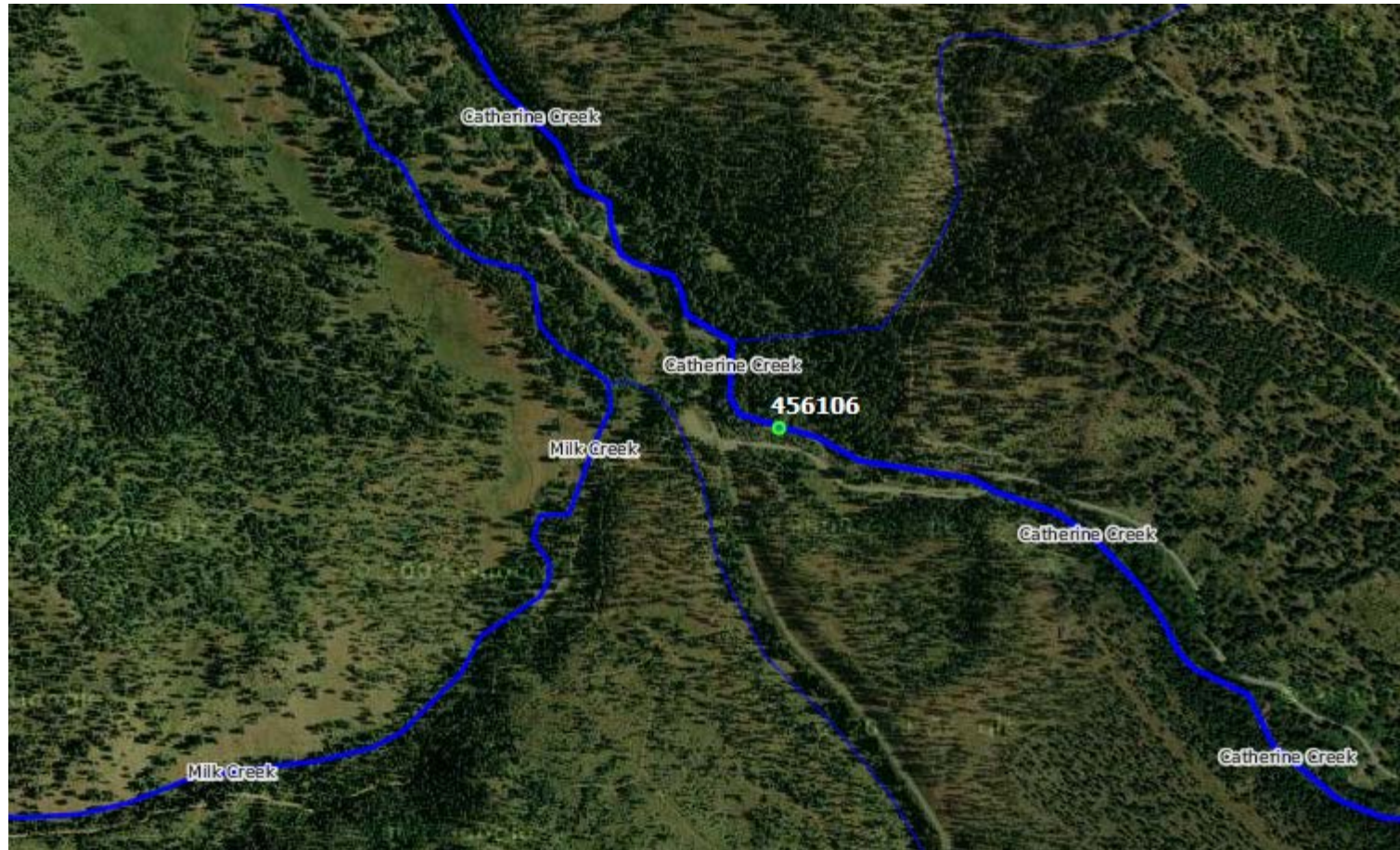


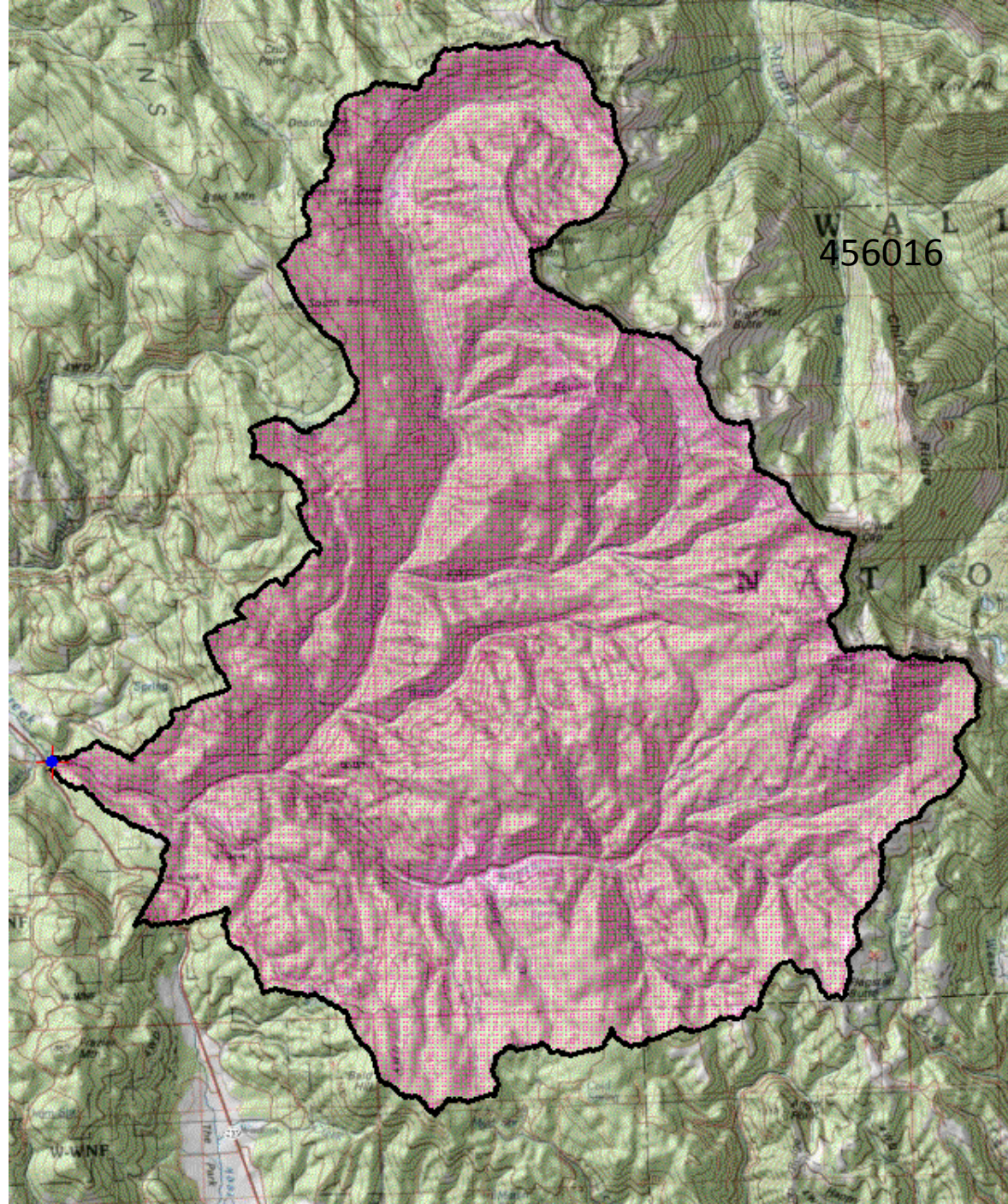


280042

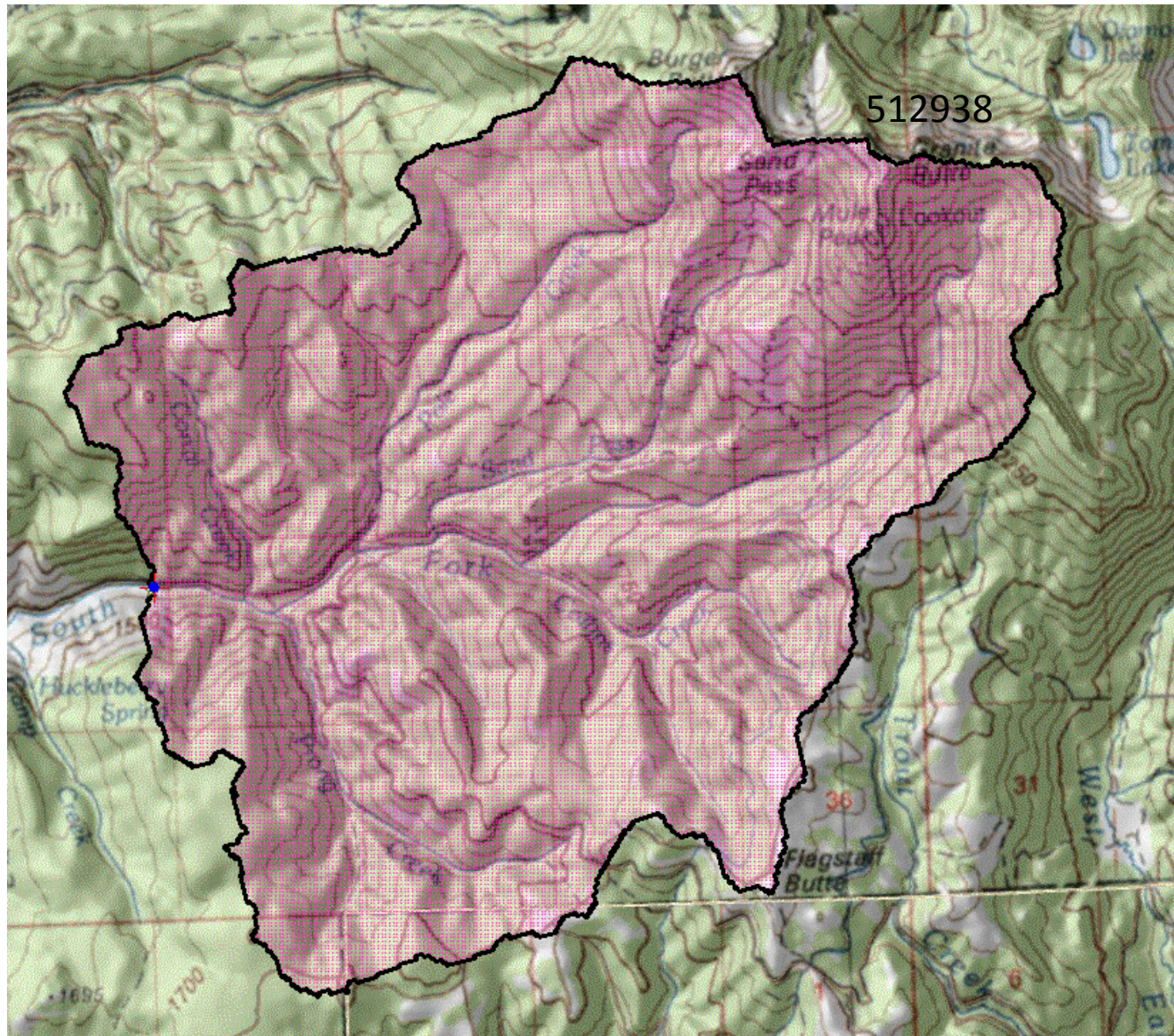


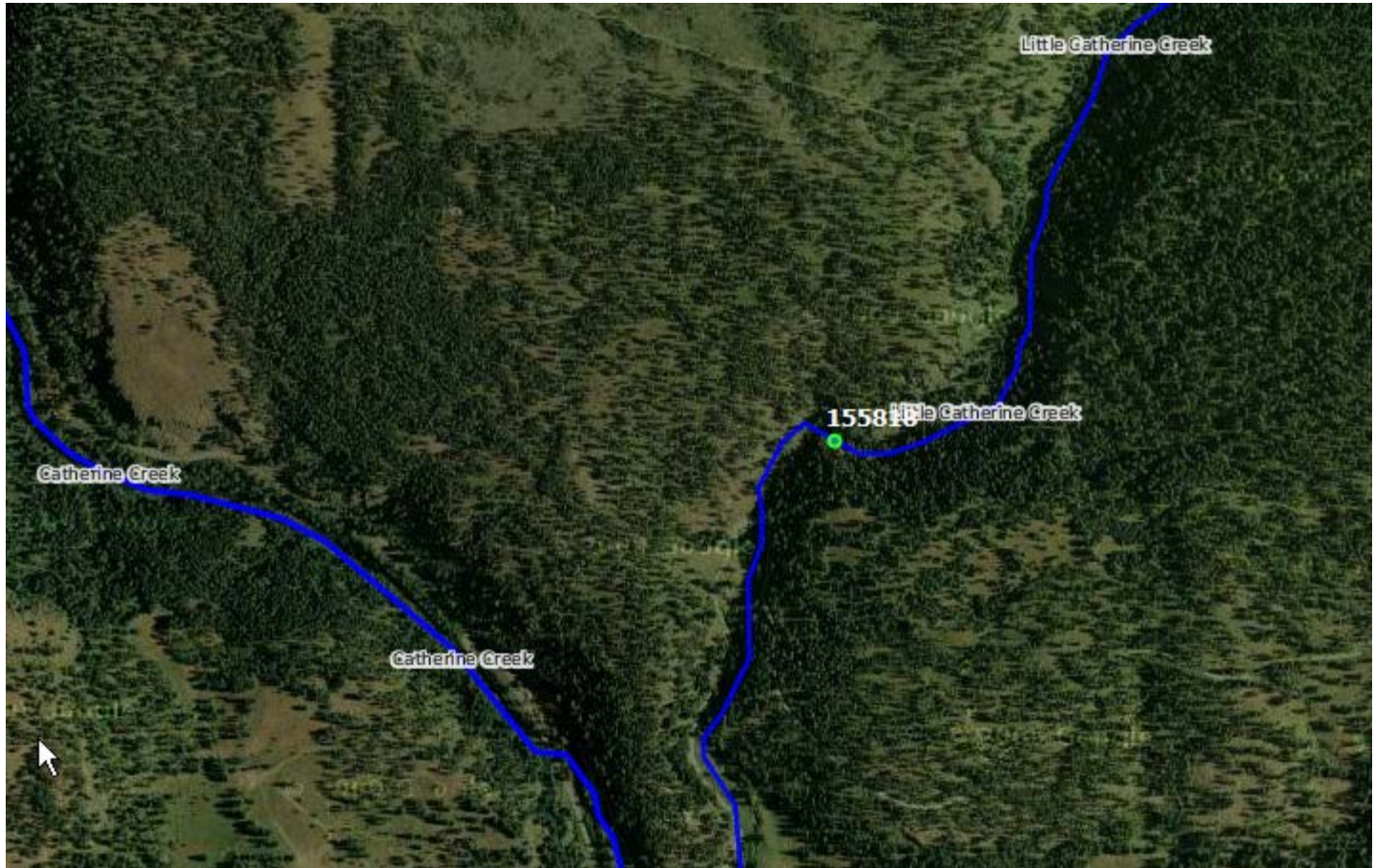


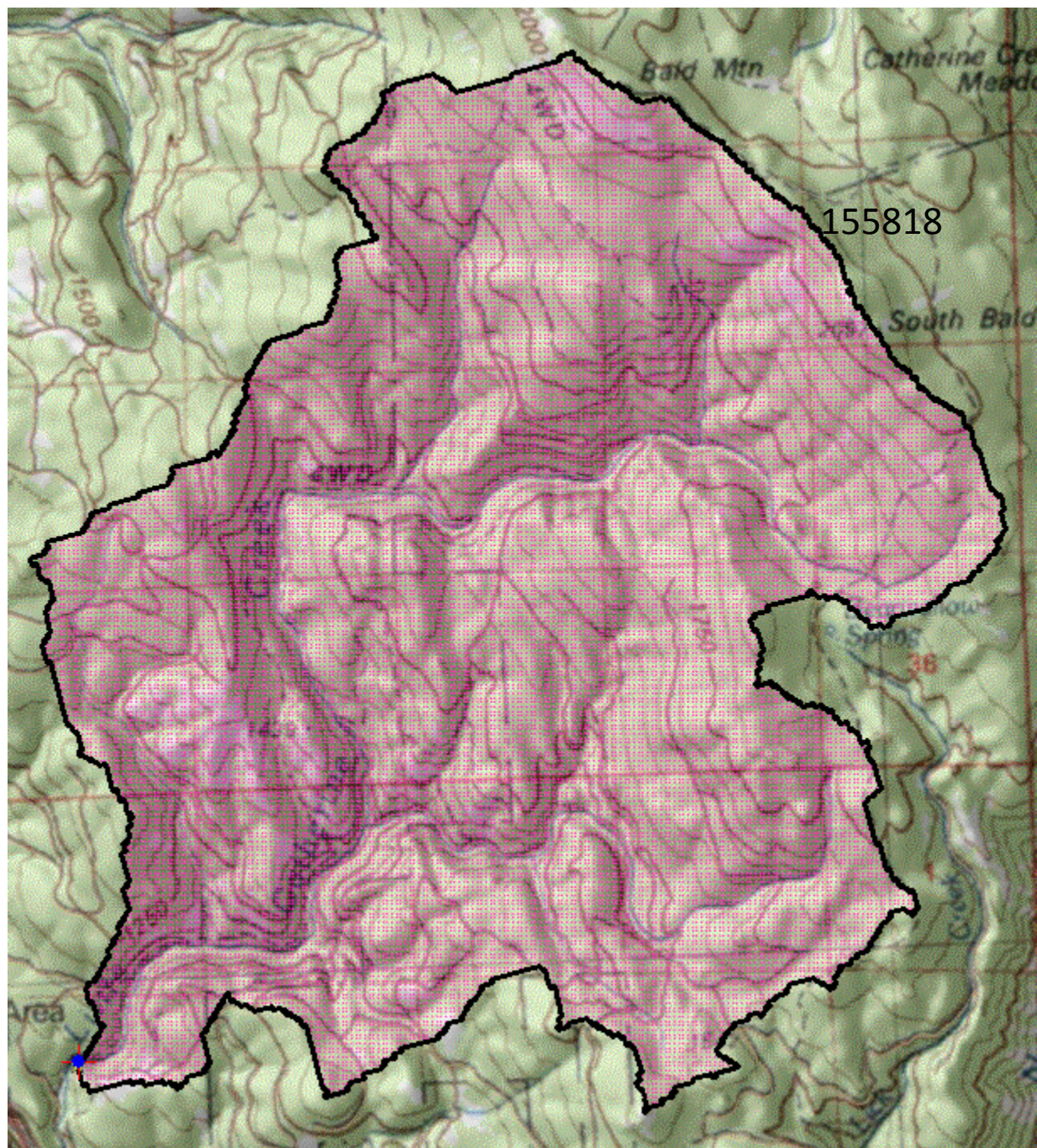


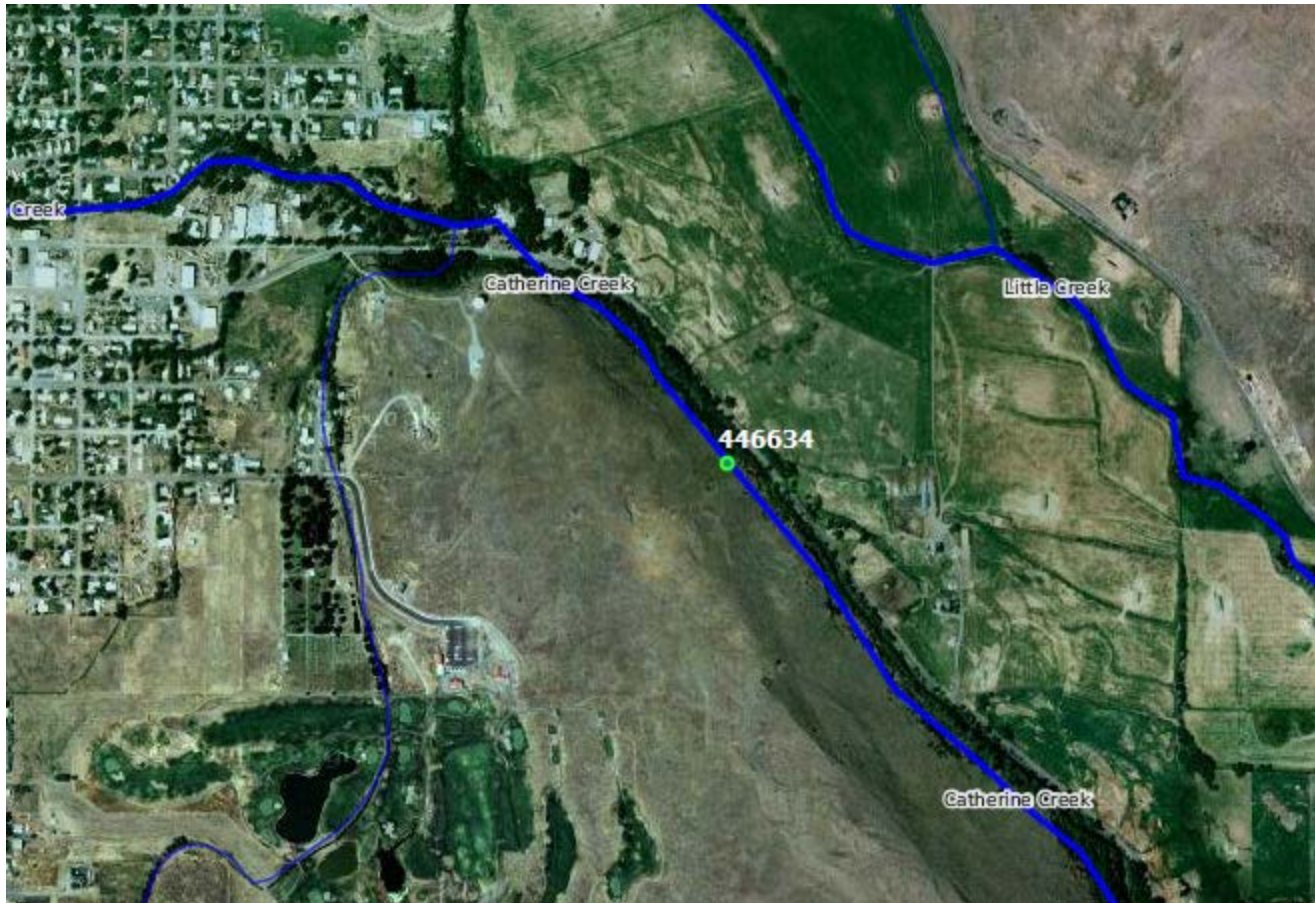


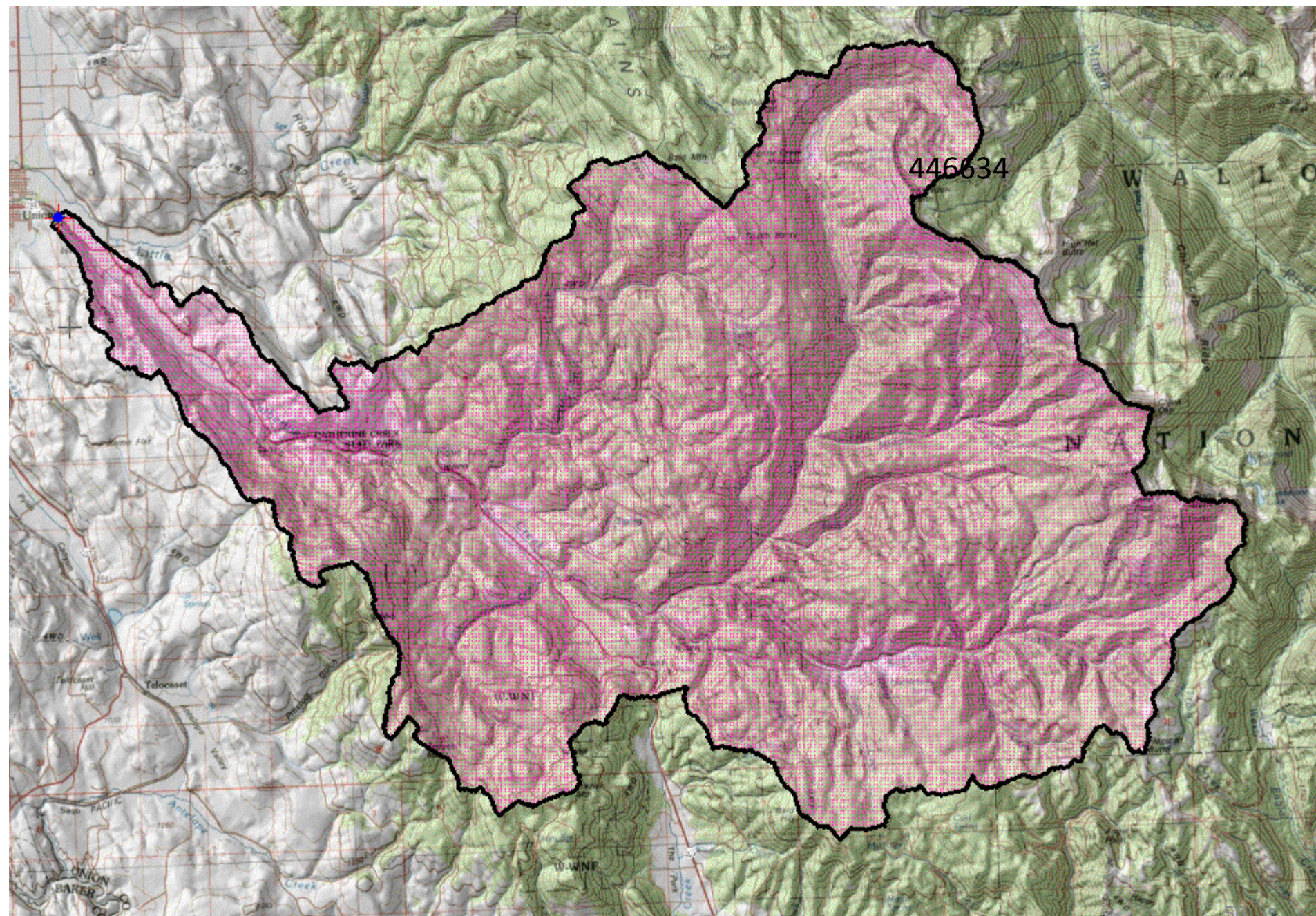


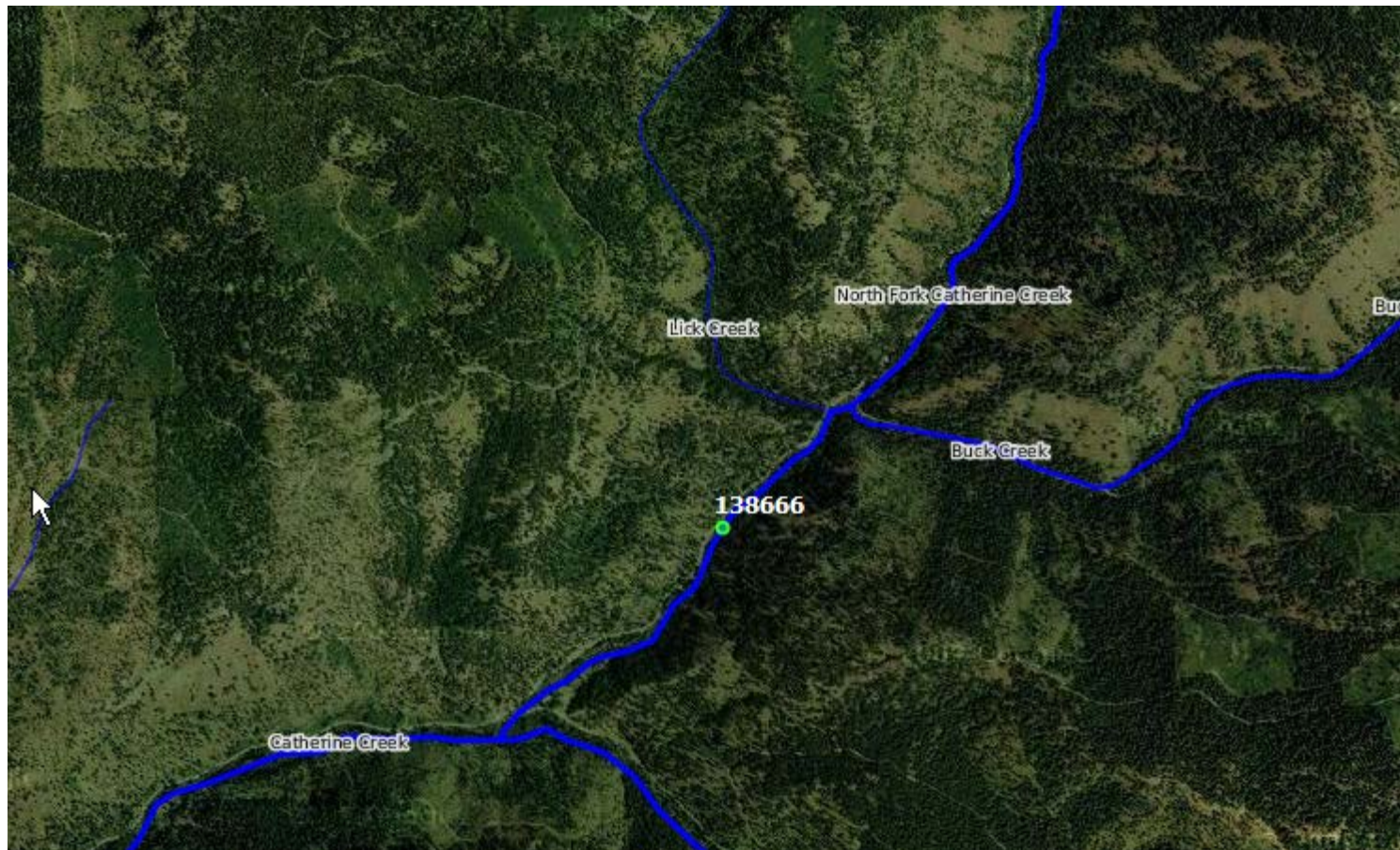


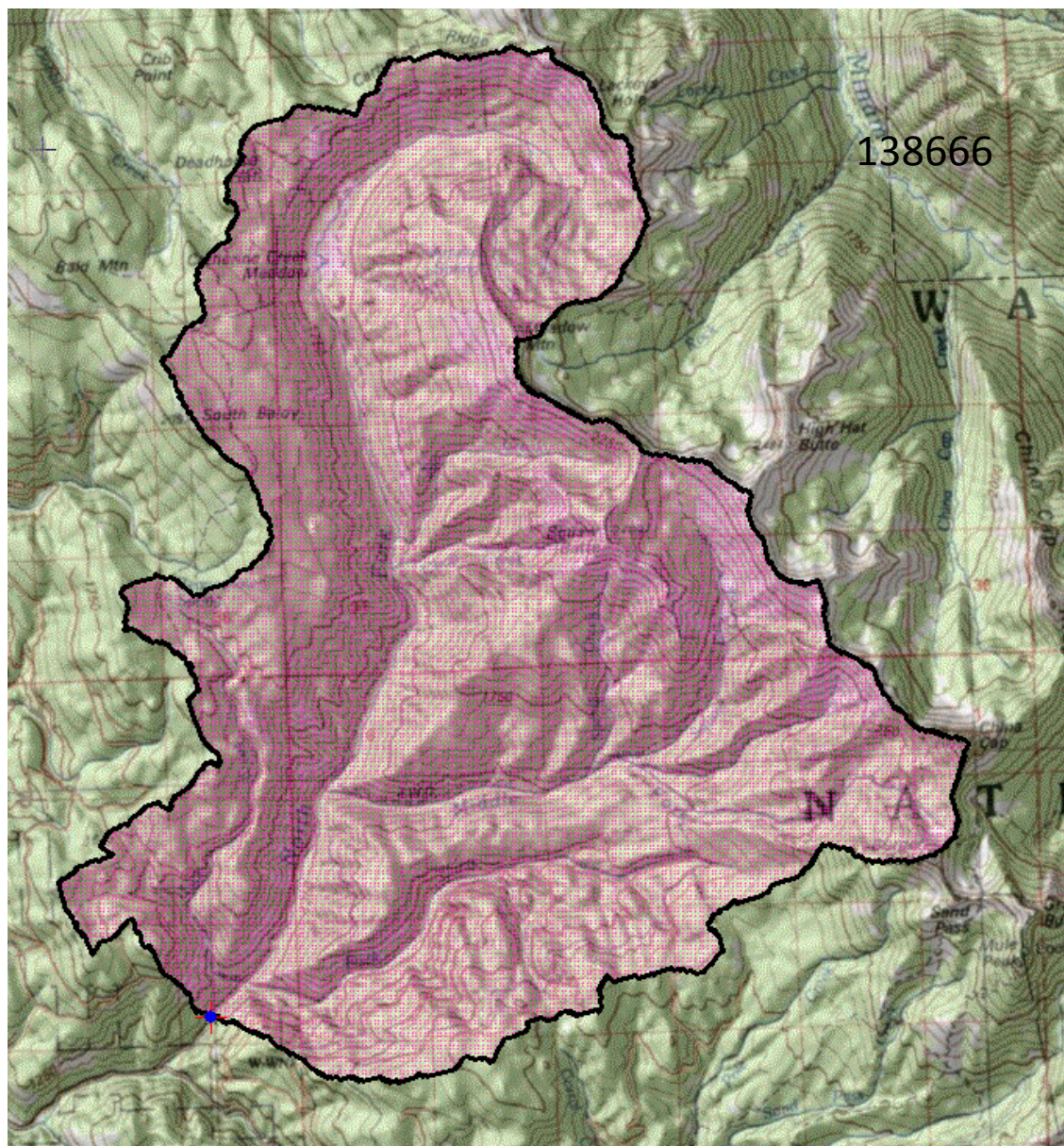


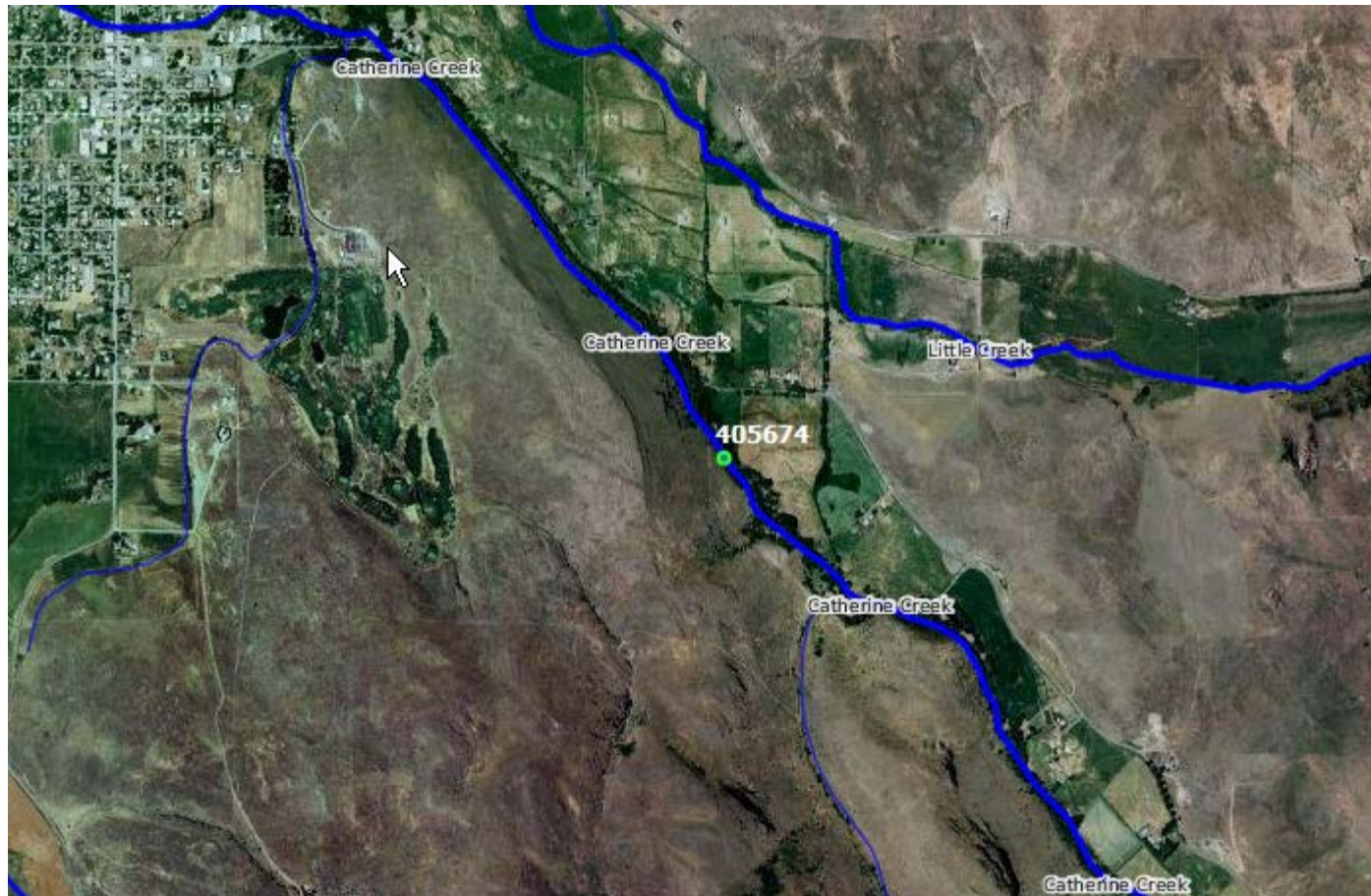


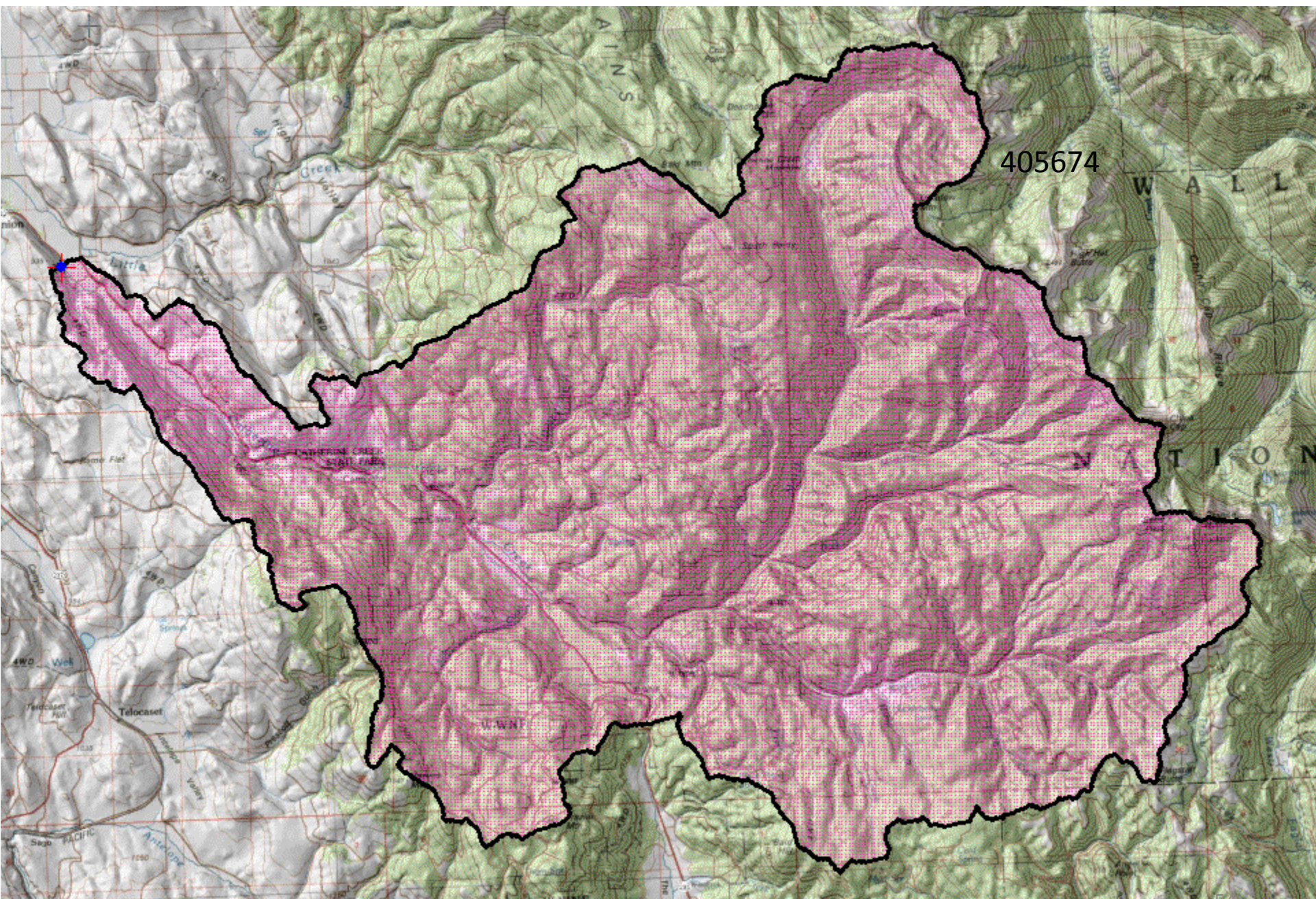


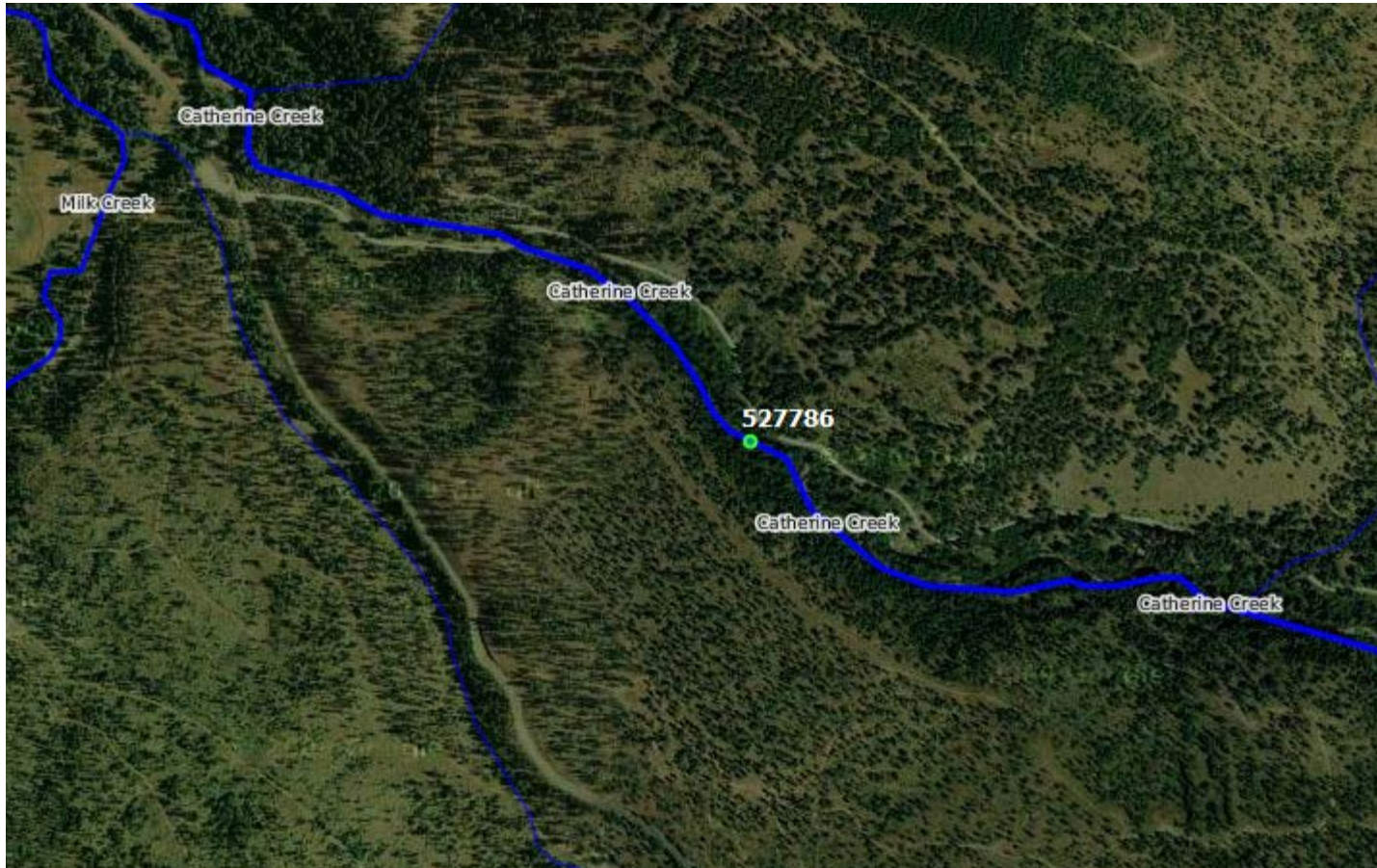


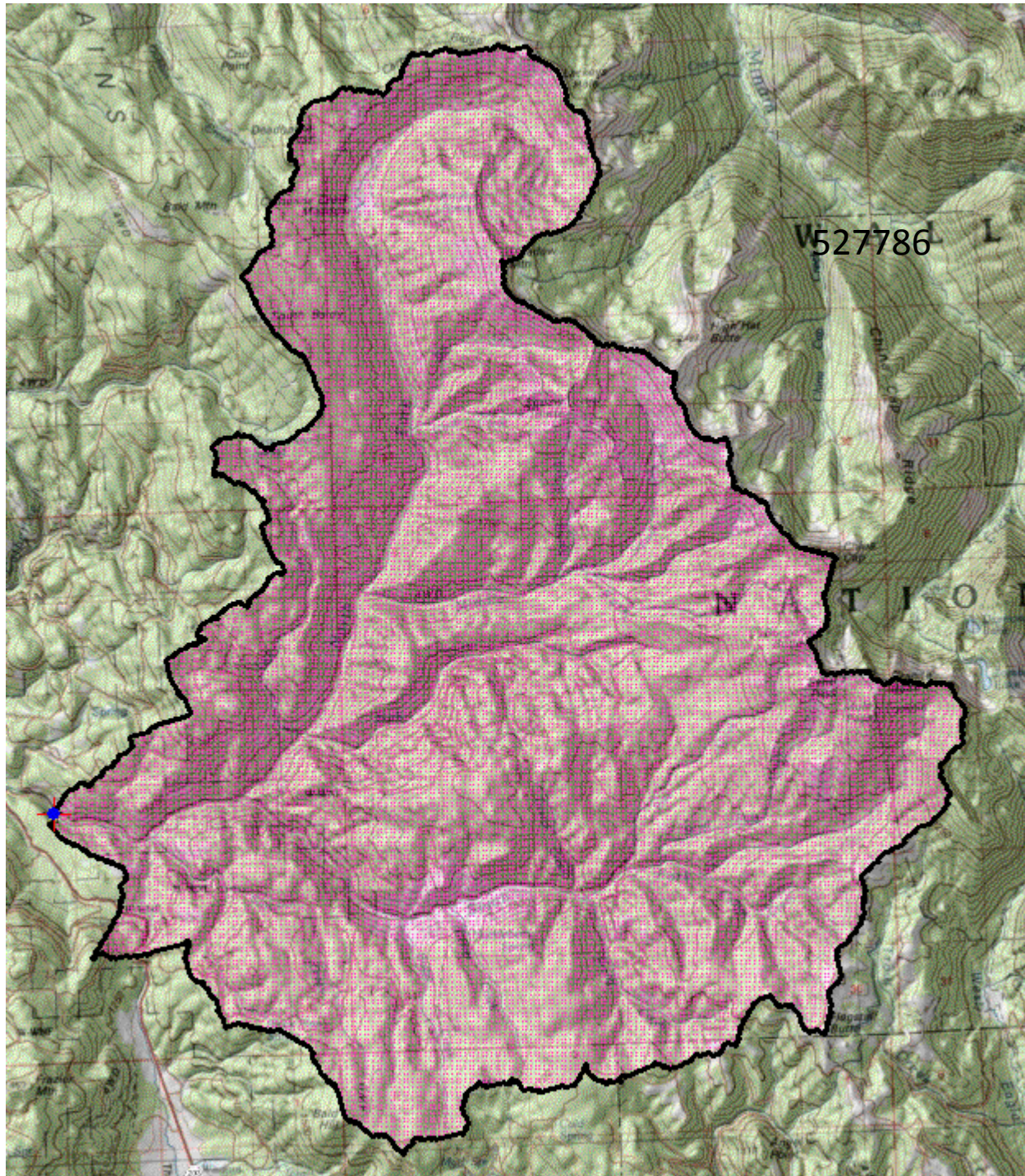


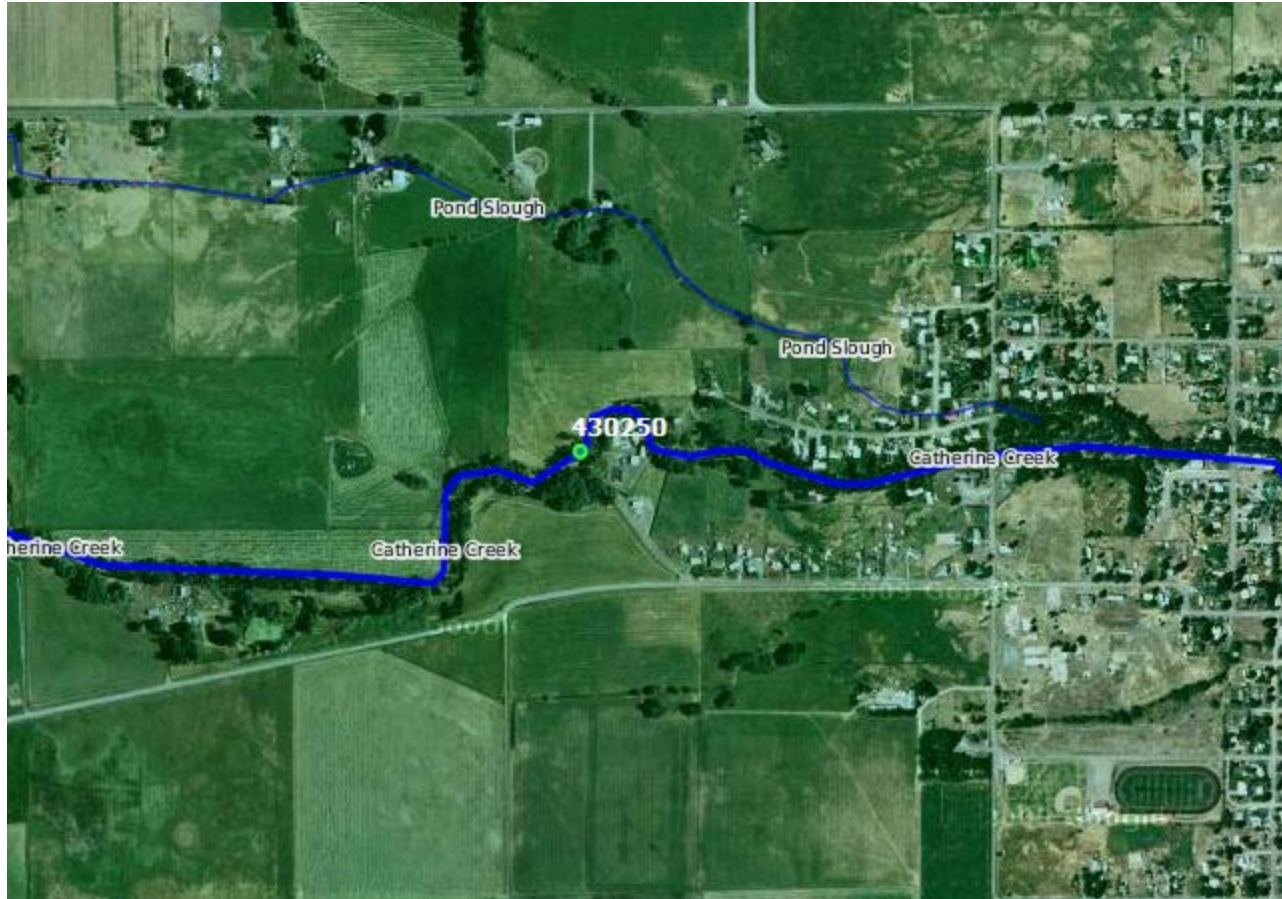


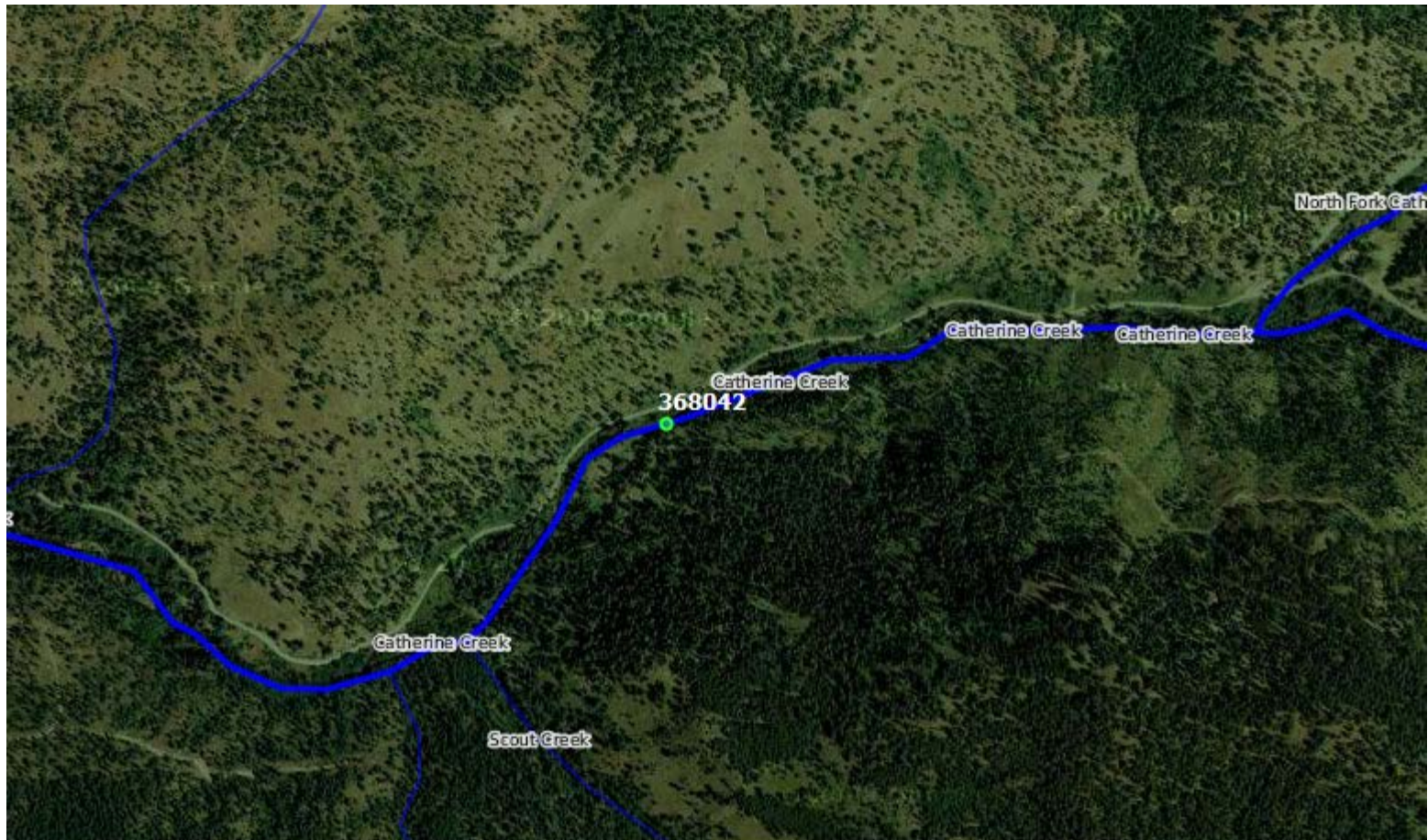


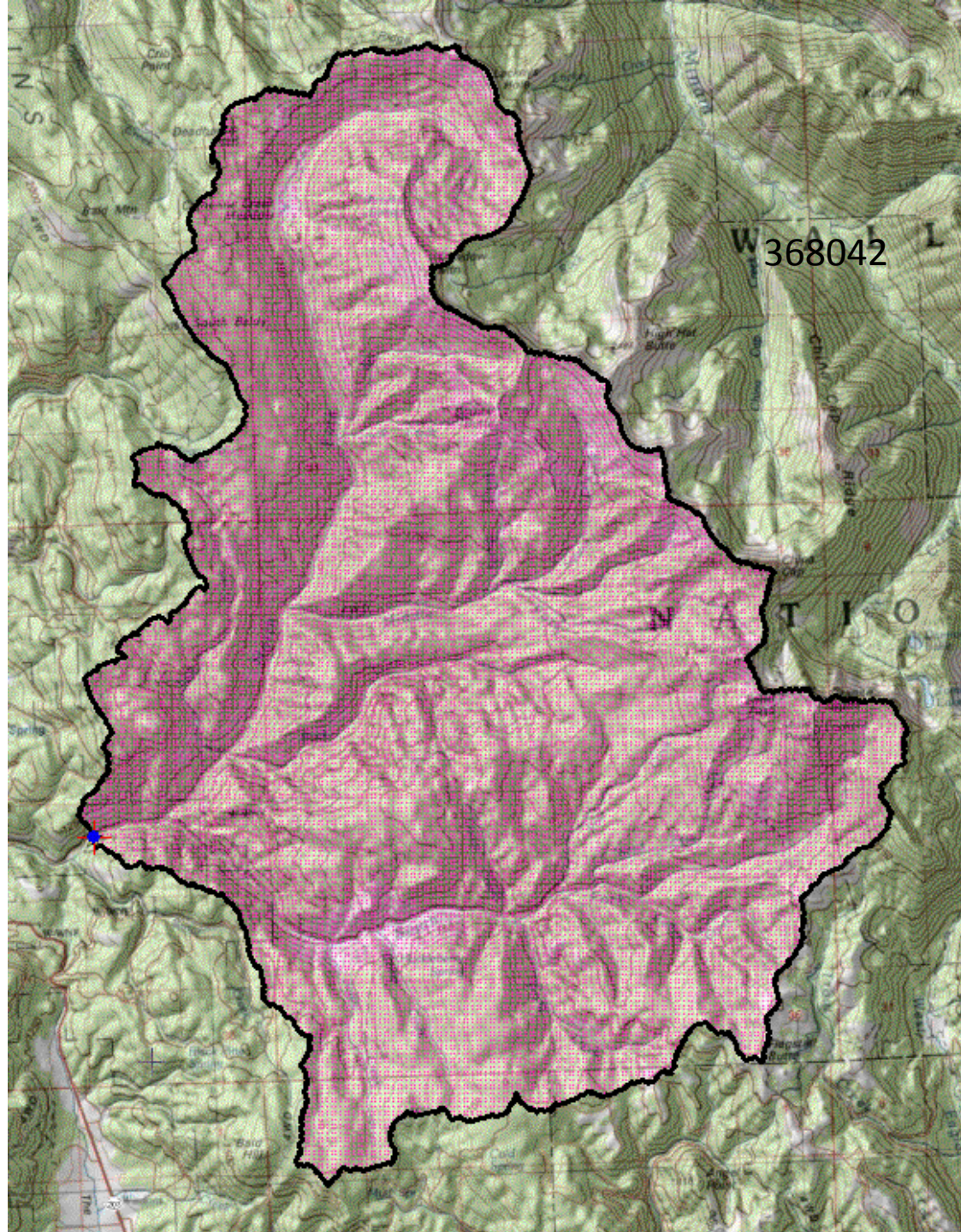




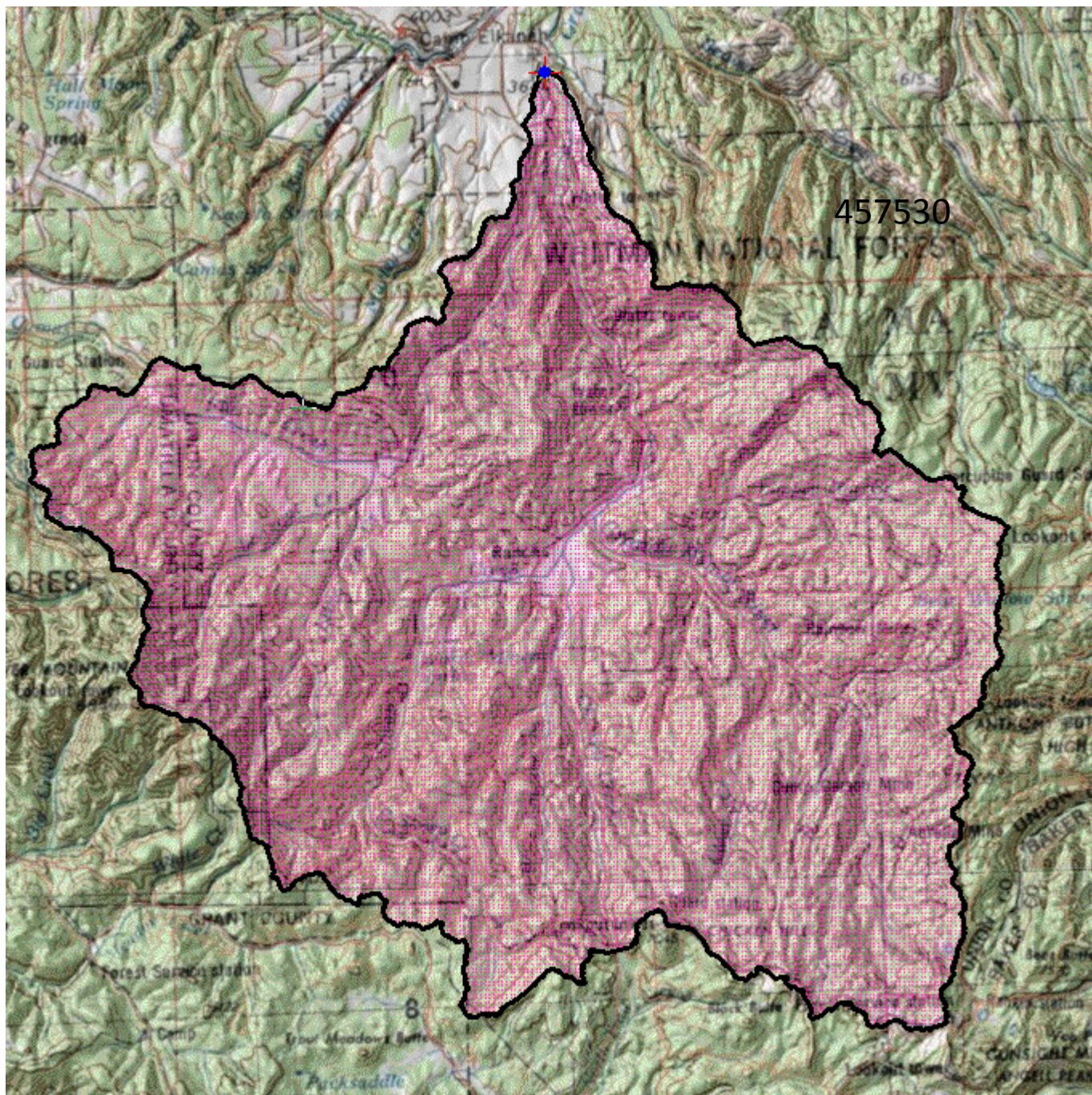


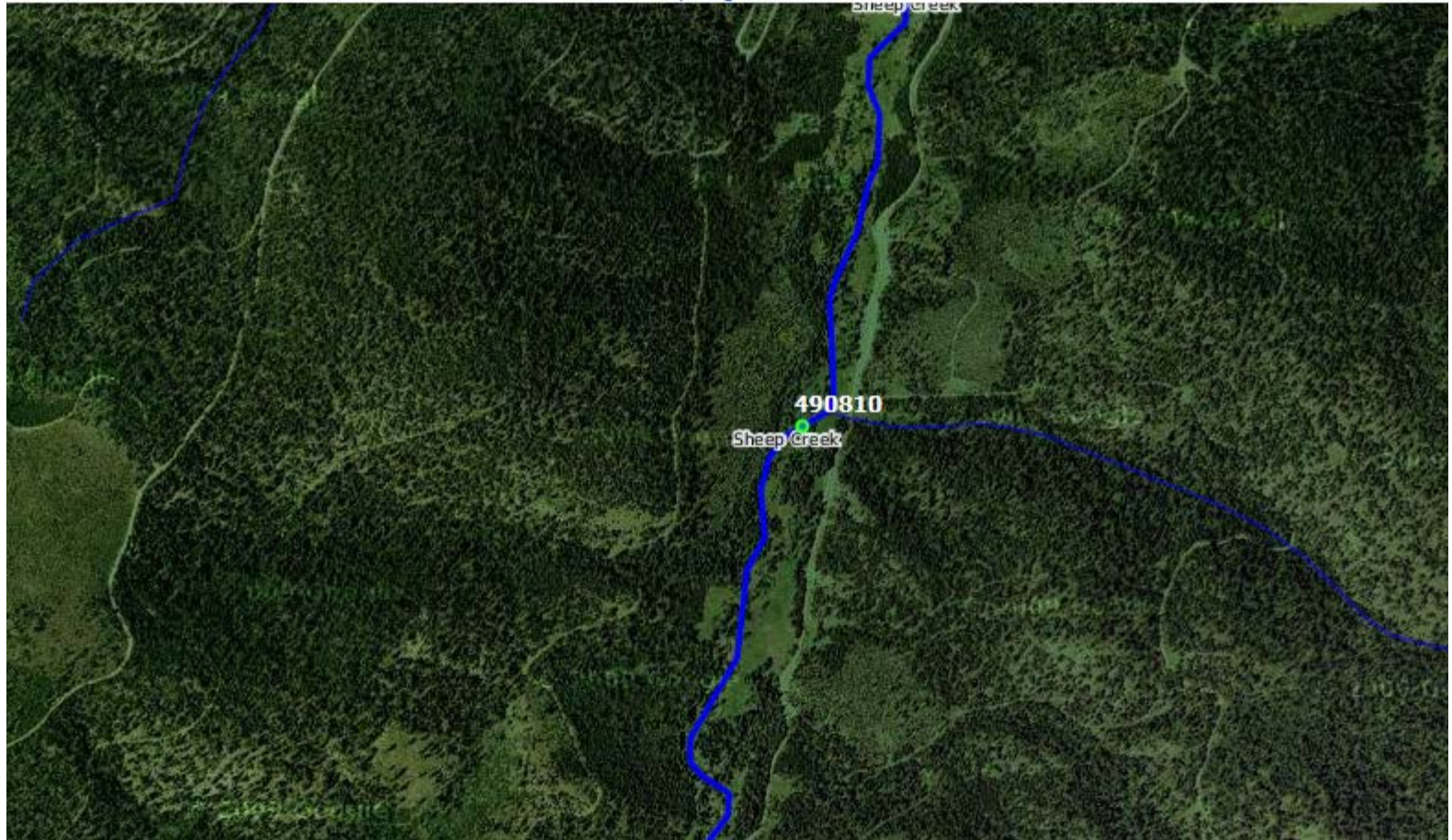


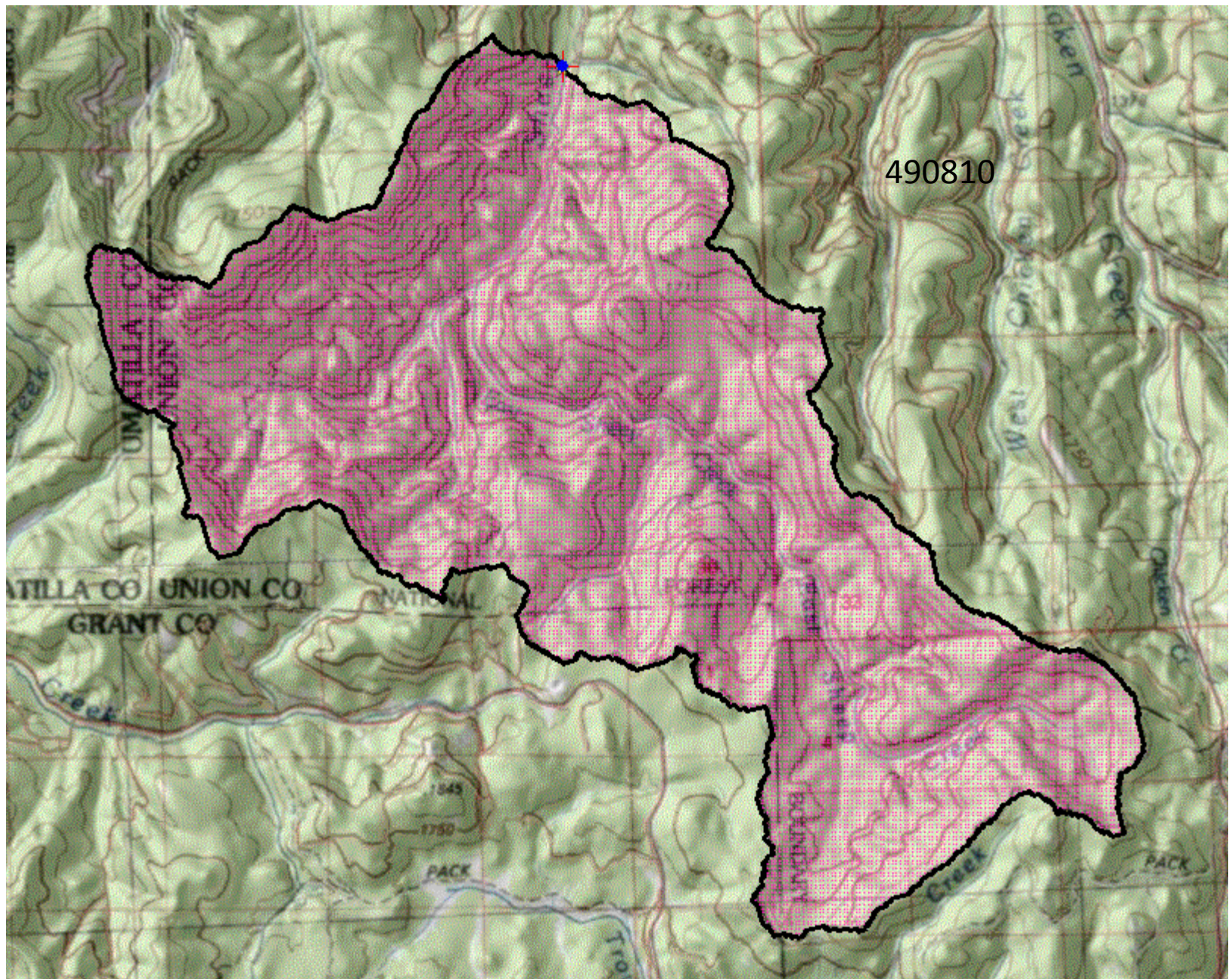




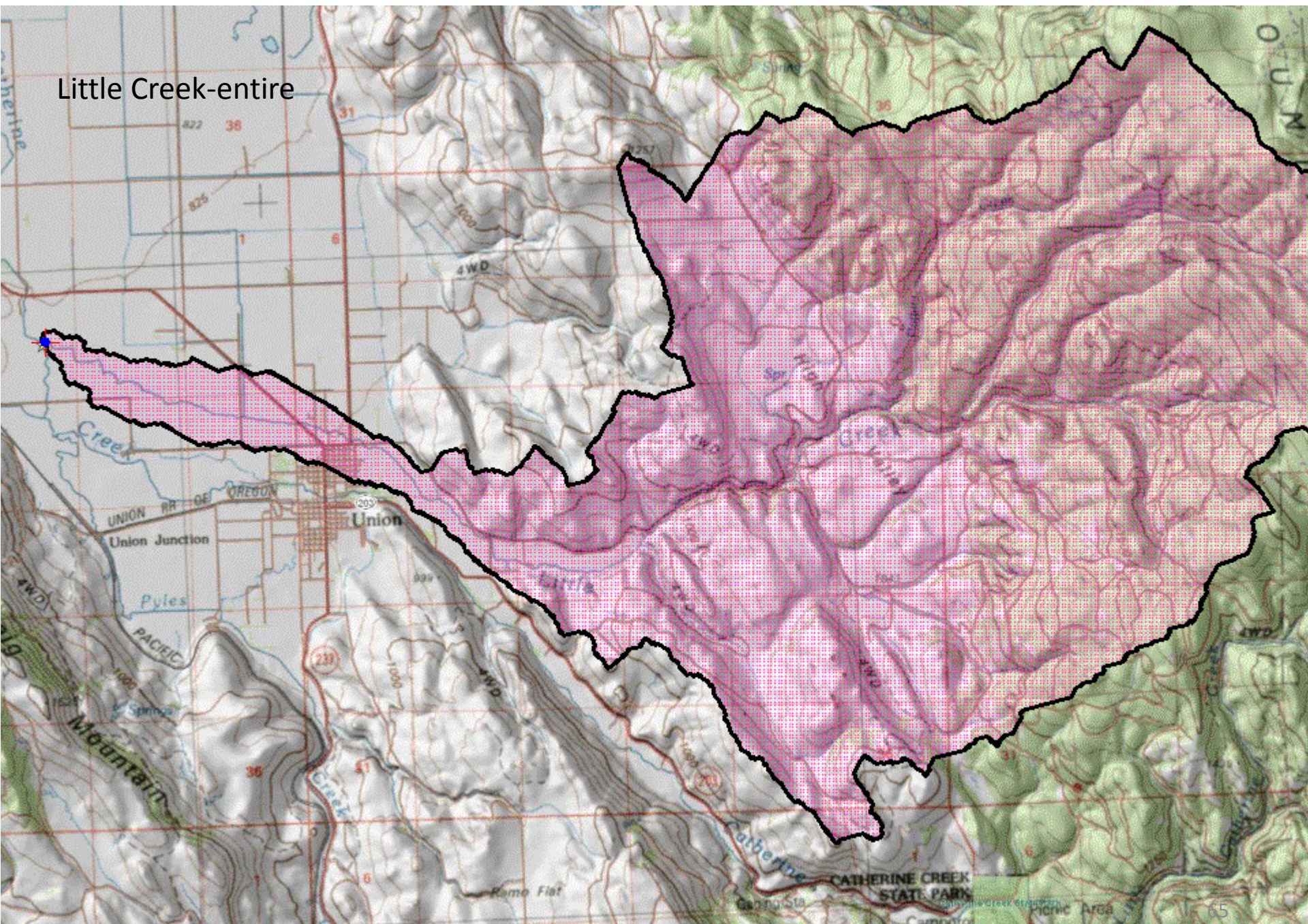






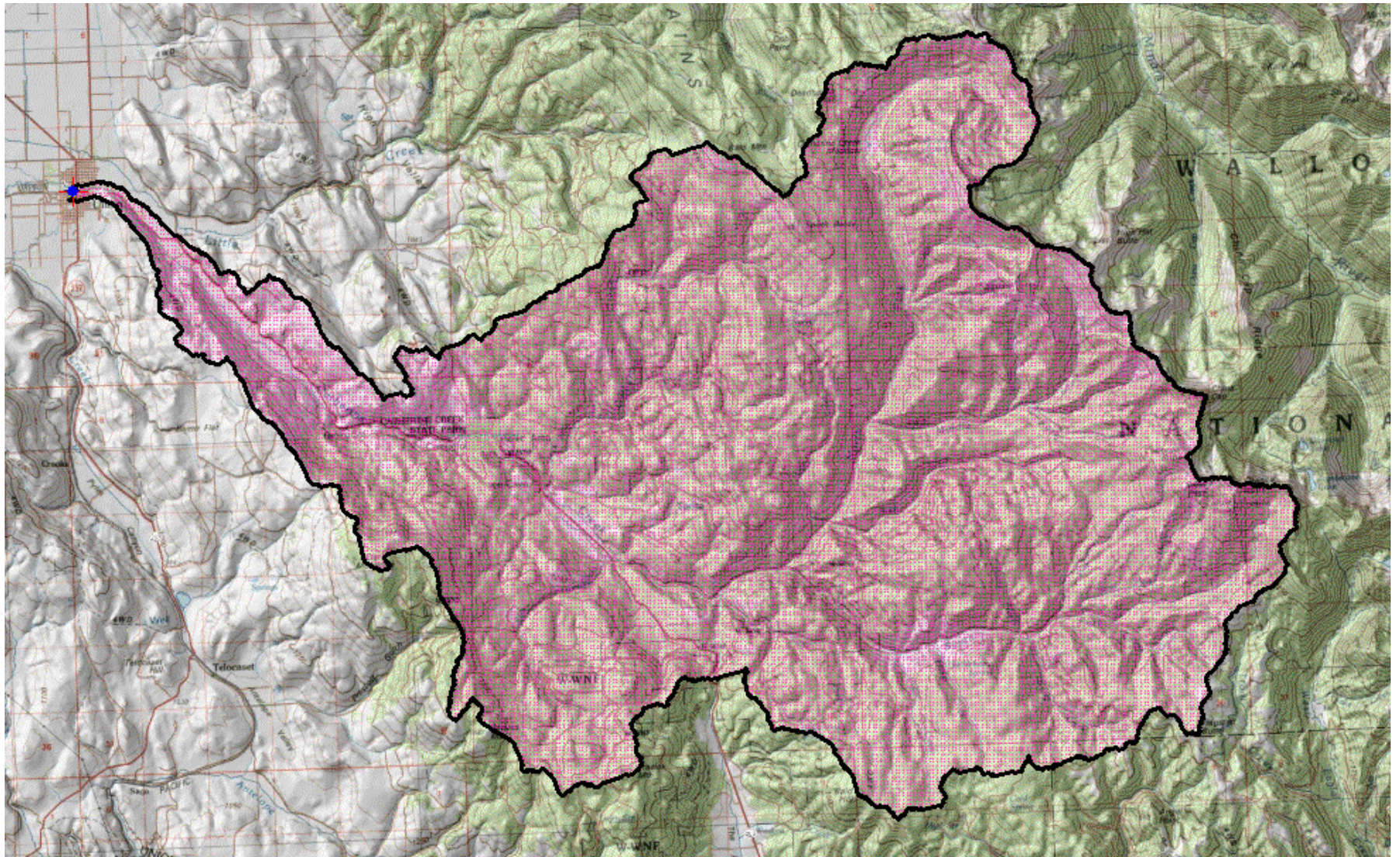


Little Creek-entire

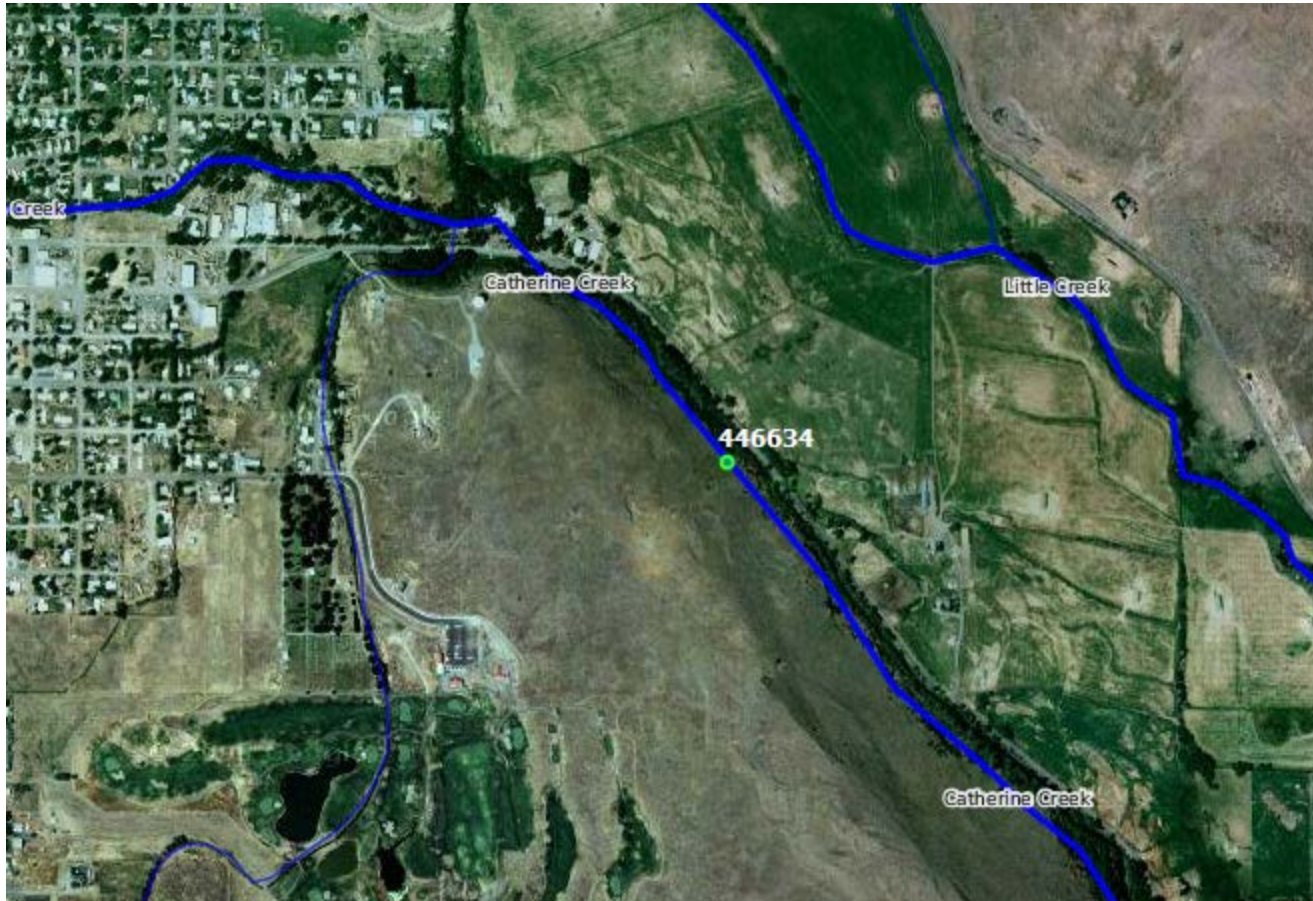


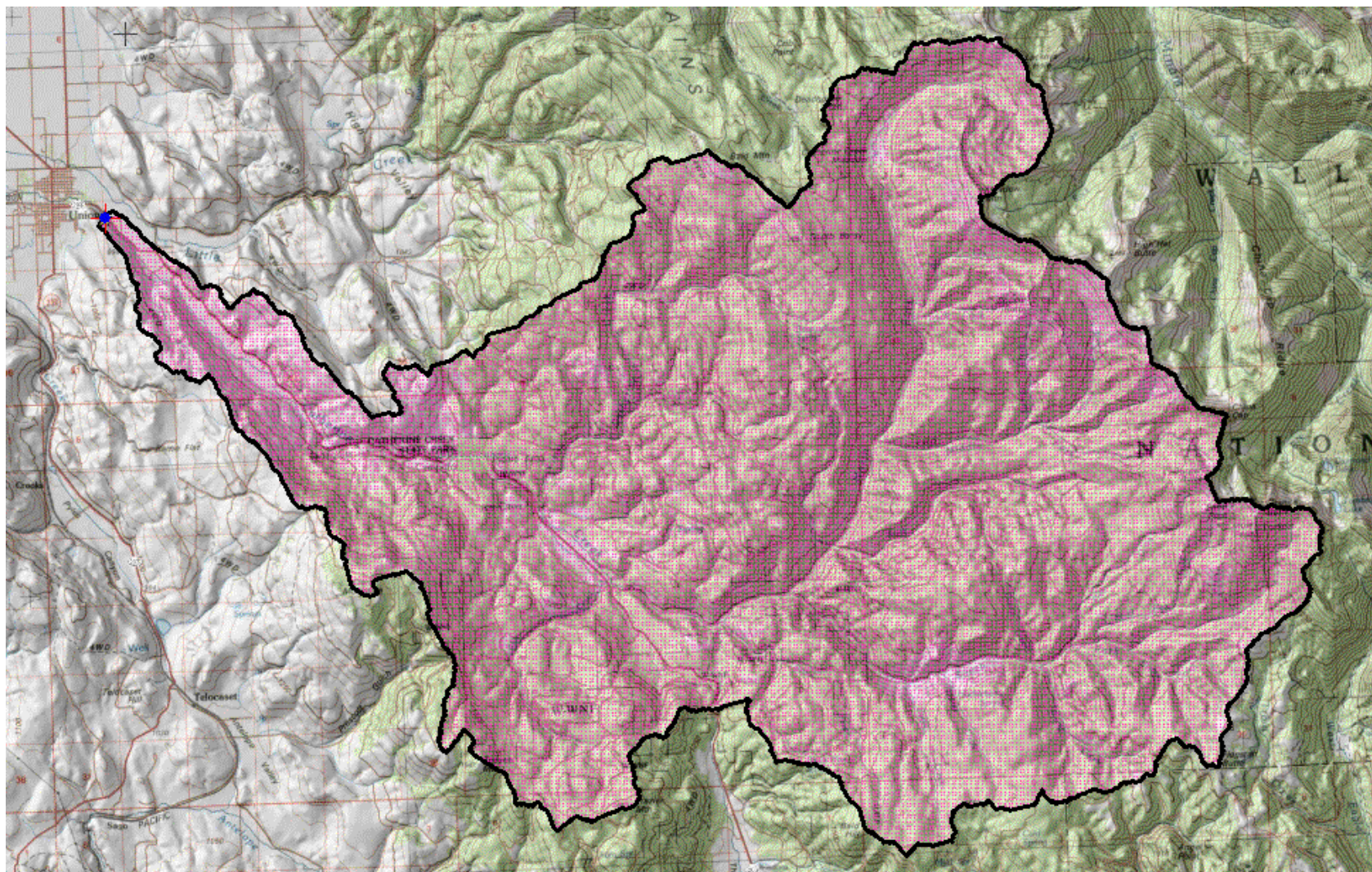
I redid this because 4 CC sites had the same DA



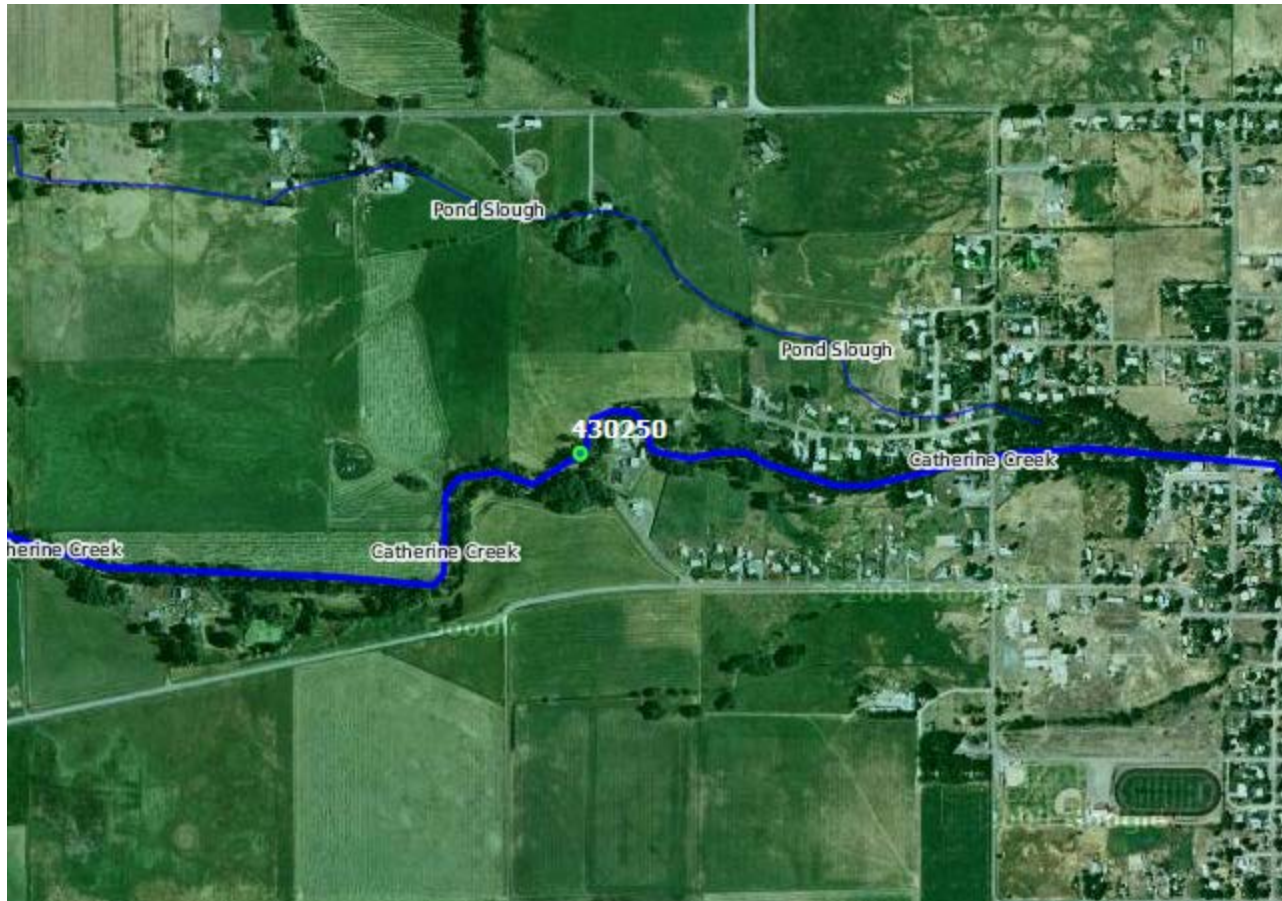


CBW05583-446634 (Catherine Creek)





CBW05583-430250 (Catherine Creek)



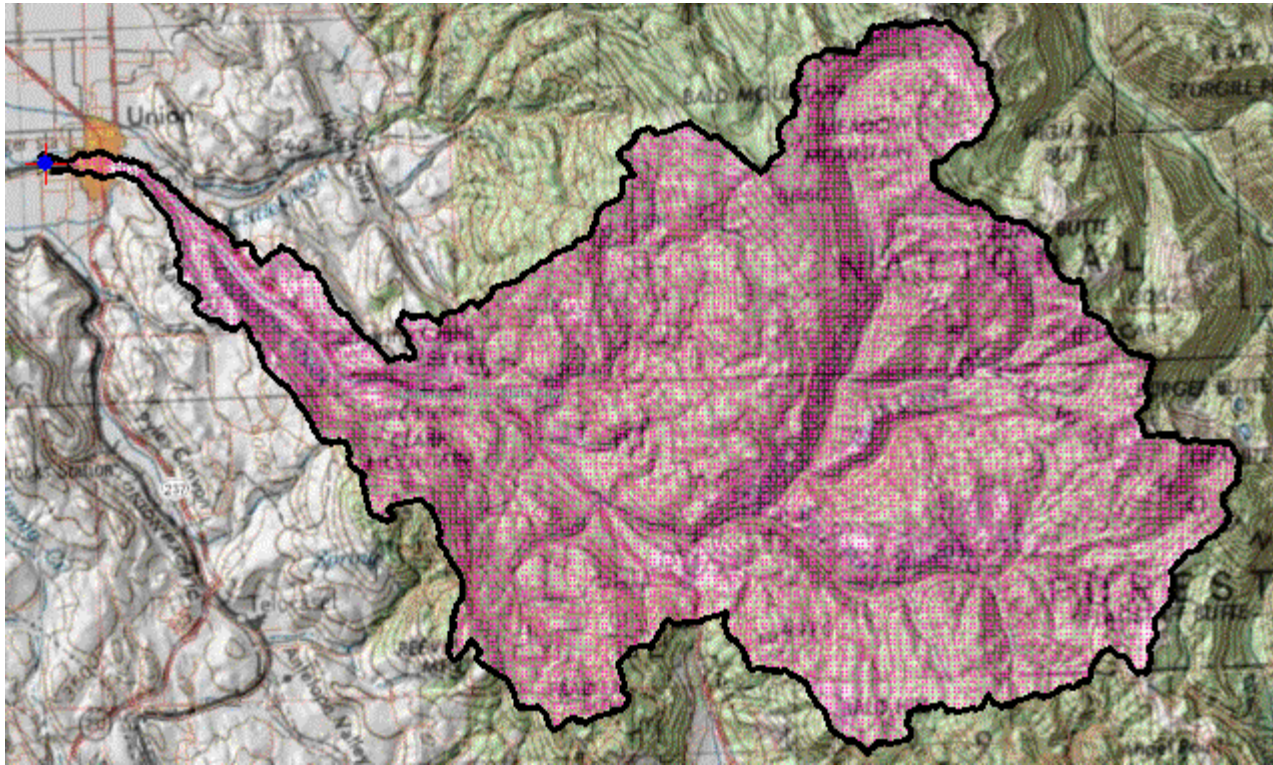


Table xx. Regression equations used in the USGS StreamStats program to calculate selected annual flow statistics for ungaged sites in the Grande Ronde basin. Flow statistics below include P values, specifying flows in cms (or m³/sec) that are exceeded 5, 10, 25, 50, and 95% of the time, and two low flow statistics. Basin characteristics used to compute these statistics include drainage area (DA), mean basin elevation (E), maximum elevation (XE), minimum elevation (NE), drainage density, and mean basin precipitation (P).

Statistic	BCF	Regression equations
		Annual
P5 =	1.04267	$*10^{-5.2458*(DA)^{0.9215}*(P)^{1.6820}*(XE)^{0.8931}}$
P10 =	1.03437	$*10^{-5.7404*(DA)^{0.9430}*(P)^{1.8401}*(XE)^{0.9049}}$
P25 =	1.03315	$*10^{-4.8728*(DA)^{1.0024}*(P)^{1.9626}*(XE)^{0.4984}}$
P50 =	1.07898	$*10^{-7.8192*(DA)^{0.9871}*(P)^{2.6103}*(XE)^{0.8823}}$
P95 =	1.25149	$*10^{-10.3790*(DA)^{0.8888}*(P)^{3.1176}*(XE)^{1.2801}}$
7Q2 =	1.22093908	$*10^{-10.0921*(DA)^{0.9904}*(P)^{2.6695}*(DD)^{-2.0861}*(E)^{1.3225}}$
7Q10 =	1.295293875	$*10^{-9.5867*(DA)^{0.9689}*(P)^{2.7912}*(DD)^{-2.4791}*(E)^{1.0945}}$

Table xx. Basin statistics calculated from USGS StreamStats program

Site	Stream	Basin	DA	P5	P5	P50	P50	7Q10	7Q10	mean ann ppt	mean ann ppt	annual runoff	Runoff (% of mean annual ppt)
			km ²	cms	cms/km ²	cms	cms/km ²	cms	cms/km ²	m	m3	m ³	
CBW05583-155818 (Little Catherine Creek)	Little Catherine Creek	CC	38.332	2.765	0.072	0.260	0.007	0.099	0.003	1.041	3.992E+07	8.212E+06	20.57%
CBW05583-512938 (South Fork Catherine Creek)	South Fork Catherine Creek	CC	40.922	4.096	0.100	0.414	0.010	0.141	0.003	1.120	4.584E+07	1.304E+07	28.45%
CBW05583-316330 (South Fork Catherine Creek)	South Fork Catherine Creek	CC	41.958	4.160	0.099	0.419	0.010	0.137	0.003	1.115	4.679E+07	1.321E+07	28.23%
CBW05583-138666 (North Fork Catherine Creek)	North Fork Catherine Creek	CC	87.283	8.751	0.100	0.964	0.011	0.441	0.005	1.166	1.018E+08	3.039E+07	29.86%
dsgn4-000001 (North Fork Catherine Creek)	North Fork Catherine Creek	CC	88.060	8.758	0.099	0.961	0.011	0.422	0.005	1.161	1.022E+08	3.031E+07	29.65%
Little Creek-entire	Little Creek-entire	CC	100.751	4.574	0.045	0.373	0.004	0.101	0.001	0.833	8.394E+07	1.177E+07	14.02%
CBW05583-368042 (Catherine Creek)	Catherine Creek	CC	152.809	13.427	0.088	1.456	0.010	0.566	0.004	1.102	1.685E+08	4.592E+07	27.26%
CBW05583-527786 (Catherine Creek)	Catherine Creek	CC	168.090	13.929	0.083	1.478	0.009	0.502	0.003	1.069	1.797E+08	4.660E+07	25.92%
CBW05583-456106 (Catherine Creek)	Catherine Creek	CC	168.608	13.968	0.083	1.482	0.009	0.486	0.003	1.069	1.803E+08	4.674E+07	25.92%
CBW05583-090282 (Catherine Creek)	Catherine Creek	CC	250.452	18.069	0.072	1.855	0.007	0.600	0.002	1.003	2.513E+08	5.848E+07	23.27%
dsgn4-000204 (Catherine Creek)	Catherine Creek	CC	287.489	18.969	0.066	1.881	0.007	0.638	0.002	0.958	2.753E+08	5.933E+07	21.55%
CBW05583-446634 (Catherine Creek)	Catherine Creek	CC	287.489	18.969	0.066	1.881	0.007	0.638	0.002	0.958	2.753E+08	5.933E+07	21.55%
CBW05583-405674 (Catherine Creek)	Catherine Creek	CC	287.489	19.054	0.066	1.894	0.007	0.644	0.002	0.960	2.760E+08	5.974E+07	21.64%
CBW05583-430250 (Catherine Creek)	Catherine Creek	CC	287.489	18.885	0.066	1.868	0.006	0.610	0.002	0.955	2.746E+08	5.892E+07	21.46%
CBW05583-217258 (Catherine Creek)	Catherine Creek	CC	290.079	19.042	0.066	1.885	0.006	0.616	0.002	0.955	2.770E+08	5.945E+07	21.46%

dsgn4-000006 (West Chicken Creek)	West Chicken Creek	GR	17.819	0.636	0.036	0.039	0.002	0.013	0.001	0.691	1.231E+07	1.229E+06	9.98%
West Chicken Cr.	West Chicken Cr.	GR	18.052	0.644	0.036	0.039	0.002	0.012	0.001	0.691	1.247E+07	1.245E+06	9.98%
Bear Creek	Bear Creek	GR	20.513	0.391	0.019	0.020	0.001	0.002	0.000	0.559	1.146E+07	6.284E+05	5.48%
East Chicken	East Chicken	GR	25.304	1.064	0.042	0.071	0.003	0.023	0.001	0.742	1.877E+07	2.244E+06	11.96%
Clear Cr.	Clear Cr.	GR	28.231	1.393	0.049	0.101	0.004	0.031	0.001	0.800	2.259E+07	3.173E+06	14.05%
CBW05583-108010 (Limber Jim Creek)	Limber Jim Creek	GR	36.260	1.601	0.044	0.117	0.003	0.051	0.001	0.795	2.883E+07	3.689E+06	12.80%
CBW05583-228666 (Sheep Creek)	Sheep Creek	GR	40.145	1.477	0.037	0.099	0.002	0.063	0.002	0.721	2.896E+07	3.130E+06	10.81%
CBW05583-490810 (Sheep Creek)	Sheep Creek	GR	43.253	1.563	0.036	0.105	0.002	0.071	0.002	0.716	3.098E+07	3.308E+06	10.68%
Chicken Cr.	Chicken Cr.	GR	46.361	1.743	0.038	0.117	0.003	0.032	0.001	0.714	3.309E+07	3.691E+06	11.15%
Dark Canyon	Dark Canyon	GR	48.692	1.237	0.025	0.081	0.002	0.022	0.000	0.688	3.352E+07	2.552E+06	7.61%
CBW05583-138554 (Sheep Creek)	Sheep Creek	GR	50.246	1.752	0.035	0.117	0.002	0.057	0.001	0.706	3.548E+07	3.695E+06	10.41%
dsgn4-000009 (Grande Ronde River)	Grande Ronde River	GR	63.196	3.619	0.057	0.295	0.005	0.050	0.001	0.861	5.442E+07	9.296E+06	17.08%
CBW05583-280042 (Grande Ronde River)	Grande Ronde River	GR	63.196	3.619	0.057	0.295	0.005	0.050	0.001	0.861	5.442E+07	9.296E+06	17.08%
dsgn4-000092 (Spring Creek)	Spring Creek	GR	63.455	1.608	0.025	0.109	0.002	0.022	0.000	0.704	4.465E+07	3.444E+06	7.71%
CBW05583-148970 (Grande Ronde River)	Grande Ronde River	GR	63.714	3.647	0.057	0.297	0.005	0.051	0.001	0.861	5.486E+07	9.371E+06	17.08%
Spring Cr.	Spring Cr.	GR	68.894	1.692	0.025	0.114	0.002	0.022	0.000	0.693	4.777E+07	3.596E+06	7.53%
GR abv Clear Cr.	GR abv Clear Cr.	GR	71.743	3.988	0.056	0.324	0.005	0.058	0.001	0.851	6.105E+07	1.021E+07	16.73%
Sheep Cr.	Sheep Cr.	GR	84.175	2.617	0.031	0.174	0.002	0.067	0.001	0.676	5.687E+07	5.480E+06	9.64%
CBW05583-206314 (Grande Ronde River)	Grande Ronde River	GR	104.118	5.396	0.052	0.439	0.004	0.091	0.001	0.831	8.648E+07	1.385E+07	16.02%
Fly Cr.	Fly Cr.	GR	135.197	3.819	0.028	0.247	0.002	0.063	0.000	0.635	8.585E+07	7.784E+06	9.07%
Rock Cr.	Rock Cr.	GR	137.010	3.583	0.026	0.236	0.002	0.056	0.000	0.645	8.839E+07	7.427E+06	8.40%
McCoy Cr.	McCoy Cr.	GR	147.370	3.163	0.021	0.208	0.001	0.043	0.000	0.640	9.433E+07	6.554E+06	6.95%
Beaver Cr.	Beaver Cr.	GR	155.917	5.337	0.034	0.397	0.003	0.084	0.001	0.732	1.141E+08	1.253E+07	10.98%
Five Pts. Cr.	Five Pts. Cr.	GR	187.515	6.403	0.034	0.503	0.003	0.111	0.001	0.765	1.434E+08	1.586E+07	11.06%
Meadow Cr.	Meadow Cr.	GR	269.359	5.252	0.019	0.342	0.001	0.077	0.000	0.607	1.635E+08	1.077E+07	6.59%
dsgn4-000277 (Grande Ronde River)	Grande Ronde River	GR	339.288	13.173	0.039	1.040	0.003	0.222	0.001	0.739	2.508E+08	3.278E+07	13.07%
CBW05583-321338 (Grande Ronde River)	Grande Ronde River	GR	349.648	13.543	0.039	1.071	0.003	0.228	0.001	0.739	2.584E+08	3.377E+07	13.07%
CBW05583-235322 (Grande Ronde River)	Grande Ronde River)	GR	362.598	13.843	0.038	1.090	0.003	0.230	0.001	0.734	2.662E+08	3.438E+07	12.92%
Meadow Cr.-entire	Meadow Cr.-entire	GR	468.788	9.187	0.020	0.637	0.001	0.135	0.000	0.625	2.929E+08	2.007E+07	6.85%
CBW05583-457530 (Grande Ronde River)	Grande Ronde River	GR	517.998	17.906	0.035	1.388	0.003	0.289	0.001	0.704	3.645E+08	4.377E+07	12.01%
dsgn4-000202 (Grande Ronde River)	Grande Ronde River	GR	528.358	18.125	0.034	1.402	0.003	0.282	0.001	0.701	3.704E+08	4.421E+07	11.94%
CBW05583-269114 (Grande Ronde River)	Grande Ronde River	GR	530.948	18.207	0.034	1.409	0.003	0.283	0.001	0.701	3.722E+08	4.443E+07	11.94%
dsgn4-000245	Grande Ronde River)	GR	1012.685	30.048	0.030	2.303	0.002	0.393	0.000	0.663	6.713E+08	7.263E+07	10.82%

The table above provides data derived using the USGS StreamStats program for drainage area above each sample point. Sample points represent a combination of major tributaries (without any numeric designations) and all CHaMP sites surveyed in 2011. Data include drainage area (km²), P5 and P50 flow statistics in cms for each site, conversion of the P5 and P50 flows to cms/km², low flow statistic 7Q10 flows (cms) and the low flow (7Q10) converted to cms/km². Also, StreamStats provides mean annual precipitation (converted to m above). This statistic was used to calculate mean annual water volume that fell on each drainage. The P50 flow was taken as a mean annual flow (although it is a median) to estimate total annual runoff. This value was then divided by mean annual precipitation (m³) to calculate the mean annual runoff as a percentage of mean annual precipitation.

Catherine Creek watersheds had significantly greater P50 values calculated as cms/km² than the Upper Grande Ronde watersheds. Catherine Creek watershed also had greater mean annual precipitation and much greater percentage runoff than all the Upper Grande Ronde watersheds.

Figure xx. Annual flows that are exceeded 50% of the time (P50) and 7Q10 low flows on an areal basis (km²) for all Catherine Creek sites evaluated between drainage area of 38 to 290 km².

Catherine Creek

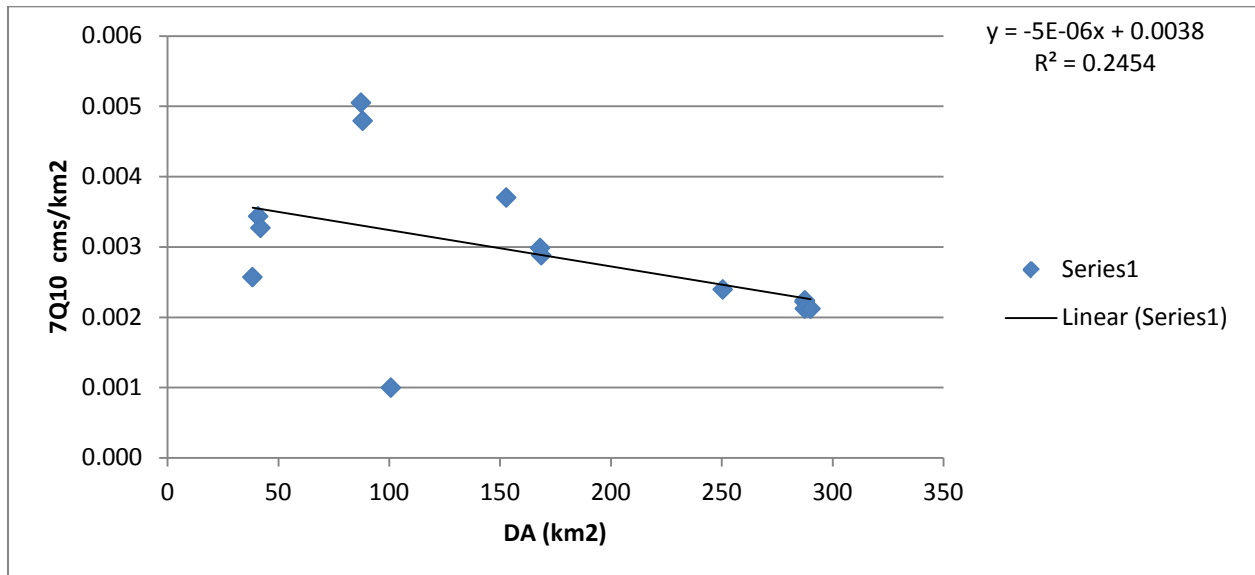
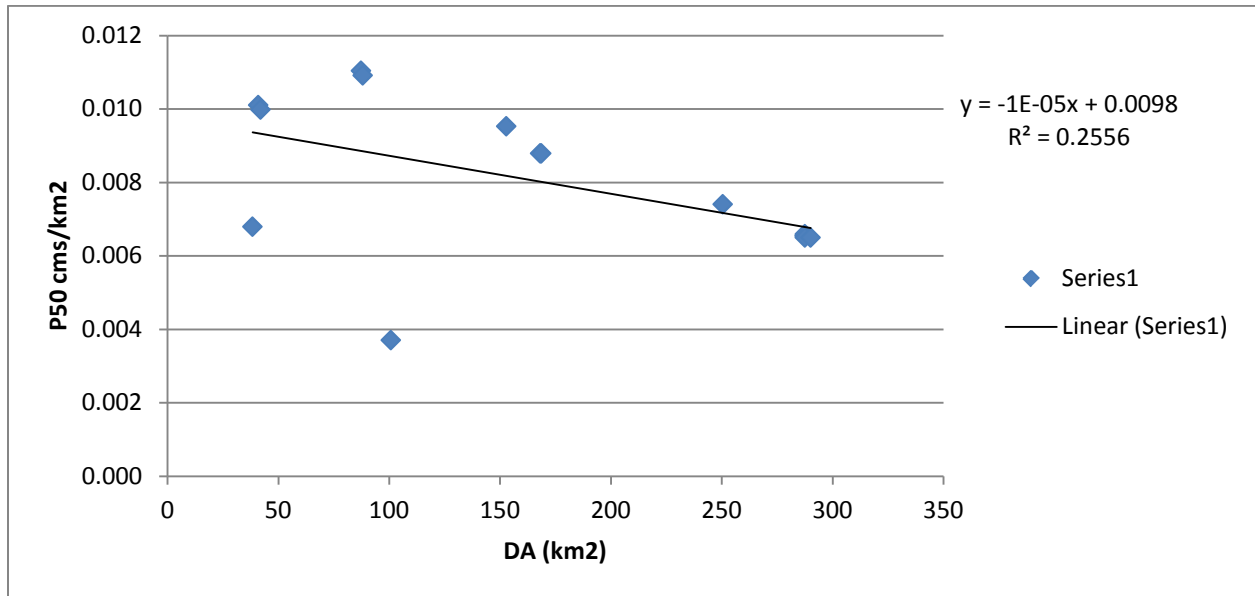


Figure xx. Annual flows that are exceeded 50% of the time (P50) and 7Q10 low flows on an areal basis (km²) for all upper Grande Ronde sites evaluated between drainage area of 17.8 to 1012.7 km².

Upper Grande Ronde

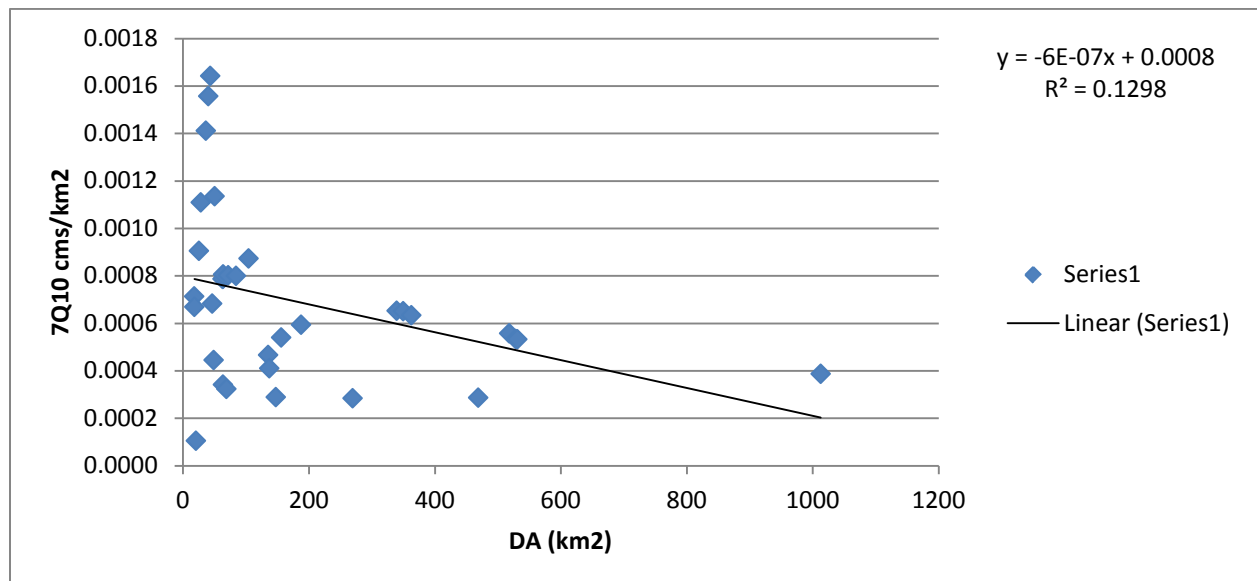
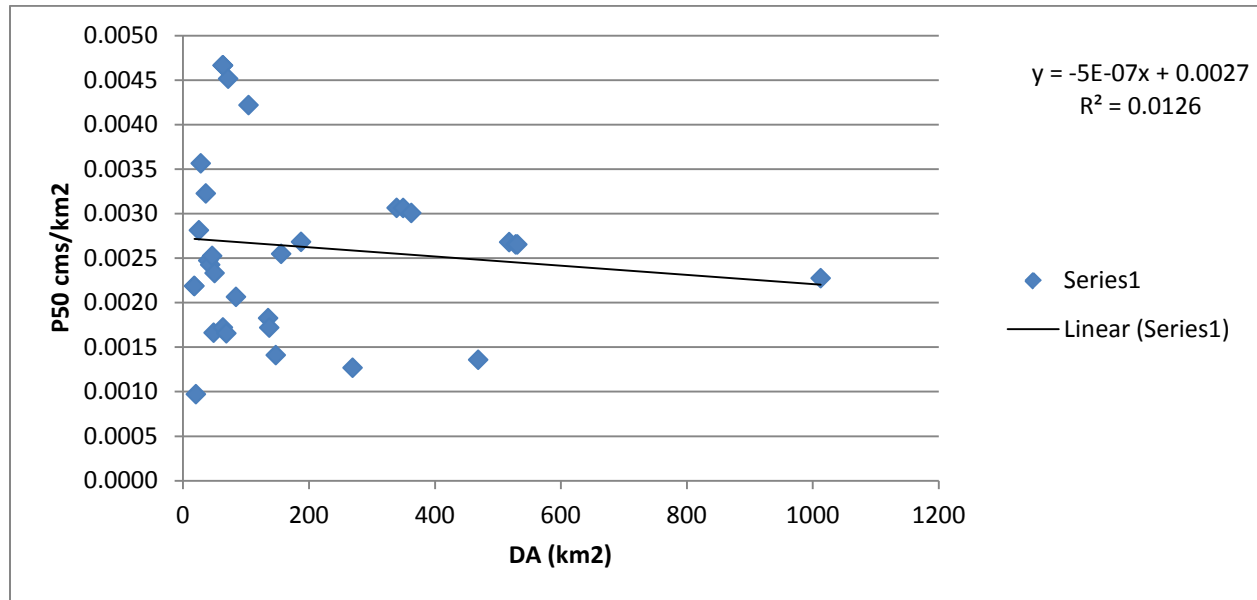


Table xx. Basin characteristics provided by www.champmonitoring.org for all CHaMP monitoring sites surveyed by CRITFC in 2011.

	Site: dsgn4- 000245	Site: dsgn4- 000006 (West Chicken Creek)	Site: dsgn4- 000092 (Spring Creek)	dsgn4- 000001 (North Fork Catherine Creek)	CBW0558 3- 235322 (Grande Ronde River)	CBW0558 3- 316330 (South Fork Catherine Creek)	dsgn4- 000009 (Grande Ronde River)
UTM	11N 392921 5013827	11N 389626 4990427	11N 400292 5020270	11N 449415 4996710	11N 391609 5001324	11N 453284 4994577	11N 397812 4989894
Township Range Section		6S 35 1/2E 10	3S 36E 2	5S 41E 23	5S 35E 1	5S 42E 29	6S 36E 9
Category	Upper Grande Ronde Chinook	Grande Ronde Steelhead- Source- Public	Grande Ronde Steelhead- Transport- Public	Catherine Creek Chinook	Upper Grande Ronde Chinook	Catherine Creek Chinook	Upper Grande Ronde Chinook
Panel	Annual	Annual	Annual	Annual	Rotating Panel 1	Rotating Panel 1	Annual
Owner Type	Private Lands	Public Lands	Public Lands	Private Lands	Public Lands	Public Lands	Public Lands
Ownership	Private Lands	Wallowa Whitman NF	Wallowa Whitman NF	Private Lands			Wallowa Whitman NF
State	OR	OR	OR	OR	OR	OR	OR
County	Union	Union	Union	Union	Union	Union	Union
HUC6	1.71E+11	1.71E+11	1.71E+11	1.71E+11	0	0	1.71E+11
Stream	Grande Ronde River	West Chicken Creek	Spring Creek	North Fork Catherine Creek	Grande Ronde River	South Fork Catherine Creek	Grande Ronde River
Strahler Order	5	2	3	3			3
Latitude	45.26978	45.0587	45.32885	45.12205	45.15707	45.10312	45.05513
Longitude	-118.365	-118.402	-118.272	-117.643	-118.379	-117.594	-118.298

CBW0558 3- 138554 (S heep Creek)	dsgn4- 000204 (C atherine Creek)	CBW0558 3- 217258 (C atherine Creek)	dsgn4- 000202 (G rande Ronde River)	CBW0558 3- 206314 (G rande Ronde River)	dsgn4- 000277 (G rande Ronde River)	CBW0558 3- 269114 (G rande Ronde River)	CBW0558 3- 321338 (G rande Ronde River)
11N 385425 4990678	11N 431989 5006622	11N 430865 5006831	11N 390773 5010804	11N 395762 4992134	11N 392576 4998661	11N 391118 5012095	11N 392691 4999647
6S 35E 12	4S 40E 18	4S 39E 13	4S 35E 2	6S 36E 5	5S 35E 13	3S 35E 35	5S 35E 12
Upper Grande Ronde Chinook	Catherine Creek Chinook	Catherine Creek Chinook	Upper Grande Ronde Chinook	Upper Grande Ronde Chinook	Upper Grande Ronde Chinook	Upper Grande Ronde Chinook	Upper Grande Ronde Chinook
Rotating Panel 1	Annual	Rotating Panel 1	Annual	Rotating Panel 1	Annual	Rotating Panel 1	Rotating Panel 1
Public Lands	Private Lands	Private Lands	Private Lands	Public Lands	Public Lands	Private Lands	Public Lands
	Private Lands		Private Lands		Wallowa Whitman NF		
OR	OR	OR	OR	OR	OR	OR	OR
Union	Union	Union	Union	Union	Union	Union	Union
0	1.71E+11	0	1.71E+11	0	1.71E+11	0	0
Sheep Creek	Catherine Creek	Catherine Creek	Grande Ronde River	Grande Ronde River	Grande Ronde River	Grande Ronde River	Grande Ronde River
	4		5		5		
45.06029	45.2098	45.21157	45.24225	45.07499	45.13325	45.25392	45.14214
-118.455	-117.866	-117.88	-118.392	-118.324	-118.366	-118.388	-118.365

CBW05583-228666 (Sheep Creek)	CBW05583-148970 (Grande Ronde River)	CBW05583-108010 (Limber Jim Creek)	CBW05583-280042 (Grande Ronde River)	CBW05583-090282 (Catherine Creek)	CBW05583-456106 (Catherine Creek)	CBW05583-512938 (South Fork Catherine Creek)	CBW05583-155818 (Little Catherine Creek)
11N 384631 4988286	11N 396628 4991086	11N 395317 4995296	11N 397642 4990189	11N 443053 4999153	11N 445093 4996877	11N 454223 4994742	11N 443666 4999598
6S 35E 14	6S 36E 4	5S 36E 29	6S 36E 9	5S 41E 7	5S 41E 16	5S 42E 29	5S 41E 8
Upper Grande Ronde Chinook	Upper Grande Ronde Chinook	Upper Grande Ronde Chinook	Upper Grande Ronde Chinook	Catherine Creek Chinook	Catherine Creek Chinook	Catherine Creek Chinook	Catherine Creek Chinook
Annual	Rotating Panel 1	Annual	Rotating Panel 1	Rotating Panel 1	Annual	Rotating Panel 1	Annual
Public Lands	Public Lands	Public Lands	Public Lands	Private Lands	Private Lands	Public Lands	Private Lands
OR	OR	OR	OR	OR	OR	OR	OR
Union	Union	Union	Union	Union	Union	Union	Union
0	0	0	0	0	0	0	0
Sheep Creek	Grande Ronde River	Limber Jim Creek	Grande Ronde River	Catherine Creek	Catherine Creek	South Fork Catherine Creek	Little Catherine Creek
45.03864	45.06569	45.10338	45.05776	45.14356	45.12323	45.10466	45.14761
-118.46478	-118.313	-118.331	-118.3	-117.724	-117.698	-117.582	-117.717

CBW05583-446634 (Catherine Creek)	CBW05583-138666 (North Fork Catherine Creek)	CBW05583-405674 (Catherine Creek)	CBW05583-527786 (Catherine Creek)	CBW05583-430250 (Catherine Creek)	CBW05583-368042 (Catherine Creek)	CBW05583-457530 (Grande Ronde River)	CBW05583-490810 (Sheep Creek)
11N 433286 5006178	11N 449908 4997197	11N 434102 5005126	11N 445880 4996414	11N 430541 5006856	11N 448013 4996286	11N 390371 5009661	11N 384880 4989154
4S 40E 20	5S 41E 13	4S 40E 20	5S 41E 21	4S 39E 13	5S 41E 23	4S 35E 11	6S 35E 14
Catherine Creek Chinook	Catherine Creek Chinook	Catherine Creek Chinook	Catherine Creek Chinook	Catherine Creek Chinook	Catherine Creek Chinook	Upper Grande Ronde Chinook	Upper Grande Ronde Chinook
Rotating Panel 1	Annual	Annual	Annual	Rotating Panel 1	Rotating Panel 1	Annual	Rotating Panel 1
Private Lands	Public Lands	Private Lands	Private Lands	Private Lands	Private Lands	Private Lands	Public Lands
OR	OR	OR	OR	OR	OR	OR	OR
Union	Union	Union	Union	Union	Union	Union	Union
0	0	0	0	0	0	0	0
Catherine Creek	North Fork Catherine Creek	Catherine Creek	Catherine Creek	Catherine Creek	Catherine Creek	Grande Ronde River	Sheep Creek
45.20593	45.12647	45.19654	45.11912	45.21177	45.11813	45.2319	45.04649
-117.84951	-117.637	-117.839	-117.688	-117.885	-117.661	-118.397	-118.462

Table xx. Basin characteristics calculated with the USGS StreamStats program for all CHaMP monitoring sites surveyed in 2011, plus the mouths of major tributaries to the upper Grande Ronde and Catherine Creek. The major tributary watersheds are those sites without numeric codes used by CHaMP.

	Meadow Cr.	Rock Cr.	Sheep Cr.	Spring Cr.	Clear Cr.	GR abv Clear Cr.	Dark Canyon	Meadow Cr.-entire
These coordinates come from after placing the points on the USGS map using StreamStats								
NAD27-Lat	45.2623	45.342	45.0931	45.3227	45.0627	45.063	45.2724	45.2645
Nad27-Long	-118.4	-118.225	-118.395	-118.259	-118.309	-118.309	-118.381	-118.377
NAD83-Lat	45.2622	45.3418	45.0929	45.3225	45.0626	45.0629	45.2723	45.2644
NAD83-Long	-118.401	-118.226	-118.396	-118.26	-118.31	-118.31	-118.382	-118.378
Drainage area in square miles	104	52.9	32.5	26.6	10.9	27.7	18.8	181
Mean Basin Elevation, in feet	4440	4460	5070	3870	5940	6050	4280	4330
Maximum elevation in feet.	5200	6070	6470	4650	7170	7920	4750	5200
Minimum elevation in feet.	3340	2930	4140	3050	4560	4560	3320	3280
Relief in, feet.	1860	3140	2330	1600	2610	3370	1430	1920
Mean basin slope measured in degrees.	8.44	9.73	11.9	9.8	11.3	12.9	10.9	8.69
Maximum basin slope in degrees.	41.1	40.3	39.6	34.7	39.9	41.6	39.8	41.1
Minimum basin slope in degrees.	0.0107	0	0.0344	0.0338	0.0107	0.0172	0.0306	0
Total stream length in miles	151	71.7	37.8	40.7	14.7	44.8	26.2	266
Total length of streams divided by total drainage area, kilometers per square kilometer	0.9	0.84	0.72	0.95	0.83	1.01	0.87	0.91
Mean basin precipitation, in inches.	23.9	25.4	26.6	27.3	31.5	33.5	27.1	24.6
Mean maximum January temperature, 1971-2000, in Fahrenheit.	33.9	32.8	32.4	35	30.3	29.9	33.3	33.8
Mean minimum January temperature, 1971-2000, in Fahrenheit.	18.7	19.2	16.4	20.1	16	15.8	19.1	18.9
Average maximum air temperature, Fahrenheit	54.2	54.5	53.2	55.7	50.7	50.2	54	54.3
Average minimum air temperature, Fahrenheit	32.1	32.8	30.7	32.9	30.3	30	32.4	32.3
Percent of area covered by forest.	61.8	65.2	83.9	44.6	84.9	75.4	69.1	63.5
Percentage of area covered by impervious surface area, from NOAA 1 km Sprawl impervious surfaces grid	0.0295	0.0815	0	0	0	0	0	0.15
Percentage of impervious area determined from NLCD 2001 impervious dataset	0.11	0.17	0.29	0.28	0.15	0.13	0.31	0.2
Percentage of urban land cover determined from NLCD 2001 land cover dataset	0.31	0.0624	0.16	1.01	0	0.37	0.28	0.23
Average Soil Permeability, in inches per hour	1.13	1.04	1.31	1.08	1.52	1.5	1.06	1.08
Available water capacity of the top 60 inches of soil - determined from STATSGO data, in inches	0.16	0.14	0.15	0.17	0.14	0.14	0.17	0.16
Percent of area covered by high permeability aquifer units.	0	0	3.34	4.48	4.66	12.2	0	0.54
Percent of area covered by high permeability geologic units.	0	0	0	0	0	0	0	0

	dsgn4-000245	dsgn4-000006 (West Chicken Creek)	dsgn4-000092 (Spring Creek)	dsgn4-000001 (North Fork Catherine Creek)	CBW0558 3-235322 (Gorande Ronde River)	CBW0558 3-316330 (South Fork Catherine Creek)	dsgn4-000009 (Gorande Ronde River)	CBW0558 3-138554 (Sheep Creek)
These coordinates come from after placing the points on the USGS map using StreamStats								
NAD27-Lat	45.2688 (45 16 08)	45.0582 (45 03 30)	45.3295 (45 19 46)	45.1217 (45 07 18)	45.1580 (45 09 29)	45.1031 (45 06 11)	45.0550 (45 03 18)	45.0597 (45 03 35)
Nad27-Long	-118.3646 (-118 21 53)	-118.4010 (-118 24 04)	-118.2715 (-118 16 17)	-117.6434 (-117 38 36)	-118.3788 (-118 22 44)	-117.5930 (-117 35 35)	-118.2960 (-118 17 46)	-118.4545 (-118 27 16)
NAD83-Lat	45.2687 (45 16 07)	45.0581 (45 03 29)	45.3293 (45 19 46)	45.1216 (45 07 18)	45.1578 (45 09 28)	45.1030 (45 06 11)	45.0548 (45 03 17)	45.0595 (45 03 34)
NAD83-Long	-118.3656 (-118 21 56)	-118.4021 (-118 24 08)	-118.2725 (-118 16 21)	-117.6444 (-117 38 40)	-118.3798 (-118 22 47)	-117.5941 (-117 35 39)	-118.2971 (-118 17 49)	-118.4555 (-118 27 20)
Drainage area in square miles	391	6.88	24.5	34	140	16.2	24.4	19.4
Mean Basin Elevation, in feet	4760	5240	3910	5950	5310	6010	6140	5400
Maximum elevation in feet.	7920	6320	4650	8620	7920	8680	7920	6470
Minimum elevation in feet.	3260	4350	3120	3680	3790	4370	4610	4370
Relief in, feet.	4670	1970	1530	4940	4130	4310	3310	2090
Mean basin slope measured in degrees.	10.8	13.8	10	19	12.4	17.1	13.2	13.6
Maximum basin slope in degrees.	45.1	32.1	34.7	51.4	41.6	50	41.6	39.6
Minimum basin slope in degrees.	0	0.16	0.0338	0.0226	0.0107	0.11	0.0172	0.0385
Total stream length in miles	562	8.91	37.4	37.6	195	20.2	40.7	21.2
Total length of streams divided by total drainage area, kilometers per square kilometer	0.89	0.8	0.95	0.69	0.87	0.78	1.04	0.68
Mean basin precipitation, in inches.	26.1	27.2	27.7	45.7	28.9	43.9	33.9	27.8
Mean maximum January temperature, 1971-2000, in Fahrenheit.	32.9	32.2	34.9	29.9	31.7	29.5	29.7	31.8
Mean minimum January temperature, 1971-2000, in Fahrenheit.	17.9	16.5	20	14.6	16.6	15	15.8	16.3
Average maximum air temperature, Fahrenheit	53.6	52.9	55.5	49.4	52.4	49.1	49.9	52.2
Average minimum air temperature, Fahrenheit	31.6	30.7	32.8	27.9	30.7	28.4	29.9	30.5
Percent of area covered by forest.	71.6	86.4	45.7	85.5	81.8	82.7	73.6	91.7
Percentage of area covered by impervious surface area, from NOAA 1 km Sprawl impervious surfaces grid	0.0672	0	0	0	0	0	0	0
Percentage of impervious area determined from NLCD 2001 impervious dataset	0.17	0.37	0.29	0.17	0.17	0.16	0.14	0.39
Percentage of urban land cover determined from NLCD 2001 land cover dataset	0.37	0	0.98	0	0.45	0	0.42	0
Average Soil Permeability, in inches per hour	1.23	1.39	1.07	1.15	1.37	1.24	1.51	1.44
Available water capacity of the top 60 inches of soil - determined from STATSGO data, in inches	0.16	0.15	0.17	0.14	0.15	0.15	0.14	0.15
Percent of area covered by high permeability aquifer units.	2.52	0	4.5	0.00204	5.13	0.53	13.8	0
Percent of area covered by high permeability geologic units.	0	0	0	0	0	0	0	0

	dsgn4-000204 (Catherine Creek)	CBW05583-217258 (Catherine Creek)	dsgn4-000202 (Gronde Ronde River)	CBW05583-206314 (Gronde Ronde River)	dsgn4-000277 (Gronde Ronde River)	CBW05583-269114 (Gronde Ronde River)	CBW05583-321338 (Gronde Ronde River)	CBW05583-228666 (Sheep Creek)
These coordinates come from after placing the points on the USGS map using StreamStats								
NAD27-Lat	45.2101 (45 12 36	45.2100 (45 12 36	45.2439 (45 14 38	45.0756 (45 04 32	45.1332 (45 07 59	45.2547 (45 15 17	45.1417 (45 08 30	45.0390 (45 02 20
Nad27-Long	-117.8655 (-117 51 56	-117.8894 (-117 53 22	-118.3891 (-118 23 21	-118.3230 (-118 19 23	-118.3649 (-118 21 54	-118.3857 (-118 23 09	-118.3638 (-118 21 50	-118.4635 (-118 27 49
NAD83-Lat	45.2099 (45 12 36	45.2099 (45 12 35	45.2437 (45 14 37	45.0755 (45 04 32	45.1330 (45 07 59	45.2546 (45 15 16	45.1415 (45 08 29	45.0389 (45 02 20
NAD83-Long	-117.8665 (-117 51 59	-117.8904 (-117 53 26	-118.3902 (-118 23 25	-118.3241 (-118 19 27	-118.3659 (-118 21 57	-118.3868 (-118 23 12	-118.3649 (-118 21 54	-118.4646 (-118 27 52
Drainage area in square miles	111	112	204	40.2	131	205	135	15.5
Mean Basin Elevation, in feet	5140	5130	5160	5970	5350	5150	5340	5500
Maximum elevation in feet.	8680	8680	7920	7920	7920	7920	7920	6470
Minimum elevation in feet.	2780	2730	3340	4390	3950	3310	3880	4500
Relief in, feet.	5900	5940	4580	3540	3970	4610	4040	1970
Mean basin slope measured in degrees.	15.5	15.5	12.6	12.5	12.3	12.6	12.3	13.5
Maximum basin slope in degrees.	51.4	51.4	43.6	41.6	41.6	43.6	41.6	39.6
Minimum basin slope in degrees.	0.0169	0.00338	0.0107	0.0107	0.0107	0.0107	0.0107	0.0385
Total stream length in miles	126	127	284	60.9	183	285	188	15.5
Total length of streams divided by total drainage area, kilometers per square kilometer	0.7	0.71	0.87	0.94	0.87	0.87	0.87	0.62
Mean basin precipitation, in inches.	37.7	37.6	27.6	32.7	29.1	27.6	29.1	28.4
Mean maximum January temperature, 1971-2000, in Fahrenheit.	31.5	31.6	32.2	30.1	31.6	32.2	31.6	31.5
Mean minimum January temperature, 1971-2000, in Fahrenheit.	16.6	16.6	17	15.9	16.5	17	16.6	16.4
Average maximum air temperature, Fahrenheit	52.2	52.3	52.9	50.4	52.3	52.9	52.4	51.9
Average minimum air temperature, Fahrenheit	30.3	30.4	31	30.1	30.7	31	30.7	30.7
Percent of area covered by forest.	81.8	81.4	79.4	78.5	81.8	79.2	82	93.5
Percentage of area covered by impervious surface area, from NOAA 1 km Sprawl impervious surfaces grid	0.0569	0.13	0	0	0	0	0	0
Percentage of impervious area determined from NLCD 2001 impervious dataset	0.23	0.29	0.15	0.13	0.17	0.15	0.17	0.44
Percentage of urban land cover determined from NLCD 2001 land cover dataset	0.58	0.82	0.44	0.26	0.42	0.45	0.43	0
Average Soil Permeability, in inches per hour	1.13	1.15	1.34	1.49	1.38	1.35	1.38	1.47
Available water capacity of the top 60 inches of soil - determined from STATSGO data, in inches	0.15	0.15	0.15	0.14	0.15	0.15	0.15	0.14
Percent of area covered by high permeability aquifer units.	2.22	2.68	3.93	9.66	5.5	4.01	5.34	0
Percent of area covered by high permeability geologic units.	0	0	0	0	0	0	0	0

	CBW0558 3- 148970 (G rande Ronde River)	CBW0558 3- 108010 (L imber Jim Creek)	CBW0558 3- 280042 (G rande Ronde River)	CBW0558 3- 090282 (C atherine Creek)	CBW0558 3- 456106 (C atherine Creek)	CBW0558 3- 512938 (S outh Fork Catherine Creek)	CBW0558 3- 155818 (L ittle Catherine Creek)	CBW0558 3- 446634 (C atherine Creek)
These coordinates come from after placing the points on the USGS map using StreamStats								
NAD27-Lat	45.0556 (45 03 20	45.1033 (45 06 12	45.0550 (45 03 18	45.1435 (45 08 37	45.1234 (45 07 24	45.1050 (45 06 18	45.1478 (45 08 52	45.2062 (45 12 22
Nad27-Long	- 118.2970 (-118 17 49	- 118.3296 (-118 19 47	- 118.2960 (-118 17 46	- 117.7231 (-117 43 23	- 117.6972 (-117 41 50	- 117.5815 (-117 34 53	- 117.7158 (-117 42 57	- 117.8485 (-117 50 55
NAD83-Lat	45.0555 (45 03 20	45.1032 (45 06 12	45.0548 (45 03 17	45.1434 (45 08 36	45.1233 (45 07 24	45.1049 (45 06 17	45.1476 (45 08 51	45.2061 (45 12 22
NAD83-Long	- 118.2981 (-118 17 53	- 118.3307 (-118 19 51	- 118.2971 (-118 17 49	- 117.7241 (-117 43 27	- 117.6983 (-117 41 54	- 117.5825 (-117 34 57	- 117.7169 (-117 43 01	- 117.8495 (-117 50 58
Drainage area in square miles	24.6	14	24.4	96.7	65.1	15.8	14.8	111
Mean Basin Elevation, in feet	6140	5490	6140	5360	5670	6030	5240	5140
Maximum elevation in feet.	7920	6550	7920	8680	8680	8680	6860	8680
Minimum elevation in feet.	4610	4350	4610	3240	3390	4530	3390	2820
Relief in, feet.	3310	2200	3310	5430	5290	4140	3470	5860
Mean basin slope measured in degrees.	13.2	12.5	13.2	15.7	17.2	16.9	14	15.6
Maximum basin slope in degrees.	41.6	34.9	41.6	51.4	51.4	50	48.2	51.4
Minimum basin slope in degrees.	0.0172	0.0683	0.0172	0.0226	0.0226	0.11	0.0578	0.0169
Total stream length in miles	40.8	16.3	40.7	113	78.3	19.7	17.9	125
Total length of streams divided by total drainage area, kilometers per square kilometer	1.03	0.72	1.04	0.73	0.75	0.77	0.75	0.7
Mean basin precipitation, in inches.	33.9	31.3	33.9	39.5	42.1	44.1	41	37.7
Mean maximum January temperature, 1971-2000, in Fahrenheit.	29.7	31	29.7	31.1	30.4	29.4	31.3	31.5
Mean minimum January temperature, 1971-2000, in Fahrenheit.	15.8	16.8	15.8	16.1	15.4	14.9	16.1	16.6
Average maximum air temperature, Fahrenheit	49.9	51.8	49.9	51.5	50.4	49	51.7	52.2
Average minimum air temperature, Fahrenheit	29.9	30.8	29.9	29.8	29	28.3	29.6	30.3
Percent of area covered by forest.	73.6	90	73.6	87.5	86.2	82.4	92	82
Percentage of area covered by impervious surface area, from NOAA 1 km Sprawl impervious surfaces grid	0	0	0	0	0	0	0	0.0102
Percentage of impervious area determined from NLCD 2001 impervious dataset	0.13	0.0328	0.14	0.19	0.16	0.16	0.24	0.2
Percentage of urban land cover determined from NLCD 2001 land cover dataset	0.42	0	0.42	0.18	0.0416	0	0	0.47
Average Soil Permeability, in inches per hour	1.5	1.52	1.51	1.13	1.15	1.25	1.14	1.13
Available water capacity of the top 60 inches of soil - determined from STATSGO data, in inches	0.14	0.14	0.14	0.16	0.15	0.15	0.17	0.15
Percent of area covered by high permeability aquifer units.	13.7	0	13.8	0.67	0.21	0.54	0	2.01
Percent of area covered by high permeability geologic units.	0	0	0	0	0	0	0	0

	CBW0558 3- 138666 (N orth Fork Catherine Creek)	CBW0558 3- 405674 (C atherine Creek)	CBW0558 3- 527786 (C atherine Creek)	CBW0558 3- 430250 (C atherine Creek)	CBW0558 3- 368042 (C atherine Creek)	CBW0558 3- 457530 (G rande Ronde River)	CBW0558 3- 490810 (S heep Creek)	Little Creek- entire
These coordinates come from after placing the points on the USGS map using StreamStats								
NAD27-Lat	45.1268 (45 07 36	45.1978 (45 11 52	45.1193 (45 07 09	45.2118 (45 12 42	45.1182 (45 07 05	45.2320 (45 13 55	45.0463 (45 02 47	45.2321 (45 13 55)
Nad27-Long	- 117.6360 (-117 38 10	- 117.8390 (-117 50 21	- 117.6869 (-117 41 13	- 117.8837 (-117 53 01	- 117.6599 (-117 39 35	- 118.3953 (-118 23 43	- 118.4613 (-118 27 41	- 117.9168 (-117 55 00)
NAD83-Lat	45.1267 (45 07 36	45.1977 (45 11 52	45.1192 (45 07 09	45.2116 (45 12 42	45.1181 (45 07 05	45.2319 (45 13 55	45.0462 (45 02 46	45.2319 (45 13 55)
NAD83-Long	- 117.6371 (-117 38 14	- 117.8401 (-117 50 24	- 117.6879 (-117 41 16	- 117.8848 (-117 53 05	- 117.6609 (-117 39 39	- 118.3964 (-118 23 47	- 118.4623 (-118 27 44	- 117.9178 (-117 55 04)
Drainage area in square miles	33.7	111	64.9	111	59	200	16.7	38.9
Mean Basin Elevation, in feet	5970	5150	5680	5130	5810	5180	5470	4260
Maximum elevation in feet.	8620	8680	8680	8680	8680	7920	6470	6770
Minimum elevation in feet.	3750	2850	3440	2750	3590	3390	4450	2710
Relief in, feet.	4870	5830	5240	5930	5090	4530	2020	4060
Mean basin slope measured in degrees.	18.9	15.6	17.2	15.5	17.7	12.7	13.6	10.6
Maximum basin slope in degrees.	51.4	51.4	51.4	51.4	51.4	43.6	39.6	44
Minimum basin slope in degrees.	0.0226	0.0169	0.0226	0.00338	0.0226	0.0107	0.0385	0
Total stream length in miles	37.1	124	77.7	127	67.8	277	16.1	48.2
Total length of streams divided by total drainage area, kilometers per square kilometer	0.68	0.7	0.74	0.71	0.71	0.86	0.6	0.77
Mean basin precipitation, in inches.	45.9	37.8	42.1	37.6	43.4	27.7	28.2	32.8
Mean maximum January temperature, 1971-2000, in Fahrenheit.	29.9	31.5	30.4	31.6	30.1	32.1	31.6	33.4
Mean minimum January temperature, 1971-2000, in Fahrenheit.	14.6	16.6	15.4	16.6	15.1	16.9	16.4	18.7
Average maximum air temperature, Fahrenheit	49.4	52.2	50.4	52.2	49.9	52.8	52	55.2
Average minimum air temperature, Fahrenheit	27.9	30.3	29	30.3	28.6	31	30.6	32.4
Percent of area covered by forest.	85.4	82.2	86.2	81.6	85.3	79.9	93.3	43.6
Percentage of area covered by impervious surface area, from NOAA 1 km Sprawl impervious surfaces grid	0	0	0	0.1	0	0	0	0.5
Percentage of impervious area determined from NLCD 2001 impervious dataset	0.17	0.2	0.16	0.27	0.15	0.15	0.42	0.44
Percentage of urban land cover determined from NLCD 2001 land cover dataset	0	0.43	0.0418	0.73	0	0.42	0	0.93
Average Soil Permeability, in inches per hour	1.15	1.13	1.15	1.14	1.16	1.34	1.46	1.05
Available water capacity of the top 60 inches of soil - determined from STATSGO data, in inches	0.14	0.15	0.15	0.15	0.15	0.15	0.15	0.14
Percent of area covered by high permeability aquifer units.	0.00206	1.89	0.13	2.44	0.15	4	0	7.71
Percent of area covered by high permeability geologic units.	0	0	0	0	0	0	0	0

Table xx. Flow statistics (annual, August, and September) for both major tributary mouth sites and all CHaMP sites (those with numeric codes) including P values, specifying flows in cfs (or ft³/sec) that are exceeded 5, 10, 25, 50, and 95% of the time, and two low flow statistics. In addition, annual P5, P50 and 7Q10 statistics are converted to a cfs/mi² basis.

	cfs							
Annual	Meadow Cr.	Rock Cr.	Sheep Cr.	Spring Cr.	Clear Cr.	GR abv Clear Cr.	Dark Canyon	Meadow Cr.-entire
P5 =	185.468	126.534	92.409	59.759	49.188	140.821	43.691	324.423
P10 =	118.943	80.898	58.938	37.958	31.511	93.052	27.520	211.513
P25 =	52.546	32.481	22.527	16.449	11.052	33.380	11.572	96.910
P50 =	12.064	8.317	6.137	4.026	3.553	11.438	2.857	22.478
P95 =	3.675	2.970	2.414	1.435	1.766	5.569	1.059	6.581
7Q2 =	-5.877	-3.323	-2.356	-1.912	-1.783	-6.597	-1.391	-10.748
7Q10 =	2.709	1.989	2.379	0.789	1.106	2.034	0.766	4.755
August								
P5 =	8.692	8.675	7.517	2.376	5.898	24.801	1.754	16.557
P10 =	7.476	7.493	6.516	2.068	5.185	21.904	1.526	14.275
P25 =	3.147	3.571	3.400	1.131	3.345	12.024	0.886	5.462
P50 =	2.389	2.646	2.495	0.871	2.446	8.946	0.675	4.220
P95 =	3.360	1.871	2.637	0.759	0.901	2.041	0.672	6.962
7Q2 =	4.491	2.857	2.877	1.275	2.610	8.524	1.145	8.046
7Q10 =	2.792	1.795	1.768	0.842	1.611	5.425	0.732	5.126
September								
P5 =	5.507	5.054	4.346	2.027	3.541	12.157	1.517	9.910
P10 =	4.042	3.901	3.439	1.489	2.963	10.443	1.122	7.276
P25 =	2.728	2.761	2.489	0.992	2.260	8.327	0.749	4.956
P50 =	1.694	1.818	1.686	0.609	1.655	6.605	0.458	3.157
P95 =	0.907	0.937	0.854	0.328	0.848	3.711	0.238	1.796
7Q2 =	5.468	3.550	3.293	1.811	2.729	8.378	1.529	9.718
7Q10 =	4.102	2.706	2.483	1.441	2.074	6.328	1.199	7.303
Annual	cfs/mi2							
P5	1.78	2.39	2.84	2.25	4.51	5.08	2.32	1.79
P50	0.1160	0.1572	0.1888	0.1514	0.3260	0.4129	0.1520	0.1242
7Q10	0.0261	0.0376	0.0732	0.0296	0.1015	0.0734	0.0408	0.0263

	cfs							
Annual		dsgn4-000006 (West Chicken Creek)	dsgn4-000092 (Spring Creek)	dsgn4-000001 (North Fork Catherine Creek)	CBW0558 3-235322 (Gorandé River)	CBW0558 3-316330 (South Fork Catherine Creek)	dsgn4-000009 (Gorandé River)	CBW0558 3-138554 (Sheep Creek)
	dsgn4-000245							
P5 =	1061.150	22.467	56.769	309.303	488.859	146.903	127.812	61.867
P10 =	713.533	13.904	36.078	215.830	326.759	100.257	84.384	39.296
P25 =	290.527	4.906	15.586	78.655	126.744	34.693	30.087	14.645
P50 =	81.331	1.376	3.856	33.940	38.502	14.791	10.410	4.138
P95 =	26.892	0.632	1.396	19.607	14.831	9.030	5.162	1.751
7Q2 =	-29.920	-0.624	-1.857	-12.374	-16.043	-6.110	-6.306	-1.632
7Q10 =	13.866	0.449	0.767	14.907	8.124	4.847	1.758	2.015
August								
P5 =	160.398	1.586	2.290	104.765	78.984	44.988	22.673	5.151
P10 =	138.625	1.377	1.996	95.002	68.869	40.652	20.045	4.482
P25 =	46.089	0.951	1.110	52.047	27.831	25.294	11.271	2.577
P50 =	34.452	0.681	0.856	40.903	20.788	19.397	8.384	1.888
P95 =	23.083	0.331	0.737	16.422	11.387	4.965	1.696	1.999
7Q2 =	27.056	0.724	1.268	28.784	18.347	12.342	8.132	2.360
7Q10 =	17.390	0.435	0.839	20.565	11.722	8.580	5.169	1.439
September								
P5 =	56.089	1.123	1.976	48.214	31.514	22.168	11.295	3.178
P10 =	45.681	0.896	1.456	44.091	26.220	20.293	9.727	2.539
P25 =	35.355	0.640	0.972	38.234	20.550	17.403	7.767	1.847
P50 =	26.852	0.419	0.599	35.738	15.907	15.744	6.174	1.259
P95 =	15.629	0.192	0.324	24.598	9.162	9.974	3.462	0.632
7Q2 =	29.178	0.863	1.790	27.536	18.837	12.156	7.936	2.621
7Q10 =	21.530	0.662	1.427	21.708	13.995	9.600	5.998	1.978
Annual	cfs/mi2							
P5	2.71	3.27	2.32	9.10	3.49	9.07	5.24	3.19
P50	0.2080	0.2000	0.1574	0.9982	0.2750	0.9130	0.4266	0.2133
7Q10	0.0355	0.0653	0.0313	0.4384	0.0580	0.2992	0.0720	0.1039

	cfs							
Annual	dsgn4-000204 (Catherine Creek)	CBW0558 3-217258 (Catherine Creek)	dsgn4-000202 (G rande Ronde River)	CBW0558 3-206314 (G rande Ronde River)	dsgn4-000277 (G rande Ronde River)	CBW0558 3-269114 (G rande Ronde River)	CBW0558 3-321338 (G rande Ronde River)	CBW0558 3-228666 (Sheep Creek)
P5 =	669.898	672.446	640.074	190.573	465.190	642.965	478.264	52.148
P10 =	465.164	466.828	428.183	126.455	310.833	430.162	319.775	33.075
P25 =	177.126	177.796	168.885	46.240	120.193	169.715	123.872	12.195
P50 =	66.440	66.568	49.511	15.510	36.713	49.750	37.819	3.505
P95 =	31.075	31.065	17.954	7.191	14.284	18.032	14.671	1.533
7Q2 =	-19.976	-20.245	-19.833	-8.179	-15.453	-19.878	-15.881	-1.293
7Q10 =	22.539	21.741	9.972	3.212	7.829	9.998	8.044	2.208
August								
P5 =	191.491	191.618	99.664	33.373	75.518	100.153	77.824	4.400
P10 =	170.762	170.836	86.554	29.413	65.886	86.979	67.898	3.836
P25 =	74.047	73.938	32.530	15.066	26.964	32.661	27.639	2.301
P50 =	57.312	57.207	24.262	11.242	20.141	24.362	20.658	1.685
P95 =	26.648	25.201	13.589	3.484	11.219	13.539	11.422	2.159
7Q2 =	33.078	32.906	21.160	10.977	17.931	21.156	18.385	2.130
7Q10 =	23.296	23.168	13.470	6.988	11.451	13.475	11.752	1.299
September								
P5 =	74.180	74.121	37.832	15.629	30.391	37.997	31.214	2.793
P10 =	65.600	65.519	31.194	13.345	25.322	31.329	26.002	2.242
P25 =	55.361	55.269	24.295	10.619	19.863	24.400	20.401	1.635
P50 =	49.135	49.007	18.606	8.412	15.397	18.690	15.825	1.119
P95 =	32.553	32.434	10.697	4.783	8.864	10.749	9.131	0.560
7Q2 =	34.273	34.142	21.944	10.747	18.344	21.968	18.811	2.351
7Q10 =	26.630	26.525	16.210	8.074	13.635	16.232	13.981	1.779
Annual	cfs/mi2							
P5	6.04	6.00	3.14	4.74	3.55	3.14	3.54	3.36
P50	0.5986	0.5944	0.2427	0.3858	0.2803	0.2427	0.2801	0.2262
7Q10	0.2031	0.1941	0.0489	0.0799	0.0598	0.0488	0.0596	0.1424

	cfs							
Annual	CBW0558 3- 148970 (G rande Ronde River)	CBW0558 3- 108010 (L imber Jim Creek)	CBW0558 3- 280042 (G rande Ronde River)	CBW0558 3- 090282 (C atherine Creek)	CBW0558 3- 456106 (C atherine Creek)	CBW0558 3- 512938 (S outh Fork Catherine Creek)	CBW0558 3- 155818 (L ittle Catherine Creek)	CBW0558 3- 446634 (C atherine Creek)
P5 =	128.777	56.532	127.812	638.093	493.281	144.659	97.648	669.898
P10 =	85.036	36.336	84.384	445.037	344.579	98.743	65.615	465.164
P25 =	30.334	13.410	30.087	169.043	128.847	34.138	24.644	177.126
P50 =	10.494	4.131	10.410	65.491	52.338	14.603	9.196	66.440
P95 =	5.200	1.927	5.162	31.792	27.283	8.958	4.983	31.075
7Q2 =	-6.296	-1.755	-6.306	-21.755	-19.288	-5.982	-3.734	-19.976
7Q10 =	1.815	1.808	1.758	21.192	17.162	4.965	3.481	22.539
August								
P5 =	22.858	5.597	22.673	193.014	158.603	44.506	15.903	191.491
P10 =	20.209	4.920	20.045	172.818	142.796	40.232	14.308	170.762
P25 =	11.347	3.040	11.271	77.228	68.993	25.158	9.026	74.047
P50 =	8.442	2.261	8.384	60.167	54.001	19.300	7.049	57.312
P95 =	1.759	1.683	1.696	27.559	20.359	5.261	3.004	27.060
7Q2 =	8.198	2.668	8.132	37.703	36.603	12.334	6.258	33.078
7Q10 =	5.212	1.681	5.169	26.662	25.957	8.578	4.386	23.296
September								
P5 =	11.377	3.605	11.295	76.533	66.442	22.008	10.129	74.180
P10 =	9.797	2.944	9.727	68.191	59.896	20.163	8.686	65.600
P25 =	7.823	2.193	7.767	58.014	51.447	17.303	6.905	55.361
P50 =	6.220	1.567	6.174	52.352	47.260	15.676	5.622	49.135
P95 =	3.490	0.827	3.462	35.389	32.330	9.941	3.526	32.553
7Q2 =	7.998	2.933	7.936	37.876	35.603	12.125	6.928	34.273
7Q10 =	6.044	2.252	5.998	29.445	27.774	9.578	5.561	26.630
Annual	cfs/mi2							
P5	5.23	4.04	5.24	6.60	7.58	9.16	6.60	6.04
P50	0.4266	0.2951	0.4266	0.6773	0.8040	0.9242	0.6214	0.5986
7Q10	0.0738	0.1291	0.0720	0.2192	0.2636	0.3143	0.2352	0.2031

	cfs							
Annual	CBW0558 3- 138666 (N orth Fork Catherine Creek)	CBW0558 3- 405674 (C atherine Creek)	CBW0558 3- 527786 (C atherine Creek)	CBW0558 3- 430250 (C atherine Creek)	CBW0558 3- 368042 (C atherine Creek)	CBW0558 3- 457530 (G rande Ronde River)	CBW0558 3- 490810 (S heep Creek)	Little Creek- entire
P5 =	309.049	672.889	491.885	666.912	474.171	632.334	55.197	161.541
P10 =	215.760	467.437	343.581	462.896	332.123	423.067	35.026	106.969
P25 =	78.631	178.049	128.450	176.205	123.926	166.745	12.961	41.625
P50 =	34.030	66.901	52.180	65.981	51.418	49.013	3.704	13.179
P95 =	19.719	31.333	27.209	30.819	27.485	17.841	1.603	5.768
7Q2 =	-12.284	-20.169	-19.018	-20.066	-18.554	-19.511	-1.312	-4.184
7Q10 =	15.569	22.755	17.724	21.553	19.982	10.212	2.509	3.557
August								
P5 =	105.268	193.084	158.116	189.907	158.082	98.821	4.637	19.962
P10 =	95.494	172.222	142.357	169.310	142.703	85.849	4.040	17.616
P25 =	52.426	74.704	68.819	73.395	70.420	32.393	2.390	9.114
P50 =	41.230	57.851	53.861	56.777	55.344	24.167	1.750	6.956
P95 =	17.498	27.609	21.371	25.120	24.616	14.072	2.499	3.469
7Q2 =	29.213	33.547	36.659	32.615	39.230	21.217	2.208	4.459
7Q10 =	20.883	23.637	25.984	22.959	27.910	13.507	1.346	3.084
September								
P5 =	48.530	74.830	66.261	73.533	67.301	37.619	2.916	11.151
P10 =	44.409	66.200	59.733	65.003	60.971	31.037	2.337	9.177
P25 =	38.541	55.896	51.307	54.830	52.645	24.186	1.703	7.009
P50 =	36.084	49.666	47.127	48.608	48.877	18.543	1.164	5.287
P95 =	24.890	32.962	32.232	32.148	33.856	10.670	0.583	3.089
7Q2 =	27.873	34.698	35.614	33.853	37.494	21.949	2.440	5.676
7Q10 =	21.975	26.961	27.775	26.303	29.278	16.215	1.845	4.533
Annual	cfs/mi2							
P5	9.17	6.06	7.58	6.01	8.04	3.16	3.31	4.15
P50	1.0098	0.6027	0.8040	0.5944	0.8715	0.2451	0.2218	0.3388
7Q10	0.4620	0.2050	0.2731	0.1942	0.3387	0.0511	0.1502	0.0914

Appendix J.

Report on the acquisition, mapping, and quality control of ODFW Aquatic Habitat Inventory data

Report on the acquisition, mapping, and quality control of ODFW Aquatic Habitat Inventory data

March 28, 2012

Laurinda Hill, Denise Kelsey, and Seth White
Columbia River Inter-Tribal Fish Commission

Introduction

In the Grande Ronde River basin and elsewhere in the state, Oregon Department of Fish & Wildlife (ODFW) has conducted spatially continuous, habitat-unit scale fish habitat surveys every decade since the 1990s. The Aquatic Habitat Inventory (AHI) surveys (Moore et al. 2008) employ rapid assessment techniques to collect coarse resolution information over large areas using modified rapid fish-habitat assessment procedures (Hankin and Reeves 1988). While more recent fish-habitat surveys such as the Columbia habitat monitoring protocol (CHaMP) (Bouwes et al. 2010) compromise extensive spatial coverage for precise measurements collected at a few, probabilistic random locations, we felt that AHI data was useful for describing coarse resolution habitat change through space and among decades. This report briefly describes our work in acquiring, mapping, summarizing metrics, and performing initial quality control procedures on AHI data. The final version of AHI data will be used by CRITFC for analysis of fish-habitat relationships, and the resulting database will be shared with ODFW, who will have the option of replacing the current dataset, which is available to the public, with the corrected dataset.

Data acquisition and mapping

The most recent spatial and tabular (habitat unit and summary reach attribute data associated the spatial data) of AHI datasets were collected from two sources for the Grande Ronde Basin. Most of the data can be downloaded from the ODFW Aquatic Inventories Project website (<http://oregonstate.edu/dept/ODFW/freshwater/inventory/>), but several years of data were only available by contacting ODFW staff. The data is in a linear spatial form built from thousands of line segments representing the habitat units or summary reaches. For CRITFC's

use, the data was organized into three decades; within a decade, data may span several years, and may or may not cover a large spatial area (Figure 1). New fields of attributes have and will be added to the original data to organize the data into landscape and Chinook population metrics that CRITFC is using for habitat analysis.

The 1990s decade spans years 1991 – 1996, skips a few years, but includes year 1999. This decade covers a very large portion of basin, with extensive coverage of CRITFC's study area. The 2000s decade has three survey years; 2002, 2003, and 2005 and covers less area than the 1990s, but added the Minam Basin and repeated surveys in our study area completed in earlier years. The present 2010s decade, has data collected in 2010 and 2011, and like the 2000s, repeats surveys in our study area and continues to add new area to the AHI dataset.

Summary of metrics and quality control procedures

Within the three decades that the AHI data spans, three different versions of the protocol were used (1990, 1998, 2008). Many of the metrics and measurements taken are common among the protocols, but there were some changes. To make the differences between the protocols more accessible and comprehensive, a list of terms, codes, and definitions was compiled (Appendix 1). The majority of the terms were acquired first from an ODFW's Habitat and Reach Data Coverages Metadata (ODFW 1997). Then we read through the protocols and data sets to add any codes or parameters that had been missed. Columns designating which decade each of the measurements was relevant to were also added. In future, linking terms between this compilation and the database may occur and make the definitions accessible directly from the data.

The AHI dataset was put into Microsoft Access for easier analysis and arranged by reach or unit scale and decades. Simple quality assurance and quality control checks were performed by using the dropdown filters at the column headings. These checks focused mainly on the unit scale data and were looking for erroneous minimum values, maximum values, codes, and characters. The data was mostly clean, but some simple changes were made to spelling and entry format. We tracked observed issues and actions taken to resolve them (Table 1).

Tables

Table 1. Quality assurance/quality control actions taken and recommended for aquatic habitat inventory data.

Decade	Topic	Concern	Action taken
1990's	Naming of basins and streams does not follow 2008 protocol	Names are inconsistent and varying among themselves (there were no guidelines in the 1990's protocol). Creek, river, fork, aren't supposed to be spelled out, but abbreviated CR, R, FK.	None
	Location codes	Inconsistent format for a few of them. Usual format ends up being "T3S-R35E-25SW," some of them are lacking dashes/ have an extra dash.	None
	Valley Form codes	Some channel form codes are used under valley form column.	None
	VEG_CL codes	Some seem to be wrong.	There is a "Y" included in some of the codes – does this mean young trees?
	LAND_DOM	Park should be "greenway"	None
2000's	Location codes	The format for most of them is as described above, but that is inconsistent with the protocol. Should follow the format T10S R5W Sec. 22 SE. One code also seems to have been mis-typed.	Location code T04S-R43E-S00NA (Should this be S00NE? S00NW? or is it right?) Made codes consistent with existing format.
	Unit type/Unit name	A code that doesn't exist in the protocol was added – MX, Mix of Habitats.	Added to spatial data fields list.
	CHANL_TYPE	In the list of descriptions channel type only goes to 12 (for secondary valley floor tributary).	I could see 13 and 14 being tertiary and quaternary valley floor tribs, but where did 22 come from?
	SLOPE	Is supposed to be percent change in elevation over the length of the unit, but there are some values over 100%	None
	DEPTH_PTC	Parameter not listed in the protocol/metadata list.	Added to spatial data fields list (assumed it meant pool tail crest depth).
	AC_EROSION	Was listed as "AE_EROSION" in protocol/metadata list.	Changed to AC_ in spatial data fields list.
	KEYPIECES	There were extra spaces in front of some of the entries.	Extra spaces eliminated.
	COMM_CODE	There are a lot of slashes incorporated into the comment codes (and notes sections). I don't	None

		know if they serve a specific purpose. Not a huge problem, but makes the data look messy.	
	NOTE_1	A lot of slashes here too, again, don't know if they serve a specific purpose and whether or not it's important to take them out.	None
	NOTE_1	There are also a lot of temperatures under the notes. I didn't compare them with the temperatures in the temp. column, but wondered if they're redundant.	None
	NOTE_1, NOTE_2	Observations don't have a consistent format (white fish or whitefish; ADLT CHNK, ADULT CHNK, ADULT CHINOOK), so it's a little messy.	Made some changes to make them a bit more consistent, but didn't focus on it.
	RCHCOM	Two of the reaches (LLIDs 1178722453139, 1169845460718) say they are un-surveyed under the reach dataset, but in the habitat unit data, there is information on all of the habitat units.	None.
2010s	LENGTH	Some seem quite long for unit lengths and don't have decimals places consistent with the rest of the lengths, so don't know if they are valid or not.	Are 5520.41 and 10603.9 valid lengths?
	SAMPL_DATE	One listed as 8/5/2020	Presumed it should be 2010 and changed it.
	WATER_TEMP	There is a value of 34.5 C, which may be plausible, but seemed a little high.	None
	PER_FLOW	High percent flow value of 150	None
	SLOPE	High slope values as in 2000's data	None

Figures

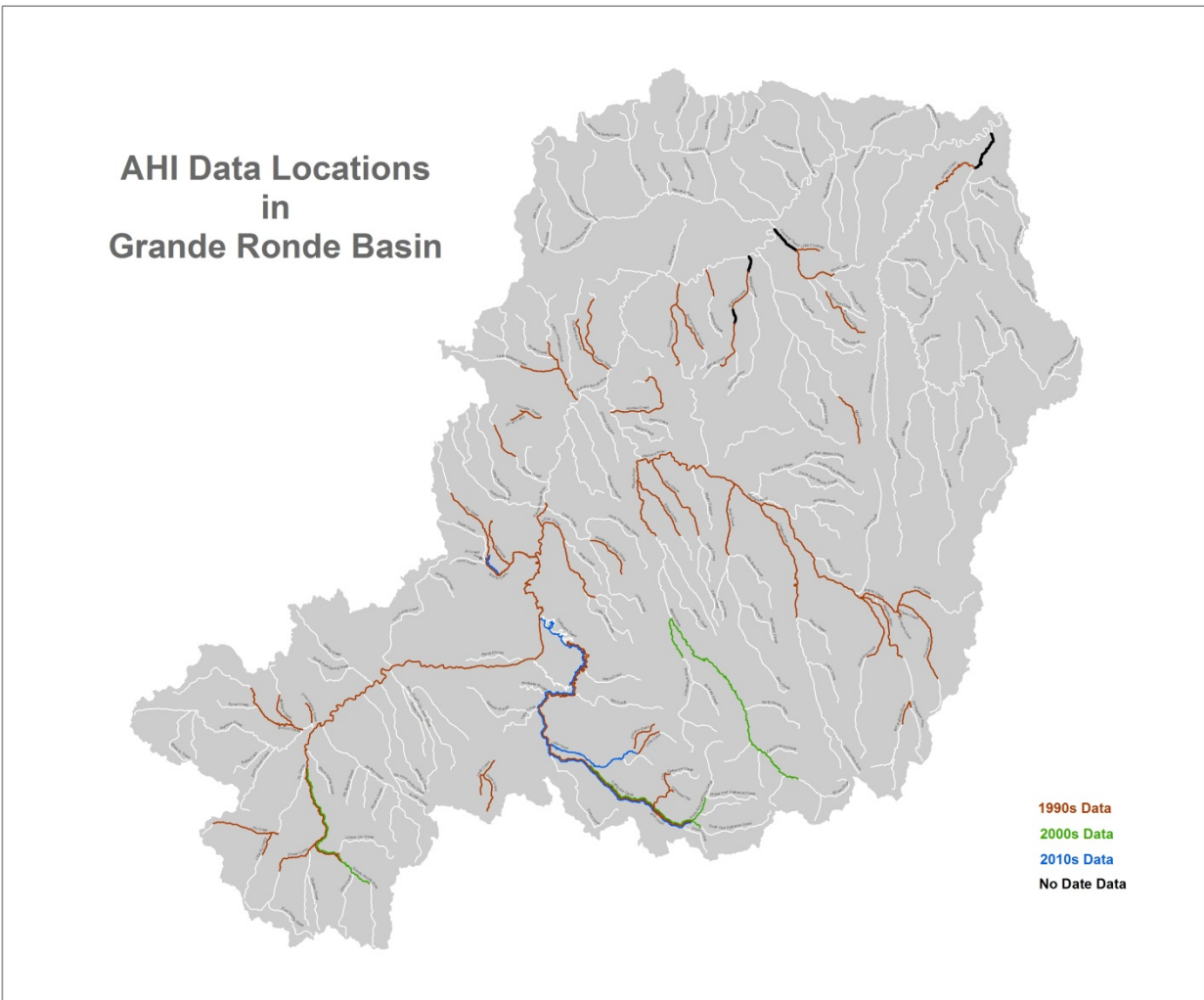


Figure 1. Three decades of Aquatic Habitat Inventory survey data collected in the Grande Ronde Basin.

References

- Bouwes, N., C. Jordan, N. Weber, S. Bennett, J. Moberg, and B. Bouwes. 2010. *Tributary Habitat Monitoring Summary Report: a Recommendation for a Standardized Fish Habitat Monitoring Program Implemented Under the Federal Columbia River Power System's Biological Opinion*. NOAA_Fisheries and Bonneville Power Authority.
- Hankin, D. G., and G. H. Reeves. 1988. "Estimating Total Fish Abundance and Total Habitat Area in Small Streams Based on Visual Estimation Methods." *Canadian Journal of Fisheries and Aquatic Sciences* 45: 834–844.
- Moore, K., K.K. Jones, J. Dambacher, and C. Stein. 2008. *Methods for Stream Habitat Surveys Aquatic Inventories Project*. Corvallis, OR: Oregon Department of Fish and Wildlife, Aquatic Inventories Project, Conservation and Recovery Program.
<http://oregonstate.edu/dept/ODFW/freshwater/inventory/pdf/files/habmethod.pdf>.
- Oregon Department of Fish & Wildlife. 1997. *ODFW Aquatic Inventories Project Stream Habitat Distribution Coverages*. Natural Production Section. Corvallis. Oregon Department of Fish & Wildlife.

Appendix 1

Reach Dataset

< basin >rch.aat (Arc Attribute Table)
 < basin >rch.bnd (Boundary – Coverage extent.)
 < basin >rch.tic (Contains tic information. Tics are a registration point for a coverage.)

Arc Attribute Item Description:

Summary: The reach dataset provides information within the context of specific stream reaches identified by the stream habitat survey crew and supported at the time of stream analysis. Reaches vary in length from ½ kilometer to more than 8 kilometers and are defined by channel and valley geomorphology, gradient, land use, land ownership, riparian characteristics, and stream flow. The survey describes the reaches in terms of hill slope constrained, terrace constrained, and unconstrained stream channels. Within each reach, the stream is described as a series of habitat units. The information present in this dataset summarizes the unit by unit data collected at the time of the survey. There are multiple calculated fields present that provide important and useful statistics which give insight into the condition of the reach. The reach information is distributed on the coverage based on the distance of the reach from the start point of the stream.

Time period columns:

X = included in the survey

/ = only included in survey for a portion of the time period

Attribute Name	Codes	Description	1990s	1998	2000s/2010s
LENGTH		Length of arc in meters	x	x	x
<BASIN>RCH#		Computer generated identification number for arc.	x	x	x
<BASIN>RCH-ID		User generated identification number for arc.	x	x	x
GROUP		Funding or Sponsor Group (blanks acceptable)	x	x	x
	BLM	Bureau of Land Management (1990 BL)	x	x	x
	BPA	Bonneville Power Administration	x	x	x
	ODF	Oregon Dept. of Forestry	x	x	x
	FED	Other Federal	x	x	x
	ODFW	Oregon Dept. Fish and Wildlife (1990 FW)	x	x	x
	OFIC	Oregon Forest Industry Council	x	x	x
	R&E	Restoration and Enhancement Program	x	x	x
	REFOG	Reference old growth reach	x	x	x

	UBFRI	Umpqua Basin Fisheries Restoration Initiative	x	x	x
	P	(1990) Private	x		
	M	(1990) Municipal	x		
	C	(1990) County	x		
	T	(1990) Tribal	x		
	SF	(1990) State Forest	x		
	NF	(1990) National Forest	x		
	WA	(1990) Wilderness Area	x		
LLID		Unique identification number which equals the longitude and latitude of the starting arc of the stream.	x	x	x
STREAM		Stream name.	x	x	x
REGION		ODFW Fish Management Region.	x	x	x
	C	Central	x	x	x
	CO	Columbia	x	x	x
	NE	NorthEast	x	x	x
	NW	NorthWest	x	x	x
	SE	SouthEast	x	x	x
	SW	SouthWest	x	x	x
ECOREGION		EPA Ecoregion and Subregion.	x	x	x
		Not a code. Short description of EPA ecoregion or subregion name. Useful or sorting to large grouping within the state. Wild card grouping and sorts i.e. "COAST" particularly useful.	x	x	x
BASIN		Major basin or watershed associated with the stream.	x	x	x
Elevation		(1990)	x		
Geology, soil types		(1990)	x		
Flow records		(1990)	x		
HUC		USGS/EPA Hydrologic Unit (8 digits).	x	x	x
NEXT_STRM		Stream that survey stream flows into.	x	x	x
OWNERSHIP		Name of individual, company, or agency that owns reach (blanks acceptable). By agreement, no ownerships are given for most Umpqua reaches.	x	x	x
		Ownership. Not a code. Short explanation of ownership as noted in field. Useful	x	x	x

		for grouping data for some reports, but does not reflect all ownerships or changes in ownership.			
REACH		Stream Reach #. It may be defined by geomorphic characteristics such as changes in valley and channel form or an area between named tributaries or by major changes in vegetation type, land use or ownership.	x	x	x
RCHCOM		Reach comments that provide additional information used for some data sorts.	x	x	x
	(W)	Winter survey also done	x	x	x
	LQ	Low Quality field work, use with caution	x	x	x
	DRY	DRY channel in this reach	x	x	x
	SS	Small Stream survey methods used	x	x	x
	UNS	UNSurveyed because access denied, most data missing	x	x	x
	RSVR	reach was a lake or ReSerVoiR	x	x	x
NODATA		Explanation code for some blank variable fields (riparian survey, wood survey, calculated fields).	x	x	x
	KP	no Key Pieces (not calculated prior to 1993).	/	x	x
	P1	Pools > 1.0 m in depth, not calculated for this reach.	x	x	x
	RP	RiParian transects missing (no riparians done prior to 1993).	/	x	x
	RI	Riffle units not present in reach.	x	x	x
	WD	Wood Debris summary data missing (no wood survey prior to 1991).	/	x	x
SURV_DATE		Survey date.	x	x	x
STREAMORD		Stream order from 7.5 min topo (blanks acceptable).	x	x	x
WATERSHED		Watershed area from 7.5 min topo (blanks acceptable).	x	x	x
PRICHNLL		Length of primary channel. This is defined as the mainstem of the stream and does not include secondary channel units, backwater, alcove or tributary unit lengths surveyed.	x	x	x
FROMDIST		From distance (m). Measures the distance from the start of the stream to the beginning of the unit.	x	x	x
TODIST		To distance (m). Measures the distance from the start of the stream to the end of the unit.	x	x	x
SECCHNLL		Length (m) of secondary channels (secondary channels are coded separately from the primary channel of the stream).	x	x	x

PRICHNAREA		Area of primary channel (m ²).	x	x	x
SECCHNAREA		Area of secondary channels (m ²).	x	x	x
PCTSCCHNLA		Percent of the total area of the stream in the reach that is associated with secondary channels.	x	x	x
LUSE1		Primary land use as determined from observation of the terrace and hill slopes beyond the riparian zone of the stream within the reach.	x	x	x
	AG	Agricultural crop or dairy land.	x	x	x
	TH	Timber Harvest. Active timber management including tree felling, logging, etc. Not yet replanted. (1990 – CC Clear-cut forest)	x	x	x
	YT	Young forest Trees. Can range from recently planted harvest units to stands with trees up to 15 cm dbh.	x	x	x
	ST	Second growth Timber. Trees 15-30 cm dbh in generally dense, rapidly growing, uniform stands. (1990 – SG)	x	x	x
	LT	Large Timber (30-50 cm dbh).	x	x	x
	MT	Mature Timber (50-90 cm dbh).	x	x	x
	OG	Old Growth forest. Many trees with 90+ cm dbh and plant community with old growth characteristics.	x	x	x
	PT	Partial cut Timber. Selection cut or shelterwood cut with partial removal of large trees. Combination of stumps and standing timber. If there are only a few live trees or snags in the unit, describe in note column. (1990 – SC Selective cut)	x	x	x
	FF	Forest Fire. Evidence of recent charring and tree mortality.	x	x	x
	BK	Bug Kill. Eastside forests with > 60% mortality from pests and diseases. Enter bug kill as a comment on the unit sheet when it is observed in small patches.	x	x	x
	LG	Light Grazing pressure. Grasses, forbs, and shrubs present, banks not broken down, animal presence obvious only at limited points such as water crossings. Cow pies present	x	x	x
	HG	Heavy Grazing pressure. Broken banks, well-established cow paths. Primarily bare earth or early successional stages of grasses and forbs present.	x	x	x
	EX	Exclosure. Fenced area that excludes cattle from a portion of range land.	x	x	x
	UR	URban.	x	x	x
	RR	Rural Residential.	x	x	x
	IN	INDustrial.	x	x	x

	MI	MIning.	x	x	x
	WL	WetLand.	x	x	x
	NU	No Use identified.	x	x	x
	GW	(1990) GreenWay	x		
LUSE2		Secondary land use, blanks acceptable. (Codes the same as LUSE1)	x	x	x
RIPV1		Primary riparian vegetation within approximately one active channel width of the mainstem of the stream.	x	x	x
	N	No Vegetation (bare soil, rock).	x	x	x
	B	SageBrush (sagebrush, greasewood, rabbit brush, etc.).	x	x	x
	G	annual Grasses, herbs, and forbs.	x	x	x
	P	Perennial grasses, sedges, and rushes.	x	x	x
	S	Shrubs (willow, salmonberry, some alder).	x	x	x
	D	Deciduous dominated (canopy more than 70% alder, cottonwood, big leaf maple, or other deciduous sp.).	x	x	x
	M	Mixed conifer/deciduous (approx. 50:50 distribution).	x	x	x
	C	Coniferous dominated (canopy more than 70% conifer).	x	x	x
		Second part of code for size class. Only the first number of the sequence shown in the reach file. <i>(These size classes correspond to dbh estimated in inches of: <1, 1-5, 6-11, 12-20, 21-35, and 36+ respectively.)</i>	x	x	x
	1-3	Seedlings and new plantings. (1990 – S)	x	x	x
	3-15	Young, established trees or saplings. (1990 – P)	x	x	x
	15-30	Typical sizes for second growth stands. West side communities may have fully closed canopy at this stage. (1990 – Y)	x	x	x
	30-50	Large trees in established stands. (1990 – M Mature)	x	x	x
	50-90	Mature timber. Developing understory of trees and shrubs. (1990 – M Mature)	x	x	x
	90+	Old growth. Very large trees, nearly always conifers. Plant community likely to include a combination of big trees, snags, downed woody debris, and a multi-layered canopy. (1990 – O)	x	x	x
RIPV2		Secondary riparian vegetation. (Codes the same as RIPV1)	x	x	x
GRADIENT		Average of unit gradients (percent slope) for reach, weighted by unit length.	x	x	x
VWI		Valley Width Index. The ratio of active channel to valley floor.	x	x	x

VALLEYTYP		Valley form or type. Describes the configuration of the valley floor.	x	x	x
	SV	Steep V-shaped valley or bedrock gorge.	x	x	x
	MV	Moderate V-shaped valley (side slopes > 30%).	x	x	x
	OV	Open V-shaped valley (side slopes < 30%).	x	x	x
	CT	Constraining Terraces.	x	x	x
	MT	Multiple Terraces.	x	x	x
	WF	Wide-active Floodplain.	x	x	x
Adjacent Feature		(1990) Description of the landform adjacent to the active channel margin on the left and right sides (looking upstream). Separate left side and right side entries by a slash (e.g. HS/FP)	x		
	HS	Hill Slope	x	x	x
	HT	High Terrace	x	x	x
	AF	Alluvial Fan	x	x	x
	FP	Flood Plain	x	x	x
	RF	Road Fill (Rip-Rap)	x	x	x
	WM	Wetlands-Meadow	x	x	x
	O	Other (make note in comment column)	x	x	x
CHANNELFO		Channel form, describes the morphology of the active channel, hill slopes, terraces and floodplains.	x	x	x
	CB	Constrained by Bedrock (bedrock dominated gorge).	x	x	x
	CH	Constrained by Hill slope.	x	x	x
	CF	Constrained by alluvial Fan.	x	x	x
	CL	Constrained by Land use (road, dike, landfill).	x	x	x
	US	Unconstrained - predominantly Single channel.	x	x	x
	UA	Unconstrained - predominantly Anastomosing.	x	x	x
	UB	Unconstrained - Braided channel.	x	x	x
	TC	Terrace Constrained. (CT – Constrained by Terrace in 1990)	x	x	x
	CA	Constrained by Alternating terraces and hill slope.	x	x	x
Stream Flow		(1990) Description of observed discharge condition. Best observed in riffles. Reference to gauging station staff gauges where possible.	x		
	DR	DRy	x		

	PD	PuDDled. Series of isolated pools connected by surface trickle or subsurface flow.	x		
	LF	Low Flow. Surface water flowing across 50 to 75 percent of the active channel surface. Consider general indications of low flow conditions.	x		
	MF	Moderate Flow. Surface water flowing across 75 to 90 percent of the active channel surface.	x		
	HF	High Flow. Stream flowing completely across active channel surface, but not at bankfull.	x		
	BF	Bankfull Flow. Stream flowing at the upper level of the active channel bank.	x		
	FF	Flood Flow. Stream flowing over banks onto low terraces or floodplain.	x		
WIDTH		Average Channel Width (m). Width of the wetted portion of the channel.	x	x	x
ACW		Active or bankfull channel width (m). The horizontal distance across the channel at the "bank full" or annual high flow line.	x	x	x
ACH		Active channel height (m). The vertical distance from the streambed to the top of the active channel.	x	x	x
TERR_WIDTH		Inter-terrace width (m). Width across stream from terrace edge to terrace edge.	x	x	x
TERR_HT		Height of terrace above the streambed (m).	x	x	x
FLOOD_WID		The floodprone width is the width of the valley floor inundated during a flood which occurs approximately every 50 years. The floodprone width is determined as the channel width measured on a level line at the level of the floodprone height. (Info not collected prior to 1998).		x	x
FLOOD_HT		Floodprone height is determined by doubling the active channel height. It is the maximum depth in the channel during a flood with an occurrence of approximately 50 years. (Info not collected prior to 1998.)		x	x
ENTRENCH		The entrenchment value is the ratio between the floodprone width and the active channel width. (Info not calculated prior to 1998.)		x	x
UNITS100		Number of habitat units/100 m stream survey. An index of stream habitat complexity.	x	x	x
NOPOOLS		Combined count of scour and dammed pools in reach.	x	x	x
PCTPOOL		Combined percentage (by area) of scour and dammed pools in reach.	x	x	x
SCRPOOLD		Average depth of scour pools.	x	x	x
PCTDBPOOL		Percent of habitat units in the reach that are backwaters or dammed pools.	x	x	x

RIFFLEDEP		Average depth of riffles.	x	x	x
LRGBLDR		Number of boulders ≥ 0.5 m diameter in reach.	x	x	x
PCTSNDOR		Average percent of sand, silt, and organics in surface substrate of all units.	x	x	x
PCTGRAVEL		Average percent of gravel in surface substrate of all units.	x	x	x
RIFSNDOR		Average percent of sand, silt, and organics in surface substrate of riffle units only. No value is given for reach without riffles.	x	x	x
PCTBEDROCK		Average percent of bedrock in surface substrate of all units. (Info not in the reach database prior to 1999).		/	x
RIFGRAV		Average percent of gravel in surface substrate of riffle units only. No value given for reaches without riffles.	x	x	x
POOLS_KMTL		Number of pools per kilometer of total stream length.	x	x	x
POOLS_KMPL		Number of pools per kilometer of primary channel length.	x	x	x
POOL1P_KM		Number of pools deeper than 1.0 meter/kilometer of total stream length.	x	x	x
COMPOOL_KM		Number of pools with ≥ 3 pieces of LWD/kilometer of total reach length.	x	x	x
CWPOOL		Channel widths/pool. A pool frequency measure calculated by dividing the number of pools by the number of active channel width equivalents in the reach.	x	x	x
SHADE		Amount of shade provided to stream by riparian vegetation and topography (percentage of 180 degrees).	x	x	x
BANKEROSI		Percent reach length of channel units with banks classified as actively eroding.	x	x	x
PCTUNDERC		Undercut bank unit average as percent of unit length.	x	x	x
PIECESLWD		Pieces of large woody debris (≥ 0.15 m diameter and ≥ 3 m long) in reach.	x	x	x
VOLUMELWD		Volume of large woody debris (m^3) in reach.	x	x	x
LWDPIECE1		Pieces of large woody debris/100 meters of primary stream length.	x	x	x
LWDVOL1		Volume of large woody debris/100 meters of primary stream length.	x	x	x
KEYLWD		Key pieces of large woody debris (≥ 0.60 m diameter and ≥ 12 m long) in reach.	x	x	x
KEYLWD1		Key pieces of large woody debris/100 m of primary stream length.	x	x	x
MAXTEMP		Maximum temperature in $^{\circ}C$ measured during survey.	x	x	x
MINTEMP		Minimum temperature in $^{\circ}C$ measured during survey.	x	x	x
POOLS100		Number of pools/100 m total stream length.	x	x	x
RESIDPD		Average residual depth of pool.	x	x	x

WDRATIO		Width to Depth ratio (calculated as active channel width to active channel depth).	x	x	x
LRGBLDR1		Large boulders (≥0.5 m dia)/100 m total channel length.	x	x	x
THARDWOOD		Total number of riparian hardwood trees in a 100 ft zone/1000 ft of stream length (30 m x 305 m).	x	x	x
TCONIFERS		Total number of riparian conifer trees in a 100 ft zone/1000 ft of stream length (30 m x 305 m).	x	x	x
CON_20PLUS		Conifers ≥ 50 cm dbh/1000 ft (305 m) of stream length.	x	x	x
CON_20TO35		Conifers ≥ 50 cm and < 90 cm dbh/1000 ft (305 m) of stream length.	x	x	x
CON_36PLUS		Conifers ≥ 90 cm dbh/1000 ft (305 m) of stream length.	x	x	x
FISH1		Code of primary fish species observed (blanks frequent and acceptable)	x	x	x
FISH2		Code of 2nd fish species.	x	x	x
FISH3		Code of 3rd fish species.	x	x	x
FISH4		Code of 4th fish species.	x	x	x
	Standard Abbreviations		Non-Standard Abbreviations		
	BG	bluegill	AM	lamprey ammocoetes	
	BLB	black bullhead	AS	Atlantic salmon	
	BR	brown trout	ATF	adult tailed frog	
	BRB	brown bullhead	BD	black dace	
	BSU	bridgelip sucker	BTH	brook/bull hybrid	
	BT	brook trout	C	crappie	
	BUT	bull trout	CF	crayfish	
	CC	channel catfish	COT	sculpin	
	CH	chinook salmon	CP	carp	
	CLM	chiselmouth	CTH	cutthroat hybrid	
	CO	coho salmon	FRG	frog (species unknown)	

	CS	chum salmon	JSU	jenny lake sucker			
	CSU	largescale sucker	LB	laregemouth bass			
	CT	cutthroat trout	LND	longnose dace			
	D	dace	MF	western mosquitofish			
	LAM	lamprey	MMS	Malheur mottled sculpin			
	MSU	mountain sucker	MS	mottle sculpin			
	OC	Oregon chub	PGS	Pacific giant salamander			
	PK	pumpkinseed	RTS	reticulate sculpin			
	PM	peamouth	RO	roach			
	PS	pink salmon	RSN	rough skin newt			
	RB	rainbow trout	SH	shiner spp.			
	RSS	redside shiner	SKB	stickleback			
	RT	redband trout	SR	sandroller			
	SP	smallmouth bass	SP	speckled dace			
	SS	sockeye salmon	SQ	northern squawfish			
	ST	steelhead	SNF	sunfish			
	SU	sucker	SF	salmonid fry (age 0+)			
	WF	mountain whitefish	SAL	salamander			
			TC	tui chub			
			TF	trout fry (age 0+)			
			TFT	tailed frog tadpole			
			UT	unknown trout			
			US	unknown salmonid			

		X	no fish found			
		YP	yellow perch			
BVR_DAM		Beaver dams. If present, give code and number of occurrences, eg. BD04		x	x	x
	BD	Two-part code BD which indicates beaver dam activity and a two-digit number indicating number of occurrences in the reach. Blank fields are acceptable.		x	x	x
BVR_ACTIV		Beaver Activity observed within reach. If present, give code and number of occurrences.		x	x	x
	BV	Beaver activity codes have two parts, the type of activity and the number of occurrences in the reach. Blank fields are acceptable.		x	x	x
CULVERT		Culvert. If present, give code and number of occurrences. Blank fields are acceptable.		x	x	x
	CC	Culvert Crossing. Primary channel goes through culvert.		x	x	x
	CE	Culvert Entry. Tributary stream enters primary channel through culvert. A two-part code indicating type and number of occurrences in the reach.		x	x	x
	CCCE	Indicates both types of culvert entry within reach.		x	x	x
MASS_FAIL		Mass Failure code for streamside earth movements. It includes code for type and a number of occurrences in reach. A comment on reach, not a useful sorting variable. Blank fields are acceptable.		x	x	x
	A	Debris Avalanche		x	x	x
	E	Earthflow		x	x	x
	L	Landslide		x	x	x
DEBRIS_JAM		Debris jams. If present, give code and number of occurrences.		x	x	x
	DD	Large woody debris jam or dam code for type and number of occurrences in reach. Includes both debris jams (3-4 pieces) and full channel damming features. Count is an index of frequency and is not appropriate for strict comparison due to the variable sizes of jams. Blank fields are acceptable.		x	x	x
HAB_STRUCT		Habitat structures. If present, give code and number of occurrences.		x	x	x
	HS	Stream habitat structure. Man-made structure intended to improve stream habitat conditions. Number of occurrences in reach given. Blank fields are acceptable.		x	x	x
HABRCH		Unique identification number for reach which equals the LLID number with reach number appended. Eg: reach 1 of stream with LLID # which equals		x	x	x

		1230144425933 would have a habrch value of 123014442593301.			
--	--	---	--	--	--

Habitat Unit Dataset

< basin >hab.aat (Arc Attribute Table)

< basin >hab.bnd (Boundary – Coverage extent.)

< basin >hab.tic (Contains tic information. Tics are a registration point for a coverage.)

Arc Attribute Item Description:

Summary: The habitat unit dataset provides all of the information collected at the unit level by the stream survey crew. Habitat units are the building blocks of reaches. Each unit is longer than one active channel width and is an area of relatively homogeneous slope, depth, and flow patter representing different channel forming processes. The channel is classified into 22 hierarchically organized types of pools, glides, riffles, rapids, steps, and cascades. The crews estimate the length and width of every habitat unit. At every unit, attributes are estimated or measured to describe gradient, substrate, woody debris, shade, features of instream cover, and bank stability. The habitat information is distributed along the length of the stream route in relation to the distance of the habitat unit from the start point of the stream.

Attribute Name	Code	Description	1990s	1998	2000s/2010s
LENGTH		Length of arc in meters	x	x	x
<BASIN>#		Computer generated identification number for arc.	x	x	x
<BASIN>-ID		User generated identification number for arc.	x	x	x
BASIN		Major basin or watershed associated with the stream.	x	x	x
STREAM		Stream name.	x	x	x
SAMPL_DATE		Date unit of stream surveyed.	x	x	x
LOCATION		Legal description of reach location. It includes the township-range-section as identified on USGS 1:24000 topographic maps.	x	x	x
REACH_NUMB		Number of reach in which habitat unit is contained. Original reach number as identified by field survey crew.	x	x	x
REACH_NEW		Reach number in which habitat unit is contained. Modified reach number determined during data analysis.	x	x	x
CHAN FORM		Channel form. It describes the morphology of the active channel, hill slopes, terraces, and flood plains.	x	x	x
	CB	Constrained by Bedrock (bedrock dominated gorge).	x	x	x
	CH	Constrained by Hill slope.	x	x	x

	CF	Constrained by alluvial Fan.	x	x	x
	US	Unconstrained-predominantly Single channel.	x	x	x
	UA	Unconstrained-Anastomosing (several complex, interconnecting channels).	x	x	x
	UB	Unconstrained-Braided channels (numerous, small channels often flowing over alluvial deposits).	x	x	x
	CT	Constraining Terraces. (Terrace height > 10% active channel width <u>and</u> terrace to terrace width < 2x active channel width).	x	x	x
	CA	Constrained by Alternating terraces and hill slope.	x	x	x
	CL	Constrained by Land use (road, dike, landfill).	x	x	x
VALLEY_FM		Valley form or type. It describes the configuration of the valley floor.	x	x	x
	SV	Steep V-shaped valley or bedrock gorge (side slopes >60%).	x	x	x
	MV	Moderate V-shaped valley (side slopes >30%).	x	x	x
	OV	Open V-shaped valley (side slopes <30%).	x	x	x
	CT	Constraining Terraces. Terraces typically high and close to the active channel. Terrace surface is unlikely to receive flood flows.	x	x	x
	MT	Multiple Terraces. Surfaces with varying height and distance from the channel. High terraces may be present, but they are a sufficient distance from the channel that they have little impact.	x	x	x
	WF	Wide-active Flood plain. Significant portion of valley floor influenced by annual floods. Any terraces present do not impinge on the lateral movement and expansion of the channel.	x	x	x
VEG_CL_DOM		Vegetation classification. Identifies the dominant vegetation located within the riparian zone of the stream based on canopy density and height.	x	x	x
	N	No Vegetation (bare soil, rock).	x	x	x
	B	SageBrush (sagebrush, greasewood, rabbit brush, etc.).	x	x	x
	G	Annual Grasses, herbs, and forbs.	x	x	x
	P	Perennial grasses, sedges and rushes.	x	x	x
	S	Shrubs (willow, salmonberry, some alder).	x	x	x
	D	Deciduous dominated (canopy more than 70% alder, cottonwood, big leaf maple, or other deciduous spp.).	x	x	x
	M	Mixed confer/deciduous (approx. a 50:50 distribution).	x	x	x
	C	Coniferous dominated (canopy more than 70% conifer).	x	x	x

	1-3	Seedlings and new plantings.	x	x	x
	3-15	Young established trees or saplings.	x	x	x
	15-30	Typical sizes for second growth stands. West side communities may have fully closed canopy at this stage.	x	x	x
	30-50	Large trees in established stands.	x	x	x
	50-90	Mature timber. Developing understory of trees and shrubs.	x	x	x
	90+	Old growth. Very large trees, nearly always conifers. Plant community likely to include a combination of big trees, snags, down woody debris, and a multi-layered canopy.	x	x	x
VEG_CL_SUB		Subdominant vegetation in the riparian zone. (Codes the same as for dominant vegetation.)	x	x	x
LAND_DOM		Dominant land use. Determined from observations of the hill slopes and terraces beyond the riparian zone of the stream.	x	x	x
	AG	Agricultural crop or dairy land.	x	x	x
	TH	Timber Harvest. Active timber management including tree felling, logging, etc. Not yet replanted.	x	x	x
	YT	Young forest Trees. Can range from recently planted harvest units to stands with trees up to 15 cm dbh.	x	x	x
	ST	Second growth Timber. Trees 15-30 cm dbh in generally dense, rapidly growing, uniform stands.	x	x	x
	LT	Large Timber (30-50 cm dbh).	x	x	x
	MT	Mature Timber (50-90 cm dbh).	x	x	x
	OG	Old Growth forest. Many trees with 90+ cm dbh and plant community with old growth characteristics.	x	x	x
	PT	Partial cut Timber. Selection cut or shelterwood cut with partial removal of large trees. Combination of stumps and standing timber. If only a few live trees or snags in the unit, describe in note column.	x	x	x
	FF	Forest Fire. Evidence of recent charring and tree mortality.	x	x	x
	BK	Bug Kill. Eastside forests with > 60% mortality from pests and diseases. Enter bug kill as a comment on the unit sheet when it is observed in small patches.	x	x	x
	LG	Light Grazing pressure. Grasses, forbs and shrubs present, banks not broken down, animal presence obvious only at limited points such as water crossings. Cow pies present.	x	x	x

	HG	Heavy Grazing pressure. Broken banks, well-established cow paths. Primarily bare earth or early successional stages of grasses and forbs present.	x	x	x
	EX	EXclosure. Fenced area that excludes cattle from a portion of range.	x	x	x
	GN	GreeNway. Designated Greenway areas, parks (city, county, state).	x	x	x
	UR	URban.	x	x	x
	RR	Rural Residential.	x	x	x
	IN	INDustrial.	x	x	x
	CR	Conservation area or wildlife Refuge.	x	x	x
	MI	MIning.	x	x	x
	WL	WetLand.	x	x	x
	NU	No Use identified.	x	x	x
	WA	Designated Wilderness Area.	x	x	x
LAND_SUB		Subdominant land use. Determined from observations of the hill slopes and terraces beyond the riparian zone of the stream. (Codes the same as for dominant land use.)	x	x	x
WATER_TEMP		Water temperature. Measured at each reach by the stream survey crew.	x	x	x
UNIT_NUMB		Unit number. Units numbers are assigned sequentially from the start to end of the survey.	x	x	x
UNIT_TYPE		Unit type. The two-letter code which identifies one of the 33 habitat types identified by the ODFW Aquatic Inventories Project Methods for Stream Habitat Surveys.	x	x	x
	PP	Plunge Pool. Formed by scour below a complete or nearly complete channel obstruction (logs, boulders, or bedrock). Substrate is highly variable. Frequently, but not always, shorter than the active channel width.	x	x	x
	SP	Straight scour Pool. Formed by mid-channel scour. Generally with a broad scour hole and symmetrical cross section.	x	x	x
	LP	Lateral scour pool. Formed by flow impinging against one stream bank or partial obstruction (logs, root wad, or bedrock). Asymmetrical cross section. Includes corner pools in meandering lowland or valley bottom streams.	x	x	x
	TP	Trench Pool. Slow flow with U or V-shaped cross section typically flanked by bedrock walls. Often very long and narrow with at least half of the substrate comprised of bedrock.	x	x	x

	DP	Dammed Pool. Water impounded upstream of channel blockage (debris jams, rock landslides).	x	x	x
	BP	Beaver dam Pool. Dammed pool formed by beaver activity.	x	x	x
	AL	ALcove. Most protected type of subunit pool. Alcoves are laterally displaced from the general bounds of the active channel. Substrate is typically sand and organic matter. Formed during extreme flow events or by beaver activity; not scoured during typical high flows.	x	x	x
	BW	BackWater pool. Found along channel margins; created by eddies around obstructions such as boulders, root wads, or woody debris.	x	x	x
	IP	Isolated Pool. Pools formed outside the primary wetted channel, but within the active channel. Isolated pools are usually associated with gravel bars and may dry up or be dependent on inter-gravel flow during late summer.	x	x	x
	GL	GLide. An area with generally uniform depth and flow with no surface turbulence. Glides may have some small scour areas, but are distinguished from pools by their overall homogeneity and lack of structure.	x	x	x
	GP	(1990) Glide with characteristics of a Pool.	x		
	GR	(1990) Glide with characteristics of a Riffle.	x		
	RI	Riffle. Fast, turbulent, shallow flow over submerged or partially submerged gravel and cobble substrates.	x	x	x
	RP	Riffle with Pockets. Same flow and gradient as Riffle, but with <u>numerous</u> sub-unit sized pools or pocket water.	x	x	x
	RB	Rapid with protruding Boulders. Swift, turbulent flow including chutes and some hydraulic jumps swirling around boulders.	x	x	x
	RR	Rapid over bedRock. Swift, turbulent, "sheeting" flow over smooth bedrock.	x	x	x
	CB	Cascade over Boulders. Much of the exposed substrate composed of boulders organized into clusters, partial bars, or step-pool sequences.	x	x	x
	CR	Cascade over bedRock. Same flow characteristics as Cascade over Boulders, but structure is derived from sequence of bedrock steps. Slope 3.5% or greater.	x	x	x
	SR	Step over BedRock (include hardpan and clay steps).	x	x	x
	SB	Step over Boulders.	x	x	x
	SC	Step over face of Cobble bar.	x	x	x
	SL	Step over Log(s), branches.	x	x	x

	SS	Step created by Structure (culvert, weir, artificial dams).	x	x	x
	SD	Step created by Beaver Dam.	x	x	x
	DU	Dry Unit. Dry section of stream separating wetted channel units.	x	x	x
	PD	PuDDled. Nearly dry channel, but with sequence of small isolated pools less than one channel width in length or width.	x	x	x
	DC	Dry Channel. Section of the main channel or side channel that is completely dry at time of survey.	x	x	x
	CC	Culvert Crossing. Stream flowing through a culvert.	x	x	x
	MT	Meadow Trench. Low gradient, low energy system with meandering channel flowing through meadow soils and peat.	x	x	x
	BR	BRaided. Multiple channels with poorly defined riffles and few pools.	x	x	x
	PR	Pool-Riffle. Low to moderate gradient. Sequence of full channel width pools and riffles; may include glides.	x	x	x
	PS	Pool-Step-pool. Moderate to high gradient. Full channel width pools separated by steps, riffles, rapids, or cascades.	x	x	x
	CA	CAscade. High gradient. Rapids, boulder strewn chutes, falls, and very small pools.	x	x	x
	CD	Colluvial Debris. Channel filled with unsorted material from the adjacent hill slopes (boulders, smaller sediments, and/or large wood).	x	x	x
	BD	BeDrock. Channel botton more than 50% bedrock.	x	x	x
	MX	Mix of Habitats.	x	x	x
UNIT_NAME		Unit name. The decoded name of the habitat unit type.	x	x	x
CHANL_TYPE		Channel type. The two-number code identifying the unit as part of the primary channel (00 or 01), a secondary channel (02-09), a backwater (10), alcove (10), isolated pool (10), or tributary (11-12).	x	x	x
	00	No multiple channels (all flow in one channel).	x	x	x
	01	Primary channel (of multiple channel reach or in the unit where a tributary enters the channel).	x	x	x
	02	Secondary channel (of multiple channel reach).	x	x	x
	03	Tertiary channel (of multiple channel reach).	x	x	x
	10	Isolated pools, alcoves, or backwater pools.	x	x	x
	11	Primary channel of valley floor tributary.	x	x	x

	12	Secondary channel of valley floor tributary.	x	x	x
PER_FLOW		Percent flow. A visual estimate of the amount of flow in the channel relative to secondary channels or tributaries, eg. flow of primary channel without tributaries/secondary channels = 100. Flow of primary and secondary channels with an equal distribution of water.	x	x	x
COR_LENGTH		Corrected length (m) is the length of the unit identified by the field crew which has been adjusted to reflect bias identified by field and map calibrations.	x	x	x
COR_WIDTH		Corrected width (m). The width of the unit measured by the field crew and adjusted based on field and map calibrations.	x	x	x
COR_AREA		Corrected area. Unit area calculated by using the corrected length and corrected width values.	x	x	x
FROMDIST		From distance (m). Measures the distance from the start of the stream to the beginning of the unit.	x	x	x
TODIST		To distance (m). Measures the distance from the start of the stream to the end of the unit.	x	x	x
SLOPE		Slope. The gradient of the water surface for the unit. It is measured as percent change in elevation over the length of the unit and is measured with a clinometer.	x	x	x
SHADE		Shade. Measures the amount of shade provided to the habitat unit from vegetation and topography.	x	x	x
Aspect		(1990) Compass heading taken while looking upstream along the central axis of the unit. Round off to the nearest 5 degrees.	x		
AC_WIDTH		Active or bankfull channel width (m). The horizontal distance across the channel at the "bank full" or annual high flow line.	x	x	x
AC_HEIGHT		Active channel height (m). The vertical distance from the streambed to the top of the active channel.	x	x	x
FP_WIDTH		The floodprone width is the width of the valley floor inundated during a flood which occurs approximately every 50 years. The floodprone width is determined as the channel width measured on a level line at the level of the floodprone height. (Info not collected prior to 1998.)		x	x
FP_HEIGHT		Floodprone height is determined by doubling the active channel height. It is the maximum depth in the channel during a flood with an occurrence of 50 years. (Info not collected prior to 1998.)		x	x

TERR_WIDTH		Inter-terrace width (m). Width across stream from terrace edge to terrace edge.	x	x	x
TERR_HEIGH		Height of terrace above streambed to the active channel (m).	x	x	x
VWI		Valley Width Index. Ratio of active channel to valley floor.	x	x	x
DEPTH		Depth of unit (m). Measured as modal depth in fast water units (glides, riffles, rapids, cascades) and maximum depth in the slow water units (pools).	x	x	x
DEPTH_PTC		Depth of pool tail crest.	x	x	x
SO_ADJ		Silt and organics adjusted. Measures the percent of substrate within the unit which is composed of silt and organics.	x	x	x
SND_ADJ		Sand adjusted. Measures the percent substrate of sand size class.	x	x	x
GRV_ADJ		Gravel adjusted. Measures the percent substrate of gravel size class. Gravel is defined as particles of between 2 and 64 mm in size.	x	x	x
CBL_ADJ		Cobble adjusted. Measures the percent substrate of the cobble size class. Cobble is defined as material between 64 and 256 mm in size.	x	x	x
BLD_ADJ		Boulder adjusted. Measures the percent substrate of the boulder size class. Boulder is defined as material 256 mm in size and larger.	x	x	x
BRK_ADJ		Bedrock adjusted. Measures the percent of substrate identified as bedrock.	x	x	x
BLDR_COUNT		Boulder count. The number of boulders ≥ 0.5 m in diameter within the unit that are exposed, but touching the water.	x	x	x
AC_EROSION		The percent of the lineal distance of both sides of the stream that is actively eroding at the active channel height.	x	x	x
UNDERCUT		Undercut bank. Percent of bank along perimeter of unit that is undercut and providing cover habitat.	x	x	x
WOOD_CLASS		Wood class. Measures the complexity of habitat provided by woody debris within the unit. (Not collected after 1997.)	x		
	1	Woody debris absent or in very low abundance. No habitat complexity or cover created.	x	x	x
	2	Wood present, but contributes little to habitat complexity. Mostly small, single pieces, creating little cover or complex flow patterns. Ineffective at moderate to high discharge.	x	x	x
	3	Wood present as combinations of single pieces and small accumulations. Providing cover and some complex habitat at low to moderate discharge, less effective at high discharge.	x	x	x

	4	Wood present with medium and large pieces comprising accumulations and debris jams that incorporate smaller root wads and branches. Good hiding cover for fish. Woody debris providing cover and complex habitat that persists over most stream discharge levels.	x	x	x
	5	Wood present as large single pieces, accumulations, and jams that trap large amounts of additional material and create a <u>variety</u> of cover and refuge habitats. Woody debris providing excellent persistent and complex habitat. Complex flow patterns will exist at all discharge levels.	x	x	x
NPIECES		Number of pieces of countable wood. Countable wood must be at least 15 cm in diameter and 3 meters long.	x	x	x
WVOLUME		Wood volume (m ³). Volume of countable wood contained within the unit.	x	x	x
KEYPIECES		Number of keypieces of wood. This includes all pieces that are at least 0.6 meters in diameter and 12 meters long.	x	x	x
Debris Configuration		(1998)		x	
	S	Single piece.		x	
	A	Accumulation. Two to four pieces.		x	
	J	Jam. More than four pieces.		x	
Debris Type		(1998)		x	
	N	Natural. Broken ends or whole tree.		x	
	C	Cut end.		x	
	A	Artificial. Part of man-made structure.		x	
	RN	Root wad attached to Natural bole.		x	
	RC	Root wad with opposite end Cut.		x	
Debris Location		(1998)		x	
	S	Side of the channel.		x	
	M	Mid-channel.		x	
	I	Island. At upstream end of mid-channel island.		x	
	F	Full channel. Completely across channel within active channel. Pieces may be above the wetted channel at the time of the survey. When part of a jam, include all pieces regardless if they are touching the water, piled up, or submerged.		x	

	O	Over channel. Suspended over the active channel with the ends above the active channel. Include debris with suspended bole but with branches in water.		x	
COMM_CODE		Comment code. Specific codes which identify important features are noted here, eg. BC = bridge crossing or TJ = tributary junction.	x	x	x
	BC	Bridge Crossing.	x	x	x
	BD	Beaver Dam.	x	x	x
	BK	Bug Kill. Patches of insect or disease tree mortality.	x	x	x
	BV	BeaVer activity (beaver den, cut trees, etc.).	x	x	x
	CC	Culvert Crossing.	x	x	x
	CE	Culvert Entry. Tributary entering through culvert.	x	x	x
	CS	Channelized Streambanks. Rip-rap or other artificial bank stabilization and stream control.	x	x	x
	DJ	Debris Jam. Accumulation of large woody debris that fills the stream channel and traps additional debris and sediment. (1990 – DD, Debris Dam)	x	x	x
	FC	Fence Crossing.	x	x	x
	GS	Gauging Station.	x	x	x
	HS	Artificial Habitat Structure. Describe type: gabion, log weir, cabled or uncabled LWD, etc. in note.	x	x	x
	MI	Mining.	x	x	x
	PA	Potential Artificial Barrier. Potential artificial or human-created barrier to upstream or downstream migration of fish.	x	x	x
	PN	Potential Natural Barrier. Potential natural barrier to upstream or downstream migration of fish.	x	x	x
	RF	Road Ford.	x	x	x
	SD	Screened Diversion (pump or canal).	x	x	x
	SS	Spring or Seep.	x	x	x
	TJ	Tributary Junction with named and unnamed tributaries.	x	x	x
	UD	Unscreened Diversion (pump or canal).	x	x	x
	WL	WildLife use of stream or riparian zone.	x	x	x
	SB	(1990) Streamside Buffer.	x		

	DC	(1990) Dry Channel (crews will attempt to make unit classifications even for dry channels).	x		
NOTE_1		Notes taken by the crew member completing the "Unit 1" sheet.	x	x	x
NOTE_2		Notes taken by the crew member completing the "Unit 2" sheet.	x	x	x
CANOPY_CL		Canopy closure. Measures the density of canopy cover in the riparian zone of the stream. This measure is taken at riparian transects which occur at least every 30 units during the habitat survey.	x	x	x
SMALLCON		Small conifers. This field contains the number of conifers counted in the riparian transect with a dbh of less than 50 cm.	x	x	x
C_50		Conifers of size class 50-90 cm. This field tallies the total number of conifers counted in the riparian transect of between 50 and 90 cm dbh.	x	x	x
C_90		Conifers of size class 90 cm and larger. This field tallies the number of conifers counted in the riparian transect with a dbh of at least 90 cm.	x	x	x
TOTHWOOD		Total hardwoods. This field contains the total number of hardwoods counted in the riparian transect taken at this unit number.	x	x	x
LLID		Unique identification number which equals the longitude and latitude of the starting arc of the stream.	x	x	x
HABRCH		Unique identification number for the reach which equals the LLID number with reach number appended, eg. Reach 1 of stream with llid# of 1230144425933 would have a habrch value of 123014442593301	x	x	x
HABUNT		Unique identification number for the unit which equals the habrch # with the unit number appended, eg. unit number 125 with habrch # of 123014442593301 would result in a habunt value of 1230144425933010125	x	x	x
Mass Movement		A two-part code. The first letter identifies the type of mass movement failure. The second letter evaluates the apparent activity of the failure. (Example: AI = inactive debris avalanche.)	x	x	x
		Type	x	x	x
	E	Earthflow. General movement and encroachment of hill slope upon the channel.	x	x	x
	L	Landslide. Failure of locally adjacent hill slope. Usually steep, broad, often shaped like a half oval, with exposed soils.	x	x	x
	A	Avalanche. Failure of small, high gradient tributary. Often appear "spoon-shaped" looking upslope.	x	x	x

		Condition	x	x	x
	A	Active. Contributing material now.	x	x	x
	I	Inactive. Evidence of contribution of material during previous winter or high flows.	x	x	x
	S	Stabilized. Vegetated scars, no evidence of recent activity.	x	x	x
Bank Classification		(1990) A general description of the stream bank at the margin of the active channel. Enter for left bank and right bank, separated by a “/”.	x		
	NE	Non-Erodible. Bedrock or boulder-lined bank.	x		
	VS	Vegetated-Stabilized. Vegetated and/or overhanging erodible bank, partly or wholly stabilized by	x		
	AE	Actively Eroding. Actively or recently eroding banks with little or no vegetative cover, mostly exposed soil.	x		

Appendix K.

Summary of Stream Temperature in the Upper Grande Ronde River and Catherine Creek During Summer 2011



COLUMBIA RIVER INTER-TRIBAL FISH COMMISSION
729 NE Oregon, Suite 200, Portland, Oregon 97232
Telephone 503 238 0667
Fax 503 235 4228

Summary of Stream Temperature in the Upper Grande Ronde River and Catherine Creek During Summer 2011

A component of

Monitoring Recovery Trends in Key Spring Chinook Habitat Variables and Validation of Population
Viability Indicators

November 2011

Laurinda Hill

Casey Justice

Dale McCullough

Seth White



Methods

We summarized stream temperature data collected from 46 sites throughout the Upper Grande Ronde River and Catherine Creek basins during the summer of 2011 (21 Jun – 5 Oct) (Table 1). Stream temperature measurements were mostly limited to areas within the range of historical spawning or rearing habitat for spring Chinook salmon as defined by the NOAA Technical Recovery Team (TRT) (Pers. Comm. Damon Holzer, NOAA). Temperature loggers were deployed at randomly selected stream reaches in coordination with a broader stream habitat monitoring program (Bouwes et. al. 2011) as well as other selected locations targeting key tributary junctions or underrepresented mainstem reaches. Continuous stream temperature data will provide critical information for assessing land use impacts on threatened salmon and steelhead populations.

Temperature data was recorded at half-hour or hourly intervals using Onset Hobo U22 Pro v2 temperature loggers (accuracy = 0.2 °C) or Onset TidBit v2 UTBI temperature loggers. Prior to deployment, we checked the accuracy of each Hobo U22 Pro logger using methods described in Ice et al. (1999). We compared the temperature measurements from each logger with measurements made with a National Institute of Standards and Technology (NIST) certified thermometer to ensure an accuracy of at least 0.3 °C. Temperature loggers were secured to the streambed using ¼ inch rebar stakes and stainless steel cable, or were cabled to tree roots along the channel margin. Most loggers were placed in PVC or steel housings to protect against physical damage and direct solar radiation. All loggers were downloaded and redeployed at the end of the summer to collect winter and spring temperatures.

After downloading data from all of the temperature loggers, we checked the data for quality assurance using methods described in Dunham et al. (2005). Specifically, we flagged all observations that fell below -1 °C or above 30 °C, or if the rate of change was greater than 3°C between successive hourly or daily measurements. All flagged observations were then verified with personnel involved in data logger programming and field sampling and obvious erroneous observations were removed from the database. Additionally, we examined plots of daily temperature observations to check for evidence of dewatering during the sampling period.

We calculated various temperature metrics to characterize thermal conditions at each sampling location during summer. Prior to calculating temperature metrics, we limited the data to include the summer period only (15 Jul – 15 Sep) to ensure that temperature conditions were comparable across sites. Twenty-two logger sites were dropped from the analysis because they were not deployed for the full summer period. This resulted in a total of 24 sites with continuous temperature data through the summer period including 3 sites in the Catherine Creek basin and 21 sites in the Upper Grande Ronde basin.

Temperature metrics included average daily temperature for the summer period (Avg), the highest instantaneous temperature recorded (Max), the lowest instantaneous temperature recorded (Min), the maximum weekly average temperature (MWAT), the maximum weekly maximum temperature (MWMT), and the greatest consecutive number of days that the daily maximum temperature exceeded the thresholds 16, 18, 20 and 24°C. MWAT was calculated as the maximum 7-day moving average of the daily average temperatures, while MWMT was defined as the maximum 7-day moving average of the daily maximum temperatures. MWMT was adopted as the statistical measure of the stream temperature standard used by Oregon Department of Environmental Quality (ODEQ) in their total maximum daily load (TMDL) evaluations (ODEQ 2000).

Results

There were very few Catherine Creek basin sites available for analysis due to eliminating those that did not record the whole summer period. This being the case, we have included the Catherine Creek basin sites in the summary tables, but have focused our analyses on the Grande Ronde basin sites. Average summer stream temperatures (mean from 15 Jul – 15 Sep) in the upper Grande Ronde basin ranged from 10.5 to 18.4 °C (mean = 14.6 °C) with the lower Meadow Creek site (DSGN4-000213) above Starkey Creek having the highest average water temperature (Table 2; Figure 1). Maximum weekly maximum temperatures (MWMT) ranged from 14.8 °C in Limber Jim Creek to 25.9 °C Meadow Creek Mouth (mean = 21.0 °C) (Figure 2).

The consecutive number of days that maximum temperatures exceeded temperature thresholds (16, 18, 20, and 24°C) was more variable than the other temperature metrics evaluated, but the general patterns

across sites were similar. For example, the number of days that maximum temperatures exceeded 24 °C in the Grande Ronde basin ranged from 0 to 12 (mean = 1.8), with the highest cumulative days exceeding 24 °C occurring in lower Meadow Creek at Meadow Creek Mouth.

Stream temperatures peaked either the first or last week of August for most sites (Figures 3-6). Some sites showed matching peak values in both the beginning and end of August. In the Grande Ronde basin, only five sites including Clear Creek, Sheep Creek, upper Limber Jim Creek, and the upper most reaches of the mainstem Grande Ronde River met the water temperature standard of 17.8 °C MWMT as defined by the Oregon Department of Environmental Quality (ODEQ 2000) (Table 2). This temperature standard represents the level above which significant impacts to salmonid spawning, egg incubation, and fry emergence are expected to occur. The three sites which met our requirements in the Catherine Creek basin all had temperatures below the ODEQ standard.

References

- Boyd, M., and B. Kasper. 2003. Analytical methods for dynamic open channel heat and mass transfer: Methodology for the Heat Source Model Version 7.0. <http://www.deq.state.or.us/wq/TMDLs/tools.htm>.
- Bouwes, N., J. Moberg, N. Weber, B. Bouwes, C. Beasley, S. Bennett, A.C. Hill, C.E. Jordan, R. Miller, P. Nelle, M. Polino, S. Rentmeester, B. Semmens, C. Volk, M.B. Ward, G. Wathen, and J. White. 2011. Scientific protocol for salmonid habitat surveys within the Columbia Habitat Monitoring Program. Prepared by the Integrated Status and Effectiveness Monitoring Program and published by Terraqua, Inc., Wauconda, WA.
- Dunham, J., G. Chandler, B. Rieman, and D. Martin. 2005. Measuring stream temperature with digital data loggers: a user's guide. General Technical Report. Fort Collins, CO: USDA Forest Service, Rocky Mountain Research Station, March.
- Ice, G., L. Dent, J. Walsh, R. Hafele, D. Wilkinson, L. Brodziak, L. Caton, T. Hunt, E. Hammond, and P. Measeles. 1999. Oregon plan for salmon and watersheds water quality monitoring guidebook. Version 2. United States Environmental Protection Agency (EPA), United States Bureau of Land Management (BLM), Oregon Department of Agriculture (ODA), Oregon Department of Environmental Quality (DEQ), Oregon Department of Forestry (ODF), National Council of the Paper Industry for Air and Stream Improvement (NCASI), Boise Cascade Corporation, and the Mid-Coast Watershed Council.
- Oregon Department of Environmental Quality. 2000. Upper Grande Ronde River sub-basin total maximum daily load (TMDL). Portland, OR: Oregon Department of Environmental Quality, Water Quality Division, April. <http://waterquality.deq.state.or.us/wq/>.

Table 1. Temperature logger sites in Catherine Creek and the Grande Ronde River Basins deployed during the summer of 2011.

Stream	Site	UTM_Easting	UTM_Northing	Start Date	Stop Date	Days
<i>Catherine Creek Basin</i>						
Catherine Creek	CBW05583-456106	445092	4996871	8/12/2011	9/20/2011	40
Catherine Creek	CC_Hwy_203	438423	5000409	7/9/2010	9/26/2011	369
Catherine Creek	CBW05583-527786	445937	4996427	8/8/2011	10/2/2011	55
MF Catherine Creek	MF_CC_mouth	451476	5000042	9/23/2010	9/26/2011	368
NF Catherine Creek	MF_CC_above_MF_CC	451504	5000096	9/22/2010	9/26/2011	368
NF Catherine Creek	NF_CC_mouth	449231	4996591	6/24/2010	9/26/2011	369
NF Catherine Creek	DSGN4-000001	449528	4996779	8/11/2011	10/2/2011	52
NF Catherine Creek	DSGN4-000168	451613	5000228	8/1/2011	10/2/2011	62
SF Catherine Creek	DSGN4-000161	455566	4994727	8/3/2011	10/2/2011	60
SF Catherine Creek	SF_CC_mouth	499252	4996530	6/24/2010	9/26/2011	408
<i>Grande Ronde River Basin</i>						
Burnt Corral Creek	CBW05583-382778	382829	5006892	7/25/2011	10/4/2011	71
Clear Creek	Clear_Cr_mouth	396784	4990798	6/29/2010	9/21/2011	365
Five Points Creek	Five_Points_Cr_mouth	404206	5022230	6/22/2010	9/22/2011	365
Fly Creek	Fly_Cr_mouth	390383	5007241	7/11/2011	9/21/2011	72
Fly Creek	DSGN4-000094	385829	4997845	6/28/2011	10/4/2011	98
Grande Ronde River	CBW05583-148970	396606	4991057	8/4/2011	9/21/2011	49
Grande Ronde River	CBW05583-206314	395754	4992143	7/15/2011	9/21/2011	69
Grande Ronde River	CBW05583-235322	391697	5001173	7/13/2011	9/21/2011	71
Grande Ronde River	CBW05583-269114	391164	5011937	8/5/2011	9/22/2011	49
Grande Ronde River	CBW05583-280042	397713	4990084	7/29/2011	9/21/2011	55
Grande Ronde River	CBW05583-321338	392694	4999615	7/13/2011	9/21/2011	71
Grande Ronde River	CBW05583-457530	390356	5009478	7/16/2011	9/21/2011	68
Grande Ronde River	DSGN4-000009	397788	4989992	7/15/2011	9/21/2011	69
Grande Ronde River	DSGN4-000202	390905	5010920	7/12/2011	9/21/2011	71
Grande Ronde River	DSGN4-000245	392853	5013613	7/11/2011	9/22/2011	73
Grande Ronde River	DSGN4-000277	392550	4998754	7/14/2011	9/21/2011	70

Stream	Site	UTM_Easting	UTM_Northing	Start Date	Stop Date	Days
Grande Ronde River	GR_above_Five_Points_Cr	404233	5022168	6/22/2010	7/13/2011	287
Grande Ronde River	GR_below_Vey	393018	4998017	6/28/2010	9/21/2011	407
Grande Ronde River	DSGN4-000205	399954	5018485	7/26/2011	10/4/2011	70
Limber Jim Creek	CBW05583-108010	395296	4995300	7/15/2011	9/21/2011	69
Meadow Creek	Meadow_Cr_mouth	391913	5013246	6/23/2010	9/22/2011	365
Meadow Creek	CBW05583-252730	389685	5012421	7/18/2011	10/4/2011	78
Meadow Creek	DSGN4-000093	374714	5015553	6/29/2011	10/3/2011	96
Meadow Creek	DSGN4-000213	390632	5013167	7/14/2011	10/4/2011	82
Peet Creek	CBW05583-013882	373300	5013214	8/4/2011	10/3/2011	60
Sheep Creek	CBW05583-138554	385429	4990674	6/30/2011	9/21/2011	84
Sheep Creek	CBW05583-228666	384614	4988282	6/30/2011	9/21/2011	84
Sheep Creek	CBW05583-490810	384890	4989128	7/14/2011	9/21/2011	70
Sheep Creek	Sheep_Cr_below_5160_Rd	385376	4990520	6/28/2010	9/21/2011	362
West Chicken Creek	DSGN4-000006	389619	4990392	6/21/2011	10/4/2011	105

Table 2. Summary of stream temperatures (°C) at 24 sites in Catherine Creek and the Grande Ronde River during the summer of 2011 (15 Jul – 15 Sep). Temperature metrics include average daily temperature for the summer period (Avg), the lowest instantaneous temperature recorded during summer (Min), the highest instantaneous temperature recorded during summer (Max), the maximum weekly average temperature (MWAT), the maximum weekly maximum temperature (MWMT), and the greatest consecutive number of days that the daily maximum temperature exceeded thresholds of 16, 18, 20 and 24°C. Values of MWMT exceeding the ODEQ temperature standard of 17.8 °C are highlighted in red.

Stream	Site	Avg	Min	Max	MWAT	MWMT	Consecutive Days Daily Max Exceeded			
							16 °C	18 °C	20 °C	24 °C
Catherine Creek Basin										
MF Catherine Creek	MF_CC_mouth	9.6	5.7	12.5	11.3	12.1	0	0	0	0
NF Catherine Creek	MF_CC_above_MF_CC	9.8	4.9	14.3	11.8	13.9	0	0	0	0
SF Catherine Creek	SF_CC_mouth	11.5	6.5	16.2	13.6	15.5	1	0	0	0
Average		10.3	5.7	14.3	12.2	13.8	0.3	0	0	0
Minimum		9.6	4.9	12.5	11.3	12.1	0	0	0	0
Maximum		11.5	6.5	16.2	13.6	15.5	1	0	0	0
Grande Ronde River Basin										
Clear Creek	Clear_Cr_mouth	10.8	5.5	15.5	12.5	14.9	0	0	0	0
Five Points Creek	Five_Points_Cr_mouth	15.6	10.6	21.7	17.4	21.2	50	26	6	0
Fly Creek	Fly_Cr_mouth	15.6	10.0	22.6	17.6	22.0	33	26	18	0
Fly Creek	DSGN4-000094	17.1	7.9	26.4	19.5	25.3	78	68	43	7
Grande Ronde River	CBW05583-206314	11.6	5.7	17.6	13.6	17.1	9	0	0	0
Grande Ronde River	CBW05583-235322	15.5	7.9	22.2	18.0	21.4	45	26	12	0
Grande Ronde River	CBW05583-321338	15.3	7.1	23.1	17.9	22.4	49	26	16	0
Grande Ronde River	DSGN4-000009	10.6	5.7	16.2	12.4	15.3	1	0	0	0
Grande Ronde River	DSGN4-000202	16.7	8.5	25.6	19.1	24.5	61	58	23	3
Grande Ronde River	DSGN4-000245	17.4	8.7	26.1	19.7	25.0	65	58	26	5
Grande Ronde River	DSGN4-000277	15.5	7.2	23.3	18.1	22.5	49	43	17	0
Grande Ronde River	GR_below_Vey	15.3	6.7	23.8	18.0	22.8	49	26	17	0
Limber Jim Creek	CBW05583-108010	10.5	5.0	15.4	12.3	14.8	0	0	0	0
Meadow Creek	Meadow_Cr_mouth	18.1	9.7	26.6	20.5	25.9	65	65	26	12
Meadow Creek	DSGN4-000093	16.3	7.6	24.8	18.6	24.1	77	30	26	5
Meadow Creek	ODFW: DSGN4-000213	18.4	11.8	24.8	20.4	24.3	62	62	44	5

Sheep Creek	CBW05583-138554	13.9	6.1	21.9	15.9	21.1	49	19	6	0
		Consecutive Days Daily Max Exceeded								
Stream	Site	Avg	Min	Max	MWAT	MWMT	16 °C	18 °C	20 °C	24 °C
Sheep Creek	CBW05583-228666	11.5	5.3	17.3	13.2	16.7	5	0	0	0
Sheep Creek	CBW05583-490810	12.5	5.8	19.5	14.3	18.7	19	5	0	0
Sheep Creek	Sheep_Cr_below_5160_Rd	13.7	5.9	22.0	15.7	21.1	49	19	6	0
West Chicken Creek	DSGN4-000006	13.7	6.4	21.4	15.7	20.3	27	22	4	0
Average		14.6	7.4	21.8	16.7	21.0	40.1	27.6	13.8	1.8
Minimum		10.5	5.0	15.4	12.3	14.8	0	0	0	0
Maximum		18.4	11.8	26.6	20.5	25.9	78	68	44	12

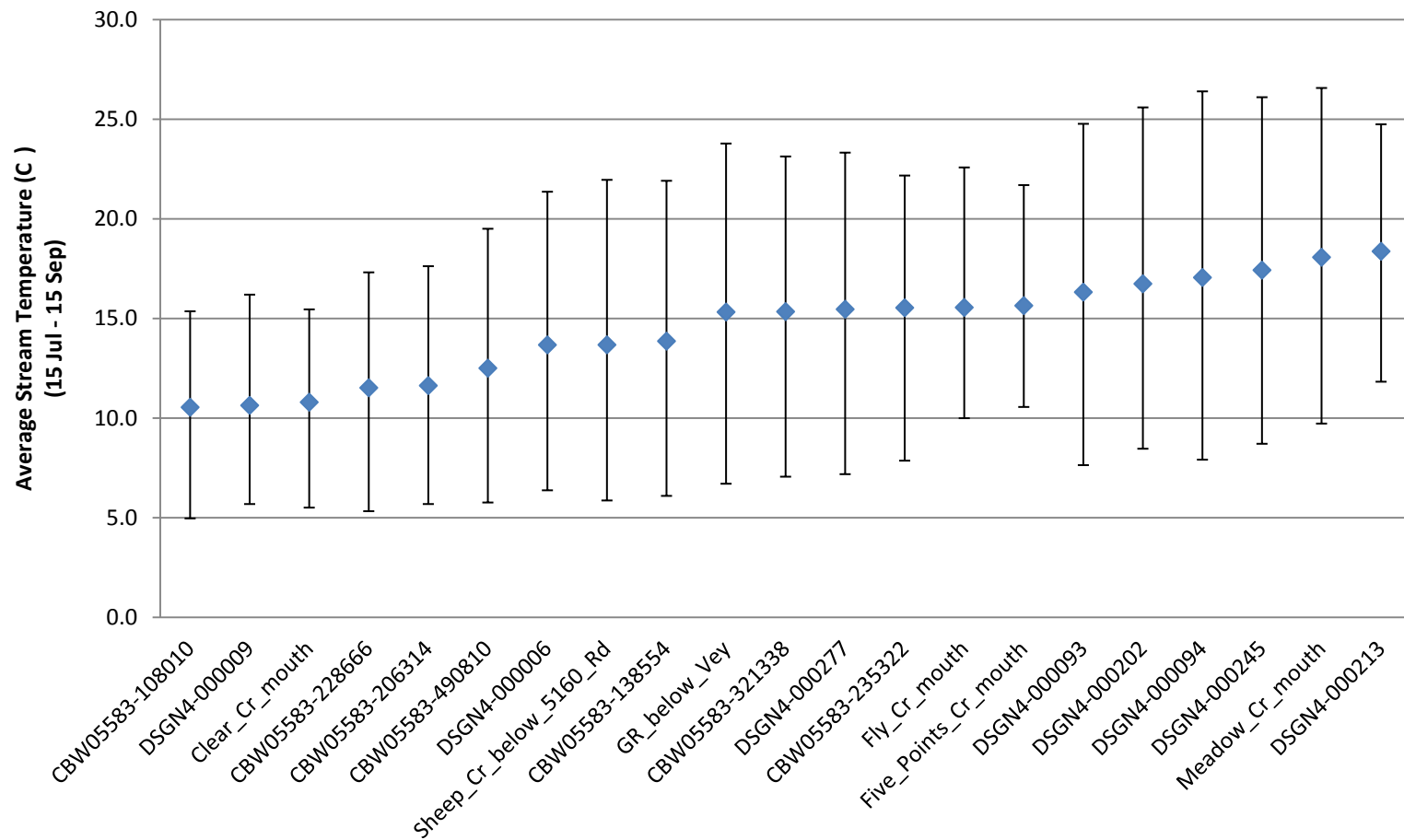


Figure 1. Average daily stream temperature (°C) at 21 sites in the Grande Ronde River basin during summer (15 Jul – 15 Sep) 2011. Error bars represent the highest (Max) and lowest (Min) instantaneous temperatures recorded during summer.

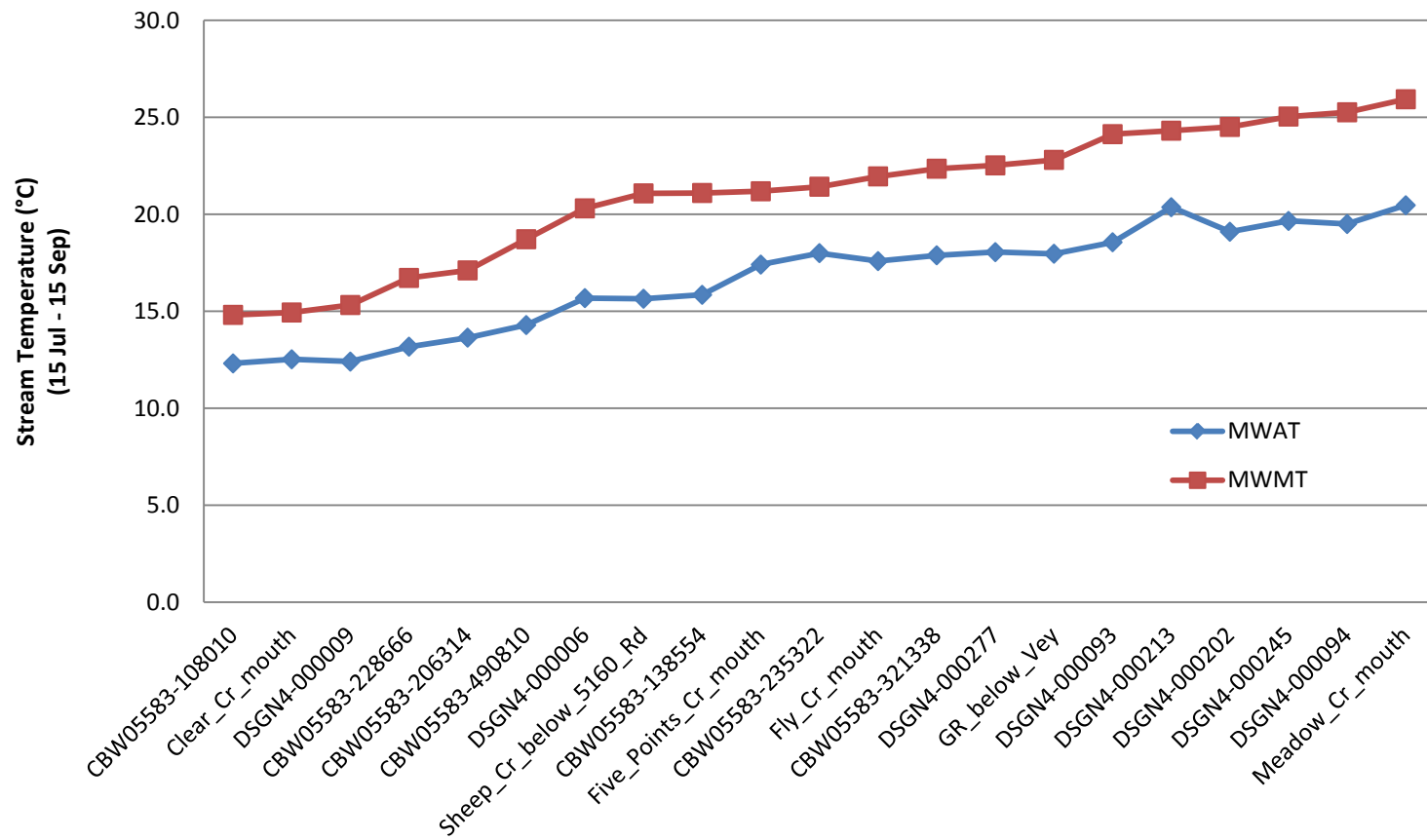


Figure 2. Maximum weekly average temperature (MWAT; °C) and maximum weekly maximum temperature (MWMt) at 21 sites in the Grande Ronde River basin during summer (15 Jul – 15 Sep) 2011. Data were sorted by MWMt in ascending order.

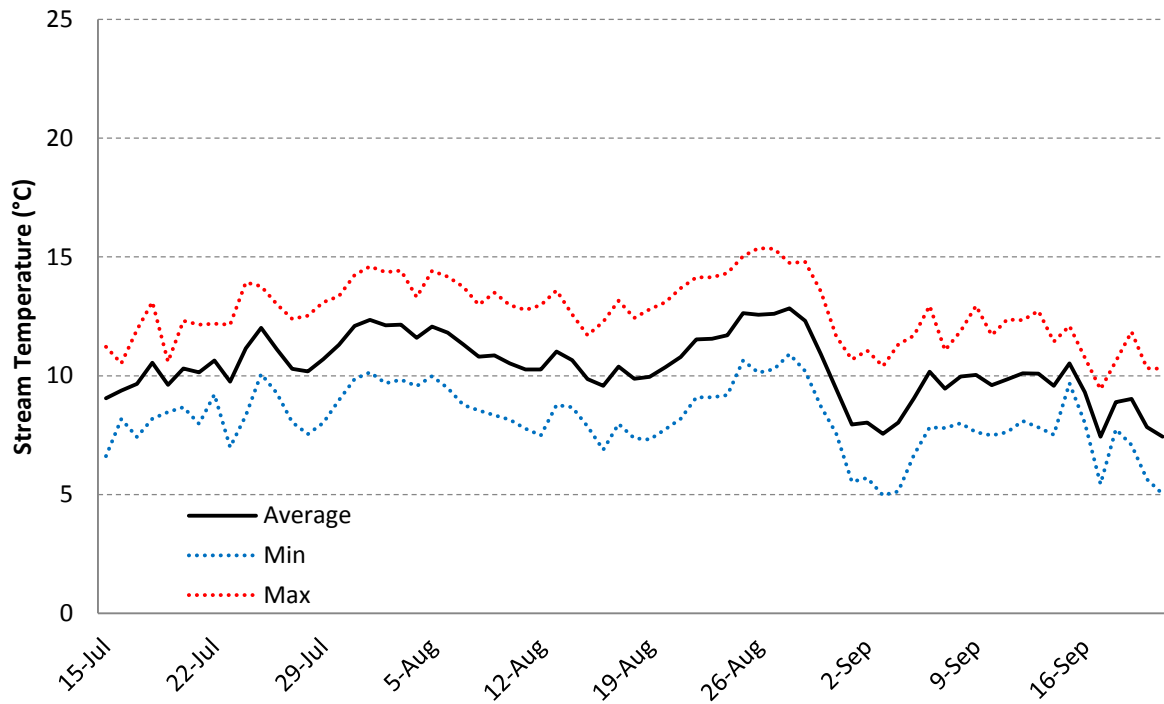


Figure 3. Daily average, minimum, and maximum stream temperatures (°C) in Limber Jim Creek from 15 Jul – 21 Sep 2011.

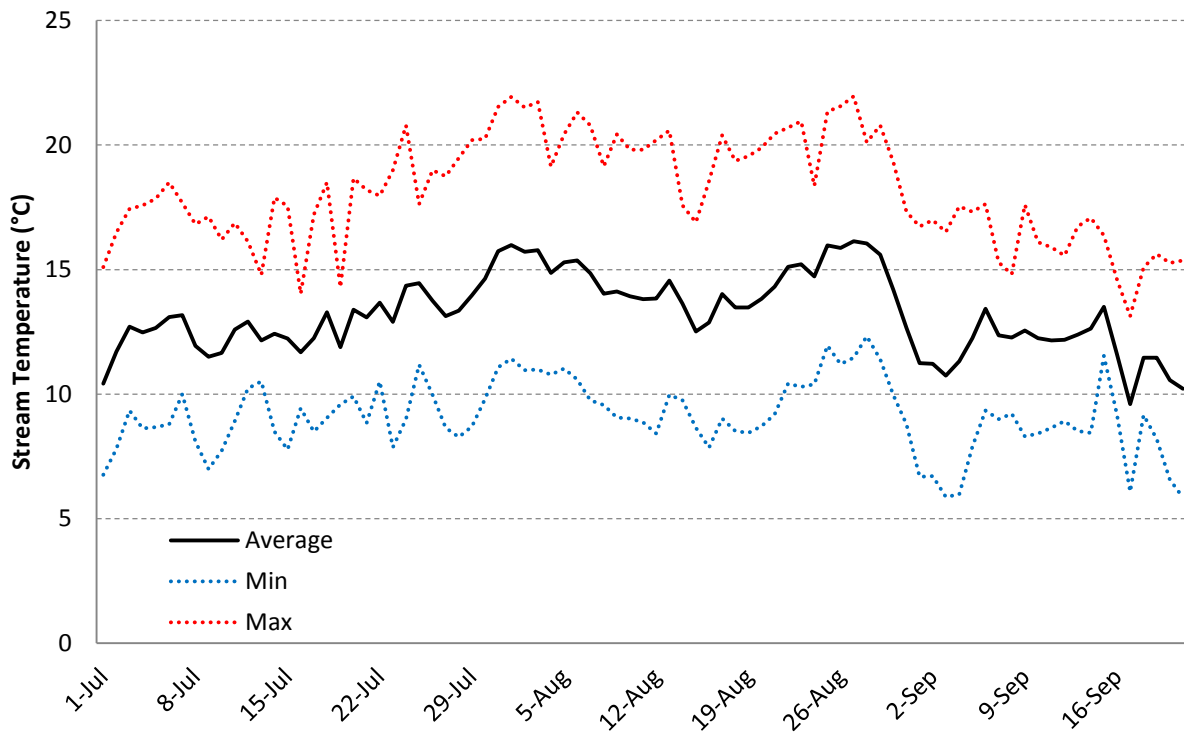


Figure 4. Daily average, minimum, and maximum stream temperatures (°C) in Sheep Creek below 5160 road from 1 Jul – 21 Sep, 2011.

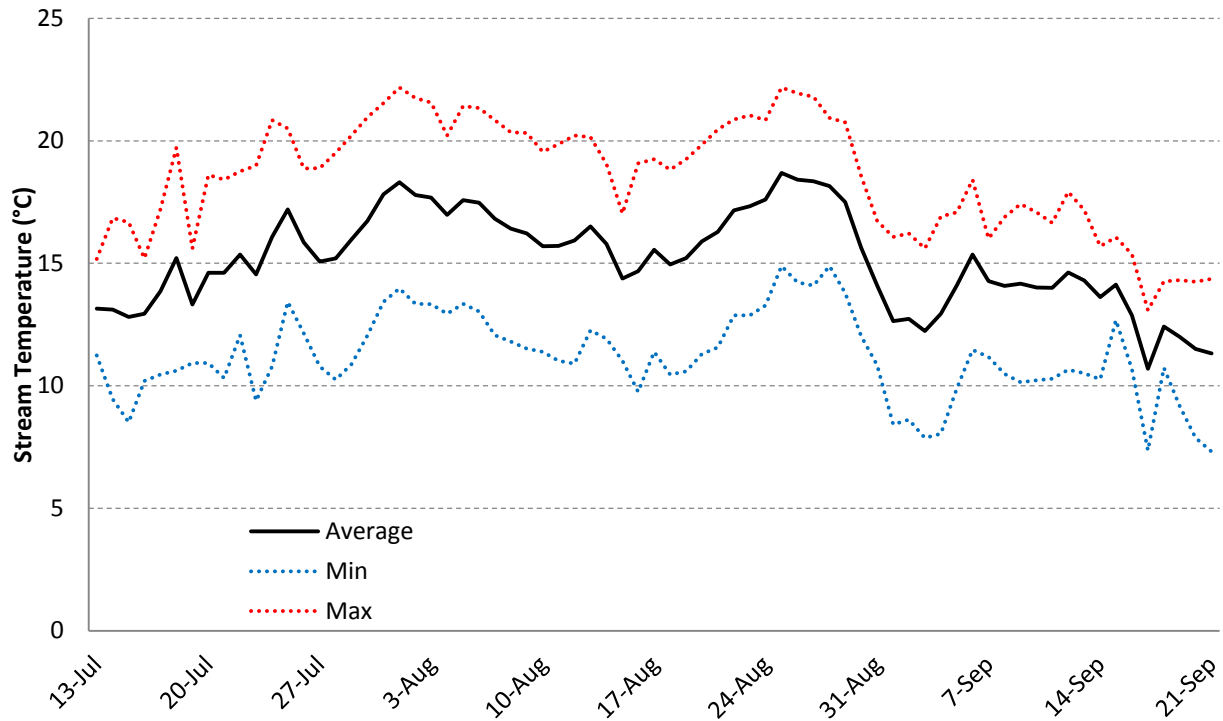


Figure 5. Daily average, minimum, and maximum stream temperatures (°C) in the upper Grande Ronde River (CBW05583-235322) from 13 Jul – 21 Sep, 2011.

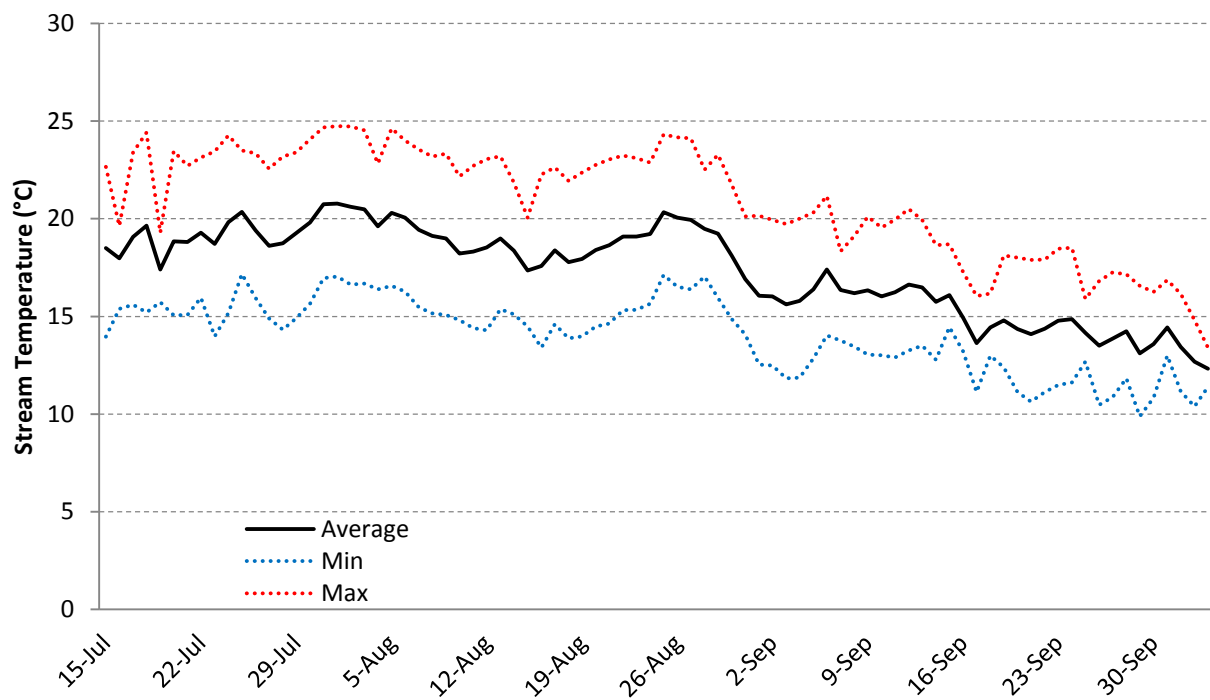


Figure 6. Daily average, minimum, and maximum stream temperatures (°C) in Meadow Creek below McCoy Creek (DSGN4-000213) from 15 Jul – 4 Oct, 2011.

Appendix L.

Joint Probabilities for Air Temperature and Streamflows

Joint Probabilities for Air Temperature and Streamflows

Percentages of mean temperatures occurring within bins of mean daily flows for the period June-October for the period of record having streamflow at USGS gage (13319000), using USGS data and NOAA air temperature data.

USGS streamflow data is available for gauge 13319000 for the period of record October 1, 1903 to September 30, 1989. These data are available from:

http://apps.wrd.state.or.us/apps/sw/hydro_report/default.aspx

and also:

http://waterdata.usgs.gov/nwis/dv?cb_00060=on&format=rdb&begin_date=1903-10-01&end_date=2011-04-12&site_no=13319000&referred_module=sw

NOAA air temperature data was available from:

<http://www7.ncdc.noaa.gov/CDO/cdo>

UNION EXP STN CoopID 358746

LA GRANDE CoopID 354622

The record for Union Exp Stn was more complete than that for La Grande at the airport. Air temperature data (maximum, mean, minimum daily) for the period October 1, 1911 to September 30, 1989 was matched with all corresponding dates having streamflow data for USGS gauge site 13319000. Using an Excel spreadsheet pivot table function, the percentage of all pairs of mean daily streamflow/mean daily air temperature data for the entire period of record were computed for June-September for this series of years as well as for all August daily values in this series of years. This computation provides an index to the long-term probability that when streamflows are at a specified low value (a specific streamflow bin), air temperature means will be within a corresponding bin.

The temperature bins were calculated so that the mean daily air temperature was divided by 2 and then rounded down to the next lower integer. By this process, a mean daily air temperature of 6.5°C would fall into bin 3. Bin 3 represents a temperature range of 6-8°C.

The streamflow bins were calculated by dividing the mean daily flow by 10 and then rounding down to the next lower integer. By this process a streamflow of 45 cfs would fall into bin 4. Bin 4 represents streamflows of 40-50 cfs.

The probability analysis shows that during the June-September period, for a 78-year period of record, one can expect streamflows as low as 0-10 cfs in the upper Grande Ronde (near USGS gauge 13319000), which is just upstream of the city of La Grande, Oregon, when air temperatures are in the range 22-26°C for 0.125% of the time. When streamflow is 10-20 cfs, mean daily air temperatures in the ranges 10-14, 14-18, 18-22, 22-26, and 26-30°C.

Table xx. Probability of Co-occurrence of combinations of air temperature (mean °C) and mean daily streamflow (cfs) for August based on the October 1, 1911 to September 30, 1989 period of record for both Union Exp Stn, Oregon (CoopID 358746) and USGS station 13319000.

			CFS																					
			0	10	20	30	40	50	60	70	80	90	100	110	120	130	140	170	180	320				
	T(° C)	T(° C)	10	20	30	40	50	60	70	80	90	100	110	120	130	140	150	180	190	330				
Bin			0	1	2	3	4	5	6	7	8	9	10	11	12	13	14	17	18	32	Grand Total			
3	6	8	0.00	0.00	0.00	0.00	0.04	0.00	0.00	0.04	0.00	0.00	0.00	0.00	0.00	0.00	0.00	0.00	0.00	0.00	2	0.09%		
4	8	10	0.00	0.04	0.09	0.09	0.09	0.00	0.04	0.00	0.00	0.00	0.00	0.00	0.00	0.00	0.00	0.00	0.00	0.00	8	0.35%		
5	10	12	0.04	0.35	0.57	0.39	0.35	0.26	0.22	0.09	0.04	0.13	0.04	0.00	0.00	0.04	0.00	0.00	0.00	0.00	58	2.54%		
6	12	14	0.04	0.96	1.57	1.18	0.66	1.05	0.35	0.09	0.13	0.13	0.22	0.09	0.09	0.04	0.00	0.00	0.00	0.00	151	6.60%		
7	14	16	0.44	1.62	3.19	2.01	1.22	0.70	0.61	0.35	0.22	0.17	0.13	0.00	0.04	0.00	0.00	0.00	0.00	0.04	246	10.76%		
8	16	18	1.18	4.81	5.42	2.93	1.49	1.57	1.01	0.79	0.26	0.22	0.31	0.09	0.04	0.00	0.04	0.00	0.04	0.00	462	20.20%		
9	18	20	1.40	4.24	6.86	3.28	1.49	1.18	1.09	0.57	0.31	0.26	0.00	0.00	0.00	0.00	0.00	0.00	0.00	0.00	473	20.68%		
10	20	22	1.44	4.63	8.09	3.41	2.01	1.92	0.70	0.44	0.22	0.00	0.04	0.00	0.09	0.04	0.00	0.04	0.00	0.00	528	23.09%		
11	22	24	0.39	2.84	4.02	2.19	0.74	0.48	0.26	0.09	0.09	0.09	0.00	0.04	0.09	0.00	0.00	0.00	0.00	0.00	259	11.32%		
12	24	26	0.13	0.70	0.92	0.44	0.44	0.39	0.09	0.17	0.04	0.00	0.00	0.00	0.00	0.00	0.00	0.00	0.00	0.00	76	3.32%		
13	26	28	0.00	0.44	0.22	0.04	0.09	0.04	0.00	0.04	0.04	0.00	0.00	0.00	0.04	0.00	0.00	0.00	0.00	0.00	22	0.96%		
14	28	30	0.00	0.00	0.04	0.00	0.00	0.00	0.00	0.00	0.00	0.00	0.00	0.00	0.00	0.00	0.00	0.00	0.00	0.00	1	0.04%		
15	30	32	0.00	0.04	0.00	0.00	0.00	0.00	0.00	0.00	0.00	0.00	0.00	0.00	0.00	0.00	0.00	0.00	0.00	0.00	1	0.04%		
			116	473	709	365	197	174	100	61	31	23	17	5	9	3	1	1	1	1	2287			
			5.07%	20.68%	31.00%	15.96%	8.61%	7.61%	4.37%	2.67%	1.36%	1.01%	0.74%	0.22%	0.39%	0.13%	0.04%	0.04%	0.04%	0.04%				

(see file: Grande Ronde flow-Union air temperature-probabilities.xlsx)

Appendix M.

Streamflow Statistics Summaries

Streamflow Statistics Summaries

USGS Station 13318500. Grande Ronde River Near Hilgard, Oregon. Streamflow statistics tabulated in USGS StreamStats.

<http://ssdev.cr.usgs.gov/gagepages/html/13318500.htm>

summarized in file: Station correlations in Upper Grande Ronde.xlsx

StreamStats Data-Collection Station Report	
USGS Station Number	13318500
Station Name	GRANDE RONDE RIVER NEAR HILGARD, OREG.
Click here to link to available data on NWIS-Web for this site.	
Descriptive Information	
Station Type	Gaging Station, continuous record
Regulated?	Undefined
Period of Record	
Remarks	
Latitude (degrees NAD83)	45.31652
Longitude (degrees NAD83)	-118.2677
Hydrologic unit code	17060104
Local Basin	-
County	061-Union

Physical Characteristics			
Characteristic Name	Value	Units	Citation Number
Contributing_Drainage_Area	505	square miles	31
Drainage_Area	505	square miles	31
Main_Channel_Length	35.2	miles	31
Mean_Basin_Elevation	4800	feet	31
Percent_Forest	86	percent	31
Percent_Lakes_and_Ponds	0.02	percent	31
Percent_Storage	0.02	percent	31
Soil_Infiltration	5.9	inches	31
Stream_Slope_10_and_85_Method	70.07	feet per mi	31

Streamflow Statistics			
Statistic Name	Value	Units	Citation Number
Peak-Flow Statistics			
10_Year_Peak_Flood	3590	cubic feet per second	31
100_Year_Peak_Flood	5510	cubic feet per second	31
2_Year_Peak_Flood	2190	cubic feet per second	31
200_Year_Peak_Flood	6130	cubic feet per second	31
25_Year_Peak_Flood	4340	cubic feet per second	31
5_Year_Peak_Flood	3010	cubic feet per second	31
50_Year_Peak_Flood	4920	cubic feet per second	31
500_Year_Peak_Flood	6990	cubic feet per second	31
Log_Mean_of_Annual_Peaks	3.346	Log base 10	31
Log_Skew_of_Annual_Peaks	0.482	Log base 10	31
Log_STD_of_Annual_Peaks	0.161	Log base 10	31
Mean_Annual_Flood	1620	cubic feet per second	31
Systematic_peak_years	19	years	31
WRC_Mean	3.346	Log base 10	31
WRC_Skew	0.187	Log base 10	31
WRC_STD	0.161	Log base 10	31

Flood-Volume Statistics			
7_Day_10_Year_Maximum	2188	cubic feet per second	31
7_Day_2_Year_Maximum	1315	cubic feet per second	31
Low-Flow Statistics			
7_Day_10_Year_Low_Flow	8.586	cubic feet per second	31
7_Day_2_Year_Low_Flow	15.31	cubic feet per second	31
7_Day_20_Year_Low_Flow	7.236	cubic feet per second	31
Flow-Duration Statistics			
1_Percent_Duration	1790	cubic feet per second	41
10_Percent_Duration	784.2	cubic feet per second	41
20_Percent_Duration	490.7	cubic feet per second	41
25_Percent_Duration	360	cubic feet per second	41
30_Percent_Duration	270.6	cubic feet per second	41
40_Percent_Duration	160	cubic feet per second	41
5_Percent_Duration	1098	cubic feet per second	41
50_Percent_Duration	82	cubic feet per second	41
60_Percent_Duration	50	cubic feet per second	41
70_Percent_Duration	37	cubic feet per second	41
75_Percent_Duration	31	cubic feet per second	41
80_Percent_Duration	27	cubic feet per second	41
90_Percent_Duration	20	cubic feet per second	41
95_Percent_Duration	16	cubic feet per second	41
99_Percent_Duration	10	cubic feet per second	41

Annual Flow Statistics			
Mean_Annual_Flow	271.6	cubic feet per second	31
Stand_Dev_of_Mean_Annual_Flow	100	cubic feet per second	31
Monthly Flow Statistics			
April_Mean_Flow	877.6	cubic feet per second	31
April_STD	321.7	cubic feet per second	31
August_Mean_Flow	28.01	cubic feet per second	31
August_STD	14.07	cubic feet per second	31
December_Mean_Flow	145.4	cubic feet per second	31
December_STD	139.1	cubic feet per second	31
February_Mean_Flow	200.2	cubic feet per second	31
February_STD	134.2	cubic feet per second	31
January_Mean_Flow	118.2	cubic feet per second	31
January_STD	89.23	cubic feet per second	31
July_Mean_Flow	98.01	cubic feet per second	31
July_STD	64.58	cubic feet per second	31
June_Mean_Flow	419.9	cubic feet per second	31
June_STD	281.7	cubic feet per second	31
March_Mean_Flow	455	cubic feet per second	31
March_STD	200	cubic feet per second	31

May_Mean_Flow	788.2	cubic feet per second	31
May_STD	422.6	cubic feet per second	31
November_Mean_Flow	72.9	cubic feet per second	31
November_STD	71.05	cubic feet per second	31
October_Mean_Flow	35.17	cubic feet per second	31
October_STD	23.82	cubic feet per second	31
September_Mean_Flow	24.89	cubic feet per second	31
September_STD	12.23	cubic feet per second	31
General Flow Statistics			
Average_daily_streamflow	271.949	cubic feet per second	41
Maximum_daily_flow	3700	cubic feet per second	41
Minimum_daily_flow	6	cubic feet per second	41
Std_Dev_of_daily_flows	393.309	cubic feet per second	41

Base Flow Statistics			
Average_BFI_value	0.638	dimensionless	42
Number_of_years_to_compute_BFI	19	years	42
Std_dev_of_annual_BFI_values	0.057	dimensionless	42
Precipitation Statistics			
24_Hour_2_Year_Precipitation	1.6	inches	31
Mean_Annual_Precipitation	24	inches	31
Temperature Statistics			
Mean_Min_January_Temperature	17	degrees F	31

Citations	
Citation Number	Citation Name and URL
31	Imported from Basin Characteristics file
41	Wolock, D.M., 2003, Flow characteristics at U.S. Geological Survey streamgages in the conterminous United States: U.S. Geological Survey Open-File Report 03-146, digital data set
42	Wolock, D.M., 2003, Base-flow index grid for the conterminous United States: U.S. Geological Survey Open-File Report 03-263, digital data set

USGS Station 13318800. Grande Ronde River at Hilgard, Oregon. Streamflow statistics tabulated in USGS StreamStats.

http://ssdev.cr.usgs.gov/gagepages/html/13318800.htm	
http://nwis.waterdata.usgs.gov/nwis/inventory/?site_no=13318800	

StreamStats Data-Collection Station Report	
USGS Station Number	13318800
Station Name	GRANDE RONDE RIVER AT HILGARD, OREG.
	Click here to link to available data on NWIS-Web for this site.
Descriptive Information	
Station Type	Gaging Station, continuous record
Regulated?	Undefined
Period of Record	
Remarks	
Latitude (degrees NAD83)	45.33902
Longitude (degrees NAD83)	-118.2441
Hydrologic unit code	17060104
Local Basin	-
County	061-Union

Streamflow Statistics			
Statistic Name	Value	Units	Citation Number
Flow-Duration Statistics			
1_Percent_Duration	1762.2	cubic feet per second	41
10_Percent_Duration	895.4	cubic feet per second	41
20_Percent_Duration	519	cubic feet per second	41
25_Percent_Duration	384	cubic feet per second	41
30_Percent_Duration	312	cubic feet per second	41
40_Percent_Duration	198	cubic feet per second	41
5_Percent_Duration	1190	cubic feet per second	41
50_Percent_Duration	109	cubic feet per second	41
60_Percent_Duration	62	cubic feet per second	41
70_Percent_Duration	43	cubic feet per second	41
75_Percent_Duration	38	cubic feet per second	41
80_Percent_Duration	34	cubic feet per second	41
90_Percent_Duration	25	cubic feet per second	41
95_Percent_Duration	21	cubic feet per second	41
99_Percent_Duration	15	cubic feet per second	41

General Flow Statistics			
Average_daily_streamflow	299.823	cubic feet per second	41
Maximum_daily_flow	3860	cubic feet per second	41
Minimum_daily_flow	9.7	cubic feet per second	41
Std_Dev_of_daily_flows	407.544	cubic feet per second	41
Base Flow Statistics			
Average_BFI_value	0.631	dimensionless	42
Number_of_years_to_compute_BFI	15	years	42
Std_dev_of_annual_BFI_values	0.061	dimensionless	42

Citations	
Citation Number	Citation Name and URL
41	Wolock, D.M., 2003, Flow characteristics at U.S. Geological Survey streamgages in the conterminous United States: U.S. Geological Survey Open-File Report 03-146, digital data set
42	Wolock, D.M., 2003, Base-flow index grid for the conterminous United States: U.S. Geological Survey Open-File Report 03-263, digital data set

USGS Station 13319000. Grande Ronde River at La Grande, Oregon. Streamflow statistics tabulated in USGS StreamStats.

<http://streamstatsags.cr.usgs.gov/gages/viewer14.htm?stabbr=GAGES>
http://waterdata.usgs.gov/nwis/nwisman/?site_no=13319000

StreamStats Data-Collection Station Report	
USGS Station Number	13319000
Station Name	GRANDE RONDE R AT LA GRANDE, OREG.
Descriptive Information	
Station Type	Gaging Station, continuous record
Regulated?	FALSE
Period of Record	1904-09, 11-15, 18-23, 26-89
Remarks	
Latitude (degrees NAD83)	45.34624
Longitude (degrees NAD83)	-118.1249
Hydrologic unit code	17060104
Local Basin	-
County	061-Union

Physical Characteristics			
Characteristic Name	Value	Units	Citation Number
Contributing_Drainage_Area	678	square miles	31
Drainage_Area	687	square miles	39
Main_Channel_Length	44.8	miles	31
Mean_Basin_Elevation	4582	feet	39
Percent_Forest	68.4	percent	39
Percent_Lakes_and_Ponds	0.03	percent	31
Percent_Storage	0.03	percent	31
Relief	5095	feet	38
Soil_Infiltration	5.6	inches	31
Stream_Slope_10_and_85_Method	46	feet per mi	38
N_Facing_Slopes_gt_30pct_from_30m_DEM	6.5	percent	39
Slopes_gt_30pct_from_30m_DEM	21.8	percent	39
Elevation_in_Thousands	4.582052	thousand feet	39
Percent_Forest_add_1_ID_ROI_Parm	69.40648	dimensionless	39
Pct_South_Facing_Slopes_add_1_ID_ROI	22.79817	dimensionless	39
Mean_Basin_Slope_from_30m_DEM	20.3	percent	39

Streamflow Statistics			
Statistic Name	Value	Units	Citation Number
Peak-Flow Statistics			
1_5_Year_Peak_Flood	2670	cubic feet per second	40
10_Year_Peak_Flood	6020	cubic feet per second	39
100_Year_Peak_Flood	10100	cubic feet per second	39
2_33_Year_Peak_Flood	3540	cubic feet per second	40
2_Year_Peak_Flood	3260	cubic feet per second	39
200_Year_Peak_Flood	11400	cubic feet per second	39
25_Year_Peak_Flood	7580	cubic feet per second	39
5_Year_Peak_Flood	4860	cubic feet per second	39
50_Year_Peak_Flood	8810	cubic feet per second	39
500_Year_Peak_Flood	13300	cubic feet per second	39
Log_Mean_of_Annual_Peaks	3.503	Log base 10	31
Log_Skew_of_Annual_Peaks	-0.072	Log base 10	31
Log_STD_of_Annual_Peaks	0.20429	Log base 10	39
Mean_Annual_Flood	2150	cubic feet per second	31
Systematic_peak_years	81	years	39
WRC_Mean	3.508	Log base 10	31
WRC_Skew	0.184	Log base 10	31
WRC_STD	0.208	Log base 10	31
Flood-Volume Statistics			
7_Day_10_Year_Maximum	3516	cubic feet per second	31
7_Day_2_Year_Maximum	2002	cubic feet per second	31
7_Day_50_Year_Maximum	5045	cubic feet per second	31

Flow-Duration Statistics			
1_Percent_Duration	3505.6	cubic feet per second	41
10_Percent_Duration	1170	cubic feet per second	41
20_Percent_Duration	615	cubic feet per second	41
25_Percent_Duration	455	cubic feet per second	41
30_Percent_Duration	338	cubic feet per second	41
40_Percent_Duration	154	cubic feet per second	41
5_Percent_Duration	1912	cubic feet per second	41
50_Percent_Duration	95	cubic feet per second	41
60_Percent_Duration	58	cubic feet per second	41
70_Percent_Duration	41	cubic feet per second	41
75_Percent_Duration	40	cubic feet per second	41
80_Percent_Duration	34	cubic feet per second	41
90_Percent_Duration	25	cubic feet per second	41
95_Percent_Duration	20	cubic feet per second	41
99_Percent_Duration	15	cubic feet per second	41
Annual Flow Statistics			
Mean_Annual_Flow	387	cubic feet per second	38
Stand_Dev_of_Mean_Annual_Flow	144.8	cubic feet per second	31
Monthly Flow Statistics			
April_Mean_Flow	1313	cubic feet per second	31
August_Mean_Flow	27.93	cubic feet per second	31
December_Mean_Flow	168	cubic feet per second	31
December_STD	172.1	cubic feet per second	31
February_Mean_Flow	307.4	cubic feet per second	31
February_STD	293.4	cubic feet per second	31
January_Mean_Flow	185.8	cubic feet per second	31
January_STD	224	cubic feet per second	31
July_Mean_Flow	95.81	cubic feet per second	31
June_Mean_Flow	443.9	cubic feet per second	31
March_Mean_Flow	752.7	cubic feet per second	31
March_STD	530.8	cubic feet per second	31
May_Mean_Flow	1044	cubic feet per second	31
November_Mean_Flow	94.26	cubic feet per second	31
November_STD	113.5	cubic feet per second	31
October_Mean_Flow	42.17	cubic feet per second	31

January Flow-Duration Statistics			
January_20_Percent_Duration	279	cubic feet per second	38
January_50_Percent_Duration	102	cubic feet per second	38
January_80_Percent_Duration	45.9	cubic feet per second	38
February Flow-Duration Statistics			
February_20_Percent_Duration	480	cubic feet per second	38
February_50_Percent_Duration	184	cubic feet per second	38
February_80_Percent_Duration	73.2	cubic feet per second	38
March Flow-Duration Statistics			
March_20_Percent_Duration	1200	cubic feet per second	38
March_50_Percent_Duration	563	cubic feet per second	38
March_80_Percent_Duration	254	cubic feet per second	38
April Flow-Duration Statistics			
April_20_Percent_Duration	1930	cubic feet per second	38
April_50_Percent_Duration	1120	cubic feet per second	38
April_80_Percent_Duration	659	cubic feet per second	38
May Flow-Duration Statistics			
May_20_Percent_Duration	1550	cubic feet per second	38
May_50_Percent_Duration	938	cubic feet per second	38
May_80_Percent_Duration	516	cubic feet per second	38
June Flow-Duration Statistics			
June_20_Percent_Duration	714	cubic feet per second	38
June_50_Percent_Duration	346	cubic feet per second	38
June_80_Percent_Duration	164	cubic feet per second	38
July Flow-Duration Statistics			
July_20_Percent_Duration	140	cubic feet per second	38
July_50_Percent_Duration	69.4	cubic feet per second	38
July_80_Percent_Duration	37.6	cubic feet per second	38
August Flow-Duration Statistics			
August_20_Percent_Duration	47.4	cubic feet per second	38
August_50_Percent_Duration	26.9	cubic feet per second	38
August_80_Percent_Duration	17.4	cubic feet per second	38
September Flow-Duration Statistics			
September_20_Percent_Duration	40.2	cubic feet per second	38
September_50_Percent_Duration	26.2	cubic feet per second	38
September_80_Percent_Duration	18.9	cubic feet per second	38
October Flow-Duration Statistics			
October_20_Percent_Duration	51.8	cubic feet per second	38
October_50_Percent_Duration	36.3	cubic feet per second	38
October_80_Percent_Duration	25.9	cubic feet per second	38
November Flow-Duration Statistics			
November_20_Percent_Duration	110	cubic feet per second	38
November_50_Percent_Duration	51.8	cubic feet per second	38
November_80_Percent_Duration	34.8	cubic feet per second	38

December Flow-Duration Statistics			
December_20_Percent_Duration	234	cubic feet per second	38
December_50_Percent_Duration	74.9	cubic feet per second	38
December_80_Percent_Duration	37.4	cubic feet per second	38
General Flow Statistics			
Average_daily_streamflow	397.26	cubic feet per second	41
Maximum_daily_flow	6300	cubic feet per second	41
Minimum_daily_flow	3	cubic feet per second	41
Std_Dev_of_daily_flows	682.892	cubic feet per second	41
Base Flow Statistics			
Average_BFI_value	0.62	dimensionless	42
Number_of_years_to_compute_BFI	13	years	42
Std_dev_of_annual_BFI_values	0.105	dimensionless	42
Precipitation Statistics			
24_Hour_2_Year_Precipitation	1.7	inches	31
Mean_Annual_Precipitation	27.57	inches	39
Temperature Statistics			
Mean_Min_January_Temperature	19	degrees F	31

Citations	
Citation Number	Citation Name and URL
31	Imported from Basin Characteristics file
38	Hortness, J.E., and Berenbrock, Charles, 2001, Estimating Monthly and Annual Streamflow Statistics at Ungaged Sites in Idaho: U.S. Geological Survey Water-Resources Investigations Report 01-4093, 36 p.
39	Berenbrock, Charles, 2002, Estimating the Magnitude of Peak Flows at Selected Recurrence Intervals for Streams in Idaho: U.S. Geological Survey Water-Resources Investigations Report 02-4170, 59 p.
40	Hortness, J.E., and Berenbrock, Charles, 2003, Estimating the Magnitude of Bankfull Flows for Streams in Idaho: U.S. Geological Survey Water-Resources Investigations Report 03-4261, 36 p.
41	Wolock, D.M., 2003, Flow characteristics at U.S. Geological Survey streamgages in the conterminous United States: U.S. Geological Survey Open-File Report 03-146, digital data set
42	Wolock, D.M., 2003, Base-flow index grid for the conterminous United States: U.S. Geological Survey Open-File Report 03-263, digital data set

Use of pivot table to calculate streamflow statistics on USGS Gauging Station Data for 13319000, Grande Ronde at La Grande, Oregon based on Streamflow Data from CIG (bias adjusted VIC stream flow data, historical). Mean monthly and mean annual flows are given. See file: Station correlations in Upper Grande Ronde.xlsx

These data are from Climate Impacts Group-bias adjusted													
http://www.hydro.washington.edu/2860/products/sites/r7climate/subbasin_summaries/4012/nat_bias_adjusted_vic_streamflow_daily_historical.dat													
Average of Historical	Column Labels												
Row Labels	1	2	3	4	5	6	7	8	9	10	11	12 (blar	Grand Total
1916	31.7	292.9	1961.0	1915.1	1401.0	657.0	163.0	47.8	29.1	25.0	43.1	49.9	551.6
1917	38.1	51.0	127.1	1331.0	1440.0	266.1	54.0	19.1	35.9	26.1	37.9	46.1	289.9
1918	639.9	464.0	1416.0	1076.3	761.1	236.0	61.7	28.2	25.0	23.9	29.9	621.0	449.6
1919	200.2	319.2	748.9	853.1	753.9	152.0	39.3	11.4	24.9	64.0	51.2	85.2	275.0
1920	98.8	283.8	602.8	1794.1	1609.0	554.1	136.0	53.2	52.1	29.0	109.9	63.1	447.8
1921	434.0	399.2	1144.0	1640.9	1458.1	424.8	112.0	30.2	24.0	73.7	75.2	79.9	491.5
1922	57.3	72.9	378.0	1242.1	826.1	208.0	36.7	23.0	16.2	29.8	32.1	542.0	289.5
1923	439.0	74.1	407.0	960.0	643.0	532.8	96.0	29.2	23.0	25.0	32.9	60.1	277.3
1924	123.1	836.9	536.1	814.1	528.7	157.0	39.1	29.1	30.0	139.9	62.9	228.9	291.2
1925	144.1	644.1	561.0	1415.0	1026.9	335.1	66.1	26.1	26.0	27.0	109.8	64.1	367.1
1926	33.0	615.0	608.0	895.1	812.9	179.0	41.9	34.2	39.9	20.0	30.1	71.8	278.9
1927	207.0	701.0	783.2	1926.1	1283.1	699.2	128.0	32.2	60.9	39.1	372.9	294.2	540.2
1928	204.2	311.9	1080.0	1525.0	733.8	255.1	69.9	22.3	26.9	164.1	325.1	151.8	405.0
1929	30.2	34.0	944.2	695.0	457.9	344.9	44.0	21.1	15.9	31.2	44.7	37.0	226.0
1930	39.3	451.0	515.0	740.1	890.1	493.0	60.0	22.1	21.1	24.1	24.2	208.0	289.0
1931	69.9	78.2	494.0	1525.0	496.3	194.1	36.9	10.3	26.9	58.0	48.0	42.1	256.0
1932	38.1	63.0	682.0	1491.0	1029.0	243.9	54.8	19.1	10.1	29.9	37.1	35.1	311.0
1933	72.9	74.9	527.0	913.9	1127.0	211.0	64.0	25.2	31.1	33.0	89.8	44.2	268.9
1934	556.0	235.1	572.1	752.9	478.9	304.1	56.0	19.3	21.9	33.1	56.1	294.0	282.0
1935	117.8	102.1	440.0	1393.0	601.0	164.1	65.3	16.2	11.1	52.1	63.9	97.2	260.0
1936	169.1	36.9	655.2	991.0	602.1	222.1	40.7	13.2	25.0	29.0	29.0	29.1	237.1
1937	12.3	24.0	640.0	1116.0	432.8	232.1	42.8	14.1	15.0	16.1	21.9	23.9	216.1
1938	197.1	456.0	954.0	1581.0	892.0	349.1	70.0	22.1	19.0	35.1	103.2	365.9	419.1
1939	68.9	257.2	630.0	756.2	384.9	121.1	37.3	10.2	17.9	35.0	70.1	67.8	203.9
1940	107.9	586.8	1110.1	1571.9	891.2	284.0	59.0	18.3	44.9	24.9	20.9	55.0	396.0
1941	224.9	363.0	541.2	956.2	1333.1	1313.0	168.9	62.8	92.0	85.0	109.0	210.9	454.0
1942	333.3	594.8	969.0	1509.0	1634.0	1007.1	204.1	47.8	32.0	95.9	161.9	515.0	591.0
1943	370.1	377.1	828.0	1744.0	1315.0	735.9	157.9	42.9	27.9	33.2	100.0	252.0	498.0
1944	46.6	209.1	477.3	916.0	425.1	368.0	58.0	24.1	26.0	59.9	61.1	56.1	226.1
1945	202.2	370.2	585.0	1193.0	1213.0	463.0	87.0	27.3	43.9	23.9	48.0	26.1	355.9
1946	268.8	270.9	630.0	1240.0	1230.9	366.0	122.0	30.4	35.0	30.2	73.8	116.0	368.0
1947	147.9	259.8	543.8	1252.9	757.8	759.1	84.0	30.3	33.0	47.1	95.1	298.0	357.9
1948	378.9	345.0	516.1	1435.0	2119.0	916.1	305.0	68.2	42.0	127.9	104.9	155.3	543.0
1949	39.4	114.9	690.0	1289.1	796.1	147.0	52.3	18.1	15.9	40.2	57.9	83.9	279.0
1950	52.3	162.8	573.0	1136.0	775.3	669.9	63.0	27.2	20.0	30.1	62.9	60.1	302.0
1951	352.0	431.1	626.0	982.0	1215.0	777.1	102.0	29.2	23.1	53.1	131.8	152.0	405.2

1952	55.9	206.2	451.2	1058.8	1149.0	443.0	103.9	24.3	23.0	51.9	50.1	71.8	307.0
1953	702.0	442.8	650.2	992.9	1342.0	824.9	112.0	41.2	23.1	18.1	26.0	28.1	433.1
1954	156.0	353.1	467.1	1056.0	668.6	452.8	81.1	38.2	28.0	37.9	58.2	243.1	301.9
1955	33.9	54.8	90.0	676.0	557.9	105.9	51.2	8.4	31.0	28.9	42.9	23.3	142.0
1956	580.0	301.0	938.0	1924.1	1745.9	668.2	159.0	58.3	26.1	37.8	156.1	516.1	593.0
1957	43.9	241.0	723.0	1420.1	1373.0	427.0	80.0	26.2	21.0	43.0	42.9	107.9	379.1
1958	365.1	961.9	801.1	1768.1	1224.0	877.0	165.0	46.2	25.0	106.9	58.9	352.0	558.0
1959	632.9	607.0	702.0	1478.9	1156.0	489.0	108.0	33.3	53.0	29.1	143.0	561.2	498.1
1960	43.2	303.3	685.0	876.0	1412.0	269.0	58.9	35.1	26.1	47.0	51.0	43.0	321.1
1961	80.0	522.0	936.1	1034.1	1164.0	357.1	66.1	22.1	21.0	39.2	149.9	54.3	369.0
1962	106.2	184.3	416.0	934.1	1253.1	222.1	58.7	23.2	22.0	29.9	44.1	85.0	282.1
1963	76.8	629.0	527.0	1510.9	1006.0	339.1	99.9	29.3	32.0	53.0	57.0	251.1	381.1
1964	108.8	81.9	317.0	844.0	384.4	184.0	49.9	32.9	30.0	35.0	75.9	46.3	182.0
1965	680.1	1291.0	779.9	1406.0	905.1	518.1	114.8	85.1	37.1	24.0	34.0	647.8	537.9
1966	182.0	99.7	487.8	461.2	152.7	91.0	30.3	14.1	32.9	42.0	65.0	43.6	142.0
1967	489.1	283.0	577.0	1074.0	898.0	260.9	60.8	20.1	20.2	35.1	81.0	572.9	365.1
1968	85.1	489.2	399.8	479.3	367.3	139.9	27.3	31.9	31.9	40.8	44.2	67.0	182.1
1969	101.2	77.1	1167.1	1743.0	1263.1	513.1	111.9	30.3	23.0	40.2	235.9	175.7	458.0
1970	1174.8	583.0	1049.0	925.0	1148.0	578.0	107.0	29.3	41.0	33.9	33.2	152.1	488.1
1971	625.9	428.3	650.0	1168.0	907.0	766.9	125.1	31.2	34.0	48.1	105.8	92.0	414.0
1972	240.7	263.1	1612.0	1269.1	1132.0	477.1	98.0	28.3	24.0	35.0	53.2	109.2	446.0
1973	122.2	137.9	323.9	588.0	485.0	99.9	28.2	9.3	49.9	34.0	47.2	219.9	178.9
1974	788.9	749.0	1214.0	2078.0	1191.9	508.2	139.0	38.2	22.0	32.8	689.1	616.1	670.0
1975	254.0	70.0	479.9	1079.9	1434.9	295.1	69.1	36.0	20.0	19.9	30.9	42.1	321.0
1976	190.1	335.1	600.9	1721.9	1009.9	354.1	78.2	52.1	25.0	51.0	45.9	264.1	392.8
1977	38.1	64.9	158.0	451.9	571.0	111.1	38.3	47.1	55.9	49.1	63.8	38.1	140.9
1978	444.1	671.1	1074.0	2106.0	1519.0	463.8	193.0	63.7	53.0	32.0	65.1	600.9	605.9
1979	21.4	129.8	1179.2	1390.8	1168.0	375.1	55.0	33.2	21.0	28.0	29.2	56.9	375.1
1980	349.2	422.1	783.0	1288.1	1509.0	676.8	145.0	42.8	47.9	41.0	56.1	188.2	462.1
1981	151.9	742.0	937.0	1102.8	1507.9	901.0	191.8	43.8	29.0	48.0	57.9	265.2	495.9
1982	487.1	1129.3	1480.0	1546.9	917.0	413.9	227.2	41.7	40.1	42.1	140.2	284.2	558.1
1983	444.7	695.3	2199.1	1666.1	1606.0	546.1	314.0	78.9	41.1	61.7	70.9	493.0	685.8
1984	297.1	266.0	1490.9	2179.0	2449.9	1215.9	200.1	67.1	66.9	39.2	153.8	185.2	718.0
1985	90.6	192.9	811.1	865.9	659.8	388.0	59.1	34.1	55.0	76.0	143.0	116.0	291.0
1986	97.0	1295.1	1680.9	898.9	1244.9	297.9	91.9	24.3	25.0	40.1	56.0	30.0	476.9
1987	97.9	445.0	785.0	655.3	842.0	298.9	63.9	21.1	10.1	33.2	186.0	56.8	290.0
1988	87.1	173.0	455.1	1159.1	872.0	277.1	66.0	20.3	22.0	21.1	40.9	43.2	269.1
1989	89.8	67.2	741.1	1784.1	1229.1	376.9	71.9	45.1	34.0	19.1	56.8	33.2	379.6
1990	168.0	158.0	421.0	620.1	1204.0	559.1	64.0	26.1	15.1	35.0	66.1	40.2	282.0
1991	128.9	170.8	522.9	663.4	1803.0	594.0	140.1	41.3	23.1	35.0	50.9	35.3	352.4
1992	142.1	490.1	539.1	872.9	538.9	162.9	76.2	27.2	30.0	34.2	339.1	120.9	279.2
1993	32.1	57.9	835.9	1648.1	1604.9	689.8	169.1	103.1	36.2	26.0	57.9	36.0	442.7
1994	207.9	158.3	531.2	674.9	1246.1	281.0	60.9	20.2	14.9	35.9	30.3	105.2	281.9
1995	359.2	564.0	1205.8	1305.0	1973.1	682.1	155.1	50.0	33.9	27.9	50.0	167.9	548.0
1996	461.1	2226.1	891.0	1697.1	1766.1	447.1	126.0	36.3	22.0	40.1	153.9	479.9	688.5
1997	1880.0	681.9	1804.0	2135.0	1440.9	739.1	300.0	61.1	37.1	35.3	354.8	343.0	818.8
1998	413.9	409.1	598.0	1020.0	1769.0	694.9	133.0	38.2	31.1	33.3	71.8	61.1	439.5
1999	477.9	451.1	740.0	1186.0	963.0	256.9	64.9	26.0	9.1	27.2	158.2	209.1	380.0
2000	185.3	479.9	1044.0	1720.0	1343.9	557.0	114.0	27.3	38.0	35.9	64.2	130.1	477.0
2001	101.0	144.8	574.1	1074.1	873.0	178.9	65.8	25.2	19.9	69.9	78.1	52.2	271.7
2002	75.9	84.0	554.0	1291.1	706.0	340.8	59.1	21.2	21.9	40.1	51.0	71.1	276.3
2003	432.8	651.1	908.1	1553.1	1202.0	458.9	91.0	27.3	21.1	22.9	32.0	66.1	453.3
2004	33.6	227.0	1416.0	1144.8	1144.0	475.0	101.9	37.3	25.0	22.1	32.2	83.8	395.9
2005	104.8	78.1	363.9	669.8	1549.0	247.9	66.0	21.1	9.1	39.9	61.0	89.1	276.9
2006	627.0	268.1	797.0	1614.0	1123.0	697.2	127.0	33.3	22.9	33.0	51.0	66.1	455.0
(blank)													
Grand Total	252.7	376.6	769.9	1232.1	1077.5	439.7	97.7	33.1	29.6	42.1	89.8	170.5	383.6

from Calculation of Return Interval of 7-day Average Low Flow Using Bias Corrected VIC Streamflow Data CIG

<http://www.hydro.washington.edu/2860/products/sites/?site=4012>

These data are from Climate Impacts Group-bias adjusted

http://www.hydro.washington.edu/2860/products/sites/r7climate/subbasin_summaries/4012/nat_bias_adjusted_vic_streamflow_daily_historical.dat

Method: <http://streamflow.engr.oregonstate.edu/analysis/annual/index.htm>

Streamflow Evaluation for Watershed Restoration Planning and Design, Oregon State University.

<http://streamflow.engr.oregonstate.edu/>

See file: Station correlations in Upper Grande Ronde.xlsx

Values										
			Ranked Max Streamflow, Q (cfs)	Rank	log Q (cfs)	(log Q - avg(logQ))^2	(log Q - avg(logQ))^3	Return Period [(n+1)/m]	Exceedence Probability (1/Tr)	
Year	Min of 7dayavg	Max of 7dayavg								
1955	8.0	811.1	8.0	1	0.903	0.136	-0.050030	92.00	0.0109	
1973	9.0	717.4	9.0	2	0.954	0.101	-0.031953	46.00	0.0217	
1999	9.0	1552.9	9.0	3	0.954	0.101	-0.031953	30.67	0.0326	
2005	9.0	2580.6	9.0	4	0.954	0.101	-0.031953	23.00	0.0435	
1931	10.0	2494.6	10.0	5	1.000	0.074	-0.020028	18.40	0.0543	
1932	10.0	1940.9	10.0	6	1.000	0.074	-0.020028	15.33	0.0652	
1939	10.0	928.7	10.0	7	1.000	0.074	-0.020028	13.14	0.0761	
1987	10.0	1164.4	10.0	8	1.000	0.074	-0.020028	11.50	0.0870	
1919	10.9	982.9	10.0	9	1.000	0.074	-0.020028	10.22	0.0978	
1935	11.0	1996.1	11.0	10	1.041	0.053	-0.012195	9.20	0.1087	
1936	12.0	1453.4	12.0	11	1.079	0.037	-0.007121	8.36	0.1196	
1937	12.0	1374.6	12.0	12	1.079	0.037	-0.007121	7.67	0.1304	
1966	13.0	662.7	13.0	13	1.114	0.025	-0.003916	7.08	0.1413	
1994	14.0	2138.7	14.0	14	1.146	0.016	-0.001974	6.57	0.1522	
1990	14.4	1889.0	14.0	15	1.146	0.016	-0.001974	6.13	0.1630	
1922	14.6	1587.0	14.0	16	1.146	0.016	-0.001974	5.75	0.1739	
1929	15.0	1452.7	15.0	17	1.176	0.009	-0.000870	5.41	0.1848	
1949	15.0	1864.3	15.0	18	1.176	0.009	-0.000870	5.11	0.1957	
1940	16.0	2437.9	16.0	19	1.204	0.005	-0.000307	4.84	0.2065	
1917	16.6	2158.1	16.0	20	1.204	0.005	-0.000307	4.60	0.2174	
1934	18.0	1110.0	18.0	21	1.255	0.000	-0.000004	4.38	0.2283	
1938	18.0	2397.4	18.0	22	1.255	0.000	-0.000004	4.18	0.2391	
1953	18.0	2120.4	15.0	23	1.176	0.009	-0.000870	4.00	0.2500	
1967	18.0	1520.1	18.0	24	1.255	0.000	-0.000004	3.83	0.2609	
1979	18.0	2214.6	18.0	25	1.255	0.000	-0.000004	3.68	0.2717	
1989	18.0	2260.3	18.0	26	1.255	0.000	-0.000004	3.54	0.2826	
2003	18.0	2355.6	18.0	27	1.255	0.000	-0.000004	3.41	0.2935	
1988	18.4	2250.6	18.0	28	1.255	0.000	-0.000004	3.29	0.3043	
1975	18.6	2037.6	18.0	29	1.255	0.000	-0.000004	3.17	0.3152	
1945	18.9	1540.1	18.0	30	1.255	0.000	-0.000004	3.07	0.3261	
1950	18.9	1299.6	18.0	31	1.255	0.000	-0.000004	2.97	0.3370	
1926	19.0	1149.7	19.0	32	1.279	0.000	0.000000	2.88	0.3478	
1930	19.0	1166.9	19.0	33	1.279	0.000	0.000000	2.79	0.3587	
1961	19.0	1451.3	19.0	34	1.279	0.000	0.000000	2.71	0.3696	
1962	19.0	2108.0	19.0	35	1.279	0.000	0.000000	2.63	0.3804	
2001	19.0	1285.4	19.0	36	1.279	0.000	0.000000	2.56	0.3913	
1986	19.1	3322.4	19.0	37	1.279	0.000	0.000000	2.49	0.4022	

1996	19.1	3777.3	19.0	38	1.279	0.000	0.000000	2.42	0.4130
2002	19.3	1609.0	19.0	39	1.279	0.000	0.000000	2.36	0.4239
2004	19.4	2346.4	19.0	40	1.279	0.000	0.000000	2.30	0.4348
1952	20.0	2046.6	20.0	41	1.301	0.001	0.000026	2.24	0.4457
1957	20.0	2047.1	19.0	42	1.279	0.000	0.000000	2.19	0.4565
1960	20.0	1808.0	20.0	43	1.301	0.001	0.000026	2.14	0.4674
1923	20.3	1361.0	20.0	44	1.301	0.001	0.000026	2.09	0.4783
1965	20.3	3114.4	20.0	45	1.301	0.001	0.000026	2.04	0.4891
1974	20.4	3134.9	20.0	46	1.301	0.001	0.000026	2.00	0.5000
1921	20.7	2512.4	20.0	47	1.301	0.001	0.000026	1.96	0.5109
1918	20.9	1853.0	20.0	48	1.301	0.001	0.000026	1.92	0.5217
1928	20.9	2073.9	20.0	49	1.301	0.001	0.000026	1.88	0.5326
1969	20.9	2727.3	20.0	50	1.301	0.001	0.000026	1.84	0.5435
1972	20.9	2473.1	20.0	51	1.301	0.001	0.000026	1.80	0.5543
1993	20.9	3282.7	20.0	52	1.301	0.001	0.000026	1.77	0.5652
1933	21.0	1685.0	21.0	53	1.322	0.003	0.000130	1.74	0.5761
1951	21.0	1743.3	21.0	54	1.322	0.003	0.000130	1.70	0.5870
2006	21.0	2687.4	20.0	55	1.301	0.001	0.000026	1.67	0.5978
1980	21.1	2415.9	21.0	56	1.322	0.003	0.000130	1.64	0.6087
1925	21.7	2192.7	21.0	57	1.322	0.003	0.000130	1.61	0.6196
1995	21.7	4230.3	21.0	58	1.322	0.003	0.000130	1.59	0.6304
1944	22.0	1326.7	22.0	59	1.342	0.005	0.000356	1.56	0.6413
1978	22.0	5419.6	21.0	60	1.322	0.003	0.000130	1.53	0.6522
1991	22.0	4452.9	22.0	61	1.342	0.005	0.000356	1.51	0.6630
2000	22.0	2311.1	21.0	62	1.322	0.003	0.000130	1.48	0.6739
1943	22.6	2649.1	22.0	63	1.342	0.005	0.000356	1.46	0.6848
1956	22.6	3775.1	21.0	64	1.322	0.003	0.000130	1.44	0.6957
1968	22.6	1051.1	22.0	65	1.342	0.005	0.000356	1.42	0.7065
1916	23.0	3268.1	22.0	66	1.342	0.005	0.000356	1.39	0.7174
1970	23.0	2856.6	22.0	67	1.342	0.005	0.000356	1.37	0.7283
1982	23.0	2487.7	22.0	68	1.342	0.005	0.000356	1.35	0.7391
1997	23.0	5245.4	23.0	69	1.362	0.008	0.000733	1.33	0.7500
1920	23.1	2461.9	23.0	70	1.362	0.008	0.000733	1.31	0.7609
1954	23.6	1398.4	23.0	71	1.362	0.008	0.000733	1.30	0.7717
1981	23.6	2387.9	23.0	72	1.362	0.008	0.000733	1.28	0.7826
1958	23.7	2680.4	21.0	73	1.322	0.003	0.000130	1.26	0.7935
1924	23.9	1056.0	23.0	74	1.362	0.008	0.000733	1.24	0.8043
1963	24.0	2016.6	22.0	75	1.342	0.005	0.000356	1.23	0.8152
1976	24.0	2657.1	23.0	76	1.362	0.008	0.000733	1.21	0.8261
1992	24.0	1224.9	23.0	77	1.362	0.008	0.000733	1.19	0.8370
1971	24.4	1622.7	24.0	78	1.380	0.012	0.001282	1.18	0.8478
1964	25.1	1211.0	25.0	79	1.398	0.016	0.002018	1.16	0.8587
1998	25.3	3380.7	24.0	80	1.380	0.012	0.001282	1.15	0.8696
1959	25.7	2097.7	25.0	81	1.398	0.016	0.002018	1.14	0.8804
1946	25.9	1588.4	24.0	82	1.380	0.012	0.001282	1.12	0.8913
1927	26.1	2638.7	25.0	83	1.398	0.016	0.002018	1.11	0.9022
1947	26.3	1702.4	25.0	84	1.398	0.016	0.002018	1.10	0.9130
1985	27.1	1318.0	26.0	85	1.415	0.021	0.002949	1.08	0.9239
1942	27.4	2659.4	27.0	86	1.431	0.026	0.004080	1.07	0.9348
1984	29.4	3283.6	29.0	87	1.462	0.036	0.006949	1.06	0.9457
1977	30.0	773.7	30.0	88	1.477	0.042	0.008685	1.05	0.9565
1983	35.9	3466.6	31.0	89	1.491	0.048	0.010618	1.03	0.9674
1948	37.4	2555.0	36.0	90	1.556	0.081	0.023085	1.02	0.9783
1941	37.9	1884.4	37.0	91	1.568	0.088	0.026102	1.01	0.9891
			19.5		1.272	sum	sum		
			average		average	1.617	-0.181724		

Tr	K(-0)	K(-0.10)	slope	K(-.0942)	Q (cfs)
2					
5					
10					
25					
50					
100	-2.326	-2.253	-0.7382	-2.257	9.31
200					

The frequency factor K is a function of the skewness coefficient and return period and can be found using the frequency factor table. The flood magnitudes for the various return periods are found by solving the general equation. The mean, variance, and standard deviation of the data can be calculated using the two formulas below.

The coefficient K is then found using tabulated values according to C_w and the return period for each discharge.

For a more detailed description of this method, please refer to the following text:

Bedient, Philip B. and Wayne C. Huber. Hydrology and Floodplain Analysis. Prentice-Hall, Inc., Upper Saddle River, 2002.

<http://hydrology.rice.edu/bedient/appendixE.html>

links to numerous hydrology websites--data and models

Flood-frequency estimates for gaged sites are computed by fitting the series of annual peak flows to some known statistical distribution. For the purposes of this study, estimates of flood-flow frequency are computed by fitting the logarithms (base 10) of the annual peak flows to a log-Pearson Type III distribution, following the guidelines and using the computational methods described in Bulletin 17B of the Hydrology Subcommittee of the Interagency Advisory Committee on Water Data (1982). The equation for fitting the log-Pearson Type III distribution to an observed series of annual peak flows is as follows:

, (1)

where

Q_t is the t-year recurrence interval discharge in cubic feet per second,

\bar{y} is the mean of the log-transformed annual peak flows,

K is a factor dependent on recurrence interval and the skew coefficient of the logtransformed annual peak flows, and

S is the standard deviation of the logtransformed annual peak flows.

Values for K for a wide range of recurrence intervals and skew coefficients are published in Appendix 3 of Bulletin 17B (Hydrology Subcommittee of the Interagency Advisory Committee on Water Data, 1982).

Based on the CIG data for VIC historical low flows, the 100-year recurrence streamflow is 9.31 cfs shown in the table above.

Use of the CIG historical streamflow (mean daily flows) for USGS (gauge 13319000) adjusted VIC data to calculate mean monthly flows.

These data are from Climate Impacts Group-bias adjusted
http://www.hydro.washington.edu/2860/products/sites/r7climate/subbasin_summaries/4012/nat_bias_adjusted_vic_streamflow_daily_historical.dat

Average of Historical	Column Labels												
Row Labels	1	2	3	4	5	6	7	8	9	10	11	12 (bl	Grand Total
1916	31.7	292.9	1961.0	1915.1	1401.0	657.0	163.0	47.8	29.1	25.0	43.1	49.9	551.6
1917	38.1	51.0	127.1	1331.0	1440.0	266.1	54.0	19.1	35.9	26.1	37.9	46.1	289.9
1918	639.9	464.0	1416.0	1076.3	761.1	236.0	61.7	28.2	25.0	23.9	29.9	621.0	449.6
1919	200.2	319.2	748.9	853.1	753.9	152.0	39.3	11.4	24.9	64.0	51.2	85.2	275.0
1920	98.8	283.8	602.8	1794.1	1609.0	554.1	136.0	53.2	52.1	29.0	109.9	63.1	447.8
1921	434.0	399.2	1144.0	1640.9	1458.1	424.8	112.0	30.2	24.0	73.7	75.2	79.9	491.5
1922	57.3	72.9	378.0	1242.1	826.1	208.0	36.7	23.0	16.2	29.8	32.1	542.0	289.5
1923	439.0	74.1	407.0	960.0	643.0	532.8	96.0	29.2	23.0	25.0	32.9	60.1	277.3
1924	123.1	836.9	536.1	814.1	528.7	157.0	39.1	29.1	30.0	139.9	62.9	228.9	291.2
1925	144.1	644.1	561.0	1415.0	1026.9	335.1	66.1	26.1	26.0	27.0	109.8	64.1	367.1
1926	33.0	615.0	608.0	895.1	812.9	179.0	41.9	34.2	39.9	20.0	30.1	71.8	278.9
1927	207.0	701.0	783.2	1926.1	1283.1	699.2	128.0	32.2	60.9	39.1	372.9	294.2	540.2
1928	204.2	311.9	1080.0	1525.0	733.8	255.1	69.9	22.3	26.9	164.1	325.1	151.8	405.0
1929	30.2	34.0	944.2	695.0	457.9	344.9	44.0	21.1	15.9	31.2	44.7	37.0	226.0
1930	39.3	451.0	515.0	740.1	890.1	493.0	60.0	22.1	21.1	24.1	24.2	208.0	289.0
1931	69.9	78.2	494.0	1525.0	496.3	194.1	36.9	10.3	26.9	58.0	48.0	42.1	256.0
1932	38.1	63.0	682.0	1491.0	1029.0	243.9	54.8	19.1	10.1	29.9	37.1	35.1	311.0
1933	72.9	74.9	527.0	913.9	1127.0	211.0	64.0	25.2	31.1	33.0	89.8	44.2	268.9
1934	556.0	235.1	572.1	752.9	478.9	304.1	56.0	19.3	21.9	33.1	56.1	294.0	282.0
1935	117.8	102.1	440.0	1393.0	601.0	164.1	65.3	16.2	11.1	52.1	63.9	97.2	260.0
1936	169.1	36.9	655.2	991.0	602.1	222.1	40.7	13.2	25.0	29.0	29.0	29.1	237.1
1937	12.3	24.0	640.0	1116.0	432.8	232.1	42.8	14.1	15.0	16.1	21.9	23.9	216.1
1938	197.1	456.0	954.0	1581.0	892.0	349.1	70.0	22.1	19.0	35.1	103.2	365.9	419.1
1939	68.9	257.2	630.0	756.2	384.9	121.1	37.3	10.2	17.9	35.0	70.1	67.8	203.9
1940	107.9	586.8	1110.1	1571.9	891.2	284.0	59.0	18.3	44.9	24.9	20.9	55.0	396.0
1941	224.9	363.0	541.2	956.2	1333.1	1313.0	168.9	62.8	92.0	85.0	109.0	210.9	454.0
1942	333.3	594.8	969.0	1509.0	1634.0	1007.1	204.1	47.8	32.0	95.9	161.9	515.0	591.0
1943	370.1	377.1	828.0	1744.0	1315.0	735.9	157.9	42.9	27.9	33.2	100.0	252.0	498.0
1944	46.6	209.1	477.3	916.0	425.1	368.0	58.0	24.1	26.0	59.9	61.1	56.1	226.1
1945	202.2	370.2	585.0	1193.0	1213.0	463.0	87.0	27.3	43.9	23.9	48.0	26.1	355.9
1946	268.8	270.9	630.0	1240.0	1230.9	366.0	122.0	30.4	35.0	30.2	73.8	116.0	368.0
1947	147.9	259.8	543.8	1252.9	757.8	759.1	84.0	30.3	33.0	47.1	95.1	298.0	357.9
1948	378.9	345.0	516.1	1435.0	2119.0	916.1	305.0	68.2	42.0	127.9	104.9	155.3	543.0
1949	39.4	114.9	690.0	1289.1	796.1	147.0	52.3	18.1	15.9	40.2	57.9	83.9	279.0
1950	52.3	162.8	573.0	1136.0	775.3	669.9	63.0	27.2	20.0	30.1	62.9	60.1	302.0
1951	352.0	431.1	626.0	982.0	1215.0	777.1	102.0	29.2	23.1	53.1	131.8	152.0	405.2
1952	55.9	206.2	451.2	1058.8	1149.0	443.0	103.9	24.3	23.0	51.9	50.1	71.8	307.0
1953	702.0	442.8	650.2	992.9	1342.0	824.9	112.0	41.2	23.1	18.1	26.0	28.1	433.1
1954	156.0	353.1	467.1	1056.0	668.6	452.8	81.1	38.2	28.0	37.9	58.2	243.1	301.9
1955	33.9	54.8	90.0	676.0	557.9	105.9	51.2	8.4	31.0	28.9	42.9	23.3	142.0
1956	580.0	301.0	938.0	1924.1	1745.9	668.2	159.0	58.3	26.1	37.8	156.1	516.1	593.0
1957	43.9	241.0	723.0	1420.1	1373.0	427.0	80.0	26.2	21.0	43.0	42.9	107.9	379.1
1958	365.1	961.9	801.1	1768.1	1224.0	877.0	165.0	46.2	25.0	106.9	58.9	352.0	558.0
1959	632.9	607.0	702.0	1478.9	1156.0	489.0	108.0	33.3	53.0	29.1	143.0	561.2	498.1
1960	43.2	303.3	685.0	876.0	1412.0	269.0	58.9	35.1	26.1	47.0	51.0	43.0	321.1
1961	80.0	522.0	936.1	1034.1	1164.0	357.1	66.1	22.1	21.0	39.2	149.9	54.3	369.0

1962	106.2	184.3	416.0	934.1	1253.1	222.1	58.7	23.2	22.0	29.9	44.1	85.0	282.1
1963	76.8	629.0	527.0	1510.9	1006.0	339.1	99.9	29.3	32.0	53.0	57.0	251.1	381.1
1964	108.8	81.9	317.0	844.0	384.4	184.0	49.9	32.9	30.0	35.0	75.9	46.3	182.0
1965	680.1	1291.0	779.9	1406.0	905.1	518.1	114.8	85.1	37.1	24.0	34.0	647.8	537.9
1966	182.0	99.7	487.8	461.2	152.7	91.0	30.3	14.1	32.9	42.0	65.0	43.6	142.0
1967	489.1	283.0	577.0	1074.0	898.0	260.9	60.8	20.1	20.2	35.1	81.0	572.9	365.1
1968	85.1	489.2	399.8	479.3	367.3	139.9	27.3	31.9	31.9	40.8	44.2	67.0	182.1
1969	101.2	77.1	1167.1	1743.0	1263.1	513.1	111.9	30.3	23.0	40.2	235.9	175.7	458.0
1970	1174.8	583.0	1049.0	925.0	1148.0	578.0	107.0	29.3	41.0	33.9	33.2	152.1	488.1
1971	625.9	428.3	650.0	1168.0	907.0	766.9	125.1	31.2	34.0	48.1	105.8	92.0	414.0
1972	240.7	263.1	1612.0	1269.1	1132.0	477.1	98.0	28.3	24.0	35.0	53.2	109.2	446.0
1973	122.2	137.9	323.9	588.0	485.0	99.9	28.2	9.3	49.9	34.0	47.2	219.9	178.9
1974	788.9	749.0	1214.0	2078.0	1191.9	508.2	139.0	38.2	22.0	32.8	689.1	616.1	670.0
1975	254.0	70.0	479.9	1079.9	1434.9	295.1	69.1	36.0	20.0	19.9	30.9	42.1	321.0
1976	190.1	335.1	600.9	1721.9	1009.9	354.1	78.2	52.1	25.0	51.0	45.9	264.1	392.8
1977	38.1	64.9	158.0	451.9	571.0	111.1	38.3	47.1	55.9	49.1	63.8	38.1	140.9
1978	444.1	671.1	1074.0	2106.0	1519.0	463.8	193.0	63.7	53.0	32.0	65.1	600.9	605.9
1979	21.4	129.8	1179.2	1390.8	1168.0	375.1	55.0	33.2	21.0	28.0	29.2	56.9	375.1
1980	349.2	422.1	783.0	1288.1	1509.0	676.8	145.0	42.8	47.9	41.0	56.1	188.2	462.1
1981	151.9	742.0	937.0	1102.8	1507.9	901.0	191.8	43.8	29.0	48.0	57.9	265.2	495.9
1982	487.1	1129.3	1480.0	1546.9	917.0	413.9	227.2	41.7	40.1	42.1	140.2	284.2	558.1
1983	444.7	695.3	2199.1	1666.1	1606.0	546.1	314.0	78.9	41.1	61.7	70.9	493.0	685.8
1984	297.1	266.0	1490.9	2179.0	2449.9	1215.9	200.1	67.1	66.9	39.2	153.8	185.2	718.0
1985	90.6	192.9	811.1	865.9	659.8	388.0	59.1	34.1	55.0	76.0	143.0	116.0	291.0
1986	97.0	1295.1	1680.9	898.9	1244.9	297.9	91.9	24.3	25.0	40.1	56.0	30.0	476.9
1987	97.9	445.0	785.0	655.3	842.0	298.9	63.9	21.1	10.1	33.2	186.0	56.8	290.0
1988	87.1	173.0	455.1	1159.1	872.0	277.1	66.0	20.3	22.0	21.1	40.9	43.2	269.1
1989	89.8	67.2	741.1	1784.1	1229.1	376.9	71.9	45.1	34.0	19.1	56.8	33.2	379.6
1990	168.0	158.0	421.0	620.1	1204.0	559.1	64.0	26.1	15.1	35.0	66.1	40.2	282.0
1991	128.9	170.8	522.9	663.4	1803.0	594.0	140.1	41.3	23.1	35.0	50.9	35.3	352.4
1992	142.1	490.1	539.1	872.9	538.9	162.9	76.2	27.2	30.0	34.2	339.1	120.9	279.2
1993	32.1	57.9	835.9	1648.1	1604.9	689.8	169.1	103.1	36.2	26.0	57.9	36.0	442.7
1994	207.9	158.3	531.2	674.9	1246.1	281.0	60.9	20.2	14.9	35.9	30.3	105.2	281.9
1995	359.2	564.0	1205.8	1305.0	1973.1	682.1	155.1	50.0	33.9	27.9	50.0	167.9	548.0
1996	461.1	2226.1	891.0	1697.1	1766.1	447.1	126.0	36.3	22.0	40.1	153.9	479.9	688.5
1997	1880.0	681.9	1804.0	2135.0	1440.9	739.1	300.0	61.1	37.1	35.3	354.8	343.0	818.8
1998	413.9	409.1	598.0	1020.0	1769.0	694.9	133.0	38.2	31.1	33.3	71.8	61.1	439.5
1999	477.9	451.1	740.0	1186.0	963.0	256.9	64.9	26.0	9.1	27.2	158.2	209.1	380.0
2000	185.3	479.9	1044.0	1720.0	1343.9	557.0	114.0	27.3	38.0	35.9	64.2	130.1	477.0
2001	101.0	144.8	574.1	1074.1	873.0	178.9	65.8	25.2	19.9	69.9	78.1	52.2	271.7
2002	75.9	84.0	554.0	1291.1	706.0	340.8	59.1	21.2	21.9	40.1	51.0	71.1	276.3
2003	432.8	651.1	908.1	1553.1	1202.0	458.9	91.0	27.3	21.1	22.9	32.0	66.1	453.3
2004	33.6	227.0	1416.0	1144.8	1144.0	475.0	101.9	37.3	25.0	22.1	32.2	83.8	395.9
2005	104.8	78.1	363.9	669.8	1549.0	247.9	66.0	21.1	9.1	39.9	61.0	89.1	276.9
2006	627.0	268.1	797.0	1614.0	1123.0	697.2	127.0	33.3	22.9	33.0	51.0	66.1	455.0

Grand Total	252.7	376.6	769.9	1232.1	1077.5	439.7	97.7	33.1	29.6	42.1	89.8	170.5	383.6
--------------------	--------------	--------------	--------------	---------------	---------------	--------------	-------------	-------------	-------------	-------------	-------------	--------------	--------------

Use of the CIG historical streamflow (mean daily flows) for USGS (gauge 13319000) adjusted VIC data to calculate maximum annual peak and minimum annual low flows.

Values			
Row Labels	Max of	Min of Average	Histori of
	Historical	cal	Historical
1916	3449	22	551.6
1917	2535	16	289.9
1918	2260	20	449.6
1919	1173	10	275.0
1920	3302	23	447.8
1921	3530	20	491.5
1922	1933	14	289.5
1923	1868	20	277.3
1924	1379	23	291.2
1925	2490	21	367.1
1926	1565	19	278.9
1927	3549	25	540.2
1928	2460	20	405.0
1929	1782	15	226.0
1930	1519	19	289.0
1931	3977	10	256.0
1932	2306	10	311.0
1933	2054	21	268.9
1934	1345	18	282.0
1935	2805	11	260.0
1936	1789	12	237.1
1937	1831	12	216.1
1938	3282	18	419.1
1939	1168	10	203.9
1940	3499	16	396.0
1941	2850	37	454.0
1942	3929	27	591.0
1943	3538	22	498.0
1944	1626	22	226.1
1945	1848	18	355.9
1946	2333	24	368.0
1947	2263	25	357.9
1948	3205	36	543.0
1949	1977	15	279.0
1950	1456	18	302.0
1951	2559	21	405.2
1952	3277	20	307.0
1953	3299	15	433.1
1954	2065	23	301.9
1955	1135	8	142.0
1956	4768	21	593.0
1957	2736	19	379.1
1958	3697	21	558.0
1959	2685	25	498.1
1960	2348	20	321.1
1961	1930	19	369.0

1962	2500	19	282.1
1963	2568	22	381.1
1964	1650	25	182.0
1965	5006	20	537.9
1966	735	13	142.0
1967	1857	18	365.1
1968	1296	22	182.1
1969	4212	20	458.0
1970	3547	22	488.1
1971	2221	24	414.0
1972	2874	20	446.0
1973	970	9	178.9
1974	4595	20	670.0
1975	2548	18	321.0
1976	3709	23	392.8
1977	1100	30	140.9
1978	9193	21	605.9
1979	2902	18	375.1
1980	3510	21	462.1
1981	3308	23	495.9
1982	3119	22	558.1
1983	5177	31	685.8
1984	3996	29	718.0
1985	1522	26	291.0
1986	4925	19	476.9
1987	1588	10	290.0
1988	3382	18	269.1
1989	3009	18	379.6
1990	2641	14	282.0
1991	6596	22	352.4
1992	1522	23	279.2
1993	4137	20	442.7
1994	3180	14	281.9
1995	6658	21	548.0
1996	4977	19	688.5
1997	8995	23	818.8
1998	4307	24	439.5
1999	2070	9	380.0
2000	3015	21	477.0
2001	1807	19	271.7
2002	1798	19	276.3
2003	3485	18	453.3
2004	3186	19	395.9
2005	3752	9	276.9
2006	3050	20	455.0

Grand Total	9193	8	383.6

Application of the CIG historical streamflow (mean daily flows) for USGS (gauge 13319000) adjusted VIC data to calculate an annual series of maximum annual peak and minimum annual low flows and use this to estimate recurrence interval for peak flows using the Oregon State University Engineering Department methodology.

Use of the OSU streamflow statistics <http://streamflow.engr.oregonstate.edu/analysis/floodfreq/mea>

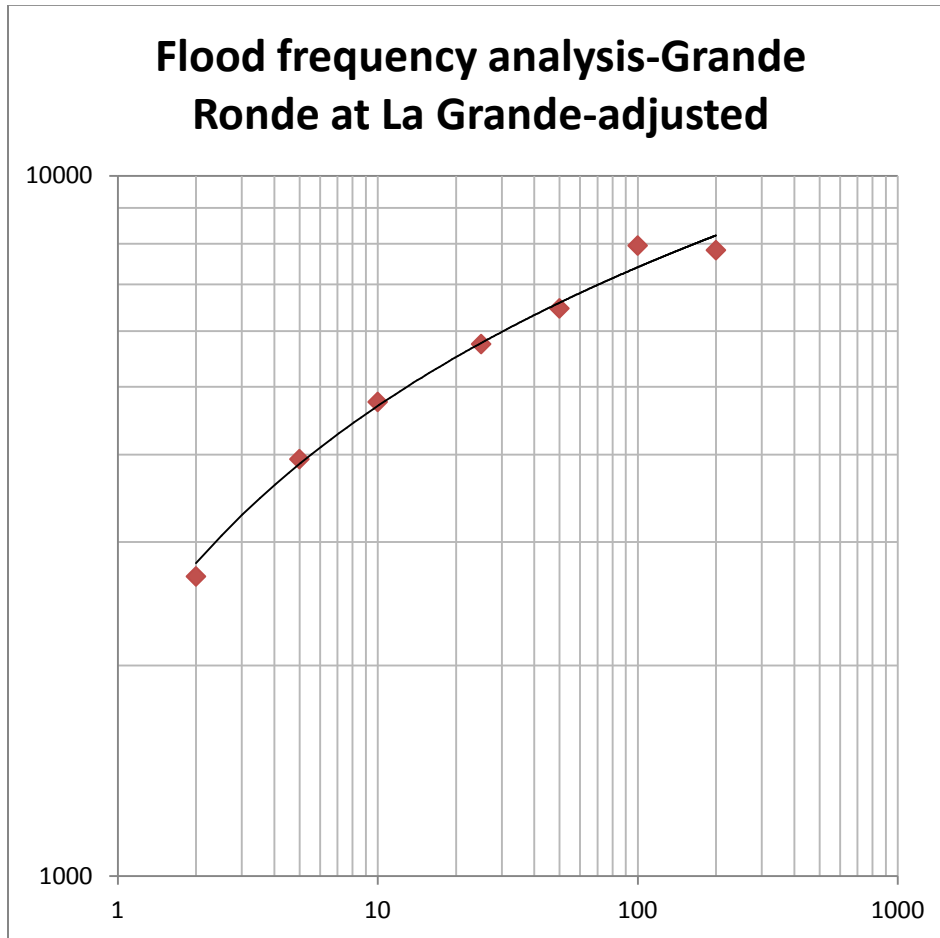
Year	Max	Min	Mean	Rank by Max	log Q (cfs)	(log Q - avg(log Q) ²	(log Q - avg(log Q) ³	Return Period [(n+1)/m]	Probab ility (1/Tr)
1978	9193	21	605.9	1	3.96	0.298	0.163	92.00	0.0109
1997	8995	23	818.8	2	3.95	0.288	0.154	46.00	0.0217
1995	6658	21	548.0	3	3.82	0.165	0.067	30.67	0.0326
1991	6596	22	352.4	4	3.82	0.161	0.065	23.00	0.0435
1983	5177	31	685.8	5	3.71	0.088	0.026	18.40	0.0543
1965	5006	20	537.9	6	3.70	0.080	0.022	15.33	0.0652
1996	4977	19	688.5	7	3.70	0.078	0.022	13.14	0.0761
1986	4925	19	476.9	8	3.69	0.076	0.021	11.50	0.0870
1956	4768	21	593.0	9	3.68	0.068	0.018	10.22	0.0978
1974	4595	20	670.0	10	3.66	0.060	0.015	9.20	0.1087
1998	4307	24	439.5	11	3.63	0.047	0.010	8.36	0.1196
1969	4212	20	458.0	12	3.62	0.043	0.009	7.67	0.1304
1993	4137	20	442.7	13	3.62	0.040	0.008	7.08	0.1413
1984	3996	29	718.0	14	3.60	0.034	0.006	6.57	0.1522
1931	3977	10	256.0	15	3.60	0.033	0.006	6.13	0.1630
1942	3929	27	591.0	16	3.59	0.031	0.006	5.75	0.1739
2005	3752	9	276.9	17	3.57	0.025	0.004	5.41	0.1848
1976	3709	23	392.8	18	3.57	0.023	0.003	5.11	0.1957
1958	3697	21	558.0	19	3.57	0.023	0.003	4.84	0.2065
1927	3549	25	540.2	20	3.55	0.018	0.002	4.60	0.2174
1970	3547	22	488.1	21	3.55	0.018	0.002	4.38	0.2283
1943	3538	22	498.0	22	3.55	0.017	0.002	4.18	0.2391
1921	3530	20	491.5	23	3.55	0.017	0.002	4.00	0.2500
1980	3510	21	462.1	24	3.55	0.016	0.002	3.83	0.2609
1940	3499	16	396.0	25	3.54	0.016	0.002	3.68	0.2717
2003	3485	18	453.3	26	3.54	0.016	0.002	3.54	0.2826
1916	3449	22	551.6	27	3.54	0.014	0.002	3.41	0.2935
1988	3382	18	269.1	28	3.53	0.012	0.001	3.29	0.3043
1981	3308	23	495.9	29	3.52	0.010	0.001	3.17	0.3152
1920	3302	23	447.8	30	3.52	0.010	0.001	3.07	0.3261
1953	3299	15	433.1	31	3.52	0.010	0.001	2.97	0.3370
1938	3282	18	419.1	32	3.52	0.010	0.001	2.88	0.3478
1952	3277	20	307.0	33	3.52	0.010	0.001	2.79	0.3587
1948	3205	36	543.0	34	3.51	0.008	0.001	2.71	0.3696
2004	3186	19	395.9	35	3.50	0.007	0.001	2.63	0.3804
1994	3180	14	281.9	36	3.50	0.007	0.001	2.56	0.3913
1982	3119	22	558.1	37	3.49	0.006	0.000	2.49	0.4022
2006	3050	20	455.0	38	3.48	0.004	0.000	2.42	0.4130
2000	3015	21	477.0	39	3.48	0.004	0.000	2.36	0.4239
1989	3009	18	379.6	40	3.48	0.004	0.000	2.30	0.4348
1979	2902	18	375.1	41	3.46	0.002	0.000	2.24	0.4457
1972	2874	20	446.0	42	3.46	0.002	0.000	2.19	0.4565
1941	2850	37	454.0	43	3.45	0.001	0.000	2.14	0.4674
1935	2805	11	260.0	44	3.45	0.001	0.000	2.09	0.4783
1957	2736	19	379.1	45	3.44	0.000	0.000	2.04	0.4891
1959	2685	25	498.1	46	3.43	0.000	0.000	2.00	0.5000
1990	2641	14	282.0	47	3.42	0.000	0.000	1.96	0.5109

1963	2568	22	381.1	48	3.41	0.000	0.000	1.92	0.5217
1951	2559	21	405.2	49	3.41	0.000	0.000	1.88	0.5326
1975	2548	18	321.0	50	3.41	0.000	0.000	1.84	0.5435
1917	2535	16	289.9	51	3.40	0.000	0.000	1.80	0.5543
1962	2500	19	282.1	52	3.40	0.000	0.000	1.77	0.5652
1925	2490	21	367.1	53	3.40	0.000	0.000	1.74	0.5761
1928	2460	20	405.0	54	3.39	0.001	0.000	1.70	0.5870
1960	2348	20	321.1	55	3.37	0.002	0.000	1.67	0.5978
1946	2333	24	368.0	56	3.37	0.002	0.000	1.64	0.6087
1932	2306	10	311.0	57	3.36	0.003	0.000	1.61	0.6196
1947	2263	25	357.9	58	3.35	0.004	0.000	1.59	0.6304
1918	2260	20	449.6	59	3.35	0.004	0.000	1.56	0.6413
1971	2221	24	414.0	60	3.35	0.005	0.000	1.53	0.6522
1999	2070	9	380.0	61	3.32	0.010	-0.001	1.51	0.6630
1954	2065	23	301.9	62	3.31	0.011	-0.001	1.48	0.6739
1933	2054	21	268.9	63	3.31	0.011	-0.001	1.46	0.6848
1949	1977	15	279.0	64	3.30	0.015	-0.002	1.44	0.6957
1922	1933	14	289.5	65	3.29	0.017	-0.002	1.42	0.7065
1961	1930	19	369.0	66	3.29	0.017	-0.002	1.39	0.7174
1923	1868	20	277.3	67	3.27	0.021	-0.003	1.37	0.7283
1967	1857	18	365.1	68	3.27	0.022	-0.003	1.35	0.7391
1945	1848	18	355.9	69	3.27	0.023	-0.003	1.33	0.7500
1937	1831	12	216.1	70	3.26	0.024	-0.004	1.31	0.7609
2001	1807	19	271.7	71	3.26	0.026	-0.004	1.30	0.7717
2002	1798	19	276.3	72	3.25	0.026	-0.004	1.28	0.7826
1936	1789	12	237.1	73	3.25	0.027	-0.004	1.26	0.7935
1929	1782	15	226.0	74	3.25	0.028	-0.005	1.24	0.8043
1964	1650	25	182.0	75	3.22	0.040	-0.008	1.23	0.8152
1944	1626	22	226.1	76	3.21	0.043	-0.009	1.21	0.8261
1987	1588	10	290.0	77	3.20	0.047	-0.010	1.19	0.8370
1926	1565	19	278.9	78	3.19	0.050	-0.011	1.18	0.8478
1985	1522	26	291.0	79	3.18	0.055	-0.013	1.16	0.8587
1992	1522	23	279.2	80	3.18	0.055	-0.013	1.15	0.8696
1930	1519	19	289.0	81	3.18	0.056	-0.013	1.14	0.8804
1950	1456	18	302.0	82	3.16	0.065	-0.016	1.12	0.8913
1924	1379	23	291.2	83	3.14	0.077	-0.021	1.11	0.9022
1934	1345	18	282.0	84	3.13	0.083	-0.024	1.10	0.9130
1968	1296	22	182.1	85	3.11	0.093	-0.028	1.08	0.9239
1919	1173	10	275.0	86	3.07	0.121	-0.042	1.07	0.9348
1939	1168	10	203.9	87	3.07	0.123	-0.043	1.06	0.9457
1955	1135	8	142.0	88	3.05	0.131	-0.048	1.05	0.9565
1977	1100	30	140.9	89	3.04	0.141	-0.053	1.03	0.9674
1973	970	9	178.9	90	2.99	0.186	-0.080	1.02	0.9783
1966	735	13	142.0	91	2.87	0.304	-0.168	1.01	0.9891

average	2929				3.42	3.871	0.011		
	Average				Average	Sum	Sum		

n	91
variance	0.0430
standard deviation	0.2074
skew coefficient	0.0016

Tr	K(0.0)	K(0.1)	slope	K(0.3460)	Q (cfs)
2	0.000	-0.017	-0.1662	0.050	2678
5	0.842	0.836	-0.0523	0.857	3938
10	1.282	1.292	0.1023	1.251	4753
25	1.751	1.785	0.3393	1.649	5749
50	2.054	2.107	0.5322	1.895	6464
100	2.326	2.400	0.7326	2.328	7948
200	2.576	2.670	0.9382	2.296	7829



Basin Statistics Calculated from Methodology in Risley et al. (2008) using USGS StreamStats Online Program.

Risley, J.C., A.Stonewall,, and T. Haluska. 2008. Estimating flow-duration and low-flow frequency statistics for unregulated streams in Oregon. U.S. Geological Survey Scientific Investigations Report 08-5126, 23 p.

Streamflow-gaging station No. Basin characteristics																					
Map No.	Region 1	A	ANT	AXT	DA	DD	E	F	G	I	JNT	JXT	NE	NS	P	R	S	SC	SP	XE	XS
276	13318500	nd	31.7	53.7	495.75	0.910	4,740	nd	0.0	0.05	18.0	32.9	3,060.5	0.00	26.2	4,863	11.2	0.155	1.25	7,923	48.3
277	13318800	nd	31.8	53.9	543.63	0.914	4,670	nd	0.0	0.05	18.2	33.1	3,001.4	0.00	26.2	4,922	11.1	0.155	1.24	7,923	48.3
278	13319000	nd	32.0	54.0	685.33	0.897	4,578	nd	0.0	0.05	18.5	33.1	2,831.3	0.00	26.4	5,092	11.2	0.153	1.23	7,923	52.6

Where the basic indices are defined as follows:

[BCF, biased correction factor; R2adj,
adjusted coefficient of determination;
SEE, standard error of the estimate;
SEM, standard error of the model;
SEP, standard error of the prediction;
P5, P10, P25, P50, and P95 are the 5th, 10th, 25th, 50th, and 95th flow-duration percentiles in cubic feet per second, respectively;
7Q2, 7-day 2-year low-flow statistic in cubic feet per second;
7Q10, 7-day 10-year low-flow statistic in cubic feet per second ;
A, percent of basin covered by high-permeability aquifer units;
ANT, annual minimum air temperature, in degrees Fahrenheit;
AXT, annual maximum air temperature, in degrees Fahrenheit ;
DA, drainage area, in square miles;
DD, drainage density, in kilometers per square kilometer;
E, mean elevation, in feet;
F, percent forest cover;
G, percent of basin covered by high-permeability geologic units;
I, percent impervious surface area;
JNT, January minimum air temperature, in degrees Fahrenheit ;
JXT, January maximum air temperature, in degrees Fahrenheit ;
NE, minimum elevation, in feet; NS, minimum slope, in degrees;
P, mean annual precipitation, in inches;
R, basin relief, in feet;
S, mean slope, in degrees;
SC, soil capacity, in inches per inch;
SP, soil permeability, in inches per hour;
XE, maximum elevation, in feet; and
XS, maximum slope, in degrees; na, not applicable]

P5 =	1.04267	$\times 10^{-5.2458}$	$\times (\text{DA})^{0.9215}$	$\times (\text{P})^{1.6820}$	$\times (\text{XE})^{0.8931}$	
P10 =	1.03437	$\times 10^{-5.7404}$	$\times (\text{DA})^{0.9430}$	$\times (\text{P})^{1.8401}$	$\times (\text{XE})^{0.9049}$	
P25 =	1.03315	$\times 10^{-4.8728}$	$\times (\text{DA})^{1.0024}$	$\times (\text{P})^{1.9626}$	$\times (\text{XE})^{0.4984}$	
P50 =	1.07898	$\times 10^{-7.8192}$	$\times (\text{DA})^{0.9871}$	$\times (\text{P})^{2.6103}$	$\times (\text{XE})^{0.8823}$	
P95 =	1.25149	$\times 10^{-10.3790}$	$\times (\text{DA})^{0.8888}$	$\times (\text{P})^{3.1176}$	$\times (\text{XE})^{1.2801}$	
7Q2 =	1.22093908	$\times 10^{-10.0921}$	$\times (\text{DA})^{0.9904}$	$\times (\text{P})^{2.6695}$	$\times (\text{DD})^{-2.0861}$	$\times (\text{E})^{1.3225}$
7Q10 =	1.295293875	$\times 10^{-9.5867}$	$\times (\text{DA})^{0.9689}$	$\times (\text{P})^{2.7912}$	$\times (\text{DD})^{-2.4791}$	$\times (\text{E})^{1.0945}$

Map No.	Streamflow-gaging station No.	Annual						
	Region 1	P5	P10	P25	P50	P95	7Q2	7Q10
276	13318500	1,101.06	792.17	355.26	81.00	16.08	15.37	8.72
277	13318800	nu	nu	nu	nu	nu	nu	nu
278	13319000	1,774.35	1,080.00	446.69	90.00	20.35	19.31	10.07
a 100-year flood freq. is a flow exceeded <1% of the time or a P1								
a 50-year flood freq. is a flow exceeded <2% of the time or a P1								
a 20-year flood freq. is a flow exceeded <5% of the time or a P1								

Table. --Description of basin characteristics used in regression equations to predict flow-duration and low-flow frequency statistics in Oregon. From: Risley, J.C., A.Stonewall,, and T. Haluska. 2008. Estimating flow-duration and low-flow frequency statistics for unregulated streams in Oregon. U.S. Geological Survey Scientific Investigations Report 08-5126, 23 p.

Basin characteristic (identifier)	Description
High-permeability aquifer units (A)	Percent basin surface area containing high permeability aquifer units; units defined as Tertiary-Quaternary sedimentary deposits, granitic saprolite of the Klamath Mountains (McFarland, 1983) and basin-fill and alluvial aquifers (Gonthier, 1985); estimated using ArcInfo Grid with a data layer created from a 1:500,000 map.
Annual minimum air temperature (ANT)	Mean annual minimum air temperature (1971-2000) over the basin surface area, in degrees Fahrenheit; estimated using ArcInfo Grid with a 800-meter resolution data layer created from the Parameter-elevation Regressions on Independent Slopes Model (PRISM). Source: http://www.prism.oregonstate.edu/ , accessed June 25, 2008.
Annual maximum air temperature (AXT)	Mean annual maximum air temperature (1971-2000) over the basin surface area, in degrees Fahrenheit; estimated using ArcInfo Grid with a 800-meter resolution data layer created from PRISM. Source: http://www.prism.oregonstate.edu/ , accessed June 25, 2008.
Drainage area (DA)	Total basin drainage area, in square miles; estimated using ArcInfo Grid with NHDPlus 30-meter resolution elevation data . Source: http://www.horizon-systems.com/NHDPlus/ , accessed June 25, 2008.
Drainage density (DD)	Basin drainage density; defined as total stream length divided by drainage area, in kilometers per square kilometer; estimated using ArcInfo Grid with NHDPlus 30-meter resolution elevation data . Source: http://www.horizon-systems.com/NHDPlus/ , accessed June 25, 2008.
Mean elevation (E)	Mean basin elevation, in feet above sea level; estimated using ArcInfo Grid with National Hydrography Dataset Plus (NHDPlus) 30-meter resolution elevation data . Source: http://www.horizon-systems.com/NHDPlus/ , accessed June 25, 2008.
Forest cover (F)	Percent basin surface area containing forest cover; estimated using ArcInfo Grid with 30-meter resolution data layers from the USGS National Land Cover Dataset (1992); forest categories included: deciduous, evergreen, and mixed. Source: http://landcover.usgs.gov/natl/landcover.php , accessed June 25, 2008.
High-permeability geologic units (G)	Percent basin surface area containing high permeability geologic units; units defined as Pliocene volcanic rocks, Upper Tertiary andesite, and Quaternary volcanic rocks; estimated using ArcInfo grid with a data layer created from a 1:2,500,000 map. Source: King and Beikman (1974), and http://pubs.usgs.gov/dds/dds11/ , accessed June 25, 2008.
Impervious surface area (I)	Percent impervious surface area of the basin; estimated using ArcInfo Grid with a 1000-meter resolution data layer from the National Geophysical Data Center, National Oceanic and Atmospheric Administration. Source: http://www.ngdc.noaa.gov/dmsp/download_sprawl.html , accessed June 25, 2008.
January minimum air temperature (JNT)	Mean January minimum air temperature (1971-2000) over the basin surface area, in degrees Fahrenheit; estimated using ArcInfo Grid with a 800-meter resolution data layer created from PRISM. Source: http://www.prism.oregonstate.edu/ , accessed June 25, 2008.
January maximum air temperature (JXT)	Mean January maximum air temperature (1971-2000) over the basin surface area, in degrees Fahrenheit; estimated using ArcInfo Grid with a 800-meter resolution data layer created from PRISM. Source: http://www.prism.oregonstate.edu/ , accessed June 25, 2008.

Minimum elevation (NE)	Minimum basin elevation, in feet above sea level; estimated using ArcInfo Grid with National Hydrography Dataset Plus (NHDPlus) 30-meter resolution elevation data . Source: http://www.horizon-systems.com/NHDPlus/ , accessed June 25, 2008.
Minimum slope (NS)	Minimum basin slope, in degrees; estimated using ArcInfo Grid with National Hydrography Dataset Plus (NHDPlus) 30-meter resolution elevation data . Source: http://www.horizon-systems.com/NHDPlus/ , accessed June 25, 2008.
Mean annual precipitation (P)	Mean annual precipitation (1971-2000) over the basin surface area, in inches; estimated using ArcInfo Grid with a 800-meter resolution data layer created from PRISM. Source: http://www.prism.oregonstate.edu/ , accessed June 25, 2008.
Relief (R)	Difference between the maximum and minimum basin elevations, in feet; estimated using ArcInfo Grid with National Hydrography Dataset Plus (NHDPlus) 30-meter resolution elevation data . Source: http://www.horizon-systems.com/NHDPlus/ , accessed June 25, 2008.
Mean slope (S)	Mean basin slope in degrees; estimated using ArcInfo Grid with National Hydrography Dataset Plus (NHDPlus) 30-meter resolution elevation data . Source: http://www.horizon-systems.com/NHDPlus/ , accessed June 25, 2008.
Soil storage capacity (SC)	Basin soil storage capacity, in inches per inch; estimated using ArcInfo Grid with a data layer created from a 1:250,000 State Soil Geographic (STATSGO) map. Source: http://www.soils.usda.gov/survey/geography/statsgo/ , accessed June 25, 2008.
Soil permeability (SP)	Basin soil permeability in inches per hour; estimated using ArcInfo Grid with a data layer created from a 1:250,000 STATSGO map. Source: http://www.soils.usda.gov/survey/geography/statsgo/ , accessed June 25, 2008.
Maximum elevation (XE)	Maximum basin elevation, in feet above sea level; estimated using ArcInfo Grid with National Hydrography Dataset Plus (NHDPlus) 30-meter resolution elevation data . Source: http://www.horizon-systems.com/NHDPlus/ , accessed June 25, 2008.
Maximum slope (XS)	Maximum basin slope, in degrees; estimated using ArcInfo Grid with National Hydrography Dataset Plus (NHDPlus) 30-meter resolution elevation data . Source: http://www.horizon-systems.com/NHDPlus/ , accessed June 25, 2008.

Basin characteristic (identifier)	Description
High-permeability aquifer units (A)	Percent basin surface area containing high permeability aquifer units; units defined as Tertiary-Quaternary sedimentary deposits, granitic saprolite of the Klamath Mountains (McFarland, 1983) and basin-fill and alluvial aquifers (Gonthier, 1985); estimated using ArcInfo Grid with a data layer created from a 1:500,000 map.
Annual minimum air temperature (ANT)	Mean annual minimum air temperature (1971-2000) over the basin surface area, in degrees Fahrenheit; estimated using ArcInfo Grid with a 800-meter resolution data layer created from the Parameter-elevation Regressions on Independent Slopes Model (PRISM). Source: http://www.prism.oregonstate.edu/ , accessed June 25, 2008.
Annual maximum air temperature (AXT)	Mean annual maximum air temperature (1971-2000) over the basin surface area, in degrees Fahrenheit; estimated using ArcInfo Grid with a 800-meter resolution data layer created from PRISM. Source: http://www.prism.oregonstate.edu/ , accessed June 25, 2008.
Drainage area (DA)	Total basin drainage area, in square miles; estimated using ArcInfo Grid with NHDPlus 30-meter resolution elevation data . Source: http://www.horizon-systems.com/NHDPlus/ , accessed June 25, 2008.
Drainage density (DD)	Basin drainage density; defined as total stream length divided by drainage area, in kilometers per square kilometer; estimated using ArcInfo Grid with NHDPlus 30-meter resolution elevation data . Source: http://www.horizon-systems.com/NHDPlus/ , accessed June 25, 2008.
Mean elevation (E)	Mean basin elevation, in feet above sea level; estimated using ArcInfo Grid with National Hydrography Dataset Plus (NHDPlus) 30-meter resolution elevation data . Source: http://www.horizon-systems.com/NHDPlus/ , accessed June 25, 2008.
Forest cover (F)	Percent basin surface area containing forest cover; estimated using ArcInfo Grid with 30-meter resolution data layers from the USGS National Land Cover Dataset (1992); forest categories included: deciduous, evergreen, and mixed. Source: http://landcover.usgs.gov/natl/landcover.php , accessed June 25, 2008.
High-permeability geologic units (G)	Percent basin surface area containing high permeability geologic units; units defined as Pliocene volcanic rocks, Upper Tertiary andesite, and Quaternary volcanic rocks; estimated using ArcInfo grid with a data layer created from a 1:2,500,000 map. Source: King and Beikman (1974), and http://pubs.usgs.gov/dds/dds11/ , accessed June 25, 2008.
Impervious surface area (I)	Percent impervious surface area of the basin; estimated using ArcInfo Grid with a 1000-meter resolution data layer from the National Geophysical Data Center, National Oceanic and Atmospheric Administration. Source: http://www.ngdc.noaa.gov/dmsp/download_sprawl.html , accessed June 25, 2008.
January minimum air temperature (JNT)	Mean January minimum air temperature (1971-2000) over the basin surface area, in degrees Fahrenheit; estimated using ArcInfo Grid with a 800-meter resolution data layer created from PRISM. Source: http://www.prism.oregonstate.edu/ , accessed June 25, 2008.
January maximum air temperature (JXT)	Mean January maximum air temperature (1971-2000) over the basin surface area, in degrees Fahrenheit; estimated using ArcInfo Grid with a 800-meter resolution data layer created from PRISM. Source: http://www.prism.oregonstate.edu/ , accessed June 25, 2008.
Minimum elevation (NE)	Minimum basin elevation, in feet above sea level; estimated using ArcInfo Grid with National Hydrography Dataset Plus (NHDPlus) 30-meter resolution elevation data . Source: http://www.horizon-systems.com/NHDPlus/ , accessed June 25, 2008.
Minimum slope (NS)	Minimum basin slope, in degrees; estimated using ArcInfo Grid with National Hydrography Dataset Plus (NHDPlus) 30-meter resolution elevation data . Source: http://www.horizon-systems.com/NHDPlus/ , accessed June 25, 2008.
Mean annual precipitation (P)	Mean annual precipitation (1971-2000) over the basin surface area, in inches; estimated using ArcInfo Grid with a 800-meter resolution data layer created from PRISM. Source: http://www.prism.oregonstate.edu/ , accessed June 25, 2008.
Relief (R)	Difference between the maximum and minimum basin elevations, in feet; estimated using ArcInfo Grid with National Hydrography Dataset Plus (NHDPlus) 30-meter resolution elevation data . Source: http://www.horizon-systems.com/NHDPlus/ , accessed June 25, 2008.
Mean slope (S)	Mean basin slope in degrees; estimated using ArcInfo Grid with National Hydrography Dataset Plus (NHDPlus) 30-meter resolution elevation data . Source: http://www.horizon-systems.com/NHDPlus/ , accessed June 25, 2008.
Soil storage capacity (SC)	Basin soil storage capacity, in inches per inch; estimated using ArcInfo Grid with a data layer created from a 1:250,000 State Soil Geographic (STATSGO) map. Source: http://www.soils.usda.gov/survey/geography/statsgo/ , accessed June 25, 2008.
Soil permeability (SP)	Basin soil permeability in inches per hour; estimated using ArcInfo Grid with a data layer created from a 1:250,000 STATSGO map. Source: http://www.soils.usda.gov/survey/geography/statsgo/ , accessed June 25, 2008.
Maximum elevation (XE)	Maximum basin elevation, in feet above sea level; estimated using ArcInfo Grid with National Hydrography Dataset Plus (NHDPlus) 30-meter resolution elevation data . Source: http://www.horizon-systems.com/NHDPlus/ , accessed June 25, 2008.

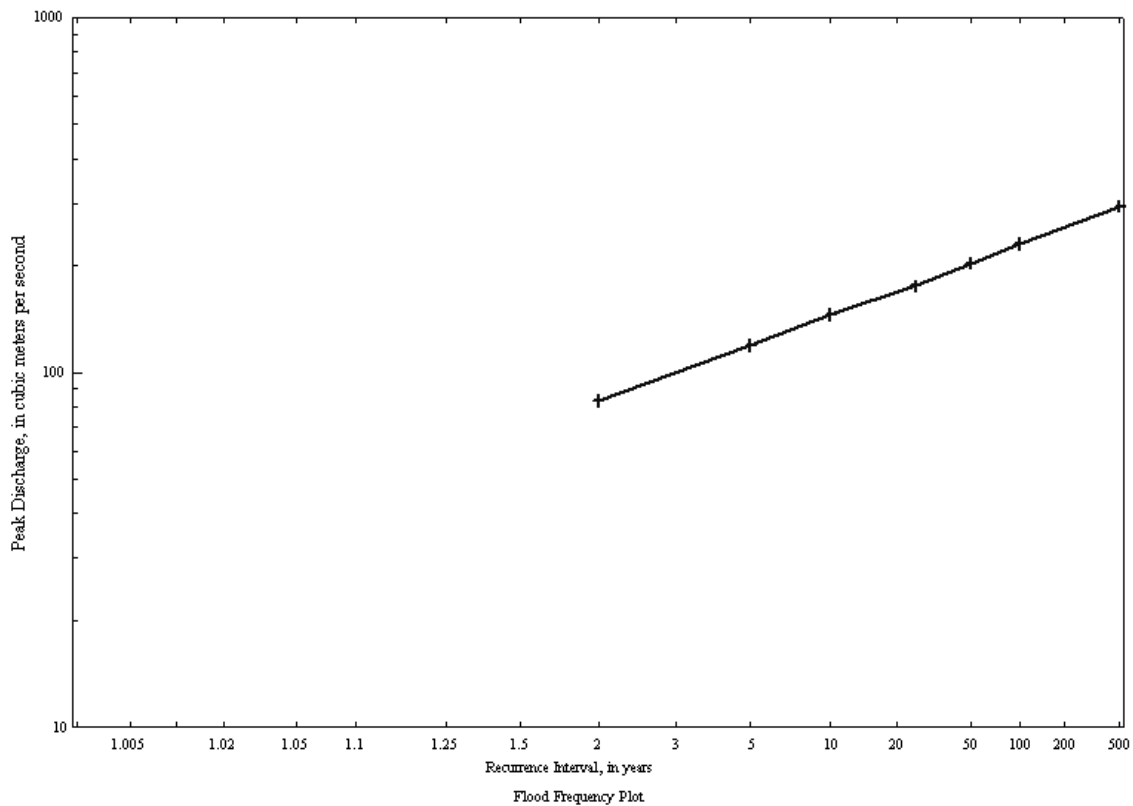
Calculation of flow statistics for gauge 13319000 using NSS (StreamStats) with physical characteristics from Risley and USGS via StreamStats

Source for NSS program: <http://water.usgs.gov/software/NSS/>

Rural 3
Basin Drainage Area: 1770 km²
1 Region
Region: Northeast_Region_Harris_1979
Drainage_Area = 1770 km²
Mean_Annual_Precipitation = 671 mm
Percent_Area_of_Forest_Cover = 68.4 percent
Crippen & Bue Region 15

Value, Standard			
Statistic	m ³ /s	Error %	ft ³ /s
PK2	83.1	65	2934.6
PK5	119	64	4202.4
PK10	145	66	5120.6
PK25	175	71	6180.1
PK50	203	72	7168.9
PK100	230	79	8122.4
PK500	294 *		

*Extrapolated value
maximum: 14800 (for C&B region 15)



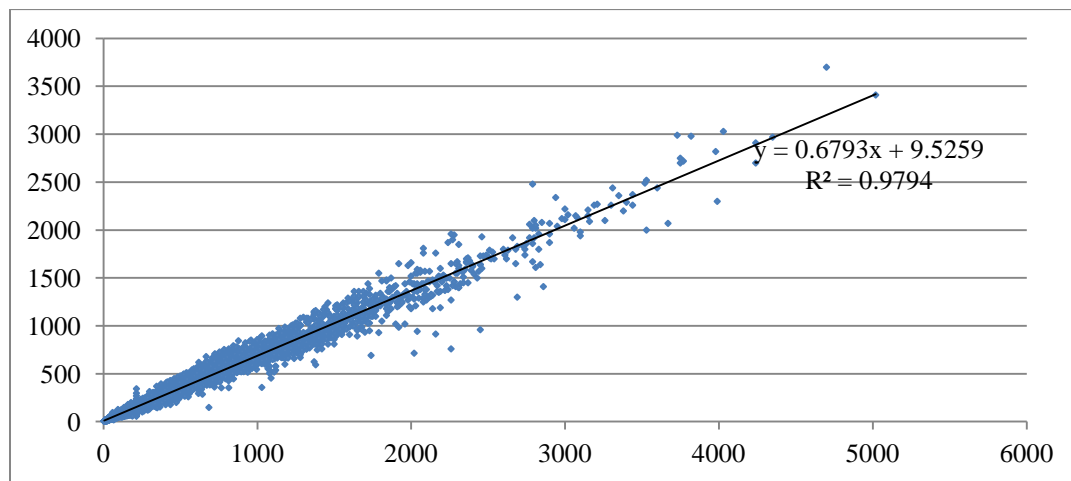
Appendix N.

Correlations among USGS stream gauges in the Grande Ronde River and Catherine Creek and selected statistics for these long term gauges.

Appendix N. Correlations among USGS stream gauges in the Grande Ronde River and Catherine Creek and selected statistics for these long term gauges.

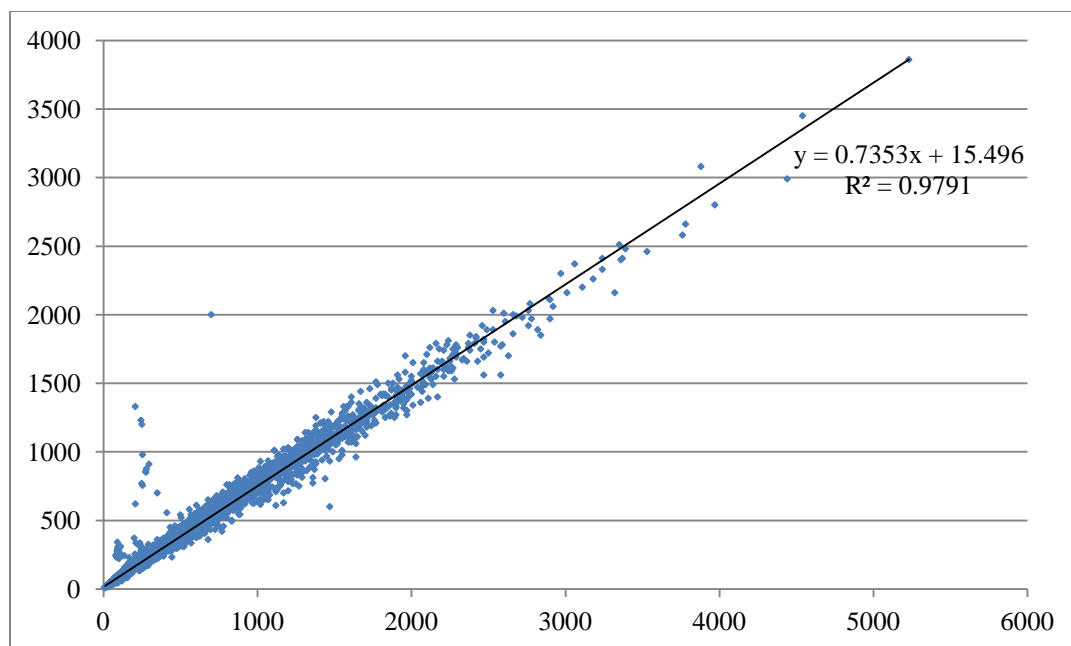
Comparison of USGS 13318500 GRANDE RONDE RIVER NEAR HILGARD, OREG. against USGS 13319000 GRANDE RONDE R AT LA GRANDE, OREG.

Regression of 13318500 on 13319000 using USGS data (see <http://waterdata.usgs.gov/or/nwis>)



Comparison of USGS 13318800 GRANDE RONDE RIVER AT HILGARD, OREG. against USGS 13319000 GRANDE RONDE R AT LA GRANDE, OREG.

Regression of 13318800 on 13319000 using USGS data (see <http://waterdata.usgs.gov/or/nwis>)



See file: Comparison of 3 UGR USGS gauges.xlsx

Comparison of Catherine Creek, OR gauge 13320000 vs. Grande Ronde at La Grande, OR gauge 13319000.

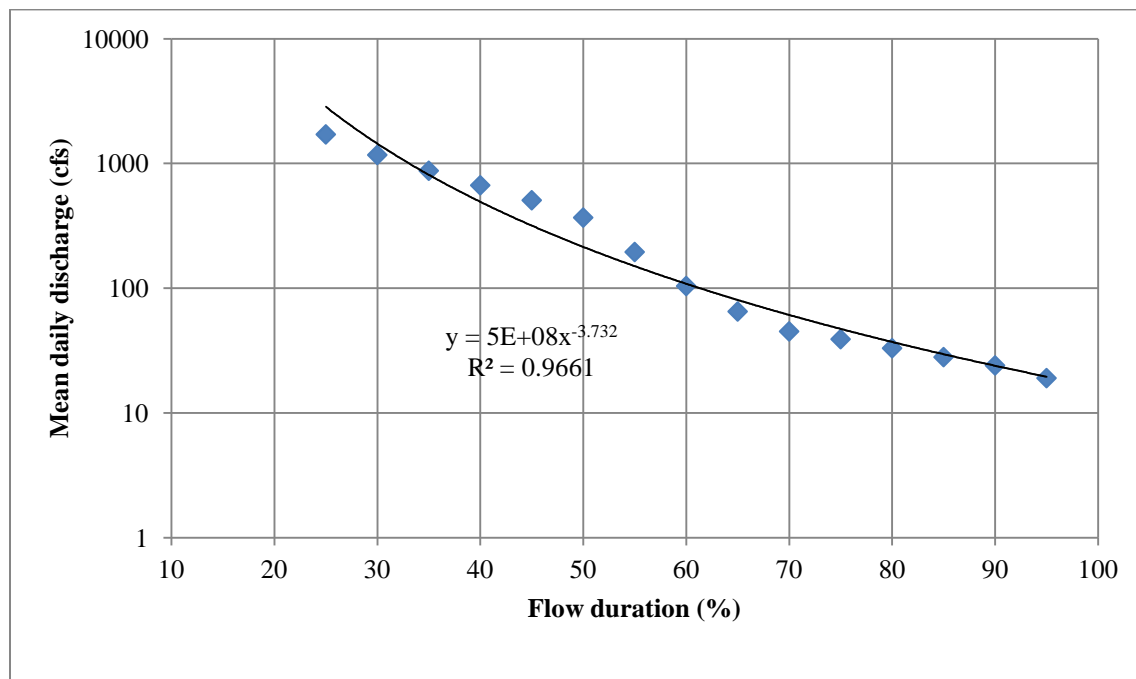
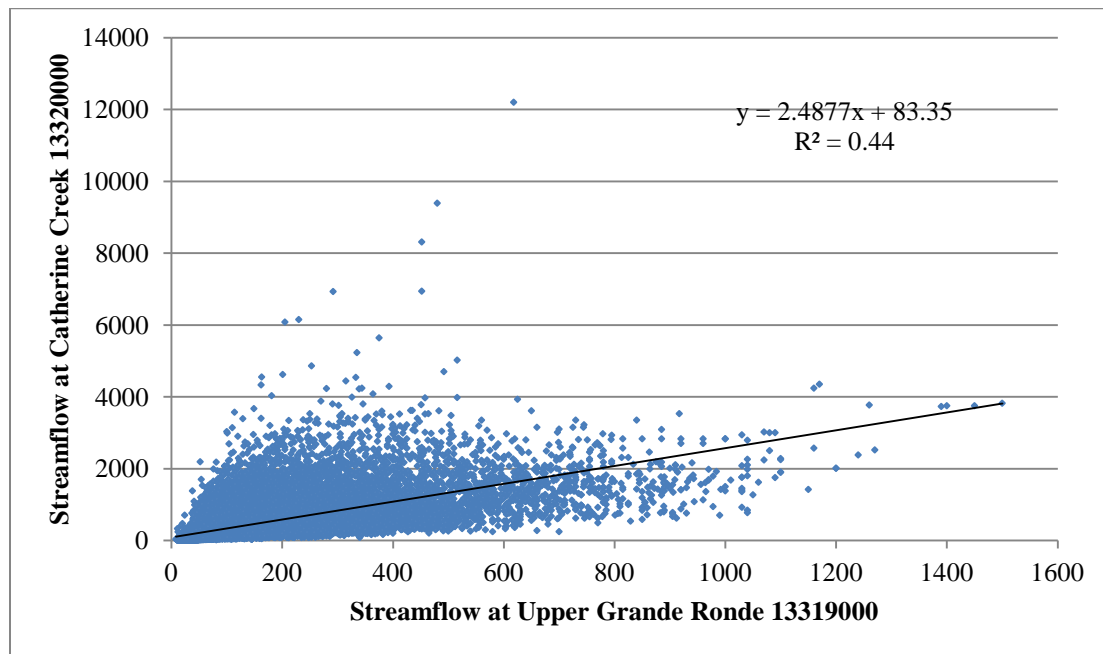


Figure xx. Flow duration curve for USGS gauge 13319000 using statistics from OWRD (http://apps.wrd.state.or.us/apps/sw/hydro_report/default.aspx)

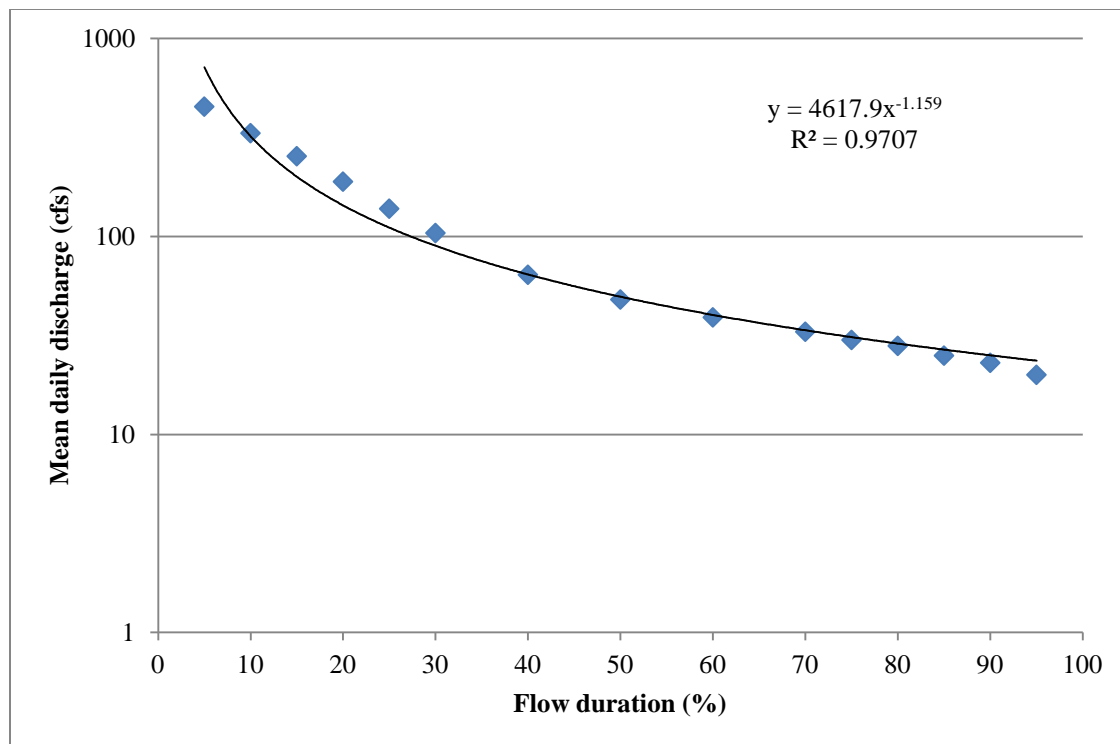


Figure xx. Flow duration curve for USGS gauge 13320000 using statistics from OWRD (http://apps.wrd.state.or.us/apps/sw/hydro_report/default.aspx)

Good Sources of Information on Basin Characteristics

HUC-8 digit code

17060104 Upper Grande Ronde River PDF | DOC 13-Sep-05

<http://www.or.nrcs.usda.gov/technical/huc-snake.html>

Good information available by HUC code

<http://www.climatesource.com/>

Source of climate data--PRISM data at highest resolution

To go to interactive map to acquire information for an ungauged site:

http://streamstatsags.cr.usgs.gov/or_ss/default.aspx?stabbr=or&dt=1302734027593

<http://water.usgs.gov/osw/streamstats/oregon.html>

Using StreamStats with address above to calculate basin stats for the 13319000 gauge location

<http://www.netmaptools.org/node/27>

Appendix O.

Upper Grande Ronde River Basin Stream Temperature Modeling: Scenarios

Upper Grande Ronde River Basin Stream Temperature Modeling



Prepared for:

Columbia River Inter-Tribal Fish Commission

729 NE Oregon Street, Suite 200
Portland, Oregon 97232

Prepared by:

Watershed Sciences, Inc.

529 SW Third Avenue, Suite 300
Portland, OR 97204



March 29, 2012

TABLE OF CONTENTS

1. Overview and Scope	1
2. Data Summary	2
2.1 Remote Sensing Data	2
2.1.1 LiDAR.....	2
2.1.2 Thermal Infrared.....	6
2.2 Ground Level Data	9
2.2.1 Hourly Temperature Data	9
2.2.2 Seasonal Variation.....	10
2.2.3 Instantaneous Flow Data	11
2.2.4 Gaged Flow Data.....	12
2.2.5 Climate Data	13
3. GIS Data Sampling for Heat Source Input - TTools.....	15
3.1 Stream Mapping	17
3.2 Wetted Edge Mapping	18
3.3 Active Channel Mapping	19
3.4 Near Stream Land Cover Mapping.....	20
3.5 Automated GIS Sampling - TTools.....	21
3.5.1 TTools Step 1	21
3.5.2 TTools Step 2	22
3.5.3 TTools Step 3	22
3.5.4 TTools Step 4	23
3.5.5 TTools Step 5	24
3.5.6 TTools Step 6	25
4. Heat Source Overview	26
5. Model Set Up and Calibration	32
5.1 North Fork Catherine Creek.....	33
5.1.1 North Fork Catherine Creek TTools	34
5.1.2 North Fork Catherine Creek Heat Source Calibration	37
5.2 South Fork Catherine Creek.....	42
5.2.1 South Fork Catherine Creek TTools Results.....	43
5.2.2 South Fork Catherine Creek Heat Source Calibration	46
5.3 Milk Creek	51
5.3.1 Milk Creek TTools Results	52
5.3.2 Milk Creek Heat Source Calibration Results.....	55
5.4 Little Catherine Creek	59
5.4.1 Little Catherine Creek TTools Results	60

5.4.2 Little Catherine Creek Effective Shade Simulation	63
5.5 Little Creek	65
5.5.1 Little Creek TTools Results	66
5.5.2 Little Creek Heat Source Calibration Results	69
5.6 Ladd Creek	74
5.6.1 Ladd Creek TTools Results	75
5.6.2 Ladd Creek Effective Shade Simulation.....	78
5.7 Catherine Creek	81
5.7.1 Catherine Creek TTools Results	82
5.7.2 Catherine Creek Heat Source Calibration Results	85
5.8 Clear Creek	91
5.8.1 Clear Creek TTools Results.....	92
5.8.2 Clear Creek Heat Source Calibration Results	95
5.9 Limber Jim Creek	99
5.9.1 Limber Jim Creek TTools Results	100
5.9.2 Limber Jim Creek Heat Source Calibration Results.....	103
5.10 Chicken Creek.....	109
5.10.1 Chicken Creek TTools Results.....	110
5.10.2 Chicken Creek Heat Source Calibration Results	114
5.11 Sheep Creek	118
5.11.1 Sheep Creek TTools Results	119
5.11.2 Sheep Creek Heat Source Calibration Results.....	122
5.12 Fly Creek.....	127
5.12.1 Fly Creek TTools Results	128
5.12.2 Fly Creek Heat Source Calibration Results	131
5.13 McCoy Creek.....	136
5.13.1 McCoy Creek TTools Results.....	137
5.13.2 McCoy Creek Heat Source Calibration Results	140
5.14 Meadow Creek	142
5.14.1 Meadow Creek TTools Results.....	143
5.14.2 Meadow Creek Heat Source Calibration Results	146
5.15 Beaver Creek	153
5.15.1 Beaver Creek TTools Results	154
5.15.2 Beaver Creek Heat Source Calibration Results.....	157
5.16 Five Points Creek	162
5.16.1 Five Points Creek TTools Results	163
5.16.2 Five Points Creek Heat Source Calibration Results.....	166
5.17 Grande Ronde River	171
5.17.1 Grande Ronde River TTools Results	172

5.17.2 Grande Ronde River Heat Source Calibration Results	175
6. Simulated Scenarios	187
6.1 North Fork Catherine Creek.....	189
6.2 South Fork Catherine Creek.....	190
6.3 Milk Creek	191
6.4 Little Catherine Creek	192
6.5 Little Creek	193
6.6 Ladd Creek	194
6.7 Catherine Creek.....	195
6.8 Clear Creek	196
6.9 Limber Jim Creek	197
6.10 Chicken Creek.....	198
6.11 Sheep Creek	199
6.12 Fly Creek	200
6.13 McCoy Creek.....	201
6.14 Meadow Creek	202
6.15 Beaver Creek	203
6.16 Five Points Creek	204
6.17 Grande Ronde River.....	205

LIST OF FIGURES

Figure 1 - Streams of interest in the upper Grande Ronde River subbasin.....	1
Figure 2 - LiDAR data coverage.	2
Figure 3 - LiDAR point cloud cross section over Beaver Creek.	3
Figure 4 - LiDAR point cloud with RGB extraction (top) and bare earth digital terrain model (bottom). .	4
Figure 5 - LiDAR digital elevation model of the Grande Ronde River near Hilgard.	5
Figure 6 - TIR data extents.	6
Figure 7 - Example of a TIR longitudinal stream temperature profile.	6
Figure 8 - Example of TIR imagery.	7
Figure 9 - Example of TIR imagery overlaid on LiDAR bare earth DTM.	8
Figure 10 - Example of TIR imagery where there is an active diversion.....	8
Figure 11 - Hourly stream temperature monitoring locations.	9
Figure 12 - Example of hourly temperature data collected by CRITFC.	9
Figure 13 - Grande Ronde River stream temperature variability during the summer of 2010.	10
Figure 14 - Catherine Creek stream temperature variability during the summer of 2010.	10
Figure 15 - Instantaneous flow measurement locations.	11
Figure 16 - Flow gage locations.	12
Figure 17- Climate station locations.	13
Figure 18 - Hourly cloud cover values recorded at La Grande airport.	13
Figure 19 - Hourly air temperature, wind speed and relative humidity data.....	14
Figure 20 - TTools sampling extents	15
Figure 21 - General workflow to prepare Heat Source model inputs.	16
Figure 22 - Raw stream polyline.	17
Figure 23 - Smoothed stream polyline.	17
Figure 24 - Stream polyline overlaid on LiDAR intensity image.	18
Figure 25 - Estimated wetted area based on LiDAR intensity image.	18
Figure 26 - Wetted channel edges (yellow) and active channel edges (red).	19
Figure 27 - Manually digitized near stream land cover polygons.	20
Figure 28 - 50-meter stream segments (yellow dots).	21
Figure 29 - Stream channel edges and the TTools point shapefile.	22
Figure 30 - Stream elevations sampled at each 50-meter node.	22
Figure 31 - Topographic features to the west (green triangles), south (red circles) and east (white squares).	23
Figure 32 - Near stream land cover radial sampling pattern.	24
Figure 33 - Example of 50-meter stream nodes and TIR data points.....	25
Figure 34 - Parameters included within the Heat Source methodology.	26
Figure 35 - Example of the TTools data input worksheet in Heat Source.	27
Figure 36 - Example of the continuous data input worksheet in Heat Source.....	28
Figure 37 - Example of the morphology data input worksheet in Heat Source.....	28
Figure 38 - Example of the longitudinal temperature output worksheet in Heat Source.	29
Figure 39 - Example of the hydraulics output worksheet in Heat Source.	30
Figure 40 - Example of heat flux output worksheet in Heat Source.....	31
Figure 41 - North Fork Catherine Creek elevation and gradient.	34
Figure 42 - North Fork Catherine Creek wetted width.....	34
Figure 43 - North Fork Catherine Creek stream aspect.....	35
Figure 44 - North Fork Catherine Creek topographic shade angles.....	35
Figure 45 - North Fork Catherine Creek land cover heights sampled from highest hit LiDAR.	36
Figure 46 - North Fork Catherine Creek TIR temperature profile.....	36
Figure 47 - North Fork Catherine Creek simulation extent.	37
Figure 48 - North Fork Catherine Creek simulated and measured hydraulics values.....	38
Figure 49 - North Fork Catherine Creek simulated and measured daily flow volumes at the gage near Medical Springs.	39
Figure 50 - North Fork Catherine Creek longitudinal stream temperature calibration.	40
Figure 51 - North Fork Catherine Creek simulated effective shade.	41

Figure 52 - South Fork Catherine Creek elevation and gradient.	43
Figure 53 - South Fork Catherine Creek wetted width.....	43
Figure 54 - South Fork Catherine Creek stream aspect.	44
Figure 55 - South Fork Catherine Creek topographic shade angles.	44
Figure 56 - South Fork Catherine Creek land cover heights sampled from highest hit LiDAR.	45
Figure 57 - South Fork Catherine Creek TIR stream temperature profile.	45
Figure 58 - South Fork Catherine Creek simulation extent.	46
Figure 59 - South Fork Catherine Creek simulated and measured hydraulic values.	47
Figure 60 - South Fork Catherine Creek simulated daily stream flow at the mouth.	48
Figure 61 - South Fork Catherine Creek simulated and measured stream temperature.	49
Figure 62 - South Fork Catherine Creek simulated and measured hourly temperatures.	49
Figure 63 - South Fork Catherine Creek simulated effective shade.	50
Figure 64 - Milk Creek stream elevation and gradient.	52
Figure 65 - Milk Creek stream aspect.	52
Figure 66 - Milk Creek topographic shade angles.	53
Figure 67 - Milk Creek TIR stream temperature profile.	53
Figure 68 - Milk Creek land cover heights sampled from highest hit LiDAR.	54
Figure 69 - Milk Creek simulation extent.....	55
Figure 70 - Milk Creek simulated and measured hydraulic values for 8/19/2010.....	56
Figure 71 - Milk Creek simulated daily stream flow at the mouth.....	57
Figure 72 - Milk Creek simulated and measured longitudinal temperatures.....	57
Figure 73 - Milk Creek simulated and measured hourly temperatures.....	58
Figure 74 - Milk Creek simulated effective shade values.....	58
Figure 75 - Little Catherine Creek elevation and gradient.....	60
Figure 76 - Little Catherine Creek stream aspect.	60
Figure 77 - Little Catherine Creek topographic shade angles.	61
Figure 78 - Little Catherine Creek TIR stream temperature profile.....	61
Figure 79 - Little Catherine Creek digitized near stream land cover.	62
Figure 80 - Little Catherine Creek simulation extent.	63
Figure 81 - Little Catherine Creek simulated effective shade.	64
Figure 82 - Little Creek elevation and gradient.....	66
Figure 83 - Little Creek stream aspect.	66
Figure 84 - Little Creek topographic shade angles.	67
Figure 85 - Little Creek land cover heights sampled from highest hit LiDAR.	67
Figure 86 - Little Creek TIR stream temperatures.....	68
Figure 87 - Little Creek simulation extent.	69
Figure 88 - Little Creek simulated and measured hydraulic values.	70
Figure 89 - Little Creek simulated flow volume at the mouth of Little Creek.	71
Figure 90 - Little Creek simulated and measured longitudinal temperatures.	72
Figure 91 - Little Creek simulated and measured hourly temperatures.	72
Figure 92 - Little Creek simulated effective shade.	73
Figure 93 - Ladd Creek elevation and gradient.	75
Figure 94 - Ladd Creek stream aspect.	75
Figure 95 - Ladd Creek topographic shade angles.	76
Figure 96 - Ladd Creek TIR stream temperature profile.	76
Figure 97 - Ladd Creek digitized near stream land cover.	77
Figure 98 - Ladd Creek simulation extent.....	78
Figure 99 - Ladd Creek simulated effective shade.	80
Figure 100 - Catherine Creek elevation and gradient.....	82
Figure 101 - Catherine Creek wetted widths.	82
Figure 102 - Catherine Creek stream aspect.	83
Figure 103 - Catherine Creek topographic shade angles.	83
Figure 104 - Catherine Creek land cover heights sampled from highest hit LiDAR.	84
Figure 105 - Catherine Creek TIR stream temperature profile.....	84
Figure 106 - Catherine Creek simulation extent.	85

Figure 107 - Catherine Creek simulated and measured hydraulic values.	86
Figure 108 - Catherine Creek simulated and measured daily flow volumes at select locations.	87
Figure 109 - Catherine Creek simulated and measured longitudinal temperatures.	88
Figure 110 - Catherine Creek simulated and measured hourly stream temperatures.	88
Figure 111 - Catherine Creek simulated effective shade values.	90
Figure 112 - Clear Creek elevation and gradient.	92
Figure 113 - Clear Creek stream aspect.	92
Figure 114 - Clear Creek topographic shade angles.	93
Figure 115 - Clear Creek land cover heights sampled from highest hit LiDAR.	93
Figure 116 - Clear Creek TIR stream temperature profile.	94
Figure 117 - Clear Creek simulation extent.	95
Figure 118 - Clear Creek simulated and measured hydraulics values for 8/19/2010.	96
Figure 119 - Clear Creek daily flow volumes at the mouth.	97
Figure 120 - Clear Creek simulated and measured longitudinal temperatures.	97
Figure 121 - Clear Creek simulated and measured hourly temperatures.	98
Figure 122 - Clear Creek simulated effective shade.	98
Figure 123 - Limber Jim Creek elevation and gradient.	100
Figure 124 - Limber Jim Creek stream aspect.	100
Figure 125 - Limber Jim Creek topographic shade angles.	101
Figure 126 - Limber Jim Creek land cover heights sampled from highest hit LiDAR.	101
Figure 127 - Limber Jim TIR stream temperature profile.	102
Figure 128 - Limber Jim Creek simulation extent.	103
Figure 129 - Limber Jim Creek simulated and measured hydraulic values.	104
Figure 130 - Limber Jim Creek simulated flows at the mouth.	105
Figure 131 - Limber Jim Creek simulated and measured longitudinal stream temperatures.	106
Figure 132 - Limber Jim Creek simulated and measured hourly stream temperatures.	107
Figure 133 - Limber Jim Creek simulated effective shade.	108
Figure 134 - Chicken Creek elevation and gradient.	110
Figure 135 - Chicken Creek stream aspect.	110
Figure 136 - Chicken Creek topographic shade angles.	111
Figure 137 - Chicken Creek TIR stream temperature profile.	111
Figure 138 - Chicken Creek digitized near stream land cover.	112
Figure 139 - Chicken Creek simulation extent.	114
Figure 140 - Chicken Creek simulated hydraulic values.	115
Figure 141 - Chicken Creek simulated flow volumes at the mouth.	116
Figure 142 - Chicken Creek simulated and measured longitudinal stream temperatures.	116
Figure 143 - Chicken Creek simulated effective shade.	117
Figure 144 - Sheep Creek elevation and gradient.	119
Figure 145 - Sheep Creek wetted widths.	119
Figure 146 - Sheep Creek stream aspect.	120
Figure 147 - Sheep Creek topographic shade angles.	120
Figure 148 - Sheep Creek land cover heights sampled from highest hit LiDAR.	121
Figure 149 - Sheep Creek TIR stream temperature profile.	121
Figure 150 - Sheep Creek simulation extent.	122
Figure 151 - Sheep Creek simulated and measured hydraulic values.	123
Figure 152 - Sheep Creek simulated flow volumes at the mouth.	124
Figure 153 - Sheep Creek simulated and measured longitudinal stream temperatures.	125
Figure 154 - Sheep Creek simulated and measured hourly stream temperatures.	125
Figure 155 - Sheep Creek simulated effective shade.	126
Figure 156 - Fly Creek elevation and gradient.	128
Figure 157 - Fly Creek wetted widths.	128
Figure 158 - Fly Creek stream aspect.	129
Figure 159 - Fly Creek topographic shade angles.	129
Figure 160 - Fly Creek land cover heights sampled from highest hit LiDAR.	130
Figure 161 - Fly Creek TIR stream temperature profile.	130

Figure 162 - Fly Creek simulation extent.	131
Figure 163 - Fly Creek simulated and measured hydraulic values.	132
Figure 164 - Fly Creek simulated flow volumes at the mouth.	133
Figure 165 - Fly Creek simulated and measured longitudinal stream temperatures.	134
Figure 166 - Fly Creek simulated and measured hourly stream temperatures.	134
Figure 167 - Fly Creek simulated effective shade.	135
Figure 168 - McCoy Creek elevation and gradient.	137
Figure 169 - McCoy Creek stream aspect.	137
Figure 170 - McCoy Creek topographic shade angles.	138
Figure 171 - McCoy Creek land cover heights sampled from highest hit LiDAR.	138
Figure 172 - McCoy Creek TIR stream temperature profile.	139
Figure 173 - McCoy Creek simulation extent.	140
Figure 174 - McCoy Creek simulated effective shade.	141
Figure 175 - McCoy Creek typical terrain and vegetation.	141
Figure 176 - Meadow Creek elevation and gradient.	143
Figure 177 - Meadow Creek wetted width.	143
Figure 178 - Meadow Creek stream aspect.	144
Figure 179 - Meadow Creek topographic shade angles.	144
Figure 180 - Meadow Creek land cover heights sampled from highest hit LiDAR.	145
Figure 181 - Meadow Creek TIR stream temperature profile.	145
Figure 182 - Meadow Creek simulation extent.	146
Figure 183 - Meadow Creek simulated and measured hydraulic values.	147
Figure 184 - Meadow Creek simulated flows at mouth.	148
Figure 185 - Meadow Creek simulated and measured longitudinal stream temperatures.	149
Figure 186 - Meadow Creek simulated and measured hourly stream temperatures.	149
Figure 187 - Meadow Creek simulated effective shade.	152
Figure 188 - Beaver Creek elevation and gradient.	154
Figure 189 - Beaver Creek wetted widths.	154
Figure 190 - Beaver Creek stream aspect.	155
Figure 191 - Beaver Creek topographic shade angles.	155
Figure 192 - Beaver Creek land cover heights sampled from highest hit LiDAR.	156
Figure 193 - Beaver Creek TIR stream temperature profile.	156
Figure 194 - Beaver Creek simulation extent.	157
Figure 195 - Beaver Creek simulated and measured hydraulic values.	158
Figure 196 - Beaver Creek simulated flows at the mouth.	159
Figure 197 - Beaver Creek simulated and measured longitudinal stream temperatures.	160
Figure 198 - Beaver Creek simulated and measured hourly stream temperatures.	160
Figure 199 - Beaver Creek simulated effective shade.	161
Figure 200 - Five Points Creek elevation and gradient.	163
Figure 201 - Five Points Creek wetted widths.	163
Figure 202 - Five Points Creek stream aspect.	164
Figure 203 - Five Points Creek topographic shade angles.	164
Figure 204 - Five Points Creek land cover heights sampled from highest hit LiDAR.	165
Figure 205 - Five Points Creek TIR stream temperature profile.	165
Figure 206 - Five Points Creek simulation extent.	166
Figure 207 - Five Points Creek simulated and measured hydraulic values.	167
Figure 208 - Five Points Creek simulated flow at mouth.	168
Figure 209 - Five Points Creek simulated and measured longitudinal stream temperatures.	169
Figure 210 - Five Points Creek simulated and measured hourly stream temperatures.	169
Figure 211 - Five Points Creek simulated effective shade.	170
Figure 212 - Grande Ronde River elevation and gradient.	172
Figure 213 - Grande Ronde River channel widths.	172
Figure 214 - Grande Ronde River stream aspect.	173
Figure 215 - Grande Ronde River topographic shade angles.	173
Figure 216 - Grande Ronde River TIR stream temperature profile.	174

Figure 217 - Grande Ronde River simulation extent.	175
Figure 218 - Grande Ronde River simulated and measured hydraulic values.	177
Figure 219 - Grande Ronde River simulated and measured flows at the gages.	178
Figure 220 - Grande Ronde River simulated and measured longitudinal stream temperatures.	179
Figure 221 - Grande Ronde River simulated and measured hourly stream temperatures.	179
Figure 222 - Grande Ronde River simulated effective shade.	185
Figure 223 - North Fork Catherine Creek simulated scenario results.	189
Figure 224 - North Fork Catherine Creek simulated effective shade.	189
Figure 225 - South Fork Catherine Creek simulated scenario results.	190
Figure 226 - South Fork Catherine Creek simulated effective shade.	190
Figure 227 - Milk Creek simulated scenario results.	191
Figure 228 - Milk Creek simulated effective shade.	191
Figure 229 - Little Catherine Creek simulated effective shade.	192
Figure 230 - Little Creek simulated scenario results.	193
Figure 231 - Little Creek simulated effective shade.	193
Figure 232 - Ladd Creek simulated effective shade.	194
Figure 233 - Catherine Creek simulated scenario results (from forks to City of Union).	195
Figure 234 - Catherine Creek simulated effective shade.	195
Figure 235 - Clear Creek simulated scenario results.	196
Figure 236 - Clear Creek simulated effective shade.	196
Figure 237 - Limber Jim Creek simulated scenario results.	197
Figure 238 - Limber Jim Creek simulated effective shade.	197
Figure 239 - Chicken Creek simulated scenario results.	198
Figure 240 - Chicken Creek simulated effective shade.	198
Figure 241 - Sheep Creek simulated scenario results.	199
Figure 242 - Sheep Creek simulated effective shade.	199
Figure 243 - Fly Creek simulated scenario results.	200
Figure 244 - Fly Creek simulated effective shade.	200
Figure 245 - McCoy Creek simulated effective shade.	201
Figure 246 - Meadow Creek simulated scenario results.	202
Figure 247 - Meadow Creek simulated effective shade.	202
Figure 248 - Beaver Creek simulated scenario results.	203
Figure 249 - Beaver Creek simulated effective shade.	203
Figure 250 - Five Points Creek simulated scenario results.	204
Figure 251 - Five Points Creek simulated effective shade.	204
Figure 252 - Grande Ronde River simulated scenario results.	205
Figure 253 - Grande Ronde River simulated effective shade.	205

LIST OF TABLES

Table 1 - LiDAR products and their applications for stream temperature modeling.	2
Table 2 - Stream flow gages within the study area.	12
Table 3 - Streams where TTools sampling was completed.	15
Table 4 - TTools steps and data sources.	21
Table 5 - North Fork Catherine Creek general Heat Source parameters.	37
Table 6 - North Fork Catherine Creek mass inflow locations and assumptions.	39
Table 7 - South Fork Catherine Creek general Heat Source parameters.	46
Table 8 - South Fork Catherine Creek mass inflow locations and assumptions.	48
Table 9 - Milk Creek general Heat Source parameters.	55
Table 10 - Little Catherine Creek general Heat Source parameters.	63
Table 11 - Little Catherine Creek land cover codes and descriptions.	64
Table 12 - Little Creek general Heat Source parameters.	69
Table 13 - Little Creek mass inflow features and assumptions.	71
Table 14 - Ladd Creek general Heat Source parameters.	78
Table 15 - Ladd Creek near stream land cover codes and descriptions.	79
Table 16 - Catherine Creek general Heat Source parameters.	85
Table 17 - Catherine Creek mass inflow and outflow features and assumptions.	87
Table 18 - Clear Creek general Heat Source parameters.	95
Table 19 - Limber Jim Creek general Heat Source parameters.	103
Table 20 - Limber Jim Creek mass inflow features and assumptions.	105
Table 21 - Chicken Creek near stream land cover codes and descriptions.	113
Table 22 - Chicken Creek general Heat Source parameters.	114
Table 23 - Sheep Creek general Heat Source parameters.	122
Table 24 - Chicken Creek mass inflow feature and assumption.	124
Table 25 - Fly Creek general Heat Source parameters.	131
Table 26 - Fly Creek mass inflows and assumptions.	133
Table 27 - McCoy Creek general Heat Source parameters.	140
Table 28 - Meadow Creek general Heat Source parameters.	146
Table 29 - Meadow Creek mass inflow features and assumptions.	148
Table 30 - Beaver Creek general Heat Source parameters.	157
Table 31 - Beaver Creek mass inflow features and assumptions.	159
Table 32 - Five Points Creek general Heat Source parameters.	166
Table 33 - Five Points Creek mass inflow features and assumptions.	168
Table 34 - Grande Ronde River general Heat Source parameters.	175
Table 35 - Grande Ronde River mass inflow and outflow features and assumptions.	178
Table 36 - Scenarios and Associated Assumptions.	187
Table 37 - Summary of scenarios that were run for each stream.	188

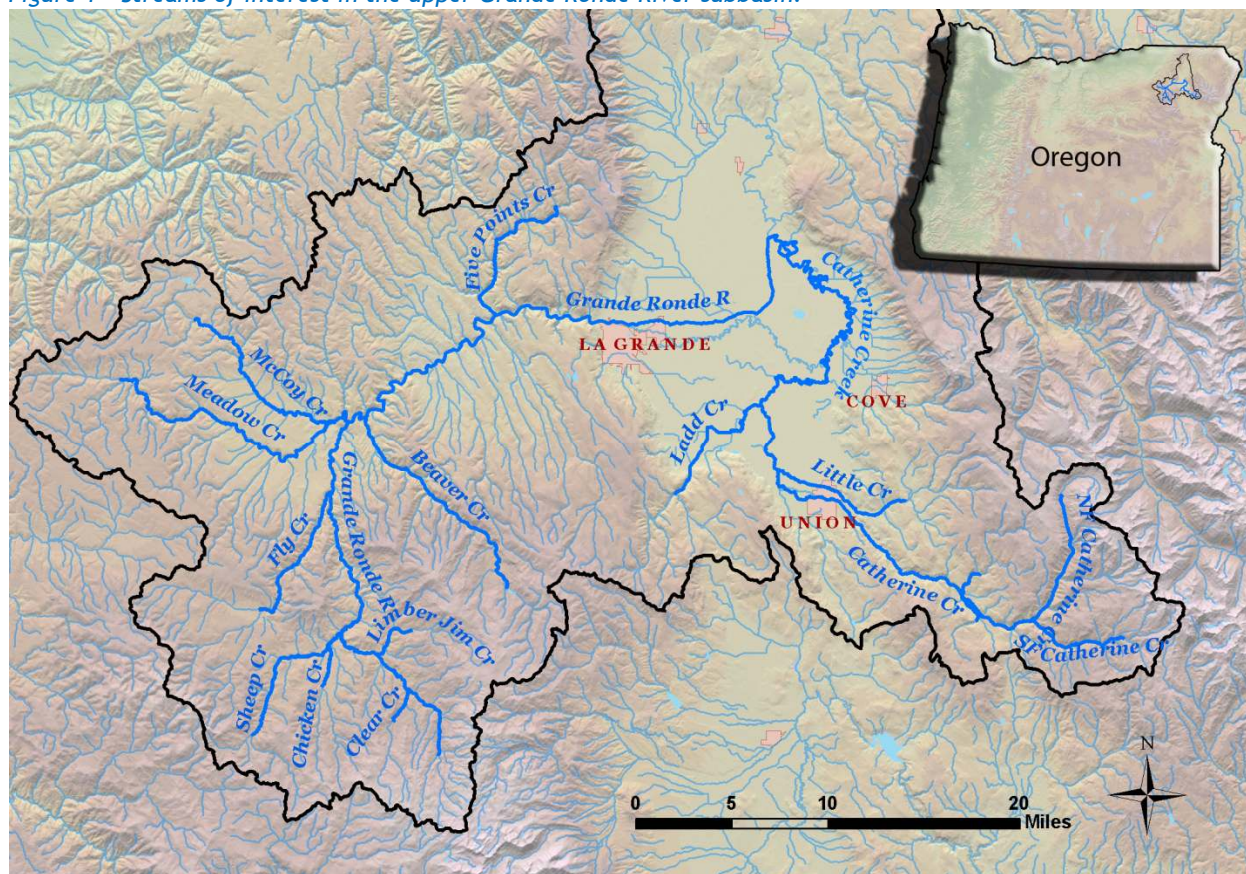
1. OVERVIEW AND SCOPE

The Columbia River Inter-Tribal Fish Commission (CRITFC) contracted with Watershed Sciences, Inc. (WSI) to collect LiDAR and thermal infrared data and simulate stream temperature in the upper Grande Ronde River subbasin in northeastern Oregon. This report summarizes the remote sensing and ground level data and describes the stream temperature modeling results.

The goal of the project was to collect high-resolution landscape and water quality data for use in the Heat Source stream temperature model. Stream temperature was simulated for the Grande Ronde River, Catherine Creek, and several of their tributaries for a 3-week period between August 6 and August 27, 2010. The simulation period is representative of low-flow and high stream temperature conditions, when salmonid habitat is at its most critical condition. A variety of scenarios were then simulated to estimate the influences of air temperature, flow, and vegetation on stream temperatures.

Figure 1 shows the location of the study area within northeastern Oregon. Approximately 247 stream miles were simulated above the confluence of Catherine Creek and the Grande Ronde River. The streams of interest are either historic or current salmonid habitat.

Figure 1 - Streams of interest in the upper Grande Ronde River subbasin.



2. DATA SUMMARY

2.1 Remote Sensing Data

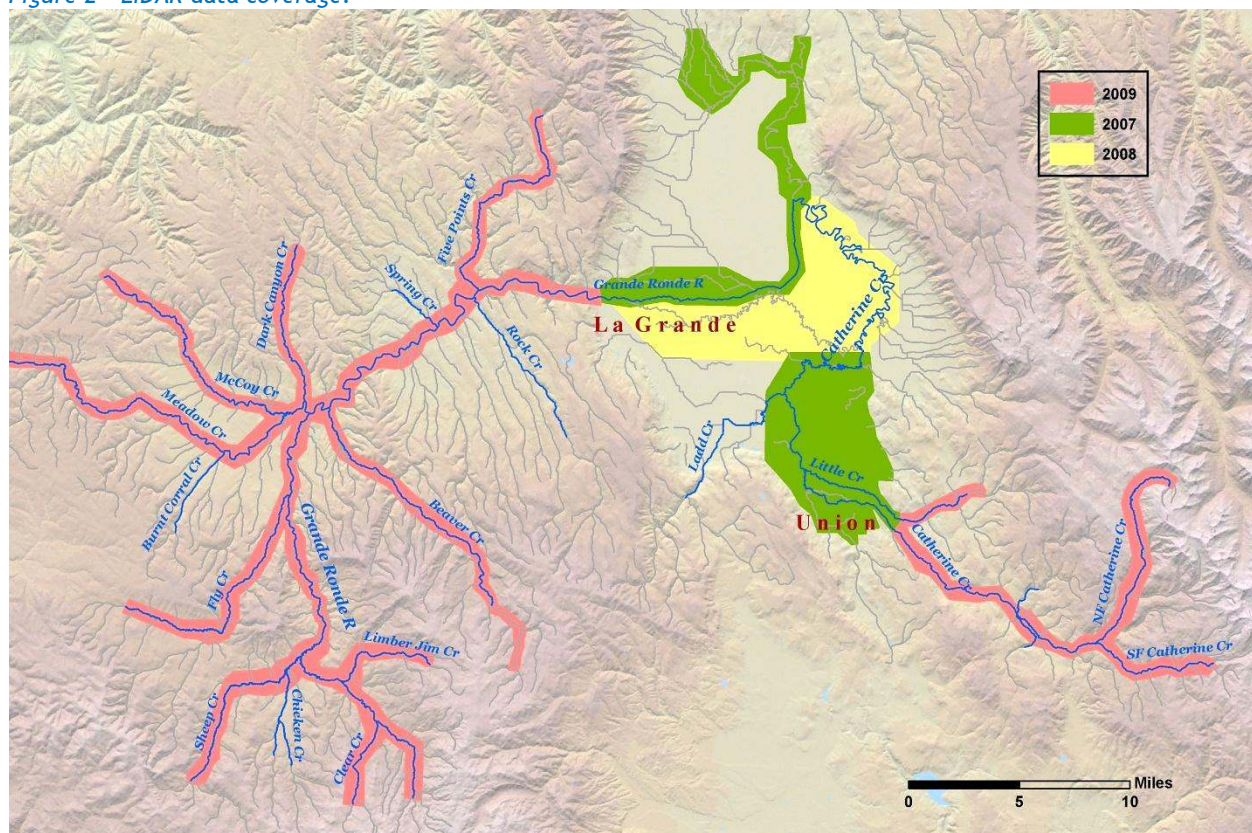
2.1.1 LiDAR

Light detection and ranging (LiDAR) data was collected by Watershed Sciences in September 2009 in order to supplement two existing LiDAR datasets that were collected in 2007 and 2008 (Figure 2). Together, the three LiDAR datasets provide high resolution land cover and bare earth elevation data for stream temperature model input. Table 1 summarizes the LiDAR products and their applicability to Heat Source modeling.

Table 1 - LiDAR products and their applications for stream temperature modeling.

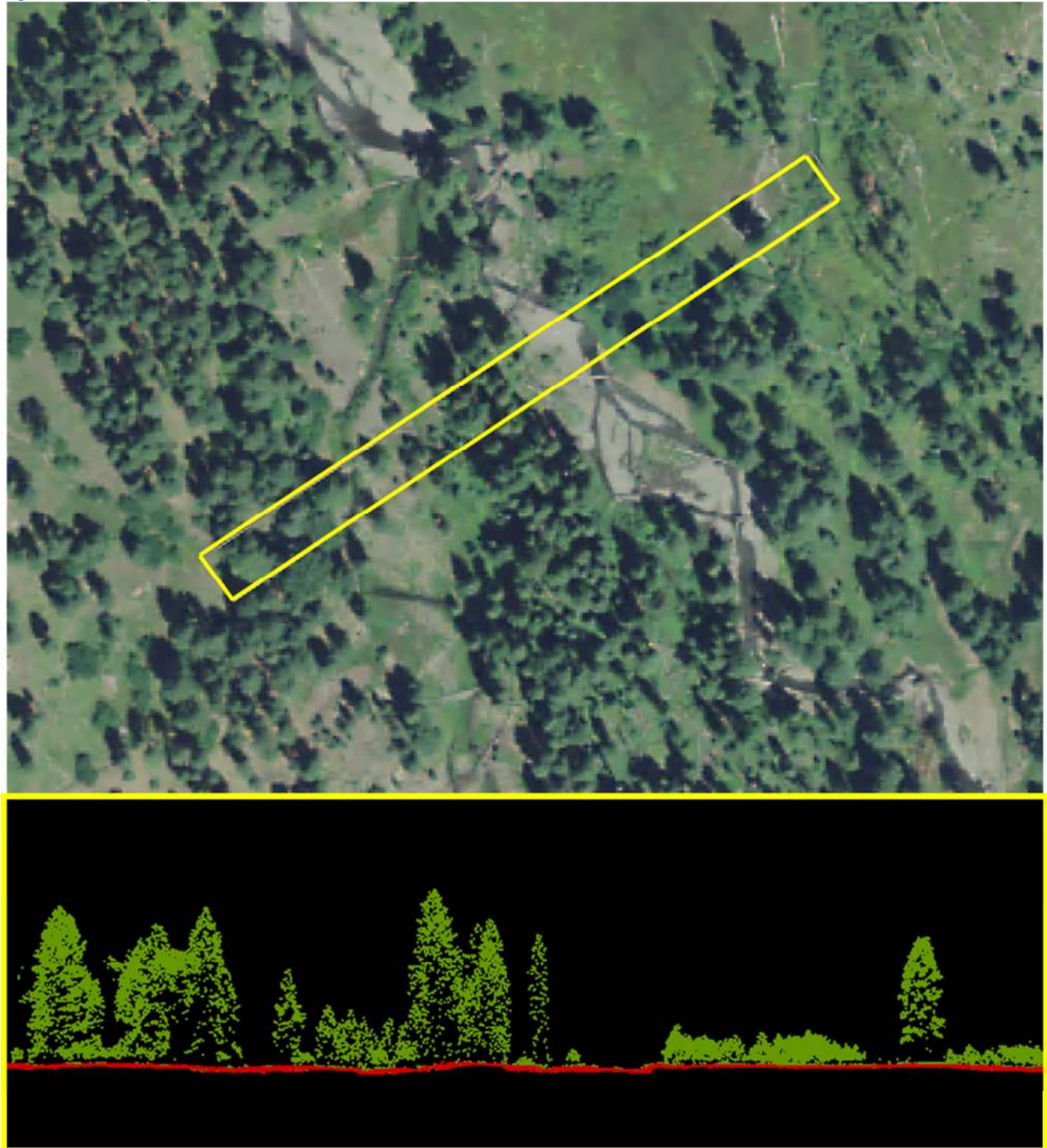
LiDAR Product	Applications
1-meter highest hit raster	Sampling near-stream land cover heights.
1-meter bare earth raster	Deriving high-resolution stream maps - including centerlines and banks. Sampling stream elevations and near-stream land surface elevations.
1-meter intensity images	Mapping stream centerlines and estimating wetted edges.

Figure 2 - LiDAR data coverage.



The LiDAR data consists of three-dimensional point clouds at approximately 8 points per square meter, with a relative accuracy of 5 centimeters. Each LiDAR data point is classified as either “ground” or “default”. “Default” includes all non-ground features such as vegetation, buildings, and other human made structures. Figure 3 shows a cross section of LiDAR data over Beaver Creek. Default points are green, while the ground points are colored red.

Figure 3 - LiDAR point cloud cross section over Beaver Creek.



LiDAR point data can be associated with RGB values from orthophotographs in order to produce more realistic or true-color oblique imagery. The default points can also be “turned off” to reveal a bare earth surface model which is useful for studying ground surface features that are normally obscured by vegetation. Figure 4 shows a LiDAR point cloud with RGB extraction and the corresponding bare earth model for a section of Beaver Creek. Complex channel geometry within the floodplain is easily visible in the bare earth LiDAR model.

Figure 4 - LiDAR point cloud with RGB extraction (top) and bare earth digital terrain model (bottom).

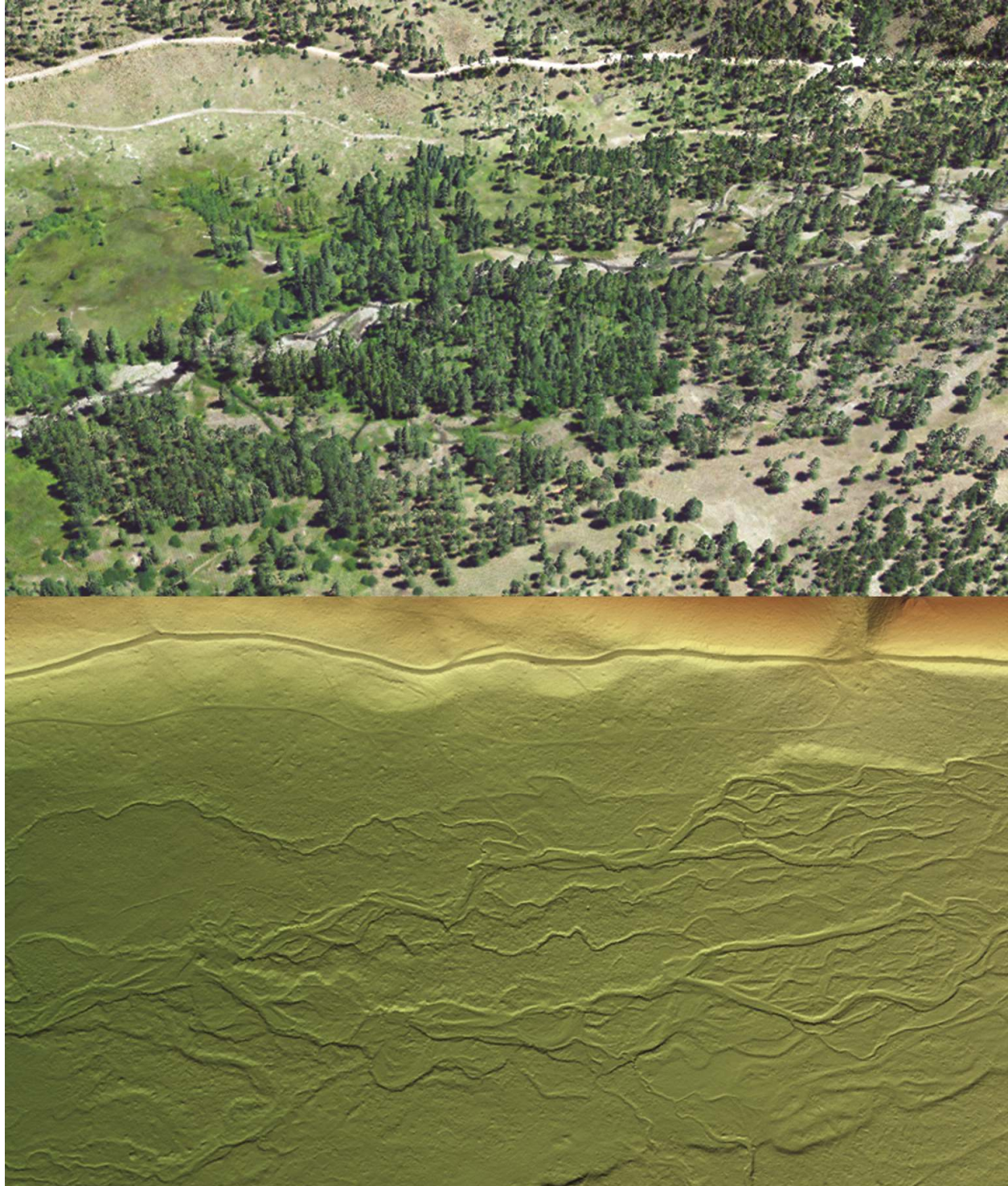


Figure 5 is another example of LiDAR digital elevation models (DEMs). The top image is the bare earth LiDAR model and the lower image is the highest hit LiDAR model. The DEM cell size is one meter. This type of raster data is commonly used within GIS applications such as ArcMap. For this project, the bare earth and highest hit rasters were used for stream mapping, tree height sampling, and other stream temperature model inputs.

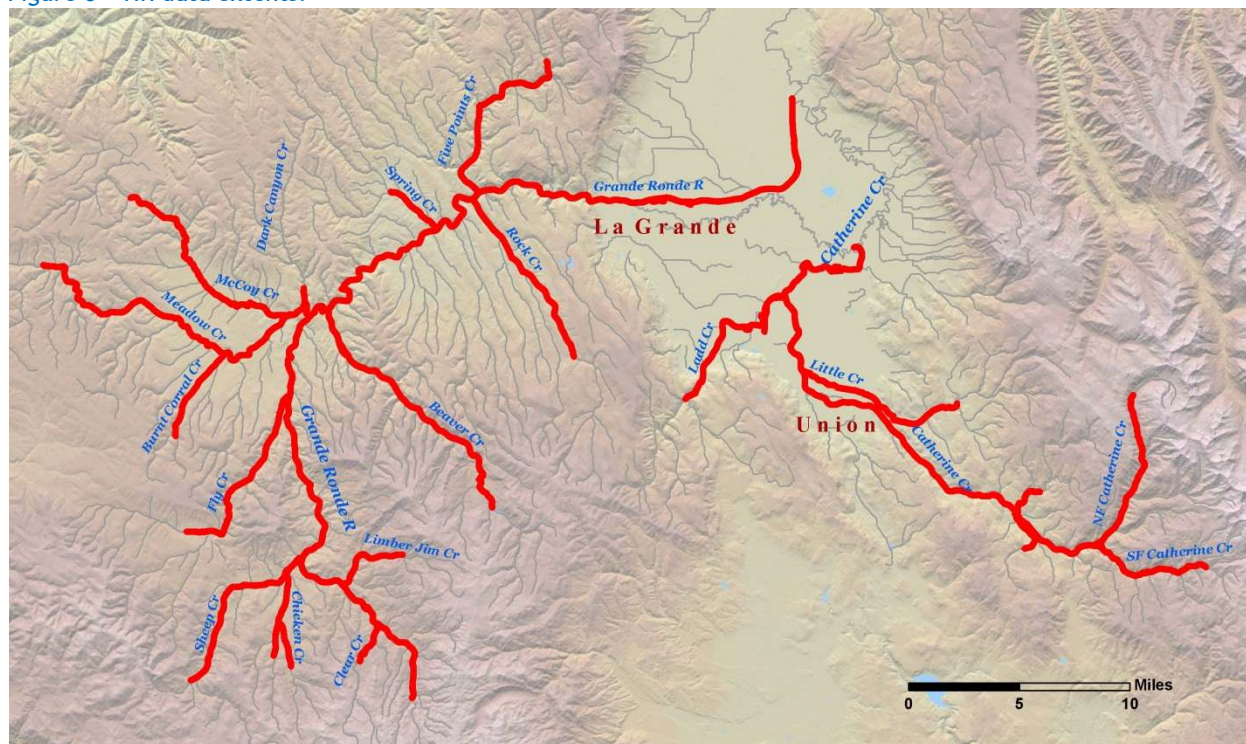
Figure 5 - LiDAR digital elevation model of the Grande Ronde River near Hilgard.



2.1.2 Thermal Infrared

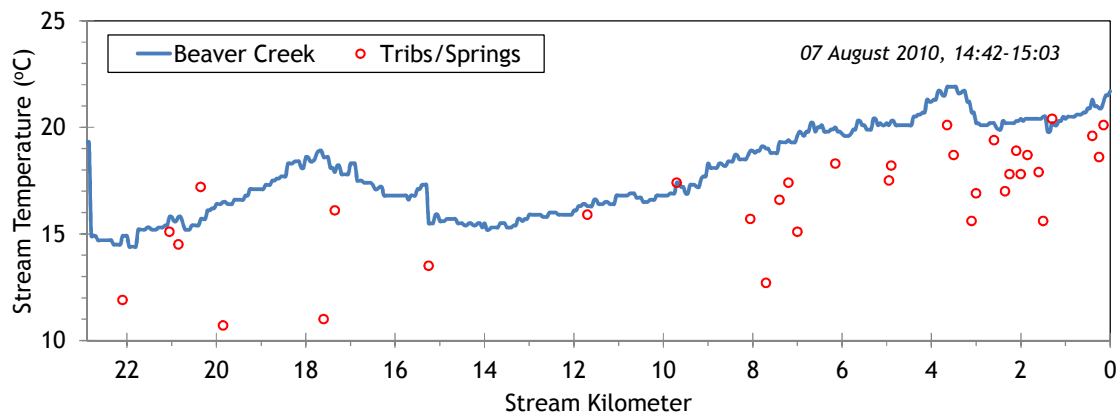
Watershed Sciences collected thermal infrared (TIR) stream temperature data for approximately 226 river miles (364 kilometers) during August 2010 (Figure 6). The TIR data was collected during the warmest part of the afternoon in order to capture near-daily maximum stream temperatures, when aquatic life is most at risk. Additionally, the August data collection was intended to target the low-flow and high seasonal temperature window when salmonid habitat is most impaired. Coinciding with the TIR data collection window, CRITFC crews were collecting ground-level flow measurements and hourly stream temperature data.

Figure 6 - TIR data extents.



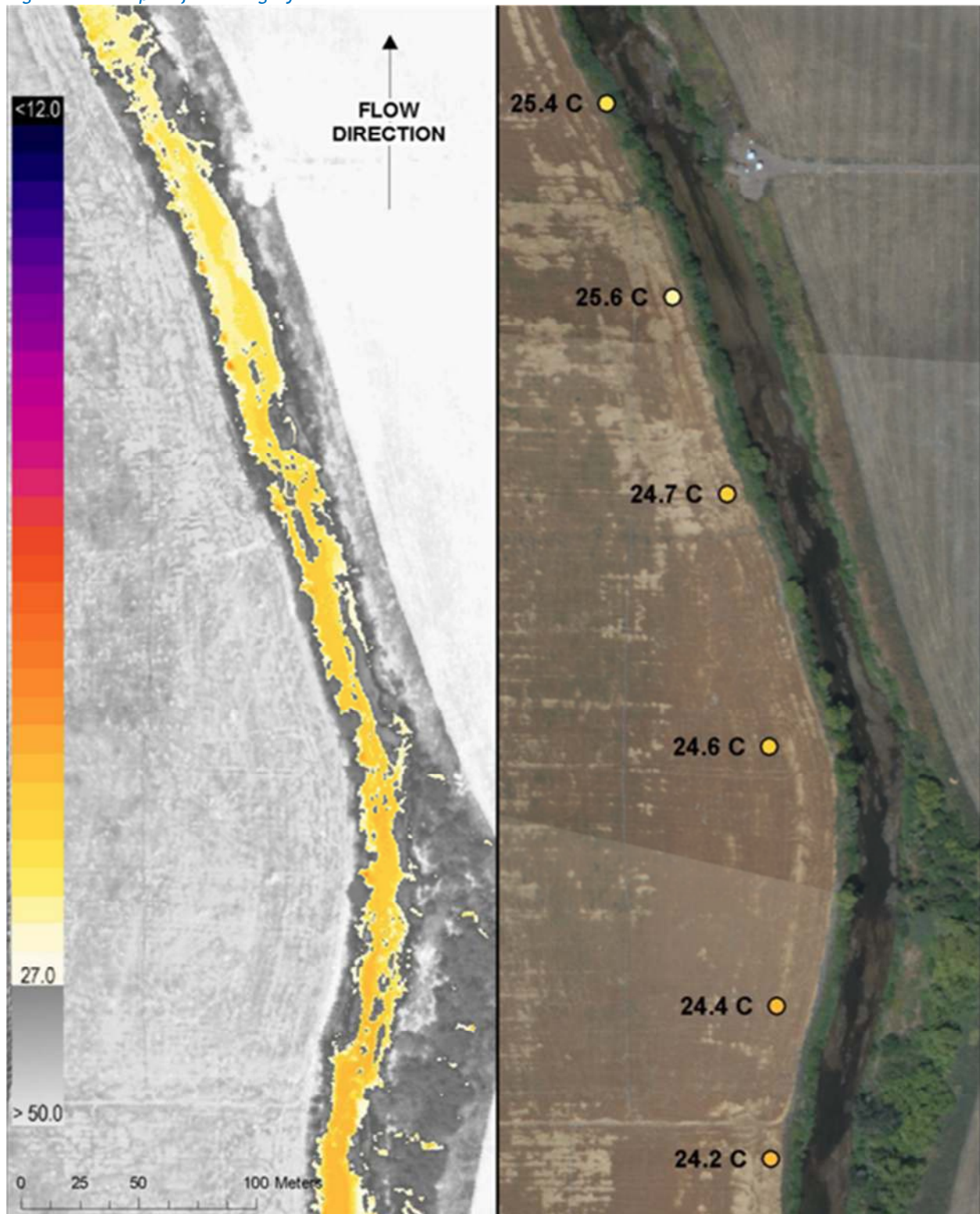
Following is an example of a TIR longitudinal temperature profile (Figure 7). In addition to the stream temperature profile, the temperatures of springs and tributaries are captured by the survey.

Figure 7 - Example of a TIR longitudinal stream temperature profile.



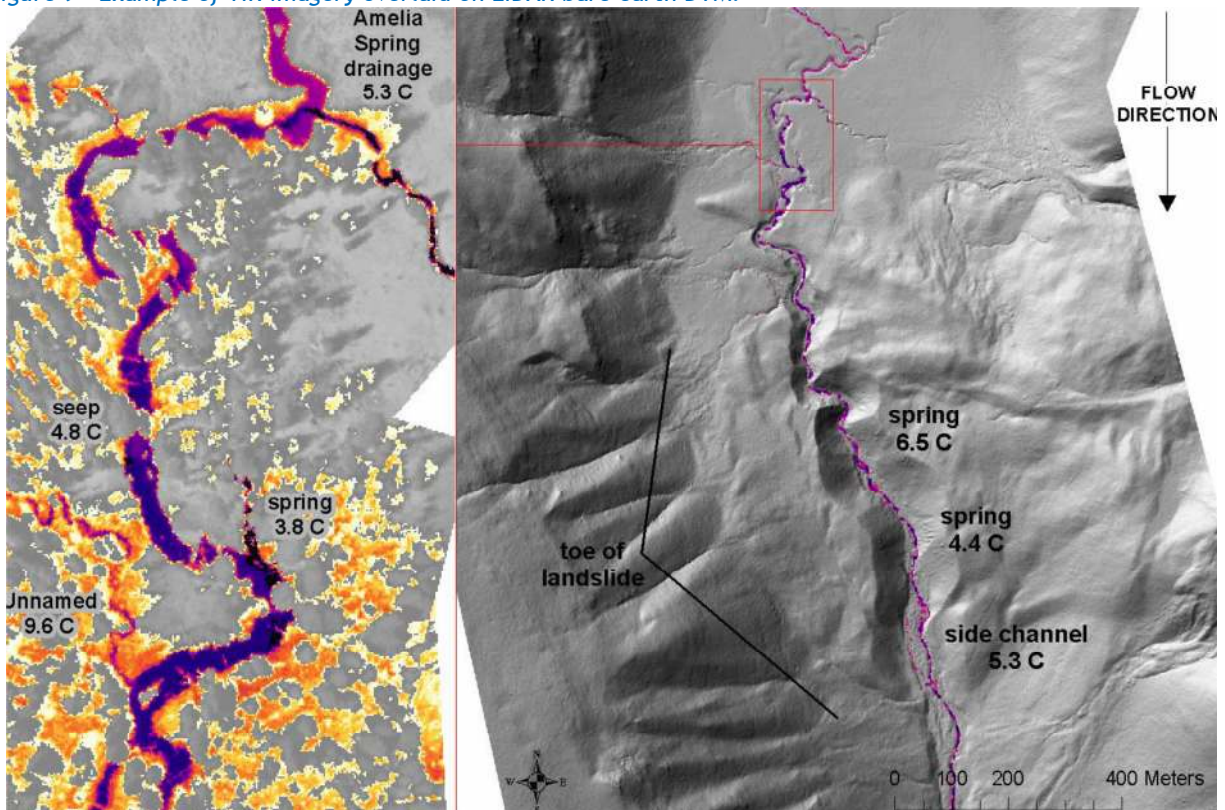
TIR surveys record only the surface temperatures and do not penetrate into the water column. Figure 8 shows an example of TIR imagery and the temperatures sampled from it. The points represent the position of the helicopter at the time the image was recorded.

Figure 8 - Example of TIR imagery.



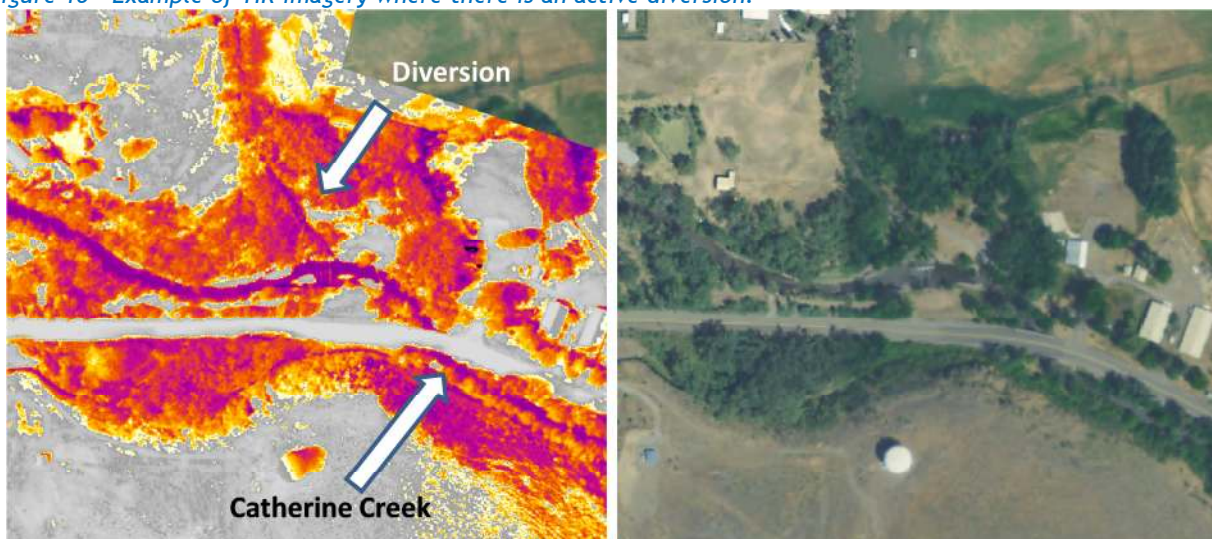
The TIR stream temperature imagery is useful for identifying features such as tributaries and springs (Figure 9). Temperatures can be sampled from those inflows and then mass balance calculations can be made to estimate their volumes. Significant inflows (ones that are large enough to accurately measure and are impacting stream temperature) are often included within the stream temperature models.

Figure 9 - Example of TIR imagery overlaid on LiDAR bare earth DTM.



The TIR imagery can also be used to identify diversion canals that were active at the time of the survey (Figure 10).

Figure 10 - Example of TIR imagery where there is an active diversion.

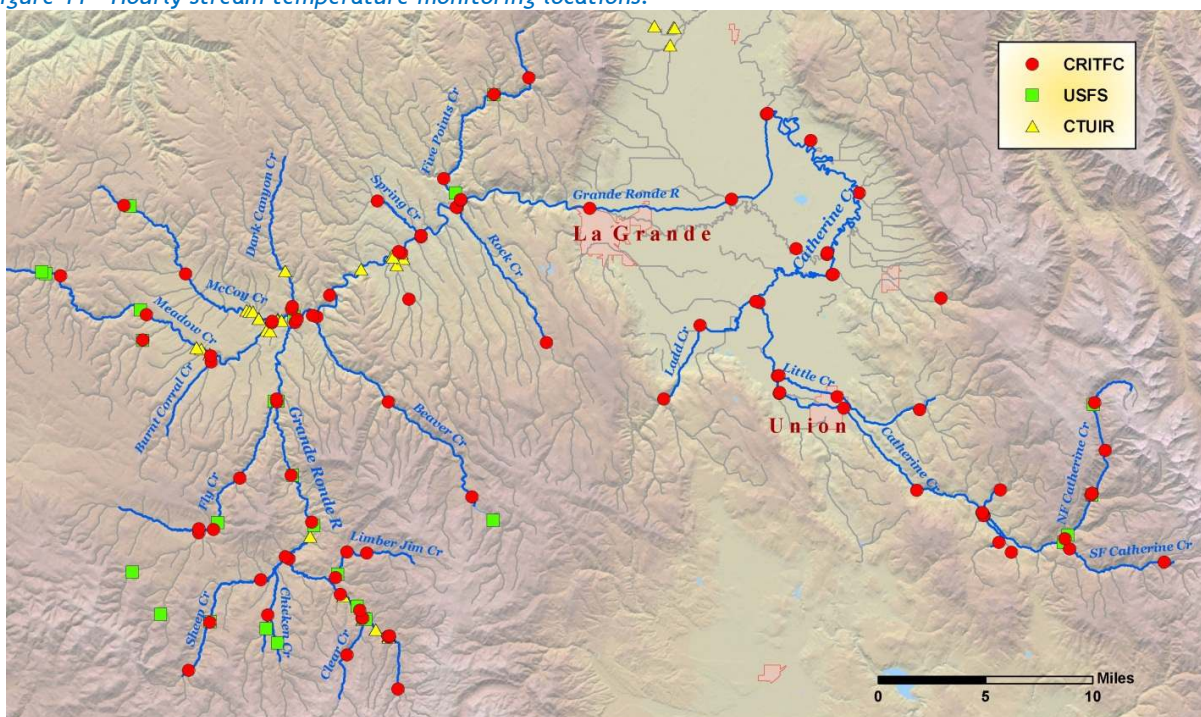


2.2 Ground Level Data

2.2.1 Hourly Temperature Data

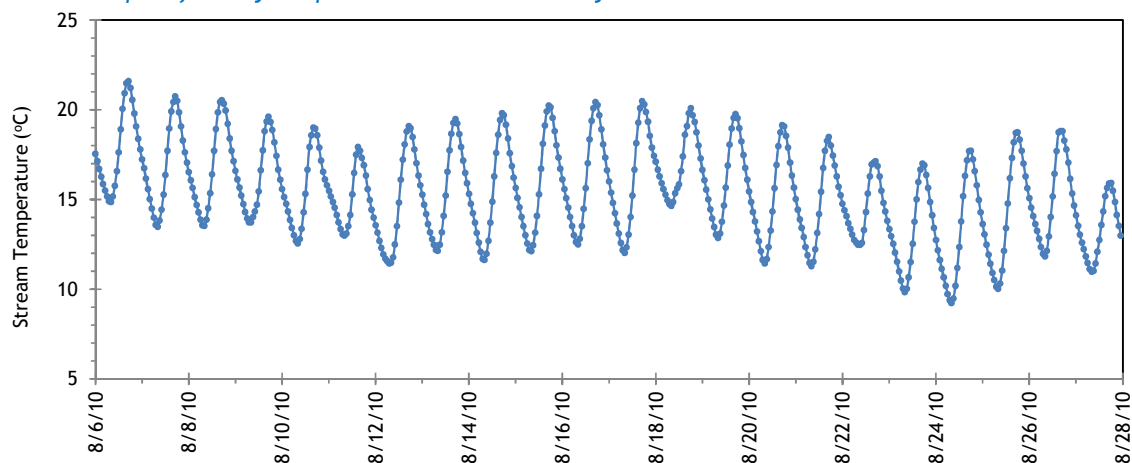
During the summer of 2010, CRITFC deployed thermistors throughout the study area in order to record hourly stream temperatures. The United States Forest Service (USFS) and Confederated Tribes of the Umatilla Indian Reservation (CTUIR) also provided hourly temperature data they had collected during that time. Figure 11 shows the hourly stream temperature monitoring locations.

Figure 11 - Hourly stream temperature monitoring locations.



Hourly stream temperature data were used to calibrate and verify the TIR data. Temperature data was also used for Heat Source input - to seed the uppermost boundary temperatures and for validating simulation results at various locations along the modeled streams. Figure 12 is an example of hourly temperature data.

Figure 12 - Example of hourly temperature data collected by CRITFC.



2.2.2 Seasonal Variation

A few stream temperature monitoring locations were selected in order to assess variability throughout the summertime period. The highest stream temperatures generally occurred in August. Figure 13 and Figure 14 display the stream temperature variability of sites along the Grande Ronde River and Catherine Creek.

Figure 13 - Grande Ronde River stream temperature variability during the summer of 2010.

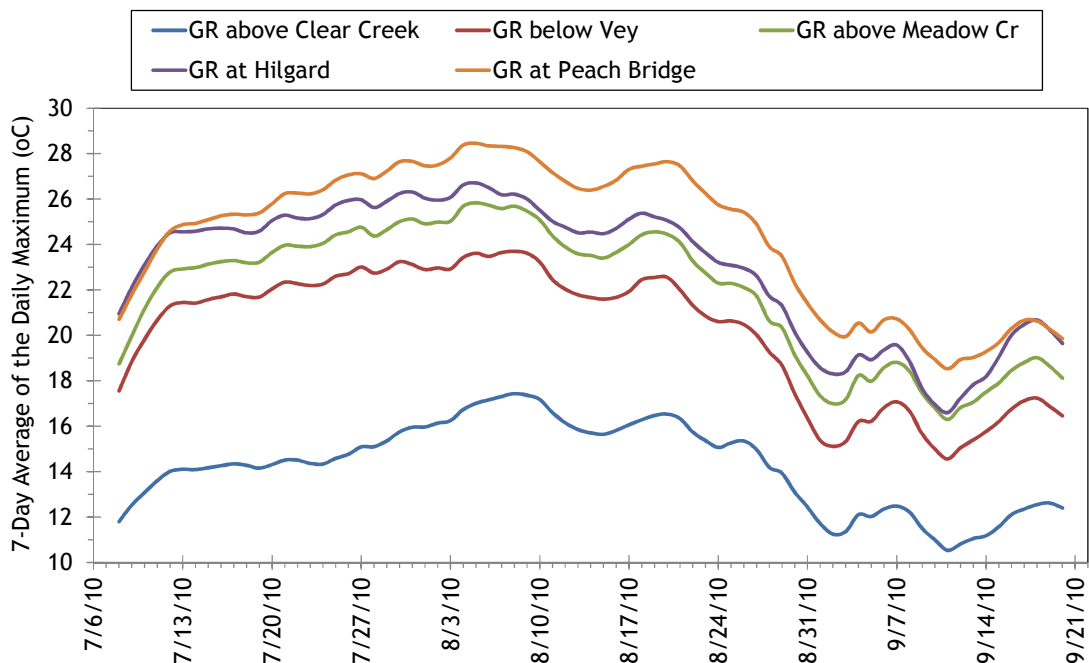
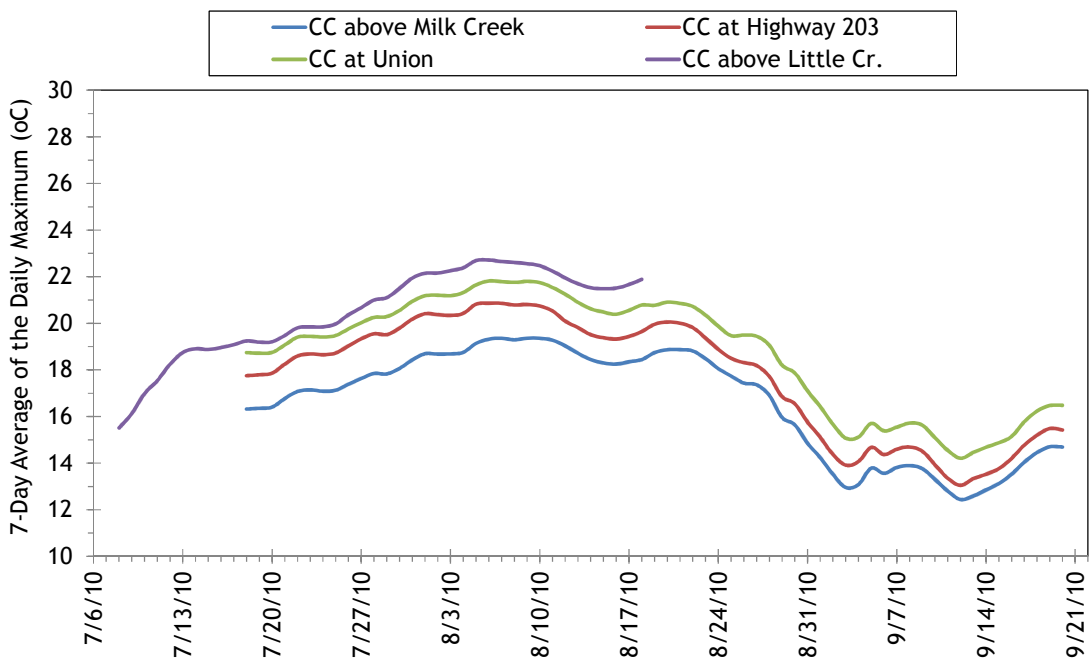


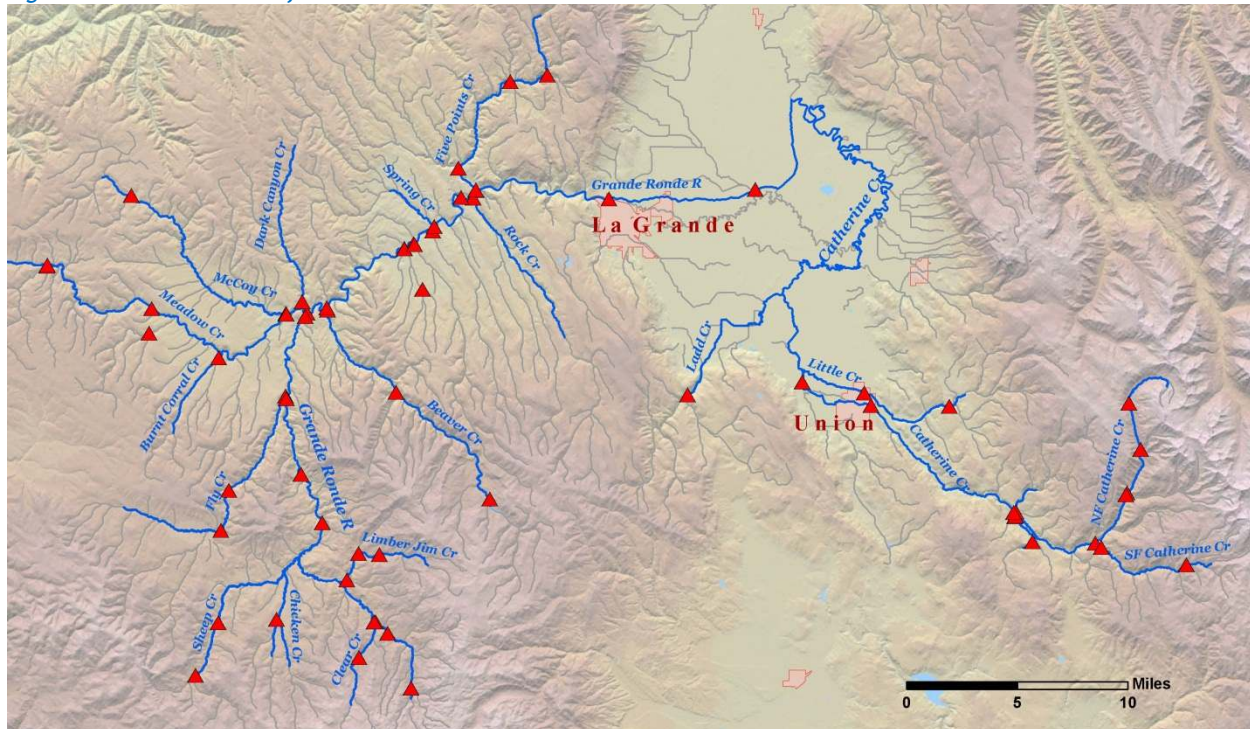
Figure 14 - Catherine Creek stream temperature variability during the summer of 2010.



2.2.3 Instantaneous Flow Data

CRITFC collected instantaneous ground-level flow data at various locations in August 2010 in order to coincide with the TIR flight window (Figure 15). Flow volume, velocity, depth and width were recorded at each location. The data were used to set up Heat Source hydraulics and to validate the simulation results.

Figure 15 - Instantaneous flow measurement locations.



The following data were recorded at each flow measurement site:

- Date and time
- Discharge volume
- Minimum, maximum and average velocity
- Minimum, maximum and average depth
- Wetted width
- Latitude and longitude

One measurement was taken at each site during the simulation time period (August 6-27, 2010). The measurements were used to “seed” mass balance calculations of daily flow volume for streams where daily gage data were unavailable. The data were also used to validate the Heat Source simulated hydraulics.

2.2.4 Gaged Flow Data

Daily flow volumes were recorded at several USGS/OWRD gages within the study area (Figure 16). The daily average flows recorded at these locations were used to set up Heat Source hydraulics and validate the simulation results.

Figure 16 - Flow gage locations.

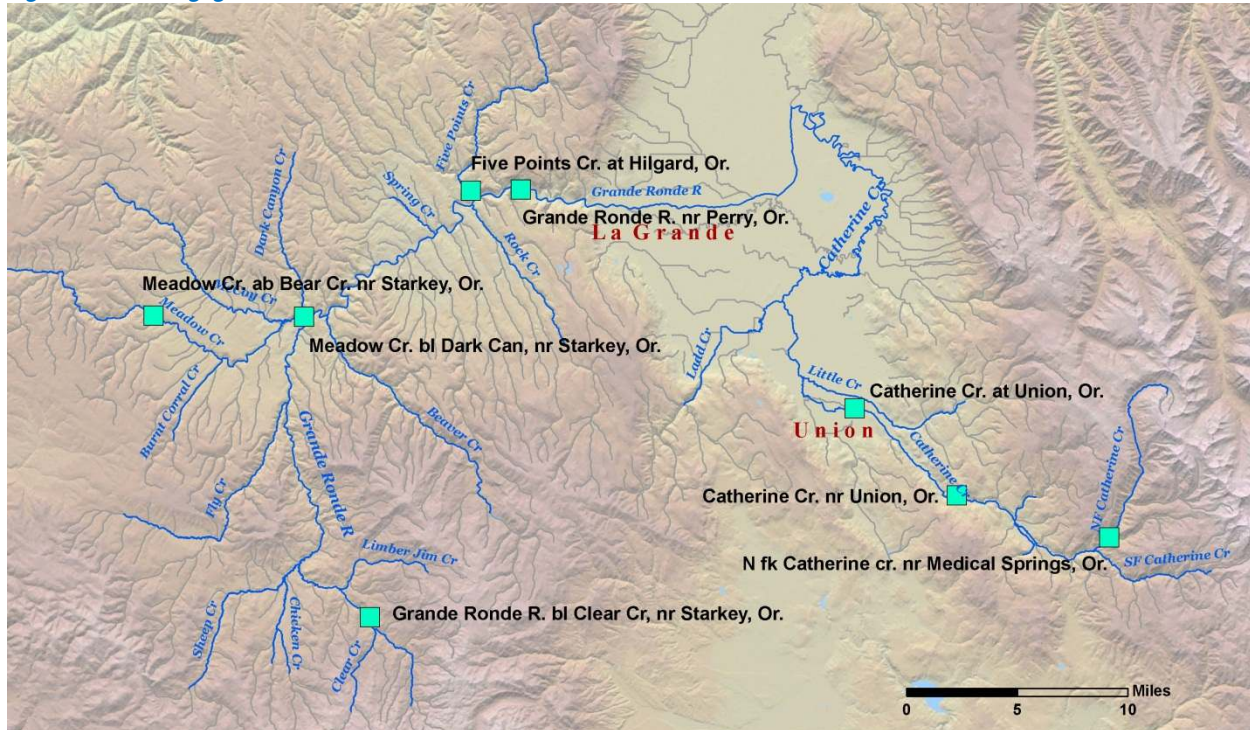


Table 2 lists the gages that were active during August 2010 within the study area. Data were downloaded from the Oregon Water Resources Department website. The original records were in 15-minute intervals and daily average values were calculated.

Table 2 - Stream flow gages within the study area.

ID #	Gage	Stream
13320300	Catherine Cr. at Union, OR	Catherine Creek
13320000	Catherine Cr. near Union, OR	Catherine Creek
13318920	Five Points Cr. at Hilgard, OR	Five Points Creek
13317850	Grande Ronde R. bl Clear Cr, nr Starkey, OR	Grande Ronde River
13318960	Grande Ronde R. nr Perry, OR	Grande Ronde River
13318060	Meadow Cr. above Bear Cr. nr Starkey, OR	Meadow Creek
13318210	Meadow Cr. below Dark Can, nr Starkey, OR	Meadow Creek
13319900	NF Catherine Cr. nr Medical Springs, OR	North Fork Catherine Creek

Hourly climate data were recorded by the National Weather Service at the La Grande airport. The U.S. Forest Service also recorded hourly temperature data at the J Ridge remote automated weather station (RAWS) site in the upper Grande Ronde basin. Figure 17 shows the climate station locations. For most Heat Source models, data from the La Grande airport were used. Some upper basin models used the USFS RAWS climate data. Further details and assumptions are provided in the following sections for each simulated stream.

This topographic map shows the region around La Grande, Idaho. The Grande Ronde River flows from the north towards the south. To the west, the J Ridge area is marked with a black dot and labeled 'J Ridge (RAWS)'. To the east, the La Grande Airport (NWS) is marked with a black dot and labeled 'La Grande Airport (NWS)'. The map includes numerous creeks such as Dark Canyon Cr., Spring Cr., Five Points Cr., Reed Cr., Little Cr., and others. The towns of La Grande and Union are also labeled. A scale bar at the bottom right indicates distances in miles (0, 5, 10).

Figure 18 - Hourly cloud cover values recorded at La Grande airport.

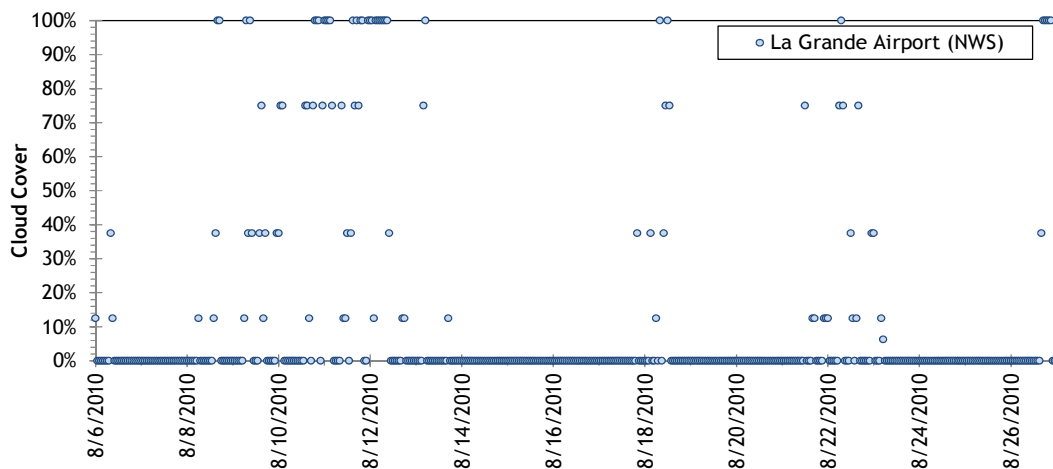
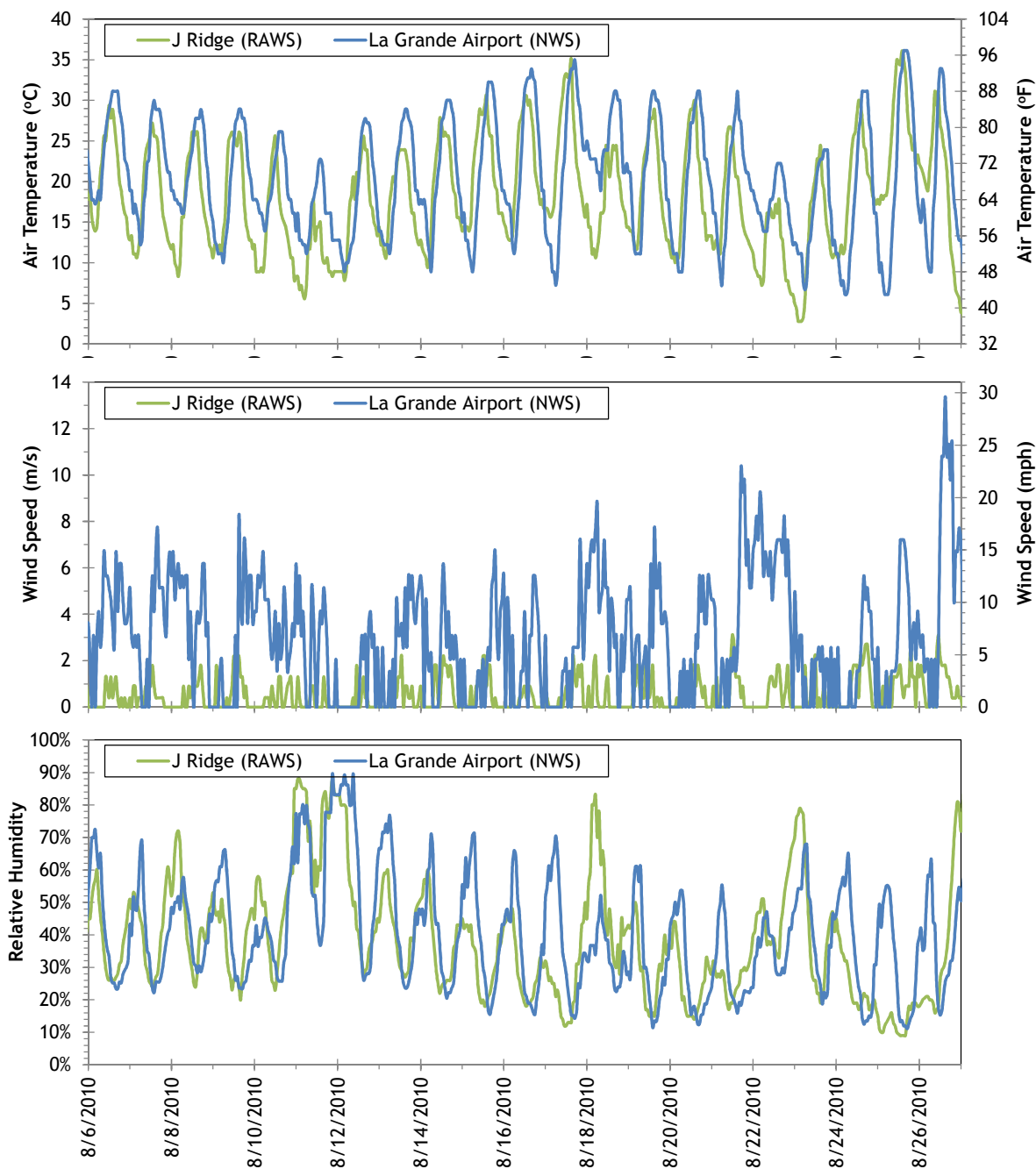


Figure 19 shows the recorded hourly air temperature, relative humidity and wind speed data recorded at the J Ridge (RAWS) and La Grande airport (NWS) weather stations between August 6 and August 27, 2010. Wind speeds at the airport were higher than at J Ridge because the airport is located in a wide open valley bottom.

Figure 19 - Hourly air temperature, wind speed and relative humidity data.



3. GIS DATA SAMPLING FOR HEAT SOURCE INPUT - TTOOLS

Streams were mapped from the bare earth LiDAR data. Then TTools, a set of automated GIS sampling tools, was used to create an input database for Heat Source model. Figure 20 is a map of where stream channels were mapped and TTools was run. Table 3 summarizes the streams and lengths that were mapped and sampled with TTools.

Figure 20 - TTools sampling extents

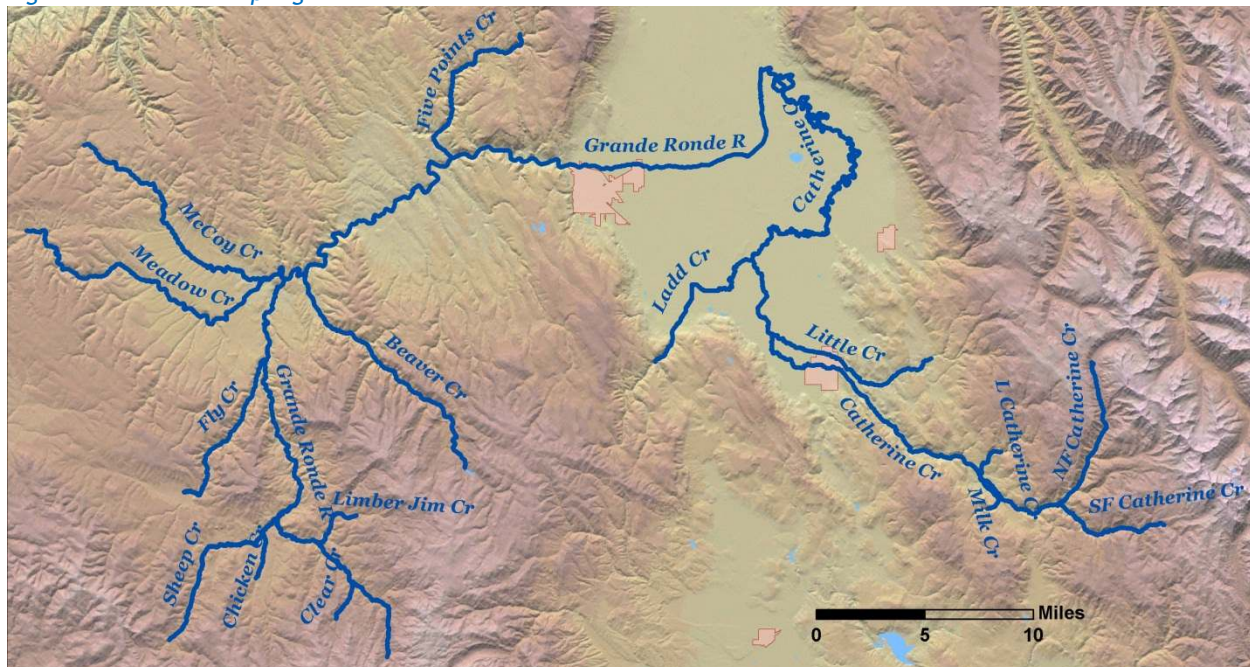


Table 3 - Streams where TTools sampling was completed.

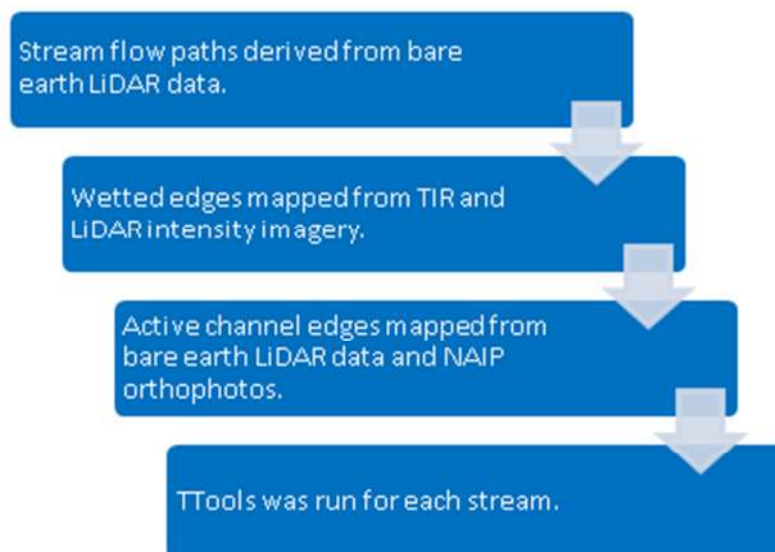
Watershed	Stream	Km	Miles
Catherine Creek	North Fork Catherine Creek	13.4	8.3
	South Fork Catherine Creek	10.4	6.5
	Milk Creek	3.4	2.1
	Little Catherine Creek	3.2	2.0
	Little Creek	16.5	10.3
	Ladd Creek	15.3	9.5
	Catherine Creek	88.7	55.1
	Clear Creek	3.5	2.2
Upper Grande Ronde River	Limber Jim Creek	5.9	3.7
	Chicken Creek	6.5	4.0
	Sheep Creek	22.2	13.8
	Fly Creek	15.5	9.6
	Meadow Creek	31.5	19.6
	McCoy Creek	23.9	14.9
	Beaver Creek	22.9	14.2
	Five Points Creek	16.4	10.2
	Grande Ronde River	98.1	61.0
	TOTAL:	397.3	246.9

Heat Source stream temperature modeling incorporates high-resolution LiDAR, TIR, and stream mapping. This section describes how stream channels were mapped from LiDAR data and how the various GIS data sources were sampled to create Heat Source input databases. Following is a brief overview of the methodology:

1. Stream flow paths were derived from 1-meter bare earth LiDAR rasters.
 - a. Smoothing algorithms were applied.
 - b. Results verified and manually corrected where needed.
2. Wetted edges were digitized.
3. Active channel edges were digitized.
4. TTools was used to segment the stream every 50 meters and sample the following:
 - a. Stream elevation, gradient, and aspect
 - b. Channel widths
 - c. Topographic shade angles
 - d. Near stream land cover heights
 - e. TIR stream temperatures

Figure 21 summarizes the general workflow used to create, assemble, and sample GIS data for Heat Source model input. Once the TTools shapefile database was created for each stream, Heat Source models were set up and the calibration process was ready to commence.

Figure 21 - General workflow to prepare Heat Source model inputs.



3.1 Stream Mapping

Existing stream layers were outdated and had fairly coarse resolutions (1:24,000 or coarser). Since Heat Source relies on high resolution LiDAR inputs, new stream layers were mapped from the bare earth LiDAR data. Following are the steps used to create the high-resolution stream layers:

1. One-meter rasters of the bare earth LiDAR were mosaicked for each stream to be modeled.
2. The bare earth rasters were filled and flow direction and accumulation rasters were derived.
3. The flow accumulation raster was then converted to polylines using a minimum drainage area.
4. The stream of interest was isolated and all extraneous segments were deleted (Figure 22).
5. Smoothing algorithms were applied to remove “kinks” (Figure 23).
6. Smoothed stream polylines were verified against LiDAR, TIR, and aerial photography and manually corrected where necessary.

Figure 22 - Raw stream polyline.

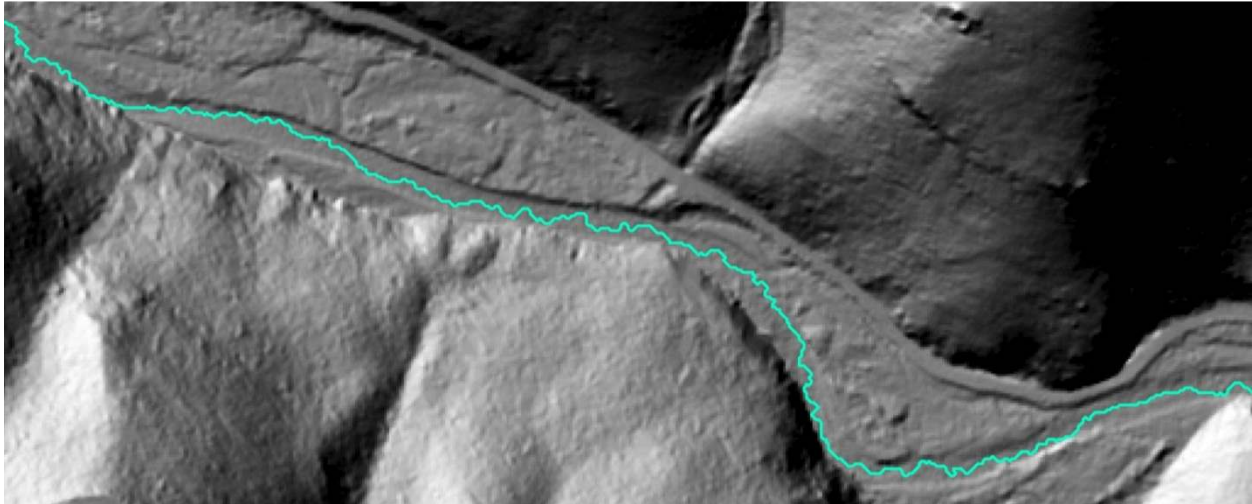
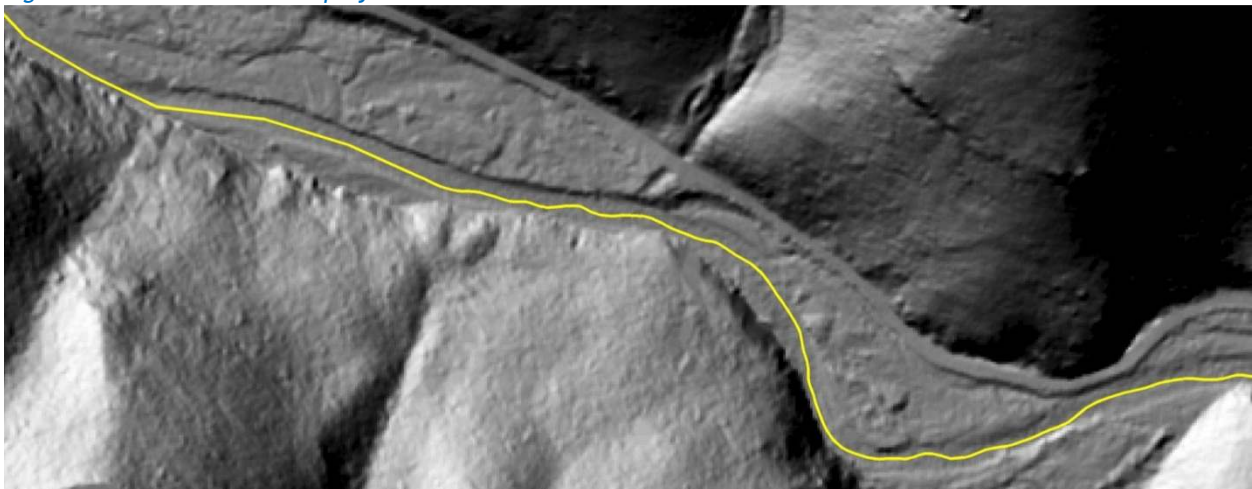


Figure 23 - Smoothed stream polyline.



3.2 Wetted Edge Mapping

Wetted widths are an important input parameter for the Heat Source model because accurate hydraulics are essential for a robust modeling effort. LiDAR intensity images and TIR imagery provided clear depictions of the stream surface in most cases. The right and left wetted edges were digitized from those sources. Then TTools was used to measure the wetted width at each 50-meter segment.

Figure 24 - Stream polyline overlaid on LiDAR intensity image.

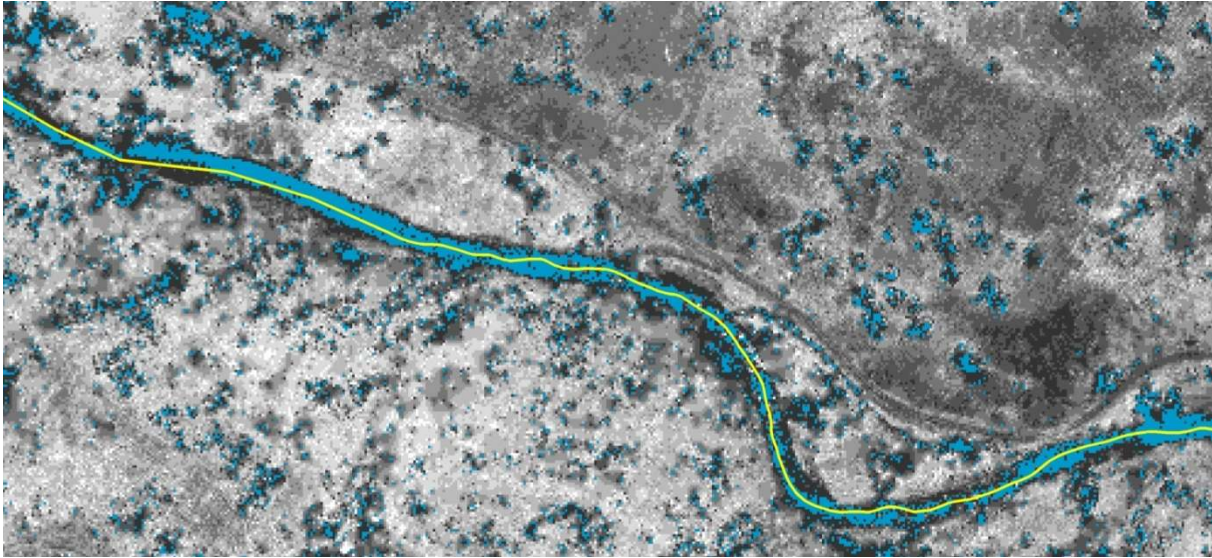
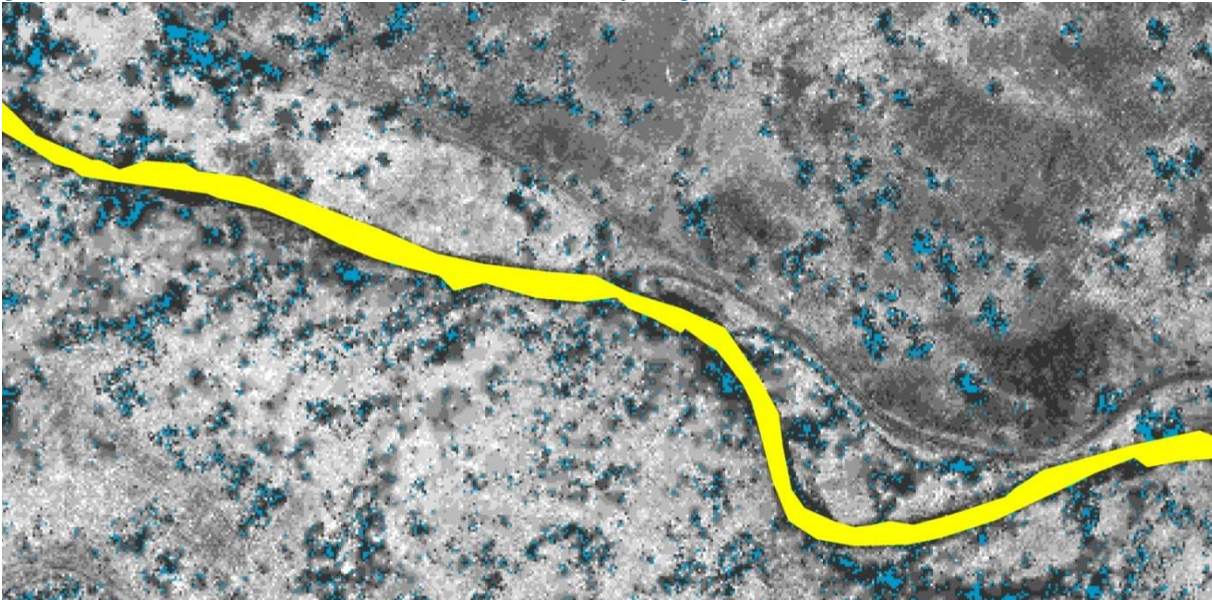


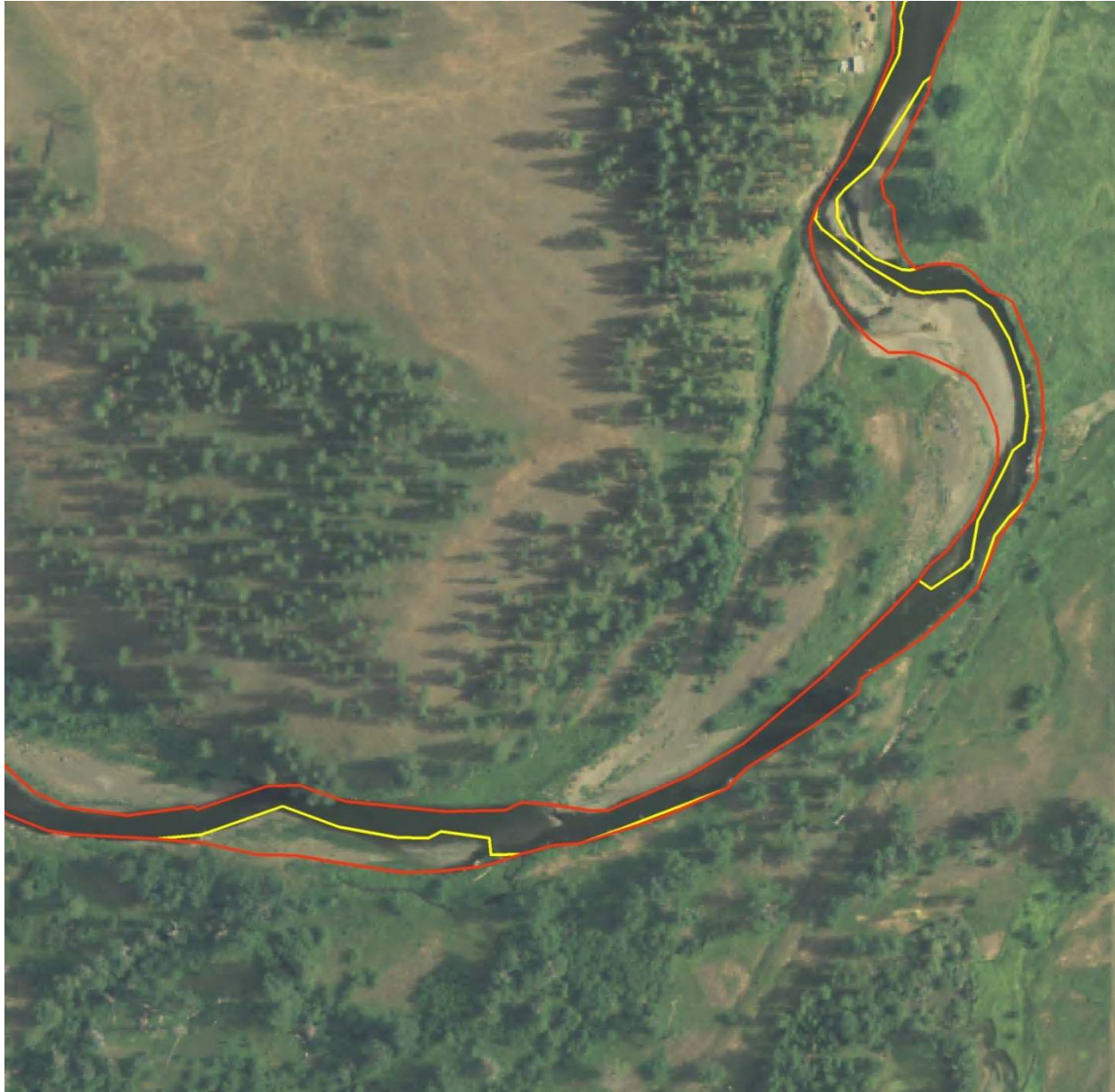
Figure 25 - Estimated wetted area based on LiDAR intensity image.



3.3 Active Channel Mapping

Active channel edges are an important consideration when applying potential vegetation for “what-if” model runs. In most cases, the active channel should remain free of vegetation during the potential vegetation scenarios. Active channel edges were digitized from the bare earth LiDAR data and aerial photography. TTools was used to sample the active channel widths at each 50-meter stream segment.

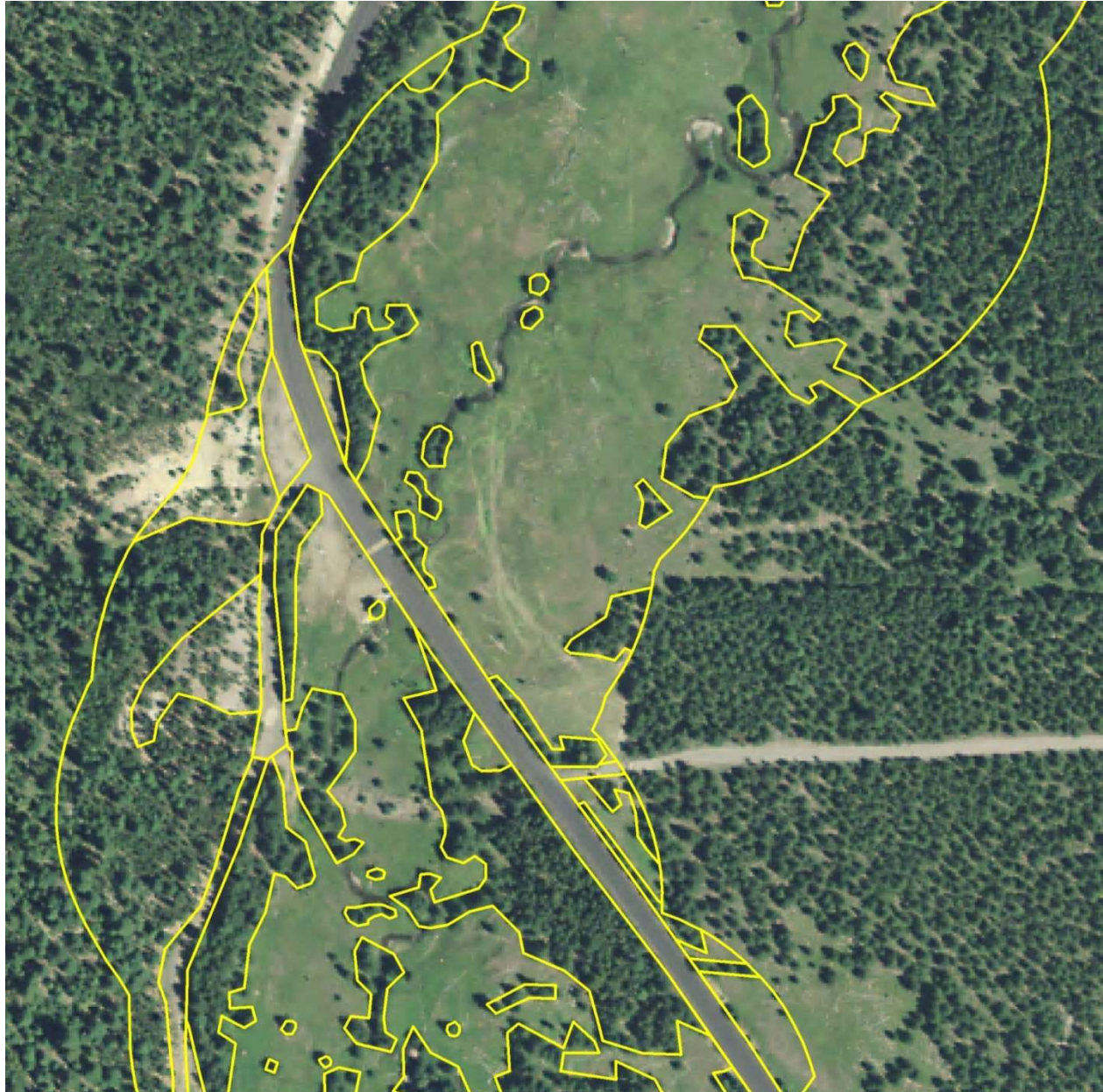
Figure 26 - Wetted channel edges (yellow) and active channel edges (red).



3.4 Near Stream Land Cover Mapping

Some streams had partial or no LiDAR data available. In those cases, the near stream land cover was manually digitized from aerial imagery (NAIP orthophotography). The stream was buffered 100 meters from each bank and that buffer was divided into polygons based on land cover type, height class, and density class (Figure 27). General height estimates were made based on nearby LiDAR data (see following sections for individual stream details).

Figure 27 - Manually digitized near stream land cover polygons.



3.5 Automated GIS Sampling - TTools

TTools is an ArcMap tool set that is designed to sample high-resolution GIS data and create an input database for Heat Source. Table 4 summarizes the TTools functions.

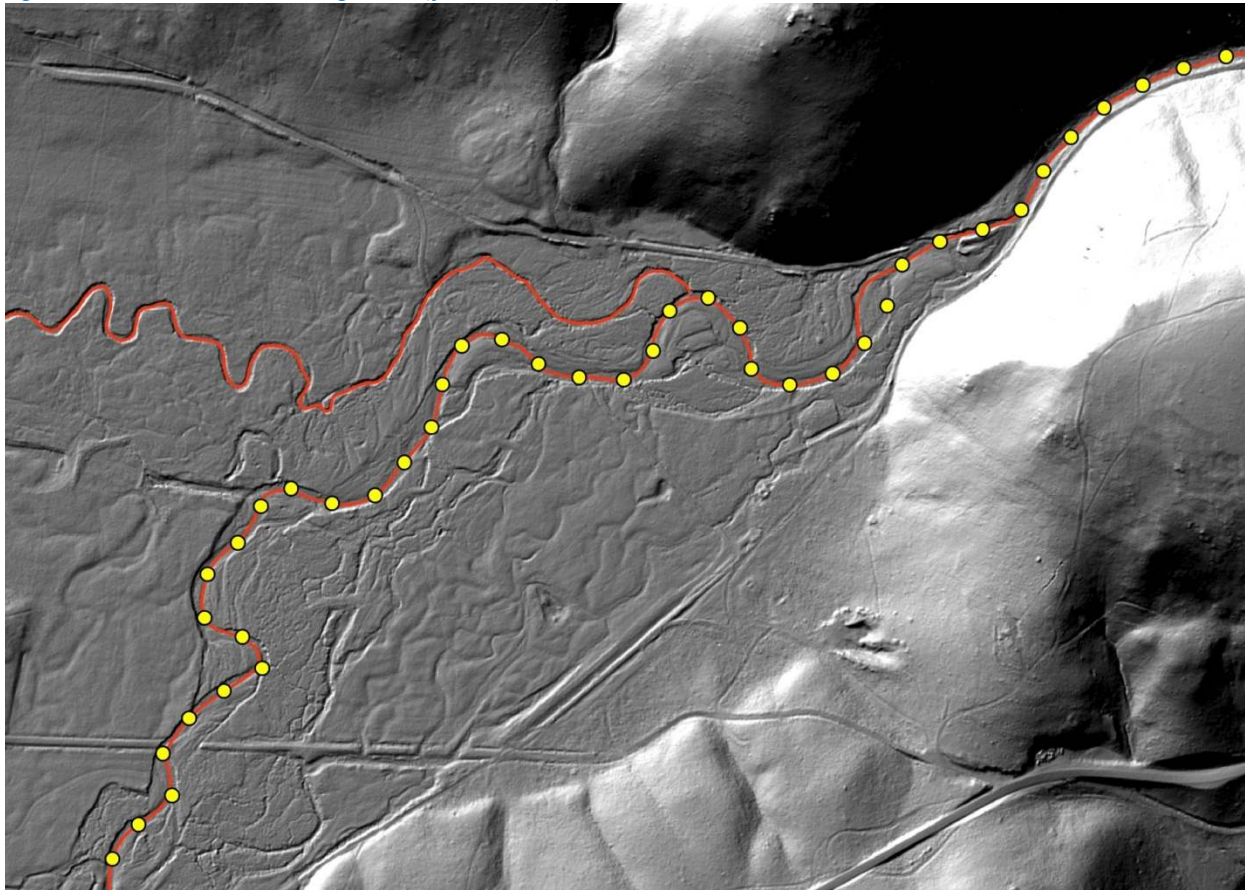
Table 4 - TTools steps and data sources.

Step	Description	Data Sources
1	Segments stream polyline every 50 meters and calculates aspect	Stream polyline
2	Measures channel width at each 50-meter node	Wetted and active channel edge polylines
3	Measures stream elevation and gradient	Bare earth LiDAR data
4	Measures topographic shade angles	10-meter DEM
5	Samples near stream land cover heights	Highest hit and bare earth LiDAR data / manually digitized polygons
6	Samples TIR temperature data	TIR point shapefile

3.5.1 TTools Step 1

In the first step of TTools, the stream polyline is segmented every 50 meters and a point shapefile is created that will house the data from all subsequent steps. Figure 28 shows an example of a stream polyline that has been segmented using TTools.

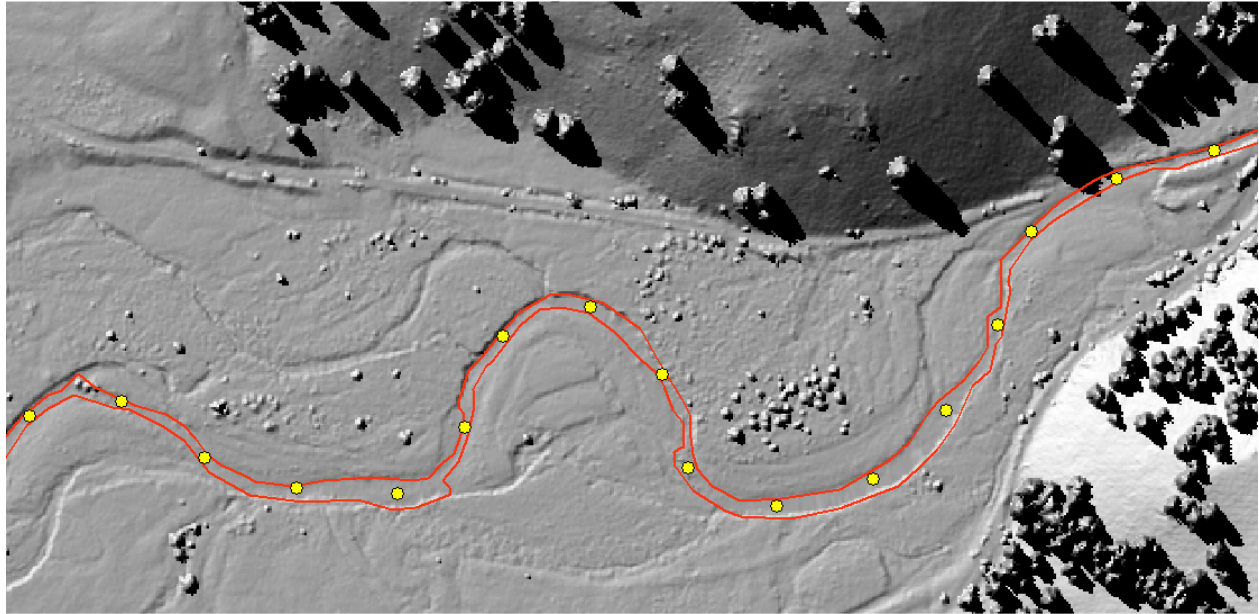
Figure 28 - 50-meter stream segments (yellow dots).



3.5.2 TTools Step 2

The second step of TTools is to sample the channel widths at each 50-meter node (Figure 29). The right and left banks or channel edges need to have been mapped and represented as individual polyline shapefiles. Channel widths are measured perpendicular to the stream flow. The user may use this step to sample wetted edges, active bank edges, floodplain widths, or various other widths relative to the stream.

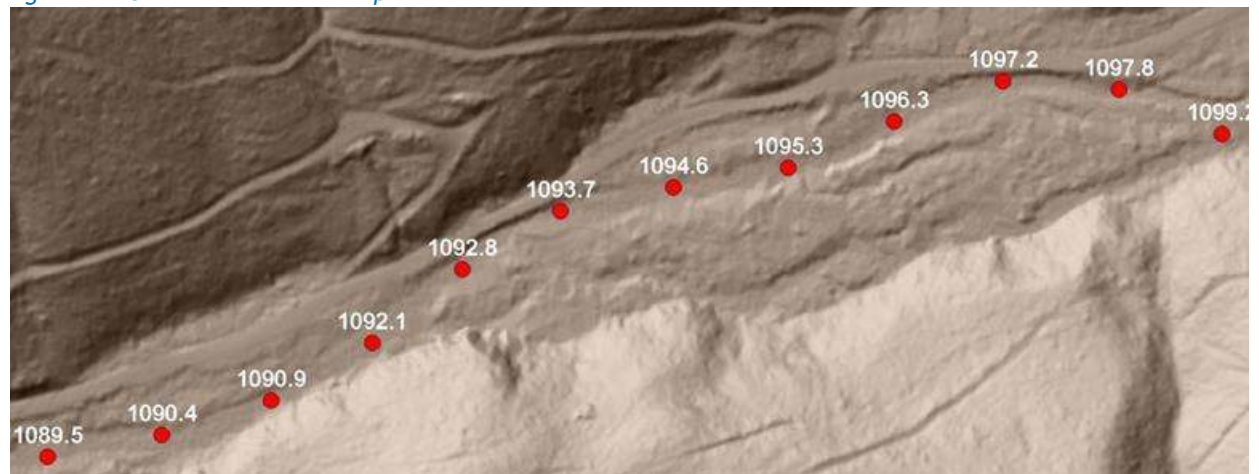
Figure 29 - Stream channel edges and the TTools point shapefile.



3.5.3 TTools Step 3

In the third step of TTools, stream elevation is sampled at each 50-meter node (Figure 30) and then the gradient is calculated as rise/run. Where LiDAR data is available, the elevations were sampled from the bare earth LiDAR data. Where LiDAR was not available, the 10-meter DEM was used.

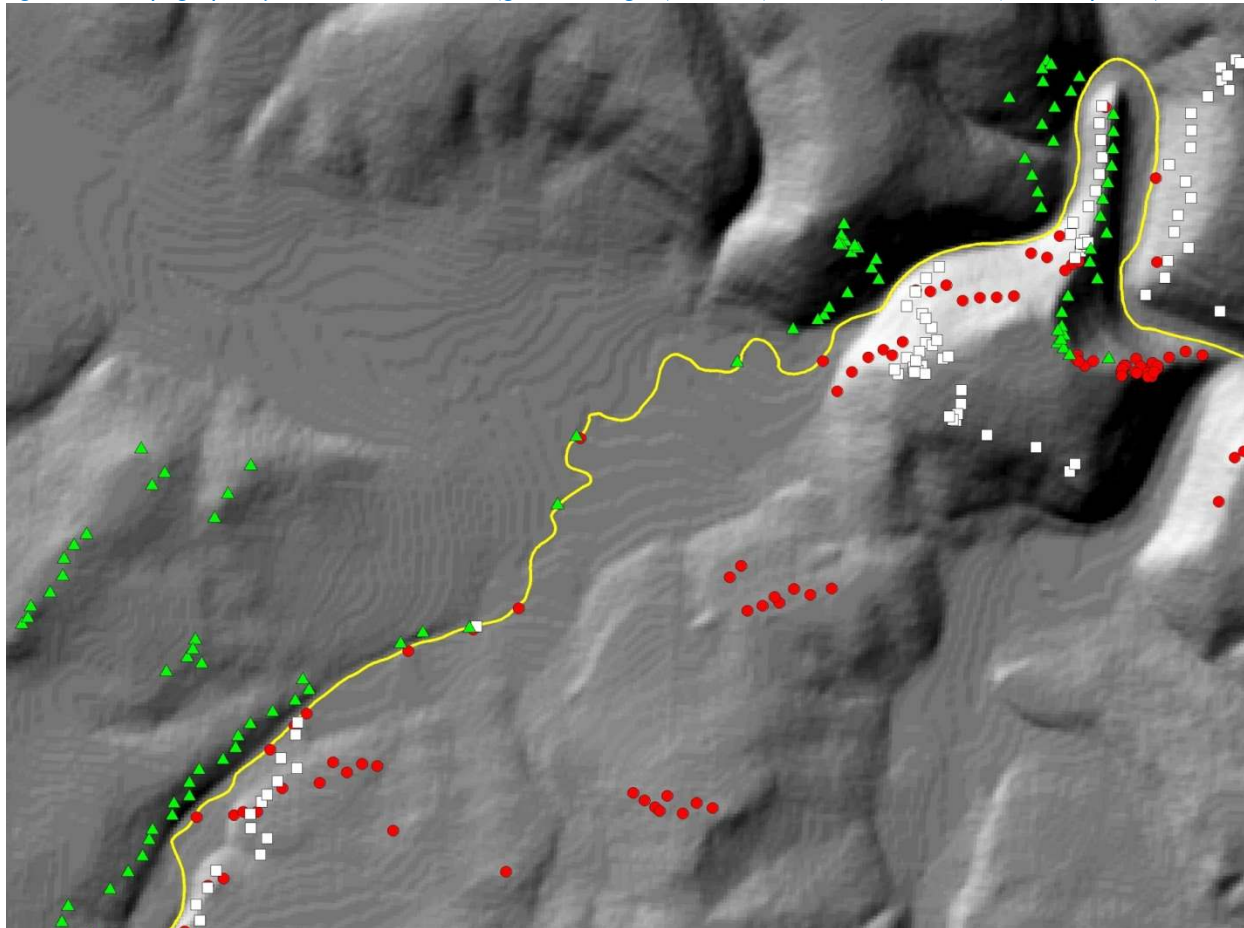
Figure 30 - Stream elevations sampled at each 50-meter node.



3.5.4 TTools Step 4

The maximum topographic angles to the east, south and west are sampled for each 50-meter node from the 10-meter DEM. The sampling routine looks up to 10 kilometers in each direction. Figure 31 shows the stream polyline (yellow) and the highest topographic shade producing features in each of the three directions. The TTools sampling routing is optimized to assess both near-field (<1 km) and far field (up to 10 km) topographic features. In many cases, the highest topographic shade feature is the bank where the stream has become down-cut or flows along cliffs.

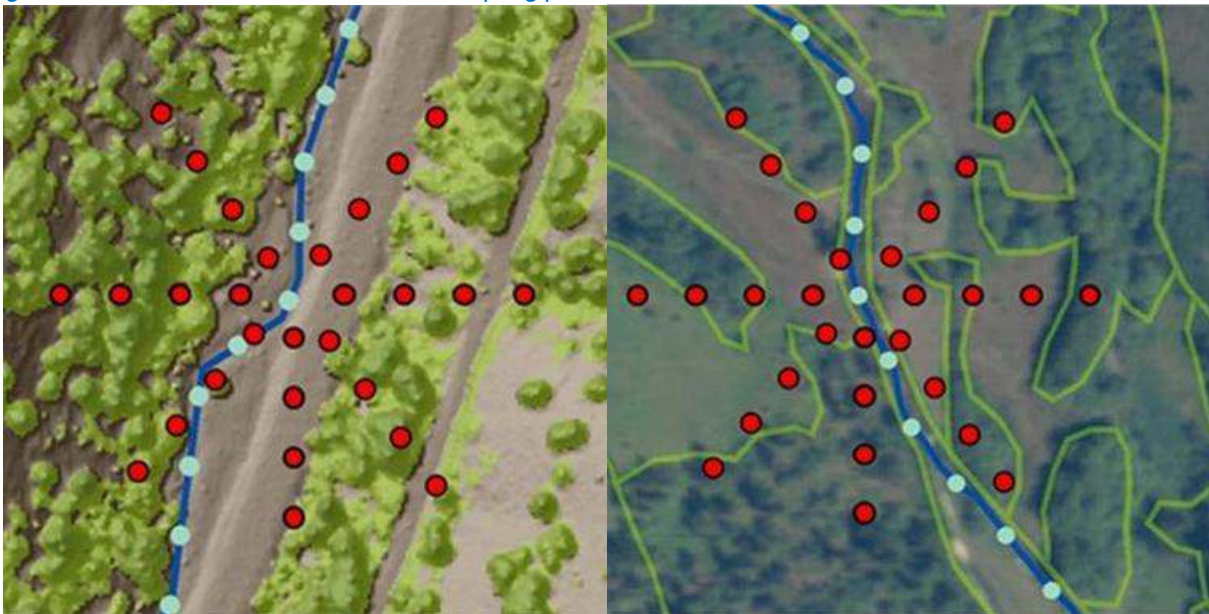
Figure 31 - Topographic features to the west (green triangles), south (red circles) and east (white squares).



3.5.5 TTools Step 5

Near stream land cover heights are sampled at each 50-meter node using a dense radial sampling pattern. Where LiDAR is available, the bare earth elevation and the highest hit elevation are both sampled and the height is calculated as the difference between the two. Where near stream land cover was manually digitized, the unique land cover code is sampled and recorded in the database. The distance between samples was either 10 or 15 meters, depending upon stream size.

Figure 32 - Near stream land cover radial sampling pattern.



The radial sampling pattern produces extensive overlap between each 50-meter node which ensures dense sampling of the near stream area. While there is no direct canopy cover input in the Heat Source model, the extensive land cover sampling and complex solar flux algorithms indirectly account for the density of tree stands within each radial sampling area. For example, in the figure above, approximately 50% of the ground is visible within the sampling area and since the model calculates solar flux through each radial sampling location for every minute of the day, the overall canopy density is indirectly accounted for and varies for each 50-meter stream node.

Note that there is an input in Heat Source for “land cover density”. This term is not the same as “canopy density” as it is classically used in the forest industry. Land cover density in Heat Source refers to the relative density of the vegetation that is being sampled. It can also be thought of as the amount of sky that is blocked by the trunk, branches, and leaves of a tree. In most Heat Source simulations of eastern and central Oregon, the land cover density value is set to 75%, which is representative of conifers in the region. Ground level solar pathfinder measurements have been used to successfully validate the Heat Source effective shade predictions using the 75% land cover density value.

3.5.6 TTools Step 6

One of the TIR deliverables was a point shapefile containing sampled stream temperatures. Step 6 of TTools associates the nearest TIR sample point with each 50-meter stream node. Figure 33 shows a section of Catherine Creek with the 50-meter nodes and the TIR data points. The TIR data points are typically more than 50-meters apart and are located according to the helicopter position at the time the TIR image frame was collected. TTools walks through each of the 50-meter stream nodes and locates the nearest TIR data point, then incorporates that data into the TTools shapefile database.

Figure 33 - Example of 50-meter stream nodes and TIR data points.

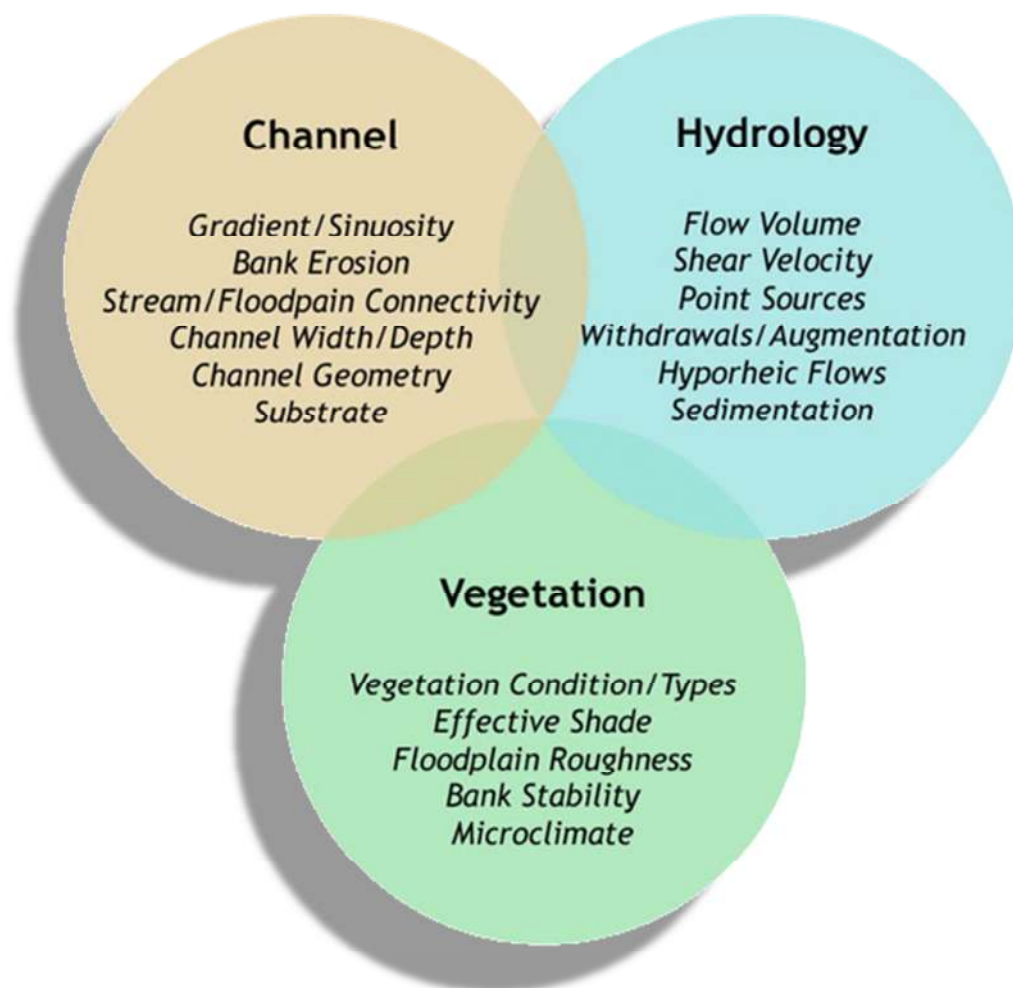


4. HEAT SOURCE OVERVIEW

Heat Source is a high-resolution stream temperature model that incorporates both remote sensing and ground level data. It has been used for stream temperature studies (including Total Maximum Daily Load development) throughout the Pacific Northwest since 1998. Some of the Heat Source characteristics are listed below:

- Input distance step = 50 meters.
- Output distance step = 100 meters.
- Time step = 1 minute.
- Hourly air temperature, relative humidity, wind speed and cloud cover inputs.
- Accommodates high-resolution LiDAR bare earth and highest hit data.
- Calibrated to TIR longitudinal profile and to hourly instream temperature measurements.
- Can be set up to simulate a connected stream network (i.e., outputs from tributaries can become inputs to receiving stream models).
- Strives to account for all factors that influence stream temperature (Figure 34).

Figure 34 - Parameters included within the Heat Source methodology.



Heat Source has a Microsoft Excel user interface and is driven by Visual Basic, Python, and C+ code. Inputs are inserted into various spreadsheet tabs within the model. Outputs are written to text files that can then be accessed within the Excel interface to be plotted or listed within the spreadsheets.

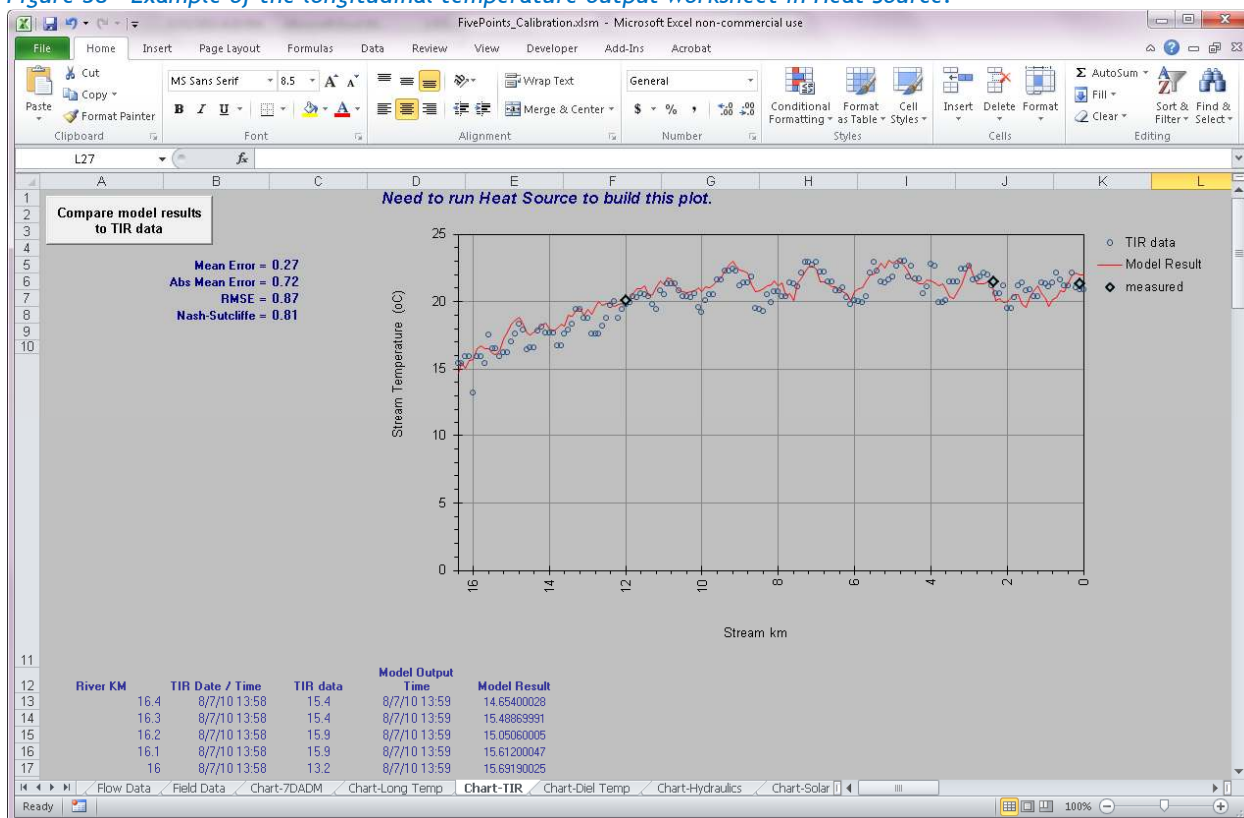
The shapefile database created from TTools sampling contains much of the information required to set up a Heat Source model. Most of the data can be copied from the shapefile database and pasted directly into Heat Source's Excel interface. Figure 35 shows one of the input worksheets where TTools data are stored.

Figure 35 - Example of the TTools data input worksheet in Heat Source.

Reach Label (optional)	Longitude (deg)	Latitude (deg)	Topographic Elev. (deg)			Emergent Veg	Veg 1	NE Veg 2	NE Veg 3	NE Veg 4	NE Veg 1	E
			West	South	East							
16.4	-118.16	45.43	30.6	9.0	28.1	0	3.2	0.1	2.5	0.5	2.2	
16.35	-118.16	45.43	29.6	9.6	29.9	0	13.8	9.8	3.5	1.9	0.4	
16.3	-118.16	45.43	28.2	10.0	31.6	0	0.9	2.6	1.7	25.7	0.6	
16.25	-118.16	45.43	28.0	10.3	25.9	0	3.7	0.5	5.4	14.7	0.6	
16.2	-118.16	45.43	28.3	10.8	13.4	0	15.6	9.2	0.3	0.3	19.1	
16.15	-118.16	45.43	29.2	11.3	15.0	0	32.0	1.7	23.7	5.2	32.1	
16.1	-118.16	45.43	34.1	18.1	15.2	0	1.4	4.8	8.0	8.2	37.6	
16.05	-118.16	45.43	34.3	22.9	19.4	0	4.7	26.7	25.2	13.9	31.0	
16	-118.16	45.43	31.2	14.0	24.5	0	1.3	0.2	2.6	0.4	8.6	
15.95	-118.16	45.43	28.9	13.2	28.8	0	1.6	0.9	0.5	0.4	0.1	
15.9	-118.16	45.43	27.8	13.7	32.3	0	1.0	0.3	0.6	0.6	0.6	
15.85	-118.16	45.43	28.6	14.5	31.5	0	9.8	16.1	15.4	18.3	0.1	
15.8	-118.16	45.43	31.2	15.4	29.6	0	0.1	0.0	5.9	0.4	0.1	
15.75	-118.16	45.43	28.9	15.8	31.9	0	4.7	19.6	5.5	2.4	5.8	
15.7	-118.16	45.42	30.2	17.0	30.2	0	1.1	23.3	13.6	11.8	13.3	
15.65	-118.16	45.42	31.1	18.0	30.8	0	3.6	2.5	19.5	0.5	3.2	
15.6	-118.16	45.42	36.6	18.1	19.0	0	0.1	0.1	0.0	0.1	0.4	
15.55	-118.16	45.42	32.1	19.7	16.1	0	0.4	2.2	2.0	0.6	0.4	

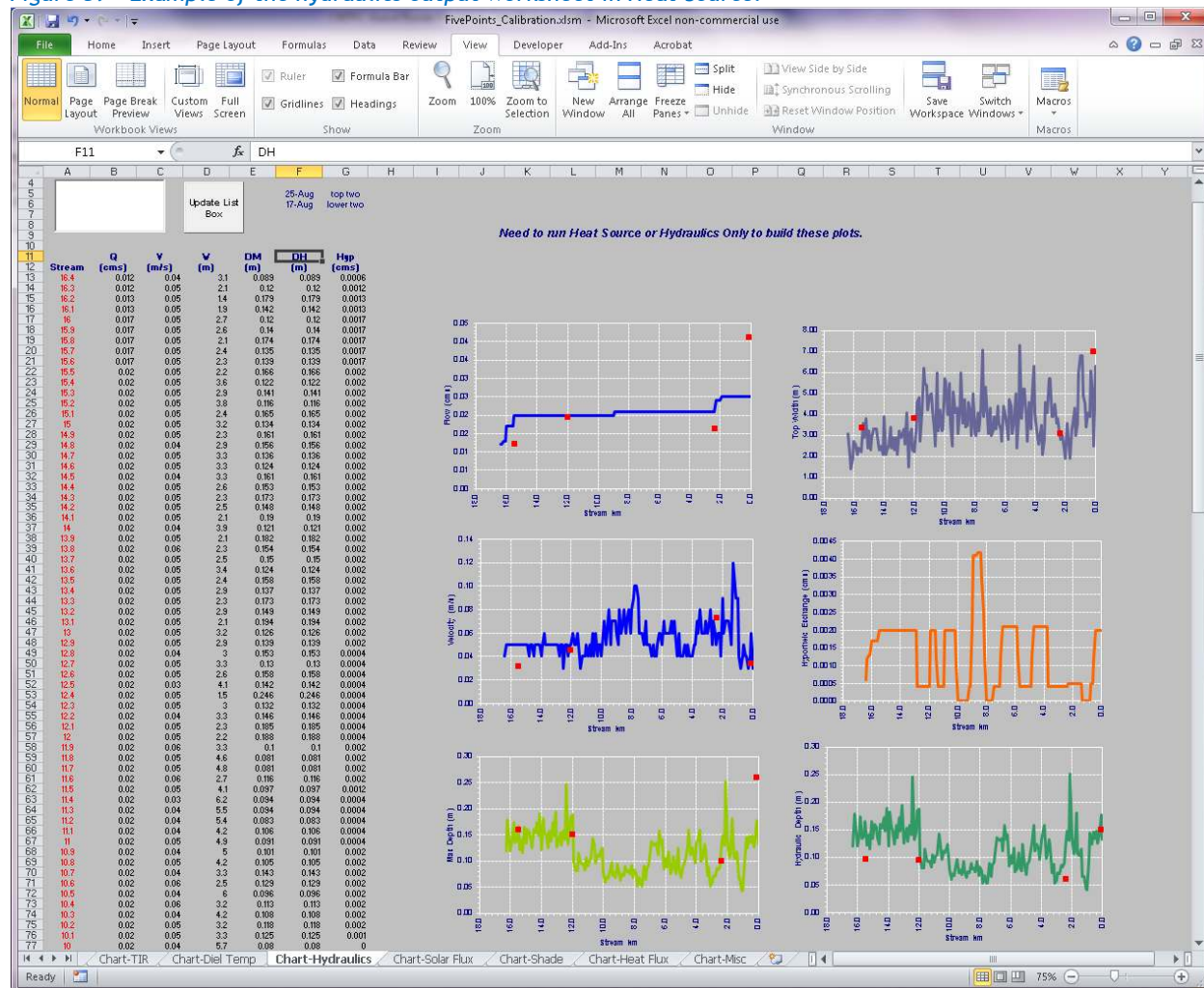
The Heat Source model contains several worksheets that use data from the output text files to display temporal and longitudinal data. Figure 38 shows the longitudinal temperature calibration worksheet. After the model is run, this chart is updated for the user to compare simulated and measured values. There are similar charts that compare the hourly simulated and measured data for each continuous monitoring location.

Figure 38 - Example of the longitudinal temperature output worksheet in Heat Source.



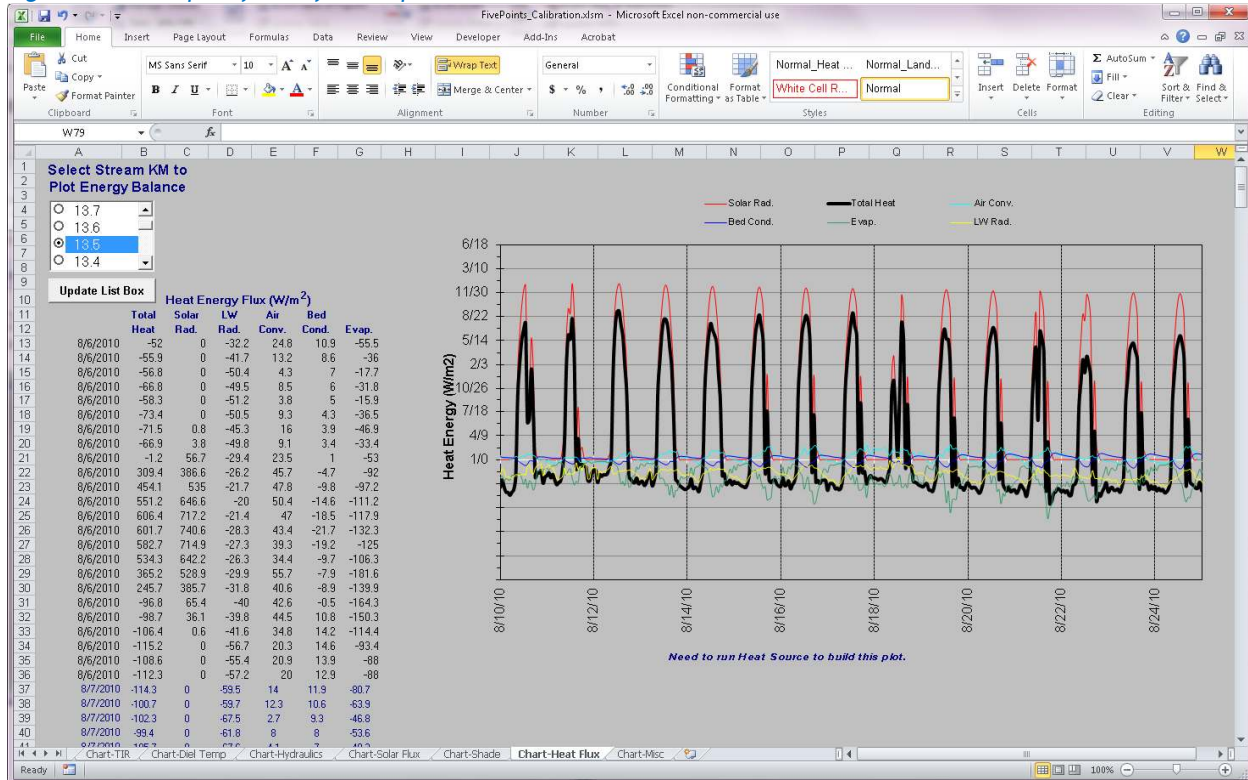
Model hydraulics is another important output worksheet in Heat Source (Figure 39). The simulation outputs can be plotted within this worksheet for model validation purposes. Any available ground level measurements can be included within these charts to compare simulated and measured values. The data can be plotted for each day of the simulation.

Figure 39 - Example of the hydraulics output worksheet in Heat Source.



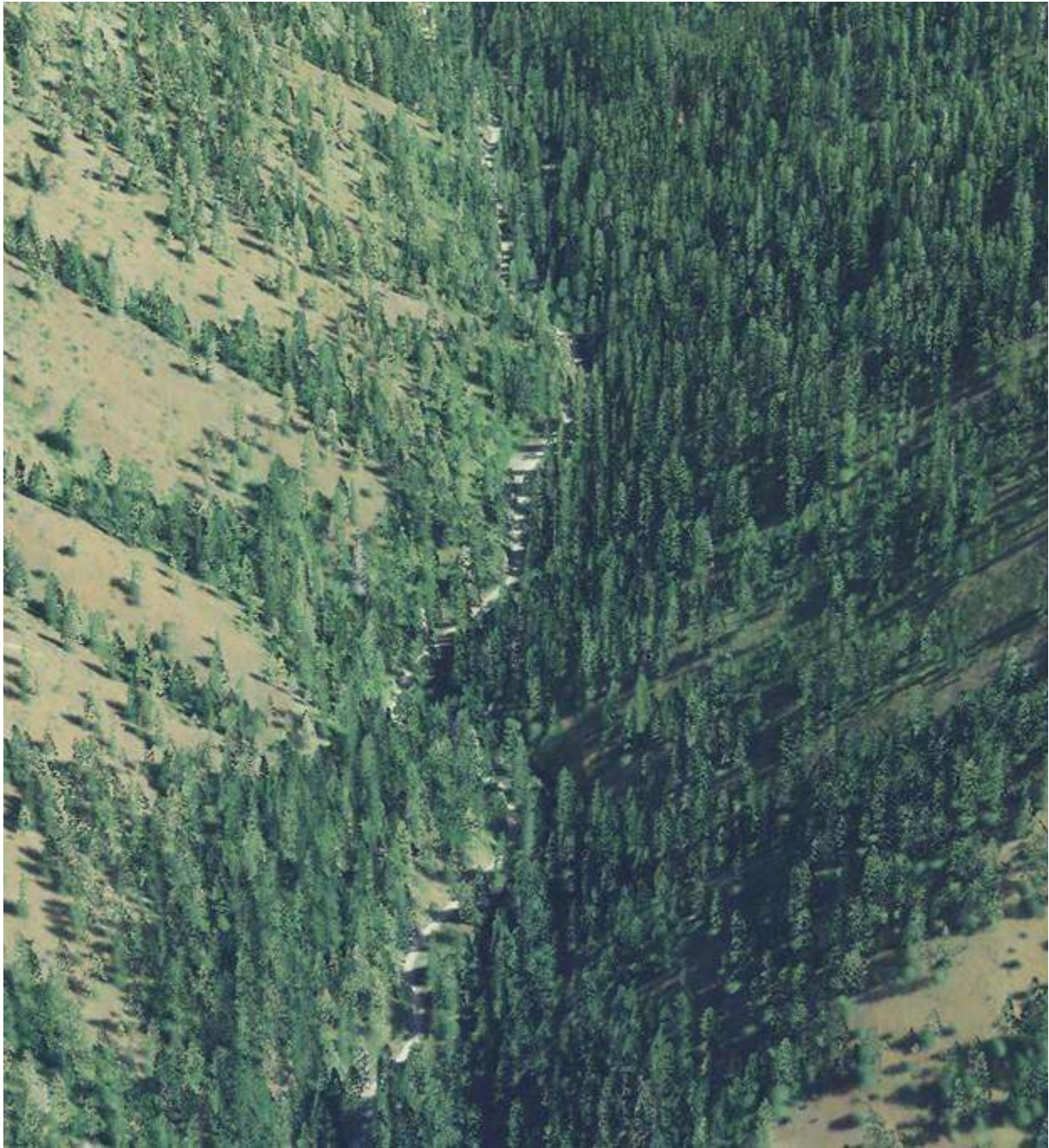
Heat Source also records the hourly heat flux values for each 100-meter output node. There is a worksheet where the user can view various simulated heat flux values (Figure 40). These outputs are useful during calibration to make sure that the simulation is within reasonable boundaries for solar flux, bed conduction, evaporation, air convection, longwave radiation, etc.

Figure 40 - Example of heat flux output worksheet in Heat Source.



5. MODEL SET UP AND CALIBRATION

5.1 North Fork Catherine Creek



RGB-colored LiDAR point cloud - North Fork Catherine Creek looking upstream just above mouth (road visible alongside stream).

5.1.1 North Fork Catherine Creek TTools

The North Fork Catherine Creek has a moderate gradient, typically between 2% and 8%. Figure 41 shows the TTools-sampled stream elevations and calculated gradients for each 50-meter node.

Figure 41 - North Fork Catherine Creek elevation and gradient.

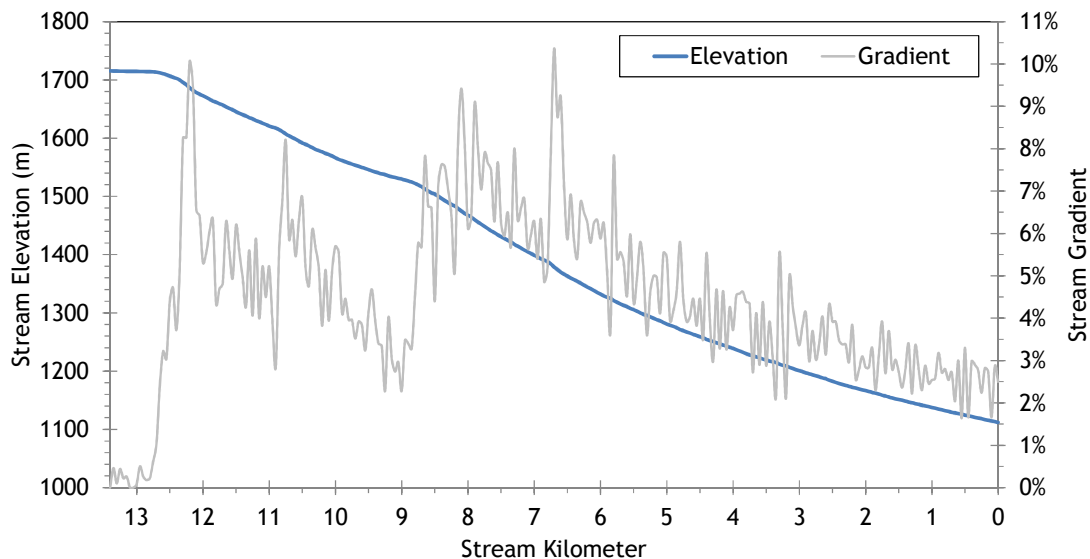
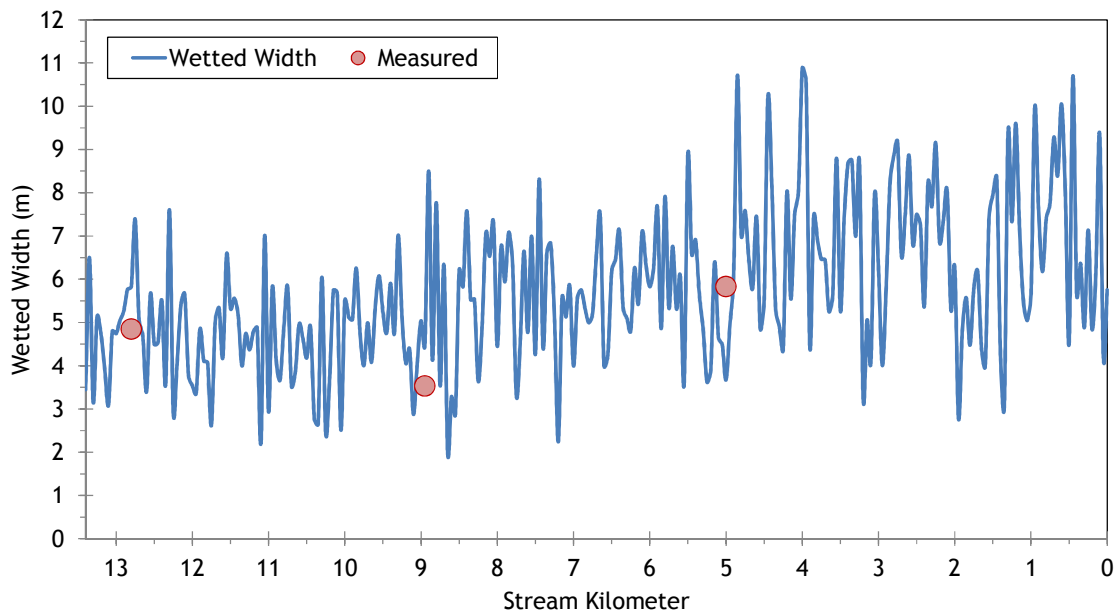


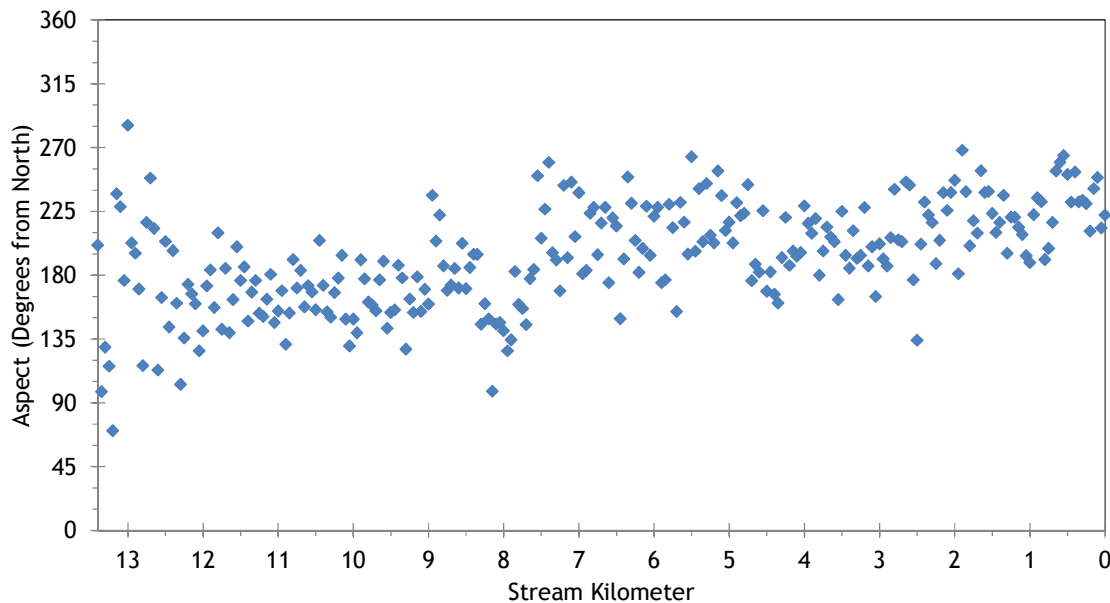
Figure 42 shows the TTools-sampled and measured wetted widths for the North Fork Catherine Creek which are used as estimates for the simulation time period. Generally, the stream was between 4 and 8 meters wide during August 2010.

Figure 42 - North Fork Catherine Creek wetted width.



The North Fork Catherine Creek generally flows from north to south. Figure 43 shows the TTools-sampled stream aspect for each 50-meter node. Aspect is an important Heat Source input parameter because it is used to calculate solar flux at the stream surface.

Figure 43 - North Fork Catherine Creek stream aspect.



The North Fork Catherine Creek flows through mountainous foothills and eastern and western topographic shade angles are typically over 20 degrees from the horizon (Figure 44). Since the stream flows down a predominately south-facing slope, the southern topographic shade angles are smaller.

Figure 44 - North Fork Catherine Creek topographic shade angles.

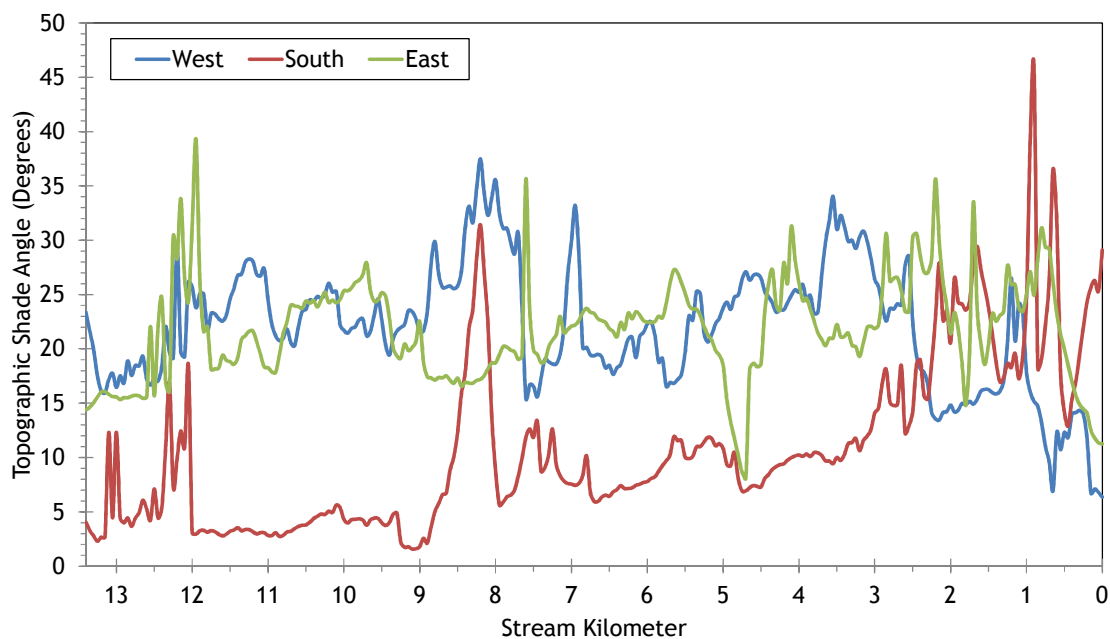
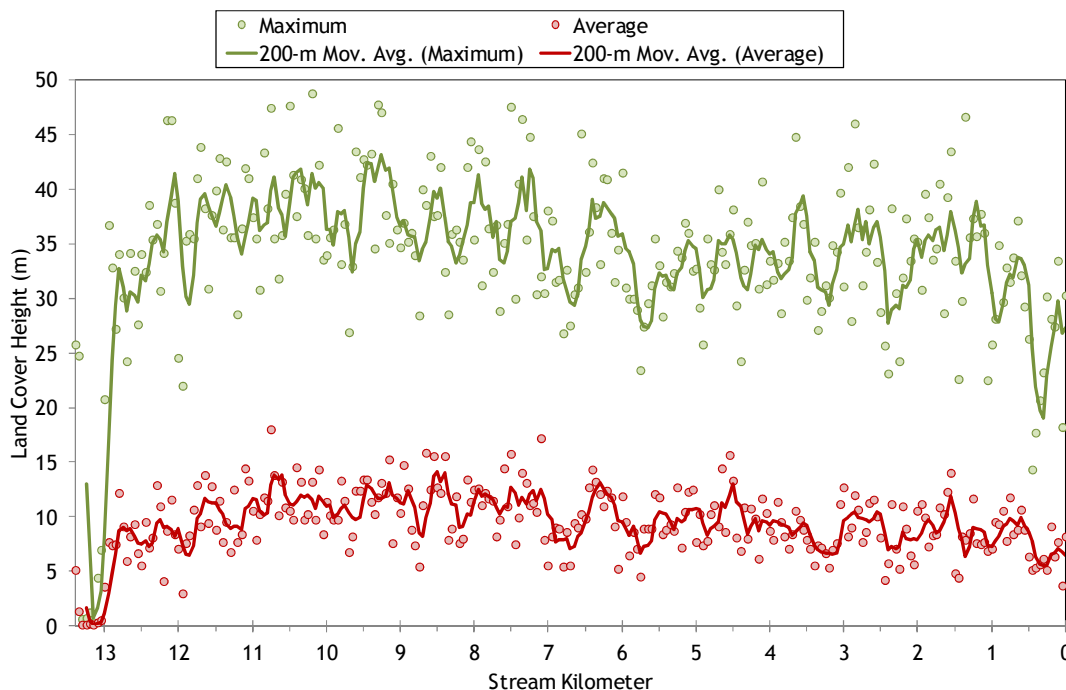


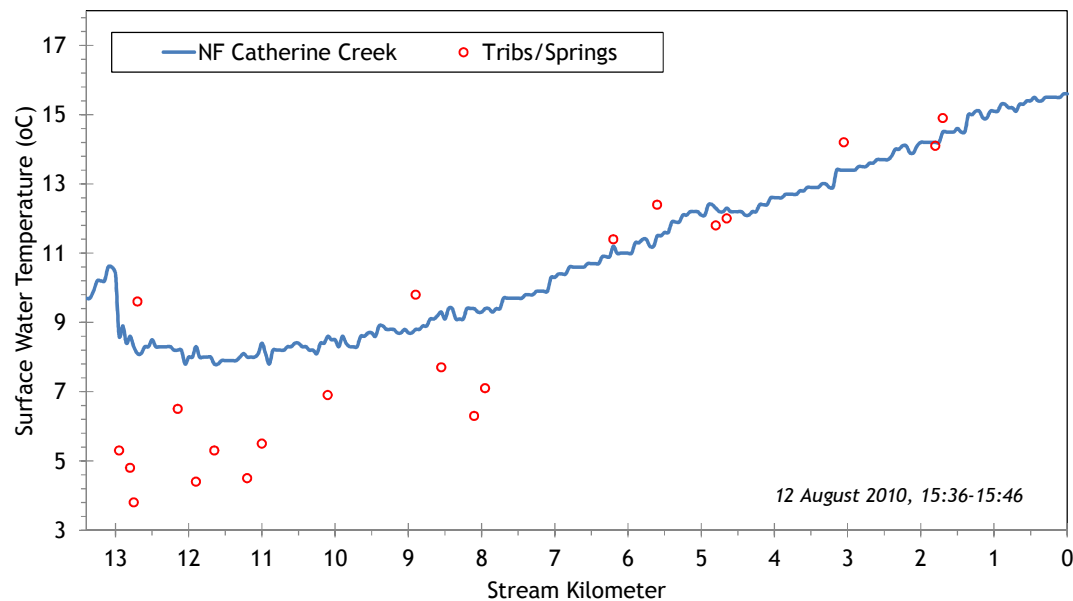
Figure 45 shows the land cover heights sampled along North Fork Catherine Creek. The maximum and average of the 28 radial samples were calculated for each 50-meter stream node. The stream is well-forested throughout most of its length. (Note: Heat Source uses each of the 28 radial samples for each 50-meter node. The maximum and average are shown here for simplification purposes.)

Figure 45 - North Fork Catherine Creek land cover heights sampled from highest hit LiDAR.



TTools was used to associate TIR temperatures with each 50-meter node (Figure 46). Heat Source is calibrated to the TIR longitudinal temperature profile. The North Fork Catherine Creek was cool, relative to other streams in the watershed at the time of the survey (12 August 2010, 15:36-15:46).

Figure 46 - North Fork Catherine Creek TIR temperature profile.



5.1.2 North Fork Catherine Creek Heat Source Calibration

The North Fork Catherine Creek was simulated from just above Amelia Spring to the mouth (13.4 stream kilometers). The largest tributaries are the Middle Fork Catherine Creek, Buck Creek, and Lick Creek. There were four sites where hourly stream temperature data collection was attempted; however there were data quality issues at some locations. Figure 47 shows the simulation extent and continuous temperature monitoring locations.

Figure 47 - North Fork Catherine Creek simulation extent.

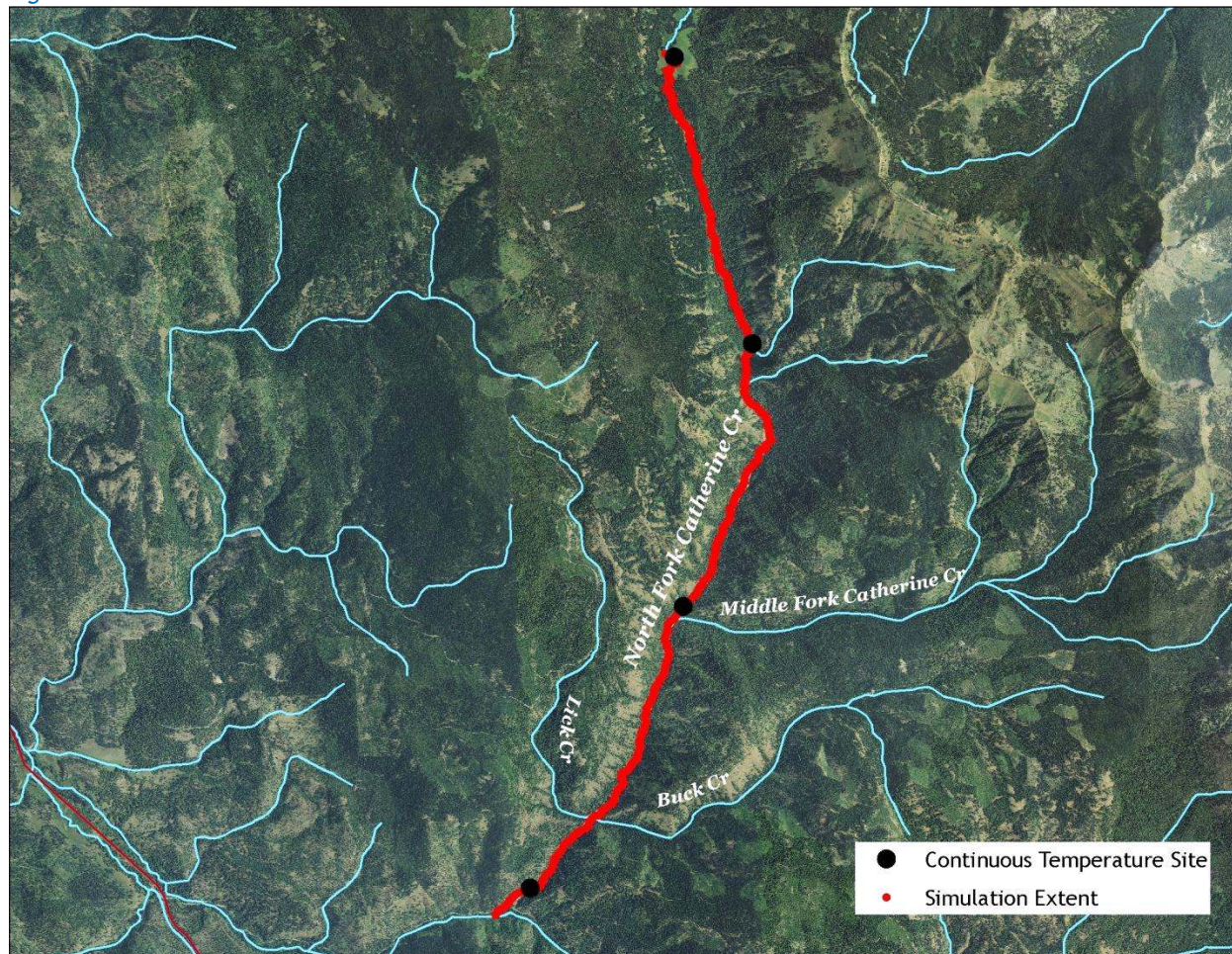


Table 5 - North Fork Catherine Creek general Heat Source parameters.

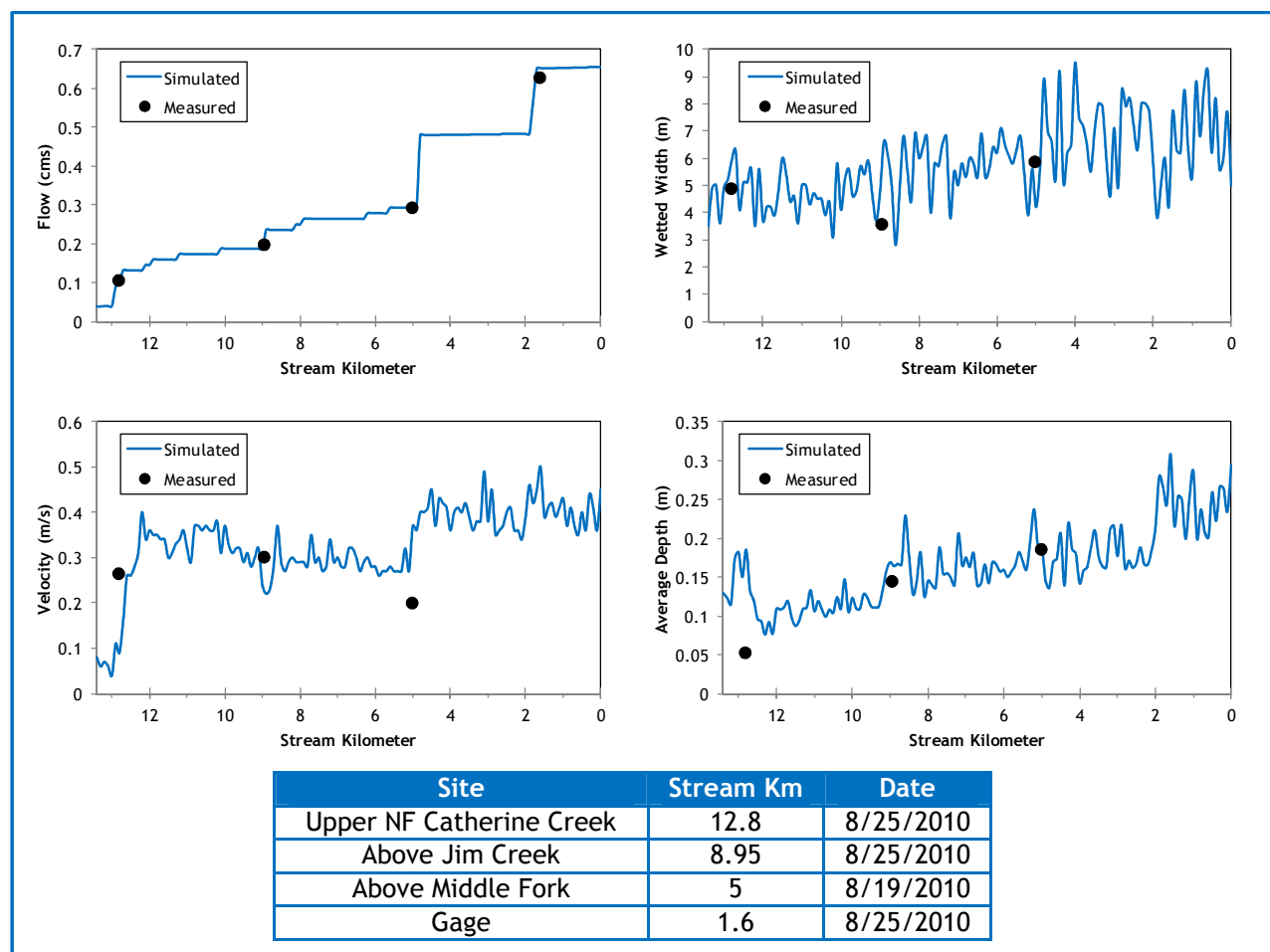
Stream:	North Fork Catherine Creek
Length:	13.4 kilometers
Time Period:	August 6-27, 2010
Input Distance Step:	50 meters
Output Distance Step:	100 meters
Time Step:	1 minute
Flush Initial Condition:	7 days
TIR Date and Time:	August 12, 2010 15:36-15:46
Land Cover Data Source:	LiDAR
Land Cover Sampling Distance Step:	15 meters

Following is a list of assumptions that were used during Heat Source calibration:

- Hourly climate data was obtained from the La Grande Airport (NWS). Air temperature was adjusted using the adiabatic lapse rate of 1°C per 100 meters elevation.
- Daily flow volumes vary based on extrapolation (back-calculation) from the gage data recorded on the North Fork Catherine Creek at Medical Springs (stream kilometer 1.6).
- There were no observed diversions or withdrawals on the stream.
- Small springs and seeps were assumed constant volumes and temperatures.
- Jim Creek, Buck Creek, Lick Creek, and Middle Fork Catherine Creek were included using daily variable flow volume and hourly temperatures (see Table 6).

Figure 48 shows the simulated and measured hydraulic values for the calibrated model. The simulated data was plotted for August 25, 2010 because that is the day most of the field measurements were collected. The simulated values vary daily based upon flow volume.

Figure 48 - North Fork Catherine Creek simulated and measured hydraulics values.



Daily flow values used in the model were based upon data recorded at the gage near Medical Springs. Figure 49 compares the simulated and measured flow volumes at the gage for the entire simulation time period. The simulated daily flow values are identical to the gage values because those gage data were used as the starting point for the stream flow mass balance calculations. Tributary and spring inflows were estimated and applied within the model in order to meet the recorded gage values.

Figure 49 - North Fork Catherine Creek simulated and measured daily flow volumes at the gage near Medical Springs.

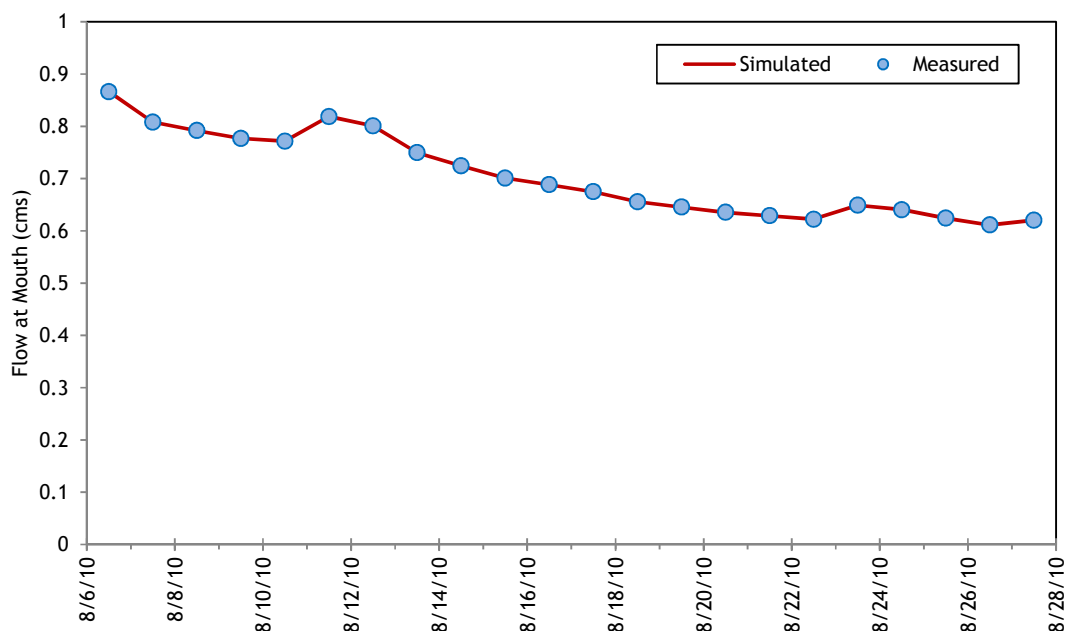


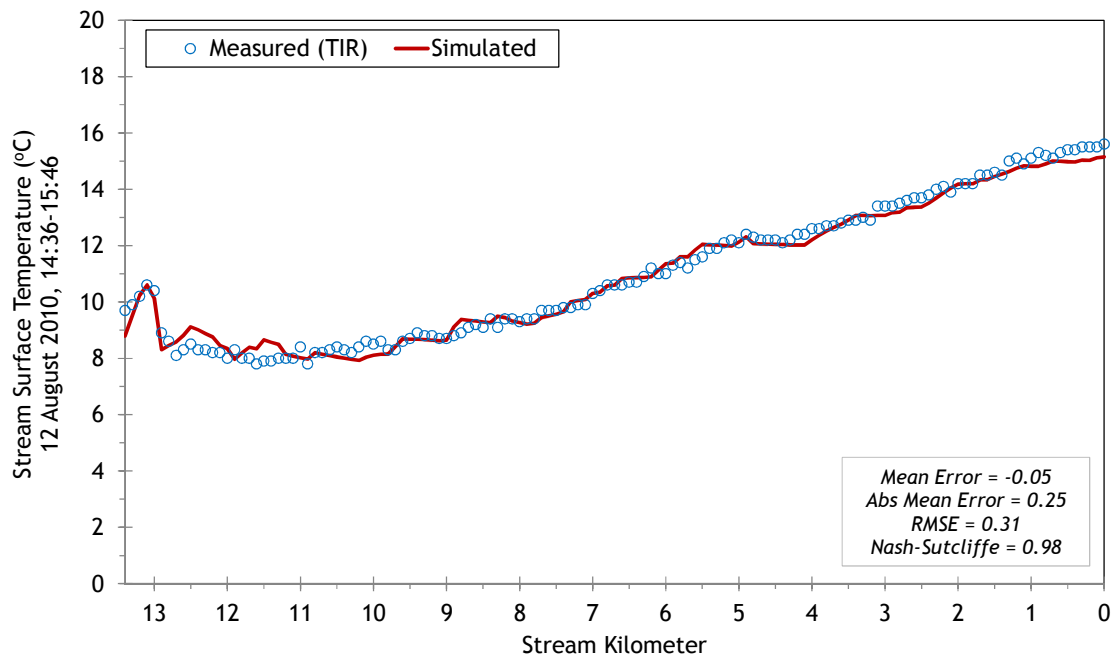
Table 6 summarizes the mass flow inputs that were included within the calibrated Heat Source model. They are features that were identified from the TIR imagery.

Table 6 - North Fork Catherine Creek mass inflow locations and assumptions.

Feature	Stream Km	Assumptions
Amelia Spring	12.95	0.05 cms at 5.3°C (constant)
Seep	12.8	0.014 cms at 4.8°C (constant)
Spring	12.75	0.014 cms at 3.8°C (constant)
Unnamed Trib	12.7	0.014 cms at 9.6°C (constant)
Spring	12.15	0.014 cms at 6.5°C (constant)
Spring	11.9	0.014 cms at 4.4°C (constant)
Spring	11.2	0.014 cms at 4.5°C (constant)
Seep	10.1	0.014 cms at 6.9°C (constant)
Jim Creek	8.9	Estimated daily flow (mass balance) and MF temperatures minus 2°C.
Spring	8.1	0.014 cms at 8.1°C (constant)
Spring	7.95	0.014 cms at 7.1°C (constant)
Unnamed Trib	6.2	0.014 cms at variable temperature
Unnamed Trib	5.6	0.014 cms at variable temperature
Middle Fork Catherine Cr	4.8	Estimated daily flow (mass balance) and measured hourly temperatures.
Buck Creek	1.8	Estimated daily flow (mass balance) and MF temperatures minus 2.3°C.
Lick Creek	1.7	Estimated daily flow (mass balance) and MF temperatures minus 3.1°C.

The North Fork Catherine Creek simulated and measured longitudinal temperatures are shown in Figure 50. Amelia Spring is responsible for the sudden temperature drop near stream kilometer 13. Then the stream gradually heats without any significant thermal fluctuations. The springs and seeps were small, while the tributaries were also relatively small and cool. The RMSE of the longitudinal temperature calibration is 0.31°C , which means the simulated instantaneous values match well to the measured TIR data.

Figure 50 - North Fork Catherine Creek longitudinal stream temperature calibration.

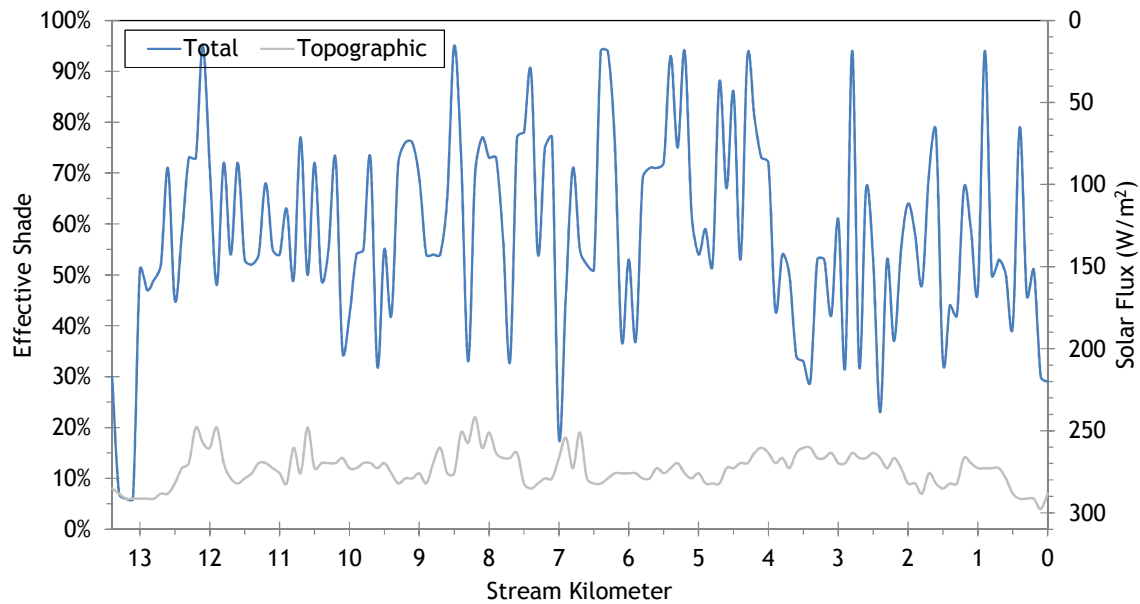


NOTE: There were no valid hourly stream temperature data available besides that which was used for the boundary condition. Data was not retrieved for the two middle sites. The data recorded at the mouth was out of the water and did not record valid stream temperatures. Therefore, there are no hourly temperature calibration results or statistics.

Effective shade is one of the Heat Source simulation outputs (Figure 51). The North Fork Catherine Creek is well-forested and the stream is shaded through much of the day, resulting in effective shade values over 50% for most areas.

Topographic shade was simulated by removing all land cover from within the model. Topographic shade was typically 10% or greater throughout the stream. The difference between the total effective shade and the topographic shade shown in Figure 51 is the amount that can be attributed to land cover.

Figure 51 - North Fork Catherine Creek simulated effective shade.



LiDAR point cloud with RGB extraction - North Fork Catherine Creek upper reach.

5.2 South Fork Catherine Creek

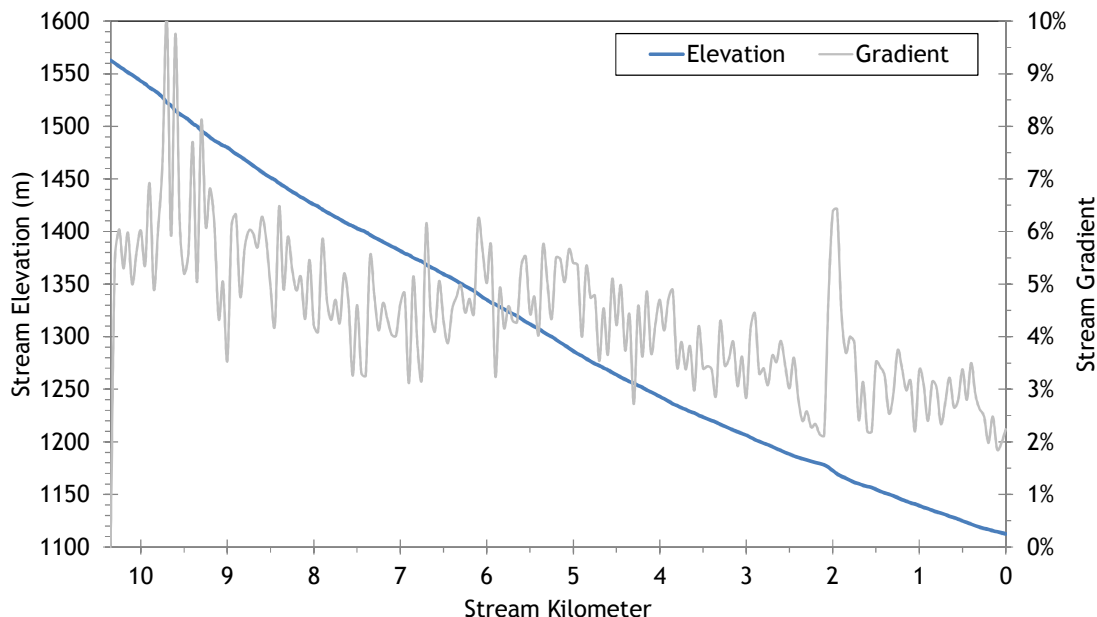


RGB-colored LiDAR point cloud - South Fork Catherine Creek looking upstream toward Corral Creek confluence.

5.2.1 South Fork Catherine Creek TTools Results

The South Fork Catherine Creek has a moderately steep gradient that ranges between 2% and 8% (Figure 52). It drops about 450 meters in elevation in the lower 10 stream kilometers.

Figure 52 - South Fork Catherine Creek elevation and gradient.



The South Fork Catherine Creek wetted widths were sampled at each 50-meter node (Figure 53). Ground level measurements are included in the chart for validation purposes. Generally, the stream is between 3 and 6 meters wide.

Figure 53 - South Fork Catherine Creek wetted width.

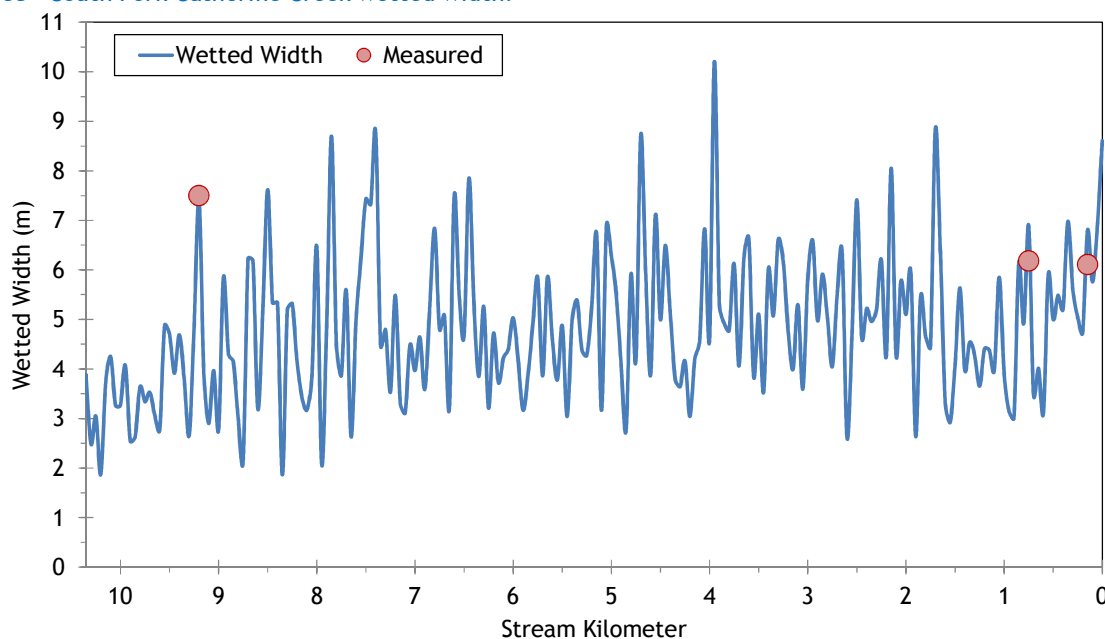
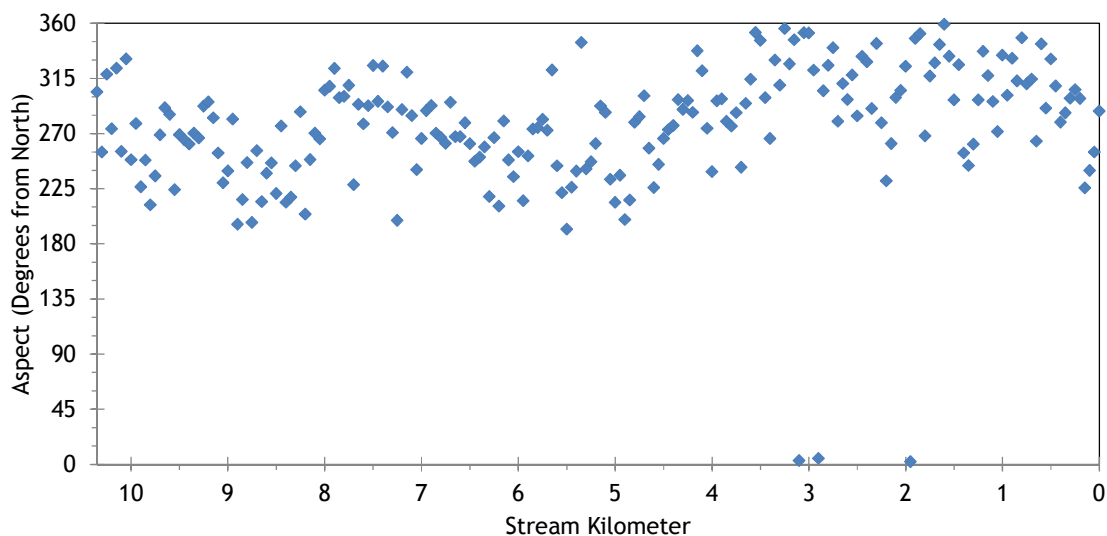


Figure 54 shows the stream aspect for each 50-meter reach of the South Fork Catherine Creek. The stream flows generally from east to west. Since it flows within a confined mountain valley, the stream meanders very little.

Figure 54 - South Fork Catherine Creek stream aspect.



Topographic shade angles of the South Fork Catherine Creek are shown in Figure 55. Since the stream flows east to west, the highest topographic shade angles are produced by hills or mountains to the south.

Figure 55 - South Fork Catherine Creek topographic shade angles.

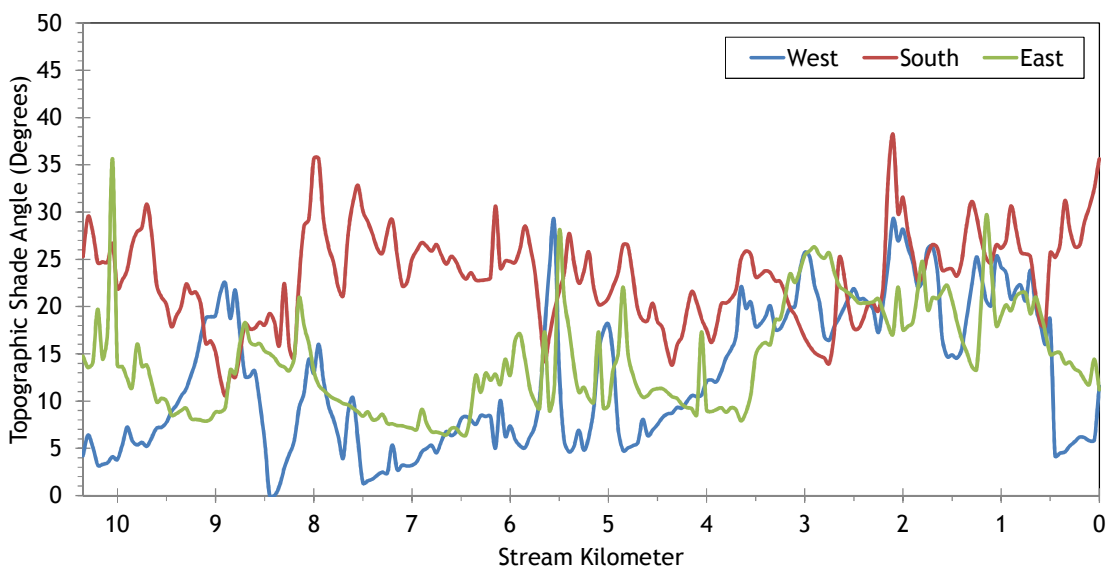
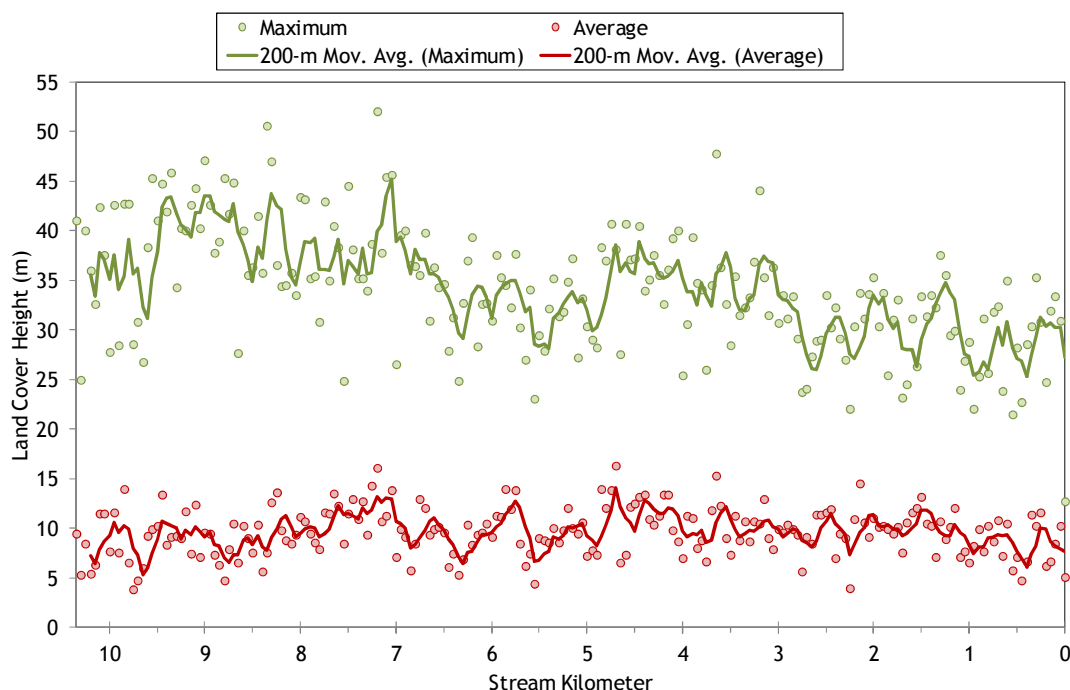


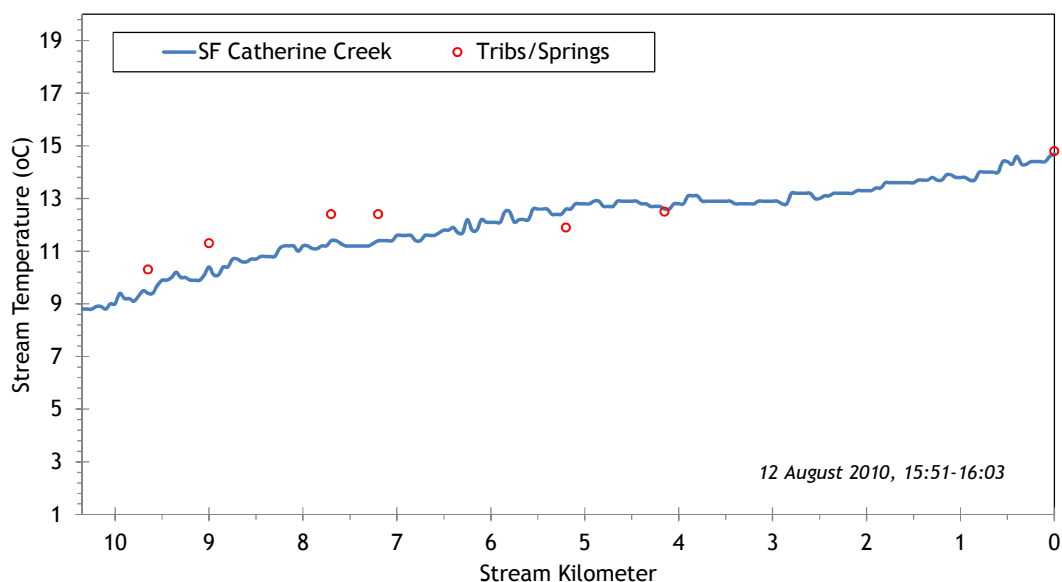
Figure 56 shows the land cover heights sampled along South Fork Catherine Creek. The maximum and average of the 28 radial samples were calculated for each 50-meter stream node. The stream is flanked by mature conifers and riparian trees through most of its length. (Note: Heat Source uses each of the 28 radial samples for each 50-meter node. The maximum and average are shown here for simplification purposes.)

Figure 56 - South Fork Catherine Creek land cover heights sampled from highest hit LiDAR.



The South Fork Catherine Creek flows through predominantly forested mountain foothills, is well-shaded and remains relatively cool compared to other streams in the watershed (Figure 57). The stream barely reached 15°C at the mouth at the time of the TIR survey.

Figure 57 - South Fork Catherine Creek TIR stream temperature profile.



5.2.2 South Fork Catherine Creek Heat Source Calibration

The lower 10.4 kilometers of South Fork Catherine Creek were simulated (Figure 58). The stream originates in the Eagle Cap Wilderness area and flows westward until joining with the North Fork to form the Catherine Creek mainstem. The South Fork Catherine Creek is primarily forested and flows within a v-shaped mountain valley. There are several small tributaries as well.

Figure 58 - South Fork Catherine Creek simulation extent.

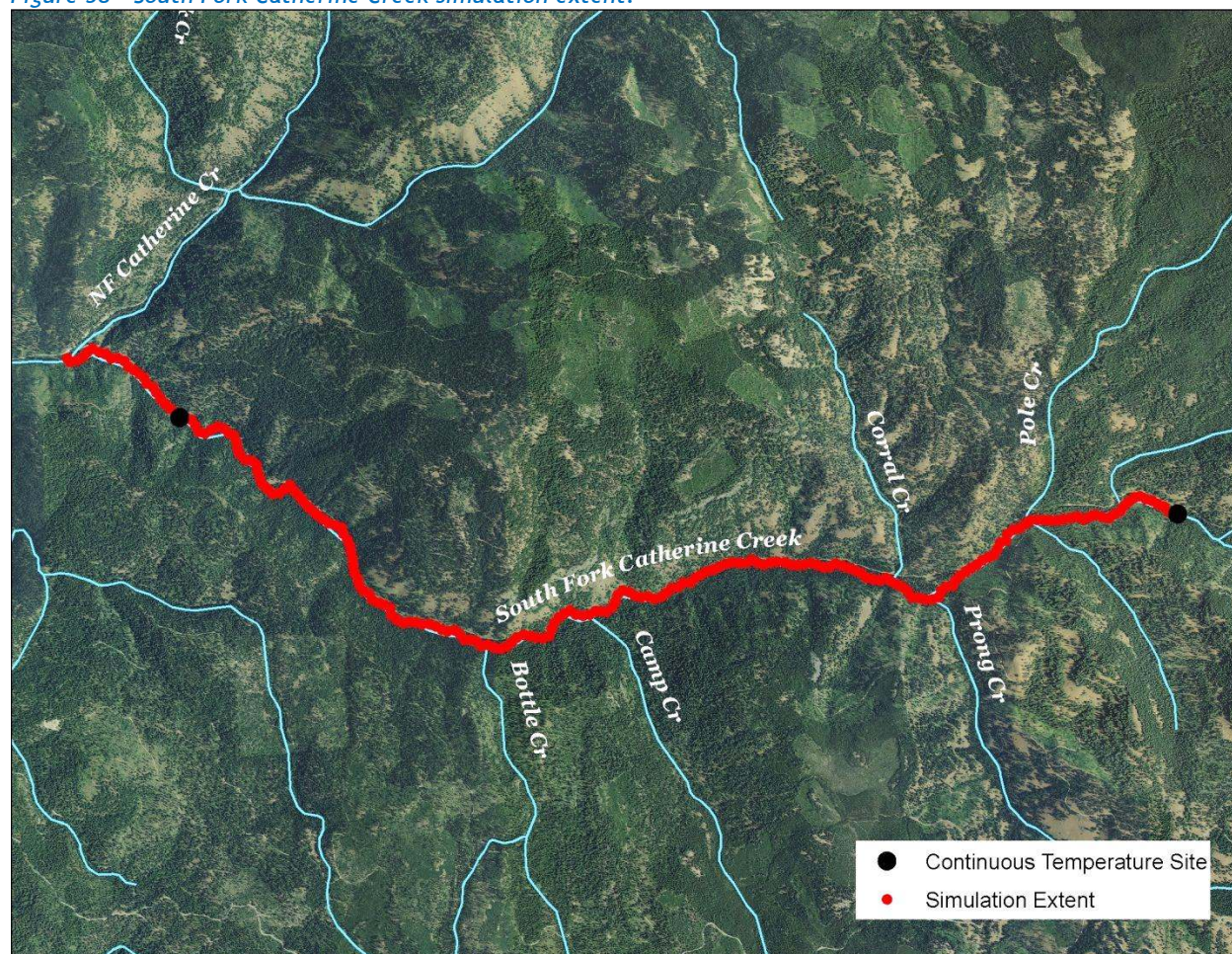


Table 7 - South Fork Catherine Creek general Heat Source parameters.

Stream:	South Fork Catherine Creek
Length:	10.4 kilometers
Time Period:	August 6-27, 2010
Input Distance Step:	50 meters
Output Distance Step:	100 meters
Time Step:	1 minute
Flush Initial Condition:	7 days
TIR Date and Time:	August 12, 2010 15:51-16:03
Land Cover Data Source:	LiDAR
Land Cover Sampling Distance Step:	15 meters

The following assumptions were used when calibrating the South Fork Catherine Creek Heat Source model:

- The upstream monitoring site had no hourly temperature data available, so 5.5°C were subtracted from the values recorded at the mouth and used as the upstream boundary condition. This assumption adds unquantifiable uncertainty to the model. However, since the stream is well-forested and the longitudinal profile has little variability, this assumption is considered a “best estimate” of actual boundary temperatures.
- Hourly climate data was obtained from the La Grande Airport (NWS). Air temperature was adjusted using the adiabatic lapse rate of 1°C per 100 meters elevation.
- Sand Pass, Pole, Prong, Camp and Butte Creek were all assumed to be contributing equal flow volumes.
- Wetted widths used in the final calibration are 130% of the raw TTools values, based on the ground level hydraulics data.
- Daily flow volumes vary based on extrapolation (back-calculation) from the gage data recorded in the North Fork Catherine Creek and Catherine Creek.

Figure 59 shows the hydraulic input parameters for the South Fork Catherine Creek for August 19, 2010. The ground level data was measured on August 19, 2010 at two locations.

Figure 59 - South Fork Catherine Creek simulated and measured hydraulic values.

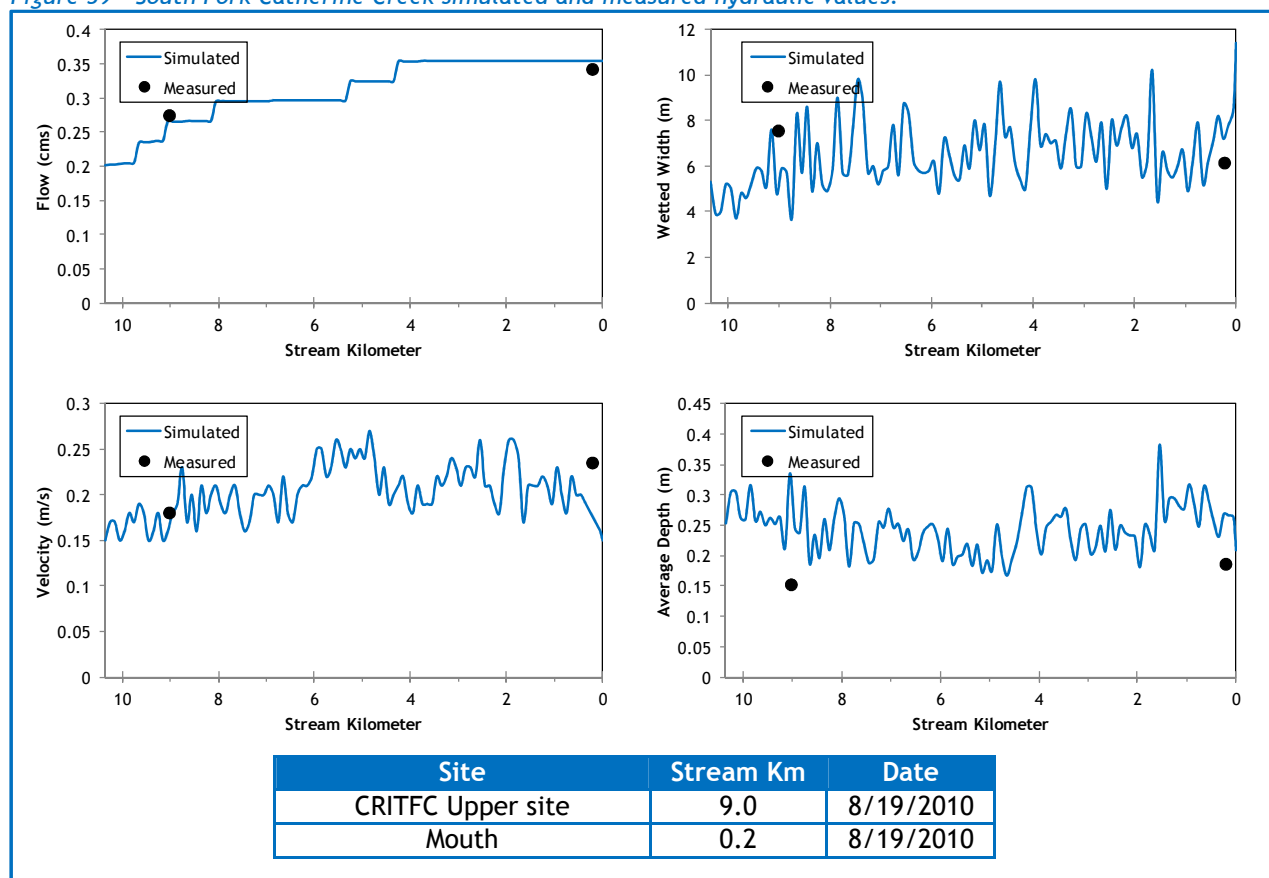
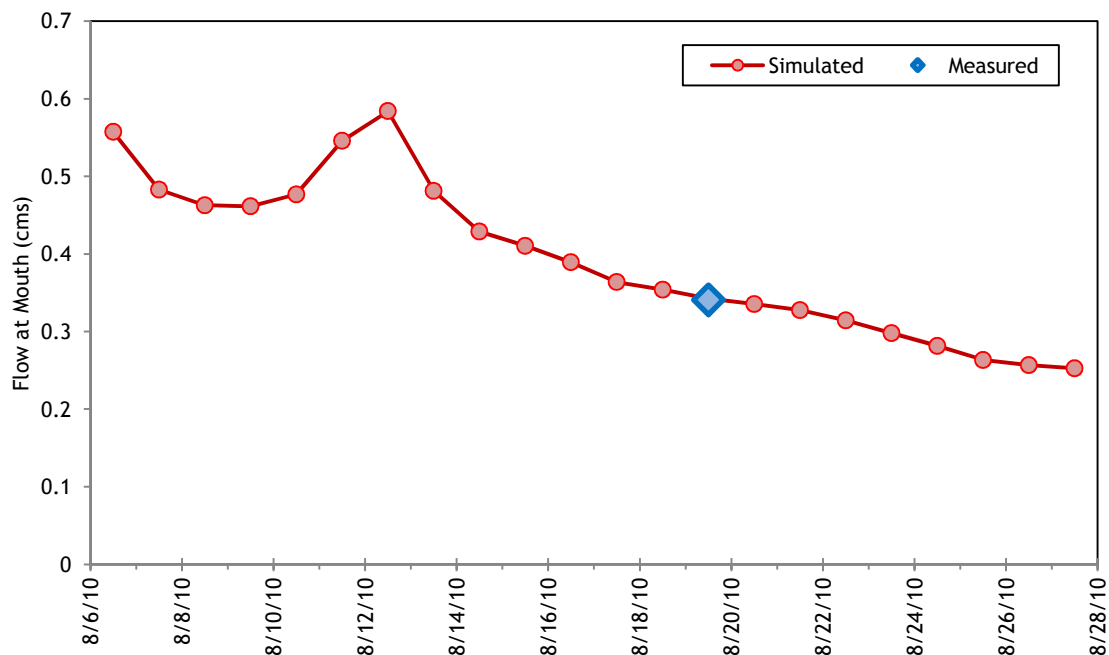


Figure 60 shows the simulated daily stream flow volume at the mouth of the South Fork Catherine Creek. Daily values for the simulation were extrapolated from gage data on the North Fork and Catherine Creek. The increased flows beginning on August 11th were caused by a small rain event.

Figure 60 - South Fork Catherine Creek simulated daily stream flow at the mouth.



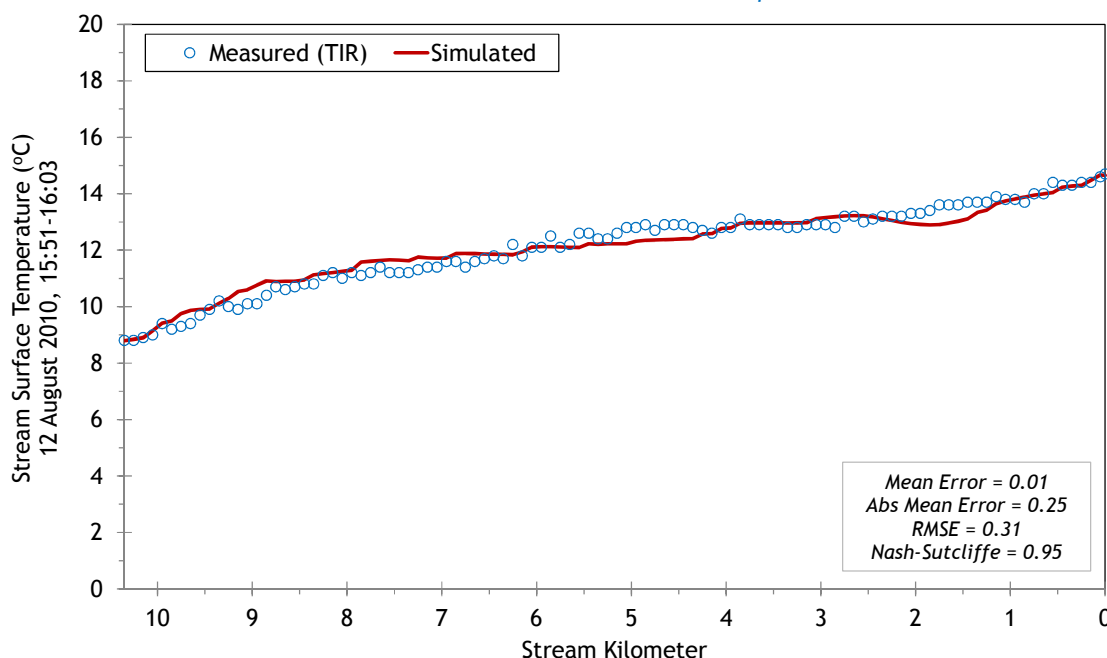
There were 5 tributaries observed in the TIR imagery. They were small enough that they did not have a measurable impact on the South Fork Catherine Creek temperatures; therefore mass balance flow estimates were not possible and simple conservative estimates were used. Hourly temperatures of the tributaries were assumed by adjusting hourly data recorded at the South Fork mouth based on temperature of the tributary observed in the TIR data.

Table 8 - South Fork Catherine Creek mass inflow locations and assumptions.

Feature	Stream Km	Assumptions
Sand Pass Creek	9.65	Daily flow estimated and hourly temperatures estimated by adjusting SF mouth data according to TIR imagery.
Pole Creek	9.05	Daily flow estimated and hourly temperatures estimated by adjusting SF mouth data according to TIR imagery.
Prong Creek	8.1	Daily flow estimated and hourly temperatures estimated by adjusting SF mouth data according to TIR imagery.
Camp Creek	5.25	Daily flow estimated and hourly temperatures estimated by adjusting SF mouth data according to TIR imagery.
Butte Creek	4.3	Daily flow estimated and hourly temperatures estimated by adjusting SF mouth data according to TIR imagery.

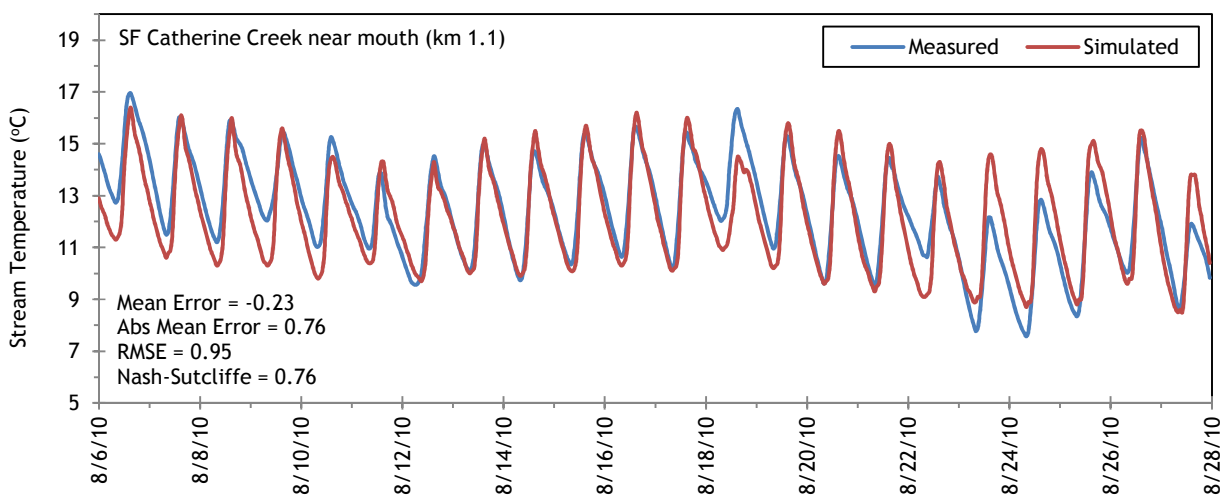
The South Fork Catherine Creek simulated and measured longitudinal temperatures are shown in Figure 61. The calibration statistics are also presented on the chart.

Figure 61 - South Fork Catherine Creek simulated and measured stream temperature.



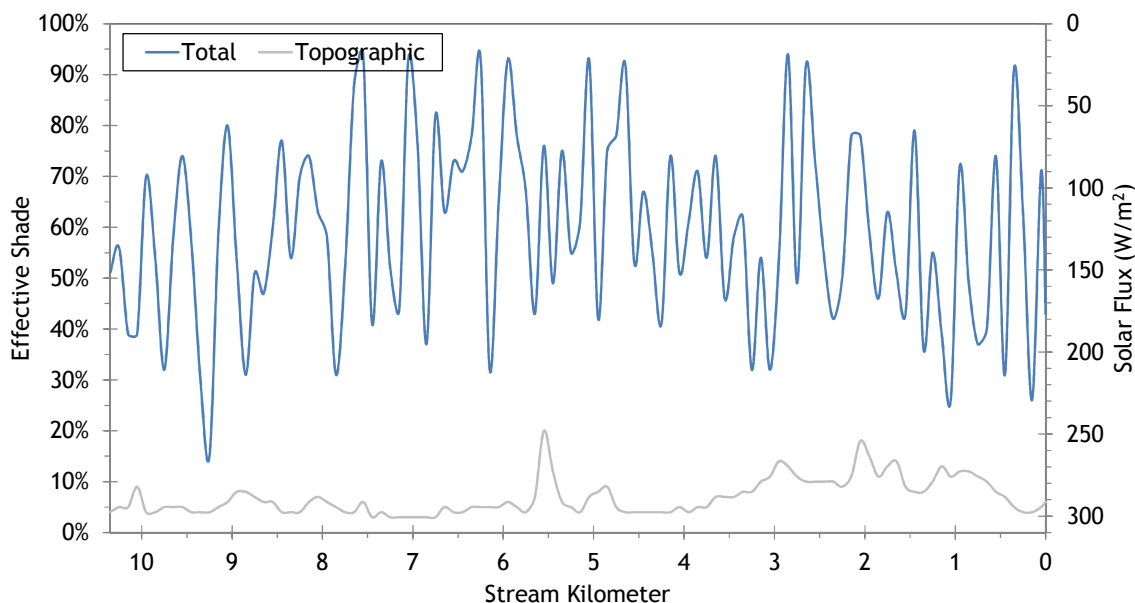
Besides the boundary condition (stream kilometer 10.4), there was one other hourly temperature monitoring site located near the mouth. Figure 62 shows the simulated and measured hourly stream temperatures near the mouth.

Figure 62 - South Fork Catherine Creek simulated and measured hourly temperatures.

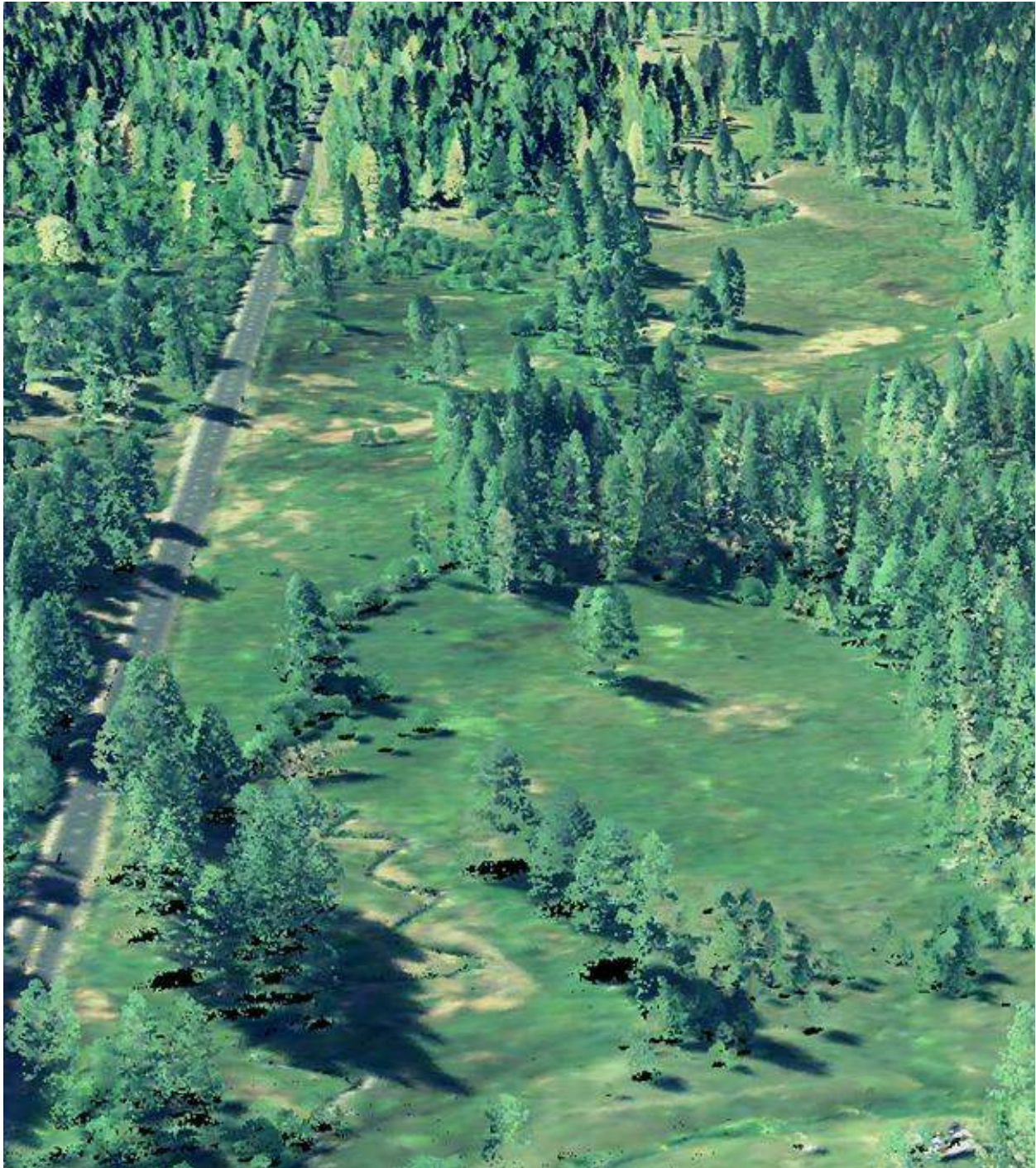


The simulated effective shade values for South Fork Catherine Creek are presented in Figure 63. The total effective shade is that which the stream experiences from both topography and vegetation. The topographic effective shade is the amount received by the stream in the absence of vegetation. The difference between the two is the amount of effective shade provided by the near stream land cover. Since the South Fork Catherine Creek is well forested, effective shade values are substantial for most of the stream.

Figure 63 - South Fork Catherine Creek simulated effective shade.



5.3 Milk Creek

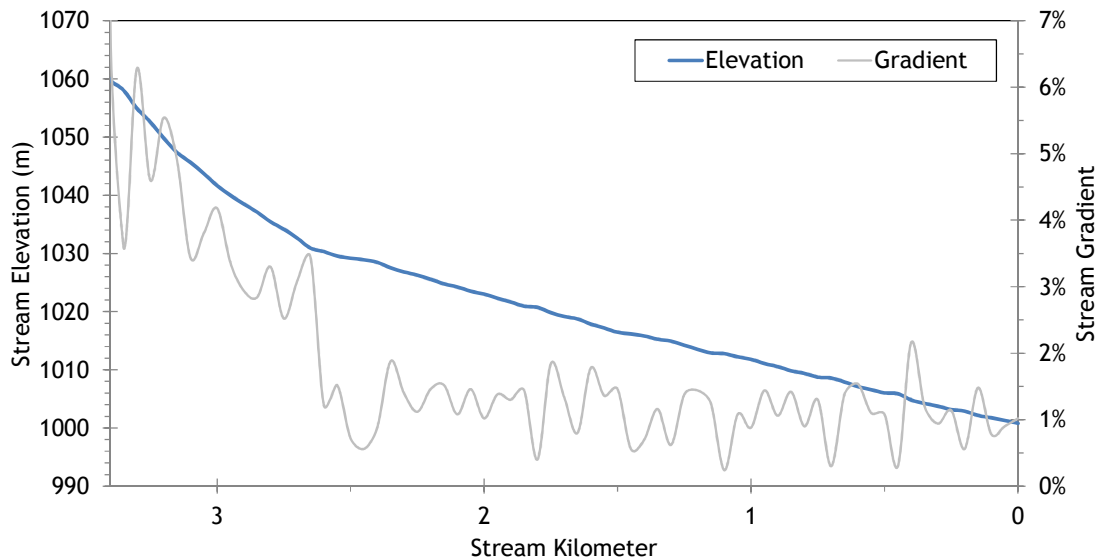


RGB-colored LiDAR point cloud - Looking upstream from mouth of Milk Creek (Medical Springs Highway on left).

5.3.1 Milk Creek TTools Results

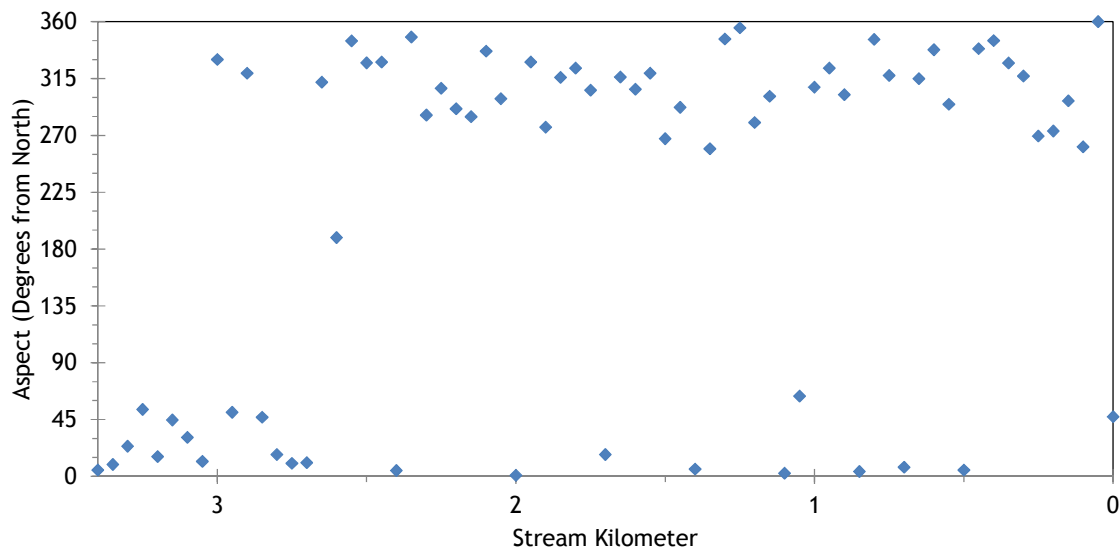
The lower 2.5 kilometers of Milk Creek flow through mostly open meadow and is low gradient. Figure 64 shows the elevation and gradient of the lower 3.4 kilometers where LiDAR data was available.

Figure 64 - Milk Creek stream elevation and gradient.



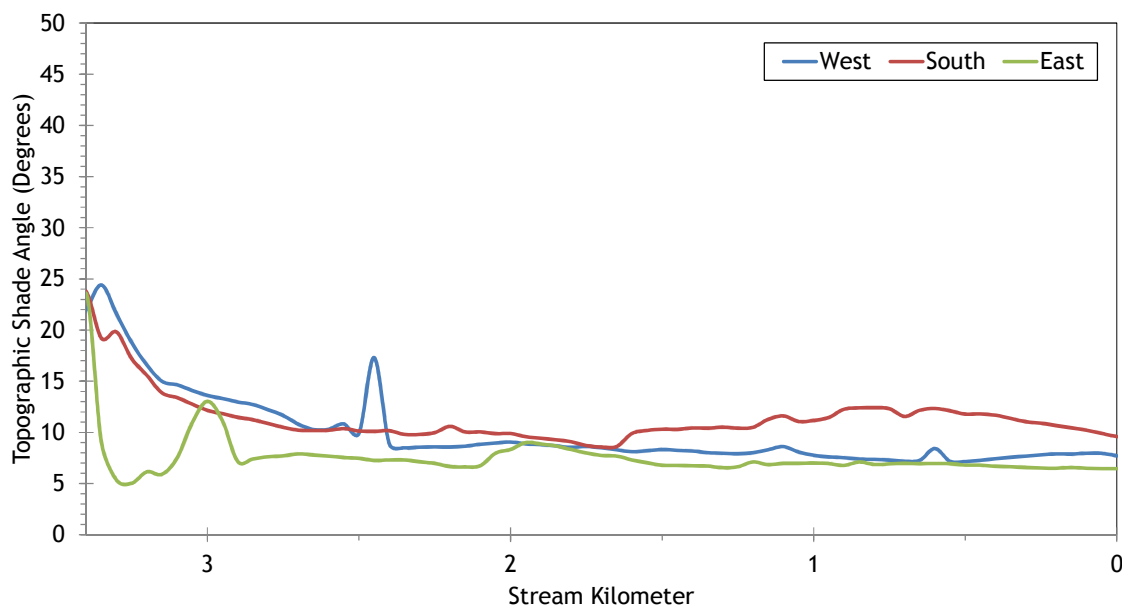
Milk creek generally flows in the northwesterly direction. Figure 65 displays the stream aspect for each 50 meter node of the lower 3.4 kilometers.

Figure 65 - Milk Creek stream aspect.



Topographic shade angles are around 10 degrees for Milk Creek (Figure 66). The highest topographic shade producing features are located to the south of the stream.

Figure 66 - Milk Creek topographic shade angles.



Milk Creek is a small stream so TIR stream temperature samples were sparser than for larger streams (Figure 67). Overall, Milk Creek was about 15-16°C during the TIR flight. This data is used for Heat Source calibration purposes.

Figure 67 - Milk Creek TIR stream temperature profile.

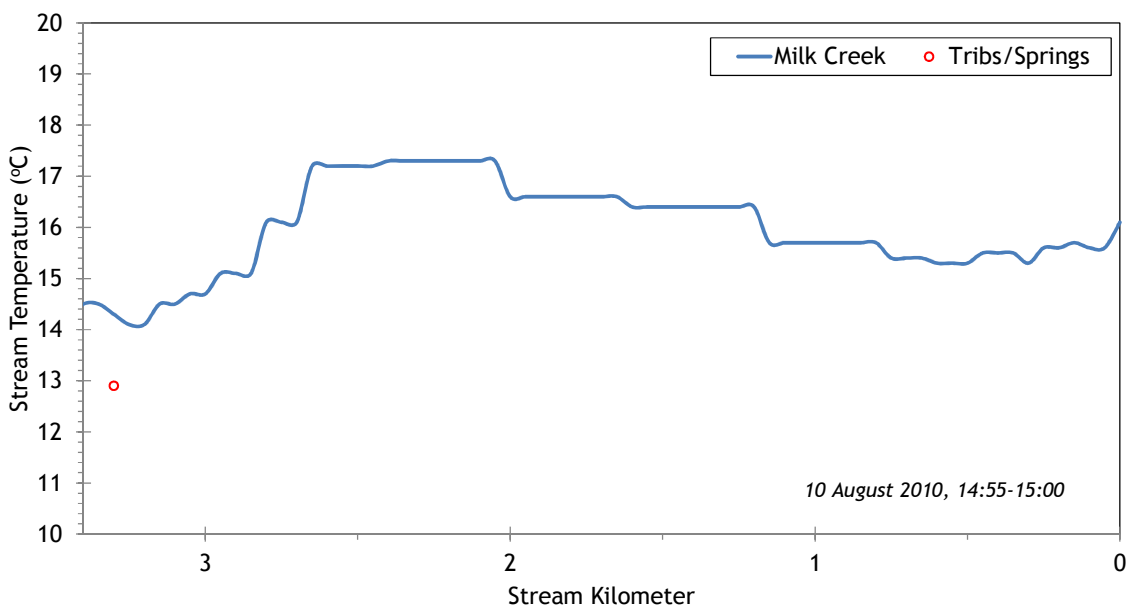
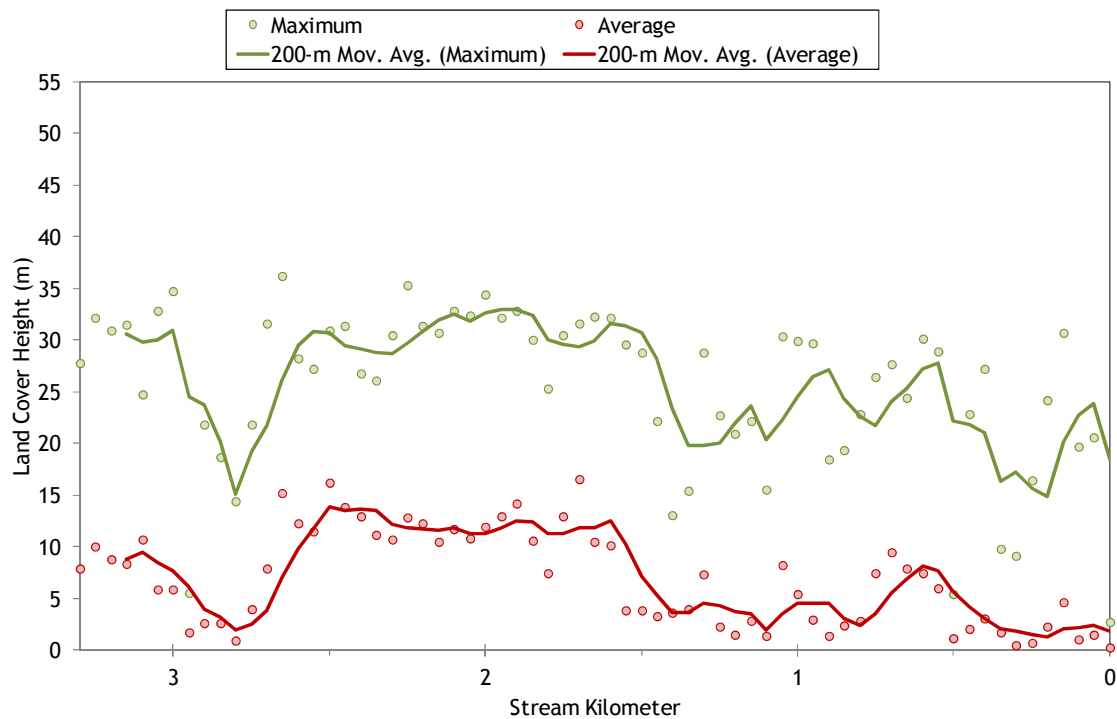


Figure 68 shows the land cover heights sampled along Milk Creek. The maximum and average of the 28 radial samples were calculated for each 50-meter stream node. Average heights are small in the lower 1.5 kilometers because there are fewer trees and many of the radial samples are of meadow grasses. (Note: Heat Source uses each of the 28 radial samples for each 50-meter node. The maximum and average are shown here for simplification purposes.)

Figure 68 - Milk Creek land cover heights sampled from highest hit LiDAR.



5.3.2 Milk Creek Heat Source Calibration Results

The lower 3.3 kilometers for Milk Creek were simulated (Figure 69). There were two ground level monitoring sites which determined the simulation extent.

Figure 69 - Milk Creek simulation extent.

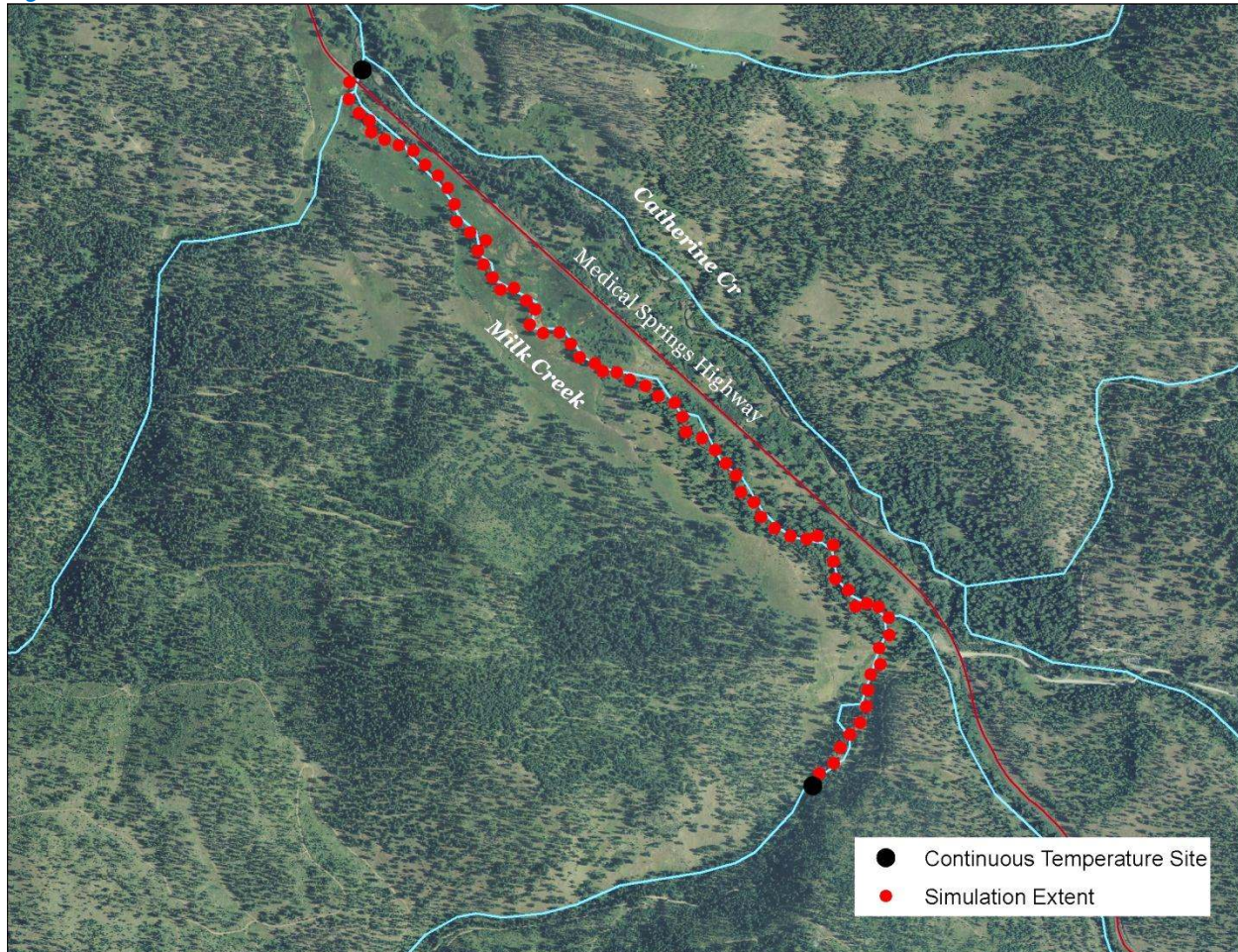


Table 9 - Milk Creek general Heat Source parameters.

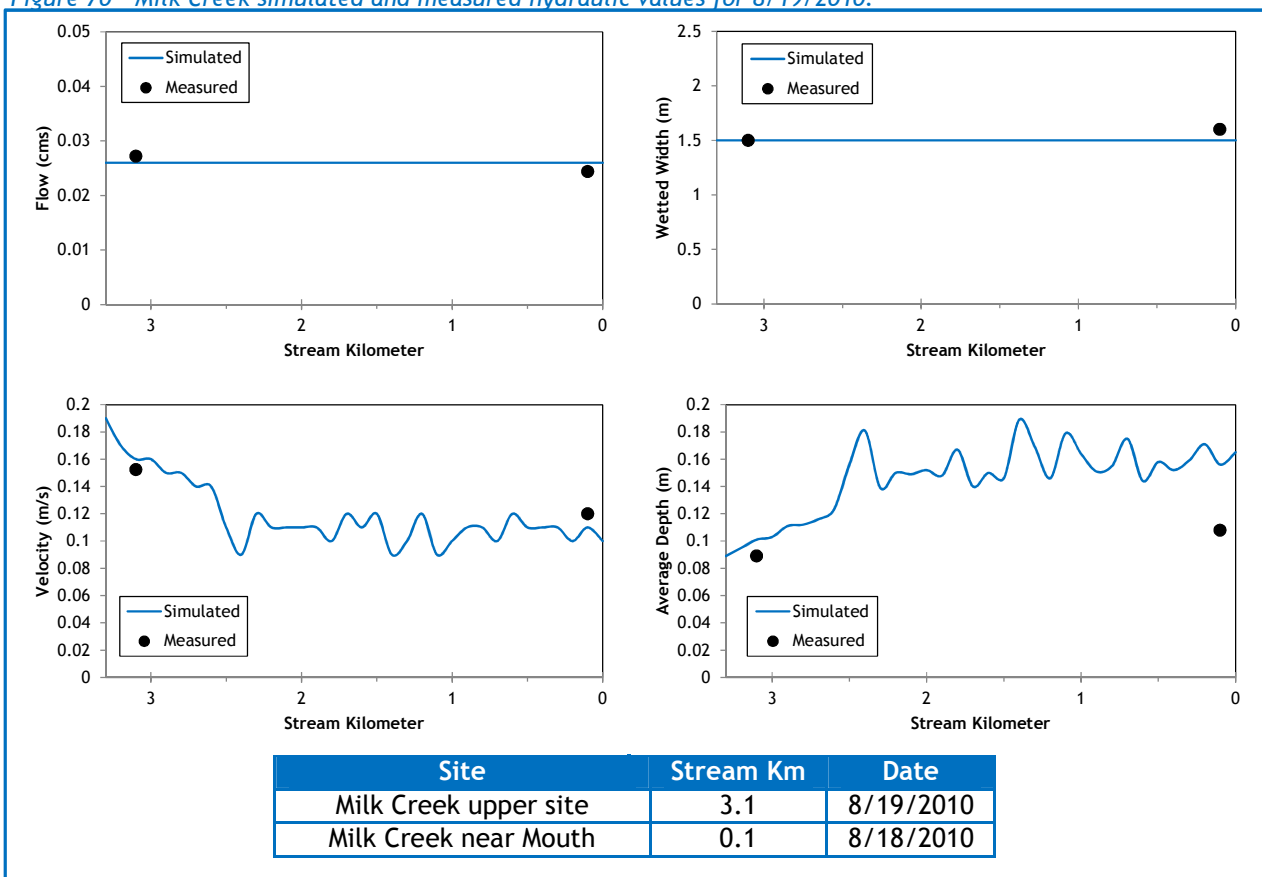
Stream:	Milk Creek
Length:	3.3 kilometers
Time Period:	August 6-27, 2010
Input Distance Step:	50 meters
Output Distance Step:	100 meters
Time Step:	1 minute
Flush Initial Condition:	7 days
TIR Date and Time:	August 10, 2010 14:55-15:00
Land Cover Data Source:	LiDAR
Land Cover Sampling Distance Step:	10 meters

The following assumptions were used when calibrating the Milk Creek Heat Source model:

- Hourly climate data was obtained from the La Grande Airport (NWS). Air temperature was adjusted using the adiabatic lapse rate of 1°C per 100 meters elevation.
- Wetted widths used in the final calibration were 1.5 meters for the entire length. The stream was too small to digitize wetted edges from the remote sensing imagery, so this value was estimated based on the two field measurements.
- Daily flow volumes vary based on extrapolation (back-calculation) from the gage data recorded in the North Fork Catherine Creek and Catherine Creek.
- Since the stream is so small, the land cover sampling distance step was reduced to 10 meters in order to capture the land cover nearest the stream.

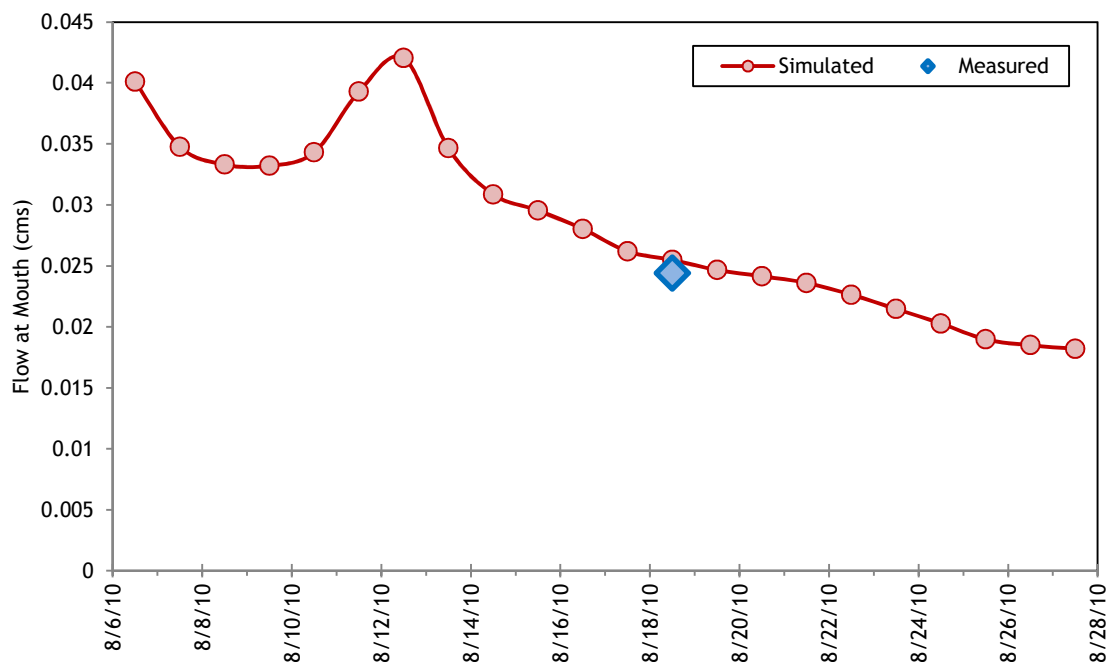
Figure 70 shows the simulated and measured hydraulic parameters for Milk Creek. The simulated data are for August 19, 2010. The field measurements were collected on August 18th and 19th.

Figure 70 - Milk Creek simulated and measured hydraulic values for 8/19/2010.



The simulated flow volumes at the mouth of Milk Creek are shown in Figure 71. The data were extrapolated/estimated from daily gage records in Catherine Creek. There was a small rain event in the basin that increased flows during the second week of August. Since there were no tributary or spring inputs to Milk Creek, these are the flow volumes that were simulated throughout the length of the stream.

Figure 71 - Milk Creek simulated daily stream flow at the mouth.



The simulated and measured longitudinal stream temperatures are shown in Figure 72. Due to the small size of Milk Creek, few TIR samples were obtained.

Figure 72 - Milk Creek simulated and measured longitudinal temperatures.

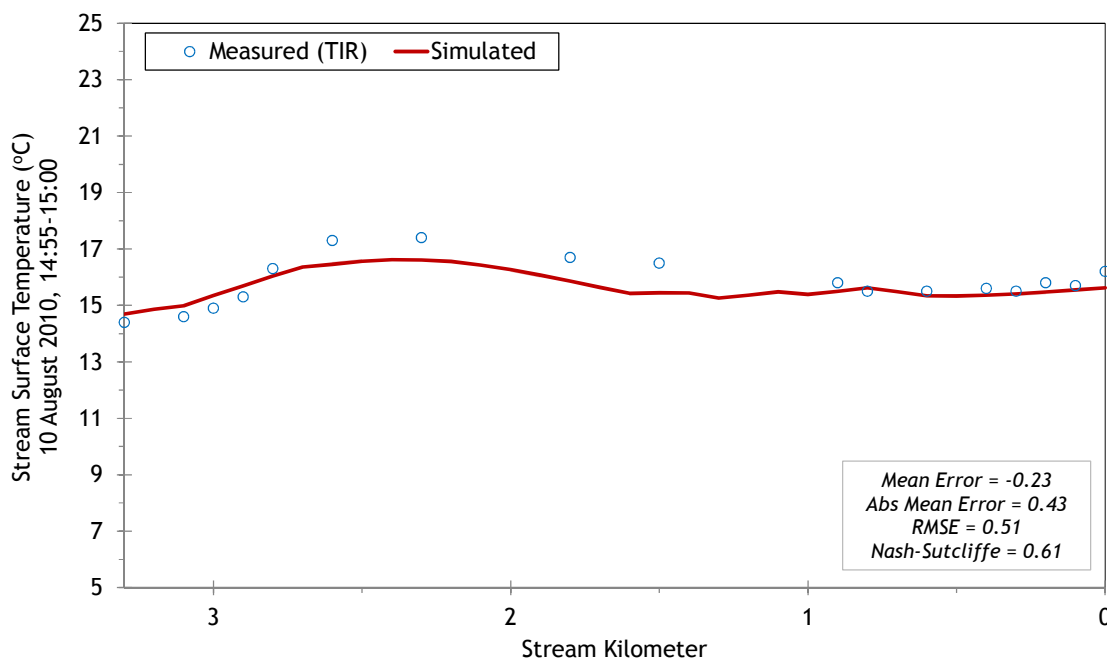
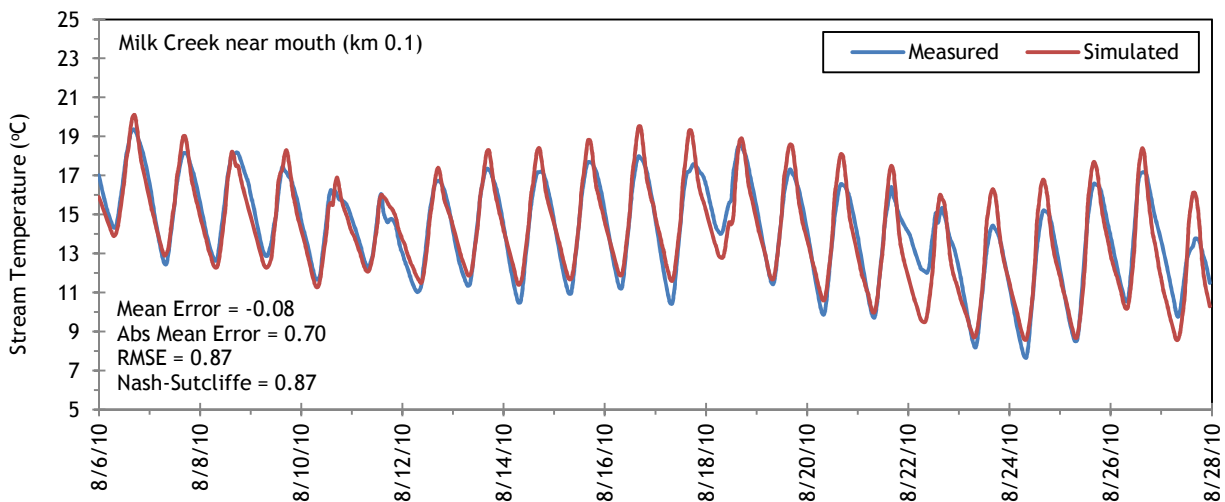


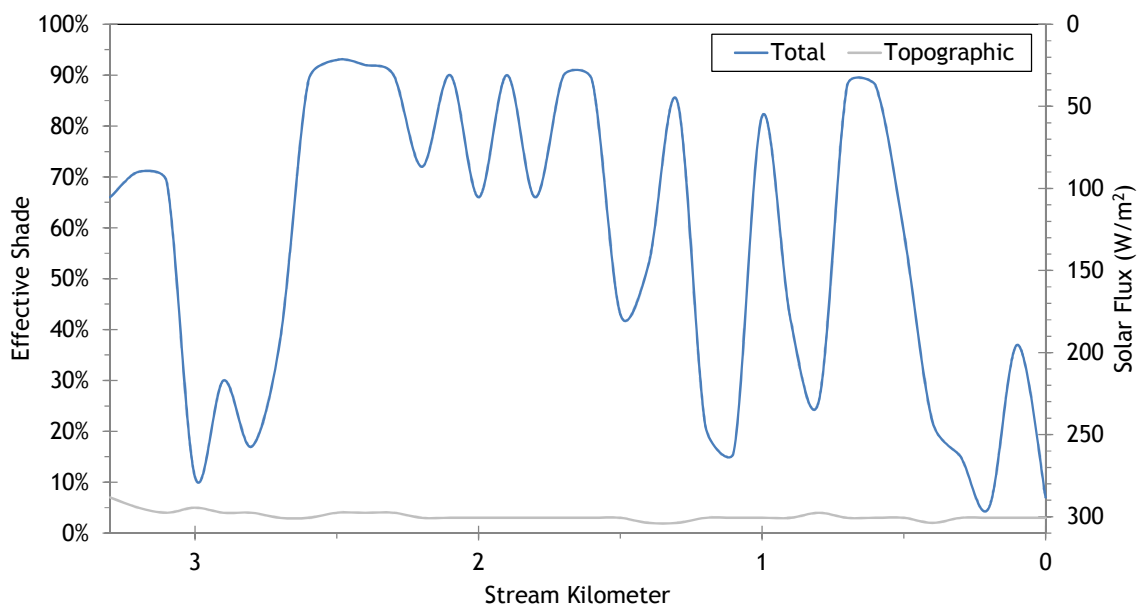
Figure 73 shows the simulated and measured hourly stream temperatures for Milk Creek.

Figure 73 - Milk Creek simulated and measured hourly temperatures.



The simulated effective shade values of Milk Creek are presented in Figure 74. The total effective shade is variable because Milk Creek is flowing through a meadow with occasional stands of trees. There is fairly little topographic shade within the meadow.

Figure 74 - Milk Creek simulated effective shade values.



5.4 Little Catherine Creek

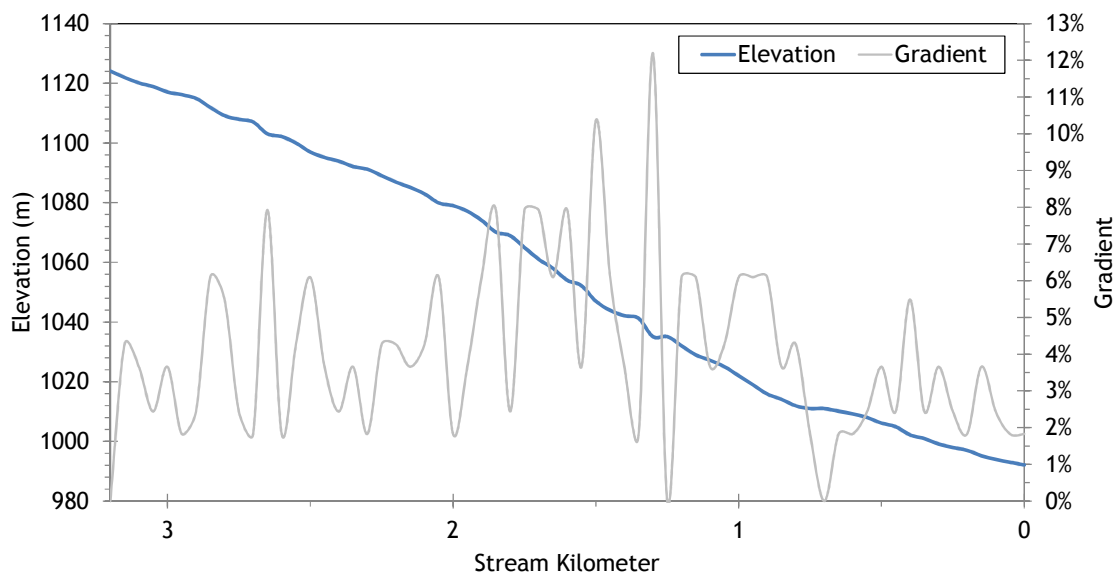


RGB-colored LiDAR point cloud - Little Catherine Creek (flowing top right to middle of image) confluence with Catherine Creek (flowing from bottom to top left of image).

5.4.1 Little Catherine Creek TTools Results

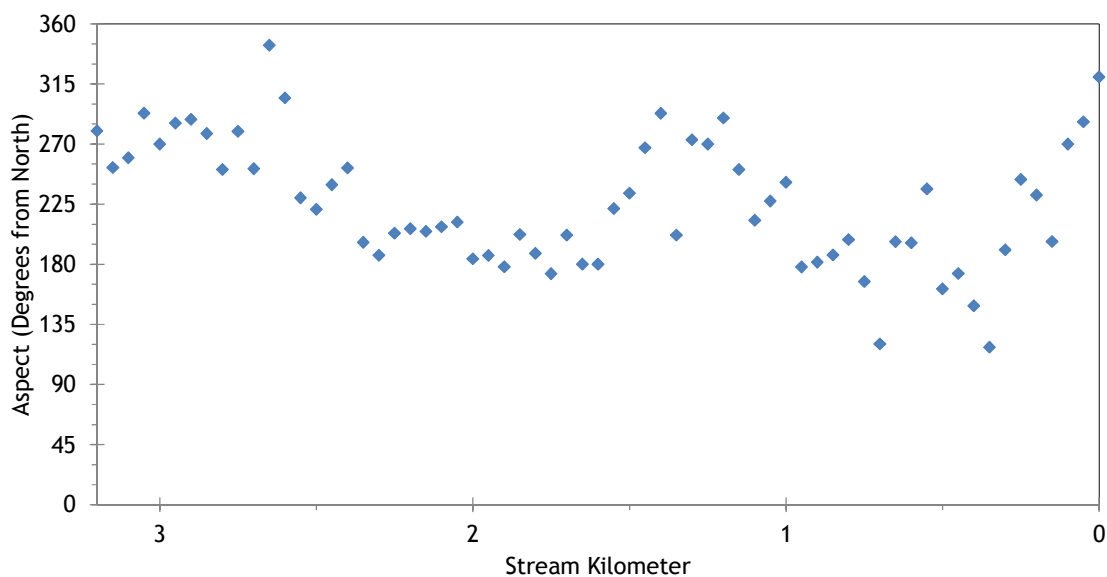
Little Catherine Creek did not have LiDAR coverage (except for a small reach near the mouth). Therefore, stream elevations and gradients were sampled from the 10-meter DEM. Figure 75 shows the elevations and gradients for Little Catherine Creek.

Figure 75 - Little Catherine Creek elevation and gradient.



Little Catherine Creek flows generally toward the southwest until it reaches Catherine Creek just upstream of the city of Union. Figure 76 shows the stream aspect for each 50-meter node of Little Catherine Creek.

Figure 76 - Little Catherine Creek stream aspect.



Topographic shade angles are relatively high on Little Catherine Creek, with some values over 30 degrees (Figure 77). This is due to the fact that the stream is flowing out of mountain foothills within a deep v-shaped valley.

Figure 77 - Little Catherine Creek topographic shade angles.

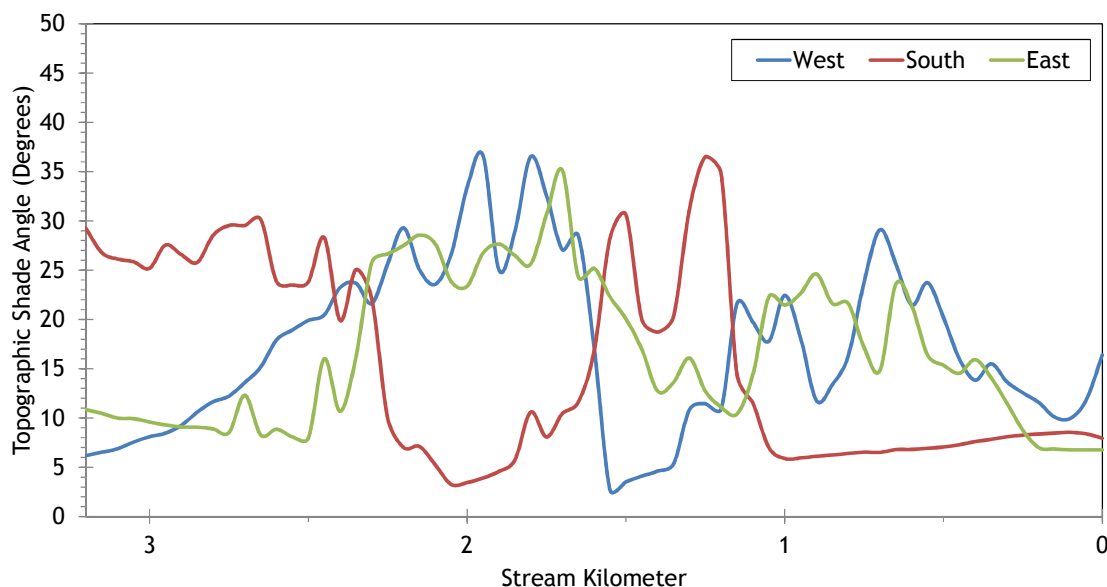
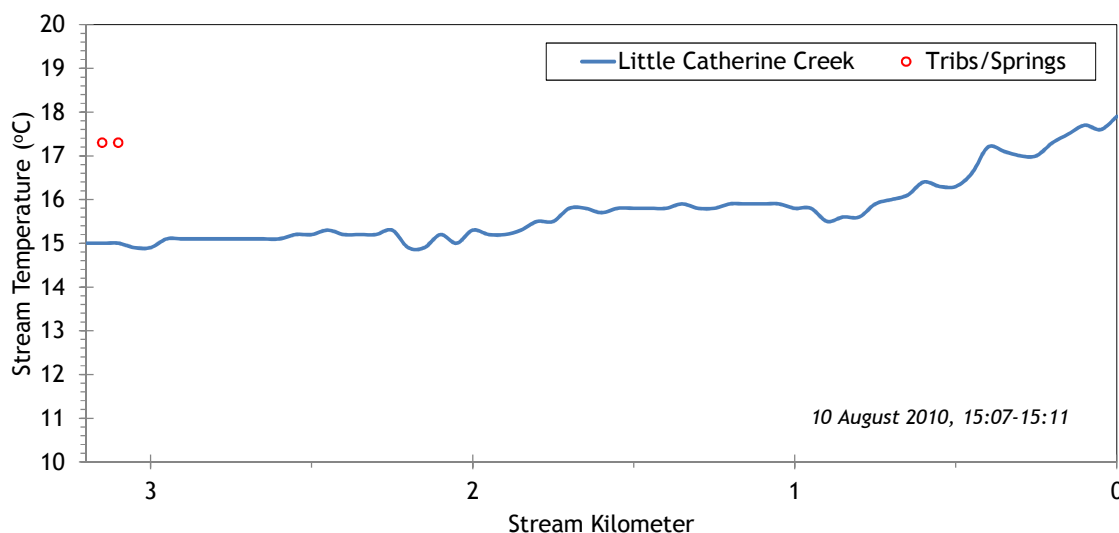


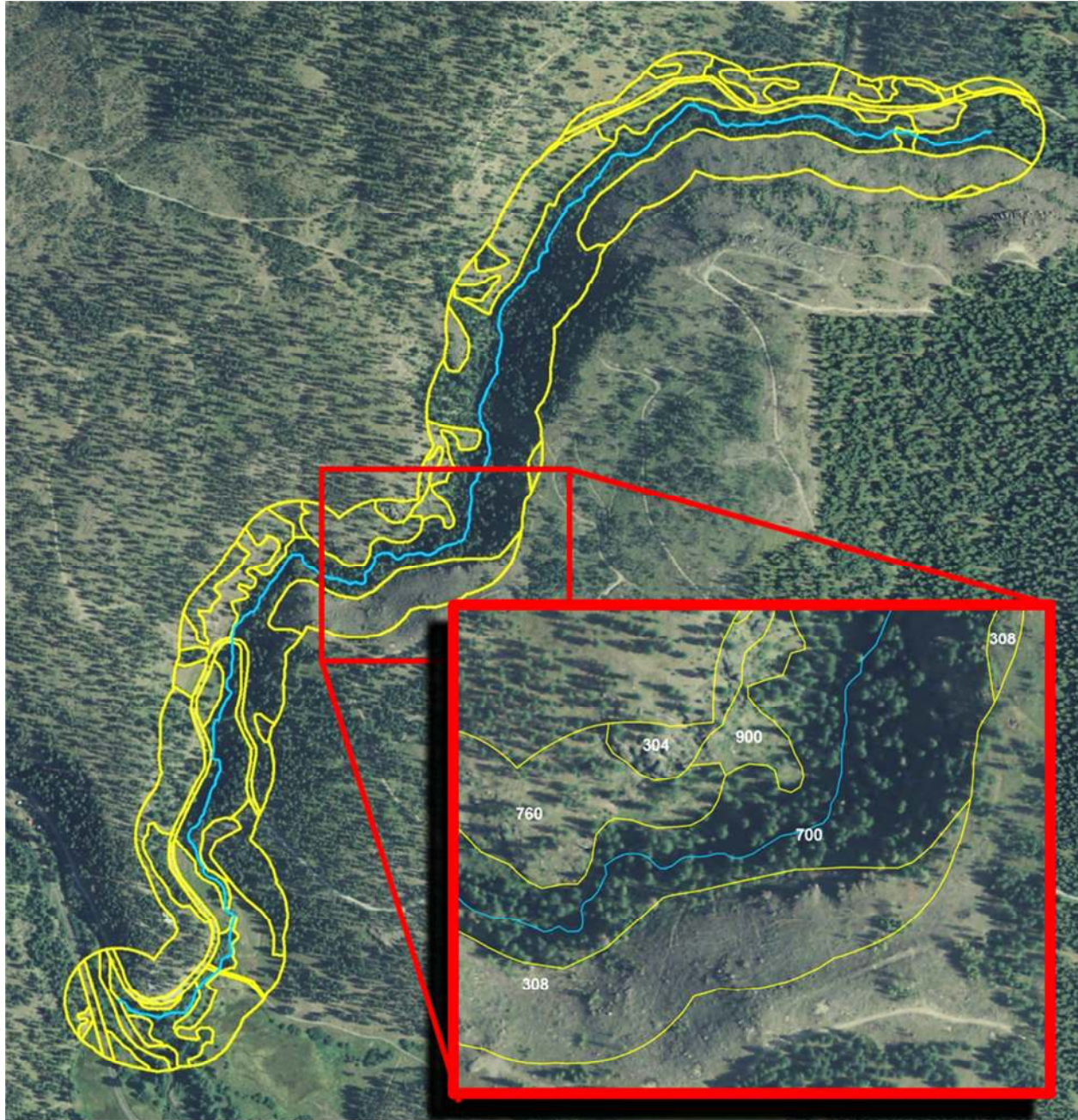
Figure 78 shows the TIR stream temperature profile of Little Catherine Creek. Stream temperature ranged from 15-18°C during the TIR flight.

Figure 78 - Little Catherine Creek TIR stream temperature profile.



Since there was no LiDAR available for Little Catherine Creek, the near stream land cover was digitized from the NAIP imagery within 100 meters of the stream. Figure 79 shows the near stream land cover polygons along Little Catherine Creek. Each polygon contains a code that signifies the land cover type, height class, and density class.

Figure 79 - Little Catherine Creek digitized near stream land cover.



5.4.2 Little Catherine Creek Effective Shade Simulation

Little Catherine Creek was simulated for effective shade only. There was insufficient ground-level flow and temperature for stream temperature modeling. Figure 80 shows the effective shade simulation extent.

Figure 80 - Little Catherine Creek simulation extent.

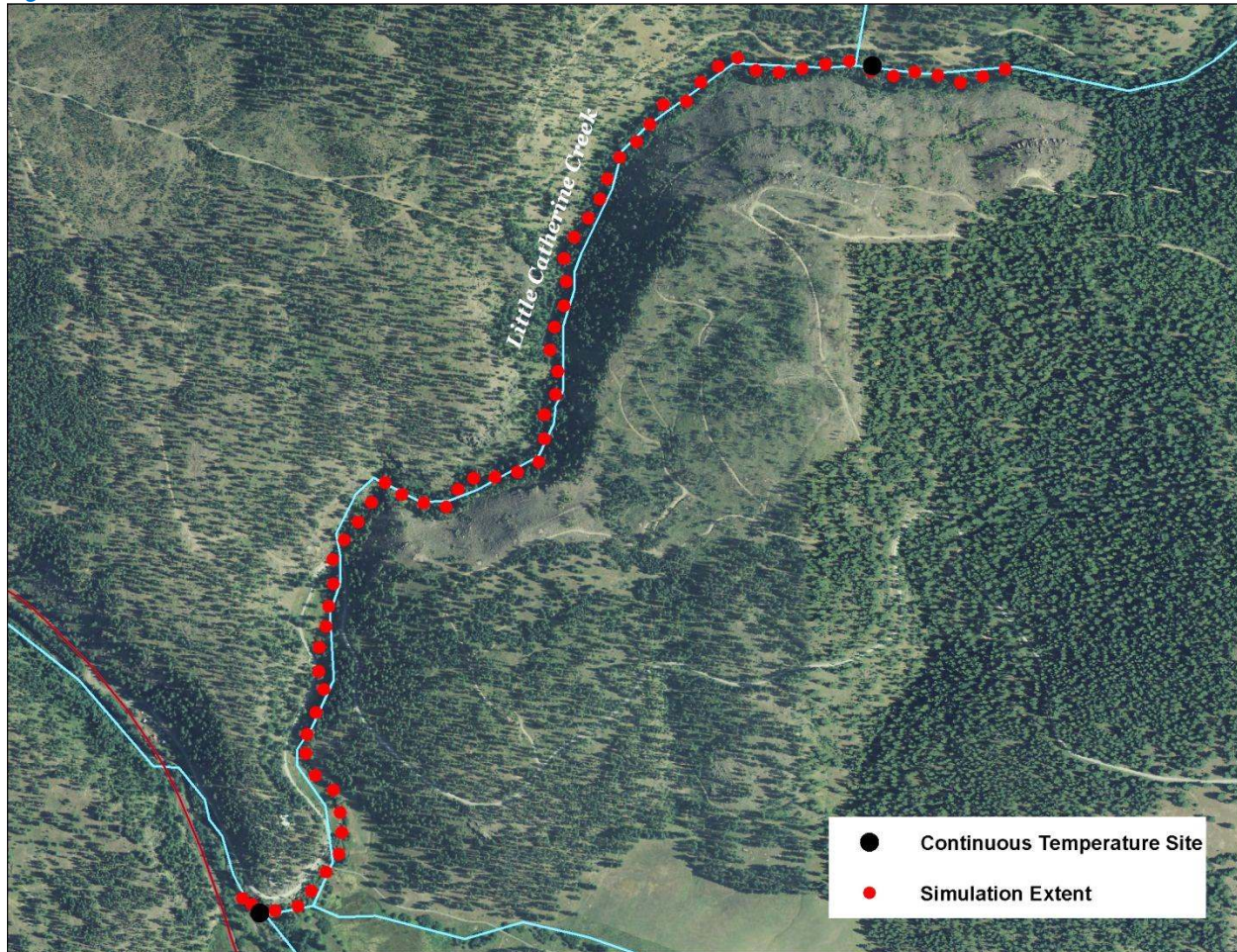


Table 10 - Little Catherine Creek general Heat Source parameters.

Stream:	Little Catherine Creek
Length:	3.2 kilometers
Time Period:	August 6-27, 2010
Input Distance Step:	50 meters
Output Distance Step:	100 meters
Time Step:	1 minute
Flush Initial Condition:	NA
TIR Date and Time:	NA
Land Cover Data Source:	LiDAR
Land Cover Sampling Distance Step:	10 meters

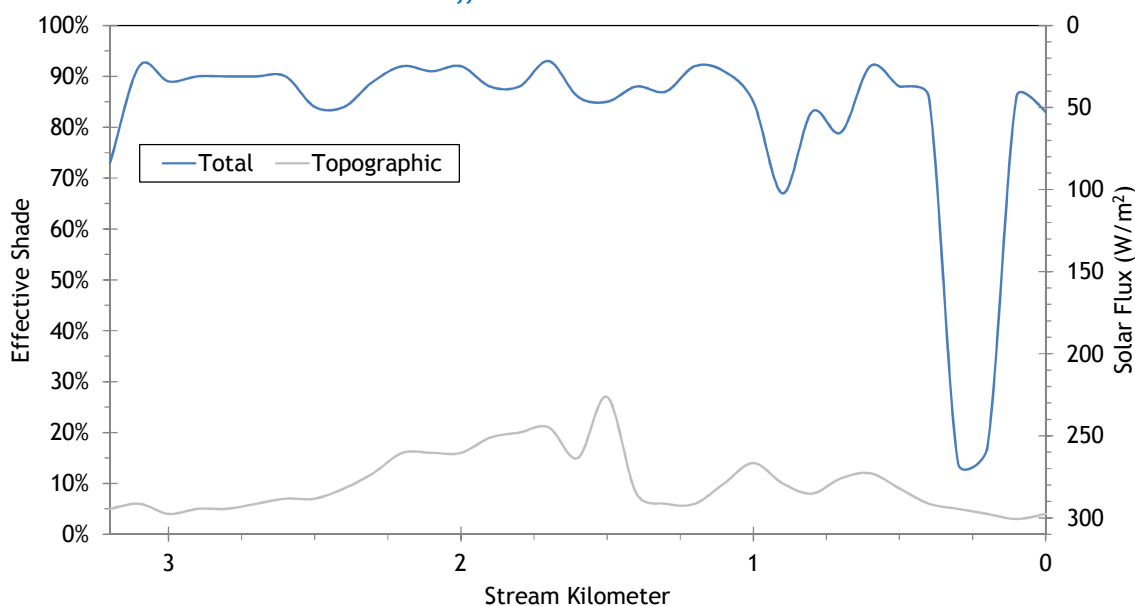
The near stream land cover codes used for Little Catherine Creek are shown in Table 11. The height values were derived from the tree heights sampled from the LiDAR data on the North Fork and South Fork Catherine Creek. The large conifer height value is the 75th percentile of all samples greater than 3 meters. The small conifer height is the 25th percentile of all samples greater than 3 meters. Density was estimated. Overhang was set at zero.

Table 11 - Little Catherine Creek land cover codes and descriptions.

Land Cover Name	Code	Height (m)	Density	Overhang (m)
Rock	304	0	0	0
Embankment	305	0	0	0
Clearcut	308	0	0	0
Road - paved	400	0	0	0
Road - unpaved	401	0	0	0
Large Conifer Forest	700	24.2	0.6	0
Small Conifer Forest	701	6.8	0.6	0
Large Conifer Forest	750	24.2	0.2	0
Small Conifer Forest	751	6.8	0.2	0
Conifer, small, sparse	760	3	0.1	0
shrubs	800	2	0.75	0
dry upland grass	900	0.5	0.9	0
floodplain grasses	901	0.5	0.9	0
active stream channel	3011	0	0	0

Figure 81 shows the simulated effective shade for Little Catherine Creek. The stream is well-forested throughout most of its length and thus well shaded by near stream land cover. Using manually digitized land cover for Heat Source inputs is less robust than using LiDAR and captures less of the natural variability. As a result, simulated effective shade also shows less variability and is more likely to be over-estimated. Ground level measurements could be used as validation if available.

Figure 81 - Little Catherine Creek simulated effective shade.



5.5 Little Creek

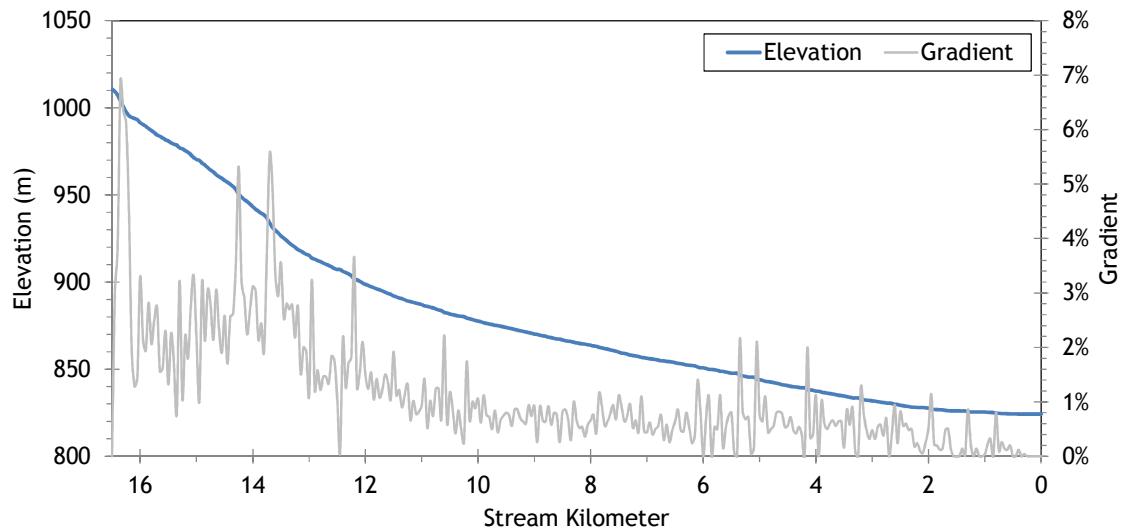


RGB-colored LiDAR point cloud - Little Creek looking downstream where it enters valley bottom.

5.5.1 Little Creek TTools Results

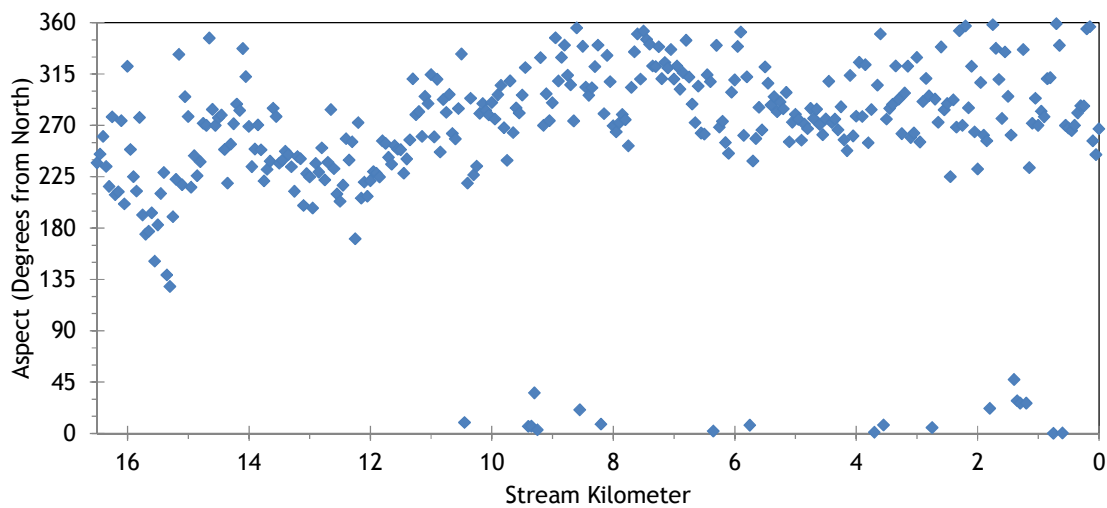
Figure 82 shows Little Creek elevations and gradients sampled from bare earth LiDAR data. The lower 10 stream kilometers are fairly low gradient because that reach flows through flat agricultural valley bottom.

Figure 82 - Little Creek elevation and gradient.



Little Creek flows mostly in the southwest-westerly direction before joining Catherine Creek below the city of Union. Figure 83 shows stream aspects for each 50-meter node.

Figure 83 - Little Creek stream aspect.



Topographic shade angles on Little Creek are highest above stream kilometer 10, where the terrain is hilly (Figure 84). The lower 10 stream kilometers have much lower topographic shade angles because the terrain is broad flat valley bottom.

Figure 84 - Little Creek topographic shade angles.

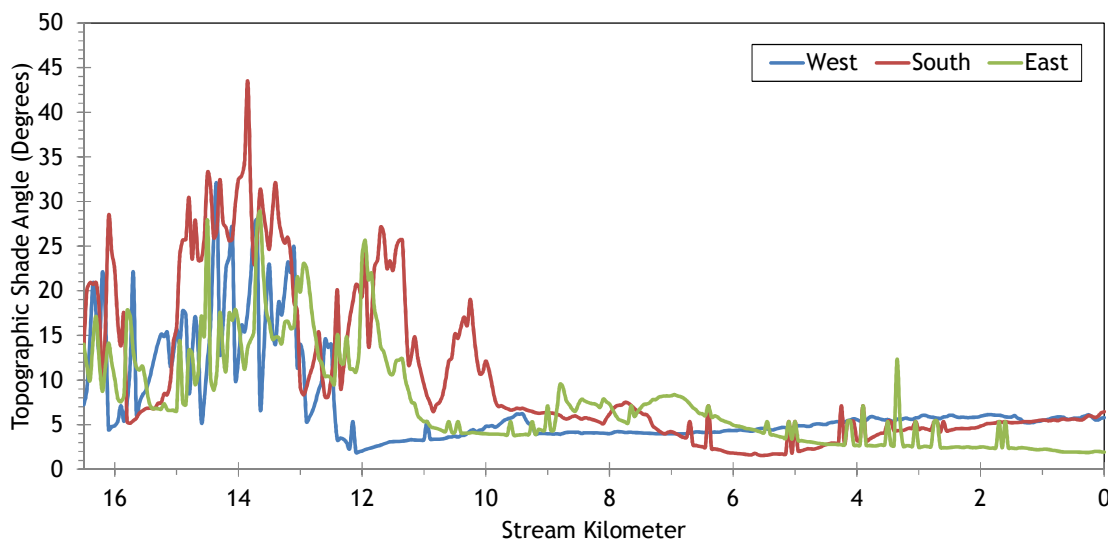
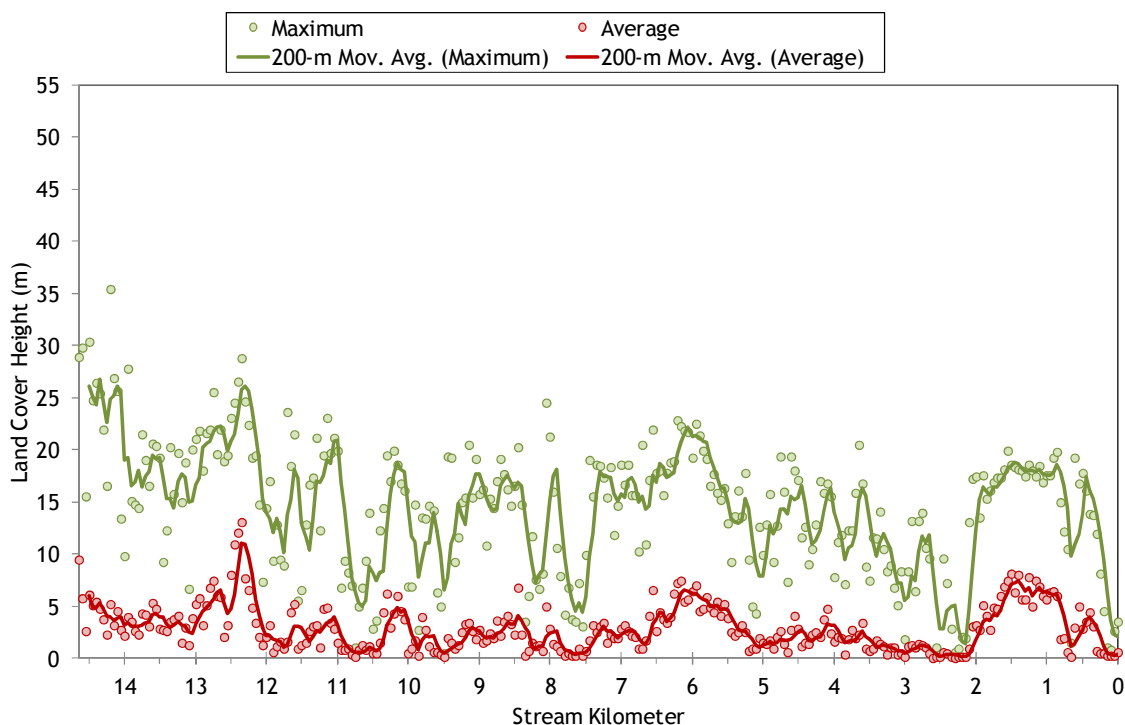


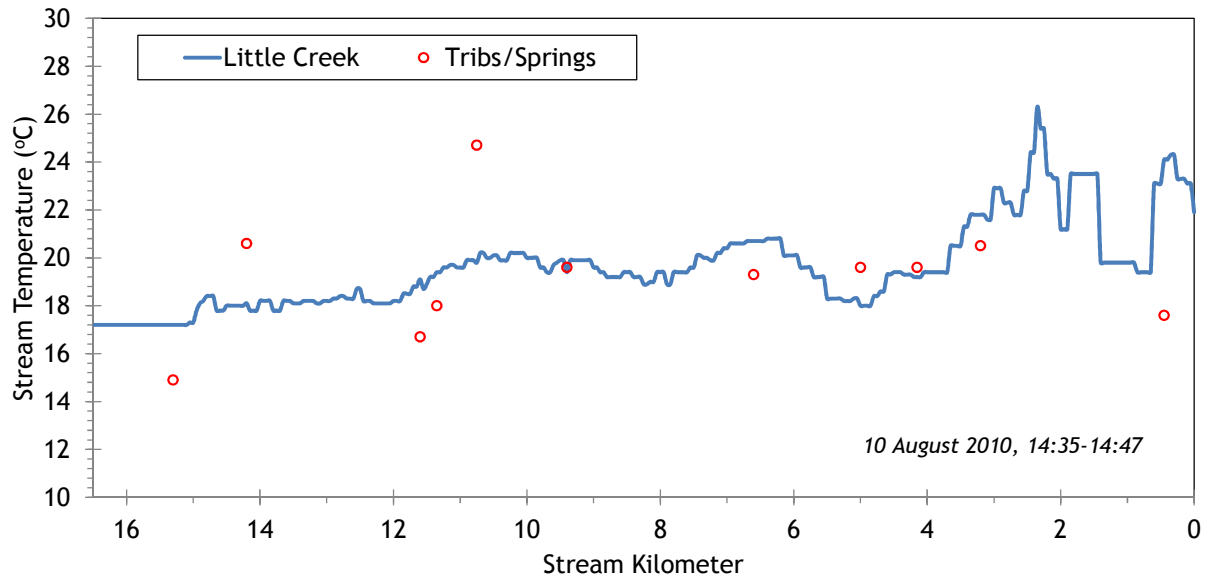
Figure 85 shows the land cover heights sampled along Little Creek. The maximum and average of the 28 radial samples were calculated for each 50-meter stream node. (Note: Heat Source uses each of the 28 radial samples for each 50-meter node. The maximum and average are shown here for simplification purposes.)

Figure 85 - Little Creek land cover heights sampled from highest hit LiDAR.



Little Creek TIR stream temperatures are presented in Figure 86. Overall, stream temperatures were 18-24°C during the TIR flight. There are areas of potential thermal stratification in the lower 3 kilometers where the stream velocities were very slow due to the low gradients. TIR only records the surface water temperature.

Figure 86 - Little Creek TIR stream temperatures.



5.5.2 Little Creek Heat Source Calibration Results

Little Creek was simulated from High Valley Road to the mouth (14.7 kilometers). Figure 87 shows the simulation extent and temperature monitoring sites.

Figure 87 - Little Creek simulation extent.



Table 12 - Little Creek general Heat Source parameters.

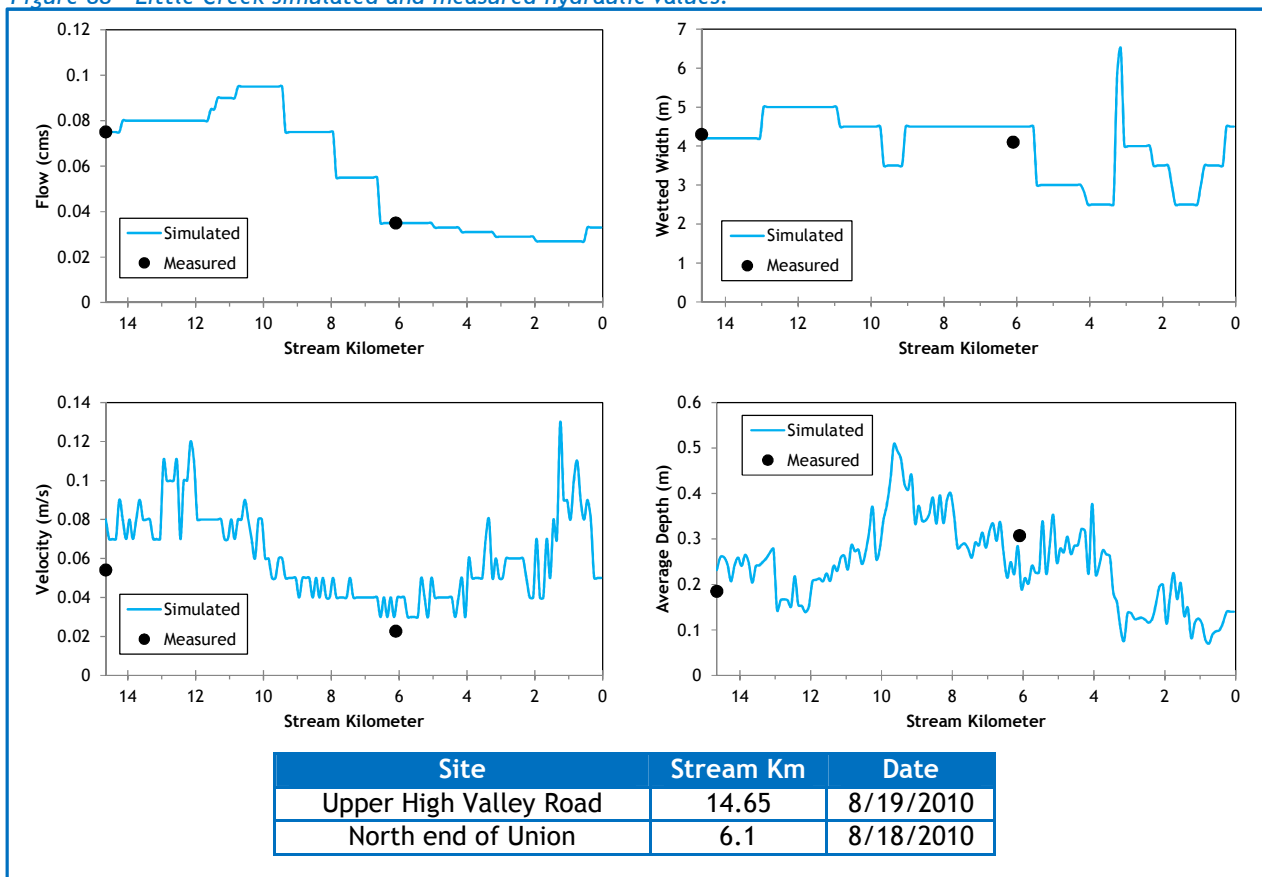
Stream:	Little Creek
Length:	14.65 kilometers
Time Period:	August 6-27, 2010
Input Distance Step:	50 meters
Output Distance Step:	100 meters
Time Step:	1 minute
Flush Initial Condition:	7 days
TIR Date and Time:	August 10, 2010 14:34-14:46
Land Cover Data Source:	LiDAR
Land Cover Sampling Distance Step:	15 meters

The following assumptions were used when calibrating the Little Creek Heat Source model:

- Hourly climate data was obtained from the La Grande Airport (NWS). Air temperature was adjusted using the adiabatic lapse rate of 1°C per 100 meters elevation.
- In many reaches, the stream was too small to digitize right and left banks. Therefore, wetted widths were estimated by taking several manual measurements from the TIR imagery.
- Since the flow of Little Creek was so small and highly regulated by irrigation withdrawals, a constant volume was used for the entire simulation time period (i.e., daily variability was not applied).
- There were 6 active diversion canals identified in the TIR imagery. The uppermost three were each assumed to withdraw 0.02 cms during the simulation time period while the lower three were assumed to withdraw 0.002 cms. No measured data was available for the canals.

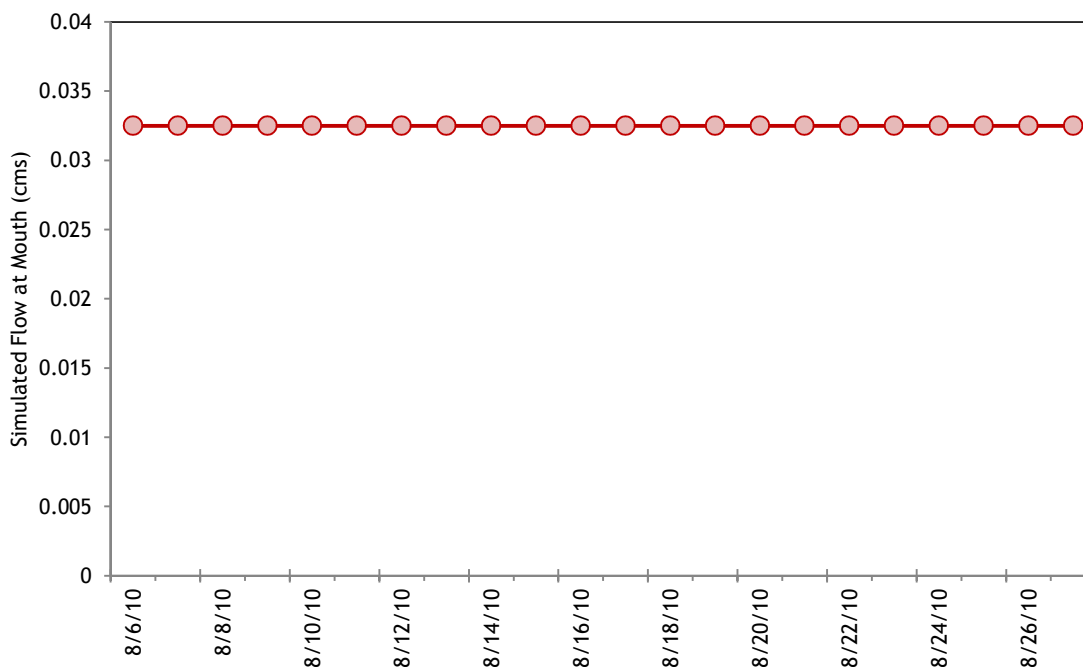
The simulated and measured hydraulic values for Little Creek are presented in Figure 88. The simulated values are for August 19, 2010. There were two ground level measurement sites, including the upstream boundary at High Valley Road, where data was collected on August 18th and 19th.

Figure 88 - Little Creek simulated and measured hydraulic values.



As mentioned previously, Little Creek simulated flows do not have daily variability. The same values were used for each day of the simulation (Figure 89). This assumption was used because of the low flow volumes and un-monitored irrigation withdrawals. (Estimating daily variability for such a stream adds unquantifiable uncertainty and also tends to make the Heat Source model unstable.) The closest field measurement was 0.035 cms on August 18, 2010 at stream kilometer 6.1.

Figure 89 - Little Creek simulated flow volume at the mouth of Little Creek.



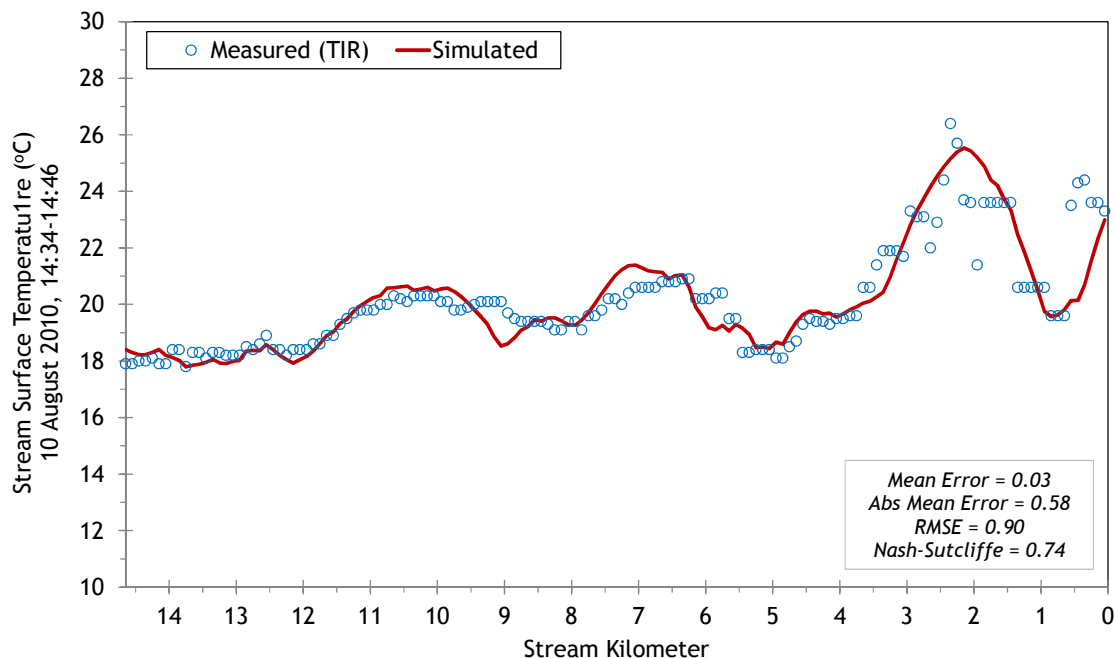
There was one unnamed tributary and several seeps identified within the TIR imagery. Those features were not large enough to compute a mass balance flow volume (i.e., did not produce a measurable thermal signature in Little Creek's longitudinal temperature profile), so volumes were estimated for each. Temperatures were measured from the TIR imagery. No daily variation was applied to these inputs because of their insignificant size relative to Little Creek.

Table 13 - Little Creek mass inflow features and assumptions.

Feature	Stream Km	Assumptions
Unnamed Trib	14.2	0.005 cms at 19.6°C (constant)
seep	11.6	0.005 cms at 16.4°C (constant)
seep	11.35	0.005 cms at 17.8°C (constant)
seep	10.75	0.005 cms at 24.4°C (constant)
seep	0.45	0.005 cms at 17.4°C (constant)

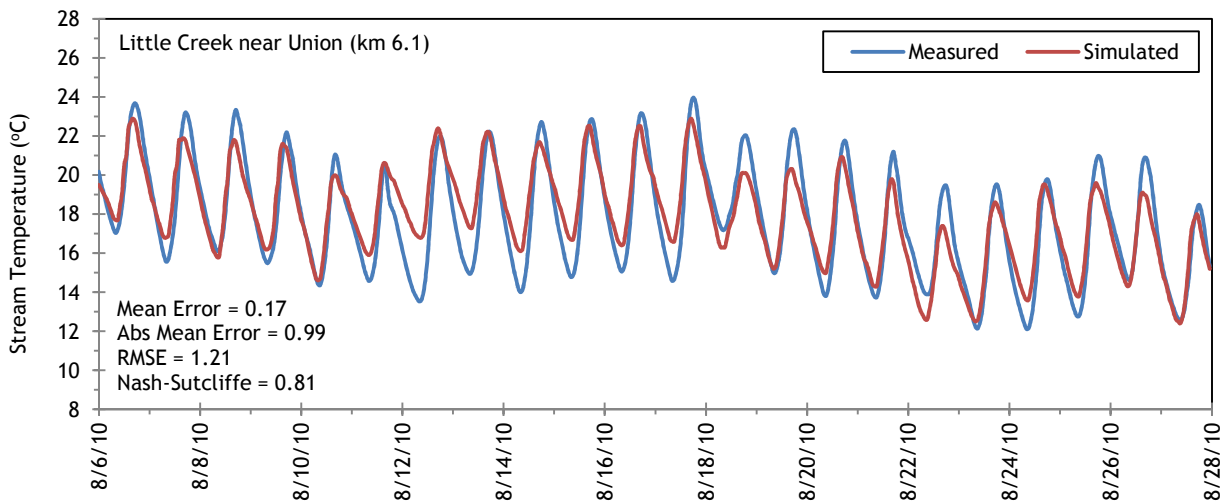
The simulated and measured longitudinal stream temperatures for Little Creek are shown in Figure 90. The lower 3 kilometers are uncertain because there is possible (but unverified) thermal stratification occurring.

Figure 90 - Little Creek simulated and measured longitudinal temperatures.



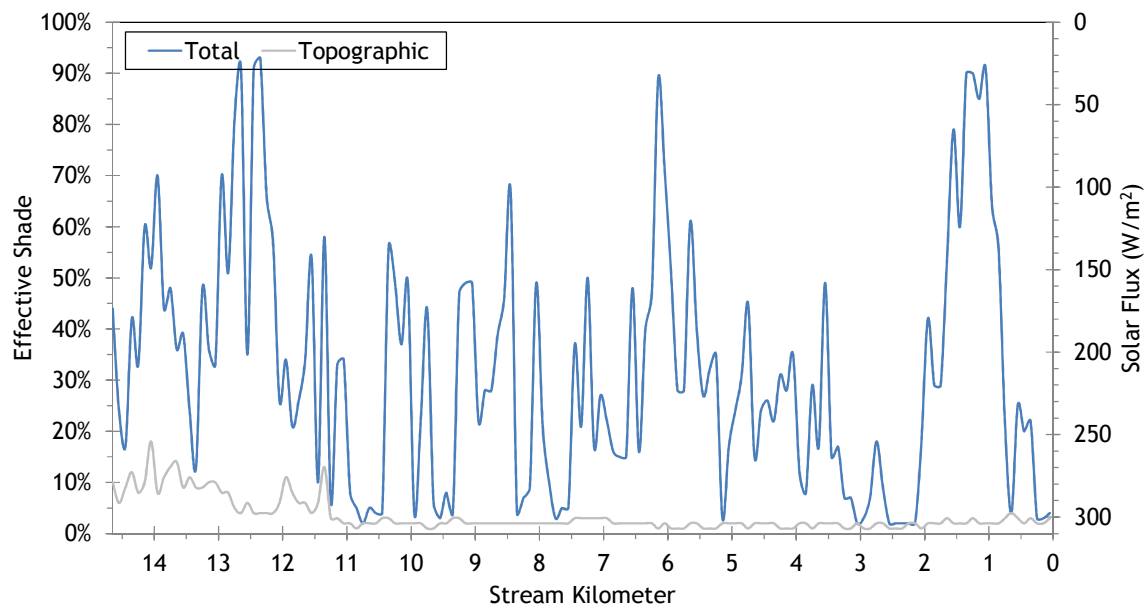
There was one site with valid hourly temperatures besides the upstream boundary condition. Figure 91 shows the simulated and measured hourly temperatures near the city of Union (stream kilometer 6.1).

Figure 91 - Little Creek simulated and measured hourly temperatures.



Simulated effective shade values for Little Creek are presented in Figure 92. The total effective shade is variable because much of the stream has intermittent riparian vegetation limited to a small strip along the banks.

Figure 92 - Little Creek simulated effective shade.



5.6 Ladd Creek



RGB-colored LiDAR point cloud - Looking downstream Ladd Creek at the mouth.

5.6.1 Ladd Creek TTools Results

Ladd Creek did not have LiDAR data available, except for a small section near the mouth. The elevations and gradients were sampled from the 10-meter DEM (Figure 93). The lower 9 stream kilometers are extremely low-gradient as they flow through agricultural lands and are often channelized.

Figure 93 - Ladd Creek elevation and gradient.

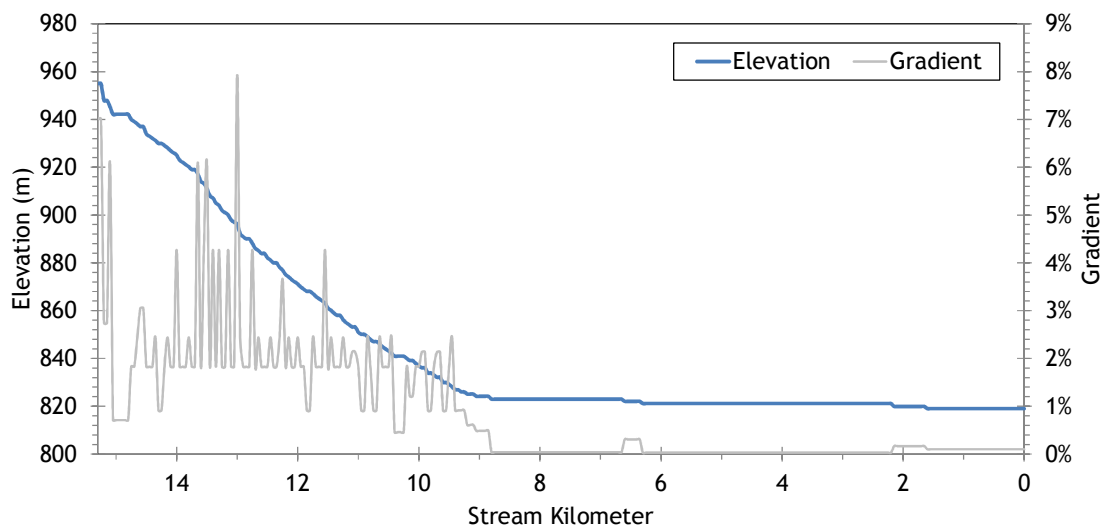
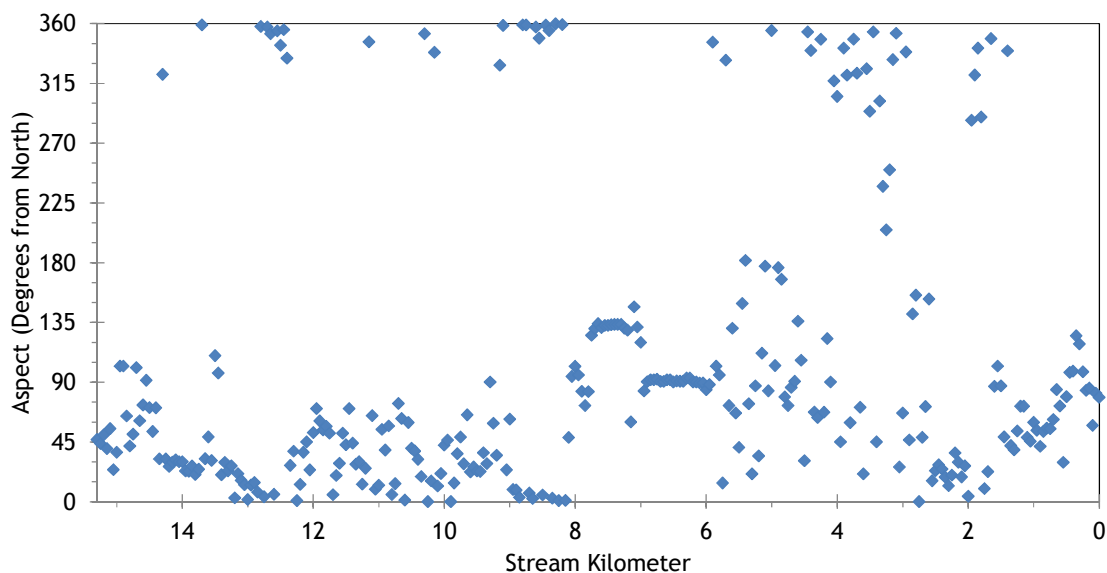


Figure 94 displays the stream aspect for each 50-meter segment of Ladd Creek. The stream flows mostly northeasterly and easterly until it merges with Catherine Creek.

Figure 94 - Ladd Creek stream aspect.



The lower 12 stream kilometers of Ladd Creek have little topographic shade because the stream is flowing through flat agricultural valley bottom (Figure 95). The upper 3 kilometers that were sampled are within more hilly terrain.

Figure 95 - Ladd Creek topographic shade angles.

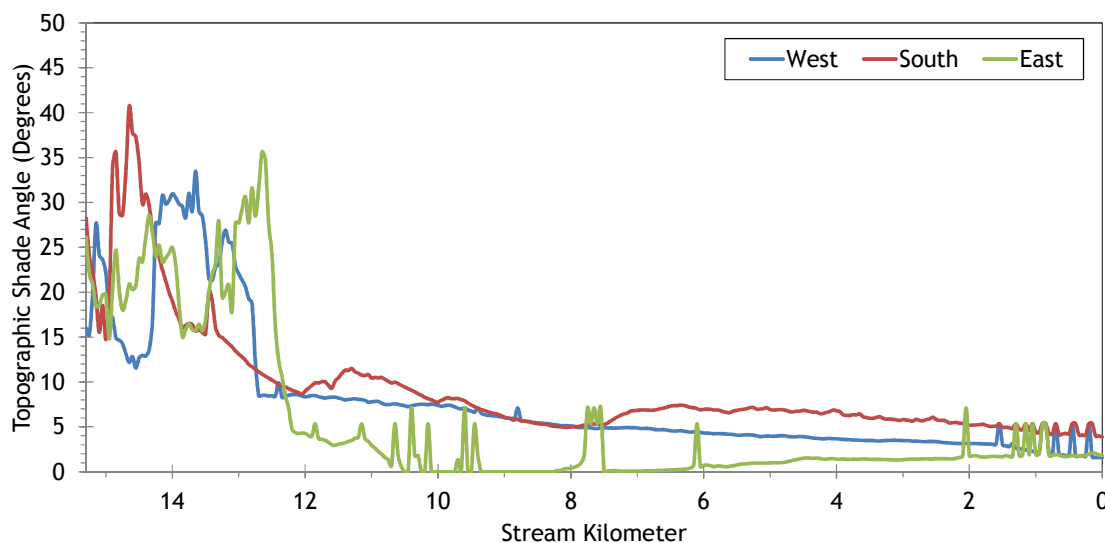
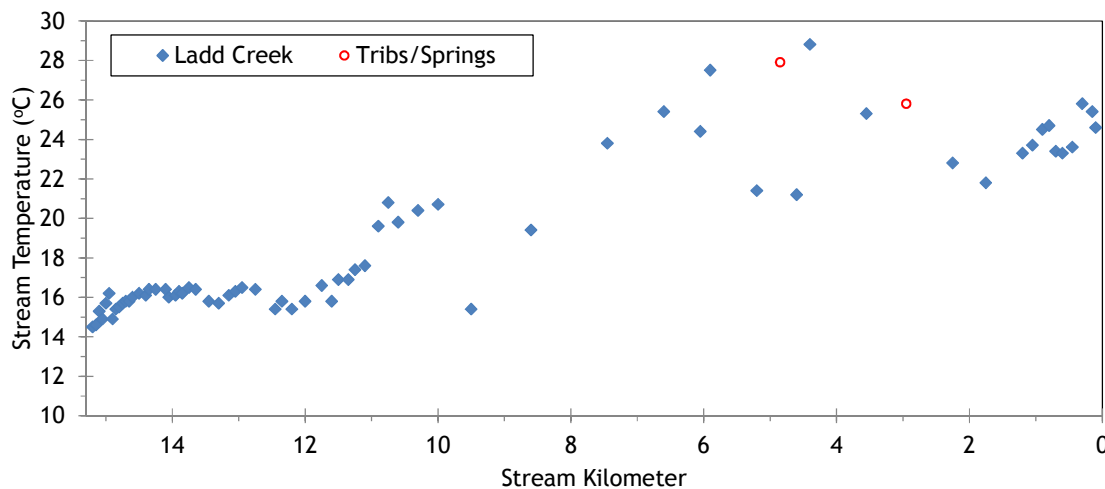


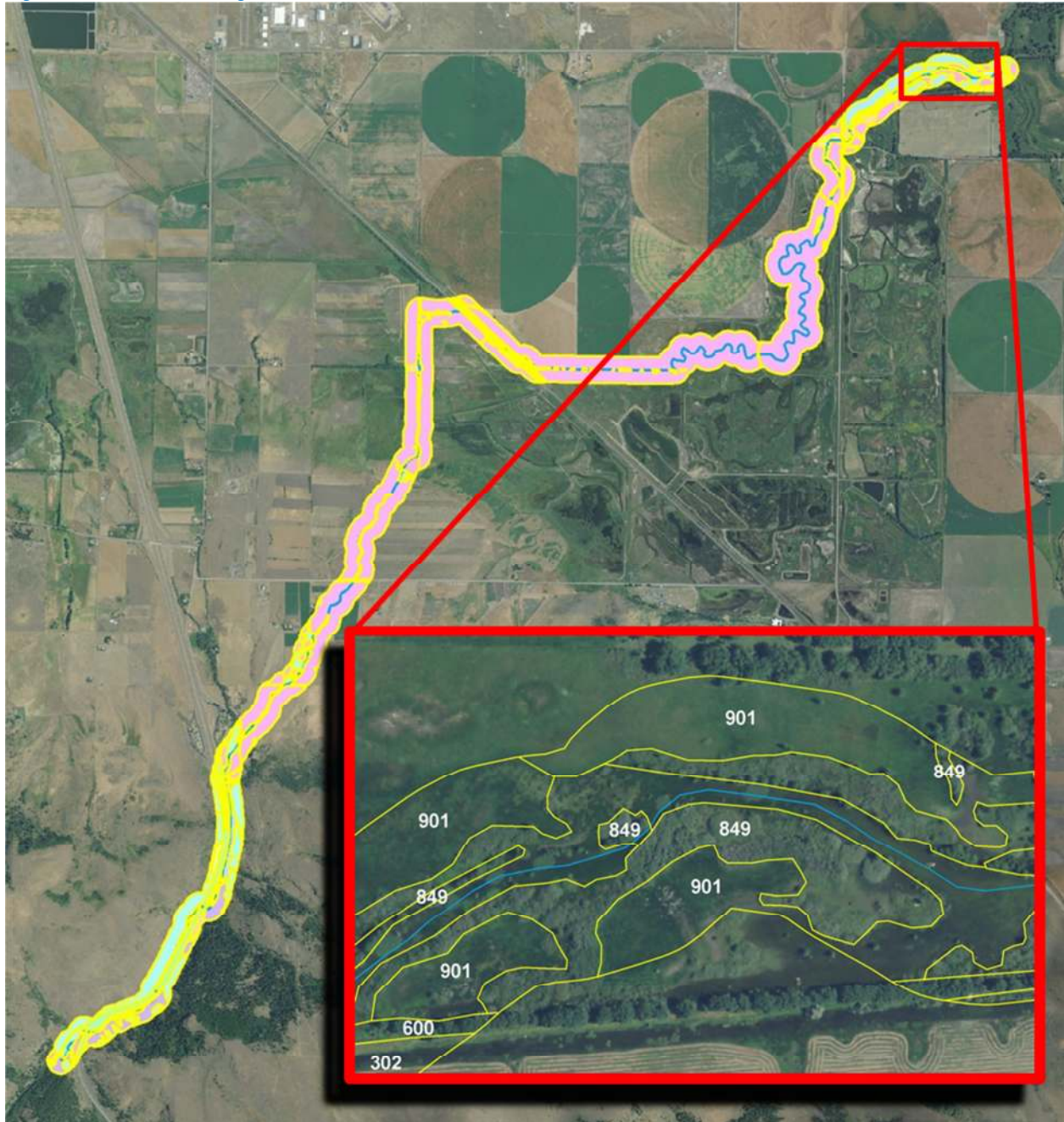
Figure 96 shows the TIR profile of Ladd Creek. The TIR temperature data is sparse throughout much of Ladd Creek and of limited value for multiple reasons. The stream flow was very low (~1 cfs) at the time of the survey. The stream is very small and difficult to sample in the TIR imagery. Much of the stream is channelized and flow volumes and paths are regulated for irrigation purposes. Many areas are very low gradient and likely to have been thermally stratified during the TIR flight.

Figure 96 - Ladd Creek TIR stream temperature profile.



LiDAR data was not available for Ladd Creek, so the near stream land cover was manually digitized from the NAIP orthophotos within 100 meters of the stream (Figure 97). Each polygon was coded to represent a specific land cover type, height class, and density class.

Figure 97 - Ladd Creek digitized near stream land cover.



5.6.2 Ladd Creek Effective Shade Simulation

Stream temperature was unable to be simulated for Ladd Creek because of its extreme low flow volume and a lack of sufficient ground level data. Effective shade was simulated for the extent shown in Figure 98.

Figure 98 - Ladd Creek simulation extent.

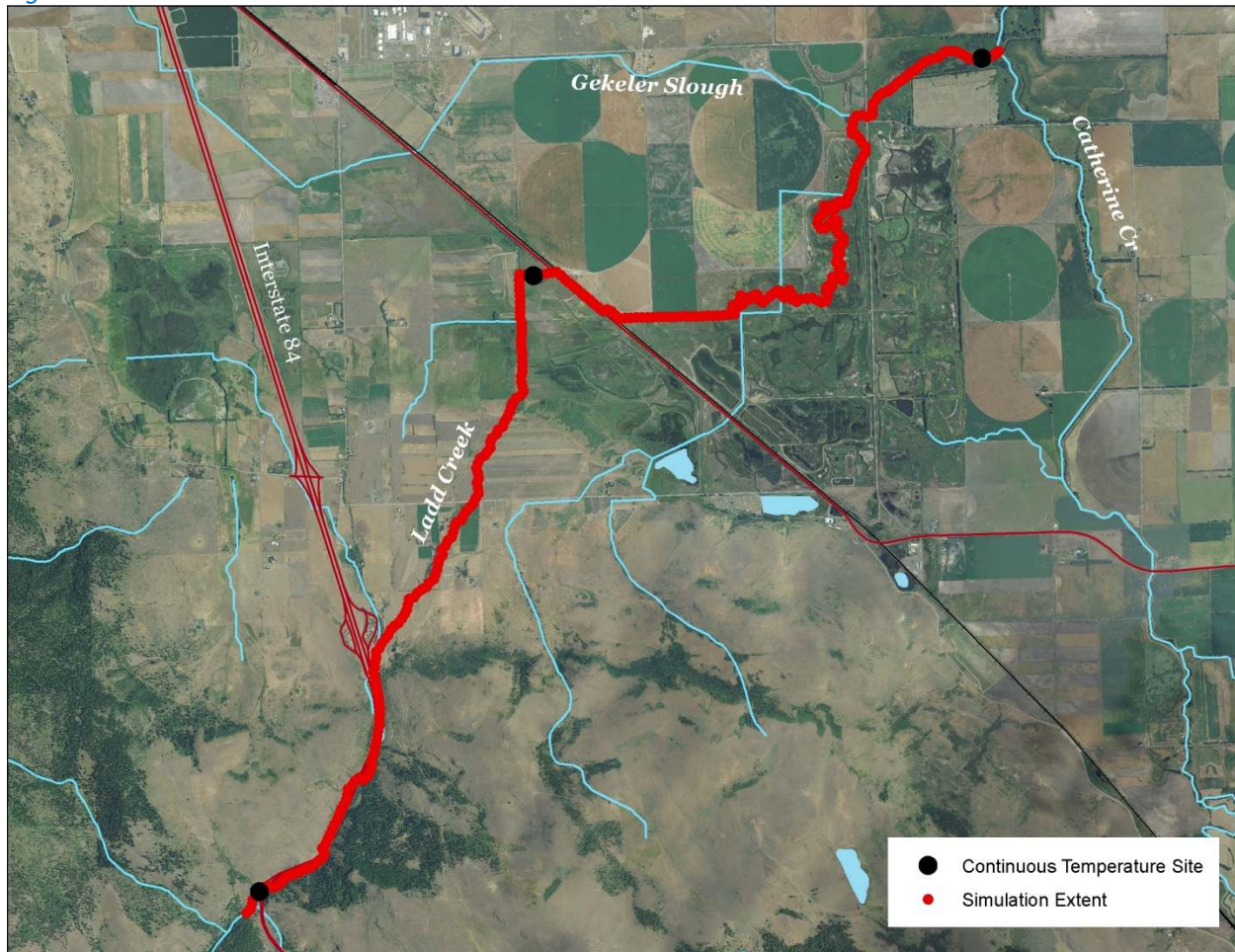


Table 14 - Ladd Creek general Heat Source parameters.

Stream:	Ladd Creek
Length:	15.3 kilometers
Time Period:	August 6-27, 2010
Input Distance Step:	50 meters
Output Distance Step:	100 meters
Time Step:	1 minute
Flush Initial Condition:	NA
TIR Date and Time:	NA
Land Cover Data Source:	LiDAR
Land Cover Sampling Distance Step:	15 meters

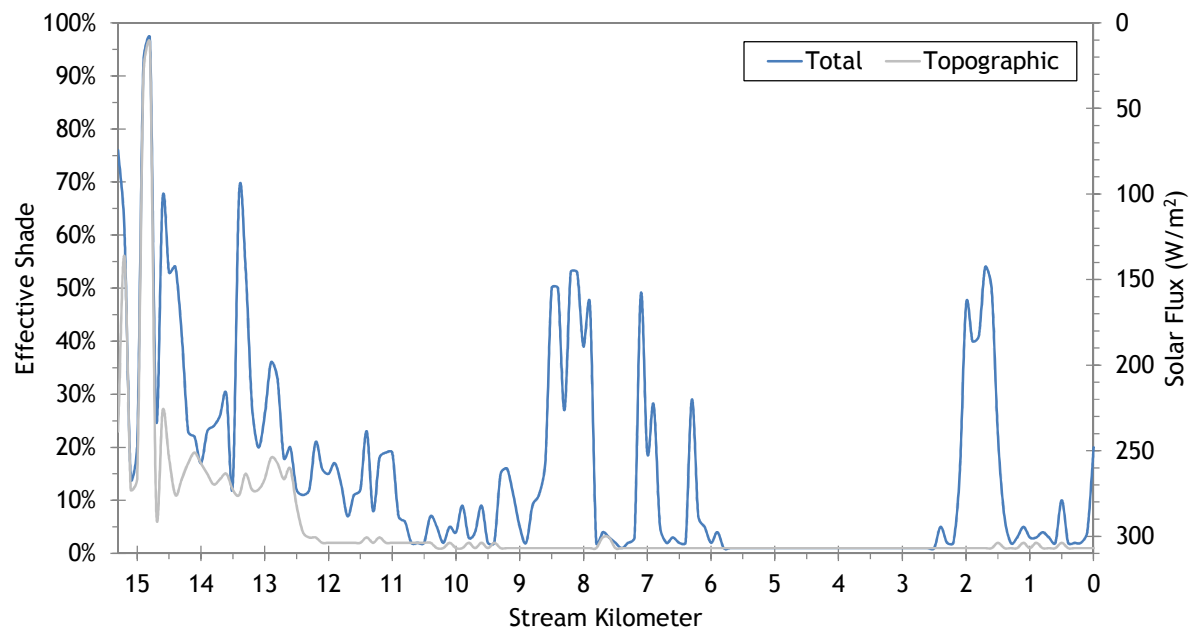
Table 15 shows the near stream land cover codes that were used in the manually digitized layer for Ladd Creek. Height values are based on the lower 66.5 kilometers of Catherine Creek, where LiDAR data were sampled. Values over 3 meters were evaluated for the 75th and 25th percentile. The large height class for Ladd Creek was 9.7 meters, which is equivalent to the 75th percentile of trees on lower Catherine Creek. The small height class used the 25th percentile of 4.4 meters. Values within the regions of Ladd Creek and lower Catherine Creek are smaller than in the upper watershed, primarily because the vegetation consists of smaller riparian shrubs and trees as opposed to large conifer stands.

Table 15 - Ladd Creek near stream land cover codes and descriptions.

Land Cover Name (optional)	Code	Height (m)	Density	Overhang (m)
water	301	0	0	0
pasture, field, cultivated, agriculture	302	0.5	0.9	0
rock	304	0	0	0
road (paved)	400	0	0	0
road (unpaved)	401	0	0	0
Road (unpaved)	403	0	0	0
mixed forest, large	500	9.7	0.75	0
mixed forest, small	501	4.4	0.75	0
deciduous, large	600	9.7	0.75	0
deciduous, small	601	4.4	0.75	0
conifer forest, large	700	9.7	0.75	0
conifer forest, small	701	4.4	0.75	0
conifer forest, large	750	4.4	0.25	0
conifer forest, small and sparse	760	4.4	0.1	0
riparian shrubs, large	849	4.5	0.75	0
shrubs	850	4.5	0.75	0
riparian shrubs, small	899	1	0.75	0
dry upland grasses	900	0.5	0.9	0
floodplain grasses	901	0.5	0.9	0
active channel	3011	0	0	0
building	3248	4	1	0

The simulated effective shade for Ladd Creek is shown in Figure 99. In the upper reaches, most of the effective shade is provided by topographic features. Below stream kilometer 12.5, the stream is flowing through the flat valley bottom and has relatively little streamside vegetation.

Figure 99 - Ladd Creek simulated effective shade.



5.7 Catherine Creek

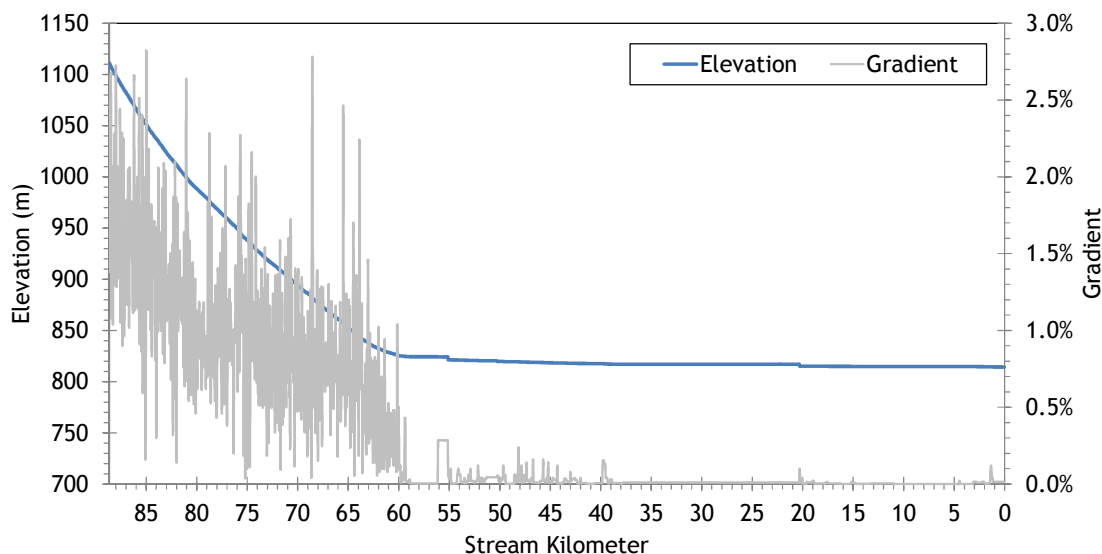


RGB-colored LiDAR point cloud - Catherine Creek in Union (looking upstream).

5.7.1 Catherine Creek TTools Results

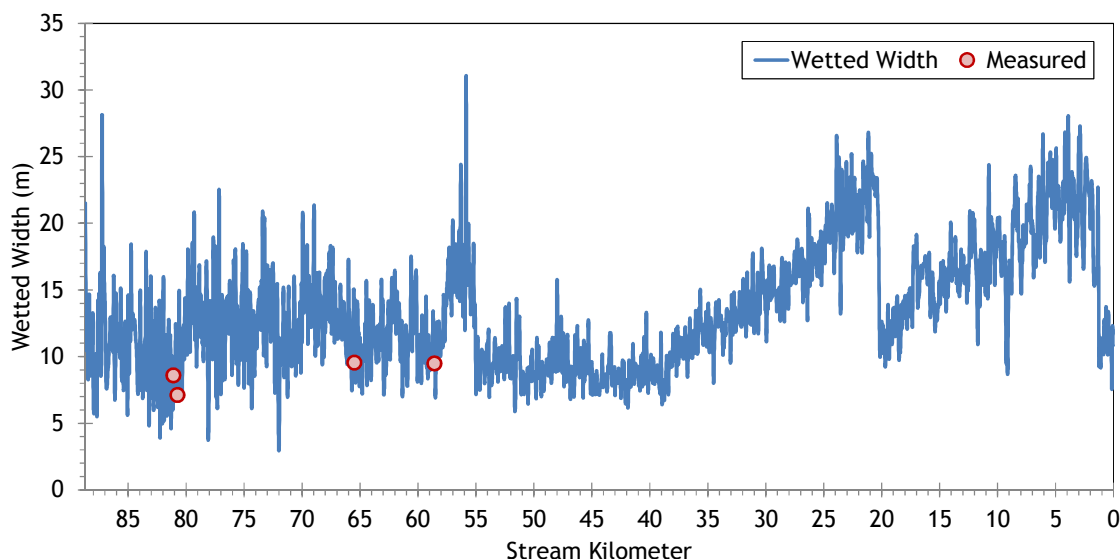
Catherine Creek elevations and gradients are shown in Figure 100. The upper reaches are flowing through mountain foothills, while the lower 60 stream kilometers run through flat agricultural valley bottom. In addition, the lower 60 stream kilometers have much higher sinuosity, thereby further decreasing the stream gradient.

Figure 100 - Catherine Creek elevation and gradient.



Wetted widths were digitized using the TIR, LiDAR intensity, and NAIP imagery. Figure 101 shows the sampled wetted widths along with the ground level measurements. These wetted widths were used as estimates for setting up the Heat Source model hydraulics.

Figure 101 - Catherine Creek wetted widths.



Overall, Catherine Creek flows northwesterly; however, there is huge variation in the lower 60 kilometers where the stream is very sinuous and has large meander bends (Figure 102).

Figure 102 - Catherine Creek stream aspect.

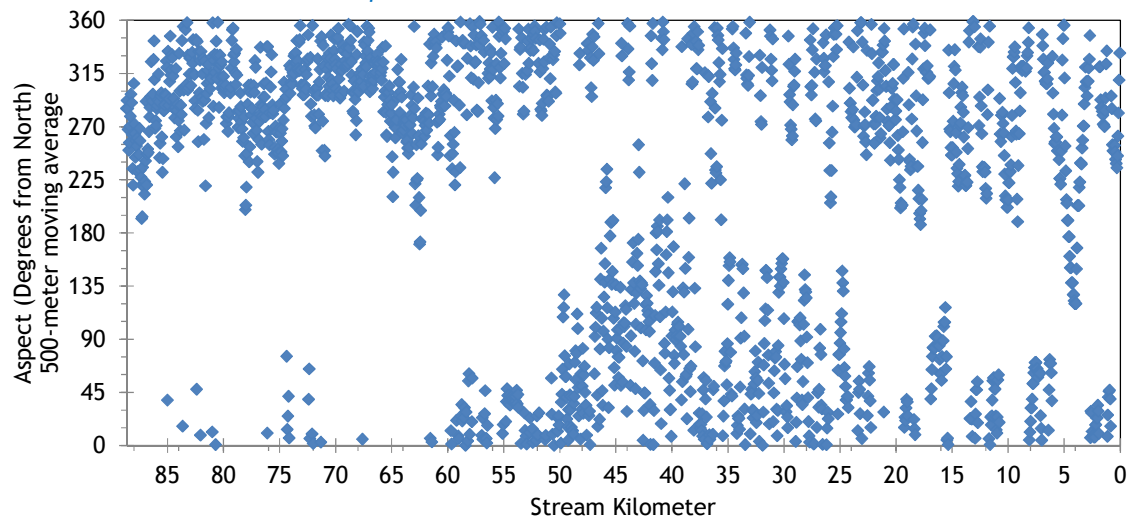


Figure 103 shows the topographic shade angles for Catherine Creek. The upper reaches have more topographic shade because the stream is flowing through a confined valley. The lower reaches have less topographic shade because they are within the Grande Ronde valley bottom.

Figure 103 - Catherine Creek topographic shade angles.

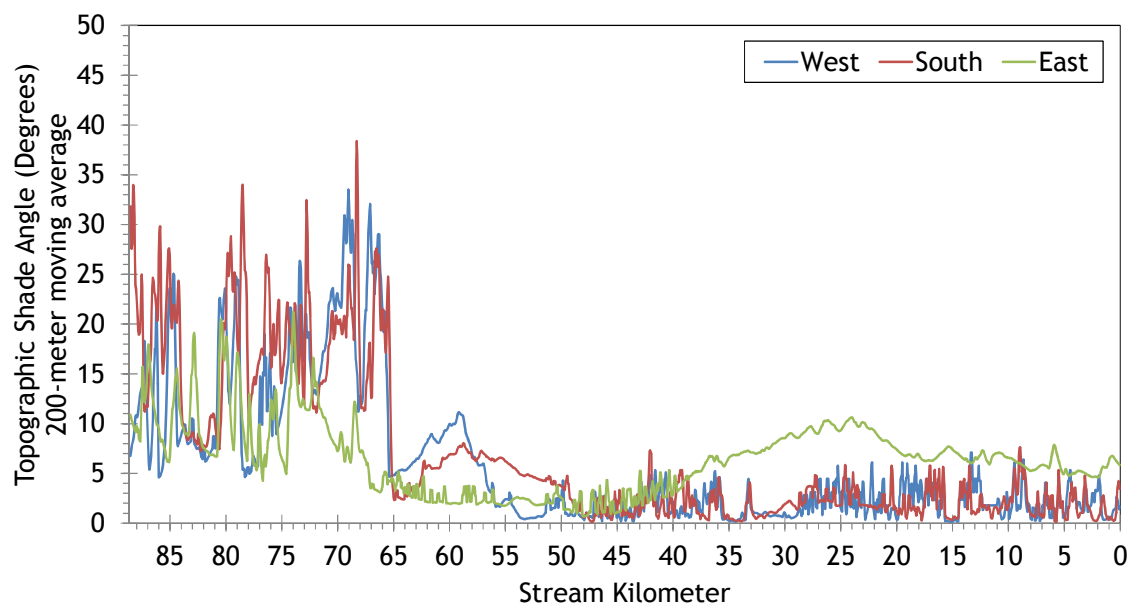
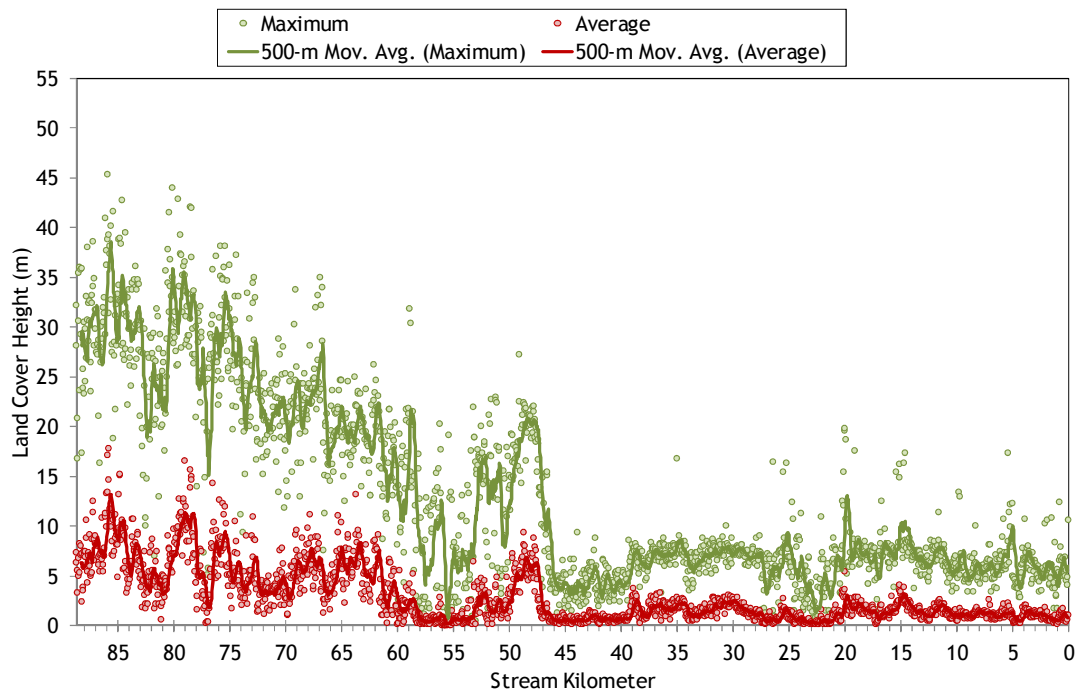


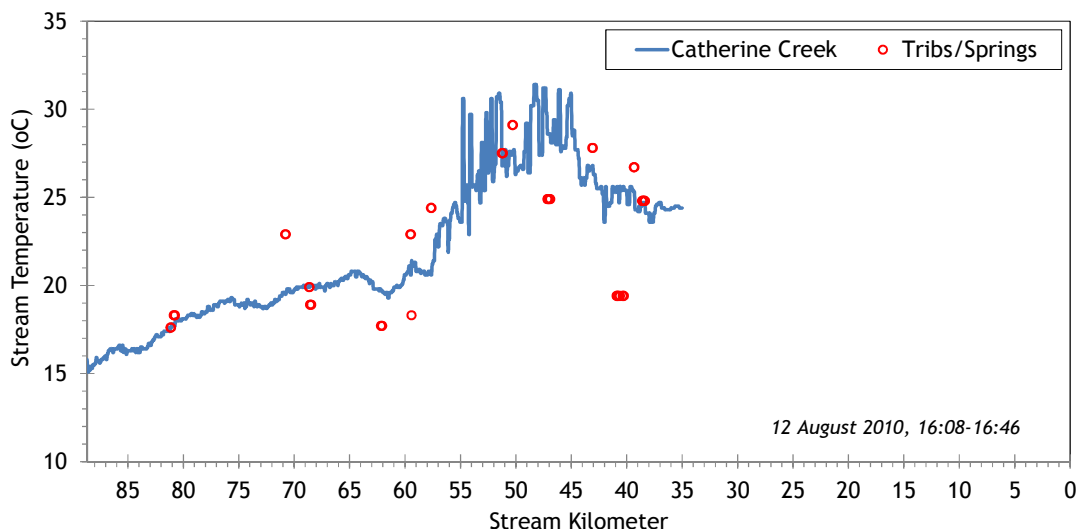
Figure 104 shows the land cover heights sampled along Catherine Creek. The maximum and average of the 28 radial samples were calculated for each 50-meter stream node. (Note: Heat Source uses each of the 28 radial samples for each 50-meter node. The maximum and average are shown here for simplification purposes.)

Figure 104 - Catherine Creek land cover heights sampled from highest hit LiDAR.



TIR data was available for approximately the upper 50 stream kilometers of Catherine Creek (Figure 105). Between the forks and the city of Union (stream kilometer 60), stream temperatures were more stable because there was more volume within the river. At Union, most of the water had been diverted for irrigation use, leaving relatively little volume in the stream. At this point, the stream temperatures rise rapidly and become variable. There are most likely areas of thermal stratification in the lower section as well.

Figure 105 - Catherine Creek TIR stream temperature profile.



5.7.2 Catherine Creek Heat Source Calibration Results

Catherine Creek was simulated for temperature from the forks to the city of Union. The entire stream was simulated for effective shade.

Below Union, the flow is heavily regulated by irrigation withdrawals which use most of the water. The reach between Union and the mouth was unable to be simulated for temperature. In addition, there are many stratified reaches below Union, which cannot be simulated using Heat Source because it is a 2-D model.

Figure 106 - Catherine Creek simulation extent.

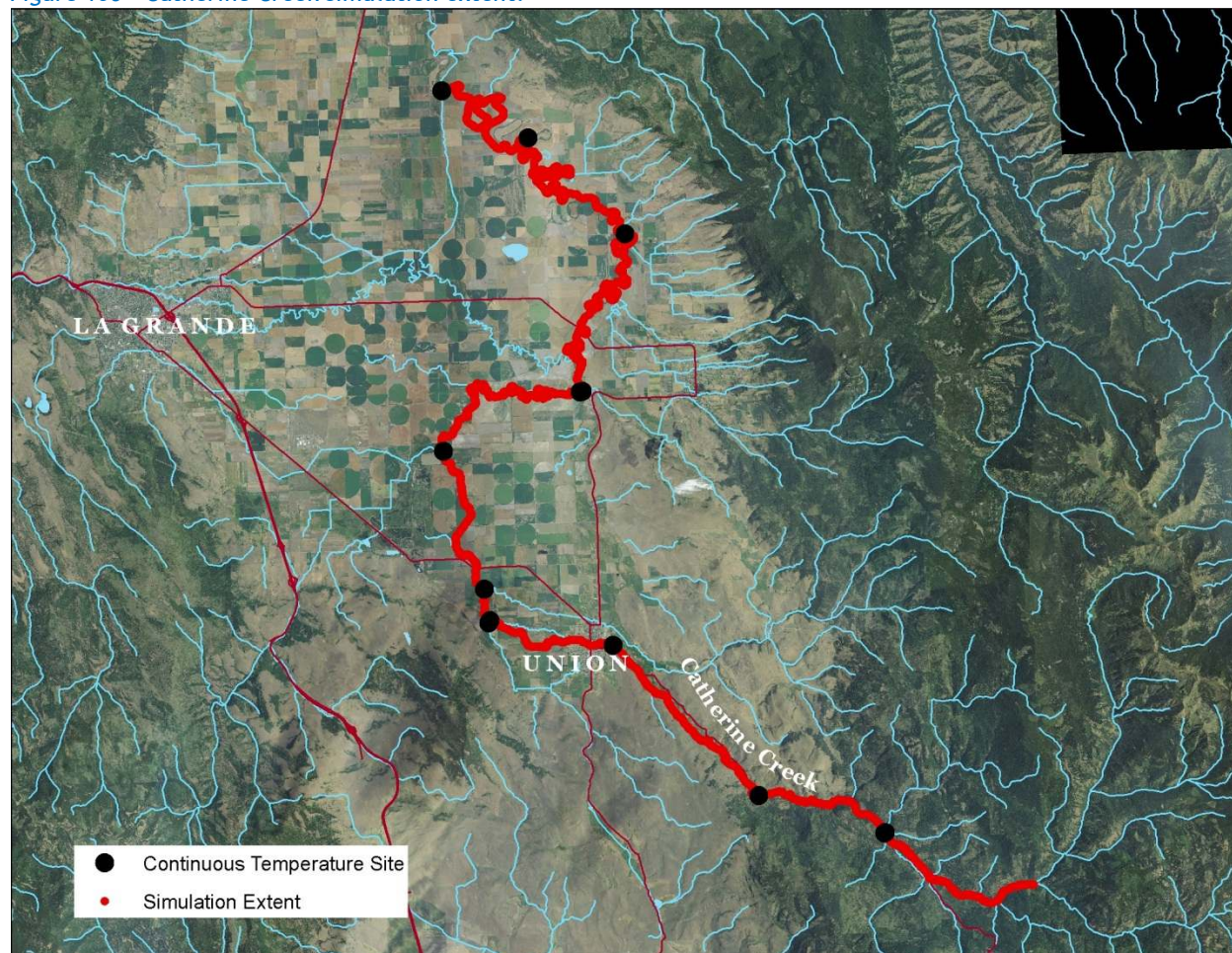


Table 16 - Catherine Creek general Heat Source parameters.

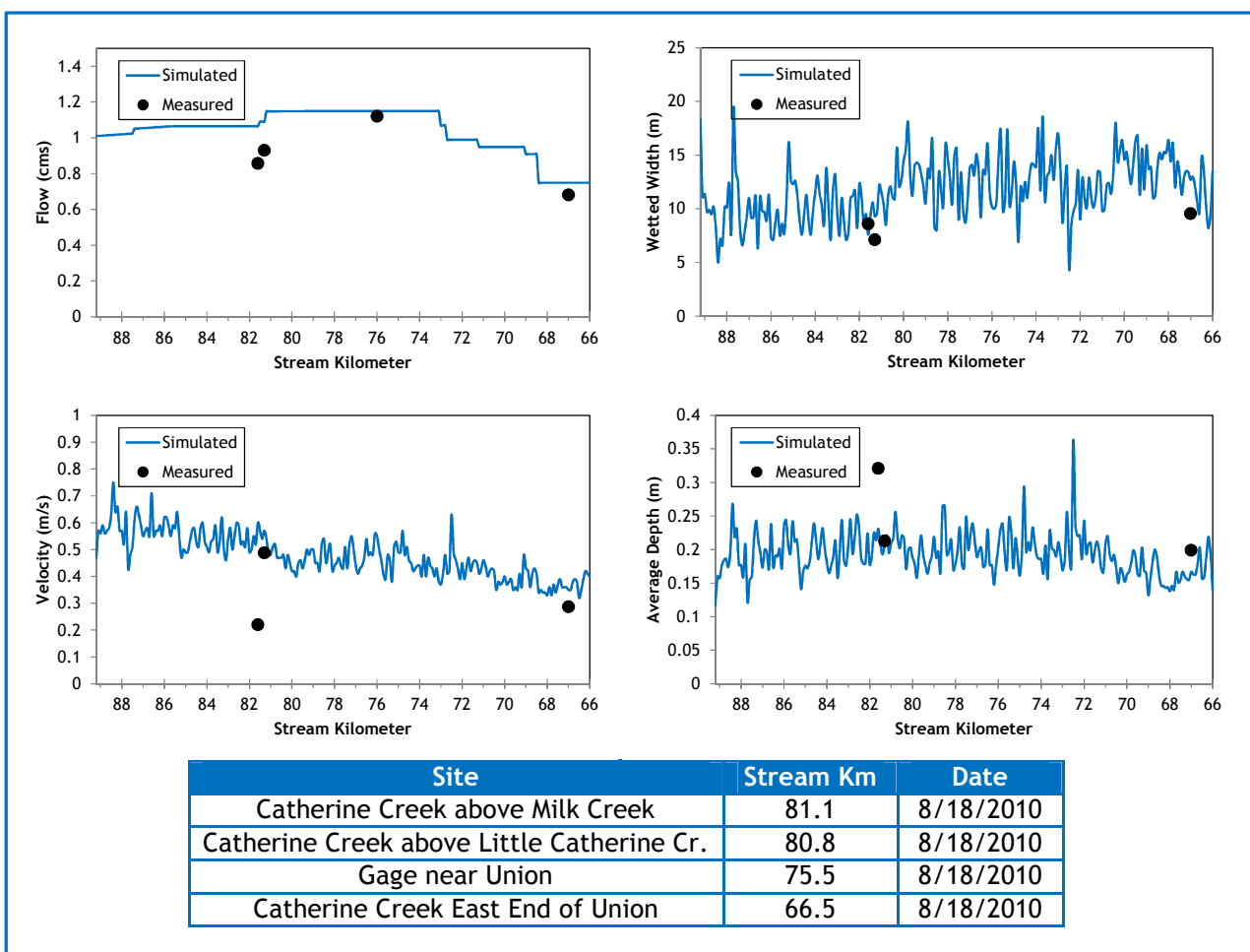
Stream:	Catherine Creek
Length:	88.7 kilometers
Time Period:	August 6-27, 2010
Input Distance Step:	50 meters
Output Distance Step:	100 meters
Time Step:	1 minute
Flush Initial Condition:	7 days
TIR Date and Time:	August 12, 2010 16:08-16:46
Land Cover Data Source:	LiDAR
Land Cover Sampling Distance Step:	15 meters

The following assumptions were used when calibrating the Catherine Creek Heat Source model:

- Hourly climate data was obtained from the La Grande Airport (NWS). Air temperature was adjusted using the adiabatic lapse rate of 1°C per 100 meters elevation.
- The upstream boundary condition is a mass balance of data from the mouths of the North and South Forks.
- There is a large diversion in the city of Union where most of the water was being diverted for irrigation use. Below this point there were additional diversions, very low flow, and thermal stratification which prohibited stream temperature modeling; however, effective shade was simulated the entire length from the forks to the confluence with the Grande Ronde River.

Figure 107 shows the simulated and measured hydraulic values for the calibrated Heat Source model for August 18, 2010. The upstream boundary flow volume is a mass balance of the North and South Forks. The Catherine Creek simulated flow volumes are based on the daily values recorded at the gage above Union (stream kilometer 75.5).

Figure 107 - Catherine Creek simulated and measured hydraulic values.



The simulated and daily gage flows for select locations are shown in Figure 108. The flow below the forks is a mass balance of the simulated flows at the mouths of the North and South Forks. The Catherine Creek simulated flows were then calibrated to target the values recorded at the gage near (upstream of) Union. There is a large diversion that was occurring between the lower end of the simulation and the gage in Union. Very little water was left in the stream and those volumes fluctuated each day. The very low flows below Union, thermal stratification, and unmonitored diversions prohibited Heat Source temperature simulation of lower Catherine Creek (effective shade was still simulated for the entire stream).

Figure 108 - Catherine Creek simulated and measured daily flow volumes at select locations.

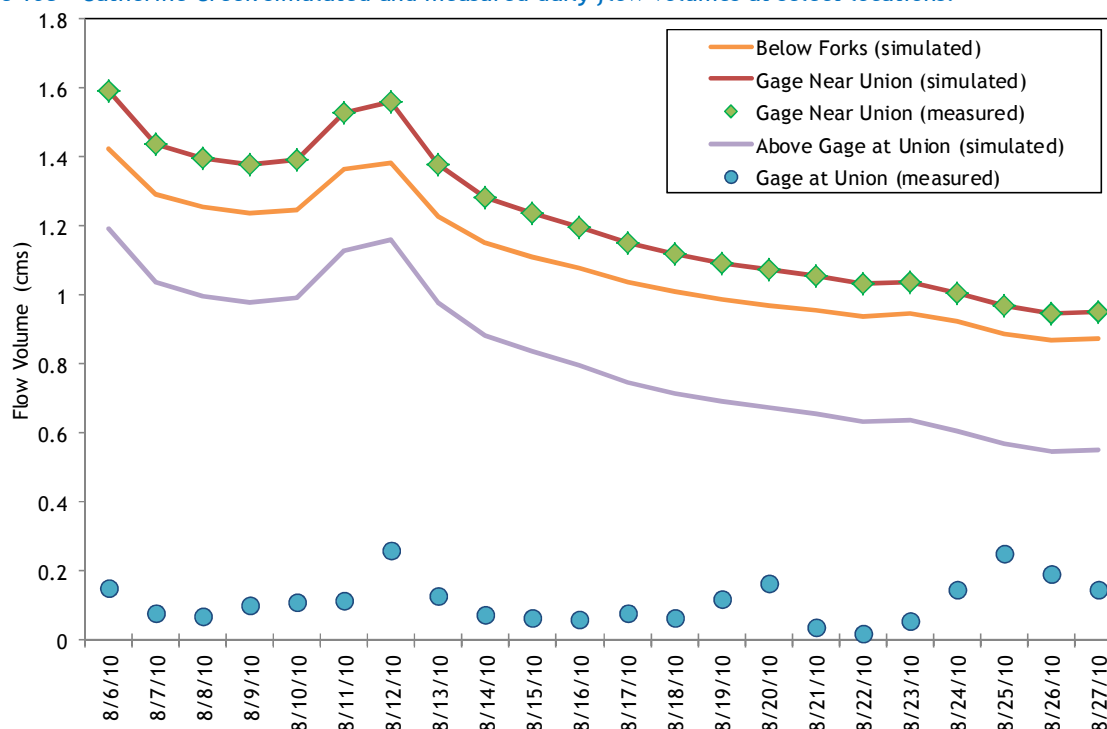


Table 17 summarizes the mass inflows and outflows included in the calibrated Heat Source model. Scout, Milk, and Little Catherine Creek flows were calculated based on the difference between the boundary condition and the gage above Union and vary daily.

Table 17 - Catherine Creek mass inflow and outflow features and assumptions.

Feature	Stream Km	Assumptions
Scout Creek	87.0	0.02-0.04 cms, used Little Catherine Creek at mouth hourly temperatures
Milk Creek	81.1	0.02-0.04 cms, measured hourly temperatures
Little Catherine Cr.	80.7	0.04-0.09 cms, measured hourly temperatures
Diversion (small)	72.5	-0.08 cms (constant)
Diversion (small)	72.2	-0.08 cms (constant)
Diversion	70.8	-0.04 cms (constant)
Hatchery / Ponds	68.5	-0.04 cms (constant)
Dam and Diversion	68.0	-0.16 cms (constant)

The simulated and measured longitudinal stream temperatures above Union are shown in Figure 109.

Figure 109 - Catherine Creek simulated and measured longitudinal temperatures.

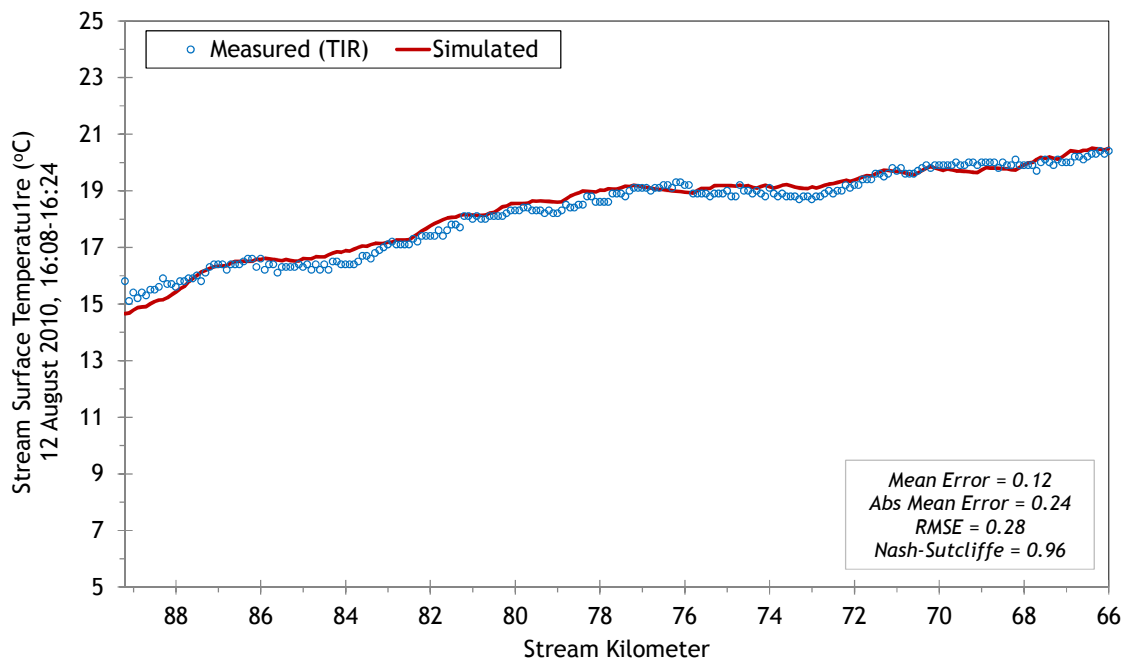
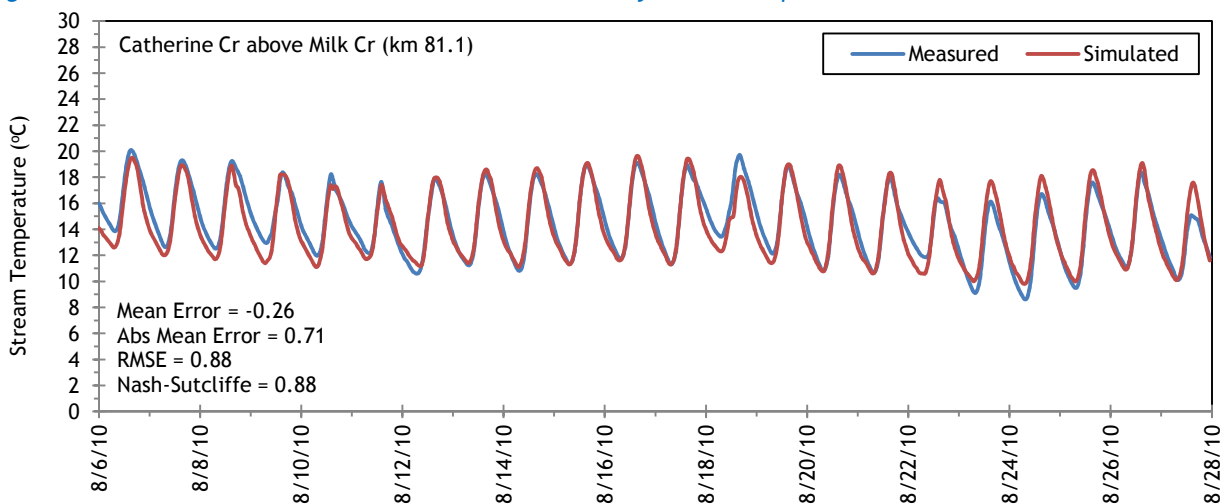
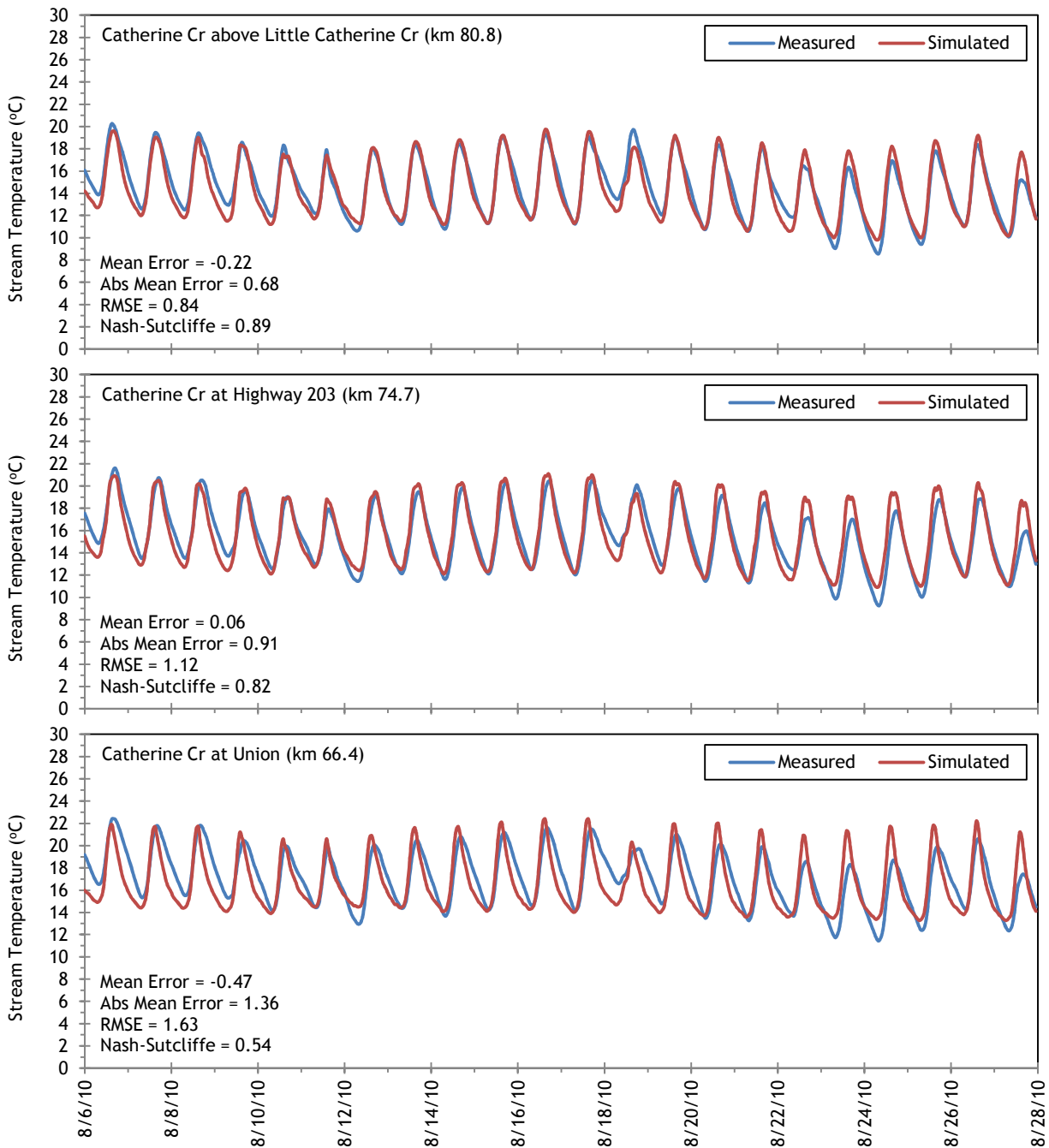


Figure 110 shows the simulated and measured hourly temperatures at 4 locations along the simulated reach between the forks and Union.

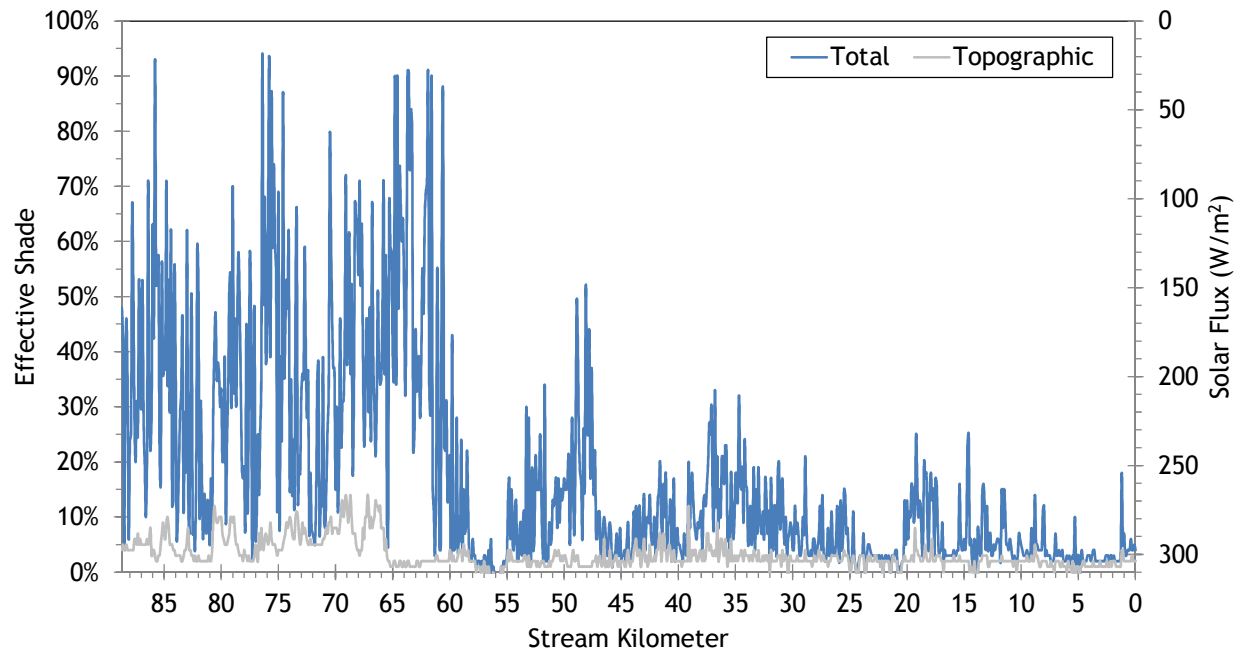
Figure 110 - Catherine Creek simulated and measured hourly stream temperatures.





The simulated effective shade values for Catherine Creek are presented in Figure 111. Above the city of Union (approximately kilometer 65) the stream is flowing through a more confined valley in the foothills and is well forested. Below Union, the land use is primarily agriculture and there is little stream side vegetation, so effective shade is lower.

Figure 111 - Catherine Creek simulated effective shade values.



RGB-colored LiDAR point cloud - Catherine Creek downstream of Warm Creek.

5.8 Clear Creek

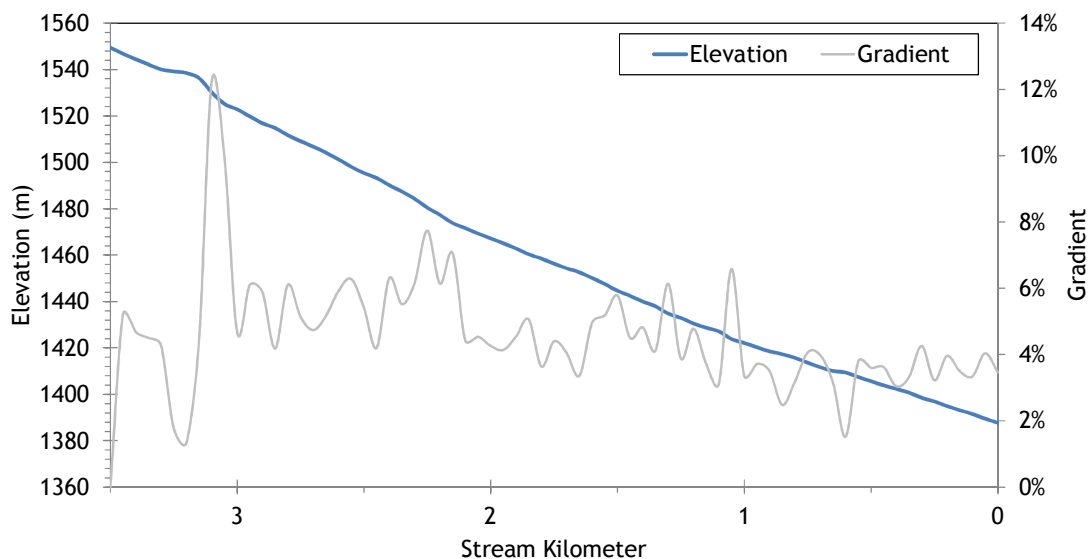


RGB-colored LiDAR point cloud - Clear Creek looking upstream from near mouth.

5.8.1 Clear Creek TTools Results

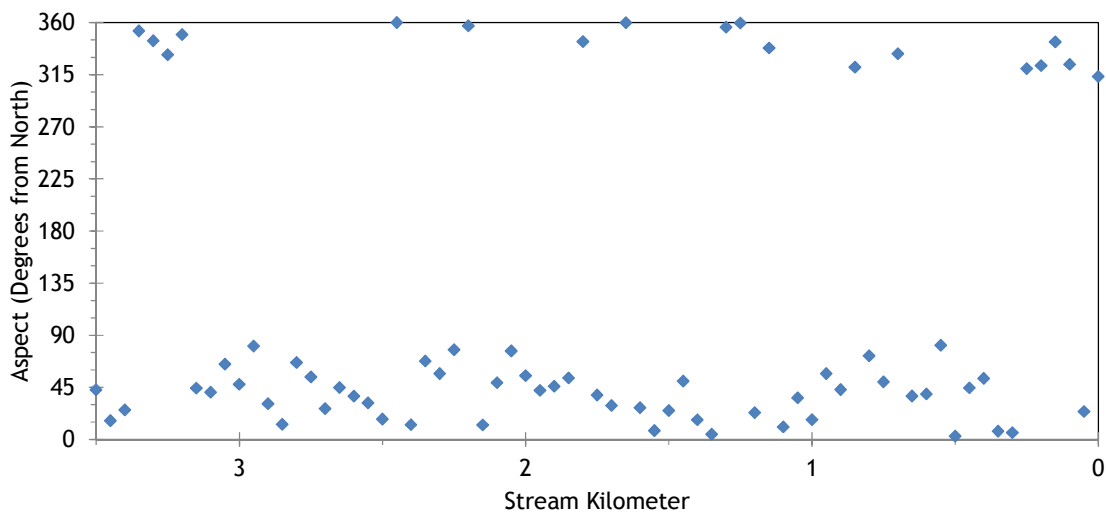
Clear Creek elevations and gradients were sampled from bare earth LiDAR data (Figure 112). The stream is located in the Blue Mountains area of the upper watershed and has a moderately steep gradient.

Figure 112 - Clear Creek elevation and gradient.



Clear Creek flows mostly toward the northeast until it reaches the Grande Ronde River (Figure 113).

Figure 113 - Clear Creek stream aspect.



Topographic shade angles for Clear Creek are shown in Figure 114. There is a significant amount of topographic shade provided by the surrounding mountains.

Figure 114 - Clear Creek topographic shade angles.

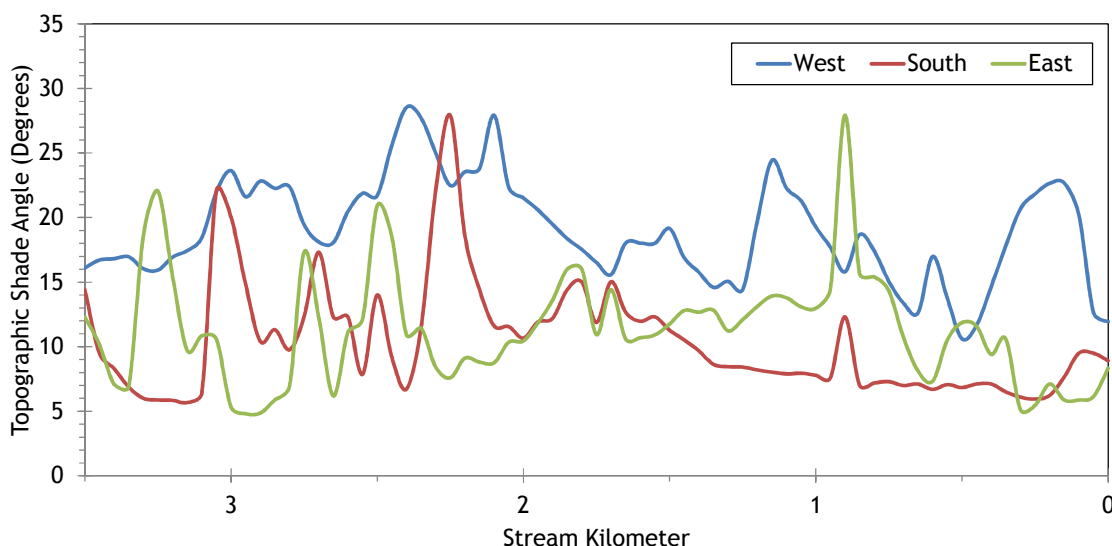
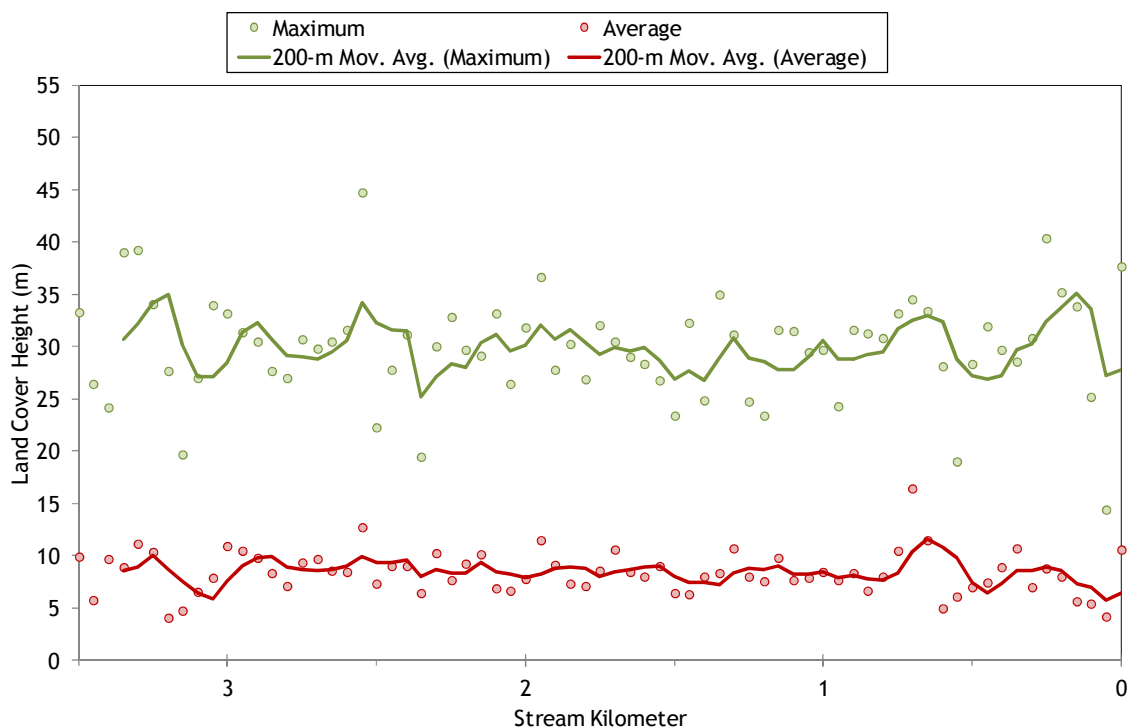


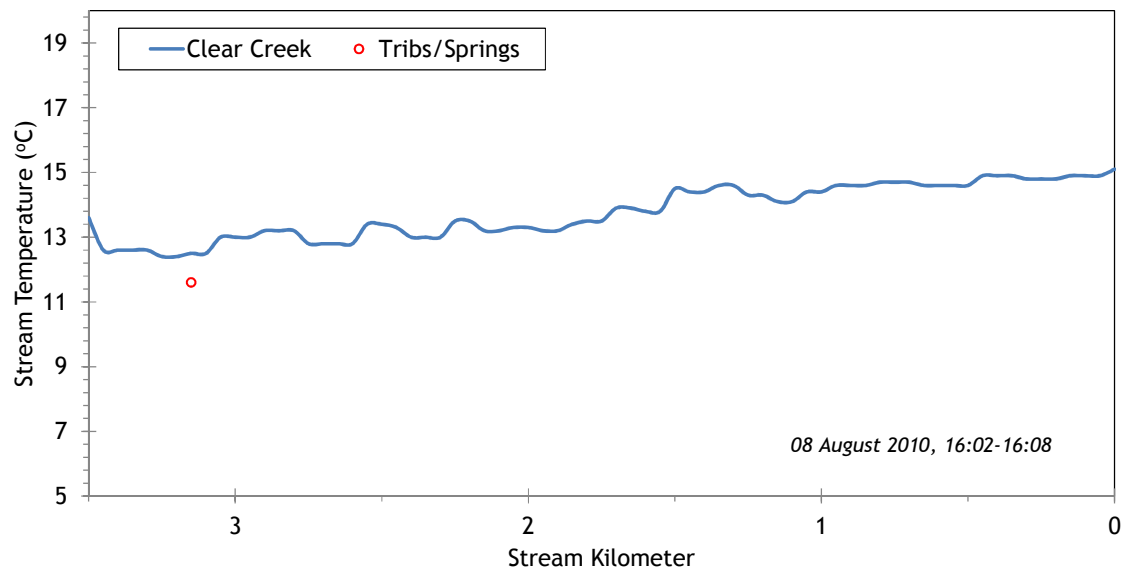
Figure 115 shows the land cover heights sampled along Clear Creek. The maximum and average of the 28 radial samples were calculated for each 50-meter stream node. (Note: Heat Source uses each of the 28 radial samples for each 50-meter node. The maximum and average are shown here for simplification purposes.)

Figure 115 - Clear Creek land cover heights sampled from highest hit LiDAR.



The TIR stream temperature profile for Clear Creek is shown in Figure 116. Clear Creek is well-forested and remains fairly cool throughout the day.

Figure 116 - Clear Creek TIR stream temperature profile.



5.8.2 Clear Creek Heat Source Calibration Results

Stream temperature was simulated for the lower 3.5 kilometers of Clear Creek (Figure 117).

Figure 117 - Clear Creek simulation extent.

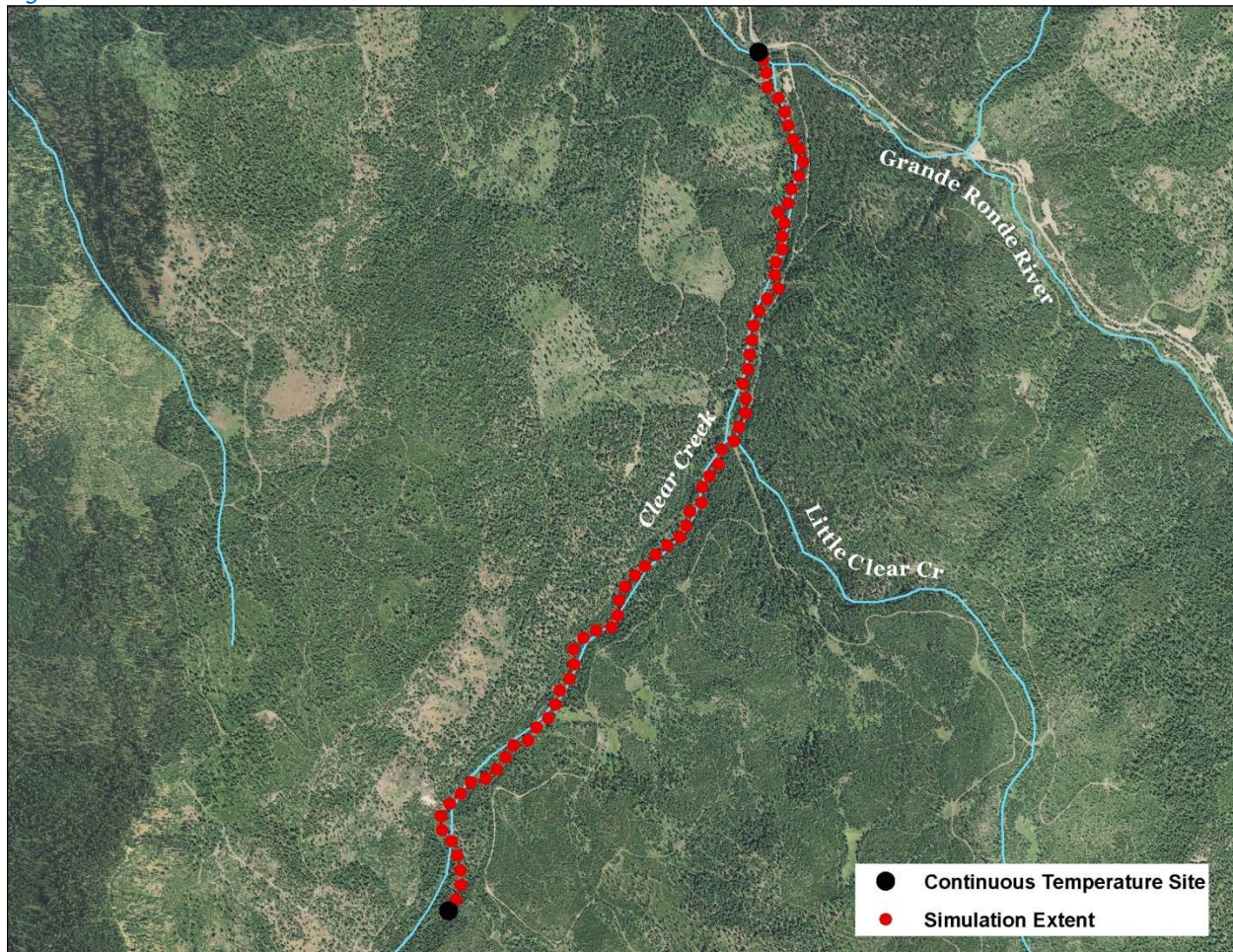


Table 18 - Clear Creek general Heat Source parameters.

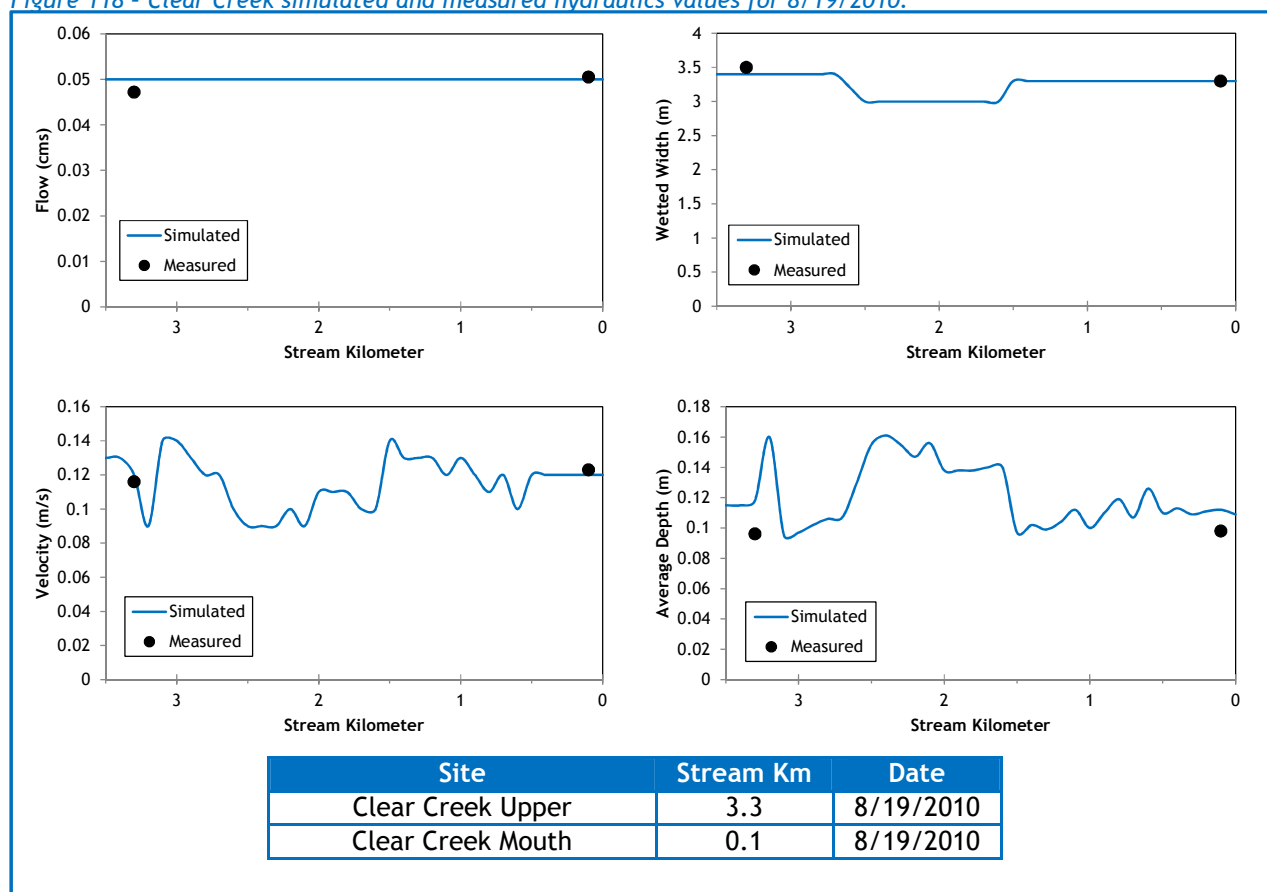
Stream:	Clear Creek
Length:	3.5 kilometers
Time Period:	August 6-27, 2010
Input Distance Step:	50 meters
Output Distance Step:	100 meters
Time Step:	1 minute
Flush Initial Condition:	7 days
TIR Date and Time:	August 8, 2010 16:01-16:07
Land Cover Data Source:	LiDAR
Land Cover Sampling Distance Step:	15 meters

The following assumptions were used when calibrating the Clear Creek Heat Source model:

- Hourly climate data was obtained from the J Ridge RAWs (USFS) site. Air temperature was adjusted using the adiabatic lapse rate of 1°C per 100 meters elevation.
- Wetted widths were too small to be digitized from the remote sensing data and were therefore estimated based on the field measurements.
- Daily flow variability was extrapolated from Grande Ronde River gage data.
- There were no significant springs or tributaries observed in the TIR imagery, and therefore none were included within the model.

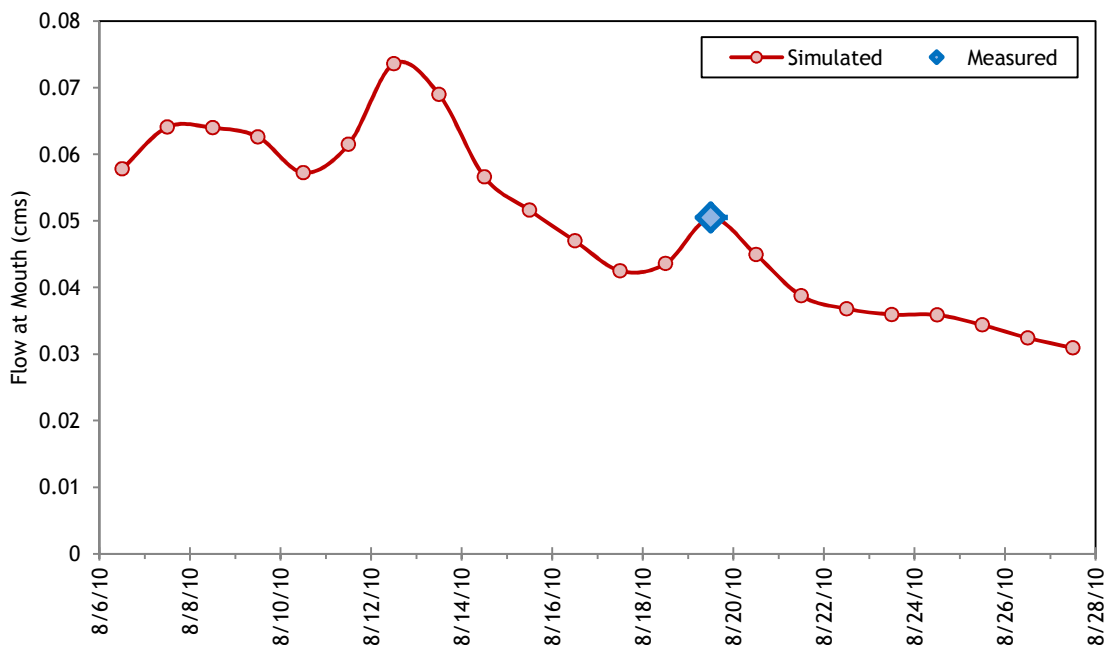
Figure 118 displays the simulated and measured hydraulic values for Clear Creek for August 19, 2010.

Figure 118 - Clear Creek simulated and measured hydraulics values for 8/19/2010.



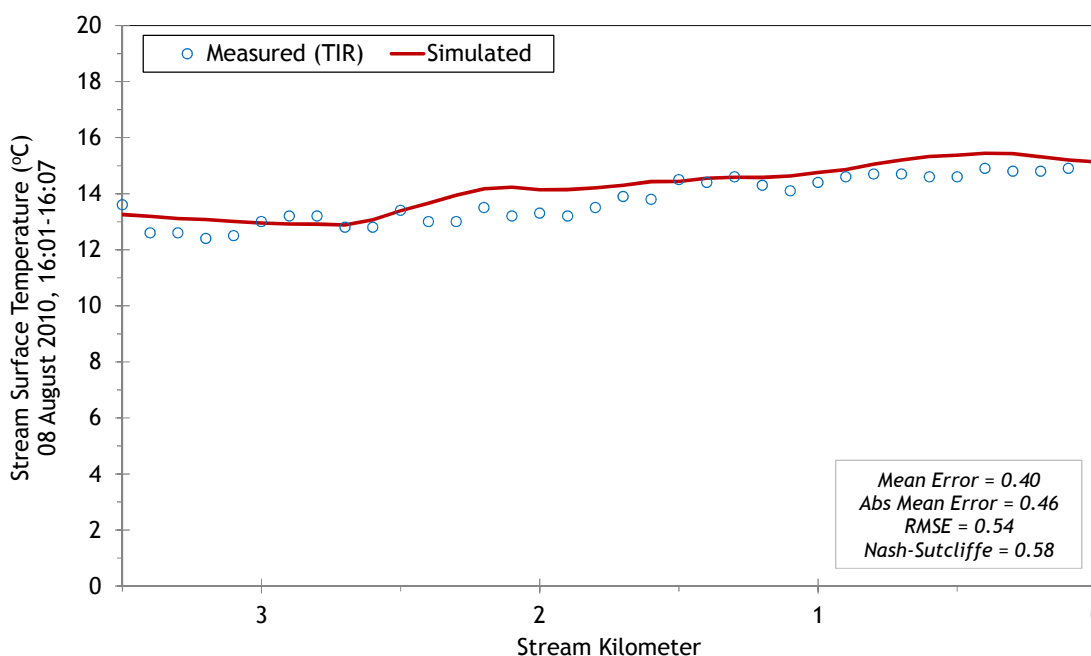
The simulated daily flow volumes at the mouth of Clear Creek are shown in Figure 119. The daily values were extrapolated from gage data recorded on the Grande Ronde River. There were two small rain events which are responsible for the slight flow increases around August 11th and 19th.

Figure 119 - Clear Creek daily flow volumes at the mouth.



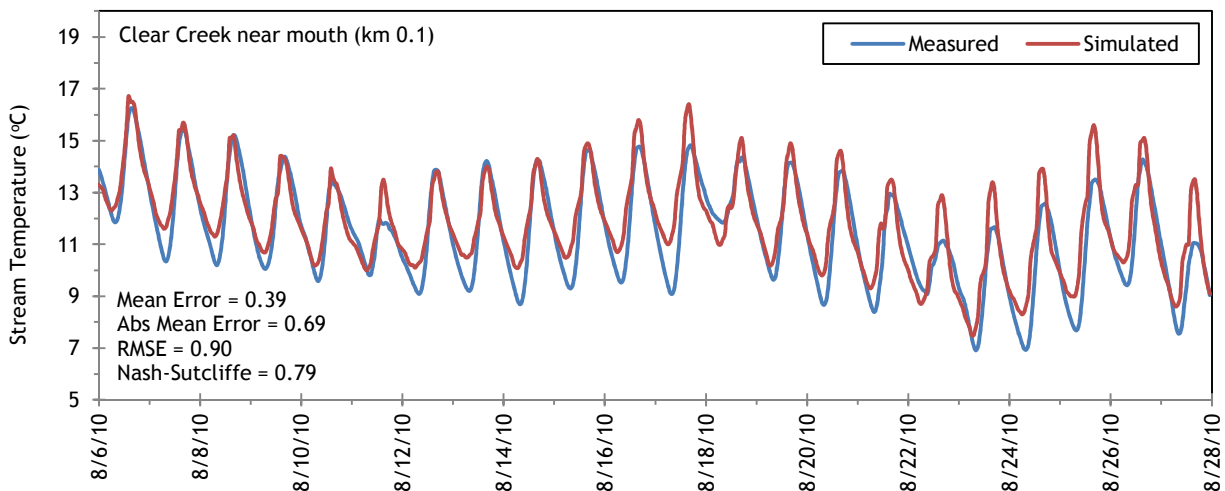
The simulated and measured longitudinal stream temperatures and calibration statistics are shown in Figure 120. There was little thermal variability in the lower 3.5 stream kilometers.

Figure 120 - Clear Creek simulated and measured longitudinal temperatures.



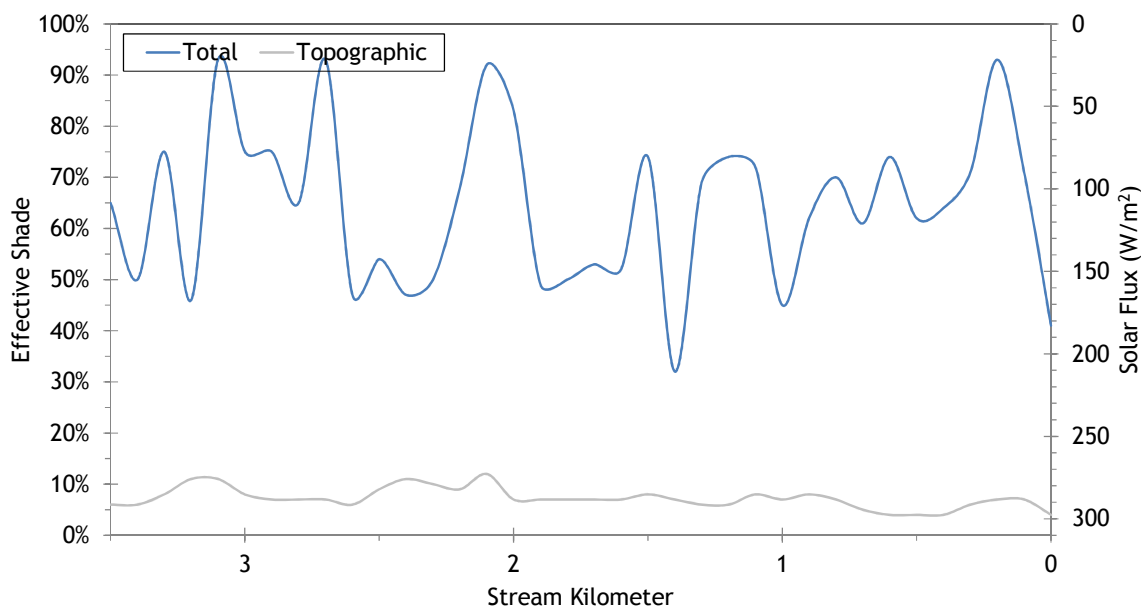
Clear Creek simulated and measured hourly temperatures are plotted in Figure 121.

Figure 121 - Clear Creek simulated and measured hourly temperatures.

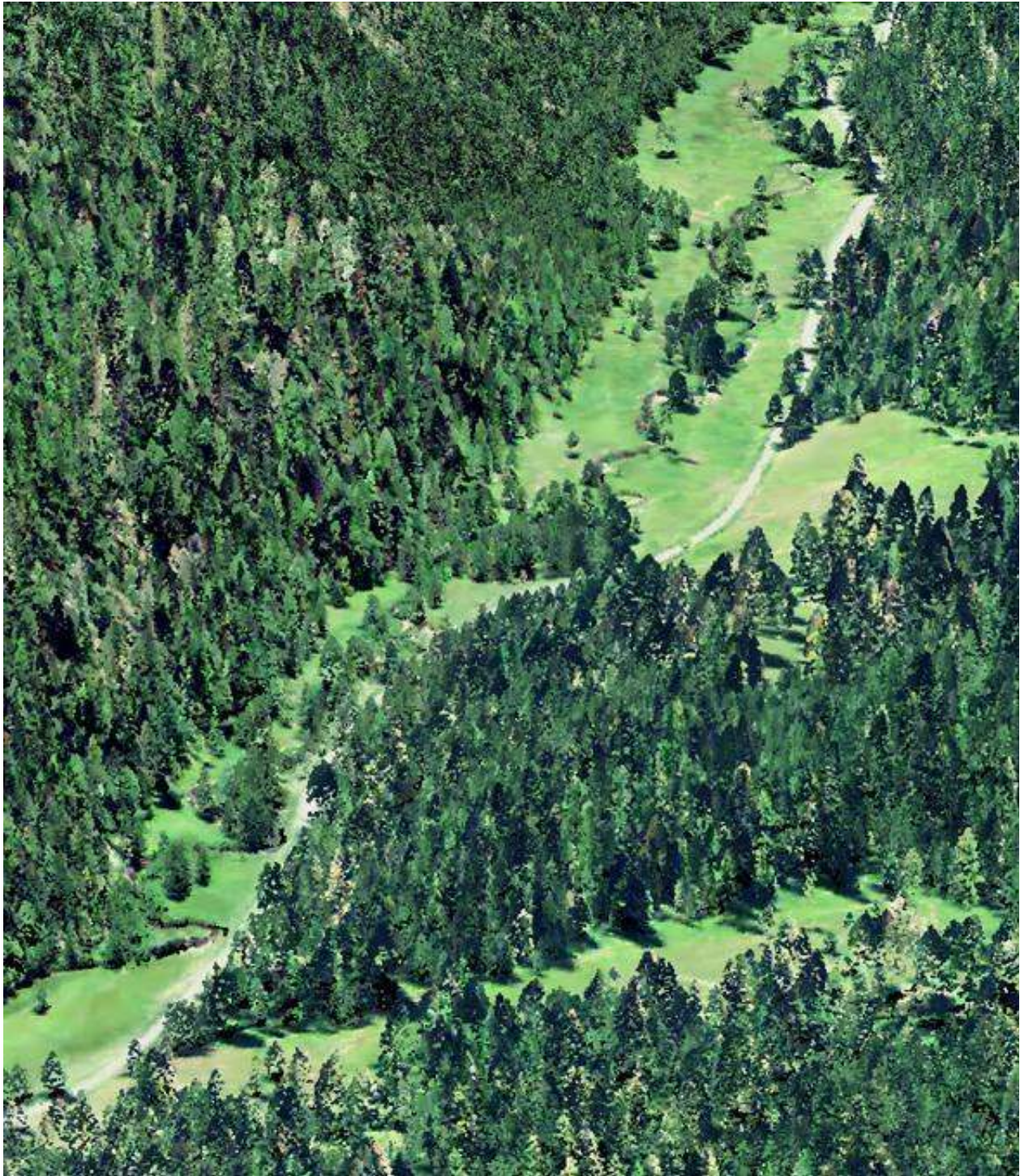


The simulated effective shade values for Clear Creek are shown in Figure 122. There is less than 10% topographic shade along the simulated reach. The majority of the total effective shade is produced by near stream vegetation.

Figure 122 - Clear Creek simulated effective shade.



5.9 Limber Jim Creek

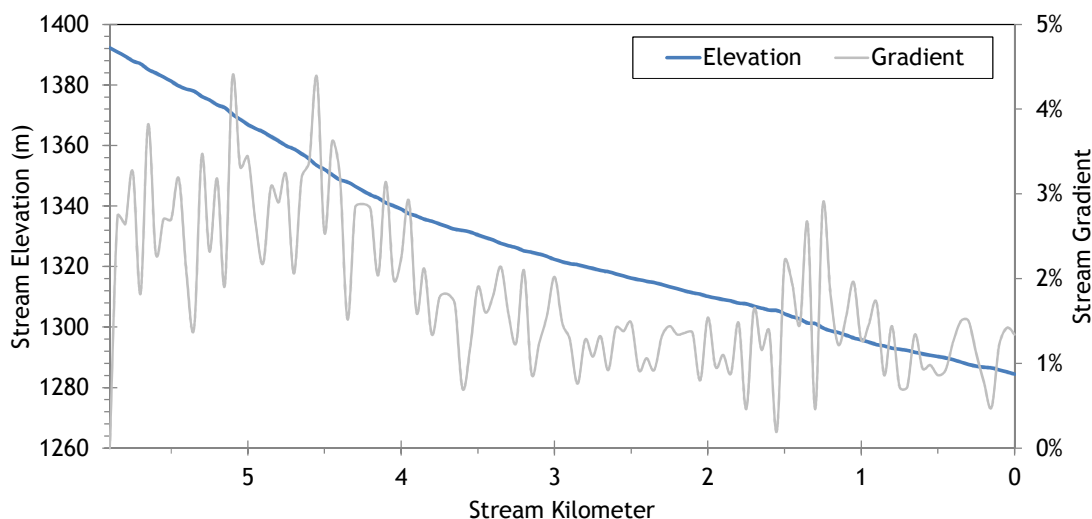


RGB-colored LiDAR point cloud - Limber Jim Creek looking downstream just below the North Fork.

5.9.1 Limber Jim Creek TTools Results

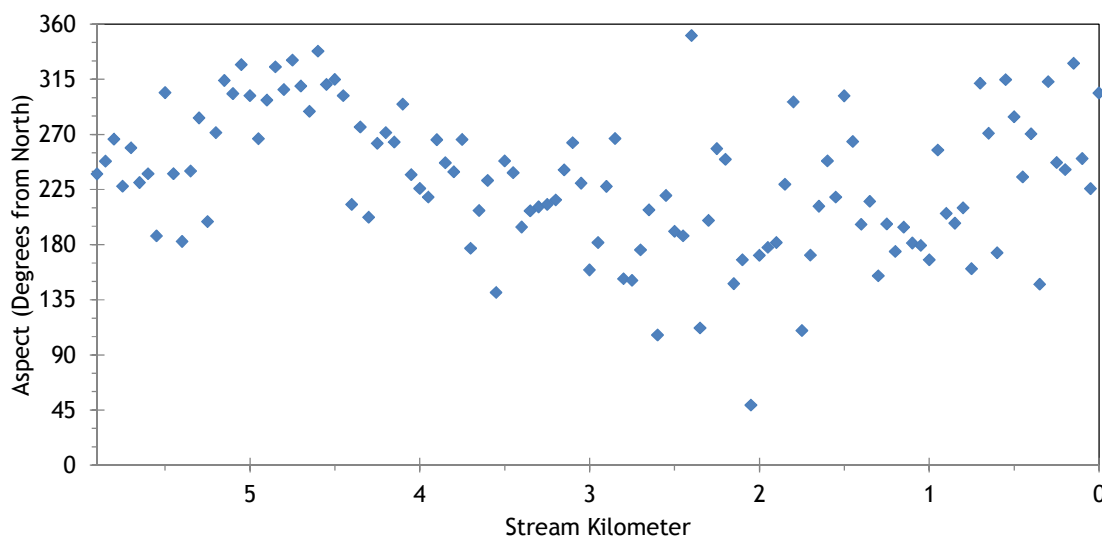
Limber Jim Creek elevations and gradients are shown in Figure 123. The values were sampled from the bare earth LiDAR data. The stream goes from a more constricted valley to a more flat valley bottom in the lower 3 kilometers, where it meanders more and has a lower gradient.

Figure 123 - Limber Jim Creek elevation and gradient.



Limber Jim Creek stream aspects are shown in Figure 124 for each 50-meter reach. Overall, the stream flows in the westerly direction before reaching the Grande Ronde River.

Figure 124 - Limber Jim Creek stream aspect.



Limber Jim Creek has a good amount of topographic shade features provided by the surrounding mountains (Figure 125). Values range between 5 and 25 degrees in general.

Figure 125 - Limber Jim Creek topographic shade angles.

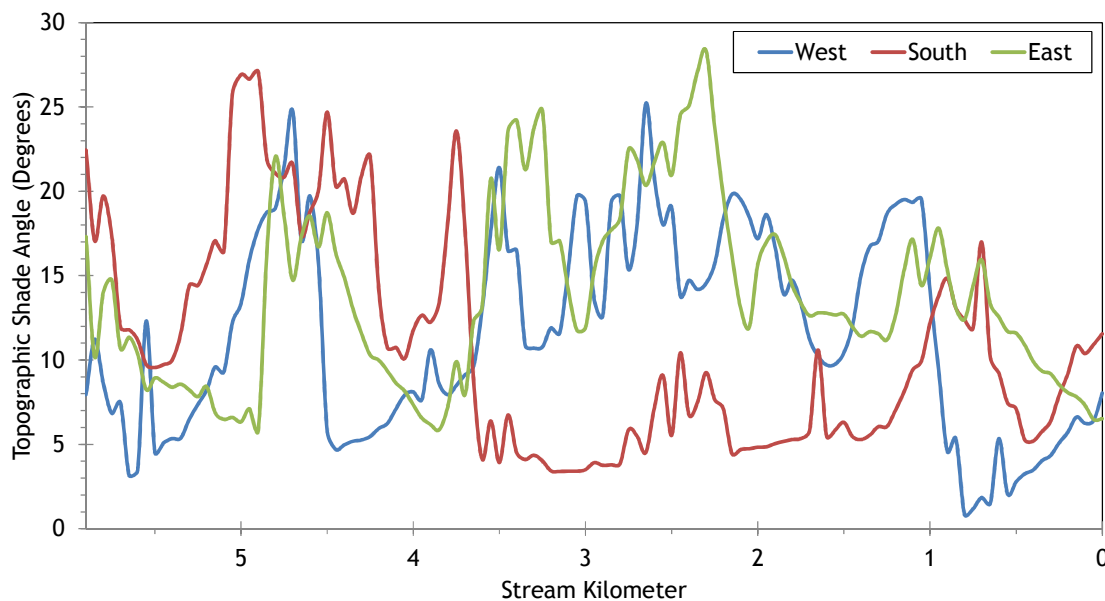
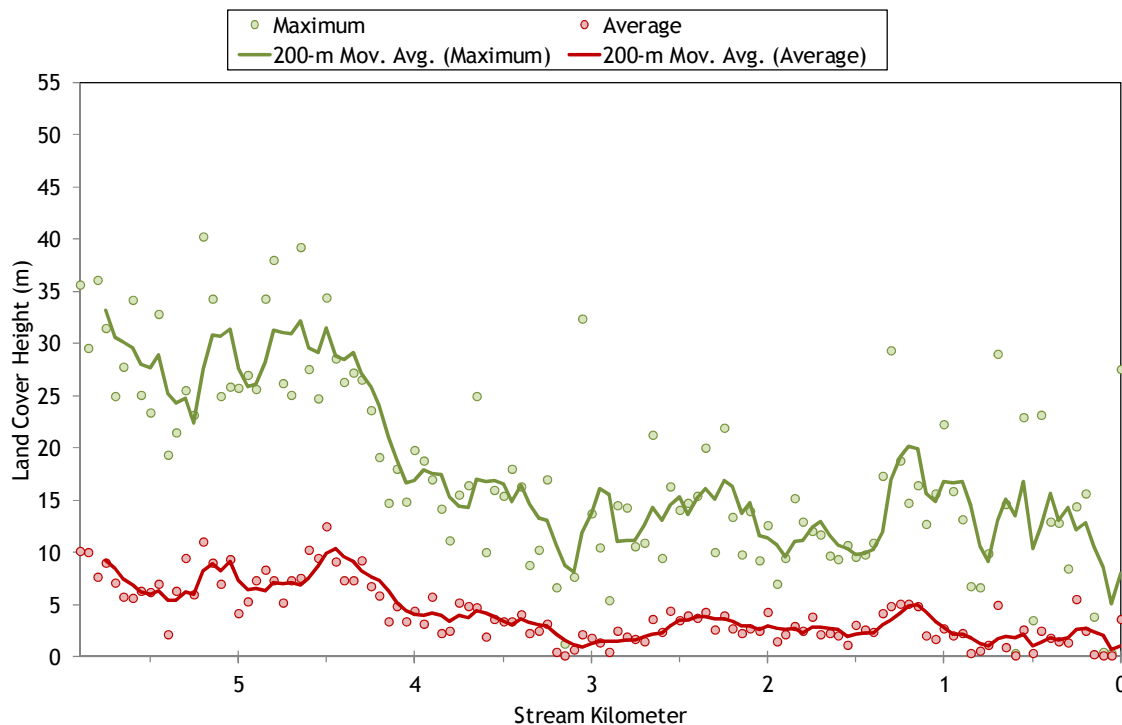


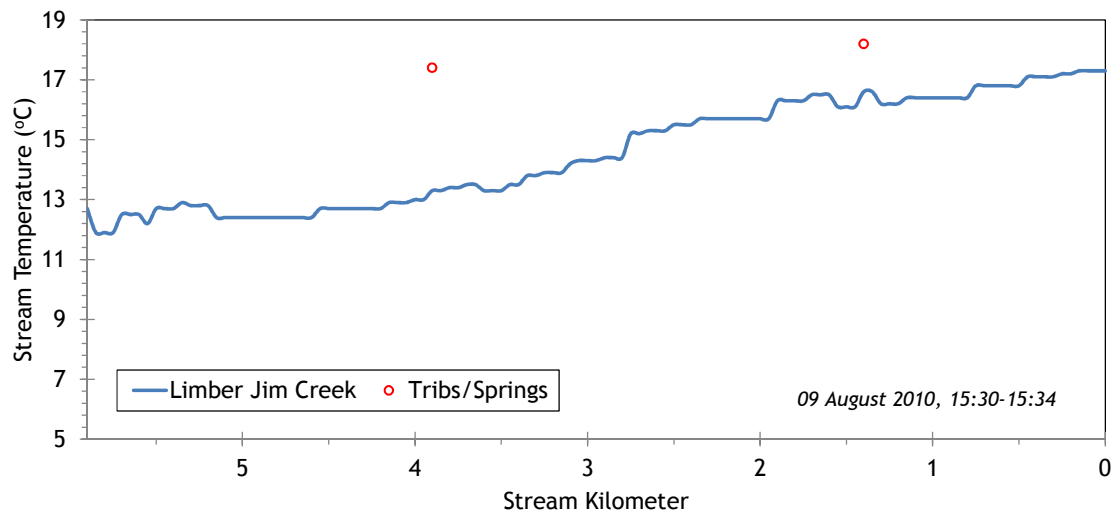
Figure 126 shows the land cover heights sampled along Limber Jim Creek. The maximum and average of the 28 radial samples were calculated for each 50-meter stream node. (Note: Heat Source uses each of the 28 radial samples for each 50-meter node. The maximum and average are shown here for simplification purposes.)

Figure 126 - Limber Jim Creek land cover heights sampled from highest hit LiDAR.



Limber Jim Creek is a fairly cool mountain stream relative to others in the basin (Figure 127). The TIR stream temperature profile shows a steady increase within the lower 6.5 kilometers.

Figure 127 - Limber Jim TIR stream temperature profile.



5.9.2 Limber Jim Creek Heat Source Calibration Results

The lower 5.9 stream kilometers of Limber Jim Creek were simulated for temperature. Figure 128 shows the simulation extent and hourly temperature data sites.

Figure 128 - Limber Jim Creek simulation extent.

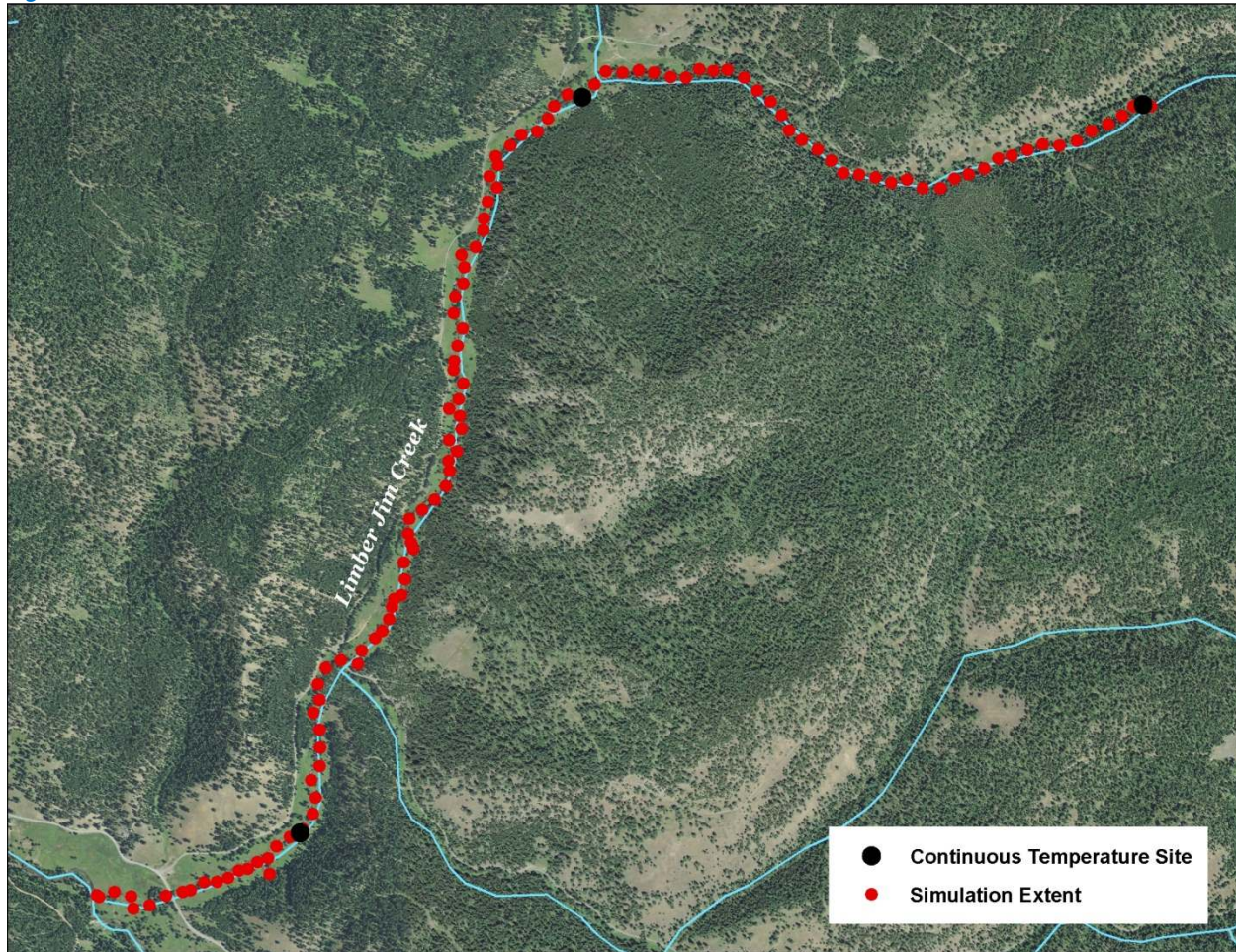


Table 19 - Limber Jim Creek general Heat Source parameters.

Stream:	Limber Jim Creek
Length:	5.9 kilometers
Time Period:	August 6-27, 2010
Input Distance Step:	50 meters
Output Distance Step:	100 meters
Time Step:	1 minute
Flush Initial Condition:	7 days
TIR Date and Time:	August 8, 2010 15:30-15:34
Land Cover Data Source:	LiDAR
Land Cover Sampling Distance Step:	10 meters

The following assumptions were used when calibrating the Limber Jim Creek Heat Source model:

- Hourly climate data was obtained from the J Ridge RAWs (USFS) site. Air temperature was adjusted using the adiabatic lapse rate of 1°C per 100 meters elevation.
- Wetted widths were digitized from the remote sensing imagery and then had to be reduced in some reaches in order to accommodate the stream hydraulics and measured data.
- Daily flow values were extrapolated from the Grande Ronde River gage data.

Figure 129 displays the simulated and measured hydraulic values for Limber Jim Creek for August 14, 2010. The ground-level data were collected at three locations, including the upstream boundary of the model extent.

Figure 129 - Limber Jim Creek simulated and measured hydraulic values.

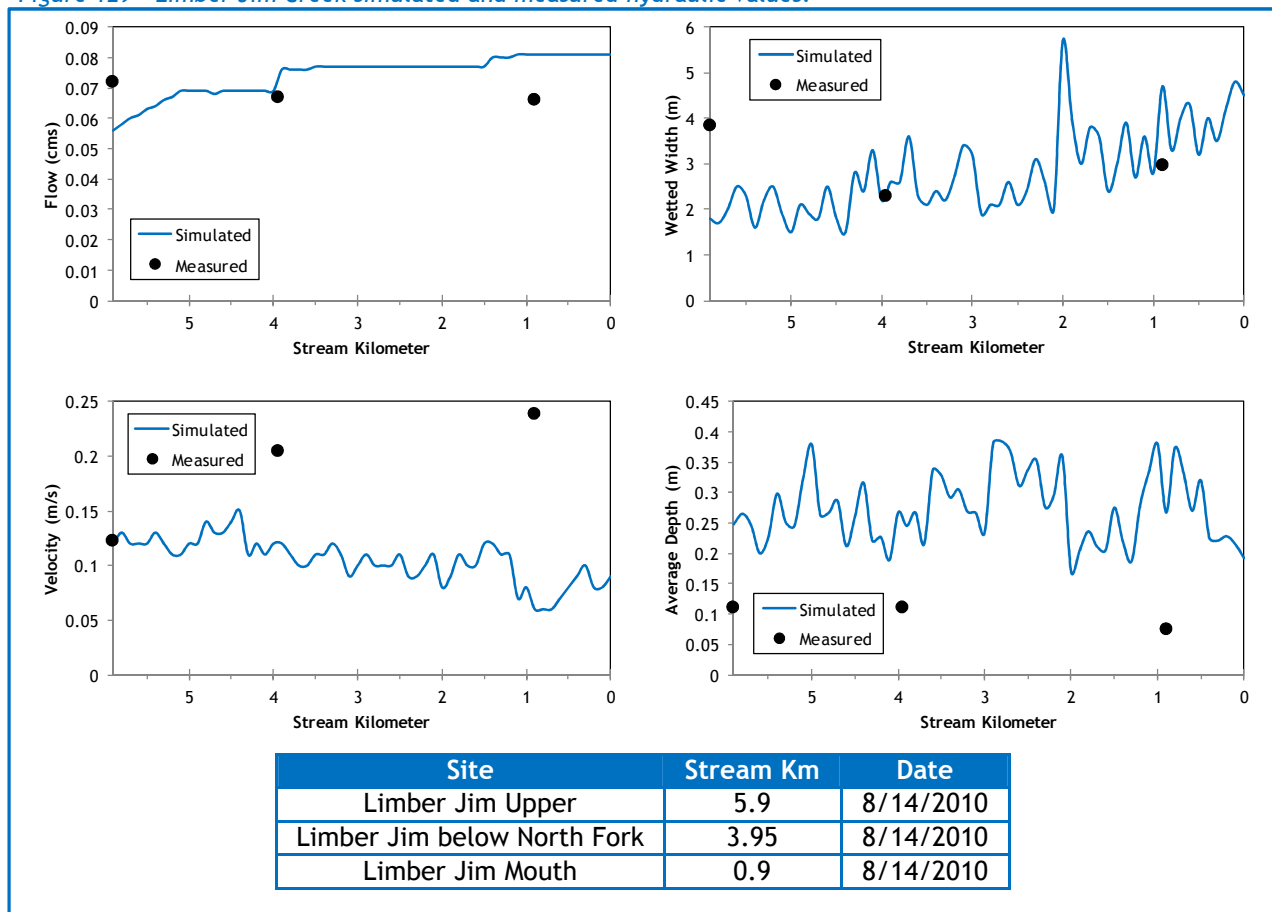
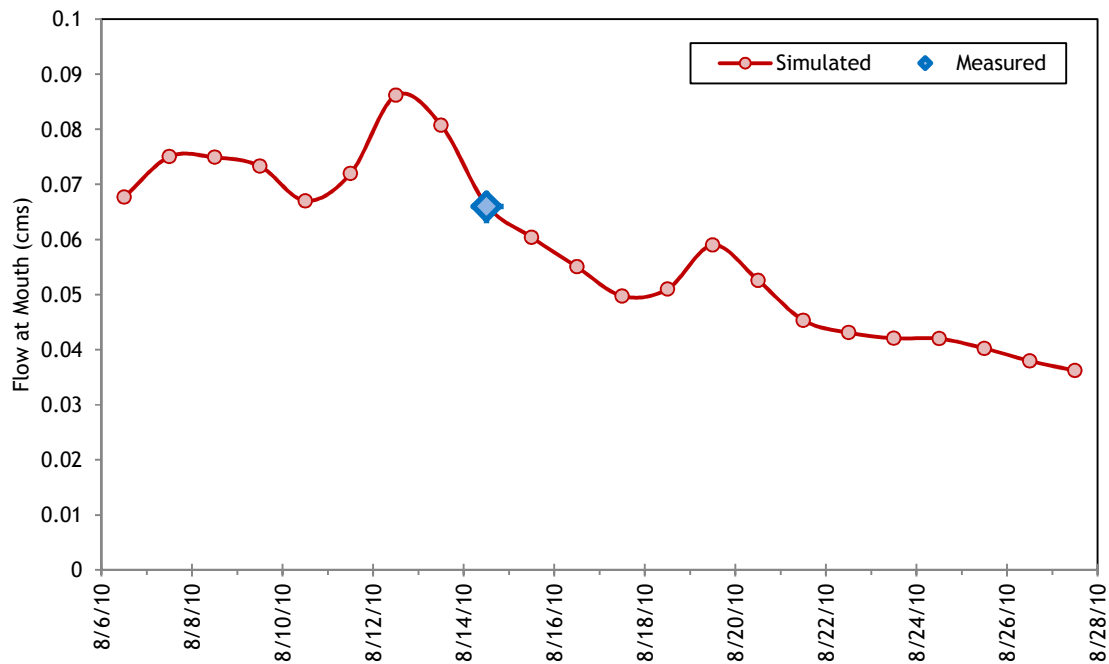


Figure 130 displays the simulated daily flow volumes at the mouth of Limber Jim Creek. The values were extrapolated from gage data on the Grande Ronde River, assuming that each stream in the watershed exhibited similar degrees of daily variability.

Figure 130 - Limber Jim Creek simulated flows at the mouth.



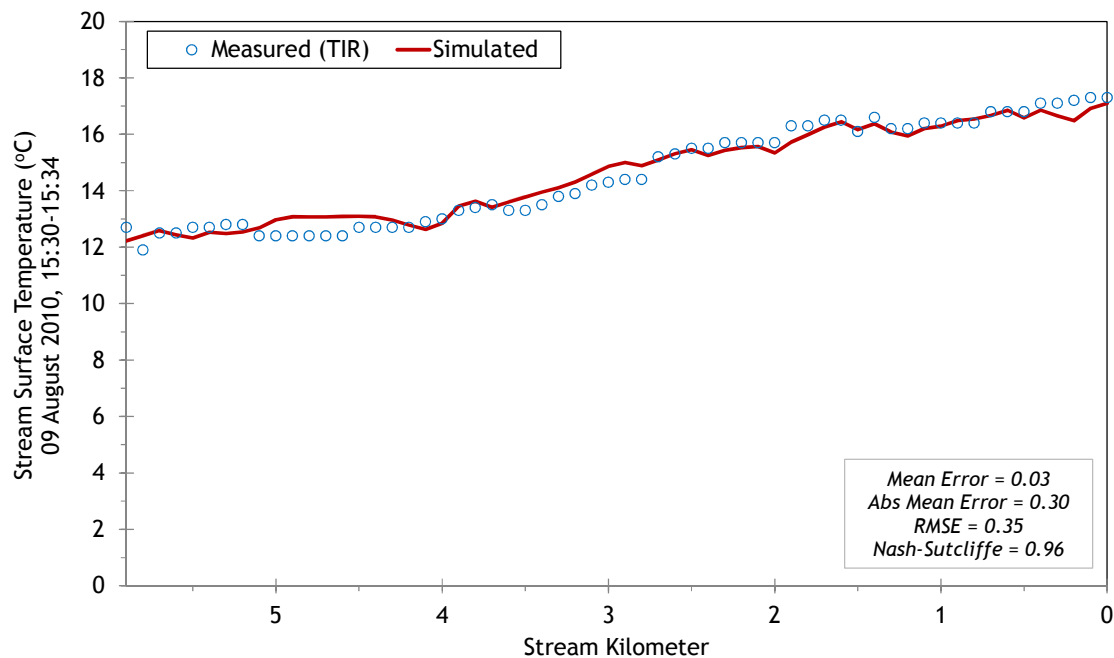
There were two tributaries observed in the TIR data (Table 20). Their daily flow volumes were estimated and daily variability was extrapolated from gage data on the Grande Ronde River. Overall, the tributaries were estimated to be much smaller than the mainstem Limber Jim Creek; therefore their flow estimates were small and temperatures were included as constants.

Table 20 - Limber Jim Creek mass inflow features and assumptions.

Feature	Stream Km	Assumptions
North Fork Limber Jim Cr.	3.9	0.004-0.009 cms at 17.4°C
South Fork Limber Jim Cr.	1.4	0.002-0.004 cms at 18.2°C

The simulated and measured longitudinal stream temperatures for Limber Jim Creek are shown in Figure 131. The stream gradually heated approximately 5°C in its lower six kilometers at the time that the TIR data were collected

Figure 131 - Limber Jim Creek simulated and measured longitudinal stream temperatures.



Simulated and measured hourly stream temperatures are presented in Figure 132. Calibration statistics are also shown in each plot.

Figure 132 - Limber Jim Creek simulated and measured hourly stream temperatures.

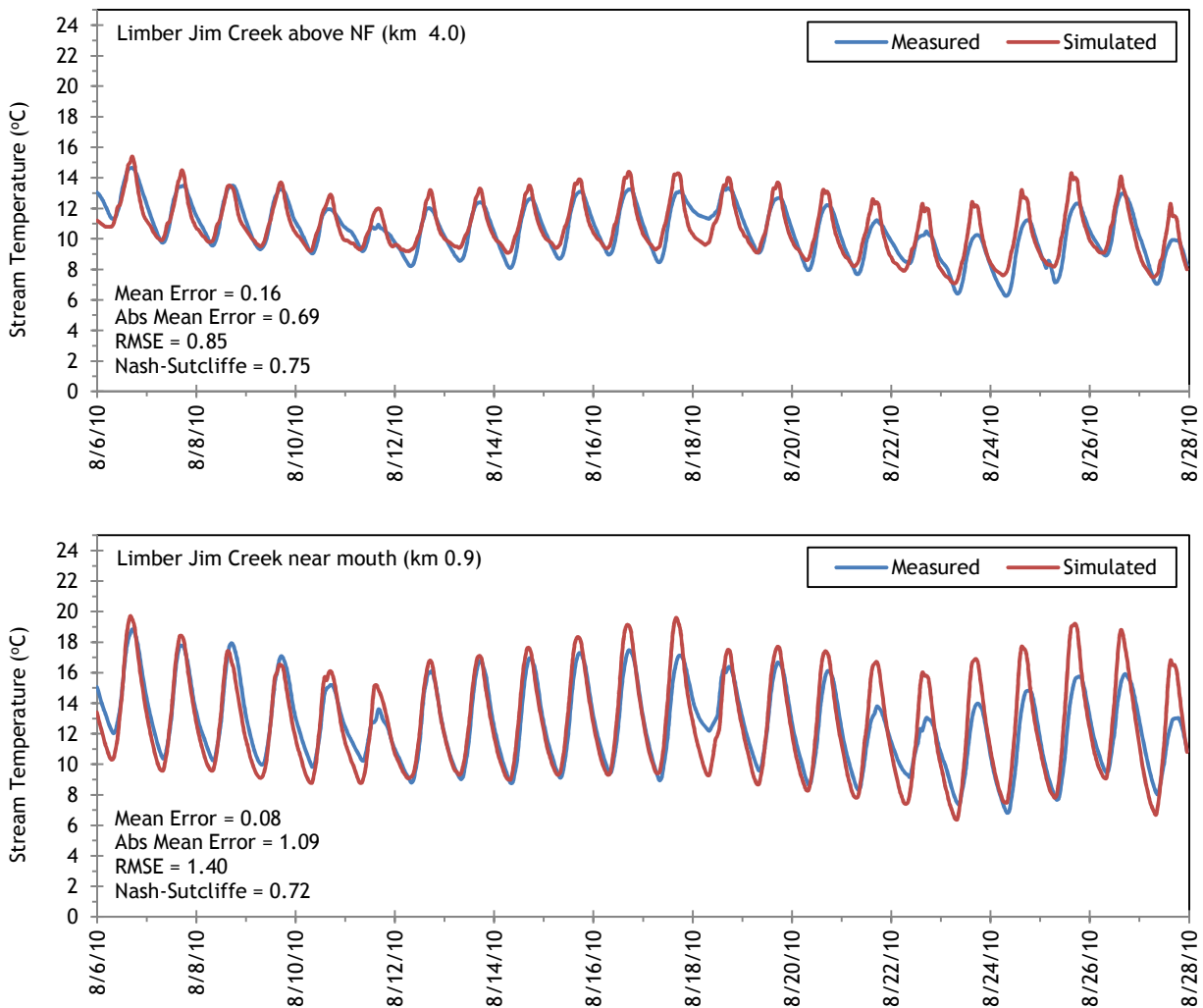
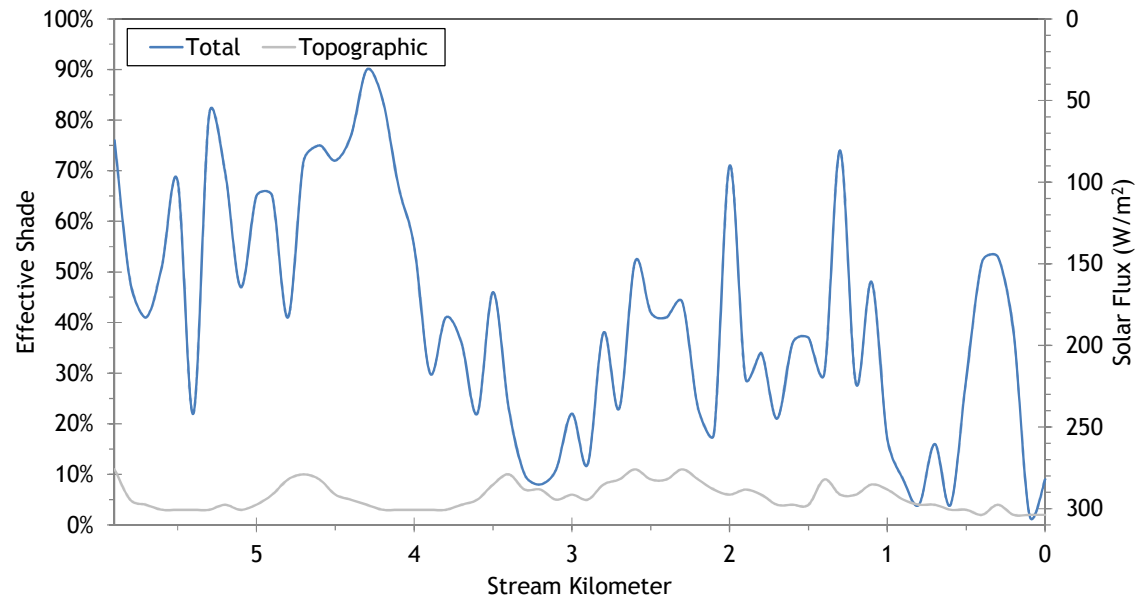


Figure 133 shows the simulated effective shade values for Limber Jim Creek. Between stream kilometer 4 and the mouth, there is less effective shade because the stream is flowing through a meadow-forest complex. Topographic shade is generally less than 10%.

Figure 133 - Limber Jim Creek simulated effective shade.



5.10 Chicken Creek

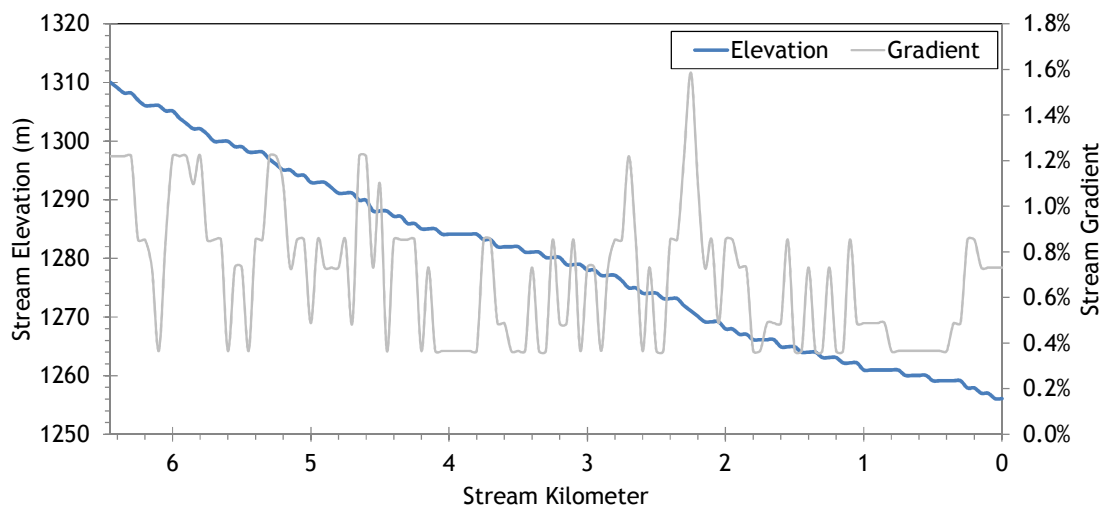


RGB-colored LiDAR point cloud - Chicken Creek (flowing from bottom of image) at confluence with Sheep Creek.

5.10.1 Chicken Creek TTools Results

Chicken Creek elevations and gradients are shown in Figure 134. The values were sampled from the 10-meter DEM because LiDAR data was only available for a short reach near the mouth. Of the sampled reach, gradients were usually less than 1%.

Figure 134 - Chicken Creek elevation and gradient.



Stream aspects for every 50 meters of Chicken Creek are shown in Figure 135. Chicken Creek generally flows northward until it reaches Sheep Creek; however there is significant small scale variation due to the meandering nature of the stream within the valley bottom.

Figure 135 - Chicken Creek stream aspect.

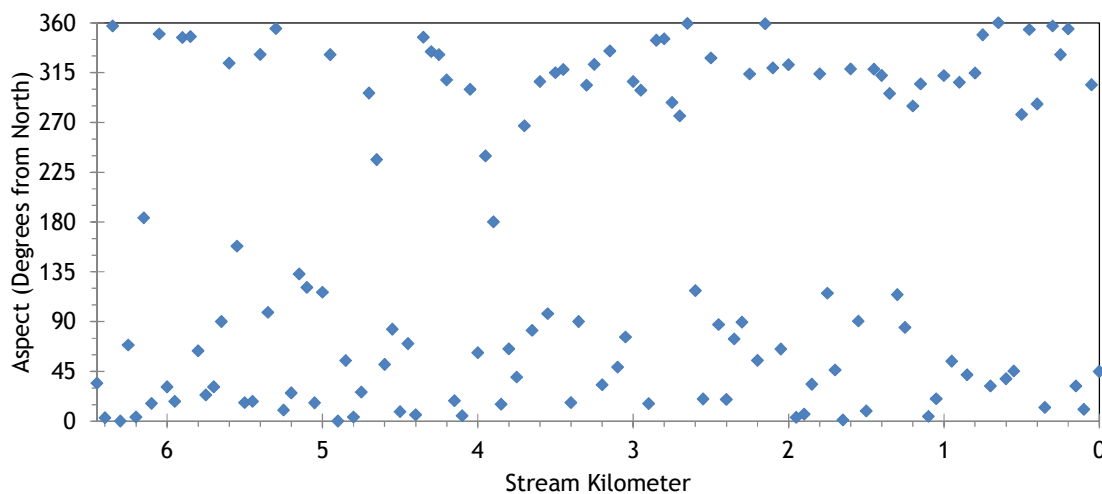
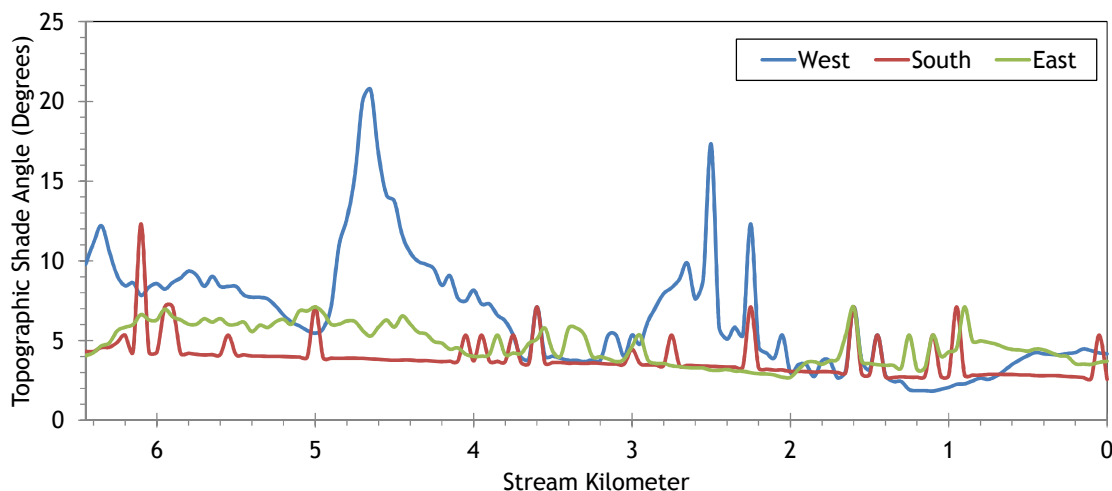


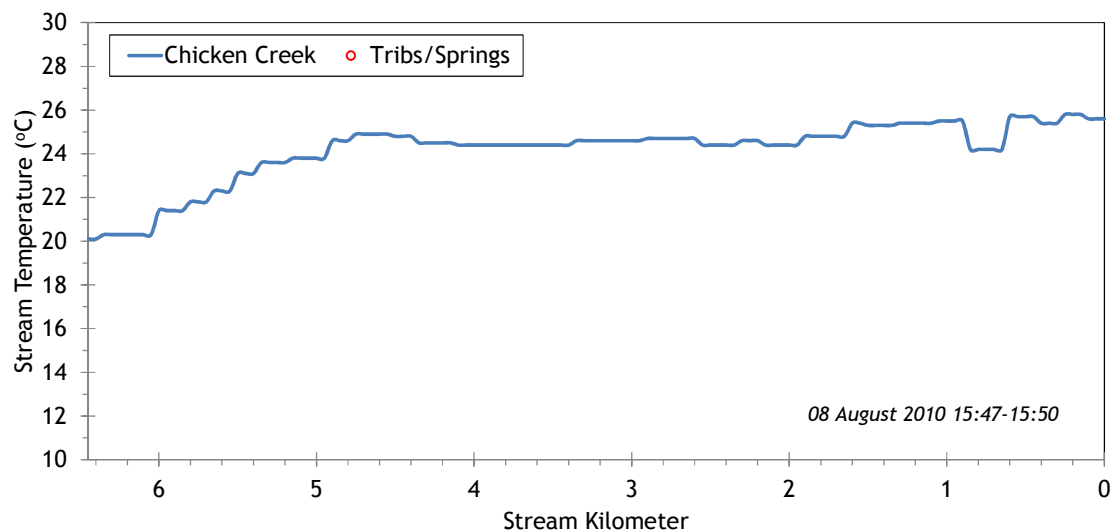
Figure 136 shows the topographic shade angles. Overall, topographic shade is minor because of the wide flat valley morphology through which this section of stream flows.

Figure 136 - Chicken Creek topographic shade angles.



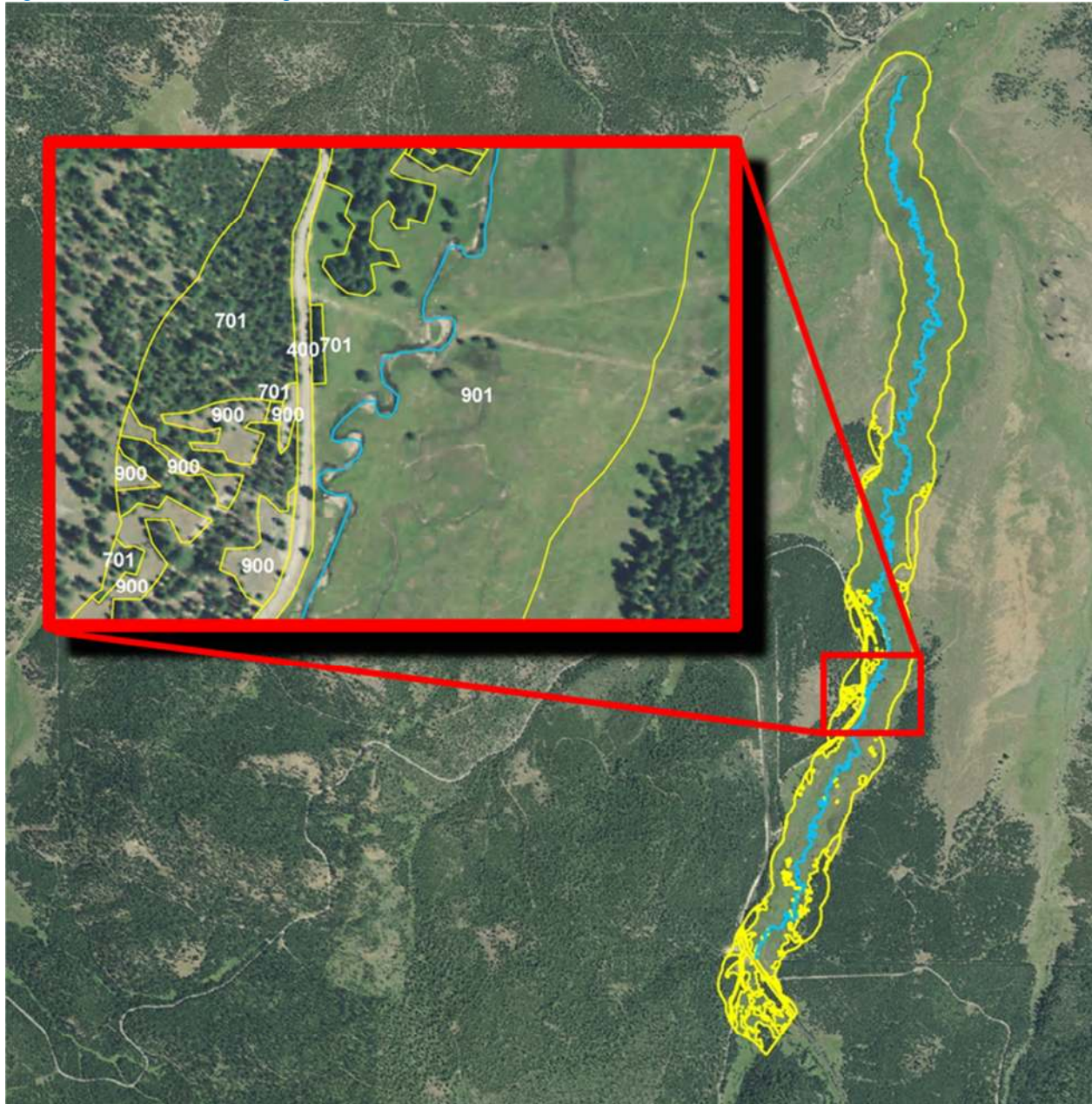
The Chicken Creek TIR stream temperature profile is shown in Figure 137. In this section of lower Chicken Creek, the temperatures were fairly warm and reached a maximum of about 25°C during the TIR flight.

Figure 137 - Chicken Creek TIR stream temperature profile.



LiDAR data were unavailable for Chicken Creek, so the near stream land cover was manually digitized within 100 meters of the stream using NAIP orthoimages (Figure 138). Most of the lower 6.5 kilometers of Chicken Creek flow through open grassy areas and has few trees.

Figure 138 - Chicken Creek digitized near stream land cover.



Chicken Creek land cover height estimates were derived from the LiDAR samples of Sheep Creek (Table 21). The 25th and 75th percentiles of values over 3 meters were calculated from the Sheep Creek TTools data. The 75th percentile was 14.1 meters, which was applied to tall tree classes for Chicken Creek. The 25th percentile was 6.3 meters, which was applied to the short tree classes for Chicken Creek.

Table 21 - Chicken Creek near stream land cover codes and descriptions.

Land Cover Name	Code	Height (m)	Density	Overhang (m)
Upland dry grasses	900	0.5	0.9	0.0
Lowland wet grasses	901	0.5	0.9	0.0
large conifer - dense	700	14.1	0.75	1.0
small conifer - dense	701	6.2	0.75	1.0
large conifer - sparse	750	14.1	0.25	1.0
small conifer - sparse	751	6.2	0.25	1.0
paved road	400	0	0	0
unpaved road	401	0	0	0
water	3011	0	0	0

5.10.2 Chicken Creek Heat Source Calibration Results

The lower 6.5 kilometers of Chicken Creek were simulated for temperature (Figure 139).

Figure 139 - Chicken Creek simulation extent.

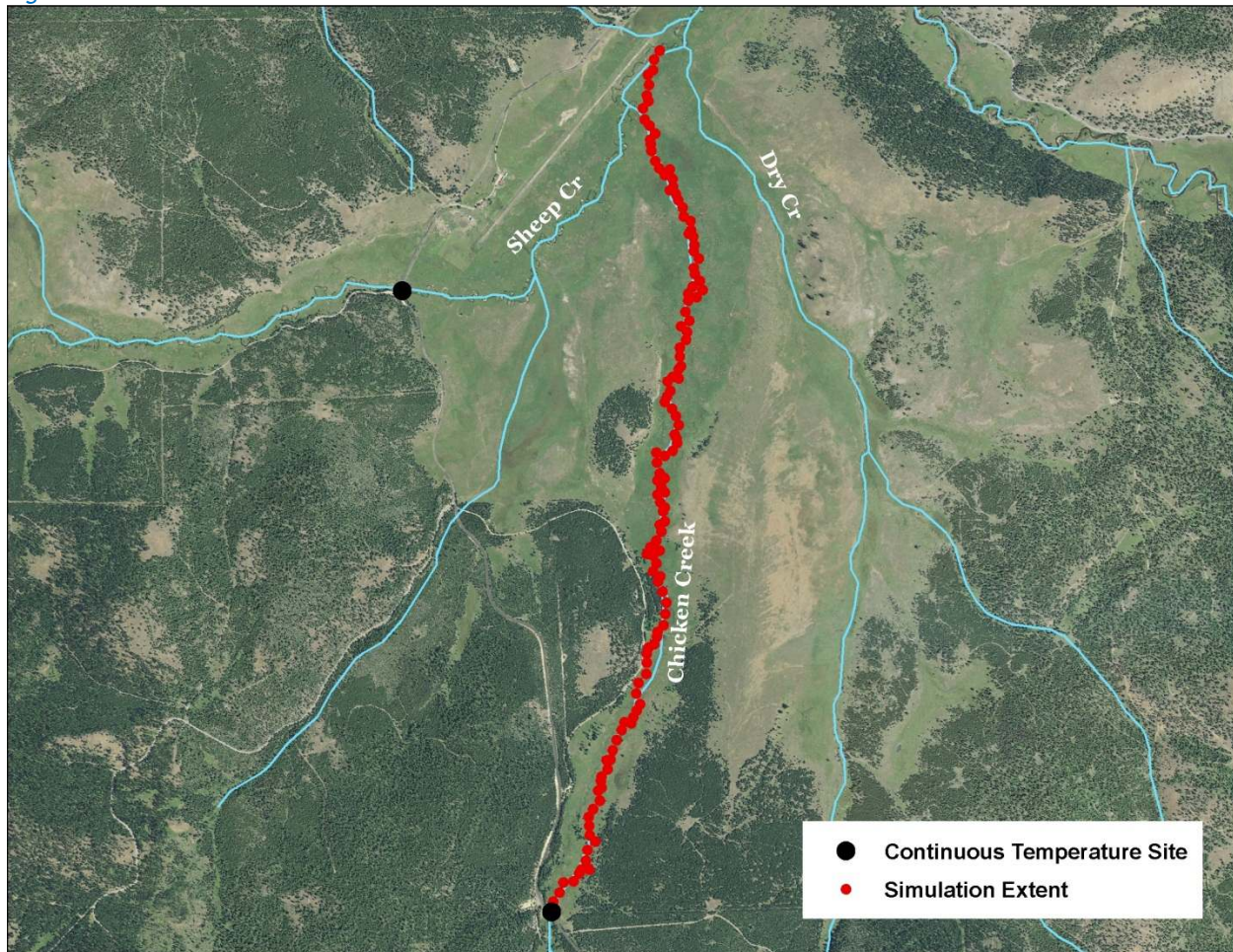


Table 22 - Chicken Creek general Heat Source parameters.

Stream:	Chicken Creek
Length:	6.5 kilometers
Time Period:	August 6-27, 2010
Input Distance Step:	50 meters
Output Distance Step:	100 meters
Time Step:	1 minute
Flush Initial Condition:	7 days
TIR Date and Time:	August 8, 2010 15:30-15:34
Land Cover Data Source:	Manually Digitized
Land Cover Sampling Distance Step:	15 meters

The following assumptions were used when calibrating the Chicken Creek Heat Source model:

- Hourly climate data were obtained from the J Ridge RAWS (USFS) site. Air temperature was adjusted using the adiabatic lapse rate of 1°C per 100 meters elevation.
- The stream was too small to digitize the banks from the remote sensing imagery. Several measurements were made from the NAIP images and the in-between values were interpolated for each 50-meter model node.
- Daily flow variability was extrapolated from Grande Ronde River gage data.
- The only available hourly temperature data was for the upstream boundary condition, therefore there is no hourly calibration validation. This model is calibrated strictly to the TIR data, which increases the uncertainty associated with it.
- Since there was no LiDAR available, the near stream land cover was digitized within a 100-meter buffer of the stream. Height estimates were applied based on values observed in the LiDAR data along other streams in the vicinity.

Figure 140 shows the simulated hydraulic parameters for Chicken Creek for August 19, 2010. There were no available ground level data for the lower 6.5 kilometers, except for the boundary condition.

Figure 140 - Chicken Creek simulated hydraulic values.

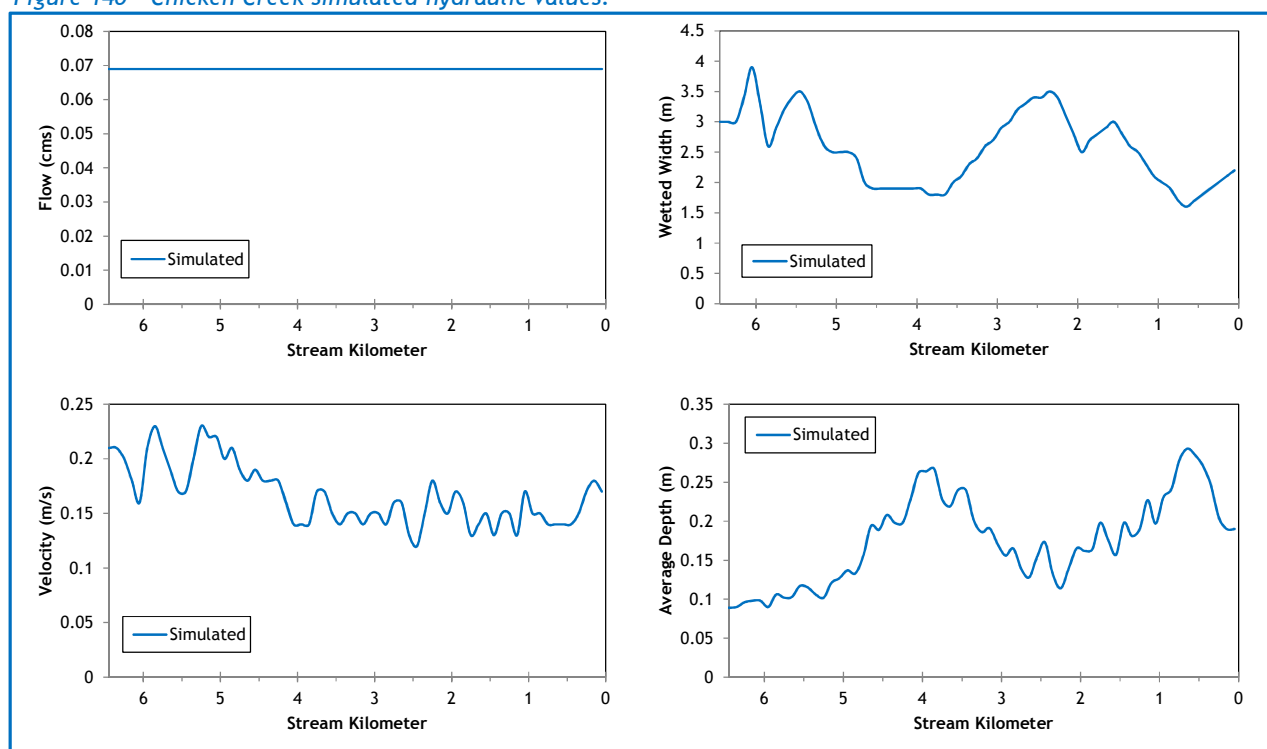
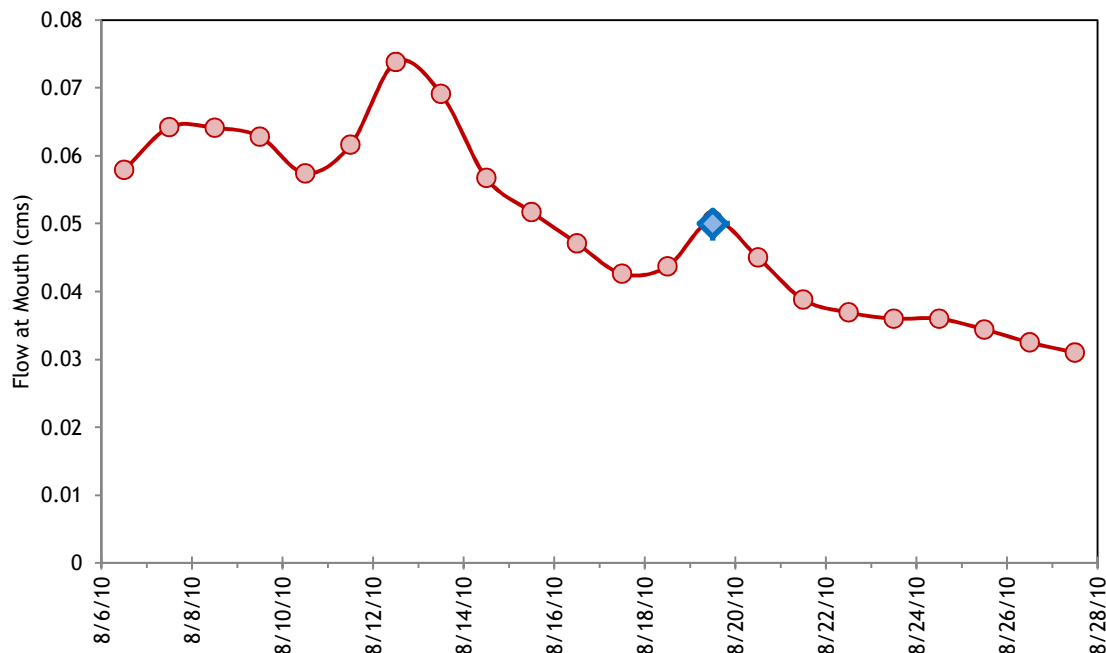


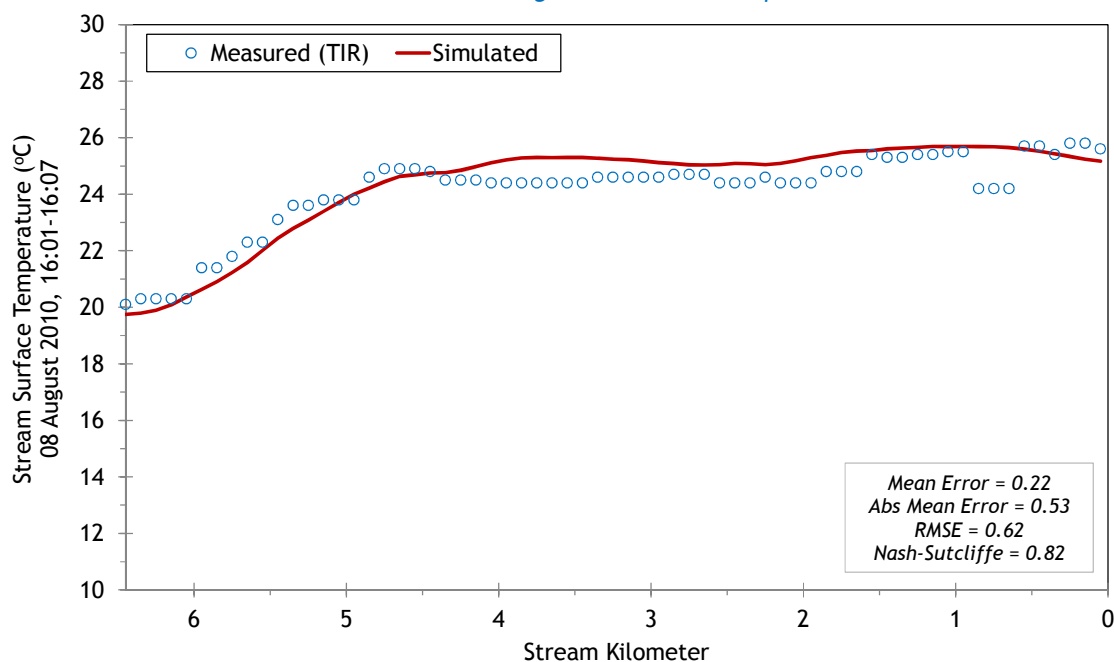
Figure 141 shows the simulated flows at the mouth of Chicken Creek. Since there were no tributaries or diversions, this is also the flow for the entire simulation length. The values were extrapolated through back-calculations from Sheep Creek. The measured flow on August 19, 2010 below the forks was 0.05 cms (1.8 cfs).

Figure 141 - Chicken Creek simulated flow volumes at the mouth.



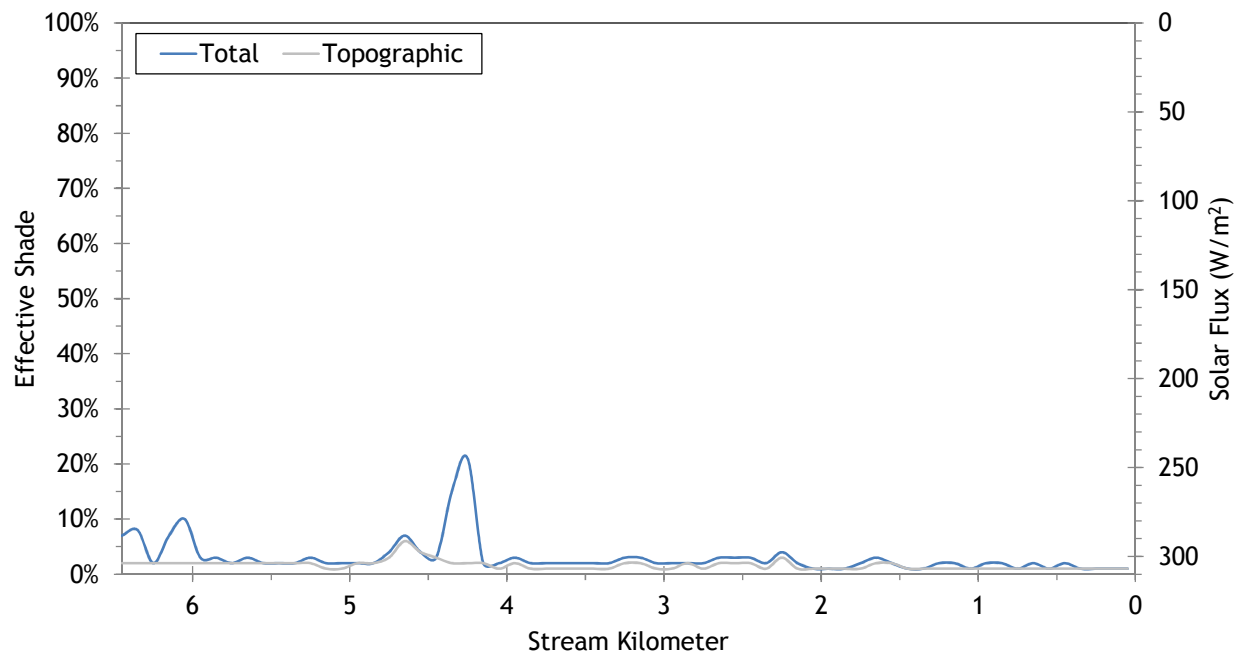
The simulated and measured longitudinal temperatures for Chicken Creek are presented in Figure 142. It appears that the stream heated more rapidly once it entered the open meadow, and then reached a maximum temperature of approximately 25°C.

Figure 142 - Chicken Creek simulated and measured longitudinal stream temperatures.



The lower 6.5 kilometers of Chicken Creek flow through mostly open meadow and hence there is very little effective shade (Figure 143).

Figure 143 - Chicken Creek simulated effective shade.



5.11 Sheep Creek

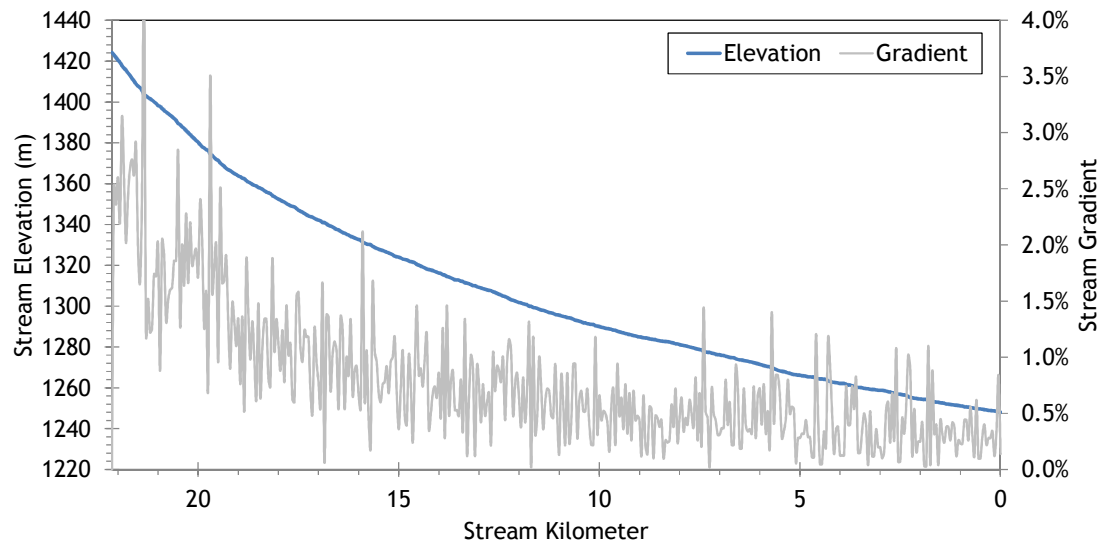


RGB-colored LiDAR point cloud - Sheep Creek downstream of East Sheep Creek (looking upstream).

5.11.1 Sheep Creek TTools Results

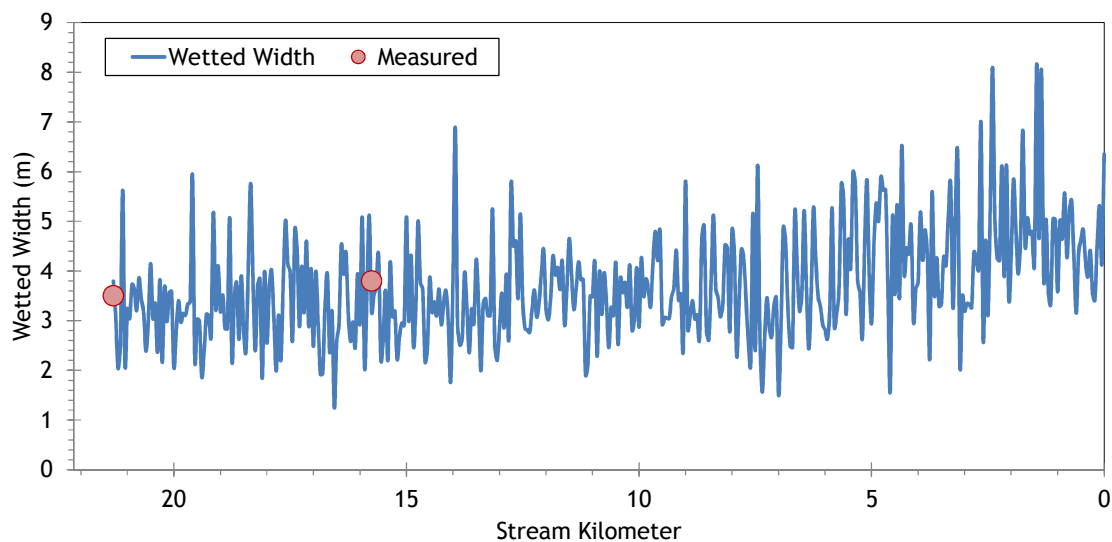
Sheep Creek elevations and gradients were sampled from the bare earth LiDAR data (Figure 144). The stream is steeper in the upper 7 kilometers, while the lower 15 kilometers meander more through a less confined valley.

Figure 144 - Sheep Creek elevation and gradient.



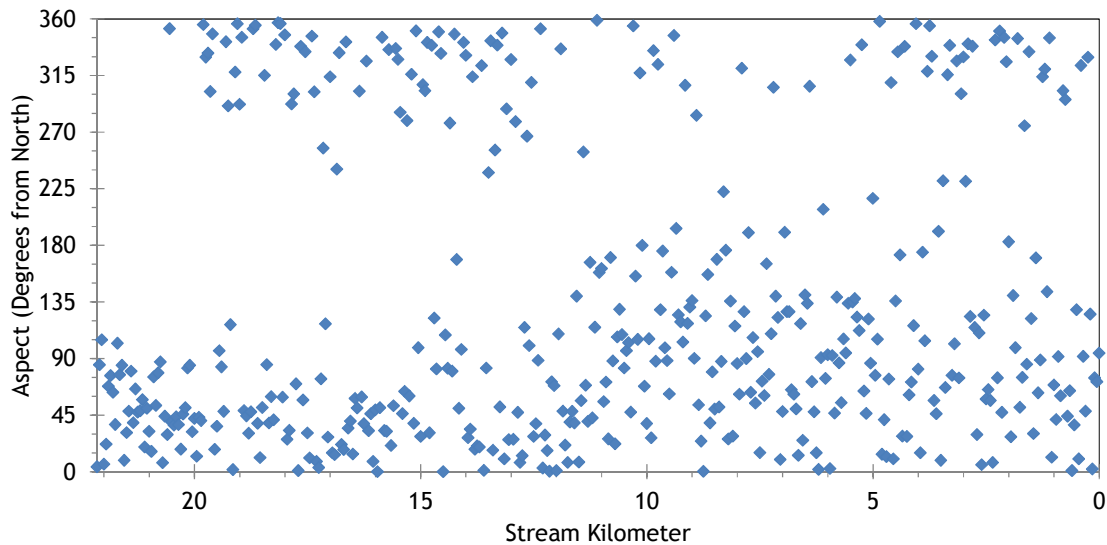
Sheep Creek wetted widths were digitized from the LiDAR intensity, TIR, and NAIP images. Figure 145 shows the sampled and measured values. Sheep Creek is a small stream, with wetted widths between about 3 and 5 meters on average during the simulation time period.

Figure 145 - Sheep Creek wetted widths.



The stream aspect for every 50 meters of Sheep Creek is presented in Figure 146. The stream is oriented northeasterly.

Figure 146 - Sheep Creek stream aspect.



Topographic shade angles for Sheep Creek are shown in Figure 147. There is a moderate amount of topographic shade produced by surrounding mountains.

Figure 147 - Sheep Creek topographic shade angles.

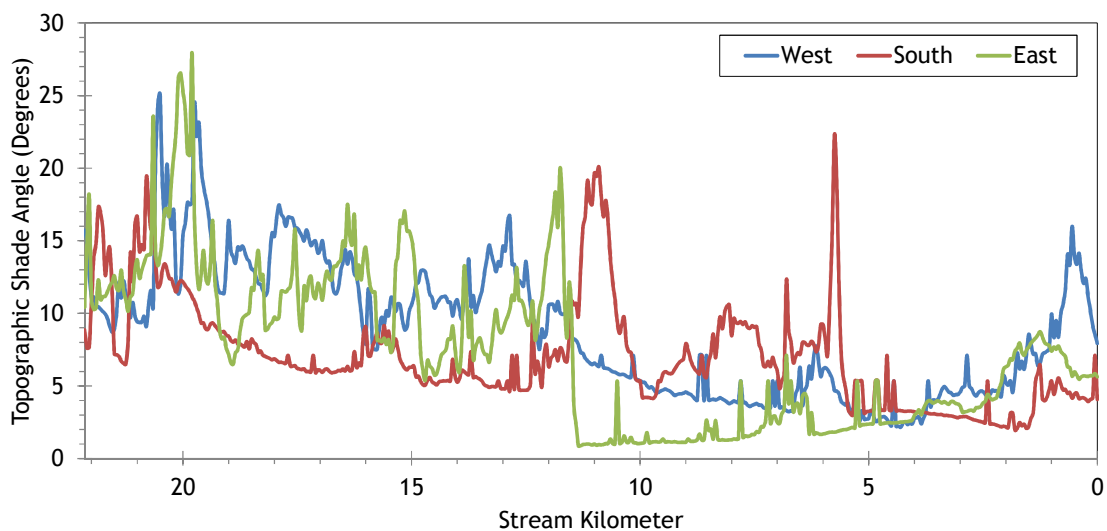
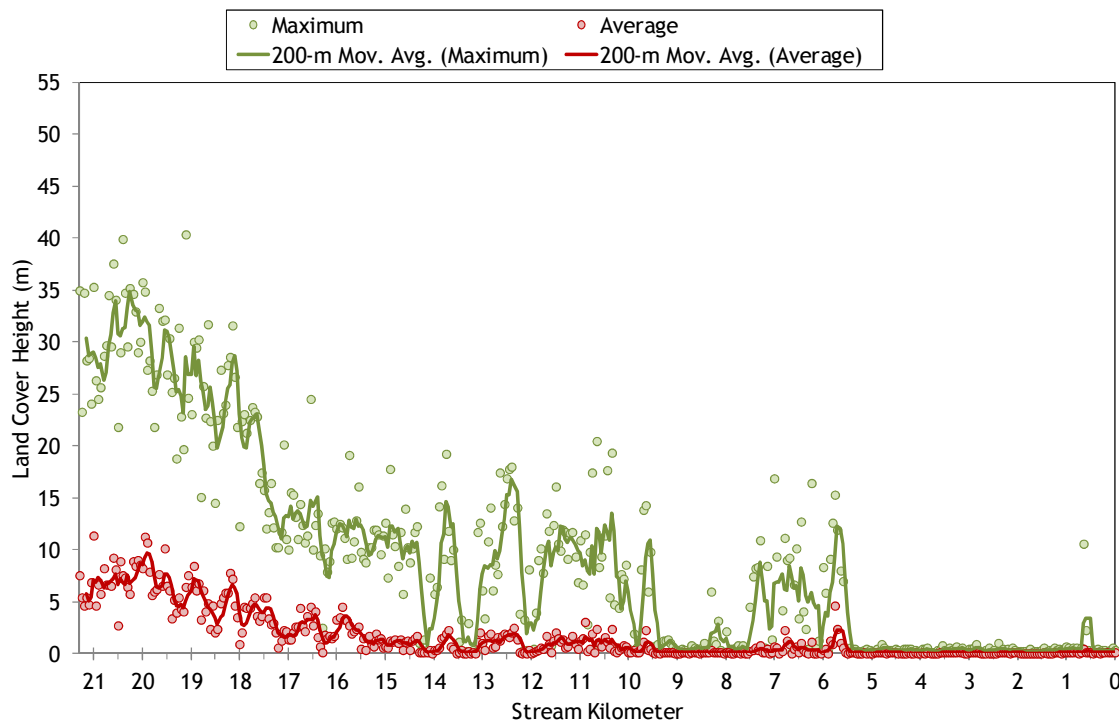


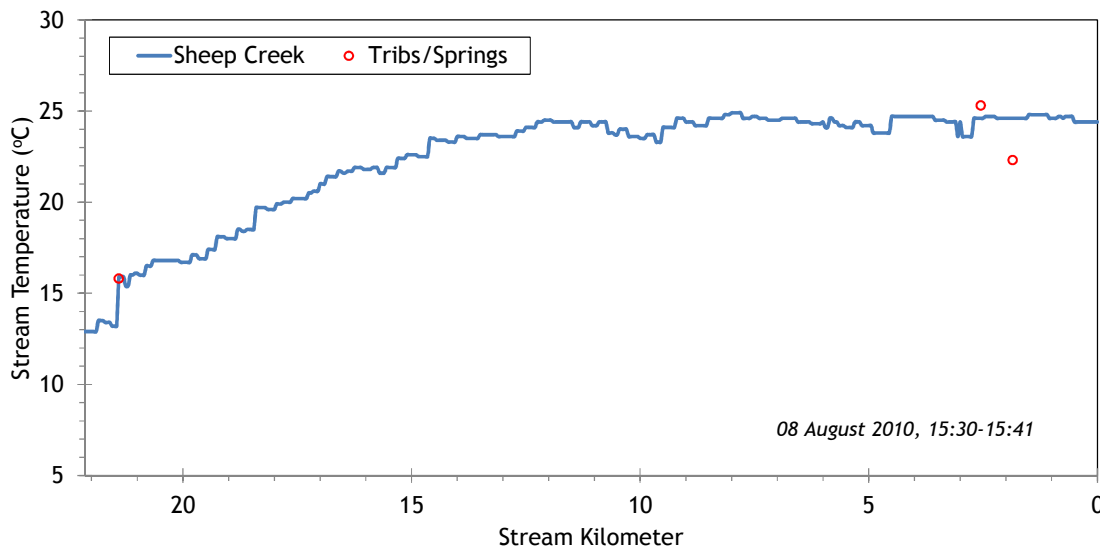
Figure 148 shows the land cover heights sampled along Sheep Creek. The maximum and average of the 28 radial samples were calculated for each 50-meter stream node. (Note: Heat Source uses each of the 28 radial samples for each 50-meter node. The maximum and average are shown here for simplification purposes.)

Figure 148 - Sheep Creek land cover heights sampled from highest hit LiDAR.



The TIR stream temperature profile of Sheep Creek is presented in Figure 149. The stream gained about 10°C between kilometers 20 and 14, and then remained around 25°C until the mouth during the TIR flight.

Figure 149 - Sheep Creek TIR stream temperature profile.



5.11.2 Sheep Creek Heat Source Calibration Results

Sheep Creek stream temperatures were simulated from East Sheep Creek to the mouth (Figure 150).

Figure 150 - Sheep Creek simulation extent.

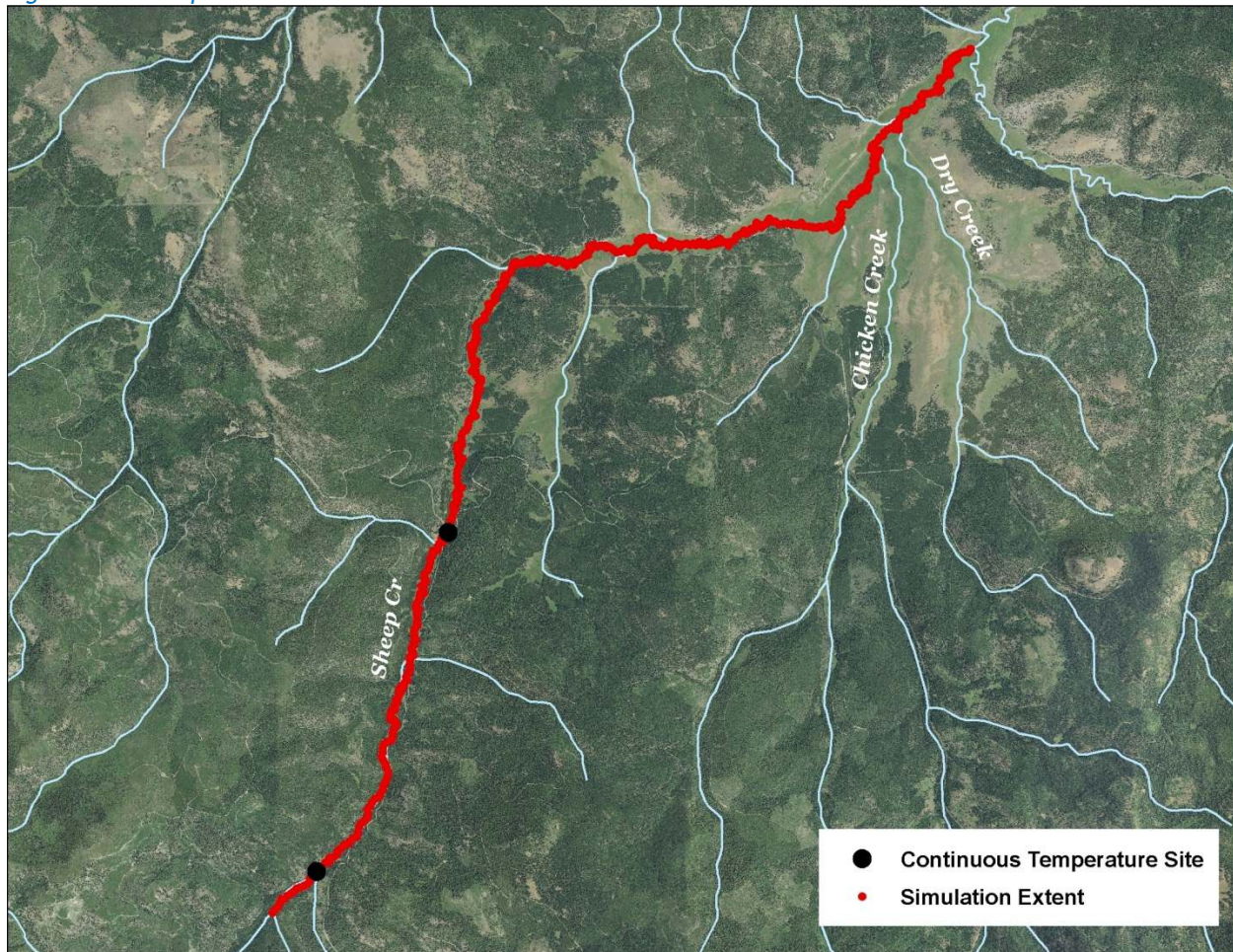


Table 23 - Sheep Creek general Heat Source parameters.

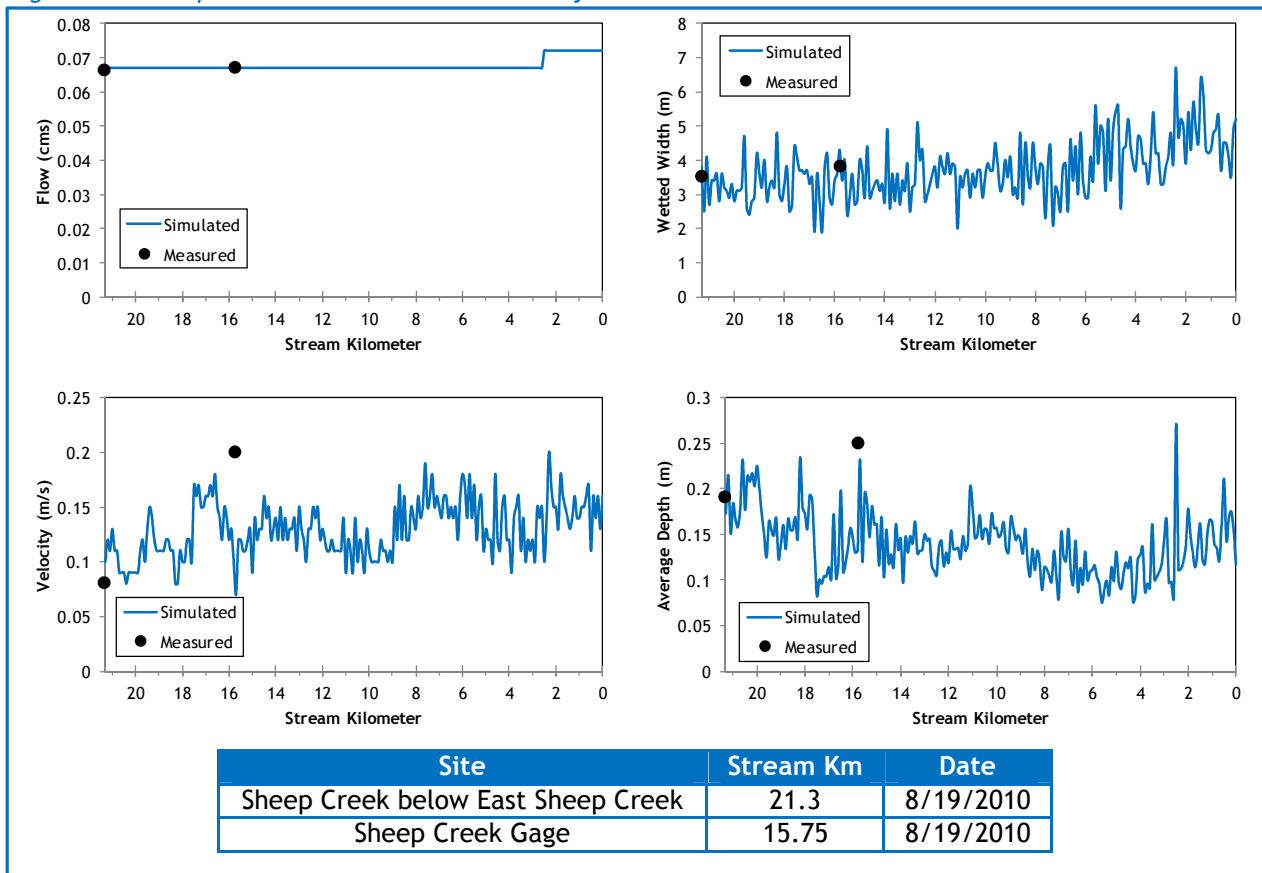
Stream:	Sheep Creek
Length:	21.3 kilometers
Time Period:	August 6-27, 2010
Input Distance Step:	50 meters
Output Distance Step:	100 meters
Time Step:	1 minute
Flush Initial Condition:	7 days
TIR Date and Time:	August 8, 2010 15:29-15:40
Land Cover Data Source:	LiDAR
Land Cover Sampling Distance Step:	15 meters

The following assumptions were used when calibrating the Sheep Creek Heat Source model:

- Hourly climate data was obtained from the J Ridge RAWS (USFS) site. Air temperature was adjusted using the adiabatic lapse rate of 1°C per 100 meters elevation.
- Daily flow variability was extrapolated from Grande Ronde River gage data.

Figure 151 shows the simulated and measured hydraulic values for the calibrated Sheep Creek model. There were only two available ground level data points, one of which was at the upstream boundary of the model. The data were plotted for August 19, 2010 when the ground level measurements were taken.

Figure 151 - Sheep Creek simulated and measured hydraulic values.



The simulated daily flow volumes for the mouth of Sheep Creek are shown in Figure 152. Daily values were extrapolated based on gage data from the Grande Ronde River. No field measurements were recorded at the mouth of Sheep Creek; however measurements were taken in the upper reaches.

Figure 152 - Sheep Creek simulated flow volumes at the mouth.

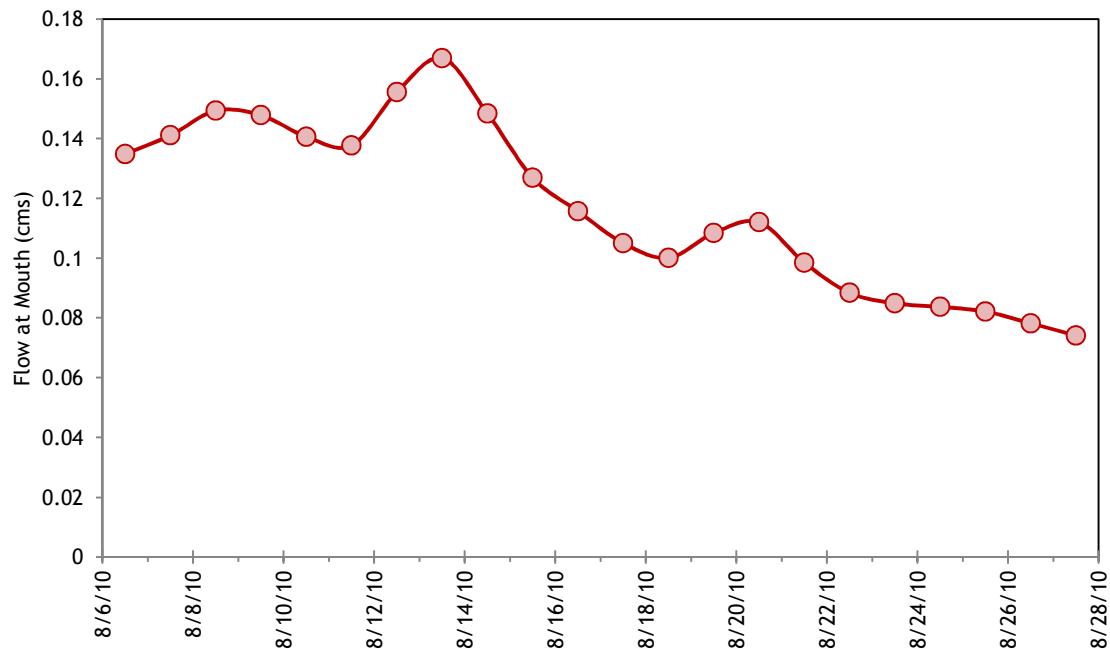


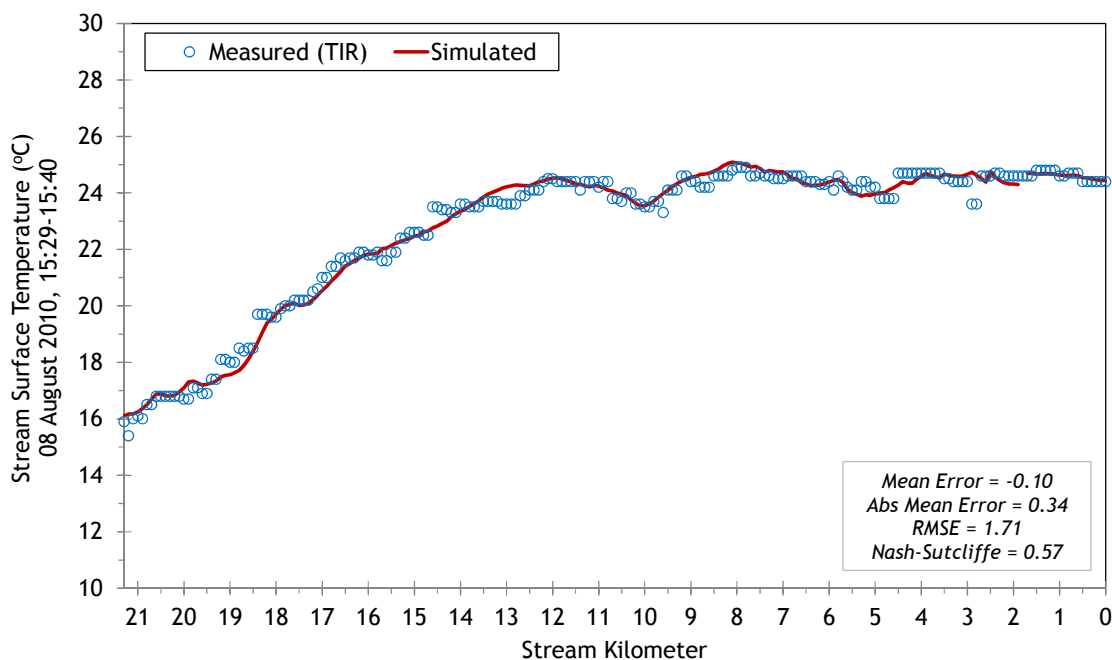
Table 24 summarizes the mass inflow input for the Sheep Creek model. There was only one significant tributary observed in the TIR data, which was Chicken Creek. There were no measured data available for Chicken Creek at the mouth, so the simulation outputs from the Chicken Creek model were used as inputs to the Sheep Creek model.

Table 24 - Chicken Creek mass inflow feature and assumption.

Feature	Stream Km	Assumptions
Chicken Creek	2.5	Used simulation outputs from Chicken Creek model as inputs to Sheep Creek model.

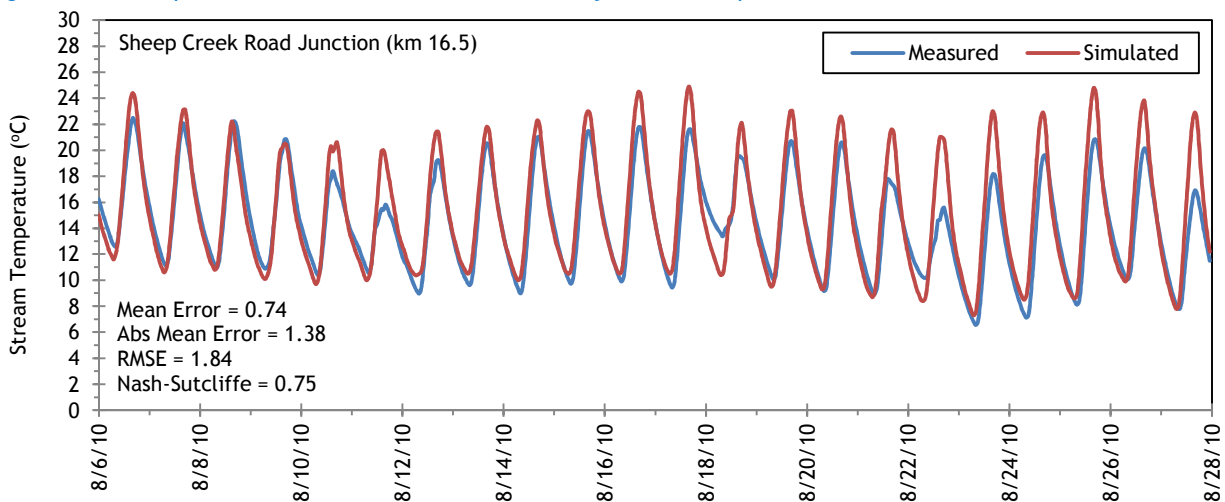
The simulated and measured longitudinal stream temperatures are shown in Figure 144. Validation statistics are also included within the plot.

Figure 153 - Sheep Creek simulated and measured longitudinal stream temperatures.



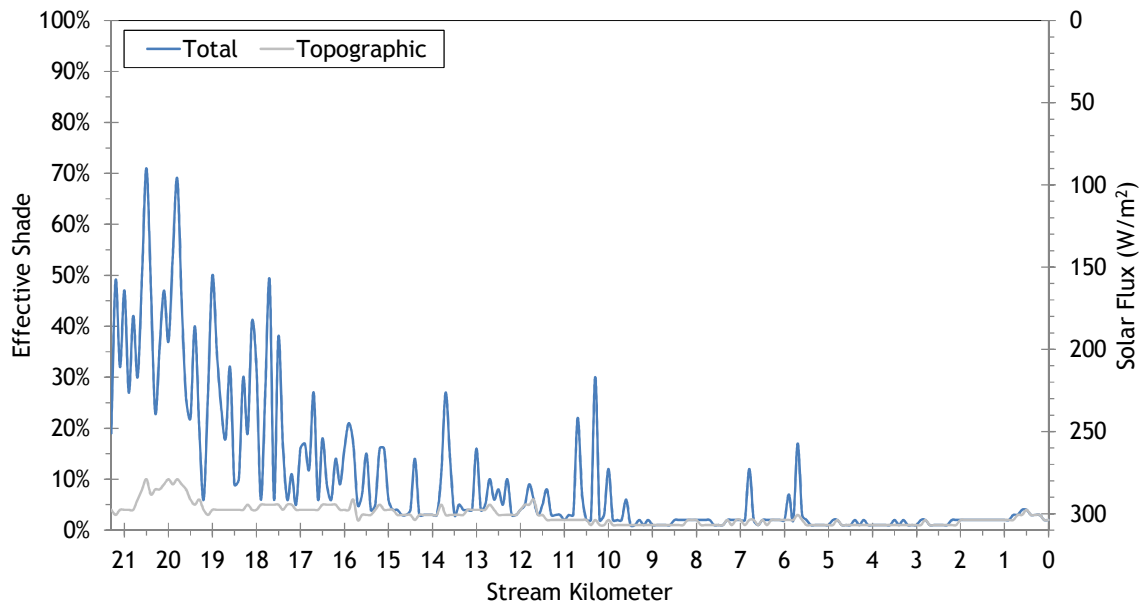
There was one site where measured hourly temperature data was available (stream kilometer 16.5). Figure 154 compares the measured and simulated hourly temperatures at that site. Validation statistics are also included in the figure.

Figure 154 - Sheep Creek simulated and measured hourly stream temperatures.



Simulated effective shade values are shown in Figure 155. Sheep Creek flows from more forested areas into wide open valley bottom meadows, so effective shade decreases in the lower reaches where there are very few trees.

Figure 155 - Sheep Creek simulated effective shade.



5.12 Fly Creek

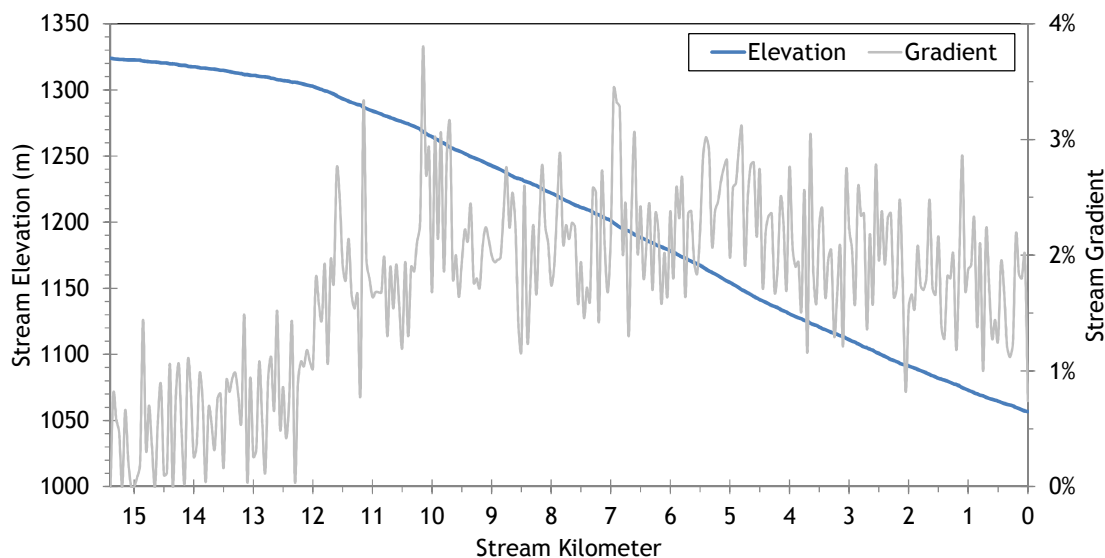


RGB-colored LiDAR point cloud - Fly Creek just above mouth (looking upstream).

5.12.1 Fly Creek TTools Results

Fly Creek elevations and gradients are shown in Figure 156. The upper 4 kilometers flow through a low-gradient meadow. The gradients are higher in the lower 12 kilometers where the stream enters steeper and more confined valley terrain.

Figure 156 - Fly Creek elevation and gradient.



The wetted widths for Fly Creek were digitized from the LiDAR intensity, TIR, and NAIP imagery. Figure 157 shows the sampled and measured wetted widths. Overall, Fly Creek is a small stream with widths between about 3 and 5 meters.

Figure 157 - Fly Creek wetted widths.

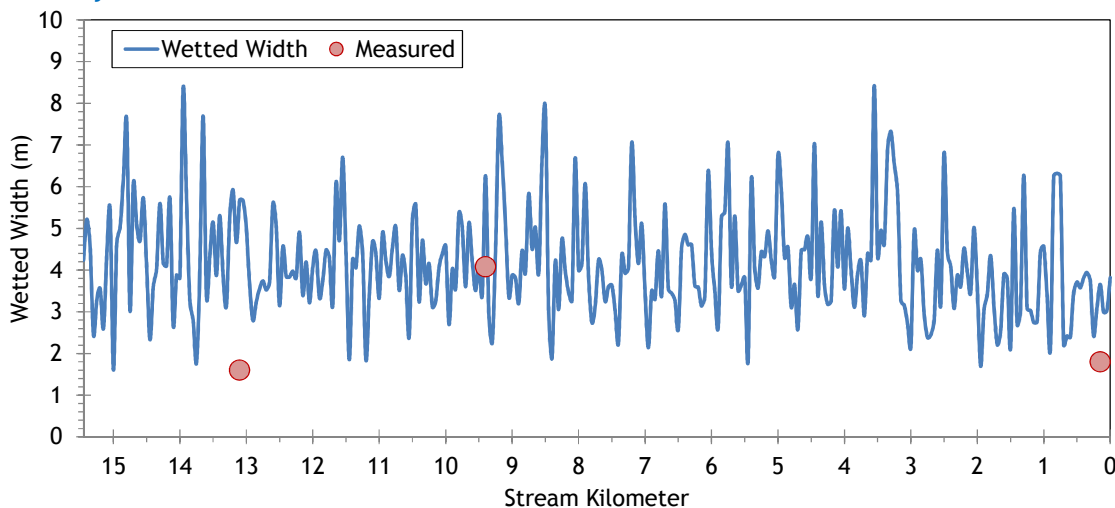
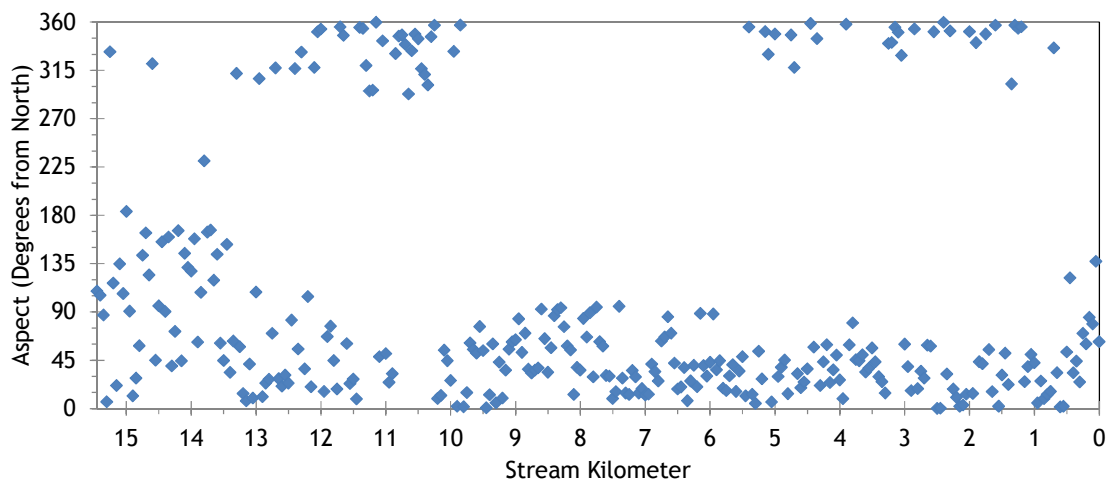


Figure 158 shows the stream aspect for every 50 meters of Fly Creek. The stream generally flows toward the northeast.

Figure 158 - Fly Creek stream aspect.



Fly Creek topographic shade angles are shown in Figure 159. The values for Fly Creek are relatively large, reaching up to 30 degrees in many locations.

Figure 159 - Fly Creek topographic shade angles.

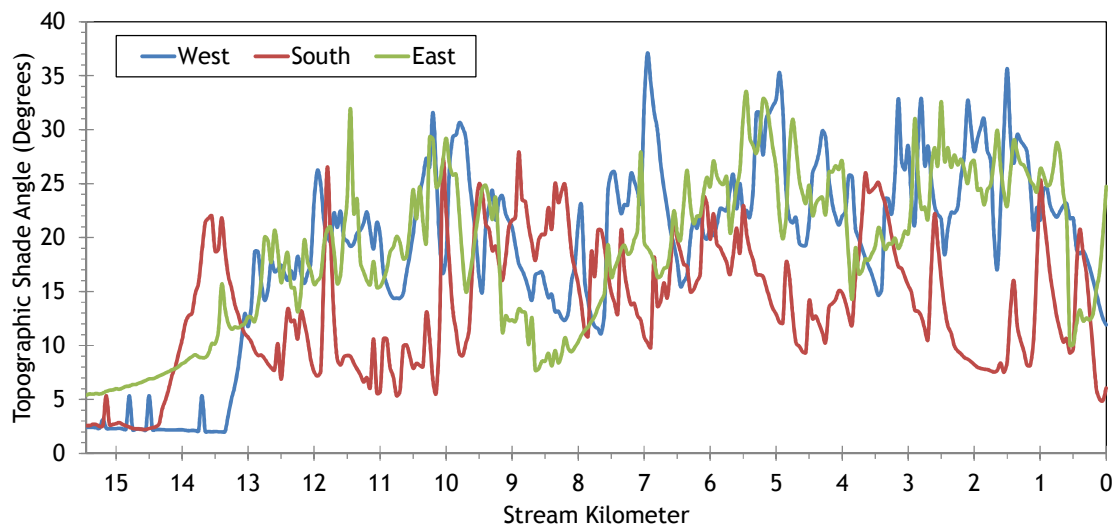
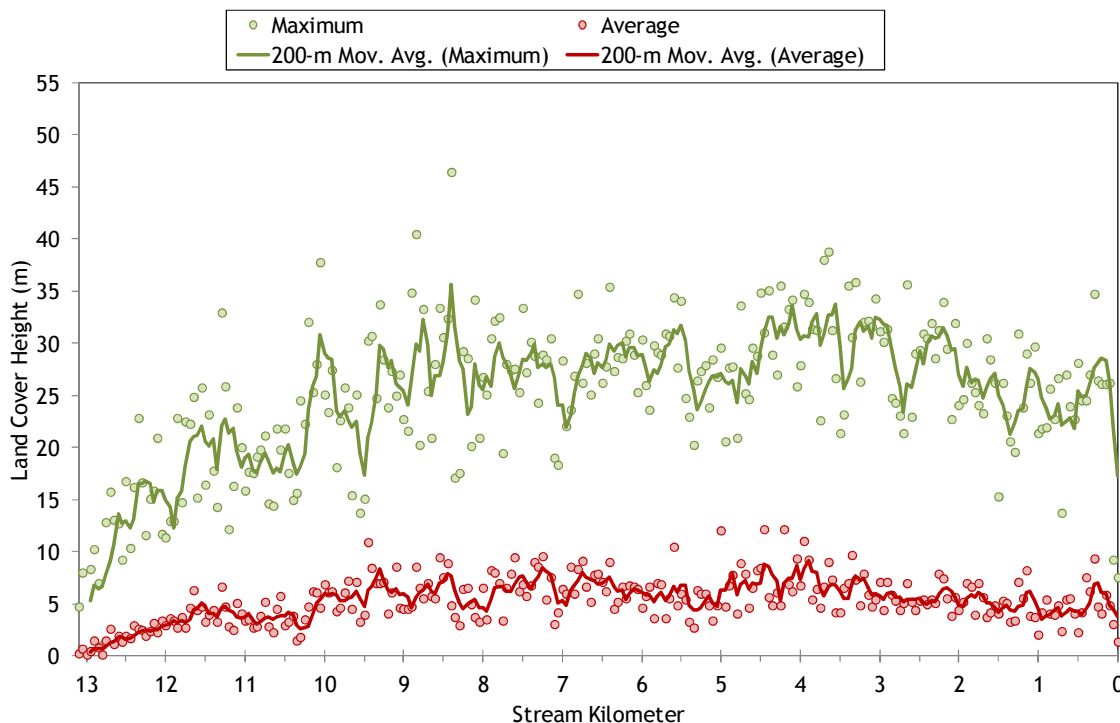


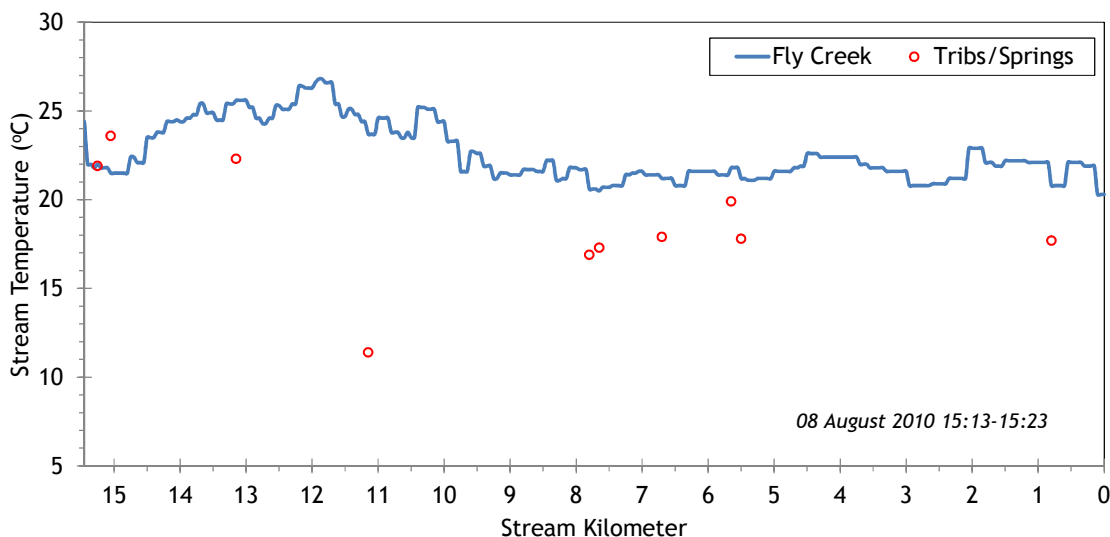
Figure 160 shows the land cover heights sampled along Fly Creek. The maximum and average of the 28 radial samples were calculated for each 50-meter stream node. (Note: Heat Source uses each of the 28 radial samples for each 50-meter node. The maximum and average are shown here for simplification purposes.)

Figure 160 - Fly Creek land cover heights sampled from highest hit LiDAR.



The TIR stream temperature profile of Fly Creek is shown in Figure 161. Interestingly, the stream temperature drops slightly in the downstream direction. The upper reaches are lower gradient open meadow, so the temperatures become quite warm. Then the stream enters a steeper and more confined valley, where some of that heat is lost from the stream.

Figure 161 - Fly Creek TIR stream temperature profile.



5.12.2 Fly Creek Heat Source Calibration Results

Fly Creek was simulated from below Little Fly Creek to the mouth (Figure 162). The total simulation length was 13.1 kilometers.

Figure 162 - Fly Creek simulation extent.

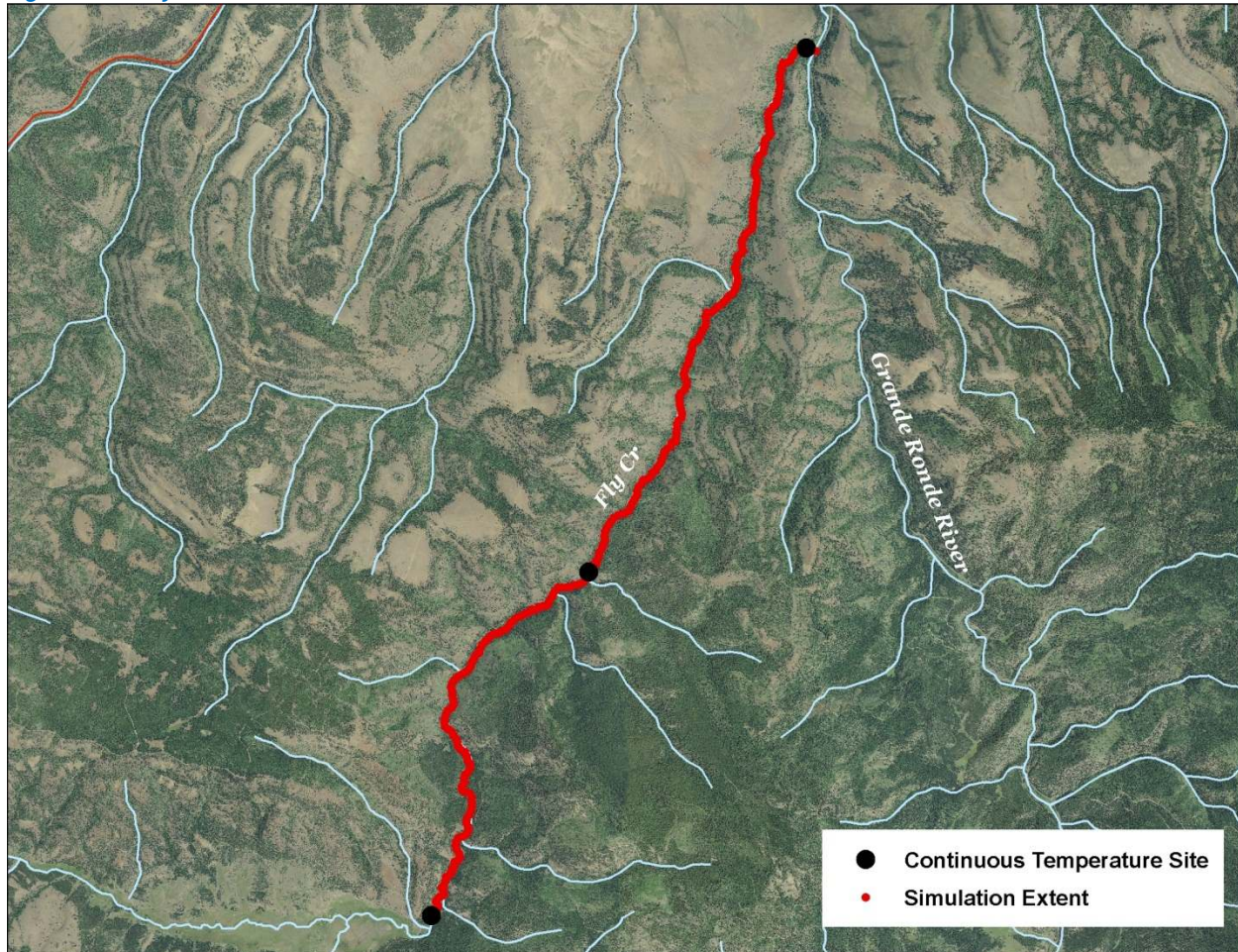


Table 25 - Fly Creek general Heat Source parameters.

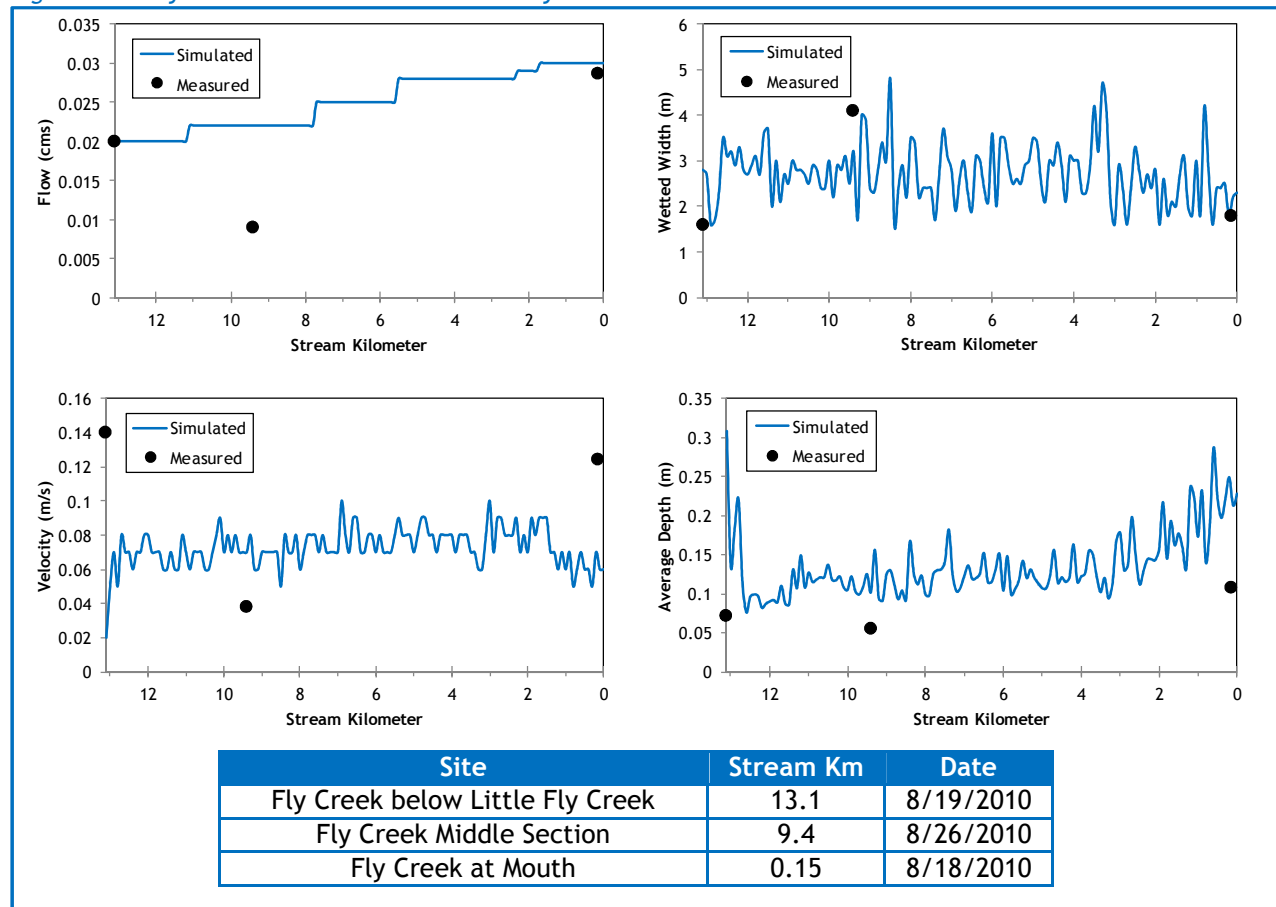
Stream:	Fly Creek
Length:	13.1 kilometers
Time Period:	August 6-27, 2010
Input Distance Step:	50 meters
Output Distance Step:	100 meters
Time Step:	1 minute
Flush Initial Condition:	7 days
TIR Date and Time:	August 8, 2010 15:12-15:21
Land Cover Data Source:	LiDAR
Land Cover Sampling Distance Step:	15 meters

The following assumptions were used when calibrating the Fly Creek Heat Source model:

- Hourly climate data was obtained from the J Ridge RAWS (USFS) site. Air temperature was adjusted using the adiabatic lapse rate of 1°C per 100 meters elevation.
- Daily flow variability was extrapolated from Grande Ronde River gage data.
- The wetted widths were reduced 33-50% from the raw TTools values in order to match the ground level measurements and calibrate the hydraulics.

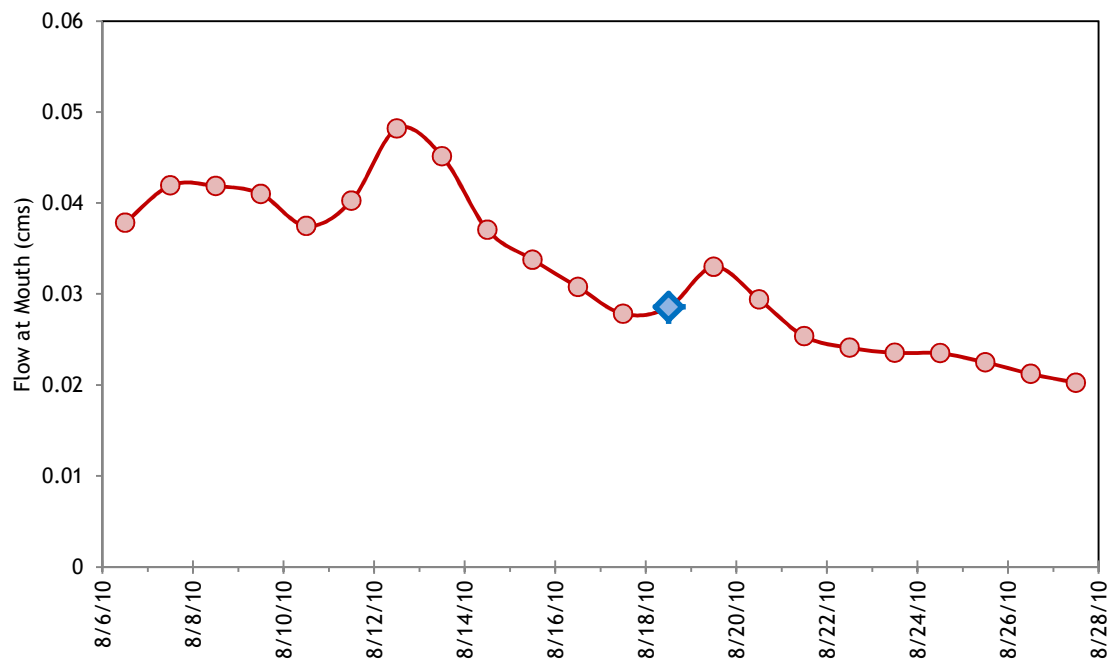
Fly Creek's simulated and measured hydraulic values are shown in Figure 163. The simulated values are from August 18th, while the measured values' dates vary. There were three ground level measurement sites. The measurements at kilometer 9.4 were taken on August 26 and do not match the simulated values for August 18 as well.

Figure 163 - Fly Creek simulated and measured hydraulic values.



The simulated daily flows at the mouth of Fly Creek are shown in Figure 164. The daily values were extrapolated from gage data on the Grande Ronde River.

Figure 164 - Fly Creek simulated flow volumes at the mouth.



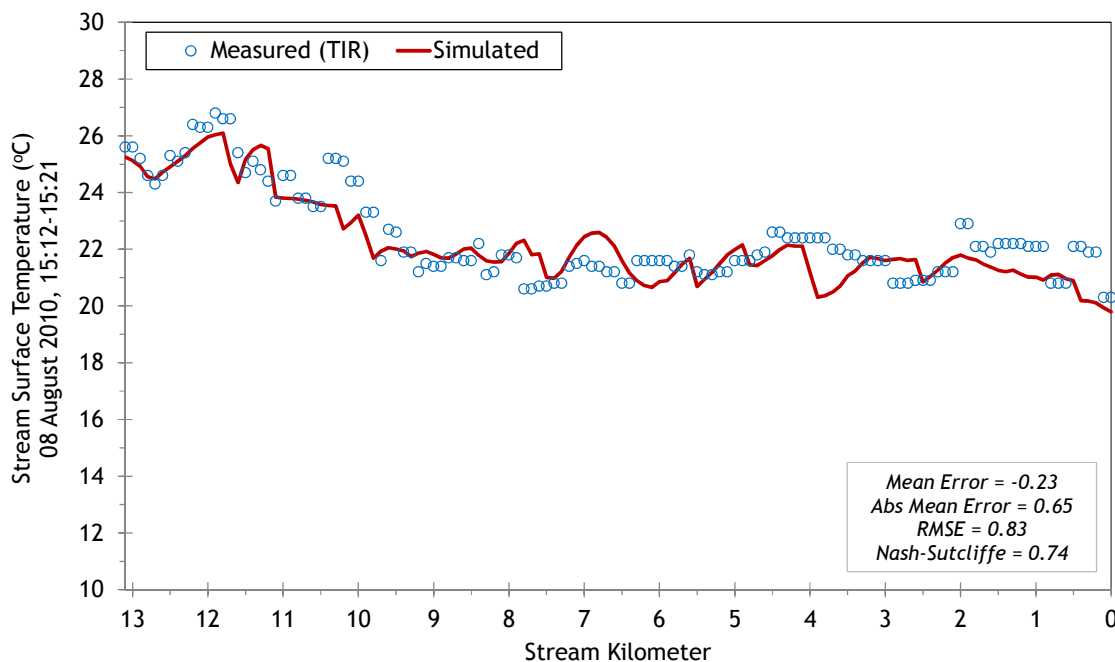
There were 2 springs and one tributary included within the Fly Creek model (Table 26). Their flow volumes were varied daily in order to mimic the variation assumed for the flows at the mouth of Fly Creek. Their temperatures were held at a constant value because of their insignificant volumes.

Table 26 - Fly Creek mass inflows and assumptions.

Feature	Stream Km	Assumptions
Spring	11.1	0.002-0.005 cms at constant 11.4°C
Spring	7.7	0.002-0.005 cms at constant 16.9°C
Unnamed Tributary	5.5	0.002-0.005 cms at constant 17.8°C

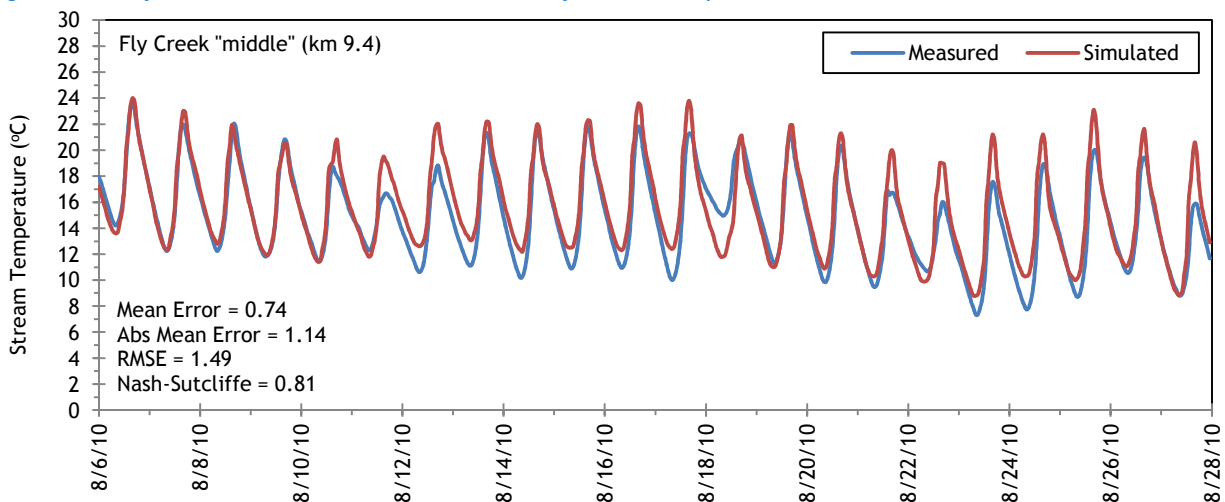
Figure 165 shows the simulated and measured longitudinal stream temperatures for Fly Creek. As previously mentioned, Fly Creek temperatures decline in the downstream direction because the stream is flowing from lower gradient meadows at the upper end into a more confined and steeper valley.

Figure 165 - Fly Creek simulated and measured longitudinal stream temperatures.



The simulated and measured hourly stream temperatures are presented in Figure 166.

Figure 166 - Fly Creek simulated and measured hourly stream temperatures.



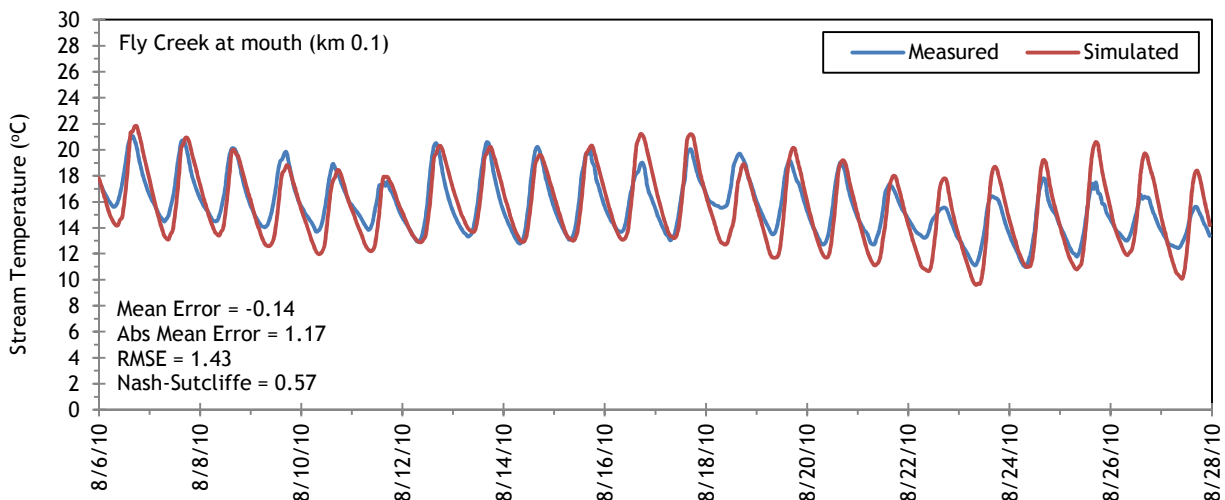
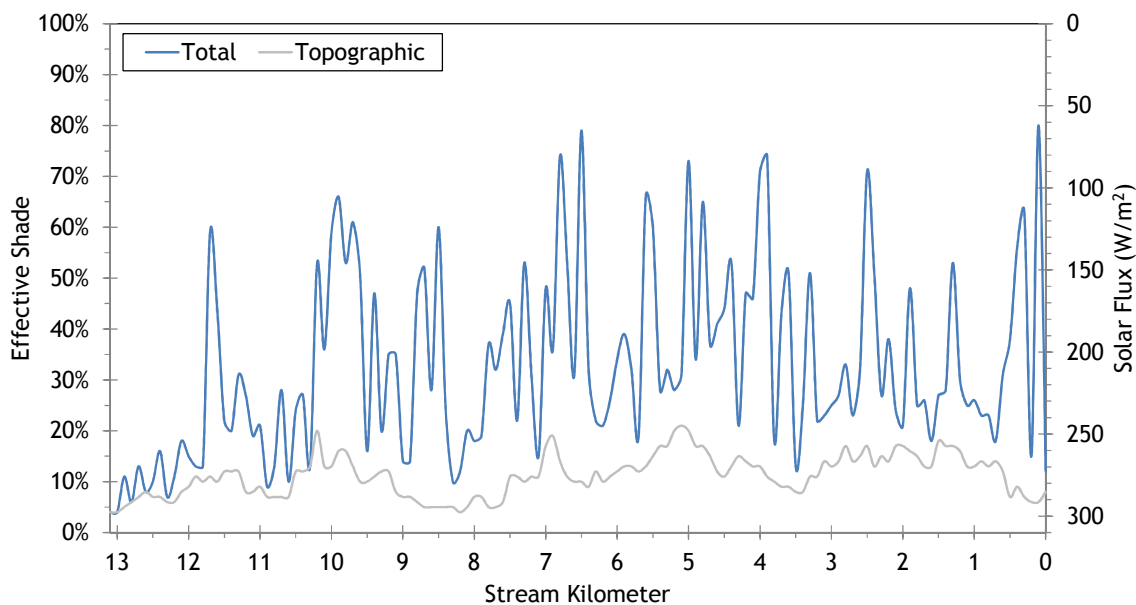


Figure 167 shows the simulated effective shade for Fly Creek. The upper few kilometers have less shade because the stream is flowing through a mixed meadow-forest complex. The lower 10 stream kilometers have more topographic shade and more total effective shade produced by the surrounding forest.

Figure 167 - Fly Creek simulated effective shade.



5.13 McCoy Creek

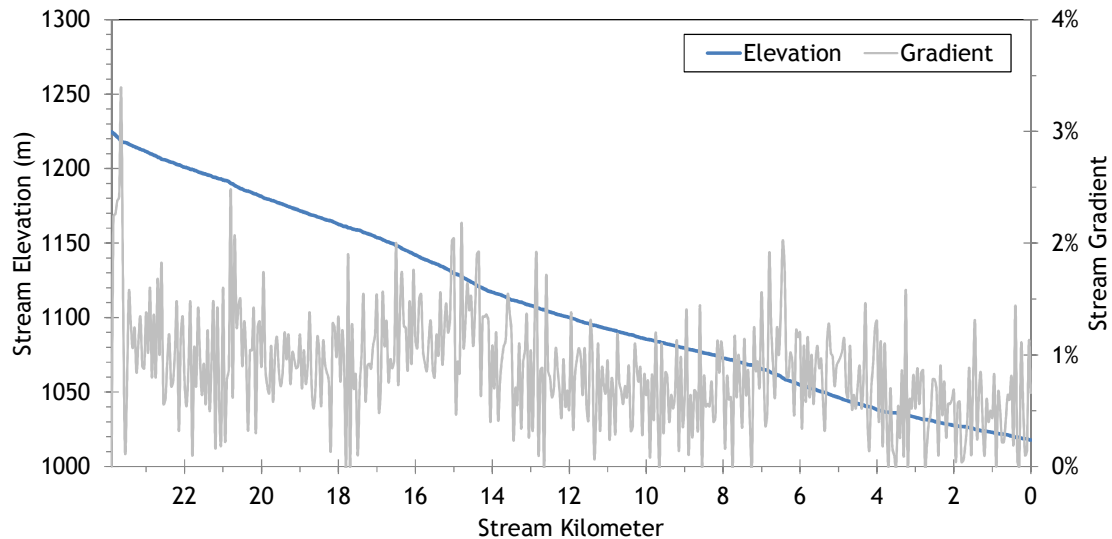


RGB-colored LiDAR point cloud - McCoy Creek just above mouth - the once channelized stream has been restored to its original channel.

5.13.1 McCoy Creek TTools Results

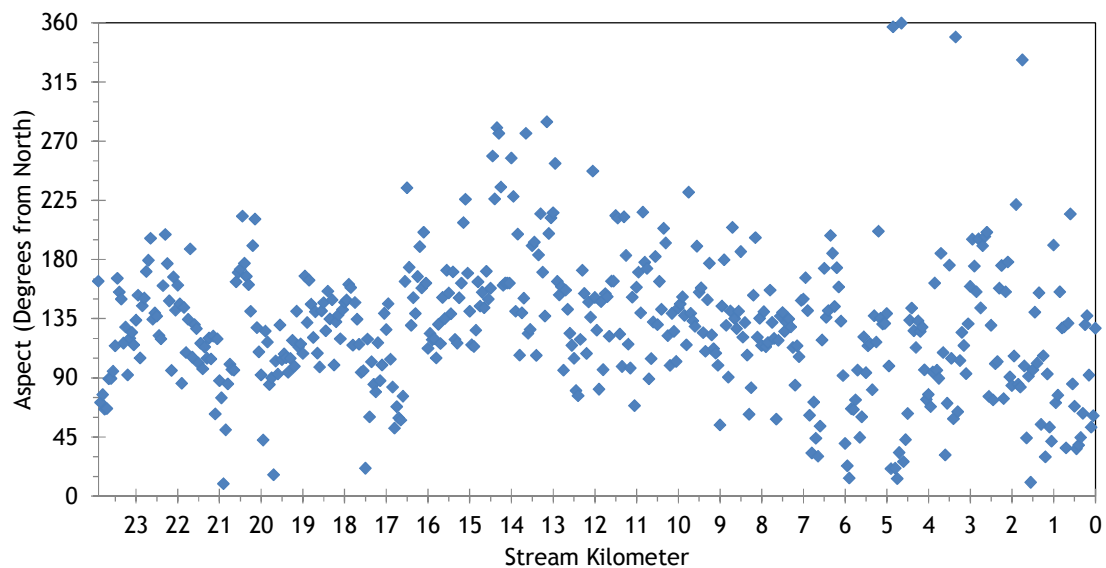
McCoy Creek elevations and gradients were sampled from the bare earth LiDAR data (Figure 168). The stream has a moderately low gradient due to the gradual elevation drop and meandering nature.

Figure 168 - McCoy Creek elevation and gradient.



McCoy Creek flows generally toward the southeast (Figure 169).

Figure 169 - McCoy Creek stream aspect.



Topographic shade is variable along McCoy Creek (Figure 170). As the stream enters more confined valleys, the topographic shade angles increase. In the lower 3.5 kilometers, the stream flows through a wide flat valley and has less topographic shade.

Figure 170 - McCoy Creek topographic shade angles.

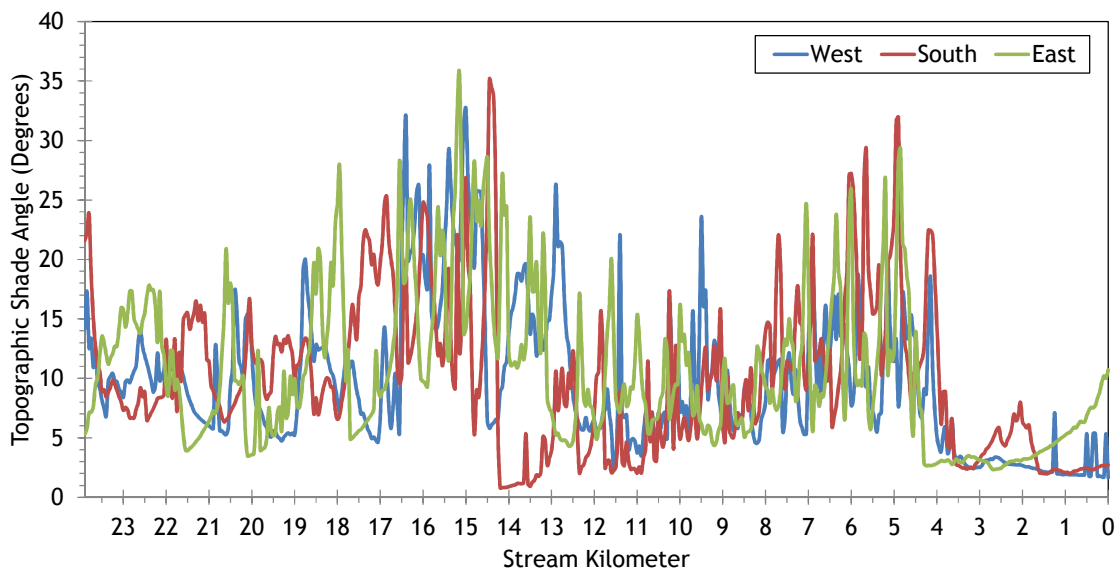


Figure 171 shows the land cover heights sampled along McCoy Creek. The maximum and average of the 28 radial samples were calculated for each 50-meter stream node. (Note: Heat Source uses each of the 28 radial samples for each 50-meter node. The maximum and average are shown here for simplification purposes.)

Figure 171 - McCoy Creek land cover heights sampled from highest hit LiDAR.

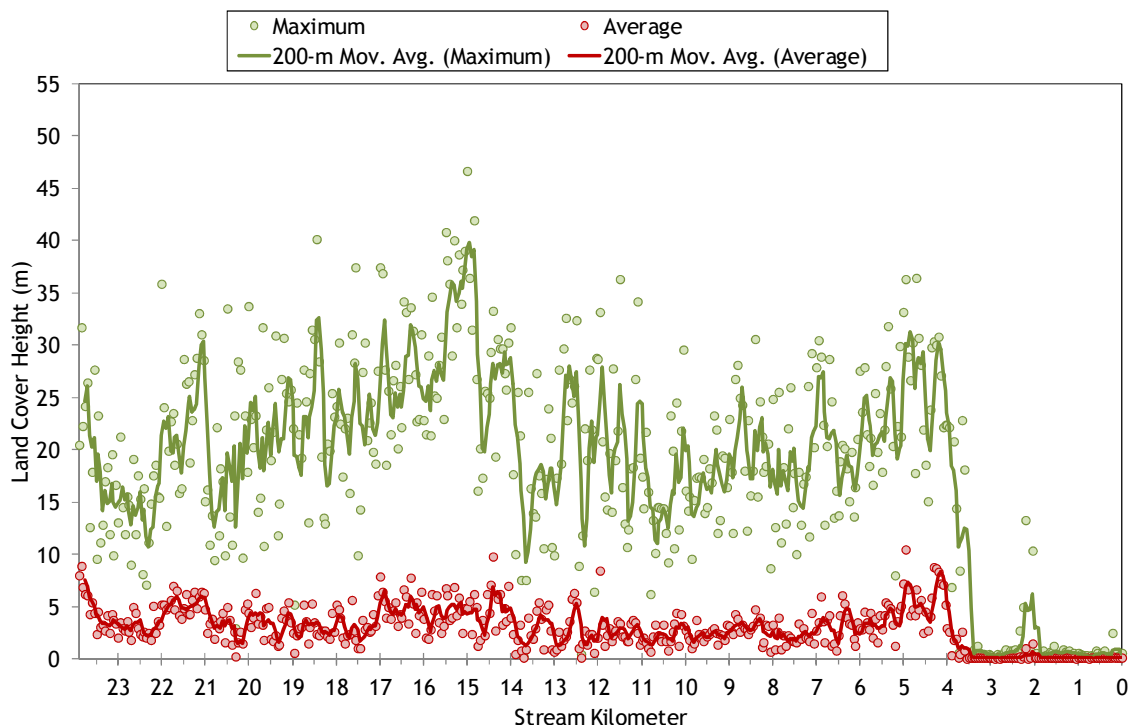
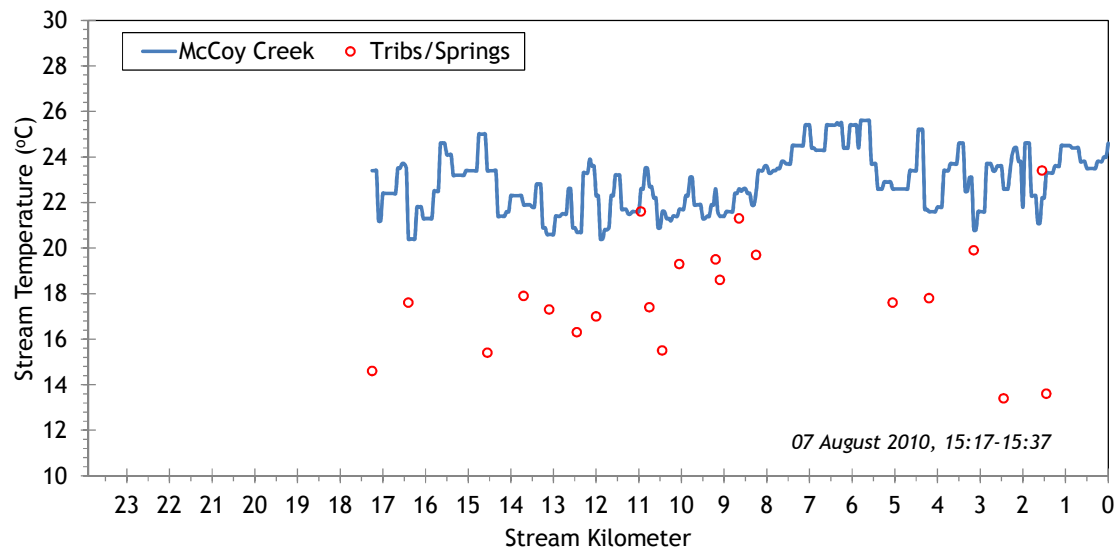


Figure 172 shows the TIR stream temperature profile of McCoy Creek. It is a fairly small stream with low summertime flows; therefore temperatures are fairly high and variable. The small flows (less than 1 cfs) are the main factor contributing to the highly variable stream temperatures.

Figure 172 - McCoy Creek TIR stream temperature profile.



5.13.2 McCoy Creek Heat Source Calibration Results

McCoy Creek effective shade was simulated for the lower 23.9 stream kilometers. The flow was too low in August 2010 to simulate temperature.

Figure 173 - McCoy Creek simulation extent.

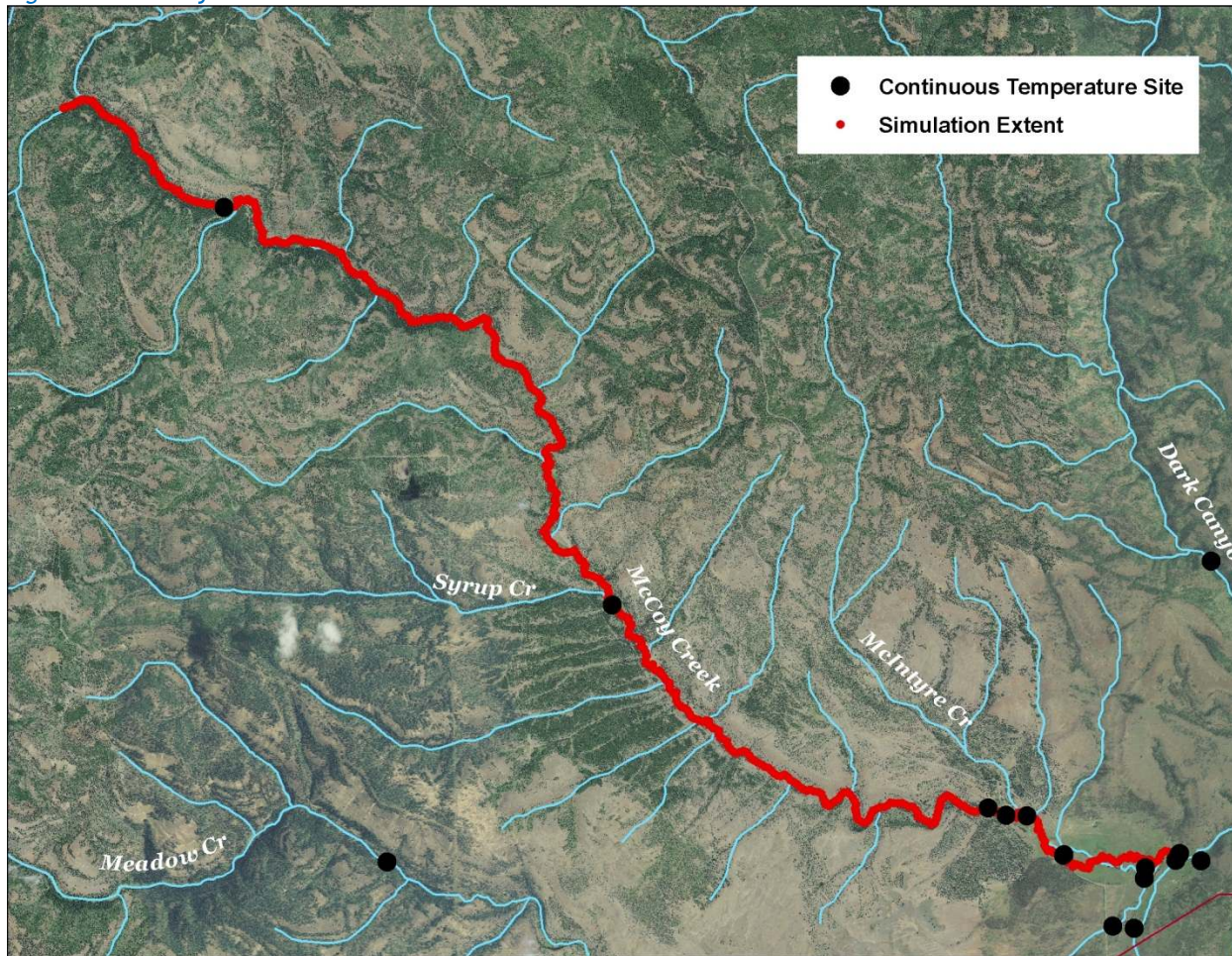


Table 27 - McCoy Creek general Heat Source parameters.

Stream:	McCoy Creek
Length:	23.9 kilometers
Time Period:	August 6-27, 2010
Input Distance Step:	50 meters
Output Distance Step:	100 meters
Time Step:	1 minute
Flush Initial Condition:	NA
TIR Date and Time:	NA
Land Cover Data Source:	LiDAR
Land Cover Sampling Distance Step:	15 meters

Figure 174 shows the simulated effective shade values for McCoy Creek. There is moderate effective shade along most of the stream, and much of the total effective shade is often created by topographic features. The lower 4 kilometers are where the stream flows in open meadow and through the restoration area.

Figure 174 - McCoy Creek simulated effective shade.

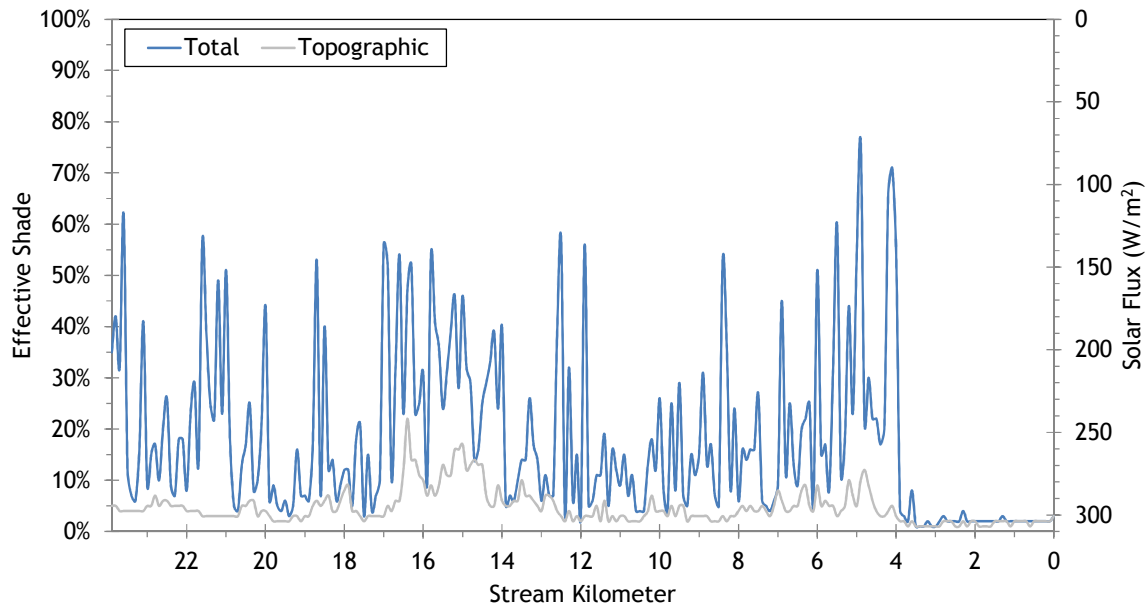
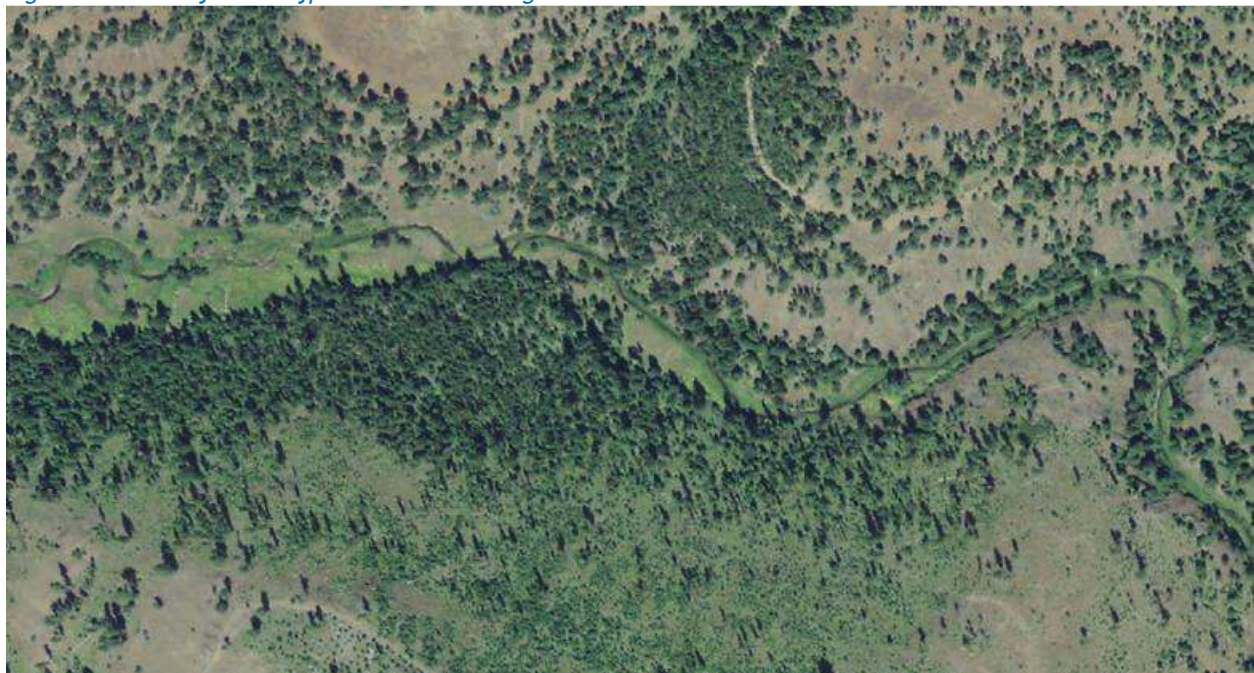
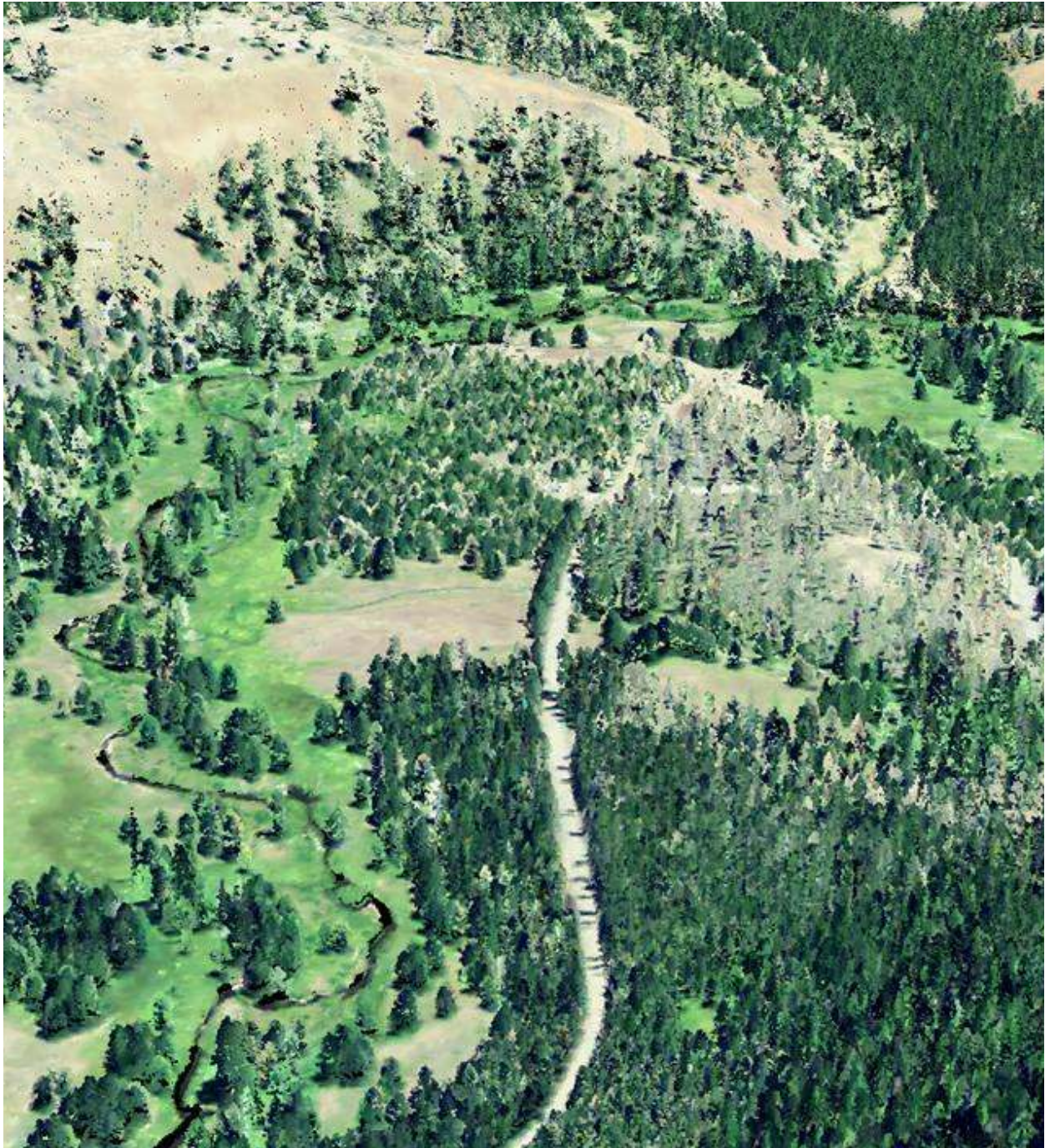


Figure 175 shows the typical terrain and vegetation along McCoy Creek. The stream often has a wide flat floodplain and intermittently is flanked by large trees. The image gives a better understanding of why effective shade is relatively low compared to other streams in the basin.

Figure 175 - McCoy Creek typical terrain and vegetation.



5.14 Meadow Creek

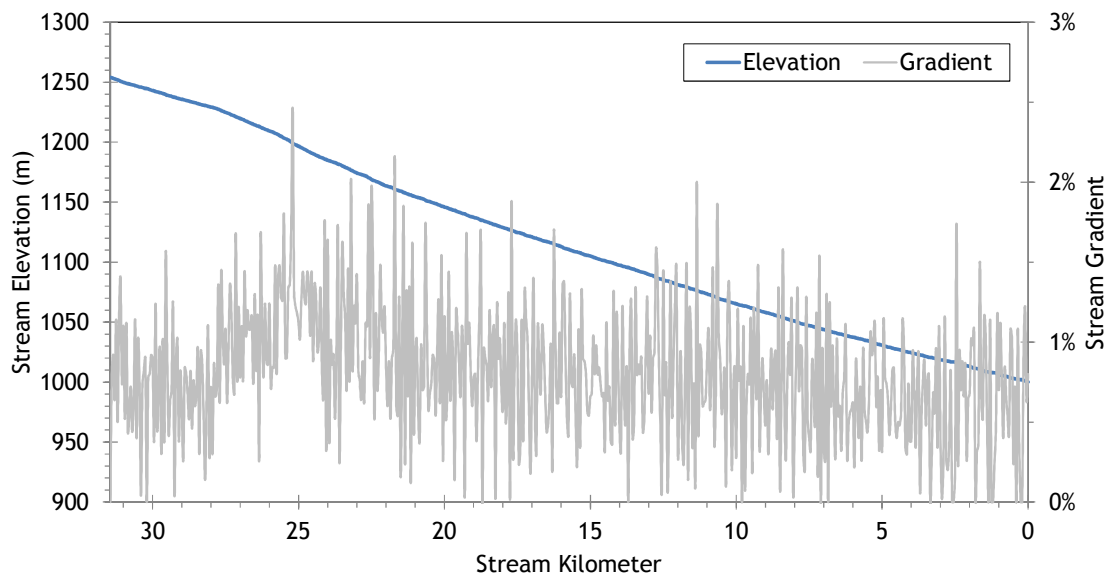


RGB-colored LiDAR point cloud - Meadow Creek looking downstream near Smith Creek.

5.14.1 Meadow Creek TTools Results

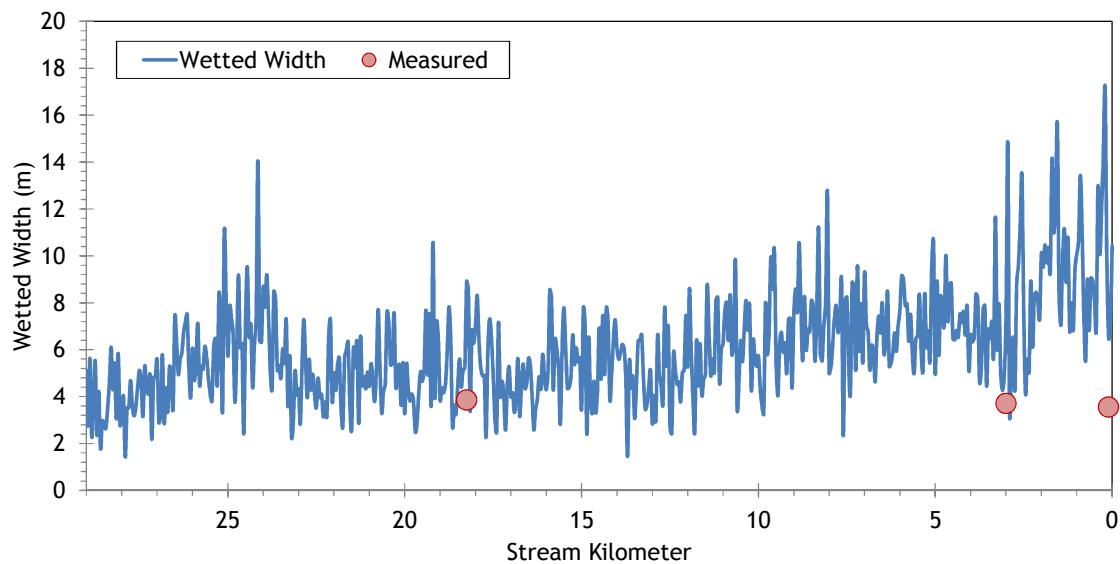
Meadow Creek elevations and gradients are shown in Figure 176. The stream has a fairly gradual descent, is moderately sinuous, and hence gradient is moderated throughout.

Figure 176 - Meadow Creek elevation and gradient.



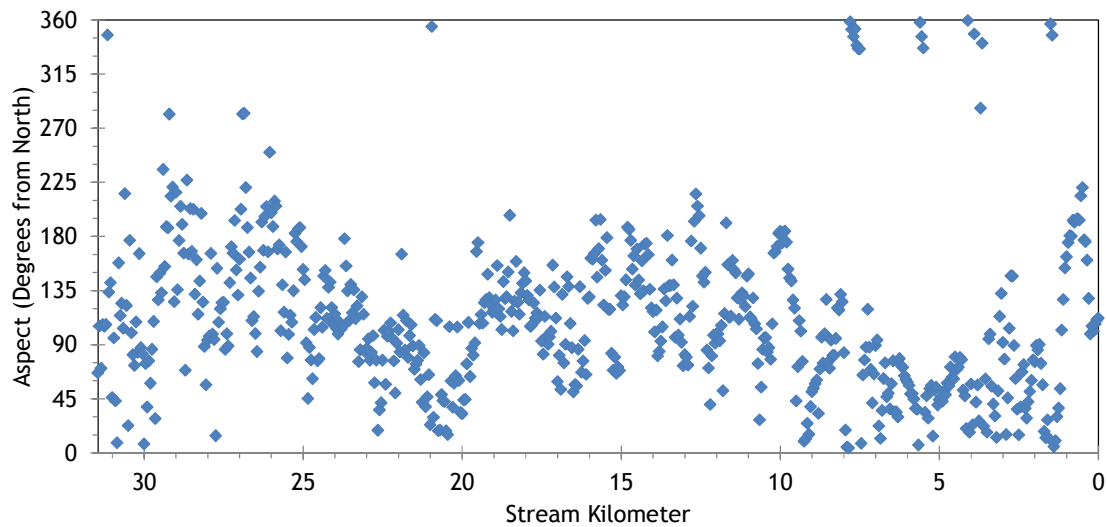
The wetted widths for Meadow Creek are shown in Figure 177. There is a slight increase in widths in the downstream direction, but overall the stream is relatively small.

Figure 177 - Meadow Creek wetted width.



Meadow Creek flows from west to east before joining the Grande Ronde River (Figure 178).

Figure 178 - Meadow Creek stream aspect.



The mountainous terrain surrounding Meadow Creek creates moderately high topographic shade angles (Figure 179). Values vary between about 5 and 30 degrees.

Figure 179 - Meadow Creek topographic shade angles.

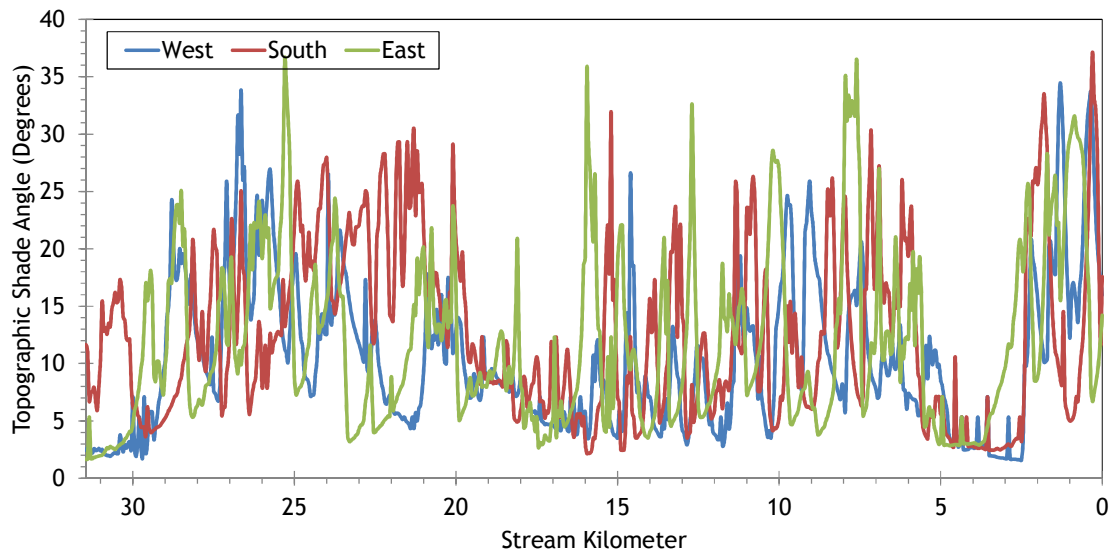
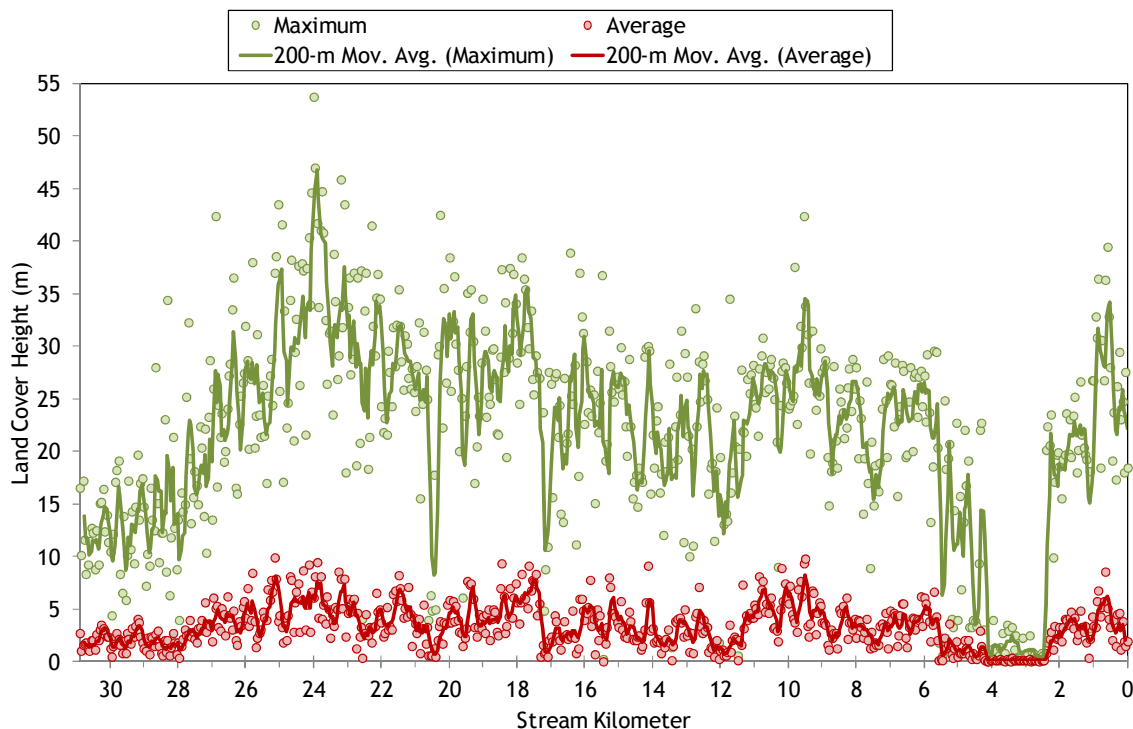


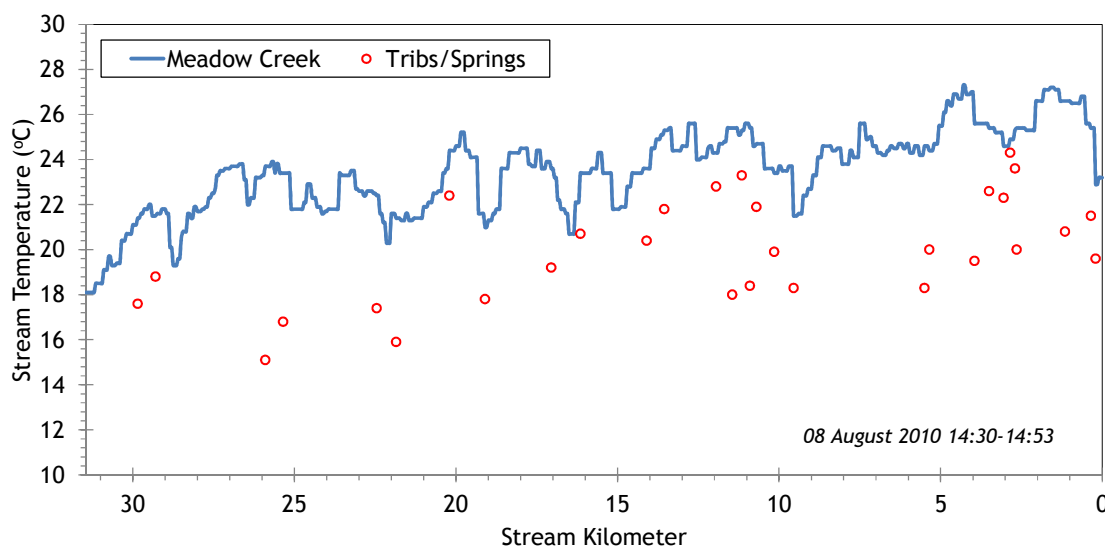
Figure 180 shows the land cover heights sampled along Meadow Creek. The maximum and average of the 28 radial samples were calculated for each 50-meter stream node. (Note: Heat Source uses each of the 28 radial samples for each 50-meter node. The maximum and average are shown here for simplification purposes.)

Figure 180 - Meadow Creek land cover heights sampled from highest hit LiDAR.



The moderate gradients and low stream flows make the longitudinal thermal profile quite variable (Figure 181). Maximum stream temperatures were about 27°C during the TIR flight.

Figure 181 - Meadow Creek TIR stream temperature profile.



5.14.2 Meadow Creek Heat Source Calibration Results

Meadow Creek was simulated from Waucup Creek to the mouth (Figure 182). The total simulation length was 30.9 stream kilometers.

Figure 182 - Meadow Creek simulation extent.

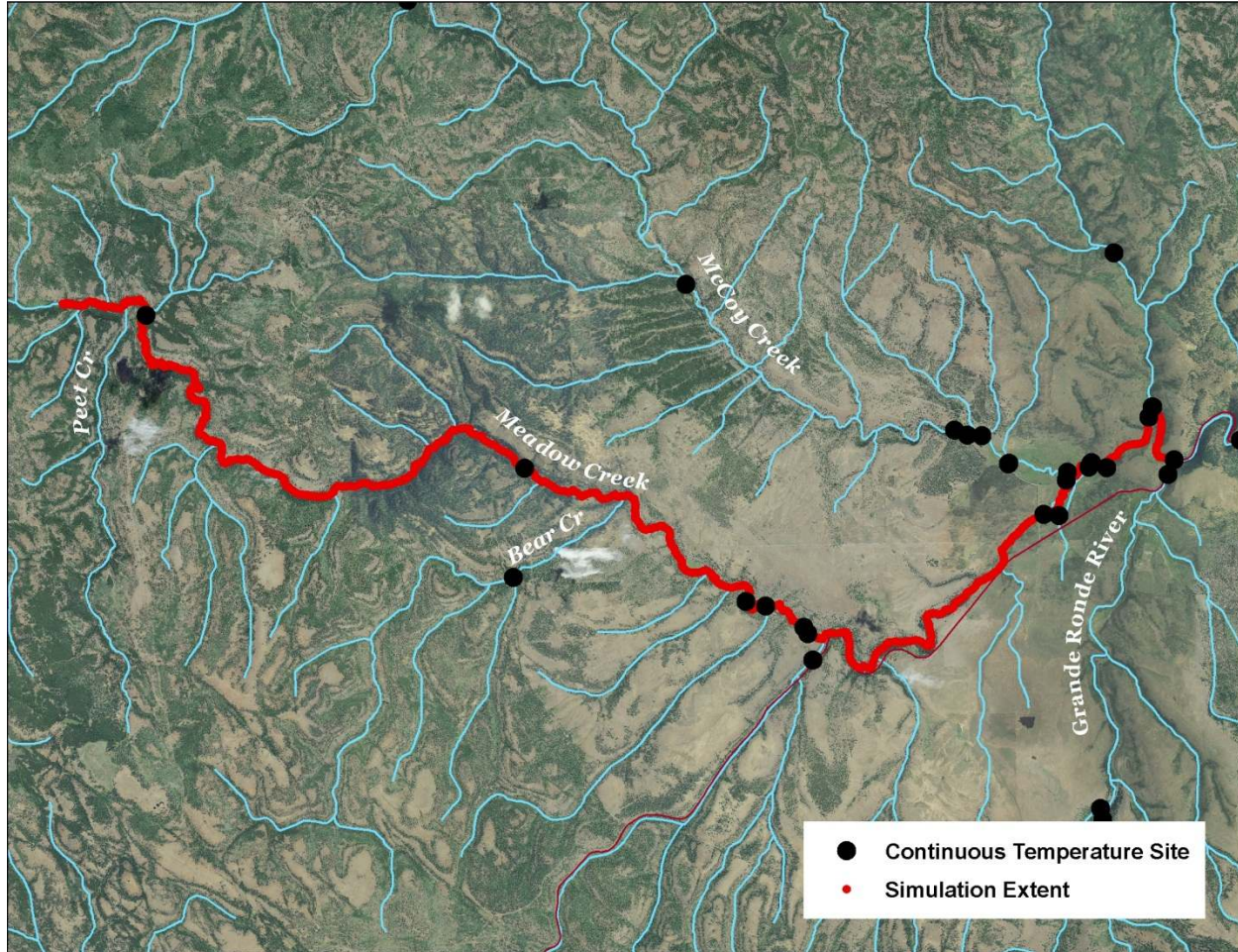


Table 28 - Meadow Creek general Heat Source parameters.

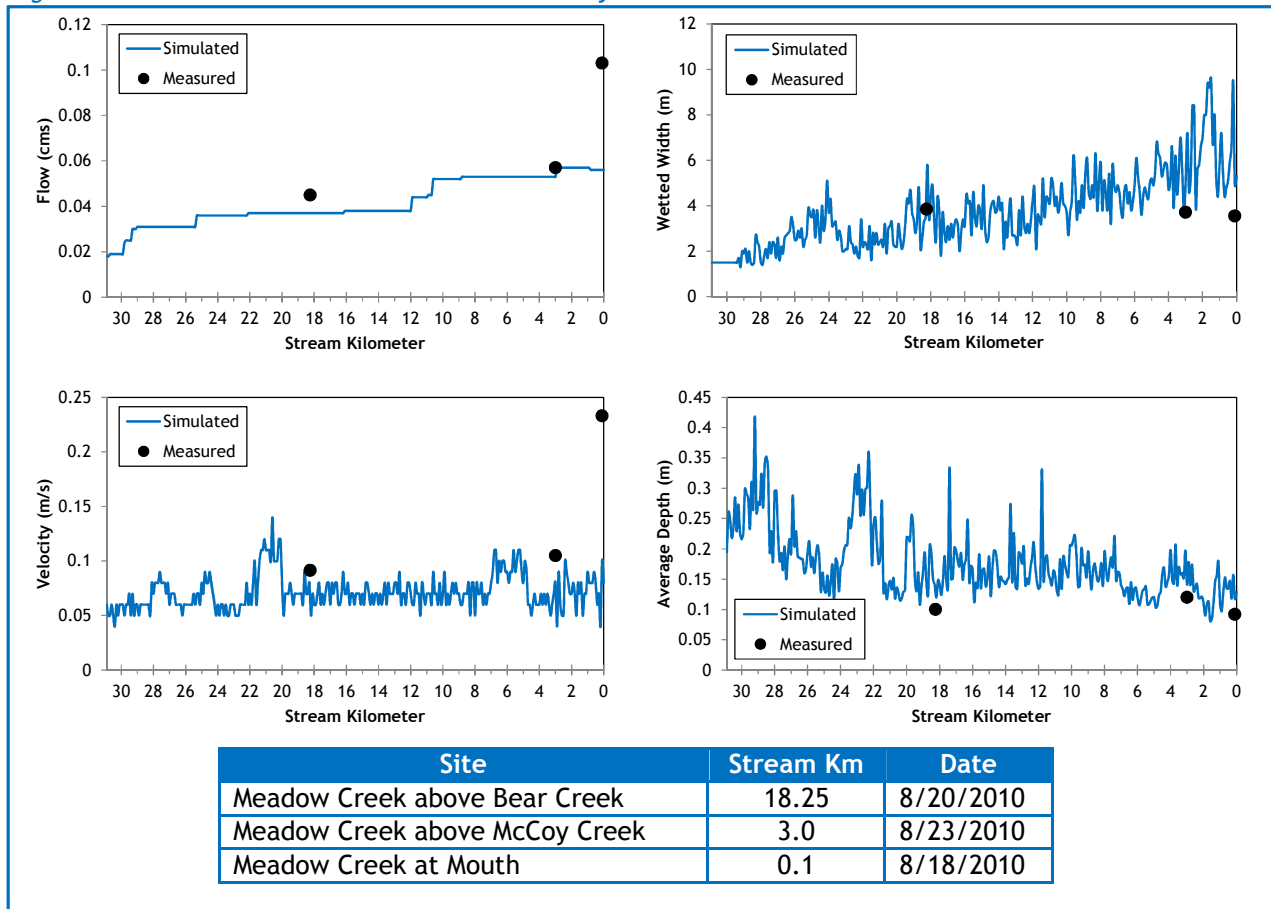
Stream:	Meadow Creek
Length:	30.9 kilometers
Time Period:	August 6-27, 2010
Input Distance Step:	50 meters
Output Distance Step:	100 meters
Time Step:	1 minute
Flush Initial Condition:	7 days
TIR Date and Time:	August 8, 2010 14:30-14:53
Land Cover Data Source:	LiDAR
Land Cover Sampling Distance Step:	15 meters

The following assumptions were used when calibrating the Meadow Creek Heat Source model:

- Hourly climate data was obtained from the La Grande Airport (NWS). Air temperature was adjusted using the adiabatic lapse rate of 1°C per 100 meters elevation.
- Daily flow variability was extrapolated from Grande Ronde River gage data.

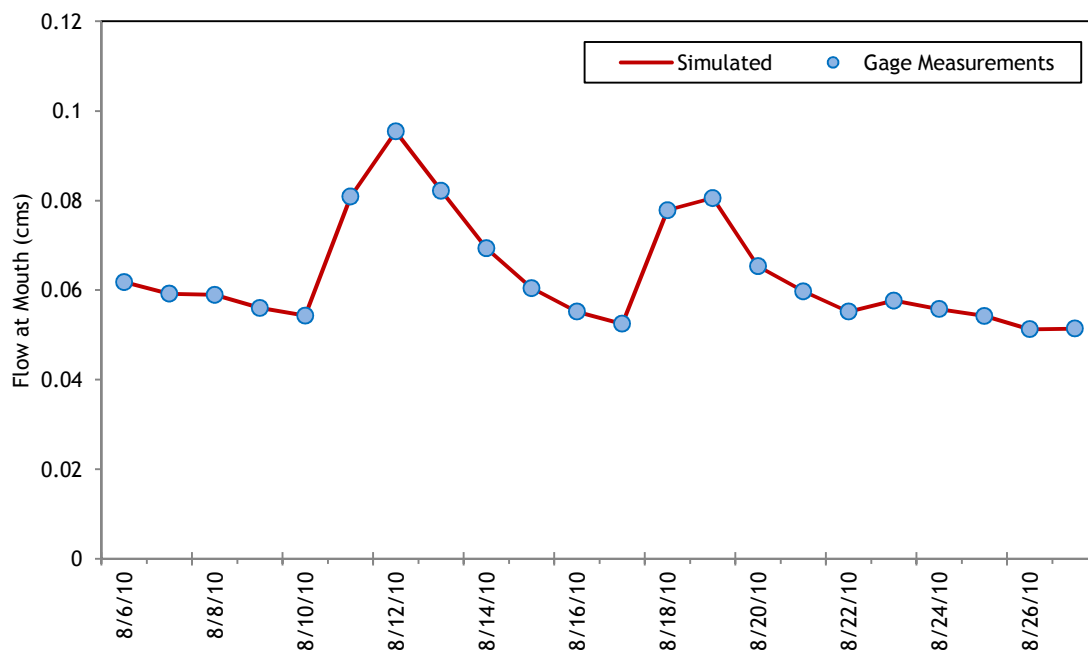
Figure 183 summarized the simulated and measured hydraulic values used in the calibrated Meadow Creek model. The simulated data was plotted for August 26th, while the ground level measurements were collected on three different days.

Figure 183 - Meadow Creek simulated and measured hydraulic values.



The simulated daily flow values at the mouth are presented in Figure 184. The daily values were extrapolated from gage data recorded on the Grande Ronde River.

Figure 184 - Meadow Creek simulated flows at mouth.



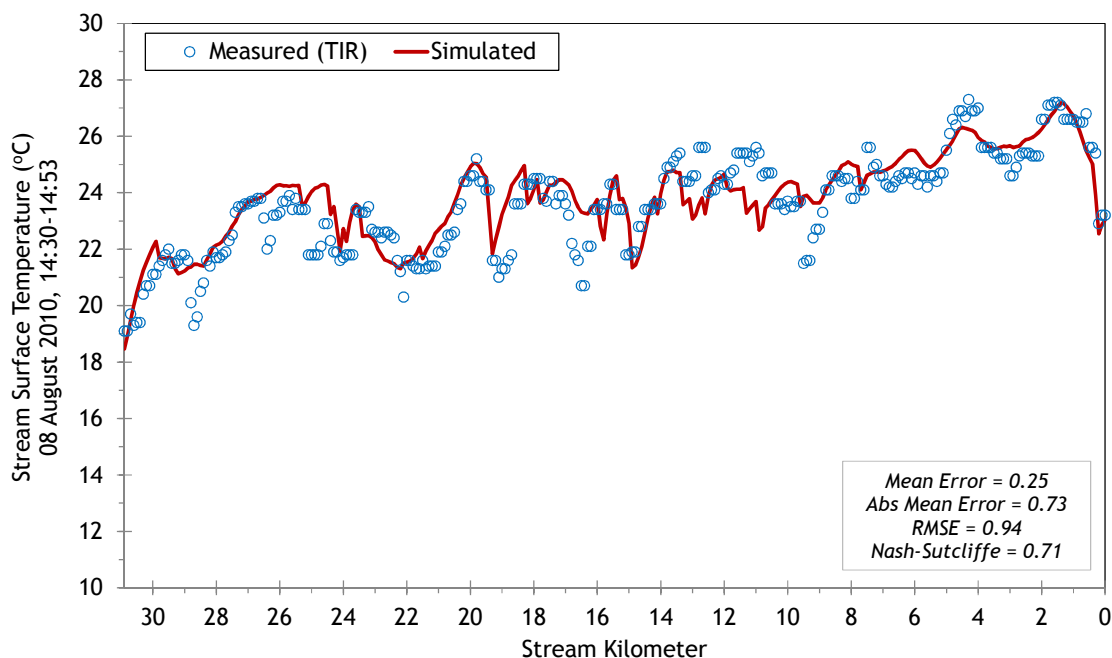
The tributaries included within the Meadow Creek Heat Source model are summarized in Table 29. Dark Canyon Creek had intermittent flow during August 2010 and was assumed dry during the simulation time period.

Table 29 - Meadow Creek mass inflow features and assumptions.

Feature	Stream Km	Assumptions
Peet Creek	29.8	0.006-0.01 cms, used Bear Cr temps
Smith Creek	29.3	0.006-0.01 cms, used Bear Cr temps
Cougar Canyon	25.3	0.006-0.01 cms, used Bear Cr temps
Bear Creek	16.15	0.0006-0.001 cms, measured hourly temps
Battle Creek	11.95	0.006-0.01 cms, used Bear Cr temps
Burnt Corral Creek	10.65	0.007-0.01 cms, measured hourly temps
McCoy Creek	2.9	0.004-0.007 cms, measured hourly temps

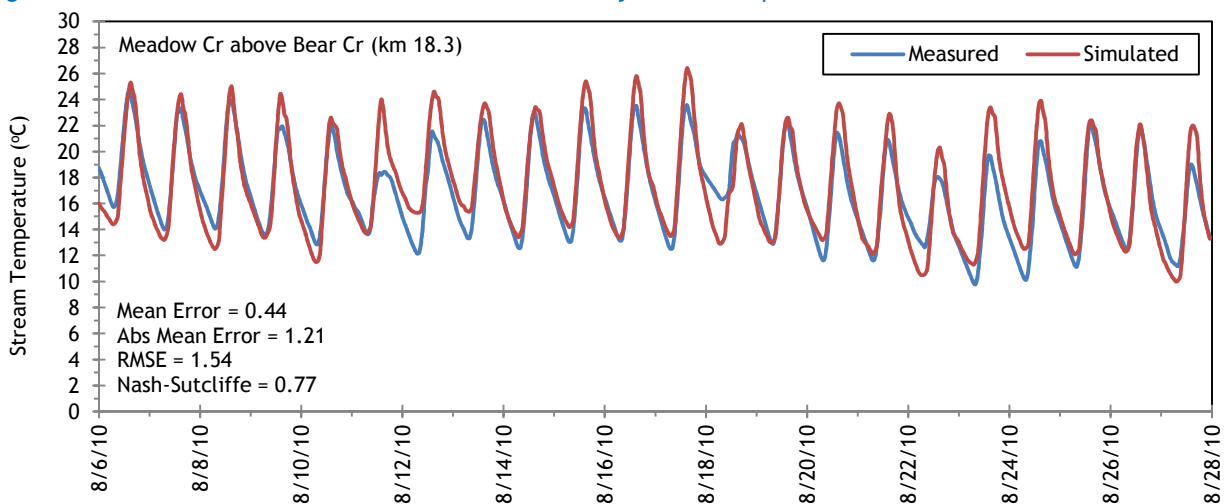
Meadow Creek simulated and measured longitudinal temperatures are shown in Figure 185. There is a great deal of variability over short distances because the stream flows were quite low during August 2010.

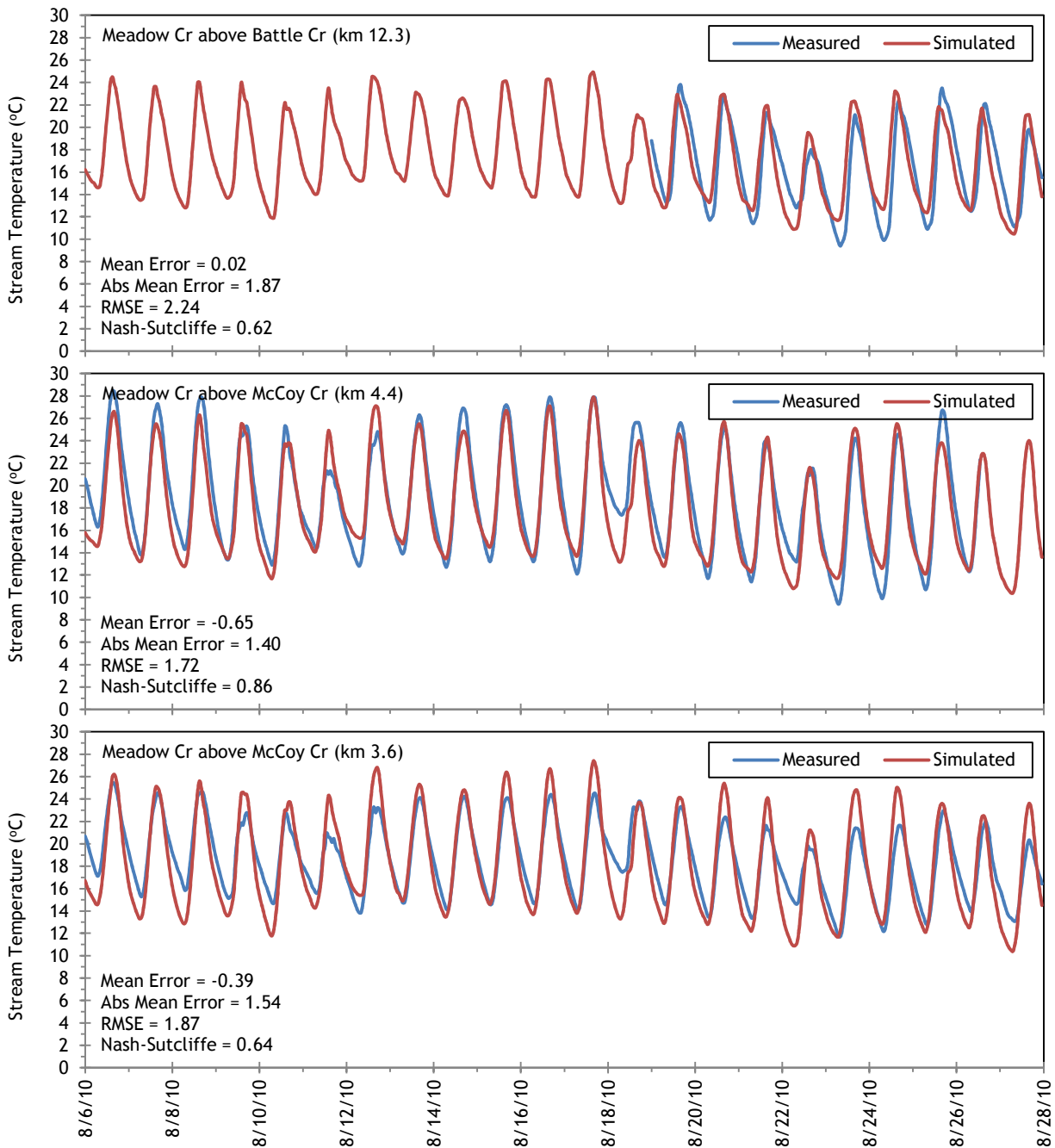
Figure 185 - Meadow Creek simulated and measured longitudinal stream temperatures.



Simulated and measured hourly stream temperatures are compared in Figure 186. Meadow Creek had very low flow which makes the stream temperatures more variable over shorter distances. Calibration of the Heat Source model was more challenging than for other streams and the resulting calibration statistics reflect that.

Figure 186 - Meadow Creek simulated and measured hourly stream temperatures.





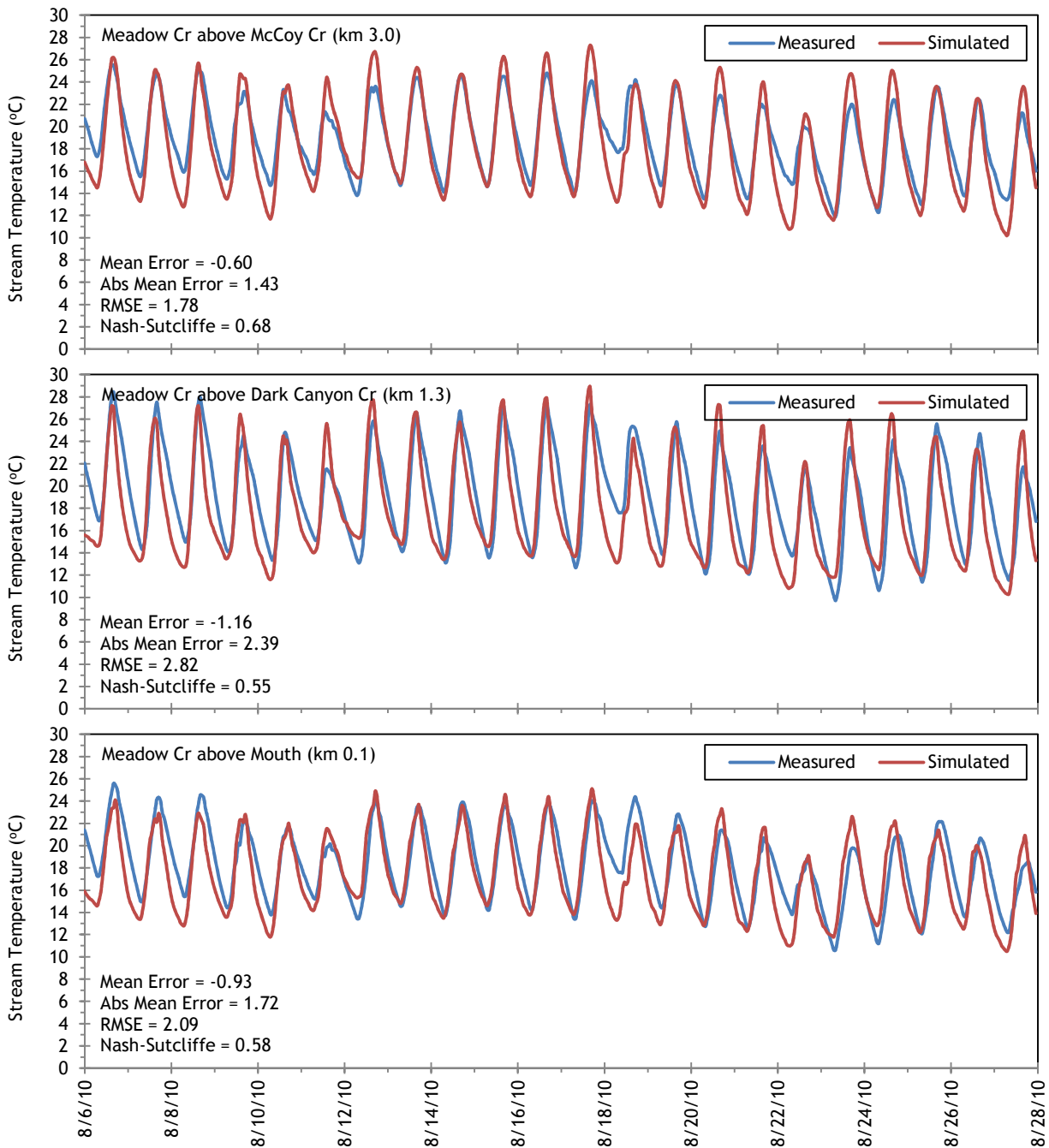
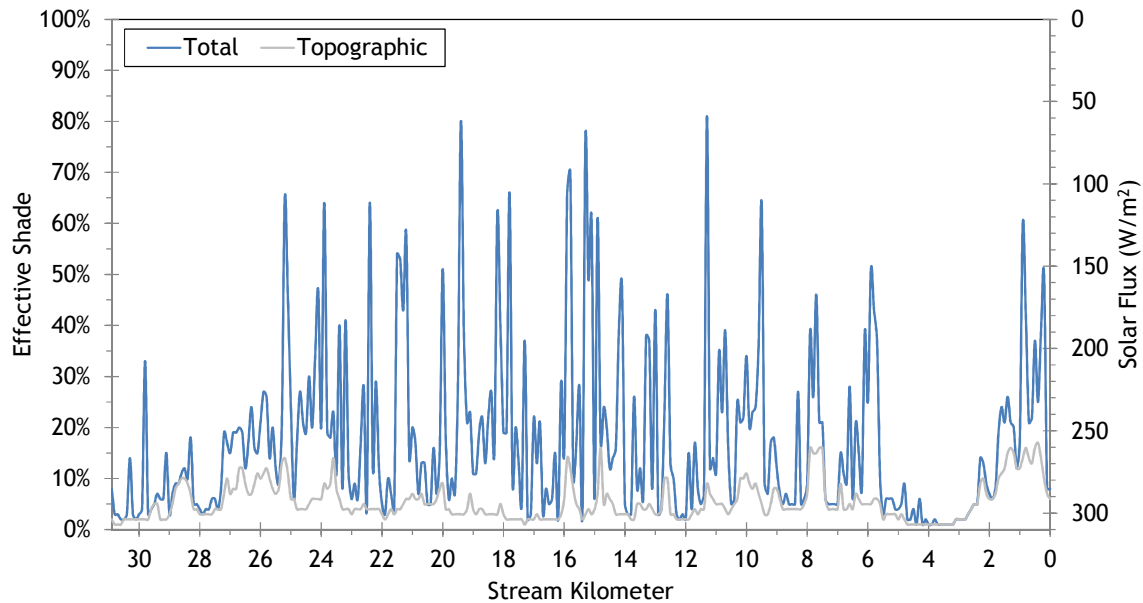
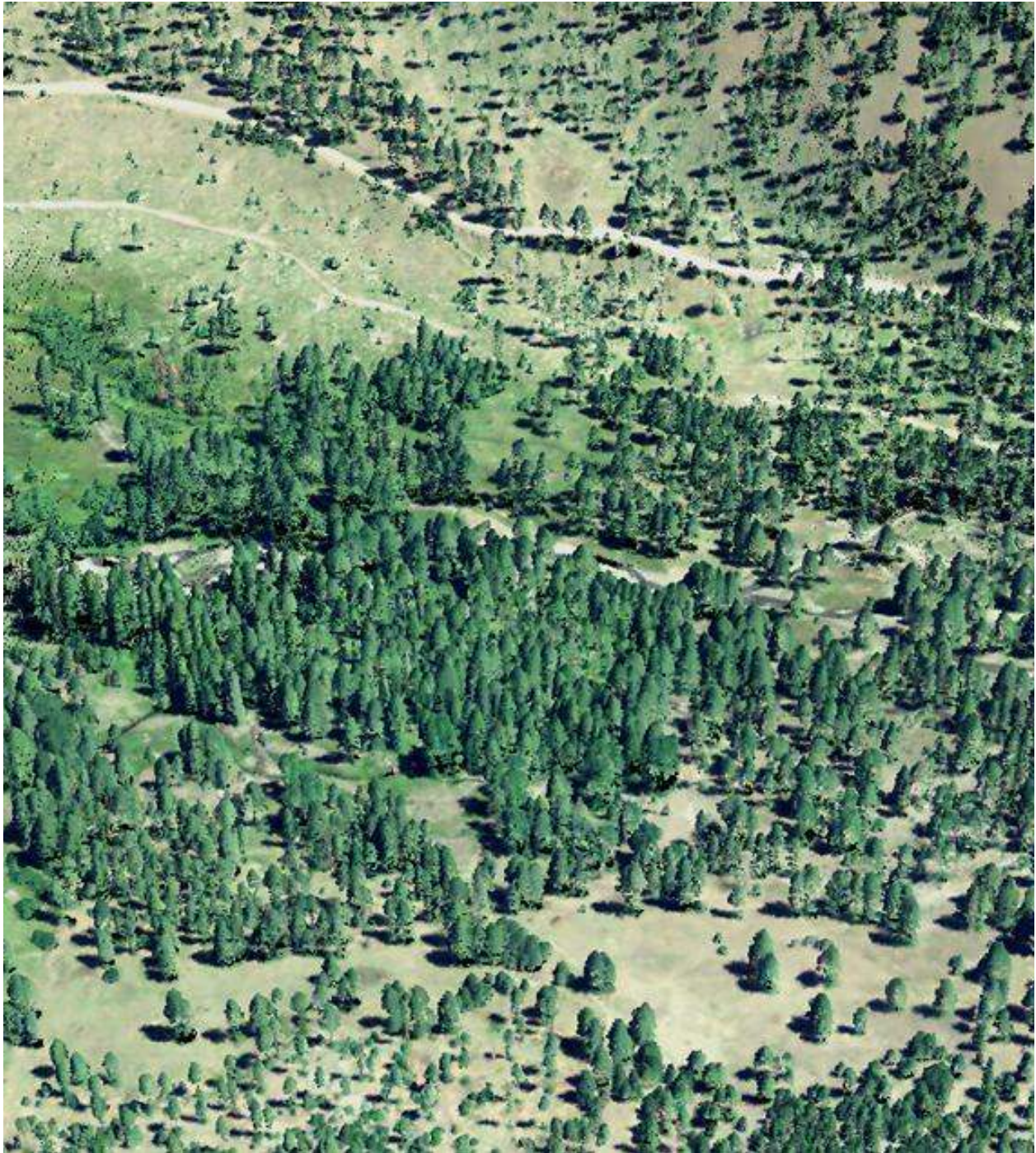


Figure 187 shows the simulated effective shade values for Meadow Creek. The total effective shade is somewhat moderate because of the meanders through meadows that are a mix of grass and trees. There is upwards of 10% effective shade produced by topography throughout much of the stream length.

Figure 187 - Meadow Creek simulated effective shade.



5.15 Beaver Creek



RGB-colored LiDAR point cloud - Beaver Creek near Little Beaver Creek (stream flowing from right to left of image).

5.15.1 Beaver Creek TTools Results

Beaver Creek elevations and gradients were sampled from the bare earth LiDAR data (Figure 188). The reaches just below La Grande Reservoir (kilometer 22.9) are the steepest, and then gradients are generally between 1% and 4%.

Figure 188 - Beaver Creek elevation and gradient.

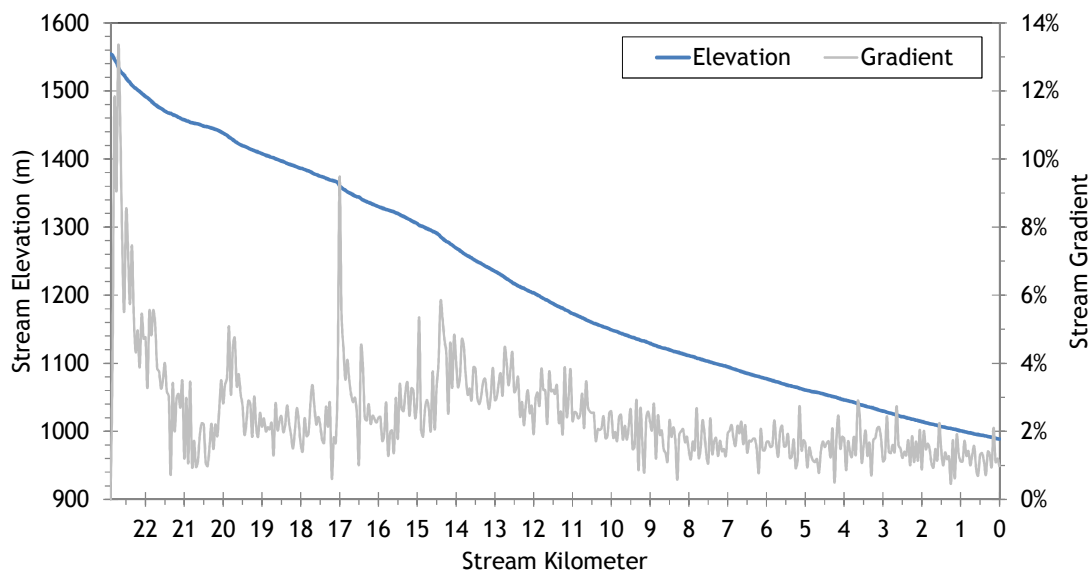
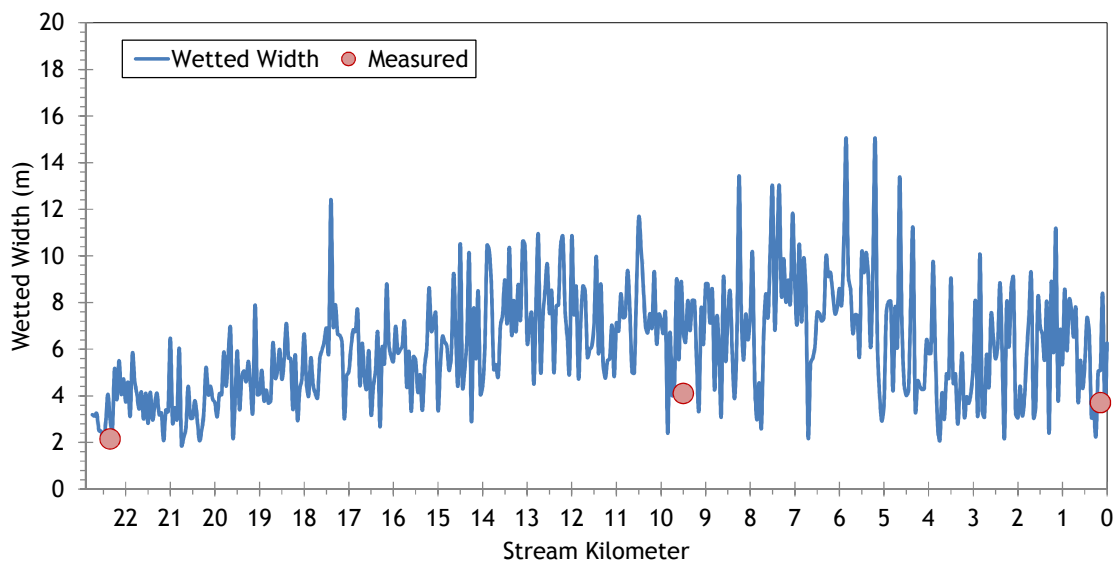


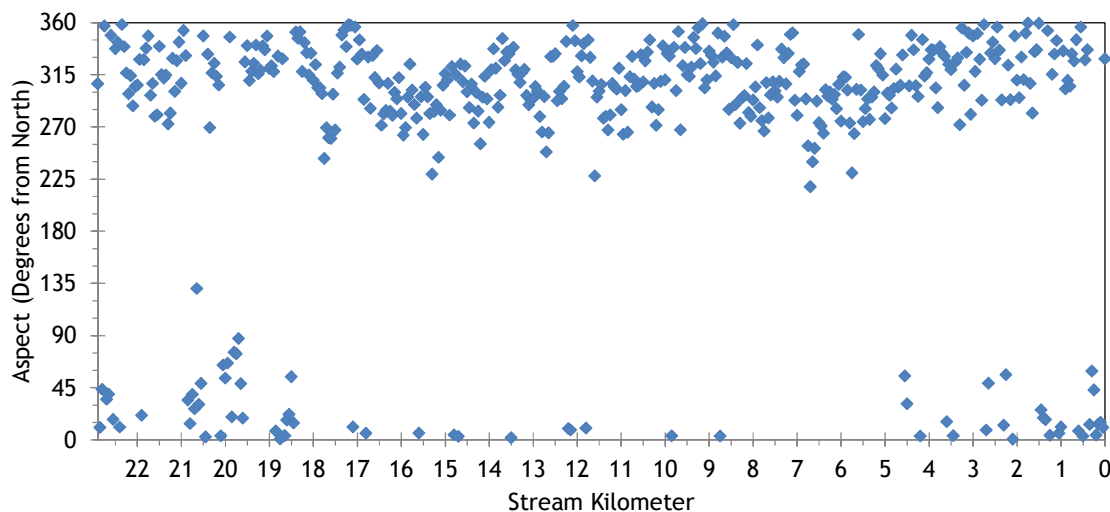
Figure 189 displays the measured and sampled wetted widths for Beaver Creek. The average width was about 6 meters during the simulation time period.

Figure 189 - Beaver Creek wetted widths.



Beaver Creek flows generally in the northwesterly direction (Figure 190).

Figure 190 - Beaver Creek stream aspect.



Topographic shade angles on Beaver Creek are somewhat higher than other streams in the watershed (Figure 191). Maximum values regularly exceed 30 degrees, while the minimums are generally above 10 degrees in most reaches.

Figure 191 - Beaver Creek topographic shade angles.

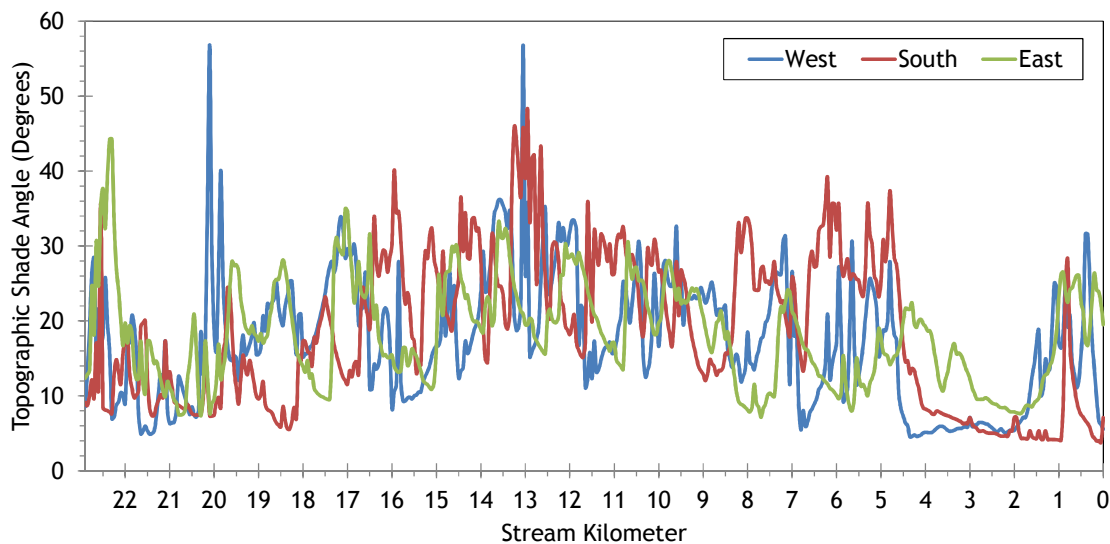


Figure 192 shows the land cover heights sampled along Beaver Creek. The maximum and average of the 28 radial samples were calculated for each 50-meter stream node. (Note: Heat Source uses each of the 28 radial samples for each 50-meter node. The maximum and average are shown here for simplification purposes.)

Figure 192 - Beaver Creek land cover heights sampled from highest hit LiDAR.

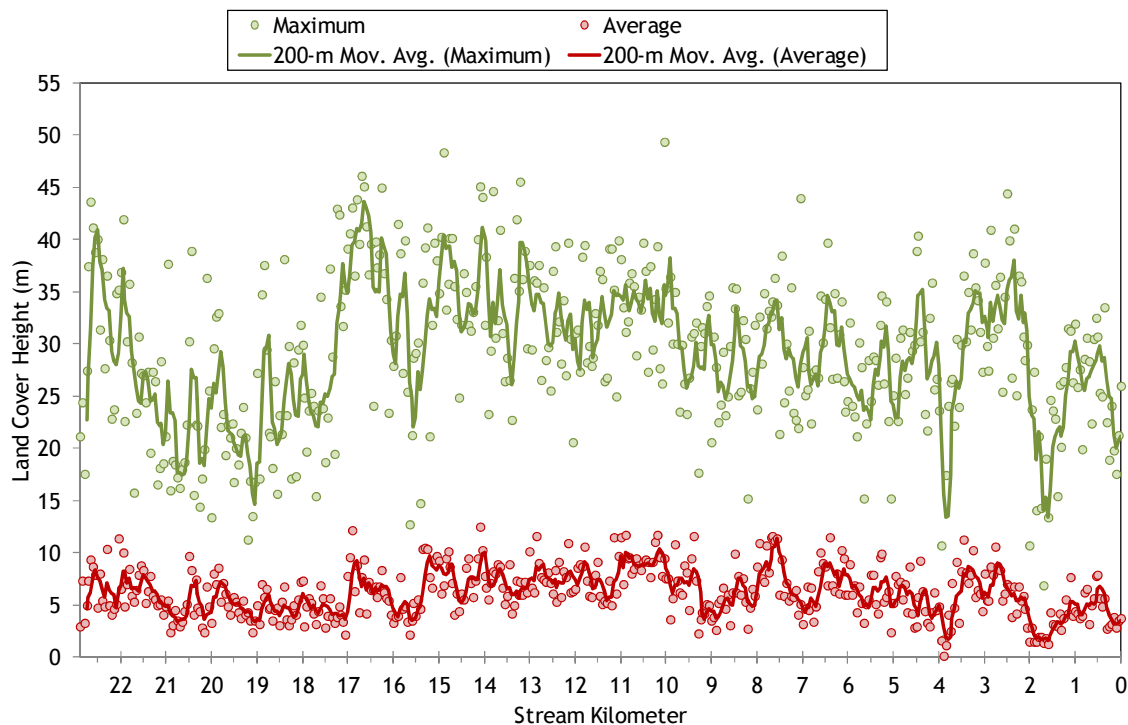
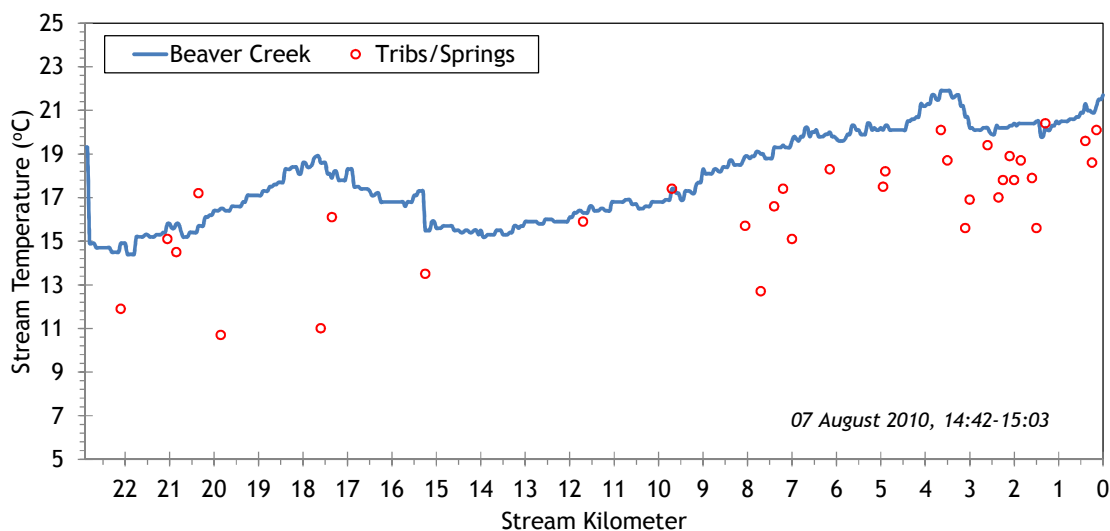


Figure 193 shows the TIR stream temperature profile of Beaver Creek. The stream was leaving the La Grande Reservoir at approximately 15°C at the time of the TIR flight.

Figure 193 - Beaver Creek TIR stream temperature profile.



5.15.2 Beaver Creek Heat Source Calibration Results

Beaver Creek was simulated from La Grande Reservoir to the mouth (Figure 194).

Figure 194 - Beaver Creek simulation extent.

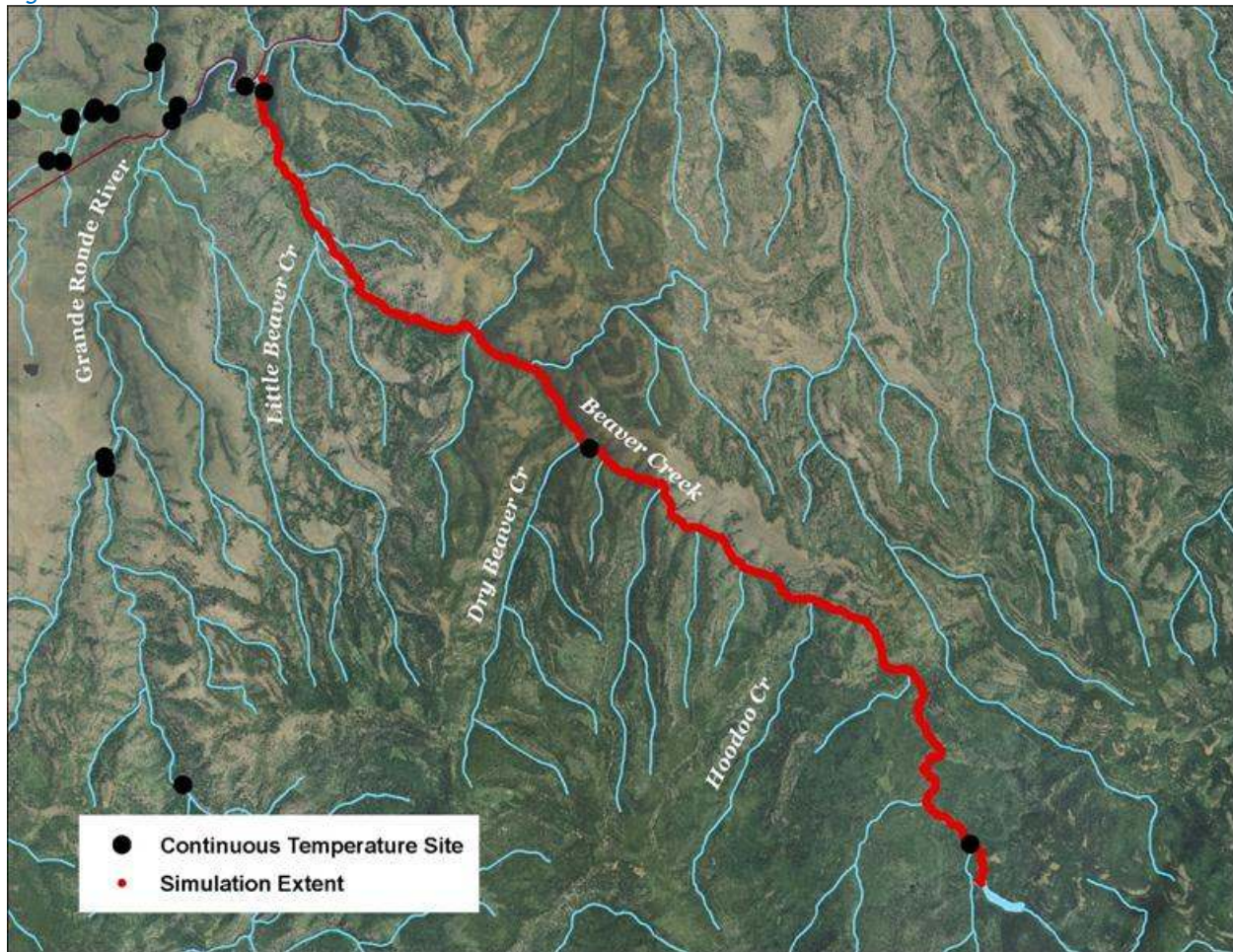


Table 30 - Beaver Creek general Heat Source parameters.

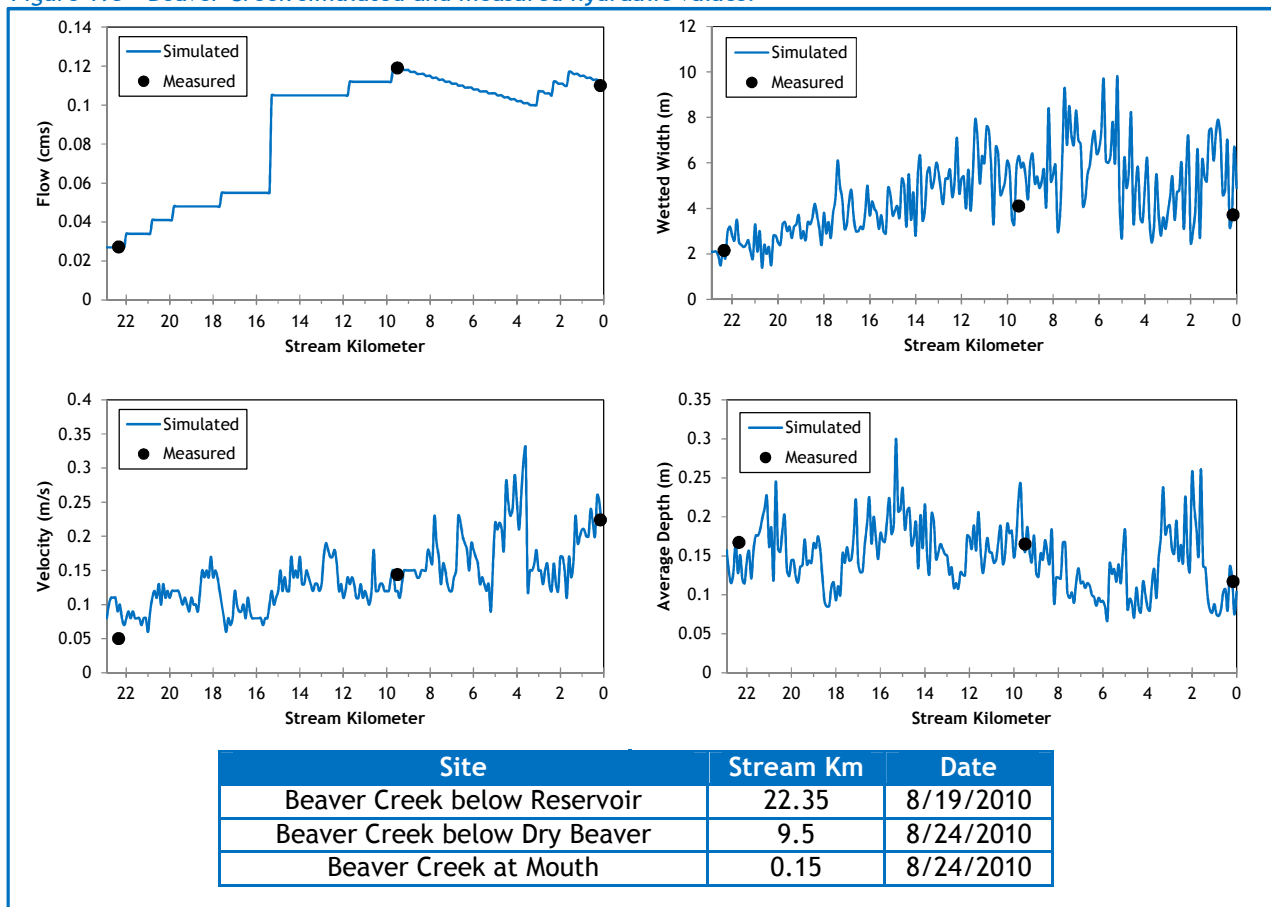
Stream:	Beaver Creek
Length:	22.9 kilometers
Time Period:	August 6-27, 2010
Input Distance Step:	50 meters
Output Distance Step:	100 meters
Time Step:	1 minute
Flush Initial Condition:	7 days
TIR Date and Time:	August 7, 2010 14:42-15:03
Land Cover Data Source:	LiDAR
Land Cover Sampling Distance Step:	15 meters

The following assumptions were used when calibrating the Beaver Creek Heat Source model:

- Hourly climate data is from the La Grande airport. Wind speeds were reduced 50% and air temperatures were adjusted using the adiabatic lapse rate.
- Wetted widths were roughly digitized from the TIR and LiDAR intensity images. The model reduced the value sampled by TTools by 20-34% in order to accommodate the other hydraulic values.

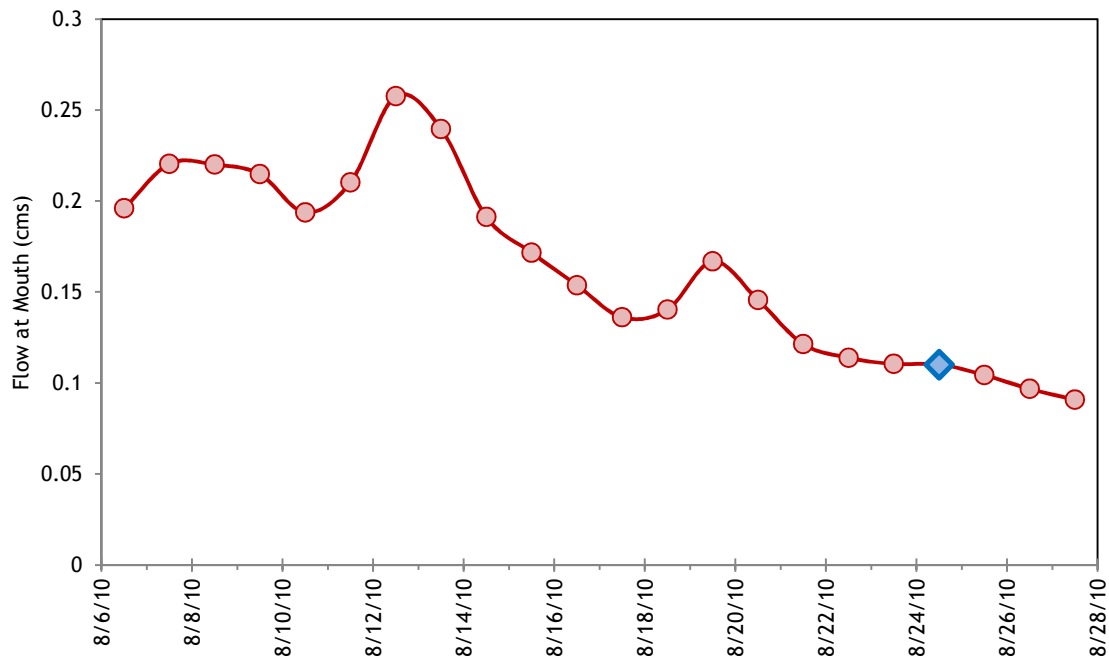
Figure 195 summarizes the simulated and measured hydraulic values from the calibrated model. The simulated values are from August 24th, while the measurements were taken on various days. There was an unverified losing reach between kilometer 9.5 and the mouth, based on measurements taken on August 24, 2010. The loss was accounted for in the simulation by gradually removing 1 cfs across the lower 9.5 kilometers.

Figure 195 - Beaver Creek simulated and measured hydraulic values.



The simulated daily flow volumes at the mouth of Beaver Creek are shown in Figure 196. The daily values were extrapolated from gage measurements on the Grande Ronde River.

Figure 196 - Beaver Creek simulated flows at the mouth.



The tributaries and springs included in the calibrated model are listed in Table 31. Hoodoo Creek was the largest tributary and created a significant thermal signature in the TIR imagery. The other tributaries were all assumed to be of equal (small) volume. Hourly temperature data was estimated by using the values recorded on Beaver Creek upstream of Dry Beaver Creek, minus the difference between the tributary (TIR temperature) and the Beaver Creek upstream of Dry Beaver Creek temperature.

Table 31 - Beaver Creek mass inflow features and assumptions.

Feature	Stream Km	Assumptions
Cove Creek	22.0	0.006-0.01 cms, hourly temps based on Beaver Cr. u/s Dry Beaver Cr. minus difference of TIR observation.
West Fork Beaver Cr.	20.85	0.006-0.01 cms, hourly temps based on Beaver Cr. u/s Dry Beaver Cr. minus difference of TIR observation.
Unnamed Tributary	19.8	0.006-0.01 cms, hourly temps based on Beaver Cr. u/s Dry Beaver Cr. minus difference of TIR observation.
Spring	17.6	0.006-0.01 cms, hourly temps based on Beaver Cr. u/s Dry Beaver Cr. minus difference of TIR observation.
Hoodoo Creek	15.3	0.04-0.1 cms, hourly temps based on Beaver Cr. u/s Dry Beaver Cr. minus difference of TIR observation.
Watermelon Creek	11.75	0.006-0.01 cms, hourly temps based on Beaver Cr. u/s Dry Beaver Cr. minus difference of TIR observation.
Dry Beaver Creek	9.75	0.006-0.01 cms, hourly temps based on Beaver Cr. u/s Dry Beaver Cr. minus difference of TIR observation.
Little Beaver Creek	3.0	0.006-0.01 cms, hourly temps based on Beaver Cr. u/s Dry Beaver Cr. minus difference of TIR observation.
Unnamed Tributary	2.35	0.006-0.01 cms, hourly temps based on Beaver Cr. u/s Dry Beaver Cr. minus difference of TIR observation.

The simulated and measured longitudinal stream temperatures are shown in Figure 197.

Figure 197 - Beaver Creek simulated and measured longitudinal stream temperatures.

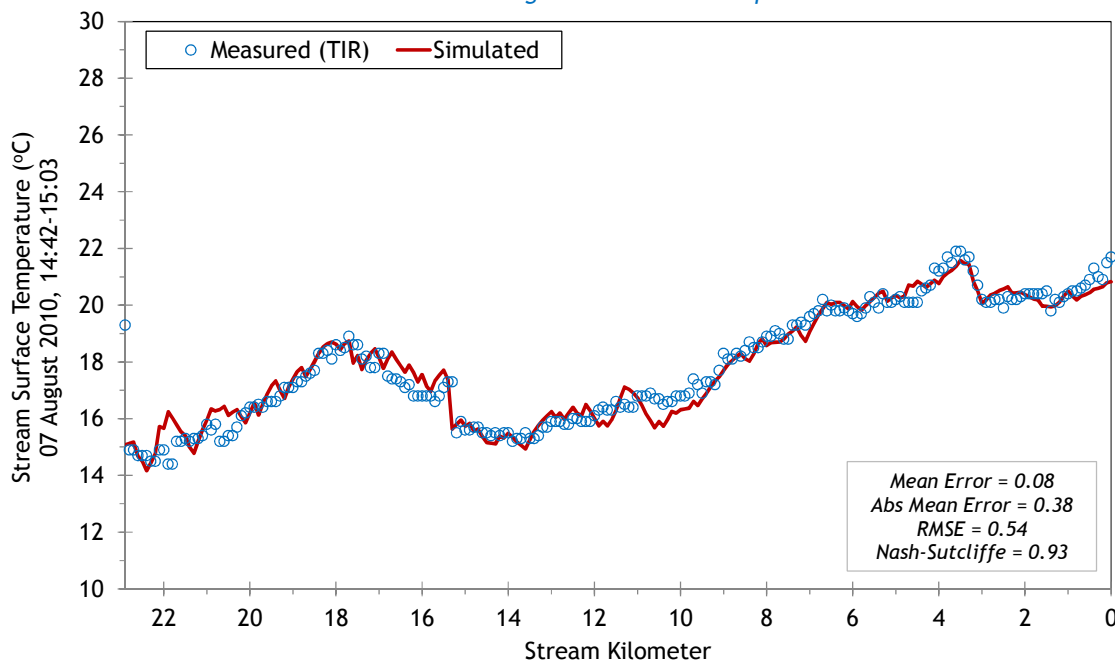
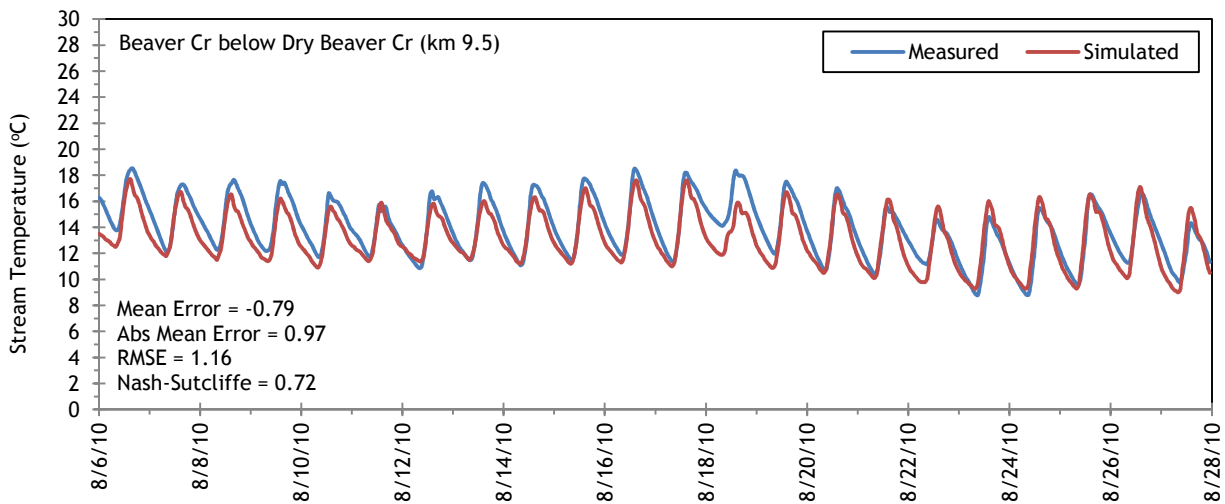
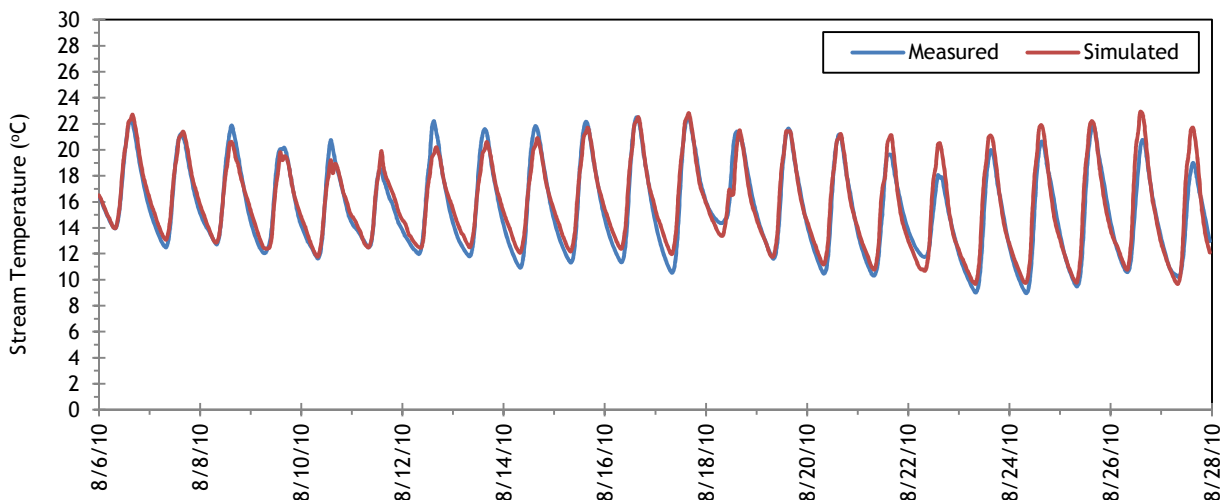


Figure 198 shows the simulated and measured hourly stream temperatures. Error statistics are also presented for each location.

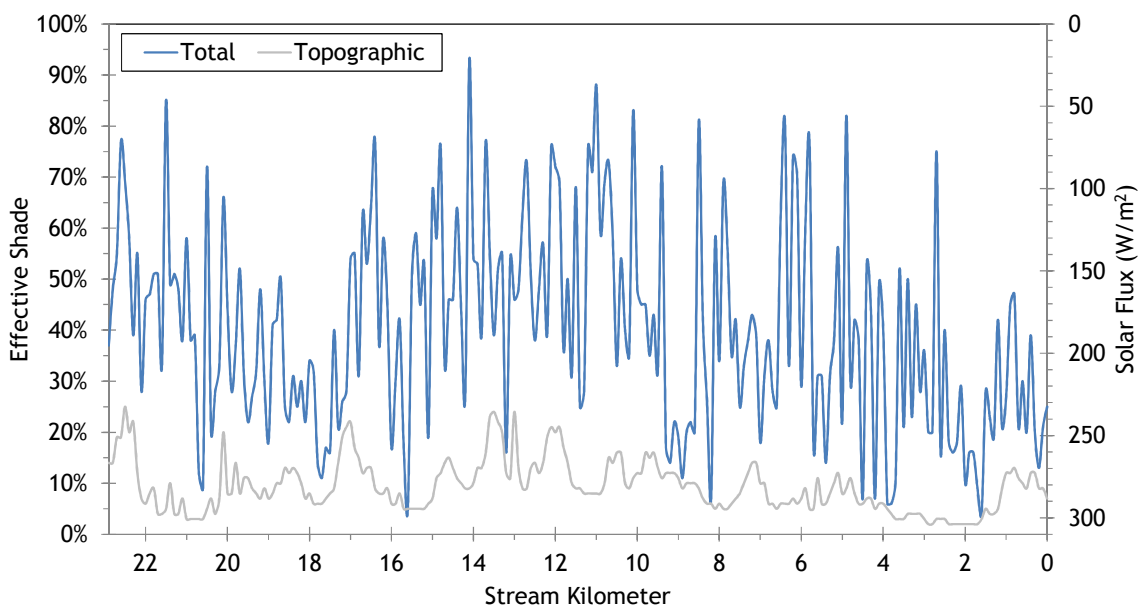
Figure 198 - Beaver Creek simulated and measured hourly stream temperatures.





The simulated effective shade values for Beaver Creek are presented in Figure 199. A fair amount of topographic shade occurs along Beaver Creek - upwards of 20% effective shade is created by topographic features in many locations. Beaver Creek is not very densely forested because of the wide grassy floodplain that occurs in so many reaches.

Figure 199 - Beaver Creek simulated effective shade.



5.16 Five Points Creek

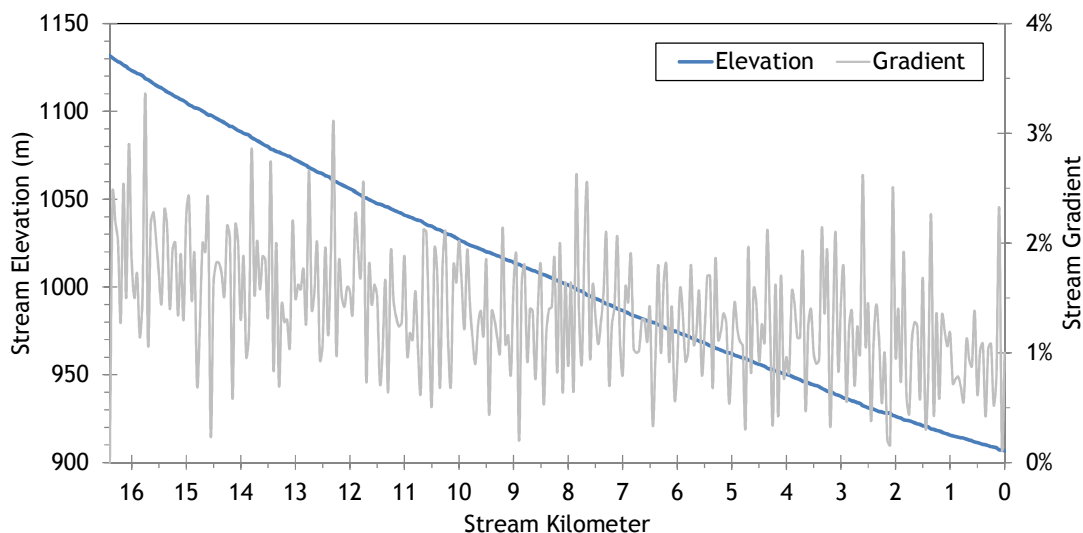


RGB-colored LiDAR point cloud - Five Points Creek below Little John Day Creek (looking downstream).

5.16.1 Five Points Creek TTools Results

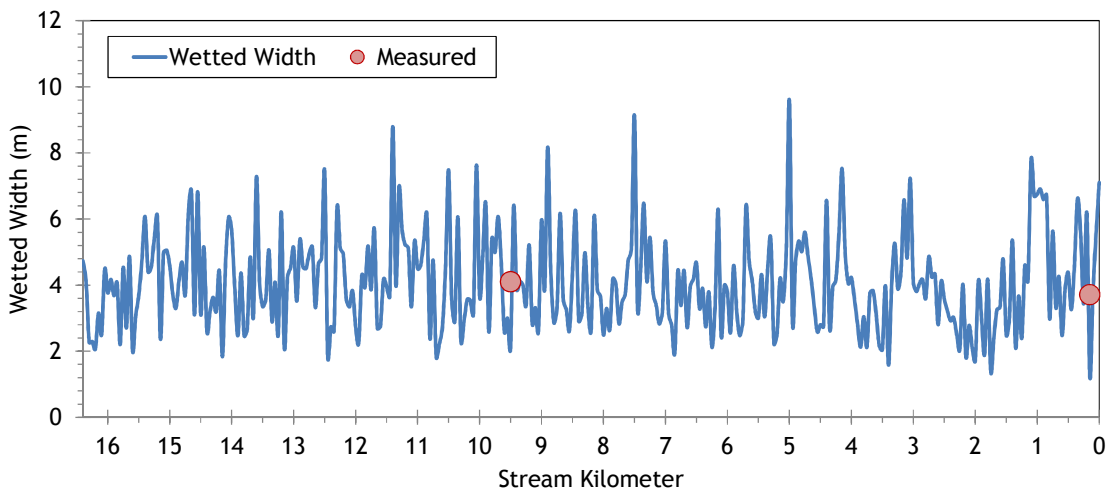
Figure 200 shows the sampled elevations and gradients for Five Points Creek. Gradients were generally between 1% and 2%. The stream flows through mostly confined valley in a mountainous terrain.

Figure 200 - Five Points Creek elevation and gradient.



Five Points Creek is also relatively small during the summertime. Figure 201 shows the measured and sampled wetted widths. The average width was about 4 meters for most of the stream.

Figure 201 - Five Points Creek wetted widths.



Five Points Creek flows from north to south, before joining the Grande Ronde River (Figure 202).

Figure 202 - Five Points Creek stream aspect.

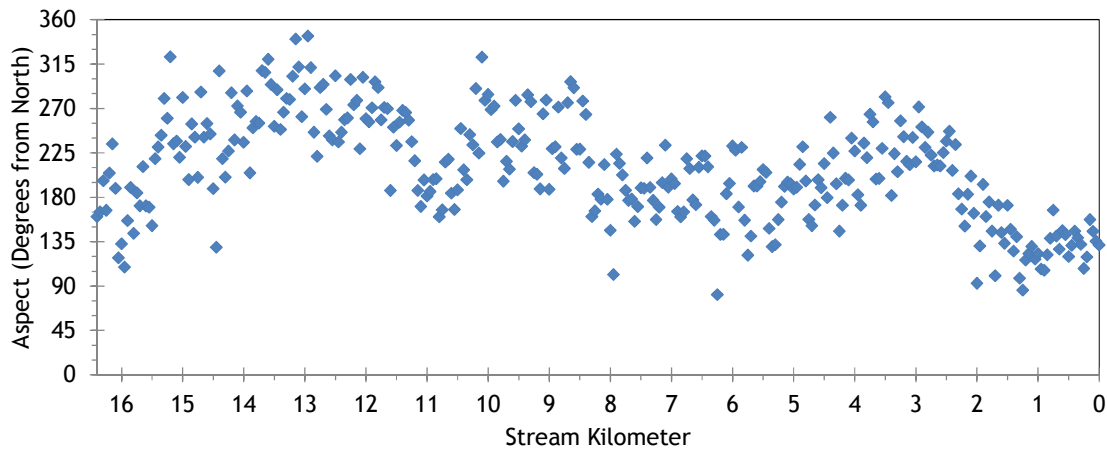


Figure 203 shows the topographic shade angles sampled for Five Points Creek. Overall, there is a significant amount of topographic shade on Five Points Creek.

Figure 203 - Five Points Creek topographic shade angles.

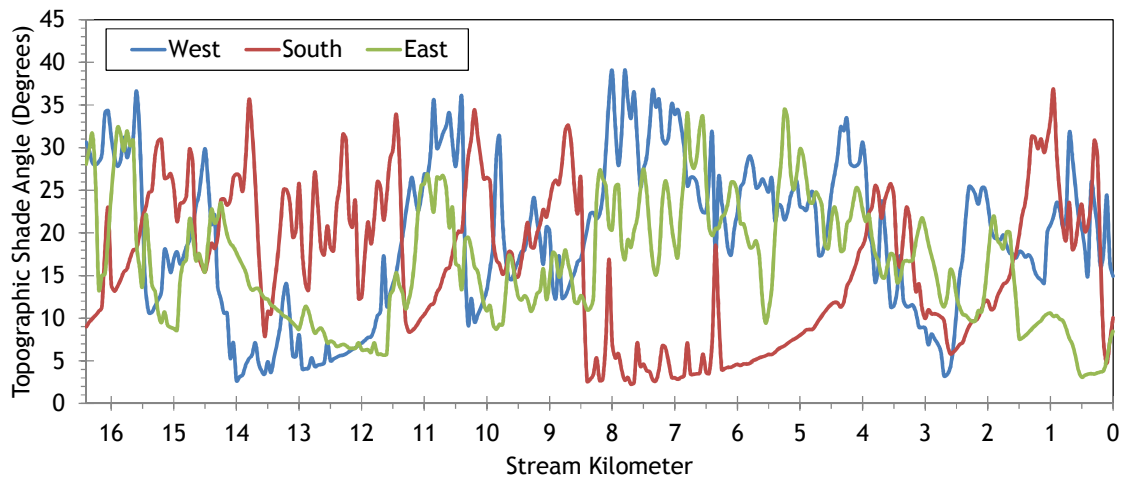
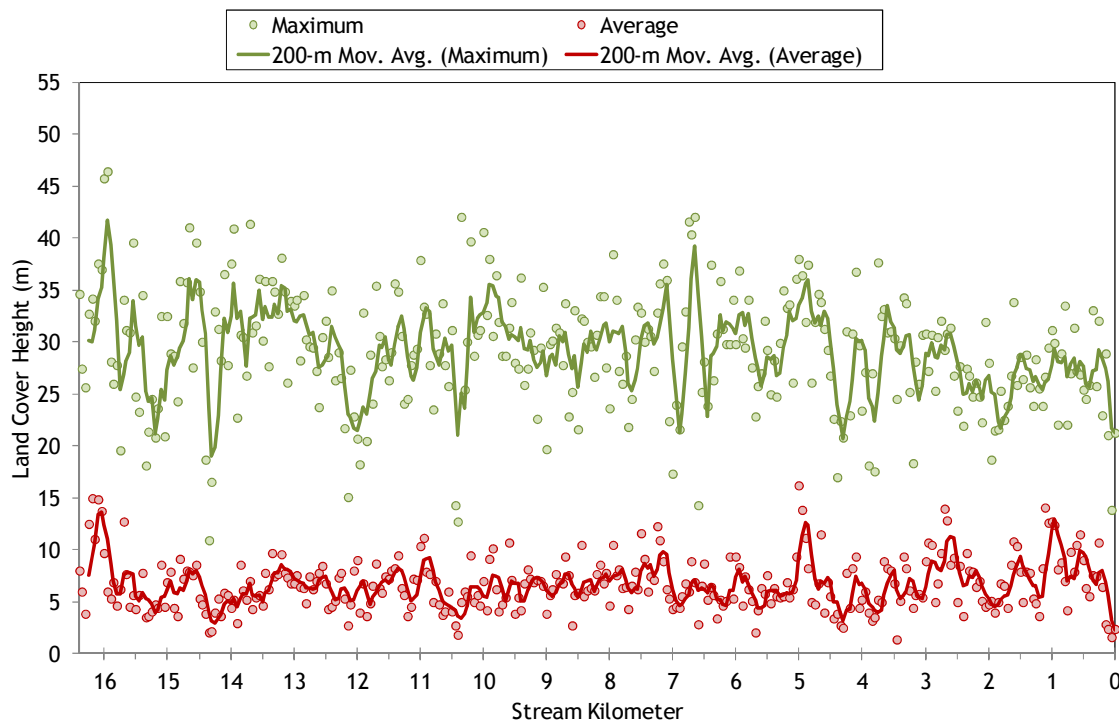


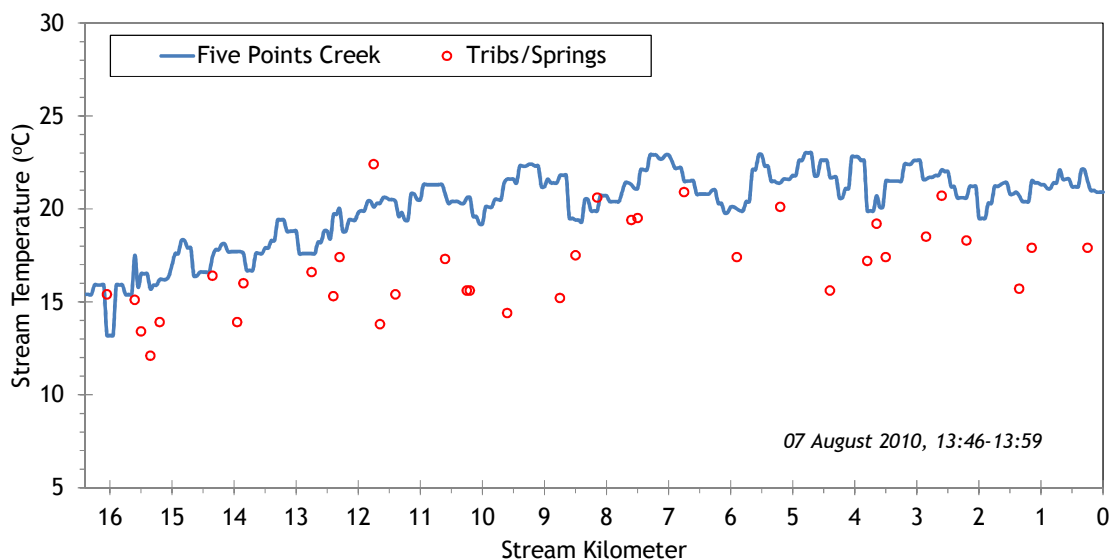
Figure 204 shows the land cover heights sampled along Five Points Creek. The maximum and average of the 28 radial samples were calculated for each 50-meter stream node. (Note: Heat Source uses each of the 28 radial samples for each 50-meter node. The maximum and average are shown here for simplification purposes.)

Figure 204 - Five Points Creek land cover heights sampled from highest hit LiDAR.



The TIR stream temperature profile of Five Points Creek is shown in Figure 205. The low flow volumes at the time of the flight are the primary reason for so much variability in the temperature profile. Smaller stream volumes are more sensitive to environmental factors that influence stream temperature.

Figure 205 - Five Points Creek TIR stream temperature profile.



5.16.2 Five Points Creek Heat Source Calibration Results

Five Points Creek flows from the north to the south and joins the Grande Ronde River. Figure 206 shows the simulation extent of the Heat Source model.

Figure 206 - Five Points Creek simulation extent.

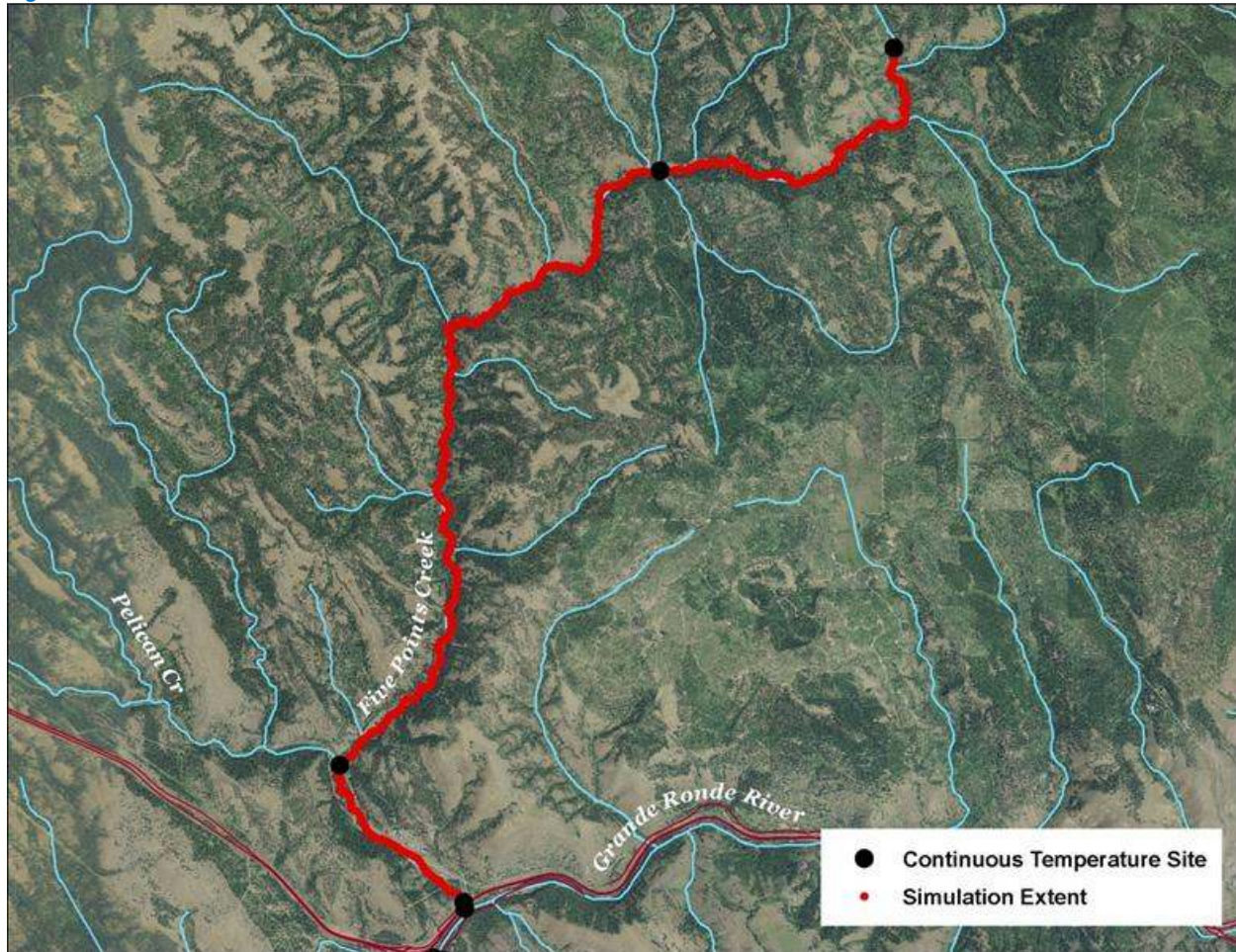


Table 32 - Five Points Creek general Heat Source parameters.

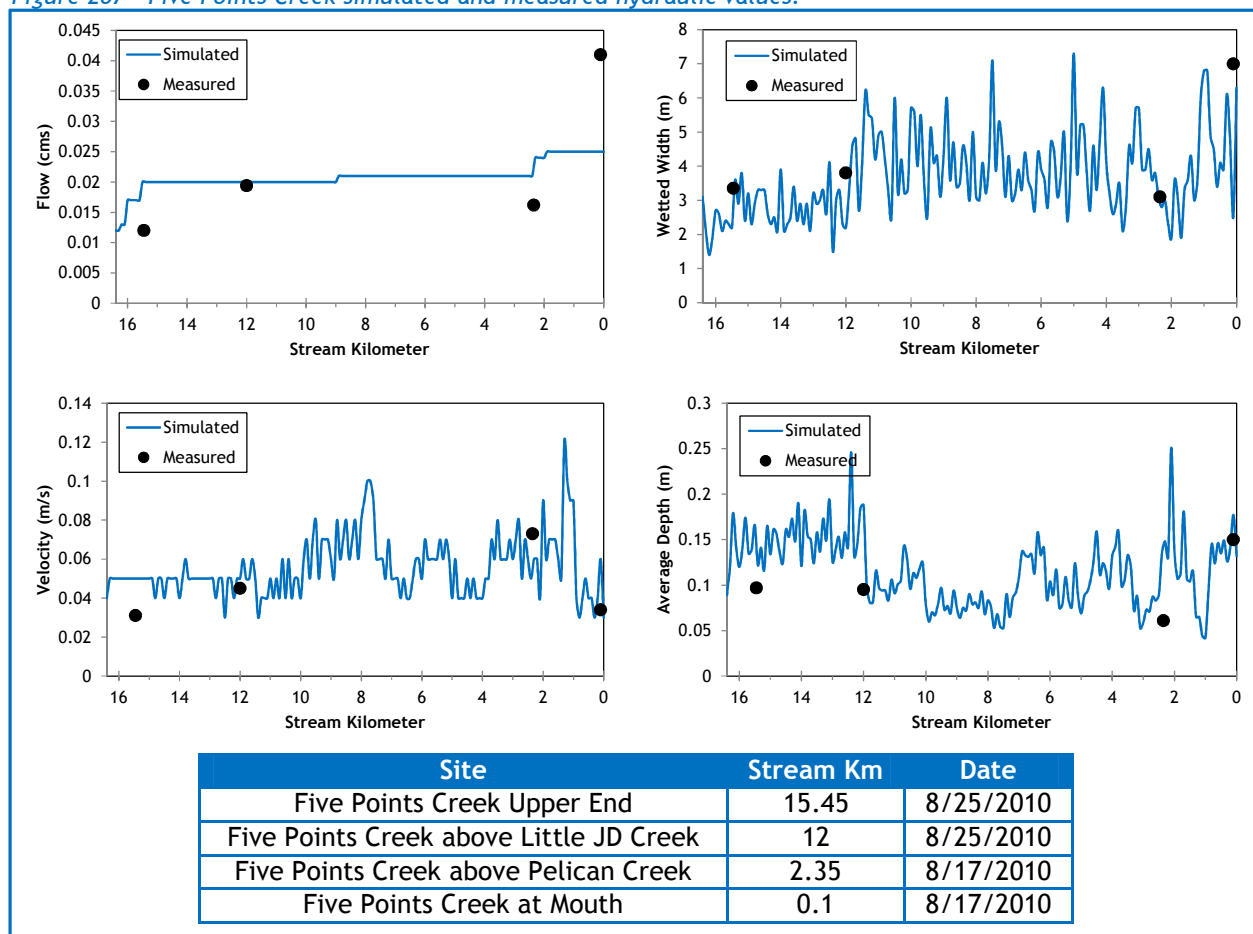
Stream:	Beaver Creek
Length:	22.9 kilometers
Time Period:	August 6-27, 2010
Input Distance Step:	50 meters
Output Distance Step:	100 meters
Time Step:	1 minute
Flush Initial Condition:	7 days
TIR Date and Time:	August 7, 2010 14:42-15:03
Land Cover Data Source:	LiDAR
Land Cover Sampling Distance Step:	15 meters

The following assumptions were used when calibrating the Five Points Creek Heat Source model:

- Hourly climate data was obtained from the La Grande airport (NWS). Wind speeds were reduced to better represent forested mountain terrain. Air temperatures were adjusted using the adiabatic lapse rate.
- Wetted widths were digitized from the TIR and LiDAR intensity images. The calibrated model used 66% of the TTools-sampled value in the upper 4.4 stream kilometers, while 100% of sampled wetted width was used in the lower 12 kilometers.

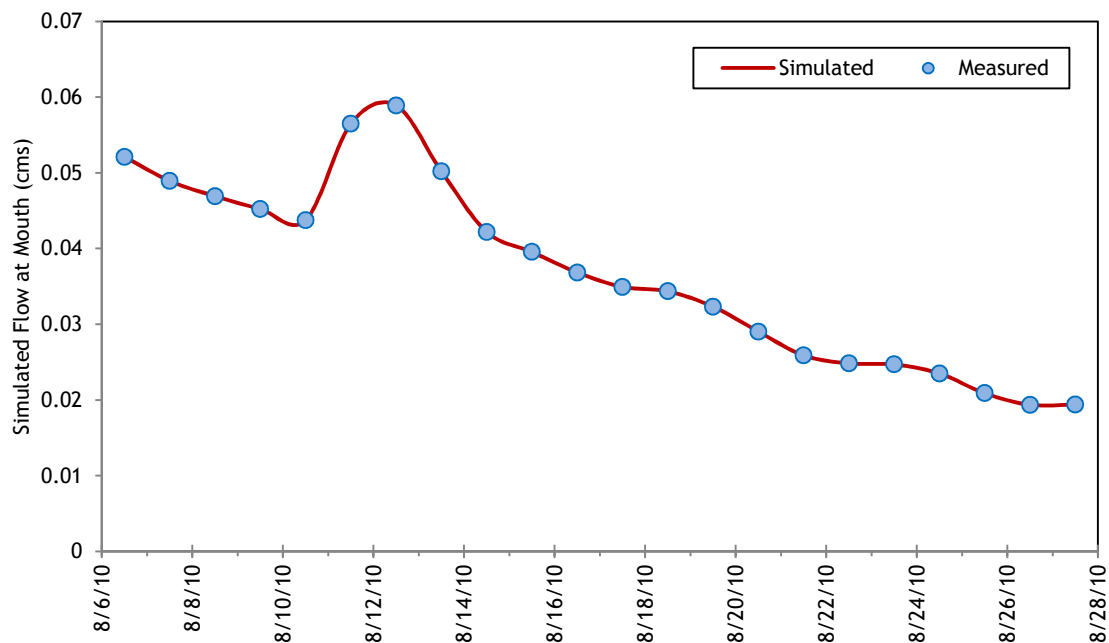
Figure 207 summarizes the simulated and measured hydraulic values for Five Points Creek. The simulated values are from August 25th, while the measured values were obtained on various dates.

Figure 207 - Five Points Creek simulated and measured hydraulic values.



The simulated daily flows at the mouth of Five Points Creek are presented in Figure 208. Daily variability was extrapolated from data measured at the Grande Ronde River gage near Perry.

Figure 208 - Five Points Creek simulated flow at mouth.



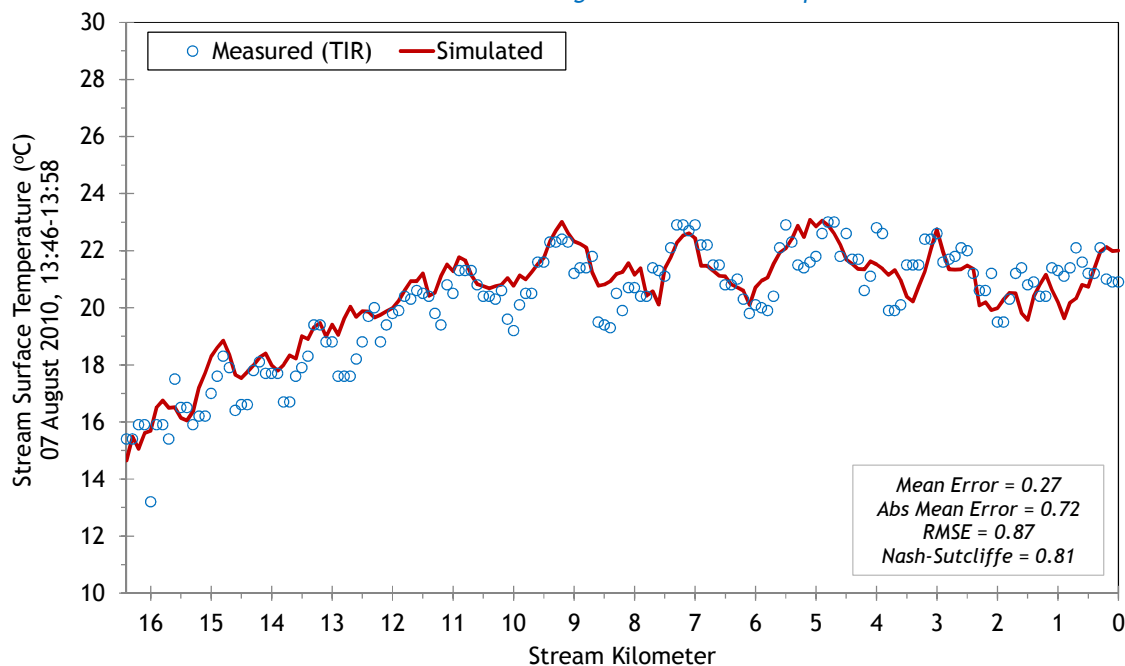
There were three active tributaries observed in the TIR imagery (Table 33). The flow volumes for each were estimated to be the same, while the TIR sampled temperatures were used for each.

Table 33 - Five Points Creek mass inflow features and assumptions.

Feature	Stream Km	Assumptions
Fiddlers Hell Creek	16.0	0.003-0.008 cms at constant 15.4°C
Tie Creek	15.5	0.003-0.008 cms at constant 13.4°C
Pelican Creek	2.3	0.003-0.008 cms at constant 18.3°C

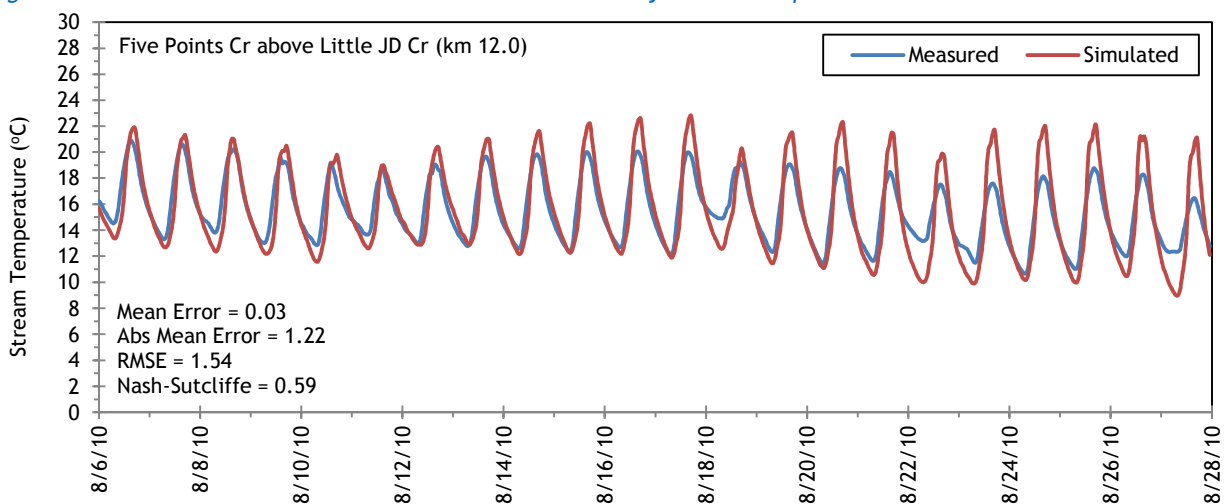
Figure 209 shows the simulated and measured longitudinal stream temperatures for Five Points Creek. There is a great deal of variability in the longitudinal temperatures mainly because of the low flow volume during the simulation time period.

Figure 209 - Five Points Creek simulated and measured longitudinal stream temperatures.



The simulated and measured hourly stream temperatures are presented in Figure 210. There were three locations where hourly stream temperatures were recorded.

Figure 210 - Five Points Creek simulated and measured hourly stream temperatures.



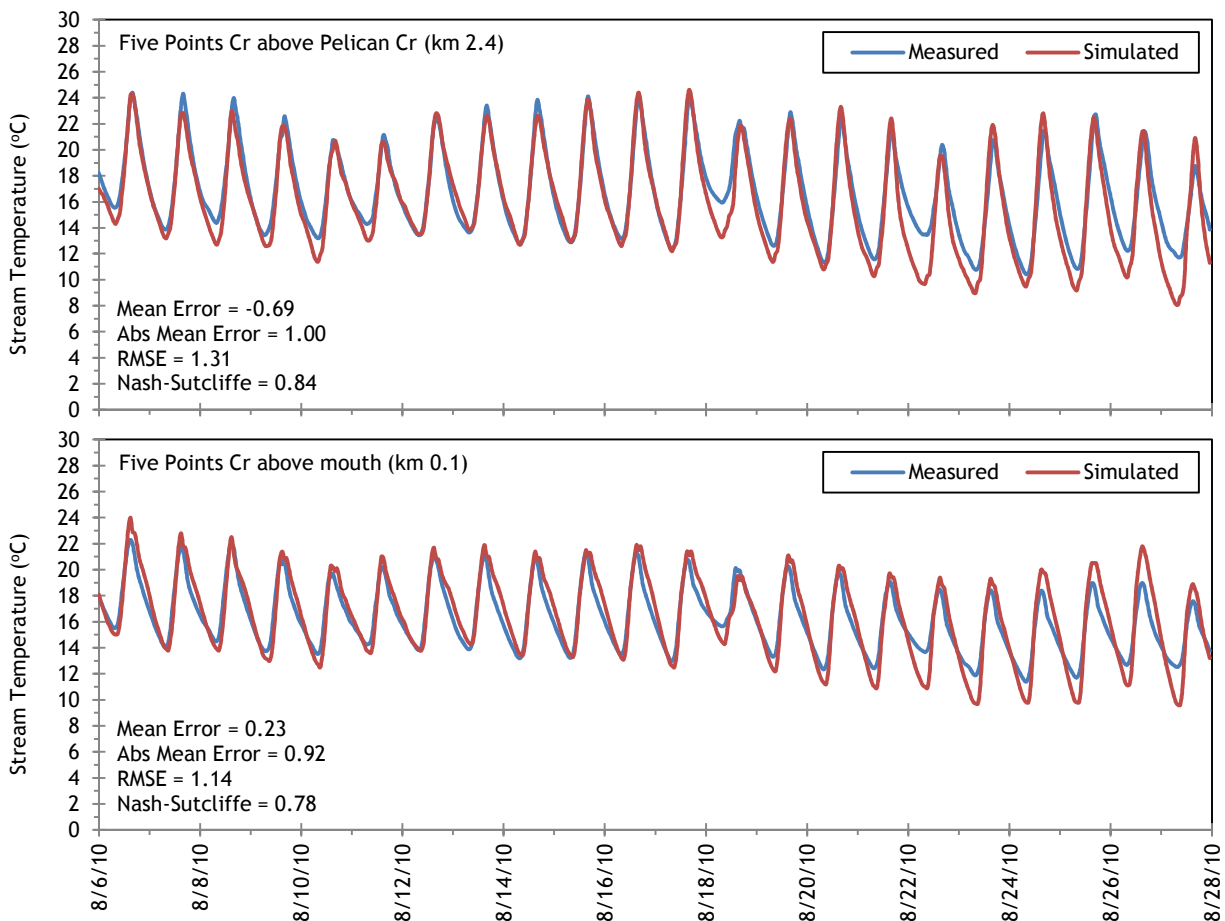
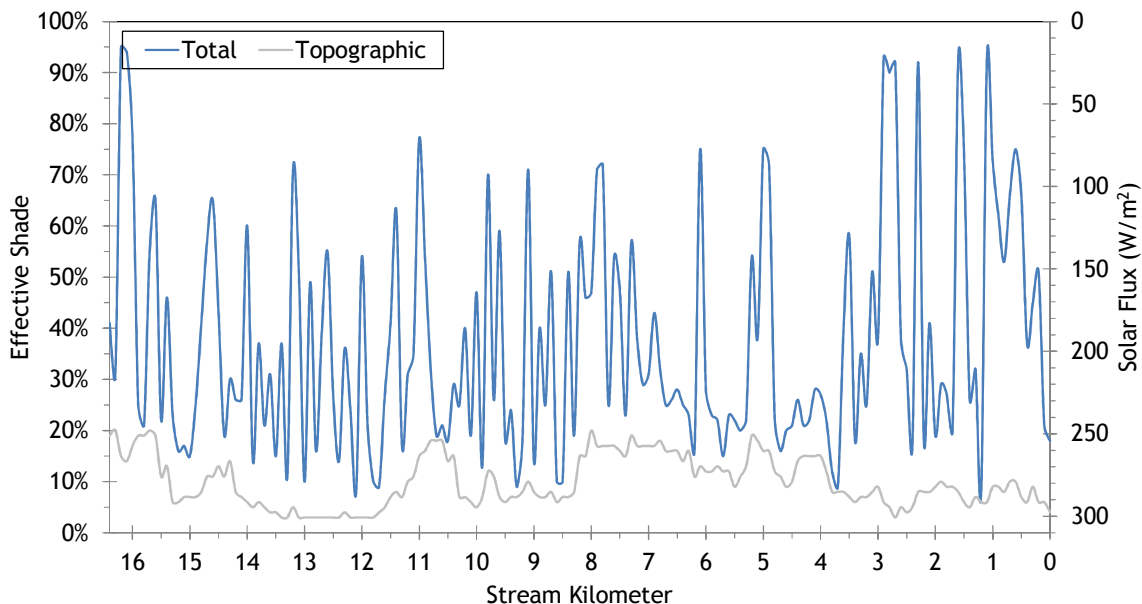
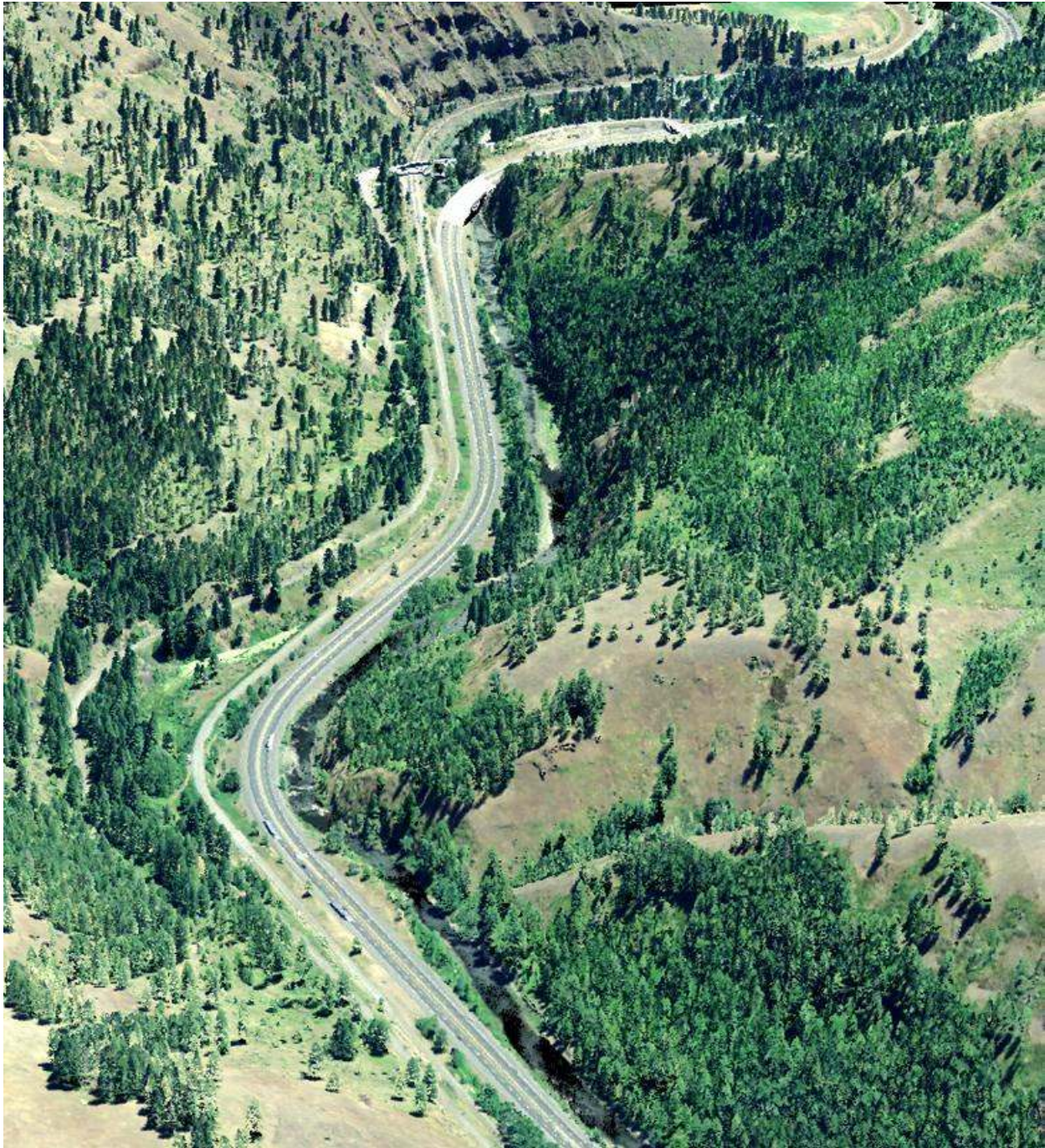


Figure 211 shows the simulated effective shade values for Five Points Creek. There is a fair amount of topographic shade created by the mountainous terrain.

Figure 211 - Five Points Creek simulated effective shade.



5.17 Grande Ronde River



RGB-colored LiDAR point cloud - Grande Ronde River alongside Interstate 84, below Five Points Creek (looking downstream).

5.17.1 Grande Ronde River TTools Results

The Grande Ronde River elevations and gradients were sampled from the bare earth LiDAR data (Figure 212). The upper reaches have a much higher gradient than the lower sections.

Figure 212 - Grande Ronde River elevation and gradient.

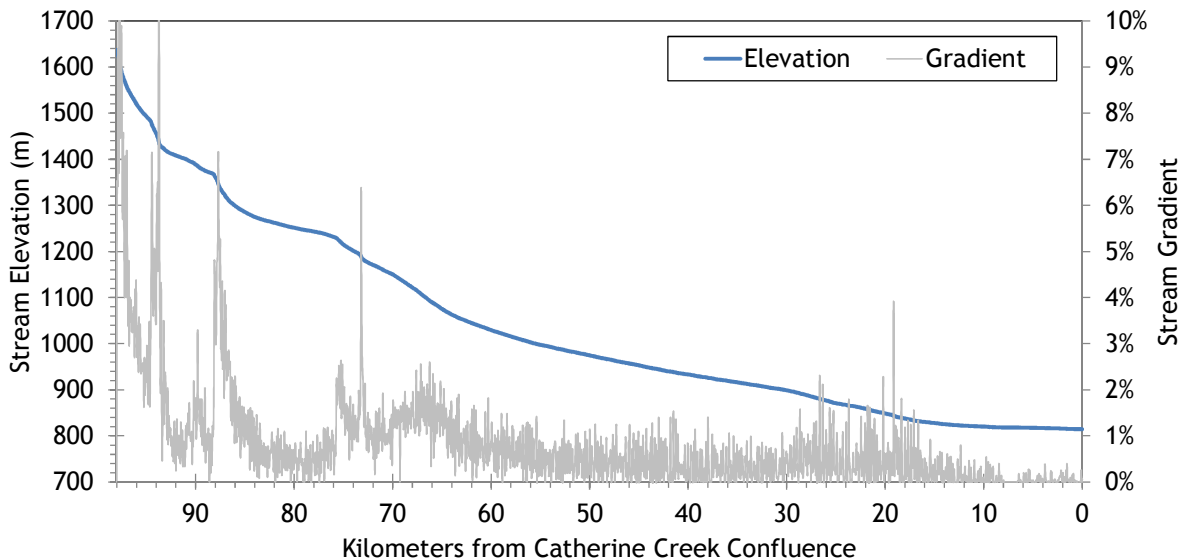


Figure 213 shows the sampled active and wetted channel widths along with the measured wetted widths. The Grande Ronde River generally gets wider as it flows downstream. Below stream kilometer 10, the channel is mostly diked and flows through a canal “State Ditch”.

Figure 213 - Grande Ronde River channel widths.

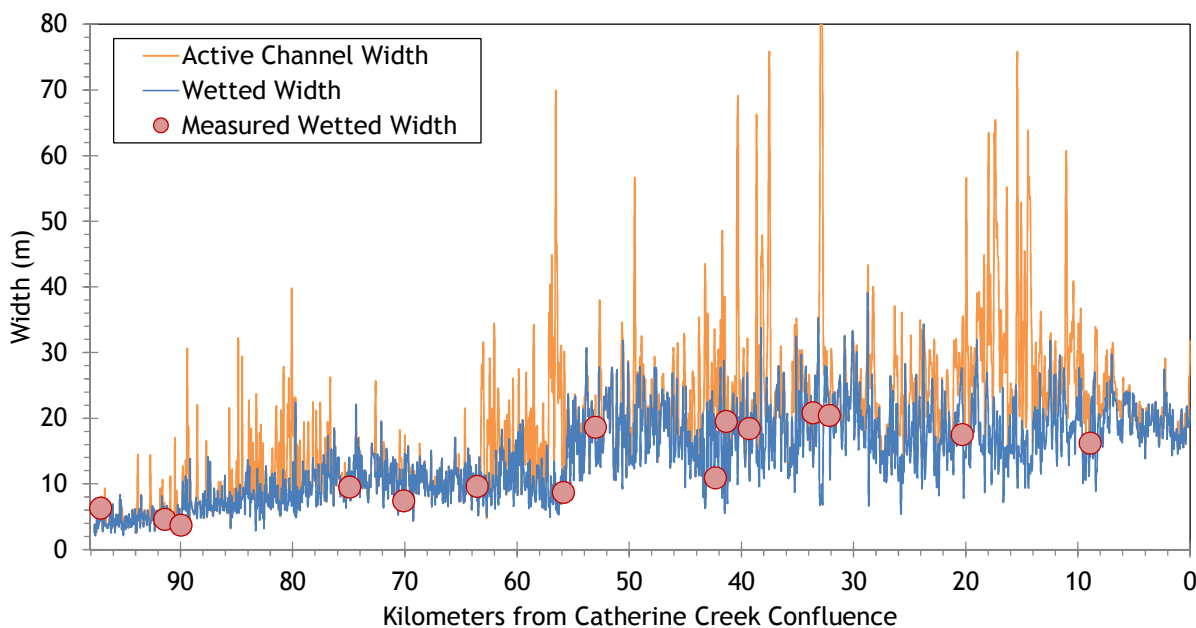
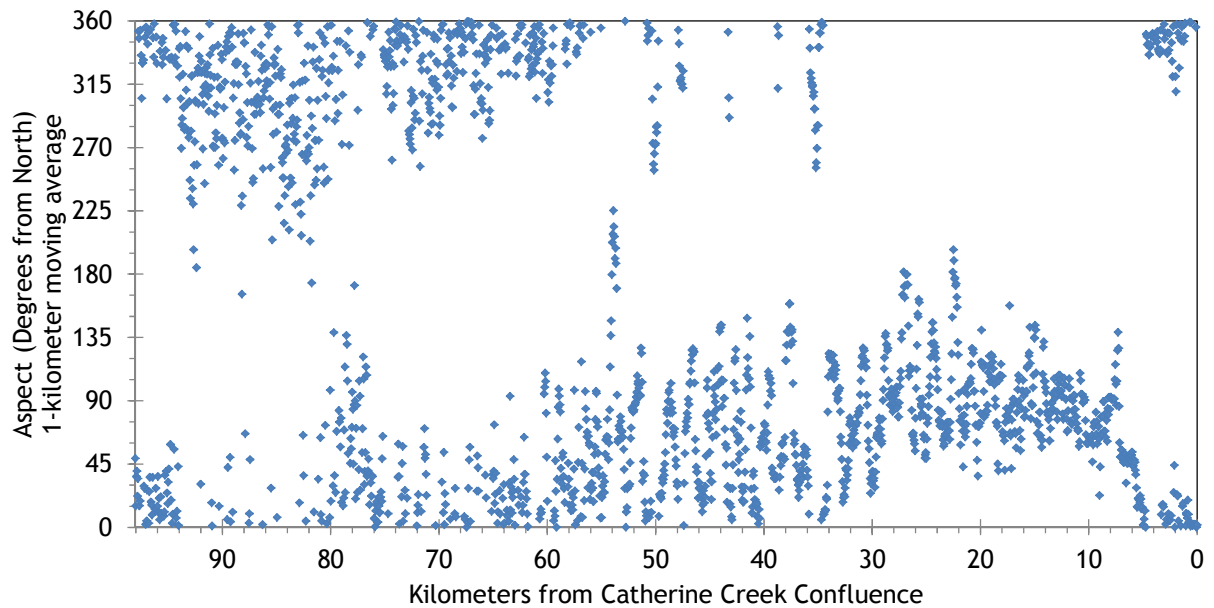


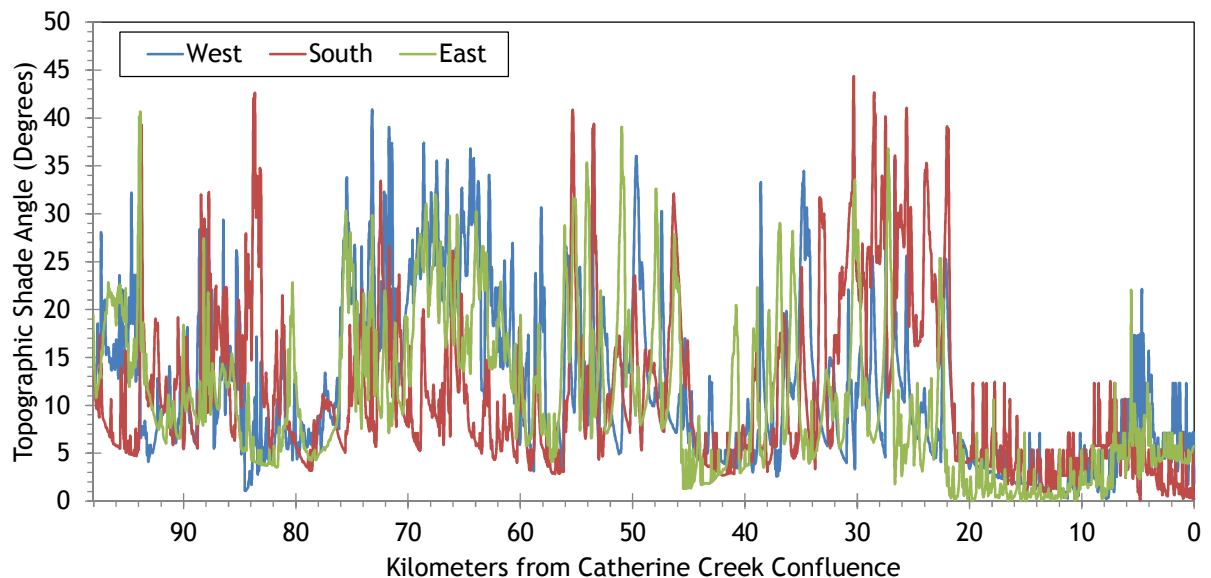
Figure 214 shows the stream aspect for each 50-meter segment of the Grande Ronde River. The river starts out flowing northerly, bends to the northeast between kilometers 60 and 30, then flows east through La Grande and the State Ditch.

Figure 214 - Grande Ronde River stream aspect.



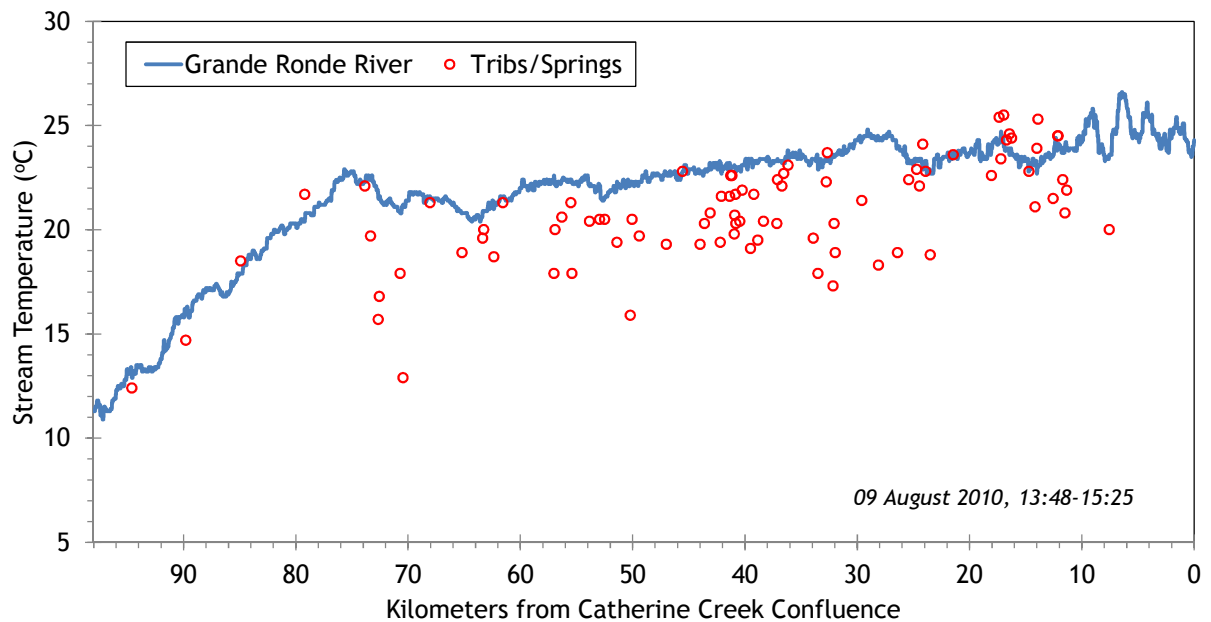
Topographic shade angles for the Grande Ronde River are shown in Figure 215. The upper river has a fair amount of topographic shade. The lower 20 kilometers are in the wide valley bottom and have much less topographic shade. In many of those lower 20 kilometers, the river banks are severely down-cut and it is the riverbanks that are producing the topographic shade.

Figure 215 - Grande Ronde River topographic shade angles.



The TIR stream temperature profile of the Grande Ronde River is shown in Figure 216. In the upper watershed, the stream is relatively cool, but heats steadily until approximately stream kilometer 75. Below that, stream temperatures hovered between 21 °C and 25 °C during the TIR flight.

Figure 216 - Grande Ronde River TIR stream temperature profile.



RGB-colored LiDAR point cloud - Grande Ronde River at Vey Meadow (flowing from right to left of image).

5.17.2 Grande Ronde River Heat Source Calibration Results

The Grande Ronde River was simulated from just below Tanner Gulch to the Catherine Creek confluence (Figure 217).

Figure 217 - Grande Ronde River simulation extent.

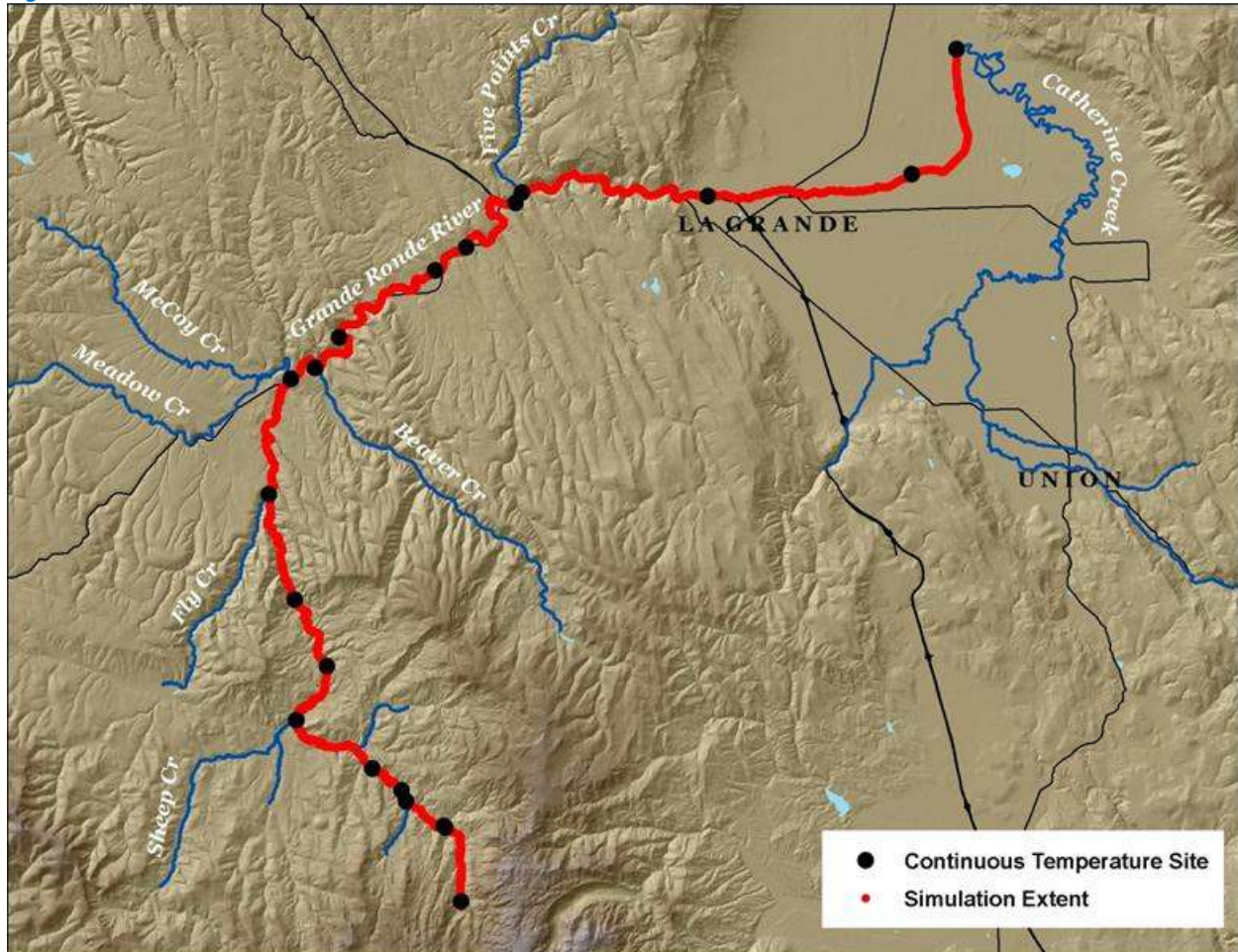


Table 34 - Grande Ronde River general Heat Source parameters.

Stream:	Grande Ronde River
Length:	97.2 kilometers
Time Period:	August 6-27, 2010
Input Distance Step:	50 meters
Output Distance Step:	100 meters
Time Step:	1 minute
Flush Initial Condition:	7 days
TIR Date and Time:	August 9, 2010 13:48-15:25
Land Cover Data Source:	LiDAR
Land Cover Sampling Distance Step:	15 meters

The following assumptions were used when calibrating the Grande Ronde River Heat Source model:

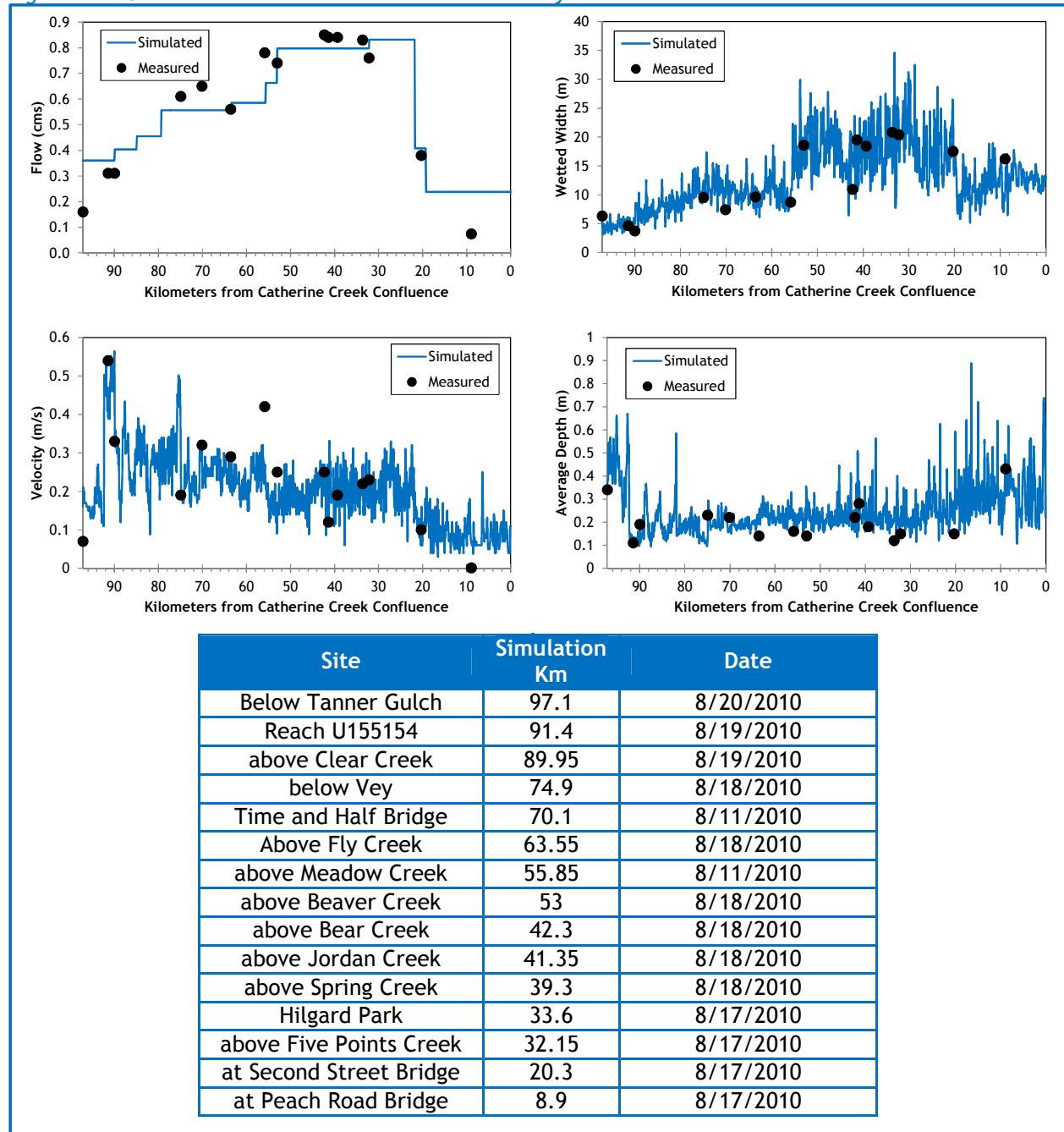
- Hourly climate data is from the La Grande airport. Wind speeds were reduced and air temperatures were adjusted for the adiabatic lapse rate of 1°C per 100 meters elevation.
- Wetted widths were digitized from the TIR and LiDAR intensity images.
- Most inflows observed in the TIR data were very small compared to the Grande Ronde River flow and did not produce measurable thermal influences. Therefore, only the larger inflows were included within the model, which includes but is not limited to the other simulated tributaries.
- There is significant withdrawal that occurs in La Grande. The withdrawals are not monitored and are likely to vary greatly during the simulation time period. Since the majority of water is consumed starting in the reaches through and below La Grande and the gradient is very low, the model exhibited instability below simulation kilometer 10. In addition, there is likely thermal stratification occurring in those low-gradient reaches below La Grande, which Heat Source is incapable of simulating. For these reasons, less water was removed at the diversions than was probably actually occurring.
- **Model results below simulation kilometer 21.75 should be considered as rough estimates only and should not be used for regulatory or planning purposes.**



RGB-colored LiDAR point cloud - Grande Ronde River above Meadow Creek (looking downstream).

Figure 218 shows the simulated and measured hydraulics values for the Grande Ronde River. Note that the measured data were collected on several different days, while the simulated values are plotted only for August 18, 2010.

Figure 218 - Grande Ronde River simulated and measured hydraulic values.



The simulated and measured flows at each gage are shown in Figure 219. The flow volumes were set up within the model to target the measured daily average flows at each gage. There were small rain events around August 11th and 18th that resulted in elevated flow volumes.

Figure 219 - Grande Ronde River simulated and measured flows at the gages.

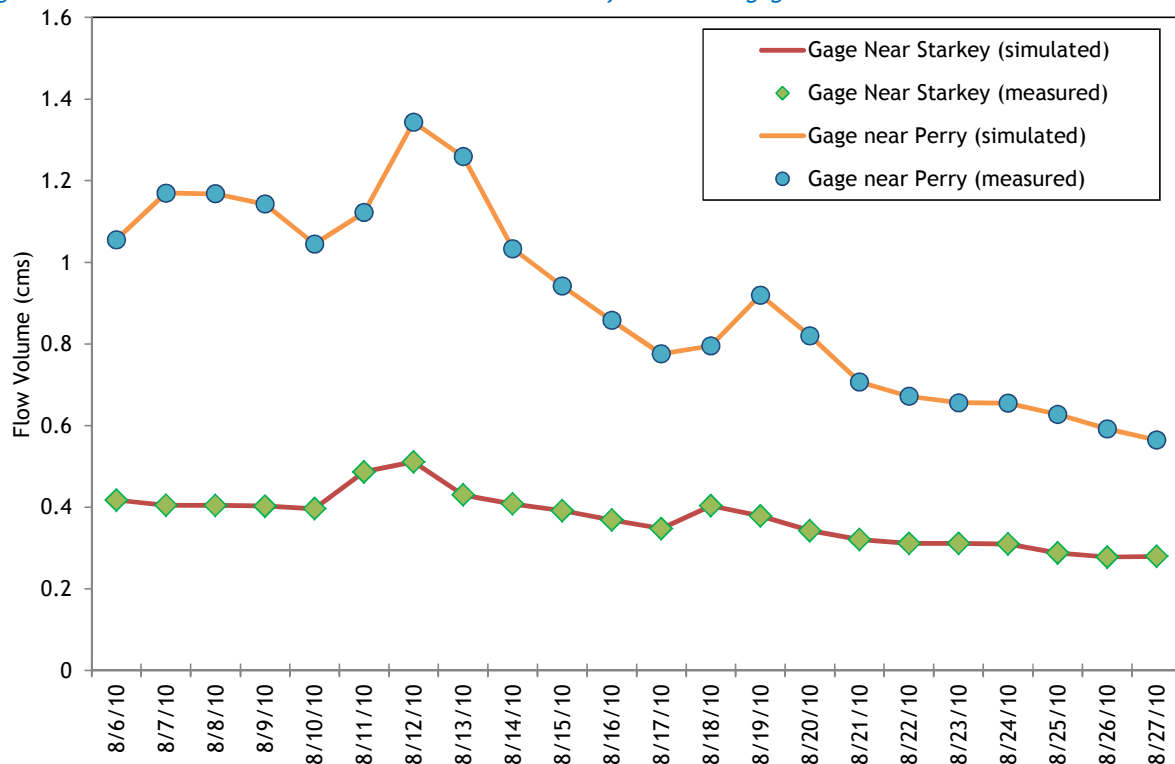


Table 1 summarizes the inflows and outflows included in the Grande Ronde River Heat Source model. All tributary flows had daily values estimated based on CRITFC measurements and patterns derived from Grande Ronde River gage data (see previous sections). Hourly stream temperatures were measured near the mouth of each tributary. The diversion rates were estimated as a constant percentage of the stream flow.

Table 35 - Grande Ronde River mass inflow and outflow features and assumptions.

Feature	Stream Km	Assumptions
Clear Creek	89.85	Simulated flow volume, measured hourly temperatures.
Limber Jim Creek	84.9	Simulated flow volume, measured hourly temperatures.
Sheep Creek	79.3	Simulated flow volume, measured hourly temperatures.
Fly Creek	63.35	Simulated flow volume, measured hourly temperatures.
Meadow Creek	55.55	Simulated flow volume, measured hourly temperatures.
Beaver Creek	52.95	Simulated flow volume, measured hourly temperatures.
Bear Creek	42.1	Simulated flow volume, measured hourly temperatures.
Spring Creek	38.95	Simulated flow volume, measured hourly temperatures.
Rock Creek	32.75	Simulated flow volume, measured hourly temperatures.
Five Points Creek	32.1	Simulated flow volume, measured hourly temperatures.
Dobbins Diversion	21.75	Estimated to be 51% of stream flow - based on 8/17/2010 CRITFC upstream and downstream flow measurements.
Diversion	19.2	Estimated to be 40% of stream flow (further reduction causes model instability)

The simulated and measured longitudinal stream temperatures are shown in Figure 220. There is an apparent “drop” in the simulated temperature near kilometer 38, but that is an artifact of the model changing times for its output data. Upstream of that location, the simulation output is for the 14:00 hour, and downstream the simulation output is for the 15:00 hour, causing an artificial temperature drop. The results below kilometer 21.75 should be considered for information purposes only because the diversions were not monitored and there is likely thermal stratification occurring.

Figure 220 - Grande Ronde River simulated and measured longitudinal stream temperatures.

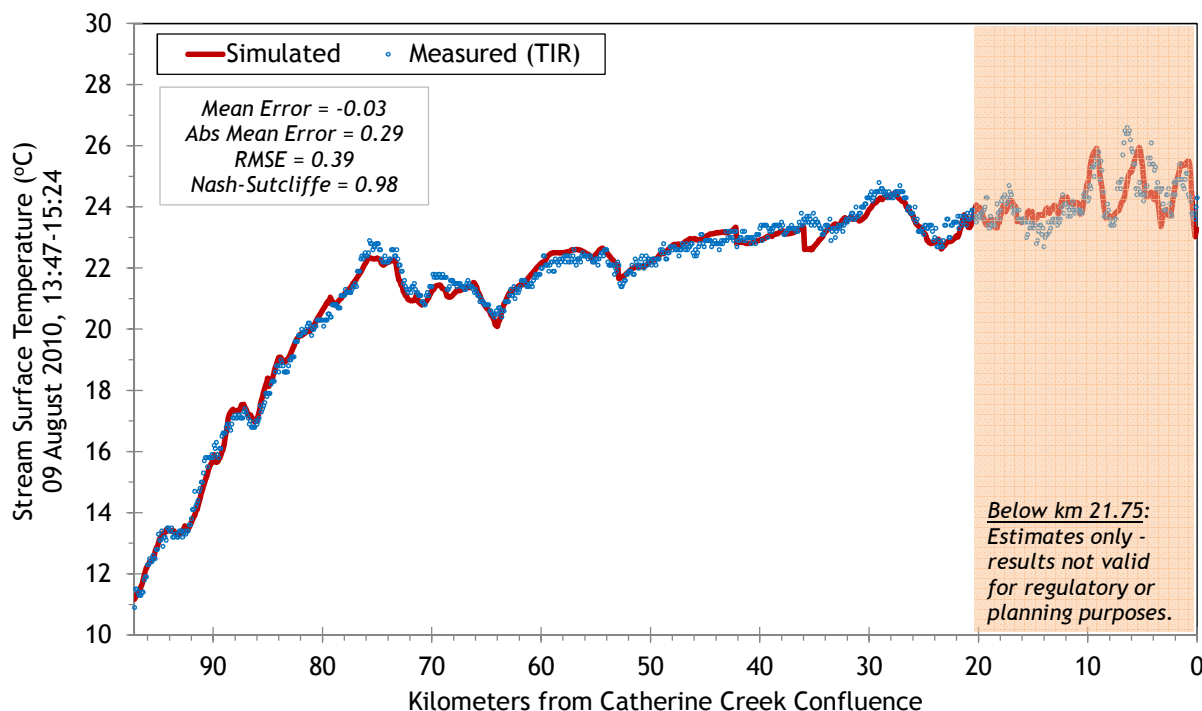
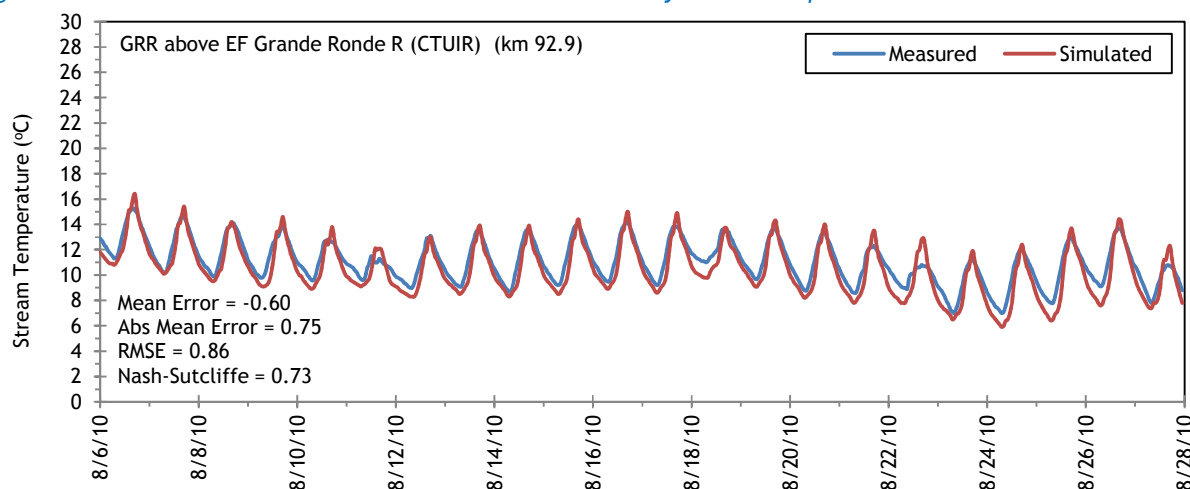
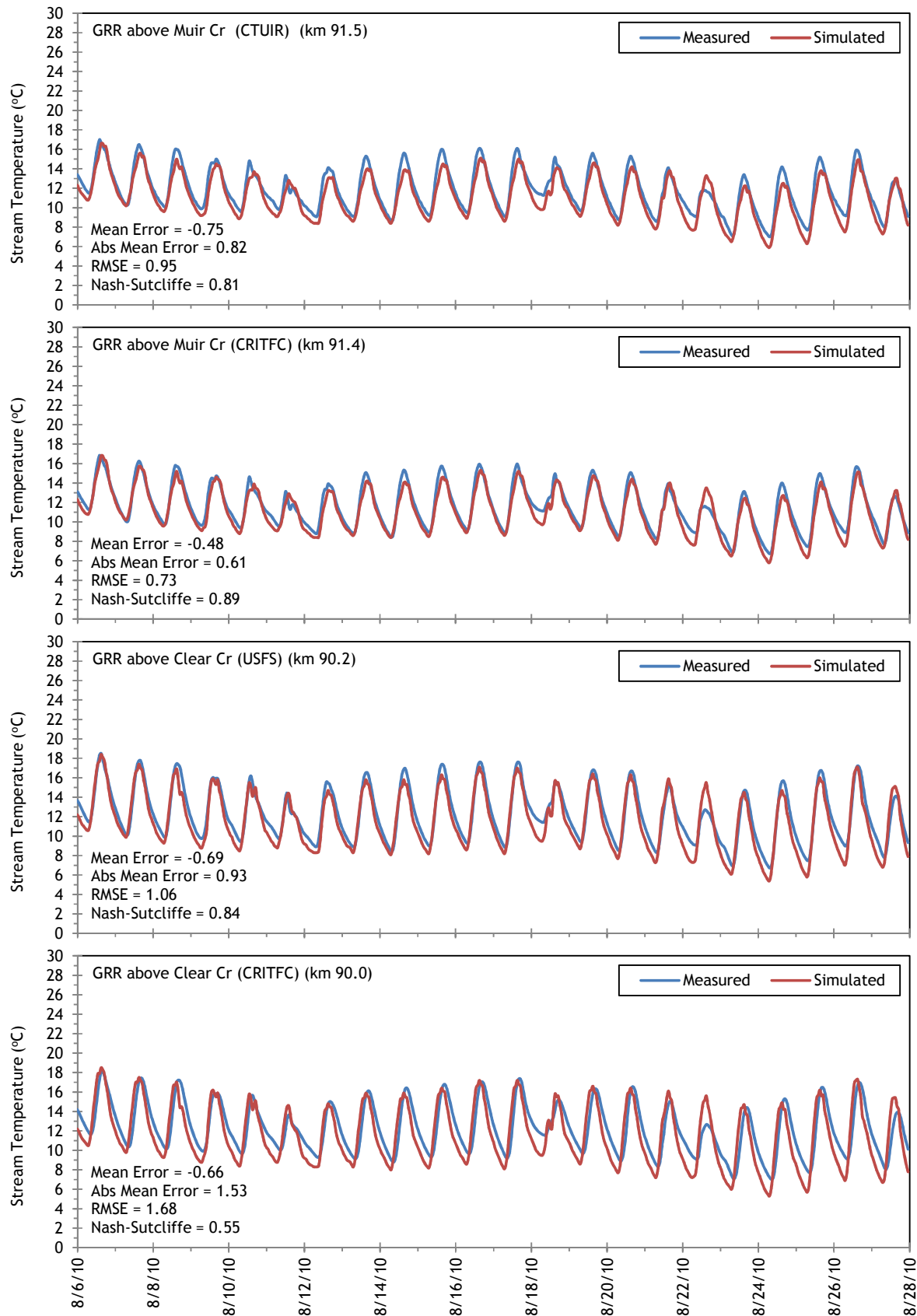
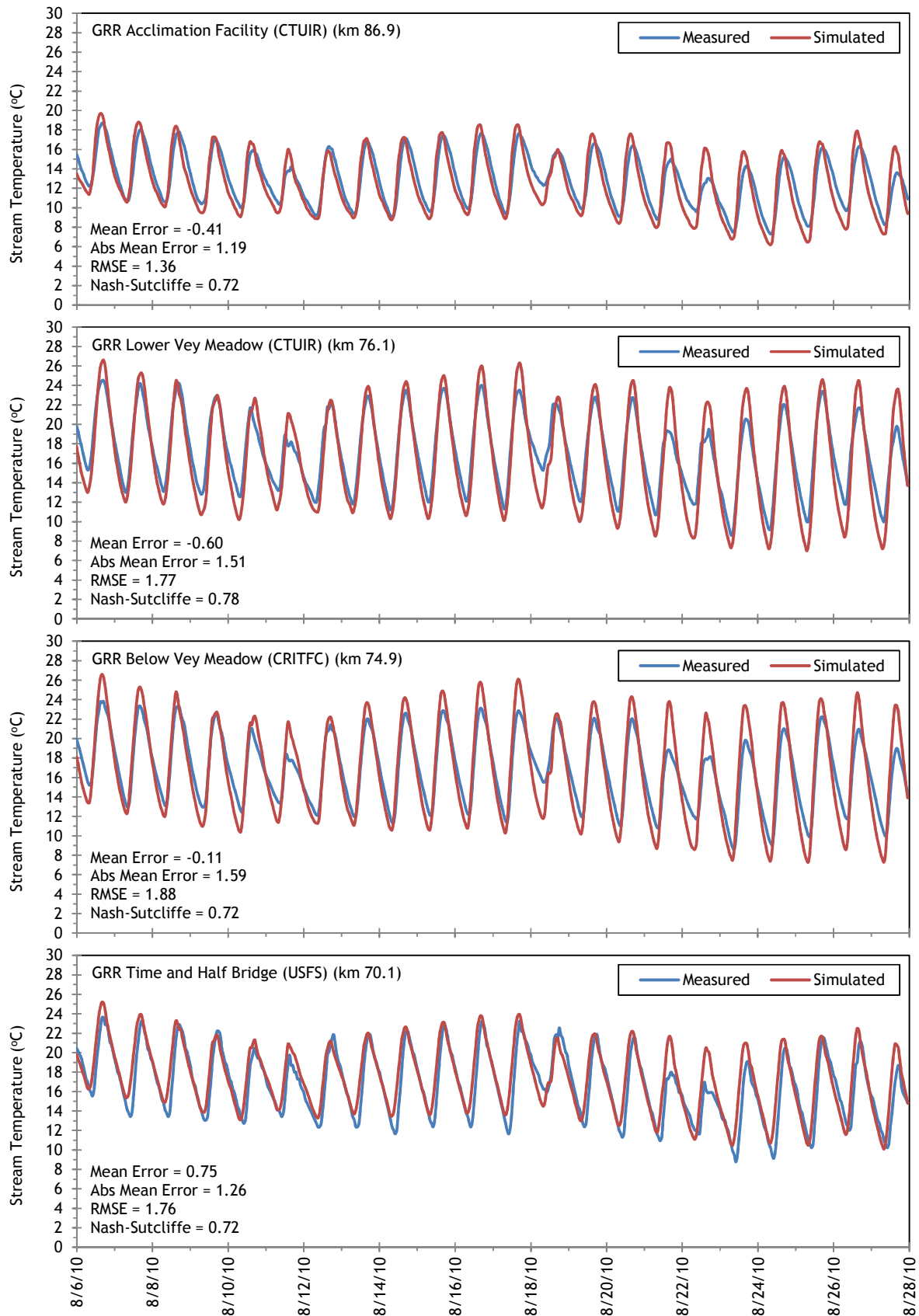


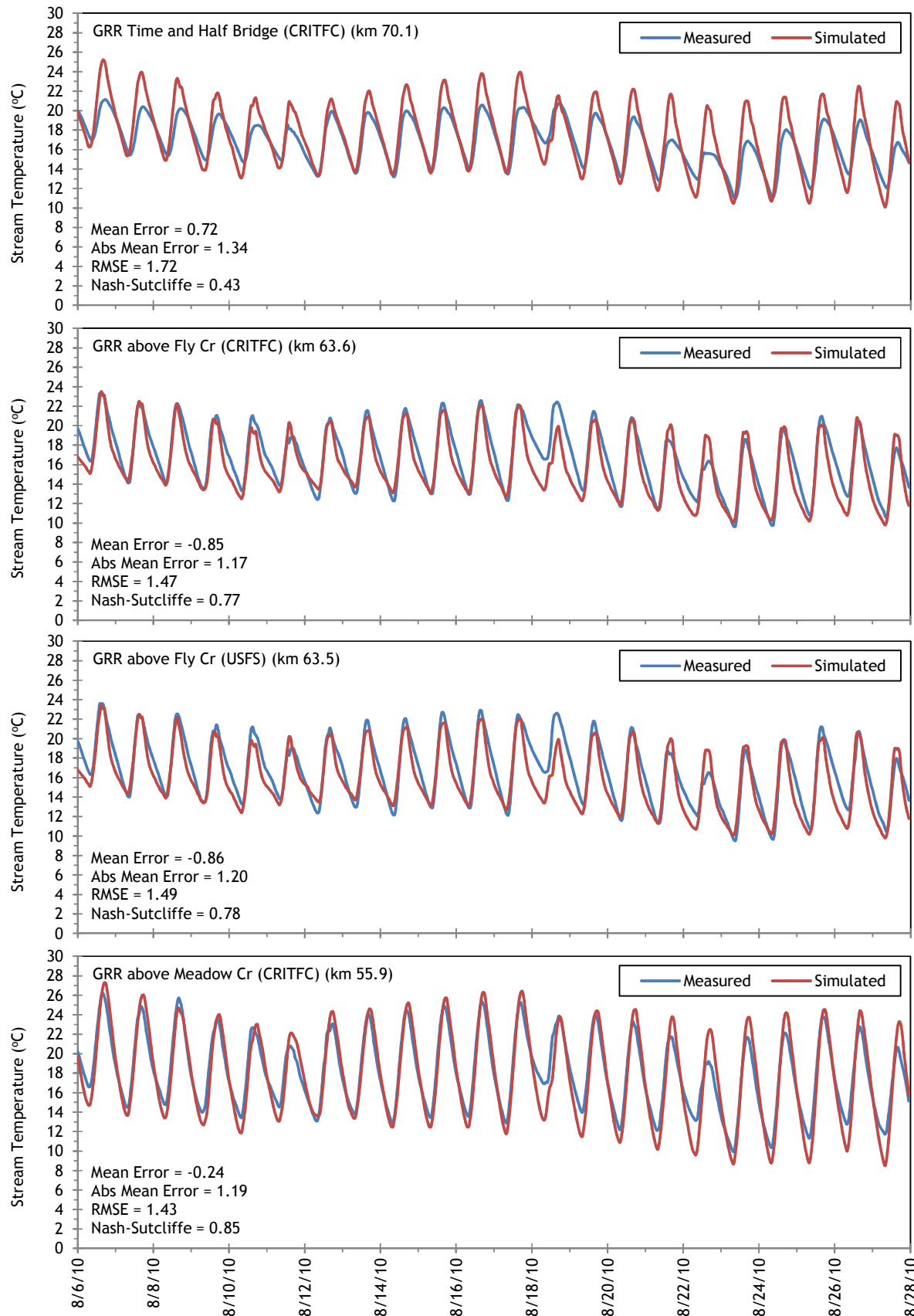
Figure 221 shows the simulated and measured hourly stream temperatures at locations along the Grande Ronde River where thermistors were deployed. Calibration statistics are included on each plot.

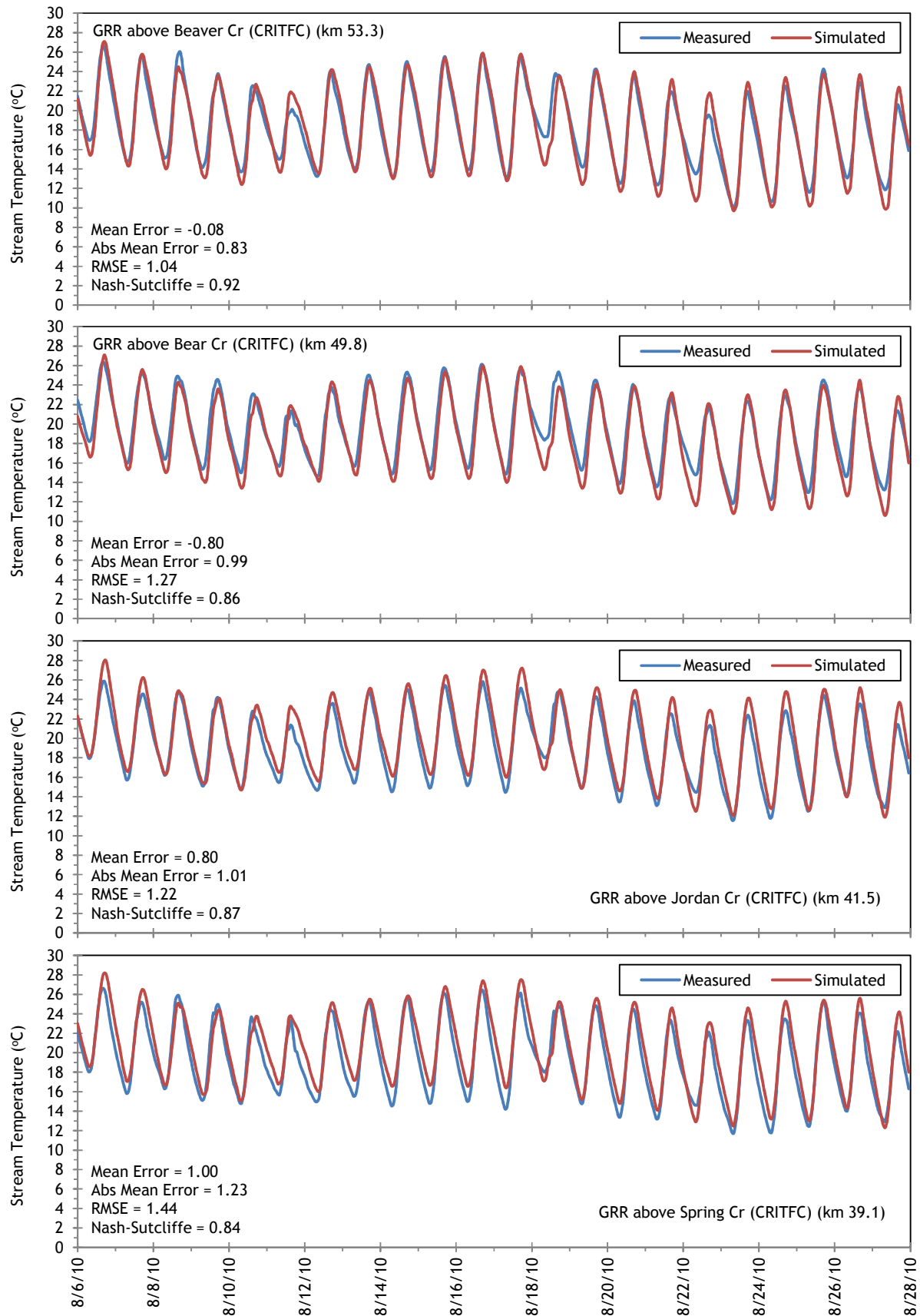
Figure 221 - Grande Ronde River simulated and measured hourly stream temperatures.

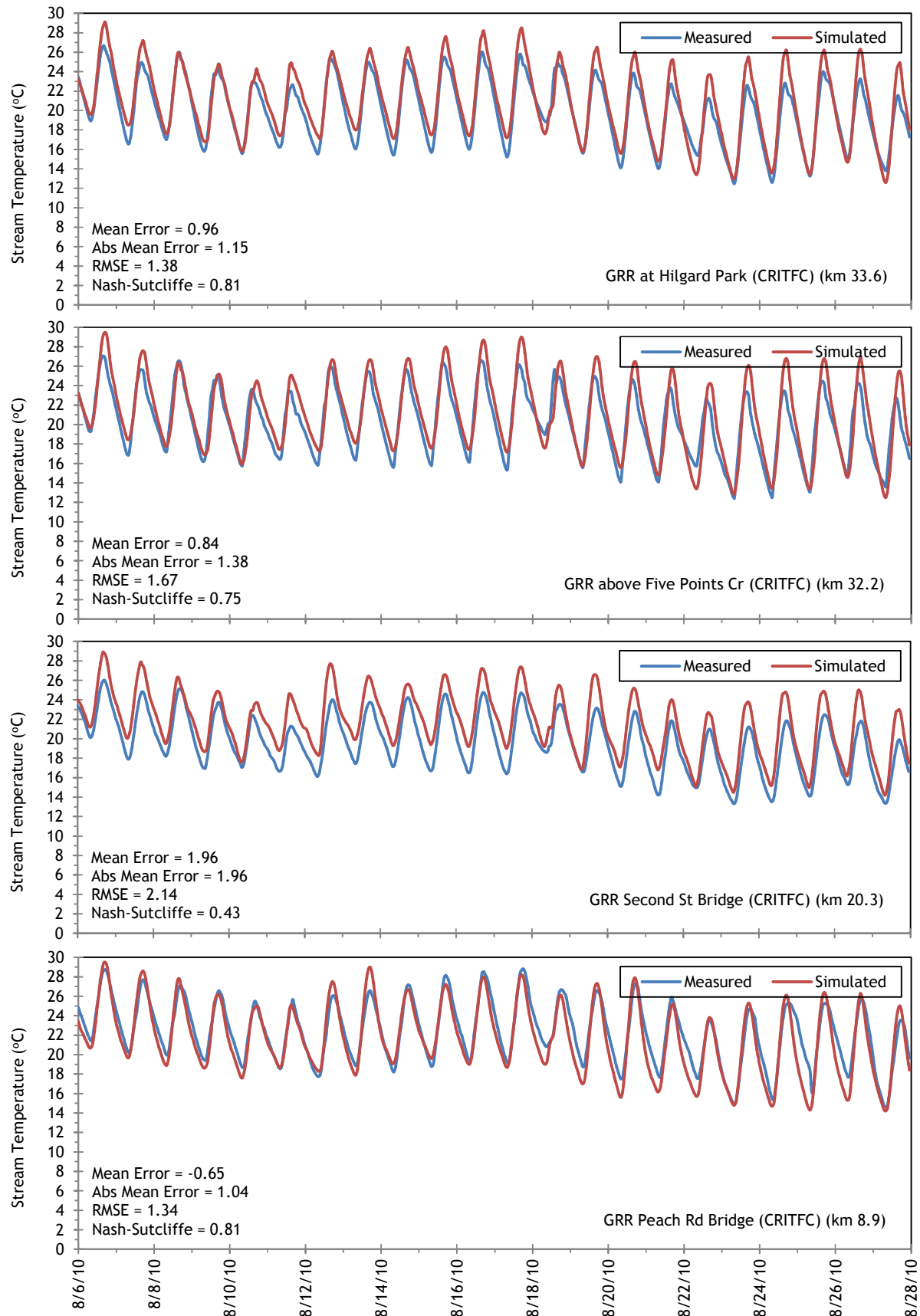






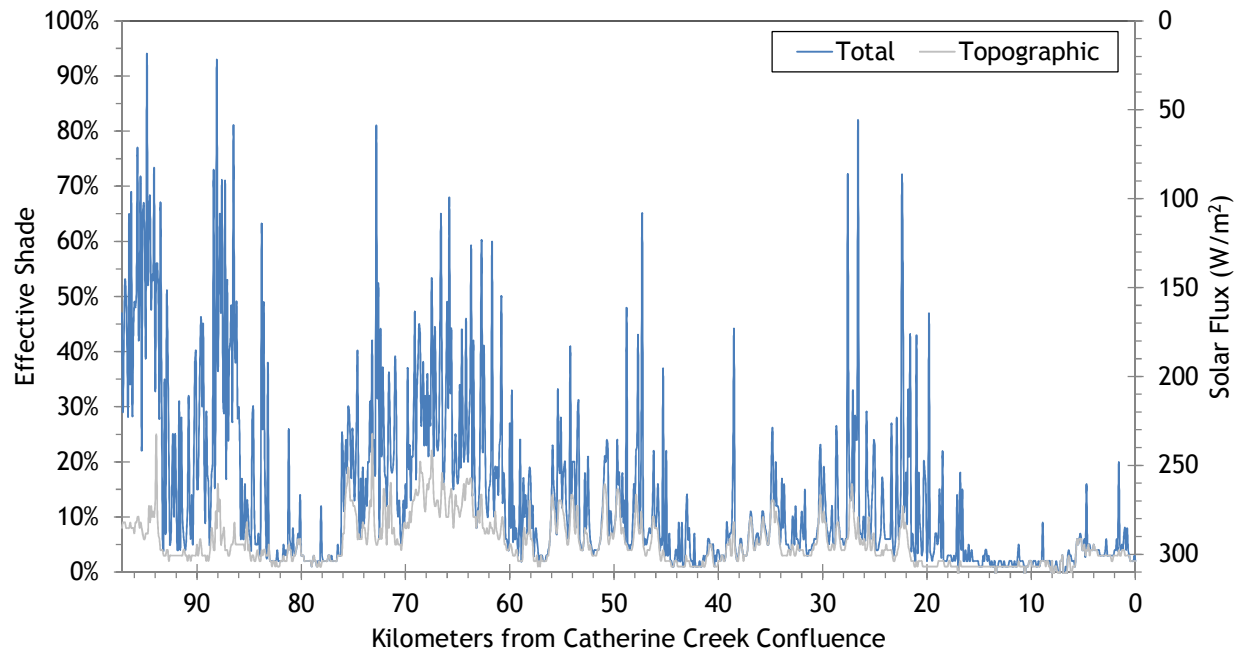


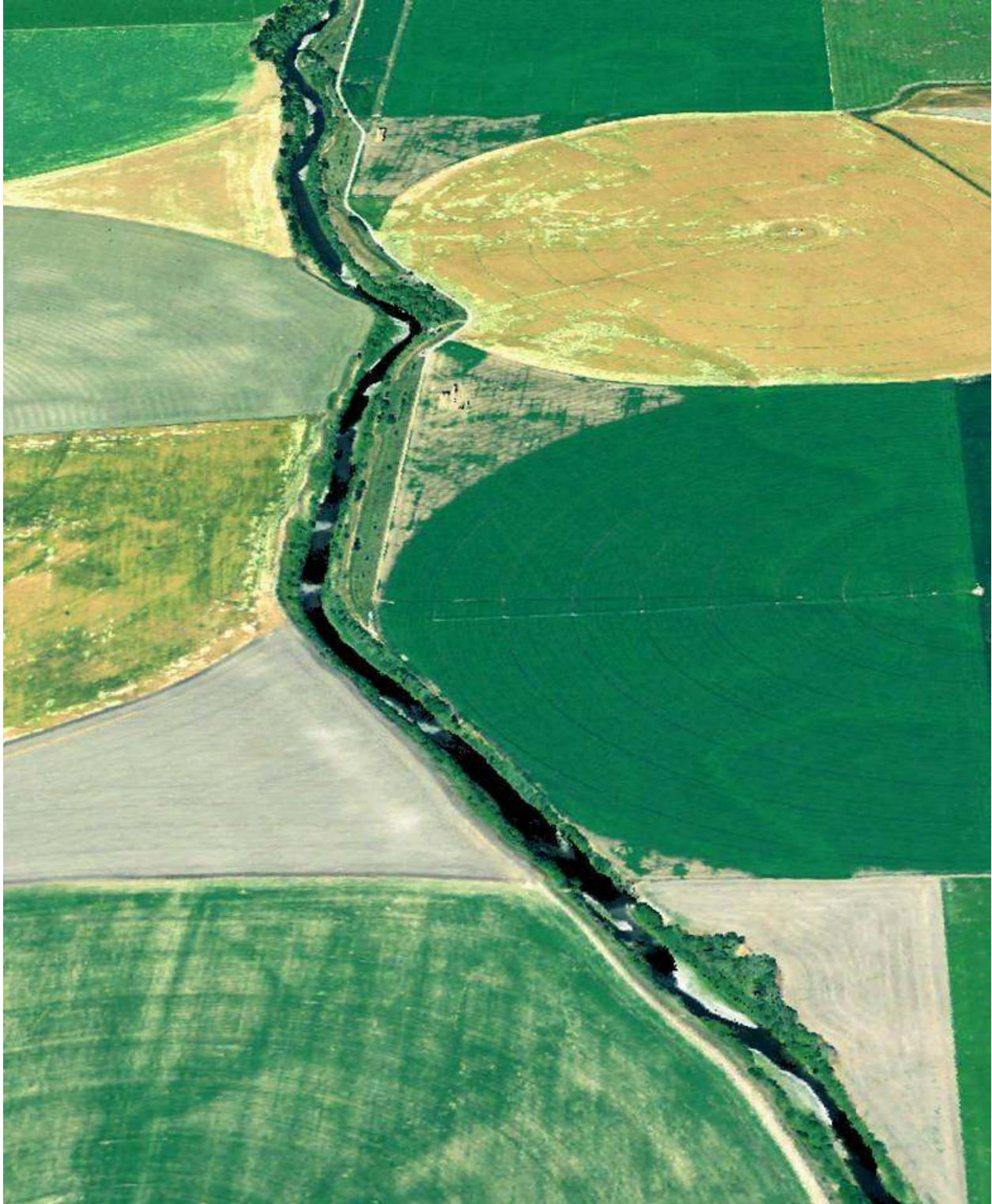




The simulated effective shade for the Grande Ronde River is presented in Figure 222. In many reaches, topography is producing the majority of effective shade. The Grande Ronde River is also wider than its tributaries and some reaches have less effective shade for that reason. Additionally, there is often a road or interstate highway alongside the river, which reduces the amount of near stream land cover. Below La Grande (approximately kilometer 22), there is less effective shade because the river is within the agricultural valley bottom where there are few large trees.

Figure 222 - Grande Ronde River simulated effective shade.





RGB-colored LiDAR point cloud - Grande Ronde River below the city of La Grande (looking upstream).

6. SIMULATED SCENARIOS

The calibrated Heat Source models were used to simulate a variety of scenarios. The results of each scenario may be considered similar to a sensitivity analysis. Parameters were changed one at a time and the model was then run for each stream. Results from the mouths of simulated tributaries were used as inputs to the appropriate simulated receiving stream (i.e., the stream network modeling approach was used). This section describes the various scenarios and presents the temperature results for each stream.

Table 36 summarizes the scenarios that were run for each stream.

Table 36 - Scenarios and Associated Assumptions.

Scenario	Assumptions
Climate (+2°C)	<ul style="list-style-type: none"> 2°C was added to the hourly air temperature at all locations.
50% Flow	<ul style="list-style-type: none"> Boundary condition flow volume was reduced 50%. Tributary inflows were reduced 50%. Diversions were reduced 50% (in order to accommodate lower stream flow volume availability).
150% Flow	<ul style="list-style-type: none"> Boundary condition flow volume was increased to 150%. Tributary inflows were increased 150%. Diversion rates were not changed.
No Diversions	<ul style="list-style-type: none"> Diversions were removed. No other flow inputs were altered.
Potential Natural Vegetation (PNV)	<ul style="list-style-type: none"> PNV values were estimated based upon the Upper Grande Ronde River Subbasin TMDL¹. Elevations above 4800 feet were assigned vegetation at 17.4 meters tall and 80% density. Elevations below 4800 feet were assigned vegetation at 33.5 meters tall and 80% density.
No Diversions & Potential Natural Vegetation	<ul style="list-style-type: none"> Combined inputs of the “No Diversions” scenario and the “Potential Natural Vegetation” scenario.

¹ Oregon Department of Environmental Quality. 1999. Upper Grande Ronde River Subbasin TMDL.

In some cases, particular scenarios were not applicable to a stream. Table 37 summarizes which scenarios were run on which streams.

Table 37 - Summary of scenarios that were run for each stream.

Watershed	Stream	Climate (+2°C)	No Diversions	50% Flow	150% Flow	Potential Natural Vegetation	No Diversions & Potential Natural Vegetation
Catherine Creek	North Fork Catherine Creek	✓	NA	✓	✓	✓	NA
	South Fork Catherine Creek	✓	NA	✓	✓	✓	NA
	Milk Creek	✓	NA	✓	✓	✓	NA
	Little Catherine Creek	NA	NA	NA	NA	Shade	NA
	Little Creek	✓	✓	✓	✓	✓	✓
	Ladd Creek	NA	NA	NA	NA	Shade	NA
	Catherine Creek (upper)	✓	✓	✓	✓	✓	✓
	Catherine Creek (lower)	NA	NA	NA	NA	Shade	NA
Upper Grande Ronde River	Clear Creek	✓	NA	✓	✓	✓	NA
	Limber Jim Creek	✓	NA	✓	✓	✓	NA
	Chicken Creek	✓	NA	✓	✓	✓	NA
	Sheep Creek	✓	NA	✓	✓	✓	NA
	Fly Creek	✓	NA	✓	✓	✓	NA
	Meadow Creek	✓	NA	✓	✓	✓	NA
	McCoy Creek	NA	NA	NA	NA	Shade	NA
	Beaver Creek	✓	NA	✓	✓	✓	NA
	Five Points Creek	✓	NA	✓	✓	✓	NA
	Grande Ronde River	✓	✓	✓	✓	✓	✓

6.1 North Fork Catherine Creek

The North Fork Catherine Creek simulated scenario results are shown in Figure 223. The lower half of the simulated stream was more sensitive to changes in flow and air temperature. The entire stream temperature was reduced under the simulated potential natural vegetation. Since tributary inputs were not changed in the PNV scenario, there are some “stair steps” where they enter the stream at their currently warmer conditions.

Figure 223 - North Fork Catherine Creek simulated scenario results.

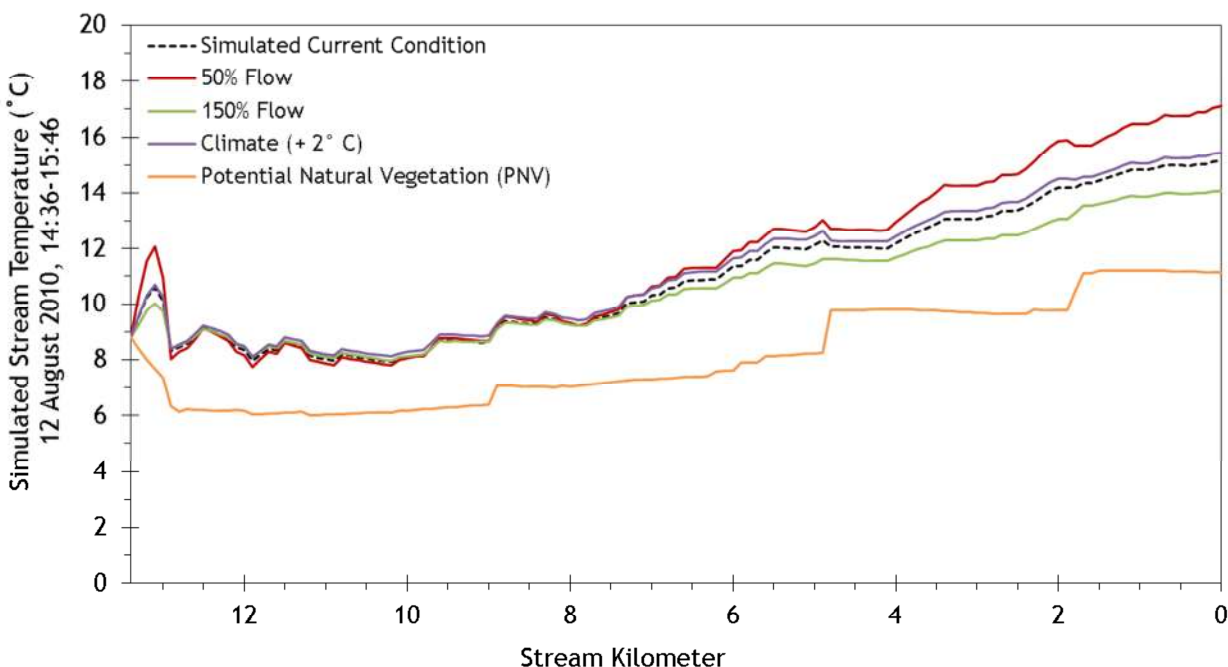
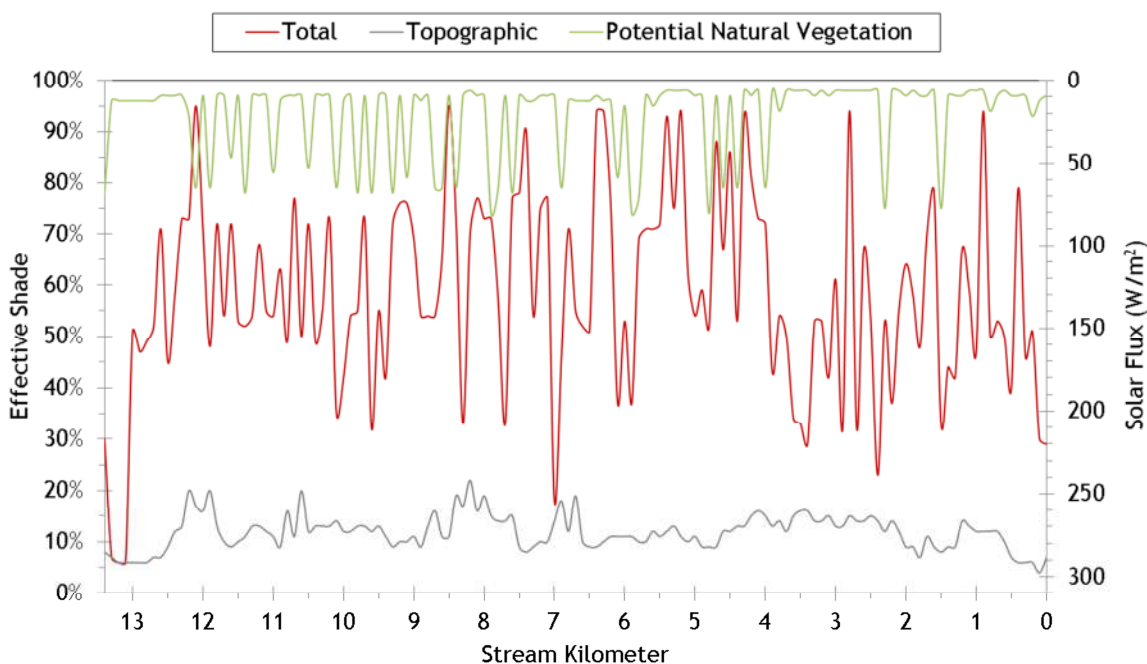


Figure 224 - North Fork Catherine Creek simulated effective shade.



6.2 South Fork Catherine Creek

The South Fork Catherine Creek scenario results are presented in Figure 225. Overall, the stream temperature was more sensitive to flow volume along its entire length. Incorporating the potential natural vegetation conditions increased shade enough that there was little longitudinal temperature increase.

Figure 225 - South Fork Catherine Creek simulated scenario results.

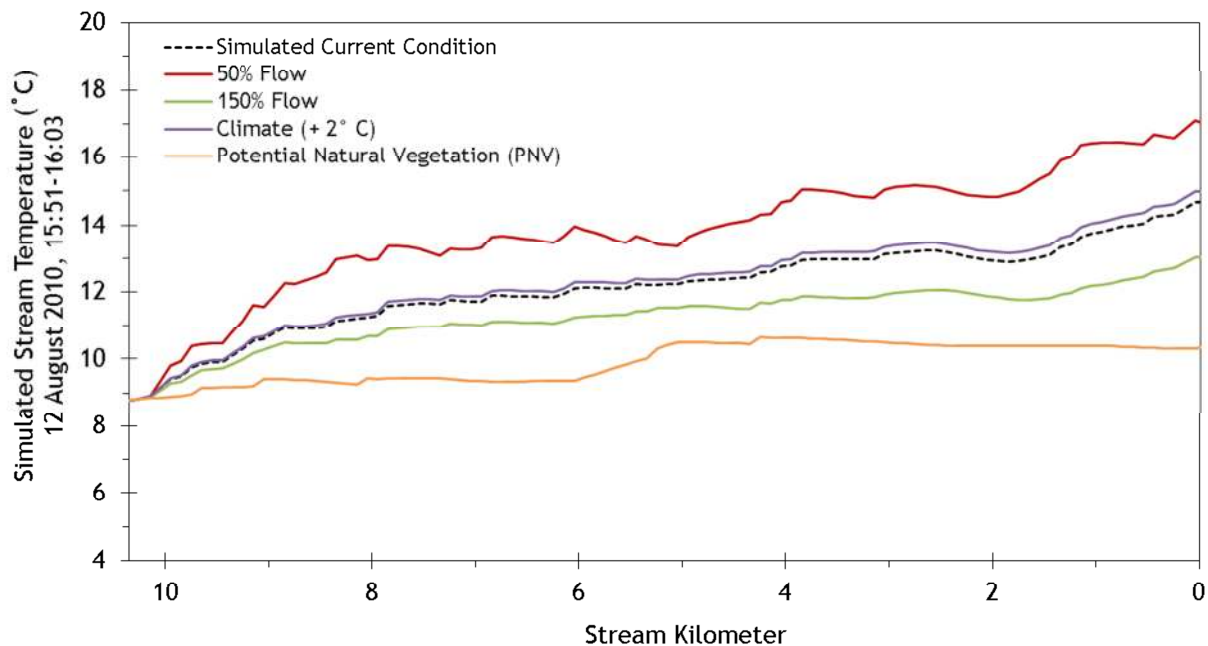
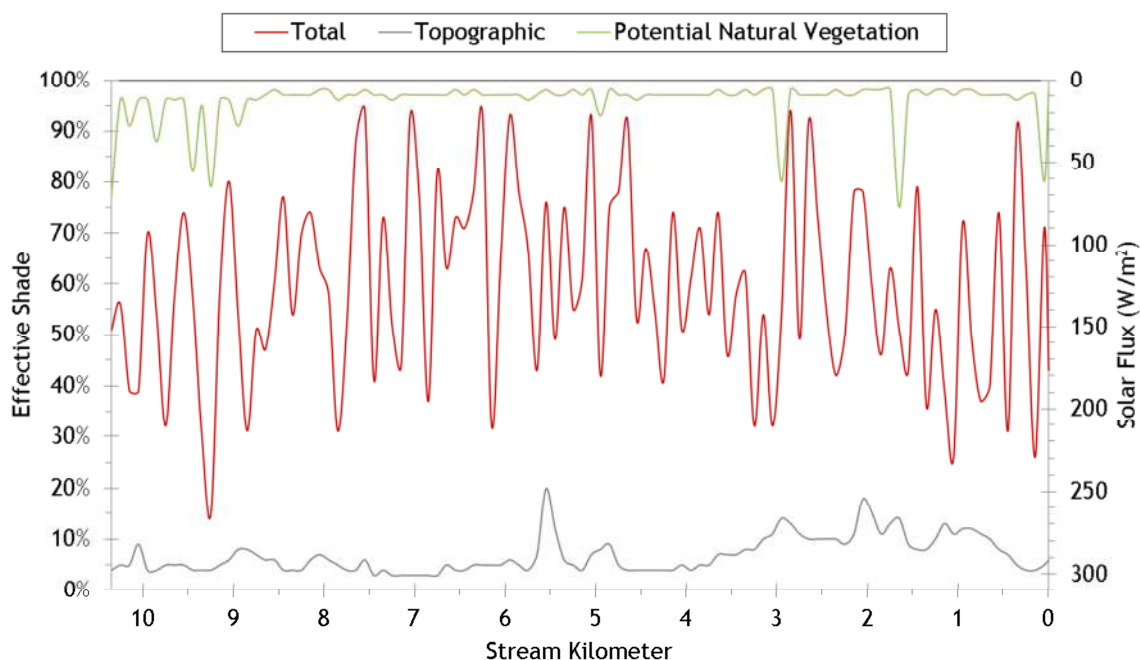


Figure 226 - South Fork Catherine Creek simulated effective shade.



6.3 Milk Creek

Milk Creek simulated scenario results are shown in Figure 227. Only the lower 3.4 kilometers were simulated, so the stream starts out at a warmer temperature than in the upper reaches. The boundary condition was not changed in any of the scenarios. As a result, the PNV scenario shows a gradual temperature decline as the simulated water mass “equilibrates” with its surroundings.

Figure 227 - Milk Creek simulated scenario results.

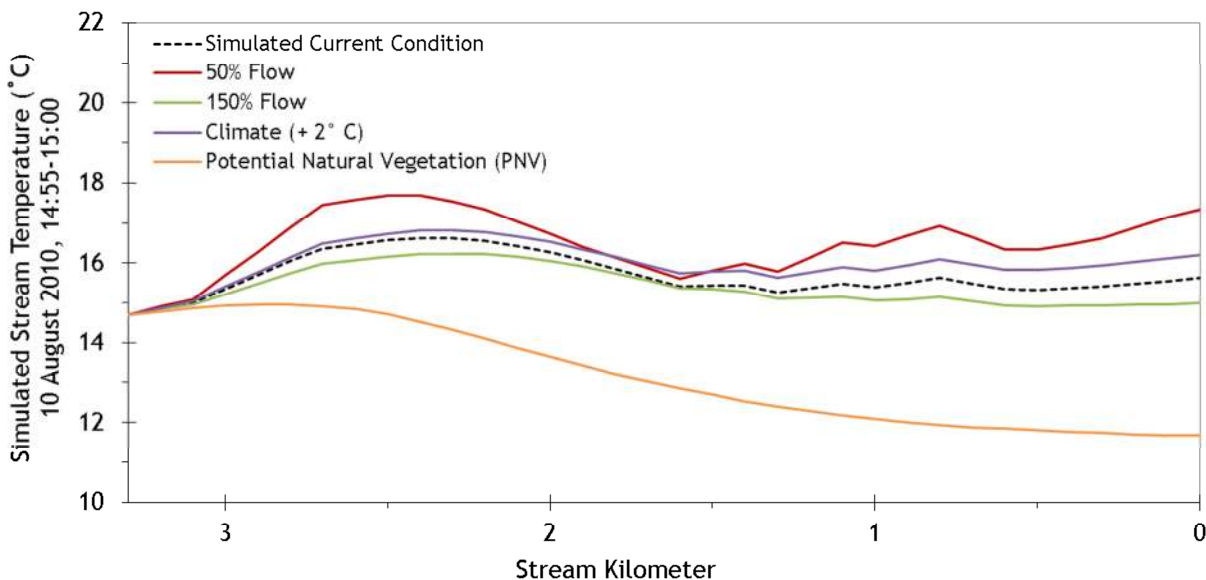
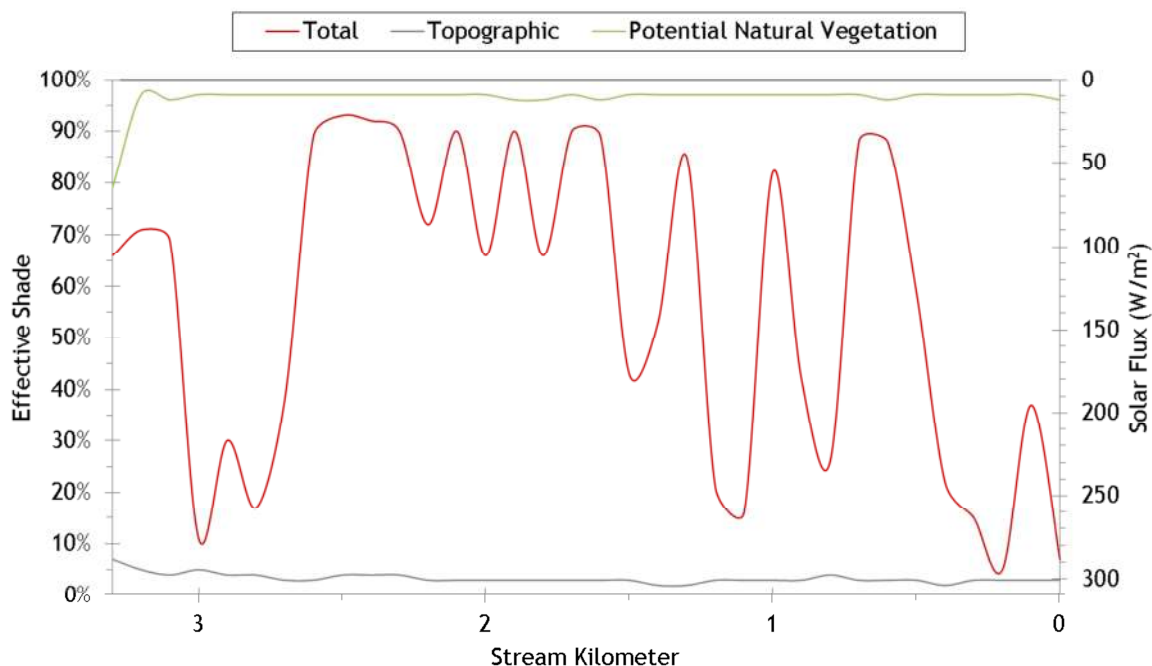


Figure 228 - Milk Creek simulated effective shade.

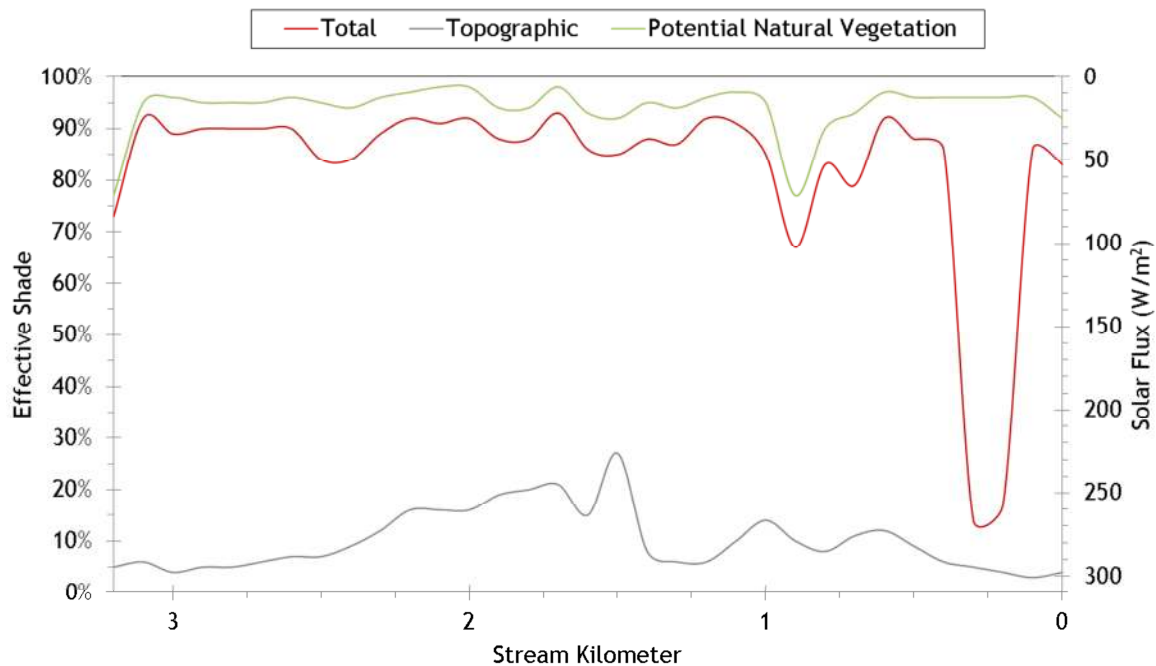


6.4 Little Catherine Creek

Stream temperature was not simulated for Little Catherine Creek due to low flow conditions and data limitations. However, effective shade was simulated for the current condition and with potential natural vegetation.

Figure 229 shows the simulated effective shade for the current condition and the potential natural vegetation.

Figure 229 - Little Catherine Creek simulated effective shade.



6.5 Little Creek

Figure 230 shows the simulated scenario results for Little Creek. There were some active diversions in the lower reaches of Little Creek during the simulation time period. In the combination scenario of PNV and no diversions, the temperature profile is moderated due to the larger instream flow volume.

Figure 230 - Little Creek simulated scenario results.

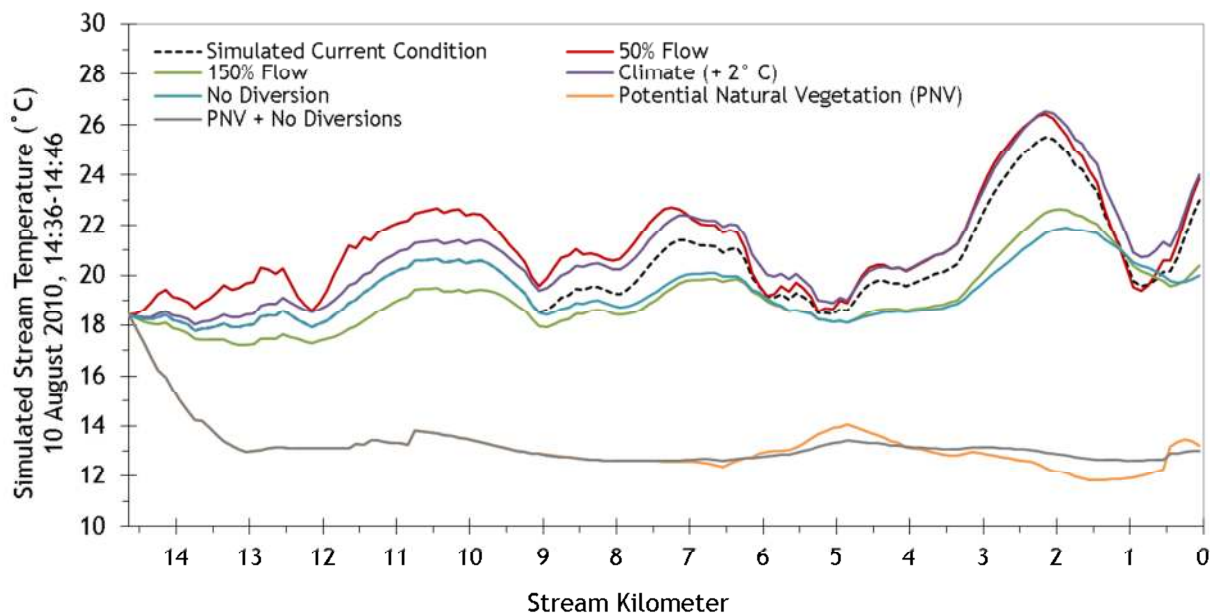
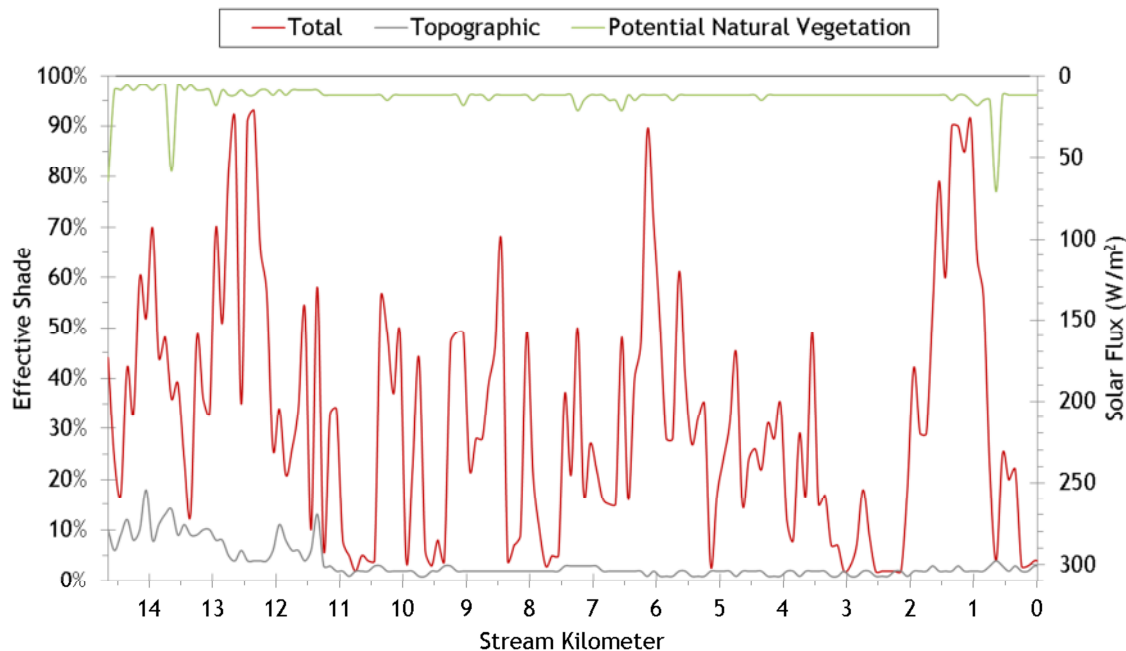


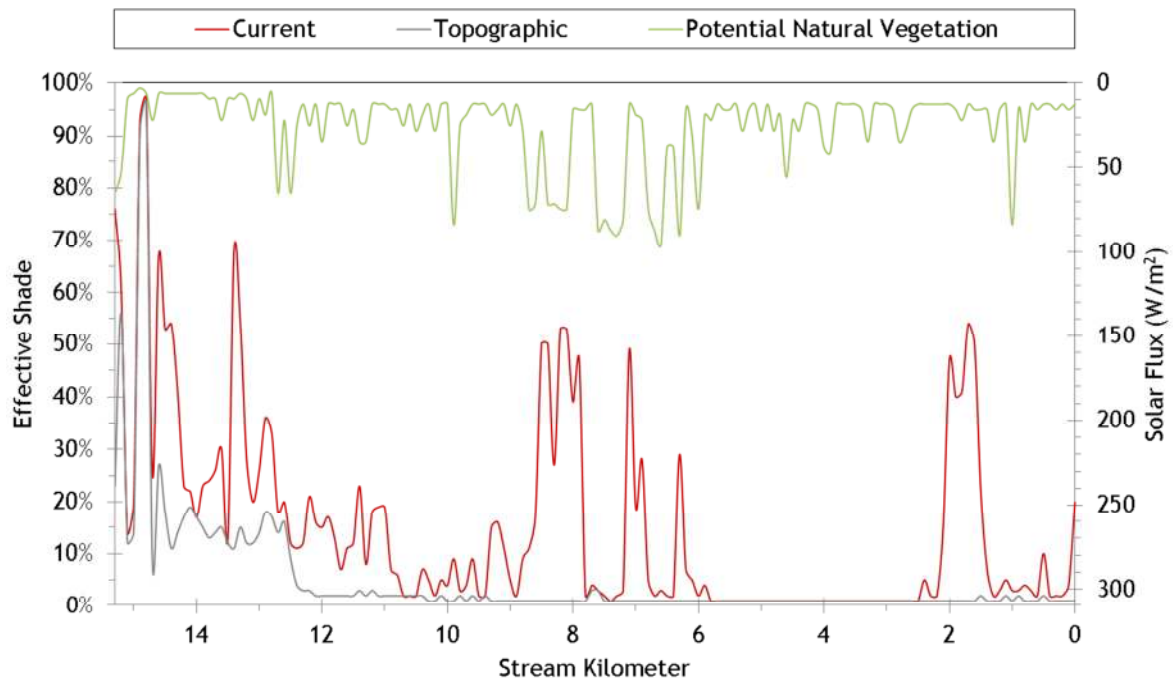
Figure 231 - Little Creek simulated effective shade.



6.6 Ladd Creek

Ladd Creek had too little flow to for temperature simulations. However, effective shade was simulated for the current and potential natural vegetation conditions (Figure 232). Currently, much of Ladd Creek is surrounded by cultivated fields and there is little effective shade. Under the potential natural vegetation scenario, there is significant effective shade along the entire stream.

Figure 232 - Ladd Creek simulated effective shade.



6.7 Catherine Creek

Stream temperature was simulated from the forks to the City of Union. Below Union, the low stream flow and thermal stratification prevented stream temperatures simulation. However, effective shade was simulated for the entire length of Catherine Creek.

Figure 233 shows the simulated scenario results for Catherine Creek between the forks and the City of Union. In this model, the boundary condition is a mass balance of the simulated results from the North and South Forks, therefore the boundary temperature varies between scenarios. There were some minor diversions occurring upstream of Union, but they had little effect on stream temperatures.

Figure 233 - Catherine Creek simulated scenario results (from forks to City of Union).

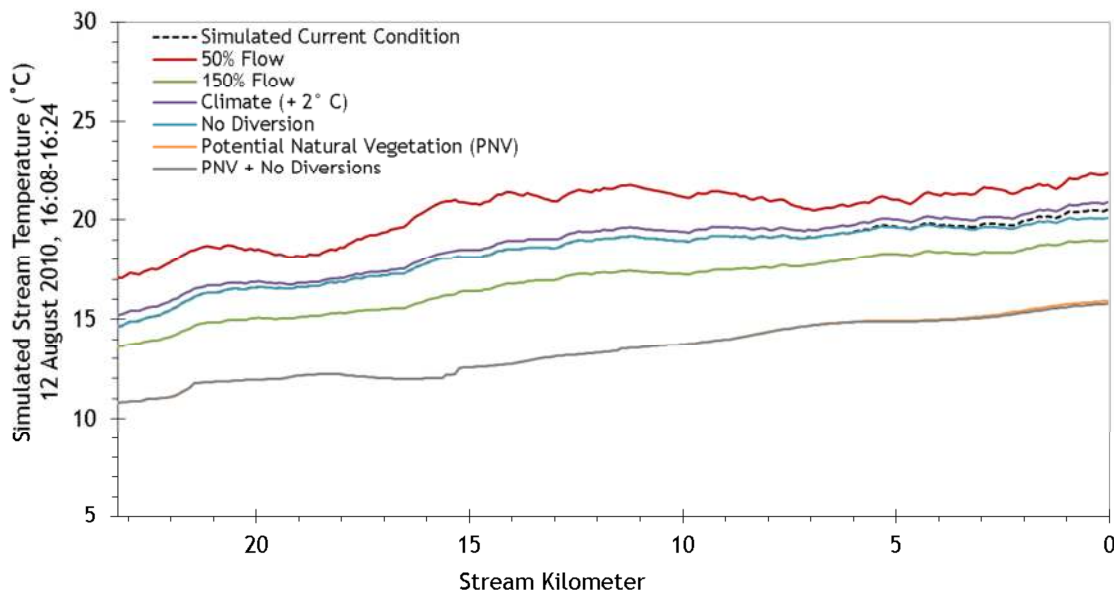
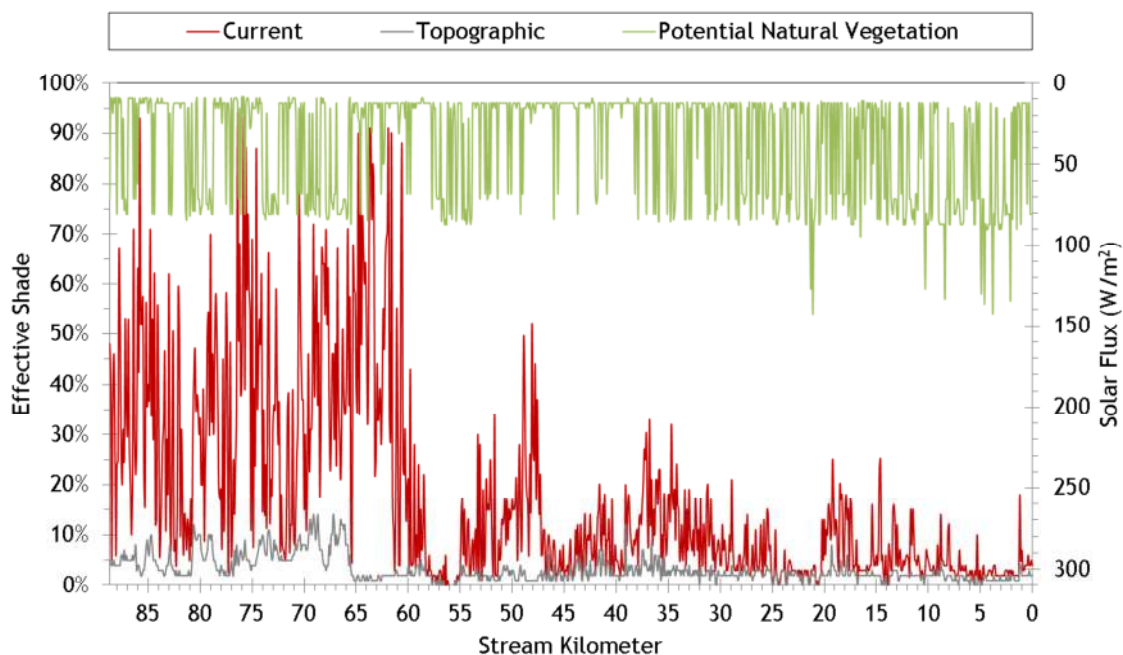


Figure 234 - Catherine Creek simulated effective shade.



6.8 Clear Creek

The simulated scenario results for Clear Creek are presented in Figure 235. Since Clear Creek is a smaller stream, it was more sensitive to the air temperature increase than the larger streams. The boundary condition was not changed in any of the scenarios and that is why there is a gradual decline in the PNV scenario.

Figure 235 - Clear Creek simulated scenario results.

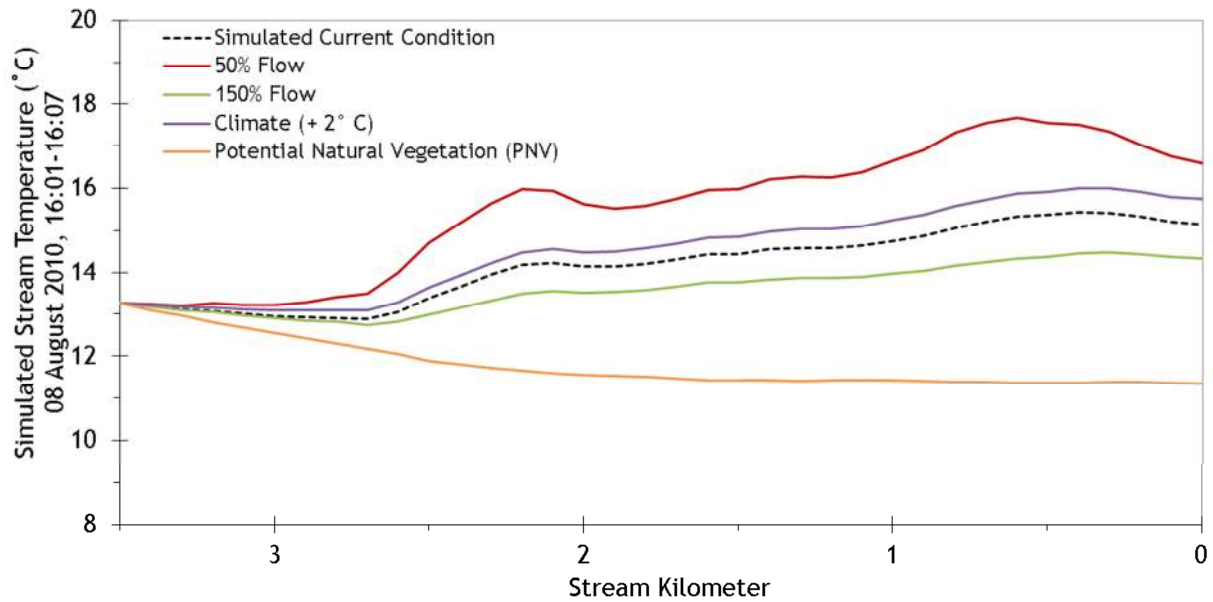
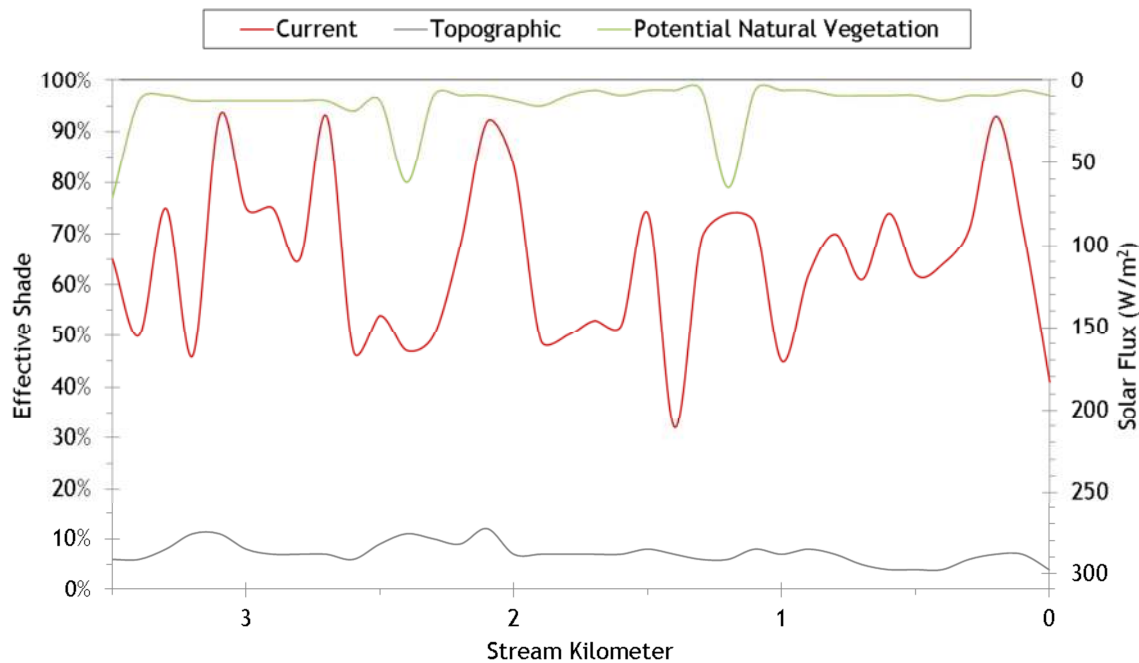


Figure 236 - Clear Creek simulated effective shade.



6.9 Limber Jim Creek

Limber Jim Creek simulated scenario results are shown in Figure 237. Stream temperatures in the PNV scenario were around 10°C at the time of the simulation. This is largely due to the small size of Limber Jim Creek and the homogenous PNV conditions assumption.

Figure 237 - Limber Jim Creek simulated scenario results.

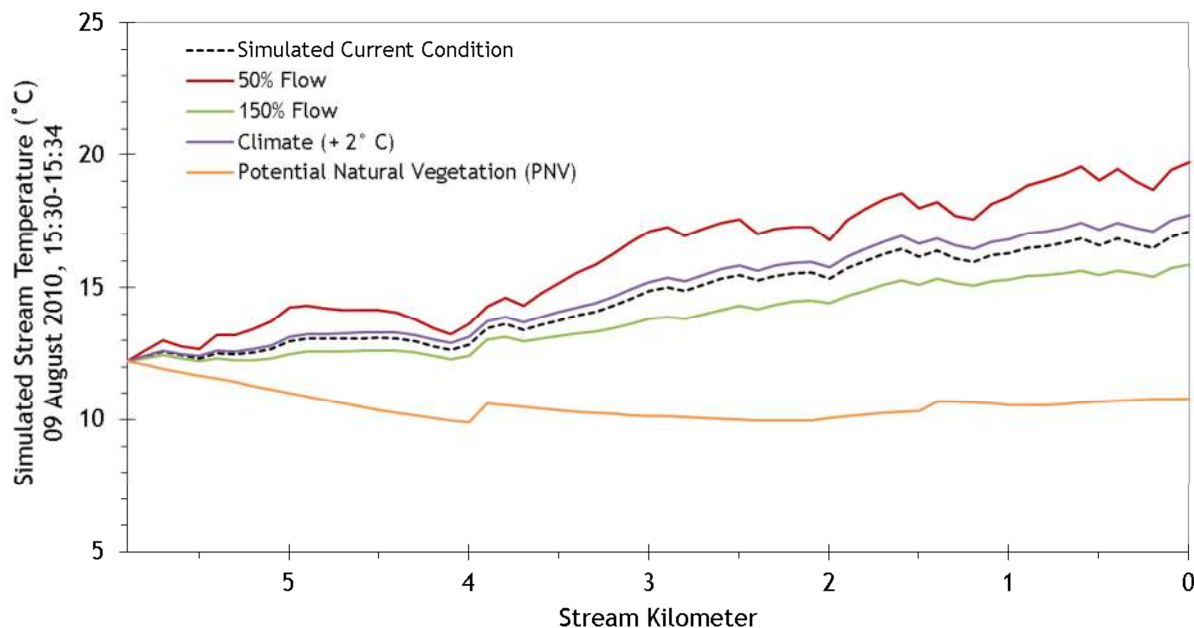
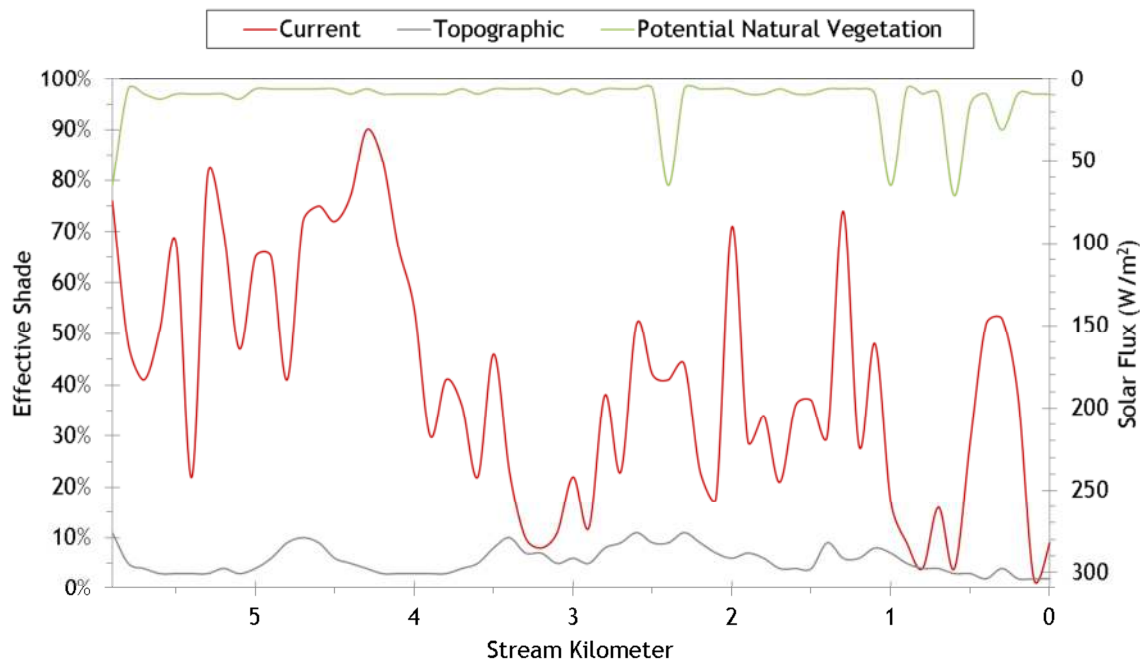


Figure 238 - Limber Jim Creek simulated effective shade.



6.10 Chicken Creek

Chicken Creek simulated scenario results are presented in Figure 239. Again, the simulated PNV temperatures decline gradually as they come to equilibrium with the surroundings. The boundary condition temperatures were not changed for any of the scenarios.

Figure 239 - Chicken Creek simulated scenario results.

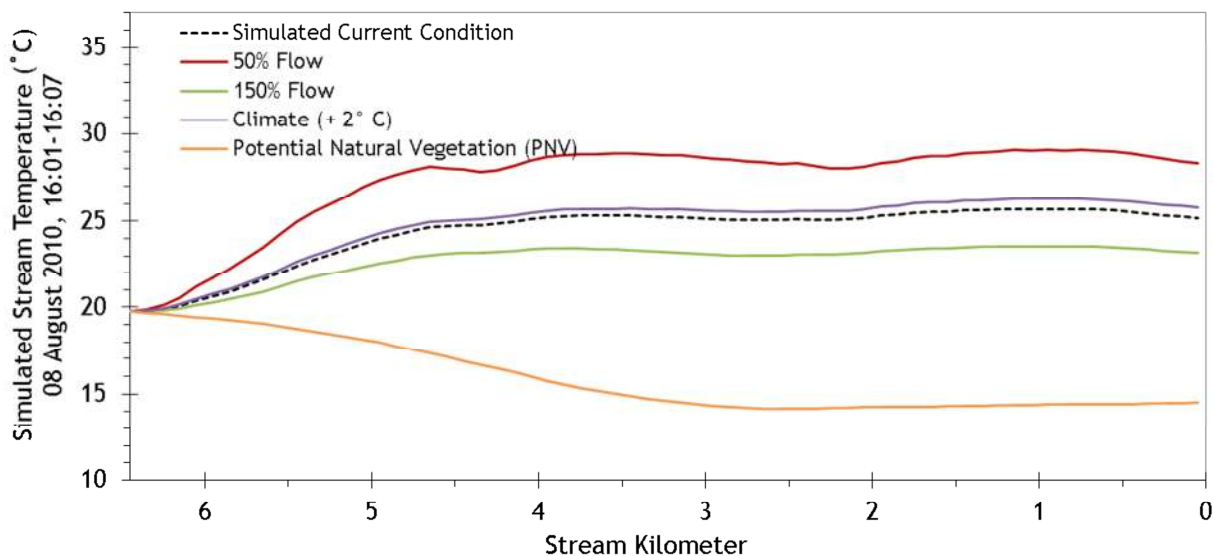
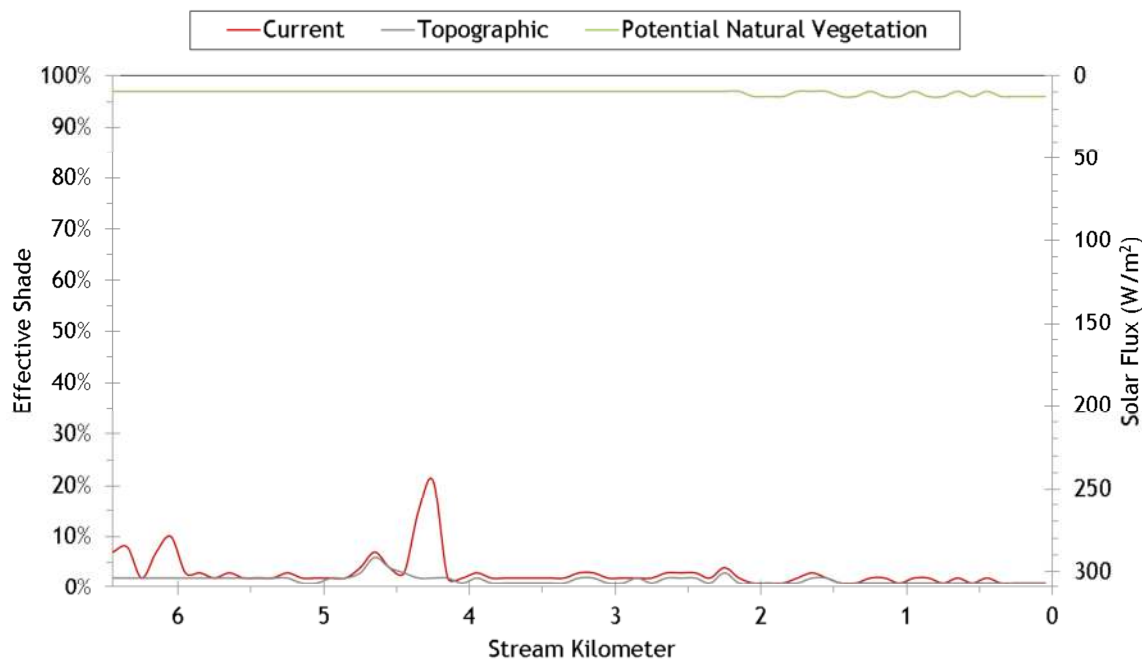


Figure 240 - Chicken Creek simulated effective shade.



6.11 Sheep Creek

Figure 241 shows the simulate scenario results for Sheep Creek. There is a big difference between the current condition and PNV simulated temperatures mainly because of the huge increase in effective shade. The simplified PNV assumptions essentially shade the entire stream throughout the day, preventing any significant heat gain.

Figure 241 - Sheep Creek simulated scenario results.

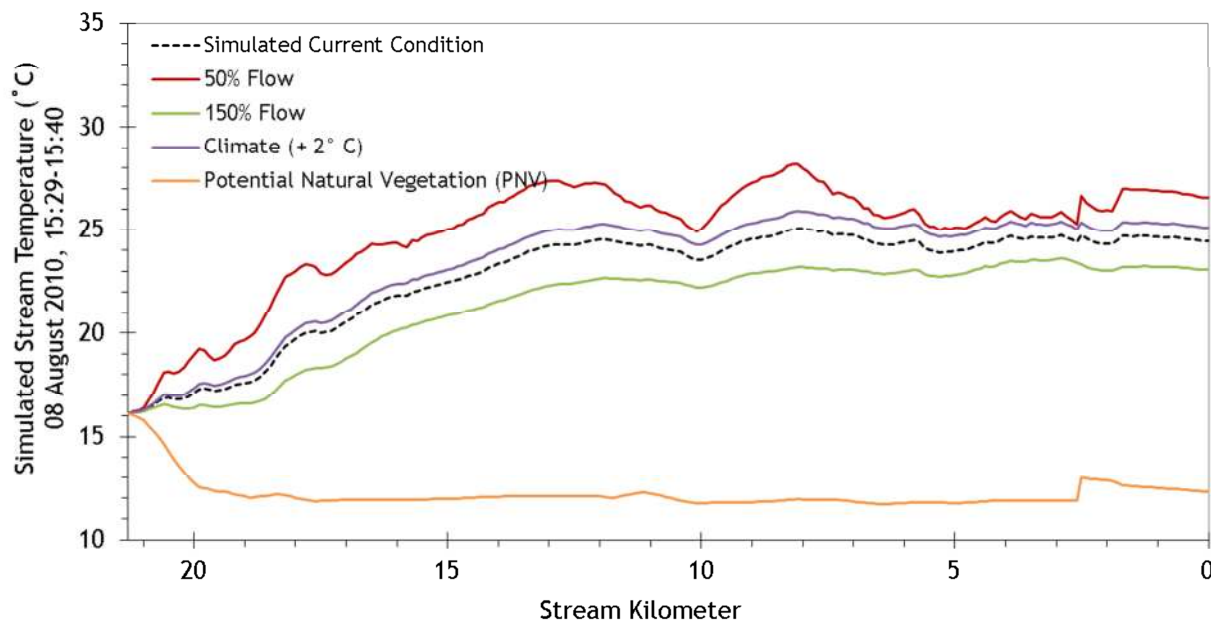
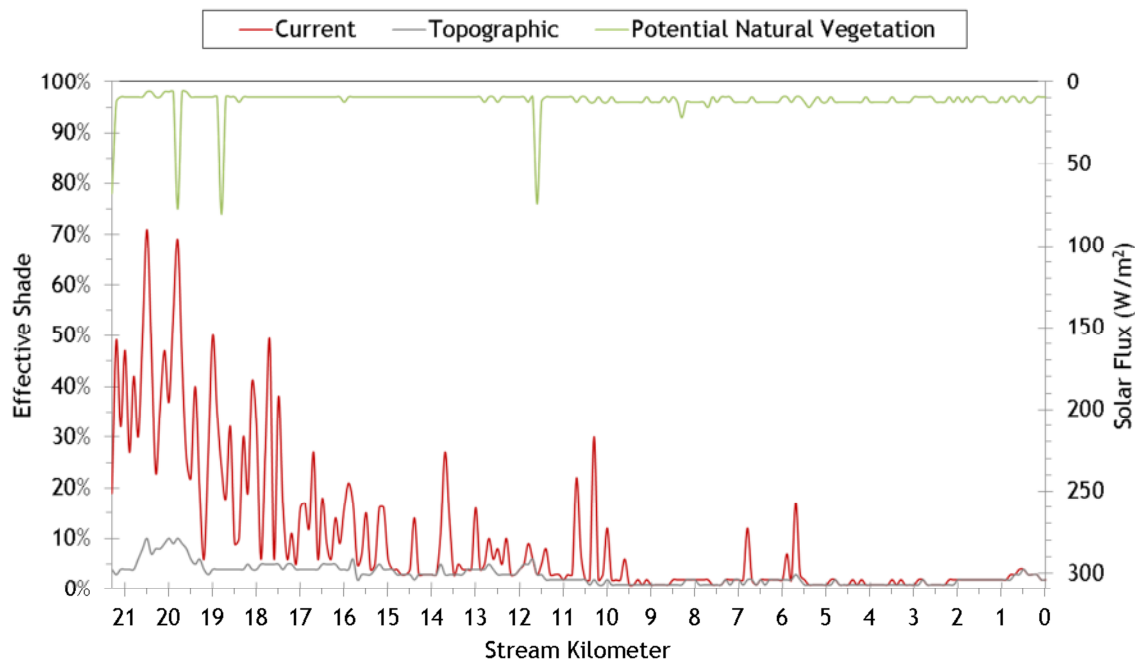


Figure 242 - Sheep Creek simulated effective shade.



6.12 Fly Creek

Figure 243 shows the Fly Creek simulation results. The boundary condition of the simulated reach starts out rather warm at 25°C. Since the boundary condition temperatures were not altered in the scenarios, there is a rapid decline and then stabilization of the simulated PNVT temperature. Again, the simplified PNVT conditions have created shade along the entire stream throughout the entire day.

Figure 243 - Fly Creek simulated scenario results.

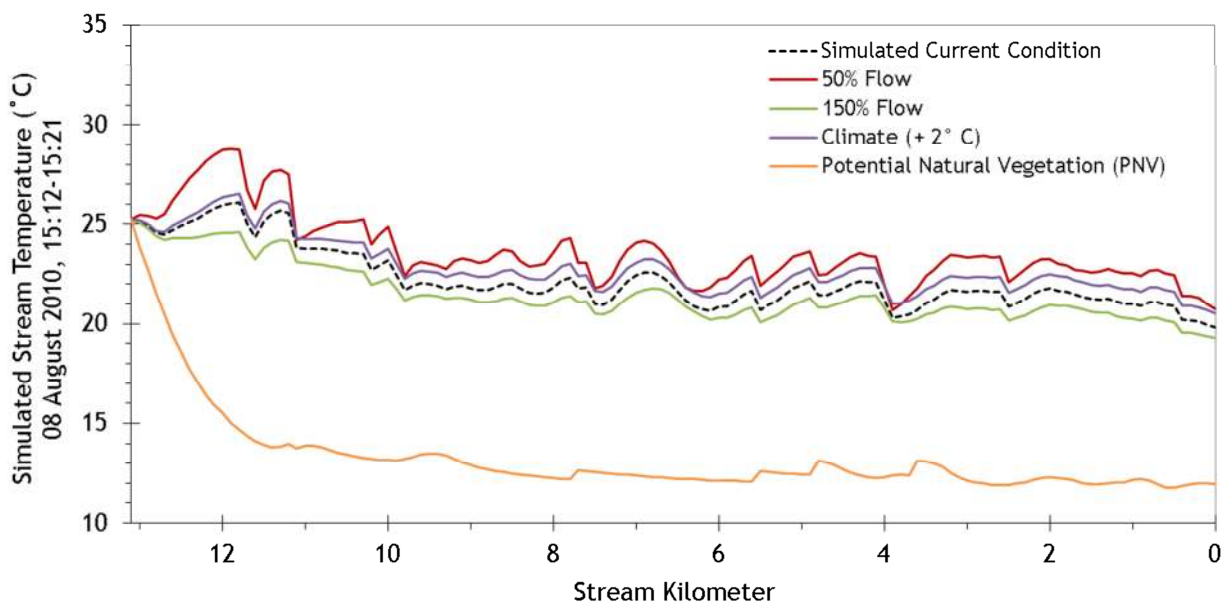
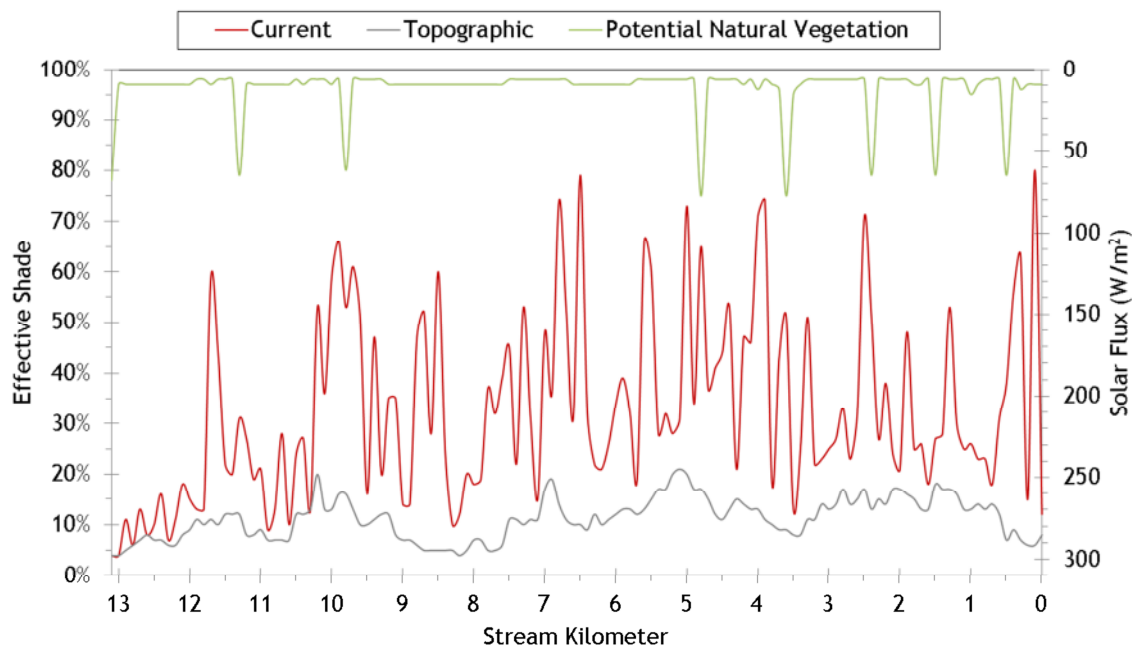


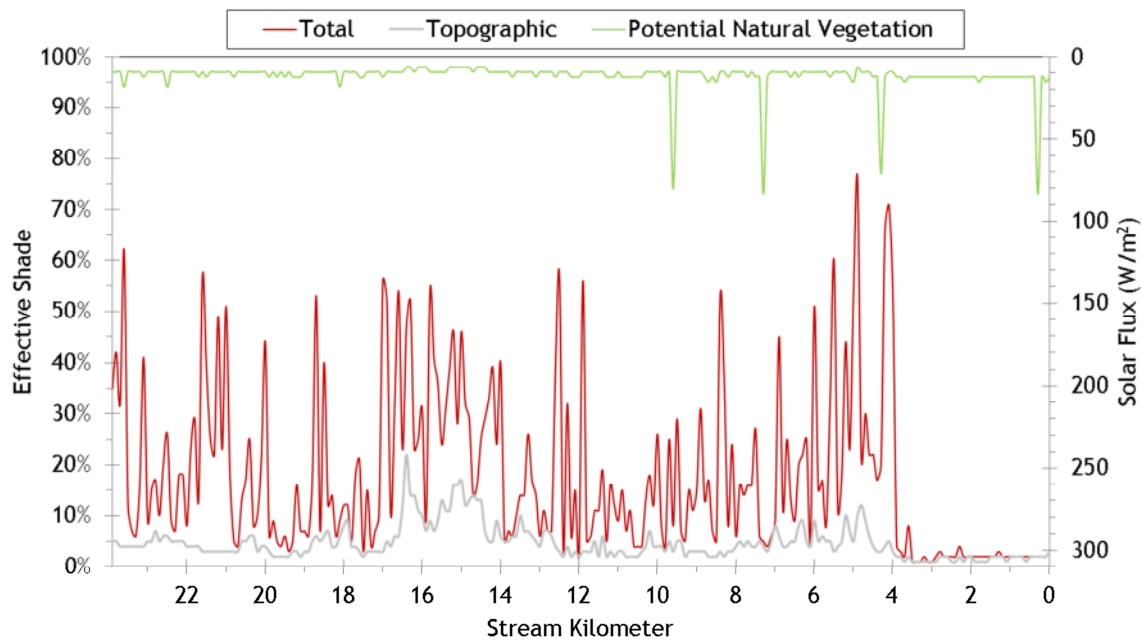
Figure 244 - Fly Creek simulated effective shade.



6.13 McCoy Creek

McCoy Creek was not simulated for temperature because the flows were too low for accurate modeling. Effective shade was simulated for the current and potential natural vegetation conditions (Figure 245).

Figure 245 - McCoy Creek simulated effective shade.



6.14 Meadow Creek

Meadow Creek simulated results area shown in Figure 246. Boundary condition temperatures were unchanged in these scenarios.

Figure 246 - Meadow Creek simulated scenario results.

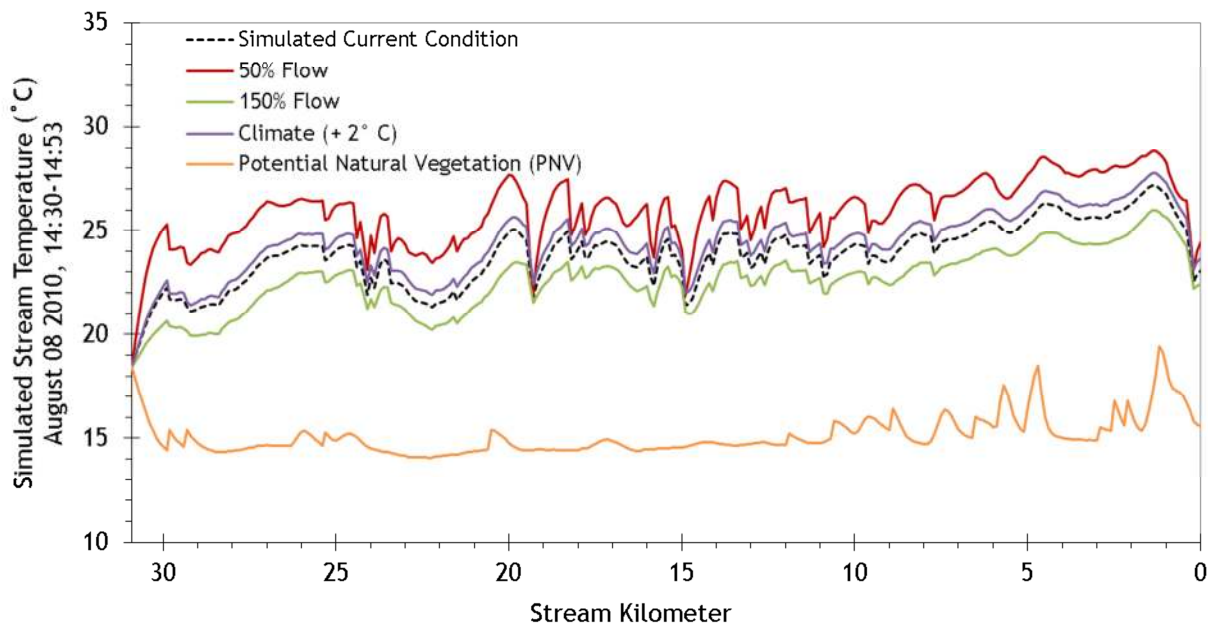
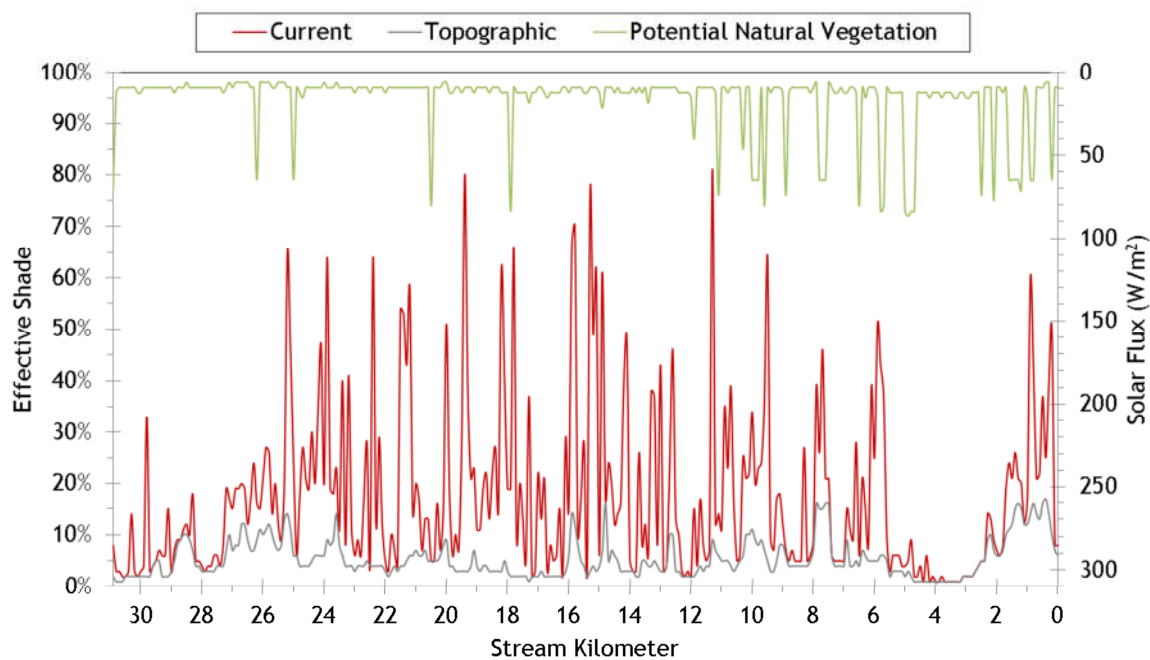


Figure 247 - Meadow Creek simulated effective shade.



6.15 Beaver Creek

Figure 248 shows the simulation results for Beaver Creek. The boundary condition and tributary temperatures were not changed within the scenarios. The coolest temperatures were obtained in the PNV simulation, where a homogenous vegetation condition was assumed throughout the entire stream length.

Figure 248 - Beaver Creek simulated scenario results.

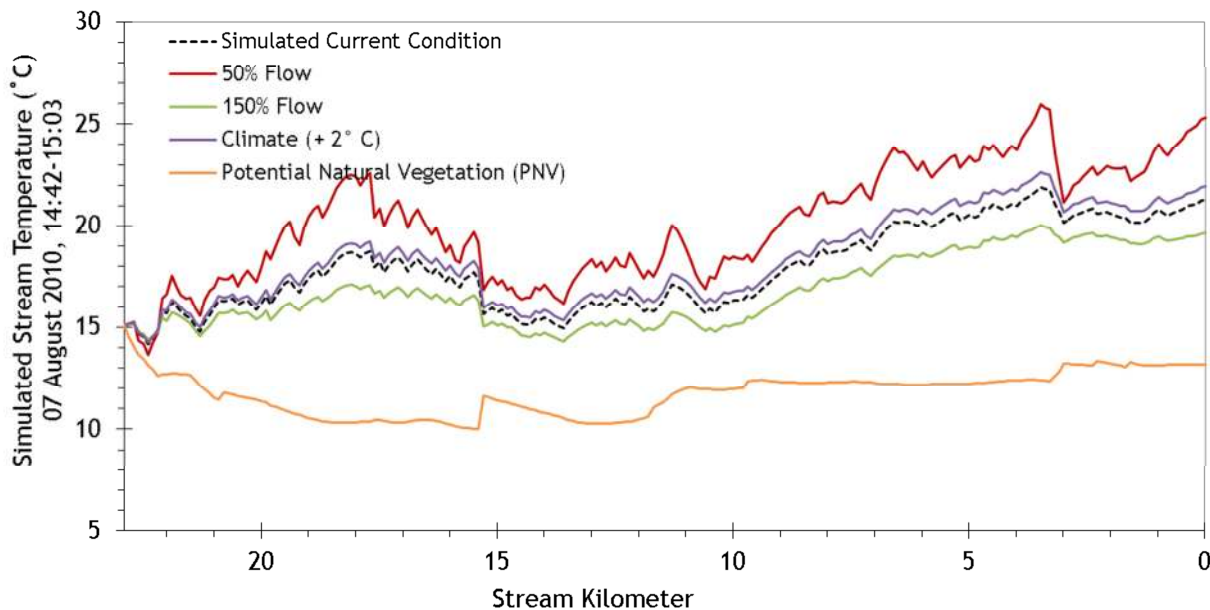
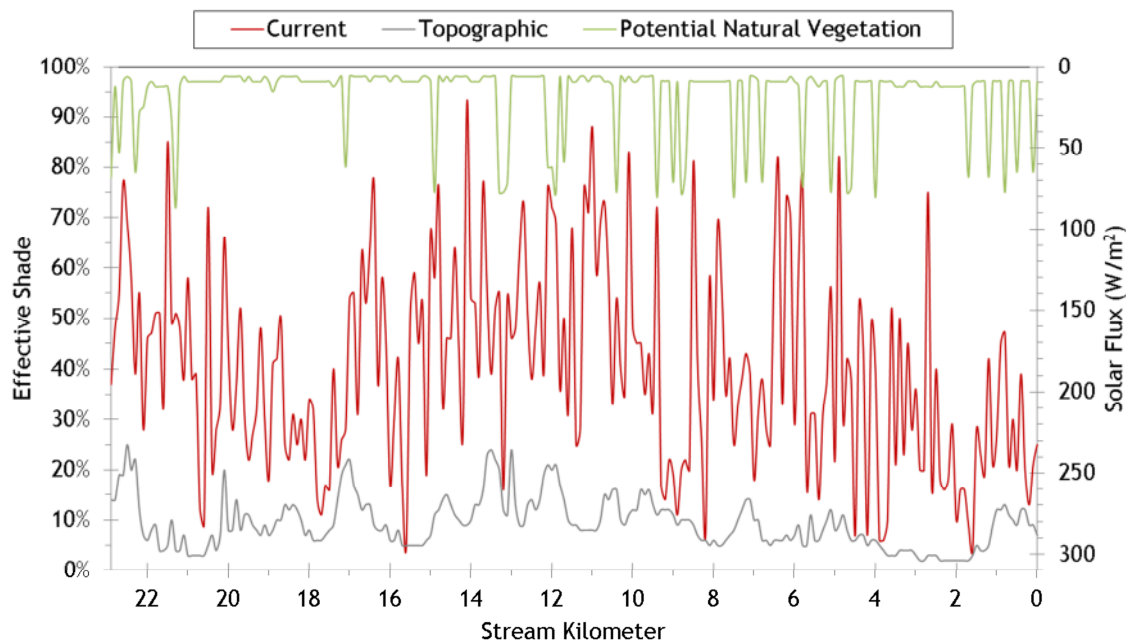


Figure 249 - Beaver Creek simulated effective shade.



6.16 Five Points Creek

Figure 250 presents the simulation results for Five Points Creek. As seen in the other simulations, the lowest temperatures were achieved in the PNV scenario due to the high levels of effective shade.

Figure 250 - Five Points Creek simulated scenario results.

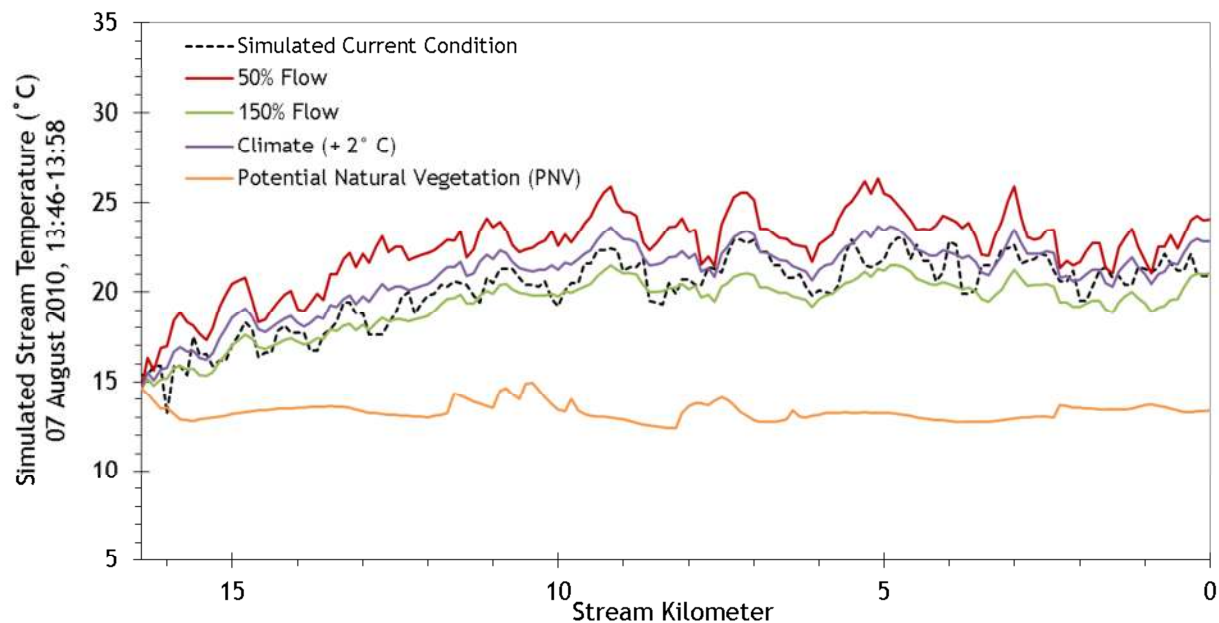
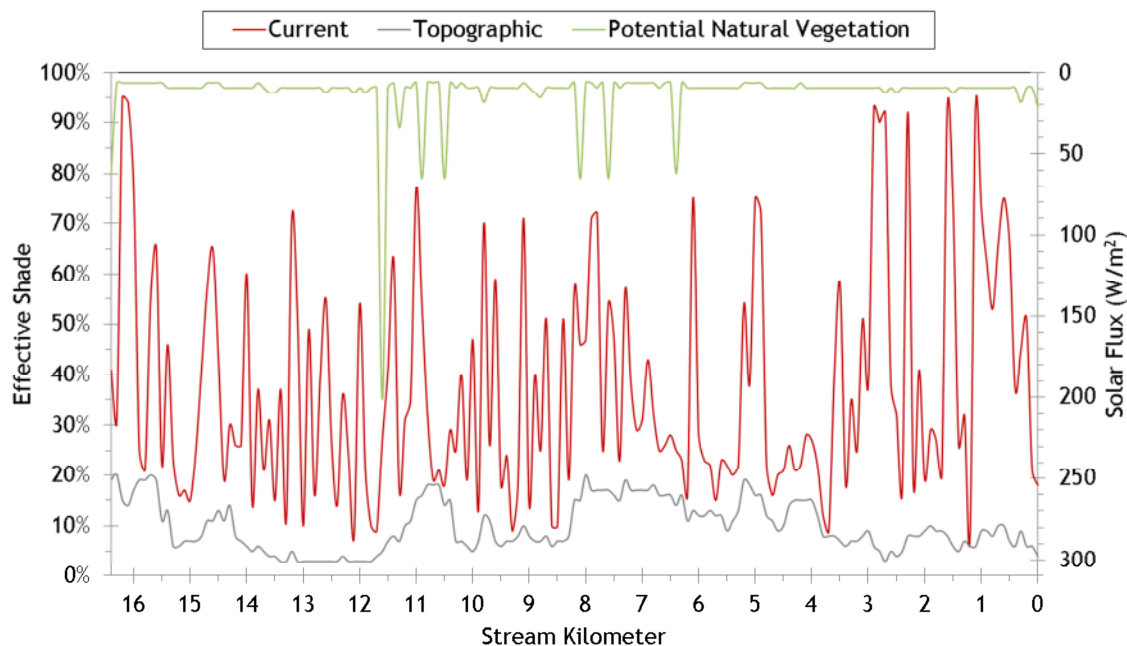


Figure 251 - Five Points Creek simulated effective shade.



6.17 Grande Ronde River

Figure 252 shows the simulation results for the Grande Ronde River. Simulated data from the mouths of tributaries were incorporated into the Grande Ronde River model where applicable. The lower 21.75 simulation kilometers are not validated because of the presence of large unmonitored withdrawals which prohibited accurate hydraulic calibration.

Figure 252 - Grande Ronde River simulated scenario results.

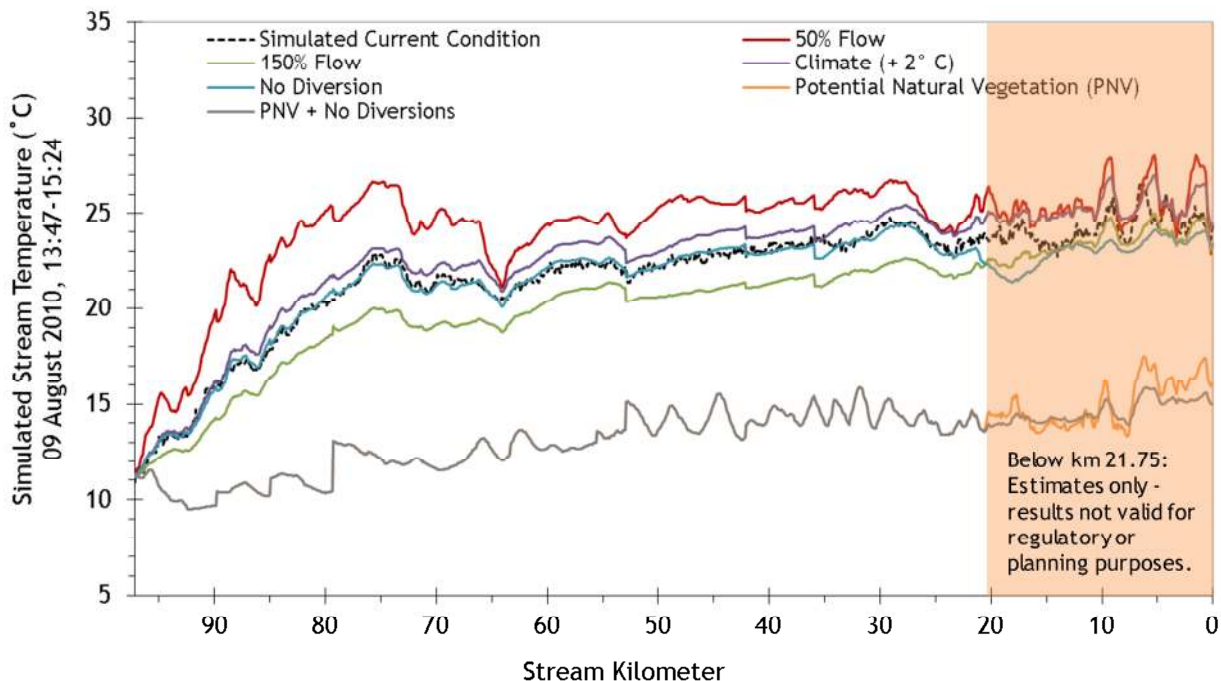
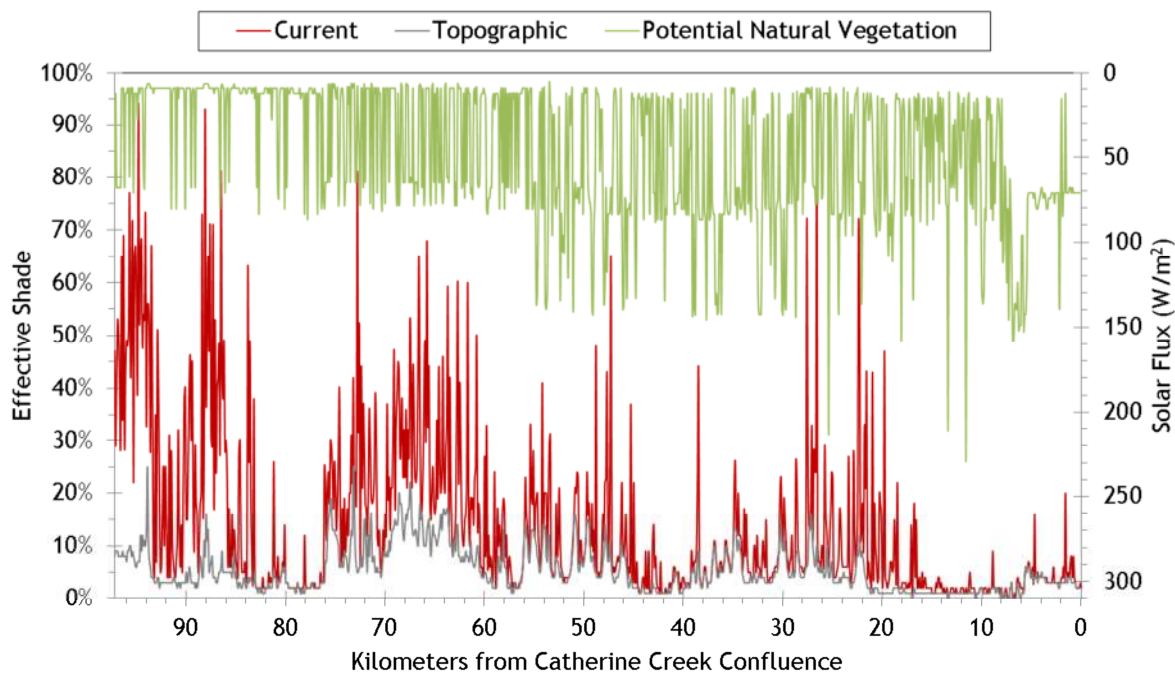


Figure 253 - Grande Ronde River simulated effective shade.



Appendix P.

Summary of Solar Input in the Upper Grande River and Catherine Creek During Summer 2011



COLUMBIA RIVER INTER-TRIBAL FISH COMMISSION

729 NE Oregon, Suite 200, Portland, Oregon 97232

Telephone 503 238 0667

Fax 503 235 4228

Summary of Solar Input in the Upper Grande River and Catherine Creek During Summer 2011

A component of

Monitoring Recovery Trends in Key Spring Chinook Habitat Variables

and Validation of Population Viability Indicators

November 2011

Tarin Lewis



Introduction

One component of the Columbia Habitat Monitoring Program (CHaMP) entails collecting solar input data at five transects for each site. Following the CHaMP protocol (Bouwes et al. 2011) this information is collected using a solar pathfinder. In addition to the solar pathfinder we collected solar data using the Solmetric SunEye.

The solar pathfinder can be difficult to use in the field because a picture must be taken directly over the pathfinder while it is held level 30cm above the stream, and you must simultaneously block the sun's glare. While it is realistic to take the photo while holding the pathfinder above the stream, it is nearly impossible to block the sun's glare without the help of another team member. Low quality images, due to certain lighting conditions such as sun glare, are a known drawback of the solar pathfinder according to Teti and Pike (2005). The solar pathfinder also does not account for gaps within the canopy, therefore omitting some solar input onto the stream. This may result in inaccurate representations of solar input at some sites.

Many of the challenges encountered with the Solar Pathfinder are eliminated with the use of the Solmetric SunEye. It is easy for one person to use, containing a built-in camera with a fisheye lens and an on-screen compass and level. Gaps in the canopy are counted as open sky either by the device, or added during the editing process, allowing for a more accurate representation of solar input. Site information and the corresponding labeled transect photos are all stored on the Solmetric, which allows for easy and organized uploading of solar data. Post-processing of images, exporting reports, and calculating wattages can be easily performed in under an hour for each site.

Methods

Field Methods:

After the Solmetric is turned on, location information is entered by either choosing the closest city, entering latitude and longitude, or using the built in GPS. Then, a new session is created; ensuring that the session name is the complete site ID and the NREL-TMY3 weather model for the closest weather station is selected. A new skyline for each transect within the session is created, making sure to add the transect number as the skyline note. If it is practical in the field, the first skyline should be the first transect and so forth (sky01=transect 1, sky02=transect 6), as this will eliminate room for error when post-processing the data. With tilt set at zero, the operator stands in the center of the stream and uses the on-screen compass to orient the Solmetric toward true south. The device is held level using the on-screen level bubble, and the image is captured using the “snap” button. The Solmetric warns you if you were not facing south, or the device was not level. The image is then viewed to check that no errors have occurred and that you are not obscuring the annual sun path.

Processing Methods:

Using the Solmetric software, sessions are uploaded into a folder automatically created by Solmetric within My Documents. It is important that these folders are not renamed or moved, as this will make them inaccessible to the solmetric software. Once a session is opened, each skyline is viewed to evaluate if editing is necessary. Most skylines did need minor editing. This was usually due to glare from the sun creating a false representation of open sky where there should be shade. Despite this error, it was easy to see where the trees were and use the editing

tool to “paint” them green, which represents shade. Sometimes the software did not catch gaps in the canopy, but these were also easy to spot and “paint” yellow, which represents open sky. The desired window of time (e.g. June-September) should be set for the session; this will limit the amount of information exported in certain .csv files. After all images are checked visually, edited if necessary, and windowed time is set, session reports are exported for each site. The report folder name will be assigned the “Client Name”, which should be the site ID.

The exported folder for the session contains a report (which can be saved in many formats), all individual images for the session, and .csv files for the corresponding skylines. Many of these .csv files are for solar panel applications and should be ignored. The .csv files do not contain notes about which transect the image corresponds to, so it is important to cross reference each skyline in the Solmetric software, and view the note, to ensure that calculations are performed for the correct transect.

The .csv files necessary for ecological purposes are Sky##Insolation.csv, and Sky##WindowedDailySolarAccess.csv. Sky##Insolation.csv lists potential insolation (irradiance) in watts per meter squared, based on NREL-TMY3 weather data which has been inputted into a daylight availability model developed by Perez et al. (1990). Our sites all used the same weather station, so this file was identical for all sites and all transects. The other relevant file, Sky##WindowedDailySolarAccess.csv, gives the daily percent of solar insolation available at each transect. Solmetric calculates that by dividing insolation accounting for shade by the potential insolation, multiplied by 100. A solar access percentage of 100 would mean there is no shade cover at that transect, all of the potential insolation is reaching the stream.

Solmetric does not export a .csv file containing Kwh/m^2 or total wh/m^2 accounting for shade, but it is fairly easy to calculate from the two .csv files listed above. To calculate wh/m^2 , I first summed each day's insolation in the Sky##Insolation.csv file, then summed all the days for each month (June-Sept.). This gave the total insolation (wh/m^2) for the entire month. This value is the total potential insolation, not accounting for shade. To find the total insolation accounting for shade at each of our transects, I took the solar access percentage for each month (June-Sept) from the Sky##WindowedDailySolarAccess.csv, divided that percentage by 100, and then multiplied that value by the total potential monthly insolation value. This produces the total monthly insolation (wh/m^2) accounting for shade for each transect. To calculate the average daily Kwh/m^2 accounting for shade for each transect I divided the total monthly insolation accounting for shade by the number of days in the month which produces the average daily insolation ($\text{wh/m}^2/\text{day}$). I then divided that value by 1000 to convert to $\text{Kwh/m}^2/\text{day}$.

Results

We found that the Solmetric SunEye is easier to use in the field than the Solar Pathfinder because an individual can easily capture the skyline without the help of another team member. Although sun glare is an issue with the Solmetric, the operator does not have to hold a camera at the same time as the Solmetric SunEye, so he/she can use his/her free hand to block the glare. In addition, trees are still visible in images with glare, so editing shade into the appropriate areas is possible. We did not conduct processing of Solar Pathfinder images, so at this time we are not able to compare processed images or insolation values. When the data becomes available, further analyses will be done to compare the Solar Pathfinder with the Solmetric SunEye. We were able

to visually compare the images from both methods, and found that the Solmetric generally produced clearer images of the skyline.



Figure 1. Left: Solmetric SunEye, Right: Solar Pathfinder. Site CBW05583-321338, Transect 11.

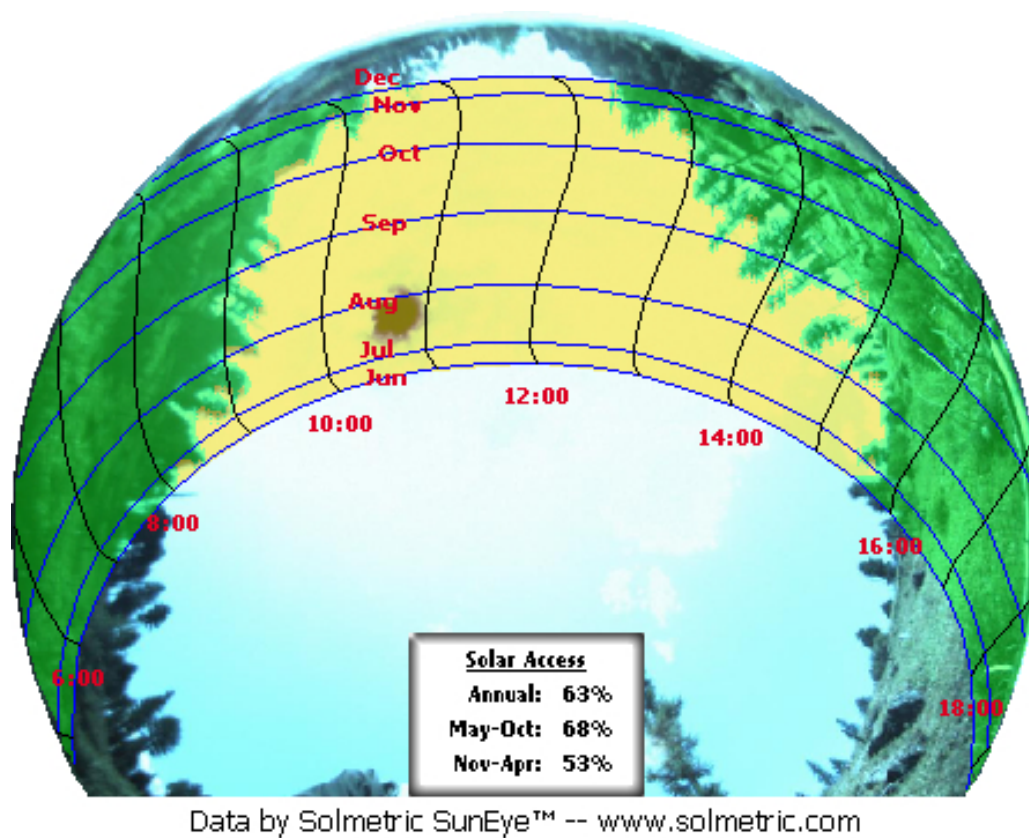


Figure 2. Solmetric SunEye image showing annual sun path and solar access percentages. This image can be viewed in field to ensure a good representation of the transect.

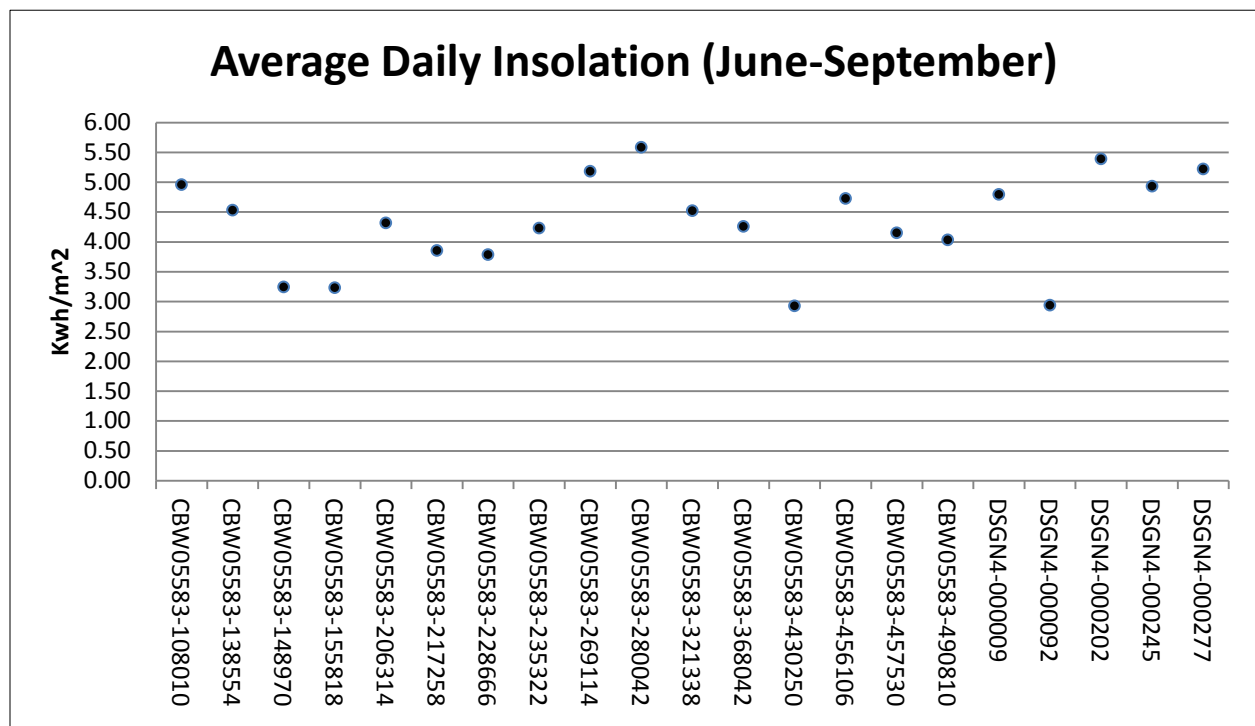


Figure 3. All transects were combined to produce site averages for each month, and then those averages were combined to produce an average for each site for June through September. See tables 4.

Calculations

Solar Access % = (Insolation accounting for shade / total potential insolation)*100

Total potential daily insolation (wh/m²) = Sum of quarter- hourly insolation values

Total potential monthly insolation (wh/m²) = Sum of daily total insolation for each day

Total actual monthly insolation (wh/m²) =

(Solar access percentage/100)*(total potential monthly insolation)

Average actual daily insolation (Kwh/m²/day) =

((total actual monthly insolation)/# days in the month)/1000

References

- Bouwes, N., J. Moberg, N. Weber, B. Bouwes, C. Beasley, S. Bennett, A.C. Hill, C.E. Jordan, R. Miller, P. Nelle, M. Polino, S. Rentmeester, B. Semmens, C. Volk, M.B. Ward, G. Wathen, and J. White. 2011. Scientific protocol for salmonid habitat surveys within the Columbia Habitat Monitoring Program. Prepared by the Integrated Status and Effectiveness Monitoring Program and published by Terraqua, Inc., Wauconda, WA.
- Perez, R., P. Ineichen, R. Seals, J. Michalsky, and R. Stewart. 1990. Modeling daylight availability and irradiance components from direct and global irradiance. *Solar Energy*, Volume 44, Issue 5, Pages 271-289.
- Teti, P.A. and Pike, R.G. 2005. Selecting and testing an instrument for surveying stream shade. *BC Journal of Ecosystems and Management*, Volume 6, Number 2, Pages 1-16.

Table 1. Total Monthly Insolation accounting for shade (wh/m²)

Site ID	Transect	Total Monthly Insolation for each Transect (wh/m ²)			
		June	July	August	September
CBW05583-108010	1	113728.8	122843.0	87062.9	61347.7
CBW05583-108010	6	192245.4	199791.1	164871.9	119037.1
CBW05583-108010	11	199244.1	204357.8	162039.1	122836.2
CBW05583-108010	16	197275.7	202531.1	158261.9	105388.6
CBW05583-108010	21	172561.5	176044.5	150141.1	116363.7
CBW05583-138554	1	174529.9	173532.9	127478.3	92584.4
CBW05583-138554	6	147628.7	157092.9	133521.7	102996.6
CBW05583-138554	11	126851.3	126039.7	100660.6	70212.2
CBW05583-138554	16	207117.6	214632.7	175825.6	125368.9
CBW05583-138554	21	143691.9	141109.6	123512.3	102011.7
CBW05583-148970	1	89670.8	90191.4	84041.2	68664.4
CBW05583-148970	6	122039.7	117591.4	89895.8	67257.4
CBW05583-148970	11	88795.9	86766.4	84607.8	65146.8
CBW05583-148970	16	150471.9	152754.6	118979.7	81609.4
CBW05583-148970	21	122695.8	118733.0	103682.3	77106.8
CBW05583-155818	1	82453.4	81058.1	55146.2	27156.2
CBW05583-155818	6	167093.8	155266.2	57412.4	17166.1
CBW05583-155818	11	154408.7	132204.6	73087.5	59237.1
CBW05583-155818	16	131225.5	129008.0	98583.2	67398.1
CBW05583-155818	21	134506.2	133346.3	121434.9	95679.9
CBW05583-206314	1	149815.8	150699.6	110481.2	69227.3
CBW05583-206314	6	121383.6	131063.0	111803.2	70352.9
CBW05583-206314	11	182403.5	182437.8	99905.2	39679.0
CBW05583-206314	16	200556.3	205727.8	164305.3	106092.2
CBW05583-206314	21	175404.8	176272.8	133332.8	57126.6
CBW05583-217258	1	145879.0	143621.3	113691.7	98212.6
CBW05583-217258	6	136693.3	131519.6	76298.1	37709.2
CBW05583-217258	11	138442.9	153896.2	88196.1	62332.7
CBW05583-217258	16	145441.6	139054.6	86496.4	50513.4
CBW05583-217258	21	166656.4	165997.9	152407.4	120725.6
CBW05583-228666	1	183278.3	187232.8	147874.8	112986.8
CBW05583-228666	6	156595.8	158691.2	125400.8	96805.6
CBW05583-228666	11	59270.2	67814.8	87440.7	85549.1
CBW05583-228666	16	111541.7	98411.4	68555.0	65146.8
CBW05583-228666	21	160532.6	162801.2	119735.1	55860.2

Table 1. Continued

Site ID	Transect	Total Monthly Insolation for each Transect (wh/m^2)			
		June	July	August	September
CBW05583-235322	1	127726.2	136543.0	121246.0	93428.6
CBW05583-235322	6	205149.2	212577.7	168837.9	106092.2
CBW05583-235322	11	107167.5	106859.7	88007.2	56423.0
CBW05583-235322	16	151565.5	156179.6	119924.0	95257.8
CBW05583-235322	21	174748.7	174674.5	118790.9	62754.8
CBW05583-269114	1	214553.7	222852.7	184324.1	127198.0
CBW05583-269114	6	141723.6	141794.6	101416.0	80061.6
CBW05583-269114	11	202306.0	210751.1	168649.0	116785.8
CBW05583-269114	16	192901.5	200247.8	170537.6	134374.0
CBW05583-269114	21	151128.1	154124.6	140131.7	108906.3
CBW05583-280042	1	212804.1	222167.7	174692.4	125650.3
CBW05583-280042	6	176498.3	180611.2	134277.1	100463.9
CBW05583-280042	11	192464.1	196366.1	165060.8	116082.3
CBW05583-280042	16	195307.3	201389.4	172048.5	133107.7
CBW05583-280042	21	205805.4	210751.1	169215.6	124946.7
CBW05583-321338	1	180435.1	185406.2	148819.1	109750.5
CBW05583-321338	6	154408.7	151156.2	132010.8	99901.1
CBW05583-321338	11	159001.6	160517.9	129366.8	85549.1
CBW05583-321338	16	136255.8	142251.3	119924.0	88363.2
CBW05583-321338	21	162719.6	170107.9	146930.5	98634.8
CBW05583-368042	1	141286.1	142251.3	105570.9	53749.6
CBW05583-368042	6	94263.7	95443.1	72709.8	32221.6
CBW05583-368042	11	209960.8	214176.1	158261.9	67116.7
CBW05583-368042	16	171249.3	181752.8	126156.3	48543.5
CBW05583-368042	21	214991.1	223994.4	175447.9	74574.1
CBW05583-430250	1	77423.1	80829.8	70821.3	57689.4
CBW05583-430250	6	115478.5	114623.0	93295.2	86111.9
CBW05583-430250	11	109135.9	107088.0	89706.9	83016.4
CBW05583-430250	16	46147.6	51603.2	21718.5	5628.2
CBW05583-430250	21	201868.6	205727.8	119735.1	50232.0
CBW05583-456106	1	208211.2	219199.4	182624.4	123680.4
CBW05583-456106	6	158564.2	159376.2	135976.8	101871.0
CBW05583-456106	11	123133.3	128551.3	100471.8	61769.8
CBW05583-456106	16	174529.9	179469.5	137298.8	91880.9
CBW05583-456106	21	198806.7	197051.1	132388.5	72182.1

Table 1. Continued

Site ID	Transect	Total Monthly Insolation for each Transect (wh/m^2)			
		June	July	August	September
CBW05583-457530	1	143035.8	149557.9	141642.5	112283.2
CBW05583-457530	6	191589.3	197051.1	160150.5	115519.5
CBW05583-457530	11	108042.3	114394.7	93295.2	74855.5
CBW05583-457530	16	107167.5	114394.7	86874.1	53046.1
CBW05583-457530	21	160313.8	157777.9	140131.7	113690.3
CBW05583-490810	1	181528.6	186091.2	145797.4	93710.1
CBW05583-490810	6	126632.6	116678.0	106515.2	80765.1
CBW05583-490810	11	159001.6	158691.2	105570.9	58111.5
CBW05583-490810	16	156377.1	161431.2	136732.3	94835.7
CBW05583-490810	21	130569.4	123528.0	84796.7	55578.8
DSGN4-000009	1	150690.6	155266.2	131633.1	105107.2
DSGN4-000009	6	158345.5	161202.9	115769.2	87519.0
DSGN4-000009	11	182840.9	179241.2	146741.7	93710.1
DSGN4-000009	16	165125.4	173304.5	156373.3	106936.4
DSGN4-000009	21	192026.7	197051.1	156562.2	112564.6
DSGN4-000092	1	110885.6	109371.4	70632.4	37709.2
DSGN4-000092	6	95138.5	98183.1	68932.7	37568.4
DSGN4-000092	11	116353.3	129464.6	109914.6	58533.6
DSGN4-000092	16	102355.9	108458.0	98394.3	74996.2
DSGN4-000092	21	101699.8	106174.7	88196.1	72744.9
DSGN4-000202	1	116790.7	119418.0	91406.6	64584.0
DSGN4-000202	6	202743.4	199791.1	160339.3	118896.4
DSGN4-000202	11	197275.7	203672.8	170915.3	129027.2
DSGN4-000202	16	213897.6	221026.1	186779.3	129590.0
DSGN4-000202	21	215428.6	224907.7	186968.1	137751.0
DSGN4-000245	1	188746.0	194311.1	159206.2	109187.7
DSGN4-000245	6	165125.4	170336.2	110670.0	71337.8
DSGN4-000245	11	166875.1	174674.5	149007.9	99056.9
DSGN4-000245	16	171905.4	176044.5	129555.7	77528.9
DSGN4-000245	21	200118.9	210522.7	179413.9	109469.1
DSGN4-000277	1	189402.2	198192.8	164494.2	113690.3
DSGN4-000277	6	166656.4	162801.2	132955.1	115097.3
DSGN4-000277	11	184371.9	187917.8	155051.4	110876.2
DSGN4-000277	16	177373.2	184036.2	160150.5	107780.6
DSGN4-000277	21	199462.8	207554.4	166571.6	103700.2

Table 2. Average Daily Insolation Accounting for Shade (Kwh/m²/day)

Site ID	Transect	Average Daily Insolation (Kwh/m ² /day)			
		June	July	August	Sept
CBW05583-108010	1	3.8	4.0	2.8	2.0
CBW05583-108010	6	6.4	6.4	5.3	4.0
CBW05583-108010	11	6.6	6.6	5.2	4.1
CBW05583-108010	16	6.6	6.5	5.1	3.5
CBW05583-108010	21	5.8	5.7	4.8	3.9
CBW05583-138554	1	5.8	5.6	4.1	3.1
CBW05583-138554	6	4.9	5.1	4.3	3.4
CBW05583-138554	11	4.2	4.1	3.2	2.3
CBW05583-138554	16	6.9	6.9	5.7	4.2
CBW05583-138554	21	4.8	4.6	4.0	3.4
CBW05583-148970	1	3.0	2.9	2.7	2.3
CBW05583-148970	6	4.1	3.8	2.9	2.2
CBW05583-148970	11	3.0	2.8	2.7	2.2
CBW05583-148970	16	5.0	4.9	3.8	2.7
CBW05583-148970	21	4.1	3.8	3.3	2.6
CBW05583-155818	1	2.7	2.6	1.8	0.9
CBW05583-155818	6	5.6	5.0	1.9	0.6
CBW05583-155818	11	5.1	4.3	2.4	2.0
CBW05583-155818	16	4.4	4.2	3.2	2.2
CBW05583-155818	21	4.5	4.3	3.9	3.2
CBW05583-206314	1	5.0	4.9	3.6	2.3
CBW05583-206314	6	4.0	4.2	3.6	2.3
CBW05583-206314	11	6.1	5.9	3.2	1.3
CBW05583-206314	16	6.7	6.6	5.3	3.5
CBW05583-206314	21	5.8	5.7	4.3	1.9
CBW05583-217258	1	4.9	4.6	3.7	3.3
CBW05583-217258	6	4.6	4.2	2.5	1.3
CBW05583-217258	11	4.6	5.0	2.8	2.1
CBW05583-217258	16	4.8	4.5	2.8	1.7
CBW05583-217258	21	5.6	5.4	4.9	4.0
CBW05583-228666	1	6.1	6.0	4.8	3.8
CBW05583-228666	6	5.2	5.1	4.0	3.2
CBW05583-228666	11	2.0	2.2	2.8	2.9
CBW05583-228666	16	3.7	3.2	2.2	2.2
CBW05583-228666	21	5.4	5.3	3.9	1.9

Table 2. Continued

Site ID	Transect	Average Daily Insolation (Kwh/m ² /day)			
		June	July	August	Sept
CBW05583-235322	1	4.3	4.4	3.9	3.1
CBW05583-235322	6	6.8	6.9	5.4	3.5
CBW05583-235322	11	3.6	3.4	2.8	1.9
CBW05583-235322	16	5.1	5.0	3.9	3.2
CBW05583-235322	21	5.8	5.6	3.8	2.1
CBW05583-269114	1	7.2	7.2	5.9	4.2
CBW05583-269114	6	4.7	4.6	3.3	2.7
CBW05583-269114	11	6.7	6.8	5.4	3.9
CBW05583-269114	16	6.4	6.5	5.5	4.5
CBW05583-269114	21	5.0	5.0	4.5	3.6
CBW05583-280042	1	7.1	7.2	5.6	4.2
CBW05583-280042	6	5.9	5.8	4.3	3.3
CBW05583-280042	11	6.4	6.3	5.3	3.9
CBW05583-280042	16	6.5	6.5	5.5	4.4
CBW05583-280042	21	6.9	6.8	5.5	4.2
CBW05583-321338	1	6.0	6.0	4.8	3.7
CBW05583-321338	6	5.1	4.9	4.3	3.3
CBW05583-321338	11	5.3	5.2	4.2	2.9
CBW05583-321338	16	4.5	4.6	3.9	2.9
CBW05583-321338	21	5.4	5.5	4.7	3.3
CBW05583-368042	1	4.7	4.6	3.4	1.8
CBW05583-368042	6	3.1	3.1	2.3	1.1
CBW05583-368042	11	7.0	6.9	5.1	2.2
CBW05583-368042	16	5.7	5.9	4.1	1.6
CBW05583-368042	21	7.2	7.2	5.7	2.5
CBW05583-430250	1	2.6	2.6	2.3	1.9
CBW05583-430250	6	3.8	3.7	3.0	2.9
CBW05583-430250	11	3.6	3.5	2.9	2.8
CBW05583-430250	16	1.5	1.7	0.7	0.2
CBW05583-430250	21	6.7	6.6	3.9	1.7
CBW05583-456106	1	6.9	7.1	5.9	4.1
CBW05583-456106	6	5.3	5.1	4.4	3.4
CBW05583-456106	11	4.1	4.1	3.2	2.1
CBW05583-456106	16	5.8	5.8	4.4	3.1
CBW05583-456106	21	6.6	6.4	4.3	2.4

Table 2. Continued

Site ID	Transect	Average Daily Insolation (Kwh/m ² /day)			
		June	July	August	Sept
CBW05583-457530	1	4.8	4.8	4.6	3.7
CBW05583-457530	6	6.4	6.4	5.2	3.9
CBW05583-457530	11	3.6	3.7	3.0	2.5
CBW05583-457530	16	3.6	3.7	2.8	1.8
CBW05583-457530	21	5.3	5.1	4.5	3.8
CBW05583-490810	1	6.1	6.0	4.7	3.1
CBW05583-490810	6	4.2	3.8	3.4	2.7
CBW05583-490810	11	5.3	5.1	3.4	1.9
CBW05583-490810	16	5.2	5.2	4.4	3.2
CBW05583-490810	21	4.4	4.0	2.7	1.9
DSGN4-000009	1	5.0	5.0	4.2	3.5
DSGN4-000009	6	5.3	5.2	3.7	2.9
DSGN4-000009	11	6.1	5.8	4.7	3.1
DSGN4-000009	16	5.5	5.6	5.0	3.6
DSGN4-000009	21	6.4	6.4	5.1	3.8
DSGN4-000092	1	3.7	3.5	2.3	1.3
DSGN4-000092	6	3.2	3.2	2.2	1.3
DSGN4-000092	11	3.9	4.2	3.5	2.0
DSGN4-000092	16	3.4	3.5	3.2	2.5
DSGN4-000092	21	3.4	3.4	2.8	2.4
DSGN4-000202	1	3.9	3.9	2.9	2.2
DSGN4-000202	6	6.8	6.4	5.2	4.0
DSGN4-000202	11	6.6	6.6	5.5	4.3
DSGN4-000202	16	7.1	7.1	6.0	4.3
DSGN4-000202	21	7.2	7.3	6.0	4.6
DSGN4-000245	1	6.3	6.3	5.1	3.6
DSGN4-000245	6	5.5	5.5	3.6	2.4
DSGN4-000245	11	5.6	5.6	4.8	3.3
DSGN4-000245	16	5.7	5.7	4.2	2.6
DSGN4-000245	21	6.7	6.8	5.8	3.6
DSGN4-000277	1	6.3	6.4	5.3	3.8
DSGN4-000277	6	5.6	5.3	4.3	3.8
DSGN4-000277	11	6.1	6.1	5.0	3.7
DSGN4-000277	16	5.9	5.9	5.2	3.6
DSGN4-000277	21	6.6	6.7	5.4	3.5

Table 3. Average Monthly Total Insolation Accounting for Shade

Average Monthly Total Insolation (wh/m ²)					
Site ID	June	July	Aug	Sept	Summer Average
CBW05583-108010	175011.1	181113.5	144475.4	104994.7	151398.7
CBW05583-138554	159963.9	162481.5	132199.7	98634.8	138320.0
CBW05583-148970	114734.8	113207.4	96241.4	71956.9	99035.1
CBW05583-155818	133937.5	126176.7	81132.8	53327.5	98643.6
CBW05583-206314	165912.8	169240.2	123965.5	68495.6	131903.5
CBW05583-217258	146622.6	146817.9	103417.9	73898.7	117689.3
CBW05583-228666	134243.7	134990.3	109801.3	83269.7	115576.2
CBW05583-235322	153271.4	157366.9	123361.2	82791.3	129197.7
CBW05583-269114	180522.6	185954.2	153011.7	113465.2	158238.4
CBW05583-280042	196575.8	202257.1	163058.9	120050.2	170485.5
CBW05583-321338	158564.2	161887.9	135410.3	96439.8	138075.5
CBW05583-368042	166350.2	171523.5	127629.4	55241.1	130186.0
CBW05583-430250	110010.7	111974.4	79055.4	56535.6	89394.0
CBW05583-456106	172649.0	176729.5	137752.1	90276.8	144351.9
CBW05583-457530	142029.8	146635.3	124418.8	93878.9	126740.7
CBW05583-490810	150821.9	149283.9	115882.5	76600.2	123147.1
DSGN4-000009	169805.8	173213.2	141415.9	101167.5	146400.6
DSGN4-000092	105286.6	110330.4	87214.0	56310.5	89785.4
DSGN4-000202	189227.2	193763.1	159281.7	115969.7	164560.4
DSGN4-000245	178554.2	185177.8	145570.7	93316.1	150654.7
DSGN4-000277	183453.3	188100.5	155844.5	110228.9	159406.8

Table 4. Average Daily Insolation Accounting for Shade

Average Daily Insolation (Kwh/m ² /Day)					
Site ID	June	July	Aug	Sept	Summer Average
CBW05583-108010	5.8	5.8	4.7	3.5	5.0
CBW05583-138554	5.3	5.2	4.3	3.3	4.5
CBW05583-148970	3.8	3.7	3.1	2.4	3.2
CBW05583-155818	4.5	4.1	2.6	1.8	3.2
CBW05583-206314	5.5	5.5	4.0	2.3	4.3
CBW05583-217258	4.9	4.7	3.3	2.5	3.9
CBW05583-228666	4.5	4.4	3.5	2.8	3.8
CBW05583-235322	5.1	5.1	4.0	2.8	4.2
CBW05583-269114	6.0	6.0	4.9	3.8	5.2
CBW05583-280042	6.6	6.5	5.3	4.0	5.6
CBW05583-321338	5.3	5.2	4.4	3.2	4.5
CBW05583-368042	5.5	5.5	4.1	1.8	4.3
CBW05583-430250	3.7	3.6	2.6	1.9	2.9
CBW05583-456106	5.8	5.7	4.4	3.0	4.7
CBW05583-457530	4.7	4.7	4.0	3.1	4.2
CBW05583-490810	5.0	4.8	3.7	2.6	4.0
DSGN4-000009	5.7	5.6	4.6	3.4	4.8
DSGN4-000092	3.5	3.6	2.8	1.9	2.9
DSGN4-000202	6.3	6.3	5.1	3.9	5.4
DSGN4-000245	6.0	6.0	4.7	3.1	4.9
DSGN4-000277	6.1	6.1	5.0	3.7	5.2

Appendix Q.

Characterizing Low-Flow Regime in Upper Grande Ronde River Basin, Oregon



Characterizing Low-Flow Regime in Upper Grande Ronde River Basin, Oregon

Prepared by:

Valerie Kelly (vjkelly@usgs.gov)
U.S. Geological Survey
Oregon Water Science Center
2130 SW 5th Avenue
Portland, Oregon, 97201
e-mail: info-or@usgs.gov

Prepared for:

Columbia River Inter-Tribal Fish Commission
729 NE Oregon, Suite 200
Portland, Oregon 97232

January 20, 2012

SUMMARY

Problem/Background

The Grande Ronde River is a tributary to the Snake River, originating in the Blue Mountains ecological province of northeast Oregon. It drains the Blue Mountains to the west and northwest and Wallowa Mountains to the southeast for a total area of about 4,000 square miles, flowing 212 miles roughly north-northeast from the headwaters to its confluence with the Snake River at Hells Canyon. Surface geology in the basin is dominated by Columbia River Basalt with older volcanic and granitic intrusive rocks largely confined to high elevation headwater areas; the Columbia Plateau aquifer system underlies about 75 percent of the basin (NPCC, 2004).

Historically, the Upper Grande Ronde River supported large runs of spring Chinook salmon (*Onchorhynchus tsawytscha*), as well as summer steelhead (*O. mykiss*), although these stocks are now much reduced (McIntosh, 1992). Snake River spring Chinook salmon in the Snake River Basin, including the Grande Ronde, were listed as threatened in 2005 under the Endangered Species Act (NOAA, 2005), and populations in the Grande Ronde River Basin are considered as high priority for recovery (NOAA, 2007). Natural spawning of spring Chinook salmon occurs in the upper Grande Ronde River and its principle tributaries: the Wenaha River, the Wallowa River with its tributaries the Minan and Lostine Rivers, as well as in smaller streams in the upper basin (CRITFC, 1995).

Funding from the Columbia Basin Fish Accords agreement between the Tribes and Bonneville Power Administration currently supports a Columbia River Inter-Tribal Fish Commission (CRITFC) project to evaluate recovery trends in important habitat variables that support spring Chinook salmon in the upper Grande Ronde River basin. The proposed work would be funded as a component of this larger project, focused on characterizing low-flow regime as a primary feature of habitat quality for salmon spawning and juvenile rearing areas throughout the year, as well as corridors and holding areas for adult migration during the summer and fall. A primary objective of this work is to develop the capacity for CRITFC personnel to conduct characterizations of low-flow regime as needed for specific stream reaches of interest. It is proposed that USGS will provide detailed analytical protocols for each step, and demonstrate their application for selected streams and reaches to be determined in collaboration with CRITFC.

Low-flow regime in the upper Grande Ronde Basin is hypothesized to fall into two general categories: surface-dominated and groundwater-dominated regimes. The range in geology across the basin indicates two large-scale geologic zones, characterized by relatively old intrusive and volcanic deposits in the headwater areas at higher elevation and younger Columbia River Basalt further downstream. These different rock types are presumed to be associated with contrasting patterns of groundwater storage, since older and less permeable formations generally store less water. Basaltic rocks, which tend to be more permeable, are more likely to function as groundwater reservoirs, capturing snowmelt and storing it during the melt season, releasing it slowly as baseflow during the summer and fall.

The characterization of low-flow regime is proposed to be conducted in stages, with the first step to examine baseflow characteristics across the regional geologic transition, especially focused on how geology may be reflected as a change in the relative importance of groundwater to summer low-flow conditions. Generation of baseflow indices and frequency distributions of low-flow volume and timing based on gaged data will provide a means to quantify and visualize the distribution of low-flow patterns across the landscape. These results will provide the basis for evaluating the relationship between low-flow regime and important watershed characteristics, which will in turn be utilized to estimate low-flow regime for ungaged stream reaches. Developing the capacity to map key elements of low-flow regime across the basin is intended to

provide a critical foundation for future work assessing the vulnerability of critical stream reaches to climate warming, which will aid in prioritizing areas for amelioration of land use impacts.

Objectives

The specific objectives for the proposed iterative protocol that can be further implemented by CRITFC personnel are as follows:

- To describe the relative importance of groundwater to baseflows across the large-scale geologic gradient in the Upper Grande Ronde River Basin
- To determine the key components of low-flow regime for gaged sites
- To identify watershed characteristics that are significantly associated with low-flow regime
- To estimate key components of low-flow regime for ungaged sites

Approach

The basic approach consists of four tasks, to be completed in collaboration with CRITFC personnel:

1. Characterize baseflow across basin to determine the importance of groundwater
2. Generate probability/frequency distributions based on gaged streamflow data for flow volume and timing of onset for annual summer 7-day low flow
3. Conduct Canonical Correlation Analysis to identify the important factors presumed to govern the low-flow regime
4. Utilize these relationships to estimate probability/frequency distributions for 7-day low-flow volume for selected ungaged stream reaches

Relevance and Benefits

The proposed work directly addresses the topic of environmental flows, which is one of the high-priority issues for the USGS Cooperative Water Program (USGS, 2010) that also aligns with the larger goals of the USGS Science Strategy (USGS, 2007). This proposal builds upon the strong foundation within the USGS of developing and testing tools for hydrologic assessment and improvement of environmental management. It also is intended to provide an approach for characterizing low-flow regime that will be relevant not only at the local scale of the Grande Ronde River Basin, but which will also be transferrable to other basins in the Pacific Northwest. As such, it represents a valuable foundation for advancing scientific understanding of the regional baseflow system in the Columbia Basin as well as supporting the recovery of salmon freshwater habitat.

FULL PROPOSAL

Characterizing Low-Flow Regime in Upper Grande Ronde River Basin, Oregon

Problem/Background

The Grande Ronde River is a tributary to the Snake River, originating in the Blue Mountains ecological province of northeast Oregon. It drains the Blue Mountains to the west and northwest and Wallowa Mountains to the southeast for a total area of about 4,000 square miles, flowing 212 miles roughly north-northeast from the headwaters to its confluence with the Snake River at Hells Canyon. Mountainous areas where headwater streams originate peak at elevations ranging from 7,500 to 10,000 feet, and two large river valleys are defined at lower elevation by the mainstem Grande Ronde and Wallowa Rivers (elevations 2,600-2,800 and 2,800-4,700 feet, respectively) (NPCC, 2004). Major tributaries include the Wenaha, Wallowa and Minam Rivers, and Catherine and Lookingglass Creeks. Much of the upper basin at high elevation is public land, primarily forested, while the lowland areas are private lands and subject to agricultural and grazing effects (McIntosh, 1992). Surface geology in the basin is dominated by Columbia River Basalt with older volcanic and granitic intrusive rocks largely confined to high elevation headwater areas; the Columbia Plateau aquifer system underlies about 75 percent of the basin (NPCC, 2004).

Climate in the Grande Ronde Basin is influenced by the diversity of topography between high mountain ranges and deep canyons, which creates localized climatic effects. Regional climate is shielded from the maritime influence of the Pacific Ocean by the Cascade Mountains, 200 miles to the east, so that the dominant climate pattern is considered to be modified Continental (NPCC, 2004). Winters are cold and wet while summers are warm and dry, with air temperature varying according to elevation. Mean annual precipitation ranges from 14 inches in the valleys to more than 60 inches in the mountains (NPCC, 2004). The range in elevation defines two snow zones in the basin: the Warm Snow Zone (between about 2,000-5,000 feet of elevation) and the Cold Snow Zone (> 5,000 feet). Snow cover may become intermittent in the Warm Snow Zone when temperatures between 50 to 60° F develop during the winter (Wissmar and others 1994). These warm conditions are often associated with moderate to heavy precipitation, so that snowmelt may be coincident with rain and result in large winter floods.

Streams in the Grande Ronde Basin are dominated by snowmelt, with peak flows occurring in the spring (April-June). Timing of snowmelt runoff varies with elevation of headwaters, with earlier runoff associated with streams originating in the relatively low elevation Blue Mountains while snowmelt peaks generally occur later in those arising in the higher Wallowa Mountains (NPCC, 2004). Runoff declines through the summer and the lowest flows generally occur in August or September, sometimes extending into the winter.

Historically, the Upper Grande Ronde River supported large runs of spring Chinook salmon (*Onchorhynchus tsawytscha*), as well as summer steelhead (*O. mykiss*), although these stocks are now much reduced (McIntosh, 1992). Snake River spring Chinook salmon in the Snake River Basin, including the

Grande Ronde, were listed as threatened in 2005 under the Endangered Species Act (NOAA, 2005), and populations in the Grande Ronde River Basin are considered as high priority for recovery (NOAA, 2007). Natural spawning of spring Chinook salmon occurs in the upper Grande Ronde River and its principle tributaries: the Wenaha River in the lower basin (river mile 45), the Wallowa River in the middle basin (river mile 81) with its tributaries the Minan and Lostine Rivers, as well as in smaller streams including Bear and Hurricane Creeks in the Wallowa Basin, Lookingglass Creek in the middle basin (river mile 85), and Catherine Creek in the upper basin (river mile 144) (CRITFC, 1995).

Snake River spring Chinook salmon life history is of the stream type, where juveniles remain in fresh water for one full year before they migrate to the ocean. Adults re-enter fresh water in late winter and early spring and move upstream to relatively high elevation areas where they rely on cool and deep pool habitat before spawning in the late summer and early fall. The most important impacts on salmon in the basin include the loss of pool habitat, degraded riparian habitat, and extreme water temperatures (high in the summer and low in the winter) (Wissmar and others, 1994). Human activities believed to be associated with these impacts include timber harvest, road construction, livestock grazing, historic splash dams and log drives, and legacy effects of mining (Wissmar and others, 1994).

Funding from the Columbia Basin Fish Accords agreement between the Tribes and Bonneville Power Administration currently supports a Columbia River Inter-Tribal Fish Commission (CRITFC) project to evaluate recovery trends in important habitat variables that support spring Chinook salmon in the upper Grande Ronde River and Catherine Creek. The proposed work would be funded as a component of this larger project, focused on characterizing low-flow regime as a primary feature of habitat quality for salmon spawning and juvenile rearing areas throughout the year, as well as corridors and holding areas for adult migration during the summer and fall. A primary objective of this work is to develop the capacity for CRITFC personnel to conduct characterizations of low-flow regime as needed for specific stream reaches of interest. It is proposed that USGS will provide detailed analytical protocols for each step, and demonstrate their application for selected streams and reaches to be determined in collaboration with CRITFC.

Low-flow regime in the upper Grande Ronde Basin is hypothesized to fall into two general categories: surface-dominated and groundwater-dominated regimes. The range in geology across the basin indicates two large-scale geologic zones, characterized by relatively old intrusive and volcanic deposits in the headwater areas at higher elevation and younger Columbia River Basalt further downstream. These different rock types are presumed to be associated with contrasting patterns of groundwater storage, since older and less permeable formations generally store less water. Basaltic rocks, which tend to be more permeable, are more likely to function as groundwater reservoirs, capturing snowmelt and storing it during the melt season, releasing it slowly as baseflow during the summer and fall.

The extent of groundwater influence on streamflow affects habitat quality for stream fishes in several ways: through augmentation of baseflow, modulation of water temperature, and provision of refugia from temperature extremes (Power and others, 1999). Groundwater augmentation of summer baseflow is beneficial because higher flows during that time provide greater volume of habitat, as well as exert a potentially significant cooling influence on stream temperature. Even a relatively small input of groundwater can provide critical protection for cold-water fishes like salmon from potentially lethal temperatures during the summer months. Baseflow augmentation is also important during the winter, especially at high elevations where streams may only maintain free flowing water with significant groundwater input. Temperature modulation by groundwater can also be important during the winter by providing refugia areas where temperatures remain above freezing.

The characterization of low-flow regime is proposed to be conducted in stages, with the first step to examine baseflow characteristics across the regional geologic transition, especially focused on how geology may be reflected as a change in the relative importance of groundwater to summer low-flow conditions. Generation

of baseflow indices and frequency distributions of low-flow volume and timing based on gaged data will provide a means to quantify and visualize the distribution of low-flow patterns across the landscape. These results will provide the basis for evaluating the relationship between low-flow regime and important watershed characteristics, which will in turn be utilized to estimate low-flow regime for ungaged stream reaches. Developing the capacity to map key elements of low-flow regime across the basin is intended to provide a critical foundation for future work assessing the vulnerability of critical stream reaches to climate warming, which will aid in prioritizing areas for amelioration of land use impacts.

Objectives

The primary intent of this work is to develop and demonstrate an iterative and staged analytical protocol that can be used by CRITFC personnel to further the analysis as appropriate. The specific objectives for that protocol are as follows:

- To describe the relative importance of groundwater to baseflows across the large-scale geologic gradient in the Upper Grande Ronde River Basin
- To determine the key components of low-flow regime for gaged sites
- To identify watershed characteristics that are significantly associated with low-flow regime
- To estimate key components of low-flow regime for ungaged sites

Approach

The basic approach is to begin by characterizing baseflow across the basin to determine the importance of groundwater, then to conduct a more structured analysis of gaged streamflow data to generate the probability distributions for 7-day low-flow volume and timing of onset during the summer months. Metrics will be derived from the probability distributions to concisely describe the low-flow regime. Further analysis will be conducted to determine the important watershed factors that are associated with these low-flow patterns. Finally, the observed relationship between low-flow metrics and watershed characteristics will be utilized to estimate low-flow volume and timing for selected ungaged stream reaches of interest. All stages of the analysis will be done in collaboration with CRITFC personnel to ensure their input.

Objective 1: Characterize baseflow across the basin

The first step will be to inventory the available streamflow data, extending to streams outside the study area as appropriate. Once the data have been identified, the potential importance of groundwater to summer low flow will be assessed by a number of different means, including evaluating the annual 7-day low volume for each year of record for individual streams. A simple baseflow index can then be calculated as the mean ratio of the annual 7-day low flow and the mean daily flow for each year of record. As appropriate, hydrograph separation techniques may be employed to provide a more clear measure of baseflow volume. Higher values of the baseflow index imply higher volume of baseflow and correspondingly more groundwater influence. These data will be evaluated within the context of the regional geologic template to determine if a natural break can be observed to identify groundwater dominated streams from those dominated by surface runoff.

Objective 2: Generate probability distributions for 7-day low flow based on gaged data

Probability distributions will be determined for volume and timing of onset for the annual summer 7-day low flow. This will include a trend analysis to identify the appropriate period of

record for frequency analysis, as well to determine if changes have occurred in the volume and timing of low flow over the period of record. Probability distributions will be generated for the data showing no trend using an index-flow procedure, based on probability-weighted moment (PWM) estimators of the Generalized Extreme Value (GEV) distribution (Hosking and others, 1985). Hydrologic metrics to describe the key features of the low-flow regime will be derived directly from the probability distributions, including (but not limited to):

- Index of baseflow stability (2-year 7-day low flow, normalized to the mean)
- Index of baseflow variability (100-year 7-day low flow, normalized to the mean)
- Index of dispersion (2-year 7-day low flow – 100-year 7-day low flow, normalized to the mean)

The metrics derived from the frequency distributions will be evaluated with standard multivariate techniques, within the context of the gradient of groundwater influence if one is observed, to determine the key components that describe low-flow regime.

Objective 3: Identify the important watershed factors related to low-flow regime

Watershed characteristics that are hypothesized to govern the low-flow-regime will be determined by and/or acquired from CRITFC for both gaged and selected ungaged sites of interest. These characteristics will include, but are not limited to, measures of climate (such as snow accumulation), geology (such as elevation and underlying rock type), and land use (such as extent of water withdrawals and grazing impacts). Additional context will be provided by other factors as appropriate, including the analysis of baseflow that describes the contribution of groundwater from objective 1. The relationship between low-flow metrics derived from the probability distributions for gaged sites and these watershed characteristics will be examined using various multivariate techniques, including simple ordinations and Canonical Correlation Analysis (CCA).

Objective 4: Estimate relationships between low-flow metrics and watershed attributes to estimate probability distributions for ungaged stream reaches

CCA provides scores on canonical watershed variates that can be matched with defined statistical measures to identify which gaged sites are appropriate to consider as part of the “hydrologic neighborhood” for ungaged sites (Ribeiro-Correa and others, 1995). Regional PWM estimators can then be determined for each ungaged site based on the correspondence of watershed data with appropriate gaged sites, and these regional estimators will be used to estimate the parameters of the GEV distribution. Metrics to describe the low-flow regime will be derived directly from the estimated probability distributions for each ungaged site.

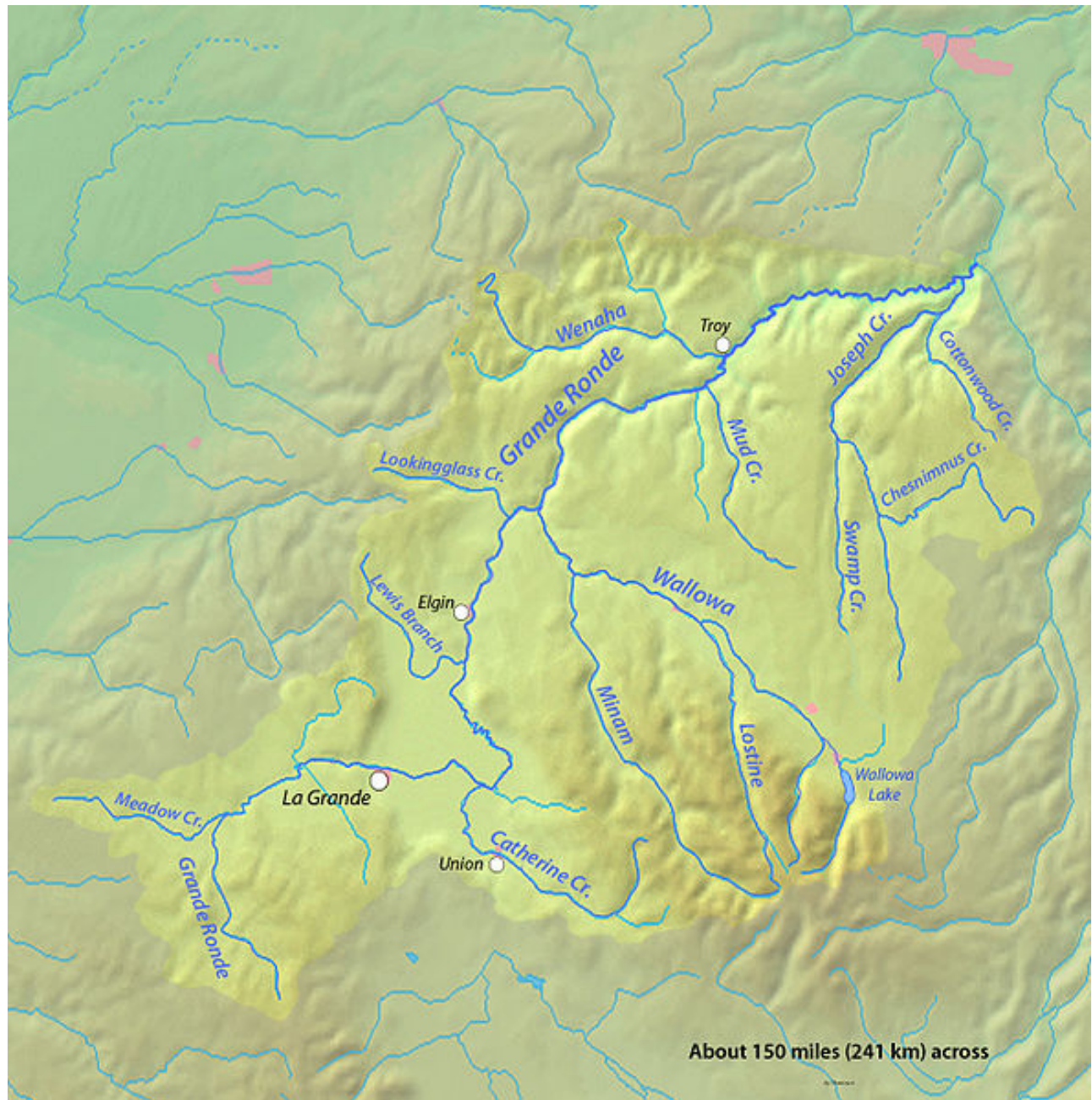
Study Relevance and Benefits

The proposed work directly addresses the topic of environmental flows, which is one of the high-priority issues for the USGS Cooperative Water Program (USGS, 2010) that also aligns with the larger goals of the USGS Science Strategy (USGS, 2007). The issue of environmental flows recognizes that human impacts on streamflow need to be carefully managed to preserve ecosystem function, especially where threatened fishes are concerned. By proposing to develop insight into the factors that determine low-flow regime in the upper Grande Ronde River Basin, this project will provide critical context for evaluating the relationship between hydrology, human land use, and the status of threatened salmon populations. This proposal builds upon the strong foundation within the USGS of developing and testing tools for hydrologic assessment and improvement of

environmental management. It also is intended to provide an approach for characterizing low-flow regime that will be relevant not only at the local scale of the Grande Ronde River Basin, but which will also be transferrable to other basins in the Pacific Northwest. As such, it represents a valuable foundation for advancing scientific understanding of the regional baseflow system in the Columbia Basin as well as supporting the recovery of salmon freshwater habitat. This work will also provide the necessary starting point for subsequent work to assess the vulnerability of critical stream reaches to climate warming, which is another key area of interest to both CRITFC and USGS.

Reports and Products

The analytical protocols and demonstration of their application will be published in an on-line USGS report to provide citable documentation while minimizing publication costs. Further analysis may be published in journal venues, in collaboration with CRITFC scientists, as appropriate.



Map of Grande Ronde River Basin.

Expenses/Personnel/Funding/Schedule

Personnel (Oregon Water Science Center)	
Valerie Kelly	70 days

Budget item	USGS FY2012			USGS FY2013			Total		
	CRITFC	Indirect	Subtotal	CRITFC	Indirect	Subtotal	CRITFC	Indirect	Total
Personnel	\$18,000	\$15,000	\$33,000	\$7,200	\$6,000	\$13,200	\$25,200	\$21,000	\$46,200
Travel	70	60	130				70	60	130
Publication				6,100	1,200	7,300	6,100	1,200	7,300
Total	\$18,070	\$15,060	\$33,130	\$13,300	\$7,200	\$20,500	31,370	22,260	\$53,630
USGS matching funds			\$22,000			\$14,000			\$36,000
Project total			\$55,000			\$34,500			\$89,500

Workplan Schedule	
Assemble streamflow data	Spring 2012
Characterize baseflow	Summer 2012
Determine key components of low-flow regime	Summer 2012
Identify important factors related to low-flow regime	Autumn 2012
Estimate low-flow metrics for ungaged sites	Autumn 2012
Report submitted for publication	Summer 2013
Progress reports provided to CRITFC	Quarterly

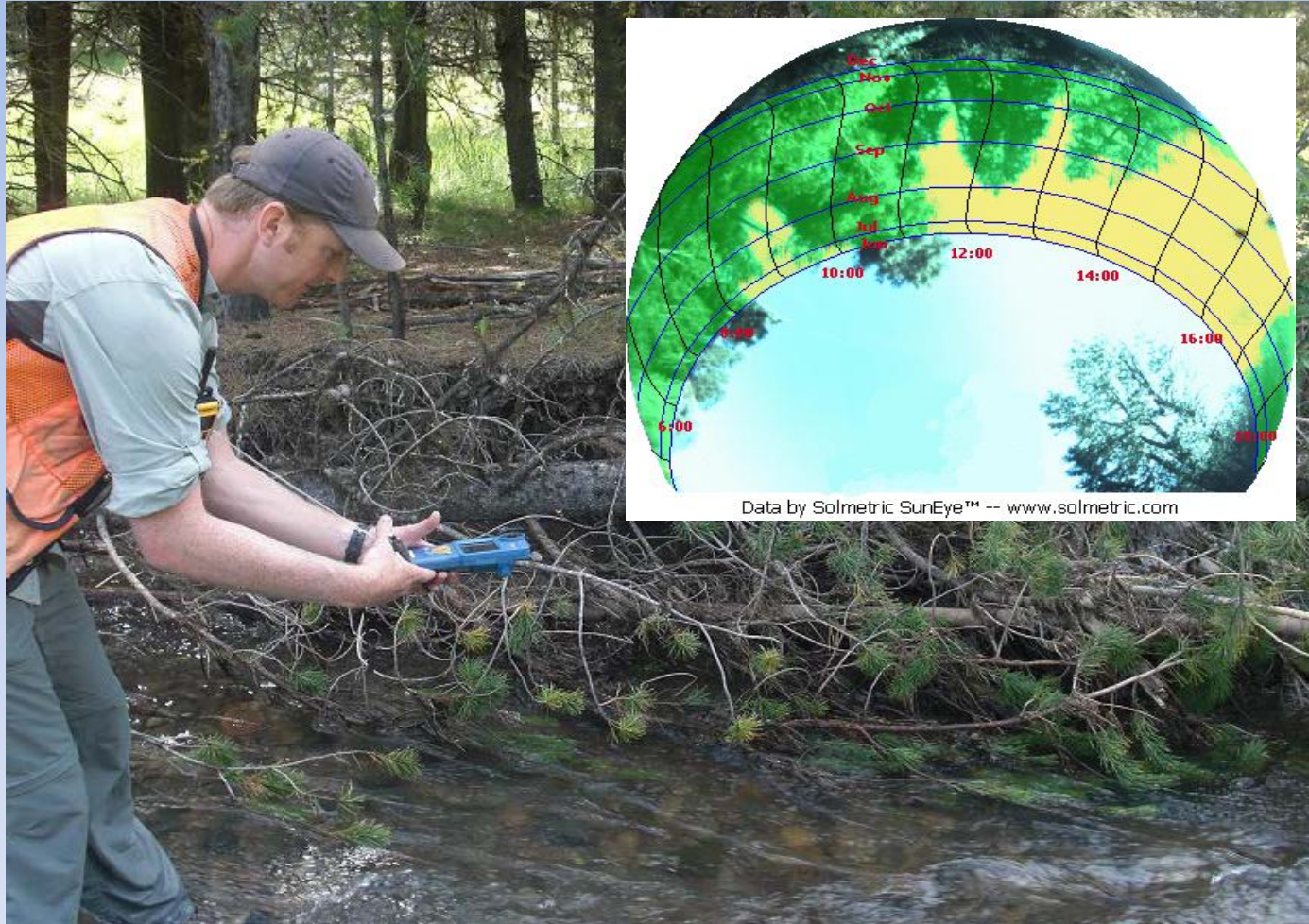
Literature Cited

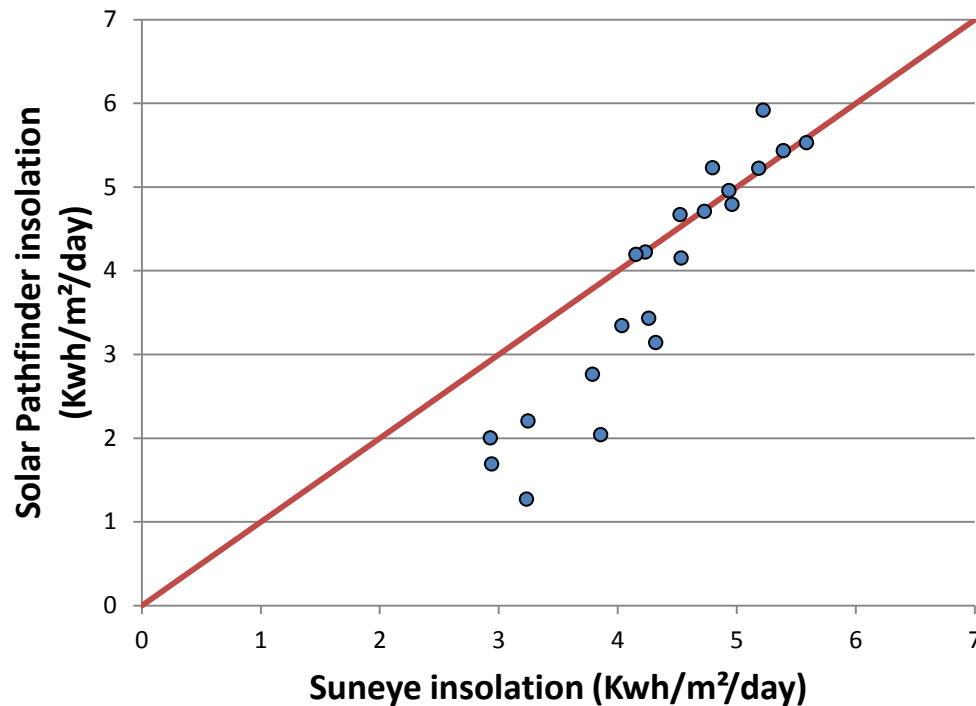
- CRITFC, 1995. Wy-Kan-Ush-Mi Wa-Kish-Wit, Spirit of the Salmon: The Columbia River Anadromous Fish Restoration Plan of the Nez Perce, Umatilla, Warm Springs, and Yakama Tribes.
- Hosking, J.R.M., J.R. Wallis, and E.F. Wood, 1985. Some statistics useful in regional frequency analysis. *Water Resources Research* 29(2): 271-281.
- McIntosh, B.A., 1992. Historical Changes in Anadromous Fish Habitat in the Upper Grande Ronde River, Oregon, 1941-1990. Corvallis OR: Oregon State University. M.S. thesis.
- National Oceanic and Atmospheric Administration, 2005. Endangered and Threatened Species: Final Listing Determinations for 16 ESUs of West Coast Salmon, and Final 4(d) Protective Regulations for Threatened Salmonid ESUS. *Federal Register* 70(123): 37160-37204
- 2007. Tributary Habitat Proposed Action Summary, May 21, 2007. NOAA, Portland, Oregon.
- Northwest Power and Conservation Council, 2004. Grande Ronde Subbasin Plan. May 2004.
- Power, G., R.S. Brown, and J.G. Imhof, 1999. Groundwater and fish—insights from northern North America. *Hydrological Processes* 13: 401-422.
- Ribeiro-Correa, J., G.S. Cavadias, B. Clement, and J. Rousselle, 1995. Identification of hydrological neighborhoods using a canonical correlation analysis. *Journal of Hydrology* 173: 71-89.
- U.S. Geological Survey, 2007. Facing tomorrow's challenges—U.S. Geological Survey science in the decade 2007-2017: U.S. Geological Survey Circular 1309.
- 2010. Water Resources Mission Area Informational Memorandum No. 2011.01: Priority issues for the Cooperative Water Program, fiscal year 2011/2012.
- Wissmar, R.C., J.E. Smith, B.A. McIntosh, H.W. Li, G.H. Reeves, and J.R. Sedell, 1994. Ecological Health of River Basins in Forested Regions of Eastern Washington and Oregon. U.S. Forest Service, General Technical Report PNW-GTR-326.

Appendix R.

Measuring Shade and Solar Radiation Using the Solmetric SunEye

Measuring Shade and Solar Radiation Using the Solmetric SunEye





T-Test Comparison:

Avg Difference
(SunEye – Solar
Pathfinder) = 0.5
Kwh/m²/day (14%)

$P < 0.001$

Image Quality Comparison

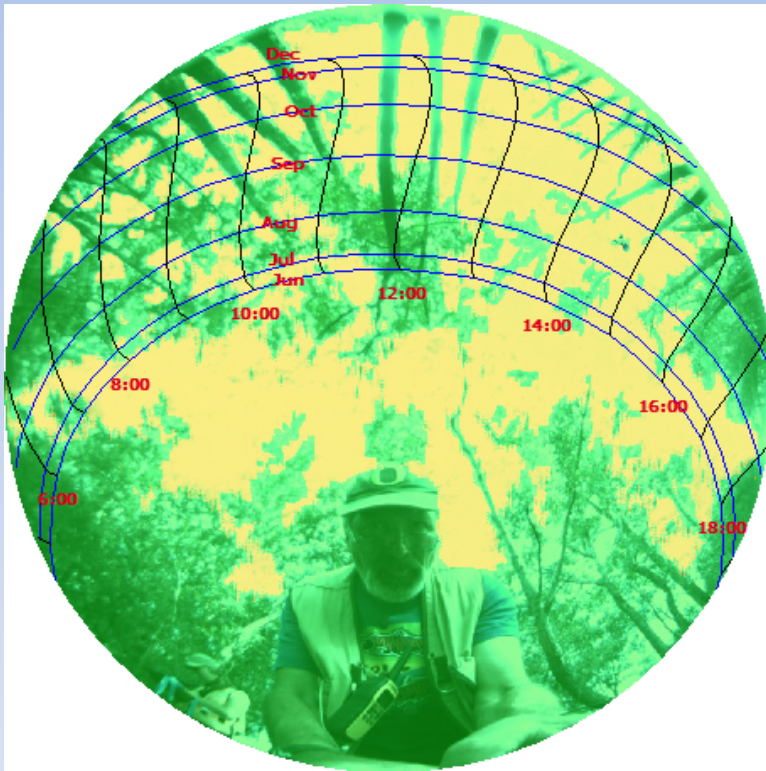
SunEye



Solar Pathfinder



SunEye



Solar Pathfinder





Importable and printable version of this report:
[CBW05583-235322 Report \(importable and printable\).htm](#)

Session Properties

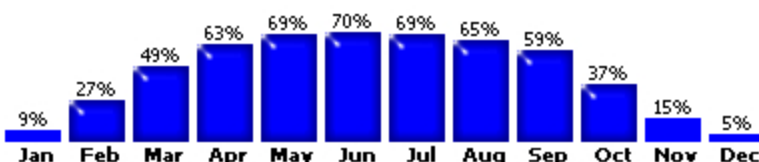
Name	CBW05583-235322
Creation Date	8/4/2011 14:20
Note	CBW05583-235322-20110809
Location	45.3°N, 118.1°W Mag Dec: 15.1°E Time Zone: GMT-08:00

Solar access averages of 5 skylines in this session

Skylines Averaged: Sky07, Sky08, Sky09, Sky10, Sky11

Monthly Solar Access Averages

Annual	May-Oct	Nov-Apr
57%	64%	39%

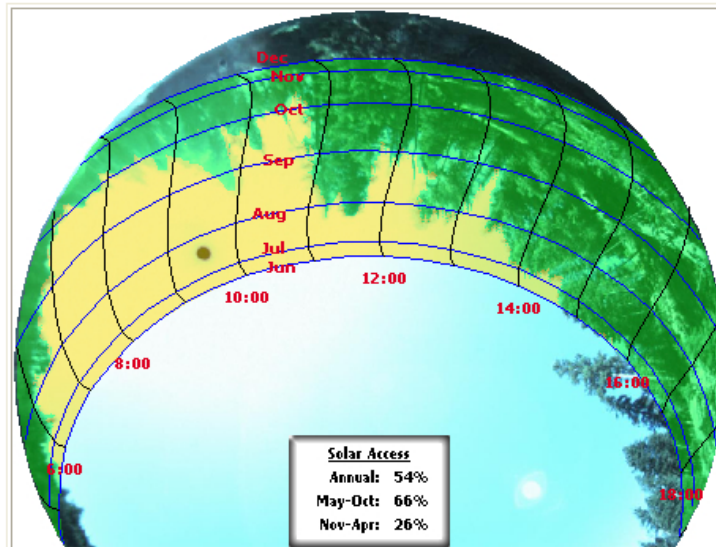


Sky11 -- 8/10/2011 10:33 -- Transect 21

Panel Orientation: Tilt=0° -- Azimuth=180° -- Skyline Heading=179°

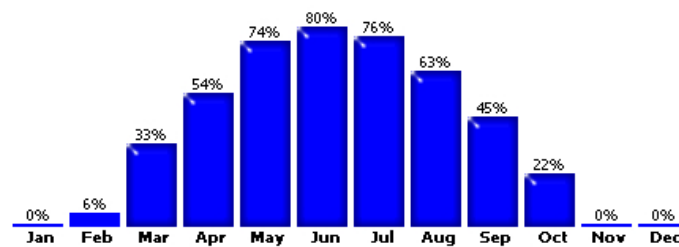
Solar Access: Annual: 54% -- Summer (May-Oct): 66% -- Winter (Nov-Apr): 26%

TSRF: 44% -- TOF: 83%



Data by Solmetric SunEye™ -- www.solmetric.com

Monthly solar access: (Fixed; Tilt=0°; Azim=180°)



Data by Solmetric SunEye™ -- www.solmetric.com

Files available for Sky11—or Transect 21

Additional Files in the ExportedFiles subdirectory:

Daily solar access data in CSV format	Sky11DailySolarAccess.csv
Windowed Daily solar access data in CSV format	Sky11WindowedDailySolarAccess.csv
Insolation (quarter-hourly) in CSV format	Sky11Insolation.csv
Shading (quarter-hourly) in CSV format	Sky11Shading.csv
Solar obstruction elevations in CSV format	Sky11ObstructionElevations.csv
Solar obstruction elevations in XML format	Sky11ObstructionElevations.xml
PV*SOL horizon angles file (.hor)	Sky11 PV SOL.hor
PVSYST horizon angles file (.hor)	Sky11 PVSYST.hor
Windowed obstruction elevations in CSV format	Sky11WindowedObstructionElevations.csv
Full resolution fish eye image	Sky11FullFishEye.jpg
Annual access fully annotated sky image	Sky11AnnualAccessFullyAnnotated.jpg

CSV Files Needed
for Calculation of
Solar Radiation

Sky11Insolation			
	A	B	C
1	Insolation 1.1		
2	Session Name:	CBW05583-235322	
3	Skyline:	Sky11	
4	Creation Date:	8/10/2011 10:33	
5	Latitude:	45.3	
6	Longitude:	-118.1	
7	Mag Dec:	15.1	
8	Tracking Mode:	Fixed	
9	Panel Tilt:	0	
10	Panel Azimuth:	180	
11	Time Zone:	GMT-08:00	
12			
13	Numbers along each		
14			
15	TMY3 Weather Station	LA GRANDE MUNI AP OR	
16	TMY3 WBAN:	726884	
17			
18	begin data	4:15	4:30
19	1-Jan		
20	2-Jan		
21	3-Jan		

Insolation (quarter-hourly) in CSV format

[Sky11Insolation.csv](#)

Note: This CSV file created for each Skyview is the **potential solar radiation** or insolation by quarter hour for every day of the year.

To calculate total solar radiation for the windowed period of interest (e.g., Jun – Sep), simply sum all values within that window.

Total potential insolation (wh/m²) = Sum of quarter- hourly insolation values

begin data	7:30	7:45	8:00	8:15	8:30	8:45	9:00	9:15	9:30	9:45	10:00	10:15
1-Jan	0	10.824	10.824	10.824	10.824	16.429	16.429	16.429	16.429	21.244	21.244	
2-Jan	0	10.824	10.824	10.824	10.824	16.429	16.429	16.429	16.429	21.244	21.244	
3-Jan	0	10.824	10.824	10.824	10.824	16.429	16.429	16.429	16.429	21.244	21.244	
4-Jan	0	10.824	10.824	10.824	10.824	16.429	16.429	16.429	16.429	21.244	21.244	
5-Jan	0	20.484	20.484	20.484	20.484	50.307	50.307	50.307	50.307	70.263	70.263	
6-Jan	0	20.484	20.484	20.484	20.484	50.307	50.307	50.307	50.307	70.263	70.263	
7-Jan	0	20.484	20.484	20.484	20.484	50.307	50.307	50.307	50.307	70.263	70.263	
8-Jan	0	20.484	20.484	20.484	20.484	50.307	50.307	50.307	50.307	70.263	70.263	
9-Jan	0	11.094	11.094	11.094	11.094	27.886	27.886	27.886	27.886	32.968	32.968	
10-Jan	0	11.094	11.094	11.094	11.094	27.886	27.886	27.886	27.886	32.968	32.968	
11-Jan	0	11.094	11.094	11.094	11.094	27.886	27.886	27.886	27.886	32.968	32.968	

Panel Azimuth: 180
Time Zone: GMT-08:00

Window Month Range: Jun-Sep

Window Time Range: 0:00-23:00

Windowed Daily solar access data in CSV format

[Sky11WindowedDailySolarAccess.csv](#)

begin data	Day	Month			
		Jun	Jul	Aug	Sep
	1	78.64	72.34	72.11	49.32
	2	78.64	72.34	72.11	49.32
	3	78.64	72.34	72.11	49.32
	4	78.64	72.34	72.11	49.32
	5	79.1	77.05	69.84	55.18
	6	79.1	77.05	69.84	55.18
	7	79.1	77.05	69.84	55.18
	8	79.1	77.05	69.84	55.18
	9	80.59	77.69	69.51	51.31
	10	80.59	77.69	69.51	51.31
	11	80.59	77.69	69.51	51.31
	12	80.59	77.69	69.51	51.31
	13	80.5	77.05	67.19	44.97
	14	80.5	77.05	67.19	44.97
	15	80.5	77.05	67.19	44.97
	16	80.5	77.05	67.19	44.97
	17	80.27	78.87	59.92	46.59
	18	80.27	78.87	59.92	46.59
	19	80.27	78.87	59.92	46.59
	20	80.27	78.87	59.92	46.59
	21	80.82	74.19	60.35	36.5
	22	80.82	74.19	60.35	36.5
	23	80.82	74.19	60.35	36.5
	24	80.82	74.19	60.35	36.5
	25	79.82	76.66	49.96	31.97
	26	79.82	76.66	49.96	31.97
	27	79.82	76.66	49.96	31.97
	28	79.82	76.66	49.96	31.97
	29	79.82	76.66	49.96	31.97
	30	79.82	76.66	49.96	31.97
	31		76.66	49.96	
Monthly totals:		79.9	76.5	62.9	44.6

Window Jun-Sep: 68.36

Solar access percentage =
(Insolation accounting for shade /
total potential insolation)*100

Average daily insolation by site for June-Sept

Average Daily Insolation (Kwh/m^2)					
Site ID	June	July	Aug	Sept	Summer Average
CBW05583-108010	5.833703	5.842372	4.660497	3.499822	4.959098246
CBW05583-138554	5.33213	5.24134	4.264506	3.287825	4.531450528
CBW05583-148970	3.824495	3.65185	3.104561	2.398565	3.244867643
CBW05583-155818	4.464584	4.070215	2.617188	1.777583	3.232392462
CBW05583-206314	5.530427	5.459361	3.998888	2.283186	4.317965544
CBW05583-217258	4.887422	4.736062	3.336062	2.463289	3.855708845
CBW05583-228666	4.47479	4.354526	3.541977	2.775656	3.786737258
CBW05583-235322	5.109047	5.076352	3.979393	2.75971	4.231125374
CBW05583-269114	6.017419	5.998521	4.935861	3.782172	5.183493275
CBW05583-280042	6.552528	6.524423	5.259964	4.001673	5.58464672
CBW05583-321338	5.285472	5.22219	4.368073	3.214658	4.522598307
CBW05583-368042	5.545007	5.533017	4.117076	1.84137	4.259117511
CBW05583-430250	3.667024	3.612076	2.550175	1.88452	2.928448631
CBW05583-456106	5.754968	5.700952	4.443615	3.009228	4.727190828
CBW05583-457530	4.734325	4.73017	4.013509	3.129297	4.151825291
CBW05583-490810	5.027395	4.81561	3.738144	2.553341	4.033622787
DSGN4-000009	5.660194	5.587522	4.561803	3.372249	4.795442056
DSGN4-000092	3.509554	3.559044	2.813356	1.877015	2.939742107
DSGN4-000202	6.307573	6.250424	5.138121	3.865657	5.390443676
DSGN4-000245	5.951806	5.973478	4.69583	3.110536	4.932912742
DSGN4-000277	6.115109	6.067757	5.027244	3.674297	5.221101852

Total actual insolation (wh/m^2) =
(solar access percentage/100)*(total potential
insolation)

Average actual daily insolation (Kwh/m^2/day) =
((total actual insolation)/# days in window)/1000

All_Sites_Insolation_Totals_tarin-Nov23-2011

Procedure:

- 1) Acquire a series of Skyviews (21) for all transects (1 min / transect)
- 2) Download the Session to the CHaMP computer (1 min)
- 3) Open SunEye software, set time window (June – Sept 4:30AM – 10PM)
- 4) Edit photo jpgs for each Skyview to correct the color designations to correctly identify sky and obstructions (0.5 – 5 min / transect)
- 5) Upload image files, total potential insolation csv file ([SkyXXInsolation.csv](#)), and daily solar access csv file ([SkyXXWindowedDailySolarAccess.csv](#)) from each transect to the CHaMP cloud (2 min)
- 6) CHaMP data managers will extract required data from the csv files and calculate actual solar insolation using the formulas described above.

Estimated data collection and processing time per site:

5 transects = 18 minutes (vs 22 min for SPF)

21 transects = 66 minutes (vs 87 min for SPF)



Optional SunEye
Extension Kit
(\$500)



Appendix S.

The landscape context of fish-habitat relationships: implications for restoring wood recruitment processes in U.S. Pacific Northwest rivers

**The landscape context of fish-habitat relationships: implications for restoring
wood recruitment processes in U.S. Pacific Northwest rivers**

DRAFT manuscript intended for *Restoration Ecology*, including preliminary analysis of 2011
Columbia Habitat Monitoring Program (CHaMP) data

March 29, 2012

Seth White, Casey Justice, and Dale McCullough

Columbia River Inter-Tribal Fish Commission

729 NE Oregon, Ste 200, Portland, OR 97232, U.S.A.

Abstract

Literature on the connections between freshwater biota and river geomorphology have long emphasized the need to link landscape-scale processes to in-stream habitat, yet restoration practitioners have been slow to adapt. This presentation describes a monitoring program in the Pacific Northwest, U.S.A., designed to evaluate whether aggregate restoration activities can positively affect threatened spring Chinook salmon. Commonly cited impediments to salmon survival are high water temperatures, fine sediment in spawning gravel, loss of riparian vegetation, channelization, lack of large woody debris in, loss of large pools, and depletion of summer streamflows. However, these factors are often inter-correlated and can be difficult or impossible to tease out using classic univariate statistics. A multivariate ordination was conducted of reach-scale habitat characteristics across eight watersheds in the Pacific Northwest to discover an appropriate landscape-level classification, which in turn helped reveal patterns of anthropogenic impacts on site-level fish habitat. In the upper Grande Ronde River, estimates of juvenile Chinook salmon density (via snorkeling) were linked to landscape classification and site-level habitat conditions. Across the entire basin, large woody debris and pools positively affected fish density through direct and indirect pathways, but were also dependent upon mean annual streamflow. These relationships varied across landscape classes, with high elevation mountain reaches behaving differently than lower elevation floodplain and constrained reaches. These findings have direct management implications for guiding the location and type of restoration within the landscape context.

Introduction

The Columbia River Inter-Tribal Fish Commission (CRITFC) is conducting a monitoring program in the upper Grande Ronde River, Catherine Creek, and Minam River basins designed to evaluate whether aggregate habitat restoration actions can positively affect ESA-listed spring Chinook salmon populations. According to literature, common impediments to salmon survival are high water temperatures, fine sediment in spawning gravel, loss of riparian vegetation, channelization, lack of large woody debris in the channel, loss of large pools for adult fish to hold in prior to spawning, and summertime depletion of streamflows. However, the effects on salmon of these and other factors are often inter-correlated and the influence of each is dependent upon the entire suite of relationships, which can be difficult or impossible to tease out using classic univariate statistics. This summary describes our process of selecting an appropriate reach-scale classification and linkages between juvenile spring Chinook salmon rearing density, pool frequency, and large woody debris in context of that classification. We employed multivariate analyses and structural equation modeling as tools for simplifying complex relationships and determining the unique effects of single habitat characteristics on salmon populations.

Specifically, our objectives were to (1) examine interrelationships among site-level CHaMP fish habitat metrics in context of several landscape-level classifications using multivariate ordination and (2) test hypotheses relating fish habitat metrics to estimates of relative fish density using structural equation modeling, specifically the direct and indirect effects of large woody debris on fish distribution.

Methods

Objective 1. Multivariate analysis of CHaMP-wide habitat metrics

We conducted multivariate ordination of CHaMP site-level habitat data collected in 2011 across eight watersheds in the Pacific Northwest (Figure 1) to discover an appropriate landscape-level classification, which in turn helped reveal patterns of anthropogenic impacts on site-level fish habitat. At the time of this preliminary analysis, 193 unique sites from the Entiat, John Day, Lemhi, Methow, South Fork Salmon, Tucannon, upper Grande Ronde, and Wenatchee watersheds were available for analysis after excluding repeat site visits and sites with missing data. We performed nonmetric multidimensional scaling (NMDS) (McCune and Grace 2002) on relativized data using Sorensen's distance measure.

Relationships among landscape-scale quantitative and categorical variables and in-stream fish habitat were then examined. Correlations with NMDS axes and landscape-level quantitative variables (e.g., mean annual streamflow, annual precipitation, etc.) were assessed by examining Pearson correlations and biplots. To test whether landscape categories (i.e., geomorphic channel type, valley class, watershed, and crews' on-site designation of bedform class) explained variation in habitat metrics, we performed multi-response permutation procedure (MRPP, a multivariate analogue to ANOVA allowing for unbalanced designs) using a rank-transformed distance matrix and Sorensen's distance to match interpretation with NMDS.

Next, we plotted univariate responses of habitat metrics grouped by appropriate landscape category (as determined from MRPP) to demonstrate how fish habitat metrics respond to

anthropogenic disturbance in context of surrounding landscape conditions. To describe land use, we used a HUC-6 landscape classification across the Pacific Northwest in two parts: a natural characteristics classification and a human disturbance classification (Whittier et al. 2011). The natural classification accounted for seven climate, land form, geologic, and stream form attributes. The disturbance classification accounted for urban land use, agricultural land use, impervious surface, and road density. The disturbance classification generated a disturbance score for each HUC-6 watershed, which was then incorporated into the CHaMP data file for each site monitored, with each site receiving the Whittier based disturbance score in its respective HUC- 6. We grouped disturbance into two classes: “low,” consisting of undisturbed, very low disturbance, and moderately low disturbance; and “high,” consisting of eastside mixed, eastside agriculture, low mountains mixed, and big valleys mixed.

Objective 2. Fish-habitat relationships in the upper Grande Ronde River basin

In the upper Grande Ronde River and Catherine Creek basins of NE Oregon (Figure 2), we linked estimates of juvenile Chinook salmon density to landscape classification and site-level habitat conditions using structural equation modeling (SEM) , an ideal statistical technique for testing complex hypothesis when variables are causally interrelated (Grace 2006). During late-summer through autumn of 2011, we conducted visual assessments of fish density via snorkeling (Thurow 1994) at CHaMP sites in the upper Grande Ronde River and Catherine Creek basins, in collaboration with Oregon Department of Fish & Wildlife, who was focused primarily on steelhead habitat. Using SEM, we examine the interrelated effects of mean annual flow, large woody debris, and frequency of pool area on the density of juvenile Chinook salmon in pools.

To meet assumptions of normality, we applied Box-Cox transformations (Box and Cox 1964) to all variables.

Results and Discussion

Objective 1. Multivariate analysis of CHaMP-wide habitat metrics

Ordination of site-level CHaMP habitat metrics using NMDS revealed a 3-axis solution that was low stress (13.57), highly stable (final instability $< 1.0 \times 10^{-8}$), and explained 86.9% of the total variation (Figure 3). Several habitat metrics that were influential on multivariate data structure were dependant on River Bathymetry Toolkit (RBT) for their calculation. NMDS axes 1 & 3 were most correlated with quantitative landscape variables precipitation (Ppt), mean annual streamflow (MeanU), cumulative drainage area above a site (CUMDRAINAG) and its square root (SqrtDrainArea), and a principal components component axis from a previous analysis of natural landscape characteristics of the Pacific Northwest (NatPrin1) (Whittier et al. 2011). Axis 1 described a gradient of sites with abundant pool tail fines, high frequency of pools, and finer substrates in all channel unit types on one end of a spectrum; and sites with large wetted volume, large wetted area, and high discharge on the other. As expected, that gradient was positively correlated with increasing mean annual streamflow and cumulative drainage area. Axis 3 described a gradient of sites with high volumes of large woody debris in pools and within the bankfull and high frequency of pools on one hand; and sites with high conductivity and highly variable bankfull dimensions on the other. That gradient was positively correlated with precipitation and negatively correlated with Whittier's natural principal components axis.

MRPP revealed that all landscape categories (valley class, channel type, watershed, and crews' on-site designation of bedform class) explained some variation the multivariate distribution in habitat metrics (Table 1). However, a simplified version of an existing channel type classification (Beechie et al. unpublished data) (Figure 4) best explained the multivariate distribution of fish habitat metrics according to a large effect size ($A\text{-statistic} = 0.17$) relative to a small number of groups (2).

When sites were categorized according to simplified channel type (mountain vs. floodplain and constrained reaches), a distinction was noted between the two groups (Figure 5). Mountain reaches were characterized by low values of NMDS axis 1; with abundant pool tail fines, smaller substrate throughout the reach, and high frequency of pools. Floodplain and constrained reaches were characterized by higher values of axis 1; with larger wetted volume and area, and greater discharge. A simplified classification of CHaMP sites such as this may be desirable for future analysis of CHaMP data; in part because the smaller number of groups helps achieve a large enough sample size within classification types.

Multivariate analyses can help guide focused univariate analyses, as demonstrated in our examination of key fish habitat variables according to level of anthropogenic disturbance. For example, an analysis of median surface particle size (D50) of sites reveals that if reach type is not taken into consideration, there appears to be no difference in D50 between disturbed and undisturbed sites; whereas the use of a channel-type classification reveals drastic differences (Figure 6). Several other habitat variables showed similar patterns (Figure 7). Bank angles were steeper with higher disturbance regardless of channel type, possibly indicating an effect of

anthropogenic stressors on channel incision. The volume of large woody debris was reduced in disturbed areas and greater in floodplain and constrained reach types. Percent fines and sand as substrate was higher in disturbed areas, possibly due to erosive inputs of sediment from the surrounding landscape into the stream channel; but substrate was also smaller in mountain reaches as expected along a river continuum (Vannote et al. 1980). In floodplain and constrained reaches, pool tail fines increased with disturbance as expected. Contrary to our initial expectations, pool tail fines decreased with disturbance in mountain reaches; possibly because the accumulation of fine sediment in higher elevation pool-riffle, step-pool, and cascade reach morphologies is a naturally occurring process. In the case of mountain reaches, anthropogenic disturbance may in fact sever the natural process of sediment delivery to the stream channel.

Objective 2. Fish-habitat relationships in the upper Grande Ronde River basin

Using structural equations modeling (SEM), we described interactive effects among stream flow, large woody debris, pool frequency, and juvenile Chinook density in the upper Grande Ronde River and Catherine Creek basins (Figure 8). As expected, the volume of large woody debris in pools and frequency of pool area both had positive effects on fish density. However, this relationship was swamped by that of mean annual flow, indicating that position of sites in the landscape needs to be accounted for when attempting to predict fish densities across an entire watershed. Mean annual flow exhibited a negative relationship with frequency of pool area, perhaps because sites at uppermost elevation (and thus lower streamflow) of our study extent were typically step pool or pool riffle channel morphologies. Mean annual flow therefore

had an indirect, negative effect on fish density through its path through pool frequency.

Contrary to our expectations, large woody debris in pools did not increase the frequency of pool area, as this relationship was insignificant.

From NMDS analysis we discovered important insights about how fish habitat metrics differ according to channel type (Figure 7) and used those findings in subsequent analyses. Using identical model specification, variables, and data as for the global SEM model, we conducted multi-group SEM and discovered very different behavior among mountain vs. floodplain and constrained reaches (Figure 9). In contrast to the global model, in mountain reaches we found large woody debris to positively affect frequency of pool area, which is in accordance with predictions of the river continuum concept (Vannote et al. 1980) that headwater streams will be more influenced by terrestrial vegetation. In headwater streams, the variables specified in our model did not predict fish density, indicating that factors other than those in our model affected fish density in those reaches. In floodplain and constrained reaches, all the hypothesized relationships among variables were significant, and slightly more variation in fish density was predicted in this model ($R^2 = 0.64$) than in the global model ($R^2 = 0.61$). In contrast to the global model, the frequency of pool area increased with mean annual flow in floodplain and constrained reaches, possibly because lower, slow water reaches were pooled up into long glides and runs because of lower gradients.

Conclusions

This paper describes an analysis of preliminary CHaMP data collected in 2011, and demonstrates the importance of incorporating a landscape context in fish-habitat relationships.

Multivariate analyses and structural equation modeling were helpful tools for simplifying complex relationships and determining the unique effects of single habitat characteristics on salmon populations. In the upper Grande Ronde River basin, we linked estimates of juvenile Chinook salmon density to landscape classification and site-level habitat conditions. Across the entire basin, large woody debris volume and frequency of pool area positively affected fish density, but their effects were swamped by mean annual streamflow. However, these relationships varied across landscape classes, with high elevation mountain reaches behaving differently than lower elevation floodplain and constrained reaches. The utility of this information can assist restoration practitioners by helping set goals for restoration and examining project effectiveness at the landscape scale. The landscape disturbance classification (Whittier 2011) and channel geomorphic classification (Beechie, unpublished data) exist for the entire Pacific Northwest and can help to identify areas of concern. The overall impact of restoration can then be tracked by the progression of the distribution of habitat metrics at restored locations toward those at the best sites. Furthermore, these results demonstrate an approach to habitat modeling that CRITFC is currently employing, with the desired outcome of supporting a habitat-based life cycle model for spring Chinook salmon.

Literature Cited

- Beechie, T. "Predicting Channel Types in the Columbia River Basin" 2010.
- Box, G.E.P., and D.R. Cox. 1964. "An Analysis of Transformations (with Discussion)." *Journal of the Royal Statistical Society B* 26: 211–252.
- Grace, J.B. 2006. *Structural Equation Modeling and Natural Systems*. Cambridge, NY: Cambridge University Press.
- McCune, B., and J.B. Grace. 2002. *Analysis of Ecological Communities*. Gleneden Beach, Oregon: MjM Software Design.
- Thurrow, R.F. 1994. *Underwater Methods for Study of Salmonids in the Intermountain West*. General Technical Report. Ogden, UT: US Department of Agriculture, Forest Service, Intermountain Research Station.
- Vannote, R. L., G. W. Minshall, K. W. Cummins, J. R. Sedell, and C. E. Cushing. 1980. "The River Continuum Concept." *Canadian Journal of Fisheries and Aquatic Sciences* 37: 130–137.
- Whittier, T.R. 2011. "Landscape Classifications _of PNW Watersheds: Natural Features _& Human Disturbance" Portland, OR.
- Whittier, T.R., A.T. Herlihy, C. Jordan, and C. Volk. 2011. *Landscape Classification of Pacific Northwest Hydrologic Units Based on Natural Features and Human Disturbance to Support Salmonid Research and Management*. Final Report for USBOR and NOAA

Interagency Agreement—Reclamation IA No: 1425-06-AA-IC-4806, NWFSC IA No:
2RLEFRE. USBor and NOAA.

Tables

Table 1. MRPP results indicating relative ability of categorical landscape designations to explain multivariate habitat metrics. Larger *A-statistic* indicates stronger group effect, whereas Rating penalizes for larger number of groups.

Group	No. groups*	<i>A-statistic</i>	Rating (<i>A/N</i>)*100	<i>P-value</i>
Channel type - simplified	2	0.17	8.50	$< 1.0 \times 10^{-8}$
Valley class (source, trans, depos)	3	0.19	6.67	$< 1.0 \times 10^{-8}$
Channel type (Beechie)	8	0.24	3.00	$< 1.0 \times 10^{-8}$
Watershed	8	0.23	2.88	$< 1.0 \times 10^{-8}$
Crew's bedform designation	5 (7)	0.08	1.60	$< 1.0 \times 10^{-8}$

*Values in parentheses are original group numbers before exclusion based on site membership < 2

Figures

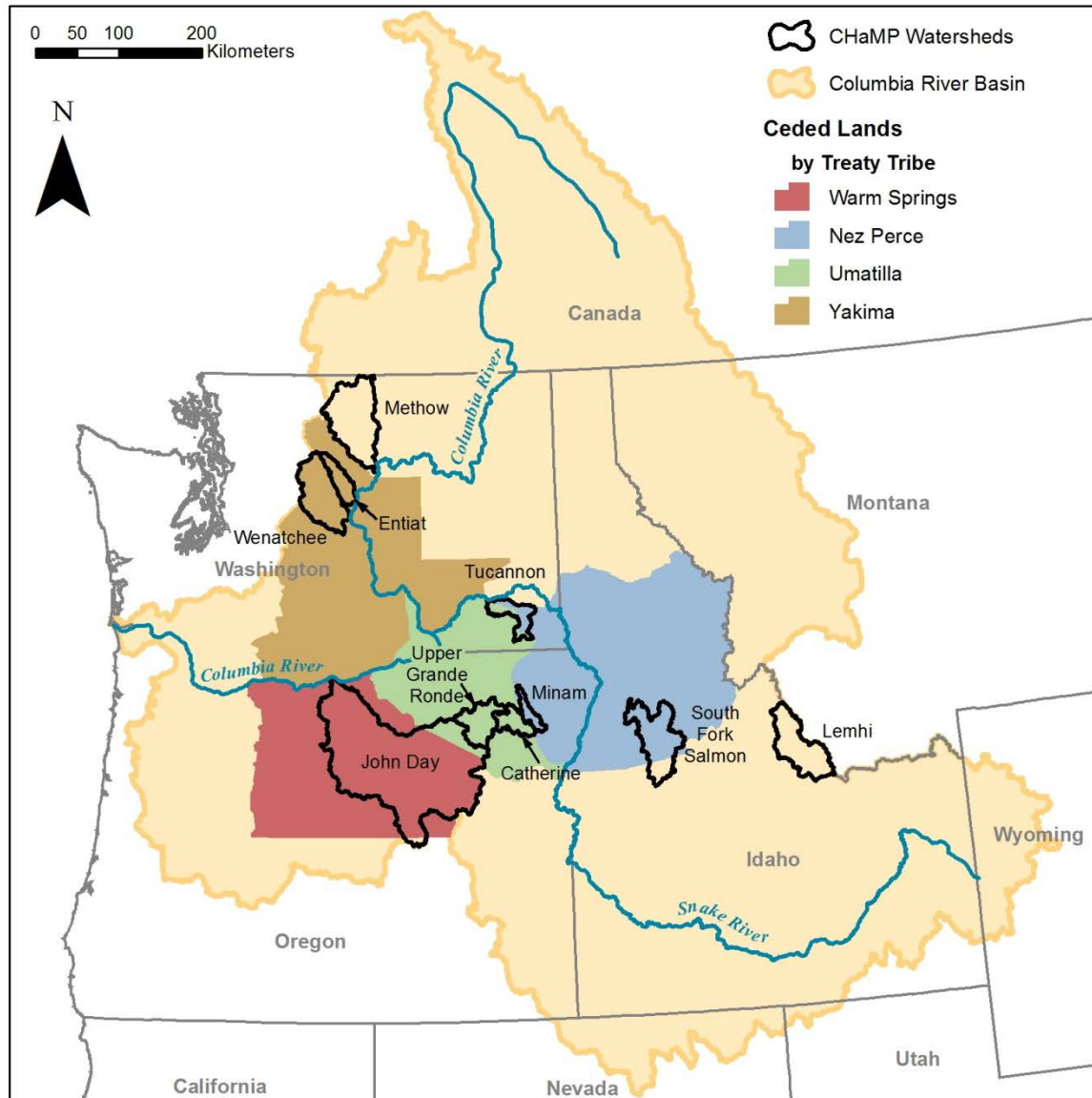


Figure 1. Location of Columbia Habitat Monitoring Program (CHaMP) watersheds in 2011 and the Minam River basin.

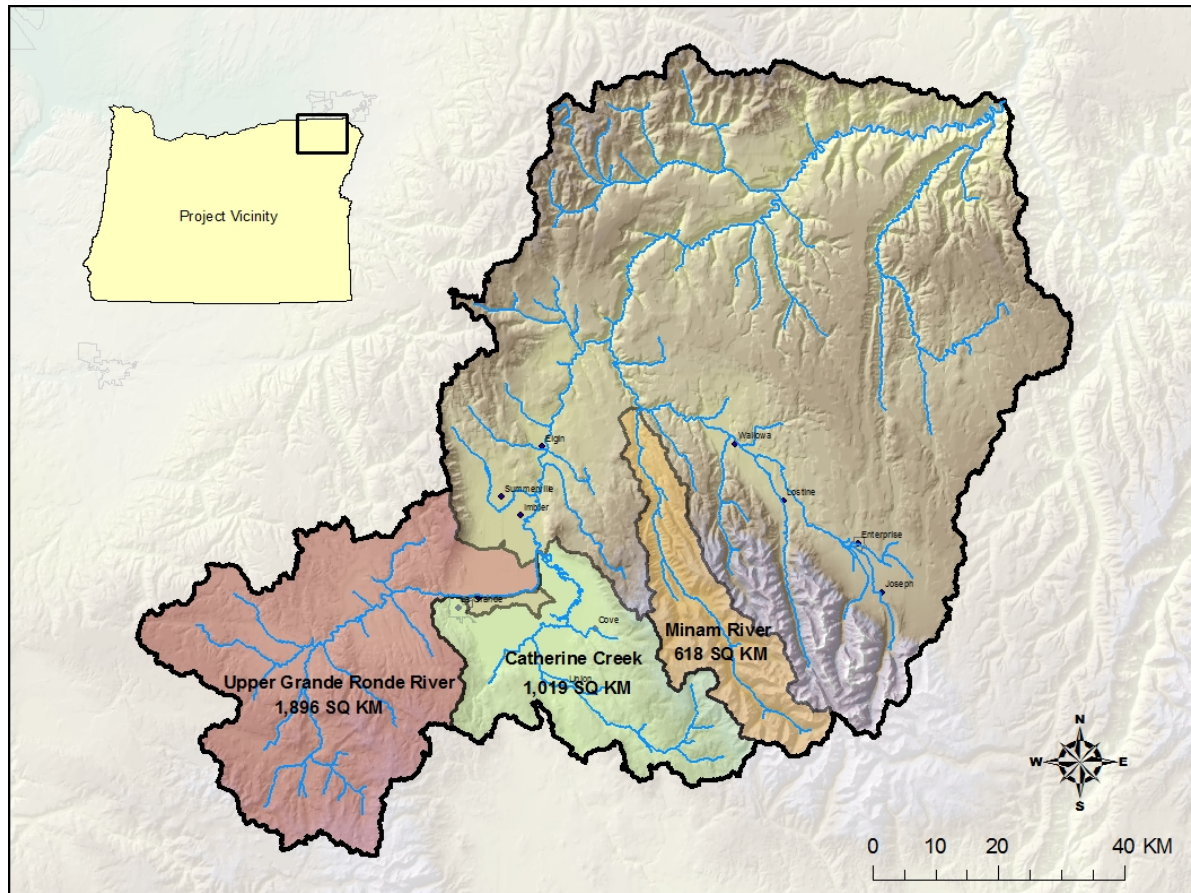


Figure 2. Map of Grande Ronde River basin in NE Oregon including CRITFC's focal watersheds upper Grande Ronde River, Catherine Creek, and Minam River.

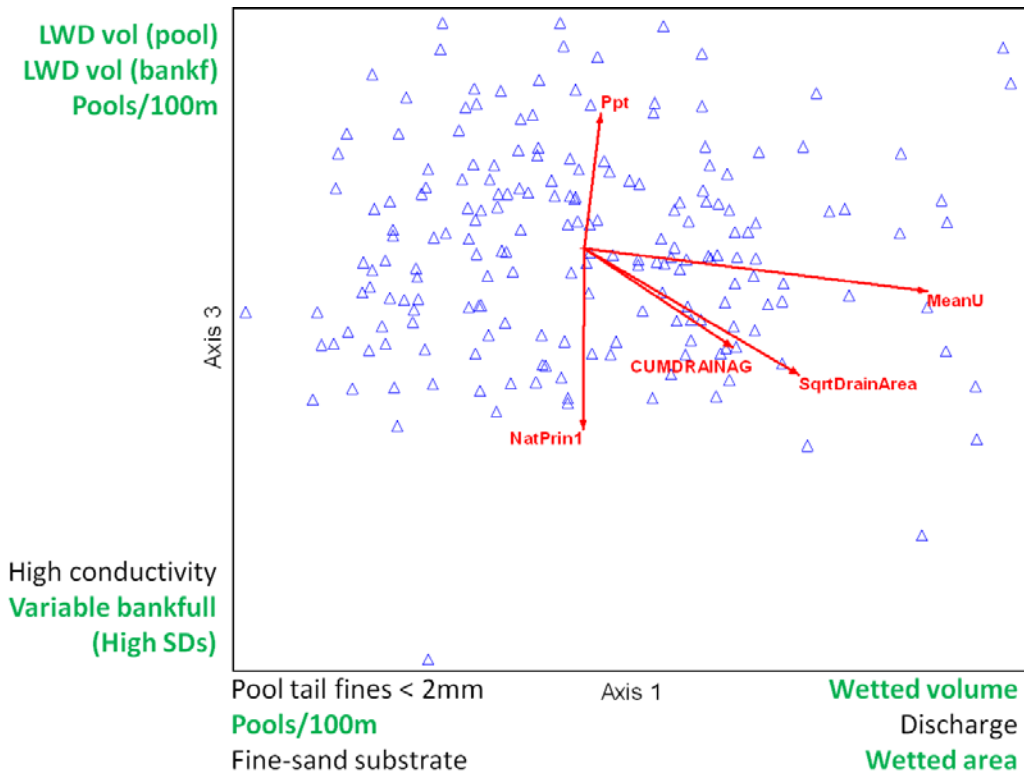


Figure 3. Biplot of site-level CHaMP sites in multivariate habitat metric space and correlations with landscape variables (see text for variable descriptions). Green text indicates habitat metrics dependant on River Bathymetry Toolkit (RBT).

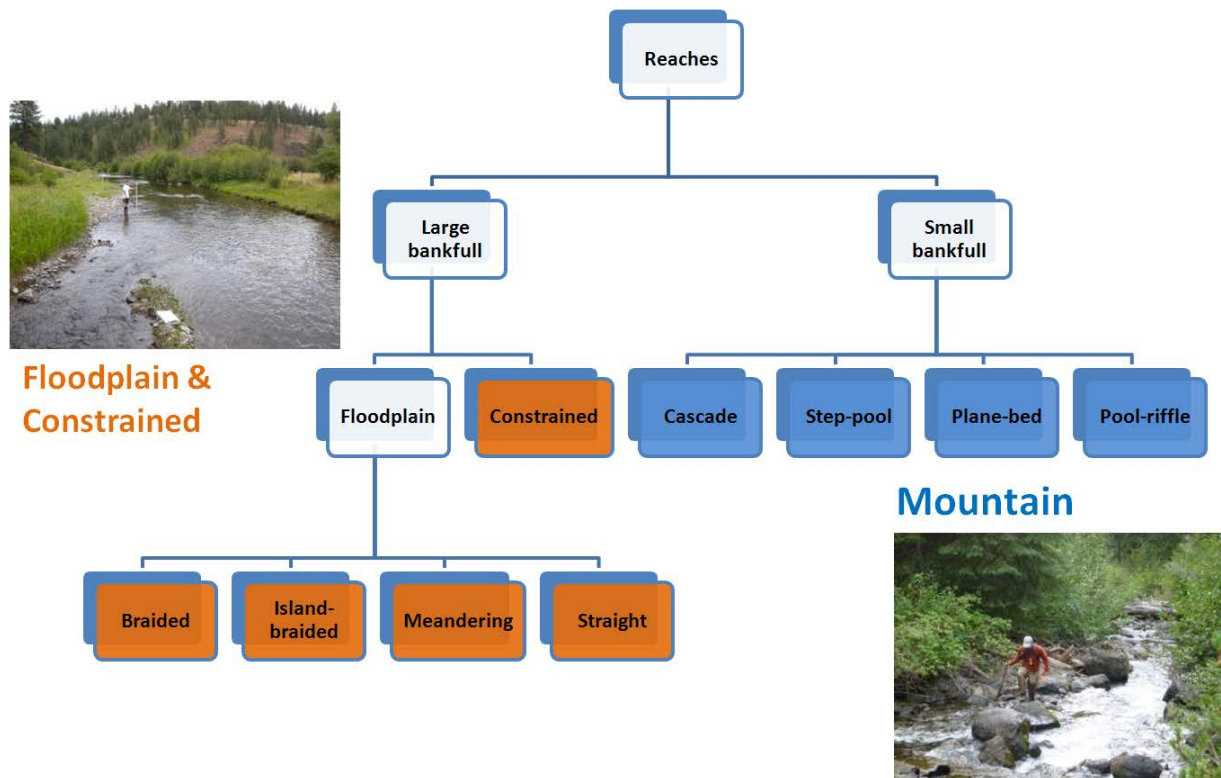


Figure 4. Simplified channel classification based on Beechie (unpublished data)

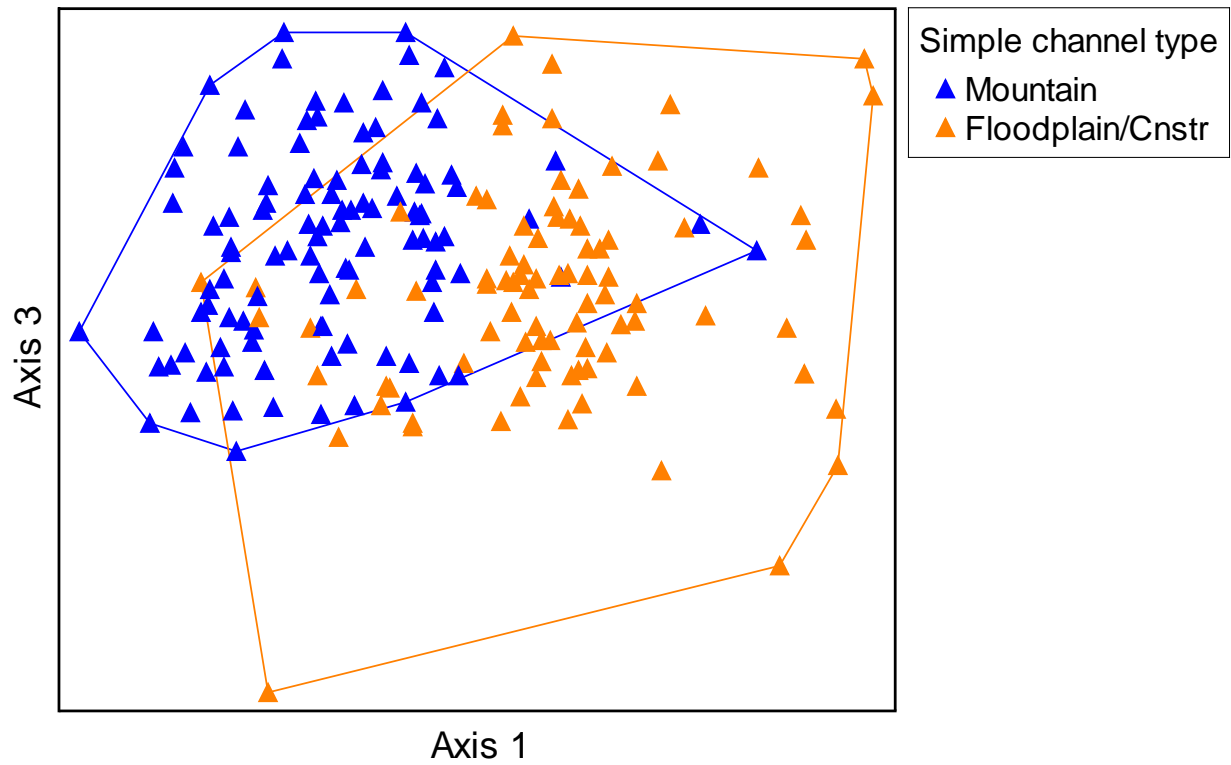


Figure 5. NMDS ordination of 2011 CHaMP sites with overlay of simplified reach type.

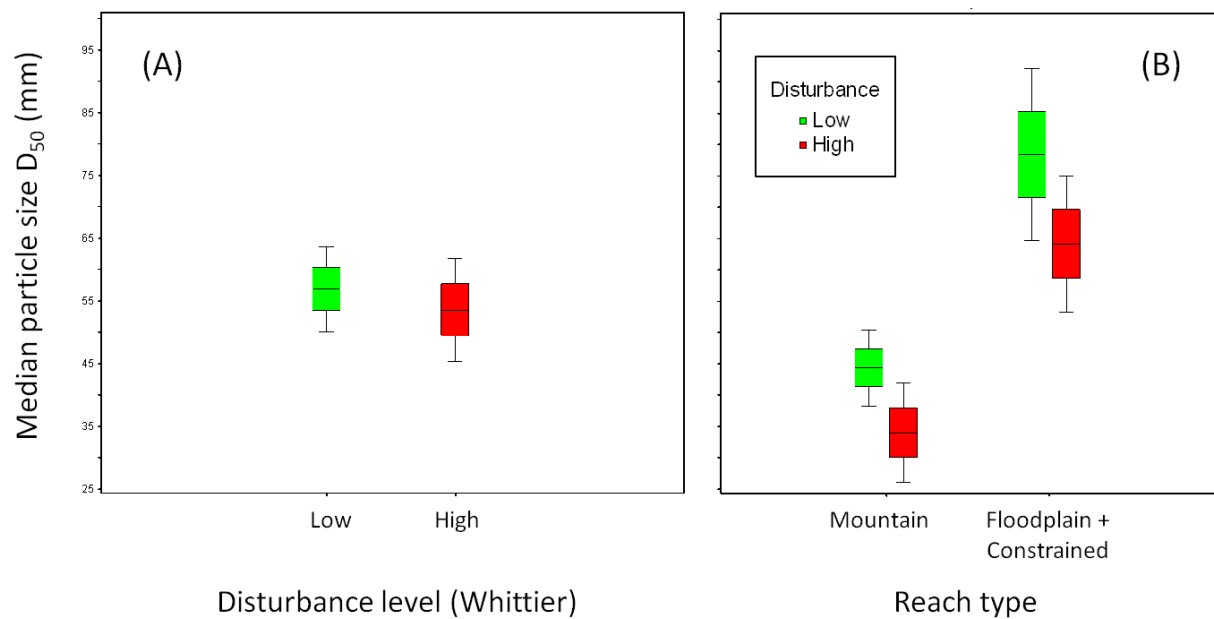


Figure 6. Difference between (A) naïve vs. (B) informed analysis of median surface particle size (D_{50}) in context of disturbance level and channel type.

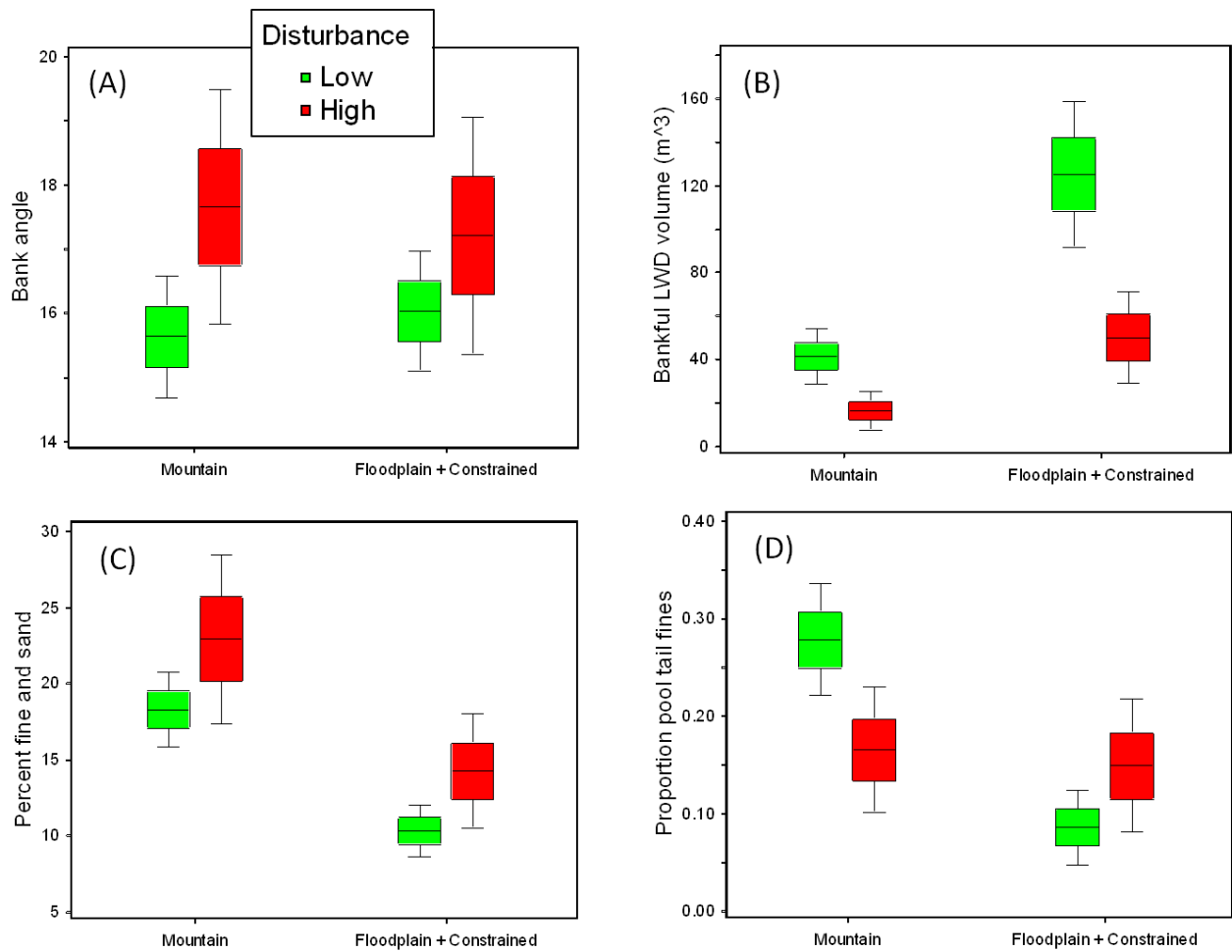


Figure 7. Boxplots of key fish habitat metrics by simplified channel type and level of disturbance.

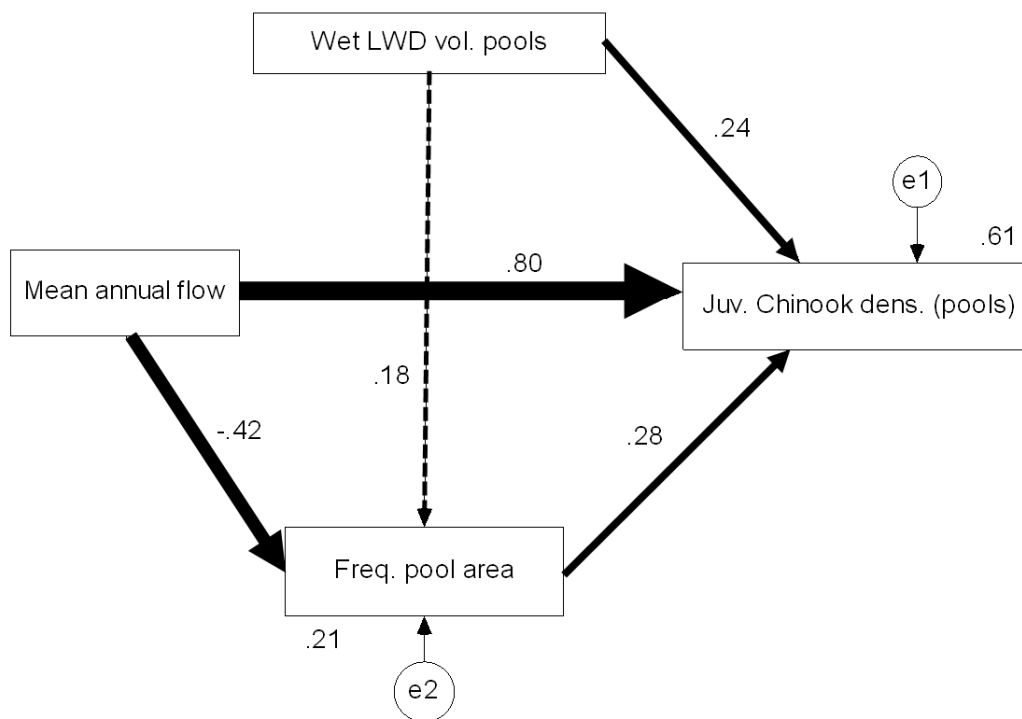


Figure 8. Structural equations modeling results linking habitat metrics with juvenile Chinook salmon density. Arrows represent direction and magnitude of causal effects among variables. Hatched lines represent non-significant interactions. Numerical values indicate standardized path coefficients and multiple R^2 correlations.

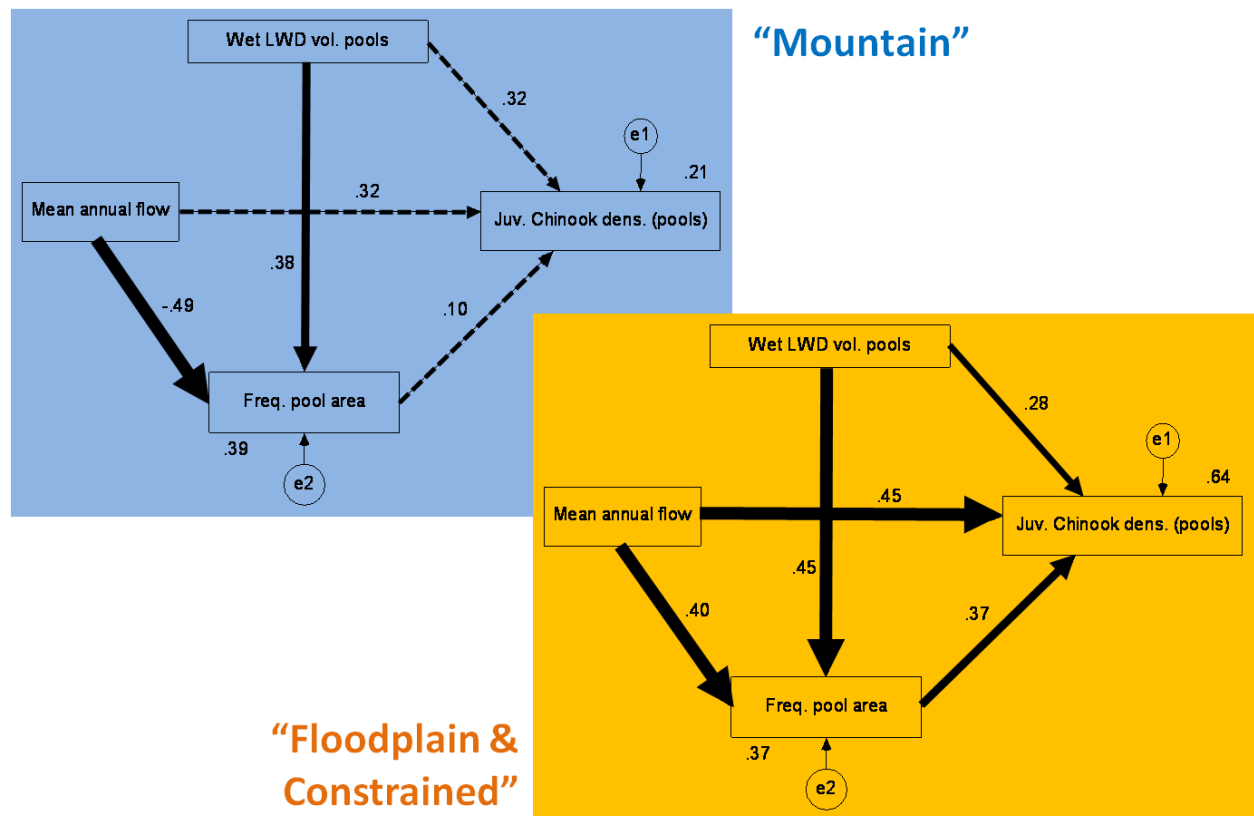


Figure 9. Multi-group SEM results by mountain vs. floodplain and constrained channel types.